



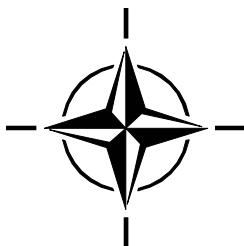
RTO TECHNICAL REPORT

TR-AVT-036

# **Performance Prediction and Simulation of Gas Turbine Engine Operation for Aircraft, Marine, Vehicular, and Power Generation**

(Estimation et simulation des performances du fonctionnement des turbomoteurs pour avions, navires, véhicules et pour la production d'énergie)

Final Report of the RTO Applied Vehicle Technology  
Panel (AVT) Task Group AVT-036.



Published February 2007





RTO TECHNICAL REPORT

TR-AVT-036

# **Performance Prediction and Simulation of Gas Turbine Engine Operation for Aircraft, Marine, Vehicular, and Power Generation**

(Estimation et simulation des performances du fonctionnement des turbomoteurs pour avions, navires, véhicules et pour la production d'énergie)

Final Report of the RTO Applied Vehicle Technology  
Panel (AVT) Task Group AVT-036.

# The Research and Technology Organisation (RTO) of NATO

RTO is the single focus in NATO for Defence Research and Technology activities. Its mission is to conduct and promote co-operative research and information exchange. The objective is to support the development and effective use of national defence research and technology and to meet the military needs of the Alliance, to maintain a technological lead, and to provide advice to NATO and national decision makers. The RTO performs its mission with the support of an extensive network of national experts. It also ensures effective co-ordination with other NATO bodies involved in R&T activities.

RTO reports both to the Military Committee of NATO and to the Conference of National Armament Directors. It comprises a Research and Technology Board (RTB) as the highest level of national representation and the Research and Technology Agency (RTA), a dedicated staff with its headquarters in Neuilly, near Paris, France. In order to facilitate contacts with the military users and other NATO activities, a small part of the RTA staff is located in NATO Headquarters in Brussels. The Brussels staff also co-ordinates RTO's co-operation with nations in Middle and Eastern Europe, to which RTO attaches particular importance especially as working together in the field of research is one of the more promising areas of co-operation.

The total spectrum of R&T activities is covered by the following 7 bodies:

- AVT    Applied Vehicle Technology Panel
- HFM    Human Factors and Medicine Panel
- IST    Information Systems Technology Panel
- NMSG   NATO Modelling and Simulation Group
- SAS    System Analysis and Studies Panel
- SCI    Systems Concepts and Integration Panel
- SET    Sensors and Electronics Technology Panel

These bodies are made up of national representatives as well as generally recognised 'world class' scientists. They also provide a communication link to military users and other NATO bodies. RTO's scientific and technological work is carried out by Technical Teams, created for specific activities and with a specific duration. Such Technical Teams can organise workshops, symposia, field trials, lecture series and training courses. An important function of these Technical Teams is to ensure the continuity of the expert networks.

RTO builds upon earlier co-operation in defence research and technology as set-up under the Advisory Group for Aerospace Research and Development (AGARD) and the Defence Research Group (DRG). AGARD and the DRG share common roots in that they were both established at the initiative of Dr Theodore von Kármán, a leading aerospace scientist, who early on recognised the importance of scientific support for the Allied Armed Forces. RTO is capitalising on these common roots in order to provide the Alliance and the NATO nations with a strong scientific and technological basis that will guarantee a solid base for the future.

The content of this publication has been reproduced  
directly from material supplied by RTO or the authors.

Published February 2007

Copyright © RTO/NATO 2007  
All Rights Reserved

ISBN 978-92-837-0061-6

Single copies of this publication or of a part of it may be made for individual use only. The approval of the RTA Information Management Systems Branch is required for more than one copy to be made or an extract included in another publication. Requests to do so should be sent to the address on the back cover.

# Table of Contents

	Page
<b>List of Figures</b>	<b>xv</b>
<b>List of Tables</b>	<b>xxviii</b>
<b>Programme Committee</b>	<b>xxix</b>
 <b>Executive Summary and Synthèse</b>	 <b>ES-1</b>
 <b>Chapter 1 – Introduction</b>	 <b>1-1</b>
1.1 Document Organization	1-1
1.2 Applications of Mathematical Engine Models	1-2
1.3 Introduction to Types of Engine Models	1-4
1.4 Computers, Software, and Recent Developments	1-5
1.5 References	1-5
 <b>Chapter 2 – Applications</b>	 <b>2-1</b>
Introductory Comments	2-1
2.1 Gas Turbine Engine Simulations for Fixed-Wing Aircraft Applications	2-1
2.1.1 Preliminary Design Synoptics	2-3
2.1.1.1 The Gas Turbine Conceptual Design Process	2-4
2.1.1.2 Mission Engine or Cycle Selection	2-7
2.1.1.3 Control System Concept Definition/Evaluation	2-10
2.1.1.4 Gas Turbine Cycle Design Methodology – Numerical Optimization	2-13
2.1.2 Design and Verification Synoptics	2-16
2.1.2.1 Technical Risk Assessment	2-16
2.1.2.2 Hardware in-the-Loop	2-22
2.1.2.3 Aircraft Simulation	2-25
2.1.2.4 Installation Effects on Full Engine	2-29
2.1.2.5 Statistical Analysis	2-32
2.1.3 System Design and Development Synoptics	2-36
2.1.3.1 Performance	2-37
2.1.3.2 Operability	2-55
2.1.3.3 Life Assessment and Durability	2-60
2.1.3.4 Adverse Weather	2-65
2.1.3.5 Controls	2-67
2.1.4 Post-Certification and In-Service Support Synoptics	2-72
2.1.4.1 The User Environment	2-73
2.1.4.2 The Need for Engine Models and User Requirements	2-74
2.1.4.3 Engine Health Monitoring and Fault Diagnosis	2-75
2.1.5 References for Fixed Wing Applications	2-91
2.2 Gas Turbine Engine Simulations for Rotary Aircraft Applications	2-93
2.2.1 History	2-93

2.2.2	Market	2-94
2.2.3	General Engine Layout	2-94
2.2.3.1	Usual Layouts	2-95
2.2.3.2	Examples of Engines Layouts	2-95
2.2.3.3	Use of Free Turbines	2-96
2.2.4	Associated Simulations	2-97
2.2.5	Rotary Application Synoptics	2-98
2.2.5.1	Adaptive Engine Model for Helicopter Turboshift Engine Control Systems	2-98
2.2.6	References for Rotary Wing Applications	2-101
2.3	Gas Turbine Simulations for Marine Propulsion Applications	2-101
2.3.1	Typical Scenarios	2-102
2.3.2	System Configurations	2-103
2.3.2.1	Gas-Turbines in Direct Drive Configurations	2-103
2.3.2.2	Gas-Turbines in Electrical Drive Configuration	2-103
2.3.2.3	Hybrid Systems	2-106
2.3.3	Propulsion System Components	2-107
2.3.3.1	Gearboxes	2-107
2.3.3.2	Clutches	2-108
2.3.3.3	Shafts, Couplings, Bearings and Seals	2-108
2.3.3.4	Propulsors	2-108
2.3.3.5	Filters and Coalescers	2-112
2.3.3.6	The Hull	2-113
2.3.3.7	Hull Propeller Interaction	2-115
2.3.4	Performance Modeling of Marine Gas Turbines	2-116
2.3.4.1	Description/Derivation of Model	2-116
2.3.4.2	Essential Differences between Marine and Aero Engines	2-117
2.3.4.3	Description of Drive Types (Overview)	2-117
2.3.4.4	Description of Installations (Overview)	2-118
2.3.4.5	Performance Model Inputs/Outputs	2-119
2.3.5	Marine Performance Model Application	2-119
2.3.5.1	SFC Level	2-119
2.3.5.2	Design Data	2-119
2.3.5.3	Intakes	2-120
2.3.5.4	Exhaust	2-121
2.3.5.5	Air-System	2-122
2.3.5.6	Testbed Design	2-123
2.3.5.7	Controls Requirements	2-123
2.3.5.8	Engine Testing	2-126
2.3.5.9	Analysis of Testdata – Referral of Operating Point	2-127
2.3.6	Synoptics for Marine Applications	2-127
2.3.6.1	Ship Propulsion System – Transients	2-127
2.3.6.2	Health Management	2-130
2.3.6.3	Condition Monitoring	2-132
2.3.7	References for Marine Propulsion Systems	2-134
2.4	Gas Turbine Engine Simulations for Vehicular Applications	2-135
2.4.1	Historical Background	2-135

2.4.2	The AGT 1500 Vehicular Gas Turbine	2-140
2.4.3	Gas Turbines vs. Diesel Engines	2-142
2.4.3.1	Performance	2-143
2.4.3.2	Weight	2-143
2.4.3.3	Signature	2-143
2.4.3.4	Reliability	2-143
2.4.3.5	All Weather Capability	2-143
2.4.3.6	Fuel Consumption	2-144
2.4.3.7	Costs	2-144
2.4.3.8	Growth Potential	2-144
2.4.3.9	Logistics	2-144
2.4.4	Vehicular Turbine Installation Specifics	2-145
2.4.4.1	Mission Profile	2-145
2.4.4.2	Weight	2-145
2.4.4.3	Environmental Conditions	2-145
2.4.4.4	Serviceability	2-145
2.4.5	AGT 1500 Cycle Overview	2-146
2.4.6	Synoptic for Vehicular Propulsion Applications	2-146
2.4.7	References for Vehicular Propulsion Systems	2-149
2.5	Gas Turbine Engine Simulations for Power Generation Applications	2-149
2.5.1	Introduction	2-149
2.5.2	Power Generation Application Synoptics	2-149
2.5.2.1	Modeling of a Combined Cogeneration Plant with Central Cooling Facility	2-149
2.5.2.2	Model Support to Industrial Gas Turbine Condition Monitoring	2-153
2.5.3	Performance Analysis Employing Adaptive Engine Models	2-154
2.5.4	Monitoring Application Cases	2-155
2.5.4.1	Modeling Industrial Gas Turbines for Operation with Different Fuels	2-157
2.5.4.2	Modeling Industrial Gas Turbines for Water Injection	2-159
2.5.5	Gas – Water Mixing	2-160
2.5.6	Turbomachinery Components	2-161
2.5.6.1	Sample Results of Effects on Performance	2-162
2.5.7	References for Power Generation Applications	2-163
2.6	Gas Turbine Engine Simulations for Manufacturing Applications	2-163
2.6.1	Introduction	2-164
2.6.2	Methodology	2-164
2.6.3	Scope of Work and Assumptions	2-165
2.6.4	Sensitivity Analysis	2-166
2.6.5	Methods of Simulating Performance Variation	2-167
2.6.5.1	Response Surface Models (RSM)	2-167
2.6.5.2	Variation Simulation Algorithm	2-168
2.6.6	Results	2-169
2.6.7	Cost Modeling	2-171
2.6.8	Conclusions	2-172
2.6.9	References for Manufacturing Applications	2-173
2.6.10	Additional Bibliography for Manufacturing Applications	2-173

## Chapter 3 – System Models

3-1

3.1	Gas Turbine Cycle Analysis	3-1
3.1.1	Ideal Joule Process	3-1
3.1.1.1	Simple Cycle	3-1
3.1.1.2	Recuperated Cycle	3-3
3.1.1.3	Intercooled Cycle	3-4
3.1.1.4	Combined Intercooling and Recuperating	3-6
3.1.1.5	Reheated Cycle	3-7
3.1.1.6	Combined Intercooling and Reheat	3-8
3.1.1.7	Combined Intercooling, Reheat and Recuperator	3-10
3.1.2	Real Joule Process	3-10
3.1.2.1	Nearly Real Joule Process	3-10
3.1.2.2	Turbine Cooling	3-12
3.1.2.3	Real Joule Process	3-14
3.1.3	Efficiency Potential of the Simple Gas Turbine Cycle	3-16
3.1.3.1	Schoolbook Wisdom	3-17
3.1.3.2	Full Cycle Calculation	3-21
3.1.4	From Power Generation to Thrust Generation	3-29
3.1.4.1	Turbojet	3-29
3.1.4.2	Turbofan	3-30
3.1.5	Quality Criteria	3-32
3.1.5.1	Propulsive Efficiency	3-32
3.1.5.2	Thermal Efficiency	3-32
3.1.5.3	Overall Efficiency	3-33
3.2	Gas Turbine Thermodynamic Engine Model	3-35
3.2.1	Selecting the Appropriate Model Type	3-36
3.2.1.1	Engine Development Cycle Considerations	3-36
3.2.1.2	Minimum, Average, New and Old Engine Models	3-37
3.2.2	General Nomenclature	3-38
3.2.3	Thermodynamic and Gas Properties	3-39
3.2.3.1	Atmosphere Definitions	3-39
3.2.3.2	Thermo Property Packages	3-39
3.2.3.3	Gas Properties Evaluation for Steam/Water Injection	3-40
3.2.3.4	Impact of Modeling Assumptions	3-42
3.2.3.5	Aero-Thermo Process Calculations	3-43
3.2.4	Steady State Performance Models	3-43
3.2.4.1	Different Types of Off-Design Steady State Models	3-44
3.2.4.2	0-D Models	3-44
3.2.5	Transient Performance Models	3-49
3.2.5.1	Solution by Explicit Euler Integration	3-50
3.2.5.2	Solution by Implicit Euler Integration	3-50
3.2.5.3	Extension of Simple Example to Include Gas Dynamics	3-51
3.2.5.4	Further Extension of the Example to Include Heat Soakage	3-53
3.2.5.5	Non-Iterative Technique	3-54
3.2.5.6	Iterative Real-Time Simulation	3-55
3.2.5.7	Other Dynamic Events	3-56

3.2.6	Iteration and Numerical Methods	3-57
3.2.6.1	Local Iterations	3-57
3.2.6.2	Global Iterations and Multi-Dimensional Newton-Raphson	3-59
3.2.6.3	Relaxation	3-64
3.2.6.4	Constraint Handling	3-64
3.2.7	Non-Component Based Parametric Models	3-64
3.2.7.1	Applications	3-64
3.2.7.2	Model Formulation	3-65
3.2.7.3	Model Synthesis Procedures	3-66
3.3	Gas Turbine Engine Performance Analysis	3-66
3.3.1	Performance Instrumentation	3-66
3.3.2	Model Validation and Calibration	3-66
3.3.2.1	Turbine Flow Capacity	3-67
3.3.2.2	Heat Balance	3-68
3.3.2.3	ISA Corrections	3-68
3.3.2.4	Accuracy	3-69
3.3.2.5	Example: Low Pressure Turbine Efficiency Analysis	3-70
3.3.2.6	Analysis by Synthesis	3-71
3.3.2.7	Summary of Analysis by Synthesis	3-76
3.3.3	Calculation of Installed Performance	3-77
3.3.3.1	Inlet Recovery	3-77
3.3.3.2	Distortion	3-77
3.3.3.3	Installed Thrust	3-77
3.3.4	Deterioration and Manufacturing Tolerance	3-78
3.3.4.1	Uncertainty of Component Performance	3-78
3.3.4.2	Change of Component Performance	3-78
3.3.4.3	Deterioration and Uncertainty in Engine Performance Level	3-78
3.3.5	Emissions	3-79
3.3.6	Bleed and Power Off-Takes	3-80
3.4	Control System Models	3-80
3.4.1	Main Engine Control	3-81
3.4.2	Afterburner Control	3-83
3.4.3	Variable Cycle Engines	3-83
3.4.4	Performance-Seeking Control (Performance Optimization)	3-83
3.4.5	Modeling Control System Components	3-83
3.4.6	Description of a Typical Control System	3-84
3.4.6.1	Sensors	3-85
3.4.6.2	Variable Geometry Actuation	3-86
3.4.6.3	Pumping	3-86
3.4.6.4	Metering	3-86
3.5	References	3-86
<b>Chapter 4 – Component Modeling for System Models</b>		<b>4-1</b>
4.1	Introduction	4-1
4.2	Gas Path Component Characteristics Required by Engine Models	4-3
4.2.1	General Program Requirements	4-3
4.2.2	Compressors	4-5
4.2.2.1	Modeling	4-5

4.2.2.2	Fixed Geometry Compressor	4-6
4.2.2.3	Importance of Compressor Maps in 0-D Models	4-7
4.2.2.4	Fan Representations	4-7
4.2.2.5	Secondary and Environmental Effects	4-7
4.2.2.6	Variable Geometry Compressor	4-7
4.2.2.7	Basic Algorithm to Determine Outlet Conditions	4-8
4.2.2.8	Precautions – Map Construction Assumptions	4-8
4.2.2.9	Precautions – Secondary and Environmental Effects	4-9
4.2.3	Turbines	4-10
4.2.3.1	Modeling	4-10
4.2.3.2	Fixed Geometry Turbines	4-10
4.2.3.3	Variable Geometry Turbines	4-10
4.2.3.4	Efficiency Definitions for Un-Cooled and Cooled Turbines	4-11
4.2.3.5	Total-to-Static Turbine Maps	4-21
4.2.3.6	Basic Algorithm to Determine Outlet Conditions	4-21
4.2.3.7	Precautions – Limitations	4-21
4.2.3.8	Importance of Turbine Maps in 0-D Models	4-22
4.2.4	Burners and Augmentors	4-23
4.2.4.1	Burners	4-23
4.2.4.2	Modeling	4-23
4.2.4.3	Basic Algorithm to Determine Outlet Conditions	4-25
4.2.4.4	Afterburner (Reheat) Simulation	4-25
4.2.4.5	Dry (Non-Burning) Operation	4-26
4.2.4.6	Wet (Burning Operation)	4-28
4.2.4.7	Flow Distribution and Cooling	4-30
4.2.4.8	Mixing and Burning	4-30
4.2.4.9	Test Analysis – Reheat Rig	4-30
4.2.4.10	Test Analysis – Gas Sampling	4-31
4.2.4.11	Test Analysis – Engine Test	4-31
4.2.4.12	Efficiency Correlations	4-31
4.2.4.13	Blow-Out	4-32
4.2.4.14	Screech	4-33
4.2.4.15	Buzz (Rumble)	4-33
4.2.5	Inlets	4-33
4.2.5.1	Inlet Function	4-33
4.2.5.2	Inlet Internal Losses: Inlet Recovery	4-34
4.2.6	Exhaust Nozzles	4-35
4.2.7	Splitters and Mixers	4-36
4.2.7.1	Splitters	4-36
4.2.7.2	Mixers	4-36
4.2.8	Ducts	4-41
4.2.9	Customer Bleeds and External Loads	4-41
4.3	Non Gas Path Component Characteristics Required by Engine Models	4-42
4.3.1	Lubrication and Fuel Systems	4-42
4.3.2	Thermal Management Systems	4-42
4.3.3	Heat Exchanger	4-43
4.3.3.1	Steady State Heat Exchanger Performance	4-43
4.3.3.2	Heat Exchanger Transient Simulation	4-44

4.3.3.3	Heat Soakage Effect Models	4-45
4.3.3.4	Recuperator Internal Wall Heat Soakage Effect Model	4-45
4.3.4	PowerTrain	4-49
4.3.4.1	Clutch Models	4-49
4.3.4.2	Loads	4-53
4.4	References	4-54

## **Chapter 5 – Examples of 0-D Numerical Simulations** **5-1**

Introductory Comments		5-1
5.1	A FORTRAN-Based Modeling System	5-1
5.1.1	Architecture	5-1
5.1.2	Database	5-2
5.1.3	Utilities	5-2
5.1.4	Block Data	5-2
5.1.5	User Interface	5-2
5.1.6	Read Data	5-3
5.1.7	Program Control	5-3
5.1.8	Engine Routine	5-3
5.1.9	Components	5-3
5.1.10	Other Routines and Functions	5-4
5.1.11	Output Control	5-4
5.1.12	Future Developments	5-5
5.2	MOPS (Modular Performance Synthesis Program) or MOPEDS	5-5
5.3	GASTURB	5-9
5.4	The GSP Object-Oriented Modeling Environment	5-11
5.5	TERTS (Turbine Engine Real Time Simulator)	5-17
5.6	Simulation Models for Engine Diagnostics	5-18
5.6.1	Examples of Results	5-20
5.6.1.1	Examining the Effects of Component Malfunctions	5-20
5.6.2	Direct Component Condition Diagnosis	5-21
5.7	Numerical Propulsion System Simulation (NPSS)	5-22
5.7.1	Overview	5-22
5.7.2	NPSS Architecture and Object-Oriented Software Design	5-23
5.7.3	NPSS and Conceptual Design	5-23
5.7.4	Standards and Zooming	5-24
5.7.5	Examples	5-24
5.8	Other 0-D Modeling Systems	5-25
5.9	References	5-25

## **Annex A – Higher Order Models** **A-1**

Introductory Comments		A-1
A.1	Detailed 1-Dimensional (1-D) Models	A-1
A.1.1	Steady State 1-D Models	A-1
A.1.2	Transient 1-D Models	A-1
A.1.3	1-D Dynamic Engine Simulations	A-2
A.1.3.1	Combustor Component – VPICOMB	A-2

A.1.3.2	Compressor Component – DYNTECC	A-3
A.1.3.3	Full Engine Simulation – ATEC	A-7
A.1.4	Benefits of 1-D vs. 0-D Models	A-10
A.2	High Fidelity 2-D/3-D Models	A-10
A.2.1	Zooming of 2-D Models	A-10
A.2.2	3-D Models (Euler and RANS)	A-11
A.3	Higher Order Modeling Applications	A-12
A.3.1	1-D Dynamic Model Applications	A-12
A.3.1.1	Rotating Stall and Surge Investigation Using 1-D Compressor Model	A-12
A.3.1.2	Engine Stall Using One-Dimensional Modeling	A-14
A.3.1.3	Combustor Dynamics	A-16
A.3.1.4	Engine-Inlet Integration	A-19
A.3.1.5	Hot Gas Ingestion	A-22
A.3.1.6	Distortion Investigation Using Parallel Compressor Model	A-24
A.3.2	Three Dimensional Model Applications	A-27
A.3.2.1	Distortion Investigation	A-27
A.3.2.2	Rotating Stall and Surge Investigation	A-30
A.3.2.3	Multi-Disciplinary Interaction for Durability	A-34
A.3.2.4	Component Aerodynamic Design	A-37
A.4	References	A-42

## **Annex B – Advanced Topics and Recent Progress** **B-1**

Introductory Comments	B-1
B.1	Compressor Systems Performance
B.1.1	Simulation of Axial Compressor Performance
B.1.1.1	Generation of Baseline Compressor Map
B.1.1.2	Effect of Axisymmetric Compressor Tip Clearance on Performance
B.1.1.3	Stationary and Rotating Distortion
B.1.1.4	Stationary and Rotating Asymmetric Tip Clearance
B.1.1.5	Effect of Compressor Axial Gap
B.1.1.6	Effect of Axial Gap on Stalling Pressure Rise
B.1.1.7	Effect of Reynolds Number and Blade Surface Roughness
B.1.1.8	Variable Stator Vane Effects
B.1.1.9	Effects of Thermal Origins
B.1.1.10	Fan and Bypass Duct System
B.1.1.11	Blade Untwist
B.1.1.12	Stratification
B.1.1.13	Parametric Analysis of Aeroengine Flutter for Flutter Clearance
B.1.2	Simulation of Centrifugal Compressor Performance
B.1.2.1	Key Centrifugal Compressor Characteristics
B.1.2.2	Effects of Tip Clearance
B.1.2.3	Effects of Surface Roughness on Performance
B.1.2.4	Effect of Erosion on Performance
B.1.2.5	Effect of Inlet Plenum on Performance
B.1.2.6	Effect of Leakage on Performance
B.1.2.7	Effect of Flowpath Steps

B.1.3	Methodologies	B-50
B.1.3.1	Approximations at Global Level	B-50
B.1.3.2	Discrete Approximations to PDE	B-51
B.1.4	Theoretical Model	B-51
B.1.5	Application of CFD and Flow Models for Compressor Performance Assessment	B-53
B.1.6	Different Levels of Modeling	B-55
B.1.6.1	Lumped Parameter (Low-Order) Models	B-55
B.1.6.2	Attributes of Macro-Level Models	B-55
B.1.6.3	Physical Level Model	B-56
B.1.6.4	Role of Each Level of Modeling	B-56
B.1.7	Compressor Overall Summary	B-56
B.1.8	Cited References for Compressor Section	B-56
B.1.9	Additional Bibliography for Compressor Section	B-58
B.2	Performance of Turbine Sub-Systems	B-60
B.2.1	Overview of Turbine Sub-System Performance	B-60
B.2.2	High Pressure Turbines	B-60
B.2.2.1	General Performance	B-60
B.2.2.2	Characteristic Generation	B-62
B.2.2.3	Rig Testing	B-63
B.2.2.4	Engine Testing	B-64
B.2.2.5	Transient and Abnormal Operations	B-65
B.2.3	Low Pressure Turbines	B-65
B.2.3.1	General Performance	B-65
B.2.3.2	Characteristic Generation	B-66
B.2.3.3	Rig and Engine Testing	B-66
B.2.4	The Exceptions	B-67
B.2.4.1	Variable Area Turbines	B-67
B.2.4.2	Statorless Contra Rotating Turbines	B-67
B.2.5	Cited References for Turbine Section	B-68
B.3	Combustor Systems	B-68
B.3.1	Flowpath and Exit Temperature	B-68
B.3.1.1	Modeling	B-69
B.3.1.2	Dissociation/Recombination/Emission	B-70
B.3.1.3	NO <sub>x</sub> Modeling	B-72
B.3.1.4	Hail and Water Ingestion	B-73
B.3.2	Transient and Dynamic Modeling	B-73
B.3.2.1	Flame Blow-Out and Relight	B-73
B.3.2.2	Modeling Relight	B-75
B.3.2.3	Combustion Efficiency and Compressor Limits	B-76
B.3.3	Reheat System	B-77
B.3.3.1	Stability and Blow-Out	B-77
B.3.3.2	Screech and Rumble	B-78
B.3.3.3	High Frequency Instabilities	B-79
B.3.4	Liner Cooling	B-81
B.3.5	Cited References for Combustor Section	B-81
B.3.6	Additional Bibliography for Combustor Section	B-82

B.4	Exhaust Nozzle Component Systems	B-83
B.4.1	Zero Dimensional Analysis	B-84
B.4.1.1	Definition of Nozzle Coefficients	B-84
B.4.1.2	Single Stream Exhaust System	B-84
B.4.1.3	Thrust Definitions	B-87
B.4.1.4	Dual Stream Engine Configuration	B-90
B.4.1.5	Mixed Flow Example	B-92
B.4.1.6	Evaluation of Nozzle Coefficients	B-94
B.4.1.7	Variable Nozzle Benefits and Examples	B-95
B.4.2	Multi-Dimensional Considerations for Variable Area Nozzle Simulation	B-98
B.4.2.1	Multi-Dimensional Representation of Convergent Nozzles	B-98
B.4.2.2	Multi-Dimensional Representation of Convergent-Divergent Nozzles	B-101
B.4.2.3	Special Considerations for Multi-Dimensional Modeling and Simulation of Nozzles	B-104
B.5	Inlet Systems	B-108
B.5.1	Diffusion and Acceleration of Airflow into the Propulsion System	B-109
B.5.2	Inlet External Loss: Spillage Drag	B-110
B.5.2.1	Subsonic Case	B-110
B.5.2.2	Supersonic Case	B-111
B.5.3	Inlet Internal Losses: Inlet Recovery	B-112
B.5.4	Cited References for Nozzles and Inlets	B-113
B.6	Aerodynamics of Air Systems	B-113
B.6.1	Introduction	B-113
B.6.2	Tappings/Bleeds	B-114
B.6.2.1	Outward Tappings	B-114
B.6.2.2	Inward Tappings	B-118
B.6.3	Pre-Swirl Systems	B-119
B.6.3.1	Pre-Swirl Nozzles	B-119
B.6.3.2	Pre-Swirl Chamber	B-120
B.6.3.3	Receiver	B-120
B.6.3.4	Coverplates	B-120
B.6.3.5	Conclusions for Tappings	B-120
B.6.4	Labyrinth Seals	B-121
B.6.4.1	Straight Through Labyrinth Seals	B-121
B.6.4.2	Stepped Labyrinth Seals	B-127
B.6.4.3	Conclusions for Labyrinth Seals	B-129
B.6.5	Rotating Holes	B-129
B.6.5.1	Sharp-Edged Holes	B-129
B.6.5.2	Rounded Holes	B-129
B.6.5.3	Discharge Coefficient Correlations	B-132
B.6.5.4	Comments on the Correlation Methods	B-135
B.6.5.5	Conclusions for Rotating Holes	B-135
B.6.6	Two Phase Flow	B-135
B.6.6.1	Pipe Flow	B-135
B.6.6.2	Bends	B-136
B.6.6.3	Mitre Bends	B-136
B.6.6.4	Stationary Orifices	B-137
B.6.6.5	Conclusions for Two Phase Flows	B-139

B.6.7	References for Aerodynamics for Air Systems	B-139
B.6.8	Additional Bibliography for Aerodynamics for Air Systems	B-141
B.7	Control Systems Modeling	B-141
B.7.1	Requirements for Modeling Control Systems	B-141
B.7.1.1	Types of Models	B-142
B.7.1.2	Equations Used in Hydraulic Control Systems	B-144
B.7.1.3	Electro-Hydraulic Servo Valves	B-145
B.7.1.4	Metering Valve	B-145
B.7.1.5	Pressure Drop Regulator	B-146
B.7.1.6	Power Actuators	B-146
B.7.1.7	Modeling a Two-Stage Servo Valve (Moog Type)	B-147
B.7.2	Control Integration with Engine Model	B-149
B.7.2.1	Common Engine Model	B-150
B.7.2.2	Using Performance (Cycle-Match) Models for Control-System Design and Analysis	B-151
B.7.3	References for Control Models	B-156
B.8	Effect of Water/Steam Injection on the Performance of Power Generation Gas	B-157
B.8.1	Introduction	B-157
B.8.2	The Physics of Operational Parameter Deviations	B-157
B.8.3	Computer Models for Water Injected Operation	B-159
B.8.3.1	Constitution of a Performance Model	B-159
B.8.3.2	Modelling for Water Injection	B-160
B.8.3.3	Estimation of Performance Deviations using Analytical Relations	B-163
B.8.4	Water/Steam Ingestion Effects Discussion	B-171
B.8.5	Conclusions for Water/Steam Ingestion	B-173
B.8.6	Further Discussions	B-173
B.8.6.1	Gas Properties	B-174
B.8.6.2	Fuel-Air Ratio	B-174
B.8.6.3	Power Output	B-175
B.8.6.4	Efficiency	B-177
B.8.6.5	Compressor Pressure Ratio	B-177
B.8.7	References in Section B.8, Water/Steam Ingestion	B-177
B.8.8	Additional Bibliography for Section B.8	B-179

## **Annex C – Computer Platforms** **C-1**

C.1	Computer Platforms	C-1
C.1.1	Hardware	C-1
C.1.2	Operating Systems	C-2
C.1.3	Development Environments	C-3
C.2	Trends and New Technologies	C-3
C.2.1	Computing Power	C-3
C.2.2	Computing Costs	C-5
C.2.3	Parallel and Distributed Computing	C-5
C.2.3.1	Multi-Threading	C-6
C.2.3.2	Distributed Computing and CORBA	C-7
C.2.4	Interfaces	C-7
C.2.4.1	User Interfaces	C-7

C.2.4.2	External Interfaces	C-8
C.2.4.3	Event Driven User Interfaces	C-8
C.2.5	Object Orientation	C-8
C.2.6	PC Technology	C-9
C.2.7	Zooming	C-9
C.2.8	Development Environments	C-10
C.2.9	Architectures	C-10
C.2.10	Configuration Management	C-11
C.2.11	Windows versus UNIX	C-11
C.3	Challenges	C-12
C.3.1	General	C-12
C.3.2	Reducing Development Effort	C-12
C.3.3	Generic Tools	C-12
C.3.4	Standardization	C-12
C.3.5	User Interfaces	C-13
C.3.6	Visualization	C-13
C.3.7	Maintainability	C-13
C.3.8	Grid Generation	C-14
C.3.9	Distributed Parallel Computing	C-14
C.3.10	Probabilistic Analysis	C-14
C.4	Future	C-15
C.5	Cited References	C-15
C.6	Additional Bibliography	C-16
C.7	Acronyms	C-17

## **Annex D – Gas Turbine Engine Simulations for Educational Purposes** **D-1**

D.1	Introduction to Transient Modeling	D-1
D.1.1	Audience	D-1
D.1.2	Format	D-2
D.1.3	Value	D-4
D.2	Introduction to Gas Turbine Cycles	D-4
D.2.1	Audience	D-4
D.2.2	Format	D-4
D.2.2.1	Module #1: Hand Calculation	D-4
D.2.2.2	Module #2: Design Point Calculation	D-5
D.2.2.3	Module #3: Off-Design Calculation	D-5
D.2.2.4	Value	D-6
D.3	Bibliography	D-7

## **Annex E – GLOSSARY** **E-1**

# List of Figures

	<b>Page</b>
Figure 1.1	Engine Model Users and Creators 1-2
Figure 1.2	Engine Models used Throughout Engine Life Cycle 1-4
Figure 2.1	Historical Trends in Computerized Analysis Capability 2-5
Figure 2.2	Transient Simulation of Fan Deceleration Operating Lines 2-9
Figure 2.3	Optimization Strategy 2-14
Figure 2.4	Typical Thrust and SFC Performance for High Bypass Transport Engine 2-19
Figure 2.5	Military Aircraft Flight Envelope 2-20
Figure 2.6	Engine Thermal Efficiency Variations 2-20
Figure 2.7	Effect of Engine Thrust-to-Weight on Aircraft Weight 2-22
Figure 2.8	Incorporation of the Simple Dynamic Engine Mode into the Thrust Vectoring Simulation 2-27
Figure 2.9	Comparison of Net Propulsive Force at 35,000 ft., Mach 0.2, no Vectoring 2-28
Figure 2.10	Comparison of Nozzle Pressure Ratio at 35,000 ft., Mach 0.2, no Vectoring 2-28
Figure 2.11	Effects of Tip Clearance on Compressor Characteristics 2-30
Figure 2.12	Power Off-Take and Bleed Effects on HPC Operating Points at Sea Level and at Altitude 2-31
Figure 2.13	Engine Station Numbering Nomenclature 2-34
Figure 2.14	Monte Carlo Study Result 2-36
Figure 2.15	Lines of Constant Spool Speed Overlaid on the Altitude Mach Number Envelope 2-39
Figure 2.16	GSP Model Window with Simple Turbofan Model 2-39
Figure 2.17	Effect of Compressor Bleed on Take-Off Performance 2-40
Figure 2.18	ATEST Component Level Modeling Approach 2-41
Figure 2.19	ATEST Typical Engine Cut-Off and Re-light Comparison 2-42
Figure 2.20	Schematic of Overall Fault Detection Process 2-45
Figure 2.21	Abrupt Change in Compressor Exit Pressure during Steady Engine Operation 2-45
Figure 2.22	Typical Environmental Condition Variances in an Altitude Test Facility 2-47
Figure 2.23	Effectiveness of Adjusting Thrust for Environmental Variances 2-47
Figure 2.24	In-Flight Transients, Idle-to-Max Snap, Altitude 40,000 ft., Mach 0.52 2-49
Figure 2.25	Schematic of Empirical Start Model 2-50
Figure 2.26	Empirical Model versus Flight Test Data 2-51
Figure 2.27	Simulation of the Effect of Erosion on Single Stage Compressor Performance 2-53
Figure 2.28	Simulation of the Effect of Erosion on Multi-Stage Compressor (J85) Performance 2-54
Figure 2.29	Effects of Surface Roughness and Tip Clearance on Compressor Performance 2-54

Figure 2.30	Surge Cycles during Engine Re-Acceleration	2-57
Figure 2.31	Schematic of the Coupled Inlet-Engine Codes	2-58
Figure 2.32	Cross-Section View of the 4060 Inlet and J85-13 Turbojet Installation	2-58
Figure 2.33	Inlet Shock Location	2-59
Figure 2.34	Compressor Pressure Ratio as a Function of Compressor Inlet Corrected Mass Flow Rate	2-60
Figure 2.35	Schematic Overview of the Integrated Analysis Tool	2-61
Figure 2.36	Measured Variation of Fuel Flow and Altitude	2-63
Figure 2.37	Effect of HPT Deterioration on FTIT	2-64
Figure 2.38	Comparison of FTIT as Measured by FACE and Calculated by GSP	2-64
Figure 2.39	Effect of HPT Deterioration on Creep Strain Accumulation	2-65
Figure 2.40	Effect of 4% Humidity on Major Engine Parameters, Thrust, Fuel Flow, and SFC	2-67
Figure 2.41	PSC Implementation and Process Flow Diagram	2-68
Figure 2.42	Component Efficiency Scaling Factor, Found from Engine Test Analysis	2-72
Figure 2.43	Calculation of Influence Coefficients using an Engine Performance Model	2-82
Figure 2.44	Flowchart of the Adaptive Modeling Procedure	2-85
Figure 2.45	Derivation of Modification Factors by an Adaptive Model	2-87
Figure 2.46	Layout of Mixed Flow Turbofan for Application of Adaptive Modeling	2-89
Figure 2.47	Modification of Map Initially Used, in Order to Adapt the Model to Engine Data	2-90
Figure 2.48	Deviations in Measured Quantities Caused by Component Faults	2-90
Figure 2.49	ALOUETTE II Powered by ARTOUSTE II	2-94
Figure 2.50	Example of Turboshift Engine Layout Tm333, Turbomeca	2-95
Figure 2.51	Example of a Tree Turbine Engine: Arriel 2S1, Turbomeca	2-96
Figure 2.52	Example of a Tree Turbine Engine: Makila, Turbomeca	2-97
Figure 2.53	Simulation of the Engine, Coupled with its Limitations, Control System and Helicopter Rotor	2-97
Figure 2.54	Simulation of the Helicopter Rotor	2-98
Figure 2.55	New vs. Deteriorated Engine – Shaft Horsepower vs. Gas Temperature Characteristic	2-99
Figure 2.56	LP Compressor Model Showing Adaptive Features	2-100
Figure 2.57	Some System Architectures	2-103
Figure 2.58	Simple Electric Propulsion System	2-105
Figure 2.59	Integrated Full Electric Propulsion System for the Type 45 Destroyer	2-105
Figure 2.60	COGES System for Large LNG Carrier (After Reynolds and Tooke)	2-106
Figure 2.61	Combined Diesel Electric and Gas Propulsion System	2-107
Figure 2.62	Combined Diesel Electric or Gas Propulsion System	2-107
Figure 2.63	$K_T/K_Q$ and Open Water Efficiency ( $\eta_o$ ) Curves for B4-70	2-110
Figure 2.64	Four Quadrant Diagram for the B4-70 Propeller at a Number of Different Pitch/Diameter Ratios	2-111
Figure 2.65	Controllable Pitch Propeller Operation	2-111

Figure 2.66	Typical Waterjet Application	2-112
Figure 2.67	Bow and Stern Wave Generation	2-113
Figure 2.68	Bow and Stern Wave Interaction	2-113
Figure 2.69	Typical Resistance Curve	2-114
Figure 2.70	Surface Effect Ship in OOD Condition	2-115
Figure 2.71	Hydrofoil Vessel at Speed	2-115
Figure 2.72	Particle Motion in a Water Wave	2-116
Figure 2.73	Water Particle Motion Beneath a Wave	2-116
Figure 2.74	Power Turbine Operating Lines	2-118
Figure 2.75	Engine Inlet Pressure Distortion from Radial Intake	2-120
Figure 2.76	Exhaust Collector Preliminary Design	2-121
Figure 2.77	Turbine Exit Flow Modeling – Bearing Support Strut Vane Wake	2-122
Figure 2.78	Power Turbine Overspeeds for Rapid Offloads – Inertia and Fuel Response Effect	2-124
Figure 2.79	Power Turbine Overspeeds for Rapid Offload – Heatsoakage Effect	2-125
Figure 2.80	Power Turbine Overspeeds for Coupling Shaft Failure	2-126
Figure 2.81	Figures 6 and 7 Pulled from the Referenced Document	2-129
Figure 2.82	Figures 8 and 9 Pulled from the Referenced Document	2-129
Figure 2.83	Derived Performance Curves	2-131
Figure 2.84	Poseidon Desktop Simulator GUI	2-131
Figure 2.85	System Overview	2-132
Figure 2.86	Raw Data Processing (Gas Generator Exit Thermocouple)	2-133
Figure 2.87	Generic Condition Monitoring and Diagnosis Process	2-133
Figure 2.88	Early WWI Vintage Tank	2-136
Figure 2.89	Renault FT Tank	2-136
Figure 2.90	M-4 Sherman Tank	2-137
Figure 2.91	Panther Tank	2-138
Figure 2.92	M60 Tank	2-138
Figure 2.93	MBT 70 Tank	2-139
Figure 2.94	M-1 Abrams Tank	2-139
Figure 2.95	AGT 1500 Gas Turbine	2-140
Figure 2.96	AGT 1500 Line Replaceable Units and Recuperator	2-141
Figure 2.97	AGT 1500 Gas Path Cycle Schematic	2-146
Figure 2.98	Schematic of the Alternative Regeneration Cycle	2-147
Figure 2.99	Performance of Various Cycles as a Function of Turbine Inlet Temperature	2-148
Figure 2.100	Combined Cycle Using Gas Turbine, HRSG	2-150
Figure 2.101	Comparison of Simulation Results with Design Data	2-151
Figure 2.102	Predicting the Amount of Steam Supplied to the Campus for Different Duct Burner Outlet Temperatures	2-152
Figure 2.103	Comparison of Net Power Produced by Gas Turbine with Inlet Air Cooled by Absorption Chiller and Electric Chiller and Without Inlet Air-Cooling	2-153

Figure 2.104	Health Indices Percentage Deviation, for a Gas Turbine, which has Suffered Severe Turbine Fouling, Caused by Fuel Additives	2-155
Figure 2.105	Evolution of Power Turbine Degradation over the Initial Period of Engine Operation	2-156
Figure 2.106	Example of the Variation of Compressor Efficiency Derived by Employing Adaptive Modeling	2-156
Figure 2.107	Measured and Predicted Values of Gas Turbine Performance Parameters for Different Fuels (NG: Natural Gas and Diesel)	2-158
Figure 2.108	Deviation of Health Indices Derived by Processing Natural Gas Data are by Adaptive Model using Diesel Oil	2-159
Figure 2.109	Schematic Representation of a Twin Spool Gas Turbine and Discrimination of its Components	2-160
Figure 2.110	Overall Performance Parameters Predicted by a Computer Model, including Operation with Water/Steam Injection	2-162
Figure 2.111	Percentage Change of Performance Related Quantities, in Function of Water/Inlet Air Flow Ratio, when Intercooling Occurs	2-162
Figure 2.112	High Pressure Compressor Operating Point for Constant Load (45 MW) and CIT	2-163
Figure 2.113	Percent Total Effect on Specific Fuel Consumption	2-166
Figure 2.114	Design Space Limitations	2-167
Figure 2.115	Simulation Algorithm Using an Optimization Plan	2-168
Figure 2.116	Normalized Tolerance Range Results	2-170
Figure 2.117	Cost Modeling Results	2-171
Figure 3.1	Ideal Joule Process in the Enthalpy-Entropy Diagram	3-1
Figure 3.2	Influence of Burner Exit Temperature $T_4$ on Specific Power	3-2
Figure 3.3	Thermal Efficiency and Specific Power of the Ideal Joule Cycle	3-2
Figure 3.4	Joule Cycle with Recuperator	3-3
Figure 3.5	Thermal Efficiency and Specific Power of the Ideal Cycle with Recuperator	3-4
Figure 3.6	Ideal Joule Cycle with Intercooler	3-5
Figure 3.7	Efficiency of the Ideal Cycle with Intercooler	3-6
Figure 3.8	Efficiency of the Ideal Cycle with Intercooler and Recuperator	3-7
Figure 3.9	Efficiency of the Ideal Cycle with Reheat	3-8
Figure 3.10	Ideal Cycle with Intercooling and Reheat	3-9
Figure 3.11	Efficiency of the Ideal Cycle with Intercooling and Reheat	3-9
Figure 3.12	Efficiency of the Ideal Cycle with Intercooling, Reheat and Recuperator	3-10
Figure 3.13	Ideal and Real Cycle for the Same Specific Work $H_{LPT}$	3-11
Figure 3.14	Thermal Efficiency of the “Nearly Real” Simple Cycle	3-12
Figure 3.15	Simulation of a Cooled Turbine	3-12
Figure 3.16	Cooling Effectiveness for Different Cooling Configurations	3-13
Figure 3.17	Cooling Air Amount for Constant Metal Temperature of 1200 K	3-14
Figure 3.18	Performance of the Real Cycle with Constant Turbine Metal Temperature	3-15

Figure 3.19	Thermal Efficiency of the Recuperated Cycle with Constant Turbine Metal Temperature	3-15
Figure 3.20	Thermal Efficiency of the Intercooled and Recuperated Cycle with Constant Turbine Metal Temperature	3-16
Figure 3.21	Core Stream Process of a Turbofan	3-17
Figure 3.22	Thermal Efficiency Evaluated with Constant Gas Properties	3-19
Figure 3.23	Thermal Efficiency Evaluated with Temperature Dependent Gas Properties	3-20
Figure 3.24	Thermal Efficiency with Steam Injection (Steam-Fuel-Ratio = 1), Evaluated with Temperature Dependent Gas Properties	3-21
Figure 3.25	Thermal Efficiency Defined with $W_F \cdot FHV$	3-22
Figure 3.26	Burner Exit Temperature for Different Fuels ( $T_3 = 800 \text{ K}$ )	3-23
Figure 3.27	Thermal Efficiency with Hydrogen as Fuel with Lines of Constant Equivalence Ratio	3-24
Figure 3.28	Burner Temperature for Maximum Thermal Efficiency, Pressure Ratio = 60	3-25
Figure 3.29	Thermal Efficiency with Cooling Air Simulation	3-26
Figure 3.30	NGV Cooling Air $W_{CL}/W_{gas}$	3-27
Figure 3.31	Specific Power	3-28
Figure 3.32	Turboshaft and Turbojet	3-29
Figure 3.33	Turbojet Performance at 11 km	3-30
Figure 3.34	Turbofan with $T_4 = 2000 \text{ K}$ , Alt = 11 km, $M_n = 0.85$	3-31
Figure 3.35	Fan Tip Diameter and LPT Pressure Ratio. Constant Thrust @ alt = 11 km, $M_n = 0.85$	3-31
Figure 3.36	Transmission Efficiency for Turbofans with Constant Core Efficiency	3-33
Figure 3.37	Breakdown of Engine Efficiencies	3-34
Figure 3.38	Historical Trend in SFC	3-35
Figure 3.39	Model Types based on Engine Life Cycle	3-37
Figure 3.40	Values of Specific Heat $C_p$ and Isentropic Exponent $\gamma$ , for Temperatures Usual in the Hot Section of Gas Turbines	3-40
Figure 3.41	Change in Gas Properties for Different Amount of Injected Water ( $f = 0.02$ )	3-41
Figure 3.42	Ratio of Specific Heats of Steam and Combustion Gases	3-42
Figure 3.43	Indicative Aeroderivative Power Turbine Characteristic	3-49
Figure 3.44	Model of Non-Iterative Calculation Process	3-55
Figure 3.45	0-D Modeling of a Free Turbine Turboshaft Engine	3-57
Figure 3.46	Multi-Dimensional Newton-Raphson Iteration	3-60
Figure 3.47	0-D Modeling of a Free Turbine Turboshaft Engine	3-62
Figure 3.48	Turbofan Station Designation	3-67
Figure 3.49	Effect of Fan Temperature Measurement Accuracy	3-71
Figure 3.50	Matching the Measured Data to a Map	3-73
Figure 3.51	Typical Control System Architecture	3-85
Figure 4.1	Station Designation for Single Spool Turbojet and Turboshaft and Twin Spool Turbofan	4-4

Figure 4.2	Station Designation for Twin Spool Duct Heater and Free Turbine Turboprop/Turboshaft	4-4
Figure 4.3	Station Designations Auxiliary Power Unit Types; Two-Spool and with Separate Stream Inlet Particle Separator	4-5
Figure 4.4	Representative Compressor-Map, with Surge-Line, Speed-Line, Efficiency Contours, and Flutter Boundary	4-5
Figure 4.5	Schematic of a Single-Stage Cooled Turbine	4-12
Figure 4.6	Enthalpy-Entropy Diagram for a Single-Stage Cooled Turbine	4-13
Figure 4.7	Efficiency Change for Cooling Air Re-Distribution	4-14
Figure 4.8	Schematic of a Two-Stage Cooled Turbine	4-15
Figure 4.9	Enthalpy-Entropy Diagram for a Two-Stage Cooled Turbine	4-15
Figure 4.10	Exchange Rates of Efficiency with Cooling Air Amount	4-16
Figure 4.11	Calculation of the Thermodynamic Turbine Efficiency	4-17
Figure 4.12	Exchange Rates of Efficiency with Cooling Air	4-17
Figure 4.13	Differences between the Efficiency Numbers for Different Methodologies	4-19
Figure 4.14	True and Equivalent Stator Exit Temperatures	4-20
Figure 4.15	Cycle Parameter Studies with Differently Defined Turbine Efficiencies Held Constant	4-20
Figure 4.16	Afterburner Nomenclature	4-27
Figure 4.17	Ideal Temperature Rise	4-28
Figure 4.18	Fundamental Pressure Loss	4-29
Figure 4.19	Empirical Efficiency Model	4-32
Figure 4.20	Stability Limits	4-33
Figure 4.21	Inlet Recovery Loss	4-34
Figure 4.22	Energy Available to Produce Thrust from Thermodynamic Cycle	4-35
Figure 4.23	Thrust Gain from Ideal Mixing of Two Streams with Equal Total Pressure	4-36
Figure 4.24	Mixer Nomenclature	4-37
Figure 4.25	Total Pressure after Mixing Two Streams with Equal Pressure (200 kPa)	4-38
Figure 4.26	Effect of Friction Pressure Losses on the Thrust Gain Due to Mixing	4-39
Figure 4.27	Effect of Nozzle Back Pressure on Theoretical Thrust Gain ( $P_8 = 200$ kPa)	4-40
Figure 4.28	Simulink Powerplant Heat Management System Model (top level)	4-43
Figure 4.29	Internal Wall Heat Soakage Effect Model	4-45
Figure 4.30	Clutch Model Algorithm	4-51
Figure 4.31	Lift-Fan (Dis)Engagement Clutch Response	4-52
Figure 4.32	Lift-Fan (Dis)Engagement Lift-Fan and N1 Response	4-53
Figure 5.1	FORTTRAN Modeling Procedure	5-2
Figure 5.2	Standard Output Format	5-5
Figure 5.3	MOPS Architecture	5-6
Figure 5.4	Program Structure of MOPEDS	5-8

Figure 5.5	GasTurb Model Selection Window	5-10
Figure 5.6	GasTurb Architecture	5-11
Figure 5.7	GSP Model Window with Simple Turbofan Model	5-12
Figure 5.8	Standard Component Architecture	5-13
Figure 5.9	Engine System Model Architecture	5-14
Figure 5.10	GSP Model Window with Recuperated Turbo-Shaft Engine Model	5-15
Figure 5.11	Compressor Component Window	5-15
Figure 5.12	Component Performance Output Results	5-16
Figure 5.13	GSP Interface Architecture	5-16
Figure 5.14	NLR TERTS Thermodynamic Engine-Model, with Sub-Levels	5-17
Figure 5.15	The Structure of a Modeling Environment Offering the Possibility of Fault Diagnosis	5-18
Figure 5.16	Main User Interface of TEACHES Package	5-19
Figure 5.17	Interface Architecture Schematic	5-19
Figure 5.18	The Operational Parameters Input Section of the Visual Interface	5-20
Figure 5.19	Output from a Compressor Model	5-21
Figure 5.20	Examples of Graphic Information Related to Diagnostics	5-21
Figure 5.21	Overview of NPSS	5-22
Figure 5.22	Output from ENG10 Modeling Tool	5-24
Figure 5.23	ALLSPD Simulation of a Combustor	5-25
Figure A.1	DYNTECC Control Volume Technique	A-4
Figure A.2	Typical Set of Stage Characteristics	A-5
Figure A.3	Schematic of DYNTECC Explicit Split Flux-Differencing Scheme	A-6
Figure A.4	Compressor with Circumferential Segments and Applied Inlet Distortion	A-6
Figure A.5	ATEC Code Compared to Component Level Modeling Technique	A-7
Figure A.6	Comparison of ATEC and Engine Model Results	A-8
Figure A.7	System Response with Small Lag	A-9
Figure A.8	System Response with Large Lag	A-10
Figure A.9	Model Attributes for Design and Analysis	A-11
Figure A.10	Post-Stall Dynamic Event – DYNTECC	A-13
Figure A.11	Surge Cycles during Engine Re-Acceleration	A-15
Figure A.12	Grid of Reverse Flow Burner	A-17
Figure A.13	Effects of an Imposed Fuel Flow Oscillation on Combustor Pressure	A-17
Figure A.14	Grid for Dump Combustor	A-18
Figure A.15	Ignition Event	A-18
Figure A.16	Blowout Event	A-19
Figure A.17	Schematic of the Coupled Inlet-Engine Codes	A-20
Figure A.18	Cross-Section View of the 4060 Inlet and J85-13 Turbojet Installation	A-20
Figure A.19	Inlet Shock Location	A-21

Figure A.20	Compressor Pressure Ratio as a Function of Compressor Inlet Corrected Mass Flow Rate	A-22
Figure A.21	Schematic of TF30 Compression System Modeled	A-23
Figure A.22	Ops Line Migration due to Temperature Ramps	A-24
Figure A.23	Static Pressure Signature	A-24
Figure A.24	Parallel Compressor Theory	A-25
Figure A.25	Imposed Distortion Pattern, Produced by Distortion Screen	A-26
Figure A.26	Model Prediction and Comparison	A-26
Figure A.27	General Technical Approach for 3-D Dynamic Compression System Model, TEACC	A-28
Figure A.28	Grid and Performance for Three-Stage Fan at 80-percent Corrected Speed	A-29
Figure A.29	Point Inlet Performance and Corresponding Flow-Field for a Typical Three-Stage Military Fan	A-29
Figure A.30	Predicted Performance with Imposed 90° Circumferential Distortion	A-30
Figure A.31	Typical Blade Row Characteristics	A-31
Figure A.32	Euler Approach with Body Forces	A-32
Figure A.33	Model Prediction of Stall Inception Process for Short Wavelength (Spike) Stalls	A-33
Figure A.34	Experimental Data of Stall Inception Process for Short Wavelength (Spike) Stalls	A-33
Figure A.35	The Effects of Co- and Counter-Screen Rotation on Compressor Stability Limit	A-34
Figure A.36	Effect of Inlet Unstart on Aircraft Wing Assembly	A-36
Figure A.37	Overall Performance Characteristic	A-39
Figure A.38	Individual Stage Pressure Rise Coefficient	A-40
Figure A.39	Axisymmetric Flow Variables, Exiting the Second Stage Rotor	A-41
Figure B.1	Basic Compressor Map	B-1
Figure B.2	Types of Compressors	B-2
Figure B.3	Polytropic Efficiency for Various Types of Compression Systems	B-3
Figure B.4	Compressor Configuration as a Function of Flow and Pressure Ratio	B-3
Figure B.5	Representative Compressor-Map, with Surge-Line, Speed-Line, Efficiency Contours, and Flutter Boundary	B-4
Figure B.6	Effect of Increased Tip Clearance on Overall Compressor Performance for a Low-Speed Compressor	B-7
Figure B.7	Effect of Tip Clearance on Overall Compressor and Fan Performance	B-7
Figure B.8	Effect of Tip Clearance on Overall Compressor and Fan Performance	B-8
Figure B.9	Correlation of Rotor Pressure Rise Capability Against Flow Blockage Associated with Tip Leakage Flow	B-9
Figure B.10	Effect of Tip Clearance on Pressure Ratio, Surge Line and Efficiency of 6-Stage, High-Speed Compressor	B-9
Figure B.11	Influence of Tip Clearance on Performance – Measurements from HPC-Rig	B-10
Figure B.12	Non-Axisymmetric Tip Clearance: (a) Stationary Caused by Off-Centered Rotor and Oval Casing; (b) Rotating Caused by Whirling Shaft and Non-Uniform Rotor Heights	B-11

Figure B.13	Effects of Circumferential Inlet Distortion on Multi-Stage Axial Compressor Performance	B-12
Figure B.14	Effect of Circumferential Distortion Sector Angle on Surge Pressure Ratio	B-13
Figure B.15	Effect of Number of Sectors, on Surge Pressure Ratio	B-13
Figure B.16	Flow Coefficient at Stall versus Distortion Rate, for Single-Resonance-Peak Type of Compressor	B-14
Figure B.17	Flow Coefficient at Stall versus Distortion Rate. Two Resonance Peak Type of Compressor	B-15
Figure B.18	Effect of Engine Presence on Total Pressure Distribution within Inlet	B-16
Figure B.19	Effect of Tip Clearance Distribution on Pressure Rise Characteristics and Stall Margin	B-17
Figure B.20	Changes in Stalling Pressure Rise with Axisymmetric and Non-Axisymmetric Clearance	B-18
Figure B.21	Changes in Flow Coefficient with Axisymmetric and Non-Axisymmetric Clearance	B-18
Figure B.22	Effect of Tip Clearance Distribution on Compressor Efficiency	B-19
Figure B.23	Changes in Peak Efficiency with Asymmetric Clearance, with the Flow Condition Corresponding to the Peak Efficiency Points in Next Figure	B-19
Figure B.24	Variation of Compressor Efficiency (top) and Pressure Rise (bottom) for Closely-Spaced (dashed lines) and Widely-Spaced (solid lines) Blade Rows	B-20
Figure B.25	Effect of Axial Spacing on Stalling Pressure Coefficient	B-20
Figure B.26	Range of Operational Reynolds Number of a High-Pressure Compressor within the Flight Envelope	B-21
Figure B.27	Effect of Boundary Layer Condition on Compressor Behavior	B-22
Figure B.28	Effect of Surface Roughness on Compressor Pressure Characteristics	B-23
Figure B.29	Effect of Blade Surface Roughness on Compressor Efficiency	B-24
Figure B.30	Effect of Variation in Blade Surface Roughness on Pressure Ratio versus Mass Flow Characteristics at 70-Percent Span	B-24
Figure B.31	Effect of Reynolds Number on the Performance of: (a) A Three-Stage Intermediate Pressure Compressor; and (b) A Six-Stage High Pressure Compressor	B-25
Figure B.32	Effect of Reynolds Number on Compressor Stalling Pressure Rise Coefficient	B-25
Figure B.33	Impact of Stator Position on Flow and Efficiency as a Function of Speed for a Particular Operating Line	B-26
Figure B.34	Advanced Fan-By-Pass Core-Engine Duct System	B-28
Figure B.35	Fan O. D. Map	B-28
Figure B.36	Fan Exit Guide Vane (FEGV) Map	B-29
Figure B.37	Low Pressure Compressor Map, including Fan ID	B-29
Figure B.38	Super Charging Curve for Primary Stream	B-30
Figure B.39	Level of Untwist for a High Bypass Fan	B-31
Figure B.40	Impact of Pressure and Mechanical Loading on Blade	B-31
Figure B.41	Definition and Conventions for Untwist Angle	B-32
Figure B.42	Blade Untwist Effect vs. Speed	B-32

Figure B.43	Effects Associated with Stratification	B-34
Figure B.44	Trends of Performance Map Flutter Boundary with $K0^*$ and $g/\rho^*$ from Full-Scale Engine Data	B-36
Figure B.45	Comparison of Centrifugal and Axial Stage Flowpaths	B-37
Figure B.46	Impeller Exit Tip Speed vs. Stage Pressure Ratio	B-38
Figure B.47	Stage Pressure Ratio vs. Impeller Exit Blade Angle	B-38
Figure B.48	Comparison of Centrifugal Compressor Maps with 0 deg and 45 deg Exit Blade Angles	B-39
Figure B.49	Impeller Exit Temperature vs. Impeller Tip Speed Material Capability	B-40
Figure B.50	Load Compressor Auxiliary Power Unit Engine Cross-Section	B-40
Figure B.51	Integral Bleed Auxiliary Power Unit Engine Cross-Section	B-41
Figure B.52	Impeller-Diffuser Matching	B-42
Figure B.53	Swirl Pattern Entering a Centrifugal Compressor from a Typical Plenum	B-43
Figure B.54	Improved Clearance Sensitivity by Reduced Blade Loading	B-44
Figure B.55	Single-stage Centrifugal Compressor's Loss versus Reynolds Number	B-45
Figure B.56	First-Stage Impeller Leading Edge Sand Erosion	B-46
Figure B.57	Inlet Plenum Cross-Section	B-46
Figure B.58	Effect of Plenum Aspect Ratio and Area Ratio on Plenum Loss	B-47
Figure B.59	Effect of Plenum Area Ratio on Compressor Efficiency	B-47
Figure B.60	Cross-Section of Centrifugal Stage Showing Leakage Paths	B-48
Figure B.61	Independent Drag Coefficient of Various Sheet Metal Joints, Based on Thickness, "h"	B-49
Figure B.62	Duality of Local and System Calculations	B-53
Figure B.63	Physical Model of Multi-Stage Compressor	B-54
Figure B.64	Typical Secondary-Air-System Returns to Main Throughflow Bleed Network	B-61
Figure B.65	Region of Stable Ignition	B-74
Figure B.66	Energy Available to Produce Thrust from Thermodynamic Cycle	B-83
Figure B.67	Turbojet Schematic Showing Engine and Nozzle Station Designations	B-84
Figure B.68	Single Stream Control Volume for Thrust Definition	B-87
Figure B.69	Representative Thrust and Flow Coefficients vs. Nozzle Pressure Ratio	B-90
Figure B.70	Schematic of a Dual-Stream Bypass Engine	B-90
Figure B.71	PW4000 Example of Dual-Stream Exhaust System	B-92
Figure B.72	Schematic of Mixed Flow Turbofan Engine	B-93
Figure B.73	Mixed Flow Configuration Example, PS-90P	B-93
Figure B.74	Mixed Flow Example, V-2500	B-93
Figure B.75	Military Mixed Flow with Augmentor Example, PW-F-100	B-94
Figure B.76	Sea Level Engine Test Facility to Measure Thrust, Airflow and Nozzle Coefficients	B-94
Figure B.77	Altitude Engine Test Facility to Measure Thrust, Airflow, and Nozzle Coefficients	B-95

Figure B.78	Nozzle Coefficients with Variable Jet Nozzle Area	B-95
Figure B.79	Schematic Showing Pressure-Forces on C-D Divergent Section	B-96
Figure B.80	Theoretical Improvement for C-D Relative to a Convergent Nozzle	B-97
Figure B.81	F-119 Example	B-97
Figure B.82	Schematic of Variable Convergent Nozzle	B-98
Figure B.83	Geometry of Variable Convergent Divergent Nozzle	B-101
Figure B.84	Over-Expanded Operation of a Convergent-Divergent Nozzle	B-102
Figure B.85	Test Result for Nozzle Velocity Coefficient Using 1-D Geometry Model	B-104
Figure B.86	Nozzle Strut Forces; Positive when Struts are Compressed	B-105
Figure B.87	Thrust Gain Due to Flow Detachment at Low Nozzle Pressure Ratios	B-105
Figure B.88	Schematic of Divergent Nozzle Wall Section with Pressure Instrumentation Locations	B-106
Figure B.89	Correlation of Static Pressure near the Nozzle Exit with Nozzle Pressure Ratio	B-107
Figure B.90	Adjusted Correlation for Nozzle Velocity Coefficient	B-108
Figure B.91	Fixed Inlet Area Schematic	B-109
Figure B.92	Flight Velocity and Inlet Contribution to Engine Cycle	B-109
Figure B.93	Schematic of Sea Level Test Inlet	B-110
Figure B.94	Inlet Spillage Drag is a Function of Mass Flow Ratio	B-111
Figure B.95	Fixed Area Inlet in Supersonic Flow	B-111
Figure B.96	Supersonic Inlet with External Compression	B-112
Figure B.97	Supersonic Inlet with External and Internal Compression	B-112
Figure B.98	Inlet Recovery Loss	B-113
Figure B.99	Example for an Outward Tapping	B-115
Figure B.100	Influence of a Diffuser on the Cd-Value	B-116
Figure B.101	Comparison of a Rectangular with an Angled Hole	B-116
Figure B.102	Influence of Slot Length on the Cd-Value	B-117
Figure B.103	Influence of Step Height and Slot Length on the Cd-Value	B-117
Figure B.104	Inward Tapping with Tubes	B-118
Figure B.105	Ideal Labyrinth Flow	B-122
Figure B.106	Carry-Over Factor from Hodgkinson	B-122
Figure B.107	Correction Term for Carry-Over Factor	B-123
Figure B.108	Discharge Coefficients for $n = 2$	B-124
Figure B.109	Discharge Coefficient for $n > 2$	B-124
Figure B.110	Correction Factor for Straight-Through Labyrinth Seals with Stator Grooves	B-125
Figure B.111	Mass Flow Differences for Honeycomb Layers on the Stator	B-125
Figure B.112	Effect of Rounding Radius	B-126
Figure B.113	Effect of Chamber Depth	B-126
Figure B.114	Discharge Coefficients for Stepped Labyrinth Seals (single fin)	B-127
Figure B.115	Correction Factor for Cd	B-127

Figure B.116	Influence of Step Height	B-128
Figure B.117	Comparison of Different Cd Correlations, Absolute Frame of Reference	B-131
Figure B.118	Comparison of Different Cd Correlations, Relative Frame of Reference	B-131
Figure B.119	Cd,rot,rel Referred to Cd,static as Function of U/Cax,id	B-132
Figure B.120	Cd,rot,rel Referred to Cd,static as Function of U/W,id	B-132
Figure B.121	Cd,rot,rel Referred to Cd,static as Function of U/Cax	B-133
Figure B.122	Comparison of U/Wid vs. U/Cax	B-134
Figure B.123	Comparison of Available Correlations with Air/Oil Measurements	B-136
Figure B.124	Pressure Loss of a 90° Bend – Comparison of Available Correlations with Air/Oil Measurements	B-136
Figure B.125	Pressure Loss of a 90° Mitre Bend	B-137
Figure B.126	Subcritical Mass Flow Rate through an Orifice – Comparison between Prediction and Measurement	B-137
Figure B.127	Critical Mass Flow Rate through an Orifice – Comparison between Prediction and Measurement	B-138
Figure B.128	Two Phase Orifice Flow Characteristic	B-138
Figure B.129	Mass Flow Function of Critical Orifice Flows	B-139
Figure B.130	Fixed Displacement Pump Characteristic	B-143
Figure B.131	Centrifugal Pump Characteristic	B-143
Figure B.132	Avoidance of Algebraic Loops	B-144
Figure B.133	Hydraulic Control System Equations	B-144
Figure B.134	Single Stage Flapper Valve	B-145
Figure B.135	Metering Valve	B-146
Figure B.136	Schematic of Main System Components	B-147
Figure B.137	A Two-Stage Moog Valve	B-147
Figure B.138	Two-Stage Servo Valve Block Diagram	B-148
Figure B.139	Valve Control Laws	B-148
Figure B.140	Engine Model Imported (Embedded) in Controls Development Environment	B-150
Figure B.141	Engine and Control-System Models Running Together with Inter-Process Communication	B-151
Figure B.142	A General Form of Dynamic Model using External Integration for Simulation	B-152
Figure B.143	Performance Model Showing Steady-State Mode	B-153
Figure B.144	A Performance Model Running in Transient Mode using Internal Integration	B-154
Figure B.145	Control-System Model Imported (Embedded) into Performance Modeling Environment	B-155
Figure B.146	Compressor Operating Point of a Single Shaft Gas Turbine. Constant TIT, Operation with Different Fuels and Water Injection	B-159
Figure B.147	Schematic Representation of a Twin Spool Gas Turbine and Discrimination of its Components	B-160
Figure B.148	Values of Specific Heat $C_p$ and Isentropic Exponent $\gamma$ , for Temperatures Usual in the Hot Section of Gas Turbines	B-161

Figure B.149	Change in Gas Properties for Different Amount of Injected Water ( $f = 0.02$ )	B-162
Figure B.150	Typical Variation of Fuel/Air Ratio, with Water and Steam Injection (TG20 Simulation). Operation with Fuel Oil and Natural Gas. Points: Computer Model, Lines: eq (1)	B-164
Figure B.151	Ratio of Specific Heats of Steam and Combustion Gases	B-165
Figure B.152	Power Output Deviation with Diluent Injection. (a) As a Function of Water/Fuel Ratio, (b) As a Function of Water/Air Ratio. Points: Computer Model, Lines: eq (6)	B-167
Figure B.153	Gas Turbine Efficiency Deviation with Diluent Injection	B-168
Figure B.154	Variation of Compressor Pressure Ratio as a Function of the Amount of Injected Steam for a Single Shaft Gas Turbine	B-169
Figure B.155	Change of Compressor Pressure Ratio with Water Injection for a Twin Shaft Gas Turbine. Points: Computer Model, Line: Eq. B-109	B-170
Figure B.156	Change of Compressor Operating Conditions with Diluent Injection for a Twin Shaft Gas Turbine. ° Operating Points when Water is Injected at Constant TIT	B-171
Figure B.157	Deviation of Power Output with Water Injection, for a Twin Shaft Gas Turbine	B-171
Figure B.158	Range of Variation of Power Deviation for Existing Gas Turbines. Single Shaft, Constant Geometry	B-172
Figure B.159	Range of Variation of Efficiency Deviation for Existing Gas Turbines. Single Shaft, Constant Geometry	B-173
Figure B.160	Schematic of the Gas Turbine Layout Studied	B-174
Figure B.161	Control Volume for Application of the SFEE over the Combustion Chamber	B-175
Figure C.1	Model Fidelity and Computing Platforms (Status Year 2005)	C-2
Figure C.2	Trends in Computing Power	C-4
Figure C.3	Spatial versus Temporal Resolution for a Given Computing Power	C-4
Figure D.1	The Exercise Model	D-2
Figure D.2	The Exercise Model, with Implicit Integration Added	D-3
Figure D.3	Results from Module #2	D-6

## List of Tables

		Page
Table 2.1	Cycle Parameter Summary	2-15
Table 2.2	Measurement Repeatability	2-35
Table 2.3	Standard Deviation for Component Efficiencies	2-35
Table 2.4	Original Mean and Optimized Values	2-169
Table 2.5	Results	2-169
Table 3.1	Thermodynamic Property Representation Effect on Model Capability and Execution Speed	3-36
Table 3.2	Model Fidelity, Accuracy and Detail Needs through the Engine Life Cycle	3-36
Table 3.3	Values for Iteration	3-63
Table 4.1	Table of Component Model Requirements and Characteristics by Level of Fidelity	4-1
Table 4.2	Table of Component Model Requirements and Characteristics by Engine Life Cycle Application	4-2
Table 4.3	Table of Secondary Effects Potentially Required by Component Models	4-2
Table 4.4	Turbine Design Data	4-18
Table B-1	Method of Turbine Characteristic Measurement	B-65
Table B-2	Simplified Method Results	B-72

# Programme Committee

## Chairman

Prof. Walter O'Brien  
Virginia Polytechnic Institute and State University  
Room 109 Randolph Hall-MC 0238  
Blacksburg, VA 24061  
UNITED STATES

[walto@vt.edu](mailto:walto@vt.edu)

## Members

### CANADA

Mr. D. Rudnitski  
Structures, Materials and Propulsion  
Laboratory  
Institute for Aerospace Research  
1500 Montreal Road, Building M-7  
National Research Council of Canada  
Ottawa, Ontario K1A 0R6

### FRANCE

Mr. P. Masson  
Head of Toxicology Dept.  
CRSSA, BP 87  
38702 La Tronche Cedex

### GERMANY

Dr. J. Kurzke  
MTU Aero Engines  
665 Dachauer Street  
80995 Muenchen

### GREECE

Prof. Dr. P.N. Kotsiopoulos  
Hellenic Air Force Academy  
Dekelia, Attiki

### UNITED KINGDOM

Mr. Marc Horobin  
Rolls-Royce plc  
P.O. Box 3  
Filton, Bristol BS34 7QE

### UNITED STATES

Mr. F. Csavina  
USAF  
2530 Loop Road West  
Wright Patterson Air Force Base  
Ohio 45433-7101

Mr. D. Popgoshev  
Naval Air Systems Command  
Propulsion and Power Engineering  
22195 Elmer Road, Unit 4  
Patuxent River, MD 20670-1534

Mr. A.D. Stramiello  
M/S 404-241  
Honeywell Engines  
111 South 34<sup>th</sup> Street  
Phoenix, AZ 85034

## Contributors

### CANADA

Dr. R. Angus  
Defence Research Establishment Suffield  
P.O. Box 4000, Station Main  
Medicine Hat, Alberta T1A 8K6

Dr. R. Evans  
Mechanical Engineering  
University of British Columbia  
2324 Main Mall  
Vancouver, B.C. V6T 1W5

**GREECE**

Prof. K. Mathioudakis  
National Technical University of Athens  
9 Iroon Polytechniou  
Athens

**ITALY**

Ing. C. Vinci  
FIATAVIO s.p.a.  
Corso Garibaldi  
0034 Colleferro

**PORTUGAL**

Prof. M.N.R. Nina  
Department of Mechanical Engineering  
Instituto Superior Tecnico  
av Rovisco Pais  
1049-001 Lisboa

**THE NETHERLANDS**

Wilfried P.J. Visser  
Gas Turbine Engine Modeling Specialist  
Dee Pinckart 54  
5674CC Nuenen

**TURKEY**

Prof. O.C. Eralp  
Middle East Technical University  
Mechanical Engineering Dept.  
Inonu Bulvari  
06531 Ankara

**UNITED KINGDOM**

Colin Edmunds  
Senior Marine Systems Engineer  
Naval Systems and Product Strategy Dept.  
Rolls-Royce plc  
PO Box 31  
Fishponds, Bristol BS16 1XY

**UNITED STATES**

John Roberts  
Senior Technical Fellow  
Pratt & Whitney Aircraft  
MS 162-14  
400 Main St.  
E. Hartford, CT 06108

Prof. Choon Tan  
Dept. of Aeronautics and Astronautics  
Massachusetts Institute of Technology  
77 Massachusetts Avenue  
Cambridge, Massachusetts 02139

Mr. R. White  
CKMSYS LLC  
203 – 9211 Bayberry Bend  
Fort Myers, Florida 33908

**Technical Editor & Member**

Dr. M. Davis  
Aerospace Testing Alliance, ATA  
AEDC MS9013  
1099 Avenue C  
Arnold Air Force base  
TN 37389-9013  
UNITED STATES

---

# **Performance Prediction and Simulation of Gas Turbine Engine Operation for Aircraft, Marine, Vehicular, and Power Generation**

## **(RTO-TR-AVT-036)**

### **Executive Summary**

Through the years, computer models for the prediction of gas turbine performance and the simulation of operational characteristics have evolved into a very wide range of applications. The present document is addressed to the operators and users of gas turbines in the field, for whom user-friendly, accurate and fast PC-based engine simulation tools are now available. These tools can help one to understand the engine performance behavior and to identify the causes of possible deficiencies in engine performance in a highly cost-effective manner. They have also become very useful for efficient mission analysis, the preliminary design studies of engines, and their matching to applications. This document is the second document published by the RTO on this subject.

The present document incorporates and updates material included in the previous report RTO-TR-044, and includes new material and an improved organization. The initial document, RTO-TR-044, concentrated on gas turbine engine modeling as it applied to aircraft applications, only.

Since the technology of this subject changes rapidly, the material can easily become outdated and obsolete. The original Task Team (AVT-018) recognized this fact and suggested that RTO continue to update this document, periodically, to include new information, and, in fact, to consider this a "living document". However, under the current RTO specifications, document revision is not an option. It was decided by the members of AVT-036 to develop a more comprehensive document by expanding the scope of the original document to include gas turbine engine modeling for Land, Sea, and Air Applications as applied to military weapon systems, as well as to update previous material where needed. That approach was accepted by RTO and as a result this document was developed. In addition to being more comprehensive, this document has been reorganized to produce a more readable document.

# **Estimation et simulation des performances du fonctionnement des turbomoteurs pour avions, navires, véhicules et pour la production d'énergie**

## **(RTO-TR-AVT-036)**

### **Synthèse**

Au fil des années, les modèles informatiques utilisés pour l'estimation des turbomoteurs et la simulation des caractéristiques opérationnelles ont évolué vers une très large gamme d'applications. Le présent document s'adresse aux exploitants et aux utilisateurs de turbomoteurs sur le terrain, pour qui des outils conviviaux, précis et rapides de simulation de moteurs sur PC sont désormais disponibles. Ces outils peuvent les aider à comprendre le comportement des moteurs et à identifier les causes de défaillances éventuelles au niveau des performances, de manière rentable. Ils sont également devenus très utiles pour une analyse de mission efficace, les études préliminaires de conception de moteurs et leur adaptation à leurs applications. Ce document est le second édité par la RTO sur ce sujet.

Le présent document prend en compte et actualise les informations contenues dans le rapport précédent RTO-TR-044, et contient de nouvelles informations ainsi qu'une meilleure organisation. Le document initial, RTO-TR-044, était ciblé sur la modélisation des turbomoteurs car il ne concernait que les applications sur avions.

Compte tenu de l'évolution rapide de la technologie dans ce domaine, les informations sont susceptibles de devenir très facilement périmées et obsolètes. L'équipe de travail initiale (AVT-018) était consciente de ce fait et avait suggéré que la RTO poursuive la mise à jour de ce document périodiquement, afin d'y inclure de nouvelles informations et, en fait, de le considérer comme un « document vivant ». Toutefois, dans le cadre des spécifications RTO actuelles, la révision du document ne constitue pas une option. Les membres de l'AVT-036 ont décidé de rédiger un document plus complet en élargissant le périmètre du document d'origine afin d'y inclure la modélisation des turbomoteurs pour les applications terrestres, maritimes et aériennes appliquées aux systèmes d'armes militaires, et d'actualiser les informations précédentes le cas échéant. Cette approche a été acceptée par la RTO, ce qui a donné lieu à l'établissement du présent document. Outre le fait d'être plus complet, ce document a été réorganisé afin d'être plus lisible.

## Chapter 1 – INTRODUCTION

### 1.1 DOCUMENT ORGANIZATION

Much of this document focuses on the gas turbine engine simulation known as a cycle code. It is also referred to in this document as a “Zero-Dimensional” or “0-D” simulation. Other codes ranging from one-dimensional to three-dimensional numerical simulations which were originally discussed in the main chapters of RTO-TR-044 [1.1] are now discussed in the Annexes of this document. In fact, the material that is in RTO-TR-044 has been largely maintained within this document but has been expanded and reorganized to produce a more focused document on cycle analysis simulations.

The main document is arranged such that examples of the use of gas turbine engine simulations are presented first in **Chapter 2**. This organizational structure allows the reader to decide which example most closely resembles his particular application. Once the reader has decided how he might use a simulation, he can dig further into the document to understand the ramifications of using the cycle code and what it might mean to his analysis process. Listed below is a brief explanation of each of the chapters and annexes so that the reader can select how he wishes to proceed.

**Chapter 2 (Applications)** focuses on application of gas turbine engine cycle codes as they are applied to:

- Fixed Wing Aircraft;
- Rotary Wing Aircraft (Helicopters);
- Marine (Ship) Propulsion;
- Vehicular Propulsion;
- Power Generation; and
- Performance Based Optimized Manufacturing.

**Chapter 3 (System Models)** introduces all the different types of cycles (Ideal Joule, Real Joule with and without reheat, regeneration) that can be utilized for gas turbine engines in the various applications (turbojet, turbofan, turboprop, and turboshaft). In addition, **Chapter 3** introduces the concept of the cycle code and how it is formulated.

**Chapter 4 (Component Models)** deals with how the various components (compressor, burner, turbine, inlet, nozzle, re-heaters, regenerators, clutches, secondary airflow, splitters and mixers, etc.) are modeled that are simulated within the cycle code. Each component modeling technique is detailed and provides a measure of how each is connected to each other.

**Chapter 5 (Examples of 0-D Numerical Simulations)** introduces several current cycle code systems and provides a Web link to those that can be downloaded for use by any interested individual.

There are five Annexes that go into detail on the following subjects:

**Annex A (Higher Order Models)** describes the 1-D dynamic modeling concepts along with applications for compression system and engine operability issues. In addition, 2-D, 3-D and CFD codes are discussed and several examples of applications are provided.

**Annex B (Advanced Topics and Recent Progress)** is for the advanced reader. This annex provides great detail into the recent research in computational modeling for all components especially for compressor performance and operability. Here one finds detailed information on subjects such as the effects of tip

## INTRODUCTION

clearance on stage performance, stationary and rotating distortion, surface roughness effects, thermal effects, and many other research areas of concern. Modeling of other components (turbine, combustor, inlets, nozzles, and secondary air systems) are treated in great detail as well.

**Annex C (Computer Platforms)** provides the reader with a look at the multitude of potential computer platforms that can be utilized in computing engine cycle analysis. This annex compares the different types of computers and operating systems as well as indicating the advantages of each. The reader is exposed to parallel computing concepts, zooming of higher fidelity models into the cycle code, distributed networking concepts, and user interfaces or GUIs.

**Annex D (Gas Turbine Simulations for Educational Purposes)** gives the reader an example of using an engine cycle code for to educate engineers. The example is taken from an engine manufacturer in-house training process and walks the reader through the process of how to teach gas turbine engine performance using a cycle code.

**Annex E (Glossary)** provides an in-depth explanation of the terms used in this document.

## 1.2 APPLICATIONS OF MATHEMATICAL ENGINE MODELS

Engine models are defined here as mathematical descriptions of the physical behavior of a turbine engine. These can either be *paper* engines in their design phases or *real* engines in operation. Engine components, such as the compressor, can also be separately modeled. During the design integration process, the component characteristics have then to be matched, for instance with respect to mass flow and shaft speed.

**Figure 1.1** shows a conceptual relationship between the users of (mathematical) engine models and the creators of these models at various levels. The present document is addressed in particular to the model users in the upper level, and to those dealing with *preliminary engine and application design studies*. Those in the upper level tend to deal with *engine operation and maintenance*, while others deal with matters including health monitoring and test bench analyses, where model complexity can still be avoided while providing usable answers. Examples are performance sensitivity studies, mission analysis and the development of engine control systems.

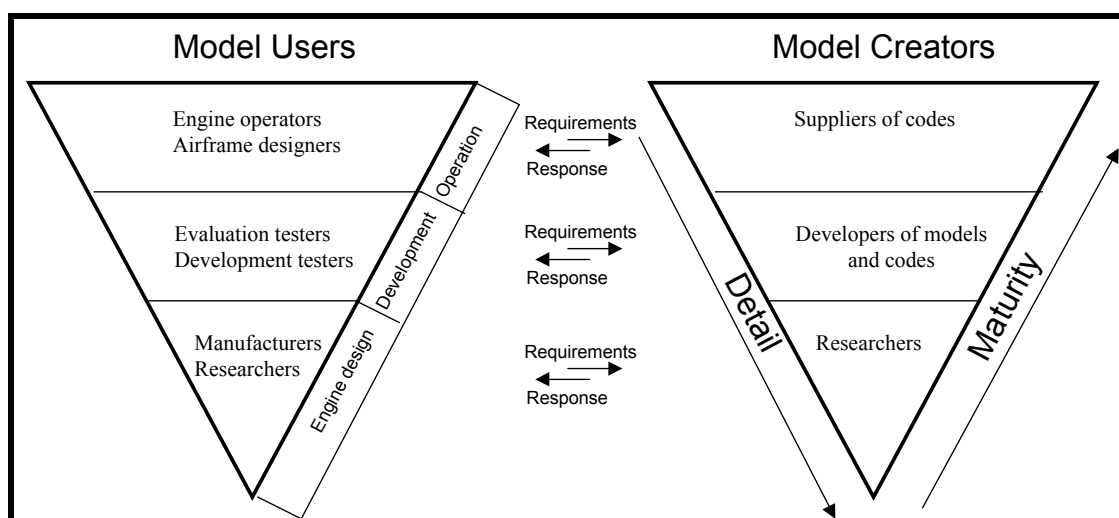


**Figure 1.1: Engine Model Users and Creators.**

For the operator, to support specific applications, such as engine diagnostics, the engine manufacturers usually supply engine-specific codes. For preliminary engine and application design studies generic tools are available, which are also in the public domain.

For engine maintenance, health monitoring, and diagnostics models the nominal condition of the specific engine is described by a mathematical model involving the indications of the various sensors (pressures, temperatures, shaft speeds) in the engine. Deviations from the nominal values indicate the state of health of the engine that can be used for diagnostics and repair on condition.

A dedicated computer model is then a very cost-effective tool to carry out an appropriate diagnosis to identify degraded or defective engine components. This application is current practice at major airline companies. Some have developed their own maintenance-on-condition system with add-ons to the basic health monitoring system offered by the engine manufacturer. The cost-effectiveness of the maintenance of military engine systems also increasingly benefits from these developments.

The application designers may use generic engine models for mission analysis as part of an application performance model in the preliminary design phase. In that case, engine sizing and sensitivity analyses are the key words. The engine designer may also do this exercise to identify requirements for possible new engines.

Other uses of engine models by the application designer are:

- To check and confirm projected engine performance data provided by the engine manufacturer while the engine is still in the design and test phase;
- To assess installation effects; and
- To assess engine performance.

Test bed engineers may also profit from a computer model that simulates their engine, and that can be run as a virtual engine in parallel to the actual engine. Such a *virtual* engine can also be used as a part of the software for (real time) aircraft flight simulators. For that application, modeling of the transient behavior (e.g. the response to a slam-acceleration) is essential. This applies, in particular, to flight simulators for the latest generation of fighter aircraft with high agility, in combination with close coupling of engine thrust and aerodynamics.

These real-time engine models are also useful for engine control design and development testing, including a hardware control system (e.g. a fuel control system) coupled to a *software* engine.

Another group of users is the evaluation and development testers. The evaluation testers generally represent the interests of future engine users, including the application designers and manufacturers. The development testers are part of the engine manufacturer's organization. They use the engine models to identify unsatisfactory component performance (like the health monitoring application mentioned earlier) and to 'tune' the whole-engine performance model made available as a performance *card deck* to the potential customers.

The engine manufacturers may use the relatively simple models in the early phase of the design only. In the detailed design phase highly sophisticated models are used, combined with in-house experience. These models are mostly based on computational fluid dynamics (CFD) describing detailed flow and combustion phenomena. In the present document these models will be referred to mostly in a qualitative way.

Researchers also make use of engine and engine component models. In many cases experimental work and theoretical modeling go hand in hand in that area. The research community may use this document to put their work into a wider scope. This also holds for trainees and students.

**Figure 1.2** shows the cycle simulations used throughout the engine life cycle. The model users identified in **Figure 1.1** are now associated with the life cycle elements of the engine and the related activities. In the lower left hand corner rather simple cycle models, of the type suitable for preliminary engine and application studies are used. In the upper part of **Figure 1.2** the most sophisticated design tools are employed, constituting the latest state of the art of the engine designers. In the top right of the figure, the activities of the development and certification testers find their place. Mission and life analysis and health monitoring are found in the lower right hand corner as activities of the engine operators.

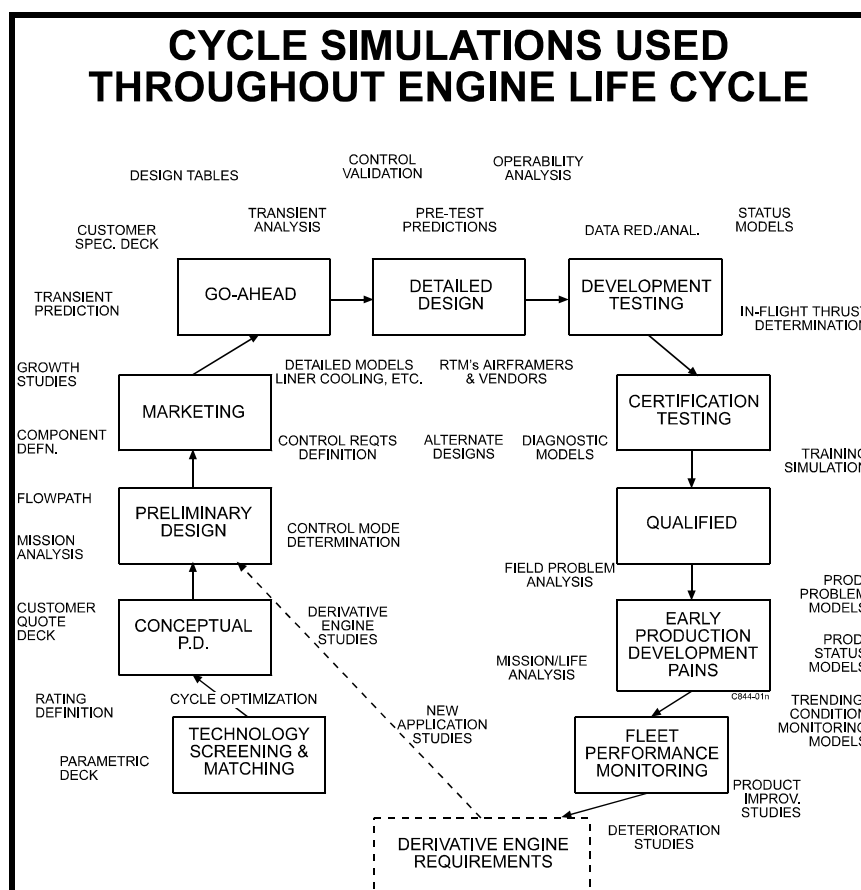


**Figure 1.2: Engine Models used Throughout Engine Life Cycle.**

## 1.3 INTRODUCTION TO TYPES OF ENGINE MODELS

A simple way of engine modeling is found in the performance data as provided by the engine manufacturer. These performance data are generally provided in the form of PC-based *cycle codes* from which performance charts or tables can be extracted. The charts are mostly three-parameter charts, using corrected parameters. These corrections are for engine inlet pressures and temperatures that are different from standard sea level conditions. An example is a chart where the corrected net thrust is given as a function of the flight Mach number for a series of engine pressure ratio values. Limits like the maximum turbine entry temperature or maximum shaft speed are included and form the operational limits of the engine. Simple thermodynamic relations can predict the performance of a generic gas turbine engine. Such a model may be *tuned* to a specific engine by using values for the component efficiencies that depend on the operational condition of the engine. On a test stand, engine component defects may show up when comparing measured pressures and temperatures with those of the *standard* engine model. An example is

a higher compressor exit temperature than expected for the measured pressure ratio, indicating degraded compressor efficiency.

In the above models, only thermodynamic parameters are considered, i.e. pressures and temperatures, as related to engine performance and performance analysis. The engine shaft speed is another important engine parameter. Modeling of the thermodynamics depends on the shaft speeds and vice versa, and requires knowledge of the actual design of the turbomachinery. In this case generalized semi-empirical engine component models (maps) may be used that relate the number of stages, the tip speed and the axial flow velocity (or specific flow) to the aerodynamic performance, say compressor pressure-ratio and turbine work. Since the maximum shaft speed is an important engine limit, inclusion of the engine shaft speed in an engine model is important for identification of its performance envelope.

One further step is to include the mechanical and thermal mass of the engine. In this case, the transient behavior can be studied; for instance, the responses of the engine to a sudden increase in fuel flow. The increase in back pressure in the combustion chamber while the compressor is still accelerating may then lead to compressor stall. To maintain safe operation and, at the same time, maximum responsiveness of the engine the behavior of the compressor should be known in order to avoid compressor stall while increasing the fuel flow.

These and other areas of interest to the engine designer lead then to component modeling. The present document will give attention to component modeling in the context of applications to whole engine performance modeling, and as a separate subject in a later chapter.

## 1.4 COMPUTERS, SOFTWARE, AND RECENT DEVELOPMENTS

All present-day gas turbine engine performance models are executed on computers, and the capabilities of modern computers have extended the applications and the range of use of the models. For users wishing to adapt models to their application, and to delve deeper into the present and future possibilities, a discussion of computers and software is provided. Because of the electronic format of the document, it has been possible to provide executable examples of some performance models. For those users wishing to model that which has not yet been modeled, and to examine the frontiers of the component and engine modeling technology, recent progress in the modeling of both whole engines and of the major sub-systems are described in *Annexes A* and *B*.

## 1.5 REFERENCES

- [1.1] RTO-TR-044, 2002, Performance Prediction and Simulation of Gas Turbine Engine Operation, RTO Technical Report 44, April 2002, AC/323(AVT-018)TP/29, ISBN 92-837-1083-5.

## INTRODUCTION

---



## Chapter 2 – APPLICATIONS

### INTRODUCTORY COMMENTS

As initially mentioned in *Chapter 1* of this report, engine mathematical models may have many applications. This chapter has been subdivided into six major sections that reflect the different applications:

- Fixed Wing Aircraft Applications, see *Section 2.1*;
- Rotary Wing Aircraft Applications, see *Section 2.2*;
- Marine Applications, see *Section 2.3*;
- Vehicular Applications, see *Section 2.4*;
- Power Generation Applications, see *Section 2.5*; and
- Manufacturing Applications, see *Section 2.6*.

Each major section provides an introduction into the particular applications followed by a variety of summaries or synoptics of published papers. Since the section on Fixed Wing Aircraft Applications comes from the previous document, [2.1], it by far has the most applications synopsized. In the section for simulations for Fixed-Wing Aircraft, the section is organized from an engine life-cycle perspective. Provided in each of the life cycle phases are synopses (summaries) synopses of published and open literature papers, from a variety of authors that provide examples of the different uses and applications of engine and component simulations. In the other sections synopses are also given but not necessarily tagged to the gas turbine engine life cycle. If an example from the Fixed-Wing Aircraft Section suffices for other applications, it will be referred to in that section.

### 2.1 GAS TURBINE ENGINE SIMULATIONS FOR FIXED-WING AIRCRAFT APPLICATIONS

For the following discussion, modeling and simulation applications are approached from the engine life-cycle perspective. The nature of the models may differ at each life-cycle phase, to reflect the specific needs of the phase. The propulsion system lifecycle can be subdivided into the following phases:

- Preliminary Design;
- Design and Verification;
- System Design and Development; and
- Post Certification and In-Service-Support.

These phases represent all the aspects of a propulsion system's life; from mission need assessments through to the eventual retirement from service. Throughout the propulsion system's life modeling and simulation are used to reduce the time, resources, and risks of the acquisition process and to improve the quality of the systems being acquired and sustained. The life-cycle phases represent a logical continuum of progress, and all programs tend to go through each of the phases in order, provided they survive long enough to see each phase. A thorough consideration of any real engine program must include the technical, managerial and contractual structure of the program.

Three major parties are typically involved in the development of any new propulsion system: the engine manufacturer, the air vehicle manufacturer, and the user service. The relationships between the parties can vary considerably from program-to-program, depending on the circumstances. For example, an engine

## APPLICATIONS

---

development program for a new engine type will probably be structured very differently from that for a derivative engine. Another program may involve an eventual competition between air vehicles, and a competition between engines for an air vehicle. The relationships between these parties tend to drive the exact location and the nature of the program decision milestones.

Decision milestones tend to be one-way gates, and while a program may backtrack through a gate, it is usually at great expense. Models are a critical contribution to the milestones because they provide critical ‘packets of information’ about engine performance and physical characteristics, for exchange between all parties involved. For example, a cycle deck might be such a packet exchanged at the completion of the Preliminary Design phase. At this point the air vehicle manufacturer has baseline engine performance characteristics that will be integrated into the design of the aircraft. The engine manufacturer uses this cycle deck as a baseline for overall engine performance that must be achieved. The engine component designers will use this data in the next phase to help determine the eventual configuration of their components. Models are used to understand the physics of the engine, as well as serve as the basis for configuration control and establish agreements between the various parties involved in the life of the engine.

A very diverse group of model makers and users works across and within the life cycle phases. In general, the manufacturers dominate the Preliminary Design through Development and Verification phases, and the using service dominates the Post Certification or In-Service-Support phase. While the specific needs and expectations of each group of users are different, there are common considerations. Models must be:

- Credible;
- User friendly;
- Flexible; and
- Robust.

There is no single ‘master model’ that does all for everyone. Instead, many different types of models are integrated into the process of designing, manufacturing, and sustaining aircraft engines. Various types of performance related models include performance and operability, aerothermal component, control system, and hardware-in-the-loop through manned flight simulator models, and engine health monitoring and life usage models. The results of these models are integrated with non-performance models such as: structural, fuel and thermal management, mechanical system and secondary power system, electrical power system, manufacturing, and cost models.

The **Preliminary Design** phase is also known as the **Concept Exploration** phase. This phase typically consists of competitive, short-term concept studies. The focus of these efforts is to define and evaluate the feasibility of alternative concepts, and to provide a basis for assessing their relative merits (i.e. advantages and disadvantages, degree of risk, etc.) at the next milestone decision-point. The analysis of alternatives is used as appropriate to facilitate comparisons of alternative concepts. Because this is the time to explore diverse concepts, many iterations need to be run. This in turn means that the turn around time per iteration needs to be relatively short, typically less than one day. The fidelity of the models is balanced with the need to run many iterations quickly. The most promising system concepts are defined in terms of initial, broad objectives for cost, schedule, and performance, opportunities for trade-offs, overall acquisition strategy, and test and evaluation strategy. This phase may be the shortest, and is typically less than two years.

The **Design and Verification** phase is also known as the Program Definition and Risk Reduction phase. During this phase, the program becomes better defined as one or more concepts, design approaches, and technologies are pursued. Most major parameters become fixed, such as the number of stages of each aerothermal component, and the control scheme is fixed. A wider range of models is run, including non-

performance models and individual models now go into more detail. Assessments of the advantages and disadvantages of alternative concepts are refined. Prototyping, demonstrations, and early operational assessments are considered and included as necessary to reduce risk so that technology, manufacturing and support risks are well in hand before the next decision point. Cost drivers, life cycle cost estimates, cost-performance trades, interoperability, and acquisition strategy alternatives are key considerations. This phase is longer than the Preliminary Design phase, and longer model turnaround times are tolerated in order to achieve increased accuracy.

The ***System Design and Development (SDD)*** phase has also been previously known as Engineering and Manufacturing Development (EMD). The primary objectives of this phase are to: translate the most promising design approach into a stable, interoperable, producible, supportable, and cost-effective design; validate the manufacturing or production process; and demonstrate system capabilities through testing. Low Rate Initial Production (LRIP) typically occurs while the SDD phase is still continuing as test results, design fixes, and upgrades are incorporated. The objective of LRIP is to produce the minimum quantity necessary to:

- Provide production configured or representative articles for operational tests;
- Establish an initial production base for the system; and
- Permit an orderly increase in the production rate for the system, sufficient to lead to full-rate production upon successful completion of operational testing. The model diversity and turn-around times are probably highest in this phase.

The ***Post Certification and In-Service Support*** phase includes production, deployment, and operational support. The objectives of this phase are to achieve an operational capability that satisfies the previously developed mission needs. This will be the longest phase of all and with derivatives can typically span from 12 to 40 plus years. Deficiencies encountered in developmental or operational testing should be resolved and fixes verified early in this phase. It is key to consider that the potential for modifications to the deployed system continues during deployment and throughout operational support of the propulsion system. Modeling and simulation plays a large role in the implementation of a propulsion system's life management plan. For example, the Low Cycle Fatigue (LCF) life prediction approach typically used by aircraft engine manufacturers can be described as consisting of seven tasks: materials characterization, stress analysis, thermal analysis, mission analysis, life analysis and operating experience. Each of these tasks can utilize a variety of modeling and simulation tools. Apart from all the above, modeling and simulation plays a significant role in maintenance practices. This includes health monitoring on-board and in-flight, and diagnostic ground stations. A key evolving area is prognostics and health monitoring.

Each phase of an engine's life is discussed in terms of the use of modeling and simulation. Example synopses (summaries) synopses with references are presented in each section to give the reader a feel for typical uses of modeling and simulation in each phase. Within each synopsis there is a format that is generally followed: Each synopsis describes a specific application, and addresses each of the following:

- ***Modeling Technique;***
- ***Potential Benefits;***
- ***Cited Example(s);*** and
- ***Limitations of the Modeling Technique Chosen.***

### **2.1.1 Preliminary Design Synoptics**

In the initial stages of an engine's gestation, a specification may not be available. Much of preliminary design activity is concerned with looking at the potential market and working with commercial areas in identifying new opportunities and customers. This involves keeping a close eye on changing market forces

## APPLICATIONS

---

and military strategies, and of course, the competitor's position. Requirements may be, initially, generic and may be understood in terms of the ability to competitively fulfill a particular mission. As a concept emerges, the requirements will become more explicit in terms of the usual constraints (e.g. cost, size, and mass, life, performance, growth capability, maintainability, emissions, stealth, and program risk). The detailed specifications are developed jointly with the potential customer, and should reflect not only what the customer requires, but also what is technically achievable.

The customer is interested in whole-system performance, and so from the outset there must be an effort to place any new engine in the context of an aircraft and a mission. Mission analysis involves the analysis of each phase of a mission to which is associated a particular aircraft configuration and payload. Such analysis can yield fuel burn and flight times that can form the basis for economic comparison between alternatives. It can also identify parts of the mission where certain design parameters are critical, e.g. specific fuel consumption (SFC), handling, thrust (for particular maneuver capability), noise (for civil applications), etc. A mission analysis can also yield throttle movement profiles, which feed into component life assessment, and the propulsion system Life Cycle Cost (LCC) activities. The interactions between engine and airframe can significantly affect whole-system performance. An early understanding of such effects can save costs in later development work.

The cycle selection process starts with consideration of the engine design point. Past experience is used to set a starting point for an iterative process. Leading cycle parameters, flows, efficiencies and temperatures are chosen, and the corresponding geometry generated by component areas. Component geometry is allied to component performance, but overall layout and envelope considerations, together with component interactions will force compromises. The component teams will redesign and refine assumptions, which will lead to refinement of the performance model so that the next iteration starts with revised boundary conditions for each component. The aircraft role may also imply conflicting requirements; the requirements for effective loiter and dash-to-intercept are fundamentally opposed in cycle definition terms. Computer generation of meaningful exchange rates to trade-off design parameters to achieve a workable compromise is a prime activity in the preliminary design phase.

Off-design performance modeling may initially use generic component characteristics, suitably scaled to meet the design point requirements. As component synthesis and rig work refines these assumptions, the performance model is updated and the iteration continues.

Certain decisions must be taken in the early stages on the inclusion (or exclusion) of some engine features. Performance models can provide the basis for these decisions. Reference 1 cites the example of offsetting of mission improvements against mass penalty of a convergent-divergent nozzle. The benefits included a geometric effect on the aircraft drag characteristics, as well as a thermodynamic benefit of an optimally expanded nozzle at certain flight cases.

Cycle selection primarily addresses the steady-state performance of an engine. The implications on maneuvering between operating points are wide ranging, impacting on compressor stability, combustion stability, mechanical and thermal loading, etc. which have to be controlled to achieve spec-compliant transient handling. Controls studies in the preliminary design phase are discussed in detail elsewhere in this section.

### 2.1.1.1 The Gas Turbine Conceptual Design Process

The conceptual design process of gas turbine engines is complex, involving many engineering disciplines. Aerodynamics, thermodynamics, heat transfer, materials science, component design and structural analysis are a few of the fields employed when selecting an appropriate engine configuration. Because of the complexity involved, it is critical to have a process that reduces engine options without missing the optimum. Various steps are required, including:

- Propulsion requirements definition;
- Engine cycle analysis;
- Component design;
- Flow-path and weight prediction;
- Installation analysis; and
- Analysis of the influence of the engine design on the size and performance of the aircraft.

The engine design process is not linear since the steps are interdependent. A number of iterations are usually necessary in selecting a final engine configuration.

### *Modeling Techniques Used*

The advent of the computer has made early examination of numerous propulsion characteristics possible. Illustrated in **Figure 2.1** is an estimate of when various computerized techniques became widely available. In the early years of computer based analysis, engine selection was based primarily on cycle trade studies and the design engineer's experience. Elements such as installed performance, flow-path, and weight were delayed until the detailed design part of the overall engine-development process. This could result in the selection of an engine configuration that was not fully optimized. In the worst case, the selected engine could not satisfy the aircraft requirements, necessitating a costly and time-consuming redesign. Today, many computerized tools are at the design engineer's disposal for considering component and engine design characteristics, weapon system trade-offs, and most recently, life cycle cost.

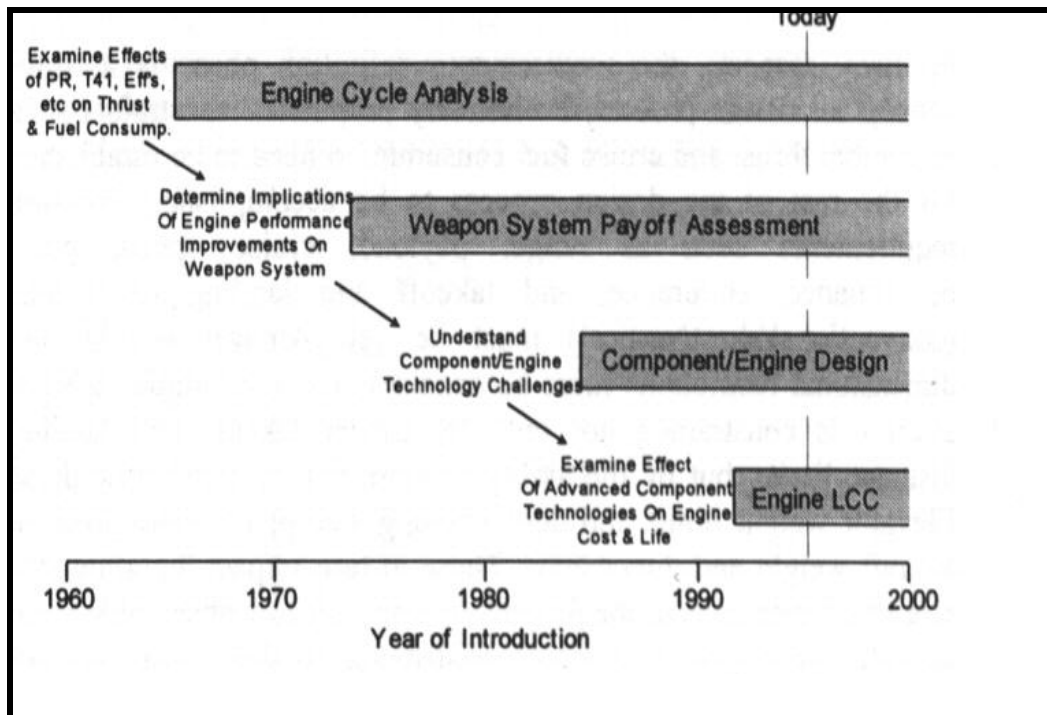


**Figure 2.1: Historical Trends in Computerized Analysis Capability.**

### *Potential Benefits*

Many different methods exist to integrate various design elements into an overall process. Ideally, designers like to perform all design steps concurrently in order to minimize the overall time required to

## APPLICATIONS

---

conduct a study. However, several steps must be performed in series since the results of one must feed into the next. Installation and component design analyses can be performed simultaneously, and the hope is that up-front costs (R&D and Acquisition) can be integrated into the process at an earlier stage.

### *Cited Examples*

- Stricker, J.M., “The Gas Turbine Engine Conceptual Design Process – An Integrated Approach”, Design Principles and Methods for Aircraft Gas Turbine Engines, RTO-MP-8, February 1999. [2.2]
- Schaffler, A. and Lauer, W., “Design of a New Fighter Engine – The Dream in an Engine Man’s Life”, Design Principles and Methods for Aircraft Gas Turbine Engines, RTO-MP-8, February 1999. [2.3]

#### *2.1.1.1.1 The Paper by Stricker*

This paper deals with a multi-disciplinary, iterative approach to gas turbine design along with the emerging importance of computer tools. Of these the author says:

*“The computer is a mixed blessing. Because of the many different design characteristics that can now be considered at the very early stages of the engine selection process, it is more difficult to provide a process that can properly address their interdependency.”*

There is an emphasis on the provision of good requirements: “An over-constrained or poorly defined set of requirements can lead the design team on a wild goose chase, focusing on the wrong criteria.... In many respects, the requirements definition phase is a mini-conceptual design process”, suggesting that modeling tools are an essential part of the requirements definition process.

The interaction between engine and aircraft is an important area. Sensitivity analysis tools are fundamental here. Models for affordability, maintainability and environmental concerns can also feed the requirements definition process. Following the requirement definition, uninstalled performance prediction is the first activity that uses models to generate cycle trends and exchange rates. The example of a ‘Global Strike Aircraft’ is given. The example illustrates the cycle options and the superimposed design constraints. A simple aircraft analysis yields estimates for fuel burn, range and take-off weights. A narrowing of options is achieved, which can lead to consideration of the installed performance (although some consideration of installed performance can be made alongside the activity described above). Installed performance is dependent on many engine and airframe effects, e.g. ram recovery, spillage, wave drag, friction, over and under expansion, shock losses, separation, etc. for which modeling facilities are required. The point is made that careful bookkeeping is essential at this point to prevent double accounting of losses (which can be accounted as aircraft drag or engine thrust).

Aircraft mission analysis is another step, which may result in refinements to the chosen design, and indeed may dictate compromise as encountered in the first example above.

Life-cycle cost comprises:

- Research and development costs;
- Acquisition costs;
- Operations and support; and
- Disposal.

Efficient or smart integrated modeling in early design may reduce the first two of the above items.

#### *2.1.1.1.2 The Paper by Schaffler*

This paper describes the early work undertaken in the definition of the Eurojet EJ200 military turbofan. Eurojet emerged as a 4-nation consortium (UK, Germany, Italy and Spain) in the mid 1980's and the EJ200 was proposed and subsequently accepted as the powerplant for the all-new European Fighter Aircraft (EFA) – later renamed Eurofighter 2000 (EF2000).

The paper summarizes the task. The engine had to be optimized for a specific role, a low cost of ownership and “set new standards on life and maintainability and testability”, as well as demonstrating carefree handling and being designed for later thrust growth of 15%. Of the missions that had to be fulfilled – the inevitable compromise had to be made in trading the design requirements for air-superiority roles against those for supersonic interception. The specific thrust requirements in these cases are contradictory.

The correlation of cost of ownership with aircraft mass became a fundamental design driver, which underpinned much of the iterative design process. The aircraft nominal thrust was fixed at an early stage and the fundamental cycle parameters: fan pressure-ratio, bypass ratio and turbine-rotor inlet-temperature were all varied to give a selection of options. Such trade studies require an efficient means of cycle modeling. Fine detail may not be appropriate at this stage; assumptions can be refined later. Examination of the trends in SFC and other key cycle parameters resulted in the down-selection of the optimum cycle, when considered in overall aircraft terms.

The technology level of the engine was the highest achievable, and the mechanical and material constraints followed.

The mechanical architecture was heavily influenced by the mass consideration (naturally) and Life-Cycle Cost (LCC), with resultant decisions concerning compressor variable geometry, compressor disc-blade fixing, bearing arrangements, parts count and shaft rotation.

The author concludes that the initial phase of engine design is “...an effort full of technical excitement and interesting interaction”.

This design phase requires quick answers to questions that are perhaps put in rather non-specific terms. Modeling tools must be available for quick generation of design information. Interfaces with modeling systems for LCC and physical design are highly desirable.

#### ***Limitations of Chosen Modeling Technique***

Conceptual design of a new engine has become an increasingly complex and sophisticated task. When engine performance and the whole aircraft system are to be optimized for the mission requirements, the designer is faced with conflicting targets and an overwhelming number of parameters to be considered. The designer has a multitude of computerized design tools to aid in the analysis of uninstalled and installed performance, component and flow-path design, aircraft trade-offs and engine life cycle costs. The limitations at this point of the process are usually based upon the level of analysis and the experience of the user.

#### **2.1.1.2 Mission Engine or Cycle Selection**

A modern fighter engine has stringent requirements for performance, operability and durability. To meet these conflicting requirements and to ensure a balanced design, simulations can be exercised during flow-path design, control-mode design and development testing. Use of a simulation helps to ensure problem prevention and reduces development costs. Representative engine models, which accurately account for off-design and transient effects, can be used early in the design phase for judicious configuration selection

## APPLICATIONS

---

and control-mode design. Favorable component matching is ensured before hardware fabrication and thus costly mistakes can be prevented. Special flow-path design considerations in fast-response twin-spool-afterburning-turbofan engines can be analyzed. In addition to flow-path design, simulation trade-off studies can be used to optimize the control system to satisfy system requirements. Novel control modes can be analytically evaluated across the operating spectrum and made practical with appropriate activation criteria that are readily implemented in digital-control logic. Simulation applications during development and flight-testing include calculation of hard-to-measure engine parameters using test-data driven transient-engine-models, thus facilitating design verification.

### *Modeling Techniques Used*

The modeling technique used in this example was a component level cycle code with additional modeling to allow for transient effects not ordinarily allowed for in standard transient cycle codes. The key relationships that were required to be satisfied are summarized below:

- Power-balance equation for each rotor with the rotor inertia term (turbine power = compressor power + parasitic power + acceleration power).
- Continuity equation for each component with transient mass storage term.
- An accounting for transient metal heat transfer of each component.
- Assurance of static pressure balance at the mixing surface boundary of the duct and core flows.

A multi-dimensional Newton-Raphson iteration technique was used to simultaneously satisfy all the relationships to achieve cycle balance at each instantaneous point. The component dynamics, including the moment-of-inertia of rotors and the heat transfer characteristics used in the equations were obtained from the manufacturer's design technology groups. In addition to the above relationships, the model had to be modified to accurately model off-nominal variable geometry effects, and the turbo-machinery performance and compressor stall line were also adjusted for the deviation of transient clearance from that obtained during steady state operation.

### *Potential Benefits*

Engine transient simulations which properly account for non-equilibrium conditions can provide system analysis and trade-off studies for judicious configuration selection and control-mode design, thereby effectively preventing operational problems and reducing costs. System design and optimization can be particularly challenging for an afterburning turbofan fighter engine with fast rotor response and augmentor transient requirements. Under transient conditions, the engine components can operate in far off-design conditions. To prevent any aerodynamic matching problems and adverse component interactions, engine configurations are thoroughly evaluated using transient simulations before hardware fabrication commitment. This ensures timely identification of the required flow-path modifications and compensatory control actions.

### *Cited Example*

- Khalid, S.J., "Role of Dynamic Simulation in Fighter Engine Design and Development", Journal of Propulsion and Power, Vol. 8, No. 1, January-February 1992, pp. 219-226. [\[2.4\]](#)

One example in the cited reference deals with bypass duct and fan deceleration stall margin. The fast deceleration rates of a fighter engine make the decrease in fan flow lag the decrease in compressor flow with a resulting increase in transient bypass ratio. The bypass duct pressure loss is a non-linear function of the bypass duct entrance Mach number, which increases with increasing bypass ratio. This non-linearity causes large increases in duct pressure loss during the bypass ratio excursion of a deceleration.

There is approximately a one-to-one relationship between duct pressure loss increase and fan stall margin loss. Illustrated in **Figure 2.2** is the simulated deceleration fan operating lines, stall line, and steady state operating lines with low duct loss representations evaluate on the F100-PW-229 engine model. It should be noted that the deceleration operating line with the initially proposed 'high blockage' duct rises significantly above the steady-state operating line (13%) in spite of opening the exhaust nozzle area. With a high blockage duct, a bigger exhaust area during deceleration further increases the duct Mach number, causing an increase in pressure loss. However, when the duct was streamlined to increase the effective flow area, the simulation showed a deceleration operating line rising only 2% above the steady state level. A low duct loss also increases the effectiveness of exhaust nozzle action in increasing fan stall margin. It should be noted that the effect of duct pressure loss characteristic on the deceleration operating line is more pronounced than on the steady-state operating line due to the higher duct-corrected-flow to fan-corrected-flow relationship during deceleration.

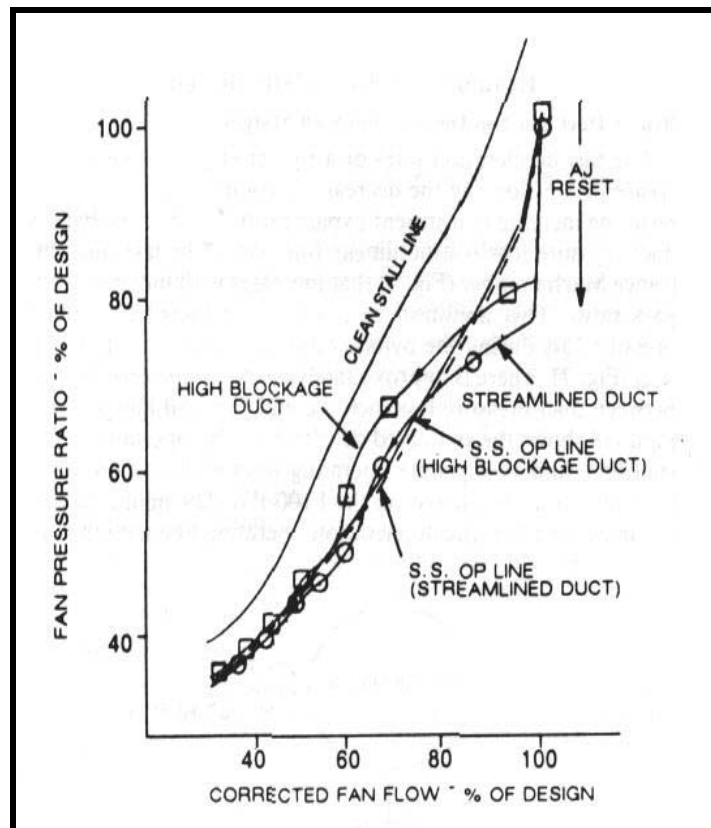


**Figure 2.2:** Transient Simulation of Fan Deceleration Operating Lines.

### *Limitations of Chosen Modeling Technique*

The major limitation is the reliance on component steady state maps. These maps are generated while the engine is running at steady state and thus have to be modified for transient behavior. A model for transient clearance is required to be able to adjust the steady state maps for transient effects. The turbomachinery performance and compressor stall-line were adjusted for the deviation of transient clearances from the steady state clearance. This deviation occurred because the rotor thermal growth is much slower than the case thermal growth. The engine model used in this investigation incorporated an algorithm to calculate transient clearances as a function of rotor speed and internal pressures and temperatures. Component performances and the stall line were correspondingly adjusted using empirically established clearance sensitivities.

## APPLICATIONS

---

### 2.1.1.3 Control System Concept Definition/Evaluation

A particular engine type or cycle is selected on the basis of its ability to produce the required steady-state installed thrust and SFC for its particular application. Clearly, other engine attributes must be considered, (mass, noise, price, dimensions, etc.) but the performance aspects are fundamental. Thrust requirements typically exist at a number of flight points, and perhaps for a range of ambient temperatures, and at various ratings (e.g. maximum dry power, idle, maximum afterburner). The agility requirements of an aircraft may place requirements on the transient times between ratings. Retention of all aspects of performance over the life of the engine may also be specified.

It is possible to define an engine operating point in terms of any gas-path parameter, or combination of parameters. Each combination may have different implications in terms of how the engine operation will be affected by external influences such as customer bleed, power-extraction and inlet airflow distortion. Stator outlet temperature (SOT) is traditionally used in early stages to define an operating level in view of its relevance to 'technology level'. However, gas temperatures such as SOT (apart from being difficult to measure) are not closely related to thrust, and so are not necessarily ideal parameters upon which to base a control scheme. It is clearly important to consider, early in the preliminary concept definition phase, how specification criteria can be achieved, i.e. how the engine must be controlled to achieve the functionality required by the customer.

#### *Modeling Technique Used*

Engine models used for control viability determination must have certain capabilities as described below.

**Representation** – An engine model must model the physical processes to a degree, to allow the derivation of meaningful steady-state sensitivities. Engine models used for controls investigations are not necessarily the same as those used for performance studies, although there is a trend towards the wider use of cycle-match models for all functional design work. As the cycle selection process is focused on the steady-state performance of the engine, dynamic modeling is not a prime consideration. However, the main dynamics associated with an engine are generic, and once the methods are established, they require engine-specific data such as shaft inertia and gas-path geometry. Therefore, a 0-D dynamic representation of up to 30 Hz is easily established. High-order models such as these are not necessarily required for initial control-loop selection. However, some candidate schemes, which appear viable under steady-state conditions, may become less so when gas-dynamics are considered. This is especially true for variable-cycle engines where power level (or operating point) is being dictated by variable geometry. In a conventional gas turbine, the dominant dynamic associated with power level is shaft inertia; if the power level can be changed at a constant shaft speed, then other dynamic terms dictate the design of the control loop. Gas dynamics are also relevant when considering the finer details of control-system implementation, e.g. actuator response.

Thermodynamic models are usually confined to the normal operating range of the engine. However, a model that is capable of running down to zero speed (or steady windmilling speed) is needed for exploration of starting strategies. Overspeed control is fundamental to engine integrity, and so a model should be capable of running to the conditions arising from system failures. Similarly, control of the engine to recover or avoid compressor stall or surge requires the post-stall behavior to be modeled. It could be argued that these aspects are not a prime part of control studies in the preliminary design phase, and so just the normal operating range may be adequate. However, if one thinks in terms of capability acquisition, generic full range models should be available so that control strategies (or part-strategies) are 'on-the-shelf' ready for maturation on forthcoming projects.

All likely sensor stations must be modeled. This requires geometry assumptions for flow areas for static pressures. Detailed gas temperature (2-D) profiles are not required at this stage, but may become relevant as a design matures. The modeling of the sensors themselves is not directly relevant to the choice of

control-loops, their own dynamics may influence the detailed design of a control-loop but ought not to impact on the overall control concept.

**Compatibility** – Controller design tools and methods are commonly based on linear methods. A linear representation of the sensitivities across the dynamic frequency spectrum can be obtained through manipulation of the engine model using a process known as linearization. This is explained in the cited reference, using a simple worked example based on the shaft and volume dynamics of a single spool turbojet modeled using iterative methods.

**Versatility** – A model should be able to generate steady-state points. This can be achieved by iteration (time fixed) or by stabilization over time. Cycle-match models have an advantage in their ability to run to a specified level of an output quantity, not just in steady-state mode but also in dynamic simulation mode. A typical thrust transient profile can be specified, perhaps in conjunction with a fan working-line constraint. Consequently, the requisite control input profile is generated (e.g. fuel and final nozzle area), which can be useful in determining the level of controller complexity required, or for investigating the potential to simplify or relax control constraints during transients.

### ***Potential Benefits***

Early consideration of control-system issues can lead to a better final product at reduced cost. Product specifications can be developed with potential (realistic) control schemes in mind; promises of unrealistic levels of performance may thus be avoided. For example, the sensor set should be chosen alongside control-law definition activities. Late consideration of control-laws may lead to a position with a sensor or a control-law incompatibility. Even if soluble, this can cost money and program time. Exposure of engine handling qualities to potential pilots using real-time whole engine-system simulation can provide early identification of control-system shortcomings, which can be rectified at more cheaply if identified in the preliminary design phase.

### ***Cited Example***

- Horobin, M., “Cycle-Match Models Used in Functional Engine Design – An Overview”, Design Principles and Methods for Aircraft Gas Turbine Engines, RTO-MP-8, February 1999. [\[2.5\]](#)

The definition of a control-system can be conveniently broken into:

- Requirements; and
- Implementation.

**Requirements** come from many sources and cover issues such as functionality, physical features, safety, cost, etc. The fundamental role of the controller is to enable the engine to deliver thrust or power as required, and so functionality is (arguably, perhaps) the prime consideration. Again, conveniently, requirements can be split into two parts: *control at a point* – or perhaps more correctly *prescription of steady-state operating point* – and *maneuver between points*. The former is the basis of control-scheme definition.

At the highest level, an engine can be considered as a process that converts inputs (e.g. instantaneous fuel and geometry) into outputs (measurable and immeasurable parameters). It is unfortunate that the output parameter of most interest (net thrust) is not directly measurable. If a certain level of thrust is required at a certain flight case, then a suitable measurement, which is related to net-thrust, must be identified to allow pseudo closed-loop control of thrust. Open-loop control, relying on specific levels of input to achieve an output may be viable for some inputs, for example some variable geometry features, but is not considered realistic for fuel flow for several reasons:

## APPLICATIONS

---

- The mass flow rate of fuel is difficult to measure;
- Fuel-heating values vary;
- Engine deterioration; and
- Engine-to-engine scatter, etc.

Engine deterioration and engine to engine scatter also apply to inputs other than fuel flow, which suggests closed-loop control of all inputs. The drive for simplicity, which may lead to lower cost and greater reliability, suggests a combination of open and closed-loop implementations. However, with the increasing complexity of engines (e.g. variable-cycle designs) and the potential rewards for tighter control of the engine operating point (e.g. life management, fleet uniformity, etc.), closed-loop control of all engine inputs is becoming more desirable.

Control-loop interaction is a hazard when multiple closed-loops are used. Ideally, each control-loop should be isolated. That is, the input should only have an effect on its own feedback parameter. Realistically, this cannot be the case for a gas-turbine engine where an increase in fuel flow has a direct effect on many parameters, some of which may be used as feedback terms for variable geometry (say). There are mathematical techniques that can reduce interaction. However (natural) interaction should be minimized by careful selection of control parameters. It is here that there may have to be a compromise between ideal performance requirements, and the feasibility of implementing certain combinations of control-loops in a robust fashion, with adequate stability margins.

The engine must be controlled within its safe operating range – critical parameters must be measured and demands overridden if necessary. The control laws must also be designed to be able to accommodate possible system failures.

Control of a demanded transient could involve relaxation of some control-loops; open loop scheduling from an appropriate engine parameter might control some inputs. Transient constraints (limits) are typically associated with compressor and burner stability, although, depending on the specific case, appropriate ‘shaping’ of an acceleration or deceleration can have an impact on engine life.

It is trades such as these that can be explored in the early design stages, using suitable engine models to establish exchange rates and sensitivities. An understanding of the engine thermodynamic cycle helps to identify a short-list of candidate schemes for control. However there are ‘black box’ techniques that can identify viable schemes.

### ***Limitations of Chosen Modeling Technique***

Any engine model that exists at such an early stage in the design process is preliminary by definition. It may contain assumptions and omissions in the steady state or dynamic modeling which could result in a non-viable control scheme being pursued, through lack of data or rig tests. For example, variable geometry features are not always well understood in the early stages of design in terms of the relationship between the geometry setting and the thermodynamic effect. At the cycle design stage, the effect of geometry can be investigated by directly varying the known consequence of the variable, such as change in flow capacity of a compressor, at a given speed. For control studies, the true input quantity must be the instantaneous geometry, which requires the true effects to be modeled. This can be difficult for some features like blocker doors and mixer valves, where sufficient work has not yet been done to establish a realistic model. Detailed CFD or rig tests might be required for this. Hence there may be significant uncertainties in the sensitivities implied by the overall model. Consequently, there is a risk that some control strategies initially identified as viable may not be so (and vice versa). This risk has to be accommodated in the context of the activity being preliminary, as opposed to in-depth, as is encountered in later phases of development.

#### 2.1.1.4 Gas Turbine Cycle Design Methodology – Numerical Optimization

In gas turbine performance simulations the following question often arises: ‘What is the best thermodynamic cycle design point?’ This is an optimization task, which can be attacked in two ways. One can analyze a series of parameter variations and pick the best solution, or one can employ numerical optimization algorithms that produce a single cycle that fulfills all constraints. The conventional parameter study builds strongly on the engineering judgment and gives useful information over a range of parameter selections. However, when values for more than a few variables have to be determined within several constraints, numerical optimization routines can help to find the mathematical optimum faster and more accurately.

The traditional way to select the thermodynamic cycle of a new gas turbine employs extensive parameter variations. For a complex engine with many design variables this is a time consuming task. One looks for the optimum solution in a certain respect. Instead of screening a wide range of potential solutions for the design variables with systematic parameter variations it is also possible to do an automatic search for the optimum engine design with the help of numerical optimization routines. A numerical optimization algorithm will only find the optimum of the mathematical model, rather than the ‘true’ optimum. If the result of an optimization run is an exotic cycle, it usually hints to a deficiency in the model. In such cases, most probably a design constraint has been overlooked when defining the problem. In addition, it is always of interest to know about the neighborhood of the optimum solution. From a parametric study, limited to the region of interest it becomes obvious which design variables and constraints have the biggest impact on the result. One of the advantages of numerical optimization is that the region where parameter studies should be performed is significantly reduced.

##### *Modeling Techniques Used*

When numerical optimization is chosen, one must define the optimum in a mathematical sense. In a parametric study the optimum is not known at the start. In a numerical optimization process, a figure of merit must be clearly defined before the calculation can commence. The figure of merit might be the specific fuel consumption of a turbofan at cruise, which is to be minimized. For a fighter engine it might be that the specific thrust should be maximized. One can also think of a weighted combination of these parameters. When values for more than a few variables have to be determined while several constraints exist, then numerical optimization routines can help to find the mathematical optimum, the minimum or maximum of the figure of merit, faster and more accurately. For a case with only two variables it is easy to find an optimum solution. If there are three variables the situation is not so clear. (When hill climbing in fog, it is difficult to see whether the hill one is standing on is the highest in the neighborhood.)

With more than three variables, the picture may get obscure. In complex studies, the true optimum may never be found with the conventional parametric study. There are many numerical optimization algorithms known from the literature. They can be divided basically into the following two major groups:

- Methods that use gradient information; and
- Others.

In the program GasTurb, there is one method from each group implemented. The gradient search algorithm implemented in GasTurb follows the procedure illustrated in **Figure 2.3**.

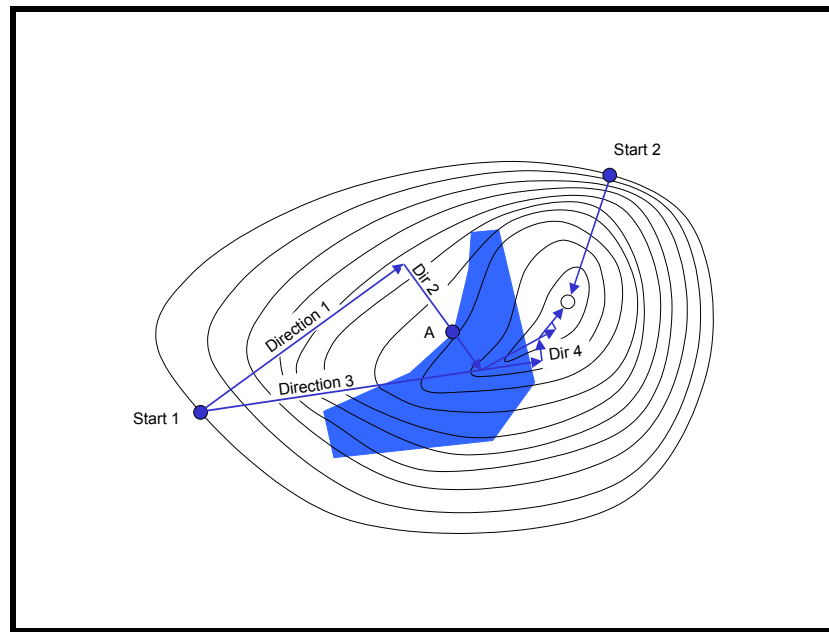


**Figure 2.3: Optimization Strategy.**

The gradient search method is initiated at the point marked ‘Start 1’ and looks for the direction of the steepest gradient (‘Direction 1’). The process follows this direction until the highest point is reached. At this point, the direction changes by 90 degrees (orthogonal). This is done without evaluating the local gradient. Following this direction, the procedure goes to the highest point. The third direction is defined from the experience of the first two directions. The ‘Start 1’ point is connected to the optimum point found in the previous step and the process is followed for as long as the search continues to optimize the figure of merit. This process is followed until the search steps or the change in the figure of merit becomes very small.

The optimization process requires the use of a numerical simulation of the gas turbine engine. The gas turbine engine simulation described in the cited example is a component-level cycle code known as GasTurb, and was developed by the author, Kurzke.

### ***Potential Benefits***

With a conventional parametric study, it is often very difficult to find the optimum solution for a problem as soon as four or more design variables and several constraints are involved. With the help of numerical optimization algorithms, one can easily find the mathematically correct solution to the problem. Extensive parametric studies around the solution will help to understand why this combination of design variables is the best choice and how sensitive the figure of merit is to small deviations from the optimum. The parametric variation is best suited for presenting the sensitivity of the results in the neighborhood of the optimum cycle design point. Sometimes this leads to a redefinition of the figure of merit or the constraints imposed on the solution. In rare cases an outstanding solution, which was overlooked while doing a preliminary parametric study, may be found.

### ***Cited Example***

- Kurzke, J., “Gas Turbine Cycle Design Methodology: A Comparison of Parameter Variation with Numerical Optimization”, Journal of Engineering for Gas Turbine and Power, Vol. 121, January 1999, pp. 6-11. [\[2.6\]](#)

A very common design task is to adapt an existing engine for a new application. It is quite obvious that in this case there are more constraints than during the design of a completely new engine. The case study is an unmixed-flow turbofan engine for a business jet. This type of engine has a rather low overall pressure ratio and a moderate burner exit temperature when compared to the big turbofan engines used on commercial airliners. Besides the pressure ratios of the new booster and the fan, among the design variables of the growth engine there will be the bypass ratio and the burner exit temperature. A new low-pressure turbine will be required while the gas generator remains unchanged. The core compressor of the new engine will not necessarily operate at the same operating point as in the basic engine. In fact, that might even be impossible because doing that would require an increase in the mechanical spool speed beyond the limits of the original design.

There are several constraints to be observed for the new engine design. The common core of the basic engine requires that both high-pressure turbines have practically the same airflow capability. The Mach number at the core exit should also be nearly the same, with the consequence that the flow capacity of the low-pressure turbine of both engines must also be very similar. A further constraint is that the low-pressure turbine inlet temperature must be below 1150 K to allow for an uncooled low-pressure turbine, which can then be manufactured from inexpensive materials. Another constraint may come from the nacelle in which the engine has to be installed. This will limit the fan diameter of the growth engine. The ‘figure-of-merit’ is the specific fuel consumption (SFC) for Max Climb rating and is to be minimized. This will automatically result in low fuel consumption for cruise.

The optimum growth engine chosen for this cited example was influenced by three of the design constraints. The growth engine has a fan diameter of 0.75 m, which conformed to the largest fan allowed in this exercise. The second constraint that had an impact on the design of the growth engine was the compressor exit temperature, which was limited to 750-K for the hot-day Take-Off case. The third constraint was the minimum high-pressure turbine flow capacity. All design variables remained within the predefined range during the optimization. The thrust increase for Max-Climb rating at altitude is 25% and at Take-Off even 29% as illustrated **Table 2.1**. Note that both engines run during Take-Off with 7% more mechanical high-pressure spool speed than at Max-Climb in this example. The specific fuel consumption at altitude is nearly 5% better for the growth engine.

**Table 2.1: Cycle Parameter Summary**

	Basic Engine		Growth Engine	
	Max Climb	Hot Day Take-Off	Max Climb	Hot Day Take-Off
<b>Thrust (kN)</b>	3.61	13.10	4.50	16.94
<b>SFC (g/(kNs))</b>	19.65	14.23	18.93	13.33
<b>Bypass Ratio</b>	4.5	4.65	5.06	5.23
<b>Fan (P13/P2)</b>	1.775	1.62	1.73	1.6
<b>Ideal Jet Vel. Ratio</b>	0.781	0.886	0.726	0.839
<b>Booster (P24/P2)</b>	1.5	1.33	1.80	1.61
<b>HPC (P3/P25)</b>	12	11.36	12.3	11.67
<b>T4 (K)</b>	1350	1479	1393	1530
<b>W41 (Rstd)</b>	1.35	1.35	1.31	1.31
<b>W45 (Wstd)</b>	4.98	4.96	5.01	5.00
<b>T3 (K)</b>	610	708	649	750
<b>T45 (K)</b>	973	1076	1000	1108

### ***Limitations of Chosen Modeling Technique***

The major limitation of this modeling approach is the reliance upon component maps. These maps must be previously generated in order to try to predict performance. For the design process, these maps must be somewhat generic and based upon previous experience. However, once a set of performance characteristics is available, predictions can be tuned via some of the mechanisms discussed in the cited reference to improve the model's accuracy.

### **2.1.2 Design and Verification Synoptics**

This phase is also known as the ***Program Definition and Risk Reduction phase***. During this phase, the program becomes better defined as one or more concepts, design approaches, and parallel technologies are pursued. Assessments of the advantages and disadvantages of alternative concepts are refined. Prototyping, demonstrations, and early operational assessments are considered and included as necessary to reduce risk, so that technology, manufacturing and support risks are well understood before the next decision point. Cost drivers, life cycle cost estimates, cost-performance trades, interoperability, and acquisition strategy alternatives are considered.

The phases represent a logical continuum of progress, and all programs tend to go through each of the phases in order, provided they survive to see each phase. The exact location of program decision milestones may be dependent on the program contract structure. For example, an engine 'EMD' contract may start after the completion of a 'Concept Exploration' contract. This means the aspects of a Design and Verification phase have been integrated into either one of the contracts, or into both. The contract structure may vary depending on whether the customer has contracted directly with the airframe manufacturer for everything, or whether there are separate airframe and engine development contracts.

Moving from the Preliminary Design phase to the Design and Verification phase represents the transition from the consideration of many concepts to the commitment to refine and select from a few of the best. At this point models are driven primarily by customer requirements. The trade-offs being considered can be broad; and while they may focus on hardware characteristics, they do not yet focus on a detailed hardware configuration. Issues such as overall cycle performance, cost, manufacturability, supportability, and tolerable technical risk (e.g. blisk or Integrally Bladed Rotors vs. bladed rotors) are important.

Throughout this phase, specific hardware configurations emerge. Trade-off studies and risk assessments need to be conducted. This is a very important time for the use of models, because the outcomes of the studies will refine the hardware configuration pursued. The need to make major configuration changes in later phases may kill the program because of the large cost and time required. This phase contains the majority of component testing that will be conducted. Rig tests will typically be used to gauge a 'realization' factor on various technologies scaled to the engine size. The rig tests are used in conjunction with the models and to refine the models. Engine testing may also be conducted during this phase.

The goal of this phase is to select, from the possibilities that have already been extensively studied, a single configuration to pursue in detail in the Development and Validation phase. In order to select wisely, one must understand the strengths and weaknesses of the proposed system, especially in terms of what the customer expects. Customer involvement is essential during this phase because the trade-offs are often complex and intertwined.

#### **2.1.2.1 Technical Risk Assessment**

When defining the cycle parameters and calculating the performance of a real engine, there are numerous practical constraints to be taken into account. These fall into two main categories: the limitations of available component technologies, and the operational considerations that are dependent on the aircraft application. In applying thermodynamic principles to specific applications, the gas turbine designer must take a multitude of practical factors into account in order to select the most appropriate cycle parameters.

Most obviously, the available component technologies impose aerodynamic, thermal and mechanical limits that set upper bounds on cycle pressure ratios and temperatures. Gas turbine research and development (R&D) is being pursued vigorously in government laboratories, manufacturing companies, universities and other research institutes. This research is pushing back technical barriers with little sign that a plateau of technology is being reached. While the acceptable limits may move with time, there remain firm limits which the designer must observe, his only freedom being the judgment of precisely where to set them for the envisaged application at the time of the design freeze. The application itself is equally important. The type of aircraft – military combat, civil or military transport, helicopter, etc. – and the planned service life and mission operating requirements will all have a major influence on the choice of cycle parameters.

### ***Modeling Techniques Used***

A variety of modeling techniques will be used when a design of a new cycle is being contemplated. Because the gas turbine engine is composed of several components, which can be optimized either through computational means or through component experimentation, many times the final product is a compromise between best component performance and optimum cycle performance. In the design of a component, computational fluid dynamics (CFD) will quite often be employed to obtain the finest details of the flow. In many instances, ‘rules-of-thumb’ or previous experience will be used to start the process. CFD will then be used to modify or optimize from the ‘last best solution’. Once the performance characteristics are computed, they must be integrated within an engine simulation to understand the component performance in relation to the engine cycle.

### ***Potential Benefits***

There is a multiplicity of factors, both technical and economical, that the engine designer must take into account and which will affect his mechanical constraints, such as shaft torque loading and overspeed limits, vibration avoidance and damage containment. The economic issues include perceived market size and the possibility of alternative applications, availability and cost of raw materials, processing methods and fabrication techniques, etc. When all such aspects are taken into consideration, the engine cycle may deviate significantly from the optimum indicated by simple design practices.

### ***Cited Example***

- Philpot, M.G., “Practical Considerations in Designing the Engine Cycle”, AGARD Lecture Series, Steady and Transient Performance Prediction of Gas Turbine Engines, AGARD-LS-183, May 1992. [\[2.7\]](#)

#### ***2.1.2.1.1 Component Technology Considerations***

For any engine, choice of compressor design is one of the crucial issues facing the designer at the start of the engine definition process. It involves a complex compromise between efficiency targets, number of stages, surge margin requirements across the intended flight envelope, and various mechanical considerations such as stress limits, and vibration. In general, increasing the work done per stage reduces compressor efficiencies, although thanks to considerable improvements in the understanding of detailed compressor aerodynamics and in CFD design methods, this effect is less marked than it used to be. On the other hand, reducing the number of stages tends to bring advantages in reduced engine length, weight and costs. For combat aircraft, weight and cost considerations generally dominate and high stage-loading designs are almost always chosen, at least for the core. For civil applications, while cost and weight are still important, the need to minimize fuel burn places more stress on high component efficiencies and leads to more modest core compressor stage loading. From a practical point of view, it is essential that the fan and core compressors are each provided with sufficient working surge margin to ensure stable operation

## APPLICATIONS

---

over the entire flight envelope and under all likely transient conditions. Achieving this at high stage loading is always a challenge.

The turbine introduces few cycle modeling problems. For example, Reynolds number effects are small and can safely be ignored. The main concern is to achieve proper representation of the bleed flows in cooled turbines. In modern, high temperature engines, the cooling bleeds are extracted from the compression system at two or more points and returned to the cycle at several points through the turbine system. Up to 25% of the core entry flow may be used in this way. The flows provide cooling for two or more nozzle guide vane rows, at least one and probably two rows of rotor airfoils, and the front and back faces of the associated rotor discs. The bleed in-flows have complex effects on the turbine aerodynamics due to flow disturbance, boundary layer thickening, etc. Turbine specialists using a mix of CFD and empirical methods can estimate these effects. Typically, in-engine aerodynamic turbine efficiencies are some 2% lower than might be measured on a cold turbine rig, with no simulation of the cooling flows.

Combustors are designed to promote the re-circulation and turbulent mixing on which the whole burning process depends, while at the same time ensuring adequate cooling of the metal walls. With flame temperatures in the primary zone reaching 2300-K or more, well above the melting point of any usable alloy, this is no mean feat. Nevertheless, it has so far been achieved with sufficient success for combustor wall temperatures not to replace the turbines as cycle temperature limiters. Despite the extreme conditions, combustion efficiency is almost always close to 100%, falling off significantly only at flight idle or below, and often not even then.

Afterburners or augmentors are used in the majority of high performance combat aircraft as a means of greatly increasing thrust for short periods of time, albeit at the cost of a huge increase in fuel consumption. Outwardly simple, the augmentor is in practice a sophisticated piece of engineering design with a long and careful development cycle. The burner is placed close to the bypass and core stream mixer plane, so that the outer radii are working with un-vitiated bypass air, while the center section is using the core exit gas, in which the fuel/air ratio may already be around 0.025. In principle, fuel/air ratio can be increased until both streams are close to the stoichiometric limit of 0.0687. In practice, it becomes increasingly difficult for the fuel droplets in the core stream to find oxygen molecules to react with and combustion efficiency begins to fall. Also, rising augmentor temperature requires more bypass air to pass round the burning zone in order to cool the liner and nozzle, thus reducing the quantity available for combustion. Thirdly, high heat release in the augmentor leads to the burning stability problems known as ‘rumble’ and ‘screech’, when severe pressure oscillations in the augmentor duct cause rapid structural failure. The precise limits on augmentor operation are dependent on the precise geometry and aerothermodynamic parameters. There is also a minimum operation limit determined by burner blowout characteristics. Although combustion efficiency falls off towards a minimum, over most of the range a good augmentor design will give close to 100% efficiency.

### 2.1.2.1.2 *Cycle Choice Considerations*

#### 2.1.2.1.2.1 Transport Application

For any application, a decision about the cycle must be made. For a transport, the high bypass turbofan or turboshaft is the most appropriate cycle. Most current civil engines have bypass ratios of around 5 or higher. For virtually all transport engines, there are two pre-eminent requirements – minimum fuel consumption, and long life between overhauls. Engines are designed for a careful balance between these two properties and as a result the core cycle parameters are largely optimized around three operating conditions:

- Maximum thrust condition at nominal cruise flight condition;
- Average thrust rating for normal cruise at steady speed and altitude; and
- Maximum thrust at sea level static conditions for take-off on a hot day.

For measuring these conditions, specific fuel consumption and thermal efficiency are good indicators of performance. Specific fuel consumption is effectively the reciprocal of overall engine efficiency. Illustrated in **Figure 2.4** is the relationship between SFC and percentage thrust at cruise flight conditions. Two curves are shown, one assumes constant component efficiency, the other assumes typical variations in fan and core compressor efficiencies along the engine operating line. Both show a characteristic catenary shape, with minimum SFC occurring at around 70% thrust. This is convenient because the engine will normally be throttled back at least to around 80% thrust at the start of steady, level cruise and will be gradually throttled further back as fuel is burned off and the aircraft becomes lighter. The shape of the curve stems from the opposing behavior of propulsive efficiency and thermal efficiency. As the engine is throttled back and the turbine exit temperature (TET) drops, propulsive efficiency increases and dominates, but below about 70% thrust, the thermal efficiency effect becomes increasingly dominant. Thermal efficiency can be defined as the energy delivered by the core divided by the energy supplied by fuel. The thermal efficiency turns out to be a function of total pressure ratio and total temperature ratio as presented in **Figure 2.6**. At the cycle conditions appropriate to a modern high bypass engine at altitude, thermal efficiency will increase with both cycle pressure ratio and temperature, although a law of diminishing returns operates for both parameters.

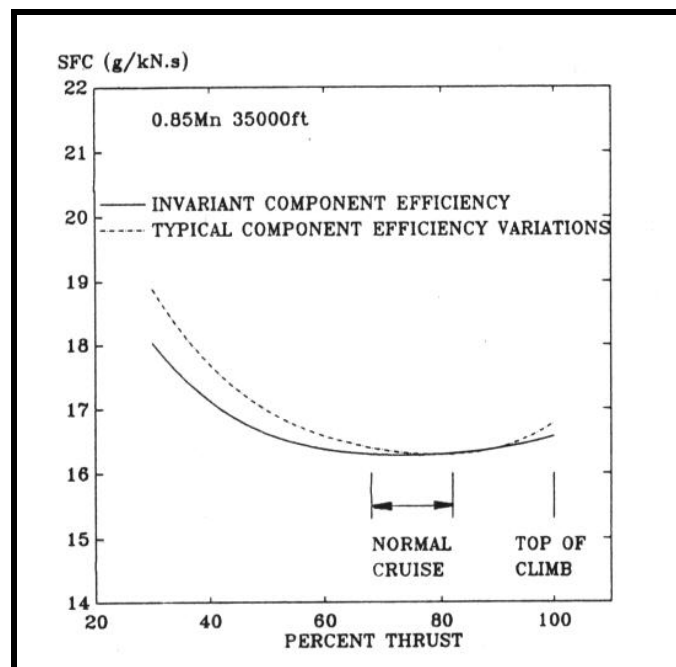


**Figure 2.4:** Typical Thrust and SFC Performance for High Bypass Transport Engine.

#### 2.1.2.1.2.2 Military Combat Engines

The basic principles for transport engines – thermal, propulsive and transfer efficiency and the effects of cycle parameters – apply with equal force to combat engines. However, both operational needs and cycle selection criteria are quite different. Combat aircraft are required to operate effectively and efficiently over a wide range of flight conditions as illustrated in **Figure 2.5** and **Figure 2.6**. While the transport engine has only about three critical flight conditions to satisfy, the military engine may have to meet 20 or more cardinal points. In addition, the predominant aim is almost always to achieve high aircraft thrust-to-weight ratio, in the interests of speed, agility and weapons carrying capability. This means engine thrust-to-weight ratio needs to be high, but more importantly, engine specific thrust is emphasized. High specific thrust means small engine cross-section and hence reduced aircraft fuselage cross-section. Any growth in engine size has a considerable effect on airframe size and weight.

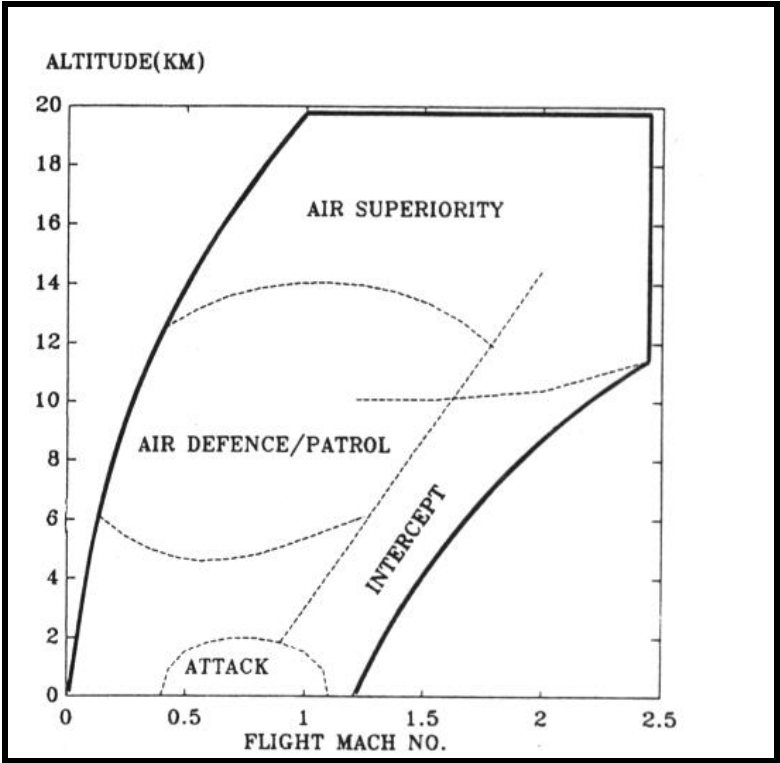


Figure 2.5: Military Aircraft Flight Envelope.

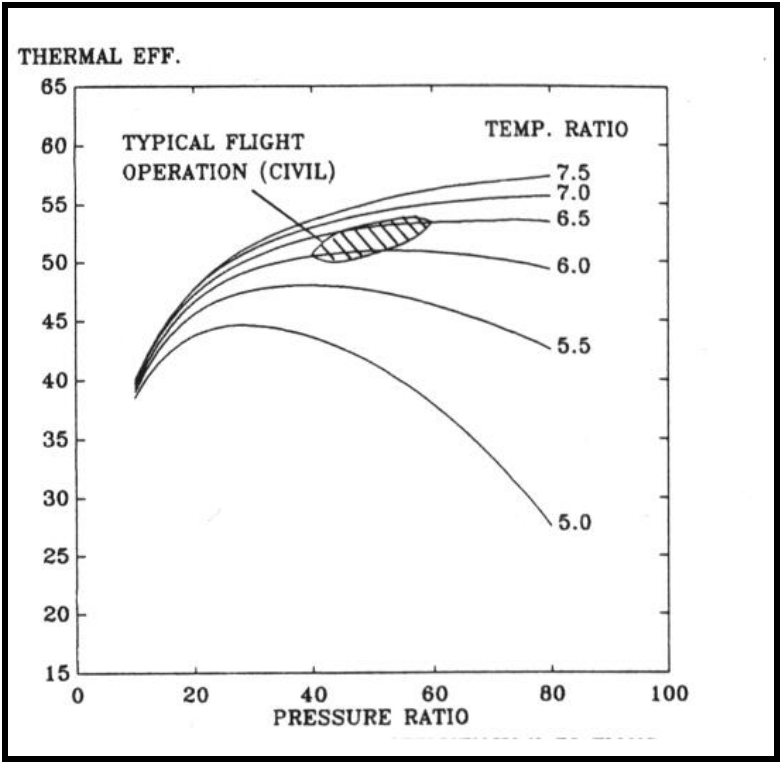


Figure 2.6: Engine Thermal Efficiency Variations.

This does not mean that fuel consumption is unimportant; far from it – the military operator is always seeking more range and endurance. Cycle choice remains a careful balance between thrust capability and endurance; engines optimized for different roles can have quite different cycle parameters. Nevertheless, the first priority is usually to satisfy the aircraft requirements for thrust and size, leaving the engine designer to achieve the best mission fuel burn that he can.

Despite the importance of specific thrust, fuel consumption cannot be neglected. It comes as no surprise that the trends are in generally the opposite sense. For military engines with augmentors, specific fuel consumption can get quite high when the augmentor is operated. Using fuel to heat the low-pressure bypass air is a highly inefficient process, whose only attractions are that it is basically simple and it provides the engine with a greatly increased thrust capability without increasing diameter. Because of the high fuel consumption, afterburning can seldom be used for more than a few minutes to provide short bursts of power for take-off, high rate climbs, acceleration and high angle of attack combat maneuvering.

Engine thrust-to-weight ratio is one of the commonly quoted measures of technical progress for combat engines. The engines in current operational fighters, which are mostly based on designs dating from the mid-1970s, generally have thrust-to-weight ratios around 7. This is based on the nominal maximum SLS thrust on full augmentor.

The current classes of engines being developed for the new generation of fighters have thrust-to-weight ratios of around 10. Foreseen technology developments will bring a thrust-to-weight of 15 within reach in the foreseeable future and advanced research and technology programs are set 20 as a longer-term goal. Achieving high thrust-to-weight has a significant direct benefit in terms of aircraft size, but it also symbolizes gains in other ways. One of these – the progressive increase in attainable cycle temperatures and hence in specific thrust – means that more thrust can be generated from a given size of engine. At the same time, improvements in internal aerodynamics have enabled the job to be done with less turbo-machinery and this also contributes to an improved thrust-to-weight ratio. However, with stage numbers now becoming quite low, there is less to be gained by this means in the future. Further direct weight reductions will be gained through the use of radically new materials like metal composites and non-metallics. A generalized plot, encapsulating the published trends and assuming constant airframe technology, is shown in **Figure 2.7**. Raising the engine thrust-to-weight from 10 to 20 will save around 15% of the aircraft weight for the same mission. This represents appreciable savings and helps to explain why the thrust-to-weight ratio attracts so much attention.

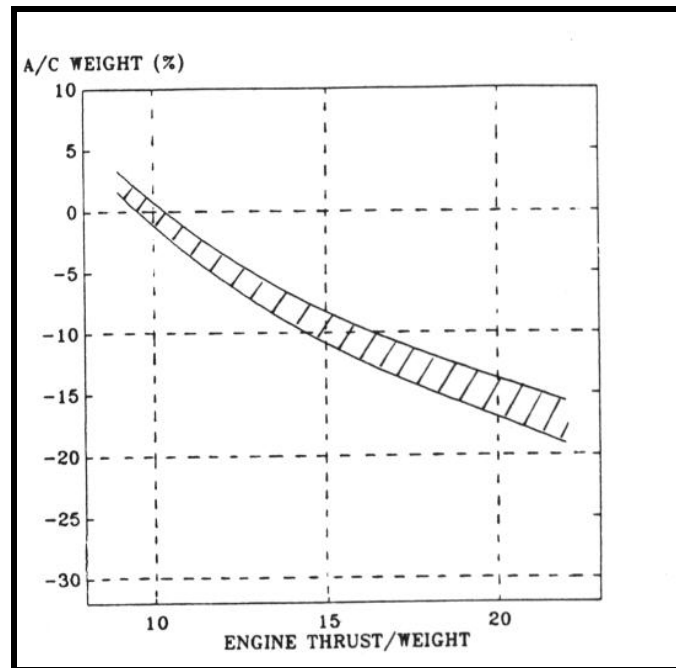


**Figure 2.7: Effect of Engine Thrust-to-Weight on Aircraft Weight.**

### *Limitations of Chosen Modeling Technique*

In general, the only computational tool available for this integration process is the 0-D or component-level code. The averaging process that must be accomplished to obtain component performance maps may smear the design improvements obtained by the more complex CFD process.

#### **2.1.2.2 Hardware in-the-Loop**

Real-time models (RTM) are models where the outputs of a transient performance computer program are generated at a rate commensurate with the response of the physical system it represents. RTMs are required for a range of applications. This synopsis attempts to summarize the real-time scene as described in detail in the reference document AIR4548 [2.8].

The following five (5) applications are summarized, and their requirements are examined in terms of 4 model attributes:

- Consistency – the model’s accuracy with respect to the reference database;
- Versatility – the adaptability of the model to fit new data, and its capacity to model over a wide range;
- Bandwidth – the range of frequencies for which the model is valid; and
- Execution rate – rate at which the model must execute to produce accurate and numerically stable results.

##### *2.1.2.2.1 Control Development Bench*

The non real-time controls development activity – based exclusively on the simulation of components – easily extends into the real-time arena when real hardware such as actuators and metering valves are used. This hardware may be of a generic nature or of a pre-production standard. Either way, early real-time HITL testing can help reduce the risk of new control technologies without placing an engine at risk.

The various bits of hardware are connected to various slave load generators (mechanical loads, pressures and temperatures) such that the operating environment of each component is reproduced. The ability to rapidly re-configure a rig (e.g. to replace a simulated component with a real one) is desirable.

There is always a trade-off between model accuracy (consistency) and execution rate. The latter is also linked to bandwidth, which for this application must encompass all the transient events that the controller can sense and control, and is driven by its own operating cycle rate.

#### *2.1.2.2.2 Integrated Flight and Propulsion Control Evaluation Tools*

In some aircraft systems, the flight and propulsion-control systems are integrated. Integrated system tests are required at several levels:

- Digital simulation – a non real-time simulation environment;
- Electronic bench – see above; and
- Iron bird – an extension of the above to include hardware-in-the-loop.

An example of the application of these development environments is in the design of the autoflight controls, particularly the auto-throttle.

#### *2.1.2.2.3 Embedded Engine Models*

Engine models can be embedded in an aircraft control-system, and can be used to improve the controllability of the aircraft through the predicted performance and response characteristics of the engine. The extent to which an engine model is exploited can vary – and so too the requirements in terms of all the standard criteria. A steady-state model may suffice in some applications; a dynamic model may be required in others.

#### *2.1.2.2.4 System Model Within Engine Control*

This is a subset of the above covering:

- Fault Detection – a model is used to generate expected values against which sensor outputs are compared. A check failure may result in reduced functionality or response; the modeled value being substituted for the failed sensor in some cases.
- Sensor and Parameter Synthesis – an extension of above. Derived parameters can be used in advanced control laws or be used to provide a better signal where measurement is difficult.
- Performance Tuning – using an appropriate model in combination with aircraft data such as angles of attack and sideslip, advanced control modes can be invoked to cash margins in return for performance.
- Trend Monitoring or Maintenance Aid – the state of the engine is monitored using on-line analysis. This provides data for maintenance crew and also can update the model used for control. Thus the advanced control modes are optimized to a particular engine.

Models supporting the functions above may have different forms (e.g. a deterioration trending model may be a detailed low bandwidth model executing a few times per flight, while a model used for performance searching may be of a different level of detail and bandwidth, running within the controller execution loop).

The trade-off between execution rate and accuracy is particularly important with embedded models. The hardware must be able to support the required integration time-step (to satisfy stability and output

## APPLICATIONS

---

criteria) with the modeling complexity required for the task. Otherwise, the control function will be degraded. Optimal consistency can be obtained by trimming models to the observed performance. It is fundamental that the model should be accurate enough to resolve the performance improvements being sought, and so the accuracy requirements for embedded models are usually more stringent than for bench testing.

### 2.1.2.2.5 *Engine and Control Models in Flight Simulators*

These fall into three general categories:

- **Engineering Development Simulators** – used for man in-the-loop studies to indicate overall general handling qualities, they can also be used in procedural studies for emergency scenarios.
- **Crew Training Simulators** – a refinement of the above used to train crew in the proper use of aircraft systems, using models to generate cockpit displays.
- **Maintenance Training Simulators** – an extension of the above to give training on the use of the increasingly sophisticated cockpit built-in-test-equipment and procedures.

Models in this group must interface with or include representations of associated systems such as air and oil systems. Cockpit indications such as vibration amplitude, and malfunction cues need also to be modeled. The transient modeling of such signals is important. The engine representation can be simple, perhaps with only thrust as an output to drive the aircraft dynamic model, although greater complexity may be required in some cases. Many simulators are for training in emergency procedures, in which case the engine performance representation may be secondary. The important functionality is in the aircraft system, and so the engine model must provide the appropriate inputs into these system models. In some cases these subsystems include ‘real’ control boxes which will reject any unrealistic inputs. This may place extra consistency requirements on the engine model. The need to model the simultaneous operation of up to four engines may present execution time challenges!

### ***Modeling Techniques Used***

The reference document outlines three methodologies, each of which has distinct advantages and disadvantages. The main aim of modeling is to provide a quality product, within cost, accuracy and execution speed constraints. The high level of interaction with users and hardware drives the first of these attributes. In setting any two of the remaining constraints, the third ‘comes in the wash’ – thus there is some compromise involved. Also, a common methodology throughout a project may be desirable, but not always achieved – the commonality may only exist at the source data level. The trade-off between the three constraints is discussed in the referenced document. The three methodologies covered are:

- **Aerothermodynamic** – This may be a cycle-match model that has been extended into transient operation by the inclusion of appropriate dynamic terms. Such models use iteration in the mathematical solution. Alternative forms of model exist, which are not rooted on steady-state synthesis and which are not iterative. Both forms represent the engine at component level and can include dynamic terms for heat capacitance of the metal components, shaft dynamics and gas dynamics. Operation outside of normal operating regimes can be modeled if component data (characteristics) are known. The level of aerothermal detail can be varied to suit the application and constraints, e.g. bleed systems may be simplified, or secondary effects removed.
- **Piecewise Linear** – These are also known as state-space models and consist of sets of matrices of partial derivative terms, which describe the engine’s operation about a series of base points. Interpolation between base points results in a model covering a specific power range. Clearly, more base points are required for greater accuracy and range. This impacts on storage and execution constraints. This sort of model can be used as an observer model by rearranging the calculations and using Kalman filtering (say) to trim the base points. The dynamic order of these models can vary:

some include only shaft dynamics; others include gas dynamics terms. The partial derivatives may be obtained by direct linearization of the full, non-linear, aerothermal model, or by employing system identification techniques to data obtained from engines which have been subjected to known (small) perturbations on input parameters.

- **Transfer Function** – As with state-space models, the engine is not represented at component level but in terms of overall engine response. The steady-state relationships are represented using exchange rates and curves which are derived using the full model, or from scaling or experimental data. The transient response between steady conditions is modeled using a system of leads and lags (transfer functions). The time constants are derived using terms from a state-space or full aerothermodynamic model.

### *Cited Example*

- Aerospace Information Report: AIR 4548: Real-Time Modeling Methods for Gas Turbine Engine Performance, Prepared by SAE S-15 Committee 1995. [2.8]

This document states in its foreword: ‘Current practices vary greatly in terminology and methods depending upon application. The document is intended to provide a vehicle for presentation of model types and definitions to be used as a basis for communication between customer and supplier. It is also intended to complement Aerospace Standard AS681 – Gas Turbine Engine Steady-State and Transient Performance Presentation for Digital Computer Programs, [2.9], and Aerospace Recommended Practice (ARP) 4148 – Gas Turbine Engine Real Time Performance Model Presentation for Digital Computers. [2.10]

### *Limitations of Chosen Modeling Technique*

There is much discussion in AIR4548 [2.8] of the relative merits of each modeling technique for each application – there is a whole section devoted to the selection of the appropriate methodology. However, there is a greater interest emerging in the use of aerothermodynamic methods for all modeling applications perhaps owing to the greater capacity of modern computers, and the drive towards multi-disciplinary interaction where the use of a common engine model is advantageous.

AIR 4548 states ‘...there are few, if any, limitations on aerothermal real-time models other than those imposed by the processor’. Iteration may be seen as an undesirable feature of a real-time model. However, as long as the iteration is controlled, and uses a robust and efficient method (e.g. multi-variable Newton-Raphson with bisection and Broyden update) real-time operation can be achieved by disallowing more than a fixed number of iteration passes per time-step. Piecewise linear models are easily scaled or adapted to match new sets of data, but are not easily adaptable to extremely non-linear processes. Transfer function models are compact but may be difficult to ‘tune’ in the dynamic sense owing to the lumping of the dynamic terms. They present no initialization problems because the steady-state conditions are explicitly defined.

There are some certification and safety issues arising from the real-time use of engine models in engine controllers. For example, reliance may be placed on the model to cash operating margins up to a critical point, or to indicate that deterioration has reached a critical level. Either way – any inaccuracy in the model can impact on the overall safety assessment. This is not so much a comment on the modeling technology, but on the application of engine models in general.

#### **2.1.2.3 Aircraft Simulation**

A representative engine model was required to run in real-time as part of an aircraft simulation. The aircraft, a modified F-18, featured thrust vectoring and flew as a research aircraft under the NASA

## APPLICATIONS

---

HARV (High Alpha Research Vehicle) program. This program was aimed at investigating the high angle-of-attack flight regime. The thrust vectoring enabled sustained flight at angles of attack (AOA) of up to  $70^\circ$ . 3 vanes per engine located in place of the divergent nozzle petals provided the multi-axis (axisymmetric) thrust vectoring.

The model was used for the development of control-laws associated with the extended flight regime and for real-time simulation (man and hardware in-the-loop testing) for evaluation of the modified control-system. The engine modeling is very simple but was considered adequate for its purpose. The model is a top-level representation of the thrust effect only. Components are not modeled. A few internal engine parameters are derived for use in the aircraft drag calculations.

An attempt had been made to make use of the full, iterative, component-level model supplied by the engine manufacturer (GE) but this more detailed model was found not to execute within the required timing criteria on the target processor. It required 4 ms per 20 ms, which was deemed unacceptable. The engine model was required to execute well within the flight control-system loop-execution rate. This became the primary drive towards a simpler model. The accuracy constraints on an alternative model were that it should perform within 5% of the steady state, and 25% of the transient response of the complete non-linear component-level dynamic model. The engine model had also to represent the effects of thrust vectoring in terms of the increased drag and loss of axial thrust.

### *Modeling Techniques Used*

The engine model was based on steady state relationships of various engine parameters tabulated against Altitude (ALT), flight Mach number (XM) and Power Lever Angle (PLA). These relationships were generated using the full model (which include the HARV thrust vectoring nozzle system) running at standard day conditions over the flight envelope.

Tables (vs. ALT, XM) generated were:

- Gross thrust (FG);
- Ram drag (Fram);
- Nozzle pressure ratio (NPR); and
- Convergent nozzle throat area ( $A_8$ ).

Tables at power levels (discrete PLA values):

- Flight idle (FI);
- Mil power (intermediate);
- Minimum afterburner (min AB); and
- Maximum afterburner (max AB).

The simple mode also included tables of the following, which were looked up with the parameters generated by the engine model section:

- Inlet spillage drag ( $D_{inl}$ ); and
- Nozzle aft-end drag increment ( $D_{noz}$ ).

The dynamic response of the engine was represented in the simple model by applying a variable response to the applied PLA shaping model. PLA input was converted to PLA' using a transfer function and rate-limiter, and tuned using the full model operating at the four corners of the flight envelope. PLA' was then applied to the look-up tables to generate dynamic behavior. Note that PLA is used as an input to the model. This means

that the engine control-system is also being characterized. The time-constants associated with a control-system are likely to be insignificant in terms of gross (long-range) engine thrust response.

### Cited Example

- Johnson, S.A., "A Simple Dynamic Engine Model for Use in a Real-Time Aircraft Simulation with Thrust Vectoring", NASA Technical Memorandum 4240, AIAA Paper # 90-2166. [2.11]

The overall model structure is shown in **Figure 2.8**. On examination of the response of the full model to changes in PLA, the judgment was made that the engine's dynamic response was approximately 1<sup>st</sup> order on the parameters of interest. Additionally the rate of response of the engine in afterburner mode was faster than in dry mode. Modulation in each case was by a different mechanism – spool speed change in dry mode, and nozzle area modulation in afterburner mode. Also, deceleration was faster than acceleration. (An engine might naturally exhibit this, but the response of the engine model to power-lever represents a controlled intent.)

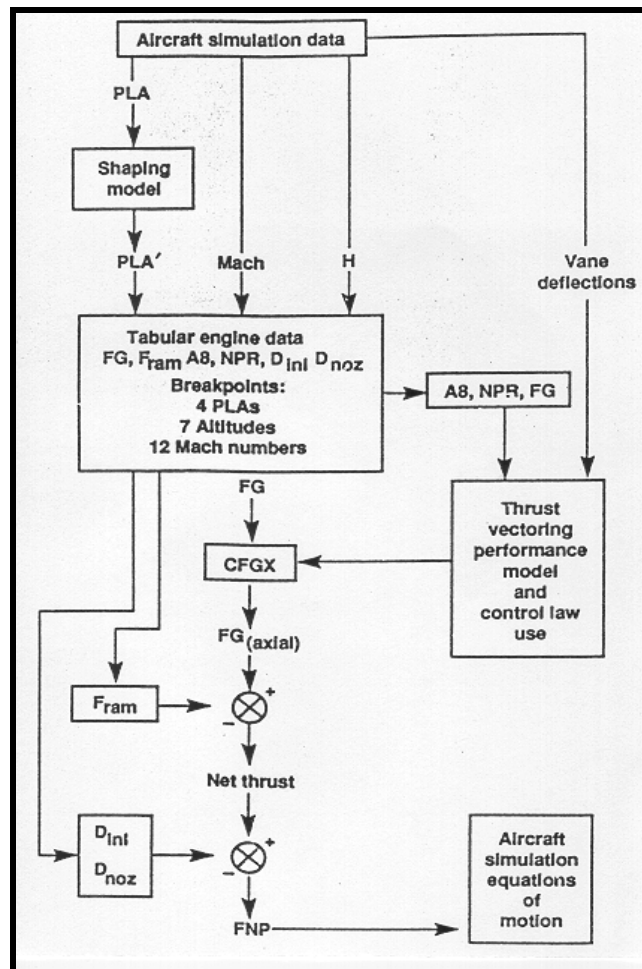


**Figure 2.8: Incorporation of the Simple Dynamic Engine Mode into the Thrust Vectoring Simulation.**

The approach described above was validated against the full model by applying similar PLA time histories, which cycled through the power range at various flight conditions typical for an aircraft with thrust vectoring. There is reasonable agreement between FG traces but the A8 and NPR terms do not line

## APPLICATIONS

up so well. This is due to the complex control laws used to control the nozzle (especially on reheat light up and shutdown).

**Figure 2.9** and **Figure 2.10** below show a time-based comparison between the full and simple models for the following PLA input profile: Flight Idle to Military Power to Maximum Afterburner back to Minimum Afterburner back to Flight Idle.

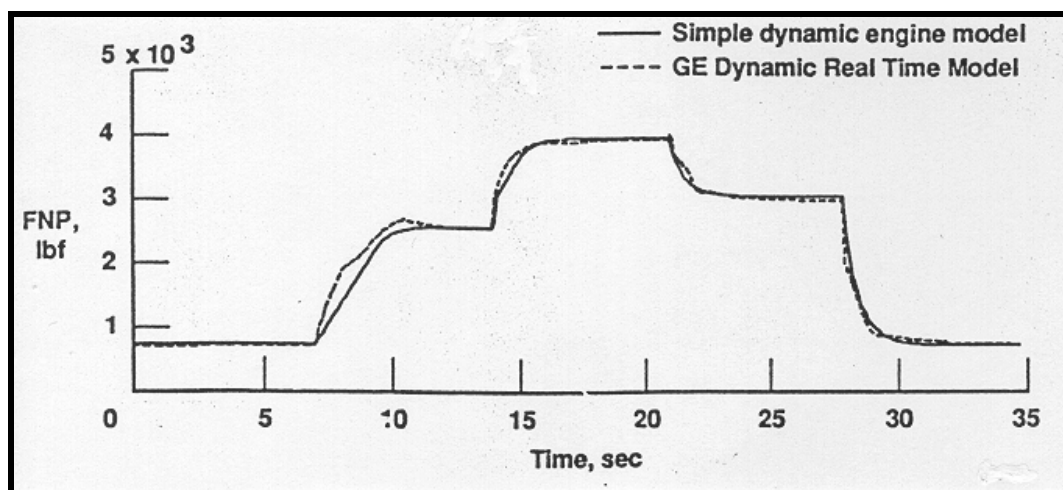


**Figure 2.9:** Comparison of Net Propulsive Force at 35,000 ft., Mach 0.2, no Vectoring.

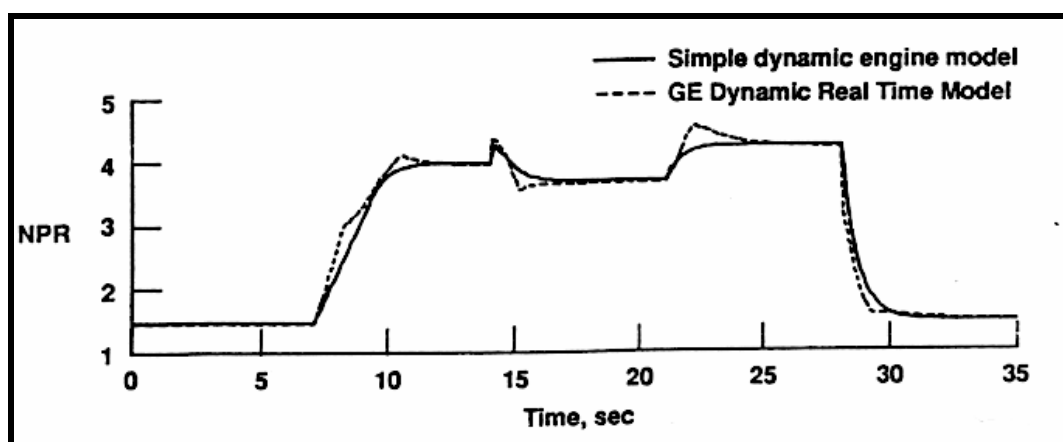


**Figure 2.10:** Comparison of Nozzle Pressure Ratio at 35,000 ft., Mach 0.2, no Vectoring.

The simple model took 0.3 ms per 20 ms to execute and was deemed acceptable for inclusion in the whole vehicle simulation. The reduction was achieved through no iteration, a reduction in code (FORTRAN in both cases) to 25% of the full model, and a similar reduction in storage memory requirement. The accuracy was inside the specification, with the steady-state being within 3%, and the transient agreeing within 20 – 25% of the full model.

### *Limitations of Chosen Modeling Technique*

This modeling technique (essentially a model of a model) can be used to great effect in the right application. However there are obvious shortcomings. A potential trap is to try to refine such a model to an extent where the advantages of simplicity are lost! Advantages of this type of model are:

- It's ease of tuning to represent gross behavior;
- It's mathematical robustness; and
- It's compact nature.

This was achieved at the expense of aerothermal detail – both steady state and dynamic.

The problem identified with the mismatch of A8 (and therefore NPR) terms is explained by the implied assumption that in dry operation, the A8 response is allied to the primary thrust modulation mechanism (shaft speed). This not necessarily the case as the nozzle is not a direct function of shaft speed. Thus, truer representations of internal parameters require regression back to component-level understanding. Also, there may be complications arising from the 'lumping' of the control-system behavior with the engine behavior. Some applications of this type of model may not require a control-system representation. In these cases, the model inputs would be the 'true' engine inputs (e.g. instantaneous fuel-flow and nozzle area). The dynamic representation would be constructed in a similar way by applying transfer functions to either the inputs or outputs (or both).

In situations where detailed dynamics are required, this method may not be most appropriate, and reversion to component-level representation may be essential. In these cases, measures must be taken to reduce execution time – either by reducing program size or extent of iteration, or by specifying a faster target processor.

#### **2.1.2.4 Installation Effects on Full Engine**

Gas turbine engine components such as compressors, combustors, and turbines are usually tested in rigs prior to installation into an engine. In the engine, the component behavior is different due to a variety of reasons. The installation effects are caused by small geometric differences due to non-representative rig operating temperatures and pressures, by different gas properties and Reynolds numbers, and by radial as well as circumferential temperature and pressure profiles at the inlet to the component. For highly accurate performance predictions, these rig-to-engine effects have to be taken into account.

Traditionally, the term, 'installation' has been also used for describing all the differences in engine operation and behavior between testbed and aircraft. Intake and after-body drag, power off-take and bleed, in-take pressure losses and inlet flow distortion all have significant impact on airflow, thrust, specific fuel consumption and compressor stability. Using modern performance synthesis programs all these effects can be simulated reasonably well.

#### ***Modeling Techniques Used***

A performance calculation computer program is sometimes also called a 'synthesis' program, because performance is synthesized from lots of ingredients. Those ingredients are the components of the engine such as compressors, turbines, burners, ducts, and nozzles. The behavior of the component is described by their characteristics. In case of a compressor, for example, the characteristic is the compressor map with pressure ratio plotted as a function of corrected airflow rate for several values of corrected speed. Efficiency contours can be plotted on the same map. In a simple synthesis program the component characteristics are used as calculated or measured on a rig without applying any corrections. That however, does not give very accurate results. To match such a model to measured data from an engine test adjustments to the rig data sometimes have to be made. Sometimes these adjustments are used either within the model or applied to the results with no physical justification. For accurate performance synthesis, one should make corrections to the component characteristics that take into account any difference between the in-engine operating conditions and the conditions for which the characteristic was originally set up.

### Potential Benefits

Engine manufacturers are mainly interested in the operating conditions of the engine components. During engine development there needs to be a mechanism to determine which component is responsible for performance shortfalls and how the components are matched. To predict the effects of a variety of installation effects, computer modeling will be used throughout an engine development program. Aircraft manufacturers are interested in the aircraft performance in terms of achievable turn rates, specific excess power, and mission fuel consumption. For that purpose they need computer programs which calculate installed engine performance.

### Cited Example

- Kurzke, J., "Calculation of Installation Effects Within Performance Computer Programs", AGARD Lecture Series, Steady and Transient Performance Prediction of Gas Turbine Engines, AGARD-LS-183, May 1992. [\[2.12\]](#)

For accurate performance synthesis one needs to make corrections to the component characteristics for any difference between the in-engine operation conditions and the conditions for which the characteristic originally was set up. The cited reference gives a complete summary of all rig-to-engine effects. The author shows how introducing those effects into the performance model should minimize the need for adjustments to component performance and thus provide the best performance synthesis model of an engine. The author discusses installation effects from a rig-to-engine component perspective then the integration of the components into the simulation where effects that cannot be attributed to a single component are described.

Under rig-to-engine differences there are differences due to geometric component differences. The author describes models for tip clearances, blade untwist, thermal expansion, bleed off-take, and cooling air injection. The effect of tip clearance on compressor characteristics as an example of a rig-to-engine difference is presented in [Figure 2.11](#).

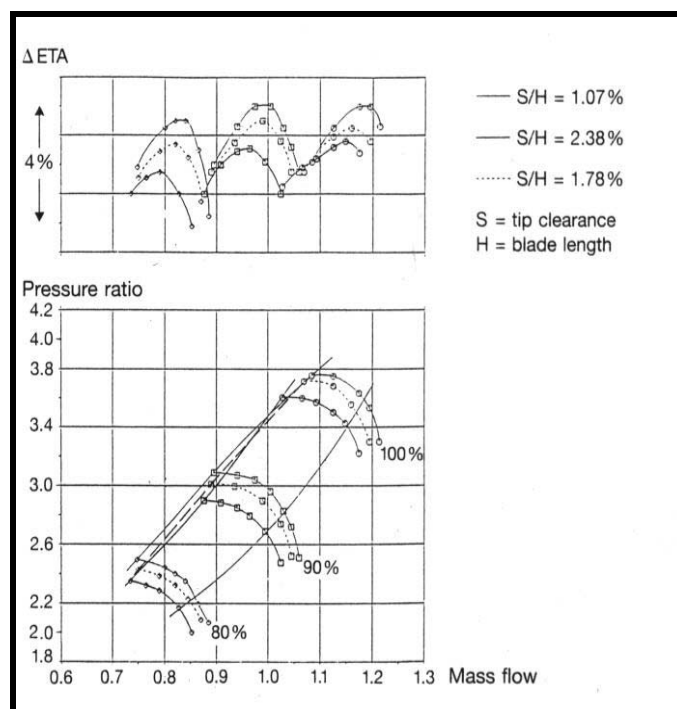


**Figure 2.11: Effects of Tip Clearance on Compressor Characteristics.**

In the second part of the cited reference, the author takes a look at those effects that cannot be attributed to a single component. Areas of concern are thrust-drag bookkeeping, power off-take, bleed effects, intake losses, flow distribution, and inlet flow distortion on stability and performance.

As an example of these types of effects, let's look at the effect of power off-take and bleed air. It is no problem at all to simulate the effect of power off-take within a performance synthesis program. One should be aware that taking off a fixed power can have quite different effects on the cycle. At high altitude flight conditions such as 50000 ft and Mach Number of 0.7, the power off-take is only 14% of the power available at sea level static conditions. Such a power off-take has a severe effect on the cycle: the operating point in the high-pressure compressor is moving towards a lower spool speed and in direction of the surge line, see **Figure 2.12**. While at sea level static conditions, the power off-take is limited by mechanical restrictions within the gearbox, at high altitude it is limited by the compressor stability limit. For calculations at high altitude the power consumption of the engine gearbox and the attached accessories need to be modeled in a better fashion than just with a constant mechanical efficiency of the high pressure spool.

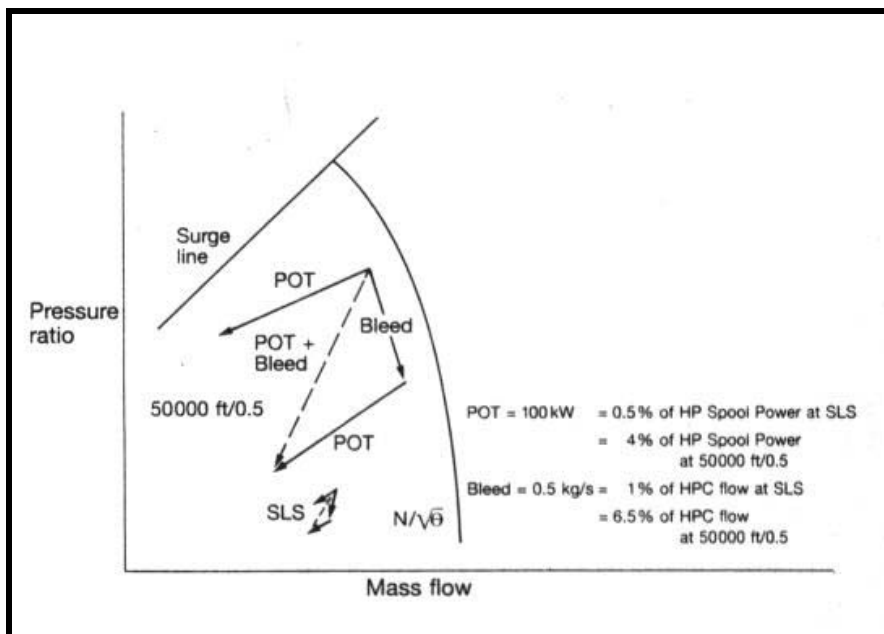


**Figure 2.12: Power Off-Take and Bleed Effects on HPC Operating Points at Sea Level and at Altitude.**

Bleed air used for aircraft cabin pressurization alleviates the compressor stability problem, but weakens the cycle. Again, the bleed air requirements in terms of mass flow rate are fairly independent of flight condition. However, the effect of bleed air is much more severe at altitude. Illustrated in **Figure 2.12**, is the impact of both power off-take and bleed air on the high-pressure compressor map for both sea level and altitude. The absolute amount of bleed air and power off-take is the same for both flight conditions. Bleed air pressure and temperature are important for the aircraft designers. There are both maximum and minimum limits for the pressure and sometimes there is also a not-to-exceed bleed air temperature.

On a modern civil engine it can be necessary to have two customer bleed air off-takes which are switchable. At idle compressor exit bleed is used, and at max climb rating an inter-stage bleed port is used. Bleed air conditions at aircraft and engine interfaces have to be calculated with sufficient care. The local pressure – where the air is taken off – is dependent on the specific design; it is seldom the total pressure. The pressure losses within the bleed manifold and pipe system are very much mass flow dependent.

***Limitations of Chosen Modeling Technique***

The major limitation of this modeling approach is the reliance upon component maps. These maps must be generated in advance, in order to try to predict performance. For the design process, these maps must be somewhat generic and based upon previous experience. However, once a set of performance characteristics is available, predictions can be tuned via some of the mechanisms discussed in the cited reference to improve the model's accuracy.

**2.1.2.5 Statistical Analysis**

Gas turbine performance models are normally used in a straightforward manner. Unambiguous direct questions about the operating conditions, intended engine modifications, modified control schedules, etc. yield equally unambiguous answers. However, the data from a single engine cycle are sometimes not sufficient because the statistical distribution of a parameter is also needed.

When some input data for a cycle performance model are statistically distributed, the calculated parameters will also be statistically distributed. The correlation between the standard deviation of the input parameters with those of the results can be calculated with the widely used 'root-sum-squared' approach, which uses influence factors for the correlation between the input and the result. This procedure implies that the influence factors are all statistically independent from each other. In practice this is not always the case, especially when control system interactions must be taken into account.

An alternative to the 'root-sum-squared' approach is the Monte Carlo method. This method works such that random numbers with prescribed statistical distributions are generated and fed into a mathematical model of arbitrary complexity. The statistical distribution of the calculated parameters is then analyzed, and the statistical outputs form the result of the Monte Carlo simulation.

***Modeling Techniques Used***

For the analysis of the measurement uncertainty of a gas turbine performance test, for example, one needs a thermodynamic cycle program. Depending on the question to be answered, one needs a simple cycle design program or a full off-design simulation including some aspects of the control system.

The input into the program must offer the option to generate random numbers with a prescribed statistical distribution. It is an advantage when the performance program can also analyze statistically the computed results. However, the statistical analysis can also be done as a post-processing task, with any other suitable tool.

Many of the input data are statistically independent of each other, but some are not. For example, when the series production of compressors is being simulated, there is a correlation between the efficiency and the flow capacity, which should be taken into account when producing random numbers for these two model input quantities.

***Potential Benefits***

The Monte Carlo method can handle simulation models of arbitrary complexity. It will automatically take into account all interactions between the input parameters and the calculated results correctly. Contrarily, the 'root-sum-squared' approach assumes that all influence factors are independent of each other, and this is not always true. For example, the control system interacts in a very complex manner with the individual engines of a series.

***Cited Example***

- Kurzke, J., “Some Applications of the Monte Carlo Method to Gas Turbine Performance Simulations”, ASME Paper # 97-GT-48, Presented at the ASME International Gas Turbine Institute’s Turbo Expo, Orlando, FL, June 1997. [\[2.13\]](#)

Engine tests are performed to evaluate the overall characteristics in terms of thrust and specific fuel consumption. However, during the development phase the main purpose of performance testing is to find the efficiency of the engine components. The analysis result has a tolerance, which is affected by both random and systematic measurement errors. This tolerance can be found with the help of the Monte Carlo method as will be shown for the example of an unmixed flow turbofan.

**Random Errors** – When a measurement is repeated several times, the instrument readings will not agree exactly but will show some scatter. In gas turbine tests this scatter is caused not only by random effects in the measurement chain, but also by small changes in engine geometry and operating conditions. A running engine is never absolutely stable because of small changes in inlet flow conditions, variable geometry settings, thermal expansion of casings and disks, etc. The unintended (and undetectable) changes to the engine during re-assembly for a back-to-back test can also be regarded as random errors of an experiment.

Obviously the magnitudes of these errors have an effect on the confidence interval for the test analysis result. Compressor efficiency, for example, is calculated from the four measurements of inlet and exit total temperature and pressure. How should the individual measurement precision errors be propagated to an efficiency confidence interval? Abernethy describes some alternative solutions to the problem, and reports that the recommended method has been checked with Monte Carlo simulations. This recommendation implies that a Monte Carlo simulation is superior to other methods.

**Systematic Errors** – In a carefully controlled engine performance test the random errors mentioned above are not negligible, but are smaller than the systematic errors caused, for example, by incorrect positioning of the probes. There is seldom space in an engine to put enough pressure and temperature pickups at the component interface plane. Although every effort is made to correct the measurements for all known effects, an uncertainty remains.

The difference between the measurement (after applying all known corrections) and the true mean value is called a bias. There is no data available to calculate the magnitude of the bias and therefore it is usually estimated from experience with component rigs. For example, Abernethy discusses the problem in some detail and concludes that bias limits should be root-sum-squared when the confidence interval must be estimated for a quantity that is calculated from several individual measurements.

Using the root-sum-squared approach for estimating confidence intervals implies that the bias of every element to be combined in the sum has a normal distribution. Both normal and non-normal bias errors can be simulated with the Monte Carlo method.

**Engine Simulation** – During an engine performance test all temperatures and pressures on the cold side of the engine (stations 2, 13, 25 and 3, see [Figure 2.13](#)) are measured. Furthermore, fan mass flow and fuel flow, and inlet and exit total pressures of the low-pressure turbine are normally available for test analysis. Temperatures that are eventually measured around the low-pressure turbine are not used in the analysis because the severe gradients, both circumferentially and radially, make the mean value rather inaccurate. For the cycle program one needs as additional input data, the internal air system and mechanical losses, which must be estimated or analyzed separately from detailed measurements.

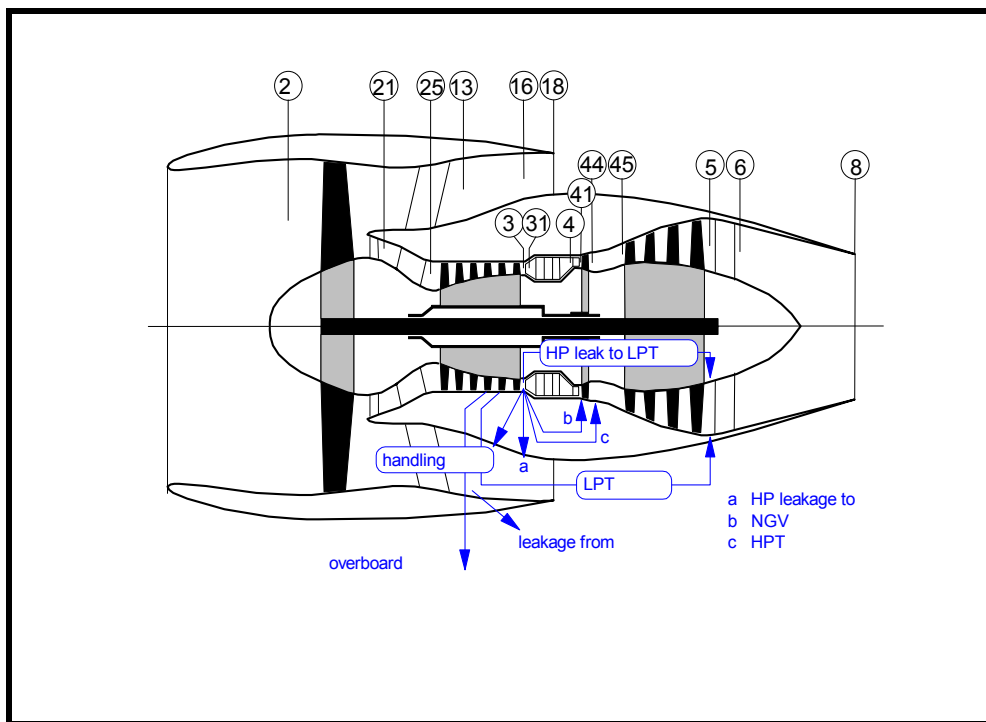


**Figure 2.13: Engine Station Numbering Nomenclature.**

From the pressures and temperatures on the cold side of the engine all compressor efficiencies can be derived. For the analysis of the turbine efficiencies one needs to know the turbine shaft power. The power balance with the compressors yields that information when the bypass ratio is known.

**Core Flow Analysis** – In the test analysis process one can find the bypass ratio in several ways by iteration. For example, one can calculate the bypass ratio in such a way that the continuity at the bypass nozzle exit is fulfilled. Such an analysis method needs the exact dimension of the bypass nozzle area  $A_{18}$  and the nozzle discharge coefficient.

Often the high-pressure turbine nozzle-guide-vane throat area is known more precisely than the effective bypass nozzle area and is therefore used as a basis for the core flow analysis. However, this method requires a good knowledge of the secondary air system, because the amount of air that bypasses the turbine throat influences the result found for the bypass ratio.

As input data for the Monte Carlo simulation the standard deviations  $\sigma$  of the individual measurements is needed. Those data complemented by assumptions for the engine internal measurements are used here for the simulation of tests on a sea-level testbed (**Table 2.2**).

**Table 2.2: Measurement Repeatability**

Parameter	Symbol	Std Deviation [%]
Inlet Pressure	P2	0.1
Inlet Temperature	T2	0.1
Fan Exit Pressure (Core)	P21	0.2
Fan Exit Pressure (Core)	P21	0.2
Fan Exit Temperature (Core)	T21	0.2
Fan Exit Pressure (Bypass)	P13	0.15
Fan Exit Temperature (Bypass)	T13	0.15
HP Compressor Exit Pressure	P3	0.2
HP Compressor Exit Temperature	T3	0.2
Fan Mass Flow	W2	0.4
Fuel Flow	WF	0.7
HP Turbine Exit Pressure	P45	0.2
LP Turbine Exit Pressure	P5	0.2

Two engines with bypass ratios of 4 and 7 respectively have been simulated. The pressure ratios of the booster and the high-pressure compressor were assumed to be the same ( $P_{21}/P_2 = 2.5$  and  $P_3/P_{25} = 12$ ) for both engines. However, the fan pressure ratios are necessarily different ( $P_{13}/P_2 = 1.84$  for bypass ratio 4 and  $P_{13}/P_2 = 1.49$  for bypass ratio 7). All the other details like the burner exit temperature and the component efficiencies are also the same for both cycles and at typical levels for modern high bypass engines.

In the Monte Carlo simulations a scatter for the parameters listed in **Table 2.3** is produced in such a way that they are normally distributed with the prescribed standard deviation,  $\sigma$ . The random numbers generated for each quantity are independent from each other in this example. When the random number generator produces a value outside of the range  $\pm 2 \sigma$  then this value is discarded. In one pass of the simulation up to 441 cycles are evaluated. A typical output chart is shown in **Figure 2.14**. The standard deviation for the component efficiencies found by the Monte Carlo simulation is shown in **Table 2.2**. It is obvious, that the measurement tolerances from **Table 2.3** do not yield acceptable accuracy for the efficiency of the fan and the low-pressure turbine when the bypass ratio is high.

**Table 2.3: Standard Deviation for Component Efficiencies**

Component	Bypass Ratio 4	Bypass Ratio 7
Fan	0.80%	1.40%
Booster	0.82%	0.82%
High Pressure Compressor	0.50%	0.50%
High Pressure Turbine	0.52%	0.52%
Low Pressure Turbine	0.82%	1.19%

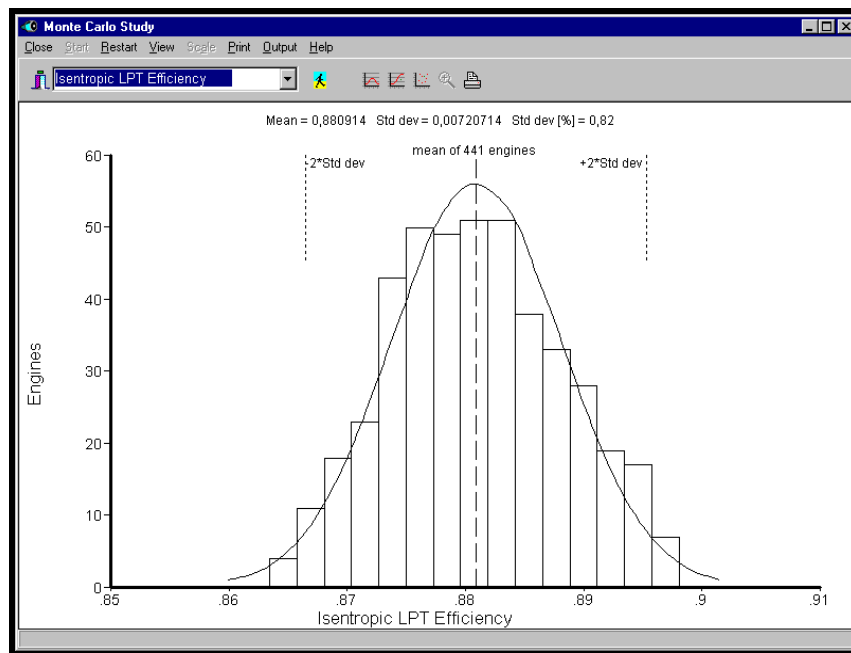


**Figure 2.14: Monte Carlo Study Result.**

### ***Limitations of Chosen Modeling Technique***

For the input into a Monte Carlo simulation one needs the standard deviation, which may be difficult to acquire for some quantities. Moreover, not all quantities necessarily follow a standard distribution. However, there is no basic problem with feeding a performance simulation code with non-standard distributed data. The use of the Monte Carlo method should be preferred to the traditional 'root-sum-square' approach because it automatically takes arbitrarily complex interactions between the parameters of the problem into account.

### **2.1.3 System Design and Development Synoptics**

A primary objective of System Design and Development (SDD) is to home in on the most promising design approach and begin to evaluate a preliminary design configuration with regard to its performance, operability, and maintainability through the test and evaluation process (T&E). Much of the T&E mission is centered on enhancing test analysis capability in order to conduct turbine engine tests more efficiently. Many of the test objectives conducted in any turbine engine development program are concerned with stable and safe engine operation.

Because of the mission of military aircraft, the propulsion system must operate in a harsh environment such as severe inlet dynamic pressure and temperature distortion. To address the operation in these harsh environments, the T&E process requires the application of a variety of test resources as well as analytical and computational tools. Testing for airframe-propulsion integration, and in particular inlet-engine compatibility, generally requires complementary component tests conducted in wind tunnels and engine altitude facilities.

Through the use of modeling and simulation technology, coupled with the baseline information provided by current wind tunnel and test cell test procedures, a fusion of computational and experimental data can be accomplished. This will make more information available to the design engineer for system development and risk reduction. Such an approach is key to the successful understanding of high performance engine

phenomena such as High Cycle Fatigue (HCF), and inlet and integration issues associated with tomorrow's highly integrated flight systems.

The use of modeling and simulation in conjunction with test information results provides the following capabilities to the T&E community:

- Enhanced aircraft inlet and turbine engine capability for integrated test and evaluation on military weapon system tests.
- Improved ground test operational efficiency by providing accurate pre-test predictions and post-test analysis to support pre-and post-test decisions and optimize test matrix.
- Enables correlation of isolated inlet and engine simulated ground test results to provide a pre-flight release assessment of integrated airframe and engine performance in a dynamic flight test environment.
- Provides affordable or reduced test costs through improved planning, optimizing test matrix, and smarter test analyses and decisions.
- Improves knowledge-based IT&E applications to provide integrated aircraft in-flight performance assessments.

#### **2.1.3.1 Performance**

One of the first requirements for an engine program is to predict the performance of the engine over the full range of conditions from take-off to a variety of flight regimes such as low altitude penetration, high altitude cruise and combat maneuvering with maximum afterburning. This requires sophisticated modeling which can be done with a high level of confidence before the engine has run; both design point and off-design-point performance must be accurately predicted. This must be done before any component testing has been carried out and the component performance changes between test rigs and actual engine operation will be discussed.

##### *2.1.3.1.1 Steady State Performance*

Engines are steadily becoming more complex, as the need to improve aircraft performance drives the engine designer to improve engine performance. Variable stator compressors, for many years found only on GE engines, are now used on virtually all high performance engines to cope with steadily rising pressure ratios. Blow-off valves are frequently used on starting or when operating at low power. Variable final nozzles are becoming more sophisticated, with the first variable convergent-divergent nozzle introduced on the Olympus 593 for the Concorde aircraft. Variable geometry turbines have not yet been introduced in aeroengines, but have been used for some years in industrial engines for performance improvement at part load.

Future military, and probably civil, engines will introduce variable cycle technology. As an example, to minimize noise a future supersonic transport engine will need to operate at a high by-pass ratio and low jet velocity at take-off; while for efficient supersonic cruise, it will need to operate with a very low by-pass ratio and high jet velocity. The evaluation of all of these new technologies requires an increasing use of mathematical models at not only the design stage, but throughout the development phase as well. Many initially promising schemes may turn out to be impractical, but considerable human effort and machine computation may be required to provide the information to support or abandon a new concept.

#### ***Modeling Techniques Used***

Nearly all steady state performance modeling is accomplished using a component level simulation. Two excellent component level models are described in the following paragraphs.

## APPLICATIONS

---

**GASTURB** is a PC program developed by Kurkze. It is user friendly and easy to use for the analysis of the thermodynamics of gas turbines. It covers all-important aspects of engine design cycle selection, off-design behavior, test analysis and monitoring, and engine stability and transient operation. The number of input data required is limited to the important items. Real compressor and turbine maps are used to yield representative results. For off-design calculations, iterative methods with up to twenty (20) variables are implemented. The user, however, is not confronted with the difficult task of setting up the iteration. The program simulates the most common types of aeroengines, including single and two-spool turboshafts, turboprops, turbojets, and turbofans. Both mixed and unmixed flow engines can be simulated. Afterburners and convergent-divergent nozzles are available for mixed flow turbofans and turbojets. In the latest version of the program, even a variable cycle engine and an intercooled, recuperated three-spool turbofan are included.

**GSP** or '*Gas Turbine Simulation Program*' is a component-based modeling environment for gas turbines. GSP's flexible object-oriented architecture allows steady-state and transient simulation of any gas turbine configuration using a user friendly drag and drop interface with on-line help, running under Windows 95/98/NT/ME/2000/XP. GSP has been used for a variety of tasks such as various types of off-design performance analysis, emission calculations, control system design, and diagnostics of both aircraft and industrial gas turbines. More advanced applications of GSP include analysis of recuperated turboshaft engine performance, lift-fan STOVL propulsion systems, control logic validation and analysis of thermal load calculation for hot section life consumption modeling.

### *Potential Benefits*

The two programs described above provide an ease of use to the user that makes any analysis task easier. These programs are ideally suited for basic studies and for getting a fundamental understanding of the principles underlying the design and operation of gas turbines. They are suited to both professional applications in the gas turbine industry and to the student in an educational setting. The flexibility built within the codes will provide ease of adaptation to future applications such as performance analysis of complex recuperated intercooled cycles, multi-stage combustion, detailed simulation of STOVL propulsion systems and tilt-rotor propulsion system simulation.

### *Cited Example*

- Kurkze, J., "Advanced User-Friendly Gas Turbine Performance Calculations on a Personal Computer", ASME Paper # 95-GT-147, June 1995. [2.14]
- Visser, W.P.J. and Broomhead, M.J., "GSP, A Generic Object-Oriented Gas Turbine Simulation Environment", ASME Paper # 2000-GT-0002, May 2000. [2.15]

Using the simulation by Kurkze, steady state performance can be obtained for a variety of configurations. One such configuration cited in the reference was a turbojet and the matching of components. The calculation of each off-design point requires iteration. Several input variables for the thermodynamic cycle must be estimated. The number of variables is calculated as follows. The result of each pass through the cycle calculation is a set of errors. Inconsistencies are introduced through the use of imperfect estimates for the variables. The number of errors equals the number of variables. A Newton Raphson Iteration scheme is used to drive the errors to zero. One way that off-design information can be presented is by plotting lines of constant mechanical speed on an altitude-Mach number flight envelope as illustrated in **Figure 2.15**.

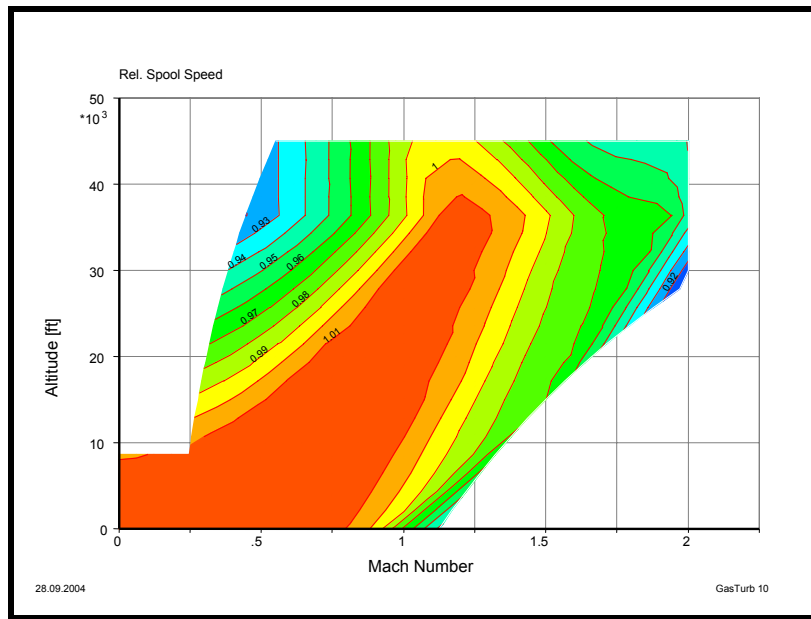


**Figure 2.15: Lines of Constant Spool Speed Overlaid on the Altitude Mach Number Envelope.**

A relatively simple example of using GSP is the analysis of off-design performance of a typical high-bypass turbofan engine. The GSP demo model, BIGFAN is depicted in **Figure 2.16**. Generic component maps were used and then scaled to the BIGFAN design point. The code can calculate sea level take-off performance at varying ambient temperatures and compressor bleed flows. This was accomplished by the calculation of steady-state points at a series of different ambient temperatures, with the engine running at either maximum total turbine inlet temperature,  $Tt4$  (or TIT) or maximum burner pressure  $Ps3$  (i.e. a flat rated engine).

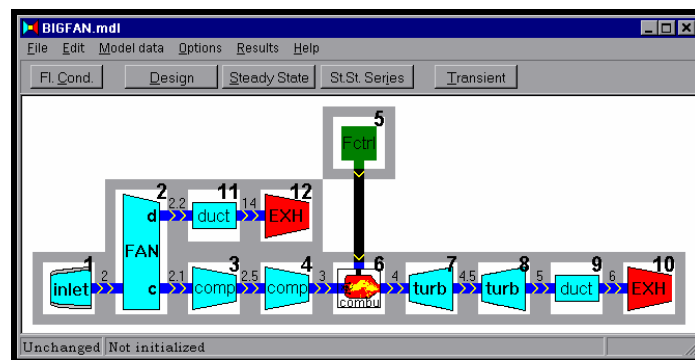


**Figure 2.16: GSP Model Window with Simple Turbofan Model.**

A flat rated temperature (FRT) was assumed, in which the engine is at both maximum  $Tt4$  and maximum  $Ps3$  for an inlet temperature of 288 K. The procedure calls for the calculation of a design point, with a  $Tt4$  of 155 K. An ambient temperature parameter sweep from 280 K up to 320 K was then performed, while maintaining the  $Tt4$  at 1554 K. The parameter sweep was performed both for no-bleed and for 5% compressor bleed. The results in **Figure 2.17** show the typical turbofan trends for fan speed  $N1$ , compressor speed  $N2$ , engine pressure ratio EPR, and net thrust  $FN$ , used for specifying take-off performance at temperatures above FRT.

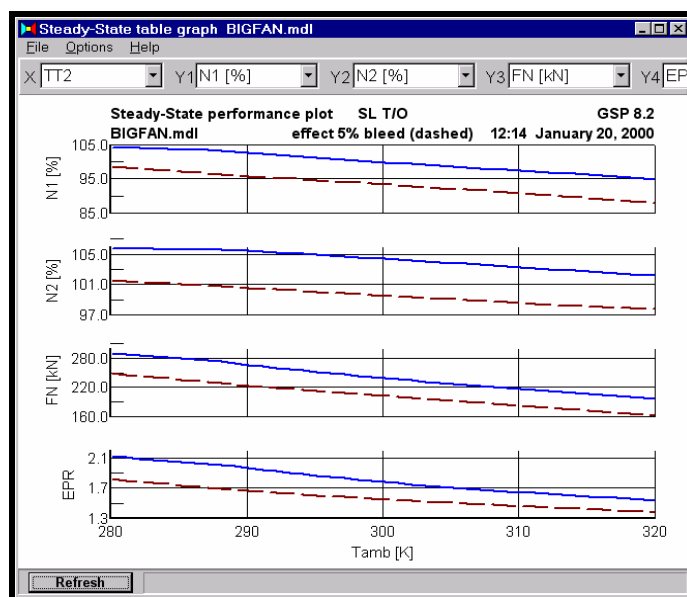


**Figure 2.17: Effect of Compressor Bleed on Take-Off Performance.**

## Limitations of Chosen Modeling Technique

Both the models cited are component level models and as such require component performance maps. Much of the labor-intensive process for providing input and getting output has been minimized through the use of user-friendly graphical interfaces. Compressor and turbine maps within GSP are compatible with the GasTurb map format. This allows the use of the SmoothC and SmoothT program utilities for editing and smoothing maps.

### 2.1.3.1.2 Transient Behavior

Successful and quick starting of turbine engines is essential for safe operation of an aircraft and the activation of auxiliary power systems for ground use. A simulation of the starting process can provide valuable information such as the torque required to accelerate to and away from self sustaining speeds, and the time required to start over a wide variety of starting conditions. In addition, a component-level aerothermodynamic simulation of the starting process can provide:

- An indication of compression system stall-margin and turbine temperature-margin during an engine start; and
- An indication of the ability of the engine control to execute and monitor a successful engine start.

## Modeling Techniques Used

An existing engine simulation technique, AEDC Turbine Engine Simulation Technique (ATEST), was selected as a basis for providing an engine starting simulation because of its overall capabilities. The ATEST program provides a one-dimensional component-level transient simulation (0 to 20-Hz frequency response) applicable to arbitrary engine configurations as illustrated in **Figure 2.18**. The ATEST program is also capable of simulating off-running line engine operations and utilizes widely accepted component-matching principles. The ATEST program includes the effects of rotor dynamics, volume dynamics, and heat transfer, and it is capable of accepting an engine control simulation as an additional program module.

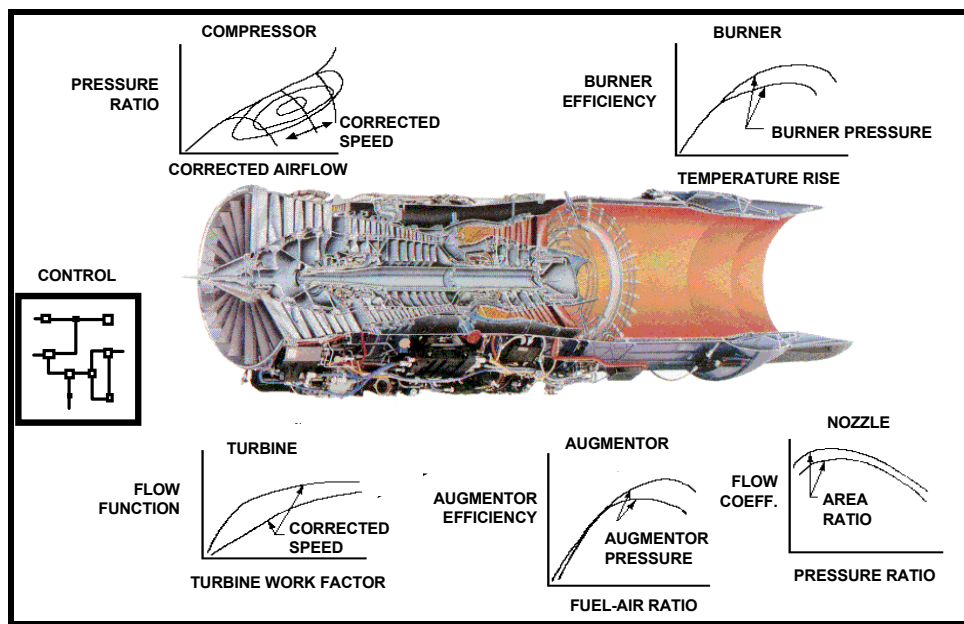


**Figure 2.18: ATEST Component Level Modeling Approach.**

Fundamentally, engine windmilling is a steady-state process and engine starting is a transient process subject to the same aerothermodynamic principles as above-idle engine operation. The original ATEST program provided the capability of simulating normal above-idle engine steady state and transient operations. An expansion of ATEST to include the simulation of engine starting and unfired (no combustion) windmilling processes provides the ability to simulate continuous engine operation from startup to maximum power to shutdown with a single tool.

### **Potential Benefits**

ATEST provides the means to quantitatively understand the following, during the engine start process:

- The combined effects of operating line excursions;
- Turbine temperature fluctuations;
- Engine control operation;
- Component interactions; and
- Power and air extraction effects.

ATEST can be used for arbitrary engine configurations and can simulate turbine engine operation continuously from startup to shutdown. The approach expands widely accepted component-matching principles to simulate sub-idle, windmill, and engine-starting operations and preserves the existing one-dimensional steady state and transient capabilities and simulation accuracy for above-idle operations.

ATEST was validated using test data for:

- Steady state windmilling operation;
- Windmill starts;
- Spool-down starts; and
- Starter-assisted starts.

## APPLICATIONS

The processes required to characterize gas turbine engine starting, and to predict the boundary between starter-assisted and windmill starts, prescribed by the engine manufacturer's performance specification, were successfully simulated.

### Cited Example

- Chappell, M.A. and McLaughlin, P.W., "Approach to Modeling Continuous Turbine Engine Operation from Startup to Shutdown", *Journal of Propulsion and Power*, Vol. 9, Number 3, May-June 1994, pp. 466-471. [2.16]

A generalized approach, to modeling gas turbine engine operation continuously from startup to shutdown, for arbitrary engine configurations, is described in this article. The approach preserves existing steady state and transient capabilities, and simulation accuracy for above-idle operations. This article will focus on the approach used in applying conventional component-matching simulation principles to the starting process. The approach is applied to a military flight-type two-spool after-burning turbofan engine, and simulation results are compared to engine test data.

The ATEST model was applied to a military-type two-spool after-burning turbofan engine and included a simulation of the engine control. Model results were obtained by prescribing throttle position as a function of time, and prescribing flight conditions in terms of altitude and Mach number. Model results were compared to engine test data for steady state windmill operation and windmill, starter-assisted, and spool-down starts.

The ATEST model results were compared to engine test data to evaluate the ability of the model to simulate engine-starting phenomena as illustrated in **Figure 2.19**. The more important aspect of the evaluation was the ability of the model to reproduce the general shape of time-varying performance, including the existence of inflections, breakpoints, and overshoots. The comparison of absolute levels of performance was evaluated, but was less important in demonstrating the capability of simulating fundamental engine start processes.

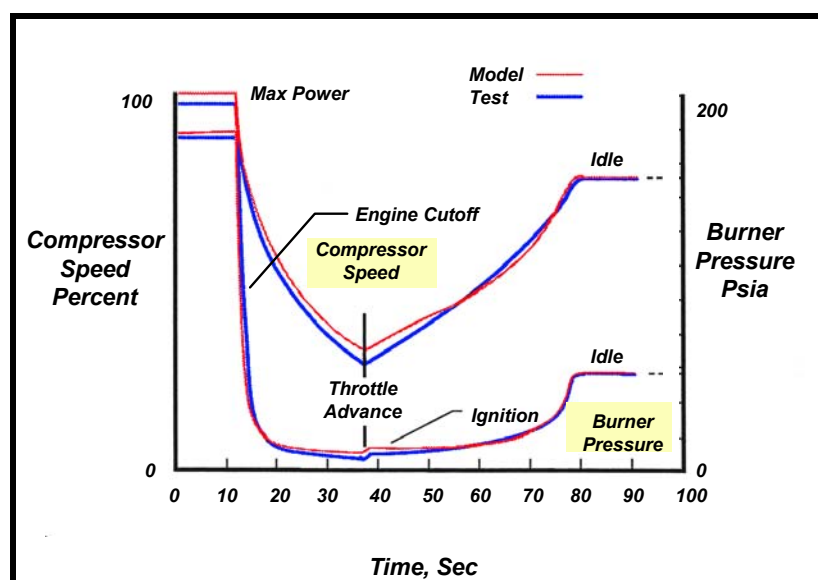


**Figure 2.19:** ATEST Typical Engine Cut-Off and Re-light Comparison.

Expanding the component models attained the level of agreement illustrated. Further improvements to the level of agreement would result from revision of the control system simulation to match control system

revisions specific to the tested engine, and the inclusion of off-schedule geometry effects on component performance.

### ***Limitations of Chosen Modeling Technique***

The simulation of combustor ignition and blowout is a key area of modeling continuous engine operation from startup to shutdown. Combustor ignition is a complex phenomenon and is not well understood in the industry. Simple one-dimensional correlations that form ignition boundaries are highly empirical and unique to specific combustor configurations. Additional development is required in this key area to provide a more accurate determination of combustor ignition characteristics.

The ATEST model described in this article is capable of simulating windmilling speeds to less than 10 rpm. However, a simulated start from static conditions (absolute zero speed) is complicated by the indeterminate nature of the relationship between torque and power when speed approaches zero. It is expected that the simulation of engine operations at zero and near zero speeds can be attained by representing component performance in terms of torque, which is a form of specific power, rather than temperature ratio.

#### ***2.1.3.1.3 Model Based Diagnostic Test Support***

Turbine engine testing is conducted to evaluate engine operation at a wide variety of simulated altitude conditions. Hundreds of sensors, each producing measurements at rates in excess of one hundred samples per second, are typically installed in the engine and test facility to measure aerothermodynamic performance. Consequently, a typical 8-hour test can produce 30 million samples of aerothermodynamic performance data. The challenge is to ensure the validity of the data, monitor the condition of the engine, and to promptly identify anomalies.

The countless variations in steady-state and transient engine operation and the necessity to delineate between sensor anomalies and abnormal engine deterioration, combined with the large volume of data, overwhelms the capabilities of traditional data validation methods. Although traditional methods produce meaningful results, they are labor-intensive and time-consuming. Consequently, application of the methods is typically restricted to a fraction of the available data, which diminishes the ability to detect anomalous data and intermittent events. An automated approach that emulates the traditional data validation and engine condition monitoring processes is needed to ensure a comprehensive assessment. Nonlinear component-matching engine models embody the physical relationships employed in the data validation and engine condition monitoring processes and can provide a basis for automating them. However, in order to provide a sound basis, the models must accurately represent the test engine.

A fault identification approach is described. The approach relies on an automated real-time model calibration technique and emulates traditional fault identification processes. The technique focuses on single faults as each occurs rather than on the estimation of an optimal combination of all possible faults (AGARD-CP-448). The approach is adaptable to changes encountered in developmental turbine engine testing and relies on a basic component-matching model that represents the engine cycle (e.g., turbofan, turboshaft, and turbojet). Industry-accepted engine modeling practices are combined with advanced fault diagnostic algorithms and parallel computer techniques to provide real-time fault identification including data validation and engine condition monitoring for steady state and transient engine operation.

### ***Modeling Techniques Used***

To be effective, gas path analysis tools must identify component performance deviations and measurement errors. The model-based fault identification process consists of two main phases. The first phase of the fault identification process relies on a real-time model-based evaluation of test data to detect a probable fault resulting from:

## APPLICATIONS

---

- Measurement errors;
- Engine component events; and
- A combination of the two.

After a fault is detected, automated model simulation studies are performed to diagnose the most probable cause of the fault in near-real time. This detailed diagnostic information allows the analysis engineer to assess the relative probability of the fault and, in most cases, quickly identify and verify the actual cause of the fault. If necessary, additional test data may be acquired from previously tested stabilized engine operating conditions to increase the fidelity of the diagnosis.

A component-level model (CLM), capable of simulating steady state and transient engine operation, serves as the basis for the fault identification process. The CLM combines the physical relationships that govern engine operation with empirical relationships that describe individual component performance. The result is an adaptable model in which the effects of changes to engine attributes, such as components, configuration, and controls, are incorporated by making corresponding changes to the model attributes. Additionally, the component matching approach quantifies the changes to engine performance inter-relationships, which provides a prediction capability for the fault identification process.

### *Potential Benefits*

Hundreds of individual sensors produce an enormous amount of data during developmental turbine engine testing. The challenge is to ensure the validity of the data and to identify data and engine anomalies in a timely manner. An automated data validation, engine condition monitoring, and fault identification process that emulates typical engineering techniques has been developed for developmental engine testing. The result is an ability to detect data and engine anomalies in real-time during developmental engine testing. The approach is shown to be successful in detecting and identifying sensor anomalies as they occur and distinguishing these anomalies from variations in component and overall engine aerothermodynamic performance.

### *Cited Example*

- Malloy, D.J., Chappell, M.A. and Biegl, C., “Real-Time Fault Identification for Development Turbine Engine Testing”, ASME Paper # 97-GT-141, Presented at ASME International Gas Turbine Institute’s Turbo Expo, Orlando, FL, June 1997. [\[2.17\]](#)

A new capability for real-time fault identification during developmental turbine engine testing has been developed and demonstrated. A schematic of the overall process is presented in [Figure 2.20](#). The capability automates a model calibration process and emulates traditional manual approaches. A parallel computing approach permits real-time operation of the processes. The model-based fault identification approach was demonstrated on steady state and transient test data, successfully detecting and identifying anomalous measurements and distinguishing these from unusual variations in component and overall engine performance. A component-level model provided the basis for fault identification and an automated model calibration process ensured adequate model fidelity. In addition, the component-level model enables automation of fault detection and diagnostic techniques that generally rely on engine cycle-matching principles.

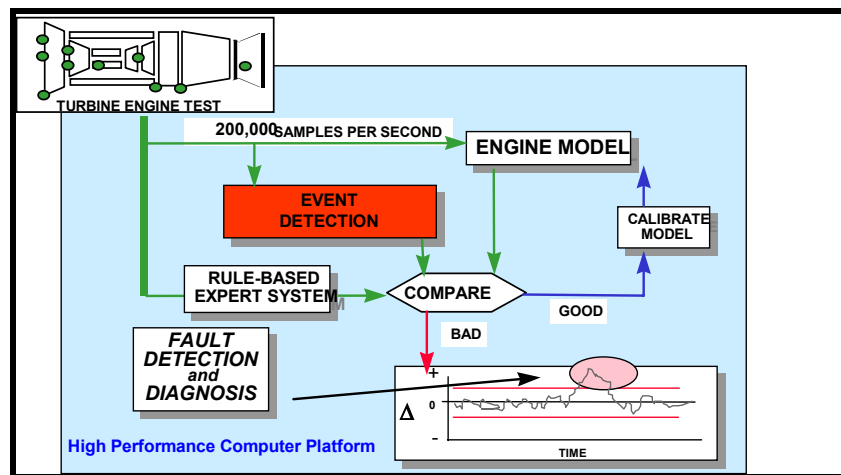


**Figure 2.20: Schematic of Overall Fault Detection Process.**

The technique was demonstrated during developmental turbine engine testing at simulated altitude conditions. The viability of the approach in terms of the functionality of the model-based approach, and the required computational speed were assessed. The results indicate that the technique is capable of detecting and diagnosing abrupt changes in measurements as illustrated in **Figure 2.21**.

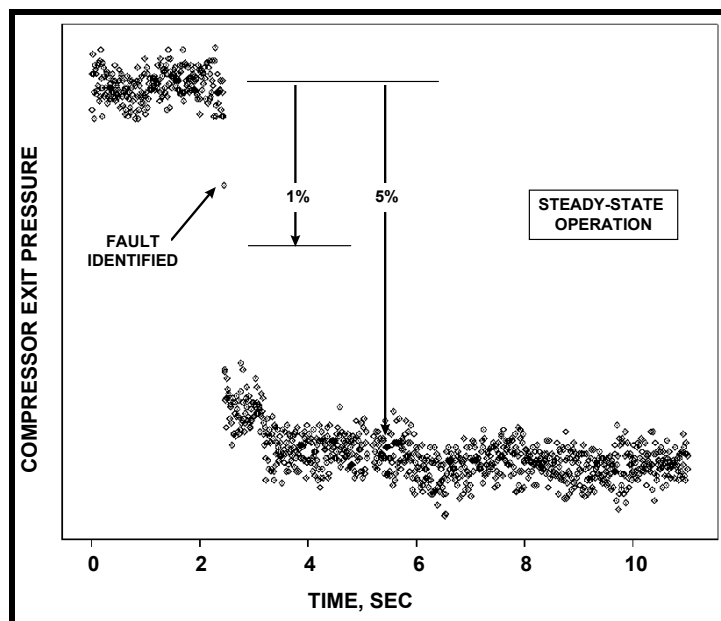


**Figure 2.21: Abrupt Change in Compressor Exit Pressure during Steady Engine Operation.**

### *Limitations of Chosen Modeling Technique*

A variety of interactive tools, that permit more detailed diagnostics of steady-state data (and if necessary, backward chaining to identify the fault), is currently available for use in developmental engine tests. Due to observability constraints, imposed by the specified instrumentation and test conditions at the time of the identification, some loss of diagnostic resolution of data anomalies occurs. This is the result of lumping together component modifiers and measurements used in the model-based diagnostic system. For example, burner fuel flow (WFB) is a function of measured fuel heating value, specific gravity,

## APPLICATIONS

---

viscosity, fuel temperature, and turbine flow meter output. Future work includes linking the model-based fault identification approach with other fault diagnostic systems to better analyze all available information.

### *2.1.3.1.4 Performance Recovery*

The role of an aeropropulsion altitude test facility is to duplicate or simulate environmental factors that affect propulsion system operational behavior. Typically, variances from specified environmental conditions occur during ground testing and affect the measured performance of the engine. Perturbations in engine inlet pressure and temperature and ambient pressure can influence engine performance calculations such as gross and net thrust, time-to-thrust, airflow, fuel flow, turbine temperature, combustor pressure, rotor speeds and fan and compressor operating lines. Maintaining specified environmental conditions during engine transient operation is much more demanding than when steady state testing. The ability to control environmental conditions in directly connected test installations is primarily a function of environmental temperature, pressure levels, excursion rates, engine airflow rate excursions, test facility hardware configuration and facility active control characteristics. The ability to control test cell environmental conditions is especially important in flight clearance testing and engine specification compliance testing.

### *Modeling Techniques Used*

A detailed transient component-level model of a dual-spool afterburning turbofan engine was developed and validated with representative test data to determine the effect of environmental variances. The model included a simulation of the engine control and performance characteristics for all the major components (fan, compressor, burner, high and low-pressure turbines, and exhaust nozzle). The effects of Reynolds number for the rotating machinery and off-schedule geometry effects for the fan and compressor were included in the simulation. The model accounts for turbine cooling-air, heat transfer within the turbine section, and engine internal power requirements. The model was validated by comparing model results to representative-engine transient-performance data, in terms of the characteristic response of thrust, fuel flow, rotor speeds, and combustor pressure.

### *Potential Benefits*

The effects of environmental variances can be determined for gross and net thrust, time-to-thrust, airflow, fuel flow, turbine temperature, combustor pressure, rotor speeds, and fan and compressor operating lines, using a calibrated component-level simulation of a gas turbine engine. A transient data adjustment method based on simplified turbine engine cycle interrelationships was employed to compensate engine performance parameters for the combined effects of variances in inlet pressure and temperature and ambient pressure. The adjustment method was applicable to both steady state and transient operation.

### *Cited Example*

- Chappell, M.A. and McKamey, R., “Adjusting Turbine Engine Transient Performance for the Effects of Environmental Variances”, AIAA Paper # 90-2501, July 1990. [\[2.18\]](#)

In general, at altitude test facilities, either referred parameters are used to adjust transient data or no adjustments are made. Referred parameters address the effects of variances in inlet conditions ( $P_2$  and  $T_2$ ) but fail to address the effects of variances in exit conditions ( $P_0$ ). The adjustment method that was applied for the cited example was based on fundamental gas turbine cycle interrelationships. These relationships were developed specifically for determining performance changes with respect to changes in the environment (or in the control) for steady state and transient engine operation. As a result, the relationships were easily adapted as a transient data adjustment method for transient engine testing in a direct-connect

altitude testing facility. The adapted method addresses variances in inlet pressure and temperature and exit pressure. Typical environmental variances for sea-level-static conditions are illustrated in **Figure 2.22**.

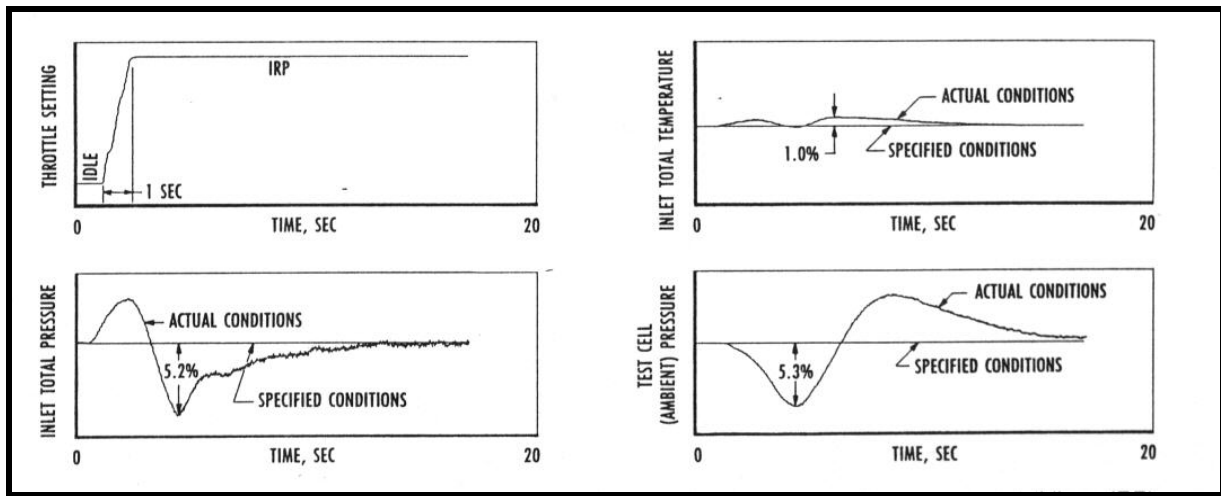


**Figure 2.22:** Typical Environmental Condition Variances in an Altitude Test Facility.

The adjustment method was applied to performance obtained at *unadjusted* actual environmental conditions for conditions near extreme corners of the engine operational envelope and two cruise conditions. *True* engine performance was defined as performance determined by the model at specified conditions. *Adjusted* performance is compared to *true* performance and to *unadjusted* performance in **Figure 2.23**. The effects of the variances on gross and net thrust are characterized by the difference in thrust response between *true* and *unadjusted* performance. By adjusting the data the maximum thrust variation was reduced from 6.1 percent to 1.1 percent and eliminated most of the effects of environmental variances on thrust. This is indicated by how closely *adjusted* performance approximates *true* performance.

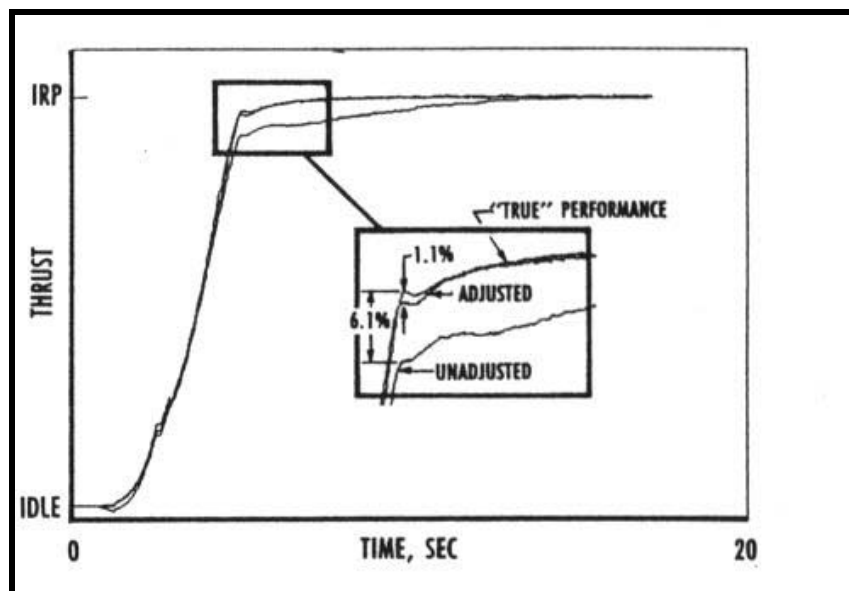


**Figure 2.23:** Effectiveness of Adjusting Thrust for Environmental Variances.

### ***Limitations of Chosen Modeling Technique***

A method based on simplified turbine engine cycle inter-relationships was adapted for use as a method of adjusting transient performance for the effects of variances in environmental conditions. The method was demonstrated throughout the operational envelope for variances in inlet temperature and pressure, and ambient pressure of up to 18%, 1%, and 32%, respectively. The adjustment method may be applicable to larger pressure variances. However larger variances were not investigated. Applicability of the adjustment method was limited to small ( $< 1.0\%$ ) temperature variances because larger variances produced unacceptable results. The demonstration was restricted to choked nozzle operation and to environmental variances that have a minimal effect ( $< 1.0\%$ ) on fan rotation speed. The adjustment method was found to be applicable to both steady state and transient engine operation.

#### ***2.1.3.1.5 In-Flight Thrust Certification***

During development testing, it is necessary to verify the design quantified by the various measures of merit and to refine the design. The test engines are usually instrumented with both steady state and transient instrumentation to evaluate engine performance and operability. Determining figures of merit from engine measurements is not always easy and practical. For example, turbine inlet gas temperature used in engine performance analysis is based on a flow-path area weighted average of a spatially varying environment. To determine the flow-weighted average from measurements is a very difficult task. It would require a large number of temperature probes covering the gas path station and each probe must be able to survive in a high temperature environment. By using flight test data as the input to a modeling technique, these difficult engine merits of performance can be calculated.

### ***Modeling Techniques Used***

The modeling technique used was a component level cycle code with additional modeling to allow for transient effects not ordinarily allowed for in standard transient cycle codes. The key relationships that were to be satisfied are summarized below:

- Power-balance equation for each rotor with the rotor inertia term, (turbine power = compressor power + parasitic power + acceleration power);
- Continuity equation for each component with transient mass storage term;
- An accounting for transient metal heat transfer of each component; and
- Assurance of static pressure balance at the mixing surface boundary of the duct and core flow.

A multi-dimensional Newton-Raphson iteration technique was used to simultaneously satisfy all the relationships to achieve cycle balance at each instantaneous point. The component dynamics, including rotor moments-of-inertia and heat transfer characteristics used in the equations were obtained from the manufacturer's design technology groups. In addition to the above relationships the model was changed to accurately represent off-nominal variable-geometry effects, and the turbomachinery performance and compressor stall line were also adjusted transient clearance changes.

### ***Potential Benefits***

Engine transient simulations, which properly account for non-equilibrium conditions, can provide system analysis and trade-off study tools for judicious configuration selection and control-mode design, thereby effectively preventing operation problems and reducing costs. System design and optimization can be particularly challenging for an afterburning turbofan fighter engine with fast rotor response and augmentor transient requirements. Data driven engine models aid design verification by calculating hard-to-measure parameters. The calculated average flow-path parameters, such as in-flight thrust and turbine inlet temperature provide a means to quantify engine performance from rudimentary flight test instrumentation.

*Cited Example*

- Khalid, S.J., "Role of Dynamic Simulation in Fighter Engine Design and Development", Journal of Propulsion and Power, Vol. 8, No. 1, January-February 1992, pp. 219-226. [2.19]

The modeling technique described in the cited reference was successfully used to calculate the in-flight transient thrust of a modern fighter engine installed in the F-15 flight-test aircraft. The analysis was of snap engine acceleration from flight idle to military power, performed at an altitude of 40,000 ft. and Mach number of 0.52. The installation effects of compressor bleed and horsepower extraction were included in the analysis. The measured flight-test data for flight conditions; engine fuel flow, variable geometry, and exhaust nozzle area were used as input to the transient engine model. Model calculations for transient thrust, exhaust nozzle inlet pressure, (PT6M), and fan rotor speed (N1) are presented in **Figure 2.24**. The model calculations of PT6M and N1 are compared to flight-test data and show excellent agreement. Since PT6M is reflective of gross thrust and N1 is reflective of total engine airflow, it may be inferred that the calculated net thrust, FN, is representative. It may also be inferred from **Figure 2.24** based upon the accuracy of the compressor exit total pressure, PT3, and the use of actual fuel flow rates, that the calculated combustor exit temperature TT4 is also representative.

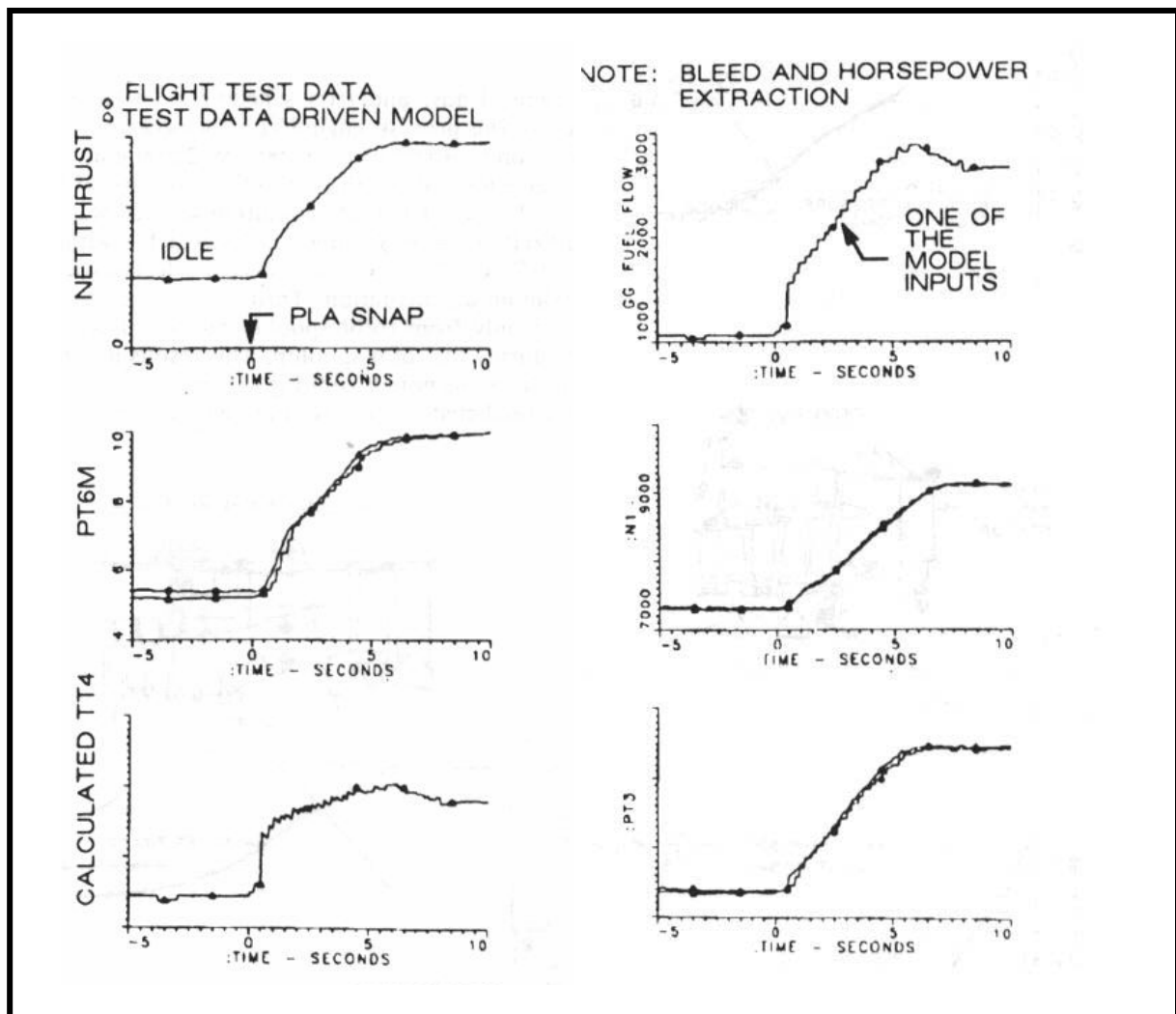


**Figure 2.24:** In-Flight Transients, Idle-to-Max Snap, Altitude 40,000 ft., Mach 0.52.

### *Limitations of Chosen Modeling Technique*

The major limitation is the reliance on component steady state maps. These maps are generated while the engine is running at a steady state and thus have to be modified for transient behavior. The turbomachinery performance and compressor stall line were adjusted for the deviation of transient clearances from the steady state clearance. This deviation occurred because rotor thermal growth is much slower than the case thermal growth. The engine model used in this investigation incorporated an algorithm to calculate transient clearances as a function of rotor speed and internal pressures and temperatures. Component performances and stall line were correspondingly adjusted using empirically established clearance sensitivities.

#### *2.1.3.1.6 Fighter Engine Airstarting Capability*

The ability to airstart a fighter engine successfully and quickly is of paramount importance to flight safety. Even though stall-free operation and stall recoverability are demonstrated during development engine testing and flight testing, there could be instances of engine flame-out in the field, due either to the aircraft exceeding the flight envelope or to an interruption in fuel flow. This latter could be caused by a fuel system malfunction or an inadvertent PLA movement to cut-off. Under these eventualities, an airstart has to be completed before the aircraft loses too much altitude. Fast start times increase the pilot's confidence in recovering the airplane from an engine-out condition and thus enhance the safety and dependability of single engine installations.

### *Modeling Technique Utilized*

A start model is required for pre-test predictions and for arriving at start schedules for test evaluation. Component operation in the far off-design sub-idle region makes the definition of accurate sub-idle component maps difficult, thus precluding the construction of the conventional aerothermodynamic model for the starting regime. Instead, an empirical model was constructed using correlations developed from available spool-down and airstart data. Corrected torque relationships were developed both for the unlit and lit conditions using time derivatives of HP rotor speed. The algorithm, using these relationships in conjunction with engine parasitic loads, starter torque and aircraft loads, is summarized in **Figure 2.25**.

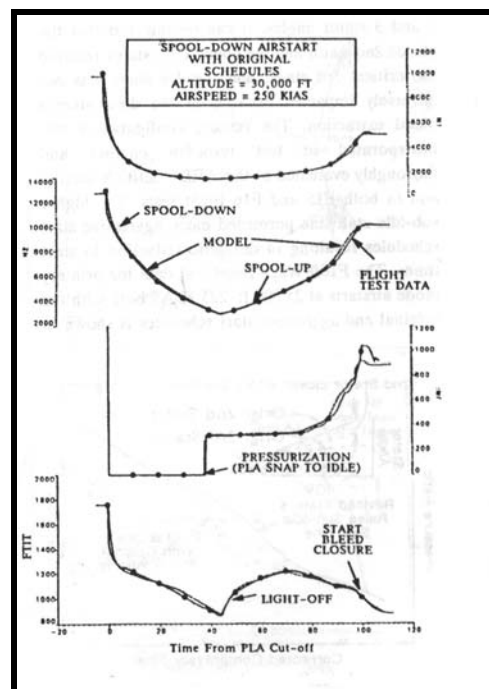


**Figure 2.25: Schematic of Empirical Start Model.**

### Potential Benefits

The success criteria for starting include: good ignitability, combustion stability, adequate stall margin, ability to spool-up from a low compressor speed at acceptably low airspeed, and short acceleration time to idle to prevent excessive altitude loss in the engine-out condition. Meeting all these conflicting requirements in the far off-design sub-idle region are the systems engineer's challenge. A model that is suited for this type of off-design condition is a tremendous aid to the analysis process.

### Cited Example

- Khalid, S.J. and Legore, R.T., "Enhancing Fighter Engine Airstarting Capability", International Journal of Turbo and Jet Engines, Vol. 10, 1993, pp. 225-233. [2.20]

The modeling technique described in the cited reference was successfully used to calculate an in-flight spool-down and re-light. The fidelity of the empirical model is evident from **Figure 2.26** which shows a comparison of model results with flight-test data for the 25% spool-down airstart at 30,000 ft., 250 KIAS. The results showed good agreement with flight test data and thus the empirical model was found adequate to obtain pre-test prediction of start transients with start logic revisions.

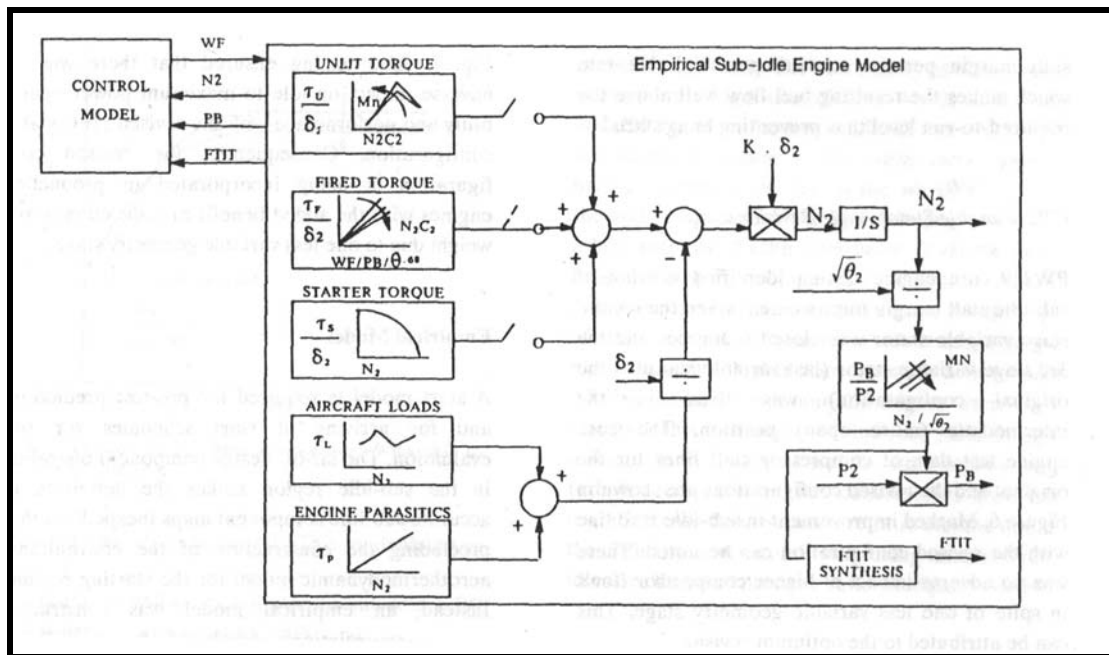


**Figure 2.26:** Empirical Model versus Flight Test Data.

### Limitations of Chosen Modeling Technique

The major limitation is the reliance on component steady state maps. These maps are generated while the engine is running in steady state conditions and thus have to be modified for transient behavior. The turbo-machinery performance and compressor stall line were adjusted for the deviation of transient clearances from the steady state clearance. This deviation occurred because rotor thermal growth is much slower than the case thermal growth. The engine model used in this investigation incorporated an algorithm to calculate transient clearances as a function of rotor speed and internal pressures and temperatures. The component performances and stall-line were correspondingly adjusted using empirically established clearance sensitivities.

## APPLICATIONS

---

### 2.1.3.1.7 Performance Deterioration

The effects of deterioration on engine performance can be significant from an operational, economic and safety point of view. The ingestion of particles suspended in the air, such as sand, dust, water droplets, ice, fly ash, and salt, is the single most important factor causing performance deterioration in all types of gas turbine. Since gas turbines use roughly half a ton of air for each horse power output for every twenty four hours of operation, even if one part per million (ppm) enters the compressor, a 10,000 HP unit will ingest ten pounds of foreign material in a single day. With such a high rate of foreign particle ingestion, even a highly efficient filtering system can only mitigate, but not eliminate the problem of gas turbine deterioration. Among the different gas turbine applications, aircraft gas turbines are affected the most by the ingestion of dust not only during flight but also during landing and take-off. Because of the high power setting during take-off, a strong suction zone is induced at the engine inlet due to a vortex formed between the inlet and the ground. This suction pressure ingests runway gravel, puddles of water and ice, and salt spread on the runway during winter. Similarly, during landing, the thrust-reverser efflux blows runway dirt into the air. This is sucked into the engines. Generally, performance deterioration in gas turbines is due to:

- Fouling, due to minute dust particles, pollen, salt spray and insects, which gets deposited on blade surfaces;
- Erosion of blade sources caused by particulate ingestion;
- Tip clearance increase of blade tips caused by particulate ingestion;
- Water ingestion during rain; and
- Foreign Object Damage (FOD) caused by hailstones, runway gravel and bird ingestion.

### *Modeling Techniques Used*

Two models in the cited references deal with performance deterioration. Both models deal primarily with damage and wear caused by suspended particles using a stage-by-stage stacking procedure. The simulations at both design and off-design conditions are based on a mean line row-by-row model, which incorporates the effects of blade roughness and tip clearance. The results indicate that the increased roughness reduces the pressure ratio as well as the adiabatic efficiency of the compressor at all speeds, with the largest influence at 100% speed. Increased tip clearance has a more pronounced effect on the compressor adiabatic efficiency and a lesser effect on the pressure ratio.

The paper by Singh et al., uses a simple mean line method to model the effects of increased blade roughness and tip clearance due to erosion, on compressor performance. The model can predict the compressor stage performance, given the blade inlet and exit metal angles, blade stagger, camber, chord, solidity, thickness to chord ratio and hub to tip diameters. The model developed by Singh was validated using experimentally measured performance data obtained before and after erosion caused by the ingestion of 25 Kg. of sand. The model was then used to predict the effect of increased blade roughness and tip clearance due to erosion on two other single stage compressors with higher blade loading.

The paper by Lakshminarasimha et al., uses a stage stacking method where the stage characteristics are synthesized from a generic stage characteristic which is then modified by the design point information.

### *Potential Benefits*

From operational, economic and safety considerations, gas turbine performance deterioration has emerged as a very important topic of research. From an economic point of view, a one percent increase in specific fuel consumption (SFC) for a 45 aircraft fleet of single engine aircraft, could increase the expenditure due to additional fuel by a million dollars a year. Using models to aid in the determination and prediction of deterioration effects is very economical way of analyzing this problem.

### Cited Examples

- Lakshminarasimha, A.N., “Modeling and Analysis of Gas Turbine Performance Deterioration”, ASME Paper # 92-GT-395, June 1992. [2.21]
- Singh, D. et al., “Simulation of Performance Deterioration in Eroded Compressors”, ASME Paper # 96-GT-422, June 1996. [2.22]

In general, blade erosion is a complex function of the physical properties of the particles, blade material and aerodynamic parameters such as particle mass flow, particle size, shape, velocity and direction of impingement, the geometry, and the material of the blade row. In view of this complexity, the prediction of erosion and the subsequent change in compressor performance is a complicated task.

The method as described by Lakshminarasimha, was initially validated against a single stage compressor as illustrated in **Figure 2.27**. Considering the simplicity of the method, a good comparison can be seen between measured and simulated results.

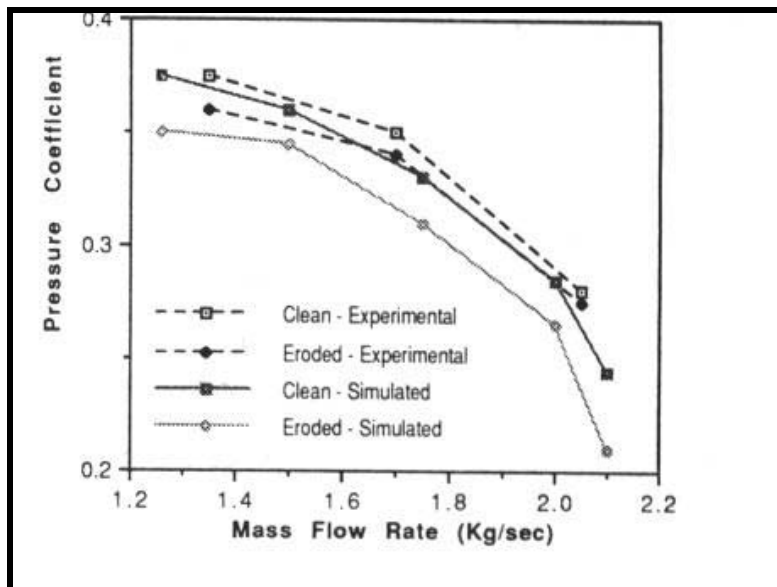


**Figure 2.27: Simulation of the Effect of Erosion on Single Stage Compressor Performance.**

This procedure was extended to a multi-stage compressor (a J-85). Results of this comparison are presented in **Figure 2.28**. The compressor erosion results in a reduction of both compressor mass flow rate and pressure ratio. Also, it can be concluded that the reduction in mass flow and pressure ratio is dependent upon compressor speed, being higher at higher speeds. Additional numerical experiments were carried out, by simulating cases when only front or rear stages were eroded. These results indicated that front stages have a greater impact on overall compressor performance compared to rear stages, because a front stage affects all the stages following it. This is an important conclusion from both safety and economic viewpoints. If a gas turbine is to operate in dusty environments, it is more advisable to use expensive highly erosion resistant compressor blade material or coating in front rather than rear stages thus reducing both time between overhaul periods and increasing the safe operation time.

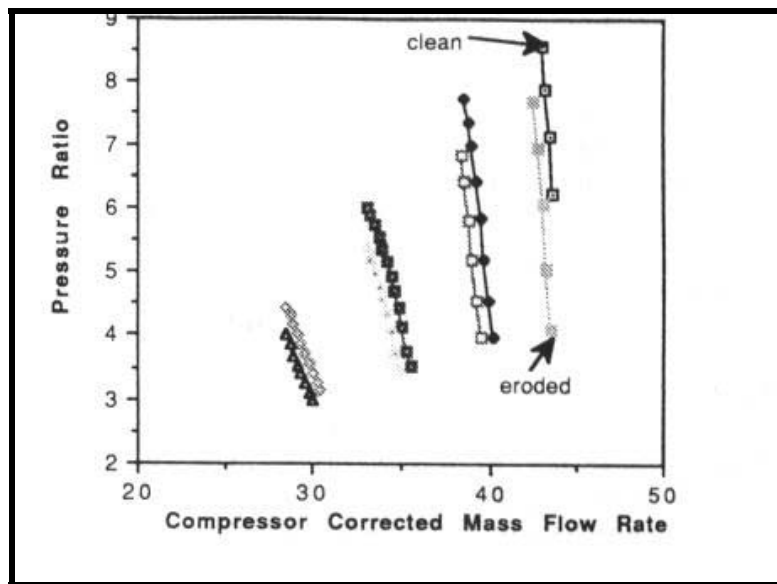


**Figure 2.28:** Simulation of the Effect of Erosion on Multi-Stage Compressor (J85) Performance.

The method described by Singh was used to analyze the combined effects of increased tip clearance due to erosion and moderate roughness. Results of that investigation are presented in **Figure 2.29**. Increased tip clearance is predicted to have a more pronounced effect on the stage adiabatic efficiency with an additional 2 to 2.5% drop over the operating range. In comparison with other test cases where the loading was not as severe as indicated in the cited example, it was concluded that the loss in aerodynamic performance increases with increased blade loading.

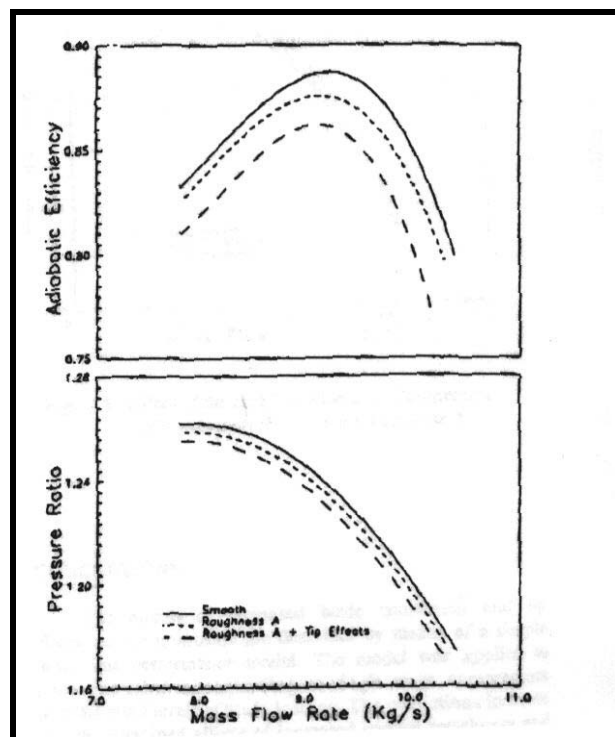


**Figure 2.29:** Effects of Surface Roughness and Tip Clearance on Compressor Performance.

### ***Limitations of Chosen Modeling Technique***

The performance of compressors is normally depicted by means of the compressor characteristics, which describe the variation of compressor pressure ratio and efficiency with engine mass flow rate. In performance deterioration studies, the variation in the compressor map with engine usage is sought. Since performance maps are not supplied to the operator, any simplified map generation technique would be extremely useful to the operator to aid in meaningful maintenance scheduling and trending of the performance variation of the component.

The stage stacking method takes into account interrelationships among stages through compatibility of speed, mass flow and energy. Thus, it provides a logical basis for examining the behavior of a multi-stage compressor subjected to deterioration in one or more stages. Additionally, it is possible to study the effect of different types of deterioration using this method. Usually, a gas turbine user has neither the compressor performance maps nor the stage characteristics for performance simulations. In such a situation, one can use the on-site performance measurement values of baseline compressor flow, efficiency, and the annulus area of the compressor gas path together with the generalized stage compressor characteristics for compressor performance simulation. However, this means of obtaining performance can only be used for trending since the accuracy is in doubt.

### **2.1.3.2 Operability**

An important component of the gas turbine engine is the compression system. In today's military turbine engines, the compression system consists of one or more axial compressors. These axial compressors must operate in a stable manner even with severe inlet pressure or temperature distortion. Many experimental and analytical investigations have been conducted in the past three or four decades to separately quantify the effects of pressure or temperature distortion on the compression system. While little experimental work has been performed on combined time-variant total pressure and temperature distortions, some investigations have been carried out to examine the effects of combined steady-state pressure and temperature distortion on compression system stability. With the advent of highly agile maneuvering aircraft with weapons release near the engine inlets, there will exist a requirement to quantify the combined effects of severe pressure and temperature distortion, both transiently and in the steady state. Although the traditional cycle code doesn't have the capability to handle engine/compressor instabilities, there have been several methodologies that have been developed to analyze engine surge and rotating stall.

*Most cycle or 0-D codes may indicate when an engine transient may reach unstable operation such as surge by flagging that event to the user and possibly stopping execution. The modeling of stall or surge within a cycle code is usually highly dependent upon empirical data. However, 1-D Codes have been developed to go beyond the stall point and are more dynamic in nature. Two examples are presented in the next sections.*

#### **2.1.3.2.1 Engine Stall Using One-Dimensional Modeling**

The gas turbine engine has played a significant role in the advancement of the flight capabilities of modern day aircraft. In order for a gas turbine engine to operate at the performance, operability, and durability level for which it was designed, stable operation of the various engine components must be ensured. Transient and dynamic instabilities, which could push the engine components beyond their operational limits, could result in loss of thrust, loss of engine control, or possible engine damage due to high heat loads and high cyclic stresses. The influence of operating instabilities must be quantified not only from the individual component considerations, but also from the point of view of any interaction between the various components.

### ***Modeling Techniques Used***

The turbine engine modeling technique was the Aerodynamic Turbine Engine Code, or ATEC, a time-dependent turbine engine model and simulation capable of simulating a turbojet engine operating in both transient and dynamic modes. Other gas turbine engine models and simulations have typically focused on providing a transient, component-level representation of the overall engine, or a dynamic representation of a single component. The ATEC simulation provides a bridge between the two types of simulations. It provides the computational efficiency that is desired when simulating the gas turbine engine during transient events, but it also provides the appropriate simulation techniques to address overall engine operation during a dynamic event such as compressor surge or combustor blow-out. ATEC provides the detailed system resolution needed to analyze a dynamic event (such as a stage-by-stage representation of the compression system), but uses the same type of component performance information used in standard transient simulations.

The Aerodynamic Turbine Engine Code (ATEC) solves the one-dimensional, time dependent, compressible, inviscid flow-field solution for internal flows by solving the Euler equations for the conservation of mass, momentum, and energy. The solution is obtained over the computational domain using both implicit and explicit numerical integration routines. The effects of the various engine system components are modeled using turbomachinery source terms in the governing equations.

### ***Potential Benefits***

The ATEC model and simulation can simulate on and off-design steady-state operation, as well as transient and dynamic engine responses to perturbations in a wide range of operational and control conditions. By example, it has been shown that the ATEC simulation can handle a wide variety of conditions that occur during normal and abnormal gas turbine engine operation. The benefits of the variable time-step routine, which uses a combination of the explicit and implicit numerical solvers, were also demonstrated. Test cases were presented that demonstrated that the ATEC simulation could: be calibrated to a steady-state data set; extended the steady-state calibration to a transient fuel variation; presented results from an engine operation that resulted in compressor surge; and addressed a turboshaft engine going through the start process. The ATEC results were shown to agree closely with test data where available.

### ***Cited Example***

- Garrard, G.D., “ATEC: The Aerodynamic Turbine Engine Code for the Analysis of Transient and Dynamic Gas Turbine Engine System Operations – Part 1: Model Development”, ASME Paper # 96-GT-193, June 1996. [2.23]
- Garrard, G.D., “ATEC: The Aerodynamic Turbine Engine Code for the Analysis of Transient and Dynamic Gas Turbine Engine System Operations – Part 2: Numerical Simulations”, ASME Paper # 96-GT-194, June 1996. [2.24]

This example demonstrates the real benefit of a dynamic simulation, by computing post-stall operation of a compressor and engine system, which cannot be modeled with a cycle-type simulation. The test case simulated a transient throttle movement using the T55-L-712 that resulted in the gas generator portion of the engine decelerating from 100 percent speed to approximately 90 percent speed. After a brief pause at the 90 percent speed, the engine was accelerated back to the 100 percent speed condition. The change in fuel flow rate during the acceleration was fast enough to force the compressor into surge cycles. The relative compressor pressure ratio as a function of time is illustrated in the figure below. The multiple surge cycles cause a significant drop in the total pressure throughout the engine and a corresponding flow reversal as indicated in **Figure 2.30**.

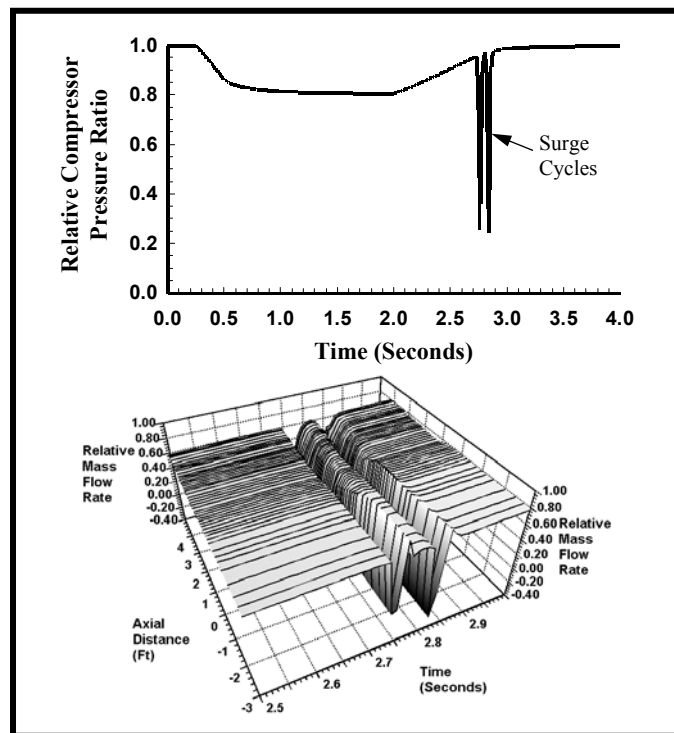


**Figure 2.30: Surge Cycles during Engine Re-Acceleration.**

### *Limitations of Chosen Modeling Technique*

The simulation described in the cited reference uses a one-dimensional approach. Thus, the interaction associated with inlet spatial distortion can not be analyzed with this modeling technique. It is, however, an excellent technique to investigate control actions that can be initiated because of some destabilizing event such as an inlet by-pass door malfunction or an engine surge.

#### *2.1.3.2.2 Engine-Inlet Integration*

The economic viability of a commercial supersonic transport, such as the High Speed Civil Transport (HSCT), is highly dependent on the development of a high-performance propulsion system. Typically, these propulsion systems mate a supersonic mixed-compression inlet with a turbojet or turbofan engine. The nature of such propulsion systems offers the potential for undesirable component interactions, which must be thoroughly understood for proper design. Therefore, it is imperative to have tools that allow investigation of inlet-engine integration issues.

The inlet must provide the engine with the correct mass flow rate at the highest possible pressure with minimum drag. Additionally, flow angularity and distortion must be minimized at the compressor face if the engine is to function appropriately. Maximum thrust with a minimum of fuel consumption will not be obtained without the inlet operating close to peak performance. Unfortunately, operating near peak performance can result in an inlet unstart (expulsion of the normal shock) followed by engine stall and possibly surge. When that happens, proper control action must be taken to recover the system as quickly as possible. Thus the operability of the overall system must also be addressed, because stable time dependent operation of the system must be ensured for both scheduled and non-scheduled events.

Because of the complexity of the inlet and engine systems, and the high cost of experimentally determining overall performance, numerical simulations of the components can be of significant benefit. For example,

dynamic simulations provide a means for investigating the potential interactions mentioned above, as well as providing a test bed for guiding the design, testing and validation of propulsion controls.

### *Modeling Techniques Used*

The simulation system, operating under the Application Portable Parallel Library (APPL), closely coupled a supersonic inlet with a gas turbine engine. The supersonic inlet was modeled using the Large Perturbation Inlet (LAPIN) computer code, and the gas turbine engine was modeled using the Aerodynamic Turbine Engine Code (ATEC) as illustrated in **Figure 2.31**.

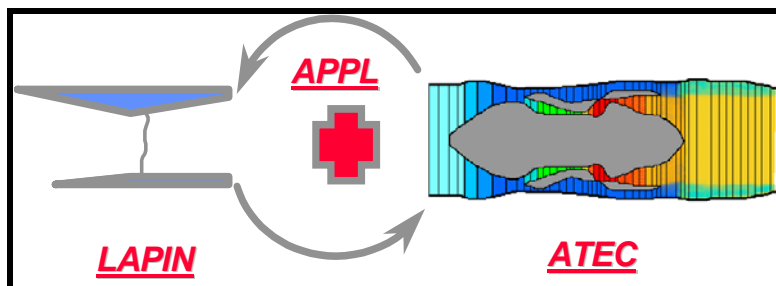


**Figure 2.31: Schematic of the Coupled Inlet-Engine Codes.**

Both LAPIN and ATEC provide a one-dimensional, compressible, time dependent flow solution by solving the one-dimensional Euler equations for the conservation of mass, momentum, and energy. Source terms are used to model features such as bleed flows, turbomachinery component characteristics, and inlet subsonic spillage while unstated. High frequency events, such as compressor surge and inlet unstart, can be simulated with a high degree of fidelity. The simulation system was exercised using a supersonic inlet with sixty percent of the supersonic area contraction occurring internally, and a GE J85-13 turbojet engine as illustrated in **Figure 2.32**.

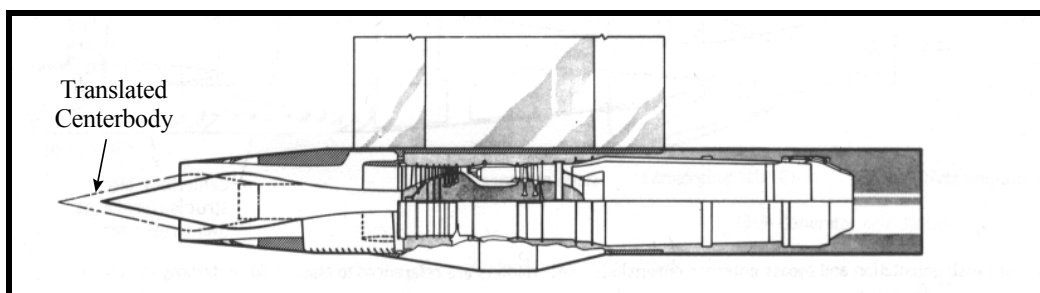


**Figure 2.32: Cross-Section View of the 4060 Inlet and J85-13 Turbojet Installation.**

The cited paper [2.25] describes the general modeling techniques used in the simulations, and the approach taken to implement the simulations under the APPL environment. It presents results from selected test cases.

### *Potential Benefits*

Traditionally, aircraft inlet performance and propulsion performance have been designed separately and latter mated together via flight-testing. In today's atmosphere of declining resources, it is imperative that more productive ways of designing and verifying aircraft and propulsion performance be made available to the aerospace industry. One method of obtaining a more productive design and evaluation capability is with numerical simulations. Numerical simulations can provide insight into physical phenomena that may

not be understood by test data alone. Simulations can fill information gaps and extend the range of test results to areas not tested. In addition, once a simulation has been validated, it can become a numerical experiment and the analysis engineer can conduct ‘what-if’ studies to determine possible solutions to performance or operability problems.

### Cited Example

- Garrard, G.D., Davis, Jr., M.W., Wehofer, S. and Cole, G., “A One-Dimensional, Time Dependent Inlet/Engine Numerical Simulation for Aircraft Propulsion Systems”, ASME Paper # 97-GT-333, June 1997. [2.25]

The simulation system was exercised using a supersonic inlet with sixty percent of the supersonic area contraction occurring internally, and a GE J85-13 turbojet engine. The inlet-engine simulation combination of LAPIN and ATEC was compared to experimental results. A transient event was initiated at a flight Mach number of 2.5 by pulsing the bypass doors in the closed direction. The result was an inlet unstart followed by an engine compression system stall. During the given transient, the majority of the system instabilities can be traced to the fact that the normal shock, located initially downstream of the inlet throat, was expelled outside of the inlet. The location of the shock is plotted as a function of time in **Figure 2.33**. The shock location is normalized by the inlet cowl lip radius, and referenced to the centerbody tip. The cowl lip is axially located two cowl-lip-radii downstream of the centerbody tip. The act of closing the bypass valve forces the shock structure to be expelled from the inlet. Moving the centerbody forward in conjunction with proper modulation of the bypass doors allows the shock to be re-ingested.

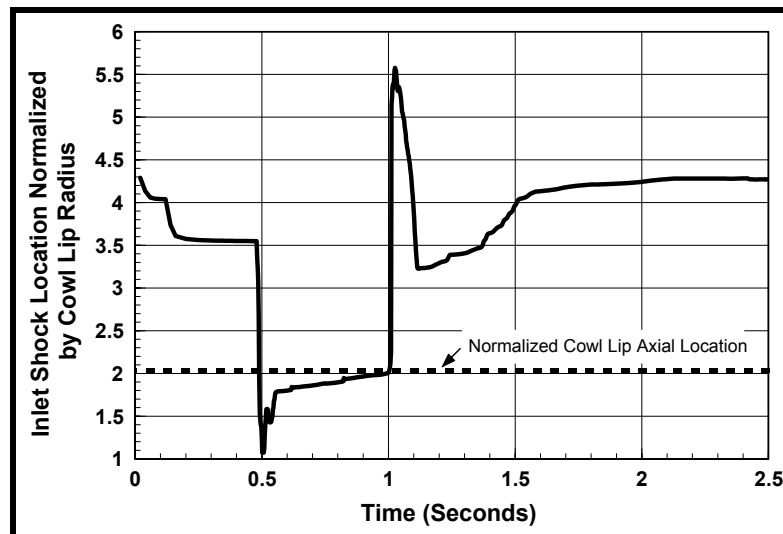


**Figure 2.33: Inlet Shock Location.**

Total pressure across the compressor is lost once the inlet system unstarts. At the instant of unstart there is a sharp spike in pressure ratio to a value exceeding 5.0 which (probably) exceeds the steady-state stall line, resulting in stall. Although the system begins to recover the original level of compressor operating pressure ratio, the compressor total pressure ratio is lower. The relative compressor pressure ratio is plotted as a function of the inlet corrected mass flow rate, expressed as a percentage of the design mass flow rate, in **Figure 2.34**. It is evident from the figure that there is one engine surge cycle, with a rotating stall event. Recovery takes place at a lower corrected inlet mass flow rate due to the lower engine shaft speed.

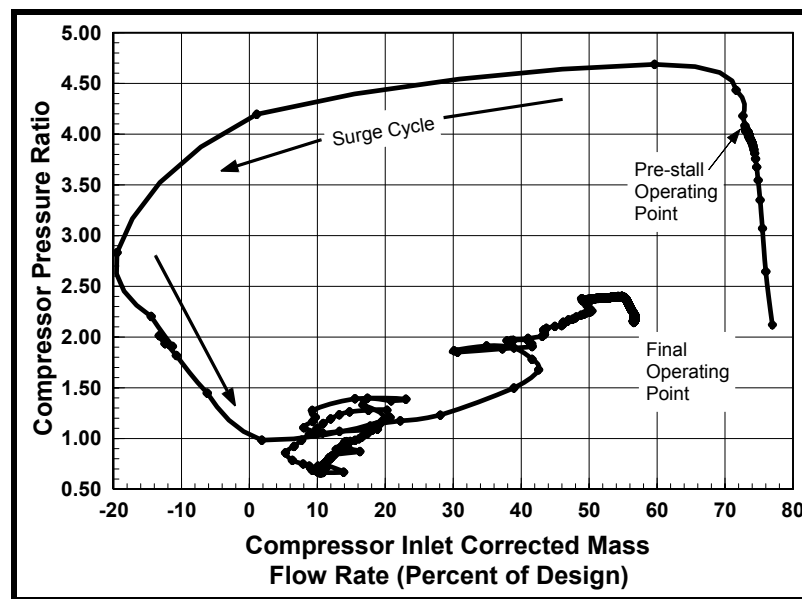


**Figure 2.34:** Compressor Pressure Ratio as a Function of Compressor Inlet Corrected Mass Flow Rate.

### *Limitations of Chosen Modeling Technique*

The simulation described in the cited reference uses a one-dimensional approach. Thus, the interaction associated with inlet spatial distortion cannot be analyzed with this modeling technique. It is, however, an excellent technique to investigate control actions that can be initiated by some destabilizing event such as an inlet by-pass door malfunction or an engine surge.

### **2.1.3.3 Life Assessment and Durability**

Life cycle costs have emerged as a primary factor in the design of gas turbine powerplants. The recognition of repairs and rebuilds and lost availability as major recurring costs suggests that some means of getting more use from the engine would be attractive. The concept of 'on-condition' repair and maintenance has emerged as a common ownership philosophy for both military and industrial equipment. Such a philosophy can only be put into practice if the tools to accurately assess engine condition can be assured. Furthermore, these tools must be tailored to the needs and capabilities of the personnel who must use them.

#### *2.1.3.3.1 Integrated Analysis Tool for Gas Turbine Component Life Assessment*

A major part of aircraft engine operating costs is related to maintenance. Maintenance cost would be significantly reduced if inspection intervals could be extended and component service life increased. Inspection intervals and service life are commonly based on statistical analysis, requiring a limited probability of failure (a certain level of safety) during operation. However, in many cases this approach leads to conservative inspection intervals and life limits for the majority of parts or components. Having an appropriate analysis tool offers a way to attempt to reduce maintenance costs and improved safety by applying usage monitoring to predict operation component condition and thereby facilitating 'on-condition maintenance'.

### **Modeling Techniques Used**

An integrated analysis tool implemented by the National Aerospace Laboratory of The Netherlands consists of a sequence of software tools and models, which is presented in **Figure 2.35**.

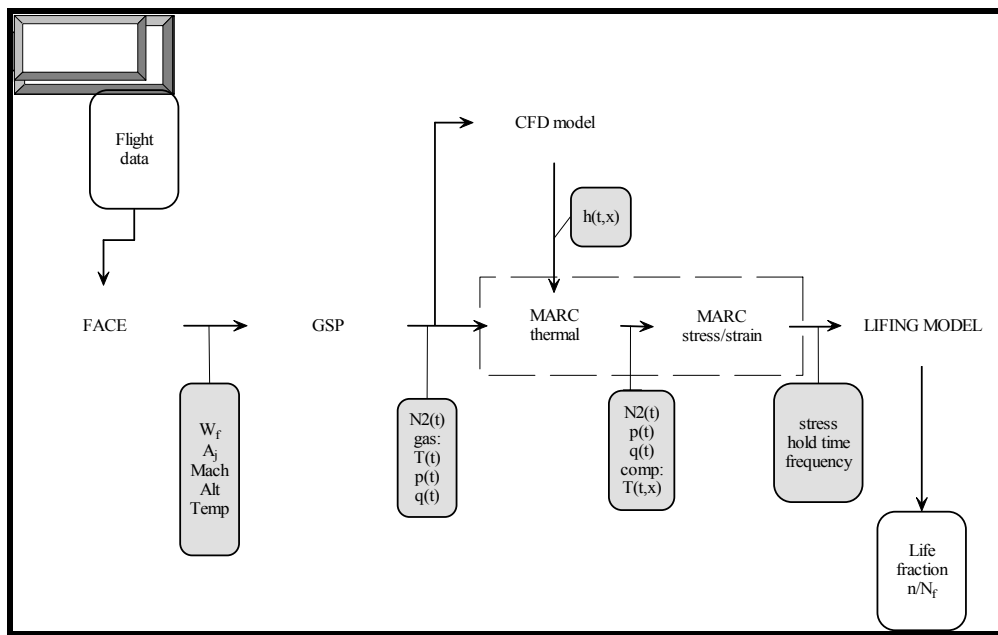


**Figure 2.35: Schematic Overview of the Integrated Analysis Tool.**

The sequence ranges from the measurement of operational engine data by the FACE system to ultimately predicting the life consumption during the analyzed mission. The following tools must be subsequently applied to process the data:

- FACE for Monitoring Engine Data;
- GSP for Calculating Gas Turbine Performance Data From FACE data;
- CFD Model for Calculating Heat Transfer to Hot Section Components;
- MARC for Calculating Thermal and Mechanical Stress in Hot Section Components; and
- Lifing Model for Deriving Life Consumption Data from the Stress History Data.

The FACE system consists of both on-board and ground-based hardware. In the aircraft two electronic boxes are installed: the Flight Monitoring Unit, (FMU) and the Data Recording Unit (DRU). The FMU is a programmable unit that determines which signals are stored and how they are stored. The relevant signals stored by the DRU are engine parameters from the engine's Digital Electronic Engine Control (DEEC) and avionics data. The DEEC signals can be sampled at a maximum frequency of 4 HZ. The following signals, which together fully describe engine usage are stored.

- Fuel flow to the gas generator;
- Fuel flow to the augmentor;
- Exhaust nozzle position; and
- Flight conditions – Mach, altitude and air temperature.

These parameters, as a function of time, are used as input to the GSP model, which is the next tool in the sequence.

The Gas Turbine Simulation Program (GSP) is a tool for gas turbine engine performance analysis, which has been developed by the NLR. This program enables both steady state and transient simulations for any

## APPLICATIONS

---

kind of gas turbine configuration. The simulation is based on one-dimensional modeling of the processes in the different gas turbine components with thermodynamic relations and steady-state characteristics (component maps). GSP can be used to calculate gas temperatures, pressures, velocities, and composition at relevant engine stations from measured engine data. This particularly applies to stations for which no measured data is available, such as the critical high-pressure turbine entry temperature. Also, GSP is able to accurately calculate the dynamic responses of these parameters (critical to engine life) where measured data is not available or has unacceptably high time lags or low update frequencies. The GSP output is used for further processing by the CFD and MARC finite element models.

The Computational Fluid Dynamic (CFD) model is used to accurately calculate the heat transfer from the hot gas stream to the component. For this calculation it is important to have detailed information on the geometry of both the flow channel and the different components that disturb the flow (blade vanes). From CFD analysis of the gas flow through the gas turbine, values for the heat transfer coefficient are obtained at specific locations in the component. The heat transfer coefficient value varies significantly along the flow path, due to variations in the flow conditions (gas velocity, type of flow – laminar or turbulent, etc). An engineering approach, which results in a number of functions that describe the approximate distribution of the heat transfer coefficient across the blade surface, is followed. This heat transfer model is based on, and validated with, heat transfer results obtained by the CFD model.

The Finite Element (FE) model consists of two interrelated models. The thermal model calculates the temperature distribution in the component, based on the heat input from the hot gas stream. The mechanical model calculates the stresses and strains in the component, caused by the varying temperature distribution and the externally applied loads. The finite element code used is MARC, which is a commercially available, multi-purpose finite element package.

The thermal model calculates the temperature distribution in the component. For each finite element on the surface of the component, the heat-transfer coefficient follows from the CFD model. Given the thermal conductivity of the material, the temperature distribution in the component can be calculated. A transient thermal analysis can be performed for the complete flight under consideration with the time-variant ambient gas temperature as input.

The mechanical model calculates the stress and strain distribution in a component. Both rotational frequency and the temperature distribution as functions of time are input for the model with stress and strain distribution as output. The temperature distribution is obtained from the results of the thermal analysis and the values of the rotational frequency are obtained from GSP.

A lifing model generally calculates either total time to failure or number of cycles to failure for a certain component subjected to a specific load sequence. A large number of specific life prediction models have been developed over the last twenty years, where each model is appropriate for a specific application. The major division in lifing models is between total life models and crack growth models. Total life models only calculate the time to failure and do not consider the way failure is reached. On the other hand, crack growth models represent the Damage Tolerance philosophy, which accepts the presence of material defects and aims to monitor crack growth and suggests removing the component before the crack become unstable. In the end, the choice of the lifing model depends on the expected failure mechanism of the component under consideration.

### ***Potential Benefits***

The potential of the analysis tool presented within the cited example is twofold. Firstly, the tool can be used to examine and support on-condition maintenance. The load history of every individual component can be tracked and can be used to determine the inspection interval or actual life limit of that specific component. The general and mostly very conservative life limits supplied by the manufacturer are based

on an assumed usage, to which a safety factor has been applied to account for heavier usage. This safety factor can now be quantified and possibly decrease, leading to a huge saving in spare parts and inspection costs. Secondly, the tool can be used to compare different mission types or maneuvers with respect to life consumption. The results can be used to optimize operational use of the aircraft.

### Cited Example

- Tinga, T. et al., “Integrated Lifting Analysis Tool for Gas Turbine Components”, ASME Paper # 2000-GT-646, May 2000. [2.26]

The analysis process described in the cited example has been demonstrated by applying it to the F100-PW-220 engine of the RNLAf F-16 fighter aircraft. The component selected for analysis is the 3<sup>rd</sup> stage turbine blade, which is the first stage rotor of the high-pressure turbine (HPT) module. To demo this capability, a random mission was selected and illustrated in **Figure 2.36**.

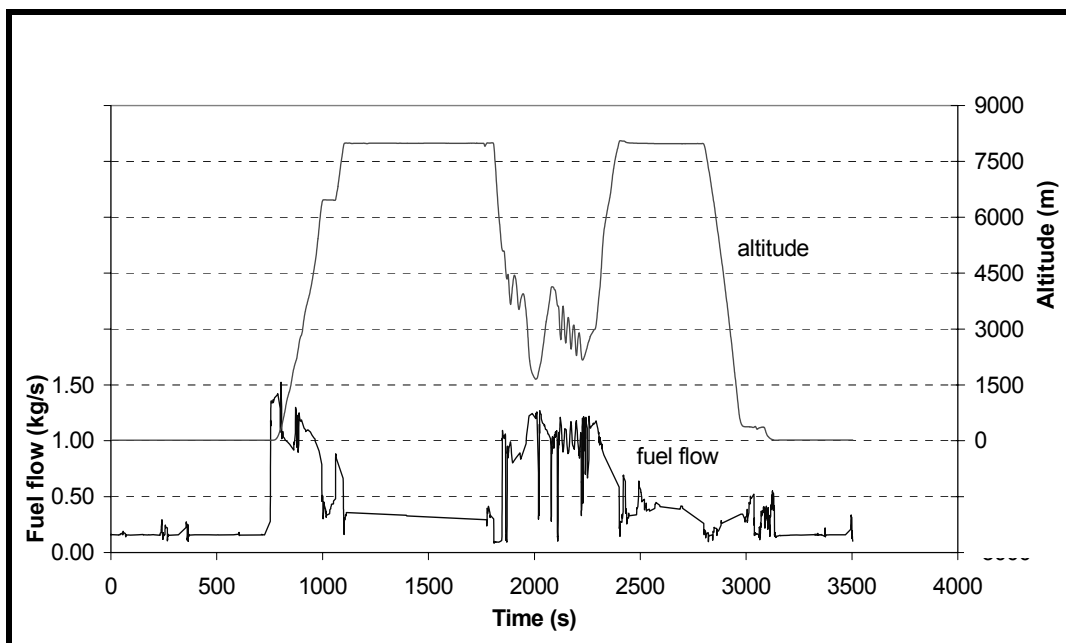


**Figure 2.36: Measured Variation of Fuel Flow and Altitude.**

The study was conducted to show the effect of HPT deterioration on the life consumption of the 3<sup>rd</sup> stage blade. HPT deterioration can be incorporated in GSP by applying a +1% change in HPT flow capacity and –2% change in HPT isentropic efficiency. The engine control is usually designed to compensate for loss of performance due to deterioration by maintaining compressor or fan rotor speed or another thrust related parameter. With the F100-PW-220, fan rotor speed is maintained, which means thrust is virtually unaffected by HPC, HPT, or LPT deterioration. However, to maintain fan rotor speed with a deteriorated HPT, turbine inlet temperature (TIT) and fan turbine inlet temperature (FTIT), levels must increase while compressor speed may drop. This implies that in order to analyze deterioration effects on thermal loads during operation, integration of the control system into the gas turbine performance model is required.

The effect of HPT deterioration is shown in **Figure 2.37**, which shows a comparison between the GSP calculations for a new and a deteriorated engine. The FTIT appears to increase by 25 to 35 degrees in the deteriorated engine. The calculated temperatures (FTIT) can also be compared to measured values obtained from FACE. This is illustrated in **Figure 2.38**.

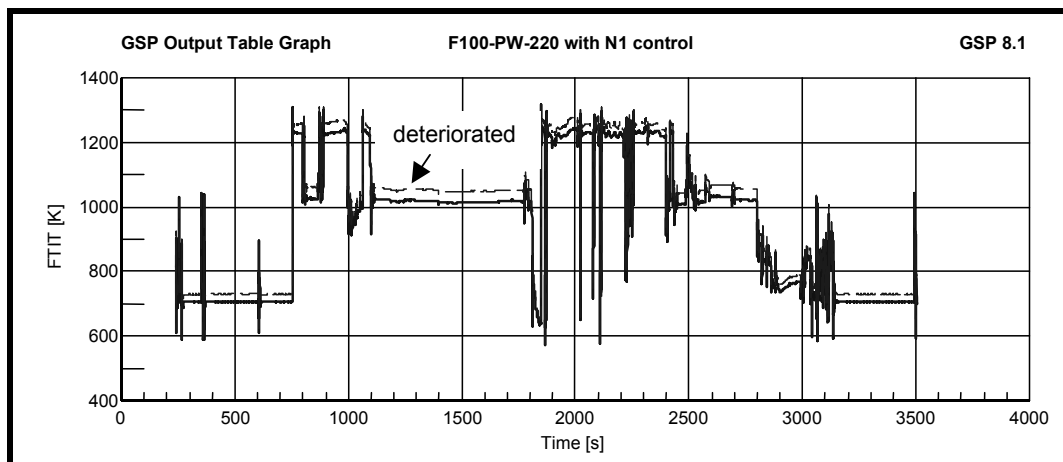


**Figure 2.37: Effect of HPT Deterioration on FTIT.**

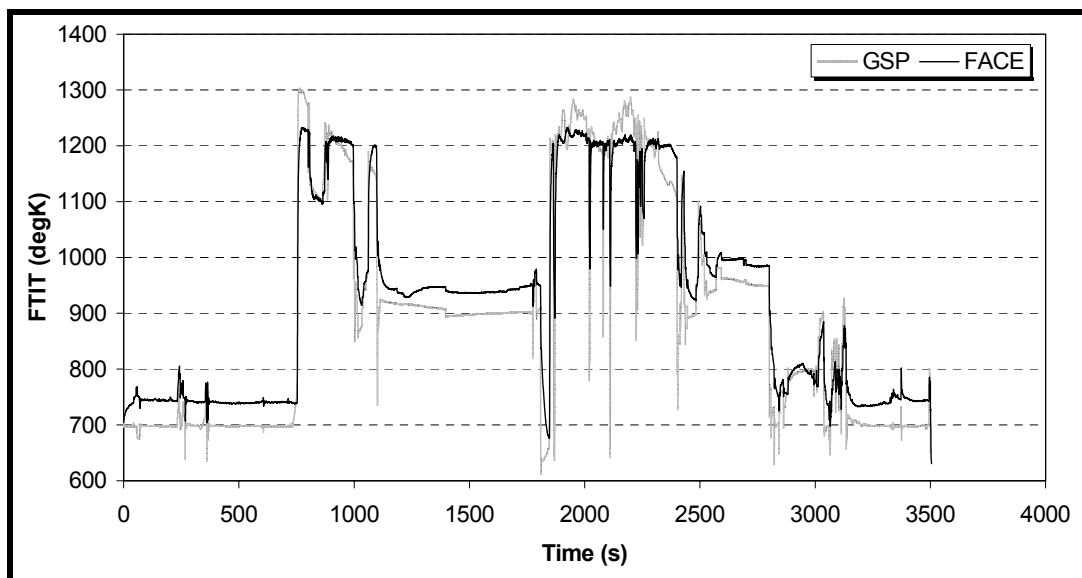


**Figure 2.38: Comparison of FTIT as Measured by FACE and Calculated by GSP.**

From the GSP output (FTIT), the finite element models determine the temperature distribution, its variation in time and the stress and strain distribution together with its variation in time. In the mechanical model the creep phenomenon is incorporated, because creep is assumed to be the life-limiting factor for the 3<sup>rd</sup> stage turbine blade. For a new component the amount of creep strain is nil and after sustaining a certain amount of creep failure occurs. Therefore, the creep strain is a damage parameter and the evolution of creep strain represents damage accumulation. The results of the integrated analysis are shown in **Figure 2.39**, which shows the accumulation of creep strain in the blade during the mission for both a new engine and a deteriorated engine. The creep strain accumulation appears to be faster in the deteriorated engine, which implies that the rate of life consumption is higher by a factor of 1.9.

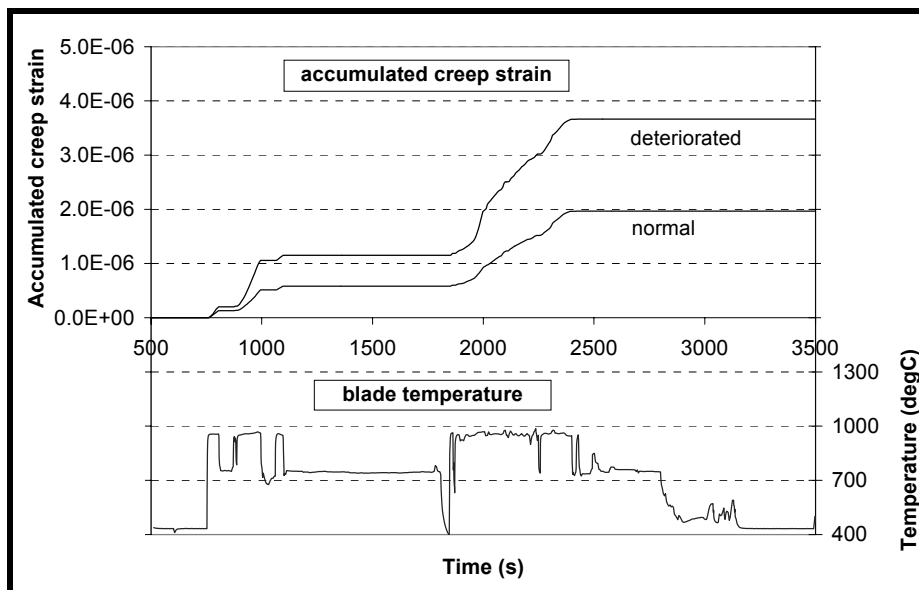


**Figure 2.39:** Effect of HPT Deterioration on Creep Strain Accumulation.

### ***Limitations of Chosen Modeling Technique***

An important point of discussion for this tool is the accuracy of the calculated results. The accuracy of the integrated tool is obviously dependent on the accuracy of the separate tools and models. The measurements of the FACE system combined with the data reduction algorithm introduce a maximum error of about 1%. The GSP model inaccuracy is considered to be less than 2%, provided that a suitable integration time-step has been chosen. The accuracy of the temperatures calculated with the thermal FE model is mainly determined by the accuracy of the heat transfer coefficient. Using the approximation functions for the heat transfer, the uncertainty in heat transfer coefficient is about a factor of 2, which is caused by uncertainty about the degree of turbulence. This may be less when a CFD model is used to calculate the heat transfer. The uncertainty in heat transfer coefficient will cause uncertainty in the temperatures during transients. However, the steady state temperatures of blades and vanes are unaffected by the heat transfer rates. This means that for creep life calculations the value of the heat transfer coefficient is not very important, but for fatigue life calculations, it is of crucial importance.

#### **2.1.3.4 Adverse Weather**

An aircraft gas turbine and its control are ordinarily designed for operation with air as the working fluid. The presence of humidity in ambient air, causing changes in molecular weight, and the ratio of specific heats of the working fluid, can generally be accommodated within a given design. Severe condensation in the engine inlet can cause water to be ingested into the engine. An air-water mixture may also enter an engine under other circumstances, such as during a rainstorm, during take-off and landing and in flight. Water may be present then, along the gas path of the engine, in droplet, film, or vapor form, in different proportions at various locations. The performance and operability of the engine can be expected to undergo changes due to aerothermodynamic and mechanical effects caused by the ingestion of water. Changes may be significant immediately, over a short period or over a long period due to sustained or repeated ingestion of water. Water in the working fluid may directly affect the performance of engine components and the matching characteristics or it may affect them indirectly through a sensor providing an incorrect input to the control, and thus an inappropriate response.

## APPLICATIONS

---

### *Modeling Techniques Used*

The model used in the first cited reference was a 0-D cycle code, capable of transient operation. The cycle model incorporated a time-dependent gas-path analysis of the engine, including its control. The cycle code included four processes related to the presence of water droplets in the working fluid:

- Aerodynamic performance changes due to ingestion, impact, surface flow, and rebound of water, along with modification of acoustic speed caused by the presence of droplets;
- Displacement of water due to blade and flow rotation;
- Inter-phase heat and mass transfer; and
- Droplet size adjustment based on Weber number considerations.

The model used in the second cited reference was a stage-by-stage compression system model based upon the solution of the 1-D Euler equations for mass, momentum, and energy. Humidity correction was based on the similarity laws and assumed that for a particular inlet Mach number and corrected speed the following was true:

- The work coefficient was held constant; and
- The stage efficiency was held constant.

The similarity laws were used to convert the humid speed and flow conditions to ‘equivalent dry’ conditions. These ‘equivalent dry’ conditions were then used to determine the ‘dry’ enthalpy rise and efficiency from the stage characteristics, which were based upon dry operation. Thus, operating under humid conditions yielded modified equivalent dry operating points on the characteristics resulting in the re-matching of stages.

### *Potential Benefits*

Through modeling, the effects of water ingestion on engine performance can be calculated and potential control actions may be built into the engine control. A model can be used to determine the changes in performance due to water ingestion. Further, it can show the effects of the design characteristics of the compressor, the water mass fraction, the residence time of the mixture in the individual blade passages, and the operating conditions.

### *Cited Examples*

- Haykin, T. and Murthy, S.N.B., “Transient Engine Performance with Water Ingestion”, Journal of Propulsion, Vol. 4, No. 1, January-February 1988, pp. 81-88. [\[2.27\]](#)
- Ludorf, R.K. et al., “Stage Rematching as a Result of Droplet Evaporation in a Compressor”, ASME Paper # 95-GT-194, Presented at the IGTI Turbo Expo in Houston Texas, June 1995. [\[2.28\]](#)

An illustration of the effects of water ingestion on key performance parameters is presented in [Figure 2.40](#).

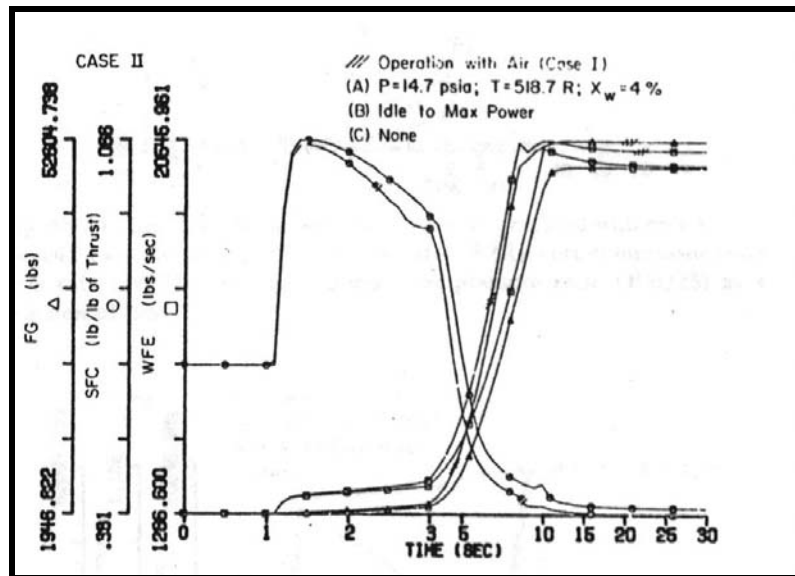


**Figure 2.40:** Effect of 4% Humidity on Major Engine Parameters, Thrust, Fuel Flow, and SFC.

The following effects were also observed in the cited papers:

- The extent of changes in compression subsystem performance due to water ingestion is significant and varies nonlinearly with the amount of water ingested.
- The effects of changes in compression subsystem performance on engine performance can become unmanageable with the ingestion of large amounts of water, especially during engine deceleration.
- Evaporation of water in the burner, during water ingestion into an engine, can have a serious effect on performance. This includes surging of the compressor and a drastic fall in power output combined with large increases in specific fuel consumption, especially when the phase change occurs at the exit of the burner.

Errors in input to the control system can arise due to the effect of water on sensors. Thus, the thermocouple (located at the casing of the core compressor), which provides an input to the control for determining the setting of the stator vane angles may register a temperature close to that of the water instead of that for the gas phase. The result is a drastic change in the performance of the control and, hence, the engine.

### ***Limitations of Chosen Modeling Technique***

The major limitation is the reliance on component steady state maps. These maps are generated while the engine is running steady with dry air. Adjustments were made based upon correlation for the effects of humidity. Substantial changes in compressor performance can arise with small quantities of water and those changes vary non-linearly with the amount of water. No simple scaling laws can be established for the various effects of water ingestion among vastly different compressors, although some similarity can be found for a given compressor under different operating conditions.

### **2.1.3.5 Controls**

With advanced engine types which feature many control inputs *viz.* fuel flow, compressor variable geometry, final nozzle area, etc. it is particularly important to ensure the correct setting of these inputs to attain optimum performance through the life of the engine. When the engine and airframe control inputs are optimized as a single mathematical problem (rather than being controlled independently as two distinct

## APPLICATIONS

systems), there are highly significant gains. In order to optimize these control inputs, the particular engine and airframe characteristics must be understood.

### 2.1.3.5.1 Embedded Model in Control System

In this example a Performance Seeking Control (PSC) algorithm was used, in an adaptive model-based control-system that optimizes the quasi-steady performance of an aircraft propulsion system. This allowed the whole engine and aircraft system to operate in various modes:

- Minimum fuel flow at constant thrust;
- Minimum fan turbine inlet temperature (FTIT) at constant thrust; and
- Maximum thrust (for acceleration).

The PSC system was implemented on an F-15 supersonic research airplane that was powered by two PW1128 afterburning turbofan engines. The engines are controlled by Full Authority Digital Electronic Control systems (FADEC). The FADEC provides control by:

- Open-loop scheduling of compressor (LP and HP) variable guide vanes (VGV);
- Closed-loop control of engine pressure ratio (EPR) via nozzle area (A8); and
- Closed-loop control of corrected fan speed (NLRT) via fuel flow (WFE).

The PSC system operates by applying trims as follows:

- For subsonic conditions, trims are applied to LPVGV, HPVGV, NLRT and A8; and
- For supersonic conditions, trims are applied to LPVGV, HPVGV, EPR, calculated airflow (W2calc), afterburner fuel flow (WFAB), inlet geometry: cowl (1st ramp) and 3rd ramp, and also stabilizer (horizontal tailplane) position.

### Modeling Techniques Used

The PSC algorithm uses the conventional EEC sensed parameters and the algorithm estimates other parameters as required. The process consists of estimation, modeling and optimization as illustrated in **Figure 2.41**.

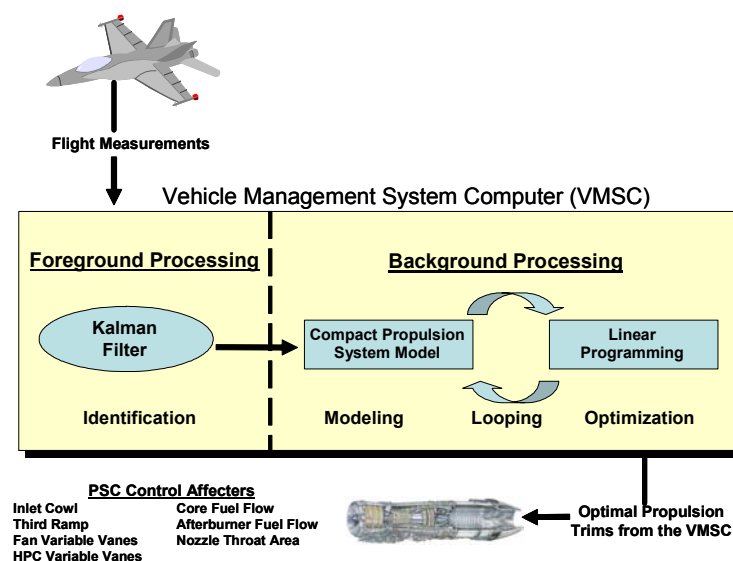


**Figure 2.41: PSC Implementation and Process Flow Diagram.**

Estimation concerns the assessment of the engine's performance in terms of the deviations of turbine efficiencies, compressor flows and HP turbine capacity. This is achieved using a Kalman filter. A piecewise-linear model is used as the basis of the estimator and is constructed as:

- States  $[x]T = [\text{HP speed, LP speed, turbine metal temp, 5 component deviation parameters}]$ ;
- Inputs  $[u]T = [\text{control inputs}]$  (as measured); and
- Outputs  $[y]T = [\text{pressures, temperatures, speeds}]$  (as measured).

Modeling derives the engine outputs required for the optimal solution. This requires formulation of the Compact Propulsion System Model (CPSM) which combines the Compact Engine Model (CEM) and the Compact Inlet Model (CIM).

The CEM consists of a linear steady-state variable model (SSVM). This is essentially a matrix of exchange rates linking the input vector comprising: measured fuel flows, turbine exit pressure, compressor variable position, and component deviations obtained from the estimator, to the response vector comprising: speeds, nozzle area, pressures, temperatures and airflows. Non-linear parameters, e.g. reheat parameters, thrusts, effective nozzle area, ram and nozzle drag, are calculated via analytical expressions and from data tables using outputs from the SSVM and engine measurements. These are linearized in real-time with respect to the input vector. These partials are used in the optimization process.

The CIM consists of equations, which relate inlet geometry and calculated flow to observed inlet conditions.

The airframe model is only invoked at supersonic conditions (the geometry is near optimum for subsonic), and is used to derive compensation in pitch control (via the stabilizer) arising from changes in inlet geometry. The model comprises tabulated relationships between pitching moments and drag effects for the cowl and stabilizer positions.

Optimization is performed using linear programming to determine the local optimum in terms of control inputs and output variables, within the accuracy of the models and defined constraints. Some iteration between the optimization and modeling functions is necessary. The primary constraints are set by the particular mode of operation, such as minimum fuel burn, and engine hardware, such as limits on actuator travel. The basis of the optimization is the Propulsion System Matrix (PSM) which is formed by combining the linear (steady-state) models from the CEM and CIM.

### ***Cited Example***

- Gilyard and Orme, "Performance-Seeking Control: Program Overview and Future Directions", NASA Dryden Research Facility, 1993. [\[2.29\]](#)
- Orme and Schkolnik, "Flight Assessment of the Onboard Propulsion System Model for the Performance Seeking Control Algorithm on the F-15 Aircraft", NASA Dryden Research Facility, 1995. [\[2.30\]](#)

The subsonic test program was conducted in 1990 – 1991 and was followed by the supersonic program during 1992. Only one engine was subject to the PSC algorithm. The ability of PSC to compensate for deterioration was demonstrated by using a degraded engine in the subsonic test phase. Most of the testing was carried out under cruise conditions. Trim update rate was slower in supersonic phase owing to the increased computing load for the inlet model. The claims for each of the three modes can be summarized as:

- Maximum thrust mode (accelerating) – up to 15% subsonic and 10% supersonic;
- Minimum FTIT mode (constant thrust) – reductions of  $\sim 100^\circ\text{F}$  observed at high altitudes; and
- Minimum fuel flow mode (constant thrust) – 2% reduction subsonic and 10% supersonic.

### ***Limitations of Chosen Modeling Technique***

The demonstrated PSC system is based on open-loop estimations and predictions and is thus sensitive to the accuracy of the engine model and the accuracy of measured parameters. The basis of the performance gain obtained from the engine is the change in EPR. That is, the increase in fan pressure-ratio towards stall. The calculation of surge margin is therefore fundamental to ensure surge-free operation. To assess this accuracy, an in-flight stall was provoked and the model output compared with the analyzed stall point. Up to 10% error in surge margin was observed – possibly due to measurement error and some contribution from the assumptions made for random errors. The surge-margin errors happened to be negative, so safety was not an issue (surge margin was always underestimated). Consequently the PSC system did not necessarily identify the full potential. Pratt & Whitney suggested that a reduction in design fan surge-margin requirement could lead to 3% increases in aircraft thrust-to-weight or 1.2% fuel burn reduction; this underlines the requirement for high accuracy in the assessment of surge-margin.

The thrust calculation accuracy of the PSC algorithm was assessed by comparing the PSC-calculated thrust to the value obtained using the excess thrust method. This relies on assessment of aircraft drag and weight, and measurement of acceleration. The accuracy was found to be within 3%.

The modeling technique appears to be fit for purpose, although it is generally recognized that a non-linear model, rather than the various linearized representations used in this example, has benefits in modeling fidelity terms. There is however a computing load issue as illustrated by the inclusion of the inlet model in the supersonic testing. This caused a reduction in trim update rate from 5 to 2 per second for supersonic operation.

Greater model accuracy may be achieved using higher accuracy sensors, or perhaps by using different measurements. The measurements taken were from the standard engine sensor set. More advanced adaptive control techniques that can identify measurement biases and compensate for model inaccuracy are being considered.

#### ***2.1.3.5.2 Control System Development and Analysis-by-Synthesis (ANSYN)***

Reheat or afterburning is used in military gas-turbine engines as a lightweight means to boost thrust by increasing the exhaust gas temperature and consequently its velocity. The reheat system (fuel flow and nozzle area) has direct and indirect influences on the fan operating point. The amount of fuel burned in the reheat system is critical to safe operation of the engine. If too much is burned, there is a risk of fan surge. If there is too little, there is a risk of combustion instability and wasted performance through low fan pressure ratio.

Two reheat control approaches have been taken on engines: closed-loop where the fuel is controlled to achieve a prescribed fan operating point, or open-loop where fuel is metered in accordance with the measured final nozzle area (which can also be controlled using open-loops). Both methods have advantages and disadvantages, this paper deals with the challenges in the open-loop method, and is linked to work carried out in the development of the Eurojet EJ200 turbofan for Eurofighter 2000 (Typhoon). Derivation and refinement of control laws is conveniently carried out using an engine simulation.

In order to conserve fan safety (freedom from surge), it is necessary to build-in safety margins in the reheat fuel control laws, commensurate with the accuracy of the simulation. Clearly, a greater confidence in the model will allow minimization of these margins, which can lead to better performance levels. Although all elements of the engine model contribute to the definition of the fan operating point, for reasons of clarity and brevity, only the building and the calibration of the nozzle and reheat components of the whole-engine model are covered here.

### ***Modeling Techniques Used***

The whole engine model is built in a modular fashion using component maps which include corrections for Reynolds number effects, tip clearance changes and inlet swirl (arising from variable guide van position). As such the engine is a 0-D representation.

Reheat fuel is introduced into three areas: two in the bypass stream, one in the core stream; and is progressively introduced through the reheat modulation range. Bypass and core air streams are combined to give a mixed stream, and cooling air is re-introduced at various points along the reheat liner. Correct accounting of mixing and cooling streams is essential to correctly model pressure losses which directly affect fan operating point for a given nozzle area. Pressure loss, bleeds and mixing calculations are handled differently in dry and reheated conditions. Afterburner burning efficiency is modeled without taking account of the burning location, but differences are modeled between low and high powers.

The nozzle model is very important in terms of internal engine parameters and in the prime external parameter – thrust. It is important to understand the physical construction in order to model correctly its functionality; for example gaps between petals can open up under some conditions and change the effective throat area. It is important to understand the changes in the nozzle flow-field for different nozzle geometry, in order to model correctly an essential control feedback parameter – PS7 (nozzle entry static pressure).

The simulation model is used to analyze dry and reheated test data from a variety of flight conditions. The process used is known as ANSYN (*Analysis by Synthesis*), which is a form of model calibration. The model's thermodynamic assumptions are automatically varied to match selected measured parameters. There are several ways of approaching this, each of which may have different inherent assumptions. Examples include placing more emphasis on certain measurements, or placing greater dependence on the quality of modeling for a certain component. For analyzing reheat performance, P7 and P161 are used as 'anchors' in the ANSYN process. In reconciling test data with the model, care must be taken to reasonably account for uncertainties. In this example, bypass stream pressure loss coefficient is used as a 'dump'.

### ***Potential Benefits***

An accurate model is essential to derive open-loop reheat schedules. Schedules must be set to reflect the uncertainty in the model. Consequently the better the model, the smaller are the margins that are required to guarantee thrust for the worst engine and to guarantee a safe fan operating point. Using an accurate model to derive schedules can decrease expensive altitude testing time, and help reduce program time-scales.

### ***Cited Example***

- Kurzke, J. and Riegler, C., "A Mixed Flow Turbofan Afterburner for the Definition of Reheat Fuel Control Laws", May 1998, Design Principles and Methods for Aircraft Gas Turbine Engines, RTO-MP-8, February 1999. [\[2.31\]](#)

The main idea of Analysis by Synthesis (ANSYN) is to match an engine simulation model to test data automatically. Scaling factors are applied to the component models, to close the gap between the calculated and the measured component performance. For example, corrected spool speed and specific work give the operating point of a compressor on its map. Both can be derived from measured data. The corrected mass flow and the efficiency in the model are calculated using the compressor map and corrections for Reynolds Number effects. The scaling factors then result as the particular ratio of measure to calculated value. Illustrated in [Figure 2.42](#) is an example of the scaling factors for the HPC efficiency versus corrected HPC spool speed resulting from the analysis of many scans. The small scatter of the scaling factor shows that the HPC efficiency model accounts for the most important physical phenomena

and may be used for high quality performance predictions over a wide range of engine ratings and flight conditions.

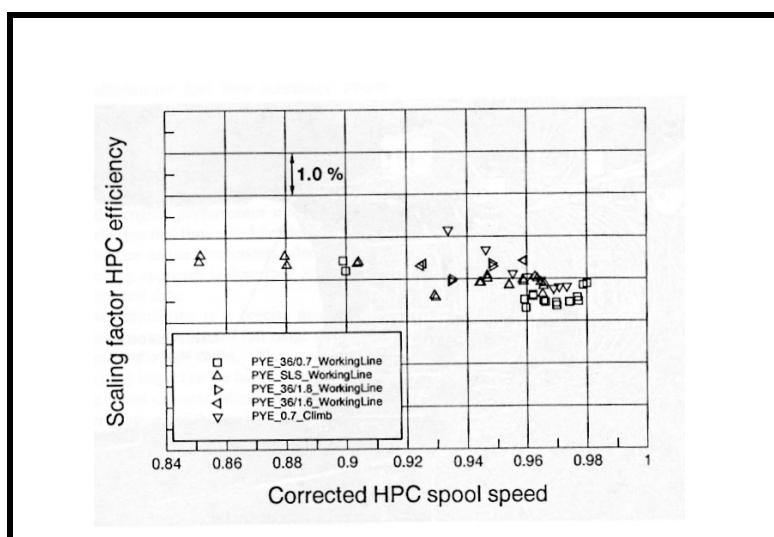


**Figure 2.42: Component Efficiency Scaling Factor, Found from Engine Test Analysis.**

The control schedules for a mixed flow turbofan with an open-loop afterburner fuel control system, can only be derived from a performance model of the engine. Any inaccuracy of the simulation must be covered by safety margins in the afterburner fuel flow schedules. Poorly designed fuel schedules can cause a loss of thrust and may require additional turbine inlet temperature clearance for compensation. The key to a good simulation is a precise model of the convergent-divergent nozzle over the full range of pressure ratios encountered during flight. The nozzle flow characteristic has a big impact on the fan surge margin, while understanding the thrust characteristic is a prerequisite for optimizing the performance of the engine.

## ***Limitations of Chosen Modeling Technique***

The modeling technique described is 0-D and steady state, although the technique is easily extended to include dynamic terms. Fuel staging and mixing, and geometry effects are not taken into account explicitly in the modeling. Although not a limitation, care must be taken to account for the modeling uncertainties in a realistic and reasonable manner in the calibration method. A good understanding of the nozzle performance over a full range of nozzle pressure ratios is essential to be able to understand and predict engine thrust characteristics.

## **2.1.4 Post-Certification and In-Service Support Synoptics**

Life cycle costs have emerged as a primary factor in the design of gas turbine powerplants. The recognition of repairs and rebuilds and lost availability as major recurring costs suggests that some means of getting more usefulness from the engine is desirable.

The concept of on-condition repair and maintenance has emerged as a common ownership philosophy for both military and industrial equipment. Such a philosophy can only be put into practice if the tools to accurately assess engine condition can be provided. Furthermore, these tools must be tailored to the needs and capabilities of the personnel who must use them.

The analysis of performance data has remained complex. If one considers the typical military fighter engine with at least two and often three elements of controllable variable geometry in addition to control

of fuel, it becomes apparent that old simple ‘rules of thumb’ in diagnosis will not apply. This state of affairs suggests that analytical methods must be sought to provide a more systematic approach to engine fault diagnosis. The complexity of modern engines is such that no single failure or degradation mode can be described as dominant. While a number of failure modes such as Low Cycle Fatigue (LCF) are purely mechanical phenomena, a great many others directly affect engine performance and are best diagnosed through performance measurements.

#### 2.1.4.1 The User Environment

The user environment consists of various activities. Each of them provides an opportunity for the use of EHM (Engine Health Monitoring) methods but each, at the same time, has different requirements. These activities can be categorized as *flight line*, *engine repair shop* and *engine test cell*, and are briefly discussed in the following.

The *flight line* is primarily the domain of the aircraft and engine technicians. It is organized around the concept of a quick fix. Engine designers make every effort to make line replaceable units (LRUs) accessible and easy to change. In this environment, the technician is compelled to work with some combination of pilot reported problems and whatever recorded limit-exceedance or alarm information is available. The latter implies that the aircraft has been fitted with a flight recorder, which is usually the case for modern aircraft.

Time is of the essence at the flight line. The technician typically has only one or two hours in which to effect a repair and put the airplane back into service. Based on the available information, backed up with on-wing inspections, the technician makes a preliminary diagnosis and conducts whatever tests he deems necessary, to substantiate his hypothesis. It is also common practice to begin simply by changing a suspect LRU. On-wing testing follows this and, if successful, the aircraft is released to fly. If unsuccessful, the technician may elect to replace another LRU and try again, or he may elect to replace the entire engine and send it to the engine repair shop for more involved repair. In either case, the flight line actions trigger demands on spares and consume engine life during on-wing tests.

From an EHM requirement viewpoint, a number of things are clear:

- Unless the problem is quite obvious, the flight line repair is a process with very poor diagnosis success rates.
- Diagnosis must be quick and very convenient for the technician. The technician is not necessarily an engineer.
- Diagnosis must focus on those problems for which exchanging an LRU will affect a repair or else clearly indicate the need for engine removal.

The *engine repair-shop* is, in effect, the nearest available repair area that provides service to the flight line. This service consists of stripping the engine and replacing life expired parts (scheduled repairs) and dealing with all engines removed from the aircraft because a quick fix could not be effected at the flight line (unscheduled repairs).

The repair-shop management is judged on its ability to complete repairs in a timely manner. This, in turn, is quite dependent on a timely flow of the right spare parts at the right time. Bearing in mind the high cost of spare parts, this translates to ‘just in time’ spares management. Clearly, the key to success in this endeavor is the accurate prediction of the workload and the type of work in the engine shop.

The unscheduled engine repairs sometimes represent 50% or more of the engine repair-shop workload. Without adequate means of assessment and prediction, this workload will appear quite suddenly and will require large spares inventories and many personnel. It is, therefore, evident that some means of providing early warning of the arrival of unscheduled engines would have a very substantial impact on the entire

## APPLICATIONS

---

range of concerns of the engine repair shop. From an EHM requirement viewpoint, the engine repair-shop is quite different from the flight line:

- The time frames of concern are substantially longer, making parameter trending very useful.
- A more sophisticated level of diagnosis is possible with the support of engineering personnel.
- Proper data management offers a feed-forward information loop to the flight line.
- The essence of EHM at the engine repair shop is proper planning of resources.

The **engine test cell** is an expensive facility provided for the primary purpose of ensuring safety. The engine undergoes a ‘go-no go’ test, which checks the engine in accordance with the repair level. Since the express purpose of the test is to ensure flight safety, two major aspects of engine operation are examined. First, the mechanical integrity of the engine is established. This may include possible hydraulic and oil leaks, loose bolts and vibration levels. Secondary, the static and dynamic performance of the engine is examined. These tests consist of establishing throttle settings and maneuvers and then recording speeds, pressures, and temperatures, etc. for purposes of comparison with acceptable standards of performance.

During the course of the tests, allowable control adjustments are made and the engine is re-tested. If the engine passes all tests, it is declared ‘ready for installation’. If, however, it fails and subsequent adjustments do not cause it to fall within acceptable limits, it must be partially or completely stripped and reworked. The engine test itself is quite straightforward. Analysis of the data follows the normal practice recommended by the manufacturer. However, the diagnosis used in current test cells is little better than that available on the flight line. The requirement for diagnostic techniques in the test cell is self-evident:

- Test cells provide a larger complement of engine measurements than most flight recorders.
- Diagnosis requirements are similar to those for the flight line, progressing from simple adjustments to the replacement of LRUs while the engine is on test.
- Test cell diagnosis can and should progress to fault identification deep within the engine. It can help to eliminate unnecessary testing and direct attention to repairs.
- Data obtained during engine testing will provide quantitative assessment of the available engine margins. These data are important in establishing a first estimate of when the engine will next need work, and for what reason.

### 2.1.4.2 The Need for Engine Models and User Requirements

There are essentially two primary factors that suggest that computer-modeling techniques are the only practical approach to the development of reliable diagnostic techniques. These are:

- System complexity; and
- Time.

Concerning complexity, it is worthwhile drawing an analogy with control systems development. For a modern engine, an engine control system will typically consist of about 15 – 20 sensors and 2 – 4 actuators. Including engine start-up and limit exceedance protection, the complete control package will comprise 40 – 50 interrelated functions for which design tools are well developed. A modern EHM system relies on the same sensor configuration as the control system with perhaps a few additional measurements such as fuel flow. The process of diagnosis is expected to segregate parameter deviations caused by engine degradation, and simultaneously to distinguish between faulty engines and faulty control units. This suggests at least a doubling of system complexity. It also suggests that the models used to understand engine behavior will be useful to design diagnostic algorithms.

The second major reason that computer-modeling methods are essential to the successful development of diagnostic algorithms is time. The job at hand is to provide a method of recognizing, with minimum effort, the existence of any of the common faults through the measurement suite available on a modern engine. This gives the user the benefits of maintenance downtime and cost reduction, and increases operational service time.

It is appropriate at this point to consider the requirements for a successful mathematical model, bearing in mind that the model should be kept as simple as possible, consistent with the needs of the particular user. The main important requirements from a model include:

**Accuracy** – The prime requirement of any model is that it should accurately represent the behavior of the engine over its complete running range and flight envelope.

**Flexibility** – The simulation must be capable of handling all the obvious requirements, such as scheduled accelerations and the operation of variable geometry devices. It must also be capable of dealing with situations that were not anticipated initially, such as failures that have led to an incident.

**Credibility** – The simulation must be readily understandable to performance, development and management engineers who are not simulation specialists. For this reason, the simulation should produce results in a form similar to a real engine and should use commonly available data.

**Availability** – Once the simulation has been verified it must be capable of being rapidly brought into use whenever required, without needing lengthy setup times.

**Reliability** – A high degree of reliability and repeatability is clearly essential. The simulation must be easily checked to ensure that it is functioning correctly. This is especially important for complex engine simulations.

**Supporting Documentation** – The program supplier should deliver the User's Manual with the program. The User's Manual shall stand-alone and be independent of previous User's Manuals. SAE AS681, [2.9], has standardized information that should be included in the User's Manual.

### **2.1.4.3 Engine Health Monitoring and Fault Diagnosis**

#### *2.1.4.3.1 Application Aspects of Monitoring System*

In the practical world of engine support, a system designer must ultimately satisfy the engine technicians. These people have no patience with systems that do not provide them with a useful tool. Thus there are really only two major ingredients for success in this endeavor:

- A user friendly software package that can implement the concepts in use; and
- An effective fault identification system.

The former requirement recognizes that most technicians are not specifically interested in computers and will use them only if they provide an advantage. The latter requirement reflects the inevitable impatience of the same group with systems that provide wrong answers.

In general, the application systems fall into three categories:

**Assessment of Periodic Engine Tests** – The most fundamental element of the performance monitoring system is the ability to assess data obtained from periodic inspection. In the aircraft application, this test is conducted either on the wing or more commonly in an engine test cell after a repair. The measured and

## APPLICATIONS

---

corrected health index values are presented along with their respective baseline values. Parameters that exceed pre-determined limits are assigned a 'status' value that is dependent on the magnitude of the performance deviation. The status indicators are then related to potential component problems and a written recommendation is presented to the operator for decision or action purposes. It is noteworthy that the test cell operator still exercises final judgment, but is guided in his decision by the recommendations provided by the diagnostic system.

***Trending of Health Indices*** – A working trend package consists of the ability to collect data, compute the health indices and to present deviations in these health indices as a function of time. Once the data falls outside preset limits a flag is set by the software, indicating to the operator that a fault is developing. The fault type is identified and, where possible, the rate of progression is tied to a number of hours before action must be taken. The ability to provide some early warning of pending faults is critical to the success of a monitoring system. Despite the obvious statistical and operational variation, a health index only becomes truly worthwhile when it provides the operator with some advance warning of the event.

***Dynamic Event Analysis*** – Intuitively, operators of gas turbines are aware that the first signs of engine distress are most likely to occur during transients. Under these conditions, the operating point of the compressor is traversing a path relatively close to surge. The temperatures are typically 100 to 200 K hotter than steady-state conditions. Similarly, the rate of growth of the casing is different from the rotors, which changes blade tip clearances, seal clearances, etc. These physical effects are difficult to quantify. Under these conditions, dynamic events such as compressor stall and over-temperature occur. These events afford an opportunity for performance analysis to be used, provided reasonable data records are available.

The availability of transient information extends the range of possible health indices. These can include such factors as rates of change, maximum values or specific fuel control parameters. However, the process of qualifying any of these as a valid health index is identical to those for steady state analysis. In general, the development of methods to assess problems related to dynamic events has proven to be remarkably productive. One must realize that the maintenance crew has to deal with the event. Without diagnostic tools, they normally resort to changing field replaceable units such as fuel controls until the problem appears to go away. This is unsatisfactory at best and usually leads to unnecessary expense driven partly by changing the wrong component and partly by the high costs of testing various attempted fixes.

### 2.1.4.3.2 *Diagnostics and its Usefulness for the Engine User*

Diagnosis<sup>1</sup> of a mechanical condition is the grasp of knowledge of the condition of parts of a machine, from information coming to the engine exterior, without dismantling the machine or getting direct access to the parts. The field of engineering science covering the techniques for achieving a technical diagnosis is called *diagnostics*.

The aim of diagnostics is to detect the presence and identify the kind of faults appearing in a machine. But what do we mean by 'fault'? A fault is a condition of a machine linked to a change in the form of its parts, or in its way of operation, from what the machine was originally designed for and was achieved during its initial operation. A fault manifests itself in the following ways:

- Change of the geometrical characteristics of parts of a machine. Such a change is inevitably linked to all commonly experienced faults, as for example when a part is broken or deformed.

---

<sup>1</sup> Diagnose is a Greek word, literally translating to 'know through', and actually meaning gaining knowledge about something that is not obvious but lies behind some barrier preventing direct access. Diagnosis is the outcome of the mental process of diagnosing. These terms have been used extensively in medicine, because humans are a typical case of systems which do not allow direct access to their interior. If one has to conclude about the condition of parts inside the human body, one has to do so from observations from the outside. The doctor has therefore to *diagnose* the causes of an illness from the external symptoms, or at least by observations which are made without getting direct access to the interior of the body.

- Change of the integrity of the material of engine parts. Typically, such a problem is the occurrence of cracks inside the material, which are not associated with any geometrical change but can nevertheless result in catastrophic consequences.
- Change of operating condition and entry to regions of unsafe operation. Although this is a situation in which there is no geometry or material problem, such problems may quickly appear as a result of bad operation. Stalled operation of a gas turbine is a situation, which can be characterized as faulty operation.

An engine free of faults is characterized as a 'healthy' engine. An engine is usually healthy when it is initially manufactured.

A distinction must be made between Machine *Diagnostics* and *Inspection*:

**Machine Diagnostics** is a procedure applied to a machine in operation and does not require that the machine is either stopped or disassembled.

**Inspection**, in contrast, refers to a procedure that involves direct access to the item of interest. Usually inspection requires either stopping machine operation or even dismantling it. Obviously, external parts of a machine can be inspected while it is in operation. While in order to inspect its internal parts, access to its interior must be gained, requiring engine stoppage in almost all cases.

The fact that diagnostic techniques provide information from a running engine is important for two particular reasons:

- Information is gathered while the engine is in operation. This is vital for engines in the process industries or energy production, as they must run without interruption for long periods.
- Incipient failures may be detected while running. This will lead to taking action necessary to prevent a catastrophic failure, which might follow.

#### 2.1.4.3.3 Basic Principles of Performance Diagnostics

Diagnosing the presence of a fault in an engine is based on the following principle:

- A change in the condition of a part of an engine will produce a corresponding change in the parameters that describe its functioning. Measurement of the changes of parameter values from their values for 'healthy' operation can in principle lead to the alterations in the parts that caused this change.

A typical example of the application of this principle by humans is the diagnosis of an abnormal condition by a machine operator from the sound produced by the machine. The operator is familiar with the sound produced by a machine in intact condition. When this sound changes, the operator knows that something has changed with the machine. If he has sufficient experience, he is able to determine what has occurred to cause the change in sound.

A diagnostic decision is usually taken at two levels:

- Detection of the presence of a fault: At this level the expert must judge whether the machine is healthy or it is suffering from a fault. Note that *fault* here also accounts for a general deterioration.
- Identification of the fault: This action specifies fault characteristics, namely location, kind and severity. This task is usually more difficult to achieve than the previous one.

In order to build a system, which can perform a diagnosis, the following stages are necessary:

## APPLICATIONS

---

- Get the basic mechanical and operational data for an engine. The full engine layout and details, and the values of various parameters of operation, for example parameters describing vibration, performance, and mechanical speed, for a healthy state, must be known. This information describes the reference condition of an engine.
- Measure the values of the variables that are necessary for describing the operating condition of an engine. The measured variables must be sufficient for producing all the information needed for diagnosis.
- Reduce the measured values to others having diagnostic value. For this task, an appropriate set of programs, which includes data reduction but modeling ones as well, must exist.
- Derive diagnostic information by combining the reduced values. This information can be for example, an array of values of differences from baseline, a parameter of a best fitting technique, a point in a feature space or other, according to the method which is followed.
- Compare the diagnostic information to existing knowledge on failures and their symptoms, and conclude about the existence of a failure. Application of this step requires previous experience, in the form of a database, and decision rules, of the symptoms of the failures that can be detected.

These stages can be followed when some kind of measurement data can be obtained from an engine. Depending on the kind of data, the techniques for the individual stages differ, as do the diagnostic techniques. An example is vibration diagnostics; namely diagnostics based on vibration measurement data.

Techniques based on data from measurements of aerothermodynamic quantities and engine performance parameters are known as *performance diagnostics* techniques. Engine performance models support such techniques in different ways, as will be discussed in detail in the following sections.

### 2.1.4.3.4 The Role of Performance Models in Performance Diagnostics

Performance models can support different aspects of diagnostic techniques. They can serve for producing baseline data and fault signatures, while they provide information supporting the set-up of a diagnostic procedure. A brief description of these tasks follows, while the role of performance models will be illustrated further when various diagnostic techniques are presented.

#### 2.1.4.3.4.1 Derivation of Baseline Information

First, important pieces of information that can be derived by a performance model are the values of engine performance variables and parameters for the entire operating range of a ‘healthy’ engine (*baseline* values). This information serves the following purposes:

- It provides the baseline values for measured quantities or diagnostic parameters; and
- It establishes therefore the reference for the diagnostics.

Variations of diagnostic parameters for reasons other than faults can be studied. A typical example is the establishment of the expected variation of such parameters for different operating conditions. A change in the operating condition causes variations, which can lead to false conclusions if attributed to faults.

#### 2.1.4.3.4.2 Derivation of Knowledge Bases

Fault signature is a general term, referring to the differentiation caused by the presence of a fault. A particular fault results in changes of parameters in a certain way. The set of these changes is the *signature* of the fault. Fault signatures must be available in order to identify the faults. The existence of a database of fault signatures is an essential part of a diagnostic system. Building up such a database is a difficult task. The main alternative approaches that can be used are:

- A posteriori observations of failures occurring in operating engines;
- Observations from experimental investigations with implanted faults, on the engines of interest; and
- Physical reasoning, which can be materialized through computational modeling and simulation of faults.

Approach a) may prove too costly, since occurrence of some of the failures can be catastrophic and engine users would have preferred it not to happen. On the other hand, if failures occur in an uncontrolled manner it is not certain that all the necessary information can be collected for constituting the signatures. Finally, it is possible that long periods may be needed before a reliable knowledge base, with a reasonable coverage of fault cases, is assembled. These drawbacks can be overcome by setting up experiments, as in approach b). Faults representative of realistic cases expected in field operation are implanted in engines and their influence on engine operation is studied. While they provide information that is useful for particular engines and faults with specific characteristics and severity, such experiments are still very costly.

An efficient alternative way of producing fault signatures is via the application of approach c); namely by computation. For this approach, the quantities employed for diagnosis are obtained by modeling both *healthy* and *faulty* operation, which are combined for the derivation of the signatures. The computed quantities and corresponding signatures should be obtained in direct correspondence to the actual measured quantities on an engine and the subsequent processing applied to the experimental data.

#### 2.1.4.3.4.3 Derivation of Background Information

Performance models can be further used to derive information useful for setting up a diagnostic system or data to support diagnostic techniques. An example of the former type of application is the assistance they can provide, for the selection of quantities to be measured and the measuring locations, when setting up a diagnostic system. The quantities have to be selected in such a way that they are sensitive to the presence of faults. The same holds for the location at which the measurement is effected. Certain locations are more suitable than others are. Calculation of influence coefficients for linear gas-path analysis methods is an application that supports diagnostic techniques (see the following section). Models are also used for measurement evaluation. Some typical applications are the checking of the consistency of test data and the generation of *virtual* measurements for sensor validation.

#### 2.1.4.3.5 Methods for Engine Performance Diagnostics

##### 2.1.4.3.5.1 Methods Based on Linearized Representation

Gas Path Analysis (GPA) methods deal with the study of the fluid (gas) aerothermodynamic changes, as it flows through the different parts of a gas turbine. The idea on which such methods are based is that any change, in the performance of the components that are in contact with the gas path, will result in a change of the aerothermodynamic parameters. If this second change is traced, the original cause can, in principle, be detected. This methodology is still widely used today and discussion about formulations currently in use can be found at Doel [2.32 and 2.33], Urban and Volponi [2.34]. In the following the main principles of this formulation are described.

Aging or specific engine failures reflect on engine performance deterioration, and result in deviations of the values of measured performance variables (pressure, temperature) from those corresponding to healthy operation (baseline values). Performance deterioration is usually represented by a change in value of some characteristic component performance parameters (e.g. efficiencies, flow capacities). The correspondence between the set of deviations of the measured variables from the baseline and the set of component

## APPLICATIONS

performance parameter deviations, constitutes the standard basis for the conventional GPA methodology, introduced by Urban, [2.35]. The ordinary mathematical formulation of the above correspondence is expressed by the well-known linear equation, which is valid at each particular operating point.

$$\Delta y = C \times \Delta x \quad \text{Eq. 2-1}$$

$\Delta y$  is a  $n \times 1$  vector of measured deviations. Each element of this vector is defined as

$$\Delta y_i = y_i - y_{i0}$$

Where  $y_i$  is the value of a measured quantity on the engine under study (e.g. a pressure or a temperature) and  $y_{i0}$  is the value of the same quantity on a *healthy* engine.  $\Delta x$  is a  $m \times 1$  vector of component parameter deviations. Each element of this vector is defined as

$$\Delta x_j = x_j - x_{j0}$$

Where  $x_j$  is the value of a component parameter on the engine under study (e.g. an efficiency) and  $x_{j0}$  is the value of the same quantity on a 'healthy' engine.  $C$  is an  $n \times m$  matrix, called the influence coefficient matrix. The elements of this matrix (called the influence coefficients) are defined as follows:

$$C_{ij} = \delta y_i / \delta x_j$$

The system of equations (**Eq. 2-1**) can be used to estimate deviations in component parameters from measurement deviations, when the number of unknown component parameter deviations equals the number of available measurement deviations namely when  $m = n$ . The solution of the system (**Eq. 2-1**) is:

$$\Delta x = C^{-1} \times \Delta y$$

The measurements used in this equation contain unavoidable noise. This fact can be taken into account to produce some formulae that give a better estimate. For example, the following relationship gives the weighted-least-square estimate of  $\Delta x$ .

$$\Delta x = M^{-1} C^T R^{-1} \Delta y$$

$R$  is the measurement error covariance matrix, and  $M$  is the so-called information matrix, defined as:

$$M = C^T R^{-1} C$$

Another possible estimate is the minimum variance Bayes estimate given by the relation.

$$\Delta = [P_0^{-1} + C^T R^{-1} C]^{-1} C^T R^{-1} \Delta y$$

when  $P_0$  is the a priori covariance matrix of  $\Delta x$

This formulation has been appropriately extended to include sensor errors.

In an effort to develop an effective diagnostic system based on GPA, practical limitations are encountered. These limitations appear when, in order to increase reliability on performance estimation and to isolate malfunctioning components of the engine, one has to increase the volume of information concerning its state. The usual approach to meet this requirement is the increase of the number of measured quantities, by installing additional sensors. In the case of engines under development, the main restriction is the cost of the additional instrumentation. In already existing engines, one additional restriction is faced: the user cannot undertake installation of new sensors, unless the engine manufacturer allows this.

Stamatis and Papailiou [2.36] have introduced a method of overcoming these practical limitations, under the name of Discrete Operating Conditions Gas Path Analysis, DOCGPA. This method uses the ignored amount of independent information coming out of measurements realized by the already existing sensors, at different operating points. To make this additional information useful, engine performance models are necessary. Such models must correlate correctly the engine observed behavior with the ‘health’ condition of its components, at all operating points. In the following, we will present how engine performance computer models can be used for providing the data needed by DOCGPA in order to perform fault diagnosis, with application to particular engines.

In order to determine the  $\Delta x$  vector, we have to solve the system equation (**Eq. 2-1**). A necessary condition for the solution of the system is  $m \leq n$ , i.e. the number of measured quantities must be greater or at least equal to the number of the unknown parameters. If however we consider that the deviations  $\Delta x$  remain the same for different operating points of the engine, we can take advantage of the non-linearity of engine performance characteristics in order to overcome this constraint. In fact, any gas turbine configuration may be considered as a system for which the measure output  $y$  is a function of the system parameter vector  $x$  and the input vector  $u$ .

$$y = G(x, u) \quad \text{Eq. 2-2}$$

The vector  $u$  determines the conditions that define the operating point (ambient conditions, load, control settings, etc.). Linearization of equation (**Eq. 2-2**) with respect to  $x$  leads to the equation:

$$\Delta y = C(u) \Delta x \quad \text{Eq. 2-3}$$

The conventional formulation of the GPA (**Eq. 2-1**) is simply the application of the equation (**Eq. 2-3**) at a particular operating point. If we apply equation (**Eq. 2-1**) at  $k$  discrete operating points we can write with the assumption of unchanged  $\Delta x$ :

$$\begin{bmatrix} \Delta y_1 \\ \vdots \\ \Delta y_n \end{bmatrix} = \begin{bmatrix} C_1 \\ \vdots \\ C_n \end{bmatrix} \Delta x \quad \text{Eq. 2-4}$$

where

$$C_i = C(u_i), i = 1, k$$

We see that we now have  $k \times n$  measurements while the unknown parameters remain the same. If the rank of the augmented coefficient matrix (now containing  $k \times n$  rows) is greater or equal to  $m$ , **Eq. 2-4** can then be used to determine  $\Delta x$ . In general, this condition is fulfilled for the case of a jet engine, because of the non-linear dependence of the influence coefficients on the engine operating point. This will be shown later. By choosing therefore a suitable number of discrete operating conditions, we can increase the number of equations in (**Eq. 2-4**), allowing thus the determination of the desired  $m$  elements of  $\Delta x$  even though  $n < m$  (parameters to be determined are more than the measured variables). The final equation is:

$$\Delta x = M_k^{-1} \Delta C_i^T R_i \Delta y_i \quad \text{Eq. 2-5}$$

$$i = 1$$

where  $M$  is the so-called information Matrix  $k$

$$M_k = \Delta C_i^T R_i^{-1} C_i \quad \text{Eq. 2-6}$$

$i = 1$

and  $R_i$  is the typical covariance matrix of the measured variables.

### 2.1.4.3.6 Performance Model and Influence Coefficients Matrix Calculation

The elements of the influence coefficient matrices  $C$  at each operating point, can either be defined analytically (for example, Urban, 1969, [2.35]), using engine parameter interrelationships, or by using an engine performance simulation code, if it is available. In this latter case,  $C$  can be produced in the following way: each independent parameter is sequentially perturbed and the corresponding percentage changes in measured variables are recorded. The derivatives involved and the influence coefficients are then numerically evaluated. The procedure is schematically shown in **Figure 2.43**.

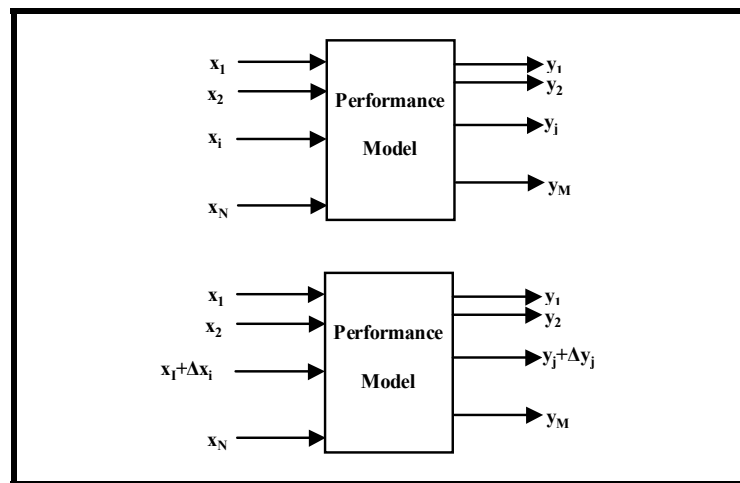


**Figure 2.43:** Calculation of Influence Coefficients using an Engine Performance Model.

The advantage of such a procedure is that all secondary effects, such as bleeds and power extraction are inherently taken into account, without the development of complicated analytical expressions. On the other hand, if one possesses a modular computer model allowing simulation of many types of engines, the technique can be applied directly, without the need to develop a new set of analytical expressions for each case. Last but not least, there is no need for simplified assumptions (for example, choked nozzle operation), which may restrict the application of Gas Path Analysis in a limited region close to full power operation.

$$\frac{\partial y_j}{\partial x_i} \approx \frac{\Delta y_j}{\Delta x_i}$$

Using this procedure, we can calculate the elements of the influence coefficient matrix at different operating points. We also have the possibility of producing and adding the information needed by equation (5) for fault diagnosis. At this point, we must emphasize the requirement for high accuracy in the calculation procedure. In fact, the corresponding performance model must be able to predict accurately the engine behavior over the whole operating range, in order to compute with acceptable accuracy the influence coefficient elements. It should be mentioned that generalized engine models, especially when built by the engine user, do not always fulfill this requirement. In order to overcome these disadvantages the models should be customized to the particular engine, as discussed in the following section.

#### 2.1.4.3.7 Models with Inherent Diagnostic Capability (Adaptive Models)

A feature of component-based computer simulation techniques is the requirement of component maps. The reliability of the predictions is highly dependent on the accuracy of these maps. It is a well-known fact that, due to assembly and manufacturing tolerances, different engines of one particular series exhibit small differences in their performance. Such differences can be of importance during the condition monitoring procedure, since deviations from baseline constitute the fundamental point of the procedure. A second known fact is that disassembly and rebuild of an engine can cause small shifts in its performance. Such shifts cannot be tracked by existing performance models. Advantages offered by this method are:

- It can accompany every individual engine, giving the possibility of a very accurate simulation of its performance.
- If the component maps are only approximately known, the exact 'on engine' maps can be reconstituted by employing engine Gas Path parameter measurements.

Although the principles of such a methodology are discussed elsewhere, the formulation of an adaptive model is briefly described here to provide the basis for understanding diagnostic applications.

##### 2.1.4.3.7.1 Formulation of an Adaptive Model

In order to build a performance model, a gas turbine is viewed as an assembly of different components (modules). Each component is identified according to the kind of thermodynamic process it accomplishes. The engine cycle at any operating point is defined by the values of the thermodynamic properties of the working fluid at stations at the inlet and exit of the components. If  $\underline{Y}_{IN}$  is the vector of independent variables at the inlet and  $\underline{Y}_{OUT}$  the corresponding vector at the exit, for each module there exists a relation of the form:

$$f(\underline{Y}_{IN}, \underline{Y}_{OUT}) = 0 \quad \text{Eq. 2-7}$$

This relation is usually derived through the conservation laws for mass, energy, and momentum, and from existing experience in component operation. It can be an analytic relation, possibly including empirical constants (e.g. duct pressure loss), or a set of curves (e.g. compressor map). Compatibility of component functioning imposes 'matching' conditions, as for example power balance and speed between turbines and compressors. A set of simultaneous equations, which have to be satisfied by the fluid parameters, is thus formed. Solution of this system for a single operating point gives the full cycle details. The solution to the system of equations is obtained numerically, since they are highly non-linear.

The approach usually followed is first guess the values of some suitably chosen variables  $v_i$ , and then explicitly solve the equations, giving the full set of parameters. Error terms are then formed from the differences of quantities calculated from different equations:

$$e_i = |P_{i1} - P_{i2}| \quad \text{Eq. 2-8}$$

where  $P_{i1}, P_{i2}$  are the values of a parameter  $P_i$  calculated by two different equations.

The data that are given as input to a model can be divided into two types:

- I** – Data related to the particular operating condition (for example ambient conditions, fuel calorific value, speed and load), which define the engine operating point.
- II** – Data related to the performance of the engine components, corresponding to equation (1), as for example, the compressor and turbine performance maps.

## APPLICATIONS

For a given set of type-II data, all cycle details and performance parameters are uniquely defined for a choice of operating condition, through a set of type-I data. This means that, once the component data are specified, for each operating point we have a unique set of calculated parameters. If these data do not represent exactly component operation of a particular engine, then the predictions will differ from actual measured values. (It is noted that type-II data are usually not available to the user, while for an engine manufacturer, the available data usually represent an average engine.) It is useful to understand why an available set of maps may not lead to accurate predictions for a particular engine. The maps may differ from the ones of a specific engine depending on their origin:

- Maps measured on isolated components – such maps may differ from actual ‘on engine’ maps, due to interactions with other components or different operating environments (e.g. heat transfer effects), inlet non-uniformity of pressure and temperature, etc.
- Maps predicted by computer programs – such maps may differ from real maps due to insufficient modeling capabilities or lack of the necessary physical data.
- Maps measured on a different engine – they may be different because of engine-to-engine dissimilarities. Such maps are sometimes difficult to measure because of practical difficulties, such as high temperatures of the hot components.

### 2.1.4.3.7.2 Model Adaptation

The performance maps of each engine component are derived from the functional relations between its characteristic performance parameters, of the form of **Eq. 2-7**. These relations can be in an analytic form or in the form of a chart. If a particular parameter has a value  $X_{\text{ref}}$  on the reference map and a value  $X_{\text{act}}$  on the actual ‘on engine’ map, then the correspondence between the two can be expressed by means of a modification factor MF defined as follows:

$$\text{MF} = \frac{X_{\text{act}}}{X_{\text{ref}}} \quad \text{Eq. 2-9}$$

It must be noted here that modification factors can be introduced either as *scalars*, multiplying the reference value as above, or as *adders*, namely values that are added to the reference value. Knowledge of the reference performance map and the values of MF offers the possibility of reproducing the actual maps. Care must be taken however in the way that these factors are introduced. They must be consistent with existing representation of the maps and the set of equations used. For example, in the case of the compressor, we can employ the following definitions:

$$\text{MF}_1 = \frac{Q}{Q_{\text{ref}}} \quad \text{MF}_2 = \frac{\eta}{\eta_{\text{ref}}} \quad \text{Eq. 2-10}$$

The value given to any component parameter used by the model is thus introduced as a product:

$$X_{\text{act}} = \text{MF} \cdot X_{\text{ref}} \quad \text{Eq. 2-11}$$

We see that a value of a component parameter is now defined by means of two numbers: its reference value and the value of the corresponding modification factor. When the reference values are available, let's see how the values of the modification factors can be determined. Having chosen a set of modification factors values  $\text{MF}_i$ , it is possible to define an optimization problem, which allows the determination of their values, needed for adapting the maps.

In a straight engine model the solution of the equations for a particular operating point, proceeds by guessing values for some variables  $v_i$  and calculating error terms  $e_i$ , **Eq. 2-8**. Besides the parameters

necessary to form the error-term, values of all cycle details are calculated. They include the values of the quantities measured along the gas path during experiments. For any measured quantity  $Y_m$  there is a corresponding calculated  $Y_c$ . We then form a cost function FC as follows:

$$FC = \sum_{i=1}^M a_i e_i^2 + \sum_{i=1}^N b_i (Y_{ci} - Y_{mi})^2 \quad \text{Eq. 2-12}$$

where  $M$  is the number of error terms of the model,  $N$  is the total number of measurements and  $a_i$  and  $b_i$  are weight coefficients depending on both measurement and desired model accuracy. If modified maps are introduced into the model, by means of a particular set of values for  $MF_i$ , the value of FC obtained, will be a function of the original guess for  $v_i$  and  $MF_i$ :

$$FC = FC(v_1, v_2, \dots, v_M; MF_1, MF_2, \dots, MF_N) \quad (7)$$

The set of independent variables that minimizes the value of this function to zero satisfies the matching conditions for the engine, while it ensures that the measured and predicted quantities are the same. A set of values for the modification factors is produced for the particular operating point. We get thus a set leading to an optimal reproduction of measured quantities, through the simulation model. The flow chart of the procedure is depicted in **Figure 2.44**. Covering the entire operating range of the engine will give the full set of MFs needed.

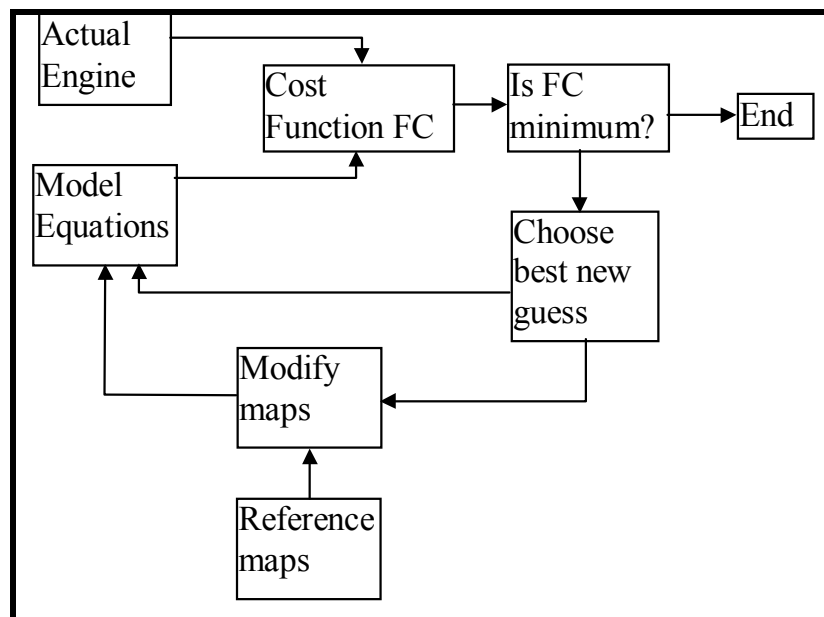


**Figure 2.44: Flowchart of the Adaptive Modeling Procedure.**

An engine model which only solves for cycle, namely it zeroes the first of the sums of **Eq. 2-12**, will be termed a *straight model*. A model that allows adaptation of component parameters to match the performance of an engine, namely it minimizes the function FC of **Eq. 2-12**, will be termed an *adaptive model*.

The method described above can incorporate a variable number of measured quantities. The number of modification factors that can be determined changes accordingly. This method can be characterized as ‘internal’ to the model: the adaptation procedure is embedded in the performance model itself, and the adaptation is performed simultaneously with the solution of the engine-matching problem. Although the

## APPLICATIONS

---

procedure in this form offers an effective method from a computational point of view, it requires that the model be built for the particular engine studied.

The adaptation can also be done ‘externally’, by requiring the minimization of the two sums of equation (6) separately. In this case the minimization of the first sum is actually achieved by the straight model. Such a procedure has the disadvantage of requiring larger calculation time. It has the advantage however, that since it is external to the straight model, it can be coupled very easily to straight models that a user already possesses. An existing engine code can be employed as it stands, and the adaptation procedure is performed by interaction with the code without intervening in it, but only through its input and output data. This allows the development of adaptive models on the basis of available generalized jet engine performance simulation codes and gives the possibility of producing adaptive models for a large variety of aeroengine configurations.

### 2.1.4.3.7.3 Using an Adaptive Model for Fault Diagnosis

The structure of the adaptive model allows the direct application to Engine Condition Monitoring (ECM). Application can be done in two different ways:

- Fault Simulation; and
- Fault Detection.

Simulation of faults is achieved by introducing deviations in component parameters (as they would be caused by the presence of a fault) and producing the resulting deviations in measured quantities (measurement fault signatures). Of course, such a possibility exists already with a straight model, but the improved reliability of the adaptive model gives more accurate results.

The determination of the modification factors can also be used for detecting faults either in the engine components or in the sensors. If for example the efficiency of a component drops this will show up in a change of the value of the corresponding modification factor and can, thus, be detected. If on the other hand a sensor fails, its reading will influence the calculated values of MFs.

To employ the method for diagnostic purposes the procedure to be applied is:

- The adaptive modeling is applied to the engine in its healthy state.
- The calculated Modification Factors and the reference performance maps employed constitute the baseline for the engine performance.
- From this point on, by using the reference data and measurements on the engine, sets of modification factors are calculated for every engine run, as shown schematically in **Figure 2.45**.
- Observation of the changes in the values of modification factors can then lead to detection of the location and the fault type.

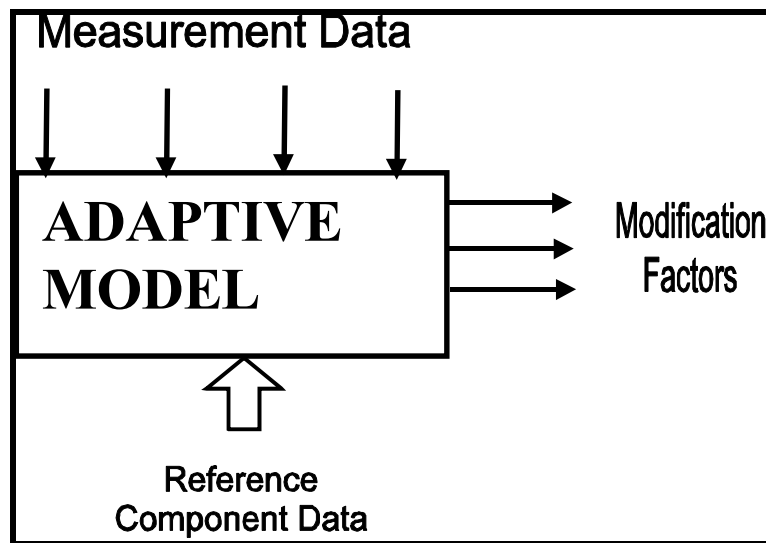


**Figure 2.45: Derivation of Modification Factors by an Adaptive Model.**

We may consider that any phenomenon such as erosion, corrosion, fouling, leakage, burning, bowed or missing blades, etc., has in a macroscopic level the effects:

- A reduction in the efficiency;
- An alteration in pumping capacity; and
- An increase in pressure drop.(in ducts).

Therefore, any problem, that is aerothermodynamically related to the gas path components, would appear as a change in the value of modification factors. The modification factors can be treated as ‘features’ and an automatic diagnosis can be performed from the clusters formed in a feature space (For example, a method of recognizing such faults by using Neural Networks has been presented by Kanelopoulos et al., 1997, [2.37]).

In order to distinguish whether a fault is due to a sensor failure or comes from an actual engine problem, the observation of shifts in the calculated MF values has to be combined with runs in the direct mode, using the obtained values. The details of such a procedure are currently under elaboration.

Finally, besides jumps in calculated values indicating the presence of a fault, continuous monitoring can also be performed using the present procedure. In this mode the values of MF must be calculated at regular intervals during engine operation. Their trending will indicate how each component’s deterioration is occurring.

Sensitivity analysis can also produce information useful for ECM. There are two different aspects of application and corresponding approaches. The first approach can be characterized as a manufacturer’s one, because it is oriented to the selection of the most appropriate measurements set, in order to ensure a good capability of in-service monitoring. The approach is the following: Having decided which are the more suitable component parameters for monitoring, we form various objective functions including different sets of global performance parameters and flow variables (Measurement Candidate Sets). The final choice is the set that gives the most sensitive objective function.

The second approach can be characterized as a user oriented approach. The user is faced with the problem of choosing the best possible set of component parameters to be estimated when a given measurement possibility exists. In that case the objective function has a standard form and its variation is examined.

## APPLICATIONS

---

The parameters giving the maximum sensitivity are the ones that should be sought when fault detection is considered. The selection procedure has been discussed by Stamatis et al., 1992 [2.38].

### 2.1.4.3.8 On-Board Engine Performance Diagnostics

Adaptive engine models can be incorporated in advanced control algorithms, which can be used for in-flight propulsion system optimization, condition management and damage accommodation. An adaptive model is fed with data as they are produced during engine operation. The model changes the values of its parameters to produce output values with the minimum possible deviation from the measured data. The deviation of parameters from their nominal values represents the condition of the engine.

Bushman and Gallops (1992) [2.39] have produced an in-flight performance diagnostic application for a PW1128 military turbofan engine. The on-board engine model is formulated as a piecewise linear state variable model. The model is based on a set of linear relationships between engine inputs and outputs, characterized by engine operating point. Perturbing a large-scale aerothermodynamic model of the PW1128, which is accurate over the full engine operating range and flight envelope, generates the model's linear relationships. The resulting linear relationships allow accurate modeling of unmeasured parameters with reduced computational and storage requirements.

Deviations in component performance can be for many reasons, such as in service deterioration, damage or engine to engine build variations. These deviations can already be estimated at an initial calibration phase, in order to accurately represent a particular engine, which is not identical to the typical average engine represented by the full-scale aerothermodynamic model. The particular model employed by Bushman and Gallops uses five parameters to represent performance deviations: a low pressure spool efficiency deviation, a high pressure spool efficiency deviation, fan airflow loss, compressor airflow loss, and high pressure turbine area change. Adaptation of the model is by employing a Kalman filter algorithm to estimate the magnitude of these deviations. Observability constraints on this method, imposed by the limited number of measured quantities available, dictated the use of combined performance parameters. For example, a single efficiency parameter per spool, instead of individual compressor and turbine efficiencies, was used.

### *Modeling Techniques Used*

Models that can be used for on-board diagnostics are essentially of the state variable type. Piecewise-linear state-variable models can be calibrated to accurately represent engine characteristics. These models are considerably faster than full-scale aerothermodynamic models, and they can thus be used for real-time, or near real-time, implementation. A full scale aerothermodynamic model, even of zero order, solves a set of non-linear equations and is not, in general, able to run as fast as real-time applications require. At this point, it must be said that future developments in microprocessor technology could make the real-time implementation of full-scale models a reality.

### *Potential Benefits*

The benefits of implementation of applications of this kind include all those expected to result from diagnostic techniques in general, while some additional advantages can be provided. The use of on-line diagnostic capabilities and through it, the on-line adaptation of the engine model, allows their incorporation into the engine controller. Performance seeking control schemes can then be implemented and through them, engine usage can be optimized.

### *Cited Example*

- Bushman, M.A. and Gallops, G.W., "I-flight Performance Diagnostic Capability of an Adaptive Engine Model", AIAA Paper # 92-3746, 28th Joint Propulsion Conference and Exhibit, AIAA/SAE/SME/ASEE, July 6-8, 1992, Nashville, TN.

### *Limitations of Chosen Modeling Technique*

A modeling technique based on state variable representation has the disadvantage that it has to be calibrated upon a full-scale thermodynamic model. If it is piecewise linear, it may also lose accuracy, unless a very fine division is used in regions of steep gradients. It is essentially a zero order model, with all the related possible drawbacks. Since it is fast in execution and has small computer requirements, providing nevertheless sufficient accuracy, it is very suitable for inclusion in on board systems and integration with the engine controller.

#### *2.1.4.3.9 Diagnostic – Ground Station*

From an implementation viewpoint, ground station applications have several advantages when compared to on-board applications. They can rely on more computational resources, and they can therefore employ techniques based on more sophisticated algorithms. Non-linear methods are suited for ground station diagnostics. Application of adaptive modeling is considered on a mixed-flow turbofan engine (a version of the P&W JT8D). The engine schematic and the stations used for modeling and interrelation to measurement data are shown in **Figure 2.46**.

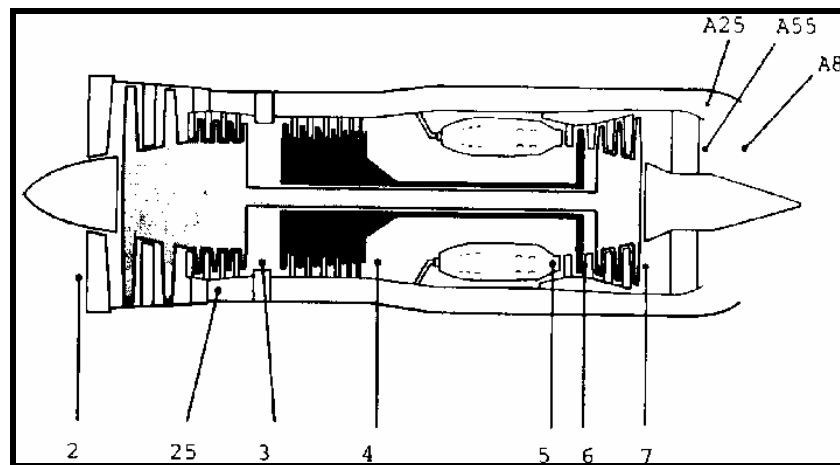


**Figure 2.46:** Layout of Mixed Flow Turbofan for Application of Adaptive Modeling.

Values of various performance variables were available at the design point, while the variation of  $N_1$ ,  $N_2$ , EGT, WF and net thrust  $F_N$  with EPR was available at off-design points. Adaptation of the model to engine data was performed in two stages, first at the design point and then at off design conditions. The adapted model predictions were compared to the manufacturer's data to show how successfully engine performance can be predicted. An example of the modification which was needed for adaptation is shown in **Figure 2.47**, where the intermediate compressor map before and after the adaptation are shown.

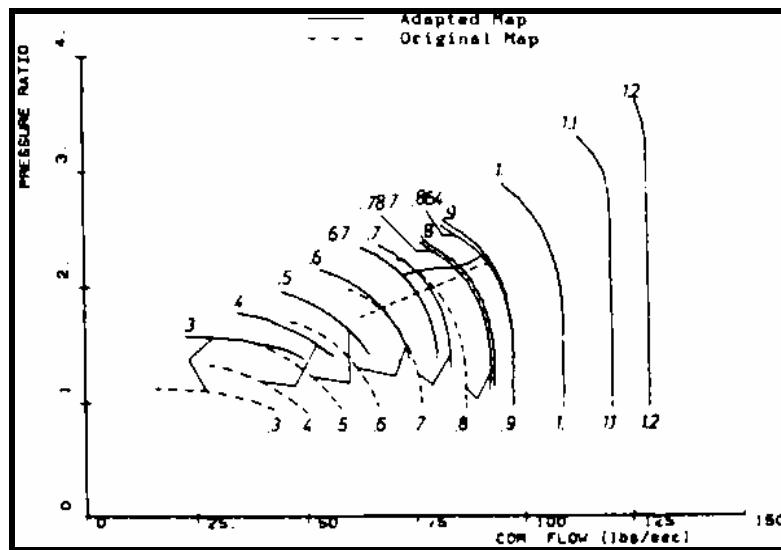


**Figure 2.47:** Modification of Map Initially Used, in Order to Adapt the Model to Engine Data.

Simulation of faults is achieved by introducing deviations in component parameters (as caused by the presence of a fault) and producing the resulting deviations in measured quantities (fault signatures). Of course, such a possibility exists also with a non-adapted model, but the improved reliability of the adaptive model gives more accurate results, as demonstrated in **Figure 2.48**. This figure shows that signatures predicted by the adaptive model are much closer to those of the manufacturer's than those predicted by the core model.

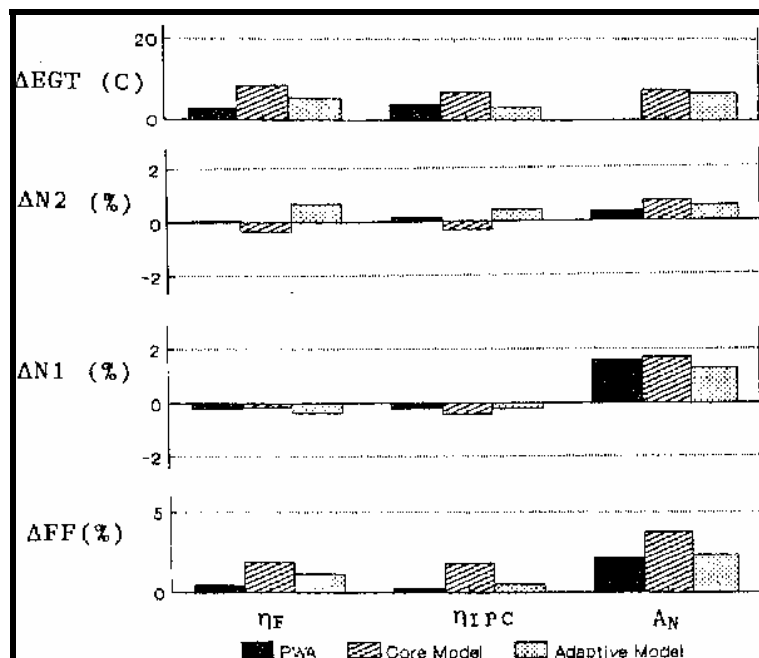


**Figure 2.48:** Deviations in Measured Quantities Caused by Component Faults.

Finally, using the adaptation capability of the model, one can use it for diagnostic purposes. When data from a faulty engine are introduced into the model previously calibrated on the healthy engine, the estimated

deviations of component parameters correspond to alteration in the engine components. These alterations are a direct indication of the presence of a fault within a component. Adaptive modeling provides one additional capability. If the deviations do not correspond to a fault but to small engine to engine differences, the corresponding component deviations are defined and the model is suitable for normal operation prediction of the particular engine considered. Therefore, the procedure is able to produce not only a model customized to a particular engine type, but also track differences of different engines of one particular series.

### **2.1.5 References for Fixed Wing Applications**

- [2.1] RTO-TR-044, 2002, Performance Prediction and Simulation of Gas Turbine Engine Operation, RTO Technical Report 44, April 2002, AC/323(AVT-018)TP/29, ISBN 92-837-1083-5.
- [2.2] Stricker, J.M., "The Gas Turbine Engine Conceptual Design Process – An Integrated Approach", Design Principles and Methods for Aircraft Gas Turbine Engines, RTO-MP-8, February 1999.
- [2.3] Schaffler A. and Lauer, W., "Design of a New Fighter Engine – The Dream in an Engine Man's Life", Design Principles and Methods for Aircraft Gas Turbine Engines, RTO-MP-8, February 1999.
- [2.4] Khalid, S.J., "Role of Dynamic Simulation in Fighter Engine Design and Development", Journal of Propulsion and Power, Vol. 8, No. 1, January-February 1992, pp. 219-226.
- [2.5] Horobin, M., "Cycle-Match Models Used in Functional Engine Design – An Overview", Design Principles and Methods for Aircraft Gas Turbine Engines, RTO-MP-8, February 1999.
- [2.6] Kurzke, J., "Gas Turbine Cycle Design Methodology: A Comparison of Parameter Variation with Numerical Optimization", Journal of Engineering for Gas Turbine and Power, Vol. 121, January 1999, pp. 6-11.
- [2.7] Philpot, M.G., "Practical Considerations in Designing the Engine Cycle", AGARD Lecture Series, Steady and Transient Performance Prediction of Gas Turbine Engines, AGARD-LS-183, May 1992.
- [2.8] SAE Standard, AIR4548: Real-Time Modeling Methods for Gas Turbine Engine Performance.
- [2.9] SAE Standard, AS681: Gas Turbine Engine Steady-State and Transient Performance Presentation for Digital Computer Programs, March 1999.
- [2.10] SAE Standard, ARP4148: Gas Turbine Engine Real Time Performance Model Presentation for Digital Computers, July 2003.
- [2.11] Johnson, S.A., "A Simple Dynamic Engine Model for Use in a Real-Time Aircraft Simulation with Thrust Vectoring", NASA Technical Memorandum 4240, AIAA Paper # 90-2166.
- [2.12] Kurzke, J., "Calculation of Installation Effects Within Performance Computer Programs", AGARD Lecture Series, Steady and Transient Performance Prediction of Gas Turbine Engines, AGARD-LS-183, May 1992.
- [2.13] Kurzke, J., "Some Applications of the Monte Carlo Method to Gas Turbine Performance Simulations", ASME Paper # 97-GT-48, Presented at the ASME International Gas Turbine Institute's Turbo Expo, Orlando, FL, June 1997.
- [2.14] Kurzke, J., "Advanced User-Friendly Gas Turbine Performance Calculations on a Personal Computer", ASME Paper # 95-GT-147, June 1995.

## APPLICATIONS

---

- [2.15] Visser, W.P.J. and Broomhead, M.J., "GSP, A Generic Object-Oriented Gas Turbine Simulation Environment", ASME Paper # 2000-GT-0002, May 2000.
- [2.16] Chappell, M.A. and McLaughlin, P.W., "Approach to Modeling Continuous Turbine Engine Operation from Startup to Shutdown", Journal of Propulsion and Power, Vol. 9, Number 3, May-June 1994, pp. 466-471.
- [2.17] Malloy, D.J., Chappell, M.A. and Biegl, C., "Real-Time Fault Identification for Development Turbine Engine Testing", ASME Paper # 97-GT-141, Presented at ASME International Gas Turbine Institute's Turbo Expo, Orlando FL, June 1997.
- [2.18] Chappell, M.A. and McKamey, R., "Adjusting Turbine Engine Transient Performance for the Effects of Environmental Variances", AIAA Paper # 90-2501, July 1990.
- [2.19] Khalid, S.J., "Role of Dynamic Simulation in Fighter Engine Design and Development", Journal of Propulsion and Power, Vol. 8, No. 1, January-February 1992, pp. 219-226.
- [2.20] Khalid, S.J. and Legore, R.T., "Enhancing Fighter Engine Airstarting Capability", International Journal of Turbo and Jet Engines, Vol. 10, 1993, pp. 225-233.
- [2.21] Lakshminarasimha, A.N., "Modeling and Analysis of Gas Turbine Performance Deterioration", ASME Paper # 92-GT-395, June 1992.
- [2.22] Singh, D. et al., "Simulation of Performance Deterioration in Eroded Compressors", ASME Paper # 96-GT-422, June 1996.
- [2.23] Garrard, G.D., "ATEC: The Aerodynamic Turbine Engine Code for the Analysis of Transient and Dynamic Gas Turbine Engine System Operations – Part 1: Model Development", ASME Paper # 96-GT-193, June 1996.
- [2.24] Garrard, G.D., "ATEC: The Aerodynamic Turbine Engine Code for the Analysis of Transient and Dynamic Gas Turbine Engine System Operations – Part 2: Numerical Simulations", ASME Paper # 96-GT-194, June 1996.
- [2.25] Garrard, G.D., Davis, Jr., M.W., Wehofer, S. and Cole, G., "A One-Dimensional, Time Dependent Inlet/Engine Numerical Simulation for Aircraft Propulsion Systems", ASME Paper # 97-GT-333, June 1997.
- [2.26] Tinga, T. et al., "Integrated Lifting Analysis Tool for Gas Turbine Components", ASME Paper # 2000-GT-646, May 2000.
- [2.27] Haykin, T. and Murthy, S.N.B., "Transient Engine Performance with Water Ingestion", Journal of Propulsion, Vol. 4, No. 1, January-February 1988, pp. 81-88.
- [2.28] Ludorf, R.K. et al., "Stage Rematching as a Result of Droplet Evaporation in a Compressor", ASME Paper # 95-GT-194, Presented at the IGTI Turbo Expo in Houston Texas, June 1995.
- [2.29] Gilyard and Orme, "Performance-Seeking Control: Program Overview and Future Directions", NASA Dryden Research Facility, 1993.
- [2.30] Orme and Schkolnik, "Flight Assessment of the Onboard Propulsion System Model for the Performance Seeking Control Algorithm on the F-15 Aircraft", NASA Dryden Research Facility, 1995.

- [2.31] Kurzke, J. and Riegler, C., “A Mixed Flow Turbofan Afterburner for the Definition of Reheat Fuel Control Laws”, May 1998, Design Principles and Methods for Aircraft Gas Turbine Engines, RTO-MP-8, February 1999.
- [2.32] Doel, D., “TEMPER-A Gas-Path Analysis Tool for Commercial Jet Engines”, ASME Paper # 92-GT-315, 1992.
- [2.33] Doel, D., “An Assessment of Weighted-Least-Squares Based Gas Path Analysis”, ASME Paper # 93-GT-119, 1993.
- [2.34] Urban, L.A. and Volponi, A.J., “Mathematical Models of Relative Engine Performance Diagnostics”, Aerotech 92, Anaheim California, October 5-8, 1992.
- [2.35] Urban, L.A., “Gas Turbine Engine Parameter Interrelationships”, HS VAL, Windsor Locks GK, 1969.
- [2.36] Stamatis, A. and Papailiou, K.D., “Discrete Operating Conditions Gas Path Analysis”, AGARD CP 448, Paper 33, 1988.
- [2.37] Kanelopoulos, K., Stamatis, A. and Mathioudakis, K., “Incorporating Neural Networks into Gas Turbine Performance Diagnostics”, ASME Paper # 97-GT-035, 42nd ASME International Gas Turbine and Aeroengine Congress and Exposition, June 2-5 1997, Orlando FL, USA.
- [2.38] Stamatis, A., Mathioudakis, K. and Papailiou, K.D., “Optimal Measurements and Health Indices Selection for Gas Turbine Performance Status and Fault Diagnosis”, Journal of Engineering for Gas Turbine and Power, ASME, Vol. 114, No. 2, April 1992, pp. 209-216.
- [2.39] Bushman, M.A. and Gallops, G.W., “I-flight Performance Diagnostic Capability of an Adaptive Engine Model”, AIAA Paper # 92-3746, 28th Joint Propulsion Conference and Exhibit, AIAA/SAE/SME/ASEE, July 6-8, 1992, Nashville, TN.

## **2.2 GAS TURBINE ENGINE SIMULATIONS FOR ROTARY AIRCRAFT APPLICATIONS**

### **2.2.1 History**

First attempts to make rotary wing aircraft dates back to the early 1900's. One can quote the works of Breguet, Cornu, and Sikorsky, however, it is not proven that these aircraft carried passengers. From this point, further progress was made in Europe, the United States and the USSR. Just before World War II, significant progress was made by Breguet and Doran (France) and Focke (Germany), but their concept of a two rotor helicopter was eventually discontinued. The modern helicopter industry was really born in United States, with the Sikorsky's VS300, ordered by the US Army. In 1941, a duration world record of 1 h 32 min was achieved. Other historic milestones were:

- 1951: First flight of a helicopter using a gas turbine engine is achieved by Turbomeca. The helicopter was the Ariel III. The drive is pneumatic which means that pressurized air is driven through hollow rotary wings. The air being expelled at the end of the wings achieves the thrust that makes the blades rotate. Compressed air is produced by a compressor, driven by the gas turbine.
- 1951: First flight of a helicopter using gas turbine with mechanical drive. It is achieved by a Kaman Helicopter with a Boeing 502 gas turbine.
- 1956: First serial production of a helicopter using gas turbine with mechanical drive. The helicopter is an Alouette II powered by an Artouste engine (Turbomeca), **Figure 2.49**.

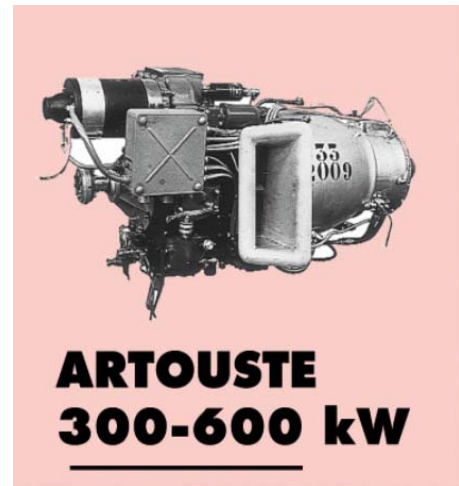


**Figure 2.49: ALOUETTE II Powered by ARTOUSTE II.**

### 2.2.2 Market

At a given medium power class, gas turbine engines have a lower weight than piston engines, and are better suited as a helicopter power plant. However, at very low power class, due to high turbine and compressor relative clearances in gas turbines, it is relevant again to use piston engines. Piston engines are only used marginally in the market of helicopters. The use of piston engines is limited to helicopter of weight below 1.2 tons and produce power below 350 shp. Thus, piston engines currently make up less than 5 percent of the helicopter market.

The civilian helicopter market remains stable. The growth of the global market is now due to the recovery of military sales. In Europe and in the United States, this sector will renew its production levels of the 1960's and 70's. We can expect the military sector to drive the growth for the 10 following years.

There are two main helicopter manufacturers in Europe, in which 4 countries take part: Eurocopter (France, Germany) and Agusta Westland (Italy and England). Three main American helicopter manufacturers are Bell, Sikorsky and Boeing. Other countries with significant helicopter industries are India, China, Japan, Korea and Russia. For emerging countries, the helicopter market is an important means of technological development. Compensation markets, which imply that customer countries will partner in the creation of the engine, are now common. Turbomeca's Ardiden engine will be designed and manufactured both in France and in India. Worldwide there are over 35,000 helicopters in service (excluding the former Soviet Union) with over 6200 operators.

### 2.2.3 General Engine Layout

Helicopters are typically used on short range missions. Their fuel usage is thus roughly half the average value for fixed-wing transport aircraft (typically 30% versus 15%). With regards to the engine itself, the weight fraction remains the same for both fixed- and rotary-wing around 4 – 5%. The engine fraction, however, grows significantly when the complete powerplant installation and its impact on the airframe are considered (engine mounts, air intakes and exhausts, filters, fireproof bulkhead, access door, etc.).

These considerations seem to suggest that for a new generation helicopter engines, weight reduction has become a more important design driving factor than fuel efficiency through a reduction in specific fuel consumption.

Another reason to have a small engine, regardless of the engine's power output, the airflow through the engine is much smaller for a turboshaft configuration than for turbofans. For example, the medium-power (1700 – 2000 shp) T700 has airflow in the region of 4.5 – 6.0 kg/sec, while medium-thrust turbofans (M88, EJ-100, F404) are in range of 65 kg-75 kg/sec.

### 2.2.3.1 Usual Layouts

Given the need for a small engine, a series of design considerations and technological choices becomes natural. Often, a centrifugal compressor design is used (see [Section B.1.2](#)). Also, a mixed layout design whereby a number of axial stages are followed by a high-pressure centrifugal single-stage compressor feeding a reverse-flow combustor and high pressure turbine. This design provides an extremely compact high pressure engine core. The centrifugal compressor has been abandoned since the early 50's in turbojet engines of reasonable thrust class. This is due to the severe limitations of possible airflow with a given frontal cross-section. It's a small drawback for helicopter engines, while the capability of a single centrifugal stage to give about three times the compressor ratio of an axial design is much more significant. With the use of first axial compressors, the air flow reaches the centrifugal stage already compressed to a much smaller volume than at the air intake, and even a small-diameter centrifugal compressor will thus offer a significant increase in total compression ratio in a very compact package.

### 2.2.3.2 Examples of Engines Layouts

The peripheral outlet of a centrifugal compressor matches perfectly with a reverse-flow annular combustion chamber containing the co-axial high pressure turbine. Examples of this layout: Pratt & Whitney Canada PT6-T, Rolls Royce Turbomeca RTM322, General Electric T700. The opposite all-axial lay-out was noticeably adopted for some large US and Russian designs, with 14 stages equipping both the General Electric T64 and the Rolls-Royce Allison T406, while the Klimov TV3-117 has twelve axial stages. In the most recent helicopter engines, such as the MTU/Turbomeca/Rolls Royce MTR390 for the Tiger and the LHTEC T800 for the Comanche, have adopted the centrifugal compressor approach. Thanks most notably to the exceptional advances in 3-D CFD (computational fluid dynamics techniques) for internal engines design, the axial low-pressure stages have been discarded, and the layout includes but two centrifugal stages. This significantly reduces the overall engine length and parts count. Shown in [Figure 2.50](#) is the Turbomeca TM333 engine as an example.

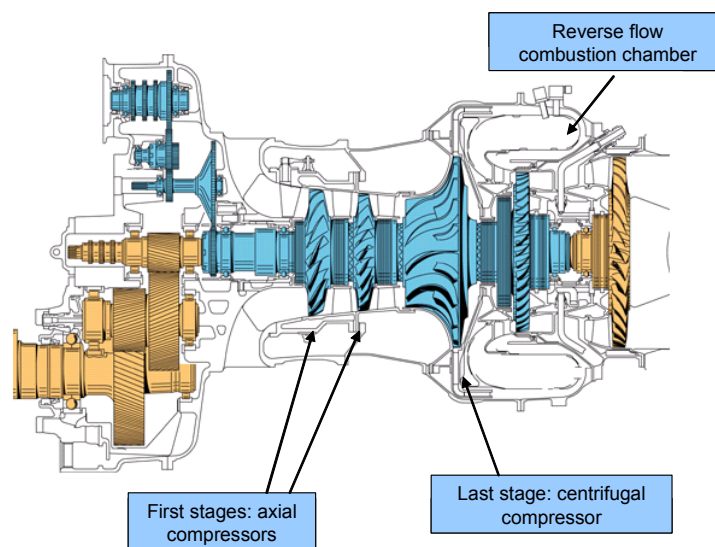


**Figure 2.50:** Example of Turboshaft Engine Layout: Tm333, Turbomeca.

## APPLICATIONS

### 2.2.3.3 Use of Free Turbines

Use of free turbines is now commonplace for helicopter gas turbines. For these engines, there are two rotating parts: the gas generator, which works like a turbo-reactor and the power turbine, which provides power to the helicopter rotor through a power drive. The free turbine has numerous advantages:

- The gas generator is independent from the power turbine; i.e. it can operate at different speeds and results in good specific fuel consumption at all power ratings.
- Starting is easier, as only the gas generator needs to be driven.
- Eliminates the need for clutches on the helicopter.

During transient maneuvers, with a single shaft turbine, there's a risk that the engine will spool down if minimum surge margin is attained. The only way to prevent the engine from stopping is to quickly decrease the power demand. There's then a need to "over-size" the engine, to stay far away from the surge line and insure safe power transients. With a free turbine, the risk of spool down doesn't exist, and there's no need of over-sizing the engine, however, time response of the free turbine engine will be longer.

The main challenge with free turbine may be to link the engine to the helicopter if the main transmission gearbox is at the front of the engine. This difficulty may be overcome by using a traversing power shaft (Figure 2.50: layout of Tm333). If no traversing power shaft is used, an intermediate gearbox may enable the power shaft to pass around the gas generator (Figure 2.51: layout of Arriel 2S1). Another solution is to install the engine back to front (which is the case of the Pratt & Whitney Canada PT-6). Of course, some helicopters feature the main transmission gearbox at the rear of the engine (Figure 2.52 layout of Makila).

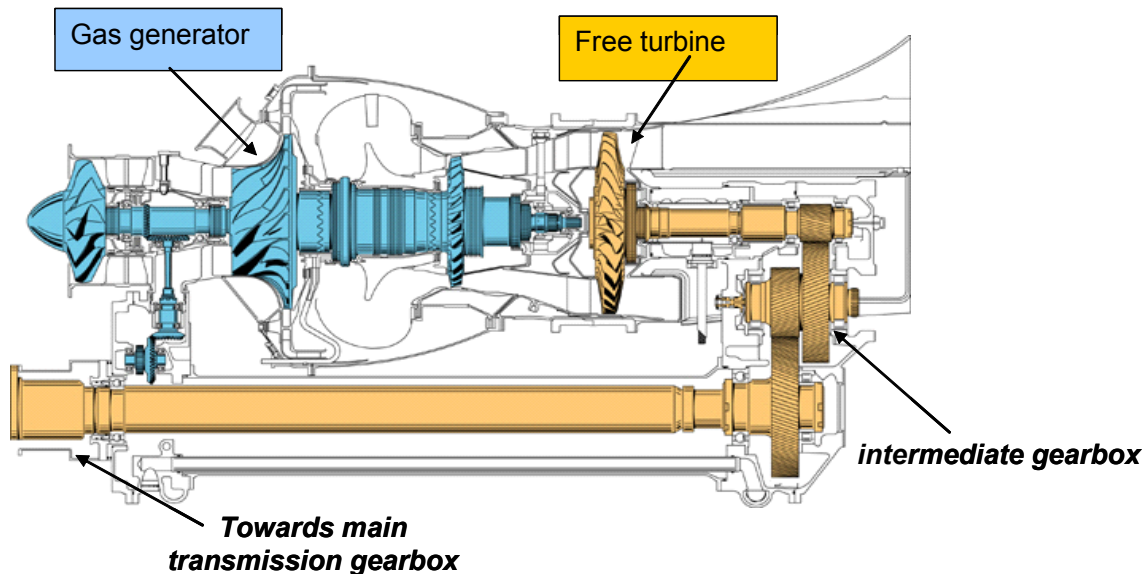


**Figure 2.51:** Example of a Tree Turbine Engine: Arriel 2S1, Turbomeca.

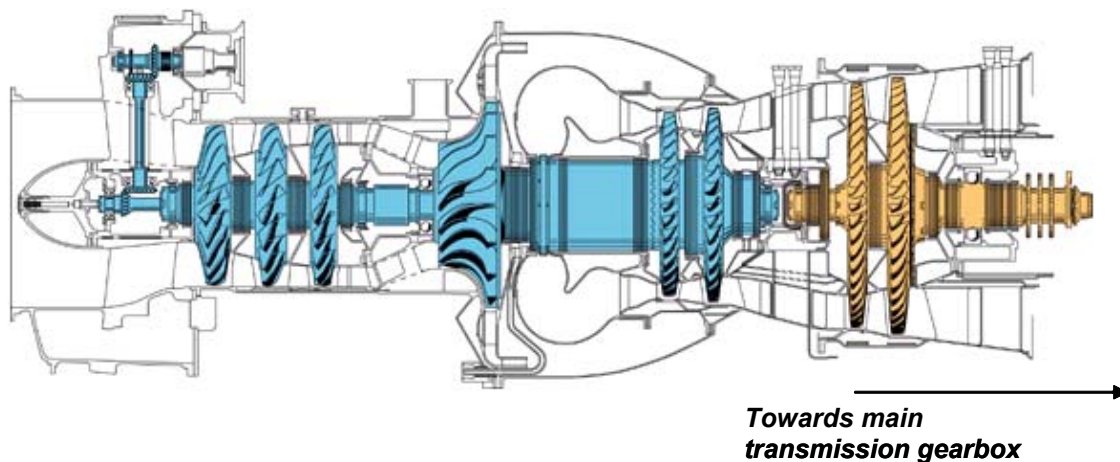


**Figure 2.52:** Example of a Tree Turbine Engine: Makila, Turbomeca.

## 2.2.4 Associated Simulations

For a free turbine engine, transient performance will be very different from the performance of a linked turbine engine. As such, they require specific simulation. The design of an engine will be a compromise, among other things, between steady state and transient performance. It is also very important that the transient performance be predicted accurately at an early stage of the engine design.

In a development phase, the quality of transient performance may be judged by:

- The time of acceleration from idle to take-off; and
- The maximum drop of the helicopter rotor speed before steady state performance is achieved. This drop delays the power available for the helicopter during the acceleration and has to be minimized.

To simulate transient performance, one may use tools such as Simulink™. The following schemes (**Figure 2.53** and **Figure 2.54**) are simplified Simulink™ schemes. Control system, per se, may be very coarse at the early stages of development. However, it doesn't matter that much, as the drop in helicopter rotor speed is mainly a consequence of acceleration limitation by the maximum fuel schedule, which can be estimated on an "open loop" basis. This limitation has to be determined in order to give maximum acceleration while respecting the engine surge margin and thermal limitations.

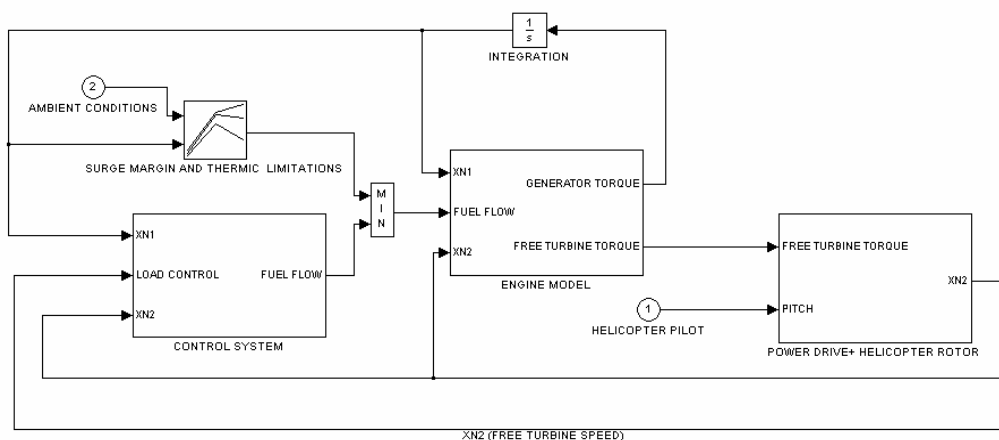


**Figure 2.53:** Simulation of the Engine, Coupled with its Limitations, Control System and Helicopter Rotor.

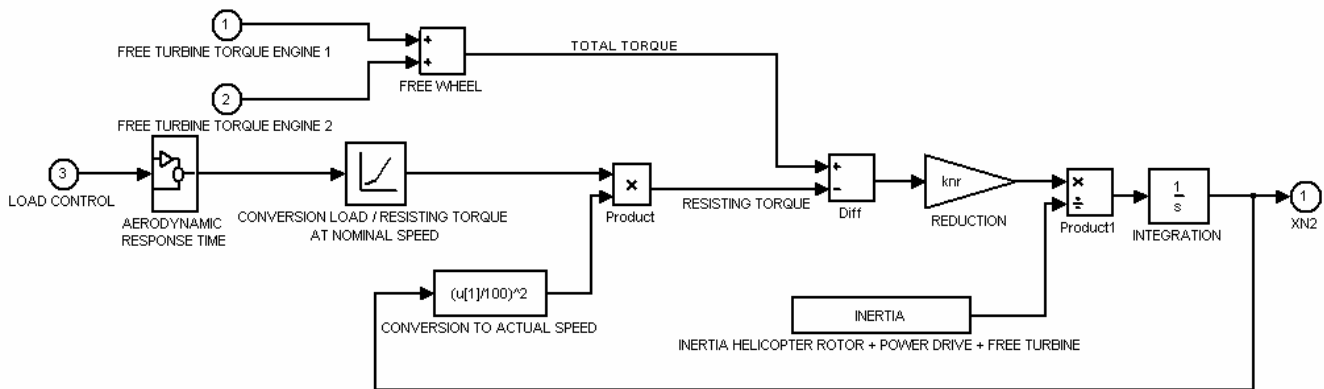


**Figure 2.54: Simulation of the Helicopter Rotor.**

Should the engine have variable geometry, such as anti-surge valves, a level of complexity is added. The laws governing the variable geometry have to be determined, in order to maximize acceleration.

Considering the resisting torque ( $T_{q\ s}$ ), and the engine torque ( $T_{q\ e}$ ), we can infer the accelerating torque with the formula:

$$T_{q\ acc} = J \cdot dN_g/dt = T_{q\ e} + T_{q\ s}.$$

Difficulties may occur in having the relevant conversion between loads and resisting torque. This conversion is specified by the helicopter manufacturer. It varies depending on ambient conditions and the speed of the helicopter. To enable the simulation, the helicopter manufacturer must also provide the inertia of the helicopter rotor. The aim of the free wheel is to disengage the clutch of a failing engine from the power shaft. A good simulation of it is not necessary at the early stage of the development. One of the major difficulties in transient performance is simulation of thermal effects, such as heat-soak. Thermal effects deprive the engine of its potential acceleration. These simulations remain difficult due to the geometric complexity and high temperatures of the elements in which are taking place. Some research remains to be conducted in this domain.

## 2.2.5 Rotary Application Synoptics

### 2.2.5.1 Adaptive Engine Model for Helicopter Turboshift Engine Control Systems

An engine model embedded in the Electronic Control Unit software that is adapted to reflect engine deterioration provides a powerful tool for estimating real-time engine performance characteristics. Besides providing maximum power available, the adaptive engine model can also provide real-time estimates for engine parameters used during back-up control mode in the event of a sensor failure. The adaptive model can also provide useful information about engine parameters that are not measured and subsequently can be used for sensor validation in a fault tolerant engine diagnostic and health monitoring environment.

An algorithm adapts engine model component (compressors and turbines) efficiencies to minimize the error between engine-measured parameters in steady state and those computed by the model. The parameters chosen for comparison are those typically available on all helicopter engine control systems.

The conventional approach of predicting maximum power available by extrapolating actual measured power at a reduced power level introduces error due to the highly nonlinear characteristics of a turboshaft engine. **Figure 2.55** shows that a typical Health Indication Test (HIT) established for a new

(non-deteriorated) engine would indicate a power reduction of 12% where the real loss is only 4% at maximum engine power.

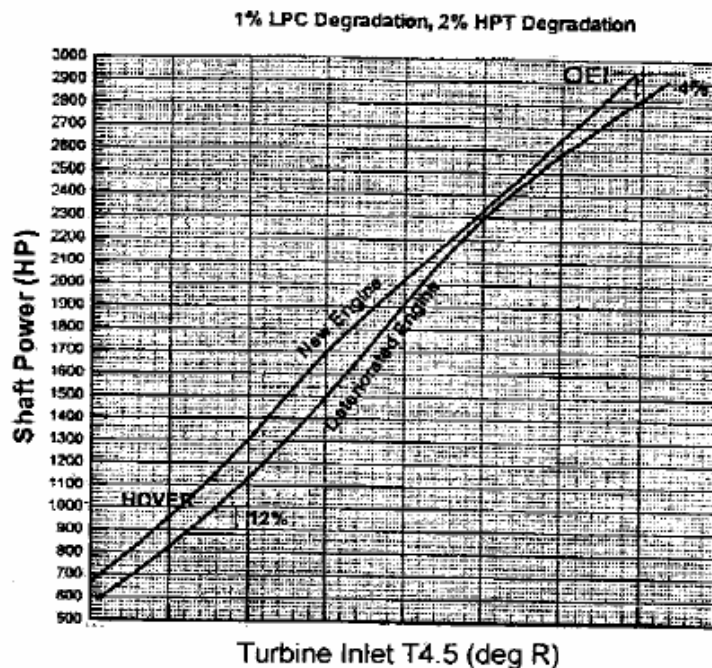


**Figure 2.55: New vs. Deteriorated Engine – Shaft Horsepower vs. Gas Temperature Characteristic.**

Using this technique, the embedded thermodynamic engine model can also be used to compensate for heat transfer effects during engine rapid transients thus minimize scheduling errors and improving transient response times.

### **Modeling Techniques Used**

A full transient thermodynamic match model poses several major challenges for use in real-time engine control systems. First, computational resource requirements inhibit the real-time capability necessary for Engine Control Unit functionality. Second, as the engine deteriorates over time, engine performance and thus control parameters change. An adaptive model that actually matches component deterioration and predicts the non-linear performance of the engine is required. Adaptation of the model is performed by modifying component efficiencies to match engine parameters with model computed counterparts at a number of steady state operating conditions. As part of the algorithm, calibration curves for measured fuel flow and inlet guide vane position are automatically generated to cancel errors due to tolerances and fuel property variations. The adaptation process is posed as a non-linear least squares minimization process which is numerically solved using a quasi-Newton method.

The engine model is a system of coupled nonlinear differential equations in eleven variables representing the compressor, combustor and turbines. Engine accessory power extractions are also modeled. Inputs to the model are fuel flow, engine inlet pressure and temperature, inlet guide vane angle, interstage bleed, power turbine speed and exit static pressure.

Model adaptation is performed by scaling component characteristics to represent the effect of deterioration with time. The major deterioration factors considered for the 3-spool turboshaft engine with the structure presented are:

## APPLICATIONS

- Loss of efficiency and flow for each of the two compressors; and
- Loss of efficiency and shift of flow capacity for each of the three turbines.

Calibration inaccuracies in IGV position can introduce errors in the model, hence IGV estimation is also a part of the adaptation procedure. **Figure 2.56** is a block diagram for the Low Pressure (LP) Compressor section of the engine.

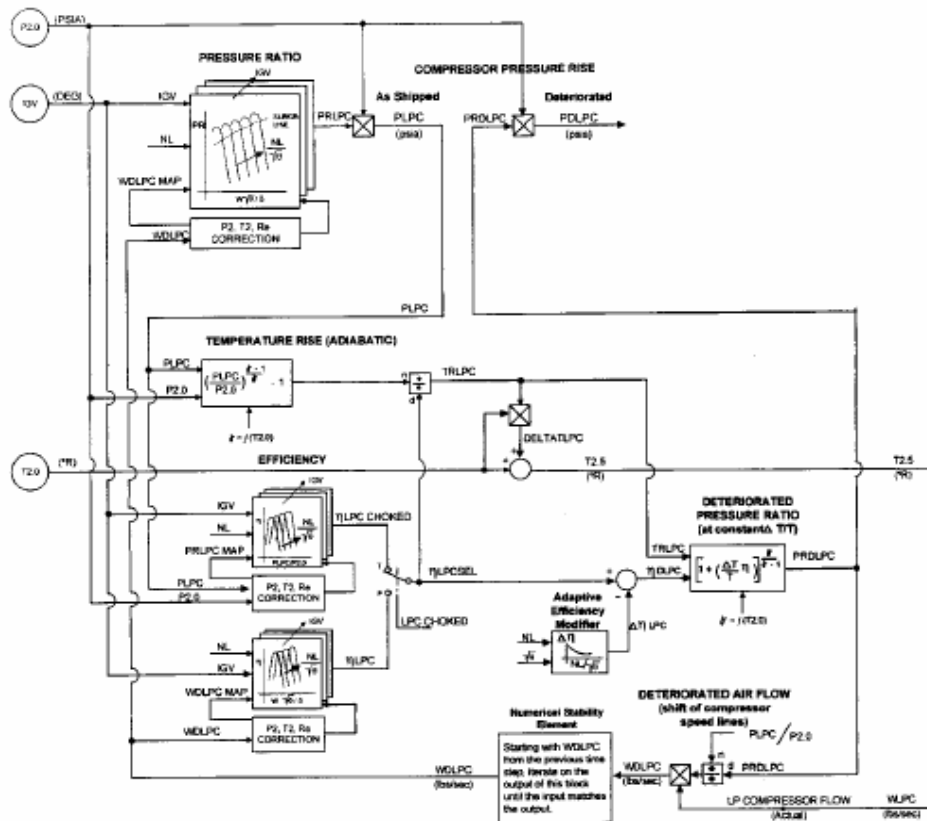


**Figure 2.56: LP Compressor Model Showing Adaptive Features.**

The adaptation is an iterative procedure where each iteration is performed as a 3-step process until the error between the measured and model-computed values are reduced to the desired level.

### Potential Benefits of Using the Simulation

A component-based thermodynamic model for a 3-spool, 3000 SHP turboshaft engine with variable compressor inlet guide vanes is developed. This form is chosen because it models the physics of individual components and is amenable to adaptation as deterioration occurs. Alternate engine models such as excess torque, which is a piecewise linear representation, are difficult to adapt to be consistent with physics.

### Cited Example

- Desai, N.C. and Crainic, C., “Adaptive Thermodynamic Engine Model for the Next Generation Control System for Helicopter Engines”, American Helicopter Society 58th Annual Forum, Montreal, Canada, June 11-12, 2002. [2.40]

An embedded adaptive engine model in the Electronic Control Unit is presented which can be used for accurately computing engine Continuous Power Assurance, engine sensor backup signals and for performance enhancement during engine accelerations from low to high power. An algorithm to estimate component efficiencies, fuel flow and IGV is shown to be robust in real time simulations.

#### ***Limitations of the Modeling Technique***

The adaptation algorithm can be applied as long as the appropriate set of measured steady state data is available. Typically, steady state data is available at a limited range of operating conditions, thus it would be beneficial to collect data at a condition of high interest, both considering power level and operating envelope. Also, the effect of measurement errors will cause a perturbation in the estimated engine component efficiencies. Finally, a microprocessor operating in the hundreds of megahertz range needs to be used if it is desired to adapt the engine model rapidly to changes that could occur during a mission.

#### **2.2.6 References for Rotary Wing Applications**

- [2.40] Desai, N.C. and Crainic, C., "Adaptive Thermodynamic Engine Model for the Next Generation Control System for Helicopter Engines", American Helicopter Society 58th Annual Forum, Montreal, Canada, June 11-12, 2002.

### **2.3 GAS TURBINE SIMULATIONS FOR MARINE PROPULSION APPLICATIONS**

The gas turbine engine first went to sea in 1953, in the shape of the surprisingly sophisticated Rolls-Royce RM60 Gas turbine, used to power HMS *Grey Goose* (using a mechanical drive). Now, for any vessel whose design function makes it speed or volume critical, the gas turbine has become a strong candidate for selection as a prime mover, due to its inherent power density and low weight. As is the case for the land-based power generation application, for marine use, the gas turbine is equipped with a power turbine to convert the energy in the exhaust gases into rotational energy. In the marine case, this rotational energy is applied, via a shaftline, to a suitable propulsor (marine propulsion), either by a direct mechanical drive system or via the intermediary of an electrical system.

In marine applications, the behavior of the gas turbine engine is perhaps more significantly influenced by the nature of the system in which it is the provider of the motive power than is the case for other applications. In particular, the prime mover may experience significant periods of operation well away from the design point as a function of the vessels operational profile and rapidly varying fluctuations of loading as a function of environmental conditions. As an example of the latter we may take the case of ship in which the gas turbine engine drives a propeller in a mechanical system. When the vessel is operating in rough seas, the propeller will be operating in a regime where the water entering the propeller disc will exhibit a significant variation in velocity and pressure due to wave characteristics. This results in a rapidly varying absorption of torque by the propeller and a consequent tendency for the shaft to constantly seek to accelerate and decelerate according to the relative position of the ship and propeller in the wave train.

Such behaviors must be identified, analyzed and quantified early on in the design process and this is the primary function of modeling and simulation of the system. Early in a project, modeling studies will have been conducted to determine the economic performance of the design and the reliability characteristics of the candidate system and the steady state performance characteristics of the system and its Individual components will naturally have been modeled as is standard engineering practice. The operational considerations however, require that extensive dynamic modeling at whole system and component level be undertaken comparatively early on in the design process. This is necessary both to validate the design

## APPLICATIONS

---

which, in many cases, will be unique and for which, consequently, an appeal to previously applied systems will not be possible, and to ensure the suitability and compatibility of system components. Once a verified dynamic model of a system has been created, it may also be used in the development of algorithms for the overall control system.

There is a further very important application of simulation techniques in the marine field that requires modeling of gas turbines, that of the use of computers in training activities in the shape of real time simulators. This technology has wide application throughout the marine field covering areas such as navigation and cargo management in addition to the application specifically relevant to gas turbine modeling, that of engine room simulators. These are used to train engineering personnel in both normal operation and deviation scenarios. This is a specialized area of simulation however, and makes much use of empirically derived data obtained from real units and referenced as look up tables, as opposed to simulating operation by operating from first principles derived from a modeling exercise. This application will not therefore, be discussed further in this document.

One of the main considerations relating to the practice of modeling and simulation in the marine environment is the wide variety of time constant that the modeler may encounter in a single modeling exercise, from microseconds for a control system through tenths of a second for the gas turbine itself up to minutes for the hull response. It is one of the skills of the modeler working in this field to settle on an appropriate level of 'granularity' for the particular task in hand.

It should be noted that merchant applications are generally simpler in both equipment fit and operational complexity than those developed for naval use. There exist, however, examples to the contrary.

### 2.3.1 Typical Scenarios

The scenarios that require modeling from a marine system point of view, relate mainly to the dynamic behavior of the system and the corresponding condition of each of the components. The information derived can be used both to inform/confirm design parameters and to assist in the development of control systems and interfaces. Those most frequently encountered are:

**Acceleration**, this is the simplest of the dynamic modeling tasks but will usually need to be carried out for a number of ship and environmental conditions.

**Crash Stop** this scenario is of interest not only for the information it can provide with regard to the safety issues attending the ship stopping distance, but will also be used to confirm the conditions experienced by different components during each stage of the maneuver to confirm that safe operating limits will not be exceeded. This scenario will again be repeated for differing environmental conditions.

**Propulsor Emersion**, the motions of a vessel in a seaway can lead to a periodic variation in the depth of immersion of the propulsor or even its partial emergence. Such phenomena will lead to a dramatic loss of thrust and torque quickly followed by a rapid reloading of the propulsor. The variations of loads consequently experienced can cause major problems for the entire propulsion train and it will be the function of modeling and simulation to identify and quantify the risk and probable magnitude of such excursions. These effects may be experienced by propulsors of any type.

**Asymmetric Behavior**; by asymmetric behavior is meant the response of a system, two areas of which are operating under differing conditions. Examples might include a vessel with twin propeller shafts in a turn, under which the condition the operating conditions of each of the propellers may be significantly different. This imbalance can cause a significant difference in the torque absorption on each shaft. This example would be used to characterize the response of the control system or would be of particular concern in the case of a system utilizing a splitting gearbox where the torque imbalance in the gearing may become problematic.

**Reversionary Mode Operation;** this refers to those scenarios in which one or more components of the system are unavailable due to fault and the system is operating with performance limitations. These are studied to investigate the potential fault recovery routines and the overall system fault tolerance levels.

### 2.3.2 System Configurations

There are a considerable number of options for the configuration of marine drive systems employing gas turbines, but a system that used a single gas turbine as the only prime mover would be a real rarity. Gas turbines are generally employed in combination with other, smaller, gas turbines or diesel engines to provide redundancy and allow some ‘staggering’ of the levels of power which can be supplied to the system without incurring the penalties attending operating gas turbines at powers significantly below their rated levels. A system of acronyms to describe the various combinations has become widely accepted. To give an example, a system using one diesel engine and one gas turbine simultaneously driving a common shaft would be described as CODAG. The acronym is formed as COMbined Diesel And Gas where “CO” (for combined) indicates the use of two engines per shaft, the “D” (for diesel) indicates the type of the cruise engine, the “A” (for ‘and’, alternatively ‘O’ would indicate ‘or’ in which case simultaneous operation is not a possible option) indicates the method of interoperating the engines and the “G” (for gas) indicates the type of the boost engine.

#### 2.3.2.1 Gas-Turbines in Direct Drive Configurations

The main consideration in modeling the behavior of gas turbine systems in direct drive configurations is the nature of the combination of prime movers in the system. Using the nomenclature outlined above, examples of direct drive systems are CODOG, CODAG, COGOG and COGAG. An example of two of these architectures are shown in **Figure 2.57**.

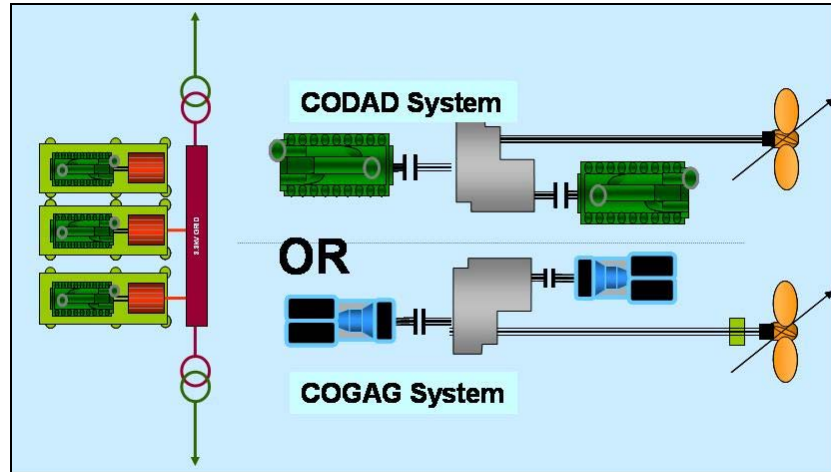


**Figure 2.57: Some System Architectures.**

**Figure 2.57** illustrates the essential differences in the system which are due to the nature of the gearbox and its associated clutch.

#### 2.3.2.2 Gas-Turbines in Electrical Drive Configuration

An increasingly common configuration for a number of ship classes is that of electric drive. The common feature here is the use of a generation facility that supplies both hotel and propulsion requirements in a ‘power station’ concept. The gas turbine lends itself well to this application, especially in those applications that are volume and/or speed critical. The electrical component of the system may or may not be carried

## APPLICATIONS

---

by both prime movers and the gas turbine in such systems may be used for power generation or may contribute to the drive requirements by a mechanical input via a gearbox with the other prime mover driving the gearbox via an electric motor. The acronym system referred to above is extended to include the electrical systems and for the case where the second prime mover is a diesel driven alternator and simultaneous operation of the electrical and mechanical components is possible, the acronym would be CODLAG, (**CO**mbined **D**iesel **E**lectrical **A**nd **G**as). Other acronyms are built in the same manner. When all aspects of drive and hotel/weapons requirements are served by a single power station, the resulting system is often referred to as **I**ntegrated **F**ull **E**lectric **P**ropulsion (IFEP). The last class of system in which electrical drive is employed, is the system where drive is totally electric and is serviced by a gas turbine, the waste heat in the exhaust of which is used to generate steam. This steam is then used in a steam turbine alternator to provide extra power. This is referred to as a **CO**mbined **G**as **E**lectrical and **S**team (COGES) system.

The demands in modeling the gas turbine as the prime mover in an electrical drive of system differ from those for the direct mechanical drive, in so far as in this configuration the output of the gas turbine is controlled to a fixed speed and fuel is adjusted to the required power level. This approach is extended in all-electrical drive systems where both the prime and secondary power plants will be controlled in this manner.

When developing an electrical system, a further level of modeling and simulation will be undertaken which studies the behavior of the electrical transmission system as power flows through it, looking at the stability of the system and issues such as the quality of the electrical supply, paying particular attention to the behavior in fault conditions. Such investigations will not usually require detailed dynamic modeling of the gas turbine.

A number of electrical drive systems exist which employ a direct drive from the motor to the propeller shaft without the intermediary of a gearbox, and system modeling in these cases will additionally be concerned with the potential vibration issues that may arise due to the interaction of factors such as torque pulsation frequency of the motor and the blade rate of the propeller.

### 2.3.2.2.1 *Simple Cycle Turbo-Electrical Systems*

The simplest example of a turbo electrical system is the direct drive situation where a single motor is directly coupled to the propeller shaft. In practice, it may be found that the size of a single motor becomes a problem and smaller motors driving through a combining gearbox are then employed. Such a system is shown in **Figure 2.58**.

### Simple Cycle MT30 & 501 electric drive

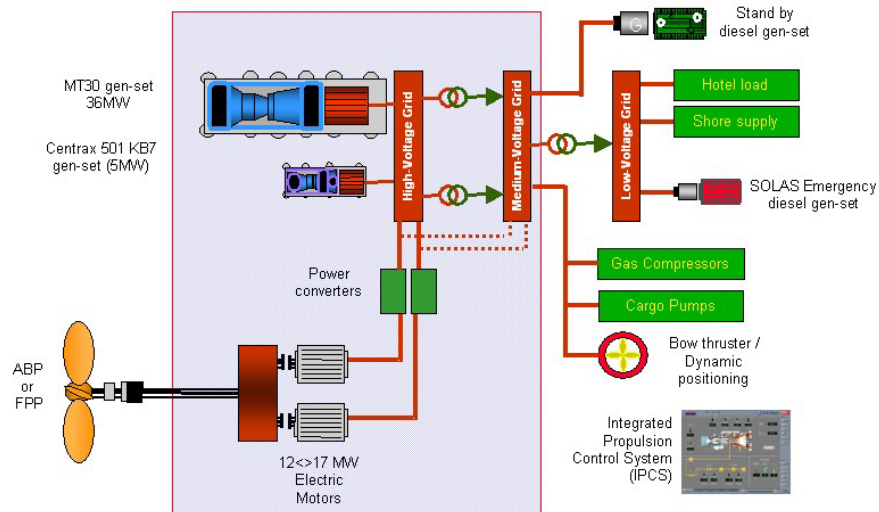


**Figure 2.58: Simple Electric Propulsion System.**

**Figure 2.59** illustrates another example of the Integrated Full Electric Propulsion system designed for the Royal Navy's Type 45 destroyer.

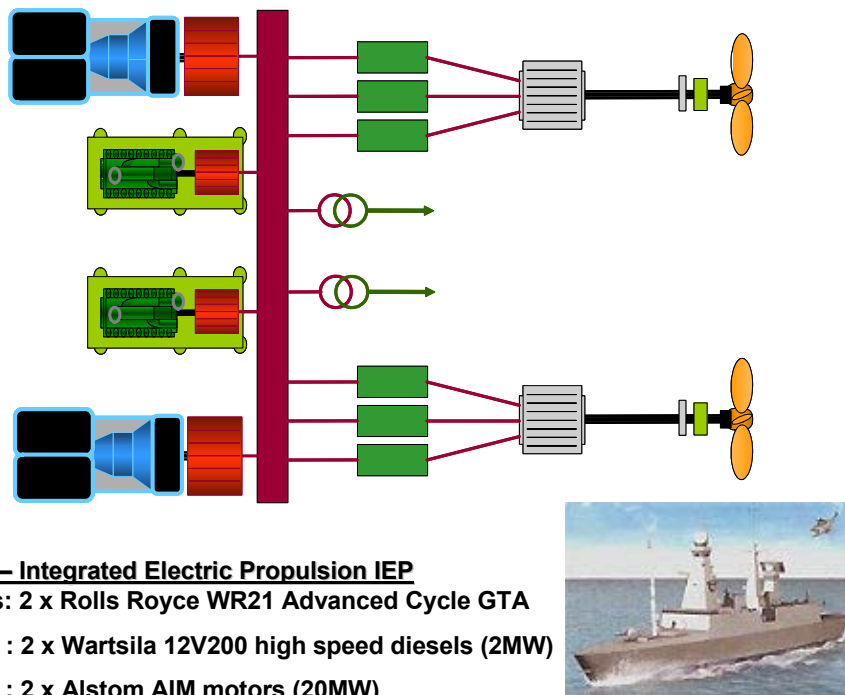


**Figure 2.59: Integrated Full Electric Propulsion System for the Type 45 Destroyer.**

#### 2.3.2.2.2 Combined Gas Electrical and Steam (COGES) Systems

This system is often referred to as 'Combined Cycle' generation. The unique feature is the use of the heat contained within the exhaust of the Gas Turbine Alternator to generate superheated steam which is

subsequently employed by a Steam Turbo-Alternator (STA), to generate additional electricity. Such systems, which are common in land based gas-fired power stations, require a large number of additional components associated with the generation of steam. The added complexity of such systems is offset by the increase in thermal efficiency over that of the simple cycle that may be obtained, raising it to 50% in some cases. COGES systems may or may not be used in combination with additional small gas turbine or diesel driven alternators which are used to ‘top up’ the power levels of the whole system or to provide a dedicated generator for use when low power levels are required. The performance characteristics of the COGES power generation system will usually be modeled separately from the ship system using specialized software packages.

**Figure 2.60** below, illustrates an integrated electrical system for a large Liquefied Natural Gas (LNG) Carrier based on a COGES system. This example is quite complex due to the use of three generation sources plus subsystems (not shown) to control the production and use of fuel gas which is derived from the cargo. This fuel gas uses both natural and forced boil off gas. A complex propulsion control system integrated with the cargo management system is necessary.

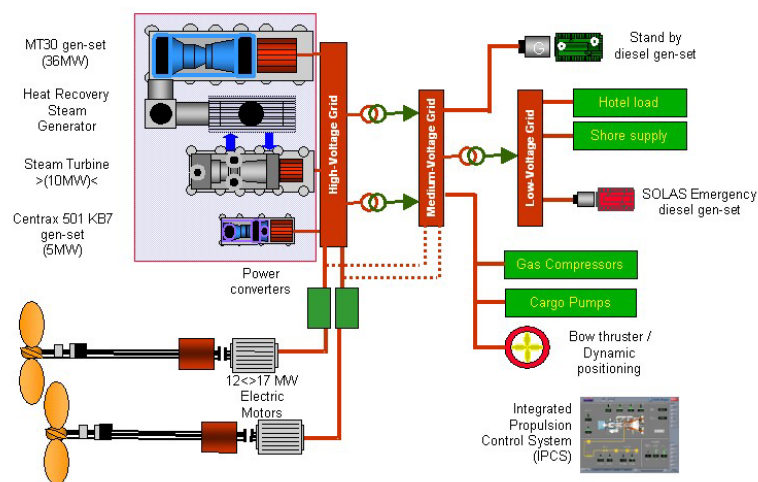


**Figure 2.60: COGES System for Large LNG Carrier (After Reynolds and Tooke, [2.41]).**

### 2.3.2.3 Hybrid Systems

There is currently a trend, particularly evident in naval vessels, towards systems that combine mechanical drive with an electrical drive component. The advantages offered by such systems include, lower structural born noise and vibration, greater flexibility in electrical load profile tolerance, and reduced prime mover count. These systems add significantly to the modeling that must be carried out to inform system selection decisions. Inspection of the two examples presented at figures five and six below, illustrate the point that the system architecture for the ‘Or’ and ‘And’ combined systems are externally similar and the essential difference lies in the gearbox. The system illustrated in **Figure 2.61**, developed for the Royal Navy’s T23 frigates, introduces an interesting option open to the designer of such systems, namely the use shaft motors. These motors, which are mounted in the shaft line downstream of a mechanical drive, can function as both generator and motor, either contributing to the drive or supplying electrical power derived from the prime mover.

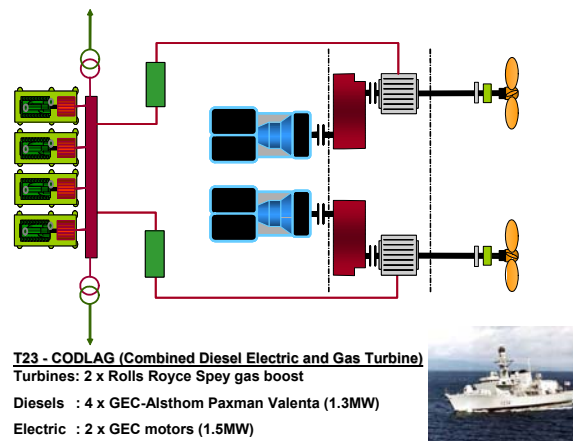


**Figure 2.61: Combined Diesel Electric and Gas Propulsion System.**

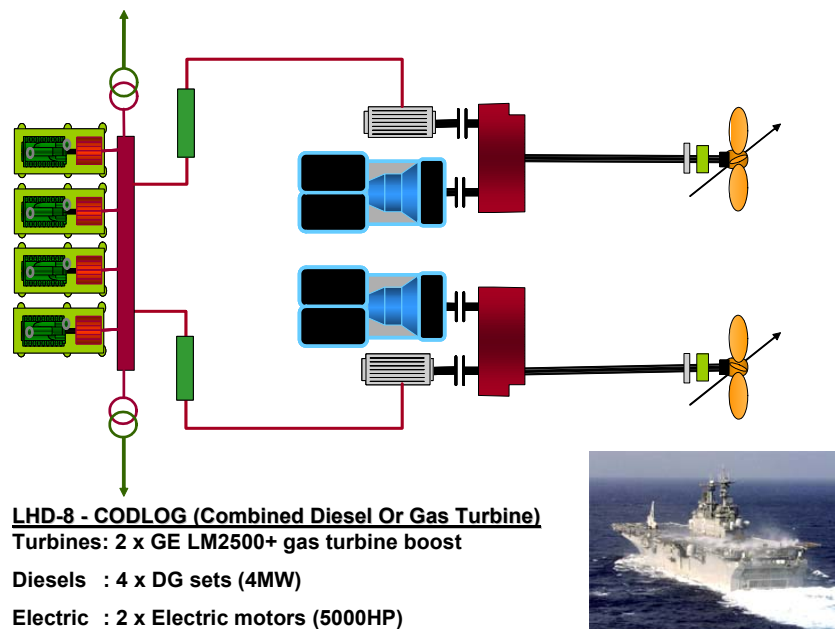


**Figure 2.62: Combined Diesel Electric or Gas Propulsion System.**

## 2.3.3 Propulsion System Components

### 2.3.3.1 Gearboxes

Gearboxes are necessary in mechanical drive systems having gas-turbine prime movers, to reduce the speed of the power-turbine output shaft down to the level of the design speed of the propulsor. The presence of a gearbox in a single shaft system has reliability implications as it adds a single point of failure mode for the vessel. Gearboxes can be of the single-input, single-output (SISO), multiple-input, single-output (MISO), single-input, multi-output (SIMO) or multi-input, multi-output (MIMO) configurations. In practice, the simplest option, SISO, is rarely met and the gas turbine is most frequently found in combination with a second gas turbine or a diesel engine, both inputting to a common gearbox. This inevitably increases the complexity of the gearbox, particularly when a diesel engine is selected as the second prime mover; as the rotational speed of the diesel will almost always be significantly lower

## APPLICATIONS

---

than that of the output shaft from the power turbine of the gas turbine. Complex gearboxes add an extra layer of complexity to the system modeling due to the need in some cases, to model the flows of torque back and through the gearbox during changes between different operating modes and disturbances to the load sharing between different prime movers. There are a number of instances of multiple input gearboxes where one of the inputs drives through a number of different selectable ratios. Fortunately, in such cases power shifting is rare and presently confined to smaller units that are seldom modeled.

### 2.3.3.2 Clutches

The comments in **Section 4.3.4.1** regarding the use of clutches with gas turbines notwithstanding, in marine applications, the clutch is an important and widely used component of the shaftline. Marine clutches will generally either be of the over-running synchronous type, or the more conventional frictional variety. Engagement and disengagement of the synchronous clutches occur at synchronous speed and hence have little influence on system dynamics and do not impose significant demands for modeling/simulation at the whole-ship level. Friction clutches however, do have a measurable effect on the dynamic performance of a system. This is due to the fact that they are generally transmitting significant amounts of torque and engagement is not rapid. Whilst this effect is, as stated, measurable it is still however, small in terms of the overall system time constant and effects at greater than component level are not significant. They cannot, however, be ignored when considering the internal dynamics of the propulsion machinery, especially when modeling changes between machinery states. (Rubis, 1970, [2.42])

### 2.3.3.3 Shafts, Couplings, Bearings and Seals

For most purposes, the characteristics of each of these components have little impact on system dynamic modeling. They are however, critical in the analysis of the vibration characteristics of the whole system (Vassilopoulos and Heliotis, 1988, [2.43]).

### 2.3.3.4 Propulsors

For use with gas turbines, there are currently only two propulsors that need to be considered, the marine propeller and the waterjet. Both types may be represented in the simplest case by a cube law relationship between the speed and power requirement, but more detailed investigations are possible. Selection between the two types of propulsor is made on the basis of the speed distribution in the vessel's operational profile.

#### 2.3.3.4.1 Propellers

This is still the most common form of marine propulsor. It exists in two basic types of configuration, the Fixed Pitch Propeller (FPP) and the Controllable Pitch Propeller (CPP). Usually in both cases the propeller is driven by the propulsion motor, either direct mechanical drive or via an electrical system, via a shaft which transits the hull via a seal. The use of an electrical drive system however, has allowed the development of another drive system in which the entire propulsion train; motor, shaft, bearings and seals is carried in an outboard gondola with the electrical generation plant retained within the hull. This gondola usually, though not universally, affects the steering of the vessel. The propeller may be arranged in tractor rather than pusher configuration. Such systems are commonly referred to as 'Pods' and have to date only employed FPPs. Such propulsion systems have little effect on the propulsion characteristics of the system once the drag and propeller characteristic differences between the pod and the shafted system have been taken into account, though there may be some interaction effects between adjacent steerable pods in some maneuvering situations (Rains, van Lamingham and Schlappi 1981, [2.44]). A further distinct class of propeller exists in the form of Surface Piercing Propellers (SPPs). This latter class could, strictly, be considered as a subset of the FPP, but for several reasons relating to the manner of their hydrodynamic operation, are generally considered separately. For modeling/simulation purposes, the critical characteristics of each propeller design are the torque absorbed and the corresponding thrust delivered. These are

conventionally derived from a set of coefficients from which the torque and thrust can be derived once vessel and rotational speed are provided. Most applications are met with a bespoke design, but there are several families of what are referred to as ‘Series’ propellers which will be used for preliminary modeling of the system, both to provide an objective measure and to allow development of the system model before details of the purpose designed propeller become available. A propeller series is established when there are a significant number of geometrically similar propellers for which there has been established a basic set of performance data and in some cases, upon which it has been possible to conduct multiple regression analysis. The results of such analyses is that the propeller coefficients can be specified as a set of polynomial coefficients from which it is possible to determine the performance of a particular example from a set of basic parameters relating to its configuration and dimensions. An alternative for some of these families is that they may also be characterised by a Fourier Series representation.

Marine propellers operate in one of four quadrants of a diagram on which the x axis carries the speed of rotation and the y axis the vessel speed. The graphed variable is the hydrodynamic pitch angle experienced by the propeller in each combination of revolutions and velocity. The definitions of the four quadrants are as follows:

- First quadrant – Ship advancing in ahead direction, shaft rotation positive.
- Second quadrant – Ship advancing in ahead direction, shaft rotation negative.
- Third quadrant – Ship advancing in astern direction, shaft rotation negative.
- Fourth quadrant – Ship advancing in astern direction, shaft rotation positive.

The characteristics derived from the polynomial or Fourier representations referred to above, relate only to operation in the first quadrant and are commonly referred to as  $K_t/K_q$  representation.

This restricts the usefulness of these approaches as first quadrant operation is only of use for certain analyses. This is due to the fact that to calculate the thrust and torque from the coefficients, the advance coefficient  $J$ , is necessary. This coefficient is derived from the vessel speed and has the propeller rate of rotation as a divisor. In dynamic analyses in which the propeller rate of rotation falls to zero, this usually results in ‘division-by-zero’ errors stopping the programme. For dynamic analyses therefore, a more general treatment of the propeller, the full four-quadrant representation, is more useful. This data is generally empirically derived for specific examples of a particular series. The thrust and torque coefficients obtained from the four quadrant diagram are in this case often referred to as  $C_T^*$  and  $C_Q^*$  respectively. A similar position can be taken when considering CPPs, but in this case since they are constrained to rotate always in the same direction, only the first and fourth quadrants need to be considered.

For manoeuvring analyses a further dataset is often encountered, in the form of the Robinson curve. These curves record the torque absorbed by the propeller plotted as a function of the propeller rate of rotation and the vessel’s speed.

The propeller is a major factor in the generation of structural vibration in ships and the generation of hydrodynamic noise. The former is of concern for all ships and latter is of concern for naval and research vessels. A limited amount of modeling and simulation is possible in studies relating to these phenomena, but it is unlikely that there will be direct interface with the gas turbine problems. There is a further characteristic of a propeller which must be taken into account when using modeling to support a vibration study, that of the added mass of the propeller. This feature is a result of the interaction between the propeller and its surrounding water. It is perceived as an apparent increase in the inertia of the propeller. This is usually defined as a factor in matrix form, but is not available for a whole series and is generally determined for specific designs by model tests.

## APPLICATIONS

### 2.3.3.4.1.1 Fixed Pitch Propellers

The fixed pitch propeller is the commonest and simplest of the three types. Perhaps the best-known example of the FPP series propeller in the public domain is the fixed pitch Wageningen 'B' Series. For this series,  $K_T/K_Q$  values can be derived by both polynomial or Fourier representations and are also available graphically (Oosterveld et al., 1969 and 1975, [2.45] and [2.46]). Figure 2.63 below illustrates the  $K_T/K_Q/\eta_o$  curves for a typical 'B' Series propeller (the B4-70). (The first figure in the identifier for this particular propeller, 4, relates to the number of blades, since the B series is defined for blade numbers from 2 to 7. The second, 70, refers to the ratio of the blade area to the disc area in terms of percentage.)

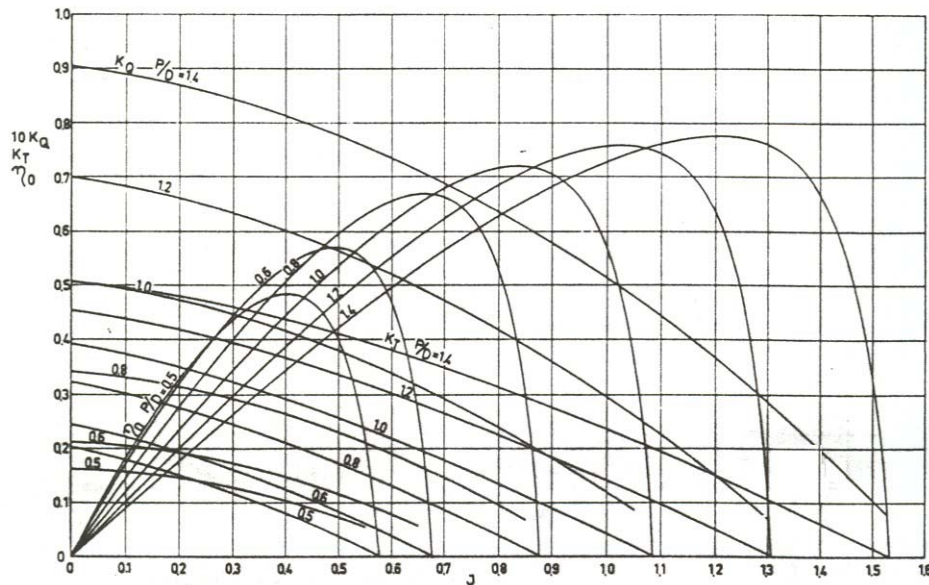


**Figure 2.63:**  $K_T/K_Q$  and Open Water Efficiency ( $\eta_o$ ) Curves for B4-70.

There is a restricted amount four-quadrant data available in the public domain for some of the propellers in the 'B' series, but this is not comprehensive. Figure 2.64 shows an example for the B4-70 propeller at a number of different Pitch/Diameter ratios. (Note that as with the  $K_T/K_Q$  for graphical purposes the  $C_Q^*$  values are scaled by a factor of ten to bring them onto a comparable scale to that of the  $C_T^*$  values, but then are inverted for purposes of clarity.)

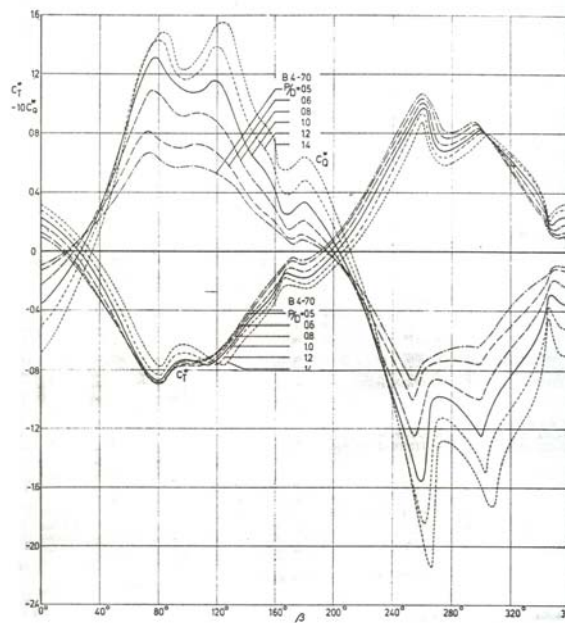


**Figure 2.64: Four Quadrant Diagram for the B4-70 Propeller at a Number of Different Pitch/Diameter Ratios.**

#### 2.3.3.4.1.2 Controllable Pitch Propellers

The CPP outwardly resembles the FPP, but the propeller is constrained to always rotate in the same direction. The blades have non-constant pitch and may be controlled to rotate about a spindle on the hub, through the zero pitch point into a reverse pitch angle thus reversing the thrust effect as shown in **Figure 2.65**. Note that because of the distribution of pitch over the blade, neutral thrust does not coincide with zero pitch, but occurs at a small positive angle. This facility is a desirable feature for mechanical direct drive configurations with gas turbines, as it obviates the need for a reversing gearbox for astern operation. There is an example of a series propeller range for the CPP, the Guttser-Schroeder series, (Porter and Strom-Tejsen, 1972, [2.47]). The rate of pitch adjustment is comparatively slow and may become a factor in some dynamic analyses.

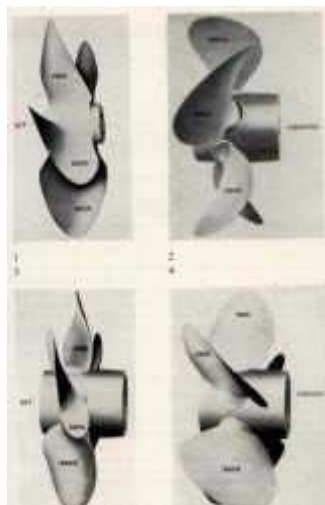


**Figure 2.65: Controllable Pitch Propeller Operation.**

## APPLICATIONS

### 2.3.3.4.1.3 Surface Piercing Propellers

The SPP operates in a very different regime from the other two classes of propeller. The centreline of the propeller shaft lies at or close to the water surface during operation. As a result, each blade enters and leaves the water once during each revolution. As the speed of rotation for such propellers is very much higher than conventional FPPs, the fatigue characteristics of such propellers become a major concern. The blade is so shaped that whilst in the water a cushion of air at atmospheric pressure covers the suction side of the blade. This is a fundamental feature of its hydrodynamic performance and it means that this type of propeller is to some extent protected against one of the main problems affecting conventional propellers, that of cavitation. There is a standard series for SPPs, the Rolla series, (Radojcic and Matic, 1997, [2.48]) but there is little other information on performance in the public domain.

### 2.3.3.4.2 Water Jets

The marine water jet is a viable candidate for propulsion of vessels with speeds of above, say, 25 knots. It consists essentially of a pump in a chamber that accelerates water taken into a tunnel, out of the vessel via a nozzle mounted at the stern. The unit also serves to steer the vessel by deflecting the flow by an adjustable extension to the nozzle. Reversing is effected by inserting a deflector into the flow, either from above or by closing from the sides. Any of the prime mover combinations used for propeller propulsion may be used as prime movers for water jet systems. The hydrodynamic characteristics of a system using a water jet propulsor differ markedly from those utilising a propeller and dynamic modeling of such systems presents a number of challenges. There is no equivalent to a series available in the public domain. Modeling of the water jet from first principles is complicated by the need for a comprehensive set of data for several of the components of the system. This data may not be readily available. For the purposes of simulations of system performance, it is probable that manufacturer's data for torque absorption, thrust and rotational speed for specific applications can be obtained and generalisations using the pump affinity laws can subsequently be employed to approximate off-design point operational characteristics. **Figure 2.66** below illustrates a typical water jet application. Note the presence of steering nozzle and reversing buckets outboard and the centre jet configured purely for thrust.

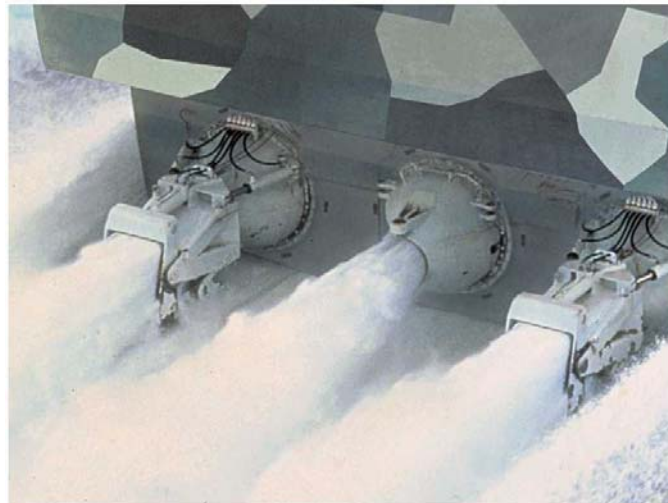


**Figure 2.66: Typical Waterjet Application.**

### 2.3.3.5 Filters and Coalescers

One of the major differences between the marine and aero application of gas turbines, is the need, in the former case, to locate the engine within a part of the ship structure where it may be protected from an

aggressive environment. This immediately imposes the need to duct both the incoming air and the hot exhaust to and from the engine. In addition, it is in many instances a requirement to fit filter/coalescers somewhere in the inlet ductwork to remove traces of corrosive seawater from the incoming air. The restriction due to these ducts and filters imposes a performance penalty on the engine, due to back-pressure and choking that must be taken into account when modeling system performance.

### 2.3.3.6 The Hull

The hull has a number of characteristics that impact on the propulsion system and its components and which must be recognised and taken into account for the effective modeling and simulation of marine systems. The most fundamental of these is the resistance of the hull to motion through the water. This is obviously speed dependent and comprises a number of factors, the most significant of which are form resistance, wave making resistance and frictional resistance. The vessel moving through the water will generate wave systems at the bow and stern as illustrated in **Figure 2.67**.

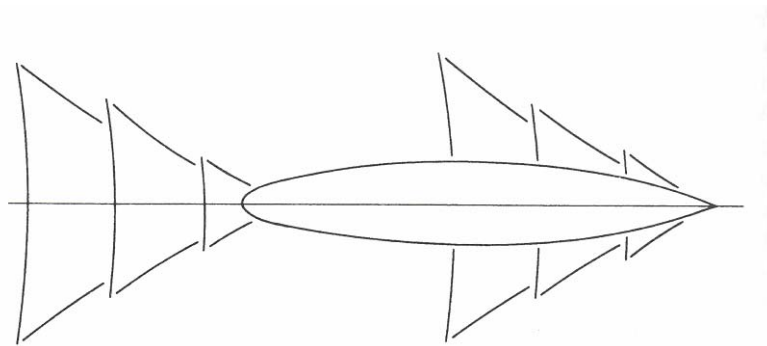


**Figure 2.67: Bow and Stern Wave Generation.**

These wave systems interact with one another as shown in **Figure 2.68**.

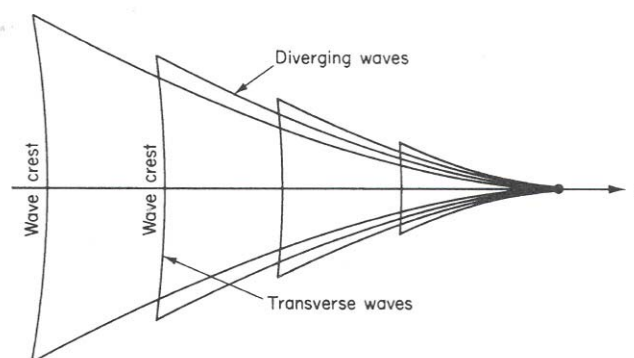


**Figure 2.68: Bow and Stern Wave Interaction.**

The wavelengths of these waves are dependent upon vessel speed and consequently, their interference both constructive and destructive modifies the resistance curve of the vessel and hence the power/speed curve. There will be several peaks and troughs superimposed onto the basic curve due to the interaction of the waves, as illustrated above. (The dominant of these, the third in the series, is often referred to as the prismatic hump). The behavior of planning vessels differs from displacement types in the behavior of the hull as the vessel speed continues to increase. In a planning hull the hump speed marks the transition to the planning condition.

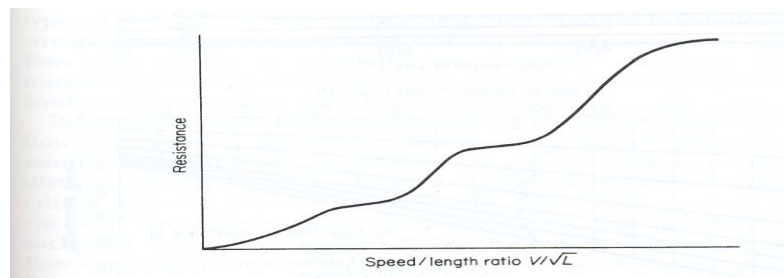


**Figure 2.69: Typical Resistance Curve.**

There are a number of differing hull configurations that must be considered as prime candidates for gas turbine propulsion. The commonest of these is the ubiquitous monohull. Vessels of this type will have hulls falling into one of three distinct subclasses, displacement, semi-displacement and planning. The former and latter of these three types are well defined and present significant differences to be taken into account when constructing models. The class of Semi-displacement hulls is not clearly defined however, and can exhibit a composite of the two sets of characteristics, depending on the operating point. The essential difference between the two classes is the way in which the mass of the vessel is supported whilst underway. In displacement vessels the hull is supported almost totally by hydrostatic effects (although there will be some limited hydrodynamic effects), whilst in the planning hull the pressure generated on flatter hull sections lifts the vessel bodily out of the water to reduce the wave-making resistance as speed increases.

The environmental response of a vessel is often modelled since, as previously mentioned, the motions imparted can have a significant affect on the behavior of the propulsor due to loss of drive/efficiency through aeration as the depth of immersion varies (Politis, G.K. 1999, [2.49]).

Two further types of hull are candidates for the use of gas turbine prime movers, the surface effect ship and the Hydrofoil. In both types of vessel the hull is wholly or partially lifted from the water to reduce wave-making resistance. In the former type, much of the vessel hull (which is of catamaran type) is bodily lifted out of the water by using the space between the sponsons as a pressure chamber by fitting seals at the bow and stern and using fans or compressors to raise the air pressure in the chamber. In the latter class, the hull of the vessel is lifted by hydrodynamic lift resulting from the action of forward motion through the water acting on lifting foils. Both types of vessel operate in the high speed range and whilst conventional propeller propulsion is an option, the higher operational speeds of these craft tends to favour the employment of water jets or SPPs. The speed/power profile of these vessels exhibit extreme 'hump' features at the point at which transition to the out-of-displacement (OOD) condition occurs. **Figure 2.70** shows a surface effect ship in the OOD condition whilst **Figure 2.71** illustrates a hydrofoil vessel raised onto its foils.



**Figure 2.70: Surface Effect Ship in OOD Condition.**



**Figure 2.71: Hydrofoil Vessel at Speed.**

### 2.3.3.7 Hull Propeller Interaction

In the case of the normal type of vessel, the presence of the hull effects the operation of the propulsor and vice versa. The first and most obvious affect is the difference in the velocity of the water flow experienced by the hull and the propulsor. As the vessel moves through the water, the effect of the friction, is that some motion is imparted to the stationary water in the direction of travel. The value of this motion may thus be subtracted from the velocity of the ship to give a value known as the Velocity of Advance ( $V_a$ ). In the case of the propeller, the value of this variation of velocity is not constant over the area of the propeller disc and it is convention to define an average fraction, known as the Wake fraction,. This factor is unique to a particular vessel and will be derived from model tests and tabulated over a range of speeds.  $V_a$  can then be used to derive the advance coefficient,  $J$ , in terms of which it is convention to describe the characteristics of a particular propulsor. The propeller does not also accelerate water in an axial direction, but also imparts some swirl. The presence of the hull in the way of the propulsor also has an effect upon the velocity of swirl. Due to the limited amount of data in the public domain and the absence of any data relating the wake behavior during transient conditions, it is difficult to take account of these factors when modeling a system in the early stages of a project, other than to use the tabulated characteristics of a hull of a similar type to that being considered.

There is a further significant effect on the velocity experienced by the propulsor, the interaction of the propulsor with the vessel's bow wave. A ship in motion inevitably gives rise to a system of waves

## APPLICATIONS

divergent and transverse waves of a length that increases with the vessel speed. Water particles in a wave describe essentially circular motions as illustrated in **Figure 2.72**.

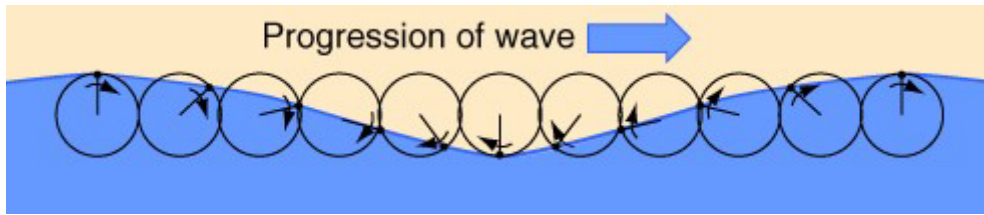


**Figure 2.72: Particle Motion in a Water Wave.**

This distribution of particle velocities is found in the upper layers of the water column and although it diminishes in amplitude as depth increases, it is still of sufficient magnitude to affect the flow conditions along the hull and at the inflow to the propeller disc. The direction of motion with depth is illustrated in **Figure 2.73**.

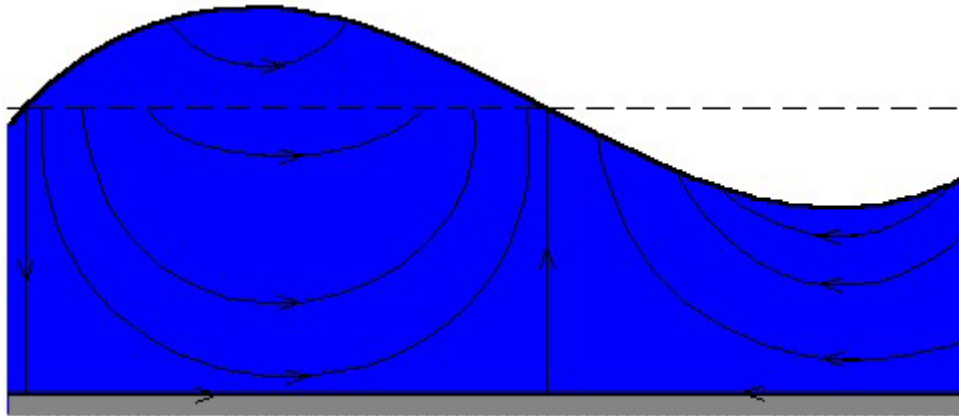


**Figure 2.73: Water Particle Motion Beneath a Wave.**

As the wave length of a ship's bow-wave increases with ship speed, the propulsor finds itself operating in different parts of the wave, eventually, the propulsor will be operating in the lower pressure region in the trough. The horizontal component of the velocity of the particles at this point will effectively reduce the apparent velocity of the water flow at the propulsor. As is the case for the wake fraction, this factor, known as the Thrust deduction Factor, is averaged and tabulated.

As is the case for the propeller, the displacement hull also exhibits the phenomenon of added mass. This can be best visualised as the effect of the water that the passage of the vessel sets in motion. This need only be taken into consideration in system dynamic simulation exercises.

### 2.3.4 Performance Modeling of Marine Gas Turbines

#### 2.3.4.1 Description/Derivation of Model

A gas turbine performance model – that is, a series of thermodynamic routines representing the steady-state and transient aerodynamic processes in the engine – is often assembled using a previous model as a basis and adding/subtracting routines and features as necessary to represent the new project. For aero

derivative marine engines, this is the obvious creation process and a first cut model of a marine variant can be created quite easily.

Initially un-validated, these models are progressively validated through testing and the associated engine analysis process (see below) which refines the modeling assumptions (e.g. component characteristics).

There are always issues with mastering off existing software: Full familiarity with the ‘parent’ software must be gained to make sure that the additions and subtractions do not invalidate/conflict with what is already present – performance models can be extremely complex. Therefore full co-operation across the organizational boundaries must be sought.

### 2.3.4.2 Essential Differences between Marine and Aero Engines

Because marine engines have a different operating profile and run under different environmental conditions to aero engines (e.g. prolonged operation at high ambient pressure) significant secondary air-system changes may be required to attain reasonable bearing loads and cooling behavior. Also, the marine environment is particularly corrosive (salt) and so coatings to some turbomachinery is required. Marine fuel has a wider variance in quality and higher sulphur content than aero fuel – this can impact on hot end life.

All this means that the first refinement of a marine performance model is to account for the marine-specifics. This will involve specialist component areas bidding a level of performance for their component operating in the marine variant.

Marine engines fall into two distinct categories: those which drive a mechanical drivetrain terminating in a propeller or waterjet (these are described in further detail in [Section 2.3.3.4](#) and those which drive electrical generators. These two drive types dictate the Power turbine operating trajectory (see [Figure 2.57](#)).

### 2.3.4.3 Description of Drive Types (Overview)

**Mechanical Drive:** Delivered power is related to speed – often assumed to be a simple cubic relationship, although more complex modeling is required in some cases (see [Section 2.3.3](#)). The PT speed at maximum power is defined by the engine maker at a level which best suits the engine cycle (especially in terms of the power turbine efficiency), as a gearbox is required in the drivetrain, selection of this design speed is not particularly critical to the rest of the drivetrain design.

**Overview of Control Approach:** Delivered power is set by controlling a fuel flow using a closed-loop control of a suitable, power-related parameter. Core engine shaft speed and PT shaft speed are potential governor parameters. Open-loop control of fuel flow could be considered but the variation in marine fuel properties would require some trimming (for each refueling) of the throttle controller gains in order to achieve a consistent throttle characteristic. Using a core parameter for the throttle is beneficial if there is variation in the absorbed power at a PT speed (the absorbed power of a propeller is dependent parameters such as immersion depth and ship speed) as this eliminates the controller ‘hunting’ which may occur for a PT speed control. Core control would result in the core engine being held steady and the PT speed varying ‘in the wash’; PT speed control could result in the core engine cycling in an attempt to keep the PT speed constant – a lifing issue. The response of the PT speed loop could be tuned (i.e. damped) to minimize this, but at the expense of disturbance rejection response. Waterjets are not as sensitive to ship speed, and so a PT speed governor may be less of a problem.

Acceleration and deceleration requirements for a mechanical driveline are not arduous in terms of required engine response (idle to maximum power may be as slow as 2 minutes or more). Cavitations of the propulsor might be the limiting issue.

**Electrical Generation (genset):** Here, the engine drives an alternator which is required to operate at a fixed speed (maintaining the grid electrical frequency at e.g. 60 Hz). Normally there would not be a gearbox between engine and alternator so the overall engine efficiency must be optimal (or near optimal) at the specified grid frequency.

**Overview of Control Approach:** PT shaft speed is controlled to the grid frequency for whatever load is demanded of the alternator. Applied load can change rapidly as different parts of the ship's overall electrical system are switched in or out (a ship's electrical system comprises many different elements: e.g. propulsion system, hotel load, weapons system, docking systems). The controller must therefore be responsive to maintain the grid frequency within the constraints given (e.g. for a load change of  $x$  MW, local grid frequency must not deviate by more than  $y$  Hz and must return to  $n\%$  of nominal frequency in  $t$  seconds). There are clearly greater transient demands placed on a genset marine engine than a direct drive variant, though unreasonable transient demands should be minimized through sensible electrical system design.

Each of the drive types described above can be subject to a rapid off-load. In the case of a propeller/waterjet, certain ship operations can result in the propeller emerging or waterjet aerating which results in a sudden loss of load. In this case a rapid de-fuelling is required to avoid PT overspeed. In the genset case, rapid load drops or, at worst, a 100% loadshed can occur which requires similar action.

A genset and direct drive engine will display different part-power fuel consumption due to the different operating lines on the PT map. **Figure 2.74** shows a typical PT map (aero-derivative) which shows the cubelaw operation running down the map close to peak efficiency, whereas the same engine in genset mode (running at constant speed) loses efficiency sooner.

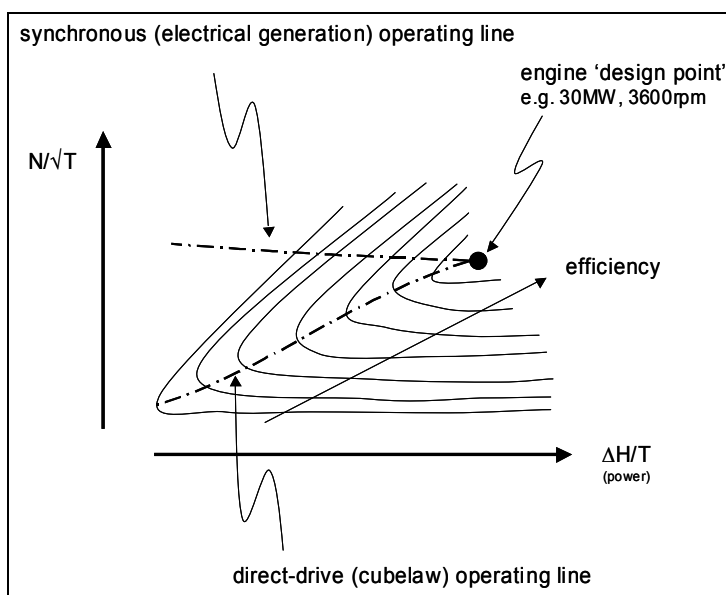


**Figure 2.74: Power Turbine Operating Lines.**

### 2.3.4.4 Description of Installations (Overview)

For a gas-turbine, ideally the air should be presented at the engine face in a well-behaved, uniform profile (pressure and temperature), however as marine engines can be located in various positions in the ship this can be difficult to achieve. Long intake ducting with bends, transitions, filters and cascades can lead to non-uniform profiles. Also, a radial intake may be necessary to turn the airstream just before the engine

face. In addition to accounting for the pressures losses of the intake system, the likely profiles and the effect on the compressor operability margins must be assessed.

Similarly, the exhaust, as with the intake, lower deck space constraints may dictate that the turbine exit flow must turn through a right-angle for entry into the exhaust stake (which may include silencers and waste-heat-recovery boilers). Again, the pressure loss effects on the engine must be understood, but also the upstream effects of the turning process; the power turbine should not be exposed to an excessive circumferential pressure profile which might arise from a poorly designed exhaust collector.

#### **2.3.4.5 Performance Model Inputs/Outputs**

Performance models are usually stand-alone engine models, i.e. they accept a required power condition expressed in terms of one or more of the following: required fuel flow, power level, shaft speed, turbine gas temperature, variable geometry, etc. and calculate flows, pressure and temperatures for the main gas path. A control system may be added so the model is run to a given operator input parameter (e.g. % power, or throttle angle). Other inputs are those defining the environmental conditions (e.g. ambient temperature, pressure and humidity).

### **2.3.5 Marine Performance Model Application**

#### **2.3.5.1 SFC Level**

From the earliest stages in an engine's development, specific fuel consumption (SFC) is of significant importance as it is a major contributor to direct operating costs (though not as critical as in an aero application). For marine and power generation projects, thermal efficiency (ratio of power out to power in) or Heat Rate (inverse of thermal efficiency) is used in preference to SFC. If SFC is used, then the calorific value of fuel must also be specified. Apart from the definition of SFC itself (see below) the accounting planes of SFC must also be defined. It is a common convention that published manufacturer's data is for an engine with no intake or exhaust stack loss. However, marine engines may be packaged to include radial intakes and exhaust collectors, so these losses should be included in the SFC accounting. Comparing published engine SFCs can be fraught as engine flange-to-flange may also be published (i.e. no intake or exhaust collector loss).

Various definitions of SFC may be used, some of which are described below:

- Brochure – a nominal level for marketing purposes;
- Average/new engine – this is usually the level generated by a performance model;
- Minimum /new engine – this includes the production scatter worst debit; and
- Guarantee – the level to which the manufacturer is willing to be contractually bound for as specific application (and which would typically include a specified level of installation loss).

#### **2.3.5.2 Design Data**

Steady-state gas path data (flow, pressure, temperature) is issued at an early stage for a variety of operating conditions for component design. Clearly, the prediction is iterative as component assumptions in the model will change to reflect the latest component design. Transient performance data is rarely used for component design – more for lifing. Transient allowances are built into worst case conditions which form the corner points of the design envelope. Having said this, some engines/applications might involve specific transient events (e.g. fast cargo ships susceptible to repeated waterjet offloads) and so transient data forms an important preliminary design input.

## APPLICATIONS

### 2.3.5.3 Intakes

The engine needs a well-behaved, uniform pressure (and temperature) profile at entry to the first compressor. This is a challenge for some marine installations where the engine is located in the depths of the ship with long and convoluted intake ducting. A performance model must include a pressure loss for the intake and preliminary/generic values of pressure loss must be refined as a particular application emerges. CFD modeling can give insight into the flow-field presented to the engine and perhaps this technique is now sufficiently robust to replace the traditional model testing route. CFD can be used to determine:

- **Pressure Loss** – A fundamental term in the definition of SFC.
- **Engine face profile**, i.e. how the pressure and temperature profile at plenum entry is transferred to the engine face. This can be an important ship/engine functional interface issue. The profile at entry to the plenum (arising from ducting) must have some design constraint to safeguard engine operability. A combined CFD model of the ducting and radial intake may be the best approach here but organizational and commercial boundaries may prohibit. Certain profiles may be present in certain power ranges and impose operability constraints. A typical ship radial intake is shown below **Figure 2.75**, comprising a plenum, centerbody (mushroom) with support sting and vanes. A CFD solution shows the non-uniform pressure field, largely created by the support struts. A circumferential distortion of this nature may excite certain blade vibration modes. The tip-low profile is interesting as it presents the compressor with an opposite effect to the aero-engine equivalent (i.e. with a low pressure compressor in front), and so this prompts questions about compressor operability for the marine variant which may restrict engine operation at higher pressure ratios.

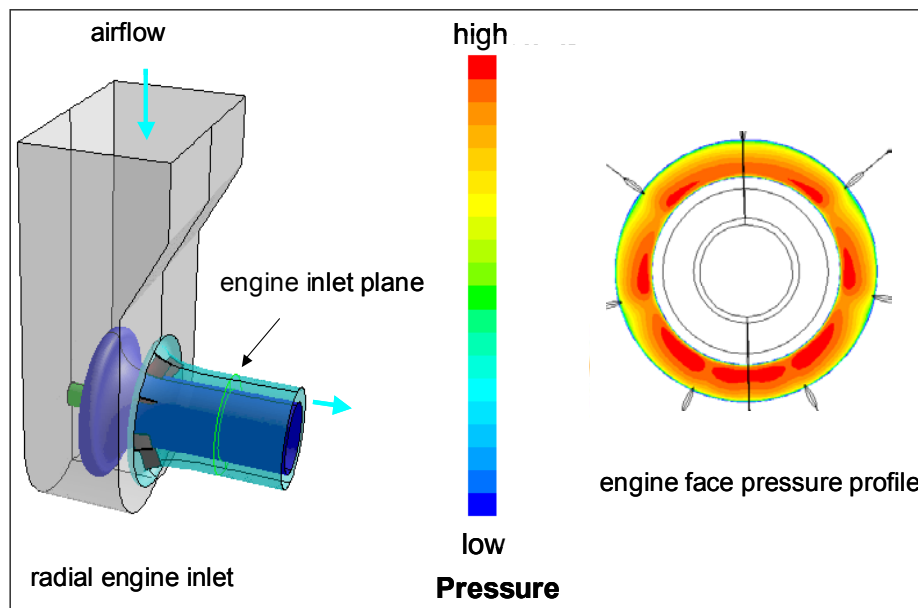


**Figure 2.75: Engine Inlet Pressure Distortion from Radial Intake.**

- **Optimum Locations for Instrumentation** – Control instrumentation is usually required to measure engine inlet pressure and temperature. CFD can be used to determine, if not the best position, the areas to avoid (e.g. in regions of recirculation or high swirl).
- **Pressure loads** – for normal, steady-state operation and for pop-surge events. The latter involves the prediction of the pressure pulse at engine face arising from compressor stall. Performance models can be used for this prediction. The pressure pulse forms the input into an unsteady CFD

solution to determine the sequence and decay of loads on the plenum walls and mushroom. This is an ideal opportunity to interface the boundary condition generator (the performance model) and the CFD solution as there is considerable interaction during the sequence of events.

#### 2.3.5.4 Exhaust

As for the intake, the space constraints imposed by the ship design can lead to significant pressure losses downstream of the power turbine. Again, this is fundamental to the SFC definition.

There are several types of exhaust collector which turn and diffuse the turbine exit flow; a dump diffuser type is shown below. During development, the pressure loss is measured using rakes at entry and exit. The CFD solution enables the pressure rakes to be designed and sited appropriately. Interpretation of results obtained from the test is made easier when the flow pattern is understood. The same solution can be used for structural and heat transfer work. Such a collector design is likely to present a reasonably uniform pressure profile at the power turbine exit.

CFD analysis needs boundary conditions which can be produced by a combination of:

- Performance model (power turbine exit conditions: temperature, pressure and flow);
- Specialist axisymmetric component models (radial and circumferential profiles); and
- Test data (e.g. swirl measured using yaw probes).

This is another opportunity to link CFD and performance predictions as the exhaust collector design process can be iterative due to the effect it can have on the upstream components. The power turbine is sensitive to circumferential exit pressure distortion which can become more pronounced with non-optimal collectors such as the one shown below **Figure 2.76** – a preliminary design of a turn and diffuse type.

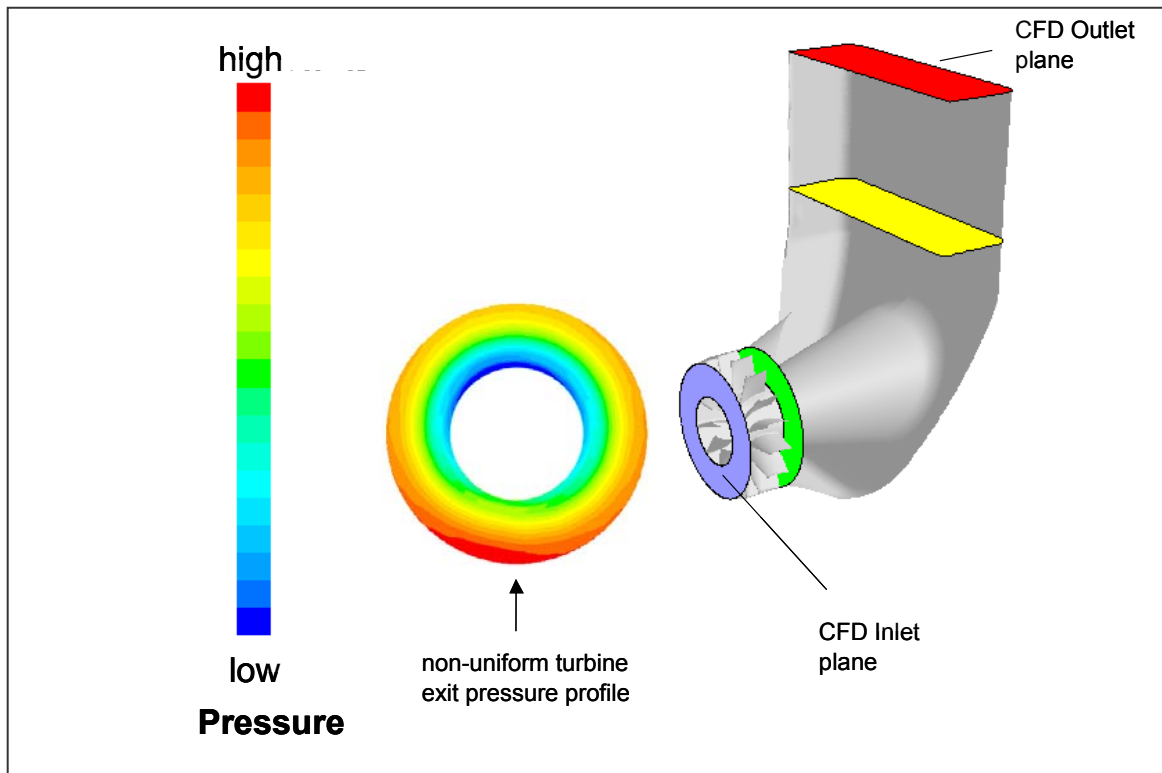


**Figure 2.76: Exhaust Collector Preliminary Design.**

## APPLICATIONS

Engine testing, in particular the assessment of PT performance, requires turbine entry and turbine exit instrumentation. Turbine exit rakes may be situated downstream of fixed vanes and can be subject to a power level and speed dependent effect owing to the wake from the vanes. CFD can be employed to help interpret performance instrumentation and hence be a valuable tool in the Performance process. At certain power levels the (fixed) exit vane incidence may not be matched to the turbine exit swirl and stall can occur (either through excessive positive incidence or, in some cases, negative incidence). A change in turbine speed (at constant power) can restore incidences but this may not be operationally feasible. **Figure 2.77** illustrates the problem, showing pressure profile variation radially, circumferentially and axially (near to the hub). The positioning of instrumentation rakes (used for performance analysis) is clearly critical – at some conditions they may be in a stalled wake, at others, they may sample clean flow. Even if the CFD solution is inaccurate in the absolute sense, it can give a useful insight to the flow conditions and exchange rates with power turbine speed for example.

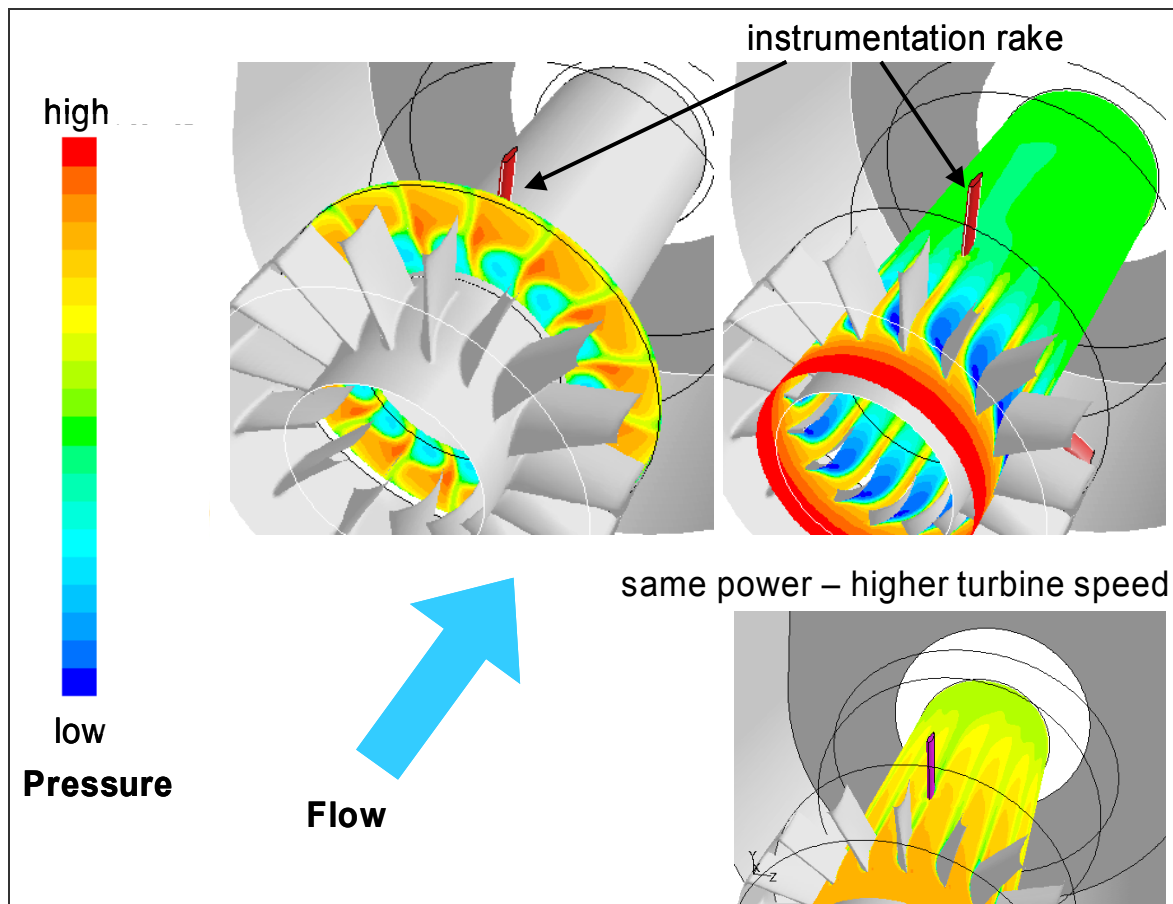


**Figure 2.77:** Turbine Exit Flow Modeling – Bearing Support Strut Vane Wake.

### 2.3.5.5 Air-System

The design of the secondary air-system is another example of an iterative process involving the performance model. Boundary conditions influence the cooling flows which in turn affect the performance and hence the boundary condition. An interface with the specialist tools – normally involving interdisciplinary boundaries – would seem to offer process advantage.

### 2.3.5.6 Testbed Design

Marine engine test-beds have fewer performance correction issues than the aero equivalent, however, the inlet airflow presentation and measurement of airflow (fundamental to a full performance understanding of a test engine) present challenges – particularly on high hub-tip ratio compressors where the flow enters in an annulus rather than a cylinder. CFD techniques can be applied to testbed design or improvement, with the aim of reducing the uncertainties present in performance determination.

### 2.3.5.7 Controls Requirements

The use of performance models to generate controls requirements has already been discussed elsewhere in this document (see **Section 2.1.1.3**). However, there are some specific and interesting control challenges in the marine application which require full and careful treatment in both mechanical and generator applications.

#### 2.3.5.7.1 Loadshed, Full and Partial

At an early stage in the control system requirements capture, the rapid flow reduction capability of the fuel system must be specified to give adequate protection against the rapid offloads mentioned in **Section 2.3.4.3**. Essentially, the requirement here is that the power turbine must not exceed the speed beyond which would result in a significant life penalty. Clearly, the degree of exposure to rapid offloads comes into consideration here – e.g. a fast cargo ship (with direct drive) may be required to experience a large number of offloads during its life on account of its hull/propulsion configuration and operating requirements. Another ship in another role may only encounter a 100% offload relatively infrequently.

A performance model can be run to a range of fuel profiles for a given set of load profiles with a range of drivetrain inertias in order to scope the requirement. The fuel must be reduced sufficiently quickly to prevent high turbine speeds but sufficiently slowly to prevent engine flameout (assuming that prevention of flameout is a requirement in this case). **Figure 2.78** shows turbine overspeeds for:

- load reduction from 100% to parasitic levels in 50 ms – black line
  - as 1. but over 100 ms – red line
  - as 2. but with 50% drivetrain inertia – green line
- ... all for a constant fuel reduction profile vs. time (from max to idle levels in around 200 ms).

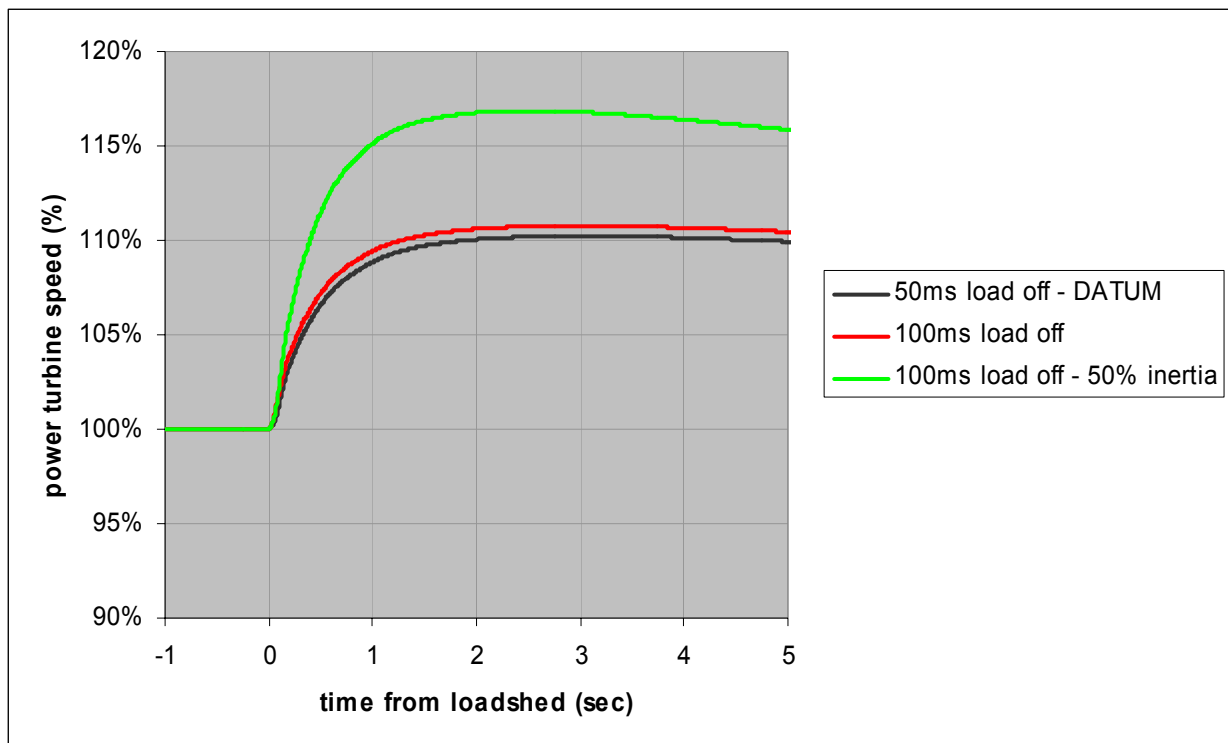


**Figure 2.78: Power Turbine Overspeeds for Rapid Offloads – Inertia and Fuel Response Effect.**

Inertia clearly has a large effect (no surprise). Driven inertia varies greatly across applications – electrical generators are generally heavier than mechanical drive systems; load-off time, in this example has a smaller effect. However, load-off characteristics vary considerably from electrical (near instantaneous) to mechanical drives (300 – 400 ms) and so the loadshed scenario must be carefully scoped. Prevention of speed rising in excess of 110% nominal speed could be considered as a reasonable target.

Partial offload may be experienced, accommodation of which may require different (perhaps less vigorous) control action.

There may be operational requirements that normal control is regained quickly after an offload, in which case, the fuel must be re-introduced rapidly otherwise the power turbine speed will droop. A full electrical offload (arising from a fault condition causing circuit breakers to open) will result in the engine returning to a state where it may be re-connected to the local grid at the command of the higher-level electrical power control system.

Normal load changes in electrical genset operation are accommodated by accelerating or decelerating the core engine within the operability constraints of the compression system. Control accel/decel limits need to be derived using the performance model which will disclose the compressor working point trajectory. In this case, an iterative approach is needed by integrating the performance model with the (emerging) controller model, so the acceleration of the engine is determined by the acceleration controller response. As such, the performance model is being used to progressively validate the emerging performance requirements for engine control. Model integration is discussed further below.

Modeling of loadshed is also sensitive to the accounting of heatsoak – that is the time-dependent modeling of energy passing between gas-stream and engine hardware (blades and casings). **Figure 2.79** shows a loadshed modeled as before (i.e. to an applied load profile and fuel profile) and with varying heatsoak models:

- The dark line represents the correct (validated) simulation.
- The purple line represents the absence of any heatsoakage modeling in the power turbine – a small reduction in modeled overspeed.
- The yellow line represents no heatsoakage modeling at all – i.e. available energy at the power turbine is dependent on the fuel input and the time-dependent behavior of the shafts (rundown following fuel reduction). The modeled overspeed is some 60% lower than the correct simulation.

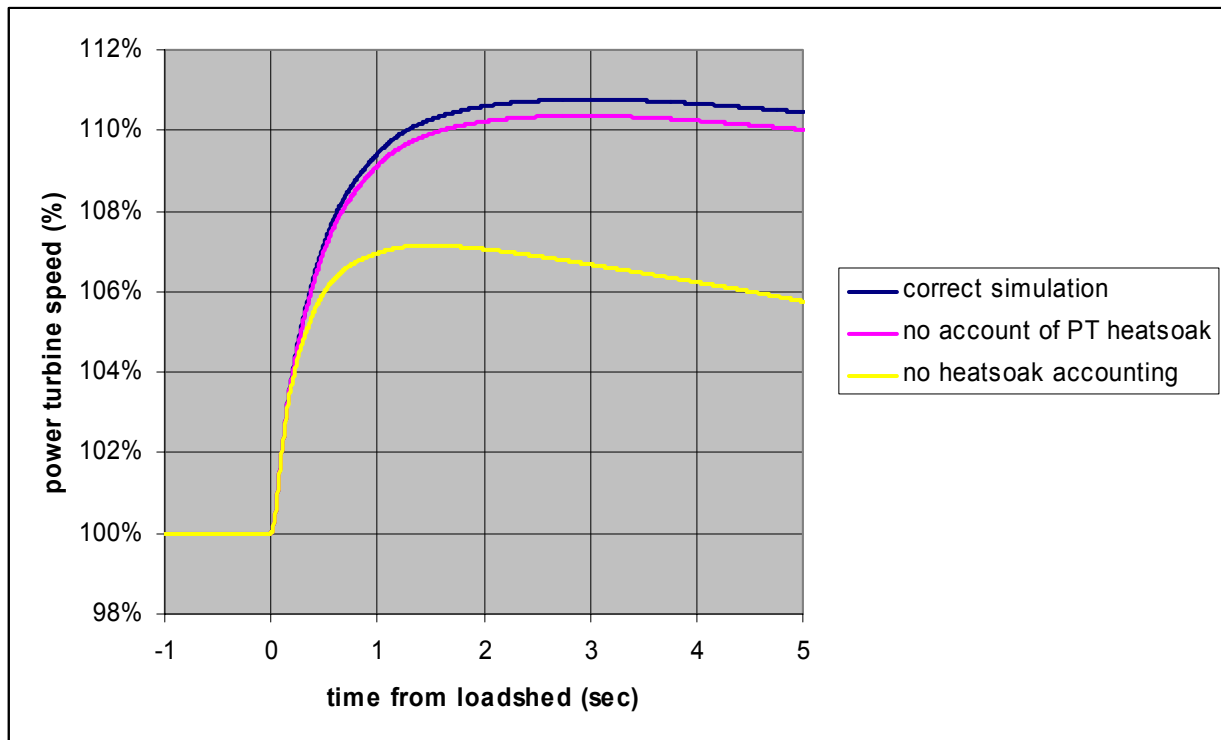


**Figure 2.79: Power Turbine Overspeeds for Rapid Offload – Heatsoakage Effect.**

Clearly, there is a need to refine the heatsoak model and validate those assumptions to gain a good predictive capability for loadshed – and perhaps more importantly – for shaft failure which is discussed below.

#### 2.3.5.7.2 *Shaft Failure*

A more critical event is a driveshaft coupling failure – either failure by over-torque or de-coupling stemming from a mis-assembly. In this case, the fuel system needs to act extremely quickly to shut the fuel as the power turbine will overspeed beyond blade-release or disc-burst speed owing to the loss of driven inertia. Control action is needed to assure margin against this hazardous event (a hazard of this type is ‘designed-out’ through capability and reliability arguments, and inspection regimes to a very low probability). A detection mechanism for this rapid action must be devised – transient modeling can help in identifying the characteristic of the event which leads to definition of controller logic. In this case avoidance of flameout is not an issue – indeed flameout helps reduce the overspeed, although only slightly as the rundown of the core compressor(s) and turbine(s) provides significant ‘blowing’ of the power turbine once the fuel effect has gone, as does heatsoak. **Figure 2.80** shows the terminal speed attained for a shaft failure case (blue line) with the fuel pull-off rate assumed for the loadshed case (i.e. the maximum fuel rate needed for normal operation). A more rapid fuel pull-off is required to avoid disc burst (pink line). This may involve analogue or mechanical triggering of fuel shut off.

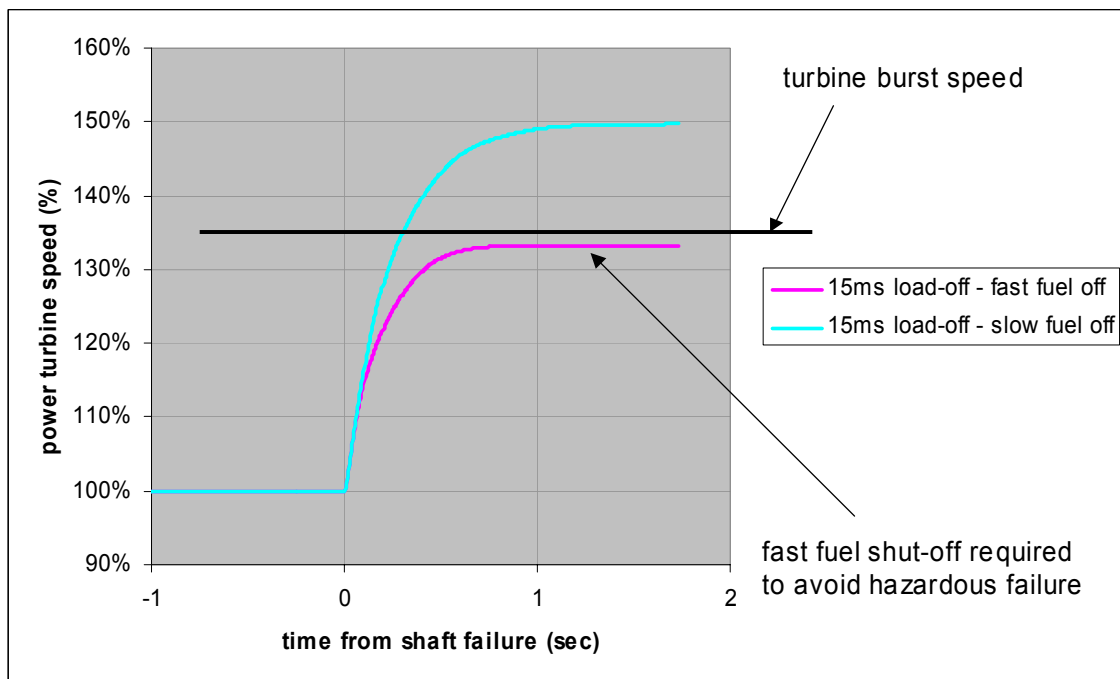


**Figure 2.80: Power Turbine Overspeeds for Coupling Shaft Failure.**

#### 2.3.5.7.3 Integrated Models (Engine + Controller)

The integration of models is covered elsewhere in this document; however it is worth summarizing the issues here. Ideally a single thermodynamic model should be capable of all functions required of an engine model in the design and validation process *viz.* performance prediction, controller design, ship integration studies, control-system validation (real-time – hardware-in-the-loop), however organizational boundaries as well as technical challenges might preclude a universal model, and so there may be different models for different purposes. Maintaining a consistency between these models and managing their differences can be time-consuming. There is a spectrum in fidelity and consistency (these terms of are discussed in [Section 2.1.2.2](#)).

- **Simple Models:** In a ship, the GT may be a small part of the overall propulsion/electrical system, a simple model may be appropriate for system studies – perhaps consisting of just a series of steady-state look-ups with a basic dynamic response (see [Section 2.3.2](#)). A similar level of modeling may also be adequate for simulators used for training purposes.
- **Detailed Models:** The in-depth thermodynamic understanding of engine performance and operability – in all GT application areas – requires detailed thermodynamic representation of components as described above.
- **The Middle Ground:** Reduced detail thermodynamic models are often used for controls-design work, some projects/organizations may use piecewise linear models which can be derived using the high detail thermodynamic model. For real-time applications where there is limited computer processing power, these models offer a good compromise between detail and consistency.

#### 2.3.5.8 Engine Testing

In order to make best use of expensive engine test time, engine tests must be carefully planned and executed. Using the integrated performance model in the test planning process can avoid nasty surprises on test, and having a model to hand during the test can help diagnose unexpected behavior. This is especially valuable for away-from-base testing where full technical-team back-up is not available.

### 2.3.5.9 Analysis of Testdata – Referral of Operating Point

Observed engine performance is required to be quoted at (referred to) standard (reference) conditions. In the marine world, it has been common practice to ‘correct’ the data using non-dimensional approach however this is unsatisfactory as turboshaft engines in particular do not necessarily display non-dimensional behaviour, e.g. consider performance at a constant shaft power, and at different installations. Dimensional corrections based on performance model exchange rates are often used. Such an approach is transparent in that it is clear how the referral has been made; this can be an advantage when it comes to customer scrutiny of claimed performance. Analysis by Synthesis (AnSyn) which is discussed at length in the aero applications chapter offers thermodynamic rigor but has the disadvantage of being somewhat opaque to those not closely associated with engine performance.

An analysis program calculates from measurements, parameters such as intake air mass flow and averaged (1 dimensional) values of total pressure and temperature at measurement planes within the engine. Some measurements comprise many individual measurements which are averaged to produce a single value. Parameters which cannot be measured directly are calculated (i.e. derived) from other measurements. For example, intake airflow is derived from total and static pressure measurements in the intake, inlet total temperature and duct area. As a result, the individual component performance can be determined. For example, high-pressure compressor (HPC) efficiency is obtained from HPC pressure ratio ( $P3/P25$ ), entry temperature ( $T25$ ) and exit temperature ( $T3$ ).

A synthesis program works in the opposite sense to an Analysis program. Using predictions of component performance (e.g. compressor, combustor, turbine and nozzle) and a set of environmental conditions (e.g. ambient temperature, pressure, humidity) the ‘synthesis model’ predicts/calculates the performance and functional behavior of a gas turbine engine. Parameters such as intake airflow, fuel flow, thrust, total pressure and temperature at specific locations in the engine (e.g. HPC entry and exit, HP turbine entry and exit) are predicted. Parameters such as compressor stability margin when the engine is subjected to intake distortion or transient engine operation (rapid throttle movements) can also be predicted.

Traditional techniques use a stand-alone Test Bed Analysis (TBA) program. The term AnSyn is used to describe a process where engine test measurements are analyzed using a synthesis program. In this case, when measured parameters such as fuel flow, compressor delivery temperature and pressure are different to the values predicted by the synthesis model, the model component design assumptions (e.g. pressure ratio, flow and efficiency on component characteristics) are varied (factored) according to a ‘matching scheme’ until agreement is reached. Thus an accurate model of each testpoint is produced which can be re-run (as a pure synthesis) at reference conditions (i.e. ‘referred’).

## 2.3.6 Synoptics for Marine Applications

### 2.3.6.1 Ship Propulsion System – Transients

#### *Modeling Techniques Used*

In order to model transient disturbances, representations of several components of the ship’s propulsion system are required to be modeled.

- **Engine:** A thermodynamic 0-D/1-D representation (including dynamic terms).
- **Gearbox:** The gear ratio is of prime importance as it affects the effective drive inertia.
- **Coupling Shaft:** Stiffness may be an issue for long shafts, breaking the shaft line into smaller elements may be required in this case.
- **Propeller:** A specific load characteristic must be applied. This is often represented at a simple level – e.g. absorbed power going with the cube of rotational speed, but additional terms can be added to give dependencies on, e.g. ship speed and propeller depth.

## APPLICATIONS

---

- **Propulsion Control System:** The action of the higher level control system can dictate how disturbances are accommodated.
- **Engines of Various Types** (gas-turbines, electric, diesel) may be combined – their combined effect must be taken into account.
- **Wave** – The frequency and size of disturbance can be taken into account.

### *Potential Benefits*

Looking at whole system response allows the optimization of response for that system and also gives an understanding on the conditions placed on each part of the system. Understanding the demands (e.g. temperature and torque transients) placed upon the gas-turbine to meet certain response requirements can influence the design process from a very early stage, and so it is important to put the effort into assembling such integrated models from early in the design process. Detail can be added as the design evolves. In addition to engine hardware (blades, etc.) the control system hardware and software logic can be progressively refined through attention to such a modeling activity.

### *Cited Example*

- Dzida, M. and Domachowski, Z., “Influence of Disturbances on Transients of a Gas Turbine Ship Propulsion System – Preliminary Investigations”, ASME Paper # 2000-GT-0325, Presented at ASME International Gas Turbine Institute’s Turbo Expo, Munich, May 2000. [2.50]

A model of a 235 kW engine operating at 24000 rpm driving a propeller through a reduction gearbox was assembled in the MATLAB/Simulink environment. The response to step changes under the influence of various control constraints was examined to establish trade-offs between response and torsional stresses in the gas generator.

**Figure 2.81** and **Figure 2.82** (Figures 6 – 9 from the published paper) show the response to engine shaft speed setpoint change. A varying speed response is seen depending on controller interaction – these differing responses imposing differing mechanical and thermal stresses in the gas generator.

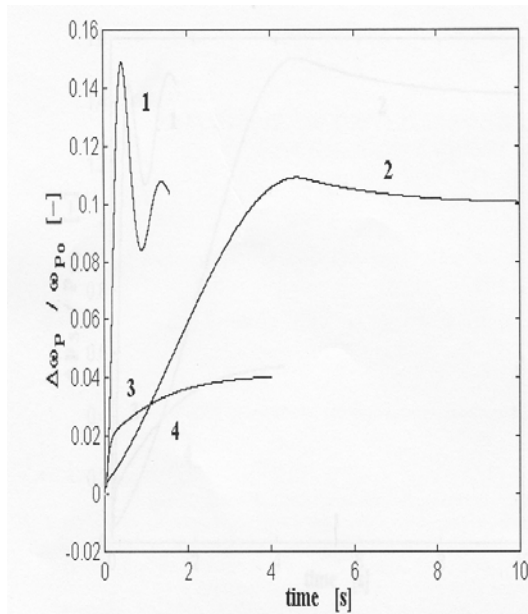


Figure 6. Ship shaft angular velocity step response to set point change

- 1 - linear controller
- 2 - influence of combustion chamber outlet temperature limiter
- 3 - influence of fuel flow limiter
- 4 - influence of both 2 and 3 limiters

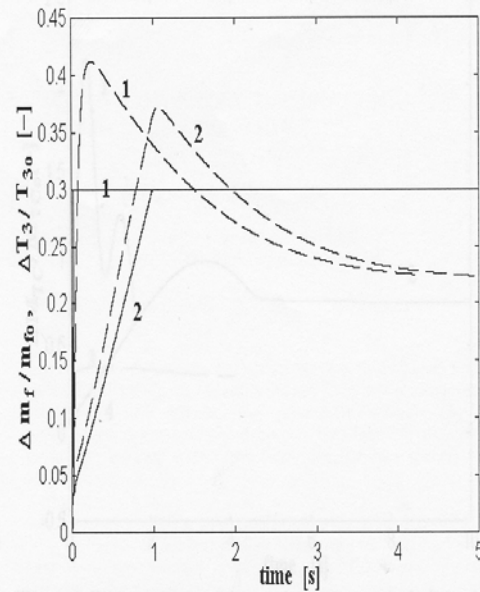


Figure 7. Step response of fuel flow rate and combustion chamber outlet temperature to ship propeller angular velocity set point change

- - fuel flow rate;
- - - combustion chamber outlet temperature
- 1 - Controller with fuel flow limiter
- 2 - Controller with the fuel flow and combustion chamber outlet temperature limiters

Figure 2.81: Figures 6 and 7 Pulled from the Referenced Document.

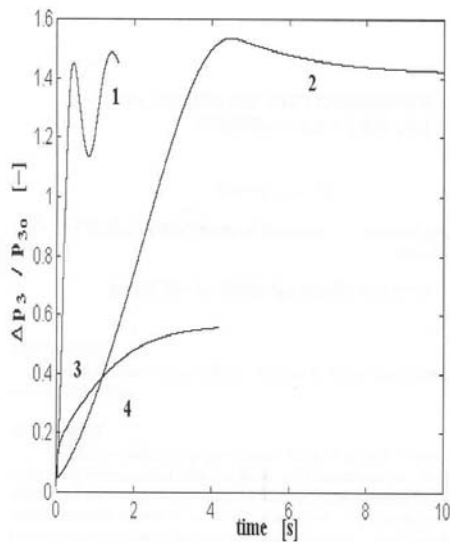


Figure 8. Combustion chamber outlet pressure step response to ship propeller angular velocity set point change

- 1 - linear controller
- 2 - influence of combustion chamber outlet temperature limiter
- 3 - influence of fuel flow limiter
- 4 - influence of both 2 and 3 limiters

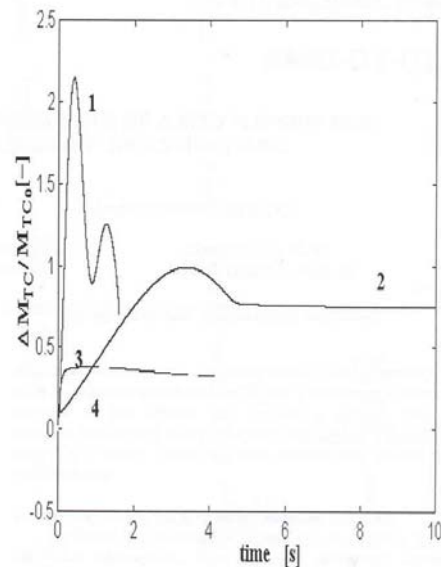


Figure 9. Step response of torque in compressor shaft to ship propeller angular velocity set point change

- 1 - linear controller
- 2 - influence of combustion chamber outlet temperature limiter
- 3 - influence of fuel flow limiter
- 4 - influence of both 2 and 3 limiters

Figure 2.82: Figures 8 and 9 Pulled from the Referenced Document.

## APPLICATIONS

---

### *Limitations of Chosen Modeling Technique*

This level of model provides a good overview of whole system design and hence a useful tool to scope the effects on the whole system by external and internal influences. It is important that the external influences, e.g. load fluctuations for certain sea states are considered representative of the particular ship operational profile.

#### **2.3.6.2 Health Management**

##### *Modeling Techniques Used*

Real-time simulation of gas-turbine performance is used with data validation/checking methods to identify faults and deterioration. Off-line processing/view facilities are also available.

##### *Potential Benefits*

On-line condition monitoring is capable of “performance and vibration diagnostics, sensor fault detection, event archiving, and maintenance reasoning” and offers the potential to “dramatically improve the condition monitoring and health management capabilities”.

##### *Cited Example*

- Kacprzyński, G.J. and Deshmukh, S., “Poseidon: The US Navy’s Comprehensive Health Management Software for LM2500 MGTs – Part 1”, ASME Paper # GT2003-38485, Presented at ASME International Gas Turbine Institute’s Turbo Expo, Atlanta, June 2003. [\[2.51\]](#)

According to the abstract: “The paper describes the initial features and capabilities of the US Navy’s conceptual condition monitoring software, called Poseidon, for its LM2500 Marine Gas Turbines”.

At the heart of the system is a real-time dynamic model of the LM2500 operating with a controller model, and driving a propeller model. These three elements are built and integrated into MATLAB/Simulink. No detail is given (in this paper) of the methods to model the gas turbine, however the various types of thermodynamic modeling approaches are well documented elsewhere.

Performance shifts can be confused with sensor faults, and so a two-pronged approach is taken to identify sensor faults. Comparisons of measured parameters against modeled parameters, along with a generic signal processing techniques (e.g. spike identification) are used in this example. Where more than one sensor error is detected, performance diagnostics are performed.

Derived parameters (e.g. compressor efficiency) are trended to form performance curves (examples are given in [Figure 2.83](#) below). Specific events, e.g. start-up profile are also captured. Examination of these trends and events can trigger maintenance action, e.g. water-wash, borescope, etc.

Performance Curves
Compressor: Compressor Inlet Mass Flow vs. Pressure Ratio vs. Ngg
Compressor: Compressor Outlet Mass Flow vs. Pressure Ratio vs. Ngg
Compressor: Compressor Inlet Mass Flow vs. Isentropic Efficiency vs. Ngg
Power Turbine: Power Turbine Speed vs. Shaft Horsepower
Power Turbine: Power Turbine Speed vs. Specific Fuel Consumption
Power Turbine: Load vs. Power Turbine Inlet Temperature
Overall: Load vs. Compressor Isentropic Efficiency

**Figure 2.83: Derived Performance Curves.**

Events captured can be viewed and further analyzed off-line with the Poseidon Desktop Simulator – see **Figure 2.84** below.

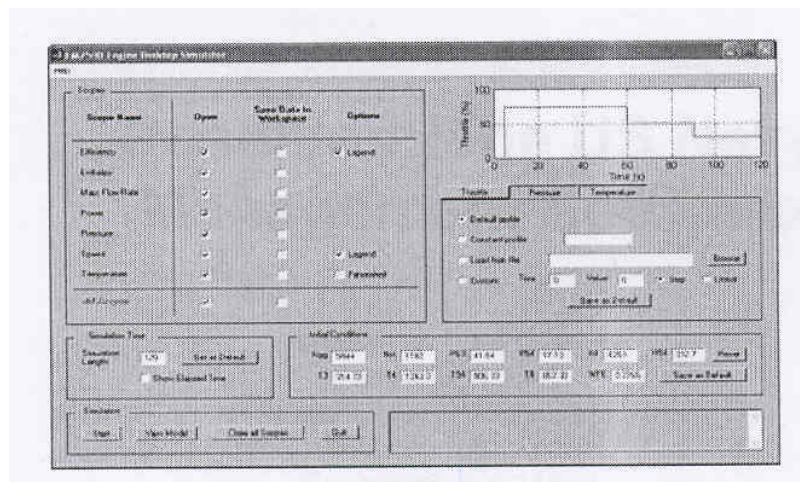


**Figure 2.84: Poseidon Desktop Simulator GUI.**

The derived parameter datasets, e.g. efficiencies, flows are compared against a library of performance ‘error patterns’, e.g. VSV mis-rigging, T2 calibration shift, compressor fouling. Kalman filter and least-square minimization techniques are used in the processing/matching of error patterns to observed/derived performance.

### ***Limitations of Chosen Modeling Technique***

In order to run real-time on a particular processor, the level of complexity of an engine model may need to be reduced from that level of complexity which is desirable. However, given the capability to re-analyze data off-line (i.e. non-real-time), this is not a fundamental problem. Also, it is worth pointing out that the purpose of this type of system is to identify a trend/event and point the finger at a likely cause, rather than account for small and subtle thermodynamic terms which have a performance effect – and for which a more detailed model is required.

## APPLICATIONS

### 2.3.6.3 Condition Monitoring

#### *Modeling Techniques Used*

As with the preceding example this example concerns the monitoring, collection and real-time processing of data to formulate a report of engine condition to contribute to an on-line through-life management of the propulsion system. Real-time modeling of the engine is used in order to provide a reference dataset to which observed parameters/behavior can be compared.

#### *Potential Benefits*

The basic aim is to provide a facility to identify faults and hence prompt remedial action. An extension to this is to provide a life expectancy which can be part of a just-in-time type of repair and overhaul regime.

#### *Cited Example*

- Grzadziela, A., Stapersma, D. and Charchalis, A., “Condition Monitoring and Fault Diagnosis of Naval Gas Turbines”, ASME Paper # GT-2002-30270, Presented at ASME International Gas Turbine Institute’s Turbo Expo, Amsterdam, June 2000. [2.52]

This paper describes the system which has been used on gas-turbine ships in the Polish Navy – Base Diagnostic System of Naval Gas-Turbine Engines (BDS) **Figure 2.85**.

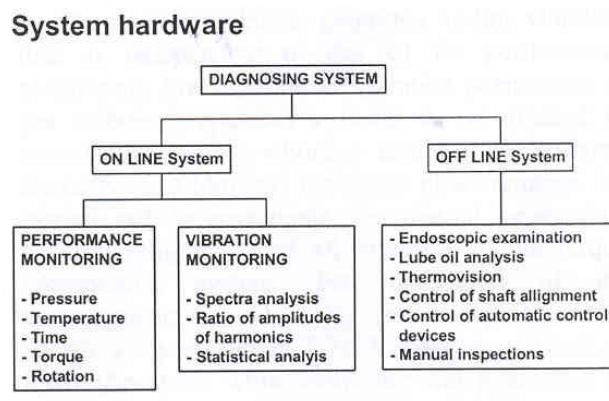


**Figure 2.85: System Overview.**

Of particular interest is the performance diagnostics section although data from, e.g. the vibration monitoring can in some cases confirm a conclusion drawn by performance function. Here performance data is gathered during various phases of operation:

- Cold rotation;
- Hot start-up;
- Engine shut-off;
- Nominal running under load;
- Transients; and
- Stopped engine.

In addition to engine parameters, ship motion parameters are also collected.

Some items of raw data are examined – an example of gas generator exit thermocouple monitoring is given below **Figure 2.86**.

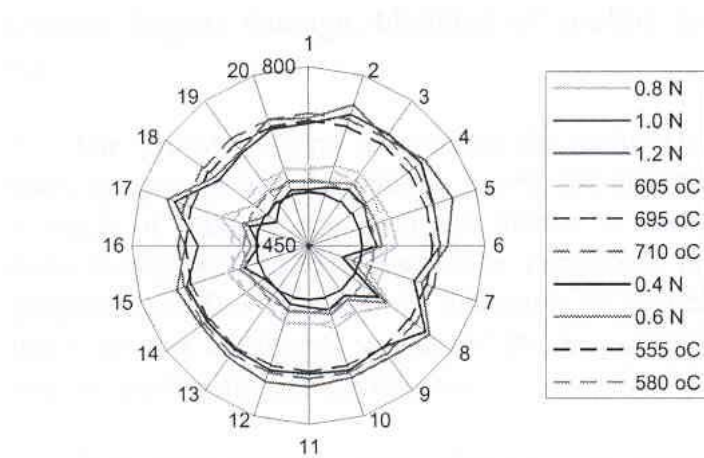


**Figure 2.86: Raw Data Processing (Gas Generator Exit Thermocouple).**

The principle of condition monitoring and diagnosis is summarized in **Figure 2.87** below:

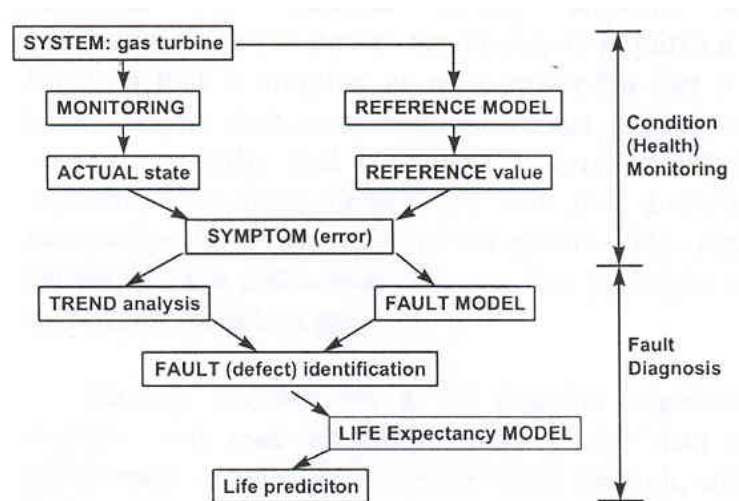


**Figure 2.87: Generic Condition Monitoring and Diagnosis Process.**

The ‘residual’, i.e. the differences between expected and observed parameters can point directly to faults, but their combination with fault models where symptoms are related to specific failures adds further diagnostic capability. Extension of failure diagnosis to life prognostics depend on further modeling which inevitably involves specialist knowledge and multi-disciplinary approaches.

The paper discusses the various levels of engine modeling:

**First Principle Model:** This type is based on physical principles such as “conservation laws (mass, energy) and constitutional laws describing material properties, e.g. the gas laws) and empirical characteristics”. There is some trade between run-time and “richness” (fidelity). The point is made that first principle

## APPLICATIONS

---

models are the norm for performance modeling/monitoring, but are beyond current expectation for vibration monitoring (for example).

**Regression Model:** These are models created from a database of data – sometimes called “statistic models”. Such models should be assembled with care to use the best/most thermodynamically sensible correlations – use of a first principle model to help in the formulation is advisable. Although most common for steady-state models, regression models can be extend to transients.

**System Identification:** This may be described as a transient regression model and is of a similar ‘black-box’ character to the SS equivalent.

**Fingerprint:** Where real data is sampled and stored, it can also serve as a model and can be used in conjunction with pattern recognition methods. This approach is suited to vibration monitoring.

**Pattern:** A fuzzy representation used in combination with pattern recognition methods.

**Neural Networks:** Akin to regression models but where the method derives the interrelationships inherent in the data itself.

There is some discussion on the use of more detailed turbomachinery models and the need to embrace iterative techniques as fidelity increases.

### *Limitations of Chosen Modeling Technique*

The discussion on differing types of model draws attention to the fit-for-purpose debate, and a conclusion is drawn that a zoom-out approach (i.e. incorporation of some higher level influence such as sea waves) would be beneficial as it seems that the performance part of the monitoring function is best at high power – the lower power region being influenced by propeller loads and external disturbances which have yet to be incorporated into the model.

The improvements in computing capability have already been cashed by incorporating models of greater fidelity.

### **2.3.7 References for Marine Propulsion Systems**

- [2.41] Reynolds, I.E. and Tooke, R.W., “Merchant Ship Applications of the MT30 Marine Gas Turbine”, *Proceedings of The Motor Ship 27<sup>th</sup> Annual Marine Propulsion Conference*, Bilbao, Spain, January 2005, pp. 175-189.
- [2.42] Rubis, C.J., “Braking & Reversing Ship Dynamics”, *Naval Engineers Journal*, Vol. 82, No.1, pp. 65-76, 1970.
- [2.43] Vassilopoulos, L. and Heliotis, A., “Modelling of Shaft Couplings for Alignment and Vibration Calculations”, *Propellers '98 Symposium*, SNAME, September 20-21, 1998.
- [2.44] Rains, D.A., van Ledingham, D.J. and Sclappi, H.C., “Hydrodynamics of Podded Ship Propulsion”, *J. Hydronautics*, Vol. 15, Nos. 1-4, pp. 18-24, 1981.
- [2.45] Oosterveld, M.W.C., van Lammeren, W.P.A. and van Manen, J.D., “The Wageningen ‘B’ Screw Series”, *SNAME Transactions*, 1969.
- [2.46] Oosterveld, M.W.C. and van Oossanen, P., “Further Computer Analyzed Data of the Wageningen ‘B’ Screw Series”, *International Shipbuilding Progress*, Vol. 22, No. 251, pp. 251-262.

- [2.47] Strom-Tejsen, P. and Porter, R., “Prediction of Controllable-Pitch Propeller Performance in Off-Design Conditions”, Paper VII B-1, *Third Ship Control Symposium*, Bath, England 1972.
- [2.48] Radojicic, D. and Matic, D., “Regression Analysis of Surface Piercing Propeller Series”, Nav. & HSMC Int. Conference, Naples, March 18-21, 1997.
- [2.49] Politis, G.K., “Ventilated Marine Propeller Performance in Regular & Irregular Waves; An Experimental Investigation”, *Chem99, Computational Methods & Experimental Measurements*, Naples, 1999.
- [2.50] Dzida, M. and Domachowski, Z., “Influence of Disturbances on Transients of a Gas Turbine Ship Propulsion System – Preliminary Investigations”, ASME Paper # 2000-GT-0325, Presented at ASME International Gas Turbine Institute’s Turbo Expo, Munich, May 2000.
- [2.51] Kacprzyński, G.J. and Deshmukh, S., “Poseidon: The US Navy’s Comprehensive Health Management Software for LM2500 MGTs – Part 1”, ASME Paper # GT2003-38485, Presented at ASME International Gas Turbine Institute’s Turbo Expo, Atlanta, June 2003.
- [2.52] Grzadziela, A., Stapersma, D. and Charchalis, A., “Condition Monitoring and Fault Diagnosis of Naval Gas Turbines”, ASME Paper # GT-2002-30270, Presented at ASME International Gas Turbine Institute’s Turbo Expo, Amsterdam, June 2000.

## **2.4 GAS TURBINE ENGINE SIMULATIONS FOR VEHICULAR APPLICATIONS**

This section will address gas turbine for vehicular applications. Although there have been applications for ground passenger vehicles (autos), most notably the foray by Chrysler in the 1960’s, this section will only address the military application – the tank.

### **2.4.1 Historical Background [2.53]**

During World War I the stalemate on the Western Front resulted in enormous losses to the infantry on both sides. During some of these battles 200,000 plus casualties were common, the French and the British lost more than one million men during this phase of trench warfare. The main cause of this stalemate was the inability of the infantry to advance over barbed wire, sometimes more than 3 feet thick, machine guns firing against the open troops, and the inability of line of fire artillery to advance with the attacking forces over this pocketed terrain.

In the past a number of suggestions were made to use steam powered armored vehicles, as well as small gasoline powered vehicles. However, the difficult terrain between the trenches made these vehicles impracticable. It did result in the development of armored cars and some mobile artillery. Unfortunately these vehicles were confined to the roads and could not overcome the battlefield terrain problems. As a result of this stalemate, the defense could prevent any significant advance without tremendous casualties. The traditional army approach of massed infantry attacks did not work and other methods were required. Beyond the immediate problem of getting the infantry through the defensive trenches, there was a need to get line of fire heavy weapons where they could be supportive of the infantry.

Several land ships were designed during the 1914/1915 period to address this problem by the British Army. They were not to successful until a large vehicle was designed with tracks installed around the outside of the armored body. This design enabled the tank to cross trenches 1.5 meters wide and pass over obstacles of 1.4 meters. This vehicle and a sister land ship successfully demonstrated the above. In 1916,

## APPLICATIONS

100 vehicles were ordered. The tank as it was now named contained two 57 mm cannon in sponsons, and 3 machine guns, see **Figure 2.88**.

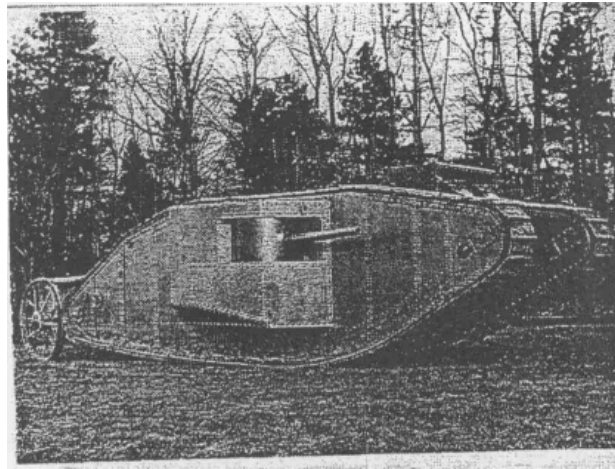


**Figure 2.88: Early WWI Vintage Tank.**

The French Army was not idle during this time and developed several designs. The design of the Renault FT tank evolved. It was a light tank of 7 tons with a top speed of 7 km/hr. It carried either a machine gun or a 37 mm cannon in a turret. This tank was a forerunner of modern tanks with a rotating turret, the engine and transmission in the rear and the tracks driven from the rear sprockets. It was used by many other governments and was still in use by some armies at the outset of W.W.II, see **Figure 2.89**.

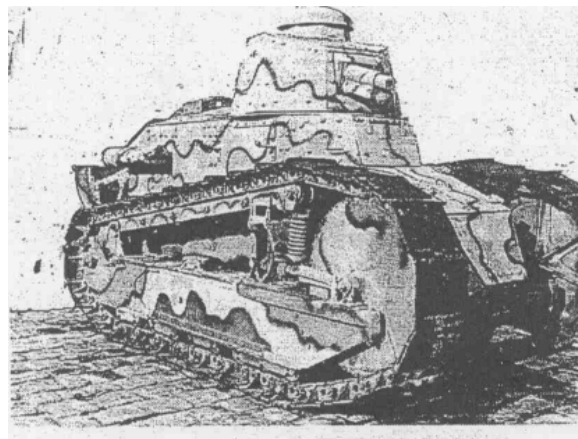


**Figure 2.89: Renault FT Tank.**

The use of tanks was not overly successful during W.W.I. The initial attack used less than 50 tanks and was not successful other than alerting the Germans that there was a new weapon being tested on the western front. A year later in 1917, approximately 500 tanks were used to attack the Germans with outstanding success. Unfortunately the army was unable to take advantage of their success because of the tanks limited range. As newer designs became available in 1918 a second major attack was made that was very successful.

At the end of World War I tanks were still only considered to be infantry support vehicles during trench warfare. Since this type of warfare would probably not occur again tanks soon started to become forgotten.

At the end of W.W.I Britain had manufactured over 2500 tanks, but had abandoned any plans to produce more.

France had almost 4000 units of the Renault FT light tank at the end of the war. Some of these were turned over to the American Army since they arrived in Europe without any heavy equipment. After the war the United States manufactured approximately 2000 copies of the French Renault FT called the M1 917 light tank. In France the role of the tank was reduced to supporting the infantry, and as such limited the potential of these vehicles to the forward speed of the infantry. Although the French Army had more tanks than any other nation from the early 20's up to the beginning of W.W.II their role was still limited to infantry support.

At the same time the American Army had adapted a similar philosophy and the majority of American tanks were a copy of the light M1 917. In fact the American Army had incorporated the armor units into the infantry in the early 20's. Although there were a number of officers in the various armies of the world that recognized the need for heavy armored divisions to fight other tanks and penetrate enemy defenses, this opinion was not generally accepted. The French relied on their Maginot Line as their first line of defense. In the case of the United States, financial constraints limited the ability to produce new armor for an unrecognized need. It has to be pointed out that an armor division is many times more expensive to equip and maintain than an infantry division.

When Hitler and the German Army achieved their blitzkrieg break through in Poland and France it immediately required a rapid rethinking of the past theories. The German breakthrough tactics, along with the American support of Britain required the United States to begin tank construction as soon as possible. This resulted in the development of the M-3 tank. Because of the immediate need, the tank did not have a movable turret, had only a 75 mm gun, and was powered by an aircraft air-cooled gasoline engine. Although obsolescent when delivered to the British in North Africa in 1942 it was still an immediate help in defending Egypt.

While the M-3 tank was being manufactured, an improved US tank, the M-4 Sherman, was being developed, see **Figure 2.90**. The M-4 had a rotating turret and the 75 mm gun. It became the main battle tank for both the American and British forces along with the rearming of the French Army. The tank was considered to be two years behind the German equipment, but it was extremely reliable. Unfortunately, the gun could not cope with the latest German armor. It has been stated that one German Panther tank could defeat 3 American M-4's. The Panther tank is depicted in **Figure 2.91** below. Although the M-4 was considered a widow maker, sheer numbers enabled the Americans to win most of the tank battles.



**Figure 2.90:** M-4 Sherman Tank.

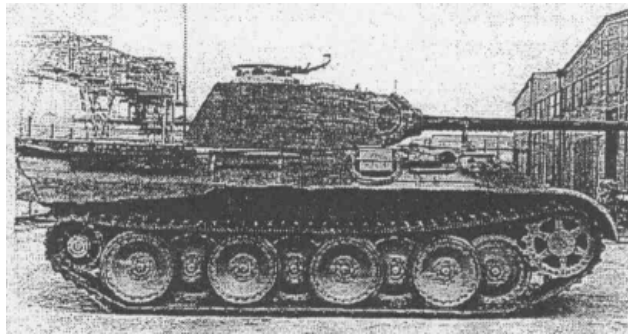


**Figure 2.91: Panther Tank.**

At the end of W.W. II the United States had superior bombers, fighter aircraft and probably the most modern Navy in the world. It also possessed more tanks than any country except perhaps Russia. However, it was clear that our armor technically was not the equal to that of the defeated Germans.

During the post war period the US Army developed two improved models over the period of 1945 to 1965. These were the M48 and the M60. The Armament was increased to a 105 mm cannon developed by the British. The power plant was a new diesel engine developed specifically for the M60, depicted below in **Figure 2.92**. This corrected a major problem due to the flammability of the fuel previously used in American tanks. The M60 was a reliable armored vehicle and was used as the Main battle tank for a long period of time. Both the M48 and the M60 were issued to our allies late in the period.



**Figure 2.92: M60 Tank.**

In the mid 60's it became apparent that the US Army main battle tank was becoming obsolete when compared to our adversary Russia. Russia had many more tanks in their inventory than the combined NATO forces, as well as more modern units than were available to the US forces.

As a result of this apparent unbalance an international effort was begun to develop a new tank for both the US Army as well as the German Army. The tank was designated the MBT 70. This tank was to contain an American engine and a German transmission with both countries sharing the development cost. The MBT70 was to be an extremely modern tank utilizing all the latest technology. It was to incorporate a gun that could fire both missiles and projectiles, a variable compression ratio diesel, and a variable height suspension system. It also placed the driver in the turret in a separate compartment. For the first time an ammunition autoloader was introduced to reduce the crew to three rather than the standard four, see **Figure 2.93** below.



**Figure 2.93: MBT 70 Tank.**

At this time the Army Tank Automotive Command (then called ATAC) initiated a proposal for a 1120 kW (1500 SHP) gas turbine for use in a future tank. A competition was held and Lycoming Division of AVCO won. This is what became the AGT 1500 turbine engine. This program in the beginning was not identified as having any connection with the MBT 70 effort but eventually became the backup engine to the diesel engine in the MBT 70 program.

It became apparent that the German/American MBT 70 program was similar to the old story that a camel is a horse designed by committee. Between the international aspect of the program that required all major decisions be reviewed by both countries, and the technical difficulties caused by the auto loader, missile firing gun, and diesel engine the program fell way behind schedule. The Germans dropped out and Congress eventually canceled the program due to the projected high cost of the vehicle.

Throughout this period the development of the AGT 1500 program had been kept going on three month minimum funding extensions as the backup engine to the variable compression ratio diesel. The US Army was requested to make a study to determine if tanks were obsolete considering the modern guided missiles that were available. The conclusion of the study indicated that with appropriate tactics, a modern tank could survive on the battlefield, in fact if atomic weapons were used it might be the only weapon that could survive. It was also determined that there was a need for mobile protected fire power, to fight other tanks. Congress then directed that a competition be held to develop a new tank that eventually became the M-1 Abrams, **Figure 2.94.**



**Figure 2.94: M-1 Abrams Tank.**

## APPLICATIONS

The two competitors were Chrysler Defense, builders of the M-60 tank, and General Motors, builder of the MBT 70. Chrysler selected the AGT 1500 engine for their tank, while GM selected the VCR diesel. In the Chrysler vehicle the turbine now had a home.

With the initiation of the competition, funding was increased for the turbine. However it was recognized that for the turbine to be successful in the tank world, it would have to be reliable, have good performance, and most importantly low cost.

### 2.4.2 The AGT 1500 Vehicular Gas Turbine [2.54]

The development and introduction of the AGT 1500 Turbine engine is closely tied to the need for a modern tank for the US Army. In the past the Army was forced to use available power plants such as truck engines, and aircraft engines. It wasn't until the introduction of the air-cooled diesel into the M-60 that the American Army had a power plant specifically designed for the tank application.

The concept of using a gas turbine power plant in an armored land vehicle is an old idea dating to the 1950's. That decade was marked by Soviet experiments with turbines and installation of a Parsons gas turbine in a British tank. Swedish tanks have used turbine engines for boost power since the 1960's. Gas turbine experimentation in the United States was stimulated by the U.S. Army, which felt that diesel technology was approaching the limits of its development potential. The Army wanted greater engine power density, reliability and a chance to translate the aviation successes of gas turbines into ground vehicular applications.

In order to achieve high power output with low fuel consumption a relatively complex cycle was used. This involved the use of a recuperator and a variable turbine nozzle. It also dictated a twin spool compressor design both for high efficiency and rapid acceleration. The final configuration is shown in **Figure 2.95**.

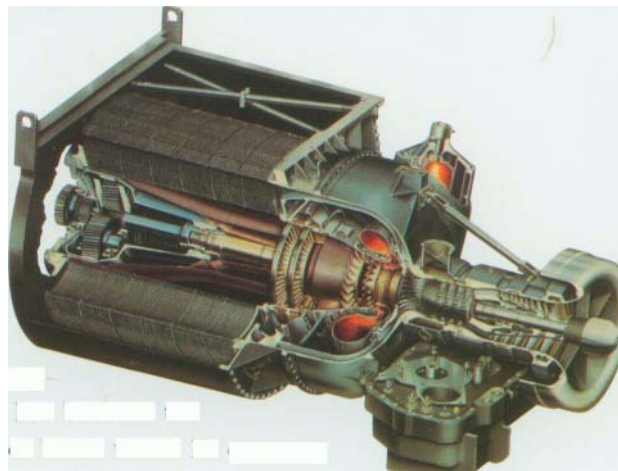


**Figure 2.95: AGT 1500 Gas Turbine.**

It was recognized from the beginning that the engine must be low in acquisition and support costs. The earlier tank program failed at least partially due to high costs of the vehicle, of which the power plant is a significant contributor. The problem was approached in several ways. The first major cost savings was in the extensive use of large commercial grade steel castings in place of the precision aircraft variety. The second was the use of commercial accessories where ever possible. The third was the use of high production machinery for the multi-wave plate recuperator, shown below in **Figure 2.96**. Also, a modular

engine design was chosen to permit maintenance to be performed on part of the units both in the field and in house.

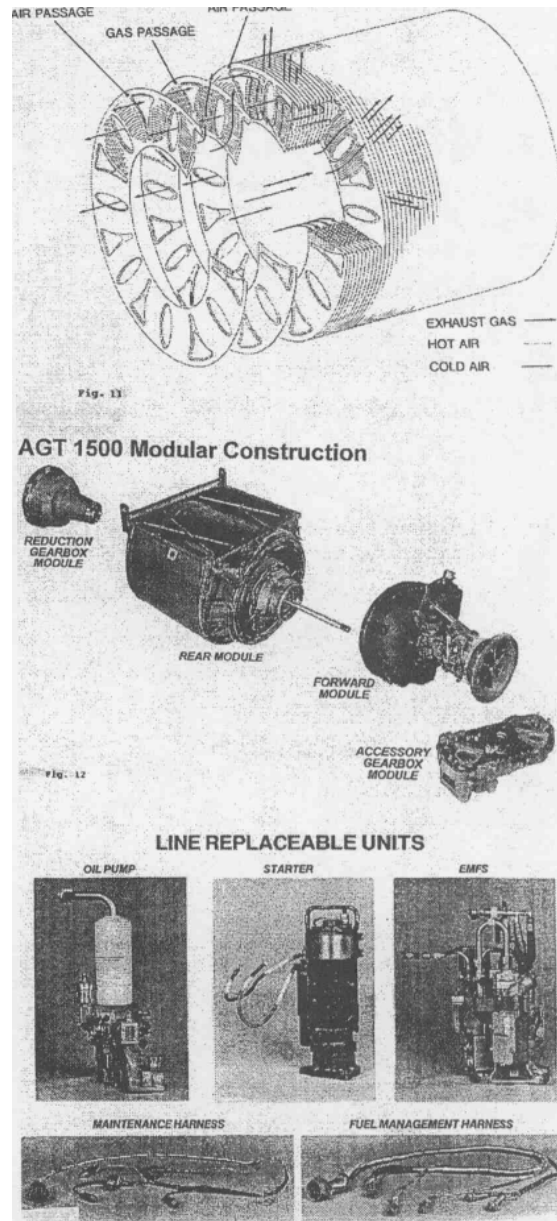


**Figure 2.96: AGT 1500 Line Replaceable Units and Recuperator.**

From the very beginning of development it was recognized that the Army tank system could not support the cost of an aircraft turbine engine. Although in the air a turbine engine is vastly superior to any of the competing engines, on the ground, turbine engines advantages are not as obvious. The question was constantly raised why is the turbine engine superior to the diesel when all previous attempts in ground vehicles have been unsuccessful. The answer is that the tank is a unique application, very different from most ground applications. As tanks require heavier armor than other vehicles, more power is required. However, the larger engines required themselves become heavier and bulkier, adding further to the weight of the tank. A gas turbine, with its smaller mass and bulk therefore offers a good compromise in this particular application.

## APPLICATIONS

---

Although this logic seems reasonable there were many dissenters. In the beginning of the XM-1 program there were many army people that did not believe that an “aircraft” engine was suitable for a tank. The main criticism of the turbine installed in the XM-1 tank was the higher fuel consumption. Although the onboard fuel capacity was increased to maintain the required range it is clear that the major fuel consumption difference in the earlier tanks was due to the more than doubling of the engine output power, and the 30 – 40% increase in weight of the tank. The other major factor in the increased fuel usage was the higher idle fuel consumption. That problem has been addressed two ways. First, the introduction of the digital fuel control reduced the idle fuel usage about 19%. Also, an auxiliary power unit (APU) was planned for the tanks’ silent watch requirements. With these two improvements fuel usage would not be a problem.

As with any new engine program all does not always go smoothly. During the early introduction phase a starting problem was experienced. This difficulty was found to be caused by heat soak back after shut down. It was quickly corrected by the introduction of insulating gaskets, and an air cooled fuel nozzle. Some of the early engines experienced significant sand and dust erosion. It is very clear that to be successful the ground environment the power plant must be protected from sand and dust ingestion. This problem applies to all power plants, be they diesel or turbine. Investigation revealed two causes. In the early tanks the fits and the seals did not match properly allowing unfiltered air to enter the engine. This was corrected, and no further problems in this area were experienced. A second problem was also identified. This involved the Army practice of running the engine external to the vehicle, with the complete power pack as part of their diagnostic testing. This practice is done before the power pack is installed to correct any leakage or wiring problems. Unfortunately the engine filter system remained in the tank so that the engine inlet air was unfiltered while running slightly off the ground. The corrective action taken was the introduction of a Ground external filter. It should be pointed out that from the beginning it was recognized that proper air filtration would be required for successful turbine operation. During the many exercises the Army conducted the turbine was less sensitive to dust ingestion than the various companion diesel engines.

The AGT 1500 provides an overall vehicle power-to-weight ratio of 23.1 HP/Ton. This is enough to accelerate the 65-ton M1A1 Abrams from 0 to 20 mph in 7.0 seconds. Top speed is governor-limited at 41.5 mph. The Abrams has excellent maneuverability and dash-to-cover capability due to its 30 mph cross-country speed and 17 mph climbing speed up a 10% grade. The turbine power plant operates with remarkably low noise and vibration. This is a difficult engine to hear running at idle, so there is little risk of audible detection in the field. Visible detection is also less likely, because the AGT 1500 has no smoke signature. It is smokeless even during acceleration and gear changes.

In 1981 the XM-1 Abrams tank became the M-1 Abrams and the official main battle tank of the US Army. Over 9000 tanks have been produced along with 12000 engines. With the introduction of the Army M-1 it was deployed to Europe to act as the first line of defense against the potential of a Soviet invasion. During the Iraqi war over 2000 M-1 tanks were deployed. They operated over a temperature range of 5 to 50 °C (40 to 124 °F), high winds and major sand storms. They were operated in both fog and burning oil. In these conditions, the engine and power train performed exceptionally well with no failures. The M-1 Abrams main battle tank performance during Desert Storm equaled or exceeded all expectations and design requirements. At the conclusion of operations not a SINGLE TANK was lost. This validated the overall design, the armor, the 120 mm gun, fire control, and the propulsion system.

### 2.4.3 Gas Turbines vs. Diesel Engines

We shall examine what is known about the relative merits of both turbine and diesel technologies with special emphasis in those areas that are important to the user. For most vehicular applications, the better part power efficiency of the Otto or Diesel cycle is the dominating factor. However, tank power plants are

a unique vehicle application. Here, the gas turbine is able to compete effectively against diesel power plants. Some of the factors that tend to favor gas turbines for tank power are as follows.

#### **2.4.3.1 Performance**

Gas turbines have the unique ability to deliver maximum torque to the sprocket at zero and low vehicle speeds. This is an attribute particularly well suited to a “shoot and scoot requirement”. The diesel engine cannot match this torque characteristic. A modern diesel engine needs to be heavily turbocharged to compete with the power density of the gas turbine. Hence it suffers from the well known “turbocharger lag” which must be compensated for by a variety of devices, which in turn, increase fuel consumption, cost, complexity, weight and under armor volume.

The AGT 1500 delivers up to 30% more power within existing envelopes. The result is more usable power to the sprocket for better acceleration, faster cruising speeds and greater hill climbing ability. It can accelerate an M1A1 from 0 – 20 mph in 7.0 seconds, which allows the tank to go from cover to cover quickly.

#### **2.4.3.2 Weight**

The AGT 1500 is 50% lighter (weighing nearly a ton less) and significantly smaller than a diesel engine of comparable horsepower. It allows the tank designer to include more armor protection for the same vehicle weight and performance. While the diesel has achieved a decrease in volume through the use of gas turbine technology in advanced turbochargers and packaging, it has not made any significant strides in weight reduction. The turbine power to weight trend for turbines continues to improve while the trend for diesels has flattened out. This weight difference is important not only in its base contribution to overall vehicle system weight, but in packaging/arrangement flexibility which may compound weight savings.

#### **2.4.3.3 Signature**

Low noise and lack of visible smoke signature are hallmarks of the gas turbine. Both turbine and diesel engines will require suppression features to meet IR signature requirements. The clean burning gas turbine engine with minimal exhaust particulates actually results in an advantage to turbine IR suppression system design. Low internal noise and low vibration of turbine contributes to crew comfort and improve crew performance.

#### **2.4.3.4 Reliability**

Compared to a diesel engine, a turbine simply has less to break and needs fewer adjustments. In a reciprocating engine, frictional wear from sliding metal-to-metal contact reduces the engine life. By avoiding sliding contact, the turbine all but eliminates this kind of wear. As a result, turbine engine reliability is significantly better than that of diesel systems. The AGT1500 had been operated successfully for 10 years and 24 million miles of operation in the M1 Abrams tank fleet. The LV100 turbine under development is expected to achieve a minimum of 70 percent better mean kilometers between hardware mission failure than the Abrams system. It is currently at almost 2 times that reliability level. The AGT1500 turbine in the Abrams demonstrated an enviable 90.4 percent readiness during all European operation and in the Desert Storm/Desert Shield combat operations.

#### **2.4.3.5 All Weather Capability**

In a free power turbine, two-spool engine such as the AGT 1500, the engine starter is not required to turn the low pressure system or the transmission. The starter turns the high pressure system only until the combustor lights off and the engine cycle is self-sustaining. In extremely cold weather, engine oil is typically as viscous as heavy grease, which in a reciprocating engine causes excessive drag on the pistons

## APPLICATIONS

---

and bearings. This condition may require pre-heater equipment to “melt” the oil. In the AGT 1500, the only oil-wetted components loading the starter are two anti-friction bearings on the high pressure rotor – a very light load. Thus, cold weather starting is a relatively fast and easy operation. This is not only an operational advantage but it avoids ancillary system cost, complexity, special logistics and reliability penalty associated with engine starting aids.

By contrast, diesels are notoriously poor starters in cold weather. They require auxiliary heaters, special lubricants and long periods of warm-up before they can be accelerated to power.

### **2.4.3.6 Fuel Consumption**

The most frequently cited advantage of the diesel engine is its fuel consumption. Improvements in materials, cycle efficiency, digital electronic control systems and recuperator design in the latest gas turbines can provide 30 – 40 percent improvements in fuel use over older turbines currently in use in army vehicles. As a result, fuel consumption is no longer a dominant factor in the engine selection process.

### **2.4.3.7 Costs**

There is a common perception that the diesel acquisition cost is less than that of an equivalent horsepower turbine. In the 1500 horsepower class to provide mobility for a 55 ton vehicle, this concept is not valid. To improve power density diesels have resorted to increased sophistication to provide turbo-charging to obtain higher internal temperatures and pressures with increased exotic material requirements in cylinder and reciprocating component parts. It is also necessary to consider the cost of other power pack components required to support the engine. For example, the engine cooling system may be significant for the diesel system.

### **2.4.3.8 Growth Potential**

A major advantage of the gas turbine engine is its horsepower growth potential. The aviation sector has repeatedly demonstrated that the gas turbine has the potential to double its initial design power within the original installation envelope. This is extremely important to provide for future weight growth or enhanced mobility without “running out of engine”. The turbine minimizes propulsion system volume under armor.

New electronics and weapons systems will greatly increase power requirements in future armored vehicles. These systems will require power on the order of 3 megawatts. Only gas turbine technology with lightweight alternators is capable of producing this power within the volume and weight required for a mobile platform. Turbine propulsion development is the logical step in the roadmap for propulsion system development for future armored vehicles.

### **2.4.3.9 Logistics**

The AGT 1500 has true multi-fuel capability, accepting diesel fuel, jet fuel, gasoline, marine diesel fuel and leaded gasoline without modification. Diesel engines are much more sensitive to differences in fuel properties, since they are designed to operate on specific types of fuels. The fuel specifications for a diesel engine must be maintained within narrow limits unless the engine and its injection system are modified for different fuel conditions.

Another revolution in field support has been achieved through the modular design of gas turbines. The diesel will not be able match the gas turbine in modular maintenance. Module transportability in the field without heavy equipment transport is an added advantage.

#### **2.4.4 Vehicular Turbine Installation Specifics**

Vehicular applications of gas turbines differ from those of aviation engines. These include differences in mission profile, packaging, and economics which result in the selection of different engine cycles and installations. The major differences in the vehicular application are discussed below.

##### **2.4.4.1 Mission Profile**

Aircraft engines are typically operated at 80% power or greater for the duration of a flight. Part power performance is not a driving issue with regard to cycle selection and design. As such, a simple cycle suits that application well. By contrast, vehicle engines spend most of their time at lower power levels or idle, yet have to be able to reach maximum power. This means that part power performance is much more important for a vehicle than an aircraft. As such, vehicular gas turbines have generally incorporated some sort of recuperator to recover the otherwise wasted exhaust energy at lower power levels. Basically, the goal is to flatten out the SFC vs. Power curve to better match the application.

##### **2.4.4.2 Weight**

A tank turbine is not as weight-sensitive as an aircraft engine, for two reasons. One, it never leaves the ground, thus it never has to overcome gravity as does an aircraft engine. Also, the engine weight is typically only about 2% of total vehicle weight. Thus, the AGT 1500, for instance, incorporates a relatively heavy recuperator (heat exchanger) to reduce fuel consumption at idle and partial power. It also uses economical steel extensively instead of titanium and other low-weight, relatively exotic and expensive metals used in aircraft turbines. However, the engine does have weight and volume constraints within the total tank package. Any savings in engine weight or volume allows addition of more ammunition, armor or fuel.

##### **2.4.4.3 Environmental Conditions**

Because a tank engine is aboard a land vehicle, it is subjected to a dirtier environment than that found in the “wild blue yonder” where aircraft engines seldom need air filtration systems. All tank engines need advanced filtering systems to avoid ingesting dirt and sand.

A second adverse environmental condition faced by tank engines is operation in water, such as fording a shallow river. A typical tank is required to ford at a depth of four feet with the engine compartment flooded. Water ingress into the engine is prevented by ducting the air inlet and exhaust openings and providing “snorkel” tubes that extend above the water line.

The primary design precaution taken by Textron Lycoming to handle fording is protection for the hot sections of the engine. Hot section components are double walled to insulate them from the thermal shock of cold water immersion. The power extraction section (high, low and power turbines) is totally isolated from potentially harmful temperature differentials of any cause. The turbines are contained within the hot section of the engine, which is enveloped by the air diffuser. This temperature gradient protection system allows the turbines and compressors to rotate freely. Otherwise, if their housings were subject to temperature-related contraction, the rotating components could seize.

##### **2.4.4.4 Serviceability**

Service conditions were another consideration during the engine design. Whereas aircraft engines are serviced in a clean environment such as a hangar, a tank is serviced wherever it is. That may be in a controlled environment, but normally it is in the field. Accessories such as the fuel pump, hydraulic pump, engine starter and oil pump can be removed and replaced from the top of the tank. There is no need to remove the engine or any related hardware.

## APPLICATIONS

The AGT 1500 engine's modular design also aids servicing. The engine is assembled in three separate main modules: forward, rear and accessory gearbox – and a reduction gearbox sub-module. Each module can be replaced independently. The combustor is designed for simple servicing, as well. Located externally on top of the engine, it contains a single heavy-duty fuel nozzle and an igniter. All or part of this assembly can be removed without disturbing the engine or related hardware. An aircraft turbine, on the other hand, has several fuel nozzles which require significant disassembly to service.

### 2.4.5 AGT 1500 Cycle Overview

The AGT 1500 engine is a typical vehicular turbine design. **Figure 2.97** illustrates how the individual engine components work together to produce the desired power output in an automotive gas turbine. The low pressure compressor is driven by a single-stage turbine. The high pressure compressor is driven by an additional single-stage turbine. This compressor arrangement is called a two-spool compressor.

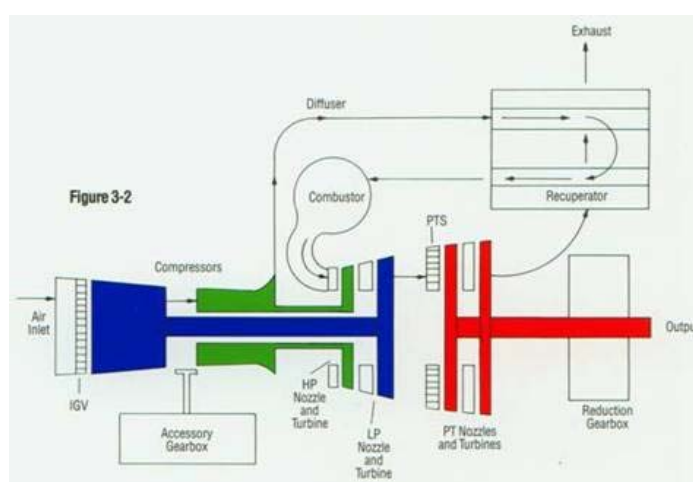


**Figure 2.97: AGT 1500 Gas Path Cycle Schematic.**

To further increase efficiency and reduce fuel consumption, a recuperator, or heat exchanger, assembly has been added. This simple device makes advantageous use of the engine's hot exhaust gases to heat the high pressure air leaving the compressor assembly, before it enters the combustion chamber. Two power turbines provide mechanical drive to the reduction gear assembly and output shaft.

### 2.4.6 Synoptic for Vehicular Propulsion Applications

#### *Improved Gas Turbine Efficiency Through an Alternative Regenerator Configuration*

Ground-based gas turbine engine applications can take advantage of innovative design configurations to improve cycle efficiencies over their airborne counterparts. Simple cycle efficiencies approaching 40% are now possible, making gas turbine engines competitive alternatives to diesel engines and Rankine steam cycles. Most ground-based gas turbines are less restricted in the space and mass requirements associated with adding regeneration to a simple cycle with the objective of even higher cycle efficiencies.

For many operating conditions, regenerators (heat exchangers) can improve gas turbine performance by recovering heat from high temperature exhaust gases. Numerous applications for the recovered heat have been devised, but on stand-alone gas turbine cycles the recovered heat is usually used for preheating the air passing between the compressor and combustor. In this way, the goal of thermodynamic design is satisfied by increasing the average temperature at which heat is added to the air during combustion, resulting in

increased cycle efficiency. Conventional regenerative cycles have traditionally used product gases leaving the final turbine stage as the source of heat so that the maximum amount of work is extracted from the high enthalpy gas stream before any heat is recovered. However, such a regeneration location is inconsistent with a fundamental lesson from Carnot-cycle thermodynamics, which is that cycle efficiency is maximized by increasing the average temperature at which heat is added, and not necessarily maximizing the work output. Thus the overall efficiency of conventional regenerative gas turbine cycles can be improved through an alternative regenerator location.

Considering the gas turbine configuration with a high-pressure turbine and a power turbine, if a heat exchanger is located between the two turbines as shown in **Figure 2.98**, then the cycle efficiency can be substantially improved beyond that available from conventional regeneration configuration.

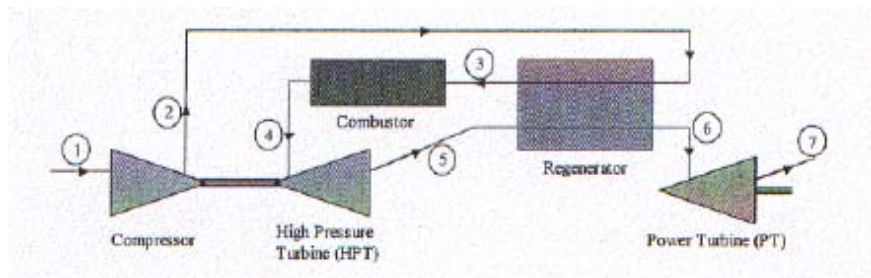


**Figure 2.98: Schematic of the Alternative Regeneration Cycle.**

### ***Modeling Techniques Used***

Computer models of simple, conventional regenerative and alternative regenerative cycles were developed to examine the influence of various parameters on the performance of the engine configuration. The models for all three cycles assumed that air is the working fluid between compressor and combustor inlets, but that beyond the combustor inlet the chemical reaction and increased temperature alter the gas properties to reflect the air-fuel mixture. All calculations further assume the isentropic compressor efficiency was 86% and the isentropic turbine efficiencies were 89%, the combustor pressure drop was 13.8 kPa (2 psi), and the compressor inlet conditions at state 1 were 21 deg C (70 deg F) and 101.4 kPa (14.7 psia). The reference case was assumed that the regenerator effectiveness was 70%, that the turbine inlet condition was 1100 deg C and that the pressure drops associated with each pass through the heat exchanger were 13.8 kPa (2 psi) each. The performance of the cycles clearly depends on the isentropic efficiencies of the compressor and turbines and it was reasonable to adopt representative values. It is noted that as the component efficiencies increase towards their isentropic limits, the alternative regeneration scheme exhibits a continuous performance advantage relative to the simple cycle and the performance gains relative to the conventional regenerative cycle are even more exaggerated than indicated.

### ***Potential Benefits of Using the Simulation***

The chosen simulation represents the most basic representation of a low fidelity, conceptual design 0-D model used to estimate steady state gas turbine performance. Yet, the ability to perform trade studies and guide conceptual design is significant.

### ***Cited Example***

- Dellenback, P.A., "Improved Gas Turbine Efficiency Through Alternative Regeneration Configuration", Proceedings of ASME Turbo Expo 2002, June 3-6, 2002, Amsterdam, The Netherlands, GT-2002-30133.

This study considers a gas turbine engine configuration with a high-pressure turbine and a power turbine. If a heat exchanger is located between the two turbines then the cycle efficiency can be substantially improved beyond that available from the conventional regeneration configuration. The thermodynamic effect is to increase the amount of heat that is delivered to the compressed air beyond what conventional regeneration is able to achieve, resulting in higher average temperature for the heat addition process in the combustor. Although there is less work produced by the power turbine in the alternative regeneration scheme due to decreases in pressure and temperature of the gas as it passes through the regenerator, the cycle efficiency is improved and the lower specific work can be compensated by using larger engine components.

It is well known that the maximum cycle temperature has a large effect on overall efficiency and this is illustrated in **Figure 2.99**. In addition to the expected trends, **Figure 2.99** shows two important results. For the reference case pressure drops, the alternative regenerator cycle is superior to the other two for any turbine engine temperature, and the conventional regenerative cycle performance falls further behind that of the other two cycles as turbine inlet temperature increases. However, the single cycle results shown could be misleading because they imply that a simple cycle could be useful at the higher turbine inlet temperatures, but the optimum pressure ratios required to achieve the efficiencies become excessive for a practical design. For example, the simple cycle requires optimum pressure ratios of 37, 58 and 90 for turbine inlet temperatures of 1100 °C, 1300 °C and 1500 °C, respectively. By contrast, the optimum pressure ratio of 30 for the alternative regeneration cycle operated at 1500 °C is feasible with current compressor designs, and results in a cycle efficiency of 54.2%.

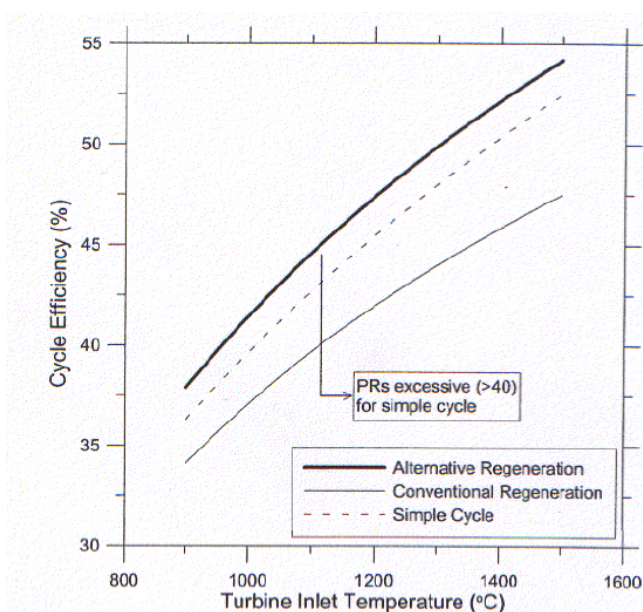


**Figure 2.99: Performance of Various Cycles as a Function of Turbine Inlet Temperature.**

### *Limitations of the Modeling Technique*

The primary goal in developing the models was to compare the performance of the multiple regenerative cycle schemes to that of the simple cycle. Consequently, the models were not comprehensive in including all details of gas turbine engine performance. As an economic analysis was beyond the scope of this paper, there is also a risk that some of the conclusions need to be further evaluated on a cost-benefit basis. Similarly, some of the performance cycle optimization results could drive design requirements beyond practical levels. For example, although the regenerator pressures and temperatures are below the levels of

existing heat exchanger designs, the demands on the heat exchanger materials are severe, which could force the use of high cost materials.

#### **2.4.7 References for Vehicular Propulsion Systems**

[2.53] Larimer, R., "The Development of a Turbine Engine for a Tank", SAE SP-1464, April 1999.

[2.54] AGT 1500 Gas Turbine, The Proven Power for Main Battle Tanks, Textron Lycoming, 1990.

### **2.5 GAS TURBINE ENGINE SIMULATIONS FOR POWER GENERATION APPLICATIONS**

#### **2.5.1 Introduction**

Gas turbines have been long used by utilities for peaking capacity, however, with changes in the power industry and increased efficiency, the gas turbine is now being used for base load power. The need for energy efficient and economic technologies with reduced environmental impact will only strengthen in this century. Moreover, with the deregulation in power generation industry worldwide, the power generation market is becoming increasingly dynamic and competitive. Manufacturers are offering larger capacity machines that operate at higher efficiencies. Some forecasts predict that gas turbines may furnish more than 80% of all new U.S. generation capacity in coming decades.

#### **2.5.2 Power Generation Application Synoptics**

##### **2.5.2.1 Modeling of a Combined Cogeneration Plant with Central Cooling Facility**

The thermodynamic cycle associated with the majority of gas turbine systems is the Brayton cycle that passes atmospheric air, the working fluid, through the turbine only once. The thermodynamic steps of the Brayton cycle include compression of atmospheric air, introduction and ignition of fuel, and expansion of the heated combustion gases through the gas producing and power turbines. The developed power is used to drive the compressor and the electric generator. Industrial gas turbines are available between 1 MW to 250 MW. They are more rugged than aeroderivative gas turbines, can operate longer between overhauls, and are more suited for continuous baseload operation.

However the simple cycle gas turbine is the least efficient arrangement since there is no recovery of heat in the exhaust gas. The trend in power plant design is the combined cycle that incorporates a steam turbine in a bottoming cycle with a gas turbine. Steam generated in the heat recovery steam generator (HRSG) of the gas turbine is used to drive a steam turbine to yield additional electricity and improve cycle efficiency. It can be seen from **Figure 2.100** that the hot exhaust gas from the gas turbine, which still has useful energy in it, is used to generate steam in a heat recovery steam generator (HRSG) or hot water in a boiler. This steam can then be used for industrial processes as well as expanded in a steam turbine to generate electricity. Moreover, since gas turbine exhaust is oxygen rich, it can support additional combustion through supplementary firing. A duct burner is usually fitted within the HRSG to increase the gas temperature and attain greater steam mass flow rates.

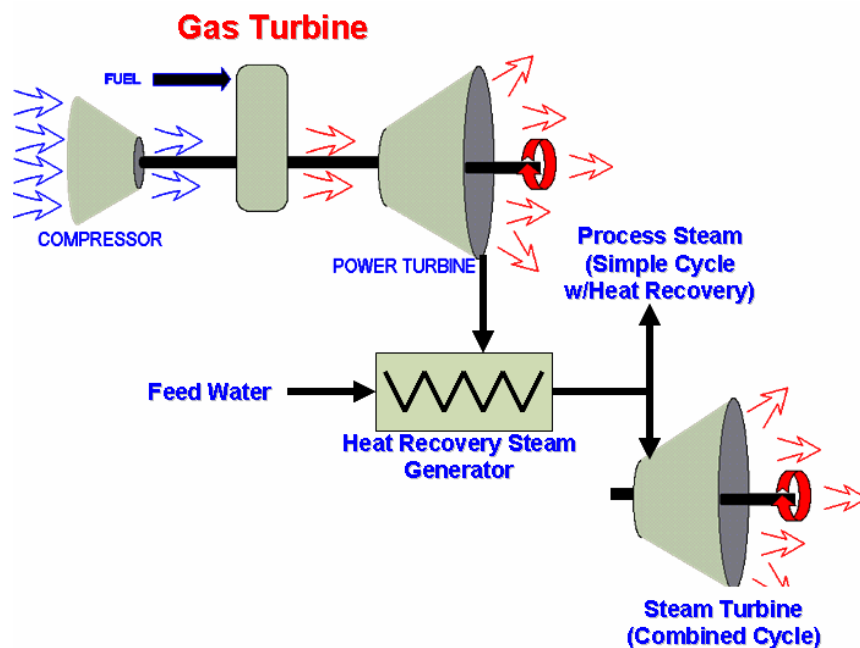


**Figure 2.100: Combined Cycle Using Gas Turbine, HRSG.**

Thus for larger gas turbine installations, combined cycles become economical, achieving about 54 – 56% electric generation efficiencies using the most advanced utility-class gas turbines. Future systems are predicted to exceed 60% in electric generation efficiency with the addition of intercoolers and the use of steam to cool the blades in the HP turbine thus improving cycle efficiency.

### ***Modeling Techniques Used***

The entire cogeneration facility was modeled and simulated using a commercially available software package. The system was modeled based on the design data available from the technical manuals of individual components such as the gas turbines, heat recovery steam generators, backpressure steam turbine, etc. The plant model was assembled by first selecting from a library of component types and then making the desired connections to create a flow sheet. After completely connecting the model, the inputs were edited describing each component based on the design data and finally solving the cycle to calculate and view the outputs.

Each gas turbine is made up of three sections, a compressor section, the combustion section and the turbine section. This modeling is consistent with gas turbine modeling discussed in the fixed wing applications section. The gas turbines for power generation have an inbuilt dual fuel system which can burn both natural gas as well as No. 2 oil fuel (which is used as back up in peak natural gas usage periods). The axial flow compressor in this example is made up of 12 stages having a high-pressure ratio of 15.6:1. The turbine section is an axial flow, three-stage reaction type, with air-cooled nozzles and blades, designed to obtain high efficiency over a wide power range. Each gas turbine generates around 11 MW of electricity while the exhaust gases at 486.6°C (908°F) are then passes to the two heat recovery steam generators to generate steam. The gas turbine model is built by connecting the individual components of the Brayton cycle.

The conditions for entry such as temperature, pressure and mass flow rates of air and fuel into the air compressor and fuel compressor respectively is entered into the air source and fuel source at the respective compressor entry. The fuel compressor or pump is normally not considered to be a part of the gas turbine

but has been included here in order to determine the amount of power it consumes at different conditions. A “heat adder” component is connected at the exit of the fuel compressor to model the gas cooler that is used to bring the temperature to 93.3°C (200°F) before it enters the combustion chamber. The heat adder component allows adding or removing heat from any type of stream such as air, combustion products, water, steam, fuels, or refrigerants. It is possible to specify the outlet phase as well as the outlet temperature of the stream in the heat adder menu. The pressure ratio and rpm of the compressor are some of the other inputs required for editing the gas turbine model. Only after successfully validating the model was it integrated into the main system model.

### ***Potential Benefits***

The commercially available software package is very flexible in nature. It is capable of modeling many thermal systems such as gas turbines, steam turbines, combined cycle or conventional steam power plants, coal-gasification systems, waste-to-energy systems, vapor compression system and other thermal systems. It can also model systems that use multiple working fluids like air, combustion products, liquid water and steam, brine, refrigerants; solid, liquid, and gaseous fuels of arbitrary composition and the products of combustion of these fuels with various oxidant streams.

In the current version of the software, the components can be modeled either in design mode, where thermodynamic criteria dictate their size; or in off-design mode, where their size dictates their thermodynamic performance. Moreover, the software package has a large library of over 90 components along with a very comprehensive gas turbine data library to choose from.

### ***Cited Example***

- Nayak, S. et. al., “Modeling of a 27 MW Combined Cogeneration Plant with Central Cooling Facility”, IJPGC 2003-40161, June 2003. [2.55]

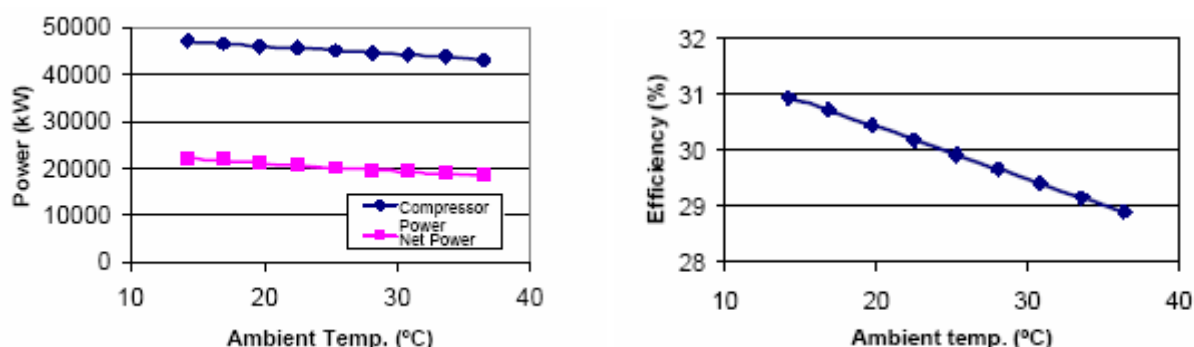
After integrating and editing all the individual component models to build the complex cogeneration system model, the model was run through a cycle to view the outputs. The simulation model was then validated and compared for accuracy with the data available from design manuals of individual components. **Figure 2.101** shows the comparison of the simulation results with the design data for some of the important parameters for a temperature of 15 °C (59 °F) and relative humidity of 60%. It can be concluded from this comparison that the simulation model agrees with the design data on which it was based to a great extent.

	Design	Simulation
GT Power Output (kW)	11002	11001.8
GT Exhaust Gas Temp. (°C)	488.8	488.7
ST Power Output (MW)	5.5	5.6
Temp. of Steam to Campus (°C)	190.5	190.3

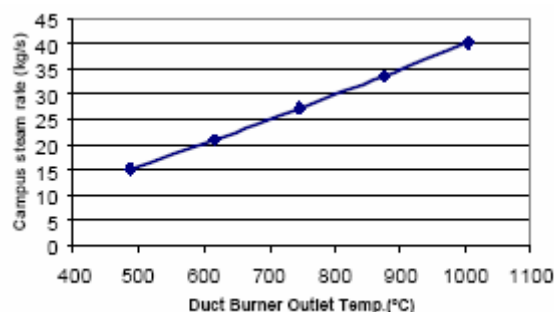
**Figure 2.101: Comparison of Simulation Results with Design Data.**

**Figure 2.102 (a), (b) and (c)** show the results of a parametric analysis conducted on the simulation model. During the parametric analysis the model is run in the off-design mode. **Figure 2.102 (a)** shows the variation in net power and compressor power required of the gas turbines for different ambient temperatures. The ambient temperature range was selected from the ASHRAE temperature bin for the Washington DC area. As the ambient temperature increases, the density of air reduces resulting in a reduction of the mass flow rate of air through the air compressor. This results in reduction of the power required by the compressor. Also the net power produced by the gas turbine decreases as temperature increases. **Figure 2.102 (b)** shows the variation in net electric efficiency based on LHV due to changes in

the ambient temperature. This graph too follows a similar trend with the efficiency dropping from about 31% at 14.2 °C to 29% when the temperature increases to 36.4 °C. The reduction in net efficiency is attributed to the reduction in the gas turbine efficiency caused by the higher specific power consumption of the gas turbine compressor. This is expected to happen in actual conditions and the model predicts this scenario very well. In **Figure 2.102 (c)**, the model predicts the mass flow rate of steam supplied depending upon the degree of duct firing in the heat recovery steam generator. The duct burner outlet temperature is used to control the amount of steam generated. It can be seen from the graph that the mass flow rate of steam supplied is about 15.2 kg/s when the duct burners are unfired (using only the exhaust gases from the gas turbines at 486.7 °C (908 °F), while the peak steam production is 40.32 kg/s when the duct burners are fully fired. The duct burner outlet temperature for this case is 1004 °C (1839 °F), which is specified in the HRSR design manual.



(a) and (b) Effect of Ambient Temperature on Power Output and Efficiency



(c) Effect of Duct Burner Outlet Temperature

**Figure 2.102: Predicting the Amount of Steam Supplied to the Campus for Different Duct Burner Outlet Temperatures.**

**Figure 2.103** shows the comparison of the net power produced by the gas turbine over a range of ambient temperature (ASHRAE temperature bin for Washington DC area), without any inlet air-cooling and when the inlet air is cooled using the absorption chiller and electric chiller. It is seen from **Figure 2.103** that without inlet air-cooling, the net power of the gas turbine decreases from 11002 kW at 15 °C to 9176 kW at 36.4 °C. When the inlet air is cooled by the absorption chiller to 15 °C always, the net power remains almost constant at 11002 kW for the entire ambient temperature range. In this case the absorption chiller uses a portion of the steam supplied to the campus. At the maximum temperature of 36.4 °C, the absorption chiller cooling load is around 686 tons and utilizes around 1.38 kg/s of steam, which is about 3.4 % of the total steam supplied to the campus. When the electric chiller is used to cool the inlet air to 15 °C, the net power of the gas turbine decreases from 11002 kW at 15 °C to 10513 kW at 36.4 °C.

The net power decreases in this case since the electric chiller uses a portion of the power produced by the gas turbine to drive its compressor. At 36.4 °C, the power consumed by the electric chiller is around 492 kW. Thus the gain in net power is 1800 kW per gas turbine if an absorption chiller is used to cool the compressor inlet air, which is about 19.6 % increase in net power compared to the case where no inlet air-cooling is used, while 1337 kW gain in net power is obtained if an electric chiller is used.

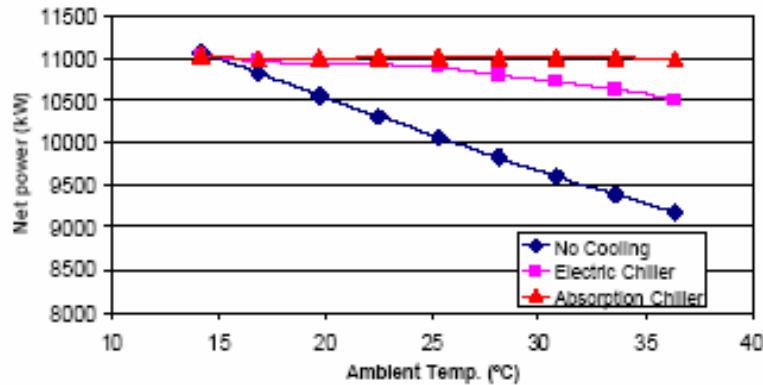


**Figure 2.103: Comparison of Net Power Produced by Gas Turbine with Inlet Air Cooled by Absorption Chiller and Electric Chiller and Without Inlet Air-Cooling.**

### *Limitations of Modeling Techniques*

With the use of the commercially available software, although flexible, it must still be validated to the thermodynamic performance of each component. Realistic losses need to be used for all subcomponents such as ducts, pipes, heat exchangers, and auxiliary pumps. System tests with adequate instrumentation to characterize the performance of each element would need to be conducted to determine adders to baseline component performance over the useful operating range for plant operation. These adders would be iterated until required accuracy for overall plant efficiency and power output is obtained. After this process, validation of the overall simulation would be completed. Accurate design data for each individual component such as the gas turbine, heat recovery, and steam generators, back pressure steam turbines, etc. would be required to successfully and accurately model a ground power generation system using a software package of the type use.

### **2.5.2.2 Model Support to Industrial Gas Turbine Condition Monitoring**

Condition Monitoring has become an essential practice for efficient management of modern industrial gas turbine installations, and control consoles are nowadays equipped with some form of monitoring capability. Although the primary target of the monitoring function is to ensure that an engine operates within safe limits of operating conditions, it is desirable that a diagnostic ability exists, so that when performance degradation occurs, its nature magnitude and cause can be identified. Having this possibility may allow operation with higher reliability, increased availability and more efficient (and consequently less costly) gas turbine operation.

A variety of methods exist today, for monitoring the condition of different parts of a gas turbine and diagnosing faults when they appear. Among those, a very important part is taken by methods monitoring the thermodynamic performance of a gas turbine. Such methods provide information about overall performance but also about the gas path components of the gas turbine.

The approach followed is similar to the one described earlier in this chapter for fixed-wing aircraft engine diagnostic support, Engine Health Monitoring and Fault Diagnostics (see *Section 2.1.4.3*). The difference

## APPLICATIONS

---

relies on the different gas turbine configuration usually encountered in ship propulsion applications: the gas turbines used are shaft power producing turbines, usually in multi-spool, multi-shaft configuration.

### *Modeling Techniques Used*

0-D models are usually employed, with modeling features similar to those described in earlier sections of this chapter. The ability to identify component performance deviations and measurement errors is the fundamental requirement here also.

A particular feature of industrial gas turbines is the possibility to employ sufficient sensors to be used for monitoring, a situation that allows for more engine health parameters to be determined simultaneously. In the case of an insufficient number of sensors existing initially on an engine, it is generally possible to implement additional ones. It can be thus considered that a closed system can be formulated for industrial gas turbine cases, a situation that is not the usual one for aircraft engines and especially when diagnosis has to be based on on-board data. A further possibility that exists in land based gas turbines is the collection of significant amount of data of continuous operation, under conditions that remain unaltered or change very slowly over time.

### *Potential Benefits*

The benefits discussed above, for marine propulsion gas turbines apply to the ones used for power generation as well. A particular aspect that applies to power generation is the fact that they operate continuously for long periods of time while their operation is critical in the sense that they produce the electricity operation is critical in the sense that they produce the electricity needed for operation of systems and installation that can be of critical nature. There are therefore aspects of optimum usage, as for example the planning of stoppages for regular maintenance or cleaning, so that they operate with minimal costs and maximum availability. Monitoring techniques employing engine models are most suitable for supporting such activities.

### *Cited Example*

- Mathioudakis, K., Stamatis, A., Tsalavoutas, A. and Aretakis, N., “Performance Analysis of Industrial Gas Turbines for Engine Condition Monitoring”, Proceedings of the Institution of Mechanical Engineers, PART A, *Journal of Power and Energy*, Vol. 215, No. A2, March 2001, pp. 173-184. [\[2.56\]](#)

This paper presents methods of analysing data from aerothermodynamic performance measurements, for the purpose of assessing the condition of the components of a gas turbine. The features of such methods are analysed in function of the measurements available and the most efficient ways of extracting information from a given measurement set are discussed. A method employing engine models is shown to be the most efficient among others. The principles discussed are highlighted and the method is substantiated by presenting results from measurements and their analysis from operating industrial gas turbines. The identification of deposits on turbine blades is discussed, with reference to a particular test case. Monitoring of compressor fouling is another industrial test case discussed in the paper.

### **2.5.3 Performance Analysis Employing Adaptive Engine Models**

The method employed is the method of Adaptive Modeling discussed earlier in this chapter. It employs the values of measured quantities in order to determine health parameters of each component. In order to employ the method for diagnostic purposes the following procedure is applied: Modification factors suitable to the particular engine and measurement situation are defined. The adaptive modeling is first applied to the engine at its healthy state. The calculated Modification Factors and the reference performance maps employed constitute the baseline for the engine performance. From this point on, by using the reference data and

measurements on the engine, sets of modification factors are calculated for every engine run. Their deviations from nominal values indicate directly the faulty component and how its operation has been altered.

For the case of the twin shaft gas turbine considered as an application, the following health indices are employed:

Compressor:  $f_1 = q_c / q_{cref}$        $f_2 = \eta_{pc} / \eta_{pcref}$

Core Turbine:  $f_3 = q_{CT} / q_{CTref}$        $f_4 = \eta_{isCT} / \eta_{isCTref}$

Power Turbine:  $f_5 = q_{PT} / q_{PTref}$        $f_6 = \eta_{isPT} / \eta_{isPTref}$

### 2.5.4 Monitoring Application Cases

First, the case of a 21 Mw twin-shaft industrial gas turbine used for electricity production in a power station is considered. The turbine suffered from the formation of deposits on gas generator and power turbine blades, very soon after it was put on operation. Adaptive modeling has been applied to the test data from this turbine and gave a clear picture of the problem. Comparison of modification factors deviation obtained from data from the initial condition of the engine and after the presence of the problem was detected, is shown in **Figure 2.104**. It is clearly shown that the swallowing capacity of both turbines has been significantly reduced, as factor  $f_3$  shows a reduction of more than 1,5% and  $f_5$  more than 3%. The reduction in  $f_1$  (of ~ 0,8%) indicates that the compressor has also suffered some deterioration.

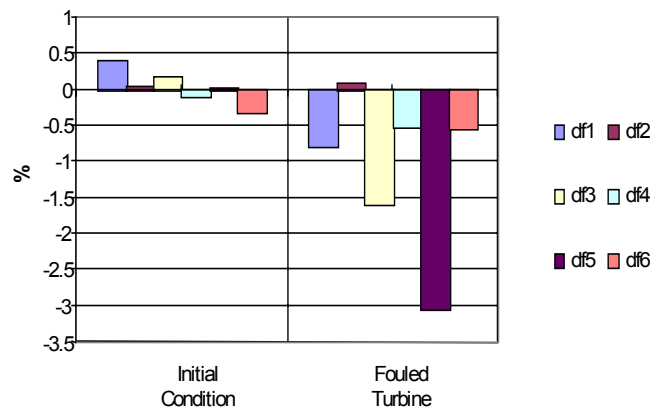


**Figure 2.104: Health Indices Percentage Deviation, for a Gas Turbine, which has Suffered Severe Turbine Fouling, Caused by Fuel Additives.**

It was further possible to analyze the rate of deterioration, by processing data over the first month of operation. The evolution of the power turbine swallowing capacity factor  $f_5$  is shown in **Figure 2.105**. The data points on this figure are produced by applying the adaptive model to each data set available. A trend line is drawn through these points. It is observed that deterioration has happened very fast, during the first month of operation.

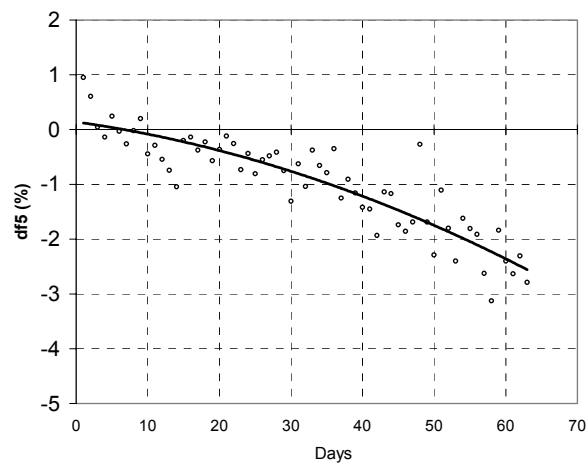


**Figure 2.105: Evolution of Power Turbine Degradation over the Initial Period of Engine Operation.**

Another application is the detection of compressor fouling and assessment of cleaning effectiveness. This is on a turbine similar to the previous one, but operating in a distillery, moving a generator which is not only supplying electricity to the network, but also feeding flue gas to a steam generator producing process steam. A typical problem for such an engine is compressor fouling, which is being taken care of through regular compressor washing.

The measured quantities fed to the adaptive model for this calculation are  $m_a$ ,  $p_3$ ,  $T_3$ ,  $T_5$ ,  $P_s$ . The modification factor corresponding to compressor efficiency is shown in **Figure 2.106**. The gradual drop of efficiency over time is attributed to compressor fouling. Application of a compressor wash is seen to restore compressor efficiency.

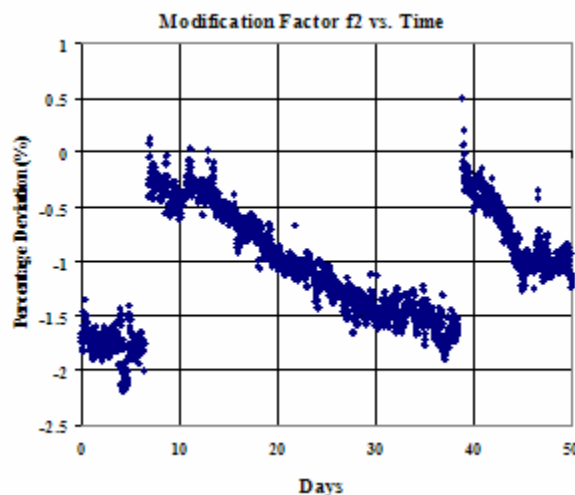


**Figure 2.106: Example of the Variation of Compressor Efficiency Derived by Employing Adaptive Modeling.**

### Limitations

Monitoring methods of this type also need information about the components of an engine. Manufacturers are in an advantageous position, as they possess such detailed information about the engine, information

not accessible to the user. The user has the possibility to produce some of this information from design data and general knowledge of component performance (for example using similarity laws or stage stacking techniques). The technique of Adaptive modeling can be used for refinement of the data, if sufficient performance data for the engine at datum condition exist.

A further limitation comes from the number of measurements available. If the measurements are not sufficient, then the health factors that can be estimated is also limited. This limitation can be alleviated by the addition of measuring instruments, which is generally possible for industrial gas turbines.

#### **2.5.4.1 Modeling Industrial Gas Turbines for Operation with Different Fuels**

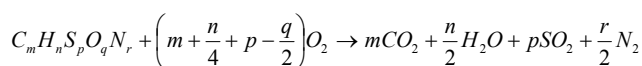
Dual fuel capability is a feature often encountered in present day gas turbines. Switching from one fuel to another can be done even during operation under load, without the need to interrupt engine operation. Engine performance is nevertheless modified, because of the change in the composition of the gases exiting the combustor and the resulting cycle alteration. Performance models should have the possibility to account for such changes, in order to accurately represent engine performance.

##### ***Modeling Techniques Used***

0-D models are usually employed, having the possibility to account for gas property and component operation changes due to altered composition. Calculations of thermodynamic processes use properties of a working medium, which is a mixture of gasses. The properties of individual mixture constituents are calculated by means of polynomial functions and the mixture properties are evaluated from its mass composition, through relations of the form:

$$P = \sum_i X_i \cdot P_i$$

$P$  is a property of the mixture and  $X_i$ ,  $P_i$  is the mass composition and the corresponding property value for the  $i$ -element of the mixture respectively. Inlet air is handled as a mixture of gases, including steam for ambient humidity. The composition of gases at the combustor outlet is computed on the basis of stoichiometric calculations, and depends on the composition of the fuel used. If the fuel can be expressed through the general formula  $C_m H_n S_p O_q N_r$  then a generalized equation for calculation of mixture composition is:



##### ***Potential Benefits***

The models can be used to predict engine performance for different type of situations and thus assist the user in assessing the effect of fuel change. Performance models can be further useful for supporting condition monitoring and diagnostics functions. For any monitoring/diagnostic system, but especially automated on-line ones, it is important that the techniques employed provide information with a high confidence level and do not produce false alarms. The deviations in performance parameters caused by fuel change will be superimposed to deviations caused by faults or deterioration of an operating engine. Diagnostic techniques based on such parameters may thus derive erroneous conclusions, unless both effects are properly incorporated in them.

##### ***Cited Reference***

- Mathioudakis, K., Aretakis, N. and Tsalavoutas, A., "Increasing Diagnostic Effectiveness by Inclusion of Fuel Composition and Water Injection Effects", ASME Turbo Expo 2002, Paper # GT-2002-30032. [2.57]

The paper investigates the impact of fuel changes or water injection on monitoring procedures for industrial gas turbines. Change of the fuel burnt by a gas turbine results in a change of the composition of the combustion gases flowing through the turbine. The consequence is that, the specific heat and the isentropic exponent change, and thus the expansion process is different. The effect of change in properties results in a different enthalpy drop (specific work produced) in the turbine, for a given pressure ratio and turbine inlet temperature. A further consequence is that the amount of combustion gases changes for a given mass flow rate supplied by the compressor. This happens when the heating value of the fuel changes, meaning that a different amount of fuel is needed to achieve the same temperature rise. This second mechanism is of marginal influence, except for cases that a large change in fuel heating value is expected.

Example results of calculations and comparisons of predictions to measurements for a single shaft gas turbine when operating with two different fuels are shown in **Figure 2.107**. Measured data come from testing a GE PG9171E gas turbine, operating with both types of fuel. It is observed that model predictions can reconstitute accurately measured quantities for operation with both fuels.

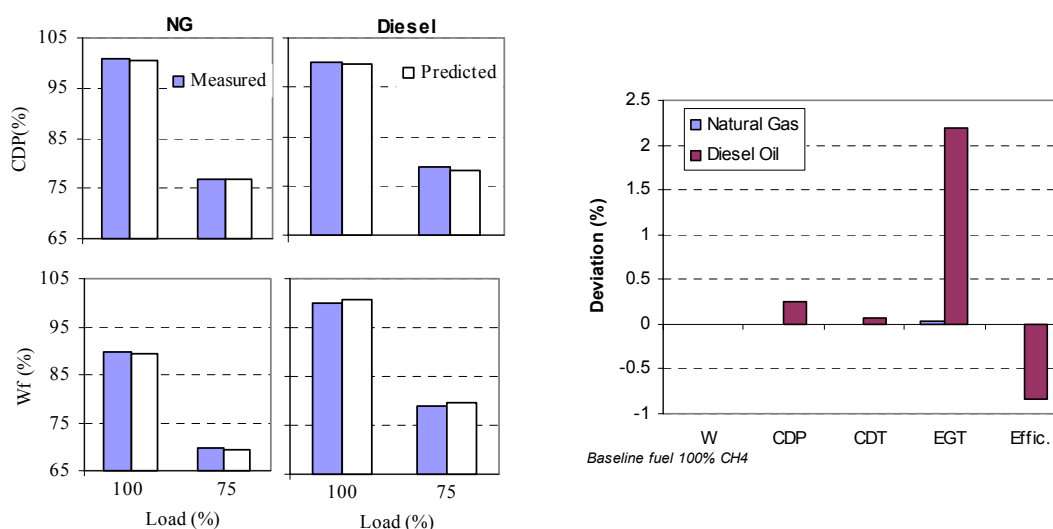


**Figure 2.107: Measured and Predicted Values of Gas Turbine Performance Parameters for Different Fuels (NG: Natural Gas and Diesel).**

The effect of changing the fuel used is assessed by comparing model predictions for operation with one fuel to the same quantities for operation with a different one. Differences for operation with fuel oil from operation with natural gas are also shown in **Figure 2.107**. The differences have been calculated for a given output power (a situation that will happen if fuel switching has to happen while the gas turbine satisfies a given power demand).

It is observed that thermal efficiency is reduced, a fact known for this fuel change. On the other hand, measured quantities deviate: compressor delivery pressure increases while a larger increase is observed in EGT.

If data for operation with one fuel are processed with an adaptive model using a different fuel, health indices non-representative of the actual component health are produced. If data from operation with natural gas are processed by a model using diesel oil, the health indices will appear deviating from the reference value as shown in **Figure 2.108**. Health indices appear to deviate, indicating an increase in flow capacity of compressor and turbine, as well as an improvement of turbine efficiency. Such deviations, if not taken into account properly, they could overshadow actual faults on the engine or produce false alarms.

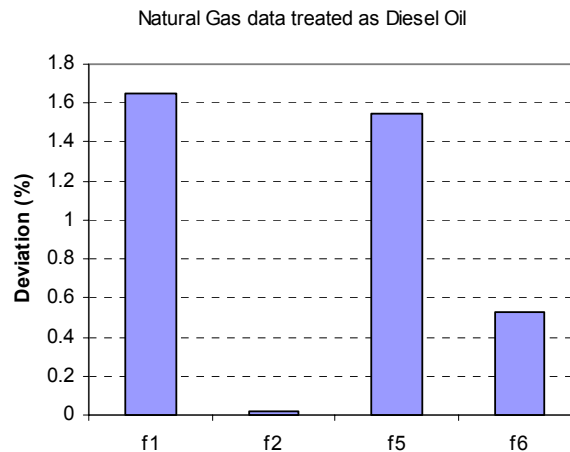


**Figure 2.108:** Deviation of Health Indices Derived by Processing Natural Gas Data are by Adaptive Model using Diesel Oil.

#### 2.5.4.2 Modeling Industrial Gas Turbines for Water Injection

The increasing use of gas turbines in the power generation industry has created an additional incentive for the further improvement of their performances. In the last years several techniques have been proposed for gas turbine power and efficiency augmentation, such as steam or water injection into the air flow or the combustion chamber. The fact that gas turbine output and efficiency drop during high ambient temperature periods, when demand usually increases, has led to the broad application of inlet air cooling through fogging.

##### *Modeling Techniques Used*

0-D models are usually employed, together with methods accounting for working medium property changes and component operation changes due to altered medium composition. The actual change resulting at the injection location needs also to be modelled, in order to define the resulting working medium properties.

##### *Potential Benefits*

Detailed overall engine performance and components behavior for multi-spool water-injected gas turbines can be obtained with the aid of engine performance models. The models can be used to forecast engine performance for different type of situations and thus assist the user in operation scheduling for most effective engine usage. Performance models can be further useful for supporting condition monitoring and diagnostics functions. The complicated layout and the many different modes of operation, imply that condition monitoring methods should be capable for accounting for all different effects. This can be achieved only if the supporting engine models can represent all different types of operation.

##### *Cited Example*

- Roumeliotis, I., Aretakis, N. and Mathioudakis, K., “Performance Analysis of Twin-Spool Water Injected Gas Turbines Using Adaptive Modeling”, ASME Paper # GT-2003-38516. [2.58]

The paper discusses the constitution of performance models for water injected gas turbines. A schematic representation of a twin spool gas turbine and its subdivision to individual components is shown in **Figure 2.109**. The layout shown has provision for inlet cooling, intercooling, combustion chamber injection and inter-turbine steam injection.

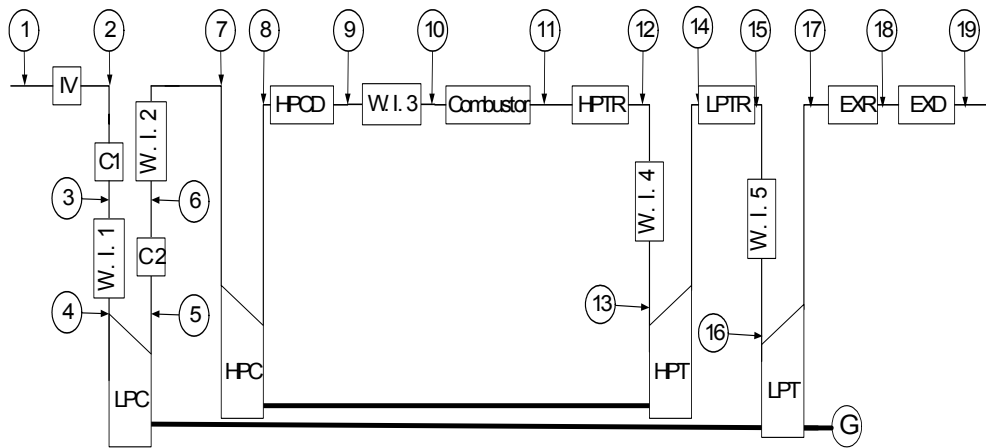


**Figure 2.109: Schematic Representation of a Twin Spool Gas Turbine and Discrimination of its Components.**

Production of a computer model for water/steam injected gas turbines necessitates the handling of the following particular aspects:

- Evaluation of state changes caused by mixing of the injected water/steam with air or combustion gases;
- Evaluation of gas properties for the resulting gas mixture; and
- Accounting for operation with a working gas different from the one they initially operated with, for turbomachinery components (compressors, turbines).

The first and third items are briefly referenced below. Gas property changes have been addressed in the corresponding section of this document.

## 2.5.5 Gas – Water Mixing

Mixing of air or combustion products with water can take place at different stations along the engine: compressor inlet, between the compressors, at compressor outlet (in the form of liquid water or steam), steam between the turbines. In zero dimensional modeling it is considered that when water is injected, it is always fully evaporated before entering the downstream component. The way that properties are calculated for mixing at any of these stations is described below.

The flow in the cooling component is assumed to be steady, one-dimensional and adiabatic. Droplet partial pressure along with the volume occupied by the droplets is neglected. At cooling component inlet (station 1) the thermodynamic conditions of the air mixture and the injected water, are considered known.



Conditions downstream of the cooling component (station 2) can be computed through the application of the conservation laws of continuity, energy and momentum which in the case of water injection form the following set of equations:

$$\dot{m}_{da}(h_{da1} + \frac{V_1^2}{2}) + \dot{m}_{v1}(h_{v1} + \frac{V_1^2}{2}) + \dot{m}_{w1}h_{w1} - \left[ \dot{m}_{da}(h_{da2} + \frac{V_2^2}{2}) + \dot{m}_{v2} \cdot (h_{v2} + \frac{V_2^2}{2}) + (\dot{m}_{w1} - (\dot{m}_{v2} - \dot{m}_{v1})) \cdot h_{w2} \right] = 0 \quad \text{Eq. 2-13}$$

$$p_1 \cdot A_1 + \rho_{m1} \cdot (V_1 \cos(a_1))^2 \cdot A_1 = p_2 \cdot A_2 + \rho_{m2} (V_2 \cos(a_1))^2 \cdot A_2 \quad \text{Eq. 2-14}$$

$$\rho_{m1} \cdot V_1 \cdot \cos(a_1) \cdot A_1 = \rho_{m2} \cdot V_2 \cos(a_1) \cdot A_2 \quad \text{Eq. 2-15}$$

These relations can express the case that no full evaporation occurs, along with the case of possible condensation. Dry air enthalpy is a function of temperature while vapor and water enthalpy is a function of both pressure and temperature and a mixing component is assumed of constant cross-sectional area.

The non-linear algebraic equations are solved through a numerical procedure, taking into consideration the variation of the composition and the variation of thermodynamic properties of the mixture. The criterion whether saturation occurs is the correlation between vapor partial pressure and vapor saturation pressure at the temperature at component exit. In the case that the mixture is saturated vapor partial pressure is equal to vapor saturation pressure at the same temperature:

$$p_{v2} = p_{sat}(T_2) \quad \text{Eq. 2-16}$$

### 2.5.6 Turbomachinery Components

Calculation of component performance parameters is based on performance maps for each component, which are expressed in a generalized form to account for the use of different gases. For example, for water/steam injection at the compressor outlet, the variation of the quantities related to the turbine is of interest, since it is the turbine that faces this gas composition changes. The quantities that remain invariable and are interrelated through the map, when gas composition changes are:

$$\left( \frac{N}{\sqrt{T}} \right) / \left( \frac{N}{\sqrt{T}} \right)_0 = \sqrt{R_0 \cdot \gamma \cdot (1 + \gamma_0) / R_0 \cdot \gamma_0 \cdot (1 + \gamma)} \quad \text{Eq. 2-17}$$

$$\left( \frac{W\sqrt{T}}{P} \right) / \left( \frac{W\sqrt{T}}{P} \right)_0 = \sqrt{\frac{R_0 \cdot \gamma}{R \cdot \gamma_0}} \cdot \left( \frac{2}{1 + \gamma} \right)^{\frac{\gamma + 1}{2 \cdot (\gamma - 1)}} \cdot \left( \frac{1 + \gamma_0}{2} \right)^{\frac{\gamma_0 + 1}{2 \cdot (\gamma_0 - 1)}} \quad \text{Eq. 2-18}$$

$$\left( \frac{\Delta h}{T} \right) / \left( \frac{\Delta h}{T} \right)_0 = R \cdot \gamma \cdot (1 + \gamma_0) / R_0 \cdot \gamma_0 \cdot (1 + \gamma) \quad \text{Eq. 2-19}$$

Subscript 0 in all the above relations denotes properties of working medium at a condition that is considered to be the reference. The choice of reference condition depends on how the map was obtained. It could be dry air, combustion gases with dry air at the inlet and reference gas fuel or other.

It is worth noting here that the expression for reduced flow rate through the turbine, **Eq. 2-18** can be used to understand some of the effects of water injection or fuel change. When the turbine is choked (which is actually the case for most gas turbines today, at least for operating conditions in the vicinity of full load), reduced mass flow remains constant. It can be easily shown that the term to the right of the radical, in the right hand side of **Eq. 2-18**, changes very little for the range of values obtained by  $\gamma$ . This means that the quantity that remains unchanged is:

$$q_d = \left( \frac{W_d \sqrt{T_d}}{P_d} \right) \sqrt{\frac{R}{\gamma}}$$

Eq. 2-20

Using this fact and also the fact that compressor inlet reduced mass flow changes very little (“vertical” characteristic on compressor map), changes in pressure ratio can be evaluated.

## 2.5.6.1 Sample Results of Effects on Performance

A model has the ability to predict overall gas turbine performances, as for example shown from the results of **Figure 2.110**. Overall performances of an LM6000 type gas turbine are shown in this figure, where comparison of predictions to manufacturer published data is shown. The deviation of different performance related quantities from their value at “dry” operation can also be predicted by a computer model. Example such results are shown in **Figure 2.111**. The change of several quantities in function of the amount of water injected between the low and the high pressure compressor is shown. As a final example, the operation of individual engine components can also be studied with the aid of a simulation code. The operating point of the high pressure compressor of the water injected gas turbine used as an example here, is shown in **Figure 2.112**, for a given power demand, at different ambient temperatures.

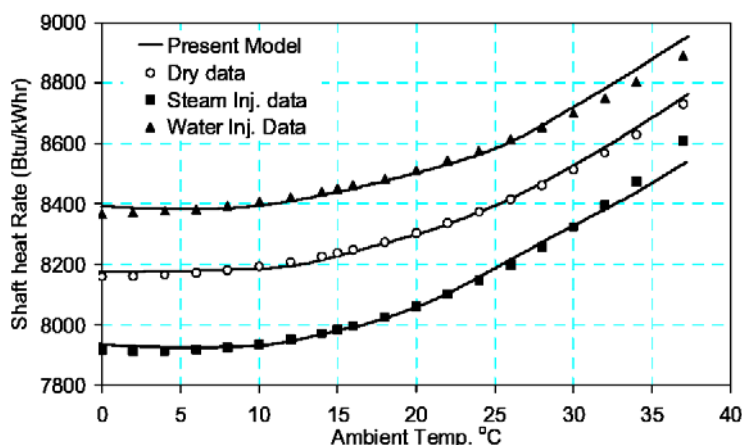


**Figure 2.110:** Overall Performance Parameters Predicted by a Computer Model, including Operation with Water/Steam Injection (from [1]).

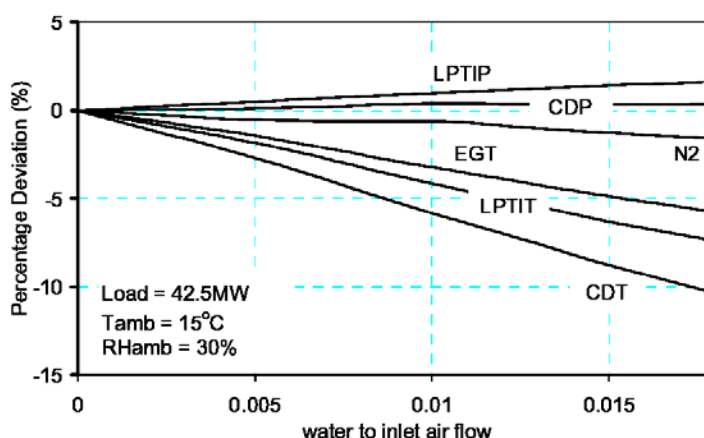


**Figure 2.111:** Percentage Change of Performance Related Quantities, in Function of Water/Inlet Air Flow Ratio, when Intercooling Occurs.

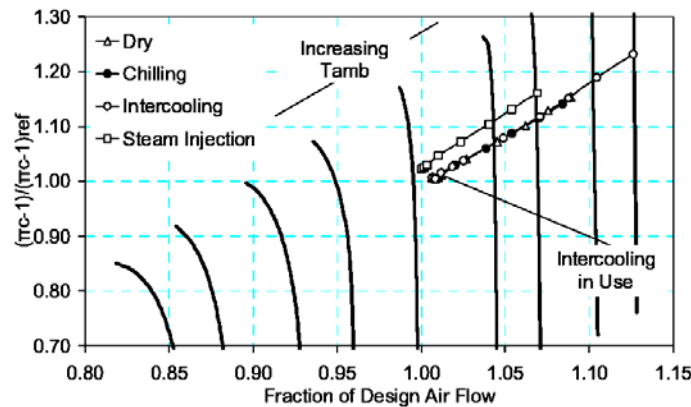


**Figure 2.112: High Pressure Compressor Operating Point for Constant Load (45 MW) and CIT.**

### 2.5.7 References for Power Generation Applications

- [2.55] Nayak, S. et. al., “Modeling of a 27 MW Combined Cogeneration Plant with Central Cooling Facility”, IJPGC 2003-40161, June 2003.
- [2.56] Mathioudakis, K., Stamatis, A., Tsalavoutas, A. and Aretakis, N., “Performance Analysis of Industrial Gas Turbines for Engine Condition Monitoring”, Proceedings of the Institution of Mechanical Engineers, PART A, *Journal of Power and Energy*, Vol. 215, No. A2, March 2001, pp.173-184.
- [2.57] Mathioudakis, K., Aretakis, N. and Tsalavoutas, A., “Increasing Diagnostic Effectiveness by Inclusion of Fuel Composition and Water Injection Effects”, ASME Turbo Expo 2002, Paper # GT-2002-30032.
- [2.58] Roumeliotis I., Aretakis, N. and Mathioudakis, K., “Performance Analysis of Twin-Spool Water Injected Gas Turbines Using Adaptive Modeling”, ASME Paper # GT-2003-38516.

## 2.6 GAS TURBINE ENGINE SIMULATIONS FOR MANUFACTURING APPLICATIONS

Few aircraft engine manufacturers are able to consistently achieve high levels of performance reliability in newly manufactured engines. Much of the variation in performance reliability is due to the tolerances of key engine components including tip clearances of rotating components and flow areas in turbine nozzles. This section ([see \[2.59\]](#)) presents analysis methods for determining the maximum possible tolerances of these key components that will allow a turbine engine to pass any reasonable number of performance constraints at a selected level of reliability. Through the combined use of a state-of-the-art engine performance code, component clearance loss models, and stochastic simulations, regions of feasible design space that allow for a pre-determined level of engine reliability can be explored. Methods for determining the bounds of any component’s feasible design space and for selecting the most cost effective combinations of component tolerances are discussed. Unique to this research is the method that determines the tolerances of engine components as a system while maintaining the geometric constraints of individual components.

### **2.6.1 Introduction**

Understanding that variation is a physical and quantifiable factor introduced by manufacturing is key to developing methods to model and analyze variation. Once the variation in a process can be accurately modeled, it can be predicted, controlled, and reduced. Variation can occur in several forms but is generally classified in two main categories: manufacturing variation and assembly variation. Manufacturing variation is the factor that is responsible for the production of individual parts that do not all have the exact same dimensions. Grinding, drilling, milling and all other manufacturing processes have limitations to their accuracy which show up as variation in the parts produced by these processes. Assembly variation is the variation responsible for the fact that not all assemblies and subassemblies are put together the exact same way. Coupling point alignment, assembly and tooling sequence, gravity and weld distortions, and even measurement error can be sources of assembly variation. Although assembly variation is relatively easy to measure, it is much more difficult to quantify and control than manufacturing variation. To conduct this research, elements from a number of different disciplines were integrated. The work presented here is not commonly found in literature as a whole, yet the pieces that comprise this work come from efforts of individuals in the field of:

- Turbine Engine Performance Modeling;
- Modeling Tip Clearance Losses in Turbine Engine Components;
- Variation Simulation Modeling; and
- Non-Linear Programming.

### **2.6.2 Methodology**

To begin assembling a model that will aid in determining the maximum tolerances of engine components, a gas turbine performance model with the ability to model geometric dimensions must be made available. It is the geometric dimensions that the user wishes to determine the maximum tolerances for that must be included in the engine model. An example of this geometric modeling is the ability to predict engine performance as a function of the tip clearance between the shroud of the inlet duct and the fan blade tip. By modeling the effect of this tip gap, the user will ultimately be able to determine the maximum tolerances that can be associated with that tip gap while maintaining an acceptable level of engine performance.

The next step in determining the widest possible tolerances of the engine components is to determine the distribution that governs the probability that a specific dimension will occur. The dimensions in question will vary as a result of manufacturing or assembly imperfections. The assumed distribution will influence the output and should be supported by evidence that substantiates the assumption. There are a number of references supporting the assumption that a Normal distribution can be used to accurately model manufacturing processes.

Once the distributions governing the probabilities have been determined, ranges of the variables describing the probabilities must be established. For example, knowing that the process governing the clearance of a fan blade is well modeled under a Normal distribution of mean 30 mils (1 mil = 0.001 inches) and a standard deviation of 2 mils, what range of means and standard deviations should be established to search for the cheapest and most reliable solution? Regardless of how the optimum is defined in this case, there are 2 design variables (mean and standard deviation) that must be manipulated while searching for the best solution. The ranges of these variables can be sufficiently bound using the experience of component design and manufacturing engineers. The larger the range of variables that is chosen to define the design space of each component, the more computational time will be required to adequately explore that space.

After constraining the ranges of the design variables and defining an objective function, an optimization algorithm must be chosen. The algorithms employed in this work are a combination of genetic and non-linear gradient based approaches. The independent variables used by the optimization algorithms are the

means and standard deviations of the tip clearances and turbine nozzle areas while the objective function is to maximize the standard deviations of the design variables. By maximizing the standard deviations of the variables describing a specific dimension, the algorithm is in essence determining the widest tolerances that can be applied to the nominal design value of that specific component. Furthermore, since tolerances are a significant driver of cost, maximizing the standard deviation is also helping to lower the manufacturing cost.

Since the computational algorithms will be required to run thousands or even millions of iterations to provide enough data for a thorough analysis, response surface models (RSM) are used. Although the engine performance code used in this analysis can run a single case in about 2 seconds, it is not fast enough to do the analysis in a time effective manner. The RSM were generated from and adequately mimic the actual performance code yet allow for computation times on the order of microseconds.

### **2.6.3 Scope of Work and Assumptions**

This example application was conducted using a state-of-the-art performance model of a small military turbofan engine capable of delivering approximately 1300 lbf of thrust. The engine in question is a twin spool machine with a fan, two centrifugal compressors, an axial high pressure turbine (HPT), and an axial low pressure turbine (LPT). Although the numeric values presented in the results are specific to this engine, the methods and tools used to conduct the research are general and would apply to any turbine engine. The engine geometries included for analysis in this work are:

- Fan Tip Clearance;
- LPC (centrifugal) Tip Clearance;
- HPC (centrifugal) Tip Clearance;
- HPT Tip Clearance;
- LPT Tip Clearance;
- HPT Nozzle Area; and
- LPT Nozzle Area.

The parameters established as design constraints are:

- Fan Minimum Cold Build Clearance;
- LPC Minimum Cold Build Clearance;
- HPC Minimum Cold Build Clearance;
- HPT Minimum Cold Build Clearance;
- LPT Minimum Cold Build Clearance;
- Turbine Inlet Temperature (T4);
- High Pressure Spool Speed (NH);
- Low Pressure Spool Speed (NL);
- Specific Fuel Consumption (SFC);
- HPC Surge Margin; and
- Fan Surge Margin.

The results presented in this document were developed at a single level of reliability. A 3 sigma (99.74%) pass rate was chosen for all the constraints. This means that 99.74% of all the engines built under the

specified tolerances must pass all of the constraints. Three-sigma was chosen due to the fact that it represents a number at which most engine manufacturers would be very satisfied with and very few achieve today. Moreover, a Normal distribution was the only distribution used in this analysis. The algorithms used in this work will easily accept the modeling of any other distribution with only minor changes.

Other assumptions associated with the simulations presented in this work include the fact that the distribution of cold build clearances in a component is a combination of the manufacturing and assembly clearances. In other words, the variance of a component may have many different sources but the solutions from this work will yield the required tolerances of the final product and not necessarily the tolerances required for each individual step of production. Secondly, all the blade clearances represent an average value for the entire component. While each blade will have a unique tip clearance, this work is limited to establishing the tolerances for the average of the tip gaps of all the blades on any single disc. Lastly, there has been no time-series analysis done in this work. All the performance conditions were calculated assuming no time dependant wear or degradation.

### 2.6.4 Sensitivity Analysis

After incorporating individual models for all the components in question, it is possible to perform a sensitivity analysis. The purpose of the sensitivity analysis is to quantify which components have the greatest affect on the engine performance parameters. Although, the sensitivity analysis presented here is percent total effect and will hide any non-linear behavior in the system, it does provide qualitative information regarding the effect of the individual clearances. **Figure 2.113** shows the percent total effect on the SFC resulting from a 5.0% variation in each component's geometry. From **Figure 2.113**, it is evident that the turbine nozzle areas and the tip clearance of the HPT play a significant role in determining the SFC. Although not shown, the turbine areas consistently played a significant role in all of the sensitivity studies.

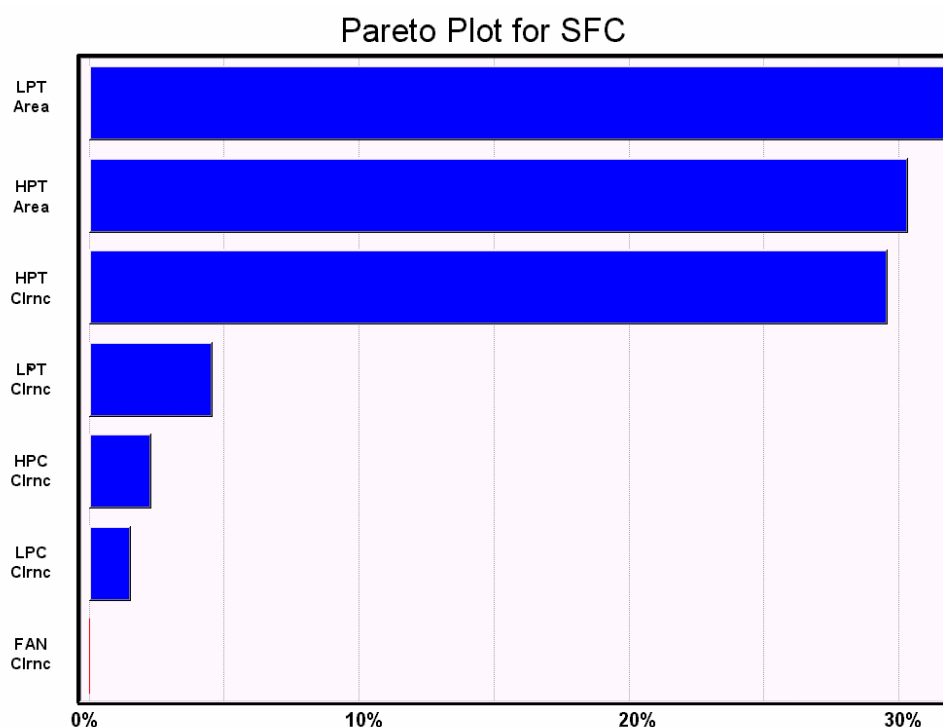


**Figure 2.113: Percent Total Effect on Specific Fuel Consumption.**

## 2.6.5 Methods of Simulating Performance Variation

### 2.6.5.1 Response Surface Models (RSM)

The advantage of using a RSM rather than an engine performance code is that the RSM can be executed with only a fraction of the computational power and speed required to run the actual code. To perform the millions of iterations required by the variation simulations, RSM are needed in place of the actual engine performance code. The reason for the decrease in computational requirements with a RSM is that the evaluation involves only the calculation of a polynomial given a set of input variables. In all, 6 RSMs were created to predict the 6 different performance parameters included as constraints. All the RSM used in this research were generated from the actual performance code and had adjusted  $R^2$  values of no less than 0.99965 with 1.0 being a perfect fit between the RSM and the actual engine performance model data.

By introducing standard deviation as a design variable, the design space that can be explored and accurately modeled by a RSM is limited. **Figure 2.114** represents the design space of a single component. The x-axis (labeled *Increasing Mean*) describes the range of mean values of a particular component's tip clearance (or nozzle area) and the y-axis (labeled *Increasing Variance*) describes the range of standard deviations of the same geometry described by the x-axis. At the same time, the range of means shown on the x-axis represents the values from which the RSM was created (labeled *Model Validity*) and is valid for. By associating a standard deviation with a mean value in certain regions of the design space, the resulting distribution may have some of its values that lie outside of the valid RSM space. This space (shaded in red) will result in performance predictions being made by certain geometries that were not considered when creating the RSM. As much as 50% of some geometric values can be outside of the valid RSM range if the maximum or minimum mean is selected with the maximum variance.

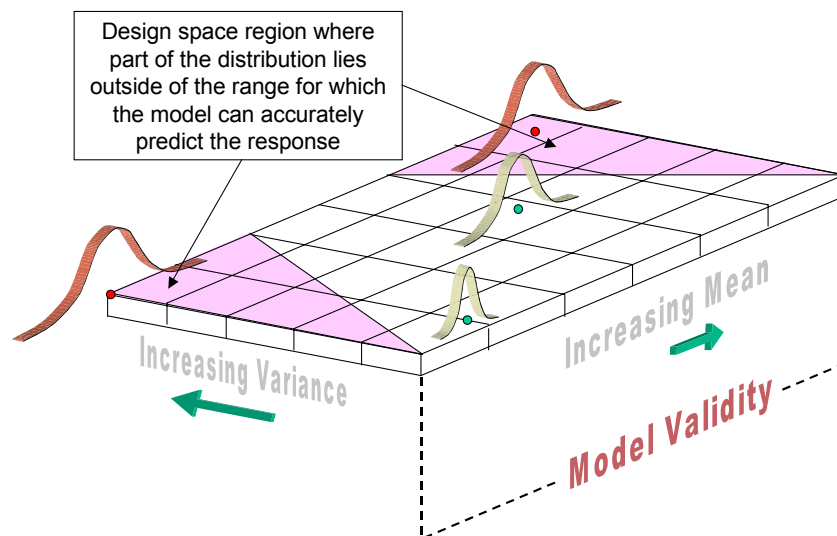


**Figure 2.114: Design Space Limitations.**

In order to employ a RSM that predicts performance outside of its valid range, a careful check of any potential solutions against the actual engine model must be made. For example, say that an optimum solution is found using a RSM with some of the responses being predicted outside of the RSM range. By taking the solution of means and standard deviations found with the RSM and plugging those solutions into the actual engine model, it is possible to determine if the solution is in fact valid. If the RSM solution and the engine model solution are identical, the implication is that the RSM prediction was still accurate even though it was outside of the RSM range. Understanding that the RSM does not necessarily go from being completely valid in the design space to being completely invalid immediately outside of the design

space is key to this approach. It is true that the further outside of the valid design space a point is evaluated, the worse the prediction will be. There is however, a small range outside of the design space where the prediction may still be relatively accurate.

## 2.6.5.2 Variation Simulation Algorithm

The optimized variation simulation was built and executed with Splus™ 4.5 and iSight™ 5.5 coupled together. **Figure 2.115** illustrates the concept of the variation simulation that includes an optimization plan.

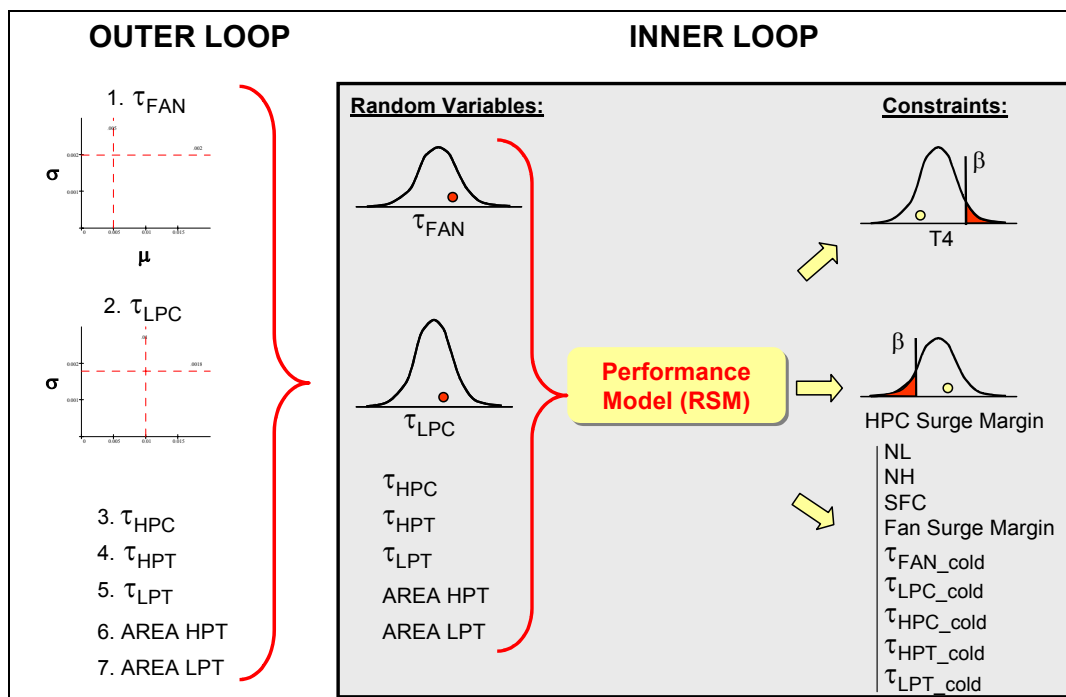


**Figure 2.115: Simulation Algorithm Using an Optimization Plan.**

Combinations of means and standard deviations that define the probability of specific clearances occurring are selected from the design space of each component in the outer loop. The distribution for the clearance of each component is then used to simulate building N engines in the inner loop. N = 50,000 was used for this work to ensure that the numbers generated from the inner loop would be consistent and repeatable. Consistency is important when employing the use of an optimization technique in probabilistic design because of the step-wise methodology inherent to gradient based algorithms. The quantities of the resulting distributions are then taken to examine their fitness relative to the constraints. If all of the distributions pass the individual constraints at a 3 sigma level or greater, the means and standard deviations of the tip clearances for that iteration are recorded as feasible. If one or more of the constraints fail, the entire combination of independent variables is declared infeasible. The objective of the optimization is to continually increase the standard deviation (tolerances) of the components until less than 99.74% of the engines meet the performance constraints.

There was more than one algorithm included in the optimization plan used to perform this work. The first was a genetic algorithm with a population size of 60 and a maximum trial limit of 2000. The genetic algorithm served as the tool that explored the entire design space and found the regions of the design space that satisfied all of the constraints. The genetic algorithm was followed by NLPQL with a maximum iteration limit of 1000. The purpose of the NLPQL algorithm was to further explore the regions of feasible design space that were discovered by the genetic algorithm.

### 2.6.6 Results

There are a number of methods to present the results of a variation simulation model that involves multiple dimensions. The results of this work exist in 14 dimensions (2 dimensions for each of the 7 design variables) so no single method of presentation will entirely capture all of the results and their association within the design space.

**Table 2.4** lists the original assumed mean values of all the components and the associated mean and tolerance that resulted from the optimized VSM.

**Table 2.4: Original Mean and Optimized Values**

<i>Component</i>	<i>Original Mean Value</i>	<i>Optimized Mean Value</i>	<i>Optimized Max Tolerance</i>
Fan Tip Clearance (mils)	30.00	31.37	± 4.65
LPC Tip Clearance (mils)	13.00	12.20	± 1.88
HPC Tip Clearance (mils)	32.00	33.25	± 2.35
HPT Tip Clearance (mils)	30.00	29.00	± 2.35
LPT Tip Clearance (mils)	20.00	21.21	± 2.36
LPT Nozzle Area (in <sup>2</sup> )	15.33	14.91	± 0.72
HPT Nozzle Area (in <sup>2</sup> )	3.38	3.49	± 0.11

By confirming the solutions with the performance code, any RSM errors can be eliminated and the results presented with greater confidence. To confirm the solutions, a Monte Carlo Simulation was used to drive the performance model under the distributions discovered by the optimization routine. It was found that performance model and the RSM returned the same values at the optimum point in the design space which confirmed that the RSM was in fact valid at the optimum solution.

**Table 2.5** lists the constraint limits, the 3-sigma quantiles of the performance parameter distributions, and the margin by which the performance parameters passed their respective constraints. **Table 2.5** was generated from the data resulting from the Monte Carlo Simulation used to confirm the results. The performance constraints and the geometric constraints are separated by the dashed line. The shaded regions of the *Limit* column in **Table 2.5** indicates an upper constraint limit while the un-shaded regions are lower limits.

**Table 2.5: Results**

<i>Constraint</i>	<i>Limit</i>	<i>3 Sigma Quantile</i>	<i>Pass Margin</i>
Fan Tip Clearance (in)	0.020	0.0357	1.7843
LPC Tip Clearance (in)	0.010	0.0138	1.3829
HPC Tip Clearance (in)	0.014	0.0351	2.5058
HPT Tip Clearance (in)	0.016	0.0311	1.9426
LPT Tip Clearance (in)	0.009	0.0236	2.6170
LPT Nozzle Area (in <sup>2</sup> )	NA	15.5797	NA
HPT Nozzle Area (in <sup>2</sup> )	NA	3.5909	NA
HPC Surge Margin (%)	20.000	20.7342	1.0367
Fan Surge Margin (%)	12.500	12.8415	1.0273
SFC (lbm/hr/lbf)	0.3950	0.3946	1.0011
T41 (Deg F)	2090	2068	1.0104
NL (RPM)	14665	14656	1.0006
NH (RPM)	44595	44579	1.0004

The 3-sigma quantile represents the limits of the distribution at which 99.74% of the data points are contained within. Since 500 engines were simulated when confirming the solutions with the engine performance model, a failure of 1 engine still constitutes a 3 sigma pass rate since  $499/500 = 99.8\%$ . However, if two or more engines out of 500 fail, then the results would be unacceptable at a 3 sigma pass rate.

The *Pass Margin* shown in **Table 2.5** is a factor quantifying the magnitude by which the 3-sigma quantile passed the respective constraint. For example, the constraint for NH was 44595 RPM and the resulting distribution had 99.74% of the engines at or below an NH of 44578.6 RPM. Since  $44595/44578.6 = 1.0004$ , the NH constraint was passed by a margin of only 1.0004. As **Table 2.5** shows, all of the pass margins are above 1.0 which indicates that all of the constraints were in fact met or exceeded by the unique combinations of optimized means and standard deviations shown in **Table 2.4**. Furthermore, it is evident that the constraints limiting the standard deviations from being increased further were the performance parameters and not the geometric parameters. All of the geometric parameters had pass margins above 1.3 while the performance parameters had pass margins no greater than 1.0367 (HPC Surge Margin). The closer the pass margin is to 1.0, the closer that particular constraint came to failing its criteria. This being the case, NL and NH appeared to be the performance parameters responsible for limiting a further increase to any of the component standard deviations.

Since the optimization algorithm was allowed to freely manipulate the mean values within the design space in an attempt to maximize the standard deviations, it is of interest to compare the resulting mean values with the original assumed mean values. The dark vertical line associated with each component in **Figure 2.116** shows the tolerance band for that component over a range that has been normalized by the nominal value of that component. The yellow horizontal line at  $y = 1.00$  indicates the relative position of the original mean value of that component. The height of the red or blue box shows the position of the optimum mean results presented in **Table 2.4**. A blue box indicates that the optimum mean was found to be higher than the original mean and a red box indicates that the optimum mean was found to be lower than the original mean. By normalizing each of the tolerance ranges by its respective nominal value, all of the components can be clearly presented in one plot. From **Figure 2.116**, it is evident that the LPT and HPT nozzle areas are some of the most sensitive components due to their relatively short tolerance band when compared to the other components.

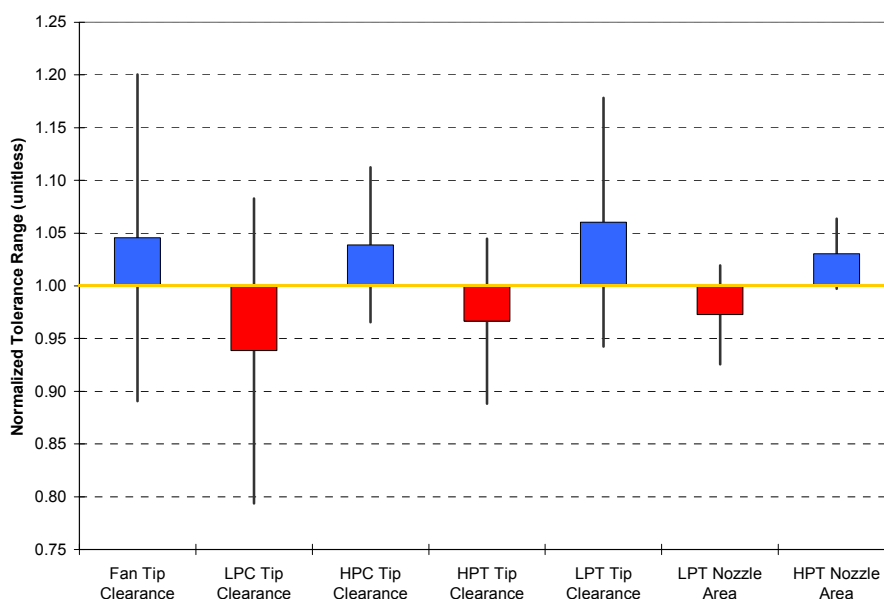


**Figure 2.116: Normalized Tolerance Range Results.**

The HPT nozzle area in particular is an issue worth exploring further. The results of this research indicate that the build specification for the HPT nozzle area that will allow for the most variation in all of the components at a 3 sigma pass rate is  $3.48 \pm 0.11 \text{ in}^2$  [3.59 to 3.37  $\text{in}^2$ ]. The original build specification for the engine was an HPT nozzle area of 3.38  $\text{in}^2$ . Essentially, the extreme limits of the allowable tolerance appear to be at virtually the same point as the mean value of the actual build specification. This implies that even very small variations in the original HPT nozzle area will force the engine to fail one or more performance specifications at a rate considerably greater than  $1 - 0.9974 = 0.26\%$ . This is an important point to consider inasmuch as if the mean value of the HPT nozzle area were set to 3.48  $\text{in}^2$  rather than 3.38  $\text{in}^2$ , any associated tolerance of the nozzle area would be much more forgiving regarding the performance of the engine. Furthermore, adjusting the mean value of a component is a relatively cheap task when compared to adjusting the tolerance of a component but can be equally beneficial.

Although not unreasonable, the optimized tolerances that are presented in **Table 2.4** are tighter than those found on many gas turbine engines. At the same time, the tolerances are established based on a 3 sigma pass rate which is a pass rate rarely, if ever, achieved by engine manufacturers. If the simulation were performed at a 2 sigma level, the tolerance ranges would certainly be much wider. Although variation simulation modeling like the type illustrated here is a powerful tool, it should only be used with respect to actual manufacturability. Like many designs that work well on paper, it is possible to discover results that are simply not possible to manufacture and can never actually be achieved. Results from an optimized variation simulation model should always be checked against the limits of real world manufacturing capability.

### 2.6.7 Cost Modeling

By assigning simple cost functions that are proportional to the inverse of the square of the tolerance, the level of reliability that results in the least cost can be explored. **Figure 2.117** shows the results of the cost minimization simulations which were done at varying levels of reliability. The blue line (diamonds) represents the least cost that can be achieved when manufacturing the engine at a given reliability. As the blue line shows, higher levels of reliability require a much greater cost to produce since the tolerances have to be much tighter. There is a unique trend seen in the blue line in that it appears to approach a constant cost value once the reliability goes below a level of 1.5. This same asymptotic relation was seen in cost modeling performed by J. R. He where he noted it was common to see an increase in cost as the tolerance was decreased and a cost that essentially remained constant as the tolerance is continually increased.

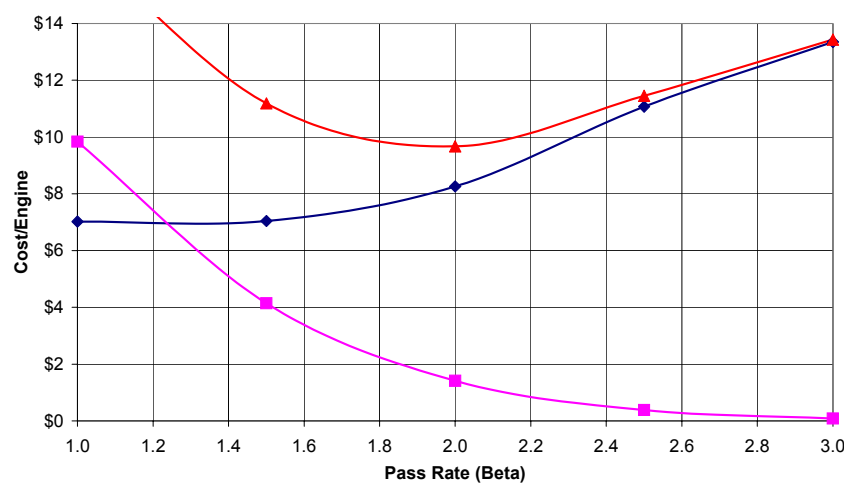


**Figure 2.117: Cost Modeling Results.**

## APPLICATIONS

---

The magenta line (squares) shows the cost associated with an engine failing some or all of its performance criteria. As the pass rate is increased, fewer engines are failing performance so there is less need to spend money scraping or fixing these engines. The red line (triangles) is the sum of the production cost curve and the failure curve and shows the reliability where the least total cost of production can be realized. Although the cost values used in the cost-tolerance model are for illustrative purposes only, the results would indicate that a pass rate of 2 sigma (95.4%) pass rate will result in the least total cost of production. Moreover, the algorithm would return the tolerances for each component associated with a 2 sigma pass rate.

### 2.6.8 Conclusions

This section has presented a performance based method for determining the maximum allowable tolerances of specific gas turbine components. Moreover, this method provides the maximum allowable tolerances based on the simultaneous interaction of all other tolerances that are included in the simulation. Specifically, this work was able to determine the maximum tolerances of 7 critical turbofan engine geometries that allowed a 3-sigma pass rate of 5 geometric and 6 performance constraints. The key points discovered throughout this analysis are:

- There exists a potential to trade tolerances on one component for the tolerances on another component. Some components offer considerable trade-off potential while others, such as the turbine nozzle areas, appear to have limits that can rarely, if ever, be exceeded. This can be a useful discovery to an engine manufacturer who is looking to cut costs on an expensive component and can do so by tightening the tolerances on a different, less costly component.
- There appears to be a limit of the total variation that can be introduced. A single simulation can contain several highly feasible solutions, each with unique component tolerances, yet the normalized sum of those tolerances is nearly constant for each simulation. In essence, the optimization algorithm is maximizing the sum of the variances and can achieve this maximum through a variety of different combinations of individual tolerances. In other words, no additional variance can be added to the system but the variation that does exist in the system can be traded between certain components.
- The use of response surface models was found to be critical to this type of work due to the sheer number of calculations that need to be performed. It was found that a RSM that has a wide range of validity when compared to the design space that will be explored is important to ensure that any associated standard deviation will allow for all of the predictions to be made within the range of model validity.
- A large number (50,000) of simulations at each selected combination of independent variables is required to effectively use a gradient based optimization algorithm. The larger the number of simulations performed at each selected standard deviation, the more consistent the quantiles of the results will be and the more accurate the prediction of the next step by the gradient based algorithm. Furthermore, a genetic algorithm with a population of approximately 4 times the number of independent variables coupled with the NLPQL algorithm appears to work well for applications like those presented here.
- A very detailed cost model and penalty function must be available if there is to be any confidence in the results of a cost modeling simulation. If these cost models exist, the methods presented here are a viable platform by which an optimization of manufacturing costs can be performed. The results from a cost modeling simulation will tell an engine manufacturer what the optimum pass rate of their engines should be to maximize profits and the tolerances that are associated with the optimum pass rate.

### **2.6.9 References for Manufacturing Applications**

- [2.59] Sheldon, K.E., Anderson-Cook, C.M. and O'Brien, W.F., "Analysis Methods to Control Performance Variability and Costs in Aircraft Turbine Engine Manufacturing", Presented at the American Helicopter Society 57<sup>th</sup> Annual Forum, Washington, DC, May 2001.

### **2.6.10 Additional Bibliography for Manufacturing Applications**

Early, J. and Thompson, J., "Variation Simulation Modeling – Variation Analysis Using Monte Carlo Simulation", Failure Prevention and Reliability, Vol. 16, September 1989.

Lakshminarayana, B., "Compressor Loss Correlations and Analysis and Effects on Compressor Performance", von Kármán Institute for Fluid Dynamics, Tip Clearance Effects in Axial Turbomachines Lecture Series 1985-05, April 1985.

Booth, T.C., "Importance of Tip Clearance Flows in Turbine Design", von Kármán Institute for Fluid Dynamics, Tip Clearance Effects in Axial Turbomachines Lecture Series 1985-05, April 1985.

Craig, M., "Managing Variation by Design Using Simulation Methods", Failure Prevention and Reliability, Vol. 16, September 1989.

Ostwald, P.F. and Blake, M.O., "Estimating Cost Associated with Dimensional Tolerance", Manufacturing Review, Vol. 2 (4), December 1989.

He, J.R., "Tolerancing for Manufacturing via Cost Minimization", International Journal of Machine Tools and Manufacturing, Vol. 31 (4), February 1991.

Rao, S.S., "Engineering Optimization-Theory and Practice", John Wiley and Sons, New York, 1996.

Schittkowski, K., "NLPQL: A FORTRAN Subroutine Solving Constrained Nonlinear Programming Problems", Annals of Operations Research, Vol. 5, 1995.

Dai, S. and Wang, M., "Reliability Analysis in Engineering Applications", Van Nostrand Reinhold, New York, 1992.

Chase, K.W. et al., "Least Cost Tolerance Allocation for Mechanical Assemblies with Automated Process Selection", Failure Prevention and Reliability, Vol. 16, September 1989.



## Chapter 3 – SYSTEM MODELS

### 3.1 GAS TURBINE CYCLE ANALYSIS

This section introduces the various gas turbine cycles as they are used for propulsion (air, land and sea vehicles) as well as for power generation. It begins with an ideal cycle and continues with more realistic cycles in which the losses that are unavoidable in real world applications are introduced step-by-step.

#### 3.1.1 Ideal Joule Process

##### 3.1.1.1 Simple Cycle

The ideal thermodynamic process of the simple cycle gas turbine is composed of three major parts: isentropic compression (stations 2 – 3), heat addition at constant pressure (3 – 4) and isentropic expansion (stations 4 – 45 – 5). Station 45 is an intermediate station which is here defined in such a way that the work done between stations 4 and 45 covers the work required for driving the compressor. Consequently the enthalpy difference between stations 45 and 5 is available as useful power. **Figure 3.1** shows this process in an enthalpy-entropy diagram. Note that the enthalpy rise in the compressor  $H_C$  equals the enthalpy drop  $H_{HPT}$  in the high pressure turbine.

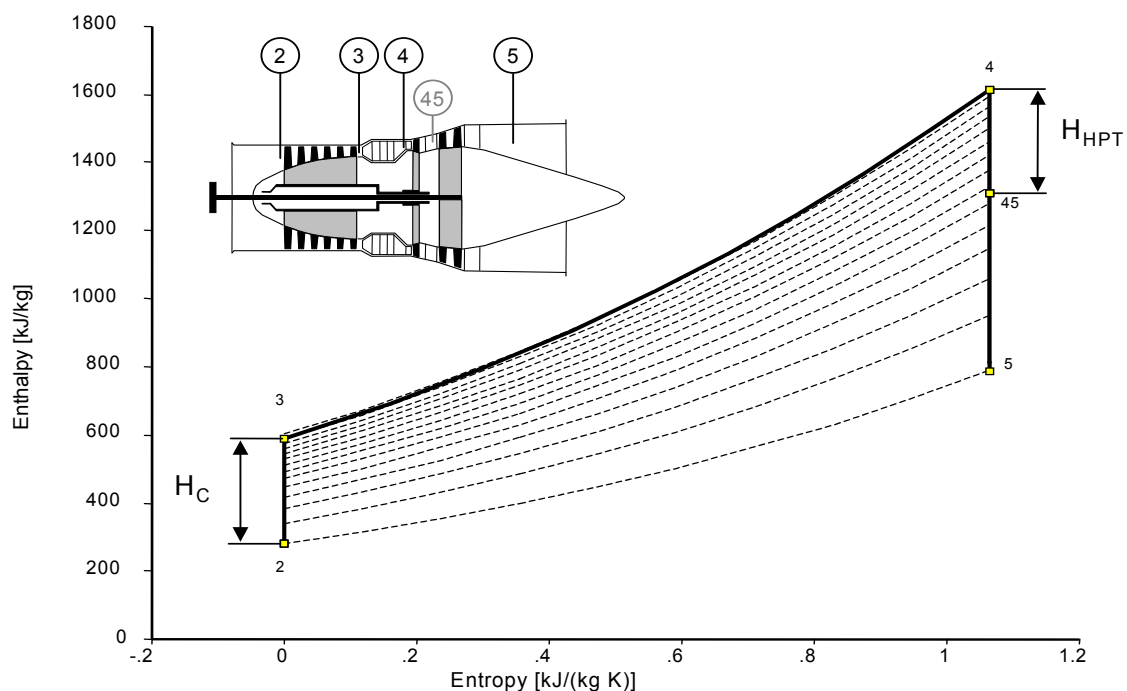


**Figure 3.1:** Ideal Joule Process in the Enthalpy-Entropy Diagram.

From the enthalpy-entropy diagram shown in **Figure 3.2** one can easily see what the main influence of burner temperature  $T_4$  on the shaft power produced is: Increasing  $T_4$  enlarges the useful work output because the isobars diverge with increasing entropy. However, the distance between stations 3 and 4 increases also and therefore more heat has to be added and thus more fuel is needed.

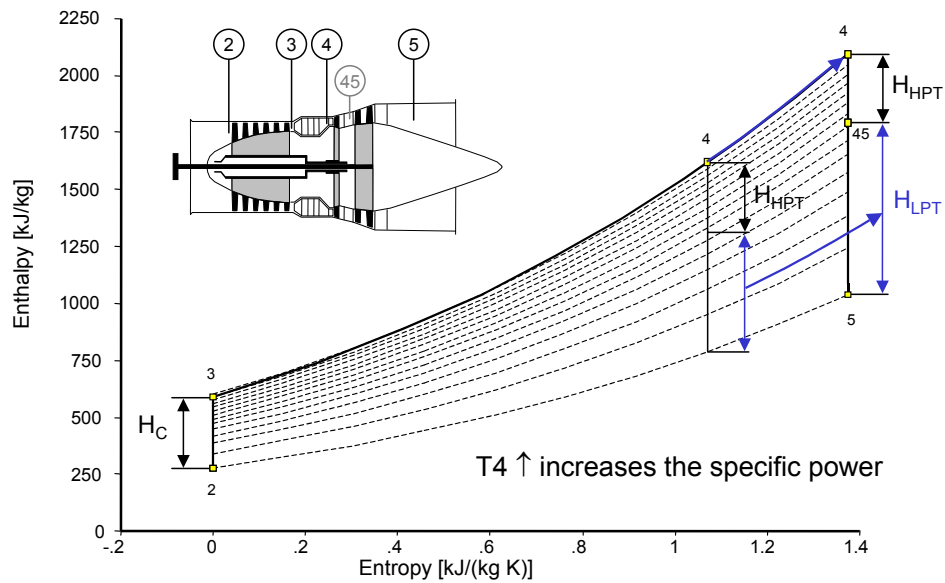


**Figure 3.2:** Influence of Burner Exit Temperature  $T_4$  on Specific Power.

With the ideal Joule process, and assuming constant isentropic exponent,  $\gamma$ , the thermal efficiency of the cycle is only dependant on cycle pressure ratio  $P_3/P_2$  and does not change with  $T_4$ . Highest pressure ratio yields the best thermal efficiency.

In reality the isentropic exponent is not constant but decreasing when temperature increases and therefore the thermal efficiency of the ideal Joule process decreases slightly with increasing burner exit temperature, see **Figure 3.3**.

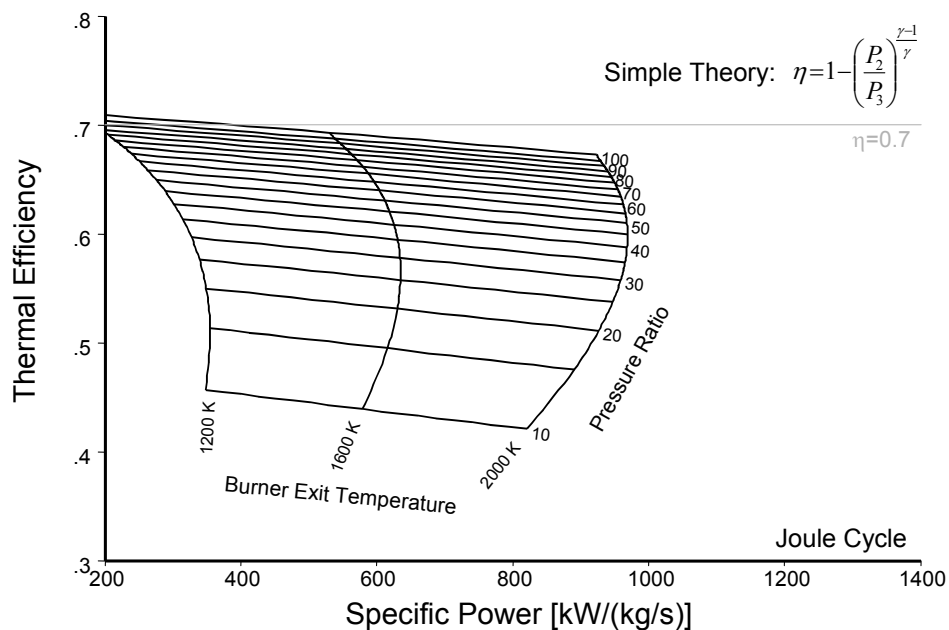


**Figure 3.3:** Thermal Efficiency and Specific Power of the Ideal Joule Cycle.

### 3.1.1.2 Recuperated Cycle

The thermal efficiency of the Joule process can be improved by adding a recuperator (heat exchanger) which recovers some of the heat in the exhaust gas and uses it to heat the compressed air before it enters the combustor at station 35 (see [Figure 3.4](#)).

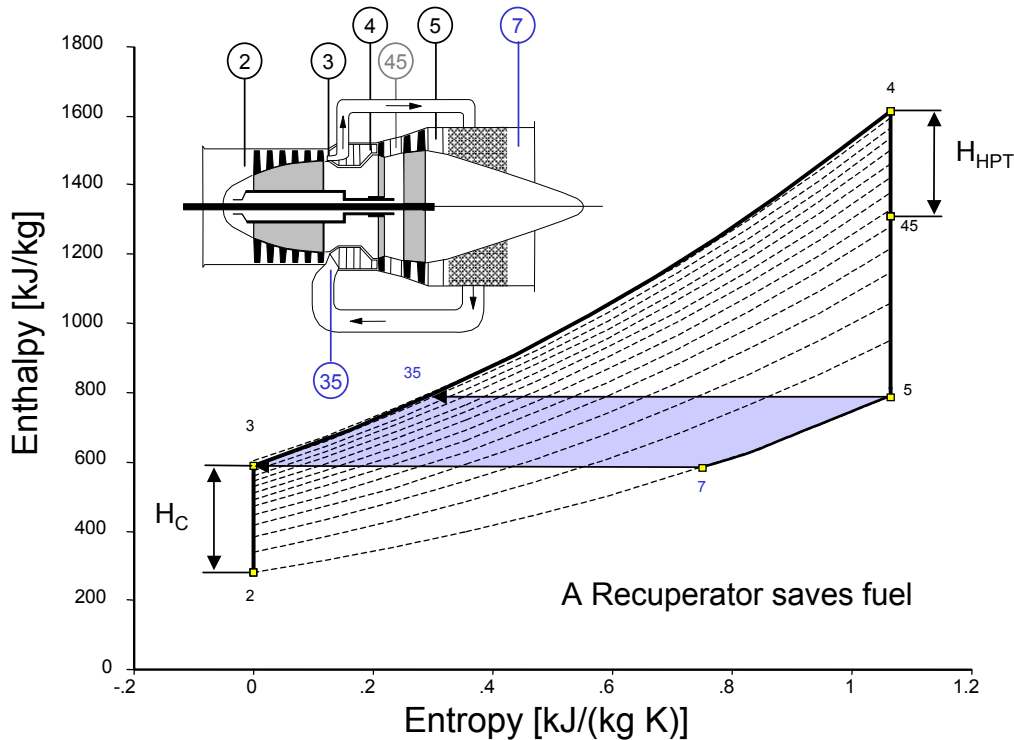


**Figure 3.4:** Joule Cycle with Recuperator.

Obviously the recuperator has no influence on the specific power produced; it reduces only the fuel consumption because the temperature difference in the burner is smaller than without a recuperator. While for the ideal Joule cycle the thermal efficiency was primarily a function of pressure ratio, with the recuperated cycle also the burner exit temperature has an influence, see [Figure 3.5](#). The pressure ratio for best efficiency is fairly low, because with low pressure ratio the temperature difference  $T_5 - T_3$  gets big and thus allows significant energy transfer from the exhaust to the burner inlet. The best achievable cycle efficiency is slightly above 70% and is connected with relatively low pressure ratios in the range of 3 to 8. The specific power at a given burner exit temperature is significantly lower than with the simple cycle, compare [Figure 3.3](#) and [Figure 3.5](#).



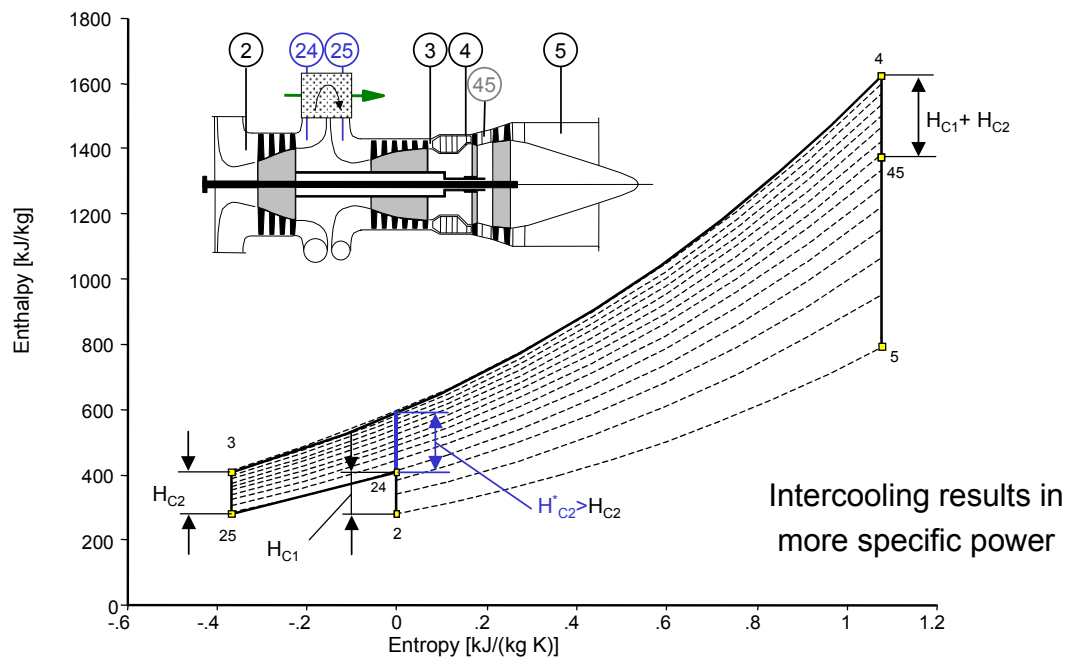


**Figure 3.6: Ideal Joule Cycle with Intercooler.**

However, the combustor inlet temperature  $T_3$  is lower with an intercooler and more fuel is needed to because the temperature difference in the burner is increased. In an efficiency analysis this effect more than compensates the net power increase and therefore the thermal efficiency of the cycle with intercooling is worse than that of the simple cycle (compare **Figure 3.7** with **Figure 3.3**).

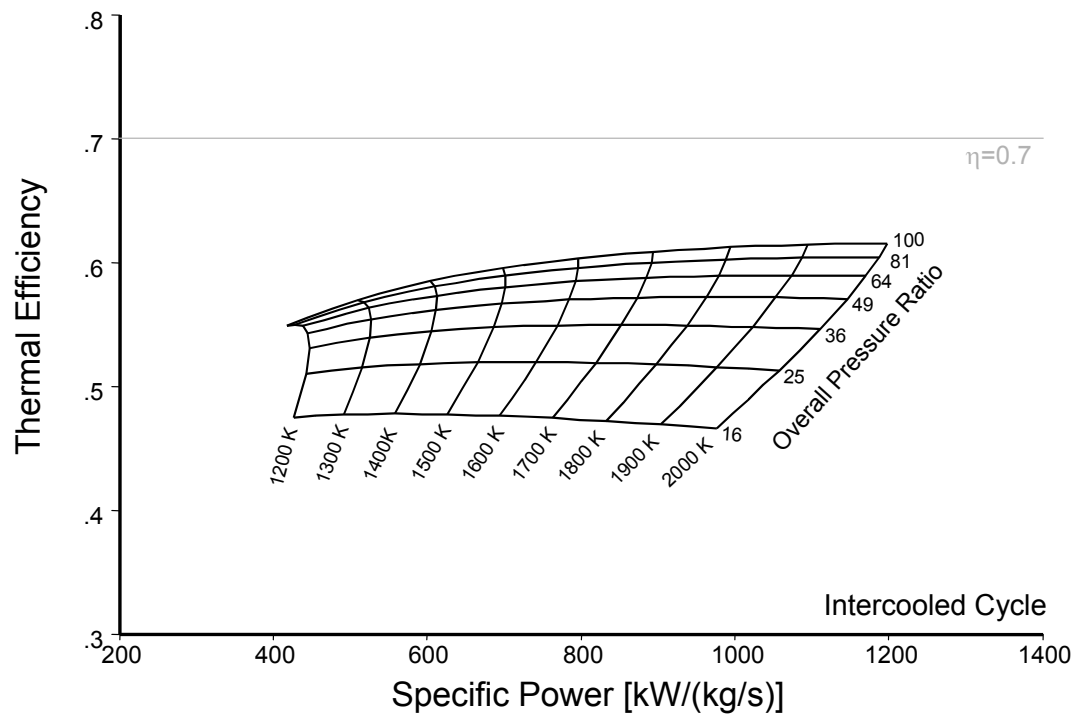


**Figure 3.7:** Efficiency of the Ideal Cycle with Intercooler.

#### 3.1.1.4 Combined Intercooling and Recuperating

The lower compressor exit temperature  $T_3$  combined with the unchanged turbine exit temperature  $T_5$  increases the temperature difference which is available for heat exchange. The efficiency of the intercooled recuperated ideal cycle is very attractive, see [Figure 3.8](#).

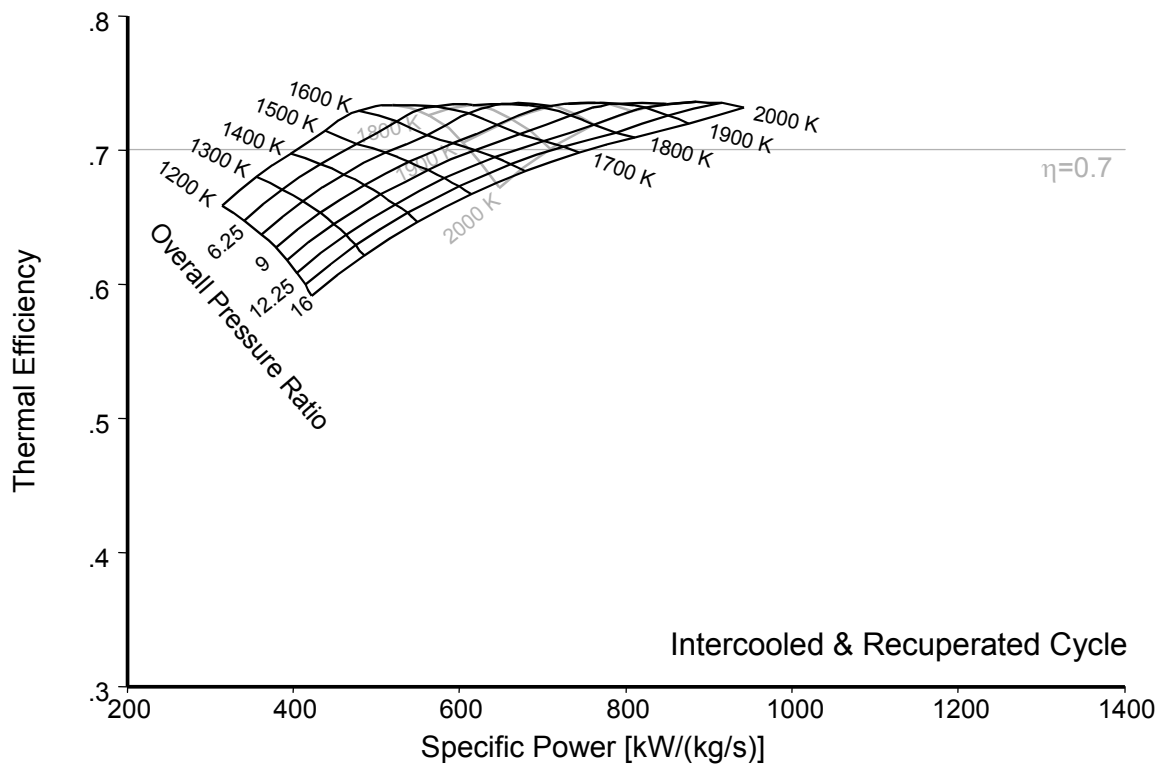


**Figure 3.8:** Efficiency of the Ideal Cycle with Intercooler and Recuperator.

Adding the intercooler and the recuperator makes the engine a rather bulky device, and the high power concentration in the turbo machines is only a minor advantage. Removing the heat from the intercooler requires a significant heat sink. In case of ship propulsion this is not a real problem since sea water can be used in the intercooler.

### 3.1.1.5 Reheated Cycle

Reheating the gas downstream of the high pressure turbine to the burner exit temperature again is equivalent to intercooling on the compressor side. The net work is increased with reheat because of the divergence of the isobar lines. The additional fuel required to get the increased power output decreases the thermal efficiency and makes it even worse than that of a cycle with intercooling. Specific power, however, is a bit higher than with the intercooled cycle, compare [Figure 3.7](#) and [Figure 3.9](#).

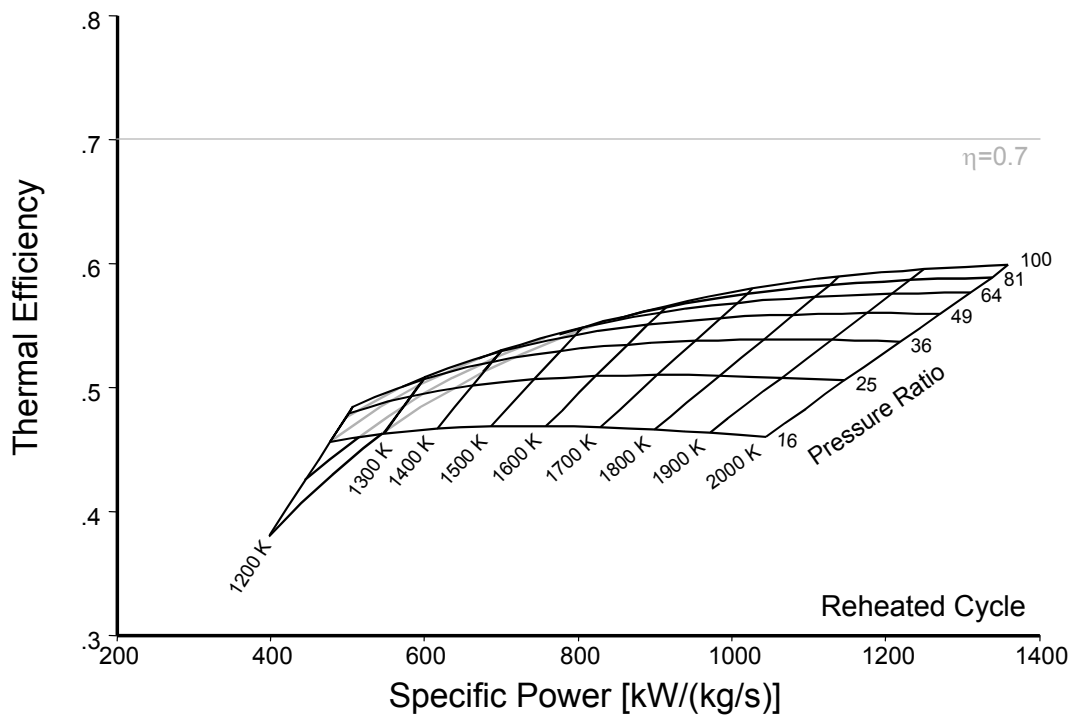


**Figure 3.9:** Efficiency of the Ideal Cycle with Reheat.

### 3.1.1.6 Combined Intercooling and Reheat

Both intercooling and reheating increase the temperature difference between turbine exit and compressor exit and thus make the use of a recuperator more attractive, see **Figure 3.10**. Without the recuperator the cycle yields very high specific work, but not a very good efficiency (see **Figure 3.11**).

Because of the high specific work for given absolute power, the compressors and turbines of this cycle would be rather small. However, especially the intercooler is a bulky device and the additional burner adds also to the volume of the machine. Overall the intercooled and reheated cycle without recuperator is not an attractive cycle.

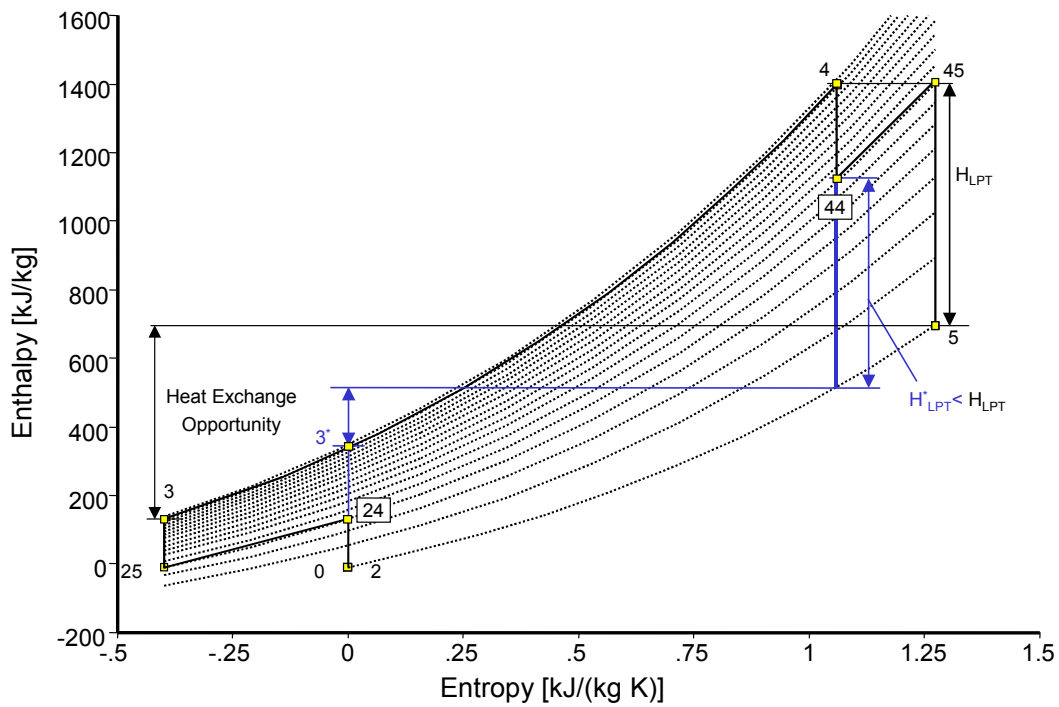


Figure 3.10: Ideal Cycle with Intercooling and Reheat.

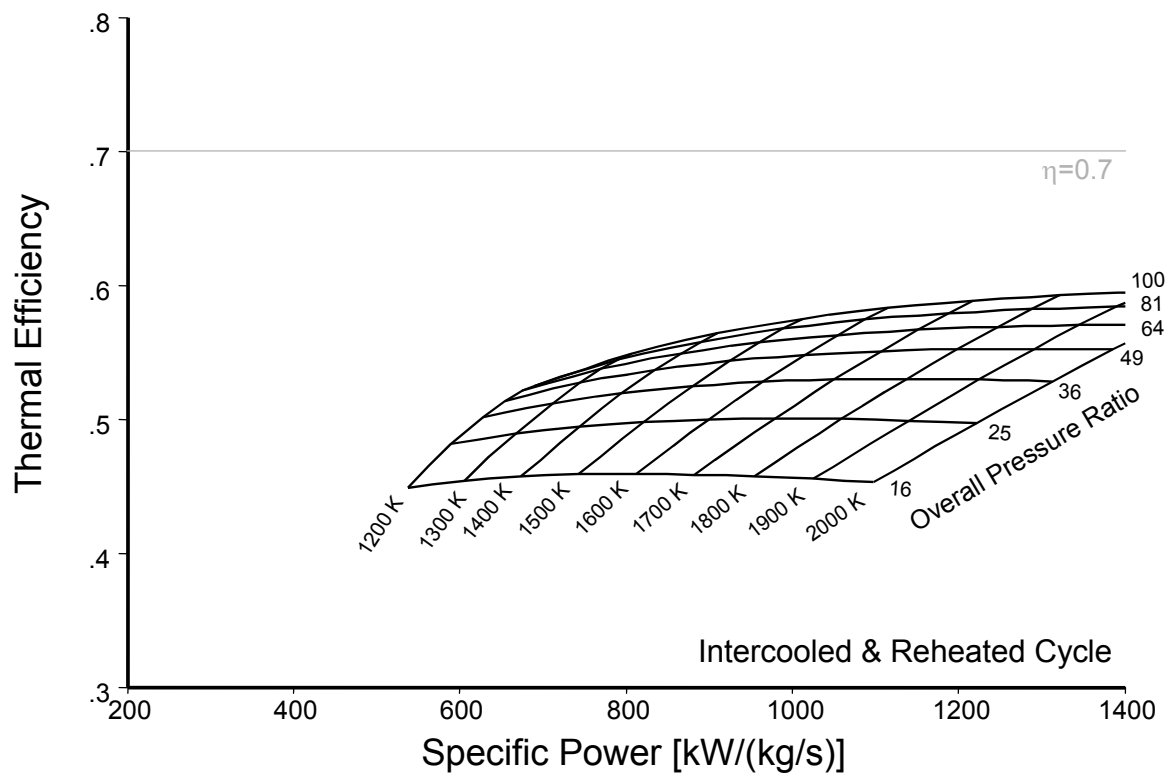
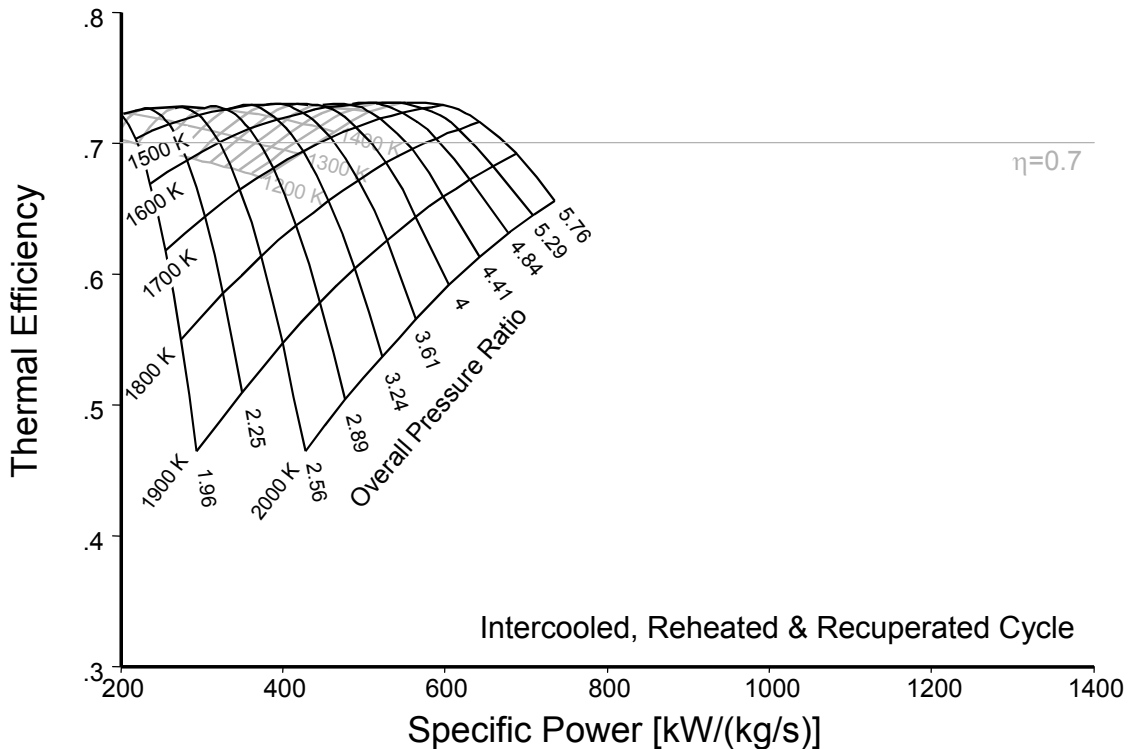


Figure 3.11: Efficiency of the Ideal Cycle with Intercooling and Reheat.

### 3.1.1.7 Combined Intercooling, Reheat and Recuperator

A machine with intercooler, reheat and recuperator yields, with a very moderate overall pressure ratio, the best efficiency (see **Figure 3.12**) of all the cycles discussed above. Certainly this machine has a significantly bigger volume than a simple Joule cycle gas turbine because of the additional components. Compared to the Joule cycle with recuperator the efficiency advantage is not very big so in summary the intercooled reheated ideal cycle with recuperator is not attractive.



**Figure 3.12:** Efficiency of the Ideal Cycle with Intercooling, Reheat and Recuperator.

### 3.1.2 Real Joule Process

In a real cycle all turbo machines have an efficiency of less than 1.0 and the other components like ducts, the burner, and the inlet and exhaust system have pressure losses. Furthermore cooling air may be required for disks and blades, sealing of the bearings consumes also some air and some leakage is unavoidable. In the following we will not go into the details of a full engine cycle simulation but concentrate on the effect of the efficiencies of the major components on the thermal efficiency.

#### 3.1.2.1 Nearly Real Joule Process

In a first step for both compressors and turbines the polytropic efficiency is set to 0.9. No further losses are assumed, neither pressure losses nor leakages and cooling air. **Figure 3.13** shows in an enthalpy-entropy diagram the comparison of the ideal cycle with the “nearly real” cycle for the same specific power. To produce the same power, a higher turbine inlet temperature  $T_4$  is required if there are losses. To achieve the higher turbine inlet temperature more fuel is needed and the consequence is decreased thermal cycle efficiency.

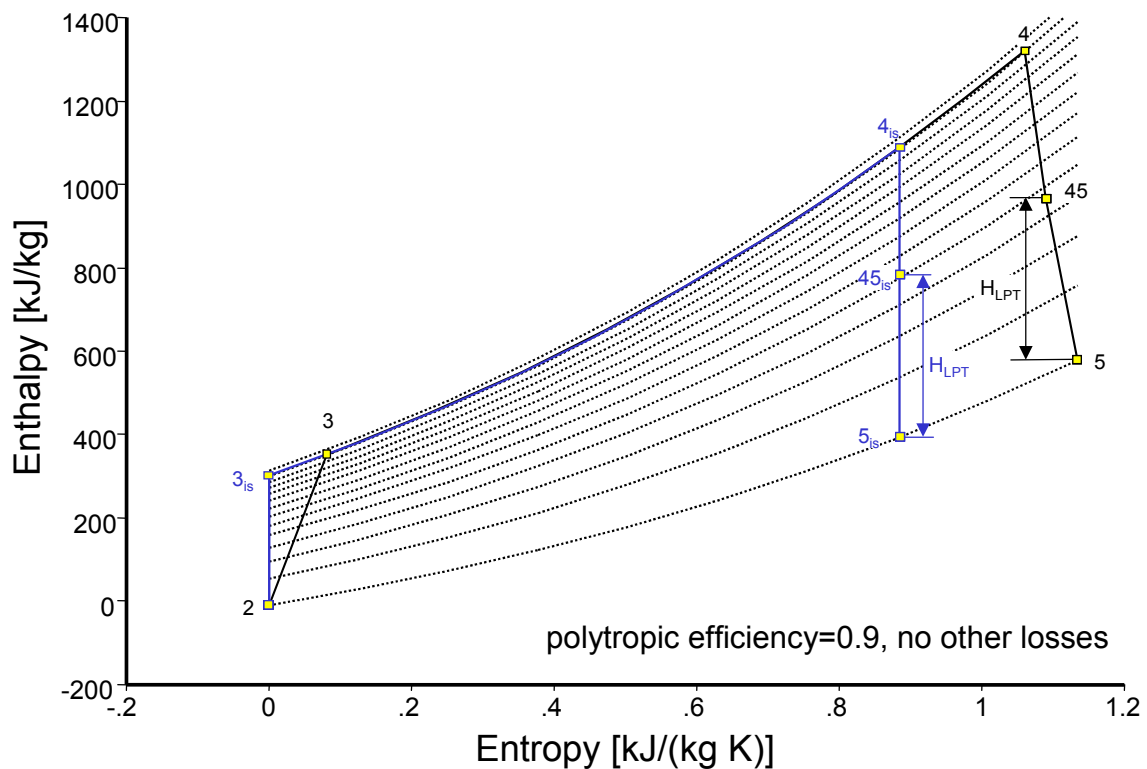


**Figure 3.13: Ideal and Real Cycle for the Same Specific Work  $H_{LPT}$ .**

While for the ideal cycle the thermal efficiency was nearly independent from turbine inlet temperature this is not the case for the real cycle. Both the thermal efficiency and the specific power are dependant on turbine inlet temperature. The maximum of the specific power is always at a lower pressure ratio than the maximum of the thermal efficiency.

For pressure ratio 50 and burner inlet temperature  $T_4 = 2000$  K the thermal efficiency of the ideal process is above 0.6 (see **Figure 3.3**) while with the “nearly real” cycle (see **Figure 3.14**) only about 0.5 is achievable. Note that both figures employ the same scale to make comparisons simple.

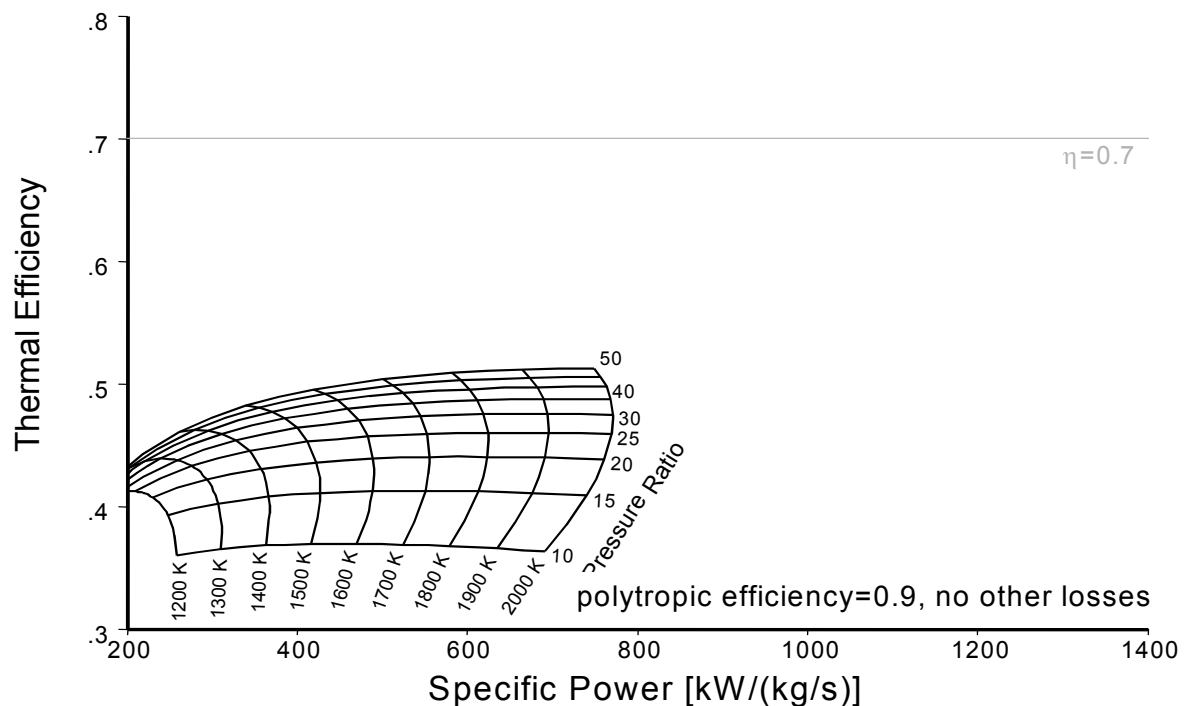


**Figure 3.14:** Thermal Efficiency of the “Nearly Real” Simple Cycle.

### 3.1.2.2 Turbine Cooling

Modern gas turbines operate at high burner exit temperatures and use significant amounts of cooling air for the high pressure turbine. This must be taken into account in more realistic cycle simulations. One often used modeling method separates the cooling and the expansion process in such a way that first the cooling of the turbine inlet guide vane is modeled, next follows the expansion and last the rotor cooling is considered, see **Figure 3.15**.

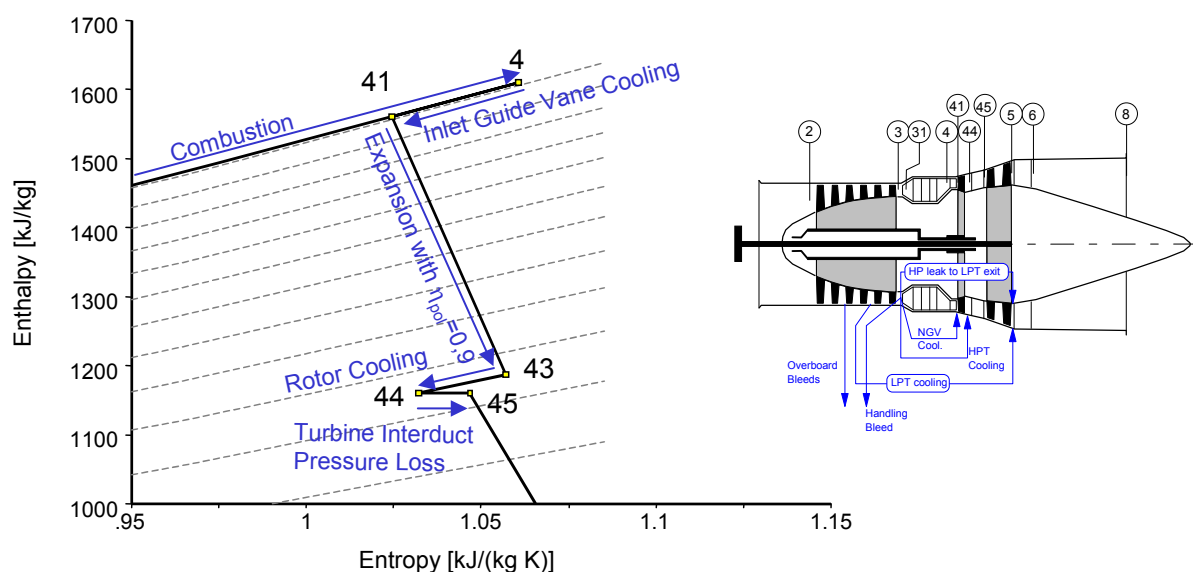


**Figure 3.15:** Simulation of a Cooled Turbine.

This modeling method works fine for single stage turbines, but requires some abstraction when applied to two stage turbines. For given compressor power and turbine pressure ratio the numbers employed for the amount of cooling air mixed upstream and downstream of the turbine rotor and the aerodynamic efficiency of the expansion process are interrelated.

The amount of cooling air must be adapted in parametric cycle design studies while high turbine inlet temperatures are considered. When constant metal temperature for the turbine inlet guide vane and the rotor blade are limitations then the relative cooling air mass flow  $W_{cl}/W_2$  must be a function of both the hot gas temperature  $T_4$  and the cooling air temperature  $T_3$  which is dependant on cycle pressure ratio. Cooling effectiveness of a row of blades or vanes can be empirically described by the following formula:

$$\eta_{cl} = \frac{W_{cl} / W_{ref}}{W_{cl} / W_{ref} + C_1} \quad \text{Eq. 3-1}$$

Using for the constant  $C_1$  a value in the range of 0.03...0.07 yields a reasonable correlation which is valid for all sorts of cooling designs beginning with simple radial holes and ending with sophisticated multi-pass configurations combined with film cooling. For the following cycle studies the mean value of  $C_1 = 0.05$  is used for finding the required amount of cooling air. This yields for 8% cooling air for the cooling effectiveness the value 0.615 and this is reasonably well in line with **Figure 3.16**.

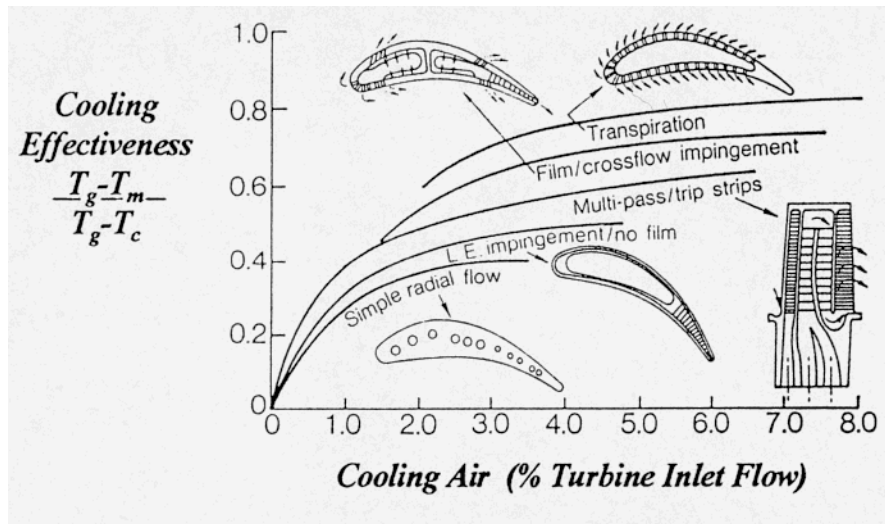


**Figure 3.16: Cooling Effectiveness for Different Cooling Configurations [3.1].**

The cooling effectiveness for the turbine inlet vane is

$$\eta_V = \frac{T_4 - T_{Metal}}{T_4 - T_3} \quad \text{Eq. 3-2}$$

and for the rotor holds

$$\eta_R = \frac{0.9 * T_{41} - T_{Metal}}{0.9 * T_{41} - T_3} \quad \text{Eq. 3-3}$$

In this correlation it is assumed that the total temperature of the hot gases relative to the rotor can be approximated by the term  $0.9 \cdot T_{41}$ .

**Figure 3.17** shows the amounts of cooling air that are calculated from the formulae above for a metal temperature of 1200 K. The rotor cooling air is less than the stator vane cooling air because of the lower main gas temperature.

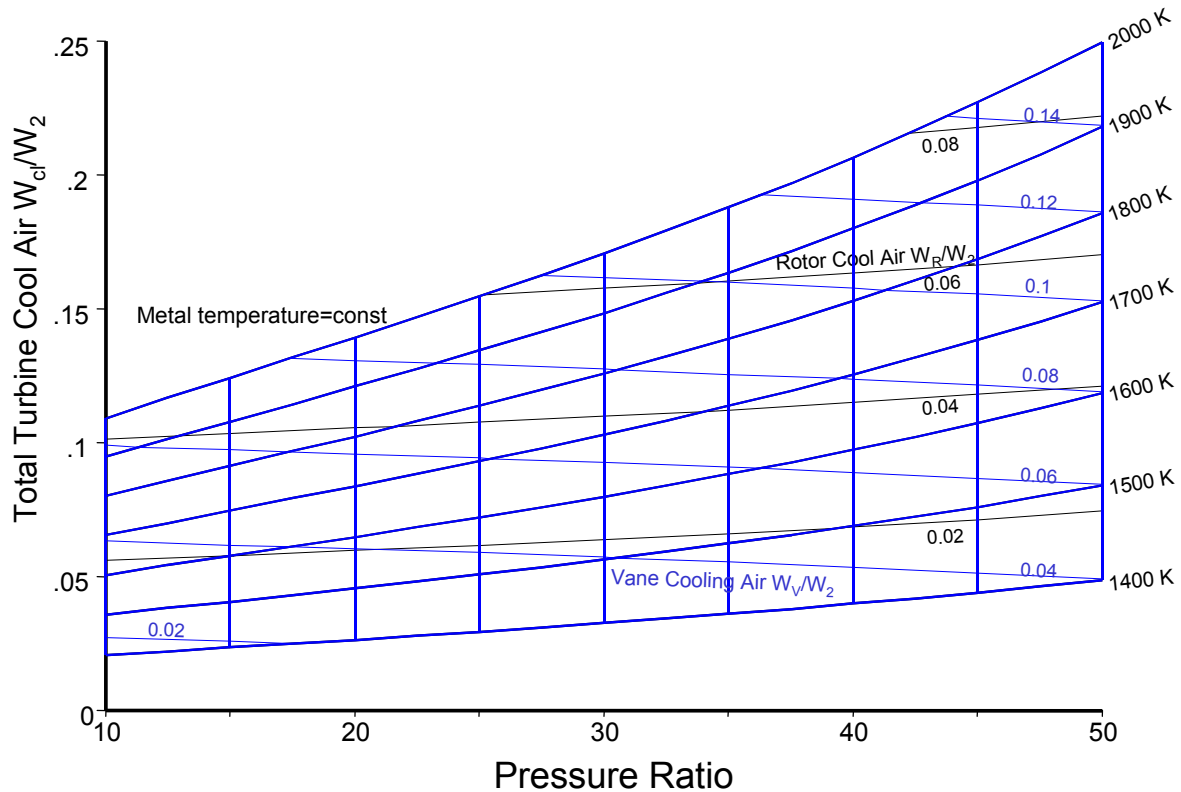


**Figure 3.17:** Cooling Air Amount for Constant Metal Temperature of 1200 K.

### 3.1.2.3 Real Joule Process

Up to now we have spoken about the losses in compressors and turbines as well as the cooling air. For a fully realistic cycle simulation also the pressure losses in the non-rotating components, some secondary air leakages and the kinetic energy of the exhaust gas stream have to be simulated. As typical numbers for the total pressure loss we introduce now 5% as the burner pressure loss and 1.02 as total/static pressure ratio at the exhaust of the turboshaft engine. Losses in the secondary air system are represented by 0.5% overboard leakage of high pressure air and the parasitic power required for driving the accessories are covered by a reduction of 0.2% of the high pressure turbine power.

**Figure 3.18** shows the resulting cycle performance which should be compared with **Figure 3.3**. Note that in spite of the progressively increasing amount of cooling air the cycle with the highest burner exit temperature and pressure ratio yields the best thermal efficiency.

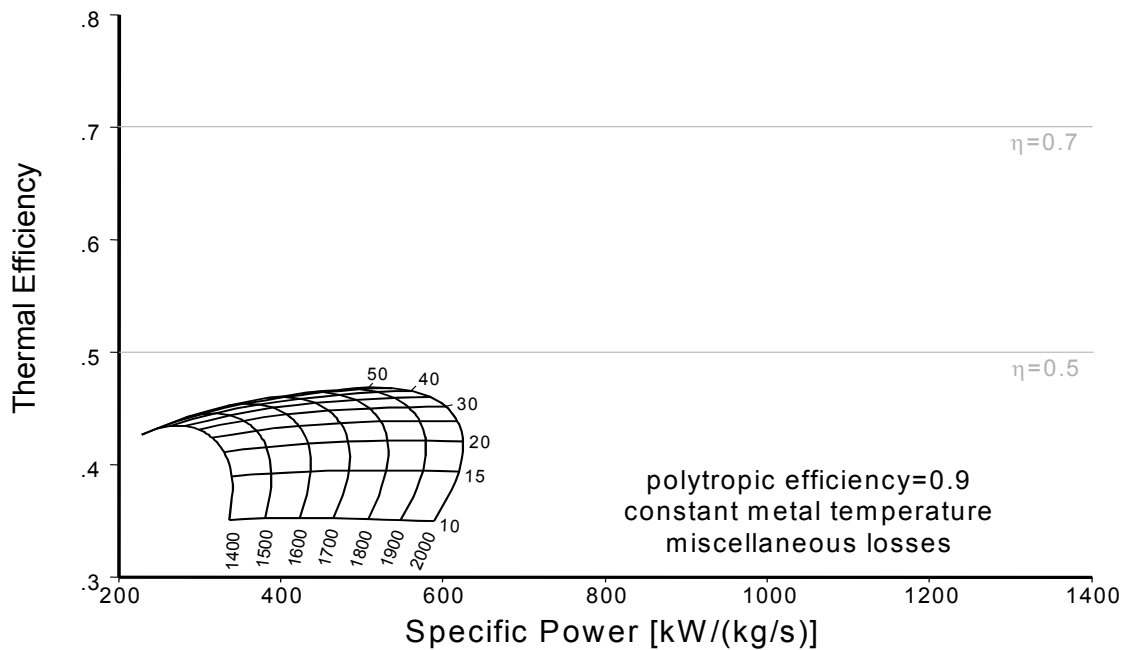


**Figure 3.18: Performance of the Real Cycle with Constant Turbine Metal Temperature.**

In **Figure 3.19** the results for the recuperated engine are shown. As can be seen the thermal efficiency is much better than that of the simple cycle, and the pressure ratio for the optimum efficiency is rather low.

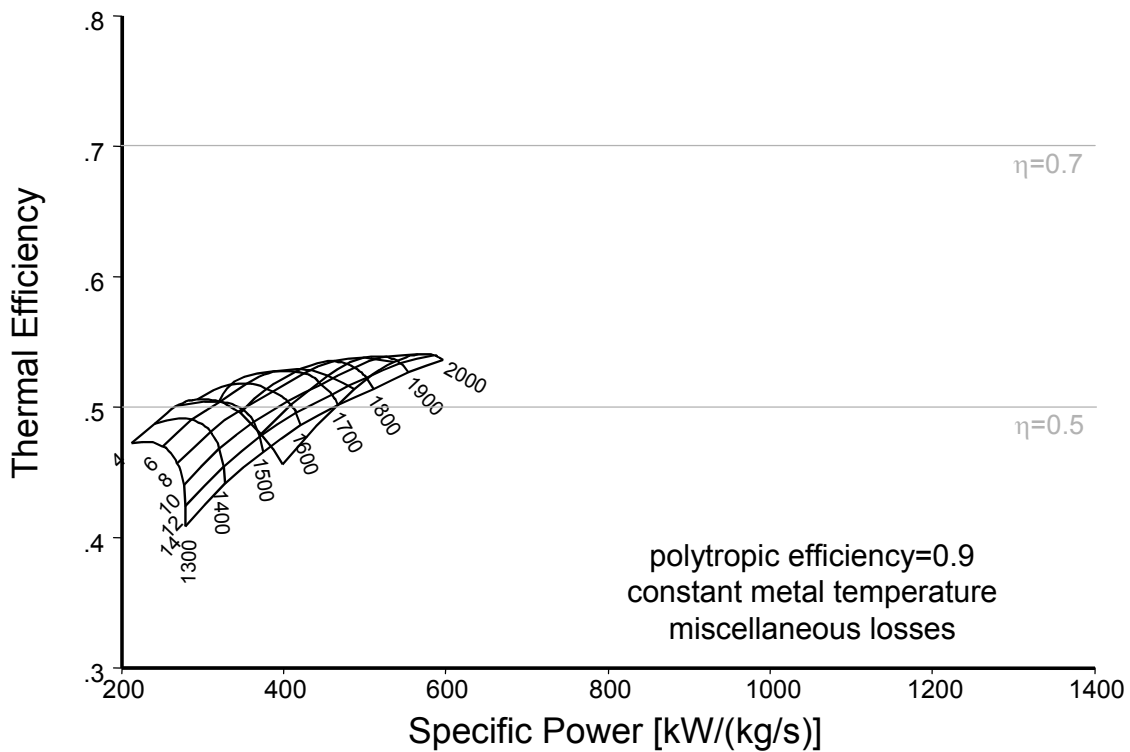


**Figure 3.19: Thermal Efficiency of the Recuperated Cycle with Constant Turbine Metal Temperature.**

Adding an intercooler increases specific work and also the thermal efficiency as can be seen from **Figure 3.20**. The pressure ratio for optimum efficiency is between the values found optimum for the simple cycle and the recuperated cycle.

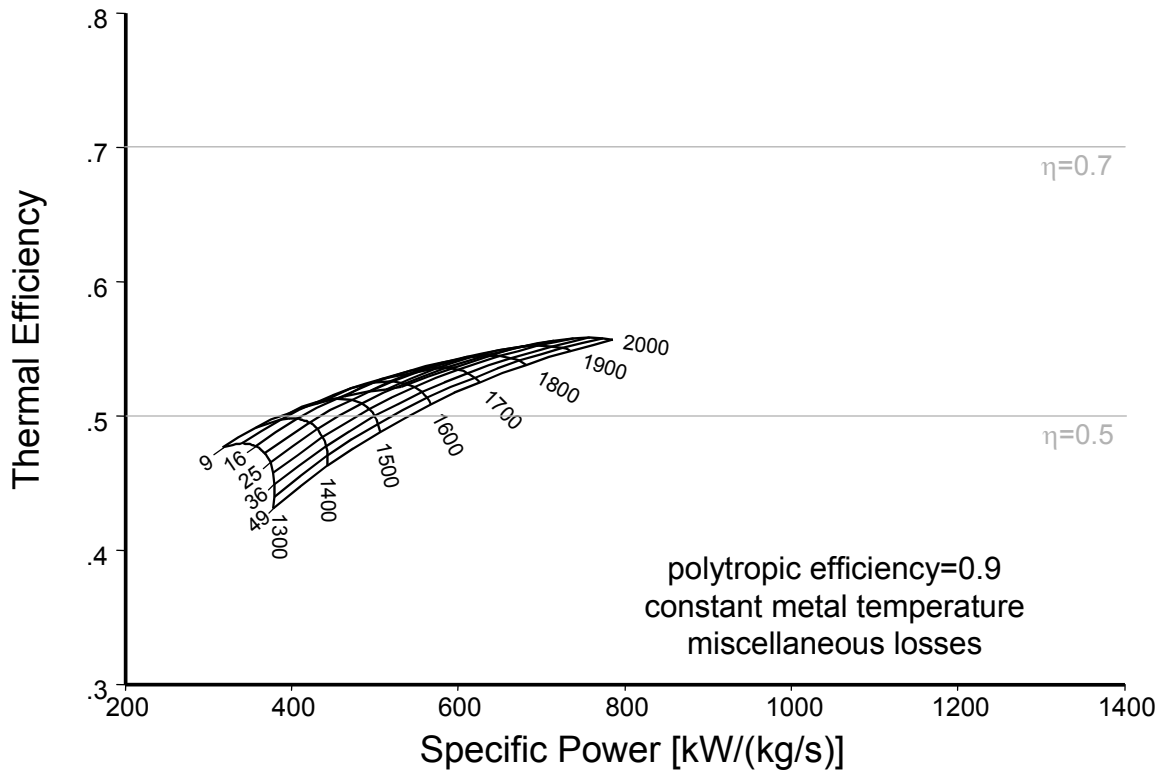


**Figure 3.20:** Thermal Efficiency of the Intercooled and Recuperated Cycle with Constant Turbine Metal Temperature.

The last three figures give an idea about which performance can be achieved with gas turbines. This however, is not the end of the story: the heat in the exhaust gas can be used for generating steam which is used to drive a steam turbine, for example. The steam can also be used for various other purposes and can even be injected into the burner of the gas turbine. The thermal efficiency of such an enhanced cycle will be better than shown above.

### 3.1.3 Efficiency Potential of the Simple Gas Turbine Cycle

The simple gas turbine cycle is of relevance for power generation, for ship, helicopter and turboprop aircraft propulsion. Moreover, considerations about this cycle give also an insight into the future of the aero engine gas turbine – which is typically a turbofan. This is because the turbofan engine cycle can be easily split into two parts: There is a core stream process (see **Figure 3.21**) which comprises of the primary flow commencing with ambient conditions up to a location within the low pressure turbine which is defined in such a way that all the compressor power needed for the core stream is covered. The second and third process parts deal with the bypass stream compression and expansion as well as with generating the core stream thrust.

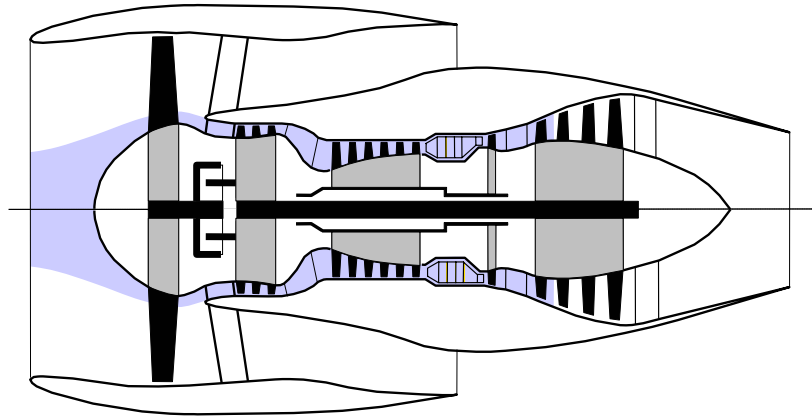


**Figure 3.21: Core Stream Process of a Turboprop.**

Apart from the compression of the incoming air from ambient conditions to inlet total pressure and temperature the core stream process is exactly the same as that of the simple cycle gas turbine.

The following discussions are restricted to the thermal efficiency of the gas turbine cycle and they do only touch shortly the specific power, i.e. the power per unit mass flow. Keep in mind that for aero propulsion applications the power developed per frontal area, per volume and per weight is an equally important attribute of any gas turbine core as its thermal efficiency.

The abstract of reference [3.2] begins with the statements: “Thermal efficiency of gas turbines is critically dependent on temperature at the turbine inlet; the higher this temperature, the higher the efficiency. Stoichiometric combustion would provide maximum efficiency”. This view about gas turbine efficiency is widely spread, however, it is incorrect. In reference [3.3] it is shown that when gas properties are modeled accurately the variation of cycle efficiency with turbine inlet temperature at constant pressure ratio exhibits a maximum at temperatures well below the stoichiometric limit.

The authors of reference [3.3] come to the conclusion that the dominant influence for this unexpected phenomenon comes from the change of composition of the combustion products with varying fuel-air-ratio, particularly the contribution from the water vapor.

Let’s begin with the findings from reference [3.3] and extend the study to effects that were not included in the referenced paper. At first the un-cooled cycle performance is discussed; the accuracy of the gas property modeling is improved in several steps with the aim of isolating the source of the efficiency maximum at temperatures well below the stoichiometric limit.

### 3.1.3.1 Schoolbook Wisdom

We consider the cycle of a simple gas turbine with 90% polytropic efficiency for both the compressor and the turbine and no pressure losses in other parts of the cycle. To simplify the considerations further the mass flow through compressor and turbine are assumed to be equal. With other words, the amount of high pressure air leakage is equal to the amount of fuel added.

#### 3.1.3.1.1 Definition of Thermal Efficiency

The thermal efficiency of this cycle is equal to the specific turbine shaft power minus specific compressor shaft power divided by the amount of heat added in the burner. For constant specific heat one can write

$$\eta_{th} = \frac{H_T - H_C}{H_B} = \frac{T_4 - T_5 - T_3 + T_2}{T_4 - T_3} = 1 - \frac{T_5 - T_2}{T_4 - T_3} \quad \text{Eq. 3-4}$$

If component efficiencies are 100% then holds

$$\frac{T_3}{T_2} = \frac{T_4}{T_5} \quad \text{respectively} \quad \frac{T_5}{T_2} = \frac{T_4}{T_3} \quad \text{Eq. 3-5}$$

This yields for the ideal Joule cycle that its thermal efficiency is only a function of pressure ratio:

$$\eta_{th} = 1 - \frac{T_2}{T_3} = 1 - \left( \frac{P_3}{P_2} \right)^{\frac{1-\gamma}{\gamma}} \quad \text{Eq. 3-6}$$

If the component efficiencies are not 100% and the gas properties (isentropic exponent  $\gamma$  and gas constant  $R$ ) are not constant then the formula becomes

$$\eta_{th} = \frac{\frac{\gamma_T}{\gamma_T - 1} * R_T * \frac{T_4}{T_2} * \left[ 1 - \left( \frac{P_2}{P_3} \right)^{\frac{\gamma_T - 1}{\gamma_T}} \right] * \eta_T - \frac{\gamma_C}{\gamma_C - 1} * R_C * \left[ \left( \frac{P_3}{P_2} \right)^{\frac{\gamma_C - 1}{\gamma_C}} - 1 \right] / \eta_C}{\left( \frac{T_4}{T_2} - \frac{T_3}{T_2} \right) * \left( \frac{\gamma_C}{\gamma_C - 1} * R_C + \frac{\gamma_T}{\gamma_T - 1} * R_T \right) / 2} \quad \text{Eq. 3-7}$$

Since the temperature ratio  $T_3/T_2$  is directly coupled with  $P_3/P_2$  and compressor efficiency it is obvious that the thermal efficiency of the simply cycle gas turbine is a function of pressure ratio  $P_3/P_2$ , temperature ratio  $T_4/T_2$ , component efficiencies and the properties of the gas.

### 3.1.3.1.2 Constant Gas Properties

The most simple model of the cycle employs constant gas properties which means in the example shown below  $\gamma_C = \gamma_T = 1.35$  and  $R_C = R_T = 287 \text{ J/kg/K}$ . Evaluating thermal efficiency over a wide range of pressure ratios and temperatures with this simple gas property model yields the results shown in **Figure 3.22**. For a better view on the optimum thermal efficiency islands the parametric study is extended to pressure ratios well beyond any realistic case. The tendency in this figure is clear: increasing burner exit temperature at constant pressure ratio yields improved thermal efficiency.

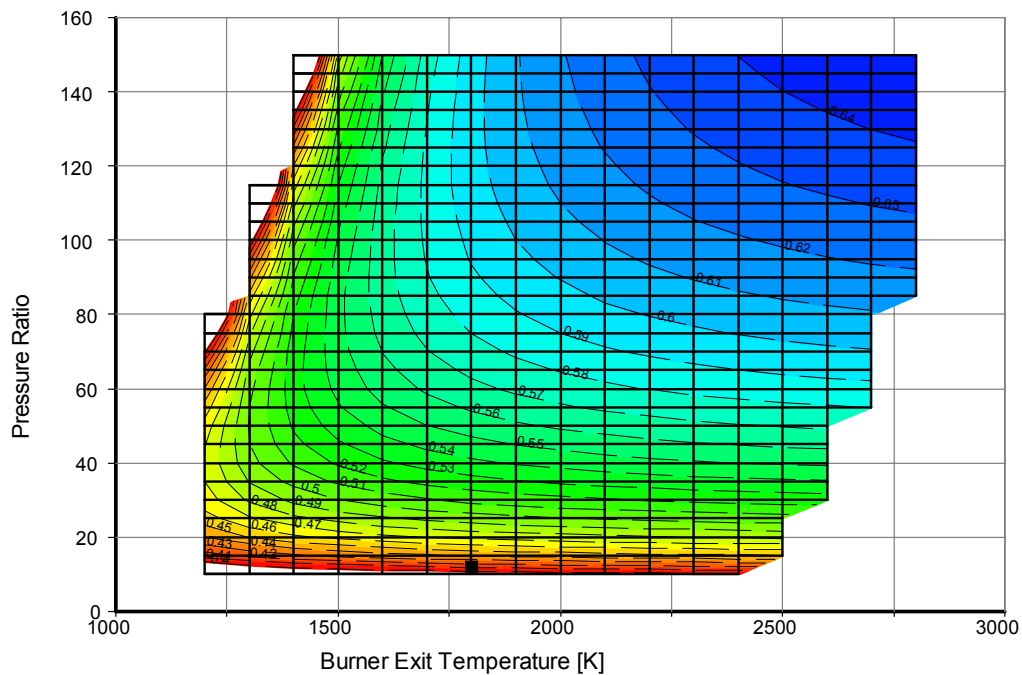


**Figure 3.22: Thermal Efficiency Evaluated with Constant Gas Properties.**

The top left corner is cut off because there the compressor exit temperature exceeds the burner exit temperature. The right border of the parametric study represents the maximum temperature achievable if Kerosene is used as fuel.

### 3.1.3.1.3 Temperature Dependent Gas Properties

Burning hydrocarbons (Kerosene, JP4 or Diesel, for example) with air leads to combustion gases that have practically the same gas constant as dry air. Thus the assumption  $R_C = R_T = 287 \text{ J/kg/K}$  is valid, but the isentropic exponents  $\gamma_C$  and  $\gamma_T$  are in reality not constant but change significantly with temperature. Moreover, the magnitude of  $\gamma_T$  depends also from the composition of the combustion gases, i.e. the fuel-air-ratio.

The gas properties of combustion gases as well as the temperature rise due to combustion used in this paper have been calculated with the NASA CEA program, [3.4 and 3.5]. The effect of pressure on the heat release is taken into account; the pressure effect on the other gas properties (isentropic exponent, gas constant, enthalpy and entropy) is neglected.

Rerunning the parametric study with variable isentropic exponents – i.e.  $\gamma_C = f(T)$  and  $\gamma_T = f(T, \text{far})$  – yields the results presented in Figure 3.23.

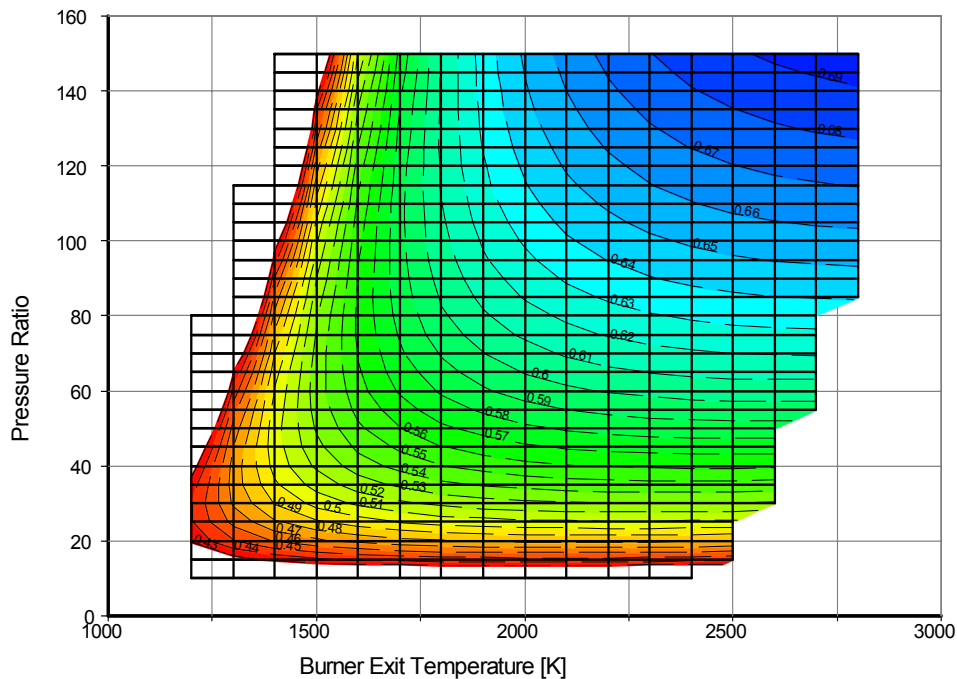


**Figure 3.23: Thermal Efficiency Evaluated with Temperature Dependent Gas Properties.**

There is not much difference between **Figure 3.22** and **Figure 3.23** and especially the tendency that the highest burner temperature yields the best thermal efficiency is the same in both models.

The question remains if a difference in the gas constant between compressor and turbine can change the basic shape of the efficiency contour lines. In the conclusions of [3.3] it is speculated that steam injection could have a mayor impact on the location of the maximum efficiency. The reasoning behind this is that the increased amount of water vapor in the combustion exhaust changes the specific heat in the expansion process significantly.

To study this effect the exercise has been repeated with steam injection (steam-fuel-ratio 1) into the burner. As can be seen from **Figure 3.24** again no significant change in the shape of the contour lines can be observed except that the maximum temperature achievable is reduced. This comes from two effects: first the percentage of oxygen in the gas consisting of a mixture of air and steam is lower than in dry air. Second some of the heat released by the chemical reaction is needed to heat the steam to burner exit temperature.

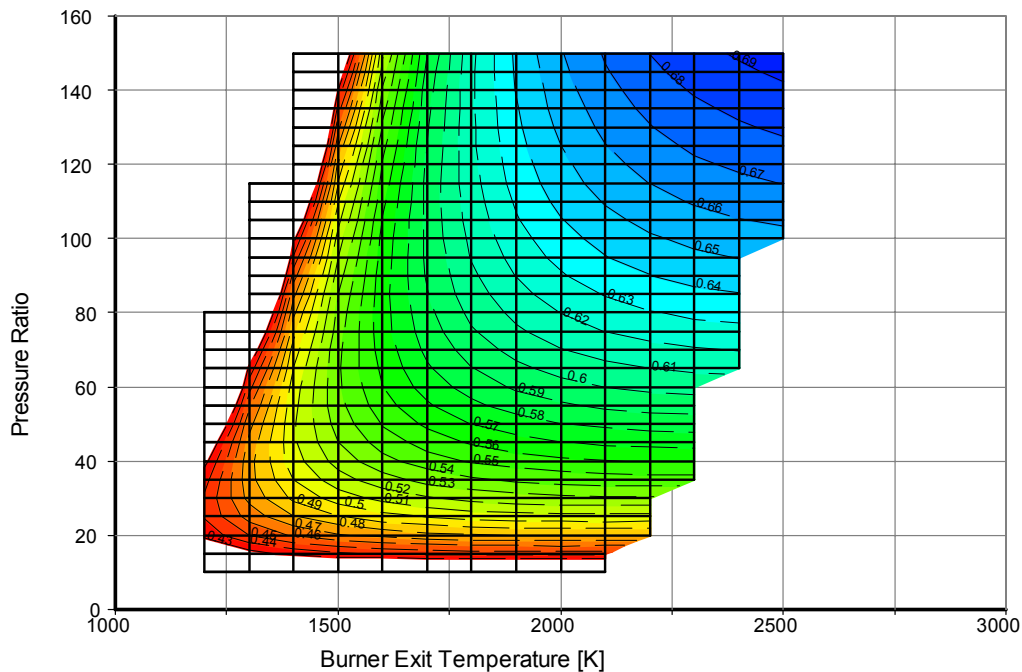


**Figure 3.24: Thermal Efficiency with Steam Injection (Steam-Fuel-Ratio = 1), Evaluated with Temperature Dependent Gas Properties.**

The authors of [3.3] come to the conclusion that the dominant influence for the thermal efficiency maximum which they have found originates from the change of composition of the combustion products with varying fuel-air-ratio, particularly the contribution from the water vapor. They make the specific heat of water vapor – which is significantly different to that of air and other combustion products – responsible for the maximum efficiency being at temperatures lower than stoichiometric.

The results shown above seem to be a contradiction to the findings from ref. 1 because no efficiency maximum below the stoichiometric temperature could be found even when the gas properties are modeled with the same accuracy as in ref. 1. Especially it has been demonstrated by the steam injection example that the gas properties of water vapor do not create an efficiency maximum at temperatures well below the stoichiometric limit.

In the calculations presented up to now only simple formulae as found in schoolbooks have been employed. Next the full blown cycle code from GasTurb [3.6] will be used for evaluating thermal efficiency.

### 3.1.3.2 Full Cycle Calculation

There is no difference between the gas property model in GasTurb [3.6] and that employed for getting the results reported above. Actually the calculations for *Section 3.1.3.1.1* of this chapter have been done with the same code which allows the user to add his own formulae as needed.

#### 3.1.3.2.1 Definition of Thermal Efficiency

In the cycle code the thermal efficiency is defined as

$$\eta_{th} = \frac{H_T - H_C}{W_F * FHV} \quad \text{Eq. 3-8}$$

The difference between this definition and the one used in [Section 3.1.3.1.1](#) is in the denominator: instead of the burner temperature difference  $T_4 - T_3$ , multiplied by the mean specific heat, here the product of fuel flow  $W_F$  and fuel heating value FHV is used. This is reasonable because in the real world one has to pay for fuel, not for a temperature difference as implied with the schoolbook definition of thermal efficiency.

The result of using this definition of thermal efficiency one gets what is reported in [\[3.3\]](#), see [Figure 3.25](#). There is an optimum of thermal efficiency at temperatures well below the stoichiometric limit! At a given pressure ratio of 40, for example, increasing burner exit temperature beyond 2000 K would decrease thermal efficiency even if no cooling air is employed.

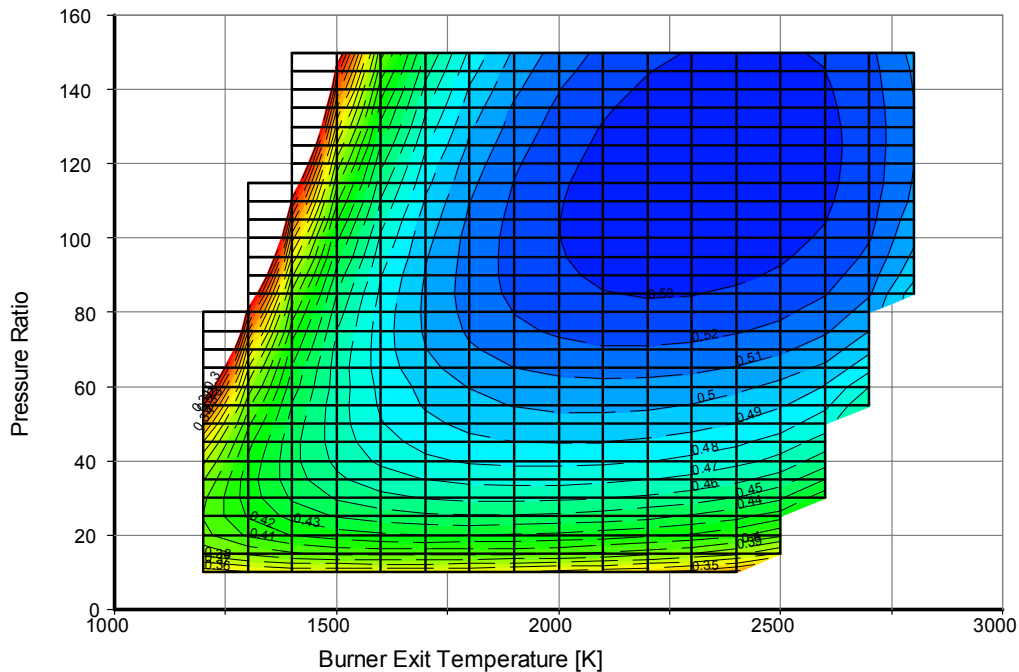


**Figure 3.25: Thermal Efficiency Defined with  $W_F \cdot FHV$ .**

This optimum is obviously caused by using  $W_F \cdot FHV$  as denominator and therefore it is adequate to study the heat release process in the burner in some detail.

### 3.1.3.2.2 Temperature Increase in the Burner

In the schoolbook definition of thermal efficiency the fuel flow is implicitly assumed to be proportional to  $C_p \cdot (T_4 - T_3)$ . In reality fuel flow respectively fuel-air-ratio is not proportional to  $T_4 - T_3$  as can be seen from [Figure 3.26](#).

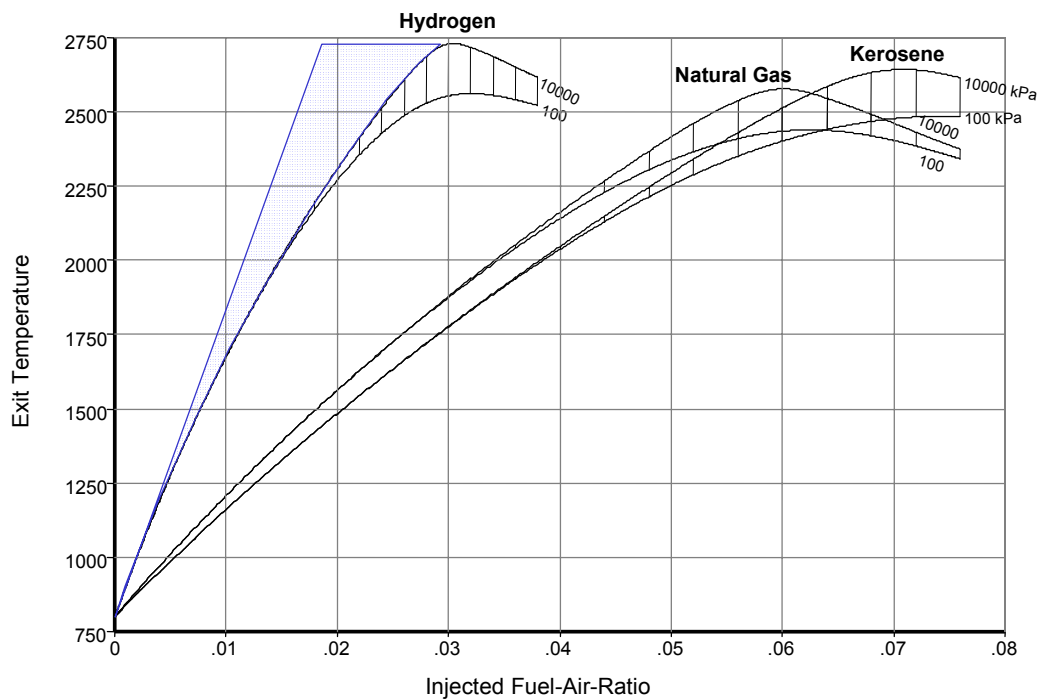


**Figure 3.26: Burner Exit Temperature for Different Fuels ( $T_3 = 800$  K).**

For example, to get 2000 K exit temperature with hydrogen as fuel would require a fuel-air-ratio of 0.0115 if the amount of fuel would be proportional to the temperature increase as the blue line indicates. However, in reality one needs the fuel-air-ratio of 0.015 – which is 30% more. Note that this effect has nothing to do with dissociation – up to 2000 K the exit temperature is nearly independent from pressure which can also be seen in [Figure 3.26](#).

The fact that for achieving high temperatures one needs over-proportional amounts of fuel is the reason for the maximum thermal efficiency being at a temperature much lower than the stoichiometric value. This effect is independent from the fuel type as can be seen from a comparison of [Figure 3.25](#) (fuel: Kerosene) with [Figure 3.27](#) which was calculated with hydrogen as fuel.

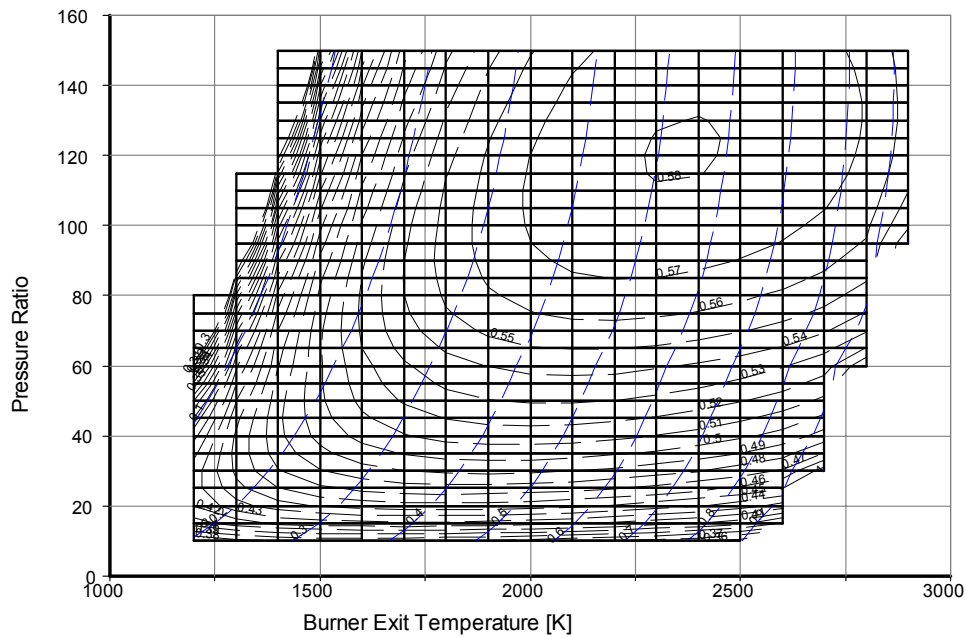


**Figure 3.27: Thermal Efficiency with Hydrogen as Fuel with Lines of Constant Equivalence Ratio.**

In **Figure 3.27** besides the lines for constant thermal efficiency also lines with constant equivalence ratio are shown. Equivalence ratio is defined as

$$ER = \frac{far}{far_{stoichiometric}} \quad \text{Eq. 3-9}$$

The optimum thermal efficiencies as function of pressure ratio are found along the line  $ER = 0.5$ . The same correlation can be observed when lines for constant equivalence ratio are plotted into **Figure 3.25**. Thus the following generally valid statement can be made:

*The maximum thermal efficiency of the simple gas turbine cycle with polytropic efficiencies equal to 0.9 and no cooling air simulation is found with fuel-air-ratios approximately equal to 50...60% of the stoichiometric value, independently from the type of hydrocarbon fuel burnt.*

### 3.1.3.2.3 Effect of Component Efficiencies

All the cycle studies discussed above were performed with the same assumption about the quality of the turbo-machinery: polytropic efficiencies were always equal to 0.9 and no further losses were considered except that the amount of air leakage was set to be equal to the amount of fuel used.

What happens if the component efficiencies are different has been already reported in **Ref. [3.3]**. As the efficiencies are increased the point of maximum cycle efficiency shifts at constant pressure ratio to lower values of  $T_4$ . **Figure 3.28** shows this for the example of pressure ratio 60.

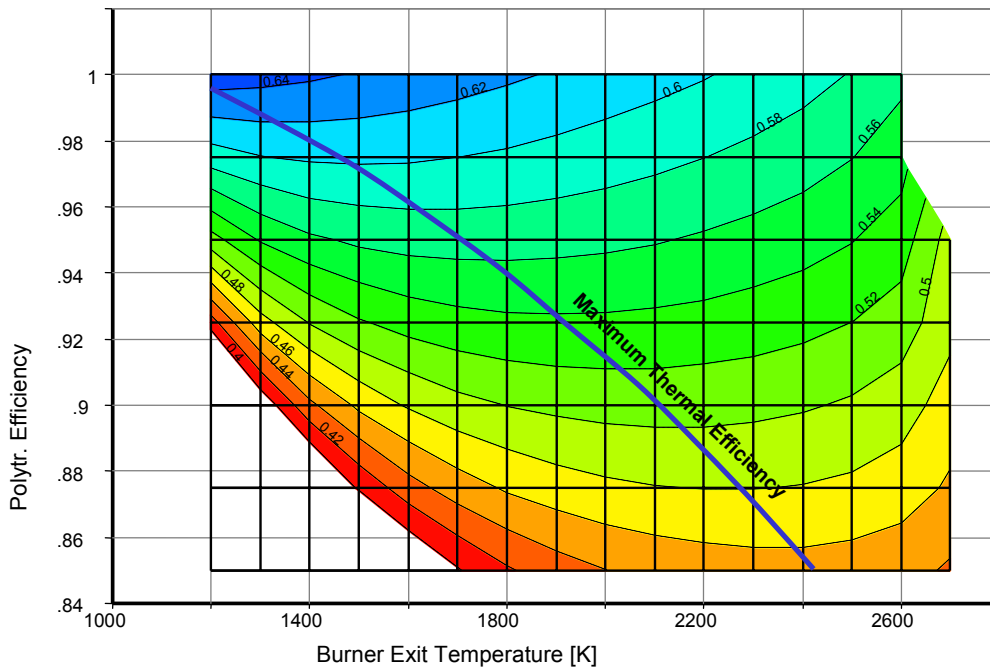


**Figure 3.28: Burner Temperature for Maximum Thermal Efficiency, Pressure Ratio = 60.**

#### 3.1.3.2.4 Cooling Air Simulation

For more accurate simulations of course the amount of cooling air needed and the associated losses must be modeled adequately. Here we employ a rather simple method for estimating the amount of cooling air which correlates permissible mean metal temperature, cooling air amount, cooling effectiveness, cooling air temperature and  $T_4$ .

Only the cooling of the first turbine stage is considered. The vane cooling air is mixed with the main stream before the first rotor and thus the rotor entry temperature  $T_{41}$  is lower than the burner exit temperature  $T_4$ . With respect to rotor cooling the relative total temperature  $T_{41R}$  is the driving parameter. Without going into the details of an aerodynamic turbine design this temperature is approximated as  $T_{41R} = 0.9 \cdot T_{41}$ .

For finding an appropriate amount of cooling air the cooling effectiveness is used:

$$\eta_{cl} = \frac{T_{gas} - T_{metal}}{T_{gas} - T_{coolant}} \quad \eta_{cl} = \frac{T_4 - T_{metal}}{T_4 - T_3} \quad \text{Eq. 3-10}$$

The amount of cooling air needed for achieving a certain cooling effectiveness depends on the design of the vane respectively blade cooling. For low cooling effectiveness it is sufficient to employ a design with convective cooling while for higher  $\eta_{cl}$  values film cooling is required. An approximate value for the amount of cooling air needed can be found from the empirical correlation which is taken from the GasTurb user's manual [3.6]:

$$\frac{W_{cl}}{W_{gas}} = C * \frac{\eta_{cl}}{1 - \eta_{cl}} \quad \text{Eq. 3-11}$$

This expression can also be found in reference [3.7] (which contains also several more similar correlations) together with quite some physical background.

The constant  $C$  in the formula is set to 0.05 which yields a reasonable amount of cooling air over the full range in the parametric study. The result for thermal efficiency is shown in **Figure 3.29**.

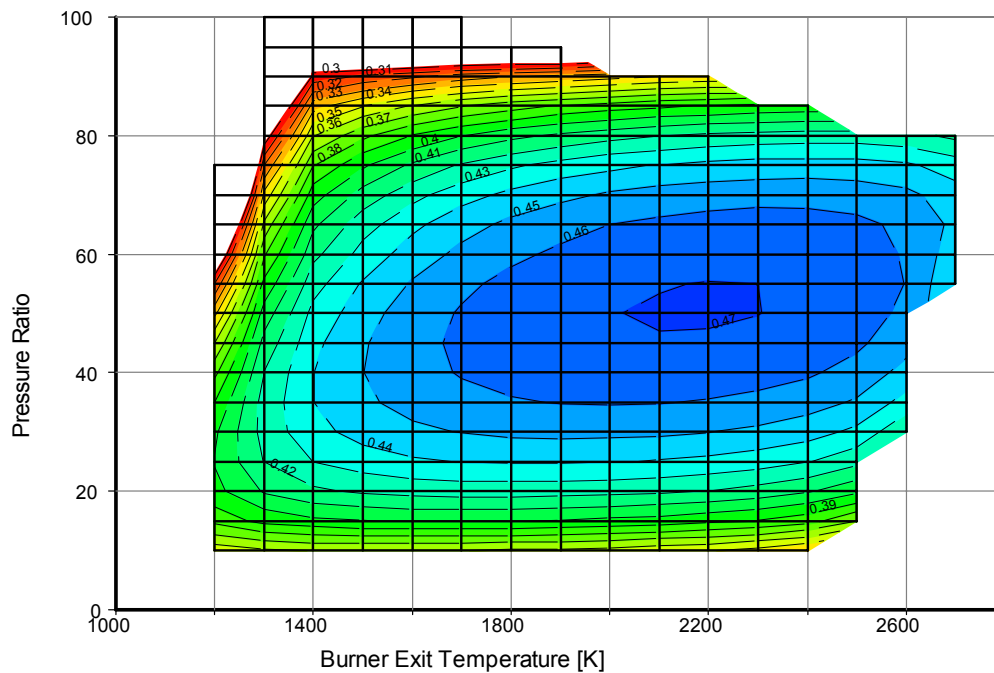


**Figure 3.29: Thermal Efficiency with Cooling Air Simulation.**

Now we see the optimum at a place which is not far from a realistic cycle. The whole top right part – where high pressure ratios are combined with high temperatures – does no longer exist. The reason is the excessive amount of cooling air which would be needed in this region; **Figure 3.30** shows the amount of NGV cooling air, the numbers for the rotor cooling air are somewhat smaller.

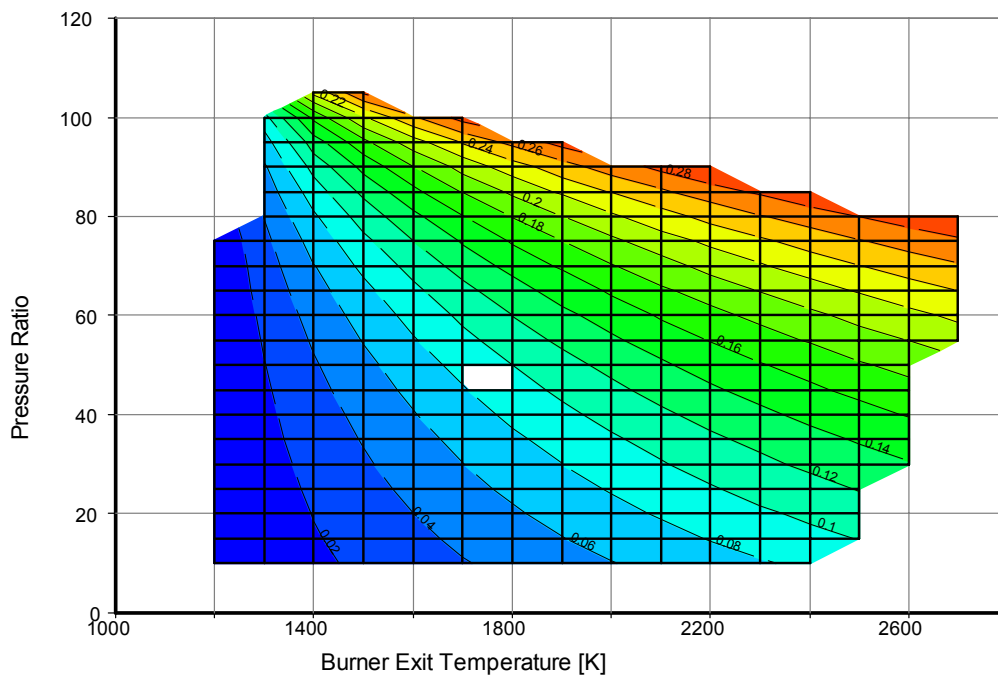


**Figure 3.30: NGV Cooling Air  $W_{CL}/W_{gas}$ .**

The equivalence ratio at the optimum thermal efficiency is  $ER_{max\ eff} = 60\%$  and thus about 10% higher than that for the un-cooled cycle, see the elaborations in the section about the temperature increase in the burner.

If **Figure 3.29** would show the design space of a real engine, and the only figure of merit would be the thermal efficiency then one would select from **Figure 3.29** as cycle design point the parameter combination  $P_3/P_2 = 50$  and 2200 K. However, since the combination  $P_3/P_2 = 40$  with 1800 K burner exit temperature yields only 1% less thermal efficiency than at the maximum it would in practice be the better choice because it requires significantly less design effort and cost.

### 3.1.3.2.5 Discussion

Optimizing an aircraft engine does not only ask for high thermal efficiency but also for low weight and low frontal area, in other words for high specific power per unit of mass flow. Specific power always increases with burner exit temperature and the maximum shows up at significantly lower pressure ratio than that required for optimum thermal efficiency. This is illustrated in **Figure 3.31** in which the dashed arrow indicates maximization of thermal efficiency while the solid arrow connects the maxima of specific power at any given burner exit temperature.

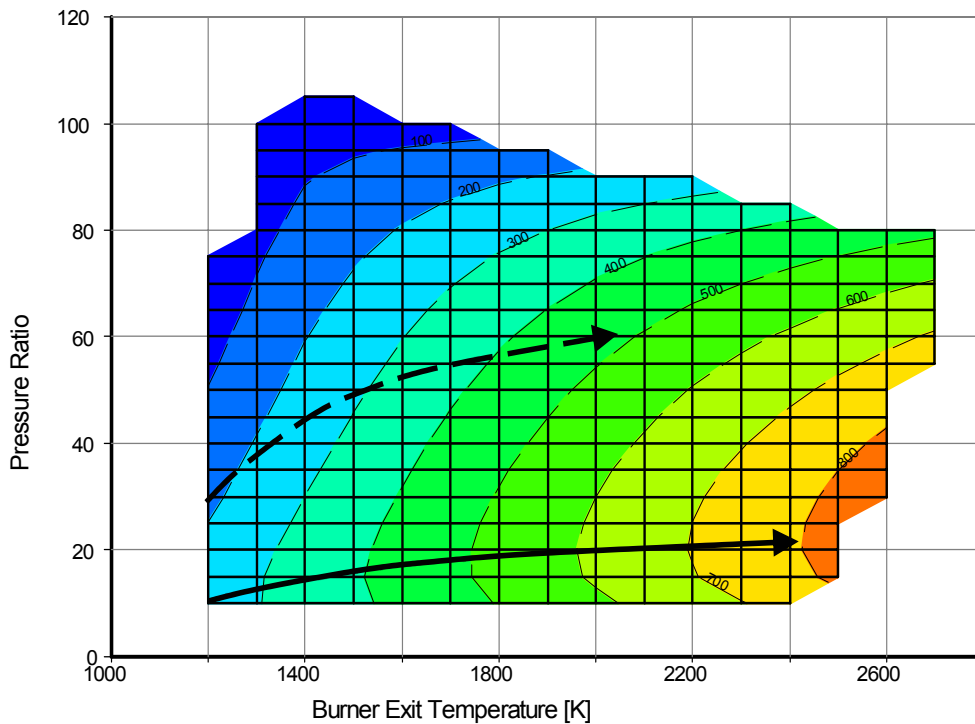


**Figure 3.31: Specific Power.**

The most economic engine designs of the future will be compromises between optimizing the core thermal efficiency and its power per unit mass flow. Dependent on the flight mission one or the other figure of merit will be more important. Both the pressure ratio and the burner exit temperature of modern engines are already near to their optimum values with respect to thermal efficiency. No significant increase in pressure ratio or burner exit temperature is beneficial for the turbofans of the future. Improvements of specific fuel consumption will be moderate since also the main element of the second process part – the bypass ratio – is already near to its practical limit for a conventional turbofan configuration.

Of course the improvement of component efficiencies and the reduction of the cooling air requirements will remain also in future important goals of any engine maker. However, success in that direction is extremely difficult since at the same time economics require that the number of parts being reduced which has the consequence that the aerodynamic loading increases. Moreover, the technical standard of today is already very high which makes further progress also very difficult.

#### 3.1.3.2.6 Conclusions

- Increasing thermal efficiency is achieved most effectively by increasing pressure ratio, not by increasing burner exit temperature towards the stoichiometric limit.
- At a given pressure ratio limit the thermal efficiency will decrease if the specific power is increased.
- The specific fuel consumption of a conventional turbofan engine can be improved by increasing component efficiencies, overall pressure ratio and bypass ratio, but not by increasing the burner temperature much above the values achieved already today. There is not much room for improvement of the component efficiencies since modern optimized 3-D blade designs are already very good. Raising the efficiency of a low pressure turbine from say 93 to 94% would mean decreasing the losses by 15% and that certainly would be very ambitious.
- There is also not much room for increasing the bypass ratio above 10.

- There is not much to expect from future increases in component efficiencies, pressure ratio and bypass ratio. An increase in burner temperature does not yield improved cycle efficiency. It must be concluded that for commercial turbofan engines significant improvements of the specific fuel consumption can only be expected if a new engine concept invalidates the findings presented in this section.

In the preceding section we considered the generation of shaft power, and its direct relevance for the propulsion system of a helicopter, a ship or a land vehicle. However, instead of creating shaft power we can also create thrust from the energy available at the exit of the high pressure turbine.

### 3.1.4 From Power Generation to Thrust Generation

#### 3.1.4.1 Turbojet

The easiest way to get thrust from a simple cycle gas turbine is to expand the hot high pressure exhaust gases in a nozzle, see **Figure 3.32**. The performance of any aircraft gas turbine depends not only on compressor pressure ratio and burner exit temperature but also very much on the flight Mach number. The air is pre-compressed by the ram effect and thus the overall pressure ratio  $P_3/P_{\text{ambient}}$  is much higher than the compressor pressure ratio  $P_3/P_2$ . Compressor inlet temperature  $T_2$  is also higher than the ambient temperature and this affects again the thermodynamic cycle.

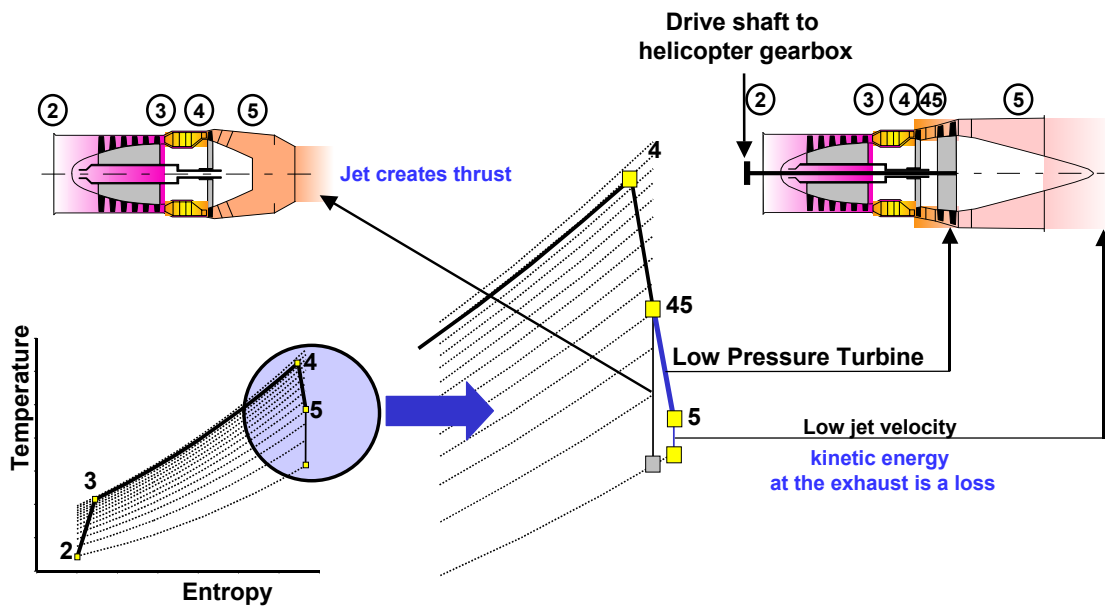


**Figure 3.32:** Turboshaft and Turbojet.

**Figure 3.33** shows performance data for a turbojet flying at an altitude of 11 km. The loss assumptions for the gas turbine are the same as described in the **Section 3.1.2**. An ideally matched convergent-divergent nozzle expands the exhaust gases to ambient pressure and the intake total pressure recovery is in case of supersonic flight dependent on Mach number  $Mn$  as described by **Mil-E-5007 [3.25]**:

$$\frac{P_2}{P_1} = 1 - 0.075 * (Mn - 1)^{1.35} \quad \text{Eq. 3-12}$$

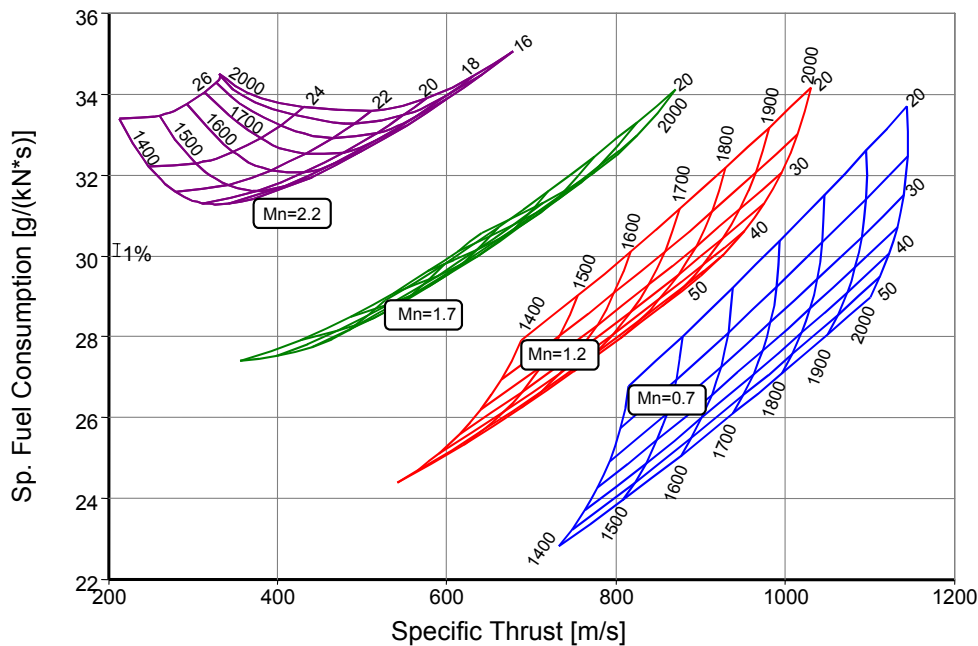


**Figure 3.33: Turbojet Performance at 11 km.**

All the gas turbines in **Figure 3.32** are of the same quality, if converted to a turboshaft by adding a power turbine with 90% polytropic efficiency they all would have the thermal efficiency shown in **Figure 3.18**. The changing thrust specific fuel consumption SFC with flight Mach number originates from the differences in propulsive efficiency. The definition of propulsive efficiency is given in **Section 3.1.5.1**.

### 3.1.4.2 Turbofan

Reducing the jet velocity is the way to increase propulsive efficiency, and this is achieved in a turbofan by extracting energy from the core stream – which decreases core jet velocity – and creating a secondary stream with moderate jet velocity. The engine can be designed such that both streams are expanded separately or they are mixed and then expanded in a common nozzle.

The loss assumptions for the gas generator calculation of the turbofans in **Figure 3.34** are the same as for the turbojet example in the previous section. For both the fan and the low pressure turbine the polytropic efficiency is 0.9; both streams are expanded through convergent nozzles.

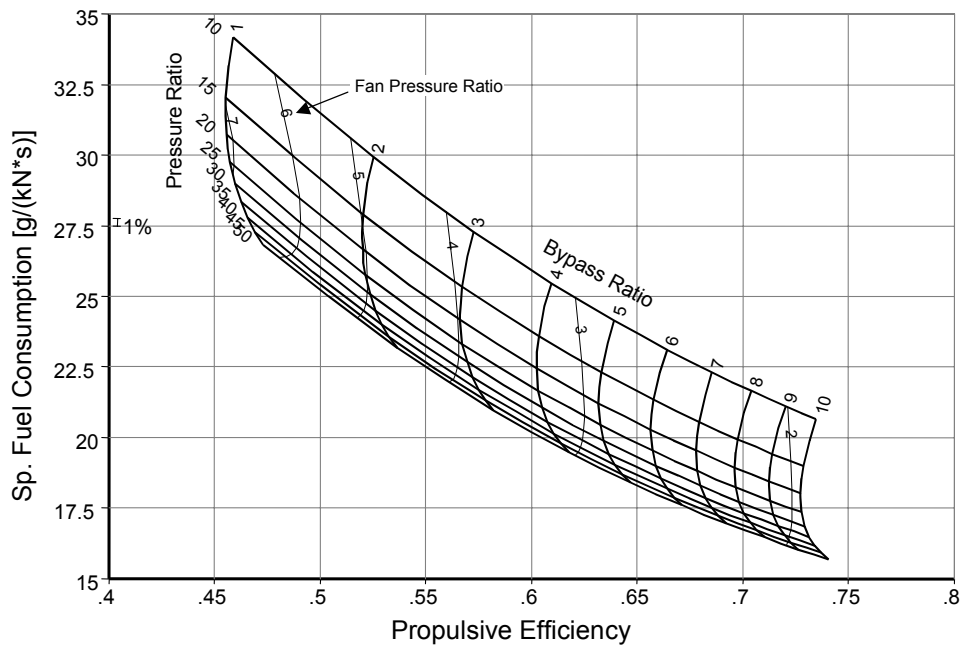


**Figure 3.34:** Turbofan with  $T_4 = 2000$  K, Alt = 11 km, Mn = 0.85.

Note, however, that the SFC improvement comes at a price: For a given thrust the size of the engine, here expressed as fan tip diameter, increases significantly with bypass ratio because the specific thrust (thrust per unit mass flow) decreases with jet velocity, see [Figure 3.35](#). Moreover, the pressure ratio of the low pressure turbine increases also and that means an increase in the turbine stage count.

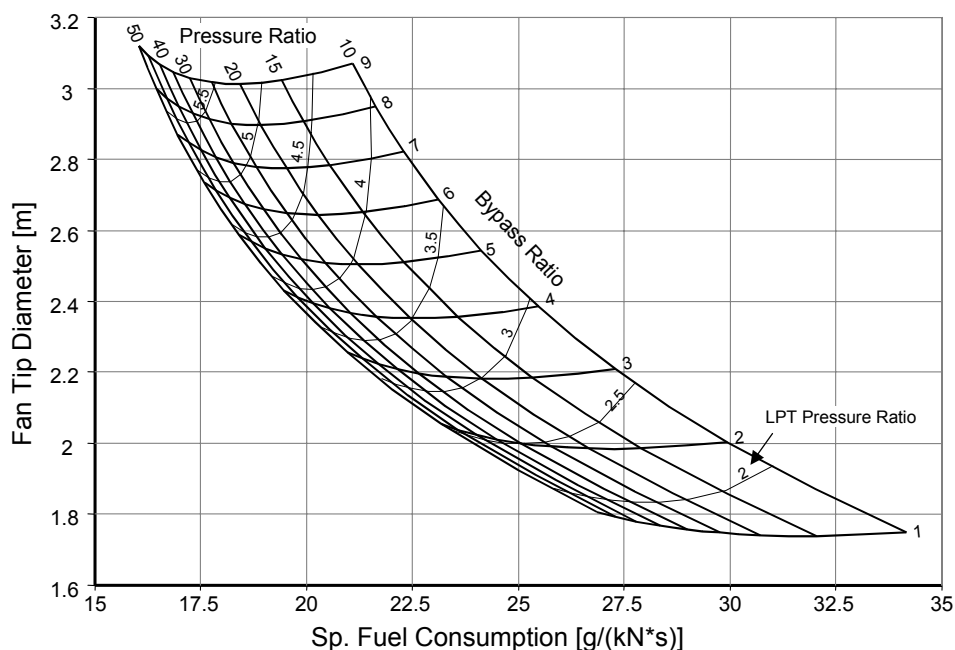


**Figure 3.35:** Fan Tip Diameter and LPT Pressure Ratio. Constant Thrust @ alt = 11 km, Mn = 0.85.

### 3.1.5 Quality Criteria

The quality of the thermodynamic cycle and its suitability for a specific task can be expressed in various types of efficiencies.

#### 3.1.5.1 Propulsive Efficiency

Propulsive efficiency is the ratio of useful propulsive energy – the product of thrust and flight velocity – compared to the sum of this energy and the wasted kinetic energy of the jet:

$$\eta_P = \frac{F * V_0}{F * V_0 + W_9 \frac{(V_9 - V_0)^2}{2}} \quad \text{Eq. 3-13}$$

If the nozzle flow is expanded fully to ambient conditions and the inlet mass flow  $W_0$  is equal to the nozzle mass flow  $W_9$  then thrust  $F$  equals  $W(V_9 - V_0)$  and the above formula can be rewritten as

$$\eta_P = \frac{2 * V_0}{V_0 + V_9} \quad \text{Eq. 3-14}$$

Propulsive efficiency is highest when jet velocity equals flight velocity; however, in this case thrust is zero.

With a turbojet at subsonic flight conditions the exhaust jet velocity is very much higher than the flight velocity of the aircraft. The high kinetic energy which the exhaust jet has relative to the air is a loss and this results in poor propulsive efficiency and finally in high thrust specific fuel consumption even if all the component efficiencies are high.

When propulsive efficiency is evaluated for an unmixed flow turbofan then the core stream and the bypass stream must be considered:

$$\eta_P = \frac{F * V_0}{F * V_0 + W_9 \frac{(V_9 - V_0)^2}{2} + W_{19} \frac{(V_{19} - V_0)^2}{2}} \quad \text{Eq. 3-15}$$

#### 3.1.5.2 Thermal Efficiency

Thermal efficiency is defined as increase of the kinetic energy of the gas stream passing through the engine by the amount of heat employed which is given as product of fuel mass flow  $W_f$  and fuel heating value FHV:

$$\eta_{th} = \frac{\frac{1}{2} W_9 * V_9^2 - \frac{1}{2} W_0 * V_0^2}{W_f * FHV} \quad \text{Eq. 3-16}$$

With turbofan engines one can split the thermal efficiency in two terms, the core efficiency and the transfer efficiency.

**Core Efficiency** is the ratio of energy available after all the power requirements of the core stream compression processes are satisfied – that means at the core exit – and the energy available from the fuel:

$$\eta_{core} = \frac{W_{core} * (dH_{is} - V_0^2 / 2)}{W_f * FHV} \quad \text{Eq. 3-17}$$

The enthalpy difference  $dH_{is}$  is evaluated assuming an isentropic expansion from the state at the core exit to ambient pressure.

**Transmission Efficiency** describes the quality of the energy transfer from the core stream to the bypass stream. It is defined as ratio of the energy at the nozzle(s) to the energy at the core exit and is equal to the thermal efficiency divided by core efficiency:

$$\eta_{trans} = \frac{\eta_{th}}{\eta_{core}} \quad \text{Eq. 3-18}$$

As can be seen from **Figure 3.36** the transmission efficiency is dominated by the efficiencies of the fan and the low pressure turbine, and both efficiencies are equally important.

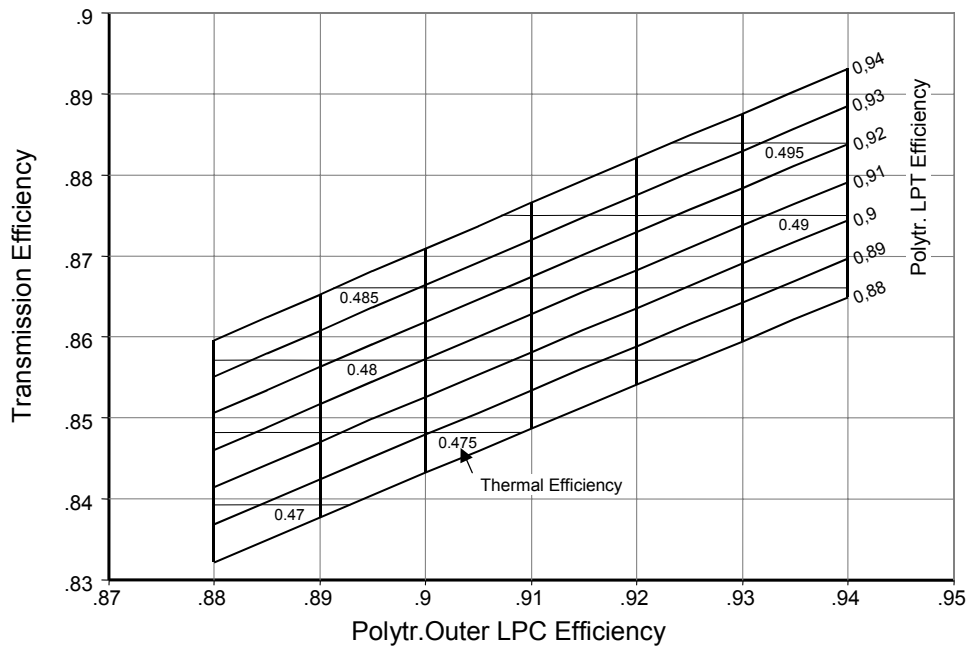


**Figure 3.36: Transmission Efficiency for Turbofans with Constant Core Efficiency.**

### 3.1.5.3 Overall Efficiency

The overall efficiency is the ratio of useful work done in overcoming the drag of the airplane to the energy content of the fuel:

$$\eta_o = \frac{F * V_0}{W_f * FHV} \quad \text{Eq. 3-19}$$

## SYSTEM MODELS

With the simplifying assumptions from **Section 3.1.5.1** it follows that overall efficiency is equal to the product of thermal efficiency and propulsive efficiency.

The efficiency of an aircraft engine is inseparably linked with the flight velocity as can be seen from the definitions listed in **Figure 3.37**. So the question arises, how to compare the quality of engines being used at different flight speeds.

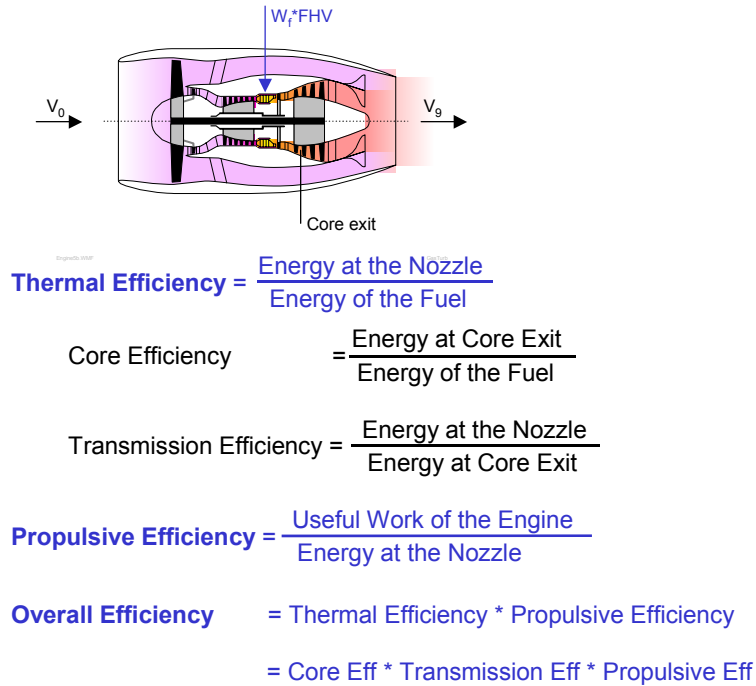


**Figure 3.37: Breakdown of Engine Efficiencies.**

We introduce the specific fuel consumption  $SFC = W_f/F$  into the formula above and get:

$$\eta_o = \frac{V_0}{SFC * FHV} \quad \text{Eq. 3-20}$$

or

$$SFC = \frac{V_0}{\eta_o * FHV} = \frac{V_0}{\eta_{th} * \eta_p * FHV} = \frac{V_0}{\eta_{core} * \eta_{trans} * \eta_p * FHV} \quad \text{Eq. 3-21}$$

In **Figure 3.38** are SFC data from many different engines shown. The big scatter in the data does not mean necessarily a big difference in thermal efficiency; it results mainly from the differences in propulsive efficiency respectively bypass ratio.

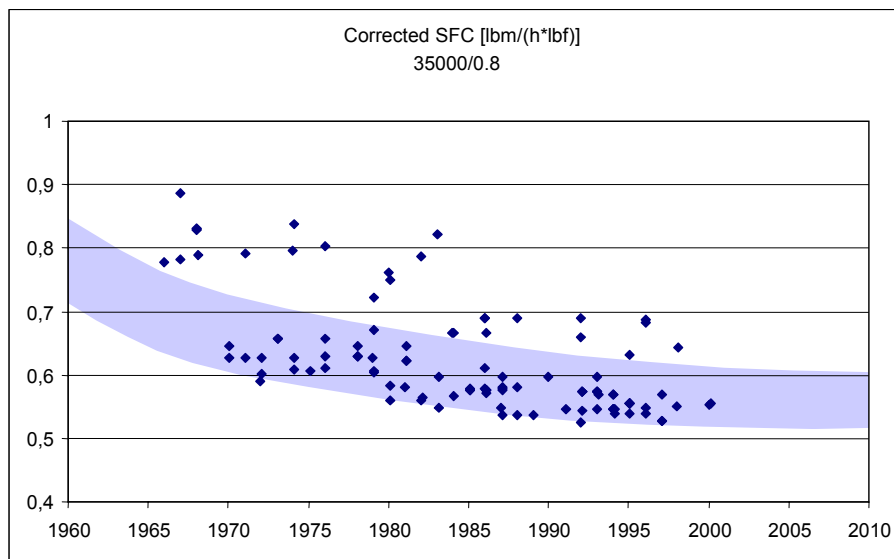


**Figure 3.38: Historical Trend in SFC [3.8].**

The historical trend of the SFC over time for the best conventional turbofans obviously flattens out and no significant improvement of fuel consumption is to be expected with today's technology.

## 3.2 GAS TURBINE THERMODYNAMIC ENGINE MODEL

The purpose of this section is to describe the key issues in engine performance simulations. The focus is to make an appropriate selection of model type and component models to meet simulation needs, and to understand the limitations and potential of various types of simulations for potential applications.

The different types of models used in the prediction and simulation of gas turbine engines operations can be classified by application and capability of the model. The range of potential applications and the types of models are shown in **Table 3.1**. Presented in **Table 3.2** are the relative requirements for some of these models in terms of accuracy, fidelity and physics detail. Detail involves how much of the engine is simulated. Fidelity refers to the depth and sophistication of the analytic representations within the model. Accuracy is the ability of the model to match tested or target values for engine and component performance or internal conditions.

**Table 3.1: Thermodynamic Property Representation  
Effect on Model Capability and Execution Speed**

	Constant Property	Limited Curve Fit	Full Range Curve Fit	Limited Constituent Equilibrium	Full Equilibrium	Full Kinetics
<b>Speed</b>	Fastest (1x)	Fast (10x)	Fast (20x)	Medium (200x)	Slow (500x)	Slowest (500x – 10000x)
<b>Accuracy / Range</b>	Limited Temperature Range (+/- 500 R)	Limited Temperature Range (< 2500R)	Wide, Limited by Complexity, Range	Wide, Limited by Extreme Disassociation (< 6000 R)	Limited by Physical Model Assumptions	Limited by Physical Model Assumptions
<b>Flexibility</b>	Low	Medium	High	High	Highest	Varies, may be limited by Kinetics Options
<b>Typical Use</b>	Simple 0-D/1-D Models, 2-D/3-D Models, Real Time or Condition Monitoring Models	Simple 0-D/1-D Models, 2-D/3-D Models	Most 0-D/1-D Models, Some 2-D/3-D Models	Some 0-D/1-D Cycle Models, Simple Combustion Models	Combustion Models, Special Application Cycle Models	Combustion Models

**Table 3.2: Model Fidelity, Accuracy and Detail Needs through the Engine Life Cycle**

	Accuracy	Fidelity	Detail
<b>Conceptual</b>	Low	Low	Low
<b>Detail Design</b>	Medium	High	High
<b>Test and Validation</b>	High	Medium	Low
<b>Fleet Support</b>	High	Low	Medium

### 3.2.1 Selecting the Appropriate Model Type

#### 3.2.1.1 Engine Development Cycle Considerations

The selection of an appropriate engine model depends on the phase of both the engine development cycle and the application (see **Figure 3.39**). Most users of engine simulations are interested in overall engine performance levels, internal conditions that have a direct influence on the aircraft and other internal engine conditions necessary to properly operate and maintain the engine. The most sophisticated models focus on the details of internal components for design purposes or special purpose analysis that is primarily of interest to engine manufacturers or government or academic researchers.

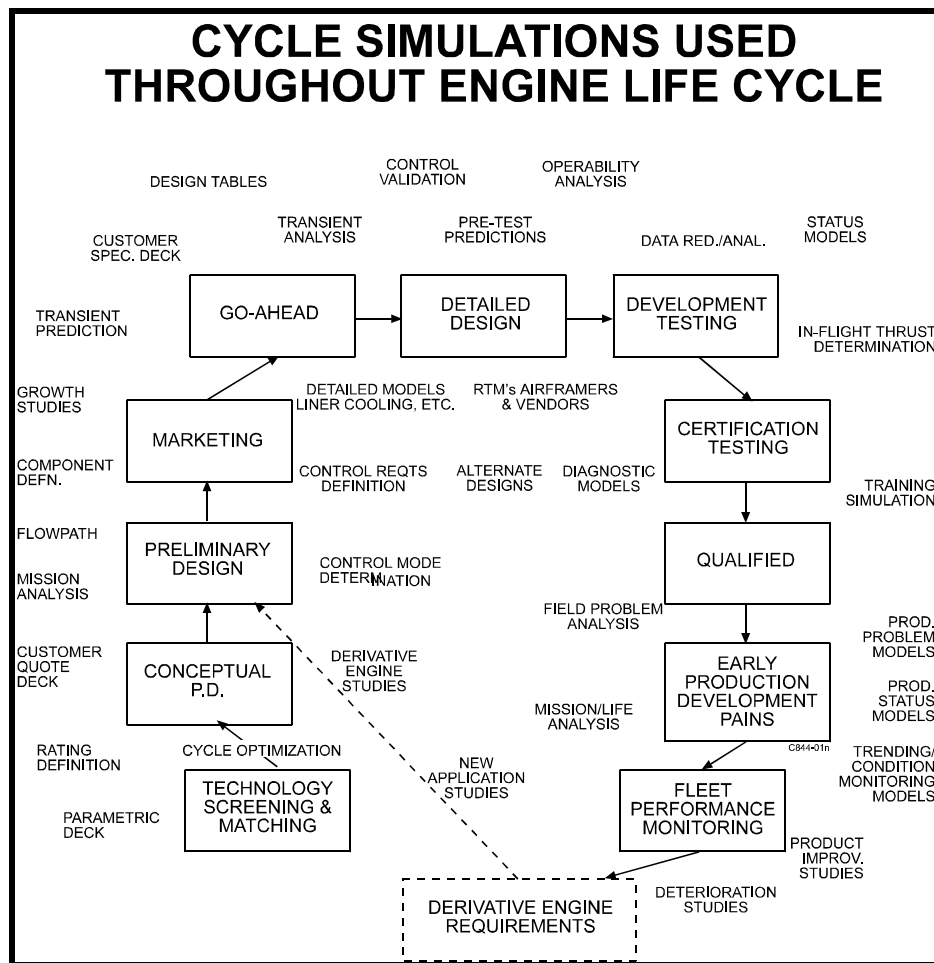


**Figure 3.39: Model Types based on Engine Life Cycle.**

Models used in the development phase are generally on the low end of the fidelity or depth of analysis spectrum, because of the uncertainty in the engine being modeled. However, for believability, these models may be required to hold very precise performance agreement with existing detailed models from which the component models are derived or will be compared. Similarly, once in production use, the primary modeling is again at the lower fidelity level but at high levels of accuracy due to large amount of data available and the need to maintain close agreement at least the overall engine performance level. The primary use of detailed models is by those involved in design improvements, failure analysis or technology development.

Although model detail tends to follow the model fidelity, the level of detail required may change with the model type shown in **Table 3.2**. A high fidelity 3-D model is often limited to just the primary flow-path while 0-D models may include each cooling flow circuit and the incremental changes in temperature and pressure in the internal cavities of the engine.

### 3.2.1.2 Minimum, Average, New and Old Engine Models

Due to production scatter and component aging, two engines of the same type, having two different usage histories, will have different performances. However, the engine manufacturer guarantees to his customer a minimum level of performance for a given Time-Between-Overhauls (TBO), or at least defines overhaul criteria that are periodically checked (as part of health monitoring).

To do this, the engine designer has to build minimum, average, new and old engine performance models. This terminology may lead to severe misunderstandings between component designers, performance engineers and customers. The key point for a good understanding of these different models, is that the only representative and accurate model that can be established by the engine manufacturer is the model for a new average engine. This is when all engine components have their average production characteristics, it is sure that the resultant engine has average performances. Conversely, the minimum performances are not necessarily obtained with an engine that has all its components at minimum level. The word *minimum* is in fact relative to an engine-level pass-off criterion (thrust, fuel consumption, TET) for global parameters and not engine components.

There are numerous combinations of component performance reductions that will cause failure of one or more of the pass-off criteria (one with highest TET, one with smallest thrust, one with maximum SFC...). A true minimum engine, at the threshold of failure for each of the criteria, will rarely if ever exist. It is better to talk of minimum *performance* model. Such models give global performance levels that any new engine will achieve. These models are obtained either by applying deltas directly to the performances of the average engine model or applying deltas to each component of the average model. The same issue arises for aged or old engine models. There is infinity of deterioration types that depend on the environment, the mission profile, and other variables that can be envisaged. Thus a general deteriorated engine model may not be possible. It may be better to talk of an *aged* performance model because such models set limits to global parameters throughout the TBO in normal operating conditions.

Although not general, deterioration models can be issued when a database of in-service engines is available. It is then possible to derive statistical deltas on either main engine parameters, or component characteristics, as a function of the number of running hours or cycles. These models are becoming more and more important because they are a basis for any diagnostic models that allow for example:

- Damage detection; and
- Engine fleet management.

A typical question is, ‘Is it better to overhaul this engine now or later?’ If the answer is now, the engine recovers its initial performance (even when not necessary for its mission, as in cold day conditions) with an economic penalty (overhaul cost). If the answer is later, the engine keeps a higher SFC and lower general performance, which can lead to a reduction in payload, range, or operating conditions, constituting an equally severe economic penalty.

### 3.2.2 General Nomenclature

The general nomenclature used in engine modeling is covered in **Aerospace Recommended Practices (ARP)** and **Aerospace Standards (AS)** published by the Society of Automotive Engineers (SAE). They have been created in a cooperative effort among the developers and users of engines to simplify the exchange of models and data. **AS755C [3.9]** defines the station definition within an engine, the application to various engine types and the nomenclature for properties and fundamental parameters. **AS681 [3.10]** provides definitions, requirements and assumptions for a class of models mostly provided by engine manufacturers to customers, often-called *customer decks*. **ARP1210 [3.11]** provides additional guidance on interface requirements for models dealing with test data, **ARP1211 [3.12]** for status models that have been matched to specific test data, **ARP1257 [3.13]** for transient models and **ARP4148 [3.14]** for real-time applications. **ARP4868 [3.15]** and **ARP4191 [3.16]** are being developed to cover the needs of newer computer systems and to define application program interface (API) standards to facilitate use with object-oriented software or in an event driven environment.

### 3.2.3 Thermodynamic and Gas Properties

Most physics based engine models make some assumptions for calculating the state properties and energy balance of the various fluid streams. These include converting typical flight conditions into the boundary conditions required by the model, and the capability required to support engine component models.

#### 3.2.3.1 Atmosphere Definitions

Most component-based propulsion system models use a standard atmosphere reference for defining operation conditions. Atmospheric properties for general use are specified in **SAE AS681F** [3.10]. The current standard atmosphere definition is **ISO 2533** [3.17]. This is generally consistent with the **U.S. Standard Atmosphere, 1976** [3.18], which was an extension of the **US Standard Atmosphere, 1966** [3.19] to higher altitudes. For non-standard atmospheric conditions the most common reference is **MIL-STD-210C** [3.20] which defines standards for extreme conditions such as arctic, desert and tropical days. Differences in air composition between these various sources is small but can be noticeable when comparing absolute properties and emissions due to the assumed percentage of CO<sub>2</sub>, as shown below:

- |                                |                     |
|--------------------------------|---------------------|
| • ISO 2533                     | 0.030%;             |
| • US Standard Atmosphere, 1976 | 0.03140 to 0.0322%; |
| • NASA TP-1906                 | 0.0319%; and        |
| • Keenan and Kayes, 1945       | 0.0000%.            |

#### 3.2.3.2 Thermo Property Packages

Multiple thermo representations may be used in a single simulation or be an integral part of component models. However, it is common to use a single separable set of routines, often called a thermodynamic property package, for the entire simulation. This is for simplicity and to ensure consistency. The package selection is typically based on the requirements of the simulation, convenience and historical reasons. **AS681** [3.10] requires that the properties be consistent with those provided in **NASA TP-1906** [3.21] and the associated computer code. The level of agreement required will depend on the application. Some considerations when selecting a package are:

- Speed;
- Accuracy over the range of operation;
- Accuracy needs of the engineering application;
- Kinetics;
- Heat transfer requiring transport properties;
- Water vapor, multi-phase water or other constituents such as solid carbon or soot;
- Non-air streams; and
- Alternate or non-hydrocarbon fuels.

The thermo property package should have no impact on the overall simulation accuracy. However, because property calculations are so pervasive in engine simulations, seemingly small speed differences can be significant. When the extra capability or range of accuracy is not required, the speed gain will often justify use of a simpler thermo package. In a typical engine simulation, the thermo property package may account for up to 30% of the execution time. Special application combinations are possible. Kinetics calculation can be based on curve fit properties, but these are normally not seen in general use property packages. **Table 3.1** contains a comparison of the various approaches and basis for selection based on the simulation requirements.

### 3.2.3.3 Gas Properties Evaluation for Steam/Water Injection

Calculations of thermodynamic processes use properties of a working medium, which is a mixture of gasses. The properties of individual mixture constituents are calculated by means of polynomial functions and the mixture properties are evaluated from its mass composition, through a relation of the form:

$$P = \sum_i X_i \cdot P_i \quad \text{Eq. 3-22}$$

P is a property of the mixture and  $X_i$ ,  $P_i$  is the mass composition and the corresponding property value for the i-element of the mixture respectively. Inlet air is handled as a mixture of gases, including steam due to ambient humidity. The composition of gases at the combustor outlet is computed on the basis of stoichiometric calculations, and depends on the composition of the fuel used. When water is injected, it is also accounted for as an additional element in the gas composition. The variation of  $c_p$  of the mixture of combustion gases and steam, for the range of temperatures of interest to gas turbine applications, is shown in **Figure 3.40**. The values have been calculated by considering the gases as a mixture of ideal gasses, and the properties of the constituents are derived by polynomial relations. The variation of isentropic exponent  $\gamma$  is also shown.

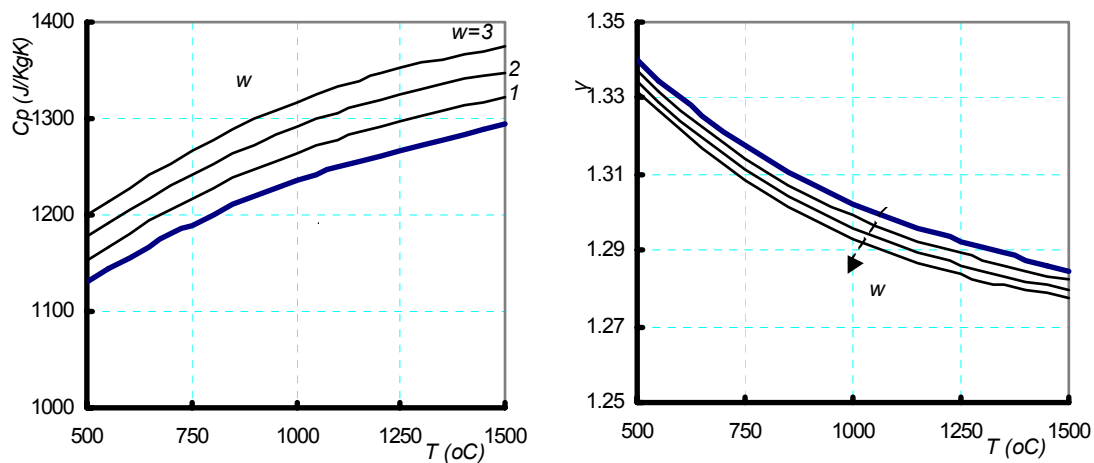


**Figure 3.40: Values of Specific Heat  $C_p$  and Isentropic Exponent  $\gamma$ , for Temperatures Usual in the Hot Section of Gas Turbines.**

Variation of gas properties for typical rates of water injection is shown in **Figure 3.41**. The changes of properties of gases after water is injected, with respect to the values with no water injected are shown.

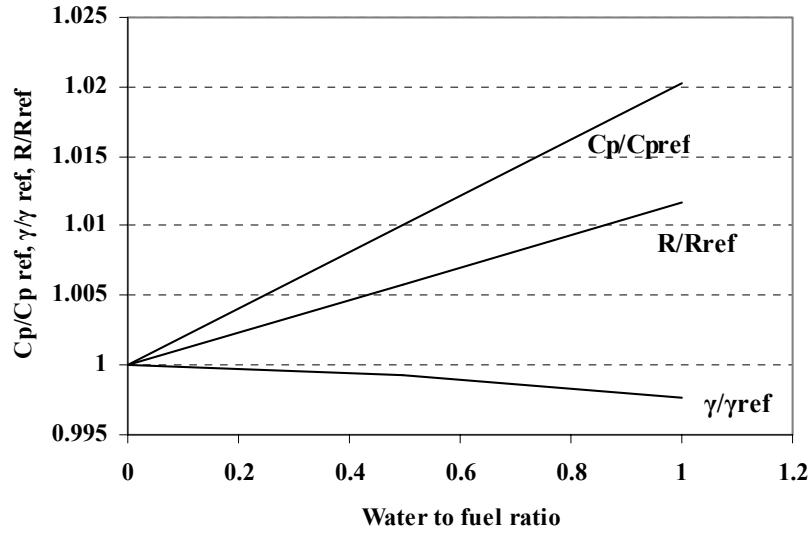


**Figure 3.41:** Change in Gas Properties for Different Amount of Injected Water ( $f = 0.02$ ).

Variation of  $C_p$  and  $\gamma$  due to the increase of water content in air can be estimated with the use of analytical relations, when the water to air ratio is small, a condition that is fulfilled in the usual gas turbine applications. Such relations have been proposed by Mathioudakis et al. [3.22 and 3.23] and express the deviation of  $C_p$  and  $\gamma$  from the dry combustion gas values in function of the water-to-air ratio  $war$ .

If property values are known for dry combustion gases, then the change of  $c_p$  because of the injection of water or steam can be evaluated by the relation:

$$\frac{\delta c_{pg}}{c_{pg}} = war \left( \frac{c_{ps}}{c_{pg}} - 1 \right) \quad \text{Eq. 3-23}$$

$C_{ps}$ : specific heat of steam,  $C_{pg}$ : specific heat of dry gas,  $\delta C_{ps}$ : change of gas specific heat, due to addition of water,  $war$  is the water to air ratio.

A similar relation can be derived for the change in the value of the gas constant  $R$ :

$$\frac{\delta R_g}{R_g} = war \left( \frac{R_s}{R_g} - 1 \right) \quad \text{Eq. 3-24}$$

The change in the isentropic exponent  $\gamma$  results from its definition and the previous expressions:

$$\frac{\delta \gamma_g}{\gamma_g} = (\gamma_g - 1) \left( \frac{\delta R_g}{R_g} - \frac{\delta c_{pg}}{c_{pg}} \right) = (\gamma_g - 1) \left( \frac{R_s}{R_g} - \frac{c_{ps}}{c_{pg}} \right) war \quad \text{Eq. 3-25}$$

Subscripts  $s$  and  $g$  denote steam and gas respectively, as in Eq. 3-23.

The above expressions can be further simplified for gas turbine combustion gases, by taking into account that the specific heat of steam is roughly double the specific heat of the combustion gases, as can be seen

from **Figure 3.42**. For the range of turbine inlet temperatures encountered in today's turbines, and representative values of fuel/air ratio,  $C_{ps}/C_{pg}$  is shown to take values very close to 2.

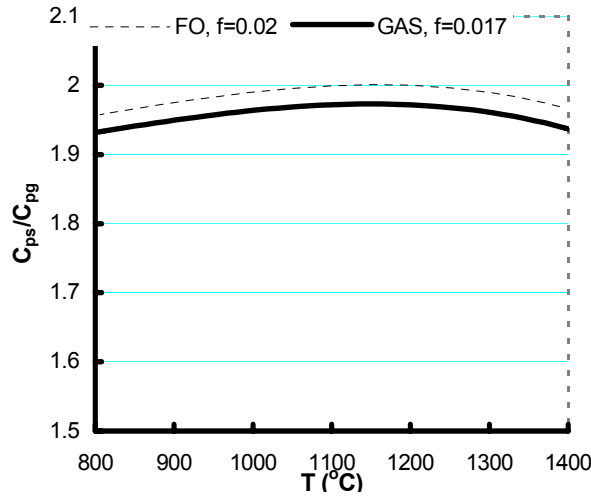


**Figure 3.42: Ratio of Specific Heats of Steam and Combustion Gases.**

By virtue of this observation, **Eq. 3-23** for  $C_p$  becomes:

$$\frac{\delta C_{pg}}{C_{pg}} \approx war \quad \text{Eq. 3-26}$$

For the gas constant  $R$ , for  $R_s = 461.5$  and  $R_g = 287$ , **Eq. 3-24** gives:

$$\frac{\delta R_g}{R_g} = 0.61war \quad \text{Eq. 3-27}$$

and for the isentropic exponent, using these relations and **Eq. 3-25**

$$\frac{\delta \gamma}{\gamma} \approx 0.33(1.61 - 2)war = -0.13war \quad \text{Eq. 3-28}$$

### 3.2.3.4 Impact of Modeling Assumptions

Besides the basic property representation, the assumptions made in applying these properties can affect the accuracy and consistency of model results. Some of the key assumptions that can change the results of simulation models are:

- Whether high temperature mixtures are assumed to be in equilibrium or frozen composition during expansion processes;
- How cooling flow mixing with the main flow is modeled; and
- Behavior with incomplete combustion products or in fuel-rich conditions.

In special circumstances, information on assumptions relative to compressibility effects, combustion product estimates, alternate fuels or operation with other fluids (water, ice, vitiated air, nitrogen diluted test stand air, etc.) may be important. When using the model for data analysis or comparison with on-line performance data generated in test facilities, the model assumptions must match those used in creating the data.

### **3.2.3.5 Aero-Thermo Process Calculations**

Independent of the thermodynamic process package, standard procedures for calculating aero-thermo processes are often used throughout a simulation and can affect the applicability of results. Reverse flow, supersonic conditions, mixer and ejector processes, swirl calculations, expansion and contraction processes are examples that may affect the range of use or accuracy of models. Models that use a thermodynamic process package may make alternate assumptions during some of these local calculations, for speed or simplicity.

### **3.2.4 Steady State Performance Models**

The gas turbine performance simulation can be sharply divided into two categories: design point analysis and off-design modeling.

The first category mainly involves the engine designer because it consists in selecting the best thermodynamic cycle in order to achieve a performance goal: delivered shaft power for helicopter engines, net thrust for airplane engines, bleed air flow at given pressure, temperature conditions for Auxiliary Power Unit (APU) starts.

This analysis is led at a *single* working point, the so called design point, which is supposed to be representative of typical customer use. The design point analysis allows optimization of the cycle and preliminary design of the engine components by:

- Selection of compressor pressure ratios and turbine inlet temperatures;
- Comparison of different engine configurations such as single spool or twin spool; and
- Varying the number and type of stages for compressors and turbines.

It is only after this analysis that a first engine geometry is defined. At this step, the engine performances are known only at design point. In order to estimate the performances under various ambient air conditions and power or thrust settings, it is necessary to create an off-design model which has the ability to describe the behavior of the engine components in conditions other than those at design point. Such modeling involves both designers and engine users (aircraft manufacturers and aircraft operators) because it is common to predict the performances during development and to define them in the whole working domain once the product definition is frozen.

It must be underlined that the importance of such off-design models has increased since the beginning of engine performance simulation. In the late sixties it was found sufficient to optimize the engine at a single working point and extensive testing permitted qualified the technologies and established the performance. But nowadays, mainly for economic reasons, an off-design model is required at a very early stage of engine design:

To match the customer specifications: it is necessary to optimize the engine within the whole working envelope and not just at one design point. For example, a turboshaft engine for a helicopter has to be optimized at both take-off rating and economical cruise power ( $\approx 50\%$  take-off) to satisfy both the maximum take-off weight, and the range requirements.

## SYSTEM MODELS

---

The meaning of the word *performance* is becoming wider and wider. It initially dealt with power or thrust and fuel consumption in steady state conditions, but the following topics are now fully part of engine performance:

- Steady state:
  - Exhaust gas emissions; and
  - Noise.
- Transient:
  - Starting time; and
  - Acceleration time.

All these types of performance have their own dimensioning points in the working domain, thus there is an increasing need for global optimization of the engine performances that implies extensive use of off-design modeling.

To reduce testing costs, many tests have been replaced by theoretical analysis in fields such as mechanics, and engine control. These analyses need off-design results as input data.

To reduce development cycles, it is necessary to design all aspects of the engine in parallel. This means that all specialists in aerodynamics, mechanics, control, and external equipment have to be provided with accurate data before the engine has any material existence, and even before the passage of components to partial test bench. The only theoretical source for these data is an off-design model.

For all these reasons, an accurate off-design model is at the heart of the engine design process and becomes increasingly critical.

### 3.2.4.1 Different Types of Off-Design Steady State Models

All off-design models aim at computing the fluid state in different locations of the mainstream in the engine, from these results, mainly W, T, P, it is possible to derive powers, thrusts, fuel consumption's and all characteristic parameters of the components.

The off-design models can be split into different categories according to the level of discretization of space. Historically, the first models belong to the 0-D category because the *averaged* fluid characteristics are computed at discrete positions inside the engine, generally at the inlet and the outlet of each component such as compressor, combustion chamber, turbine, and exhaust nozzle.

The next generation of model is the 1-D type (see *Annex A* for a detailed description of 1-D models) and introduces continuity in the computation: the fluid characteristics are still averaged in each plane, where plane means a fluid section perpendicular to the engine axis. They are computed quasi-continuously, limited by the space discretization step, along a mean line representing the average trajectory of the fluid inside the engine.

2-D and 3-D models extend this description by discretizing the whole flow path inside the engine, and not just the mean line of 1-D models. 2-D models consider there is symmetry of revolution for the stream, while 3-D models make no simplification and use the complete equations of conservation (see *Annex A* for detailed descriptions of 2 and 3-D models).

### 3.2.4.2 0-D Models

The goal of this Section is to describe the 0-D models, which are the simplest and most widely used in the industry, by analyzing the assumptions, the phenomenon modeling, the computation methods and the

limitations of such models. These models are the most widely spread in the world of turbo-machinery for many reasons:

- Historically, they were the first kind of performance model that was used.
- They do not require a detailed description of the engine geometry. Thus they can be used very early in the engine development.
- The engine description is simple and close to reality by considering it as a set of black boxes, one for each major component of the engine.
- The calculation methods are simple because the number of unknowns needed by the modeling is reduced, the goal being to compute the fluid characteristics only at the interfaces of the black boxes. The number of unknowns has the same order of magnitude as the number of individual components considered as black boxes.
- The calculation methods are natural because the fluid characteristics are computed plane by plane, or station by station, in the same order as the one used by the fluid to pass through the engine. The calculation begins at the air inlet, continues with the compressors, the combustion chamber, the turbines, and ends with the exhaust.
- Thanks to the simplicity of 0-D models, they can be run on all computer types, from the small portable PC to the workstation or the main frame. This is a very useful feature of 0-D models, because of the wide range of people who can have to run engine performance models. Such models constitute a common tool for the designer, the integrator, the customer; and the engine designer. As the main model provider, the engine designer finds issuing customer decks, based on the same approach as the one he uses for development, very convenient. This results in time and cost savings and quality gains.

First, we will analyze the steady state models which were the first developed, and which allow simulation of the engine in steady state operation, that is to say, in non time-dependent working conditions.

We will then show how to derive a transient model from the steady state one. Steady state and transient modeling are fully linked but transient modeling raises specific problems, in taking into account the physical transient phenomena. Nevertheless, the performance programs used today by designers generally allow both types of computation. Those issued for external use, engine computer decks for example, are following the same tendency albeit with some delay, as proved in AS 681 revision F aerospace standard which unifies the presentation of computer programs for both steady state and transient operation.

#### *3.2.4.2.1 General Technique*

The general technique for obtaining a 0-D solution is illustrated below by way of a simple single-spool turbojet example. The calculations employ iteration; the global iteration approach is described. The calculations can be broken into the modules described earlier in the chapter. Consider an engine represented as follows:

##### ***Compressor***

Pressure Ratio, Efficiency, Non-dimensional Flow =  $f(N\sqrt{T}, \beta)$

##### ***Combustion***

$T_4 = f(T_3, FAR, W_4)$  pressure loss =  $f(W\sqrt{T/P_3})$

##### ***Turbine***

$W\sqrt{T/P_4}$  &  $Eff_y = f(\Delta H/T, N\sqrt{T_4})$

### *Nozzle*

Entry  $W\sqrt{T}/P = f(P7/PAMB)$

### *Boundary Conditions*

Required Power Level, Altitude (ALT), Flight Mach No (XM)

(Where Req. Power Level may be expressed in terms of any engine parameter, e.g. thrust.)

A 3x3 multi-variable iterative scheme can be set up to generate steady-state performance given a specified power level. Advanced cycle match models may have very detailed matching schemes for steady-state synthesis – perhaps in excess of 30x30. For steady-state test analysis, the matching scheme can be further extended to vary model assumptions (e.g. efficiencies) to match synthesized data to measured data (see section on Model Calibration, [Section 3.2.7.3](#) or [Section 3.3.2.6.4.2](#)).

The cycle-match approach steps through the engine, front-to-back, producing flow conditions at each station. Where a parameter is not known, it is set up as an iteration variable. At the end each pass through the engine calculations, the variables are re-estimated to achieve ‘targets’ or ‘matching quantities’. Once the matching quantities are satisfied within a prescribed tolerance, the process ends.

#### *3.2.4.2.2 Steady-State Solution*

The steady state solution using the 0-D simulation technique can be obtained by the following algorithm:

- 1) Estimate values for iterative variables:
  - $N\sqrt{T}$  (compressor aerodynamic speed);
  - $\beta$  (a mapping parameter similar to outlet flow-function which allows cartesian look-up of compressor performance. The lines of constant  $\beta$  on a compressor map are arbitrary and have no thermodynamic sense. They can be derived to give optimum iterative reliability; the gradients of dependent parameters should be smooth functions of  $\beta$ ); and
  - FAR (fuel-air-ratio).
- 2) Determine inlet and ambient conditions (e.g. from Altitude and Aircraft Mach number).
- 3) Perform compressor calcs (use guessed values of  $N\sqrt{T}$  and  $\beta$ ) ... hence compressor outlet conditions.
- 4) Perform combustor calcs (use guessed values of FAR) ... hence combustor outlet conditions.
- 5) Perform turbine calcs (in steady-state, there is no excess power on the shaft so equate compressor and turbine power):
  - $W C_p \Delta T_{\text{compressor}} = W C_p \Delta T_{\text{turbine}}$ ;
  - $C_p$  is function of gas properties (known)... hence turbine  $\Delta T$ ; and
  - Read turbine chic for  $W\sqrt{T}/P4_{\text{chic}}$  and efficiency =  $f(N\sqrt{T}, \Delta H/T)$  ... hence turbine exit conditions.
- 6) Perform nozzle calcs.
- 7) Check matching conditions are within tolerance:
  - Calculated power-level = required power-level;

- $W\sqrt{T}/P4$  calculated =  $W\sqrt{T}/P4_{\text{turbine}}$  (from turbine characteristic);
- $W\sqrt{T}/P5$  calculated =  $W\sqrt{T}/P5_{\text{nozzle}}$  (from nozzle characteristic); and
- ... if not, re-run calculations above using re-estimated variables.

The process of re-estimation of variables can be complex. Various techniques can be used; the Newton-Raphson method is common. Rapid convergence can be achieved especially if guess-maps of start values are used (guess maps can generate good initial values as a function of flight case). See the section on Iterative Techniques, **Section 3.2.6**. Once a matched condition is achieved, other quantities can be derived such as thrust and surge-margin.

#### 3.2.4.2.3 *Increasing Cycle Complexity*

The principle outlined above can be easily extended to cover any engine architecture to whatever level of complexity is required. The components and thermodynamic processes are represented by characteristics, and where an independent variable is not known at any point through the engine it is set up as an iterative variable. For every extra variable there has to be a corresponding extra matching condition. Two examples of a more complex cycle are given below:

##### **Two Spool Mixed Turbofan**

The extra variables are:

- Fan outer  $\beta$  (the fan is split into 2 parts – one serving the bypass duct; one serving the core); and
- Bypass ratio.

The extra matching constraints are:

- $W\sqrt{T}/P45$  calculated =  $W\sqrt{T}/P45_{\text{turbine}}$  (from LP turbine characteristic); and
- $PS16 = PS6$  (mixer static pressure balance).

More complex representation of the same engine architecture would typically include matching pairs involved with the modeling of re-circulating bleeds, intakes, afterburning, etc.

##### **Addition of Free Power Turbine (Turboshaft Engine)**

In this case we are extracting the energy out of the gas stream leaving the (HP) turbine, and replacing the final nozzle constraint with a match to ambient pressure. The extra variables are:

- Delivered power; and
- Power turbine (PT) speed.

The extra matching constraints are:

- $W\sqrt{T}/P44$  calculated =  $W\sqrt{T}/P44_{\text{turbine}}$  (from power turbine characteristic); and
- Specified operating constraint on power turbine, e.g. turbine speed or power.

(Note: both of these are set up as iterative variables so this matching constraint could be fed into the model directly, however in the interests of flexibility the more general approach can be taken.)

The nozzle matching constraint is replaced with:

- Static pressure leaving power turbine = ambient static pressure (given).

## SYSTEM MODELS

---

The sequence of calculation is the same as in **Section 3.2.4.2.2** above, until item 6. This then becomes:

### (6) Perform Power Turbine Calcs:

W, P, T at entry (station 44) are known and so calculate power turbine exit (station 5) W, P and T

W5 = W44 (in the absence of any secondary air-system)

T5 = T44 -  $\Delta T$

where  $\Delta T$  is derived from the guessed power (i.e.  $PW/C_p.W$ ) and efficiency ( $= f(\Delta H/T, N/\sqrt{T})$ )

P5 follows from the general adiabatic relationship of Pressure ratio and Temperature ratio

### (7) Check Matching Conditions are Within Tolerance

There are now 5 matching conditions:

- Calculated core condition = required core condition (e.g. fuel flow from FAR variable = specified value);
- $W\sqrt{T}/P4$  calculated =  $W\sqrt{T}/P4_{HP}$  turbine (from HP turbine characteristic);
- $W\sqrt{T}/P44$  calculated =  $W\sqrt{T}/P4_{power}$  turbine (from PT characteristic);
- PS5 = PAMB (environmental condition); and
- Calculated PT condition = required PT condition (e.g. power from variable = specified value).

(See section above for comment on re-estimating variable for convergence.)

The choice of specified parameters will vary depending on how the model is being used:

For example, if a model is being used to generate a series of steady-state cases to form an SFC curve for a technical brochure, then running the model to Power and PT speed is most convenient (fuel flow come out ‘in the wash’ in this case). If the model is being used to model a transient maneuver (in which case the iterative scheme will need to be further expanded – see **Section 3.2.5**) then running the model to a specified fuel flow and specified power may be most appropriate. In this case, the PT speed comes out ‘in the wash’.

Beware: some combinations of driving constraints can result in a model finding multiple solutions. This is best illustrated in terms of the operating point on the PT map (see **Figure 3.43**): unless speed (y axis) and power (x axis) are specified together, there is some potential to find two feasible operating points at a common power but at a different efficiency (and hence operating speed).

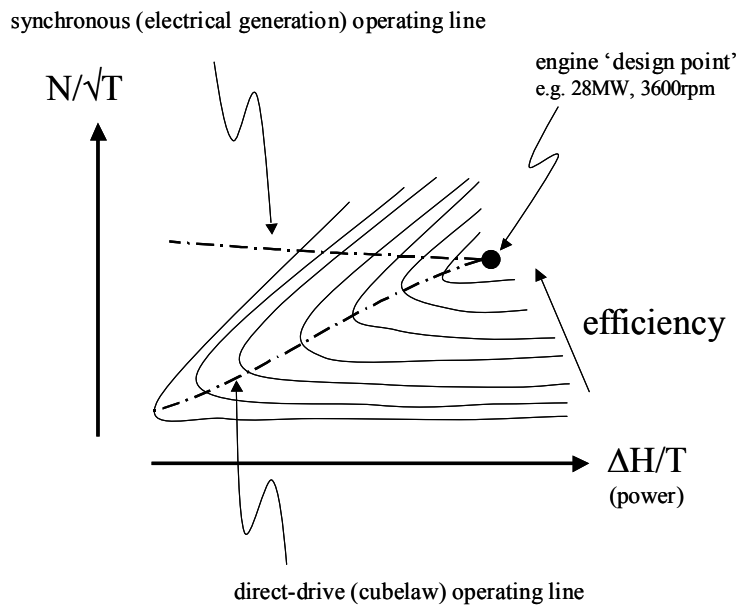


**Figure 3.43: Indicative Aero-derivative Power Turbine Characteristic.**

Another problem may arise when using power turbine characteristics looked up with  $\Delta H/T$  and  $N/\sqrt{T}$  (as above) in that turbine exit pressure may be calculated during iteration as sub-ambient. Numerically, this is of no consequence, but some thermodynamic routines may need safeguarding against this.

### 3.2.5 Transient Performance Models

This 3x3 matching scheme is easily extended for a simulation which models the dynamics associated with the shaft. In this case, required power-level must be specified as a function of time. For example WFE might be a ramp function against time.

We now have an extra descriptor of engine behavior, this time a dynamic equation that describes the behavior of a state-variable in the time domain:

$$\frac{dN}{dt} = \frac{\Delta PW}{J \cdot N} \quad \text{Eq. 3-29}$$

where:

- $\Delta PW$  is the excess power on the shaft (turbine power – compressor power);
- $dN/dt$  is shaft acceleration (state derivative);
- $J$  is moment of inertia of the shaft (constant); and
- $N$  is shaft speed (state variable).

This is the rotational form of  $F = ma$  and concerns the conservation of angular momentum.

The engine calculation process is largely unchanged. The difference lies in the treatment of shaft speed. Numerical integration is required to obtain the speed at each timestep. There are several methods of numerical integration, in the interests of clarity; Euler's explicit method is used in this example.

### 3.2.5.1 Solution by Explicit Euler Integration

Euler's explicit integration method is:

$$x(t + \Delta t) = x_t + \left. \frac{dx}{dt} \right|_t \cdot \Delta t$$

Eq. 3-30

or for our example:

$$N_{next} = N_{now} + \left. \frac{dN}{dt} \right|_{now} \cdot \Delta t$$

Eq. 3-31

where  $\Delta t$  is the chosen timestep.

Explicit methods are inherently unstable as they involve the prediction of the state variable at the next timestep based on conditions at the current timestep, however judicious selection of timestep can reduce/eliminate problems.

In our example there is now an extra matching pair:

- **Variable:** excess power on shaft; and
- **Matching Condition:** mechanical shaft speed = mechanical speed predicted from last case.

So for *time* = *t*, the calculation process can proceed as for the steady-state case, except that turbine power is now (compressor power + excess power). When the point is matched (matching conditions satisfied), the dynamic equation is used to calculate  $dN/dT$  ... hence *N* for next timestep can be calculated using Euler's equation.

Although *N* is fixed for a particular timestep (having been predicted from previous timestep), the  $N\sqrt{T}$  variable can be retained for consistency with the steady-state matching scheme. The iterative solver should not be troubled. Alternatively this variable and the speed matching condition can be extracted from the matching scheme.

The transient solution is started with a steady-state point, the first transient point (time =  $0 + \Delta t$ ) solves at the steady-state value of *N* (as excess power was, by definition, zero at  $t = 0$  hence  $dN/dt$  was also zero).

### 3.2.5.2 Solution by Implicit Euler Integration

A more stable approach can be taken which, instead of predicting forwards, looks back over the previous timestep. The implicit form of Euler's method is:

$$x(t + \Delta t) = x_t + \left. \frac{dx}{dt} \right|_{t+\Delta t} \cdot \Delta t$$

Eq. 3-32

Which can be re-written in the more useful form:

$$x_t = x(t - \Delta t) + \left. \frac{dx}{dt} \right|_t \cdot \Delta t$$

**Eq. 3-33**

or for our example:

$$N_{now} = N_{last} + \left. \frac{dN}{dt} \right|_{now} \cdot \Delta t$$

**Eq. 3-34**

At any particular timestep, the speed at time =  $t - \Delta t$  is known and Euler's equation can be solved if the current speed and acceleration ( $\dot{N}$ ) can be determined. If the speed is an iteration variable, then state-derivative can be obtained by looking backwards (rearranging implicit Euler equation):

$$\left. \frac{dx}{dt} \right|_t = \frac{x_t - x(t - \Delta t)}{\Delta t}$$

**Eq. 3-35**

The iterative/implicit approach requires the matching condition to be:

State-derivative from dynamic equation = state-derivative from Euler's implicit equation:

$$\frac{N_{now} - N_{last}}{\Delta t} = \frac{\Delta PW}{J \cdot N_{now}}$$

**Eq. 3-36**

In the interests of iterative convergence, this is best rearranged with the excess power expressed in its constituent terms:

$$\frac{J \cdot N_{now}}{\Delta t} + \frac{PW_c}{N_{now}} = \frac{J \cdot N_{last}}{\Delta t} + \frac{PW_t}{N_{now}}$$

**Eq. 3-37**

Where  $PW_c$  is the total power requirement (i.e. includes compressor power, losses and off-takes) and  $PW_t$  is the turbine power.

The bandwidth of a dynamic model, which only contains the shaft dynamic equation, has a bandwidth of around 5 Hz. For wider bandwidth, other dynamic events must be modeled. Better representation in the higher frequency ranges requires the modeling of gas dynamics (the behavior of the air in each area of the engine). For better representation in the lower frequency range, heat soakage (the transfer of heat to and from the blades and carcass) must be modeled. Gas dynamics are fast events and numerical stability of the integration method is a significant issue. The implicit approach described above is perhaps most suitable given that the cycle match process is iterative by nature. Non-iterative 0-D modeling techniques are more constrained to use explicit approaches and in these cases a more sophisticated integration method is required (e.g. Runge-Kutta 4th order).

### 3.2.5.3 Extension of Simple Example to Include Gas Dynamics

In the example so far, it is assumed that the gas is incompressible, that the flow into any control-volume at any instant is equal to the outlet flow. In reality, there is some storage of gas in a volume. There is

therefore an imbalance of gas properties (inlet to outlet) relative to the quasi-steady values encountered at each timestep in the example above. This imbalance implies a rate of change of properties within each volume.

The dynamic equations that describe these phenomena are listed below. The  $\Delta$  terms refer to inlet – outlet.

***Conservation of Mass***

$$\frac{d\bar{\rho}}{dt} = \frac{\Delta W}{Volume} \quad \text{Eq. 3-38}$$

***Momentum***

$$\frac{d\bar{W}}{dt} = \frac{\Delta(pA + Wv)}{Length} \quad \text{Eq. 3-39}$$

***Energy: Enthalpy Form***

$$\frac{d}{dt}(\bar{\rho H - p}) = \frac{\Delta(W.H)}{Volume} \quad \text{Eq. 3-40}$$

***Energy: Entropy Form***

$$\frac{d}{dt}(\bar{\rho s}) = \frac{\Delta(W.s)}{Volume} \quad \text{Eq. 3-41}$$

Some models may use simplified forms of these equations that assume low Mach number flow. A typical equation set is:

***Mass***

$$\frac{dP}{dt} = R.T \times \frac{\Delta W}{Volume} \quad \text{Eq. 3-42}$$

***Momentum***

$$\frac{dW}{dt} = \frac{A \times \Delta P}{Length} \quad \text{Eq. 3-43}$$

***Energy***

$$\frac{dT}{dt} = \frac{\Delta(W.T).\gamma}{M} - \frac{T.\Delta W}{M} \quad \text{Eq. 3-44}$$

$$\text{where } M = \frac{P.Volume}{R.T}$$

The state variables in the equations above refer to the average component properties although in some model implementations, the same equations are used in an ‘actuator volume’ sense. Rather than being applied to the average component properties, the gas dynamics are applied across a dummy volume at exit to the quasi-steady-state (qss) process.

Returning to the example, the engine can be broken down into several control-volumes, corresponding to each separate component or several components lumped together. For each control-volume there are now 3 more unknown quantities (variables) these are:

- $\Delta P$ : ‘stored’ pressure in volume (cons. of mass);
- $\Delta W$ : ‘stored’ flow in volume (cons. of momentum); and
- $\Delta T$ : ‘stored’ temperature in volume (cons. of energy).

For implicit integration, the matching quantities are set up in the same manner as for the shaft dynamic above. Essentially, the matching condition is the equality of the two expressions of state-derivative. As before, some algebraic re-arrangement helps iterative convergence.

#### **Conservation of Mass**

$$Volume. \frac{Pq_{SSnow}}{\Delta t. R. Tq_{SSnow}} + W_{outnow} = Volume. \frac{Pq_{SSlast}}{\Delta t. R. Tq_{SSnow}} + Wq_{SSnow} \quad \text{Eq. 3-45}$$

#### **Conservation of Momentum**

$$Length. \frac{W_{outnow}}{\Delta t} + A. P_{outnow} = Length. \frac{W_{outlast}}{\Delta t} + A. Pq_{SSnow} \quad \text{Eq. 3-46}$$

#### **Conservation of Energy**

$$\frac{M. T_{outnow}}{\Delta t} + \gamma_{outnow}. W_{outnow}. T_{outnow} + T_{outnow}. Wq_{SSnow} = \frac{M. T_{outlast}}{\Delta t} + \gamma_{qSSnow}. Wq_{SSnow}. Tq_{SSnow} + T_{outnow}. W_{outnow} \quad \text{Eq. 3-47}$$

where  $M = \frac{Pq_{SSnow}. Volume}{R. Tq_{SSnow}}$

It is not necessary to solve all 3 conservation equations for each volume. For around 10 Hz bandwidth, only the modeling of mass conservation may be necessary.

Note that if the momentum equation is solved, then a length term is introduced into the model, hence the model can be regarded as a 1-D representation.

#### **3.2.5.4 Further Extension of the Example to Include Heat Soakage**

The heat transfer between metal and gas can be highly significant. The long-term stabilization of the engine onto a temperature limit at a power level is important from an operational point of view, as is the behavior of the engine on hot re-slams or Bodie maneuvers (i.e. soaked high power → idle → high power). In the latter case, the metal is relatively hot compared to the shaft speeds. The aerodynamic speeds can therefore differ greatly from *normal* idle conditions. Compressor stability can be affected.

A cold slam (soaked idle → max power) modeled without heat-soakage effects can be misleading especially for large engines, as in addition to the aerodynamic speed shifts mentioned above, power lost to the heating up of engine parts results in a slower acceleration.

The temperature of a metal component in a gas stream is described the dynamic equation:

$$\frac{dT_m}{dt} = \frac{T_m - T_g}{k} \quad \text{Eq. 3-48}$$

where:

- $T_m$  is temperature of the metal component;
- $T_g$  is the temperature of the surrounding gas; and
- $k$  is a function of metal geometry, properties and gas conditions. These will be specific to the type of component being considered.

Returning to the example, we can model the effects of heat soakage within any control volume. These need not necessarily correspond to the volumes already defined for gas dynamics.

For a turbo-machine, it may be useful to consider the blades and carcass temperatures separately. So the extra iterative variables for each control volume are:

$T_{blade}$ : blade metal temperature

$T_{carcass}$ : carcass metal temperature

The associated matching quantities (for implicit Euler integration, rearranged as before) are:

$$T_g - \frac{(k \cdot T_{blade\_now})}{\Delta t} = T_{blade\_now} - \frac{(k \cdot T_{blade\_last})}{\Delta t} \quad \text{Eq. 3-49}$$

$$T_g - \frac{(k \cdot T_{carcass\_now})}{\Delta t} = T_{carcass\_now} - \frac{(k \cdot T_{carcass\_last})}{\Delta t} \quad \text{Eq. 3-50}$$

### 3.2.5.5 Non-Iterative Technique

The cycle match approach relies on iteration. A non-iterative technique can be applied to model engine performance, and such techniques are particularly suitable for real-time simulation where a fixed execution time is required.

The non-iterative approach is bound to using explicit integration (unless an outer iteration loop is provided), and also must use gas dynamics to obtain flow compatibility between components (this is achieved by iteration in the cycle-match technique). As a consequence of the gas-dynamics being present, the time step and integration method (the two are linked) must be chosen carefully to ensure numerical stability.

The following example is the simplest non-iterative implementation of a model for the example set out above. There are several variations on this approach. The model is laid out as shown in **Figure 3.44** below:

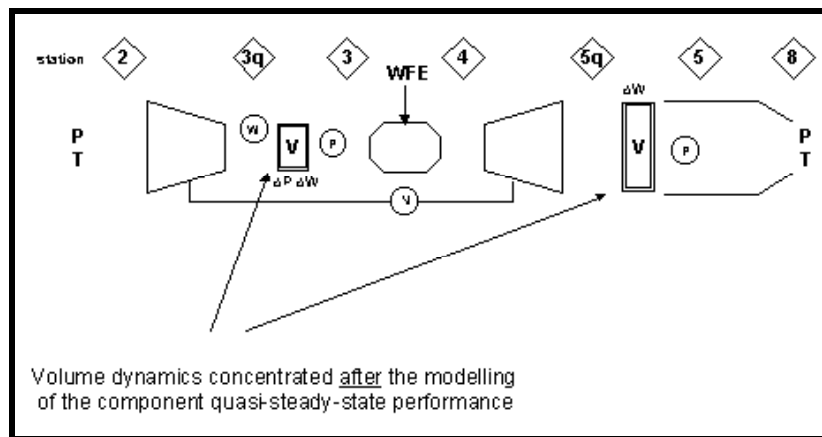


**Figure 3.44: Model of Non-Iterative Calculation Process.**

State variables:  $N$ ,  $P_3$ ,  $W_{3q}$ ,  $P_5$  (shaft dynamics, mass and momentum conservation in compressor, mass conservation in turbine – using simplified gas dynamics equations)

At time =  $t$ , the state variables are known (predicted from last case)

- 1) Perform compressor calculations:
  - The compressor must use characteristics which have been manipulated into an alternative form where pressure ratio and efficiency =  $f(W_2\sqrt{T_2}/P_3, N\sqrt{T})$ ; and
  - $W_2 = W_{3q}$  (known) ... hence  $P_{3q}$ ,  $T_{3q}$  (and  $T_3$ ), compressor power.
- 2) Perform combustor calculations:
  - Use  $W_3 = W_{4\text{last}} - W_{FE}$  now to calculate pressure loss ... hence  $P_4$ ,  $T_4$ .
- 3) Perform turbine calculations:
  - Pressure ratio is already known ( $P_{5q} = P_5$ ) ... hence  $W_4$ ,  $W_{5q}$ ,  $T_{5q}$  (and  $T_5$ ).
- 4) Perform nozzle calculations ... hence thrust, etc.
- 5) Calculate state-derivatives:
  - hence  $\Delta P$ ,  $\Delta W$  and  $\Delta PW$  now known; and
  - hence  $N$ ,  $P_3$ ,  $W_{3q}$  and  $P_5$  for next case.

Note that some calculations in this method are reliant on using values from the previous timestep (see combustor calculations above). This can force extra limitations on timestep to get sufficient accuracy and stability. Iteration avoids this problem, and is generally more flexible for performance work.

### 3.2.5.6 Iterative Real-Time Simulation

There are a number of model applications where a model must produce results in real-time. SAE AIR4548 [3.24] usefully defines a Real-Time Engine Model (RTEM) as a ‘transient computer program whose engine outputs are generated at a rate commensurate with the response of the physical system it represents’. Examples of real-time applications are:

- Embedded models for flight systems;
- Engine models within aircraft simulators; and
- Engine system integration testing.

The SAE **AIR4548** [3.24] covers the requirements of these applications in detail, and in terms of 4 criteria: *consistency*, *bandwidth*, *versatility* and *execution speed*. *Consistency* is a term used in preference to ‘accuracy’ and refers to the ability of a model to represent the *reference* source of data – whatever that reference is. *Reference* may change in various stages of the project: from the detailed performance prediction in the early stages, to engine test data later in a program. *Versatility* refers to the ability of the engine model to be refined or reworked in line with the evolving design. The model must be capable of simulating all aspects of engine behavior that the controller is capable of sensing or controlling – hence the bandwidth criteria. *Execution speed* refers to the timestep at which the simulation must run in order to produce accurate [consistent], and numerically stable results. Of course, bandwidth and timestep are linked. The advantage of cycle-match models is that if a low bandwidth is required, then the model may be stable at the large integration timesteps commensurate with the dynamics of interest, e.g. an aircraft simulator may only require outputs at 50 ms.

The prime issue at stake here, is the use of iteration in a model on which is placed strict constraints on execution time. Clearly, no specific guarantees can be made on the number of iterations to match the cycle and so a limitation has to be imposed in order to give a model that has predictable execution times. It has been shown that a model limited to as few as 2 passes is viable. Truncation of iteration in this way may lead to loss of consistency, however this discrepancy is likely to be less than the difference between the iterative model (which is taken as the reference computer definition of the engine cycle) and a separate, non-iterating real-time model.

This being so, there are also potential run-time advantages to be cashed for some model applications. A model requiring 4 passes every 50 ms uses less computing power than a non-iterative model running every 1 ms (where 1 ms may be required for stable running). The computing effort advantage amounts to a run time factor of around 10. The advantage is not so marked for applications requiring high bandwidth RTEMs. An iterative model would run 2 – 4 passes at 1 ms; a non-iterative model would typically run (1 pass) at 0.5 ms or less. The comparison in this case may not be so spectacular!

Correct handling of gas dynamics in a non-iterative model may need extremely small timesteps, perhaps 0.1 ms or less. Such a small timestep is not desirable for real-time work, a larger timestep is required. The usual way of ensuring numerical stability with a larger timestep is apply factors to selected volumes. Consequently, a larger timestep can be tolerated but at the expense of dynamic fidelity. The run time comparison for *correct* dynamics representation is still therefore in the iterative model’s favor. It must be said, however, that with the advance in computing power, run-time advantages become less of an issue; it is the benefits of commonality and versatility that come to the fore.

Why stop at real time? There is perhaps the potential to further exploit Monte-Carlo type methodology to engine and controller design where ultra-fast non-linear models could be used effectively.

### 3.2.5.7 Other Dynamic Events

There may good reason to include other dynamic terms in an engine model in order to satisfactorily replicate engine behavior, especially on analysis of gross transients such as fuel-spiking to map the compressor stall line. Fuel ignition characteristics (often modeled as pure delays) can significantly affect control stability margins. Metal growth follows on from the heat-soakage modeling described above. Turbomachinery tip clearance has a significant effect on engine performance; this behavior can also be modeled using the techniques outlined above.

### 3.2.6 Iteration and Numerical Methods

#### 3.2.6.1 Local Iterations

The example hereafter shows the loop nesting required by local iterations when that method is applied to the resolution of the compatibility equation set described in for a free turbine engine turboshaft. The algorithm is given in **Figure 3.45**. It describes four nested loops, one for each compatibility equations (the speed compatibility is directly obtained, because XNH is data) but the equations are solved one after each other.

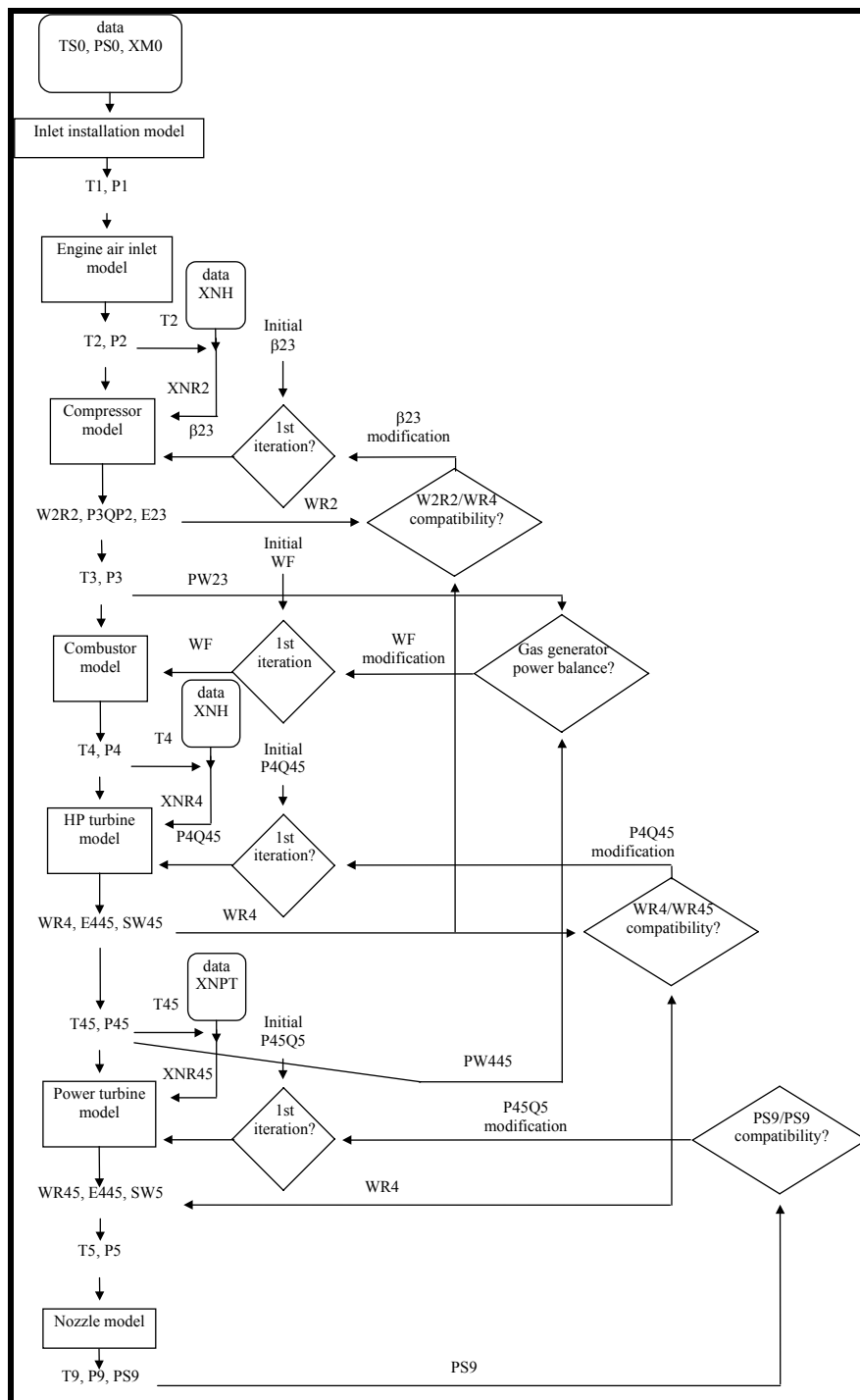


**Figure 3.45: 0-D Modeling of a Free Turbine Turboshaft Engine.**

In such a model, the calculation at given gas generator speed is privileged. In order to calculate the engine cycle at given output power, or at given HP turbine inlet temperature, etc., it is necessary to add one more loop in which XNH varies until the data parameter reaches its given value.

#### 3.2.6.1.1 *Advantages*

The local iteration method was, historically, the first one used because it is very close to the manual procedure to calculate an engine cycle. It has the following advantages:

- It is based on a very physical approach because at each step, a part of the compatibility equations are satisfied.
- It exploits all the peculiarities of the engine architecture to reduce the number of loops and to recalculate only the minimum number of components when iterating within a loop. In the turboshaft example, there is a loop iterating on P4Q45 in order to match the compatibility of flows between the HP turbine and the power turbine. Such a loop recalculates the cycle only in the turbine part and not from the air inlet. This allows timesaving, which does not now seem critical but really was at the beginning of off-design simulation.
- Solving the problem by nested loops allows the use of very simple mathematical methods to match convergence, via for example, simple gain correction, dichotomy or the 1-D Newton-Raphson method.
- Using simple methods and reducing the dimension of the problem, it was possible to run the resulting performance code on nearly any computer platforms, even with low computing resources.

#### 3.2.6.1.2 *Drawbacks*

The local iterations method is, nevertheless, being abandoned by engine manufacturers for many reasons:

- **Complexity** – The turbofan example shows that the loop nesting becomes very complex when considering multi-spool, multi-streams engines.
- **Convergence** – When numerous loops are nested, it is necessary to have high precision convergence of the internal loops so that the external loops may converge. This may reveal difficulties in the whole operating range, especially in cases where strong cross-coupling appears as in the case of mixed flow or recuperated engines.
- **Need for Decouplings** – The local iteration method can, often, be used only because the current component calculation depends only on the flow characteristics at its inlet and a reduced number of operating parameters. But, when accounting for secondary effects, like clearances or ventilation, the couplings between stations increase strongly, and it may become very difficult to find a satisfactory nested loops scheme.
- **Generality** – The local iteration method, by nature, uses all of the particularities of the engine architecture and component models. Therefore, the performance program created by this method is strictly limited to one engine type. Even for a given engine, extensive reprogramming may be necessary in case of a component modeling change. For example splitting a single compressor into two separate stages changes the size of the problem, and requires additional loops. Changing a loss model may also require reprogramming of the loops, the convergence criteria and so on. The local iteration method lacks generality and leads the engine manufacturer to have numerous performance programs to identify and maintain. Such a method is quite prohibitive for meeting actual quality requirements and prevents the designer from having a single 0-D performance code that is able to deal with various engine architectures.

Because of all these drawbacks, the local iteration method is less and less used. Global methods are increasingly used, allowing more generality and more modularity, thus avoiding the dispersion of

component models in too many programs. Furthermore, the initial computation time gains, which justified use of this method, are now less because of computer speed increases. A global method may now be run, quite instantaneously, on a portable PC.

### 3.2.6.2 Global Iterations and Multi-Dimensional Newton-Raphson

Instead of solving separately the equations, the global method is based on an iterative resolution of the whole set of equations.

The previous section, **3.2.6.1**, described how performance computation consists of identifying the values of characteristic parameters of each component. These parameters may be gathered in a vector of the unknowns, denoted  $X$  (dimension  $n$ ). The set of compatibility equations completed by the power parameters constraints, constitutes a vector denoted  $F(X)$  (dimension  $n$ ) and the performance calculation consists in solving  $F(X) = 0$ , with each line of  $F$  representing a compatibility error.

The most usual method to solve this set of equation is a multi-dimensional Newton-Raphson method:

- The first step is to initialize the unknowns. This phase may seem simple but it must be sufficiently efficient to define an initial point not too far from the real operating point, within the operating domain. This may be done by assigning constant values at the unknowns, or by using the values of the unknown parameters at the center of the maps for map modeled components, or by using an approximate tabulated working line. The successful convergence and the calculation time are dependent on the quality of this step. Let us denote  $X_0$  as the initial unknown vector.
- The second step is to apply the Newton-Raphson method. This consists of linearizing the function  $F$  around the point  $X_0$ , such that:

$$F(X) = F(X_0) + A(X - X_0), \quad \text{Eq. 3-51}$$

where  $A$  denotes the Jacobian matrix of  $F$  (dimension  $n \times n$ ). Each element  $A_{ij}$  of  $A$ , represents a correlation or influence coefficient of the  $j$ -th unknown on the error committed for the  $i$ -th equation. These  $n^2$  partial derivatives are obtained by finite difference calculation:

This matrix contains a lot of zeros, which represent all the local iterations that were exploited in the method local iteration approaches described in **Section 3.2.6.1**.

To achieve the goal, which is to have  $F(X) = 0$ , we must have:

$$\Delta X = X - X_0 = -A^{-1} F(X_0) \quad \text{Eq. 3-52}$$

By inverting the Jacobian matrix  $A$ , it is possible to calculate a variation of the unknowns  $\Delta X$  and thus to determine a new point  $X_1$ . The linearization process can then be repeated at point  $X_1$ . This procedure defines a series of values  $X_n$  that converges to the solution point  $X$  such that  $F(X) = 0$ .

The following remarks apply:

- If the Jacobian matrix is singular or ill conditioned, it means that the choice of the unknown parameters and compatibility equations is not appropriate. One of the unknowns may be not representative or an equation may be absurd, or the unknowns are not independent.
- It is often necessary to limit the variation of the unknowns at each iteration because the problem is non-linear and the solution may diverge for big variations of the unknown parameters.

The following algorithm (see **Figure 3.46**) may summarize this method. Other methods are available to solve a non-linear set of equations but Newton-Raphson is very often the most robust.

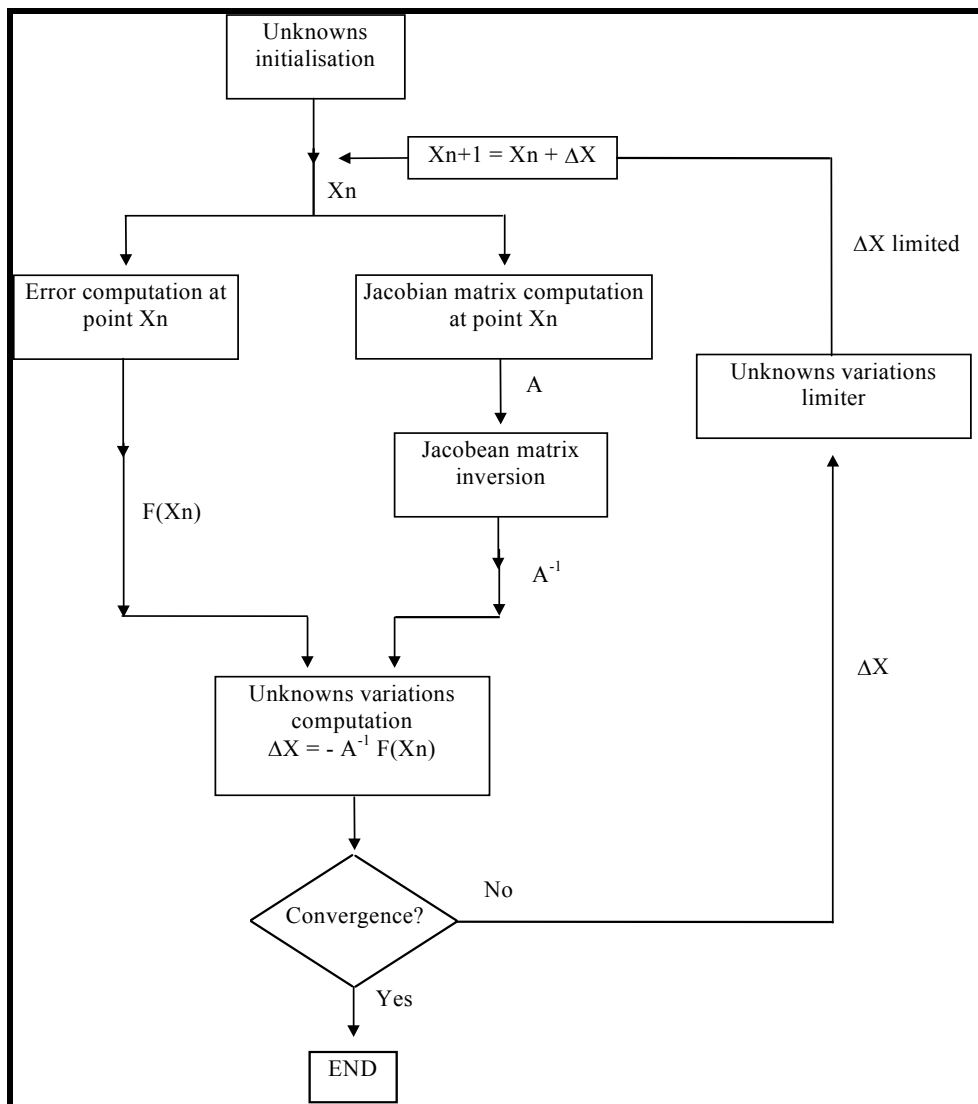


**Figure 3.46: Multi-Dimensional Newton-Raphson Iteration.**

#### 3.2.6.2.1 0-D Modeling of a Free Turbine Turboshaft Engine

The example hereafter shows an application of the global iterations method when it is applied to the resolution of the compatibility equation set described in for a free turbine engine turboshaft. Let us take the same example as in **Section 3.2.6.1**. In order to compare both methods, we will analyze the same calculation case, that is to say, taking the gas generator and power turbine real speeds as power setting parameters.

The unknown vector  $X$  is:

$$X = \begin{pmatrix} \text{XNR2} \\ \text{b23} \\ \text{WF} \\ \text{XNR4} \\ \text{P4Q5} \\ \text{XNR45} \\ \text{P45Q5} \end{pmatrix}$$

**Eq. 3-53**

The set of equations to be solved is:

Mass flow: HP compressor and HP turbine

$$\frac{WR2(XNR2,b23)P2}{\sqrt{T2}} + WF - \frac{WR4(XNR4,P4Q45)P4}{\sqrt{T4}} = 0 \quad \text{Eq. 3-54}$$

Mass flow: HP turbine and power turbine.

$$\frac{WR4(XNR4,P4Q45)P4}{\sqrt{T4}} - \frac{WR45(XNR45,P45Q5)P45}{\sqrt{T45}} = 0 \quad \text{Eq. 3-55}$$

Speed: HP compressor and HP turbine.

$$XNR2 \sqrt{T2} - XNR4 \sqrt{T4} = 0 \quad \text{Eq. 3-56}$$

Power equilibrium: gas generator spool.

$$PW23 - PW445 = 0 \quad \text{Eq. 3-57}$$

Static pressure: nozzle outlet.

$$PS9 - PS0 = 0 \quad \text{Eq. 3-58}$$

Power setting parameter 1: gas generator speed.

$$XNR4 \sqrt{T4} - XNH_{data} = 0 \quad \text{Eq. 3-59}$$

Power setting parameter 2: power turbine speed.

$$XNR45 \sqrt{T45} - XNPT_{data} = 0 \quad \text{Eq. 3-60}$$

**Figure 3.47** below shows a typical algorithm that is used to evaluate the errors.

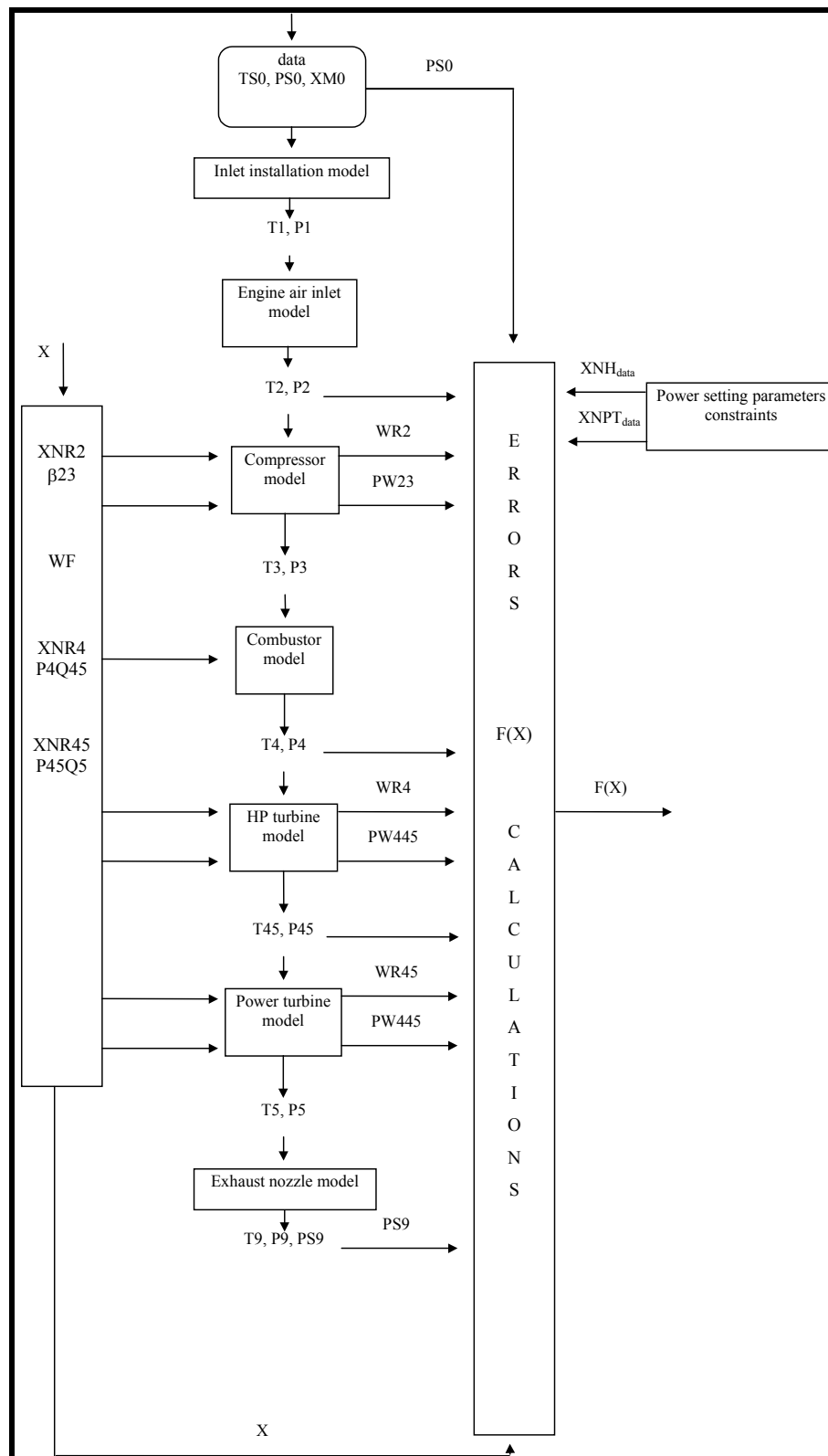


**Figure 3.47: 0-D Modeling of a Free Turbine Turboshift Engine.**

At each iteration, this algorithm is used 8 times for the following values of  $X$ :  $\beta$  ( see **Table 3.3**).

**Table 3.3: Values for Iteration**

1)	[	XNR2	$\beta_{23}$	WF	XNR4	P4Q45	XNR45	P45Q5	]
2)	[	XNR2 + dXNR2	$\beta_{23}$	WF	XNR4	P4Q45	XNR45	P45Q5	]
3)	[	XNR2	$\beta_{23} + d\beta_{23}$	WF	XNR4	P4Q45	XNR45	P45Q5	]
4)	[	XNR2	$\beta_{23}$	WF + dWF	XNR4	P4Q45	XNR45	P45Q5	]
5)	[	XNR2	$\beta_{23}$	WF	XNR4 + dXNR4	P4Q45	XNR45	P45Q5	]
6)	[	XNR2	$\beta_{23}$	WF	XNR4	P4Q45 + dP4Q45	XNR45	P45Q5	]
7)	[	XNR2	$\beta_{23}$	WF	XNR4	P4Q45	XNR45 + dXNR45	P45Q5	]
8)	[	XNR2	$\beta_{23}$	WF	XNR4	P4Q45	XNR45	P45Q5 + dP45Q5	]

The first calculation gives the error at current point  $F(X_n)$  and, combined to the following seven by finite differences, the Jacobian matrix  $A$ . It is then possible to calculate the following point  $X_{n+1}$  by applying the algorithm from the local iteration description.

#### 3.2.6.2.2 0-D Modeling of a Twin-Spool Mixed Flow Turbofan Engine

##### 3.2.6.2.2.1 Advantages

The advantages of the global method are clear when comparing the algorithms of the two method types used for the two former examples. In the global method, the cycle and components calculation is clearly separated from the mathematical resolution instead of being mixed because of numerous nested loops in the local iteration method.

Thanks to this separation, the resolution algorithm does not depend on the engine architecture under consideration. There are only small differences between the algorithms of the two former examples:

- Size and unknown types of the vector  $X$ ;
- Size and equation types of the vector  $F$ ; and
- Component calculation.

Therefore, the global method allows multi-architecture 0-D performance programs to be built easily, which was impossible with the local iterations method.

By separating component calculation and resolution, it is easier to modify the engine modeling and thus to maintain the program because the resolution part remains unchanged. This includes accounting for secondary effects.

The global method allows a simultaneous convergence of all the unknowns instead of accumulating nested loops in which only one unknown converges. This generally results in timesaving as soon as the modeled engine becomes complex or presents cross-couplings.

#### 3.2.6.2.2 Drawbacks

The global method does not have really drawbacks but its usage requires more attention.

Being based on non linear equations resolution, the global method uses more sophisticated mathematics. Thus it requires more development work than the local iterations method.

In particular, the development of the initialization step and variation limitation step requires a very careful analysis in order to ensure convergence in the whole range of computation cases (high max variation of the unknowns reduce iteration number but also stability of the method).

#### 3.2.6.3 Relaxation

Relaxation techniques use the same derivatives that are created for either local or global iteration. However, instead of solving the system at each step, the information is used to project a solution without explicitly resolving the errors. A damping factor, to reduce the sensitivity of the change in independent variables to the change in error term, drives the solution to the same result as direct iteration solution but with much less mathematical calculation. A relaxation approach is often more effective in highly non-linear regions of the simulation.

#### 3.2.6.4 Constraint Handling

The iteration schemes described above are used to satisfy continuity and the implicit nature of the simulation. They also assume the dependent and independent variables in the iteration are within the limits of the component and engine simulation. Options for constraining the iteration for these limits are to add additional iteration variables to match data or maintain other limitations.

### 3.2.7 Non-Component Based Parametric Models

These simple, fast models are used as surrogates of more complex thermodynamic models in a variety of applications that span the full range of gas turbine design, development and operation. Parametric models are employed in applications where speed is valued over accuracy or where uncertainty in the engine component characteristics or engine environmental conditions does not warrant thermodynamic model complexity. Generally, they achieve computational simplicity and speed at the expense of accuracy and resolution relative to the thermodynamic models from which they are derived. However, they typically offer equal or better accuracy than a simplified thermodynamic model of comparable speed. The formulation of parametric model always involves some form of data fitting such as polynomial functions or piece-wise linearization. In addition to speed, these models also provide a means of conveying engine performance characteristics while protecting proprietary component characteristics and modeling methodologies.

#### 3.2.7.1 Applications

Some typical applications of parametric models are discussed below. Model formulations and synthesis procedures are discussed in the following sections.

##### 3.2.7.1.1 Conceptual Design

The first parametric models were simple tabular listings or graphs of dependent versus independent performance variables. These continue in use today and in the foreseeable future in the form of multi-variate computer databases, which are used in conceptual vehicle design. The objective of the conceptual design

process is to effectively converge on an optimum vehicle design including engine system requirements for engine size, performance and operability. Detailed component requirements are defined later.

Parametric models (whatever the formulation) offer several advantages in the conceptual design process:

- Computing resource requirements are reduced for highly repetitive calculations;
- Results can be pre-certified by engine manufacturer;
- Numerical convergence issues are avoided;
- Proprietary or sensitive information can be omitted; and
- Dependent and independent variables can be transposed for inverse design.

A parametric model may be employed as a living engine specification, conveying the anticipated steady and dynamic characteristics of an engine.

#### *3.2.7.1.2 Control Design and Validation*

Parametric dynamic models have long been used in the design of control laws where linear control theory required representation of the engine dynamic behavior as a Laplace, state-space, or other linear formulation. Today, sets of these single point dynamic models are assembled with the corresponding steady-state models to provide full range transient models that are employed in the control validation process as well. These models are especially effective in the real-time validation of integrated flight/propulsion controls systems where fast execution is a requirement.

#### *3.2.7.1.3 Module Performance Analysis*

Module performance analysis (also called gas path analysis) is a process employed in fleet (on-wing) monitoring and trending to determine the health of gas turbine components and forecast operational impacts and logistics requirements. Today, statistical parameter estimation algorithms are employed to determine component performance indices that can not be computed directly from the small number of on-wing measurements. These estimation algorithms are founded in linear control theory and typically are based on state-space parametric models as described in the control application above. In deriving the estimation algorithm, the normal cause-effect relationships represented in the model are transposed mathematically into effect-cause relationships.

Module performance analysis can be applied to either steady state or transient data and can even be embedded in the real-time control.

### **3.2.7.2 Model Formulation**

A parametric model is a surrogate for a physics-based parent model and must represent the important characteristics of the parent for the intended application. In general, the physics of the parent model are represented implicitly rather than explicitly in the surrogate model. Parametric models map the complex relationships between the dependent and independent variables in the parent model into simple relationships between outputs (fluid pressures, temperatures, flows) and inputs (fuel flow, variable geometry, bleed) and internal dynamic states (rotor speeds, metal temperatures), if the model is dynamic.

The choice of input, output and state parameters is important because it determines the model accuracy and the extensibility to operating conditions beyond those where model was synthesized. The choice of parameters is commonly based on intuitive insight and experience, but can also be based on numerical analysis of parent model characteristics. Conventional gas turbine correction factors are commonly used to account for inlet conditions.

There are a variety of mathematical formulations for parametric models ranging from simple multi-variate tables for steady-state models to state-space formulations for dynamic models. In general, the state space formulation offers the greatest accuracy and flexibility and is well supported by commercially available software toolkits (XMath, MATLAB). Multiple state-space models can be assembled to cover the full engine operating range. Simple transfer function representations are a popular alternative model formulation often employed in preliminary design when engine are not well characterized. This formulation does not even require a parent model, and can be based on expected characteristics.

### **3.2.7.3 Model Synthesis Procedures**

A parametric model synthesis process can be used. In this case, the appropriate steady state and dynamic characteristics are extracted from the parent model. These characteristics may be computed using a variety of techniques such as simple mapping, factorial experiments, and system identification procedures. It is desirable to automate the synthesis procedures to reduce development time and eliminate errors. This is important because model synthesis is normally a recurring process that must be performed whenever there are substantial revisions to the parent model. The overall representation of the parametric model must be validated with the parent model. Typically, validation is performed by simply comparing the parent model with parametric model outputs for a set of input cases. Dynamic validation can be by comparing the frequency response of the parent and parametric models.

## **3.3 GAS TURBINE ENGINE PERFORMANCE ANALYSIS**

During an engine test a force, spool speeds, many pressures and temperatures at various locations along the flow-path and positions of the variable geometry (guide vanes, nozzle area) are measured. However, these values alone are of limited use without special interpretation. The task of the engine test analysis is to find the operating points of the compressors and turbines in their maps, from the measured data.

This section deals mainly with turbofans because tests of this type of engine are especially difficult to analyze. It is difficult to get a precise value for the mass flow that enters the core. This mass flow, however, is required for the calculation of the burner exit temperature, which cannot be measured directly for a variety of reasons. After a thorough test analysis the performance model can be calibrated and – if necessary – improved with newly found correlations.

### **3.3.1 Performance Instrumentation**

For a dedicated engine performance test to check the specific fuel consumption, it is not sufficient to analyze only the thrust and fuel flow. The engine inlet conditions in terms of total pressure and temperature are also needed. A precise value for the mass flow entering the engine is very important. The measured force must also be corrected for testbed specific effects, like cradle drag, to finally obtain the thrust.

Between and downstream of the compressors there must be a sufficient number of total pressure and temperature probes. In the hot part of the engine the total pressure measurements at the inlet and at the exit of the low-pressure turbine are very important. The total temperature rakes at these locations are of limited use for engine performance analysis. There are severe temperature gradients both radially and circumferentially making it extremely difficult to get a representative mean value for the total temperature of the main gas stream.

### **3.3.2 Model Validation and Calibration**

A conventional engine test analysis is quite simple and straightforward. The power required to drive the fan is calculated from the engine mass flow and the total temperature increase. The fan efficiency for the

core and the bypass stream can be found from total pressure and temperature measurements. Similarly the efficiency of the high-pressure compressor is derived.

The power required to drive the core compressor cannot be calculated without knowing the core mass flow. There are many methods to determine this flow, and the associated by-pass ratio. However, two of them are used frequently: the *turbine flow capacity* method and the *heat balance*. The indices in the formulas below refer to the station designation in **Figure 3.48**.

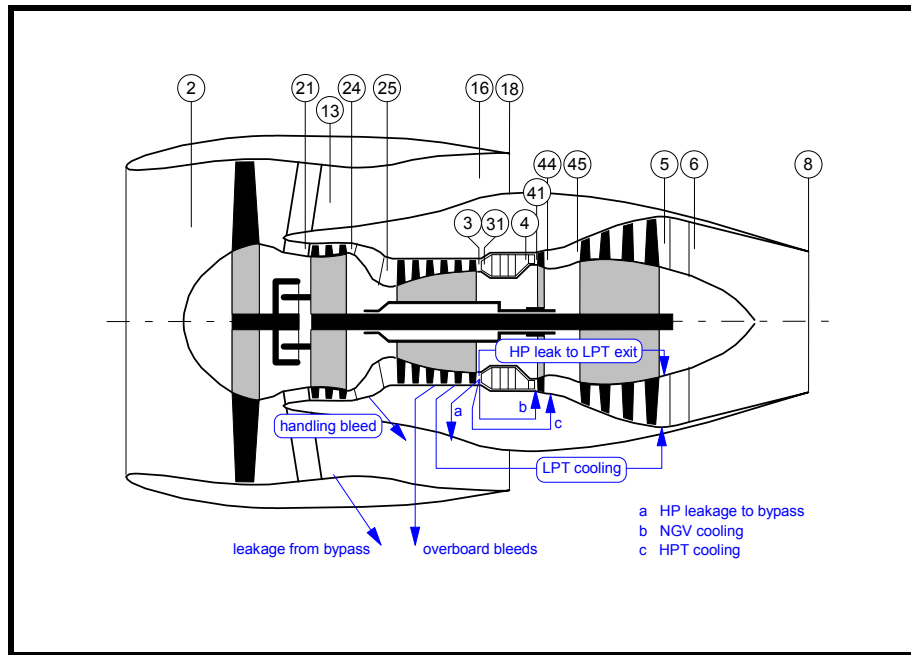


**Figure 3.48: Turbofan Station Designation.**

### 3.3.2.1 Turbine Flow Capacity

The basis of the *turbine flow capacity* method is that in the nozzle guide vane of the high pressure turbine, the flow in the throat is usually sonic or very near to sonic. For sonic flow the quantity  $W\sqrt{T}/(A^*P)$  is a function of the gas constant and the isentropic exponent only. Since we know the gas properties we only need to measure the turbine throat area to evaluate  $W\sqrt{T}/P$ . This term is the *turbine flow capacity* which gives the method its name.

When the fuel is a hydrocarbon with the hydrogen carbon ratio of kerosene the gas constant of the combustion products will be practically the same as that of air. Typically the isentropic exponent of the gas in a turbine is around 1.3 while that of air at room temperature is 1.4. This difference in the isentropic exponent has approximately the opposite effect on  $W\sqrt{T}/(A^*P)$  as the difference in temperature has on the throat size due to the thermal expansion of the metal. Therefore the term  $W\sqrt{T}/P$  is practically constant for all engine operating conditions with near sonic flow in the high-pressure turbine throat.

To make use of the known value for  $W_{41}\sqrt{T_{41}}/P_{41}$  we need some further correlations. The total pressure at the turbine throat  $P_{41}$  is calculated from the measured compressor exit pressure  $P_3$  and the burner loss characteristic.

From the fuel flow  $W_F$ , the fuel heating value FHV and the measured burner inlet temperature  $T_3$ , the turbine throat temperature  $T_{41}$  can be found:

$$T_{41} = T_3 + f(\text{far}, FHV) \quad \text{Eq. 3-61}$$

Note that for the fuel-air-ratio,  $FAR = W_F/(W_{41}-W_F)$  and for the calculation of the gas mass flow  $W_{41}$  one needs to know the secondary air system:

$$W_{41} = W_{25} - W_{\text{sec}} + W_F \quad \text{Eq. 3-62}$$

During the first pass through the test analysis computer program the core inlet mass flow  $W_{25}$  is a guess and later modified in such a way, that  $W_{41} \cdot \sqrt{T_{41}/P_{41}}$  has the prescribed value.

When  $W_{25}$  and the inter-stage bleed flows are known then the power to drive the core compressor can be determined. After taking into account gearbox drag, power off-take from the high-pressure spool and the cooling and leakage air mass flow, the work done by the turbine can be calculated. We get the ideal work from  $P_{41}$  (as calculated above) and the measured total pressure  $P_{45}$ . Turbine efficiency can be evaluated with this information.

Besides the efficiency we get a calculated value for the high-pressure turbine exit temperature  $T_{45}$ . The power balance for the low-pressure spool allows calculation of the low-pressure turbine exit temperature  $T_5$ . These two temperatures will not be identical to the measured data  $T_{45m}$  and  $T_{5m}$ . Actually, the measured hot end temperatures are ignored when doing a *turbine capacity* core flow analysis.

### 3.3.2.2 Heat Balance

The *heat balance* method is based on a measured hot end temperature and ignores the eventually known turbine capacity. This method makes sense when  $T_{45}$  or  $T_5$  is measured with many rakes. On rare occasions a rotating rake is used downstream of the low-pressure turbine which allows calibration of the standard instrumentation with only a few rakes for  $T_5$ .

Similarly to the turbine capacity method, the core-flow analysis starts with an estimated value for  $W_{25}$ . The high-pressure turbine inlet temperature  $T_{41}$  is found with the same assumptions as described above. The energy balances for the high and the low-pressure spool will yield  $T_{45}$  and  $T_5$ . The estimated value for  $W_{25}$  is modified, in such a way that after convergence the calculated value for either  $T_{45}$  or  $T_5$  equals the measured value.

### 3.3.2.3 ISA Corrections

During a normal engine test at a standard sea level testbed, for example, both the inlet pressure and the inlet temperature will deviate from ISA sea level standard conditions ( $T = 288.15 \text{ K}$ ,  $P = 101.325 \text{ kPa}$ ). The test results must be corrected to these engine inlet conditions to make the data comparable. This is often done on the basis of the Mach number similarity.

The operating conditions of a turbomachine are similar when the Mach numbers are the same everywhere in the flow-field. For a fluid with known properties of isentropic exponent and gas constant, this is the case when the corrected flow  $W\sqrt{T}/P$  and the pressure ratio are the same. Also the temperature ratios and the corrected spool speed  $N/\sqrt{T}$  will be identical for strictly similar flow-fields. Note that the variable geometry settings (guide vanes, nozzle area, bleed valve positions) must remain unchanged during any data correction on the basis of the Mach number similarity.

It can be easily shown that when the Mach numbers are the same, the terms  $F_N/P_0$  (corrected thrust) and  $SFC/\sqrt{T_0}$  (corrected specific fuel consumption) will also be the same.

With the help of these and other simple correction formulas for flow, pressures, temperatures, spool speeds, thrust, power off-take and SFC one can easily derive all engine data for a standard day.

The correction procedure on the basis of the Mach number similarity is not very accurate because the formulas are strictly valid only when: the gas properties do not change, thermal expansion of the engine has no effect on tip clearance, and Reynolds number effects do not exist. The quality of the correction procedure can be improved empirically by slight modifications of the original formulas:

$$\frac{F_N}{P_0} = F_N * P_0^{-1} \Rightarrow F_N * P_0^{-x} \quad \text{Eq. 3-63}$$

The exponent  $x$  in this formula is adjusted empirically to give the best fit to measured or calculated data. The same approach can be used with other quantities like SFC. For example:

$$\frac{SFC}{\sqrt{T_0}} = SFC * T_0^{-0,5} \Rightarrow SFC * T_0^{-y} \quad \text{Eq. 3-64}$$

After having corrected all measured data from several engine tests one has a sound basis for the calibration of the engine performance model. Engineering judgment, experience, patience and many trials are necessary to get a good match of the model to the data.

#### 3.3.2.4 Accuracy

Engine tests are performed to evaluate the overall characteristics in terms of thrust and specific fuel consumption. However, especially during the development phase, the main purpose of performance testing is to find the efficiency of the engine components and to prove that the design assumptions were valid. For such an analysis one needs to know the total pressure and temperature at all component interfaces as well as the mass flows.

Any measurement (as for example a temperature probe on a rake between two components) has an uncertainty that is affected by both random and systematic measurement errors. When it is repeated several times, the instrument readings will not agree exactly but will show some scatter.

In gas turbine engine tests random effects in the measurement chain are caused by this scatter, and also by small changes in engine geometry and operating conditions. An engine is never running in absolute stability because of small changes such as inlet flow conditions, variable geometry settings, and thermal expansion of casings and disks.

In a carefully controlled engine performance test the random errors mentioned above are not negligible, but smaller than the systematic errors caused, for example, by non-ideal positioning of the probes. There is seldom space in an engine to put enough pressure and temperature pickups at the component interface plane. Besides that, instrumentation intrusion effects must be minimized.

Every effort is made to correct the measurements for all known effects. However, an uncertainty remains.

The difference between the measurement (after applying all known corrections) and the true mean value is called a bias. There are no exact data available to calculate the magnitude of a bias and therefore it is usually estimated from experience with component rigs, for example.

### 3.3.2.5 Example: Low Pressure Turbine Efficiency Analysis

The efficiency of a low-pressure turbine (LPT) is:

$$\eta = \frac{\Delta H_{actual}}{\Delta H_{ideal}} \approx \frac{1 - \frac{T_5}{T_{45}}}{1 - \left( \frac{P_5}{P_{45}} \right)^{\frac{\gamma}{\gamma-1}}} \quad \text{Eq. 3-65}$$

where  $\gamma$  is the mean isentropic exponent of the gas.

The total pressures  $P_{45}$  and  $P_5$  must be measured with several rakes and many leading-edge probes. These measurements must be looked at in much detail. Rakes, for example, will modify the flow-field in such a way, that they increase the local pressure slightly. This must be corrected by rake position correction factors.

Further corrections to the measured values are necessary, when it is known that the rakes do not pick up a representative mean value for the relevant thermodynamic station. For example, rakes positioned in an interduct will not see the wall losses caused by the struts and thus may indicate the total pressure upstream of the interduct even when the pickups are positioned towards the end of the duct.

Also the total temperatures around the low-pressure turbine are not easy to measure. One of the total temperatures (either  $T_{45}$  or  $T_5$ ) is a direct result of the core flow analysis, which yields  $W_{45}$ . Since the total temperature measurements in the hot part of the engine are due to the severe circumferential and radial profiles, and not very accurate it is better, to derive the specific work-done from elsewhere. The work-done,  $\Delta H_{LPT}$  is proportional to the total temperature difference  $T_{45}-T_5$  from measurements in the cold part of the engine. The energy balance yields

$$\Delta H_{LPT} = \frac{W_2}{W_{45}} \Delta H_{Fan} + \frac{W_{21}}{W_{45}} \Delta H_{Booster} . \quad \text{Eq. 3-66}$$

Any error in the analysis result for the engine inlet mass flow  $W_2$  will have an impact on the LPT efficiency result.

Getting a precise value for the specific fan work  $\Delta H_{Fan}$  is very difficult for high bypass engines. It must be derived from the total temperature measurements upstream and downstream of the fan. **Figure 3.49** shows in the left part the typical temperature rise in the fan as a function of bypass ratio. In the right part one can see that a measurement error of 1 °C will cause an error in specific fan work of 1% for engines with bypass ratio of 4 and nearly 3% for very high bypass engines.

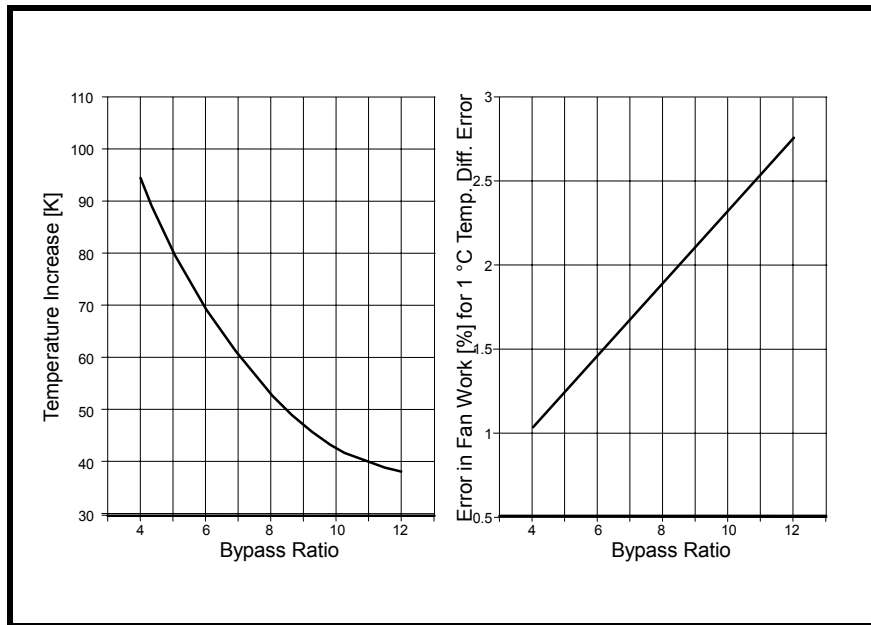


**Figure 3.49: Effect of Fan Temperature Measurement Accuracy.**

An analysis error of 1% in fan work is totally unacceptable. Therefore the temperature difference must be measured with a tolerance much lower than 1 °C and everything must be done to get the best values for the temperature increase over the fan.

The desired accuracy of the analysis dictates the number of rakes and immersions needed. A thorough static calibration of the thermocouples is required. Total temperature measurements require a recovery correction, which must be applied to the measured values as a function of the flow Mach number and density. Before using the individual pickup measurements for calculating a mean value they should be checked by coarse and fine filters. Erroneous measurements should be neglected or substituted by reasonable data, which can be derived from averaging good values.

Due to thick struts downstream of the fan, it is possible that the temperature increase may vary circumferentially. It might be necessary to apply position correction factors to the reading of the rakes, which can be found from detailed CFD calculations that provide information about wall and boundary layer effects.

In summary we need very good values for the pressures  $P_{45}$  and  $P_5$ , a precise engine inlet and core flow analysis (which sets the temperature level of the LPT) and an accurate measurement of the temperatures upstream and downstream of the fan, which yields the temperature difference  $T_{45}-T_5$ .

Even with the best effort it remains extremely difficult to find the low-pressure turbine efficiency of a high bypass engine from the measurements around the low-pressure spool components alone. However, when looking at all engine components simultaneously and comparing the results with all available information one can get a better test analysis quality.

### 3.3.2.6 Analysis by Synthesis

The conventional test analysis as described in the chapters above makes no use of information, which is available from component rig tests, for example. It will give no information about the reason why a component behaves badly. A low efficiency for the fan may be the result of either operating the fan at an

aerodynamic over-speed or a poor blade design. To improve the analysis quality in this respect is the aim of *Analysis by Synthesis* (ANSYN).

#### 3.3.2.6.1 Principle

When doing analysis by synthesis a model of the engine is automatically matched to the test data. This is done with scaling factors to the component models, which close the gap between the measured efficiency and the model. For example, efficiency scaling factors greater than one indicate that the component performs better than predicted.

Let us explain the procedure for the example of a compressor. The model of the compressor is a calculated or measured map, which contains pressure ratio over corrected flow for many values of corrected spool speed  $N/\sqrt{T}$ .

During the test analysis, we obtain from the measurements, the pressure ratio, the corrected mass flow, the efficiency and the corrected spool speed. Normally we will find that the point in the map defined by the measured pressure ratio and the measured corrected flow (marked in the figure by the open circle) will not be on the line for  $N/\sqrt{T}$  in the original map.

We can shift the line marked  $N/\sqrt{T}_{\text{map}}$  in such a way, that it passes through the open circle. This is done along a scaling line that connects the open with the solid circle. The mass flow and the pressure ratio scaling factors describe the distance between the two circles. The efficiency scaling factor compares the analyzed efficiency with the value read from the map at the solid point.

The shifting direction along the scaling line is somewhat arbitrary. There is no strict rule for defining the local gradient of the scaling line. However, it is obvious that neither strict horizontal nor strict vertical shifting would work under all circumstances.

One can try to give the scaling line some physical meaning. For example, it is possible to define the scaling line as constant corrected flow at the exit of a compressor or alternatively as a line with constant specific work over speed squared.

More important than the gradient of scaling lines is a high fidelity model of the compressor. A map is strictly valid only for the inlet temperature and inlet pressure for which it was calculated or measured. When the inlet temperature is different from the reference the isentropic exponent of the fluid will change and cause small changes in the flow-field around the blades. Since the Reynolds number of the flow in the compressor depends on both inlet pressure and temperature, there will be additional differences when the compressor is not operated at the reference inlet conditions.

Temperature and pressure differences can also result in small geometrical changes like tip clearance and blade untwist, which have an effect on the performance of the compressor.

All known effects that have an impact on the performance of any component should be modeled carefully. The better the model the smaller the distance between the two lines for  $N/\sqrt{T}$  in **Figure 3.50** will be and the gradient of the scaling line becomes an academic question.

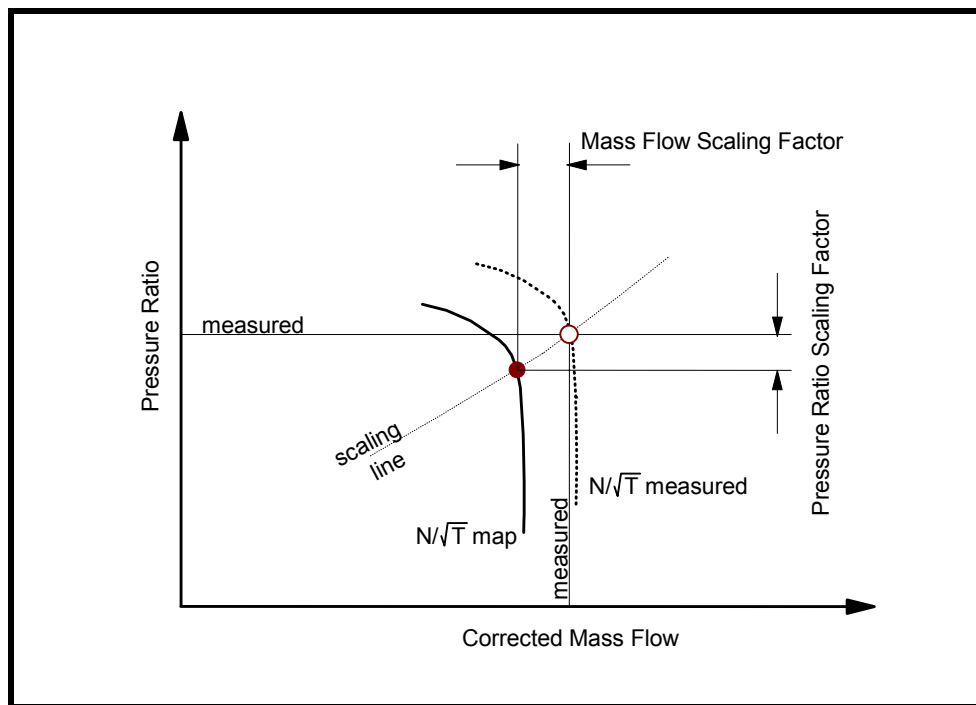


**Figure 3.50: Matching the Measured Data to a Map.**

#### 3.3.2.6.2 Mathematical Procedure

A numerical model of a turbofan requires the iterative solution of a system of equations with about six variables. Some of the measured quantities that must be consistent with the model value (like all measured pressures and temperatures) will require additional variables. With a sophisticated test analysis model one can end up with 20 to 30 variables in the numerical problem to be solved.

This is not a real problem as long as all measured values are reasonable and the model of the engine is good. However, when a measurement has a significant error, it can happen that the iteration will not converge.

Consider for example the analysis of a scan taken at idle where both static and total pressures are very near to each other. Even when the measurement accuracy is normal, it might happen – when there are not enough static pressure pickups, for example – that the mean static pressure is evaluated to be higher than the total pressure. The model will not allow for that and the consequence is that the iteration will fail to converge.

The same can happen at minimum afterburner rating when the pressure losses due to heat addition become insignificant. The model will never produce negative pressure losses. The measurements, however, might require such a result.

Other reasons for convergence problems can be that the actual hardware is different to the model assumptions.

While on the one side, it is very annoying when iteration does not converge, on the other side a very important hint is given that something is wrong either with the measurement or with the model. The conventional test analysis method does not give this information.

#### 3.3.2.6.3 *Best Match*

Analysis by synthesis can be formulated as a turbine capacity method or as heat balance method. However, these are not the only methods to find the core flow for a turbofan engine test. In fact, there are quite a lot of options:

- High pressure turbine flow capacity;
- Heat balance;
- Low pressure turbine flow capacity;
- High pressure compressor flow capacity;
- Nozzle flow check;
- Bypass loss characteristic; and
- Any other correlation of P/Ps with corrected flow.

The laws of physics require that all methods for core flow analysis give the same answer. However, the unavoidable problems with measurement biases, random scatter and misinterpretations will cause every core flow analysis method to yield a different result.

Selecting only one core-flow analysis-method, means that some information is ignored. It is very advisable to run several different methods and to compare the results. This will give many hints about the quality of the measurements and the model. The measurements should be consistent with the pre-test uncertainty-analysis.

Another option is, to use several analysis methods simultaneously. We can combine, for example, the turbine capacity method with a heat balance. Remember that the turbine capacity is based on the measured value of the turbine throat area and the heat balance method on a measured value for  $T_5$ . From a turbine capacity analysis we will get a difference between the measured and the calculated  $T_5$  and from a heat balance analysis we get a difference between the measured and the calculated turbine throat area  $A_{41}$ .

We can set up the analysis in such a way, that we minimize the weighted sum of  $[T_5 - T_{5,m}]^2$  and  $[A_{41} - A_{41,m}]^2$ . The weighting factors will be selected in such a way, that they take care of the confidence that we have in the temperature and turbine throat area measurements.

Obviously we need not restrict ourselves to the turbine capacity and the heat balance methods for core flow analysis. We can use all available measurements simultaneously, and thus we will get a compromise between all conflicting indications of the true core flow. The resulting set of ANSYN scaling factors describes the best match of the model to the test data.

#### 3.3.2.6.4 *Simultaneous Analysis of Several Data Sets*

Up to now we have discussed only the analysis of a single scan, at a single steady state operation point. For each scan, we will get a set of scaling factors for all component models. When we have to analyze a full performance curve we will get many sets of scaling factors.

When we plot the scaling factors over corrected fan speed, for example, we will normally observe that they are not equal to 1.0 (which would indicate perfect agreement between the model and the test results) and in addition to that there is a trend in the data.

There are two ways to deal with these deviations between the model and the measurements. The first is, we attempt to find the reason for the deviation. When we have found it then we can improve the model by

introducing revised or even new correlations. It might also happen, that we have to modify the way we interpret the measured data.

The second option for closing the gap between test data and model is to use representative curves for the scaling factors and thus calibrate the model.

#### 3.3.2.6.4.1 Developing Model Improvements

When we are looking for the reason why the model deviates from the test data then a straightforward core flow analysis like the turbine capacity method should be used. A *best match* core flow analysis as described in the previous chapter would make trends in the data less visible because it will, to some extent, distribute the deviations between measurements and model over all components of the engine.

How can we find the source of the discrepancies between the test results and the engine model? We must check the scaling factors against parameters that might be the reason. Compressor scaling factors should be checked against compressor parameters, and turbine scaling factors against turbine parameters. All model improvements must be based on the component inlet flow conditions (Reynolds number, temperature, pressure, etc.), the component geometry (i.e. variable vane settings, tip clearance, mechanical deformation by pressure loads, thermal expansion of rotors, blades and casings, etc.) and the operating point in the component map. Also a variable amount of bleed or cooling air which is not modeled correctly will show up in a trend of the ANSYN scaling factors.

When looking for model improvements the basis should always be the original source of the component model. For example, when a compressor map from a rig test is available, this should be the basis for all test analyses with the aim of model improvement. It would be the wrong approach to use a compressor map, which was modified during an earlier model calibration exercise. When doing that one would lose the connection to the original compressor rig data. Without realizing it, one could deviate from the precise rig test result more than is justifiable by rig to engine differences.

It must also be taken into account, that there are many interrelations between the components. An erroneous assessment of the fan work will show up in a trend of the low-pressure turbine, for example. However, it would obviously not be correct to introduce a new correlation into the model of the LPT to eliminate such an efficiency scaling-factor trend. The correction must be applied to the fan model or to the fan exit rake measurement interpretation.

A quite common problem is the efficiency split between fan and high-pressure compressor or between high and low pressure turbine. Within a certain tolerance the efficiency levels can be shifted from the high-pressure spool to the low-pressure spool or vice versa without affecting the overall compression respectively expansion efficiency.

#### 3.3.2.6.4.2 Calibrating a Model

When no further improvement of the physics within the model seems appropriate or feasible then we can introduce empirical calibration curves into the model.

The ANSYN scaling factors (i.e. the factors that make the model line up with the measurements) are a good basis for that. One can either manually draw lines through the set of scaling factors or employ a mathematical procedure. The manual approach has the advantage that spurious data will be ignored by proper engineering judgment.

The mathematical approach is a numerical optimization task. The ANSYN scaling factors are represented by some mathematical functions and the coefficients of these functions are optimally matched to the test data.

The basis of the model calibration can be one or several performance curves taken from a single engine. It might also be data from several engines. The method can be equally applied to data from a sea level testbed and to data from an altitude test facility.

Calibration does not really improve the quality of a model. It adjusts it in such a way that it reproduces the measured data of a single engine or an engine family in the best way in a mathematical sense. A model with empirical adjustment factors of significant magnitude is not very well suited for engine development work. The calibration factors represent the not understood behavior of the engine. They should be kept separate from the physically based models. One should not tweak a compressor map and thus make the calibration an integral part of the compressor model, for example. The calibration factors should always be clearly visible and easy to remove, at least for the engine model creator. The engine test analysis by synthesis should always start from a model with the not understood calibration factors removed. Otherwise it gets very difficult to find the true reason for differences between the model and measurements.

#### 3.3.2.6.5 *ISA Correction*

The correction of the measured values to ISA standard day conditions is very easy when the ANSYN approach is used. The scaling factors found from the analysis of the scan are applied to the model and then the model is run at the same corrected spool speed  $N_I/\sqrt{T_2}$  and the ISA engine inlet conditions.

The operating conditions of the engine will not be exactly the same for both the test and the calculation of the ISA corrected performance. This can be seen from the calculated value for  $N_H/\sqrt{T_{25}}$  which will be only very near to (but not exactly the same as) the measured value. The reason for that is the many small effects which do not allow strict Mach number similarity between the tested and the ISA corrected cases like:

- Gearbox drag;
- Fuel, oil and hydraulic pump power;
- Changes in gas properties;
- Reynolds number effects; and
- Thermal expansion of rotors, blades and casings.

We have discussed how the results from a single scan can be corrected to ISA conditions. However, the rated performance also has to be derived from engine performance tests. With the conventional test analysis this requires a set of scans which include the power range of interest. Then a curve fit is applied to the ISA corrected data and the resulting curve is read at the exact value of the rating parameter. This might be a rated temperature, a spool speed or an engine pressure ratio.

With the ANSYN approach one can easily evaluate the rated performance by just running the calibrated model (which is either based on single or on multiple scans) at rated power. During this evaluation one can even simulate an engine without rakes by setting the rake pressure losses to zero in the model.

#### 3.3.2.7 **Summary of Analysis by Synthesis**

The calibration of an engine performance model with test data is a time consuming task. Traditionally, special test analysis programs are employed for deriving ISA corrected performance data that are then compared with the results of a cycle program. In a second step the model is manually adjusted in such a way, that the simulation results match the test data.

The *Analysis by Synthesis* approach integrates the simulation task with the test analysis. It gives a better insight into the differences between rig and engine test results and allows automation of the process of matching the model to the test data.

### 3.3.3 Calculation of Installed Performance

The modeling of the installation boundary conditions can be handled either directly by the engine model or by an external application using an engine model. When included as part of the engine model, standard requirements are defined in the SAE AS681 [3.10].

#### 3.3.3.1 Inlet Recovery

Inlet recovery is an indication of the pressure drop in the air before it enters the engine. For supersonic aircraft this includes the losses associated with the shock and airflow capture process that may be internal or external to the physical inlet. Basic models for both sub-sonic and supersonic operation are generally correlations with a flight condition for a particular aircraft inlet system. MIL-E-5007D(3) [3.25] contains default super-sonic recovery curves for a standard inlet and is used for studies and comparison purposes. More detailed inlet models will calculate the pressure loss at a more detailed level and may include the dynamic response of the inlet to changes in the engine. An example of this at a 1-D level is the NASA LAPIN code, [3.26], which allows modeling of the high frequency inlet response to both external environment and engine inlet changes. This type of detailed model is particularly useful for examining the start/unstart process in a mixed compression inlet or in evaluating the stall and surge initiation and recovery process in conjunction with a dynamic engine model. More detailed 2-D and 3-D models allow calculation of the pressure and temperature variations that are usually collapsed into distortion indices in simpler models.

#### 3.3.3.2 Distortion

The SAE ARP 1420 [3.27] provides definitions and guidelines for addressing inlet pressure distortion in engine simulations. Some of the typical approaches are described below.

##### 3.3.3.2.1 Margins

The simplest and most common method is to consider the stall margin impact on the compression components only, by lumping the impact on component performance into the margin calculations. These are typically quoted as the difference in operating pressure ratio and the stall pressure ratio on either a constant speed or a constant flow basis. Choice of whether constant speed or flow stall margins are more meaningful depends on both the application issue and the control strategy for the engine.

##### 3.3.3.2.2 Impact on Component Performance

When the impact on component performance and stall margin is included, it will generally also include the distortion transfer effect of the components as described in ARP 1420. This includes the creation of temperature distortion that may not have been present at the inlet. This can affect other components not normally affected by pressure distortion such as the combustor pattern factor. Stall line movement with distortion is still modeled but is relative to more representative component reference conditions. This is particularly true in low to medium bypass turbofans where radial pressure distortion can have a significant impact on engine performance.

##### 3.3.3.2.3 Detail Models

Detail description of the distorted flow-field is required for 2-D and 3-D physics based models. Detailed models of inlet distortion of similar complexity to the 2-D and 3-D turbo-machinery models are often required in dynamic simulations where the engine inlet interaction becomes important.

#### 3.3.3.3 Installed Thrust

Installed thrust modeling beyond the adjustments for basic ram drag is included where the nozzle or thrust generation mechanisms cannot be adequately modeled outside the context of the aircraft installation.

The best possible estimate is desired given the uncertainty of both the measured inputs and the assumed environmental and possibly deteriorated engine condition. Often a Kalman filter or other numerical technique is used in conjunction with test data and a full aero-thermo simulation to create a simple in-flight thrust algorithm.

### **3.3.4 Deterioration and Manufacturing Tolerance**

Manufacturing tolerance effects on component performance are rarely measured for production engines. However, the uncertainty in blade and seal clearances, and coating and surface finish contribute to significant variation, even in a brand new engine. During operation, the severity and duration of use affect these characteristics. Some performance changes can be related directly to operating condition (over-speed, over-temperature, maneuver, water wash, and sand-dust-saltwater environment) while others simply follow a general long-term trend. Deterioration is typically based on some combination of continuous and cyclic operation measurement. Cyclic use measurements include throttle movement (TACs in US military engines), take-off and landing, speed excursions, augmentor light-ups). Continuous measurement can include the number of operating hours or hours of operation in a particular condition (hot time, IRP time).

#### **3.3.4.1 Uncertainty of Component Performance**

Uncertainty in measured component performance generally depends on the level of instrumentation, instrumentation accuracy, repeatability of the test conditions and the level of correction required to go from the measured conditions to the conditions at which the component performance will be compared and quoted.

Uncertainty in component performance prediction prior to test is generally based on accuracy of design and analysis tools and historical information. For derivative turbo-machinery component designs with some previous calibrated agreement, it may be possible to quantify uncertainty. Predicting turbo-machinery aero performance and operability is one of the most difficult problems in CFD, a subject of ongoing research. For new concept aero designs, the accuracy improvement over the historical spread has not been established.

#### **3.3.4.2 Change of Component Performance**

As the engine passes through its usage life, component performance changes in typical, if not predictable, ways. Engine deterioration level is easily observed. Determining the underlying component performance change is difficult, and usually impossible, without special instrumentation or analysis. In general, opening of clearances, increased leakage, surface roughness, etc. combine to reduce component performance. Although temporary improvement measures (such as a water wash to remove residue from compressor airfoils and recover performance) are possible, most component deterioration occurs gradually over the engine life. It is modeled via hours of use, or other factors such as time at high temperature, time at high power, and number of throttle movement cycles.

#### **3.3.4.3 Deterioration and Uncertainty in Engine Performance Level**

Although engine deterioration will be consistent with the implied effect of component deterioration, the engine user does not typically have the required data to separate out these component performance changes. Data is generally only available for system characteristics such as fuel burn, EGT, rotor speeds, trim settings, thrust, etc. With appropriate data and analysis, this data may be used to estimate component performance changes using simulations or other numerical analysis. However, engine level parameters are most often used directly for condition and health monitoring.

The engine level characteristics vary between engines based on the measured data and the engine control modes. Deterioration is typically based on data where there are limited effects from the standard engine

control modes. For engines controlled to measured pressure ratio, the change in rotor speeds and temperature will be monitored. For engines with exhaust temperature controls, engine speeds or variable control geometry limits may be used. Variation in these performance or monitoring parameters is generally consistent with the difference between the overhaul acceptance level and the engine removal level. This indicates a change in performance such that the aircraft performance requirements are no longer met or the reduced efficiency or potential further deterioration justifies the engine removal.

### 3.3.5 Emissions

This is a key area of detailed combustor component models. The modeling is usually done at engine level using correlations based on overall performance.

With the increasing attention to gas turbine exhaust gas pollution, exhaust gas emission levels must be predicted at varying operating conditions. On the manufacturers' side, the processes in the combustor are modeled in detail, with CFD, in order to develop new technologies to reduce emissions, such as LPP and RQL combustion. On the operational side, there is interest in how to minimize emissions by optimizing operating conditions such as engine condition, aircraft flight procedures, and fuel type and water and steam injection. The latter two variables mainly relate to ground based gas turbines, using LNG, LH<sub>2</sub> or fuel obtained from gasification of coal or bio-mass. However, it must be noted that LNG and LH<sub>2</sub> fuels for aircraft are already being considered.

ICAO tests are done for all commercial engines prior to certification. They include data for 4 points roughly corresponding to take-off, ground-idle, descent idle and max climb. The test conditions are defined in terms of a fixed percentage of certified engine thrust and may not correspond to the actual engine operation at these power settings on the aircraft.

These are done at sea level static but are used to generate the total emissions for a typical landing and take-off cycle. The ICAO points have been generalized to be applicable across all engines and may not correspond to the actual engine power settings in use. For example, the ICAO setting at 7% of rated power may not correspond to the actual descent or ground idle power setting. Furthermore, the ICAO points do not represent high altitude cruise conditions at which emissions exist for most of the time. To determine cruise condition emission levels, research is directed at both in-flight measurement methods and advanced emission models.

For more general estimates, emission coefficients can be defined as a function of engine conditions. The simplest of these make CO and HC estimates as a function of T<sub>3</sub> and NO<sub>x</sub> as a function of T<sub>3</sub>, P<sub>3</sub> and ambient humidity. These models usually represent deviation of the emissions from a reference level along with P<sub>3</sub> or T<sub>3</sub> and are often referred to as *Ratio of P3T3* models. Results can be improved by using these values along with fuel flow and airflow. These improved correlations are usually based on a combustor loading parameter that corresponds to an average residence time. These parameters are typically calculated from T<sub>3</sub>, P<sub>3</sub> as well as combustor airflow and fuel flow. Accuracy of these models generally is limited and only valid for new engines that maintain the design relationships between P<sub>3</sub>, T<sub>3</sub>, fuel flow and emissions. Deterioration and other off-design effects are not covered and for these the combustion process has to be modeled in more detail such as with CFD codes. Engine manufacturers use CFD codes to develop low emission combustors.

Emissions models are often incorporated into gas turbine performance models. A lot of work on modeling the processes in the combustor in order to predict emissions has been done. This ranges from simple relationships between engine performance parameters and emission levels to 0-D parametric models like the P<sub>3</sub>/T<sub>3</sub> or ratio models mentioned above, to complex CFD computations. The more simple, often empirical, models usually require some sort of calibration to a reference condition before they can be used for sensitivity analysis, so they can be referred to as 'off-design' or 'ratio' models. For accurate direct

prediction of emissions without any reference data, CFD calculations will be required. It should be noted that best results with combustion CFD modeling may still differ from test from by 10 – 30% on new configurations.

P3T3 and ratio models can easily be implemented in an engine performance model in order to provide a tool to directly relate operating condition to emission level, via combustor operating condition. However, the potential of the single equation ratio models to analyze a large variety of effects is very limited.

In order to obtain better insight into the effects of using other fuels, varying air properties, and deterioration, a more detailed model is required. However, the integration of CFD computations into a whole engine simulation is still very difficult and often not considered feasible due to computing power limitations.

A compromise between the CFD models and the simple empirical models is the use of multi-reactor models, which apply a limited degree of spatial differentiation inside the combustor. Multi-reactor models usually include separate flow and chemical models and offer a means of calculating a number of intermediate temperatures along the combustion process such as primary and dilution zone temperatures.

The simplest *combustor flow models* employ ‘well-stirred’ reactors that assume immediate mixing of separate user defined reactant flows. Explicit modeling of the distribution of cooling flows and the mixing processes involves a significant increase in complexity, such as multi-dimensional models.

Simple *chemical models* assume complete combustion in each reactor with no dissociation. Higher fidelity is obtained when calculating chemical equilibrium and best 1-D detail is obtained when calculating chemical kinetics. Many publications suggest multi-reactor models are valuable for the prediction of NO<sub>x</sub> emissions. These models include detailed fuel and gas composition data and NO<sub>x</sub> formation kinetics. An approach to integrate generic multi-reactor models in whole engine simulation models is presented by Visser, [3.28]. More detail on these topics is included in the combustion section in *Chapter 5*.

### 3.3.6 Bleed and Power Off-Takes

Most component-based engine models include the direct effect of bleed between components as a standard feature. For empirical models, the greater the flexibility in bleed level and location, the more tables or correlations are required to achieve the desired effects. Internal bleed must consider the impact on component performance and the method of determining the conditions of the bleed air. In trying to match bleed supply conditions to user requests, a single bleed location may not be adequate. Bleeds from multiple locations may be selected or mixed to create the required bleed with minimal impact on the overall engine performance.

External load models are generally fixed or simple relationships, and are treated by simply including them as one of the power-outputs from the rotating shaft. For some applications, these models become more complicated and are included as part of the basic engine simulation. This is particularly true where control systems are part of the model and customer load affects the ability to maintain the required conditions.

## 3.4 CONTROL SYSTEM MODELS

Early engines featured extremely simple fuel systems, often with limiting by pilot observance of cockpit gauges. Accordingly, the engine internal margins (compressor working lines) had to be large, thereby wasting performance. As engine complexity increased, the control-systems became more refined to ensure accuracy and safety as margins were cashed for greater performance. In recent years there has been a progressive shift away from hydro-mechanical systems to electronic systems, which have greater flexibility.

Modern engines have many control inputs, most of which can be categorized into two main groups:

- *Fuel Flow* – to main and reheat combustors. (Fuel may be distributed into different zones within each combustor to satisfy local combustion constraints.)
- *Geometry* – final nozzle area, both convergent and divergent, compressor inlet guide vanes, bleed valves, blocker doors, variable mixer, bypass injector, and turbine throat areas.

Other control inputs may include water or methanol injection.

The fundamental requirement for any control-system is to deliver the required (rated) level of thrust (or shaft power) at a particular flight point (e.g. Mach no, altitude combination). This is achieved by controlling certain engine parameters to prescribed levels that are related to pilot input (pilot-lever angle – PLA). Direct prescription (open-loop control) of some control inputs is clearly inappropriate, for example, relating fuel flow to pilot demand. So, closed-loop control is employed for most control inputs.

Open-loop control of some variable geometry such as convergent nozzle area, or more correctly nozzle control ring position, is common. However, it relies on the actuator position accuracy to achieve the required engine condition. Because the optimum geometry setting is unlikely to remain constant over life, open-loop schedules must be periodically trimmed, if optimum operation is to be maintained. In addition, engine deterioration and scatter, airframe off-takes (bleed and shaft power) and intake distortions, all of which are random (within acknowledged limits) conspire to make open-loop control undesirable. This said, a mix of closed and open-loops is often found; judgment on the *mix* for a specific application is made on the basis of requirement, complexity (and therefore cost) and feasibility. Multiple closed-loops can interact, and although there are standard multi-variable control techniques for compensating for this interaction, certain combinations may not be practical.

### 3.4.1 Main Engine Control

Consider a two-spool, non-afterburning, mixed turbofan: The power level is fundamentally dictated by the fuel flow. However, if thrust setting is of interest, closed-loop control of a measured parameter that is closely related to thrust is required. Common thrust-rating parameters are LP shaft speed and engine pressure ratio (EPR). Off-line prediction tools can be used to generate schedules of the chosen rating parameter against flight condition, and the fuel flow controlled to achieve the scheduled value. Other parameters may be controlled in part-dry or idle conditions as appropriate. Idle condition is commonly defined using a schedule of HP shaft speed. The suitability of some rating parameters may differ between applications. Civil engines are prime users of EPR as a main control loop. However, this is not so appropriate in the military field due to the stringent EPR measurement accuracy required in *all* parts of the flight envelope. Because this is usually much more extensive than that of a civil aircraft, a higher sensor turndown ratio is required. Also the response of the EPR measurement is likely to be slower than LP shaft speed, a consideration which may sway a decision for a fast-handling military engine.

Some engines may not use thrust-related rating parameters. Turbine exit temperature has been a common rating parameter in the past. This has the disadvantage of thrust decaying over life as the engine gets progressively hotter at a thrust. Thrust rating has the advantage of ensuring a common rated thrust across a mixed-life fleet, and can extend engine life because the engine runs cooler at the start of its life.

Limiting values of other measured parameters such as compressor delivery pressure and temperature, turbine blade temperature, and derived parameters such as aerodynamic speeds, override the rated level.

Transition between power levels is controlled to give repeatable handling times and to ensure safe compressor (HP) running line excursions. It is common to see HP shaft acceleration limiting as this is closely related to HP working line excursion, and gives repeatable handling characteristics. Other, more

aerodynamic-based transient control methods could be employed. As the rate-of-change of thrust is of prime interest from the pilot's view, LP shaft acceleration may be a more relevant control parameter, with a HP compressor exit flow-function limitation for surge protection.

Open-loop control of fuel flow is still commonly relied upon for engine starting, where fuel flow is scheduled against HP shaft speed, and for providing surge protection. Maximum fuelling limits during acceleration are expressed in terms of fuel-flow/P3, which has the property of quickly reducing fuel flow in the event of surge (P3 reduces sharply). Closed-loop control of both events is being sought, as retaining provision for open-loop fuel meter prevents simplification of the fuel system down to the ideal *Pump* and *Tap* architecture. Further simplification may be attainable, using rapidly variable capacity pumps to eliminate the *tap* element.

Compressor variable inlet guide vanes (VIGVs) are provided to ensure correct compressor operation throughout the running range. Whereas they may exhibit the property of modulating inlet flow at a given speed, their prime use is local *care* of the compressor. Vane angle is often scheduled against aerodynamic speed, according to a relationship derived on compressor rig tests. As with all control inputs, there are two issues:

- Where is the optimum position?
- Where is the safety limit?

All the disadvantages of open-loop control as discussed above apply in this case and thus impact on the safety limit. Closed-loop control may better attain the optimum, but would require a measured parameter that indicated compressor *distress* if safety were to be assured. Closed-loop control of variable geometry *within open-loop limits* is an option that may be beneficial – but at what cost to complexity? There may be some engine handling benefit in using the flow modulating properties of VIGVs especially if an engine has variable fan geometry, because fast thrust response may be achieved at constant shaft speed.

Staged combustion is emerging as a solution to stringent emissions requirements. The total fuel flow required for a demanded power level has to be distributed in the combustor to maintain flame stability and minimize emissions. There will inevitably be some interaction between differing fuel distribution (at a constant total fuel flow) and overall engine operating point. Perhaps arising from the different profile presented to the HP turbine. This is a complication that must be addressed to ensure that the staging is effectively *transparent* to the pilot. Direct, closed-loop control of measured emissions might be most desirable – but difficult! Indirect control of emissions using local fuel-air-ratio or flame temperature control is considered simpler. Open-loop distribution of fuel based upon an initial understanding of the combustion process is another option.

Control of the final nozzle area (A8) is not an issue for dry operation unless a variable nozzle has been provided for afterburning. In a dry (not reheated) engine, a variable nozzle provides a means to appropriately set the fan working-line for all flight cases. Closed-loop control of the nozzle to achieve a specified level of EPR is common (in conjunction with closed loop control of the fuel flow via the LP shaft speed – say). Open loop scheduling of the nozzle area may also be a viable approach.

For a convergent-divergent nozzle, the divergent area (A9) may be mechanically linked to the convergent part thus leading to some compromised operation at some conditions. Independent (2-parameter nozzle) control of divergent area may be justifiable. In these cases, A9 could be scheduled against nozzle pressure ratio and A8, or controlled in such a way to maximize whole vehicle performance in conjunction with the aircraft autothrottle (again, the *operation within open-loop safe limits* issue arises).

### 3.4.2 Afterburner Control

The primary purpose of reheat is to provide a thrust boost with a low mass penalty. The main premise is to increase the jet velocity by burning the remaining oxygen in the jetpipe, while ensuring stable engine operation, particularly with respect to the fan working line. In order to maintain the dry engine operating point: as jet velocity is progressively increased by modulation of reheat fuel flow, so must the nozzle area increase to compensate. Thus two extra, interrelated control loops are introduced for reheated operation. As with the main engine control-system, it is desirable to eliminate reliance on open-loop fuel metering. Closed-loop reheat control-systems could be based on EPR control of the nozzle and some means of controlling fuel flow. Direct scheduling off the actual nozzle area is common, or a closed-loop control might be employed, based on some indication of jetpipe gas velocity, e.g. total-to-static pressure, or – though difficult to measure – jet pipe gas temperature. Reheat staging to achieve optimum combustion and emissions require control of fuel distribution. As with main combustion, the distribution of the fuel may affect the overall engine operating point.

The speed at which reheat is allowed to modulate depends on how well the fuel and nozzle area modulation can be coordinated. Out-of phase modulation can upset the fan!

Reheat light-up is also potentially fan-unfriendly. Open-loop limits on fuelling may be employed to safeguard the fan operating point. Automatic sensing and compensation for dangerous reheat instabilities (buzz and screech) may also be required.

### 3.4.3 Variable Cycle Engines

So-called variable cycle engines (VCEs) could more correctly be called variable bypass-ratio engines. They employ variable geometry devices to progressively change the engine from a low bypass ratio engine (high specific thrust) to a higher bypass ratio engine (low specific thrust). This is to meet performance criteria at widely differing flight conditions. Bypass blocker doors and variable bypass exit mixers are primary features of such engines. The doors may be of the 2-position type – in which case the control task is: *when to switch* and *ensure safety in the transition* (when doors close – others might be opening and vice versa). Alternatively, doors may be of the continuously variable type, in which case the task becomes more involved. The variable mixer is positioned to ensure correct HP to LP matching for the two types of engine at either end of the operating range.

### 3.4.4 Performance-Seeking Control (Performance Optimization)

Judicious selection of control-loops and derivation of suitable schedules is seen as the basic *optimizer* of engine performance; however ‘smarter’ approaches have been demonstrated which employ searching techniques to find the minima or maxima of a particular *cost function*. The cost functions are typically: lowest temperature at a thrust, minimum fuel burn, best thrust, etc. Such techniques are reliant on the use of embedded engine models in the control system. Models included in this way are therefore also available for on-board diagnostics and fault detection. The use of smart control techniques may reap most benefit when combined with the flight control-system (which often includes any variable intake geometry) to optimize the whole vehicle.

### 3.4.5 Modeling Control System Components

Although it is often classed as an engine accessory the control-system has a fundamental role in defining what the engine does, that is, it dictates functionality. The individual components of the control-system have differing levels of influence on the functionality. However, the engine is subordinate to the control-system.

Whole-engine models (engine + control-system) are used for various purposes:

- Operability investigation, e.g. surge-margin stack-up;
- Refinement of control-system software;
- Analysis and referral of test data;
- Planning of engine testing;
- Diagnosis following of engine test *events*;
- Hardware development and validation;
- Evaluation and selection of control-system concept; and
- Pilot-in-the-loop simulation (flight simulator).

The level of model detail required for different activities may vary. For instance, actuator and sensor dynamics can often be simplified when the effects of long-range engine transients are being studied. Greater dynamic fidelity may be required in other cases such as selection of control gains to meet specific stability margins. Similarly, the requirements placed on the engine model vary for each application. Engine model requirements are covered in detail in *Chapter 2*.

The applications listed above are focused on different parts of the whole system. In some cases the reaction of the engine in response to the controller is of interest, whereas for other studies the converse applies. Accordingly, the computing environment and analysis facilities may vary. Control-system models and engine models invariably emerge from specialist departments, sometimes using different tools and programming languages. Interfacing models and systems can be an issue, although the use of CORBA-compliant tools will facilitate the co-execution of differing systems. This is discussed further in *Annex B*.

Any dynamic system model requires initialization. Initialization can be achieved by iteration or trimming, although this can be problematic. As initialization is concerned with the initial values in numerical integrators, the initialization task can be simplified by reducing the number of integrators present, by reducing the level of dynamic modeling. Such a trade-off may be acceptable for some applications – usually those that require a whole-engine model. Detailed dynamic models, with fewer shortcuts, may then be needed for detailed design and optimization of the fuel system. Such models are usually run in isolation. Fuel-systems have fast dynamic terms, which are usually insignificant in terms of overall engine response. However, where the combustion process is modeled in detail – such as for an advanced combustor type – the fuel-system dynamics may significantly interact with combustor dynamics and hence affect engine response.

### 3.4.6 Description of a Typical Control System

**Figure 3.51** below shows typical control-system architecture for a combat engine.

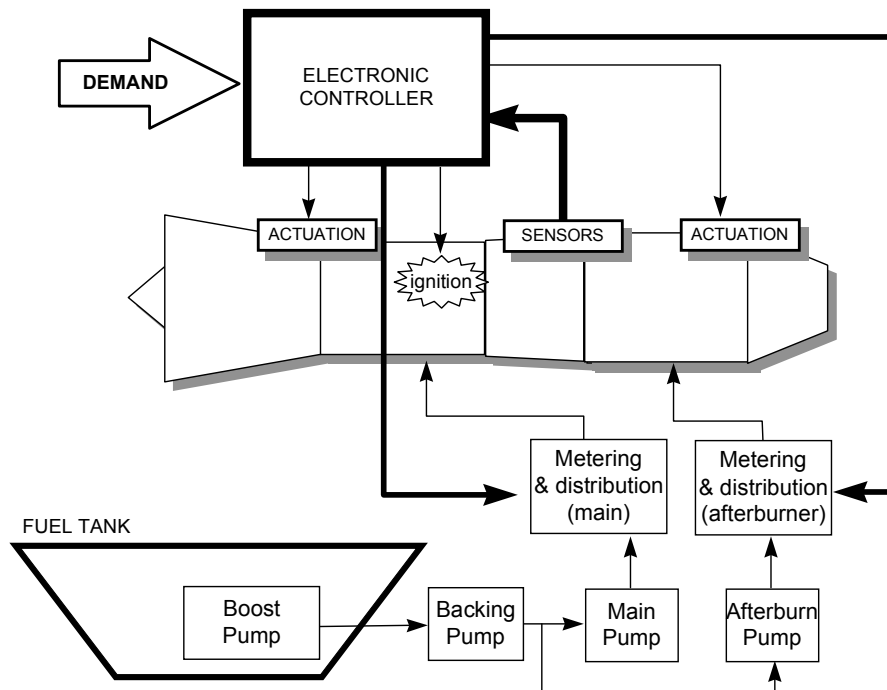


**Figure 3.51: Typical Control System Architecture.**

The main system element is the electronic control system. The control laws are now usually implemented digitally, with a degree of redundancy to meet reliability constraints. Within the electronic controller, checks are made on electrical inputs and outputs. Depending on the status of various inputs, outputs and internal flags, control model changes that may cause a significant change in engine operation may be performed. *Annex B, Section 8* discusses the selection and rationale of typical engine control-loops that are implemented electronically.

### 3.4.6.1 Sensors

An engine will carry several sensor systems, to provide feedback about the engine state to the electronic controller. A sensor is itself a sub-system containing 3 elements:

- Transducer – converting physical parameter into electrical signals;
- Interconnect; and
- Signal conditioning interface – e.g. filtering, linearization, plausibility checking.

Sensor systems may be required for any of the following:

- Shaft speed;
- Gas temperature;
- Gas pressure (total and static);
- Metal temperatures (static and rotating);
- Acoustic resonance;
- Flame detection;

## SYSTEM MODELS

---

- Fuel flow-rate; and
- Position.

Accuracy, reliability, cost and response constraints will dictate the sensing method used for each parameter.

### 3.4.6.2 Variable Geometry Actuation

Actuators can move variable guide vanes, final nozzle area, bleed valves and other variable geometry features on an engine. The common types are:

- Hydraulic;
- Pneumatic; and
- Electrical.

### 3.4.6.3 Pumping

Fuel is injected into the engine under high pressure. Pumping systems are required to overcome the back-pressure on, and the losses within the system, and to generate the required spray pattern. High-pressure fuel can also be used for servo power within the fuel system and for actuation (*fueldraulics*).

There are normally 3 pumping stages:

- Boost pump – usually electrically driven and part of the aircraft system, it ensures a constant supply of fuel to the engine fuel system at all aircraft attitudes;
- Backing pump – to provide suitable inlet conditions for the HP pump; and
- Main (high-pressure) pump – provides the main pumping effort.

Centrifugal and positive-displacement pumps are generally used for aero-engine applications, although other types such as air-jet extractor types are used for low pressure duties, e.g. accessory cooling by fuel circulation. Pumps may be driven mechanically (shaft power via gearbox), by air-turbine (using bleed or ram air) or electrically. Electrically driven pumps offer greater control of fuel flow by varying the motor speed.

### 3.4.6.4 Metering

The rate of fuel flow to the engine is the prime component of the definition of engine power output. Stable and fast responding metering is required – especially for afterburners and staged combustion systems which involve the fast selection and de-selection of burners. The most common metering system is based on a variable orifice with a regulated pressure drop – the orifice being varied by hydro-mechanical or hydro-electrical means. Valve position feedback is required for the determination of fuel flow or for closed-loop control of the valve position. In order to reduce the overall system mass, there is an effort to remove the provision for fuel metering and to provide a system based on a relatively simple *tap* that operates in a relative sense (more fuel or less fuel) rather than metering fuel in an absolute sense.

## 3.5 REFERENCES

- [3.1] Halliwell, I., “Preliminary Design of Gas Turbine Engines – An Overview”, A Tutorial for ASME Turbo Expo 2001.
- [3.2] Sandu, C. and Brasoveanu, D., “Exceeding 2000 °K at Turbine Inlet: Relative Cooling with Liquid for Gas Turbines Integrated Systems”, ASME GT 2003-38031, June 2003.

- [3.3] Wilcock, R.C., Young, J.B. and Horlock, J.H., "Gas Properties as a Limit to Gas Turbine Performance", ASME Paper # GT-2002-30517, June 2002.
- [3.4] Gordon, S. and McBride, B.J., "Computer Program for Calculation of Complex Chemical Equilibrium Compositions and Applications – I. Analysis", NASA Reference Publication 1311, October 1994.
- [3.5] McBride, B.J. and Gordon, S., "Computer Program for Calculation of Complex Chemical Equilibrium Compositions and Applications – II. Users Manual and Program Description", NASA Reference Publication 1311, June 1996.
- [3.6] Kurzke, J., "Gas Turbine Performance Simulation with GasTurb™", [www.gasturb.de/](http://www.gasturb.de/).
- [3.7] Horlock, J.H., Watson, D.T. and Jones, T.V., "Limitations on Gas Turbine Performance imposed by Large Turbine Cooling Flows", ASME Paper # 2000-GT-635, June 2000.
- [3.8] Rolls-Royce plc., Aero Data, TS 1491, February 1998.
- [3.9] SAE Standard, AS755: Aircraft Propulsion System Performance Station Designation and Nomenclature, August 2004.
- [3.10] SAE Standard, AS681: Gas Turbine Engine Steady-State and Transient Performance Presentation for Digital Computer Programs, March 1999.
- [3.11] SAE Standard, ARP1210: Gas Turbine Engine Interface Test Data Reduction Computer Programs, December 2002.
- [3.12] SAE Standard, ARP1211: Gas Turbine Engine Status Performance Presentation for Digital Computer Programs (Cancelled July 2002).
- [3.13] SAE Standard, ARP1257: Gas Turbine Engine Transient Performance Presentation for Digital Computer Programs (Cancelled July 2002).
- [3.14] SAE Standard, ARP4148: Gas Turbine Engine Real Time Performance Model Presentation for Digital Computers, July 2003.
- [3.15] SAE Standard, ARP4868: Application Programming Interface Requirements for the Presentation of Gas Turbine Engine Performance on Digital Computers, October 2001.
- [3.16] SAE Standard, ARP4191: Gas Turbine Engine Performance Presentation for Digital Computer Programs Using Fortran 77.
- [3.17] ISO 2533; Standard Atmosphere, Addendum 2, 1997.
- [3.18] U.S. Standard Atmosphere, 1976, U.S. Government Printing Office, Washington, D.C., 1976.
- [3.19] U.S. Standard Atmosphere Supplements, 1966, U.S. Government Printing Office, Washington, D.C., 1966.
- [3.20] Global Climatic Data for Developing Military Products (MIL-STD-210C), 9 January 1987, Department of Defense, Washington, D.C.
- [3.21] Gordon, S., "Thermodynamic and Transport Combustion Properties of Hydrocarbons with Air. I – Properties in SI Units", NASA TP-1906, 1982.

- [3.22] Mathioudakis, K. and Tsalavoutas, A., “Uncertainty Reduction in Gas Turbine Performance Diagnostics by Accounting for Humidity Effects”, Paper ASME Journal of Engineering for Gas Turbines and Power, October 2002, Vol. 124, pp. 801-808.
- [3.23] Mathioudakis, K., “Evaluation of Steam and Water Injection Effects on Gas Turbine Operation using Explicit Analytical Relations”, Proceedings of the Institution of Mechanical Engineers, PART A, Journal of Power and Energy, Vol. 216, No. A6, December 2002, pp. 419-431.
- [3.24] SAE Standard, AIR4548: Real-Time Modeling Methods for Gas Turbine Engine Performance.
- [3.25] MIL-E-5007D(3): Military Specification: Engines, Aircraft, Turbojet and Turbofan, General Specification for, Rev. D, Amendment 3, December 1995.
- [3.26] Varner, M.O., Martindale, W.R., Phares, W.J., Kneile, K.R. and Adams, Jr., J.C., “Large Perturbation Flow Field Analysis and Simulation for Supersonic Inlets”, NASA CR 174676, September 1984.
- [3.27] SAE Standard, ARP1420: Gas Turbine Engine Inlet Flow Distortion Guidelines, March 2002.
- [3.28] Visser, W.P.J. and Broomhead, M.J., “GSP, A Generic Object-Oriented Gas Turbine Simulation Environment”, ASME Paper # 2000-GT-0002, ASME Conference Munich, June 2000.

## Chapter 4 – COMPONENT MODELING FOR SYSTEM MODELS

### 4.1 INTRODUCTION

When a component-based engine model is used, the model capability and fidelity is generally limited by the component model characteristics available for the engine. The simulation will often be a trade-off between what is desired for system model capability and fidelity and what can be achieved with the available component models.

Component model characteristics important for consideration are:

- **Accuracy** – Does it match reality for overall component-performance?
- **Detail** – Does it provide all parts of the model at the required level? (Cooling Circuits, Seal Leakage, Purge Flows, Localized Transient Effects)
- **Fidelity** – Does it model all of the components at the required level of detail? (Average, Radial Profile, 3-D, Boundary Layer)
- **Functionality** – Does it have the required capability? (In-Stall Performance, Variable Stators and Bleed, Low Water Vapor, Vitiated Air, Rain or Ice, Clearance and Heat Transfer Effects)
- **Complexity** – Execution speed, data required, model expertise required, computer limitations.
- **Range of Operation** – Off-design, low and high speed.
- **Compatibility with System Model and Other Component Models** – Installation and use in system simulation, development overhead, consistency with accuracy and functionality of other models.

Components for modeling will be divided in the classical manner: gas path components such as inlet, compressor and turbine, and other components such as control systems and power train.

**Table 4.1** and **Table 4.2** summarize the requirements for component models for effective use in various types of simulations. **Table 4.3** identifies component model requirements for special or secondary effects within these component models. This section contains a brief summary for each of the primary component models used in turbine engine simulations.

**Table 4.1: Table of Component Model Requirements and Characteristics by Level of Fidelity**

	High Fidelity	Medium Fidelity	Low Fidelity
<b>Functionality</b>	Limited	Limited to High	Limited to High
<b>Complexity</b>	High	Medium to High	Low
<b>Range of Operation</b>	Limited	Limited to Full Range	Limited to Full Range
<b>Compatibility with External Models</b>	Low	Low to High	High

## COMPONENT MODELING FOR SYSTEM MODELS

**Table 4.2:** Table of Component Model Requirements and Characteristics by Engine Life Cycle Application

	Conceptual	Detail Design	Test and Validation	Fleet Support
<b>Functionality</b>	Limited	High	Limited to Medium	Limited
<b>Complexity</b>	Low to Medium	Medium to High	Low to High	Low
<b>Range of Operation</b>	Limited to Full Range	Full Range	Limited	Limited
<b>Consistency with External Models</b>	High	High	Low	Low

**Table 4.3:** Table of Secondary Effects Potentially Required by Component Models

Effects	Fan	Booster	Compressor	Turbine
Variable IGV/Stator Off-Schedule Effects	X	X	X	X
Reynolds Number Index Effects	X	X	X	X
Fan/Booster Effects due to BPR and O/L	X	X		
Distortion Effects	X	X	X	X
Blade Untwist Effects	X	X	X	
Clearance Variation Effects	X	X	X	X
Gas Property Variation Effects	X	X	X	X
Deterioration Effects	X	X	X	X
Inter-stage Bleed Effects	X	X	X	X
Heat Soak and Volume Dynamic Effects	X	X	X	X

## 4.2 GAS PATH COMPONENT CHARACTERISTICS REQUIRED BY ENGINE MODELS

### 4.2.1 General Program Requirements

The steady-state program is intended to represent the steady-state performance of the engine. Steady state means all inputs are constant and time derivatives are zero. The transient program is intended to provide simulation of engine response to input variables with an equivalent sine wave frequency content of up to 50 – 110 hertz (Hz). A minimum requirement of the transient program is the ability to adequately simulate the effects of normal throttle movements and operational dynamic events. Advanced transient models include starting as well as special events such as engine surge and instantaneous, non-commanded, load shed events.

A component-based engine description enables the user to identify the engine configuration and its general characteristics including operating and control limits that are functionally dependent on variable engine parameters. Critical to the accuracy of component-based models is the station identification. Station identification is a numbering system that is used to identify the points in the gas flow path that are significant to the propulsion system performance definition. Integers represent the interface planes between major components, such as the inlet exit and the compressor entry. When additional stations are needed within a component, decimals are used such as 2.7 for a compressor bleed extraction station. The system provides for the consistent definition of the process being undergone by the gas, regardless of the type of engine cycle. The six main processes specifically isolated are:

- Kinetic compression (inlet/diffuser);
- Mechanical compression/work addition/fluidic compression (compressor/propeller);
- Heat addition or exchange (combustor/augmentor/heat exchanger);
- Mechanical expansion/work extraction (turbine);
- Kinetic expansion (nozzle); and
- Mixing (mixer/ejector).

**Figure 4.1, Figure 4.2, and Figure 4.3** illustrate representative engine configurations and the associated station designations [4.1].

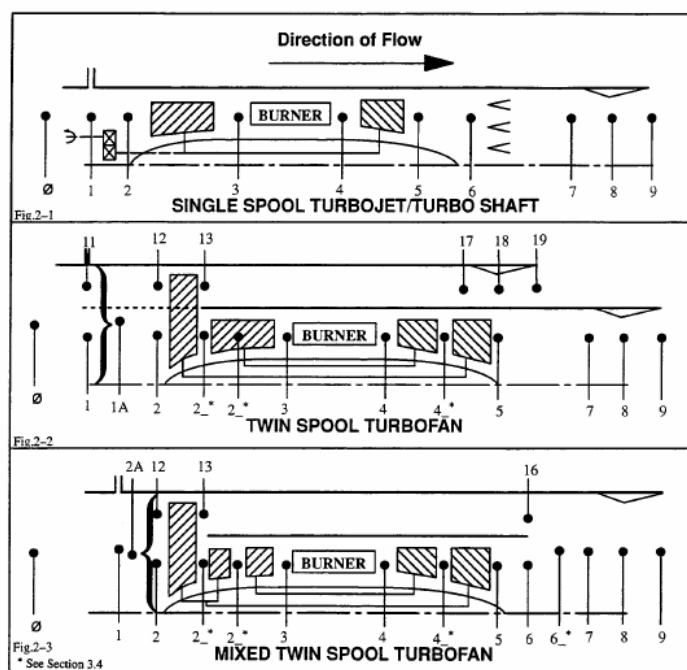


**Figure 4.1: Station Designation for Single Spool Turbojet and Turboshaft and Twin Spool Turbofan.**

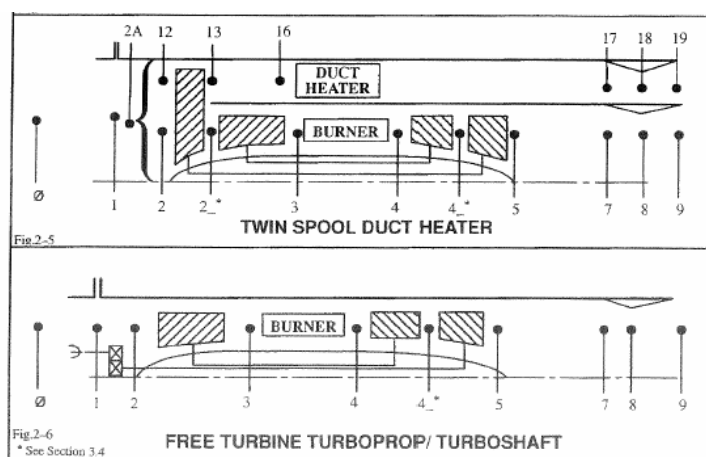


**Figure 4.2: Station Designation for Twin Spool Duct Heater and Free Turbine Turboprop/Turboshaft.**

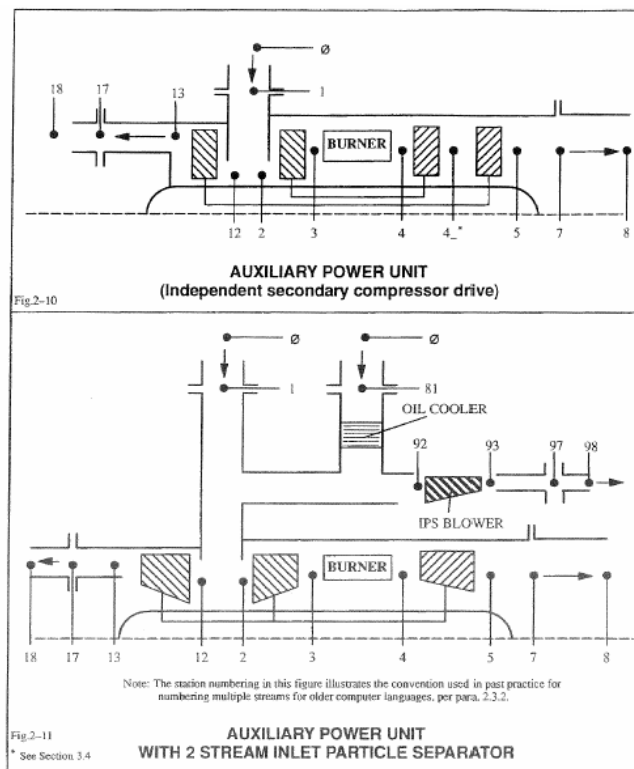


**Figure 4.3: Station Designations Auxiliary Power Unit Types; Two-Spool and with Separate Stream Inlet Particle Separator.**

## 4.2.2 Compressors

### 4.2.2.1 Modeling

A compressor map is the 0-D representation of its performance, showing the mass flow and efficiency of the compressor for a range of operating conditions. It may also include stall line operating limits and various flutter boundaries, as shown in **Figure 4.4**. The requirements for the map vary with their application. For engine and control system design, maps may be required to run from near zero speed to extreme over speed conditions that are beyond shaft break limits, and from stall down to windmill pressure ratios less than unity. For special studies, post-stall maps may be required.

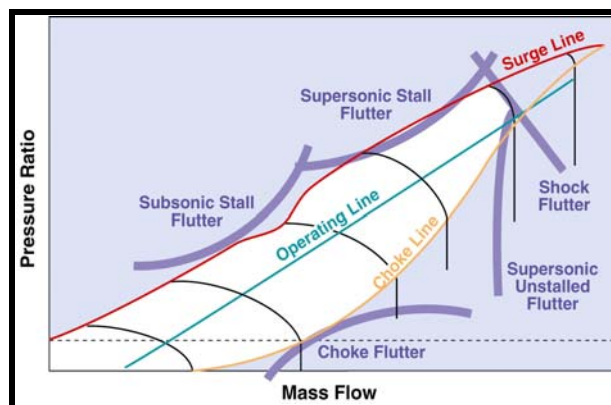


**Figure 4.4: Representative Compressor-Map, with Surge-Line, Speed-Line, Efficiency Contours, and Flutter Boundary.**

A map represents the performance for a nominal set of conditions that may include:

- Stator position;
- Bleed amount and location;
- Entrance temperature, pressure and gas properties (including Reynolds number, gas composition changes such as water vapor or combustion products); and
- Tip clearance.

Knowing the upstream conditions (T, P) and rotational speed, and eventually variable guide vane positions in case of a variable geometry compressor, compressor modeling predicts the outlet conditions (W, T, P) and surge margin.

### 4.2.2.2 Fixed Geometry Compressor

Compressor operation is characterized by the velocity triangles, on which the enthalpy rise (thus pressure ratio and efficiency) and the mass flow depend.

Dimensional analysis shows that a velocity triangle similitude must be based on a Mach number similitude.

For this reason, the classical approach to describe the compressor operation uses the two following reduced parameters:

$$W2R2 = \frac{W2 \sqrt{T2}}{P2} \frac{101.325}{\sqrt{288.15}} \quad \text{Eq. 4-1}$$

Inlet corrected mass flow, which depends only on axial Mach number at compressor inlet (in non-viscous flow).

$$XNR2 = \frac{XN \sqrt{288.15}}{T} \quad \text{Eq. 4-2}$$

Corrected speed is proportional to the tangential velocity and approximates the blade tip Mach number.

When XNR2, W2R2 are fixed, the compressor state is determined and the pressure ratio P3Q2 and the efficiency E23 are known.

This way, two maps may characterize a fixed geometry compressor:

$$P3Q2 = F(XNR2, W2R2). \quad \text{Eq. 4-3}$$

$$E23 = F(XNR2, P3Q2). \quad \text{Eq. 4-4}$$

Very often, instead of using E23 as reduced parameter, the corrected enthalpy rise H3D2/T3 is employed.

An important feature of compressor modeling is the surge line, which sets an upper limit to the pressure ratio at a given corrected speed because of aerodynamic instability. This surge line can be described within the preceding maps as one of their limits. Showing the surge line separately allows secondary effects such as Reynolds number effects, distortion or production-scatter to be taken into account, without modifying the maps.

#### 4.2.2.3 Importance of Compressor Maps in 0-D Models

The compressor map is key data in 0-D models, and one must be aware of the consequences of using insufficiently representative maps. The compressor characteristics are generally well known between 75% and 110% of the design speed. Below 75%, theoretical compressor models may lack precision. For over-speeds, compressor modeling is often limited by the inability of the partial test bench to reach these over-speeds in standard conditions, either because of insufficient driving power or mechanical risks.

Cold weather and high altitude computations often lead to operation at 125% or more of the design-reduced speed. Therefore compressor maps must be accurate in this region where efficiency is decreasing quickly. Accurate maps are also necessary at low speeds to determine the null power speed or the idle ratings; these speeds need to be accurately estimated because their influence on transient operations (acceleration times for example) and the controller design.

In a more general manner, the compressor map, like turbine maps, greatly determines the shape of the relationship between specific fuel consumption and thrust or power, and thus the range of the aircraft.

For all these reasons, the major improvements to be made to 0-D compressor models are linked to a better accounting of secondary effects.

#### 4.2.2.4 Fan Representations

Because of the downstream splitter and booster sometimes present in high bypass turbofan engines, different model representations are often used for fans rather than trying to make a conventional compressor representation work. A separate map for the fan hub, booster and tip may be used. A common approach is to create a single model of the fan hub and booster, and a separate component model of the tip. This corresponds to the way test data is typically taken and simplifies matching test data.

#### 4.2.2.5 Secondary and Environmental Effects

Secondary and environmental effects are those which are not addressed in the component model but which have a significant impact on the engine simulation, when the engine is not operating at the nominal condition assumed in the component model. The best way to address these effects is to include them directly in a component model. This is often impractical so that adjustments to the component model or model results are made to account for these operating condition differences. These models are generally closely tied to the basic component model in both methodologies. Usually they must follow a consistent approach, and provide the required accuracy.

#### 4.2.2.6 Variable Geometry Compressor

In a variable geometry compressor, 1, 2 or more stator grids have variable settings. Very often, these settings depend on compressor reduced speed, and actuators commanded by the engine controller apply the setting laws.

When the variable grid number is low (1 or 2), it is possible to add 1 or 2 dimensions, corresponding to these supplementary degrees of freedom, to the maps described in [Table 4.3](#).

This way, we have:

$$P3Q2 = F(XNR2, W2R2, CAL1, (CAL2)). \quad \text{Eq. 4-5}$$

$$E23 = F(XNR2, P3Q2, CAL1, (CAL2)). \quad \text{Eq. 4-6}$$

The setting laws  $CAL = F(XNR2)$  are then defined separately. This description is the most complete one because it allows the stator setting laws to be easily changed and optimized, without requiring a new map each time.

This first solution can be hard to apply if experimental data is lacking, or when the number of variable grids is important. In such cases, fixed geometry maps are used. Including the setting law for each stator is easier, because the data format is simpler and the data number is lower but the description is valid only for one setting law.

The more common arrangement is for all variable stators to be ganged, with changes in map performance based on a single reference stator position. There may be a series of maps for different reference stator positions relative to the nominal schedule. Alternatively, there may be a single base map for the nominal stator position and numerical corrections for other stator positions.

### 4.2.2.7 Basic Algorithm to Determine Outlet Conditions

At a given corrected speed, the reduced flow is limited between surge flow and blockage flow. To avoid computation problems during iterations, it is often preferred to use another parameter like  $W2RQPR = W2R2/P3Q2$  (close to surge margin) as the input parameter, rather than  $W2R2$ .

The outlet conditions can be calculated via the following algorithm, using  $T2$ ,  $P2$ , and  $XN1$ , as input data:

$T2, XN1$	$\rightarrow$	$XNR2$ .
$W2RQPR$	$\rightarrow$	$P3Q2, W2R2$ .
$P3Q2, XNR2$	$\rightarrow$	$E23$ .
$P2, P3Q2$	$\rightarrow$	$P3$ .
$T2, P3Q2, E23$	$\rightarrow$	$T3$ .
$T2, P2, W2R2$	$\rightarrow$	$W2$ (= $W3$ if no bleed).

The power absorbed by compressor can be calculated using the formula:

$$PW = W3H3 - W2H2.$$

### 4.2.2.8 Precautions – Map Construction Assumptions

Compressor maps are generally issued by either of two means:

- Theoretical aerodynamic models; and
- Rig testing.

In any case, the maps and surge line are often calculated as follows:

- For reference constant inlet conditions:  $T2 = 288.15$  K,  $P2 = 101.325$  kPa, that is to say Reynolds index equal to 1;
- With clean air inlet, that is to say, with low space-time pressure and temperature distortions;
- For given clearances: either constant for theoretical model or with a given (and identified) schedule for a partial test bench;

- In steady thermal operation; and
- For a rated and identified engine ventilation.

Many of these assumptions can be false in real engine operation and require specific corrections.

## 4.2.2.9 Precautions – Secondary and Environmental Effects

**Reynolds Effect** – It was said before that: reduced parameters for compressors find their origin on a Mach number similitude. But this similitude does not account for viscous effects. It is clear that boundary layer thickness and wakes have an effect on both flow and efficiency. To take into account this phenomenon, the Reynolds index is widely used:

$$IR = \frac{Re(T2, P2)}{Re(288.15 \text{ K}, 101.325 \text{ kPa})} \quad \text{Eq. 4-7}$$

The Reynolds index is 1 in standard conditions and decreases quickly when altitude increases. Therefore, the following correction is of major importance for altitude operation and is generally calibrated after either flight tests or altitude test bench trials.

The maps calculated for standard inlet conditions are modified as followed (EPOL denotes the compressor polytropic efficiency):

$$EPOL23(IR) = 1 - (1 - EPOL(IR=1)) \cdot IR^{-x} \quad 0.05 < x < 0.15 \quad \text{Eq. 4-8}$$

$$W2R2(IR) = W2R2(IR=1) \cdot \frac{EPOL23(IR)}{EPOL23(IR=1)} \quad \text{Eq. 4-9}$$

P3Q2 (IR) is then calculated at a specific work, that is to say:

$$\frac{H3D2}{T2}(IR) = \frac{H3D2}{T2}(IR=1) \quad \text{Eq. 4-10}$$

It is often necessary to correct the surge line also, especially in cases where the altitude domain is extended, as for turbofans.

**Real Gas Effects** – The real gas effects are partially taken into account because the enthalpy, specific, and entropy functions are estimated with experimental data. However, the compressor map often uses  $XN/\sqrt{T2}$  and  $W2\sqrt{T2}/P2$  as reduced parameters and these expressions only approximate Mach similitude. A better choice to account for the real characteristics of the gas would be  $XN/(\sqrt{\gamma}RT2)$  and  $(W2\sqrt{T2})/P2 \cdot \sqrt{R/\gamma}$ , for example. Even with adjustment to the corrected parameters, changes in gas properties may require additional correction as described in an AGARD report [4.2].

**Distortion Effects** – Distortion effects are difficult to account for because their analysis requires extensive testing and aerodynamic computation. Furthermore, very complete air inlet instrumentation is needed to get all distortion characteristics. Such trials allow the establishment of tabulated rules, describing the effect of distortion on maps and surge line. Such corrections are critical in cases where high angle maneuvers may happen, as with combat aircraft and certain missiles, because the aircraft body may mask the air inlet. There may be also high distortion when the engine installation is not optimal, as for APUs.

**Clearances and Ventilation Effects** – The compressor performance is highly dependent on blade tip clearances, which depend on operating conditions. These effects are not accounted for with the use of

reduced parameters (aerodynamics origin), because clearances depend on the mechanical and thermal state of solid pieces. Furthermore, clearance changes correspond to a geometry modification. The main parameters influencing the clearances are compressor speed, the temperatures of the fluid in the compressor (blades and disk temperatures), out of the compressor (ambient conditions for casings temperature) and of course, the compressor ventilation. Mainly derived from thermo-mechanical computations, tabulated laws may be usefully added to correct maps and surge line.

### **4.2.3 Turbines**

#### **4.2.3.1 Modeling**

Turbine modeling aims at determining outlet conditions, from knowledge of inlet conditions. This is the same as compressor modeling.

#### **4.2.3.2 Fixed Geometry Turbines**

From an aerodynamic point of view the turbine operation depends only on the velocity triangle. Therefore, for non-viscous flow, a good similitude is based on Mach numbers as for compressors. In fact, compressor and turbines modeling are very similar. The classical turbine description relies on the use of the following reduced parameters:

- $XNR4 = XNH/\sqrt{T4}$  reduced speed;
- $P4Q45$  : pressure ratio;
- $WR4$  : reduced mass flow; and
- $E445$  : efficiency.

In most operating conditions, the turbine nozzle guide vane is choked. Therefore,  $WR4$  is constant. To avoid computational problems,  $XNR4$  and  $P4Q45$  are preferred as input parameters for modeling. As for compressors, two maps are used:

- $WR4 = F(XNR4, P4Q45)$ ; and
- $E445 = F(XNR4, P4Q45)$ .

The reduced enthalpy rise  $H4D45/T4$  is sometimes used instead of efficiency.

These two maps are sufficient to calculate the turbine outlet conditions. Nevertheless, generally, a third map is often used in combinations with these two maps to more accurately calculate the pressure losses in the ducts behind the turbine.

Contrarily, when compared to compressors, which mostly have axial outlet flows (both axial and centrifugal compressors), the flow at the turbine outlet presents an important swirl depending on  $XNR4$  and  $P4Q45$  (swirl itself is a reduced parameter because it characterizes the velocity triangle). Thus, the third map:  $SW45 = F(XNR4, P4Q45)$  is added.

#### **4.2.3.3 Variable Geometry Turbines**

This component is relatively rare because of the difficulties due to combining variable geometry and high temperatures. Nevertheless, it can be found in free turbine turboshaft engines that include a recuperator. In such a case, a free turbine with variable nozzle guide vanes permits optimization of the recuperator, by maintenance of a constant high temperature at its inlet. This applies even at part loads, and results in a very flat  $SFC = F(RWSD)$  curve.

As indicated by the former example, the NGV position typically is not governed by the turbine speed. Thus it is not possible to reduce the modeling of 2-D maps. The number of variable NGV stages is generally lower than two. This allows the method used in certain cases for compressors, by adding dimensions (corresponding to the variable settings) to be applied.

#### **4.2.3.4 Efficiency Definitions for Un-Cooled and Cooled Turbines**

In the following sections, the commonly used turbine performance bookkeeping methods are presented. The pros and cons for the different methodologies are discussed and correlations between the definitions are shown for single and multi-stage turbines with various amounts of cooling air. Furthermore it is pointed out, that simulating a cooled multi-stage turbine with an equivalent single-stage model requires the use of an equivalent Stator Outlet Temperature  $SOT_{eq}$  which differs from the true SOT.

It depends on the bookkeeping system used what the calculated impact on turbine performance is when the amount of cooling air changes. Without carefully adhering to a unique bookkeeping system with a clearly defined control volume the probability of misunderstandings in collaborative engine development projects is not to be underestimated.

The efficiency for any machine is a number that describes the technical quality of this machine. In case of a turbine the efficiency is the ratio of the shaft power delivered  $PW_{SD}$  and the ideal shaft power  $PW_{SD,ideal}$  the turbine would deliver if there were no losses. However, this definition of efficiency is ambiguous since both terms  $PW_{SD}$  and  $PW_{SD,ideal}$  can mean different things. In the shaft power delivered the disk windage and the bearing losses may be included or not, for example, and the ideal shaft power  $PW_{SD,ideal}$  may account for the work potential of the cooling air by one of several alternative methods. Thus the number quoted as turbine efficiency will depend on how  $PW_{SD}$  and  $PW_{SD,ideal}$  are defined.

In a collaborative engine development project the partners have to agree on a unique and unambiguous definition of turbine efficiency. One might say it is not important, which definition is used as long as it is unambiguous. However, there are some practical considerations to be taken into account when picking a definition:

- When a company has to switch over to a definition that was not used in previous projects then it can be difficult to translate the experience from the past to the design goal of the new turbine.
- It must be possible to evaluate the turbine efficiency from an engine test. This can require the installation of additional temperature or pressure probes for a specific definition.
- Similarly, if a turbine rig test is part of the engine development program, then the efficiency must be measurable in the rig. The translation of the rig-measured efficiency to an in-engine value should be as unambiguous as possible.
- Not all computer codes allow for a comprehensive accounting of turbine cooling air. A well-defined process is required to translate the calculated efficiency to the “in engine” efficiency.
- Last but not least the efficiency definition must be suitable for overall engine simulation. That means that the calculated exchange rates of turbine efficiency with overall engine parameters like thrust and specific fuel consumption must be reasonable guidelines during the engine development process.

##### *4.2.3.4.1 Performance Models for Cooled Turbines*

The efficiency of a turbine is always defined as the actual work divided by the ideal work available. However, the process of cooling a turbine greatly complicates the calculation of turbine efficiency. The problems arise when attempting to properly account for the cooling air. The work that actually is

available from the turbine is reduced compared to a turbine without cooling because all of the air does not enter the turbine at the same place and with the same available energy.

There are even more complications that arise when one is attempting to calculate blade efficiency. Blade efficiency is an attempt to isolate the efficiency of the blades from the rest of the turbine losses. This requires meticulous consideration of the air that passes over the tip of the blade, the drag of the disk, the pumping of the cooling air out to the cooling holes, the cooling air mixing losses, and the mechanical losses in the shaft.

## 4.2.3.4.1.1 Efficiency of an Un-Cooled Turbine

The isentropic efficiency of an un-cooled turbine is defined as

$$\eta_{is} = \frac{\Delta H}{\Delta H_{is}} = \frac{\frac{\gamma}{\gamma-1} R^* (T_1 - T_2)}{\frac{\gamma}{\gamma-1} R^* T_1^* \left[ 1 - \left( \frac{P_2}{P_1} \right)^{\frac{\gamma-1}{\gamma}} \right]} \quad \text{Eq. 4-11}$$

In this equation the isentropic exponent of the gas  $\gamma$  is a mean value between the inlet and the exit of the turbine. The above assumes a steady state adiabatic process.

## 4.2.3.4.1.2 Stage Efficiency of a Cooled Turbine

There are two basically different methodologies for defining the efficiency of a cooled turbine: One can deal with the turbine as a sort of “black box” or go into the details of the expansion process. The first approach is discussed later, and we begin with models that describe a turbine stage by stage.

### 4.2.3.4.1.2.1 Single-Stage Turbine

**Figure 4.5** shows a cooled single-stage turbine with a typical cooling air supply system. Compressor exit bleed is the source of the cooling air, and the control volume is identical to the turbine annulus. The power created within the control volume must be bigger than the net power available at the shaft because disk windage and accelerating the cooling air to blade velocity requires some power.

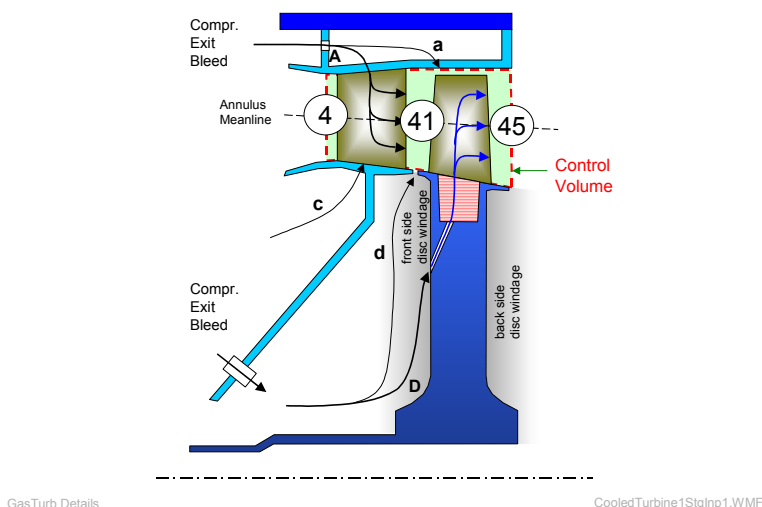


**Figure 4.5: Schematic of a Single-Stage Cooled Turbine.**

With the most widely used efficiency definition for each cooling air stream it is considered whether it does work in the turbine or not. However there is little consistency between companies on what flows are actually considered as part of the available work. One of the more common methods of accounting for the cooling air is to classify some air as “chargeable” and some as “non-chargeable”. “Non-chargeable” air is cooling air that enters before the first rotor stage and thus is available to do work. “Chargeable” air is the cooling air that enters after the entrance to the first rotor stage and thus is considered unavailable to do work. For simplification, this air is considered as mixed with the primary flow after the rotor stage.

Usually all stator (vane) cooling air is said to do work in the rotor. Thus the rotor inlet temperature (RIT, also called stator outlet temperature SOT or  $T_{41}$ ) is calculated by mixing energetically the mass flow  $W_4$  and the stator vane cooling air  $W_A$ :

$$h(T_{41}) = \frac{W_4 * h(T_4) + W_A * h(T_3)}{W_4 + W_A} \quad \text{Eq. 4-12}$$

It is assumed that the total pressure does not change while the stator cooling air is added, and thus  $P_{41}$  equals  $P_4$ , (see **Figure 4.6**). The actual expansion process begins at station 41 and yields the properties at a virtual station 415 which can only be shown in an enthalpy-entropy diagram (see **Figure 4.6**), but not in a schematic like **Figure 4.5**.

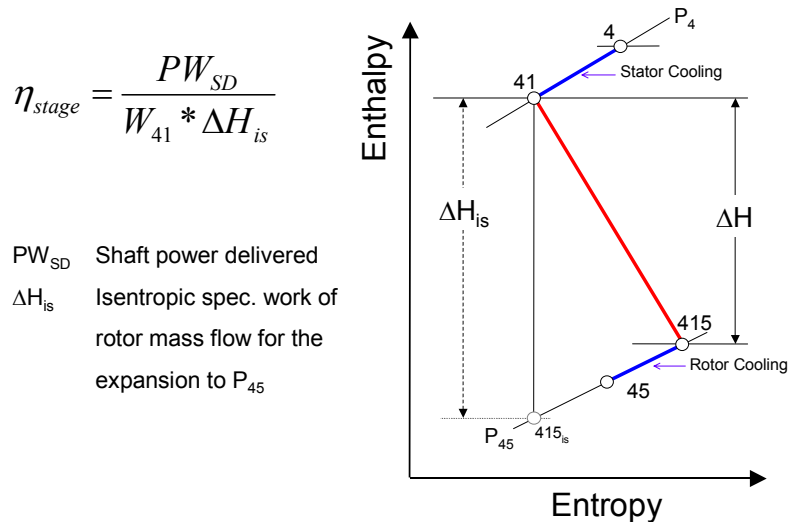


**Figure 4.6: Enthalpy-Entropy Diagram for a Single-Stage Cooled Turbine.**

Platform cooling air  $W_c$  and disk rim sealing air  $W_d$  normally are not considered when  $T_{41}$  is calculated since these parasitic flows do not have the potential to do work in the rotor because of lack of useful energy. Also the rotor cooling air  $W_D$  and the liner cooling air  $W_a$  cannot do any useful work in the rotor. Therefore these streams are not considered when calculating the expansion process from station 41 to the virtual station 415. They are mixed energetically together with the above mentioned parasitic flows downstream of the rotor between stations 415 and 45.

With this approach the expansion process in the rotor is the same as in an un-cooled turbine, and therefore the number used for the efficiency can be understood as that for an un-cooled turbine.

It is obvious that an adequate assignment of the work potential to the cooling air streams is important. For a turbine with given shaft power, fixed pressure ratio  $P_4/P_{45}$  and given turbine inlet temperature  $T_4$  one

may consider a redistribution of the cooling air between stator and rotor (constant total amount of cooling air). This hypothetical redistribution has a non-trivial effect on the corresponding turbine stage efficiency as is explained in the following.

Let us assume that the sum of stator and rotor cooling air is known to be 14% of which 8% is used for stator cooling and 6% for rotor cooling. The stage efficiency is 0.9 in this example, see **Figure 4.7**. Within limits one can debate how much of the cooling air is doing work in the rotor, whether it is chargeable or not. If the amount of stator cooling air (the non-chargeable air) is decreased from 8% to 6% and simultaneously the rotor cooling air – which does no work – is increased from 6% to 8%, then the efficiency number will change. One might assume that the turbine stage efficiency number will increase from 0.9 to 0.92 because the shaft power delivered remains fixed and the ideal power is – due to the 2% rotor mass flow reduction – smaller by exactly 2%. This linear relationship is indicated by the dashed line in **Figure 4.7**.

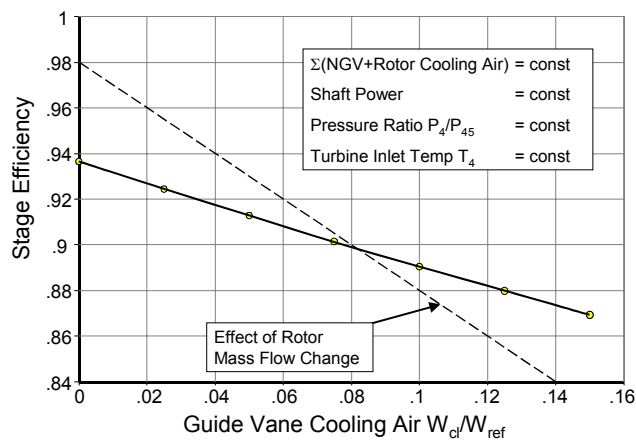


**Figure 4.7: Efficiency Change for Cooling Air Re-Distribution.**

However, reducing the stator cooling air increases the stator exit temperature  $T_{41}$  and this causes the efficiency to increase only about one percent as can be seen from the solid line in **Figure 4.7**. The reason for that phenomenon is the divergence of the isobar lines in the temperature-entropy diagram.

The rotor cooling air  $W_D$  must be accelerated to mean blade velocity  $u$  and that requires the specific pumping power  $u^2/2$ . For a proper energy balance this enthalpy change of the cooling air must be taken into account:

$$h(T_D) = h(T_3) + \frac{u^2}{2} \quad \text{Eq. 4-13}$$

Often both the pumping power and the resulting increase in enthalpy of the rotor cooling air are ignored, assuming that the effects more or less cancel each other. It is not correct to account for pumping air power and at the same time to ignore the corresponding enthalpy increase of the rotor cooling air.

### 4.2.3.4.1.2.2 Two-Stage Turbine

**Figure 4.8** shows the schematic of a two-stage cooled turbine with an associated increase in secondary air streams. Such a turbine can be modeled with two different approaches. In the first approach the two-stage turbine is simulated as an equivalent single-stage turbine. Each secondary flow is assigned a work potential. For example, the work potential of the first rotor cooling air will be approximately 50% as

opposed to the 0% for a true single-stage turbine. Consequently the calculated rotor inlet temperature will no longer be equal to the true stator exit temperature  $T_{41}$  because more than just the stator cooling air must be mixed with the main stream to get the equivalent rotor inlet temperature  $T_{41eq}$ . This temperature is used to calculate the expansion process through the equivalent single-stage turbine.

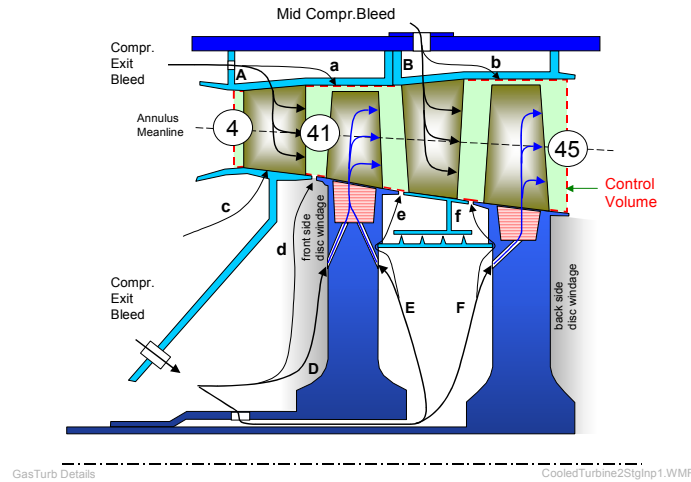


**Figure 4.8: Schematic of a Two-Stage Cooled Turbine.**

The calculation is basically the same as sketched in **Figure 4.6** and yields for given total turbine power and pressure ratio the equivalent stage efficiency of the turbine.

The second approach to model the two-stage cooled turbine follows the path shown in **Figure 4.9**. Each stage is modeled separately and the secondary airflows are mixed with the main stream at the appropriate stations. The cooling air of the first vane is mixed upstream of the first rotor, and the rest of the first stage secondary flows are mixed immediately downstream of the first rotor. Next the cooling air of the second vane is mixed, which yields the inlet mass flow  $W_{421}$  for the second rotor. At the exit of the second rotor the rest of the secondary airflows are mixed with the mainstream.

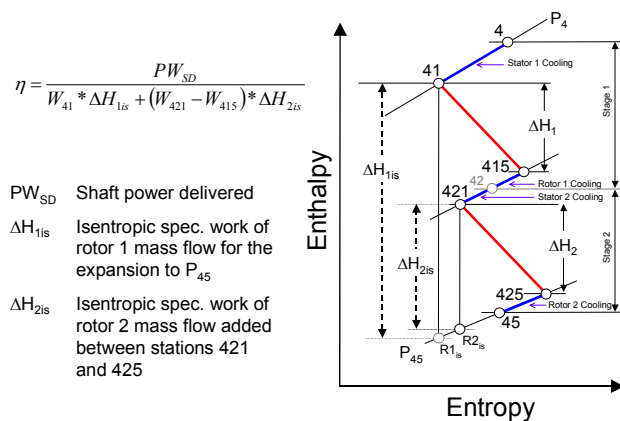


**Figure 4.9: Enthalpy-Entropy Diagram for a Two-Stage Cooled Turbine.**

With this approach one can study the effects of cooling air in a more direct way than with the equivalent single-stage approach. This, however, comes at a price: one needs to know the efficiency of each individual stage as well as the work distribution between the two rotors. During off-design simulations one needs two

turbine maps, one for each stage. These maps cannot be derived from engine tests because the required instrumentation is not available. Maps from a rig test are not fully representative because in such a test the cooling air effects on the flow are nearly never properly simulated because the temperature ratios between the cooling air and the main stream are not as in the engine. Moreover, the map of the second stage is affected by the variable exit swirl of the first stage and therefore theoretically several maps for selected inlet swirl angles are required.

What has been explained for the example of a two-stage turbine can easily be applied also to multi-stage turbines. The equivalent single-stage turbine is then an even more abstract model for the true process. The stage-by-stage approach is equivalent to **Figure 4.9** and results in a rather complex model.

The equivalent single-stage model gives quite different answers compared to the stage-by-stage model both with respect to the magnitude of the efficiency and – even more important – the change in efficiency when the amount of cooling air is changed. **Figure 4.10** shows how the two differently defined turbine efficiencies vary with changes in rotor 1 blade cooling and stator 2 vane cooling of a two-stage turbine. The calculation assumes again that the shaft power, the turbine inlet temperature  $T_4$  and the pressure ratio  $P_4/P_{45}$  are given from a cycle design table, for example. Note that in addition to the blade 1 and the vane 2 cooling air streams there are a few minor parasitic air streams. These would cause a small efficiency difference in **Figure 4.10** even if no blade 1 and vane 2 cooling air is applied.

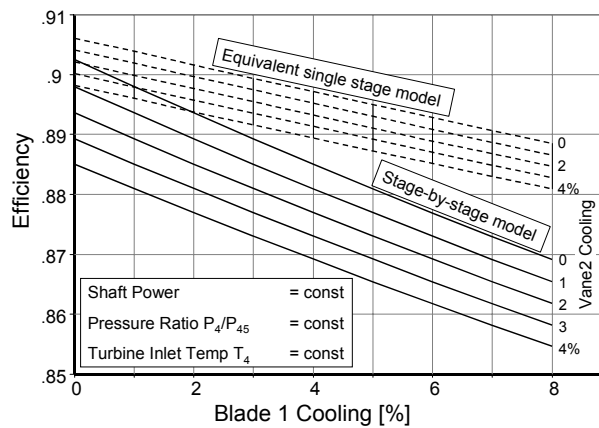


**Figure 4.10: Exchange Rates of Efficiency with Cooling Air Amount.**

## 4.2.3.4.1.3 Thermodynamic Efficiency of a Cooled Turbine

The second most used efficiency definition for a cooled turbine is called in literature the thermodynamic efficiency. In this approach the turbine is dealt with as a black box which converts thermal energy into shaft power. The input into this black box are the main stream energy flow  $W_4 \cdot h(T_4)$  and many secondary air streams  $W_i \cdot h(T_i)$ . All of these energy streams have the work potential which results from an isentropic expansion from their individual total pressure  $P_i$  to the turbine exit pressure  $P_{45}$ .

The thermodynamic efficiency is defined as

$$\eta_{th} = \frac{PW_{SD} + PW_{pump}}{W_4 \cdot \Delta H_{is} + \sum W_i \cdot \Delta H_{i,is} + \sum W_k \cdot \Delta H_{k,pump}} \quad \text{Eq. 4-14}$$

The cooled turbine process is shown in the enthalpy-entropy diagram in **Figure 4.11**. Note that within this definition no stator outlet temperature needs to be calculated.  $PW_{pump}$  is the shaft power required to

accelerate the rotor cooling air to blade velocity and  $\Sigma W_k \cdot \Delta H_{k,pump}$  is the ideal work available on these secondary streams.

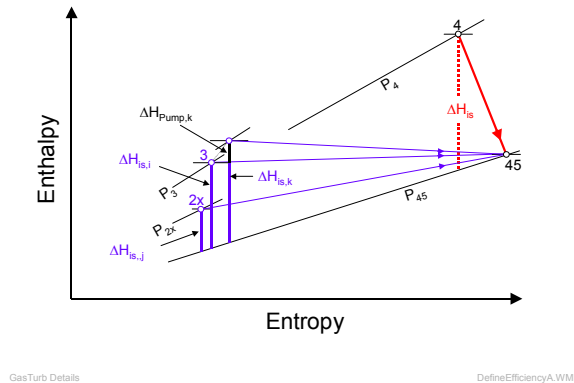


**Figure 4.11: Calculation of the Thermodynamic Turbine Efficiency.**

The advantage of this turbine efficiency definition is that no assumptions have to be made about the work potential of the individual secondary streams. The work potential of these streams is defined via their respective pressures and temperatures, which at least theoretically all can be measured. Thus the use of the thermodynamic turbine efficiency is less ambiguous than all the other methods mentioned above. Moreover, the thermodynamic turbine efficiency accounts for the pressure of the secondary streams while all the other definitions do not.

**Figure 4.12** shows for the same turbine as used for creation of **Figure 4.10** the change in thermodynamic turbine efficiency with the amount of cooling air. In comparison to the stage-by-stage model (the dashed lines are copied from **Figure 4.10**) the effect of changing the amount of cooling air on turbine efficiency is smaller. Note that the effect of 4% vane 2 cooling air on turbine efficiency is 0.007 while the effect of 4% rotor 1 cooling air is double of that. This result is due to the difference in cooling air supply pressures and temperatures.

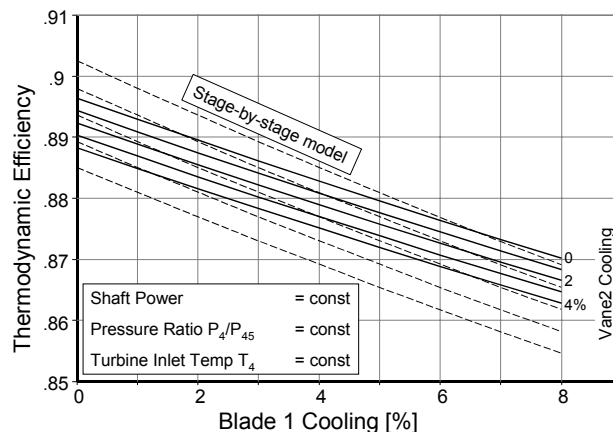


**Figure 4.12: Exchange Rates of Efficiency with Cooling Air.**

#### 4.2.3.4.2 Comparison of Turbine Efficiency Numbers

In the previous sections already a few selected comparisons between the different methodologies have been shown. Here a typical example highlights how big the differences between the efficiency numbers can be, dependent on the amount of cooling air and the number of turbine stages. Since both the

## COMPONENT MODELING FOR SYSTEM MODELS

distribution of the cooling air within the turbine and the work potential assigned to each secondary stream depend on the specific application the numbers quoted can only be a rough guideline for comparing turbine efficiency numbers that are based on different methodologies.

As examples serve two-stage and three-stage turbines which are designed for the same shaft power, mass flow, inlet temperature and pressure ratio. The most important data for the two turbines are shown in **Table 4.4**. The nomenclature for the secondary air streams of the two-stage turbine is that shown in **Figure 4.8**. The last stage of the three-stage turbine is assumed to be un-cooled with only a small parasitic flow at the disc 3 front rim and blade 3 shroud.

**Table 4.4: Turbine Design Data**

Station		Set Conditions			
Inlet Press P4		1144 kPa			
Inlet Temp. T4		1450 K			
Mass Flow W4		28,5 kg/s			
Shaft Power		11000 kW			
Spool Speed		14300 RPM			
Exit Press. P45		372 kPa			
Compr.Fl. W25		31,7 kg/s			
Compr.Exit P3		1180 kPa			
Compr.Exit T3		627 K			
Compr Midstage Press [kPa]		702 kPa			
Compr Midstage Temp [K]		537 K			
		2-Stage Turbine		3-Stage Turbine	
Cooling		% W25	%Working	% W25	%Working
NGV Cooling		5,5	100	5,5	100
Blade 1 Shroud		0,5	50	0,5	66
Vane2 Cooling		2	50	2	66
Blade 2 Shroud		0,3	0	0,3	33
NGV Platform Leak		0,4	50	0,4	66
Blade 1 Cooling (front)		5	50	5	66
Disc 1 Rim Seal (front)		0,6	50	0,6	66
Blade 1 Cooling (back)		0	50	0	66
Disc 1 Rim Seal (back)		0,2	0	0,2	33
Blade 2 Cooling		2	0	2	0
Disc 2 Rim Seal (front)		0,25	0	0,25	33
Disc 2 Rim Seal (back)				0,2	33
Disc 3 Rim Seal (front)				0,1	0
Blade 3 Shroud				0,1	0
<b>Total</b>	<b>Average</b>	16,75	58,2	17,15	66,6
Thermodynamic Efficiency		0,8757		0,8744	
Equivalent Single-stage Efficiency		0,8911		0,8841	
Stage-by-Stage Efficiency		0,8730		0,8540	
Single-stage Efficiency		0,9106		0,9106	

## 4.2.3.4.2.1 Correlations between Efficiency Definitions

In **Figure 4.13** efficiency differences are presented as a function of the cooling air amount. Note that all individual secondary air mass flows are proportional to the NGV respectively vane 1 cooling air percentage that is used as x-axis in the figure. The data corresponding to **Table 4.4** can be read from **Figure 4.13** at the x-value of 5.5%, for example.

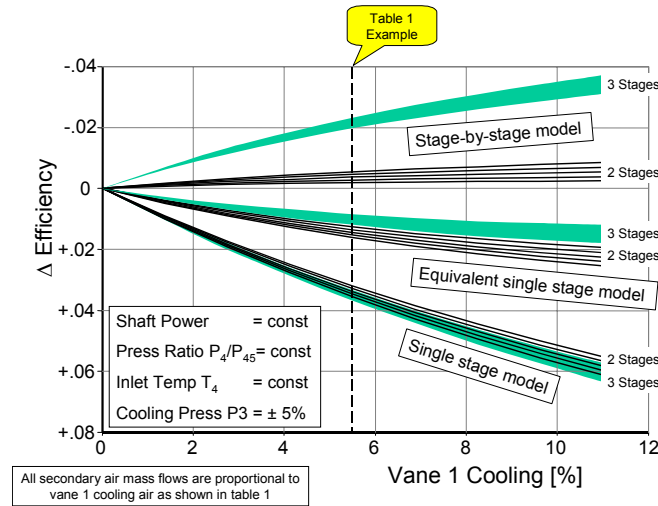


**Figure 4.13: Differences between the Efficiency Numbers for Different Methodologies.**

As a baseline the thermodynamic turbine efficiency described in **Section 1.3** is employed. The band shown about each calculation represents the sensitivity for a  $\pm 5\%$  variation in cooling air pressures which only has an impact on the thermodynamic efficiency calculation.

With the single-stage model all cooling air except of the first vane cooling air is assumed to do no work and it is mixed downstream of the rotor. Therefore the rotor mass flow is lower than that through the rotor of the equivalent single-stage model, because in this case part of the cooling air is assumed to do work. Since the shaft power delivered is the same, the single-stage efficiency is higher than the equivalent single-stage efficiency.

Note that the number of stages has only a minor effect on the efficiency difference for the single-stage methodologies, but a significant impact on the numbers consistent with the stage-by-stage model.

## 4.2.3.4.2.2 Difference between True and Equivalent T41 (Multi-Stage Turbines)

The true stator exit temperature  $T_{41}$  is calculated by energetically mixing the NGV (vane 1) cooling air  $W_{cl,NGV}$  with the turbine entry mass flow  $W_4$ :

$$h(T_{41}) = \frac{W_4 * h(T_4) + W_{cl,NGV} * h(T_{cl,NGV})}{W_4 + W_{cl,NGV}} \quad \text{Eq. 4-15}$$

As mentioned above, this temperature is used as rotor inlet temperature with the single-stage model. With the equivalent single-stage model more than just the NGV cooling air is mixed upstream of the first rotor, and therefore the calculated stator exit temperature  $T_{41eq}$  is significantly lower than the true  $T_{41}$ .

Also for the thermodynamic efficiency definition an equivalent turbine entry temperature is often calculated. This temperature is used for calculating the parameters in a turbine map like corrected spool

speed and corrected specific work. The numbers shown in **Figure 4.14** have been calculated by mixing energetically half of the secondary air with the turbine entry mass flow  $W_4$ .

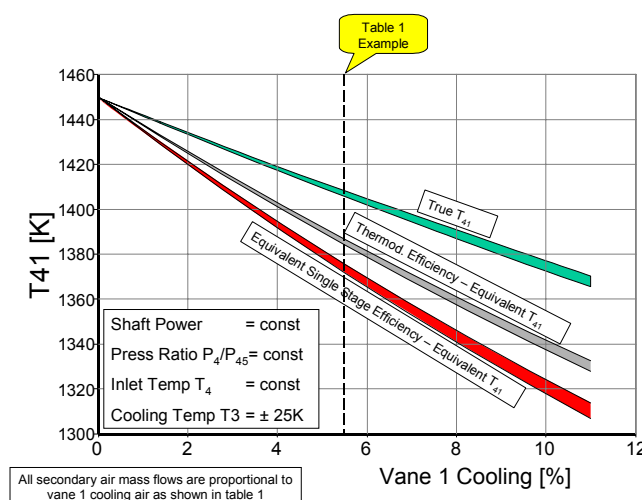


**Figure 4.14: True and Equivalent Stator Exit Temperatures.**

It has been explained above that the efficiency numbers quoted for the single-stage models depend on the amount of cooling air and thus the stator exit temperature  $T_{41}$ . By adjusting the NGV cooling air mass flow one can produce any number for the turbine efficiency. Thus it is also possible adjusting the NGV cooling air in such a way that the efficiency number consistent with the single-stage model is equal to the number of the thermodynamic turbine efficiency, for example.

## 4.2.3.4.3 Impact of the Choice of Efficiency Definition on the Results of Cycle Calculations

After having seen the differences between the various efficiency definitions it is not astonishing, that these have an important effect on the results of engine cycle calculations. **Figure 4.15** shows two carpets that were created for a high-bypass turbofan at cruise conditions with the cycle code GasTurb [4.3]. One carpet is valid for constant thermodynamic turbine efficiency, and the other for constant single-stage efficiency. Efficiencies were adjusted so that the top right corner points ( $T_4 = 1700$  K,  $P_3/P_{25} = 12$ ) agree. Because of the different mathematical definitions, the carpet plots diverge as one moves away from this set point of equality.

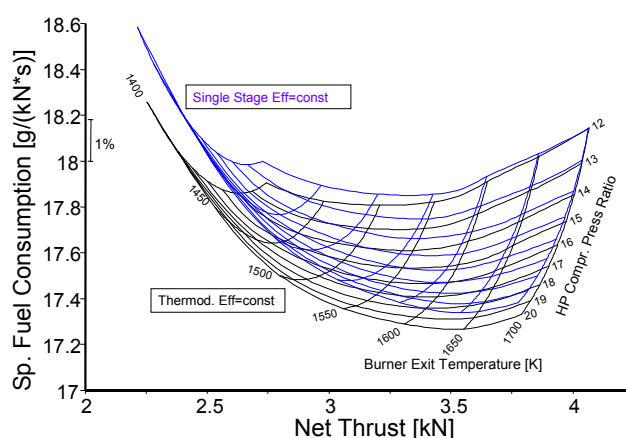


**Figure 4.15: Cycle Parameter Studies with Differently Defined Turbine Efficiencies Held Constant.**

In summary, this discussion of turbine efficiency definitions highlights the importance of choosing the definition that will be used in tracking the performance of the overall engine and at the same time defining the true technical quality of the turbine itself. The performance and turbine aero-engineer need to agree on what to choose for their application and what instrumentation is practicable and needed to verify the level of turbine efficiency attained.

As an evaluator it is also important to understand the impact of knowing what definition has been used in quoting the technical quality of the turbine, so that equal comparisons can be made from one turbine manufacturer to another.

### 4.2.3.5 Total-to-Static Turbine Maps

Generally component maps are given for total parameters, which avoid having to know the sections at inlet and outlet. Let us consider the example of a free turbine turboshaft engine.

A diverging nozzle, for slowing down the exhaust gases, follows the power turbine. The power created by the free turbine results from both total-to-total efficiency and pressure losses in the nozzle. Very often, it is difficult to evaluate the losses in the nozzle due to swirl, and the presence of struts, thus the total to total pressure ratio of the turbine is not accurately known.

To avoid this conflict between power turbine and downstream losses, a map modeling both turbine and nozzle, which uses a total to static pressure ratio  $P45Q59 = P45/PS9$ , is often used. This ratio is known more easily because  $PS9$  is equal to the ambient static pressure. In such cases, the swirl map is not given because the nozzle losses are already included in the efficiency  $E4559$ .

This total to static map is thus given in the following form at:

- $WR45 = F(XNR45, P45Q59)$ ; and
- $E4559 = F(XNR45, P45Q59)$ .

The associated drawback is that any change in nozzle geometry requires new total to static maps.

### 4.2.3.6 Basic Algorithm to Determine Outlet Conditions

The turbine outlet conditions can be calculated by the following algorithm using  $T4$ ,  $P4$ ,  $XN$ ,  $P4Q45$  as input data:

- $T4, P4, WR4 \rightarrow W4 = W45.$
- $T4, P4Q45, E445 \rightarrow T45.$
- $P4, P4Q45 \rightarrow P45.$

The power created by the turbine can be calculated by:  $PW = W4H4 - W45H45$ .

### 4.2.3.7 Precautions – Limitations

Most remarks made for compressor maps, can be applied to turbine maps. Like compressor maps, turbine maps are issued with reference inlet conditions and a reference environment expressed as clearances, ventilation. The translation of these performances to the actual engine environment is a critical problem for 0-D models, which minimize the geometry description. This translation is even more difficult for turbines than for compressors because:

## COMPONENT MODELING FOR SYSTEM MODELS

---

The design point for a turbine is at high temperature and pressure while turbine maps are often measured at partial test bench using cold and low-pressure air. Consequently, the corrections due to inlet conditions are much bigger than for compressors.

The temperature inlet condition for a turbine varies through a much wider range than for compressors because there is a combination of both ambient temperature range, due to the flight domain, and the power or thrust level range. Thus, the corrections are not only bigger than for compressors, but they have higher amplitudes within the operating envelope.

Nevertheless, there is one feature of turbines that in certain cases can ease their modeling. When a turbine stage is located between two choked fixed sections (either nozzle guide vane or exhaust nozzle), it is easy to prove, thanks to the critical mass flow formula, that the pressure ratio of the stage is fixed and does not depend on the operating conditions. Therefore the specific work  $H4D45/T4$  is also constant.

Generally, the turbine drives a compressor for which  $(H3-H2)/XN^2$  is quite constant (velocity triangle), so  $XN/\sqrt{T4}$  is nearly constant. That means that such a turbine has a single aerodynamic operating point because both  $XNR4$  and  $P4Q45$  are constant. In reality, this operating point moves a bit inside the maps because of the real gas effects and the wide temperature range. Thus, HP turbine modeling is much more of an environmental modeling problem rather than an aerodynamic one. Of course, turbines such as free turbines in turboshaft engines cumulate all difficulties because their exhaust nozzle is not choked.

Most corrections mentioned for compressors, such as Reynolds effect, clearances and ventilation corrections, can be applied to turbines. The last of these has a major impact on efficiency, because cooling flows generate local distortion and aerodynamic disturbances.

Concerning the effect of distortion mentioned for compressors, the problem is slightly different for turbines because it is not due to installation or flight conditions. Here it is due to engine design, at the combustor outlet, where there is a non-uniform temperature profile. This is because of:

- Cooling of static parts in the combustor;
- Optimization to increase turbine blade creep life;
- The presence of discrete injectors and their azimuth profile; and
- Staged combustion.

It is very difficult to account for that distortion due to lack of experiments and the severity of the environment. As with compressors, more accurate reduced parameters may be used for Mach number similitude by accounting for  $\gamma$  and  $R$  variations:

- $XN/\sqrt{\gamma RT4}$  instead of  $XN/\sqrt{T4}$ ; and
- $W4\sqrt{T4/P4} \sqrt{R/\gamma}$  instead of  $W4\sqrt{T4/P4}$ .

### 4.2.3.8 Importance of Turbine Maps in 0-D Models

As said before, what we may call a *HP turbine* has a fixed operating point. The operating point of a power turbine in a turboshaft engine, for example, is variable because the pressure ratio is not fixed. For that reason, turbine maps won't have the same criticality.

**Fixed Operating Point Turbines** – From the point of view of the customer, who considers the engine with a given turbine's matching, the HP turbine map is not as important as the environment and secondary effects. This is because the operating point is nearly constant. However, for the engine designer, it is important to have a good prediction of reduced speed and pressure ratio effects, in order to optimize the

initial matching, or to study eventual engine re-matching by NGV section changes, or simply to evaluate the production scatter effect.

**Variable Operating Point Turbines** – This case may be encountered in two configurations:

- There is one critical section behind the turbine but this section varies according to operating conditions. This is the case for an LP turbine in a military turbofan with a variable exhaust nozzle.
- There is no critical section behind the turbine. This is the case for a power turbine in a turboshaft engine.

In both cases of variable operating point turbines, the operating point may vary across a wide range within the maps and such maps will become, like compressor maps, key features of the 0-D models.

#### **4.2.4 Burners and Augmentors**

The heat addition component models typically include the primary combustor between the compressor and turbine components, and the augmentor or afterburner downstream of the turbomachinery. The component models typically differ according to the design intent and relevant operating range.

Main burners are designed for high efficiency, long life, low-pressure drop and flat temperature profiles to accommodate the downstream turbine. They must operate reliably over the aircraft envelop and all power settings.

Synonymously with *Afterburner*, the terms *Augmentor* and *Reheat* are used to describe an auxiliary burner downstream of the turbines in which the gas is reheated to provide extra thrust. These are used for limited periods, only at high power and for limited duration. Although there are many common issues, individual designs of main burner and augmentor have significant differences. A key difference between main burners and augmentors is the large variation in momentum pressure drop in the augmentor with operating condition, compared to the relatively fixed pressure drop in the main burner.

##### **4.2.4.1 Burners**

At the 0-D level, combustor representations generally model the energy rise and pressure drop across the burner, based on operating conditions and any special operating modes (number of fuel nozzles fired, number of flame-holder rings, etc.). Models may also include kinetics models for emission calculations. More detailed models may include detailed information on the temperature and pressure fields, the dilution air mixing and the fuel injection and dispersion processes.

##### **4.2.4.2 Modeling**

Modeling of combustors is relatively easier than modeling of rotating components, at least for 0-D models of classical burners, because the burning efficiency is close to 1 in many conditions. This is because they do not have any pollutant-emission constraints or non-afterburning chambers.

The combustor is considered as a black box that receives:

- Hot compressed air from an HP compressor characterized by  $W_3$ ,  $T_3$ ,  $P_3$  and eventually a non null water-air ratio  $WAR_3$ ; and
- Fuel characterized by its mass flow  $WF$  and its lower heating value  $FHV$ . This mass flow may be split in the case of a staged combustor.

The combustion is usually modeled as a heat addition at quasi-constant pressure (there are pressure losses). The real added heat depends on the burning efficiency of the combustor defined as:

$$EFB = \frac{W4H4 - W3H3}{WF \cdot FHV} \quad \text{Eq. 4-16}$$

This is the ratio of real heat over theoretical heat due to a perfect combustion. For classical combustors, EFB is close to 0.995 because the combustor is designed to have a quasi-stoichiometric primary zone, which guarantees both high efficiencies and stability.

In the case of low-emissions chambers required by new legislation for land based turbines, new concepts are being experimented with. Examples are LPP (Low Premixed Pre-vaporized) and RQL (Rich Quench Lean) where the primary zone is either poor or rich. This leads to lower burning efficiencies although still generally higher than 0.97.

To model the changes of burning efficiencies according to the chamber inlet conditions, the aerodynamic load  $\Omega$  of the chamber is often used:

$$\Omega = \frac{W3}{P3^{1.8} e^{T3/300} VOL}, \quad \text{Eq. 4-17}$$

where VOL denotes the volume of the chamber.

This parameter represents EFB as a decreasing function of  $\Omega$ :

$$EFB = EFB_0 - \alpha \Omega^\beta, \text{ with } \alpha \approx 10^{-3} \text{ and } \beta \approx 1.4.$$

$\alpha$  and  $\beta$  coefficients depend on the combustion chamber configuration.

This equation is valid for high-pressure combustion that is reaction rate limited. At lower pressures, typically below 2 atmospheres, combustion may be flame speed limited. Although this basic relation may still be useful at low pressures, the exponents in the relationship will change dramatically. In flame spreading limited regimes, the transition from laminar to turbulent burning will also affect the correlation. This relation also assumes adequate atomization of the fuel flow. At the extreme range of fuel flow for a particular burner design, the combustion efficiency may be atomization limited. This can occur at high altitudes with low fuel flow rates when the fuel delivery mechanisms has been sized and optimized for high fuel flow levels at sea level operation.

An important feature of combustion chambers is their extinguishing limit. Below a certain fuel air ratio, the flame may be blown out leading to an engine stop. This limit has to be included in any performance simulation and especially for transient simulation.

As mentioned before, the combustion is quasi isobar; the pressure losses at the design point vary typically from 3% to 10% in certain cases, where integration constraints led to a reduction in the chamber volume (for example missile engines which have to conform to an external diameter).

The diffuser, liner cooling and fundamental heat release process result in some pressure loss that can be modeled as:

$$\frac{P4D3}{P3} = CD \times \left( \frac{W3\sqrt{T3}}{P3} \right)^2 + K^*(T4/TT3 - 1) \quad \text{Eq. 4-18}$$

#### **4.2.4.3 Basic Algorithm to Determine Outlet Conditions**

The input data are:  $T_3$ ,  $P_3$ ,  $W_3$ , and  $W_F$ , and the chamber outlet conditions can be computed as follows:

$W_3$ ,  $W_F$  Mass flow conservation  $\rightarrow W_4 = W_3 + W_F$

#### **4.2.4.4 Afterburner (Reheat) Simulation**

With an afterburner the maximum thrust of a turbofan may be increased by 50 to 100% for short periods of time.

An afterburner is a fairly simple device, and it consists of only a few basic parts: a diffuser section, fuel injectors and flame-holders, a mixer, the jet pipe with a liner which controls the cooling air distribution and the nozzle.

In the diffuser section, the turbine exit guide vanes eliminate residual swirl downstream of the low-pressure turbine rotor. In the actual diffuser the Mach number is reduced from approximately 0.4 to 0.2. In this region the fuel injectors are placed in such a way that the fuel can be distributed as required.

The flame-holders stabilize the flame in the relatively high velocity environment, and the jet pipe serves as a combustion chamber, which provides time for the chemical reaction. A screech damper is necessary to suppress high-energy destructive acoustic frequencies. The screech damper is part of the liner that protects the case from high temperatures. Downstream of the afterburner a variable area nozzle is required to control the operating conditions of the turbomachinery.

The flow phenomena in a burning afterburner are extremely complex, and it is not feasible to simulate them on a purely theoretical basis with sufficient accuracy. Developing an afterburner is still an empirical task that includes the old-fashioned cut-and-try approach. An accurate simulation of the performance of an afterburner will always include some empirical correlations that are derived from engine test analysis.

An afterburner must operate over a wide range of conditions. To obtain the maximum thrust the fuel must be injected in such a way, that all of the available oxygen in the main stream is burnt. That means that the fuel-air-ratio must be very uniform at the nozzle inlet. When the fuel is not distributed evenly then there are some regions that lack fuel and others with an over-stoichiometric fuel-air-ratio. In both regions the heat release is less than maximal.

At minimum afterburner rating the fuel must be distributed stoichiometrically in the now small combustion region to prevent the flame from being blown out. In other words, the fuel must now be distributed very unevenly throughout the afterburner.

Simulation of the afterburner requires models for:

- Pressure losses in dry and reheated operation;
- Heat release of a given amount of fuel;
- Combined effect of the burning process;
- Nozzle position on the operation conditions of the turbomachinery; and
- Power requirement of the afterburner fuel pump.

For a high fidelity transient afterburner simulation the ignition process and the time needed to fill the fuel injectors that are empty during dry operation to avoid fuel coking, must also be modeled.

The following paragraphs deal mainly with the simulation of steady state afterburner operation in mixed flow turbofans. Most of the methods described are also applicable to the afterburners of straight turbojets. Practical afterburner simulation models are all of the semi-empirical type.

#### **4.2.4.5 Dry (Non-Burning) Operation**

When no fuel is injected, the afterburner behaves as a mixer, and the calculation procedures described in **Chapter 4.2.7.2** apply. However, the pressure losses are significantly higher than in an engine without reheat because the geometry of an afterburner must be optimized for best burning stability and efficiency, and not for minimum pressure losses.

##### *4.2.4.5.1 Turbine Exhaust Guide Vanes*

The pressure losses of the exit guide vanes depend on the swirl downstream of the low-pressure turbine rotor and the Mach number. This can be modeled with a loss characteristic that employs these parameters.

Alternatively, the exhaust guide vanes can be regarded as a part of the low-pressure turbine. The efficiency, as read from the turbine map, would then include the losses of the exhaust guide vanes.

##### *4.2.4.5.2 Diffuser, Spray Bars and Flame-Holders*

Flame holding and propagation requires a flame-holder system that creates a low velocity re-circulating air region. Such a system produces, as a by-product, significant pressure losses. Additional losses are created by the fuel injectors (spray rings or spray bars) placed upstream of the flame-holders, and the diffuser. All these losses are often lumped together and modeled as one. Since in this part of an engine the flow Mach number is subsonic under all conditions, the pressure losses of the core stream will vary proportionally to the turbine exit corrected flow squared.

Modeling the pressure losses of the bypass flow can be more difficult, especially in engines with a low bypass ratio. In this case, a significant part of the flow will pass behind the liner and only the remainder enters the afterburner at the bypass exit. Eventually the pressure downstream of the bypass flame-holders can be derived from the bypass exit pressure only with the help of an empirical correlation.

While all turbofans in series production employ afterburners with flame-holders, it should also be mentioned that there are alternatives. Mixing and burning in two-stream systems can be enhanced by swirl, and no flame-holders are then required. Turbofan swirl augmentors are described in some detail in the paper by Egan (1978) [4.4].

##### *4.2.4.5.3 Mixing*

The simulation of the mixing of two streams in a constant area duct is described in **Section 4.2.7.2**. From this calculation one gets the ideal nozzle inlet conditions when the afterburner is not lit. In practical afterburners the core and the bypass streams will not be fully mixed at the inlet of the nozzle. Total pressure and temperature will not be constant over the radius and this causes a thrust loss relative to the ideal case.

This thrust loss can be modeled with the help of the mixing efficiency defined in **Chapter 5**. Alternatively one can use the thrust of a nozzle with fully mixed flow as a reference, and apply a thrust coefficient that brings the calculated result in line with reality.

##### *4.2.4.5.4 Jet Pipe*

The losses due to wall friction in the jet pipe are small compared to the losses caused by the flame-holders. Mixing the liner cooling air with the main stream causes another pressure loss in the jet pipe. Mostly these

two losses are not accounted for separately, and they are combined with the bypass flame-holder loss characteristic.

## 4.2.4.5.5 Flow Distribution and Turbomachinery Matching

In a high bypass engine without an afterburner the full bypass flow joins the core flow at the edge of the mixer. When the mixer is of the confluent type, then both streams are flowing essentially in parallel, and the static pressures of both streams are equal.

The shape of a forced mixer is quite complex, and so is the flow-field in the region where the two streams join. However, for the purpose of simulating the turbomachinery-matching of such an engine, it is sufficient to calculate the mean static pressures from the invariable effective flow areas, and request that these mean pressures are equal.

In the cycle model of a turbofan the operating points of the compressors and turbines are found with an iterative algorithm. In the first pass of an iteration through the mathematical model the operating points are only estimated values, and consequently some conditions (flow continuity and energy balance, for example) are not fulfilled. In particular, the mixer inlet conditions will be such that the static pressures of the core and the bypass stream at the mixer edge are not equal, and this results in the so-called **mixing error**.

In turbofans with afterburner, **Figure 4.16**, a significant amount of the bypass air passes behind the liner and joins the main stream successively through the screech damper and the liner cooling air holes. The nozzle cooling air does not enter the afterburner at all. Thus, only a part of the bypass air enters the mixer. Moreover, at the entry to the mixer the geometry is often very complex. The flame-holders create re-circulation zones of significant size just within the region where the simple mixer model assumes static pressure balance. The question arises, what are the effective mixer areas, and are they invariable for all operating conditions?

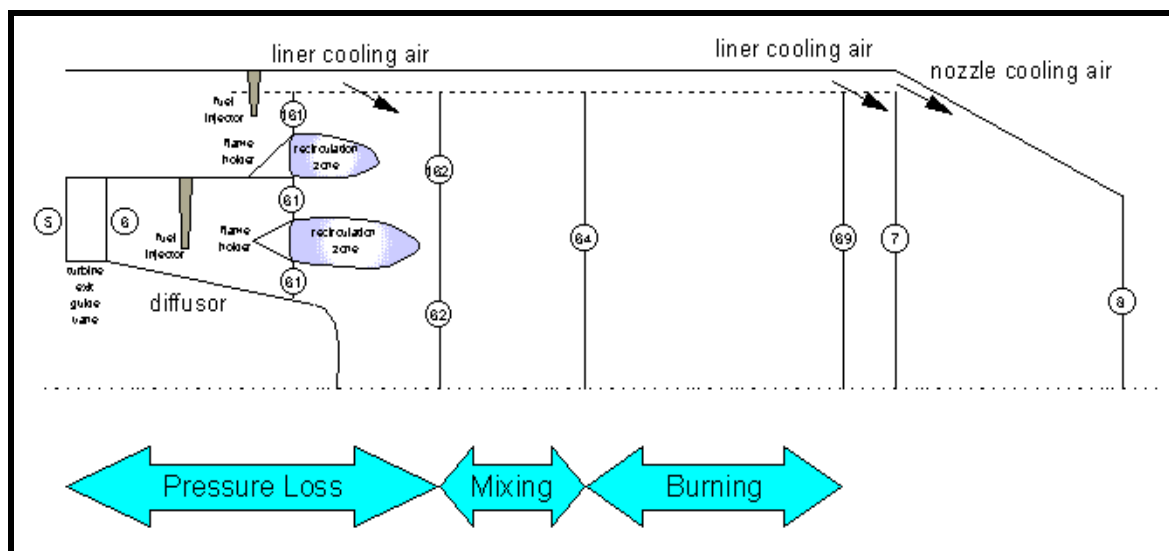


**Figure 4.16: Afterburner Nomenclature.**

For modeling real engines some empirical corrections to the simple static pressure balance assumption are unavoidable. These are dependent on the details of the afterburner design and no generally applicable advice can be given.

When iterating for an off-design operating point, it may happen that the mixer inlet conditions become quite unrealistic, because the operating points in the turbomachinery maps were estimated badly. The mathematical model of the afterburner must be able to cope with these inlet conditions and calculate the *mixing error* in such a way, that the iteration can converge. In other words, the *mixing error* must change continuously when for any fixed core inlet condition the bypass inlet pressure, temperature, and mass flow change from very low to very high. It must also change, when for fixed bypass inlet conditions the core inlet pressure, temperature and mass flow vary from very low to very high values.

### 4.2.4.6 Wet (Burning Operation)

#### 4.2.4.6.1 Ideal Temperature Rise

The ideal temperature rise due to combustion of kerosene with air depends on the air inlet temperature, the injected fuel-air-ratio and the pressure in the combustion chamber. Note that the correlation in [Figure 4.17](#) cannot be applied directly to an afterburner because, at its inlet, the combustion products of the main burner vitiate the air. Nevertheless the figure shows the decreasing return of any additional fuel injection near to the stoichiometric fuel-air-ratio of 0.068.

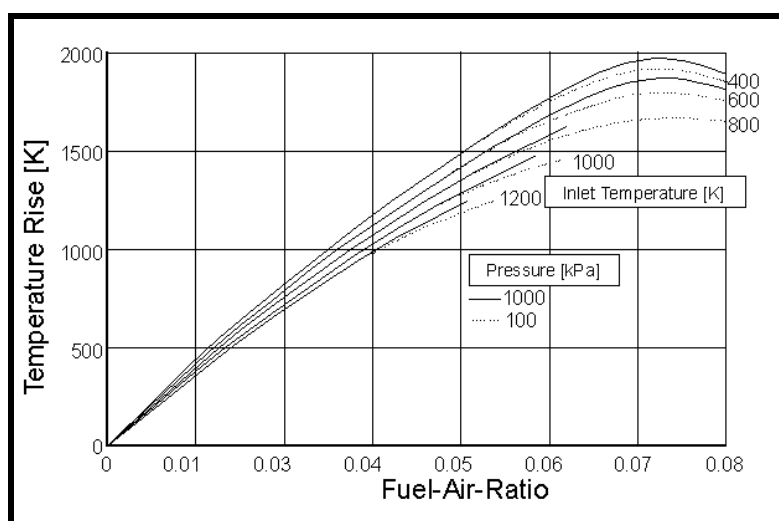


**Figure 4.17: Ideal Temperature Rise.**

When the fuel-air-ratio is over-stoichiometric, any further fuel addition will decrease the afterburner exit temperature. Keep this in mind, when iterating afterburner fuel flow for a specified nozzle inlet temperature: there are two solutions – or no solution at all when the specified temperature is too high.

#### 4.2.4.6.2 Burning Efficiency

Burning efficiency can be defined as the ratio of achieved temperature rise divided by the ideal temperature rise for a given amount of injected fuel. This definition is good in the normal range of fuel-air-ratios, but leads to peculiar numbers for over-stoichiometric cases.

Alternatively, burning efficiency can be defined as the mass ratio of ideally burning fuel divided by injected fuel. With this definition also the over-stoichiometric regime can be handled consistently. However, the question arises, what happens to the unburned fuel?

Burning efficiency depends primarily on the following parameters:

- Fuel-air-ratio;
- Pressure;
- Inlet temperature; and
- Residence time.

There are complex interactions between these parameters. For example, the fuel droplet diameter and the time needed to evaporate the droplets depends on all four of them. The fuel distribution within the afterburner has also a major effect on the burning efficiency.

Many very different attempts to correlate afterburner efficiency with the parameters mentioned above have been published, however, data required to validate these correlations is not available in the open literature.

## 4.2.4.6.3 Fuel Injection

The fuel is injected in a staged manner so that the heat addition rate can be increased gradually from min to max. Because ignition, flame stabilization and flame spreading benefit when the fuel-air-ratio is close to stoichiometric, staging is usually produced by adding fuel to successive annular stream tubes so that the mixture ratio in each tube is approximately stoichiometric.

In the core stream of a bypass engine the burning conditions are better than in the bypass stream, and therefore the fuel is injected into the core stream first.

Any fuel injection starts with a liquid. The evaporation of the fuel will cool the main stream and in a precise simulation this effect should be modeled separately, and not regarded as part of the burning efficiency.

## 4.2.4.6.4 Fundamental Pressure Loss

Adding heat to a flow in a friction-less pipe with constant cross-sectional area causes a loss in total pressure which depends on the inlet Mach number and the temperature ratio  $T_{69}/T_{64}$ , see **Figure 4.18**. This pressure loss can be calculated from the laws of mass flow, energy and momentum conservation. When these basic laws are applied to an afterburner, the fuel mass flow must not be forgotten

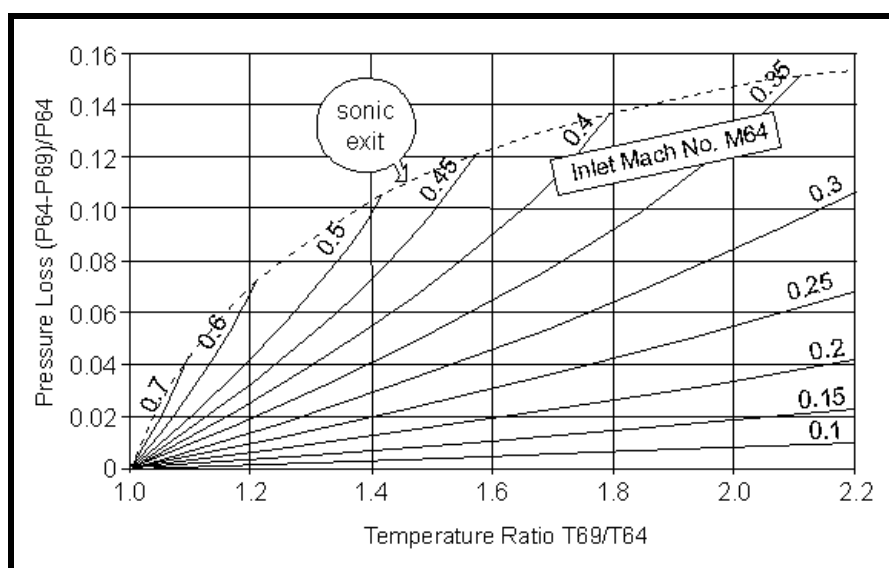


**Figure 4.18: Fundamental Pressure Loss.**

Some afterburners are not designed with a constant cross-section. In such a case a suitable *effective burning area* must be defined for the calculation of the fundamental pressure loss.

#### **4.2.4.7 Flow Distribution and Cooling**

A typical liner requires 8 to 13% of total engine airflow to cool the liner and the nozzle. With a low bypass ratio engine this means, that up to 50% of the bypass air passes behind the liner and does not participate in the burning process.

When the amount of injected fuel is increased from min to max, the afterburner exit Mach number increases, and consequently the static pressure in the jet pipe decreases. The driving pressure ratio of the liner cooling air rises and therefore more of the bypass air passes behind the liner, and less air is left for the burning process.

The nozzle cooling air passes behind the liner and joins the mainstream at the nozzle hinge. When the afterburner is lit, the nozzle cooling air will pick up some heat and therefore the cooling air temperature at the nozzle is higher than at the bypass exit.

The mixing of the liner cooling air with the mainstream is normally modeled neglecting its momentum. The total amount is split in two parts: one part is mixed before, and the rest is mixed after the heat addition calculation.

#### **4.2.4.8 Mixing and Burning**

In reality, the mixing of the core with the bypass stream, and the burning process, happen simultaneously. In the simulation, however, these processes are dealt with separately. At first the fully mixed flow conditions at station 64 are calculated. This gives the burner inlet conditions in terms of mass flow, total temperature, total pressure and Mach number. The ideal temperature rise can then be found taking into account the static pressure  $P_{s,64}$  and the injected fuel-air-ratio. Remember that some of the oxygen in the air has already been consumed in the core engine combustion chamber.

When the burning efficiency is defined as mass ratio of injected fuel over ideally burning fuel then the true temperature rise is the result of this calculation. Otherwise, the true temperature rise is found as a fraction of the ideal temperature rise.

After the temperature rise calculation the second part of the liner cooling air is mixed to the mainstream and yields the afterburner exit temperature  $T_7$ . It is obvious that any number quoted for afterburner efficiency is only meaningful together with a precise description of the liner cooling air model.

#### **4.2.4.9 Test Analysis – Reheat Rig**

For the development of afterburners, special rigs are sometimes designed. The supply of bypass air with appropriate temperature and pressure does not pose too much of a problem. However, the core inlet air must be preheated to turbine exit temperature in a burner, and this requires a smaller fuel-air-ratio than exists at the same location in the engine. Consequently there would be more oxygen available than in the engine when no corrective measures are taken (i.e. injection of steam or nitrogen, for example).

In the analysis of a reheat rig test the nozzle inlet mass flow is well known and the total pressure at this location can be derived from static pressure measurements at the end of the liner. The static pressure pickups can be calibrated with the help of CFD calculations, for example. When the effective nozzle throat area is known, one can calculate the nozzle throat temperature and thus the burning efficiency. Note that this test analysis method requires an accurate measurement of the geometric nozzle area, which is very difficult.

When the burning efficiency found from rig tests is applied within total engine simulations, one should be extremely careful. The numbers quoted for the efficiency depend on the liner cooling air model that is used in the rig test analysis.

#### **4.2.4.10 Test Analysis – Gas Sampling**

Gas analysis is a tool that gives information about local fuel-air-ratios and local efficiency. The measured values are regularly very high, but they cannot be used for performance simulations because the cooling air is not taken into account. Gas analysis is more a tool for checking the fuel distribution and for optimizing the fuel injection system.

#### **4.2.4.11 Test Analysis – Engine Test**

There are two methods to evaluate the afterburner efficiency from measurements taken during an engine test. The first method is the same as already described previously in **Section 4.2.4.9**. Instead of using the nozzle throat area measurement one can alternatively employ the measured thrust to derive the nozzle inlet temperature. This second method requires a high quality simulation of the nozzle performance, because any deficit in the nozzle model will change the numbers evaluated for the afterburner efficiency and may thus give a wrong impression of the afterburner performance.

However, during dry engine tests the nozzle simulation can be calibrated because then the nozzle inlet temperature is known very well. Therefore, a method that uses the measured thrust, to evaluate the afterburner efficiency, should be preferred. A detailed description of an engine test analysis methodology is given for example in the paper by Kurzke (1998) [4.3].

#### **4.2.4.12 Efficiency Correlations**

##### *4.2.4.12.1 One-Stream Models*

In a one-stream model the afterburner combustion process begins with the fully mixed flow conditions in station 64 (see **Figure 4.16**). A part of the liner cooling air has already been mixed with the mainstream. Then the temperature increase and the fundamental pressure loss are evaluated between stations 64 and 69. After that follows the mixing of the rest of the liner cooling air.

There is no way to calculate the afterburner efficiency from theoretical considerations with sufficient accuracy. Therefore only empirical correlations, in which the effects of the following influences must be included, can be used:

- Fuel-air-ratio;
- Inlet pressure; and
- Residence time.

For engines with fuel injection into the bypass stream, the fuel evaporation process has an influence on the afterburner efficiency. This can be taken into account by introducing the bypass exit temperature as an additional parameter.

Instead of the residence time, the inlet Mach number is often used in empirical correlations. From a philosophical point of view this is not correct, because the burning process – a chemical reaction – has nothing to do with the Mach number similarity which describes compressibility effects on a flow-field. In practice, however, since the Mach numbers at these locations are generally very low, the Mach number is proportional to the velocity and thus directly connected to the residence time.

At a given flight condition, the afterburner inlet Mach number is also directly connected with the bypass ratio, which varies with the nozzle throat area. Therefore, in empirical correlations for the afterburner efficiency, one can also use the bypass ratio as a parameter that represents the residence time, as shown in **Figure 4.19**.

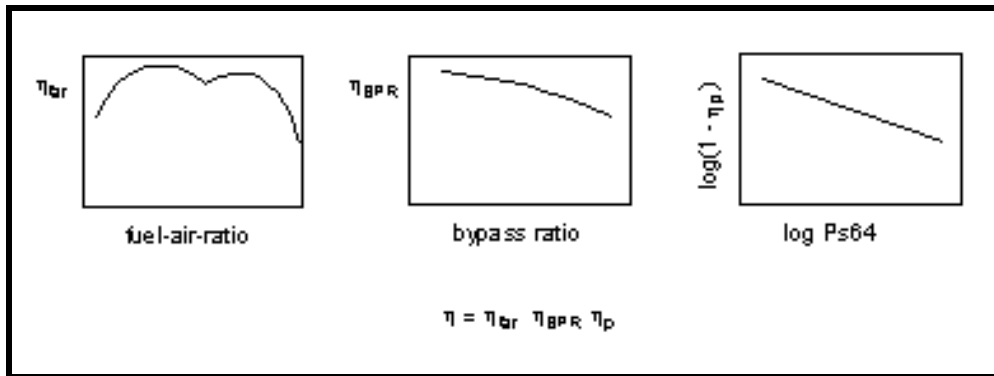


**Figure 4.19: Empirical Efficiency Model.**

#### 4.2.4.12.2 Multi-Stream Models

The conditions for fuel evaporation in particular, for the core and the bypass stream are quite different. This has led to attempts to set up simulation models that differentiate between the processes in several regions of the afterburner. Such models theoretically have the potential to provide more insight into the system. When they are validated, they could be used for optimizing the fuel staging process, for example.

However, the superiority of multi-stream models over the one-stream model described above has not yet been proven with true test data.

#### 4.2.4.12.3 3-D Codes

There exist several commercial codes, as well as company developed computer codes, for the analysis of combustors. These codes give an insight into the flow distribution and the burning process. However, for engine performance simulations they are far too complex.

#### 4.2.4.13 Blow-Out

Blowout occurs when the rate of heat release in the wake of the flame-holder becomes insufficient to heat the incoming mixture to the required reaction temperature. Important parameters are (local) fuel-air-ratio and velocity. A typical flame-holder stability limit is shown in **Figure 4.20**.

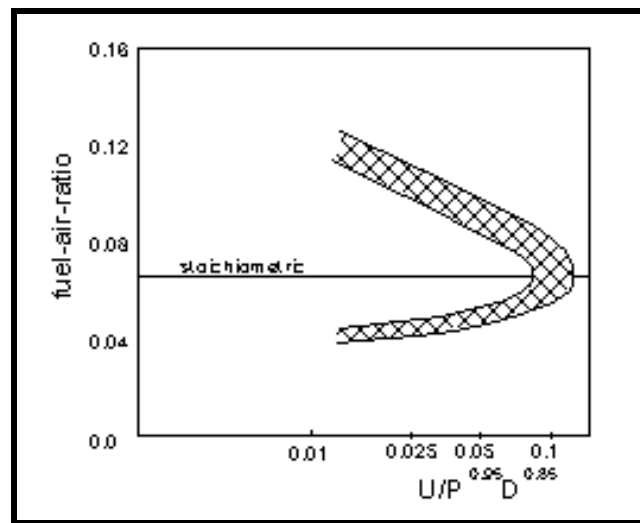


**Figure 4.20: Stability Limits.**

In the flight regime where the fan stream air flow is cold (i.e. 350 – 400 K) and the pressure is low (50 – 100 kPa), that is, in the upper left hand corner of the flight envelope, fuel vaporization is poor. Hence, uniform gaseous fuel-air mixtures are nonexistent, and two-phase mixtures create ignition and combustion problems that may result in rumble blowouts.

#### 4.2.4.14 Screech

Screech is a high frequency pressure oscillation with 1500 – 3000 Hz in radial direction, caused by variations in the heat release process. It can be very destructive to the hardware and must be avoided under all circumstances. The oscillations can be damped, by incorporating a perforated or corrugated shield in the liner just downstream of the flame-holders.

#### 4.2.4.15 Buzz (Rumble)

Rumble is a low frequency (50 – 100 Hz) pressure oscillation in a longitudinal direction caused by intermittent rich extinction. The explanation given in the paper by Hattingh (1993) [4.5] is that locally the flame goes out and a volume of unburned fuel-air mixture travels down the afterburner, explodes at some point and sends a pressure wave upstream. The pressure wave hits the flame-holder and restores light up, due to the higher pressure restoring local combustibility.

Buzz can be a problem when its frequency is in resonance with a low-pressure spool torque vibration mode.

### 4.2.5 Inlets

Inlet models generally define the engine model boundary conditions based on both environmental conditions as well as the pressure loss or flow capacity limitations of the inlet device. These models may also address distortion (both pressure and temperature) or other asymmetric boundary conditions due to the inlet or the environment.

#### 4.2.5.1 Inlet Function

The inlet aerodynamic design characteristics of the powerplant have significant effects on the engine performance and stability and are of vital concern to the engine designer. Inlets are designed to guide required engine flow into the front face of the engine with minimum loss and distortion. For sub-sonic flight

velocity this generally means properly faired inlet surfaces to minimize flow separation. For supersonic flight velocity, the design must minimize losses due to formation of shock waves. In any case to assure engine stability, the inlet design must provide low flow distortion and, in the supersonic case, stable shock structures. The inlet design will also have important effects on overall flight vehicle drag.

The inlet functions as follows in the overall powerplant system:

- It accelerates or decelerates ambient air to the engine forward flange station to achieve the entering flow Mach number that will provide most efficient operation of the engine turbomachinery.
- It is part of the cycle compression process.
- It transforms the dynamic pressure generated by flight velocity to increased cycle static pressure.
- It produces total pressure loss in the outer bypass stream.
- It produces total pressure loss in inner core stream by means of spinner scrubbing.
- It affects distortion entering the engine.
- It affects noise generated by powerplant.
- It contains instrumentation required for power setting and engine control.
- It produces 'spillage drag force' due to non-isentropic effects.
- It produces additional air vehicle drag due to scrubbing and pressure forces generated by free stream flow over the external cowl.

Inlet drag and pressure loss should be faithfully modeled in the engine simulation to calculate accurate average total pressures for the core stream and the bypass stream at the fan inlet face. Clear definitions are required for thrust-drag bookkeeping.

### 4.2.5.2 Inlet Internal Losses: Inlet Recovery

The entering flow stream tube has a stagnation point at the inlet lip. Flow within the stream tube enters the engine and scrubs the inner surface of the inlet creating a boundary layer and reducing the effective total pressure of the flow in the fan tip region. Additional loss due to flow distortion may be generated by inlet lip-separation effects. The flow also scrubs the center spinner producing an additional pressure loss in the core stream. These losses reduce  $P_{12}$  and  $P_2$  at the fan or compressor face inlet, and are correlated for simulation as functions of the corrected airflow. This is shown schematically in **Figure 4.21**.

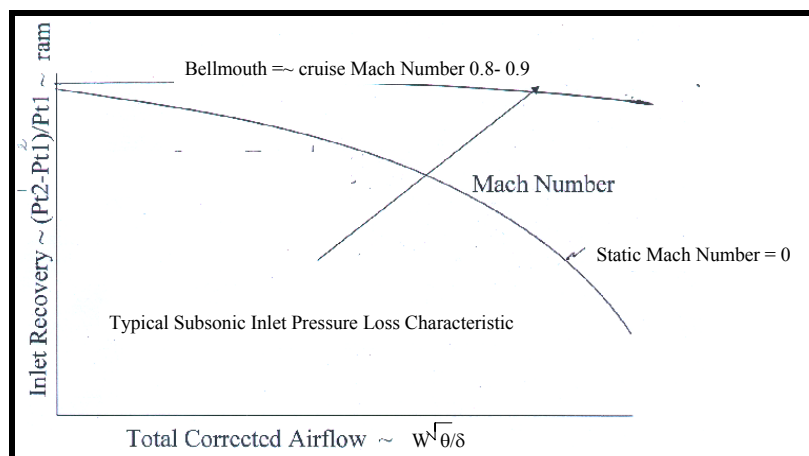


**Figure 4.21: Inlet Recovery Loss.**

## 4.2.6 Exhaust Nozzles

The nozzle exhaust system is a major component of an aircraft gas turbine powerplant. It is the device by which the energy from the gas generator is converted into useful thrust. It has efficiency just like other components. Turbofan and turbojet engines are especially sensitive to nozzle losses because they operate on all of the flow from both airflow and thrust standpoint. Careful design to keep losses low is necessary to achieve goal performance.

The exhaust nozzle component system serves the following functions in the aircraft gas turbine powerplant:

- The exhaust nozzle component contains the exit throttling area (throat) of the powerplant. It meters flow and sets the turbine back-pressure, thereby controlling turbine work. It is one of the primary metering areas in the engine, regulating the cycle. For the case of a dual stream bypass engine, the exit nozzle is the principle controller of the back-pressure to the fan thereby setting fan pressure ratio.
- The nozzle functions as an aerodynamic component that accelerates the gas exiting the turbine to produce thrust from available energy -- states 5 – 6 or 5' – 6' as illustrated in **Figure 4.22**.
- A variable area nozzle plays an important role in providing optimum performance and assuring engine operability. Variable throat area is essential for control of engine matching and fan back-pressure during augmentation.
- A variable geometry nozzle can be designed to generate pitch and yaw forces to control the air vehicle.
- The exhaust nozzle can be designed to produce reverse thrust.

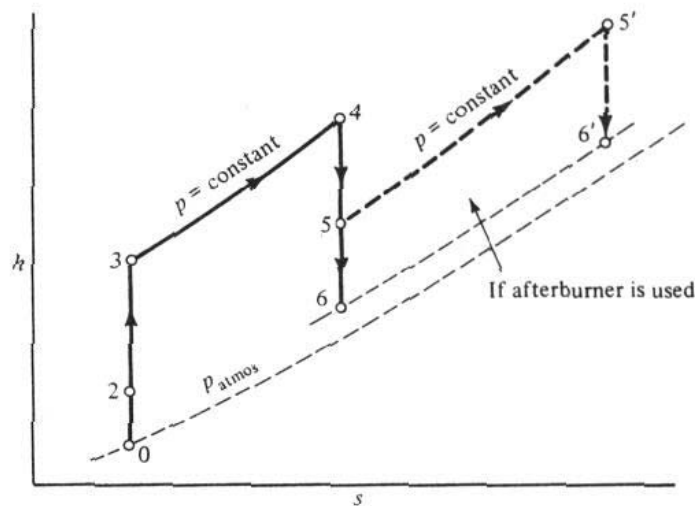


**Figure 4.22: Energy Available to Produce Thrust from Thermodynamic Cycle.**

The exhaust nozzle is generally represented like other flow restriction devices except for the special relation to thrust calculation and assumptions that can be made concerning choked flow or compatibility condition implied by the expansion to ambient conditions. Most nozzle representations that include detailed thermodynamic properties enforce frozen composition in the supersonic section downstream of the nozzle throat.

When noise is an issue, the nozzle model will generally include additional jet velocity and ejector mixing calculations.

## 4.2.7 Splitters and Mixers

### 4.2.7.1 Splitters

Splitter models are often simple bookkeeping models and require no more component-modeling effort than for simple ducts. The flow split will be iterated to match continuity conditions elsewhere in the simulation. An exception is when the splitter model is related to upstream or downstream systems. A common example is the behavior of the splitter downstream of a fan component. Here the flow split or bypass ratio may affect the fan performance via the relative axial location and other geometry details. For models addressing hail or rain ingestion, modeling of the splitter effect on capture of the liquid/solid particles is the primary driver in determining engine operability limits.

### 4.2.7.2 Mixers

Mixers are employed with high bypass turbofans for thrust increase and for noise reduction. In low bypass engines there is a mixing of two streams within the afterburner. In both cases the flow conditions within the mixer will have a dominating effect on the matching of the two spool speeds of a turbofan.

The thrust improvement due to mixing of two streams ideally – i.e. without friction pressure losses – depends on the difference in total temperature. When both streams have the same total temperature then there will be no thrust gain.

**Figure 4.23** shows the ideal thrust gain by mixing two streams with equal total pressure.

When the mixer is applied to a turbofan engine then at cruise the ideal gain in net thrust is typically twice as big as shown in the figure because 1% change in gross thrust is equivalent to 2% in net thrust.

Mixers, like any other component, perform less than ideally in practice. To fully mix two confluent streams needs a long pipe. When forced mixers (chutes) are applied, the required length becomes shorter. In practice, confluent mixers achieve about 20 – 30% mixing and forced mixers approximately 60 – 80%. Moreover, the mixing process and the additional wall friction cause total pressure losses that decrease the benefit of mixing.

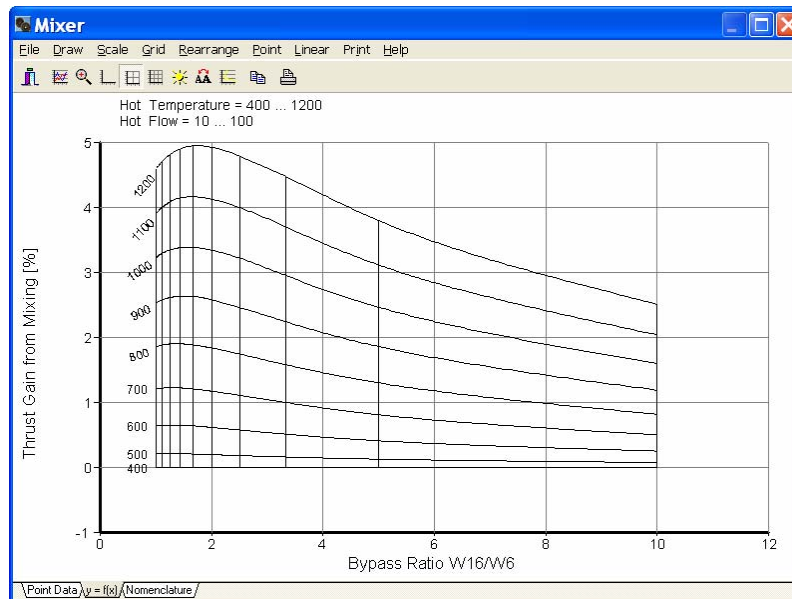


**Figure 4.23:** Thrust Gain from Ideal Mixing of Two Streams with Equal Total Pressure.

## 4.2.7.2.1 Definitions

We have spoken of the degree of mixing without defining what we mean with that term. For performance simulations the degree of mixing is defined through thrust:

$$\eta_{mix} = \frac{F_g - F_{g,unmixed}}{F_{g,fullymixed} - F_{g,unmixed}} \quad \text{Eq. 4-19}$$

The evaluation of the thrust for unmixed and ideally mixed streams must be based on a clear definition. **Figure 4.24** shows the nomenclature that we will use here.

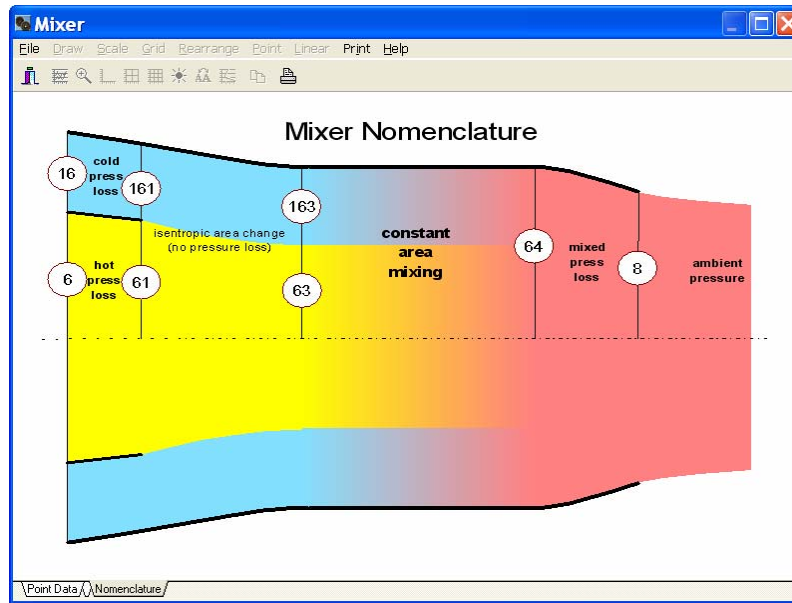


**Figure 4.24: Mixer Nomenclature.**

The ideal mixer has no pressure losses from stations 6 to 61, 16 to 161 and 64 to 8. At station 64 both streams are fully mixed and expand as a single stream without any losses through the nozzle, which might be convergent or convergent-divergent.

The total pressure and temperature of the cold stream in station 163 are the same as at station 16 and the equivalent is true for the hot stream. The ideal mixing is taking place in a frictionless duct with constant area. The following laws of physics are applied:

### Conservation of Mass:

$$W_{63} + W_{163} = W_{64} \quad \text{Eq. 4-20}$$

### Conservation of Energy:

$$W_{63} * H_{63} + W_{163} * H_{163} = W_{64} * H_{64} \quad \text{Eq. 4-21}$$

### Conservation of Momentum:

$$W_{63} * V_{63} + P_{s,63} * A_{63} + W_{163} * V_{163} + P_{s,163} * A_{163} = W_{64} * V_{64} + P_{s,64} * A_{64} \quad \text{Eq. 4-22}$$

The mixing shall take place in a duct with constant area, which gives us two more correlations:

$$A_{63} + A_{163} = A_{64} \quad \text{Eq. 4-23}$$

$$P_{s,63} = P_{s,163} \quad \text{Eq. 4-24}$$

This system of equations can only be solved by iteration.

When the flow is expanded from the conditions at station 64, through the nozzle, we will get the thrust for the fully mixed flow.

The thrust which could be developed by expanding the hot flow from station 6 through the same type of nozzle is called the *hot* thrust  $F_h$ . Similarly the cold stream expanded from station 16 yields the *cold* thrust  $F_c$ . The unmixed thrust is the sum of  $F_h$  and  $F_c$ .

## 4.2.7.2.2 Pressure Loss

The loss in total pressure, due to mixing without friction pressure loss, is shown in **Figure 4.25** for the same conditions as in **Figure 4.23**. The total pressures of both streams are the same at the inlet to the mixer.

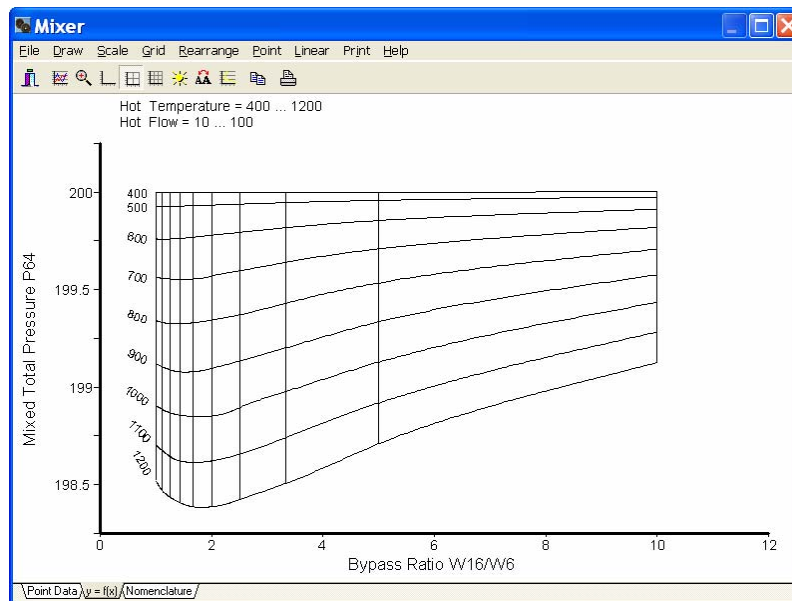


**Figure 4.25: Total Pressure after Mixing Two Streams with Equal Pressure (200 kPa).**

When the total pressures in both streams are different, then in most cases the pressure at station 64 will be between  $P_{16}$  and  $P_6$  and there is no simple way to quantify the pressure losses due to ideal mixing. However, the change in thrust gain due to ideal mixing is a good measure for the influence of the total pressure imbalance at the entrance to the mixer. In **Figure 4.26** we see from an example with  $T_{16} = 400$  K and  $T_6 = 1200$  K, that any deviation from equal pressures at the inlet will reduce the ideal thrust gain due to mixing.

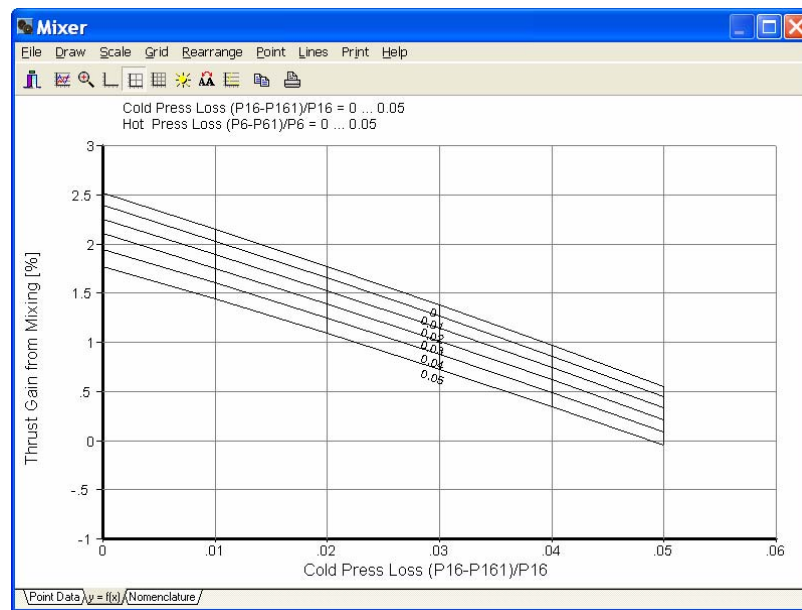


**Figure 4.26: Effect of Friction Pressure Losses on the Thrust Gain Due to Mixing.**

Unequal total pressures at the inlet to the mixer can cause significant reductions in the thrust gain potential of mixers. Note that in a bypass engine the pressure ratio  $P_{16}/P_6$  will increase when the engine power is reduced. Therefore, the aerodynamic design point of a mixer should normally be at values of  $P_{16}/P_6$  between 0.9 and 0.95.

During all previous discussions we have assumed that there are no friction losses. In reality, these obviously must be taken into account. In **Figure 4.26** (With the assumptions: equal total pressures  $P_6 = P_{16} = 200$  kPa at the mixer inlet,  $T_{16} = 400$  K and  $T_6 = 1200$  K, bypass ratio = 5, mixing efficiency = 70%,  $P_{amb} = 101.325$  kPa) the effect of cold and hot friction pressure losses on the thrust gain are shown. It becomes obvious from that figure, that friction pressure losses above approximately 1% in the bypass stream will decrease the benefit of a mixer in such a way, that the weight of the mixer is not justified from a performance point of view. Losses in the hot stream have less effect in this example with bypass ratio 5, because they affect only the smaller mass flow.

### 4.2.7.2.3 Thrust Gain of Real Mixers

In a practical mixer we will not achieve a fully mixed flow. As mentioned above, in confluent mixers we will get typically 25% and in mixers with chutes roughly 70% of the ideal thrust gain.

We have not yet mentioned the effect of nozzle pressure ratio on the performance potential of a mixer. During cruise with a subsonic high bypass engine, the nozzle flow will be sonic ( $P_8/P_{amb} > 1.85$ ), while during take-off the nozzle pressure ratio will be significantly lower. As can be seen from **Figure 4.27** this will again reduce the potential thrust gain due to mixing.

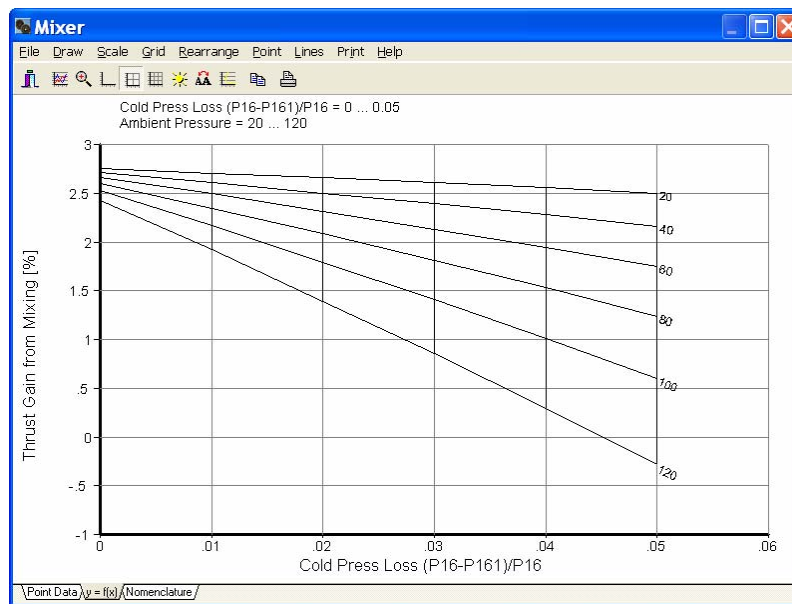


**Figure 4.27: Effect of Nozzle Back Pressure on Theoretical Thrust Gain ( $P_8 = 200$  kPa).**

In a practical mixer with chutes, the real thrust gain due to mixing will be very small for take-off conditions, and typically 1 to 2% during cruise.

#### 4.2.7.2.4 Flow Coefficients

Any flow coefficient is defined as ratio of the area needed for a mass flow at given total pressure, temperature and total-static pressure ratio, and the geometrical area through which this flow passes. Generally, flow coefficients are described by empirical correlations with geometry and total-static pressure ratio.

There are three places in a mixer where flow coefficients must be taken into account. These are the cold and the hot mixer areas  $A_{161}$  and  $A_{61}$ , and the nozzle area  $A_8$ . The upstream conditions for the cold and hot mixer inlet areas are clearly defined and the pressure ratios  $P_{161}/P_{s,163}$  and  $P_{61}/P_{s,63}$  can be easily evaluated.

The situation for the nozzle is different. The total pressure  $P_8$  at the inlet to the nozzle is only clearly defined when the two streams are fully mixed. For partially mixed flow there is no generally accepted procedure available for the calculation of the mean total pressure at the inlet of the nozzle.

Any formulae that employ the degree of mixing, for the calculation of the nozzle inlet pressure, are not fully satisfactory because the degree of mixing is defined as a thrust ratio. Thrust, however, is dominated (at a given pressure ratio) by the velocity term and thus by the temperature of the fluid, not by the total pressure.

The dilemma with the total pressure downstream of a practical mixer can be bypassed, if the nozzle discharge coefficient is defined in such a way that the ideal flow through the nozzle is calculated from the total pressure of a fully mixed flow.

#### 4.2.7.2.5 Thrust Coefficient

The thrust gain (or loss) due to partially mixing two streams can be described with the help of the *degree of mixing* as defined above. That requires three nozzle thrust calculations: two for the unmixed streams

and one for the fully mixed stream. In each of these nozzle calculations, one applies a coefficient that takes care of nozzle thrust losses, to the one-dimensional calculation result.

In principle, with this approach we use two additive thrust corrections within the calculation.

Alternatively one can use the fully mixed flow as a reference, do the nozzle calculation only once and afterwards apply an empirical correction factor. This is equivalent to the standard procedure for any turbo-machine, where we do an isentropic calculation first, and then apply an efficiency to correct the result. Such an approach eliminates any debates about the nozzle inlet total pressure for partially mixed flow.

#### *4.2.7.2.6 Static Pressure Balance*

When two parallel streams are mixed then there will be equal static pressures in both streams. This fact is used within any custom cycle calculation for mixed flow turbofan engines, as a condition for finding the match of the low and high-pressure spool speeds.

In real engines the flow in both streams will not be exactly parallel. However, this is mostly neglected and it is postulated in **Figure 4.23**, for example, that the static pressure  $P_{s61}$  equals  $P_{s161}$ .

For high bypass engines with corrugated or confluent mixers the simple static pressure balance is fully appropriate. In low bypass engines with afterburner, however, the complex flow in the region of the flame-holders can cause a local static pressure imbalance. The cycle match of such an engine must employ some empirical corrections to the conventional static pressure balance assumption.

#### *4.2.7.2.7 Mixer Test Analysis*

The analysis of mixer-component tests is rather difficult because the thrust differences between alternative configurations are rather small. For more details see Rowe, 1982 [4.6]. Comparing various mixer designs with the help of engine tests is extremely difficult. The reason is, that there are not only differences in the degree of mixing, but also (at least potentially) in the effective areas at the mixer inlet and the nozzle. These differences will cause the engine to rematch and this in turn will cause a change in fan efficiency, for example. In the end, the engine with the superior mixer design might have a poorer SFC because its effective areas are not correctly matched to the cycle.

### **4.2.8 Ducts**

Most component-based engine models include a large number of identified stations within the engines. Many of these differ only by a pressure loss or a simple extraction of flow that is not explicitly modeled. These pressure loss models are usually modeling a friction loss (Fanno line) process or a loss due to sudden expansion, separation or even an un-modeled low level mixing process. Often these are modeled as an empirical function of velocity head or flow Mach number. Most models are explicit, based only on entrance quantities and thus do not require a compatibility condition closure like nozzles, compressors and similar component models.

If flow in the duct can be choked in any operating regime of interest, this is no longer true. The duct model must address this choking and the simulation must address the implied compatibility condition or the simulation must be configured to address or avoid the issue. For higher fidelity models, the duct model must address the transfer and modification of the more detailed entrance conditions as well as the higher fidelity modeling of the processes inside the duct.

### **4.2.9 Customer Bleeds and External Loads**

Most component-based engine models include the direct effect of bleed between components as a standard feature. For empirical models, the greater the flexibility in bleed level and location, the more tables or

correlations are required to achieve the desired effects. Internal bleed must consider the impact on component performance and the method of determining the conditions of the bleed air. In trying to match bleed supply conditions to user requests, a single bleed location may not be adequate. Bleeds from multiple locations may be selected or mixed to create the required bleed with minimal impact on the overall engine performance.

External load models are generally fixed or simple relationships, and are treated by simply including them as one of the power-outputs from the rotating shaft. For some applications, these models become more complicated and are included as part of the basic engine simulation. This is particularly true where control systems are part of the model and customer load affects the ability to maintain the required conditions.

### **4.3 NON GAS PATH COMPONENT CHARACTERISTICS REQUIRED BY ENGINE MODELS**

#### **4.3.1 Lubrication and Fuel Systems**

In models where the fuel and lube system fluid conditions are of interest, these components are modeled similarly to other components except for the use of a non-air working fluid. Most performance simulation applications are not interested in these internal details. In these, fuel and lubrication systems are often empirically modeled as parasitic loads, even in fairly detailed models. In models where conditions in the engine are dramatically affected by these loads, or where the secondary systems interaction are of interest, more detailed models of the pumps and processes in these systems may be required. These models typically include pumping losses (e.g. parasitic losses) modeled as a function of fluid viscosity. Accurate modeling of these losses is particularly important for transient models that are used to predict starting and free windmilling characteristics. This is particularly important for high altitude and cold day operation, where these losses are a larger percentage of output power.

#### **4.3.2 Thermal Management Systems**

Military aircraft often have fairly extensive arrangements to reject excess heat from the aircraft and aircraft sub-systems. The engine can be part of this process, and engine models are used in optimizing these systems.

Apart from the turbine, which requires significant attention in terms of managing the cooling flows necessary to maintain component temperature levels, many other parts and systems in a gas turbine engine require management of thermal properties. There are several parts which, without special measures, would get overheated and fail. The major function of the oil system is cooling of bearings; many other parts are cooled by secondary airflows. Fuel often has to be heated to maintain favorable viscous and lubricious properties and to prevent ice formation in the fuel system, or used as a heat sink for excess heat loads. On some classes of aircraft, such as supersonic transports, rising fuel temperature may limit flight duration.

Models of these subsystems interact with the flowpath component models as required to calculate the effect on component performance and to estimate temperatures at key locations.

Separate dedicated models are also used to analyze cooling system performance. These models include heat generation sources in the engine, fuel heaters, oil coolers, fuel-oil heat exchangers and fan air flow models for air coolers. **Figure 4.28** shows a Fokker100/RR Tay engine heat management system model in Simulink. This is used for analysis of cooling performance during engine and aircraft transients. The results were used for preliminary sizing of heat exchanger components.

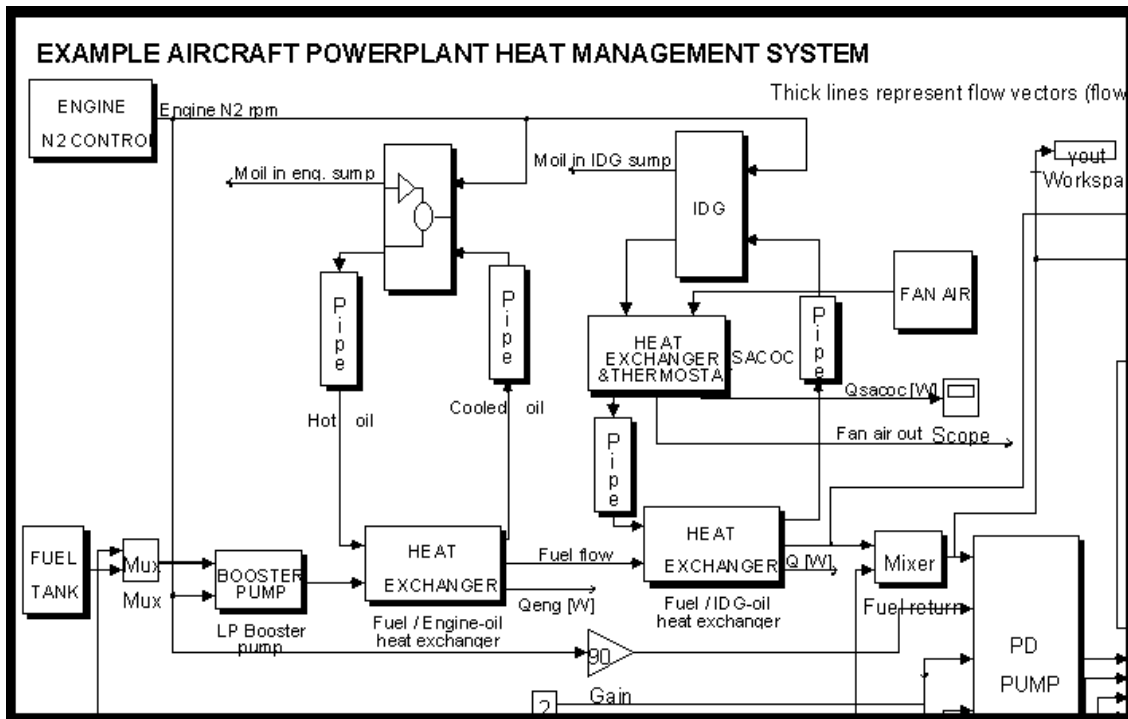


Figure 4.28: Simulink Powerplant Heat Management System Model (top level).

### 4.3.3 Heat Exchanger

Heat exchanger components in gas turbine cycle models are used to simulate components that are meant to transfer heat into or out of the gas path at some point in the cycle. Most common are heat exchangers such as recuperators or intercoolers.

For a cycle model, primarily overall heat exchanger performance is relevant, including the amount of heat transferred from one medium or heat source to another. Efficiency of the process usually is expressed with “Effectiveness” which is defined as the ratio of actual heat transfer rate  $Q$  and the maximum heat transfer that would technically be possible given the media inlet temperatures.

#### 4.3.3.1 Steady State Heat Exchanger Performance

Usually, heat exchangers in gas turbines are of the counter-flow type for maximum effectiveness. The equations for the effectiveness efficiency of a two counter-flow heat exchanger are:

$$Eff = \frac{C_{hot} \cdot \frac{T_{t_{in\_hot}} - T_{t_{out\_hot}}}{T_{t_{in\_hot}} - T_{t_{in\_cold}}}}{C_{min}} = \frac{C_{cold} \cdot \frac{T_{t_{out\_cold}} - T_{t_{in\_cold}}}{T_{t_{in\_cold}} - T_{t_{in\_hot}}}}{C_{min}}$$

with :

$$C_{hot} = C_{p_{in\_hot}} \cdot W_{in\_hot} \quad ; \quad C_{cold} = C_{p_{in\_cold}} \cdot W_{in\_cold}$$

$$C_{min} = MIN(C_{hot}, C_{cold}) \quad ; \quad C_{max} = MAX(C_{hot}, C_{cold})$$

$$Rc = \frac{C_{min}}{C_{max}}$$

Eq. 4-25

The attraction of using Effectiveness is that if the inlet temperatures and flow rates of both flows are known, the exit temperatures and heat transfer rate can be directly calculated. For a first order approach analysis, with no specific heat exchanger data, a constant effectiveness may be used, representing a typical state-of-the-art value for a particular type of heat exchanger. For detailed analysis, an effectiveness map for a specific heat exchanger may be used. This map usually represents effectiveness as a function of  $C_{hot}$  and  $C_{cold}$  or  $W_{hot}$  and  $W_{cold}$ .

After calculating the enthalpies  $H$  from the temperatures  $T$  at the entry- and exit stations of one of the flows, the heat transfer rate  $Q$  can be calculated:

$$Q = W_{cold} \cdot (H_{out\_cold} - H_{in\_cold}) \quad \text{where } H = F(Tt, \text{GasComposition}^1) \quad \text{Eq. 4-26}$$

In a cycle model, somehow a design point heat transfer rate  $Q_{des}$  must be defined. This can be done either by directly specifying  $Q_{des}$  or specifying temperature deltas, exit temperatures or effectiveness values. In either case, the design point  $Q_{des}$ ,  $Eff_{des}$  and exit temperatures can all be calculated using:

*for counterflow :*

$$Q = Eff \cdot C_{min} \cdot (Tt_{in\_hot} - Tt_{in\_cold}) \quad \text{Eq. 4-27}$$

so :

$$Eff = \frac{Q}{C_{min} \cdot (Tt_{in\_hot} - Tt_{in\_cold})}$$

Since effectiveness can be expressed as a function of heat exchanger entry temperatures only, off-design heat flux is calculated directly from a given off-design Effectiveness using **Eq. 4-27**.  $Eff$  is directly user specified or obtained from a map. An effectiveness map represents  $Eff$  depending on the flow 1 and 2 heat capacity rates  $WCp1$  and  $WCp2$ .

Depending on the interaction of the heat exchanger with the cycle, the heat exchanger operating point adds equations to the set of equations representing cycle off-design performance. For an intercooler for example, no equations are added since the coolant flow does not directly interfere with the gas path flow. However, for a recuperator, heat is transferred from one point in the gas path back to an upstream point in the gas path, which means that at least one equation is required to satisfy the energy balance in the recuperator. An extra state variable (extra unknown in the set of equations) must be added also, being part of the solution representing a valid operating point found by the solver.

Pressure losses in the flow passages usually are significant. Moreover, for transient performance analysis, with the usually large internal volume and mass of heat exchangers, volume and heat soakage effects are very significant. Therefore, heat exchanger models usually include models for pressure loss, volume and heat soakage effects.

#### 4.3.3.2 Heat Exchanger Transient Simulation

Heat exchangers in the gas path have several specific effects on transient performance. Especially with recuperators, heat soakage effects of the wall between the flows usually are significant and may well cause instabilities during severe accelerations or decelerations without special control system logic. Also volume

<sup>1</sup> This is the more exact version of the approximate calculation of heat flux using constant  $Cp$ :

$$Q = W \cdot Cp_{cold} \cdot (Tt_{out\_cold} - Tt_{in\_cold})$$

effects may be significant if the internal volumes are relatively large. Heat soakage effects of the outside walls usually are small, i.e. similar to other gas path components.

## 4.3.3.3 Heat Soakage Effect Models

An example of a 0-D heat soakage effect model for the wall between the gas flows is the GSP (NLR Gas turbine Simulation Program, [4.7]) recuperator model. Similar to the external ‘insulated wall’ heat sink model, the heat exchanger wall heat sink model is based on a first order lag behavior of the average temperature of the material. The difference is that now there are heat fluxes from both sides of the wall and also there is heat flux during steady state (this is not the case with the external insulated wall heat sink model used in other components like turbines and combustors for example).

## 4.3.3.4 Recuperator Internal Wall Heat Soakage Effect Model

The steady-state temperature of an insulated wall simply is equal to the gas temperature and also is uniform at steady-state. However, the steady-state temperature of the heat exchanger inside wall material is not uniform and normally has a value between the average temperatures of the two media flows. This average steady-state wall material temperature needs to be calculated and fed to a first order lag transfer function to obtain the actual average wall temperature. The actual heat soakage effect is then represented by the net heat flux into or out of the wall material, which is proportional to the rate of change of the average wall temperature.

Consider **Figure 4.29** displaying the temperature patterns in the flows from average flow temperature to the wall temperature.

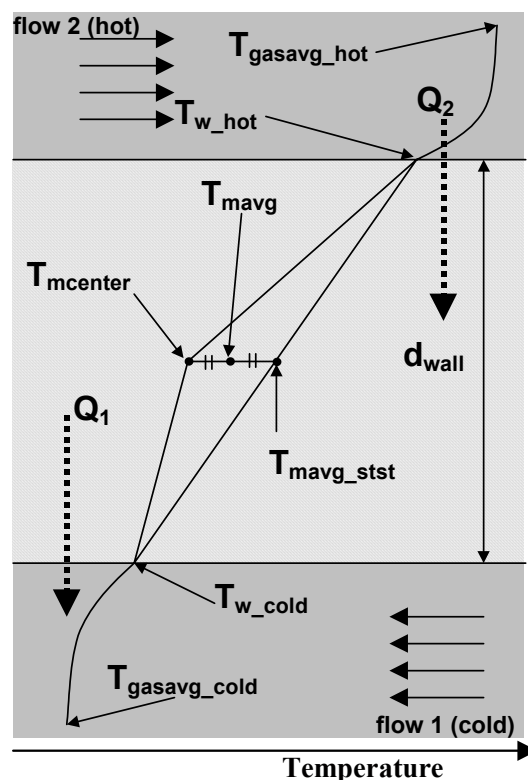


**Figure 4.29:** Internal Wall Heat Soakage Effect Model.

The temperature pattern in the wall is linear according to the relation for heat flux through a uniform material with conductivity  $K$ :

$$Q = A_{eff} \cdot \frac{K_{wall}}{d_{wall}} \cdot (T_{w\_hot} - T_{w\_cold}) \quad \text{Eq. 4-28}$$

At steady state,  $Q$  also needs to satisfy the equations for heat flux from the flows into the wall:

$$Q = A_{eff} \cdot U_{hot} \cdot (T_{gasavg\_hot} - T_{w\_hot}) = A_{eff} \cdot U_{cold} \cdot (T_{gasavg\_cold} - T_{w\_cold}) \quad \text{Eq. 4-29}$$

$A_{eff}$  is assumed equal for hot and cold sides. With a uniform wall material specific heat capacity  $Cp_{wall}$  and conductivity  $K_{wall}$ , during steady state, the average wall material temperature will be equal to  $T_{mavg\_stst}$ . During a transient, average gas temperatures and flow rates change, and the average temperature level of the wall material will change to a new level, with a certain time lag depending on the total wall material heat capacity and effective area. In view of the high gas flow rates, the effect caused by the heat capacities of the flows themselves is ignored. This assumption may cause some increase in error if one of the flows is completely shut off, resulting in a gradual change in temperature of the medium towards the other flow's inlet temperature. However, for most cases, taking only the wall heat soakage effect into account is considered sufficiently accurate for gas turbines. This assumption also applies to the external wall heat soakage effect (or 'insulated wall') model.

#### 4.3.3.4.1 Steady-State Average Wall Temperature

The average steady-state wall temperature  $T_{mavg\_stst}$  is calculated as the average of the wall temperatures  $T_{w\_hot}$  and  $T_{w\_cold}$  according to **Figure 4.29**. For calculation of  $T_{w\_hot}$ ,  $T_{w\_cold}$ ,  $T_{gasavg\_hot}$  and  $T_{gasavg\_cold}$ , the number of transfer units NTU value is calculated (note that  $0 \leq Rc \leq 1$ ):

$$NTU = \frac{\ln\left(\frac{Eff - 1}{Eff \cdot Rc - 1}\right)}{1 - Rc} \quad \text{Eq. 4-30}$$

$$\text{in case } Rc = 1: \quad NTU = \frac{Eff}{1 - Eff}$$

NTU here represents steady-state heat transfer performance. From NTU, UA can be derived:

$$UA = NTU \cdot C_{min} \quad \text{Eq. 4-31}$$

UA represents the total heat transfer coefficient and the log mean average temperature difference between the two flows then is:

$$dT_{gaslnavgstst} = UA/Q_{stst} \quad \text{Eq. 4-32}$$

From  $dT_{gaslnavgstst}$  and the known entry and exit temperatures of the two passages, two temperatures must be determined representing the average gas temperatures at the hot and cold sides of the heat transfer model ( $T_{gasavg\_hot}$  and  $T_{gasavg\_cold}$ ). Note that these are the actual GSP calculated entry and exit temperatures based on the actual heat flux state variables  $Q1$  and  $Q2$ , which include the heat soakage effect. This means that  $T_{mavg\_stst}$  represents the temperature level that the wall material would obtain for a given  $Q1$  and  $Q2$ . In reality however,  $Q1$  and  $Q2$  will change towards a steady-state value  $Q_{stst}$  eventually. In effect, an overall heat transfer coefficient UA is used based on steady-state effectiveness

data and this UA is used to calculate the wall temperatures  $T_{w\_hot}$  and  $T_{w\_cold}$  from the transient heat fluxes  $Q_1$  and  $Q_2$ .

The difference between the average temperatures  $(T_{in}-T_{out})/2$  of both flows is usually close but not exactly equal to  $dT_{gas,navgstst}$ . These must be corrected to exactly obtain  $dT_{gas,navgstst}$  as a difference between  $T_{gas,avg\_hot}$  and  $T_{gas,avg\_cold}$ .

Now  $U = UA/A_{eff}$  and for the overall specific heat coefficient  $U$  also the following relation applies:

$$\frac{1}{U} = \frac{1}{FC_{cold}} \cdot \frac{d_{wall}}{K_{wall}} \cdot \frac{1}{FC_{hot}} \quad \text{Eq. 4-33}$$

The film coefficients  $FC$  determine heat transfer between the gas and the wall. For the engine design point a ratio for the two  $FC$  is given (default = 1), so with  $U$  then the design point  $FC$  values can be calculated.

For off-design  $FC$ , the following equation is used, derived from a relation for turbulent flow Reynolds numbers obtained from ref. 2 (this equation is the same as that used for the insulated wall heat soakage effect model):

$$\frac{FC}{FC_{des}} = \frac{Cp}{Cp_{des}} \cdot \left( \frac{W}{W_{des}} \right)^{0.8} \quad \text{Eq. 4-34}$$

Now the steady state wall temperatures can be calculated using:

$$\begin{aligned} T_{w\_hot} &= T_{gas,avg\_hot} - \frac{Q_{stst}}{FC_{hot} \cdot A_{eff}} \\ T_{w\_cold} &= T_{gas,avg\_cold} + \frac{Q_{stst}}{FC_{cold} \cdot A_{eff}} \end{aligned} \quad \text{Eq. 4-35}$$

Note that the difference between  $T_{w\_hot}$  and  $T_{w\_cold}$  is proportional to  $Q_{stst}$  according to **Eq. 4-35**.

In case the flow 1 or flow 2 value for  $FC$  becomes zero (flow rate zero) the wall temperature is set equal to the temperature of the other flow (the flow medium is entirely assuming the flowing medium's entry temperature and there is no steady state heat flux).

Next the steady state average wall material temperature is calculated:

$$T_{m,avg\_stst} = \frac{(T_{w\_cold} + T_{w\_hot})}{2} \quad \text{Eq. 4-36}$$

#### 4.3.3.4.2 Transient Average Wall Temperature

A simplified approximation of the transient wall temperature profile may be represented by  $T_{w\_hot} - T_{m,center} - T_{w\_cold}$  as indicated in **Figure 4.29**. This 'linearized' profile implies all wall heat capacity is concentrated in the centre and the material between the centre and the wall has no capacity and only conducts heat from wall to centre. It is easy to derive that the actual average wall temperature representing the wall heat content then is calculated using:

$$T_{\text{mavg}} = \frac{(T_{\text{mcenter}} + T_{\text{mavg\_sst}})}{2} \quad \text{Eq. 4-37}$$

The rate of change in wall heat content dQ is equal to:

$$dQ = h_m \cdot A_{\text{eff}} \cdot (T_{\text{w\_hot}} - T_{\text{mcenter}}) + h_m \cdot A_{\text{eff}} \cdot (T_{\text{w\_cold}} - T_{\text{mcenter}}) \quad \text{Eq. 4-38}$$

with :

$$h_m = \frac{K_{\text{wall}}}{(D_{\text{wall}}/2)}$$

Eq. 4-38 can be worked into

$$dQ = 4 \cdot h_m \cdot A_{\text{eff}} \cdot (T_{\text{mavg\_sst}} - T_{\text{mavg}}) \quad \text{Eq. 4-39}$$

Since dQ in effect is the net heat flux into the material also the following equation applies (with  $C_{p_{\text{wall}}}$  and  $M_{\text{wall}}$  for wall specific heat and mass respectively):

$$dQ = \frac{\partial T_{\text{mavg}}}{\partial t} \cdot C_{p_{\text{wall}}} \cdot M_{\text{wall}} \quad \text{Eq. 4-40}$$

Eq.4-39 and Eq.4-40 can be combined into the linear differential equation for the average wall material temperature:

$$\frac{\partial T_{\text{mavg}}}{\partial t} = \frac{4 \cdot h_m \cdot A_{\text{eff}}}{C_{p_{\text{wall}}} \cdot M_{\text{wall}}} \cdot (T_{\text{mavg\_sst}} - T_{\text{mavg}}) \quad \text{Eq. 4-41}$$

Eq. 4-41 represents a first order lag system with time constant Tau:

$$Tau = F_{\text{tau}} \cdot \frac{C_{p_{\text{wall}}} \cdot M_{\text{wall}}}{4 \cdot h_m \cdot A_{\text{eff}}} \quad \text{Eq. 4-42}$$

$F_{\text{tau}}$  is a user specified factor with a default value of 1 (see below).

With Tau, now dQ becomes:

$$dQ = \frac{F_{\text{tau}}}{Tau} \cdot C_{p_{\text{wall}}} \cdot M_{\text{wall}} \cdot (T_{\text{mavg\_sst}} - T_{\text{mavg}}) \quad \text{Eq. 4-43}$$

$T_{\text{mavg}}$  now is calculated by integrating the first order lag system, using a 1<sup>st</sup> order lag transfer. Using Eq. 4-37, then  $T_{\text{mcenter}}$  can be calculated.  $T_{\text{mcenter}}$  is a purely theoretical value that is not used in the calculation.

The actual heat fluxes at the cold and hot sides into the material are calculated as follows, by correcting the steady state heat flux  $Q_{\text{sst}}$ , that is calculated using Eff as described above. Note that  $Q_{\text{sst}}$  is positive for heat flux from hot to cold flow and  $Q_1$  and  $Q_2$  are positive if adding heat to the gas flow:

$$\begin{aligned} Q_1 = Q_{hot} &= -Q_{stst} - \frac{dQ}{2} \\ Q_2 = Q_{cold} &= Q_{stst} - \frac{dQ}{2} \end{aligned} \quad \text{Eq. 4-44}$$

The deviation  $dQ/2$  of  $Q_1$  and  $Q_2$  from  $Q_{stst}$  represent the transient heat soakage effect of the heat exchanger wall. It is assumed the total heat soakage effect heat flux  $dQ$  is equally distributed to both flows, which is in accordance to the simplified temperature profile in [Figure 4.29](#).

The average heat exchanger wall temperature time constant factor  $F_{\tau}$  can be changed from the default 1, to adapt the transient heat soakage effect. The value 1 represents the case where all material heat capacity is concentrated in the centre of the wall, which in reality is not the case. The factor may well be decreased to lower values like 0.5, representing a distribution of the heat capacity towards the gas wall boundaries, resulting in faster response of the wall temperature (and smaller heat soakage effects). Also, the presence of fins on the walls can be expressed by lowering the time constant factor (effective area  $A_{eff}$  is the effective *plate surface* area excluding fins and should not be adapted for this purpose). Increase of the factor above 1 is not representing a physical meaning and therefore not recommended.

The GSP heat exchanger wall heat sink model is capable of accurately simulating heat exchanger wall heat soakage effects on gas turbine performance. It has limited accuracy in terms of representing the actual heat transfer process as such in detail and should not be used for that purpose.

## 4.3.4 PowerTrain

Typically, modeling of the power train for steady state operation is done simply by the use of a parasitic load loss function that represents the losses associated with the transfer of mechanical power from the turbine shaft to an external load via a gearbox. In the case of a lubricated gearbox, the losses may be modeled as a function of the viscosity of the lubricating fluid. For transient operation, modeling of these losses become increasingly complex as the losses may be a function of operating shaft speed. An added complexation for modeling of transient performance is the incorporation of a clutch model. This is of interest for such events as engine starting.

### 4.3.4.1 Clutch Models

A clutch is an unusual element in a gas turbine drive train system. However, there are a number of applications, where the load needs to be coupled and uncoupled from a gas turbine drive shaft during operation. In these cases, a clutch is required to allow smooth transition from the uncoupled state to the fully coupled state and vice versa, without excessive torque loads on the shafts due to high acceleration rates.

Examples of clutches in gas turbine drive trains may be found in vehicular turboshaft engines, helicopter drive trains and STOVL propulsion systems using liftfans driven by the main engine LP shaft.

In general, a clutch is a device that is able to transfer a certain (limited) amount of torque between two shafts. Several systems exist to transfer the torque including wet and dry friction plate systems and a variety of hydraulic systems (e.g. torque converters, hydro-motors). For analysis of system performance, the clutch model minimally needs to accurately represent the torque transferred. If clutch performance also itself requires scrutiny, more detailed models may well be required. This section describes the clutch model as implemented in GSP, [\[4.7\]](#), with calculation of torque transmission, clutch state and friction heat production.

## COMPONENT MODELING FOR SYSTEM MODELS

---

For the clutch model, a number of terms/parameters are introduced to determine the state of operation of the clutch.

- **Engagement Status:**

A clutch can be fully engaged or disengaged. If fully engaged, it is able to transfer maximum torque capacity; if fully disengaged, usually no torque is transferred unless some sort of residual friction loss is defined in the model. An 'engagement variable' (or engagement factor) is used, ranging from 0 to 1. 0 is fully disengaged, 1 means fully engaged.

- **Locked/Unlocked Status:**

If a clutch is locked, both shafts run at the same rotor speeds and the clutch functions as a coupling. In this case, the torque transferred does not exceed maximum static torque capacity. If the clutch is unlocked, both shafts are not running equal speeds. There is a case where the clutch is unlocked at equal speeds, but this only can occur during a very short time of transition between the locked and unlocked states, or when at least one shaft is accelerating 'past' the other shaft speed.

- **Static Torque Capacity:**

Static torque capacity is the maximum torque the clutch can transmit in the locked state. This means the friction surfaces do not move (relative to each other) and the static friction coefficient applies. Static torque capacity always is equal to or larger than dynamic torque capacity.

- **Dynamic Torque Capacity:**

Dynamic torque capacity is the maximum torque the clutch can transmit when it is unlocked, i.e. rotor speeds are not equal and the friction surfaces are moving relative to each other, so the dynamic friction coefficient applies. Dynamic torque capacity always is equal or smaller than static torque capacity.

- **Torque Demand:**

Torque demand is the torque that would be transmitted in the locked state. It can also be described as the torque that would exist in the shaft if maximum torque would be infinite and no slipping would occur.

- **Slipping:**

The clutch is slipping if the two rotor speeds are unequal and engagement is larger than 0. Torque required exceeds maximum dynamic torque capacity and therefore cannot fully be transmitted. This means friction heat is produced proportional to the torque (engagement x maximum dynamic torque) and the delta in rotor speeds.

The operation mode of interest with a clutch model is transient. For steady-state simulation, either the fully engaged or disengaged state must be assumed. For system modeling environments, this means that the reference (usually design) point state also either is fully engaged or disengaged. Prior to a transient simulation, then a fully engaged or disengaged state must exist.

For a particular clutch, a static and dynamic maximum torque must be specified. The engagement factor  $F_{\text{engagement}}$ , ranging from 0 at disengagement to 1 at full engagement, determines the actual torque capacity as a fraction of maximum torque.

The engagement factor during a transient simulation can either be obtained from user-specified time functions or result from a control system model output. With a clutch control model, accurate simulation of clutch performance in complex systems, including closed loop controlled engagement, can be performed.

Friction heat production due to clutch slipping is calculated, and with more data an accurate heat flow and conduction model can be added to analyze local heat loads and temperature levels during and after successive engagement events.

One of the challenges in modeling clutch engagement or disengagement transients is to determine whether static or dynamic maximum torque is applicable. In other words: is the clutch in a locked state or is it slipping. In the transient simulation this means the model algorithm needs to keep track of the clutch state (locked or not) history during transient simulation, i.e. save the clutch state of the prior time step. The state of the prior time step then determines whether dynamic or static maximum torque applies. For example, during a transient starting with a locked clutch but increasing torque demand, at some point this torque will exceed maximum static torque and the clutch will unlock and start slipping.

After the time step where the unlocking has been determined, the lower level of dynamic maximum torque applies, and the clutch can only lock again after the torque demand will drop below dynamic maximum torque. If torque demand fluctuates around maximum static torque levels, severe transient load effects on the clutch can be simulated. In this case however, small time steps will be required to accurately represent rapid transient effects.

In **Figure 4.30** the flow chart for the basic elements of the algorithm is shown. Starting at particular state at time  $t$ , actual static and dynamic torque depending on maximum torque capacities and the engagement factor are determined and also the rotor speed  $\Delta N$  (difference in rotor speeds) is determined.

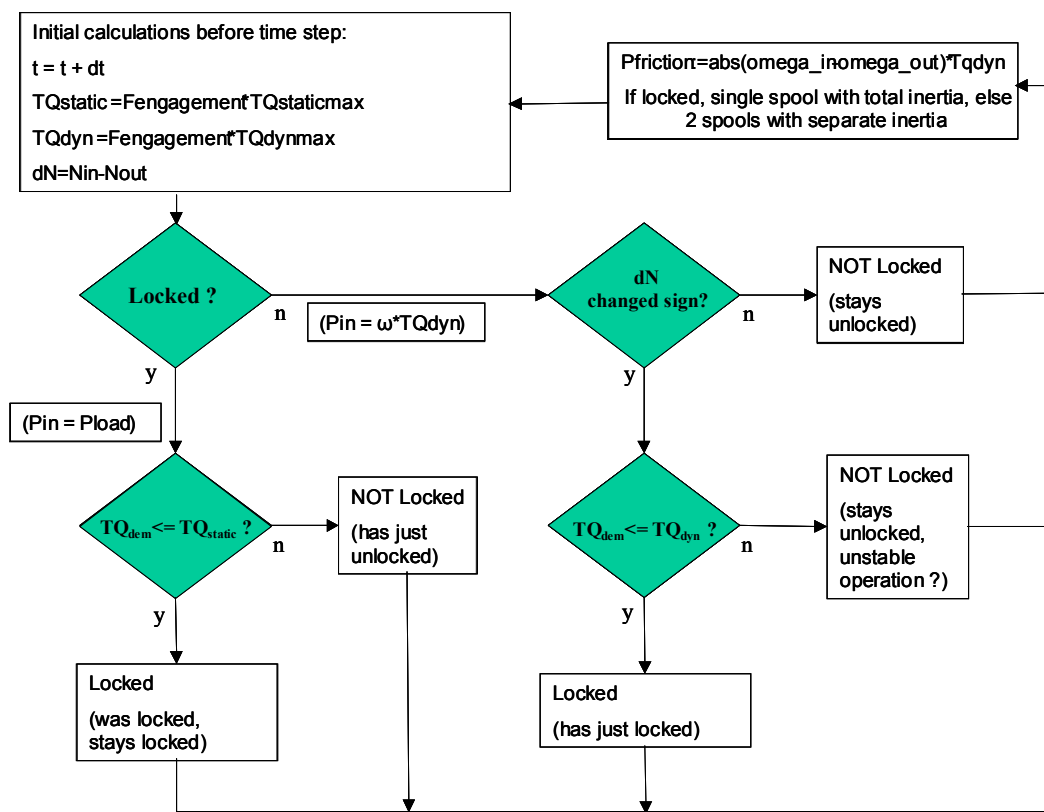


**Figure 4.30: Clutch Model Algorithm.**

Next the algorithm continues evaluating the Locked state at the prior time step ("Locked?" decision box) and then determines the new Locked state of the current time step depending on  $dN$  and the demanded

torque  $T_{Qdem}$ . There is a special case (where unstable operation may be suspected) and that is when the clutch was not Locked,  $dN$  changes sign (so the rotor speeds have been equal at some point during the last time step but locking could not be established due to excessive torque demand).

After the locked state of the new time step is determined, friction power  $P_{friction}$  can be calculated and also the distribution of inertia over the shafts can be determined. These inertia values are used when integrating rotor acceleration (at every time step) of either 2 separate shafts (unlocked) or a single shaft with the sum of 2 inertias (locked state). Furthermore, depending on the detail of the model more additional clutch data can be calculated.

In GSP, [4.7] an example is given of simulation of a turbofan driving a STOVL lift-fan through a clutch. The lift-fan is driven by the main engine fan shaft through a dry clutch that is able to disengage the Lift Fan from the engine during normal forward flight and engage during vertical flight modes.

**Figure 4.31** shows clutch parameter responses versus time for lift-fan engagement (starting at 0.2 s) and disengagement (starting at 2 s) at 100% main engine N1. The top graph shows clutch engagement in terms of (dynamic friction) torque capacity. Next actual torque delivered to the lift-fan and the heat dissipation ( $P_{friction}$ ) during clutch slipping are shown.

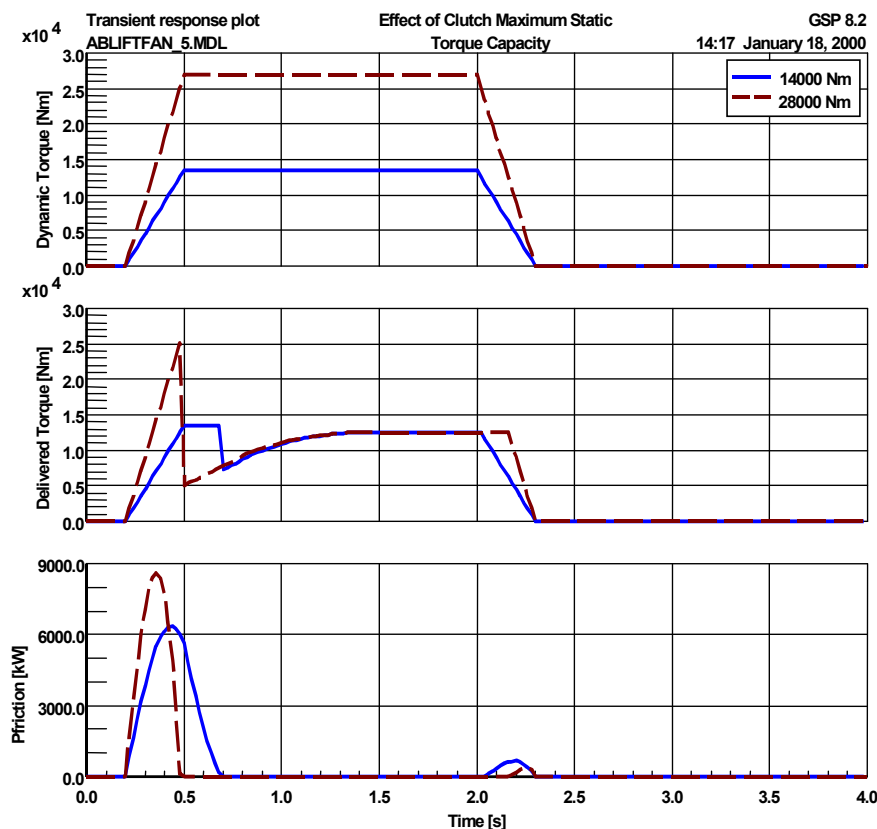


**Figure 4.31: Lift-Fan (Dis)Engagement Clutch Response.**

**Figure 4.32** shows the rotational speeds of the lift-fan and the engine fan in a single graph, effectively summarizing rotor speed and clutch performance histories.

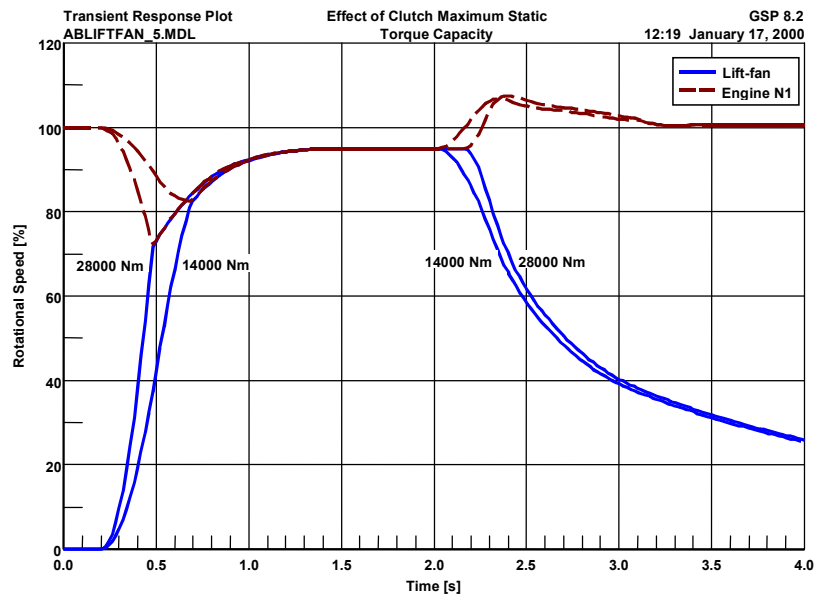


**Figure 4.32: Lift-Fan (Dis)Engagement Lift-Fan and N1 Response.**

## 4.3.4.2 Loads

There are many different types of loads, depending on the gas turbine application. For example:

- Generator for electrical power generation;
- Accessory gearbox; and
- Main transmission gearbox and rotary wing (helicopter) applications.

Accessory gearboxes drive such components as cooling fans, pumps and starter motors.

There are different levels of fidelity that can be used to model loads; from a simple constant power extraction to a more complex map for a cooling fan helicopter rotor. These models are usually provided by the load device manufacturer. They convert load demand (e.g. electrical power, mechanical power) into resisting torque or power extraction that applies to the gas turbine cycle.

Typically, load demand requirements that the gas turbine supplies for the customer's specific application change with engine power output.

Mission profiles are defined that provide typical engine power output requirements as a function of operational environment and operating mode (i.e. output power level). Mission profiles enable that analysis of:

- Life duration estimates for critical engine components; and
- Calculate tip clearance excursions for turbine and compressor and verify adequate margins throughout the flight regime.

Transient analysis must be performed in the event of a load shed event. The most severe of which would be due to a break of the power shaft. Transient simulations are used to design control systems to prevent rotor speed excursions that could damage gas turbine hardware. In cases of electrical power faults, inertia of the generator is still present so the overspeed threat is less.

### 4.4 REFERENCES

- [4.1] Society of Automotive Engineers Aerospace Standard AS755 Rev C, Aircraft Propulsion System Performance Station Designation and Nomenclature, December 1997.
- [4.2] Recommended Practices for the Assessment of the Effects of Atmospheric Water Ingestion on the Performance and Operability of Gas Turbine Engines, AGARD AR-332, 1995.
- [4.3] Kurzke, J. and Riegler, C., "A Mixed Flow Turbofan Afterburner Simulation for the Definition of Reheat Fuel Control Laws", RTO Symposium on Design Principles and Methods for Aircraft Gas Turbine Engines, Toulouse 1998.
- [4.4] Egan, W.J. and Shadowen, J.H., "Design and Verification of a Turbofan Swirl Augmentor", AIAA 78-1040, 1978.
- [4.5] Hattingh, H.V. et al., "The Design and Development of an Afterburner", ISABE 93-7041, 1993.
- [4.6] Rowe, R.K. and Kuchar, A.P., "Energy Efficient Engine, Scaled Mixer Performance Report", General Electric Company, NASA CR-167947, 1982.
- [4.7] Visser, W.P.J. and Broomhead, M.J., "GSP, A Generic Object-Oriented Gas Turbine Simulation Environment", ASME Paper # 2000-GT-2, May 2000.

## Chapter 5 – EXAMPLES OF 0-D NUMERICAL SIMULATIONS

### INTRODUCTORY COMMENTS

In the following sections, examples are given of engine simulation environments:

- A conventional FORTRAN based modeling system architecture;
- The MOPS and MOPED modeling systems;
- The GasTurb modeling architecture;
- The GSP object-oriented modeling architecture;
- TERTS, a thermodynamic real-time gas turbine modeling environment;
- Simulation models for engine diagnostics; and
- Other 0-D modeling systems.

### 5.1 A FORTRAN-BASED MODELING SYSTEM

In this modeling system, the engine is viewed as a set of interconnected gas flow passages, while engine component models are represented by subroutines. The major part of the definition of the engine performance is obtained from knowledge of the conditions pertaining at a number of engine stations in the gas flow. At each station, an array of gas conditions in terms of fuel-air ratio, mass flow, pressure, temperature, etc. is defined and used to pass information from one component to the next. The architecture is modular and provides a flexible tool to model a variety of gas turbine configurations. However, the **FORTRAN** language has limited capabilities to apply modern software development methodologies such as object orientation, modern data organization, databases and graphical user interface features.

The advantage of FORTRAN is that it is still the standard and, if no platform specific code such as user-interface shells are included (which often is the case for a command line interface), may be compiled and run on most platforms.

#### 5.1.1 Architecture

**Figure 5.1** shows the elements of the modeling system. The subroutine containing the definition of the engine is a small part of the total infrastructure. Each element is discussed below.

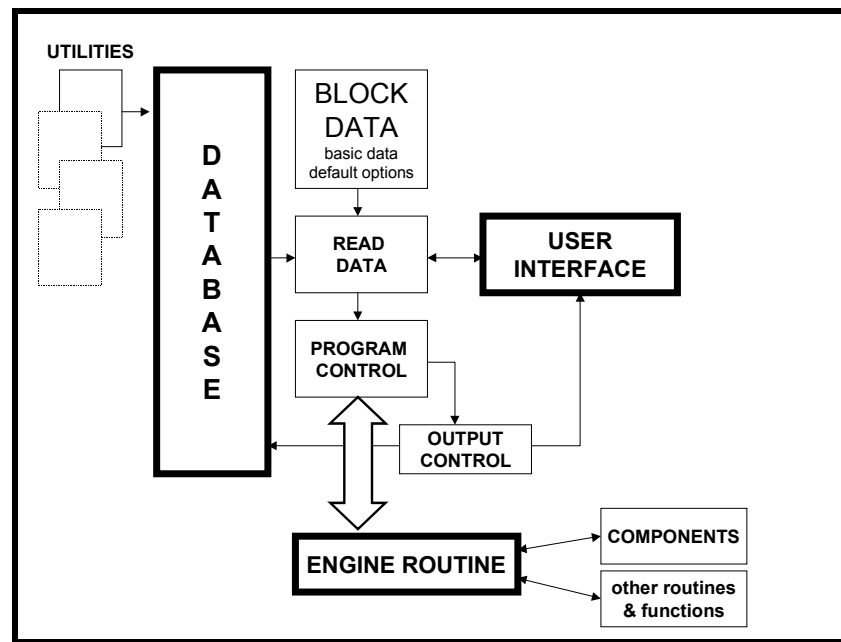


**Figure 5.1: FORTRAN Modeling Procedure.**

### 5.1.2 Database

This is not strictly part of the modeling system but a fundamental part of the Information Technology (IT) electronic infrastructure. It holds functional engine data, which is used for model definition, and also receives and stores data generated by the model. It also holds engine test data, which is required as program input for model-based analysis. Security features are essential on any database for model input or output data.

### 5.1.3 Utilities

Common utilities include data visualization (plotting, tabulation), data maintenance (deletion, addition, grouping, security), data manipulation (creation, formatting of graphical functions, etc.) and output definition (creation and storage of instruction sets for standard output formats).

### 5.1.4 Block Data

Associated with an engine-modeling program is a set of data which underpins the basic program structure, and which is independent of the standard of engine being modeled. Default options (controlled by data switches) can be set up in this dataset which is compiled with the engine routine (see below).

### 5.1.5 User Interface

The user communicates with the engine program via standard **AS681 [5.1]** interfaces and – if working in-house – by lower-level program input stores for greater flexibility. The user supplies the following information:

- Engine model (i.e. what particular standard of engine is required to be run);
- Additions to default thermodynamic definitions;
- Enabling/disabling of user options within the program or modeling system;

- Definition of points/maneuvers to be modeled (at a particular flight case or flight profile);
- Definition of output format (may include post-processing); and
- Definition of interfaces to other sub-system models (e.g. control-system) – if required.

Some of these options may not be available to some users, especially if the model is issued externally (i.e. as a customer ‘deck’).

### **5.1.6 Read Data**

The data is pulled in from the various sources: database, user, block data and presented to the program.

### **5.1.7 Program Control**

The call is made here to the engine subroutine.

### **5.1.8 Engine Routine**

This is the heart of the system. Here, the structure of the engine is defined in terms of its flow path, which is modeled at whatever detail is appropriate for the program’s application. The engineer-programmer is provided with a data structure built around the station and component subroutine structure. The engine is viewed as a set of interconnected gas flow passages, and a major part of the definition of the engine performance is obtained from knowledge of the conditions pertaining at a number of stations in the gas flow. Each station is defined in terms of fuel-air ratio, mass flow, pressure, temperature, velocity, area, flow function, etc.

Some stations may be defined as total stations in which case velocity and area terms are zero. Other stations, e.g. associated with pressure losses or mixing, may be defined as static stations in which case the pressure and temperature terms will be static values associated with the specified area or velocity. Calculations of other parameter values can be added as required.

Thus stations are handled as vectors of information. **AS755**, [5.2] is an internationally recognized standard for station numbering. Whereas this nomenclature appears on the program standard output, the programmer is given flexibility within his own program to use whatever definition is convenient.

Several FORTRAN arrays are available to the programmer. These can be used for internal working and program interfaces. The system makes use of COMMON blocks for ease of communication between different subroutines. The program structure is largely constructed to reflect the physical layout of the engine. Standard subroutines are used, with customizing being required to handle data transfer and different user options.

### **5.1.9 Components**

Component subroutines are grouped into classes such as intakes, compressors, combustors, turbines and nozzles. Although not strictly components, the following are treated as such because they follow a similar ‘control volume’ construct:

- Pressure changes;
- Multi-stream mixing; and
- Bleed network (secondary air-system).

For each class of component, several options exist within each subroutine. For example, a pressure loss may be defined in many ways. The component-subroutines model the steady-state performance of the feature.

## EXAMPLES OF 0-D NUMERICAL SIMULATIONS

---

The dynamics associated with heat-transfer (to and from the blades and casings), shafts (conservation of angular momentum) and gas dynamics (conservation of gas steam mass, energy and momentum) are handled in separate subroutines.

### 5.1.10 Other Routines and Functions

Performance programs are required to generate steady-state solutions. Dynamic/transient simulation (i.e. over a time base) is a fairly straightforward extension of the steady-state modeling principle, and so the level of thermodynamic detail is consistent with the steady-state solutions. A suite of routines, which uses an enhanced Newton-Raphson method, controls the iteration. Limits on certain parameters can be defined and the condition requested (by the user) may be overridden. In such a case, the limiting is flagged to the user. Where a control-system model is run alongside the engine model, this internal limiting action is muted.

Iteration also gives the flexibility to specify the engine operating level in an abundance of ways. Rather than specifying just the level of the ‘true’ engine input parameters such as fuel and nozzle area, the power level can be defined as a level of thrust with a specified fan surge-margin (for example). Iteration is also used in a wider sense – around the whole engine model – to vary selected component assumptions (efficiencies, flow capacities, pressure losses, etc.) to match selected model outputs to measured engine data. This process is known as AnSyn, Analysis by Synthesis, (see *Chapter 3, Section 3.2.7.3*).

Other subroutines include:

- Local, single variable iteration;
- Graph read; and
- Obtain gas or fluid properties.

The above are used within or without the component modules.

### 5.1.11 Output Control

**Figure 5.2** shows the standard output, which may generated per point. When all that may be needed is a plot of thrust vs. SFC for a series of points up a running range, such a comprehensive output may be too cumbersome. In such cases, selected parameters can be identified and extracted to the database for plotting later. Some customization of the full output is possible. Each section of the output is mutable, or may be embellished with station descriptors in plain (perhaps project-specific) nomenclature. To display a small subset of the data, an expert user may configure a summary section. Special diagnostics may be required for problem tracing, and these can either be appended to the basic output or diverted to a separate output channel.

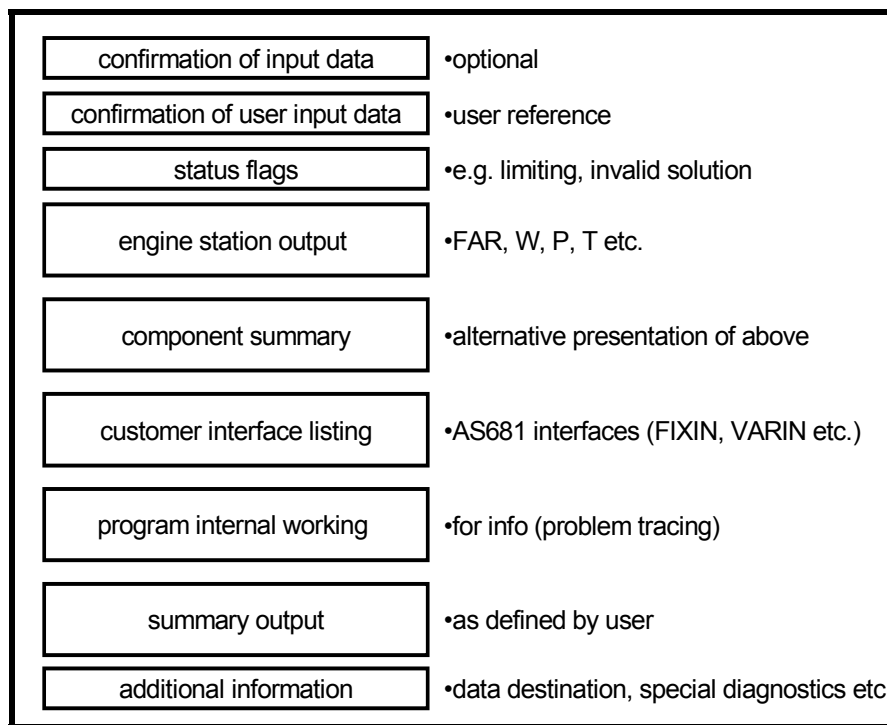


**Figure 5.2: Standard Output Format.**

Of particular importance are the status flags, which are generated to alert the user of particular program operations. These flags could indicate an invalid solution (for example if the iteration failed to converge), limiting to a condition, exceeding a limit (internal to the engine, or at a flight case level, e.g. outside normal flight envelope), invalid program input, etc. Such status flags (numerical status indicators), are generated at system level or at engine subroutine level by the engineer-programmer.

### 5.1.12 Future Developments

FORTRAN is an old computing language with limited capability especially in I/O and data organization areas. The system described above is easily envisaged in a more modern language such as C++. This would allow a true object-oriented approach and compatibility with modern computing platforms featuring graphical user-interfaces (GUIs). This said, C++ appears to have limited advantage over FORTRAN as far as the mathematical constructs required to model gas-turbine engines are concerned. A hybrid approach is feasible, and is inevitable in the short-to-medium term.

## 5.2 MOPS (MODULAR PERFORMANCE SYNTHESIS PROGRAM) OR MOPEDS

Another example with a focus on flexibility is MTU's in-house performance program MOPS (Modular Performance Synthesis Program), [5.3]. Its development started in the early 80's, and the program is presently extended to be a multi-disciplinary pre-design tool. In the beginning FORTRAN IV was used, and later FORTRAN 77. Recently added options make use of the new data structures offered by FORTRAN 90. MOPS architecture is schematically presented in **Figure 5.3**.

## EXAMPLES OF 0-D NUMERICAL SIMULATIONS

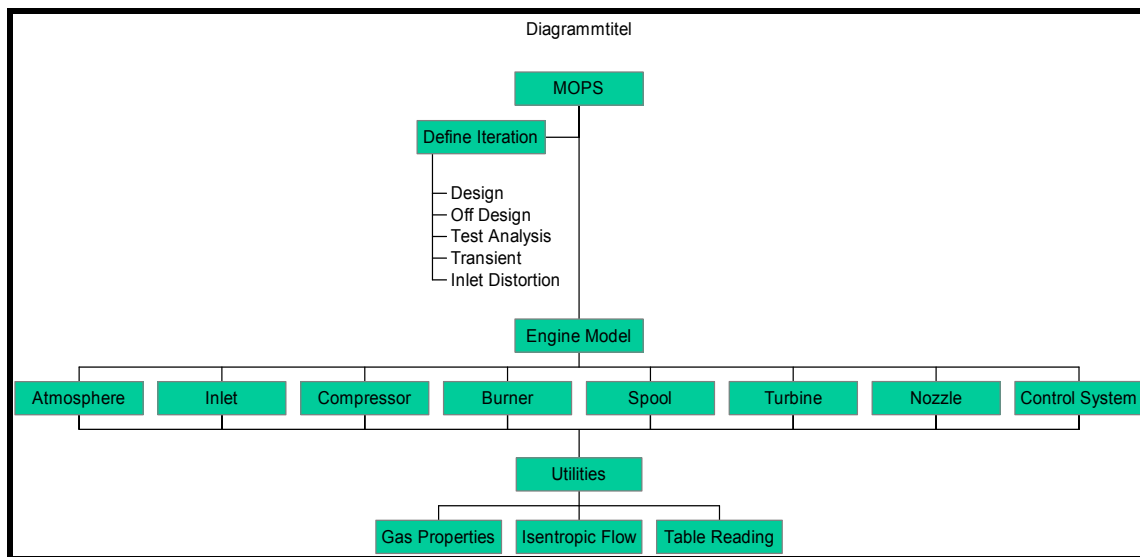


**Figure 5.3: MOPS Architecture.**

MOPS is used for a wide variety of tasks, including engine test analysis, cycle design studies, off-design and transient simulations. Moreover, MOPS is the basis for all computer decks issued by MTU.

Before actually using the program, the engine configuration must be defined with the help of a special pre-processing program. In this pre-processing the user composes his engine from modules that can be connected in any sequence. In most cases, a module is directly representing an engine-module like a compressor or a turbine. Besides the turbo-machine modules there are also other modules like ducts, shafts, control units, etc.

The primary connection between the modules is the main gas stream, and secondary connections are the shaft power transfer between modules, internal air system paths, heat transfer, control sensor signals and position commands.

The program modules are strictly isolated from each other. Normally, they can only communicate via their primary and secondary connections. The program internal nomenclature follows the **ARP 755** standard and all calculations are done in SI units. There is a sophisticated error message system built into the program, and in most cases standardized diagnostic methods allow the reason for any problem that may arise to be found rapidly.

The user has to set up an iteration scheme, which is specific for his engine configuration and the task to be performed. There are variables to be selected and errors to be defined. For example, in a mixed flow turbofan design task, the bypass ratio may be used as a variable and the difference in static pressure between core and bypass flow may be treated as the corresponding error.

Typical turbofan simulations for cycle design tasks employ iteration schemes with only a few variables, while test analysis by synthesis tasks can require over 50 variables.

Setting up the iteration scheme requires a thorough background of gas turbine theory. This is a certain disadvantage, but on the other hand, with MOPS, gas turbines of arbitrary complexity can be simulated.

MOPEDS is an extension of the in-house performance program, MOPS, and shares its program structure. Performance programs deal with all-engine effects so that their program structure generally is well suited

for such a task and the thermodynamic performance is always the backbone for any preliminary design. It was therefore obvious to base MOPEDS on MOPS. A description of MOPEDS is offered below [\[5.4\]](#).

### ***Description of the Application***

During the preliminary design phase the main parameters of the engine are set. The decisions made at that time determine most of the risks and financial resources associated with the development, manufacturing and operation of the gas turbine under concern. The preliminary design process must be carried out very quickly so that engine suppliers are able to evaluate numerous concepts with respect to the market requirements in a short time.

The preliminary design of a new engine starts with the evaluation of various thermodynamic cycles. Finally the cycle is fixed in such a way that all requirements are met at the relevant operating points of the flight mission of an aircraft, for example. Subsequently all engine components are designed aerodynamically and mechanically with respect to a good matching of the components, well behaved off-design characteristics over the whole mission, low cost, ease of manufacture, reliability, noise legislation, emission regulation, etc.

### ***Modeling Techniques Utilized***

This preliminary design task has led to the main features of MOPEDS (**MO**dular **P**erformance and **E**ngine **D**esign System), MTU Aero Engines' software package for the preliminary design:

- All major engine components and their interrelations are assessed;
- The most relevant disciplines are considered;
- Component design is may be done at various operating points; and
- Model fidelity zooming for selected components is feasible.

The program structure forms a matrix whose columns represent the engine components, whose rows represent the disciplines, and whose elements are defined to be modules (see [Figure 5.4](#)). Effectively, each module is a subroutine with a standardised interface that contains all the information about the physics associated with its position in the matrix. Somewhat outside the matrix the so-called overall-modules reside which are responsible for data that can not be related to a single discipline or engine component as for example thrust and SFC evaluation.

## EXAMPLES OF 0-D NUMERICAL SIMULATIONS

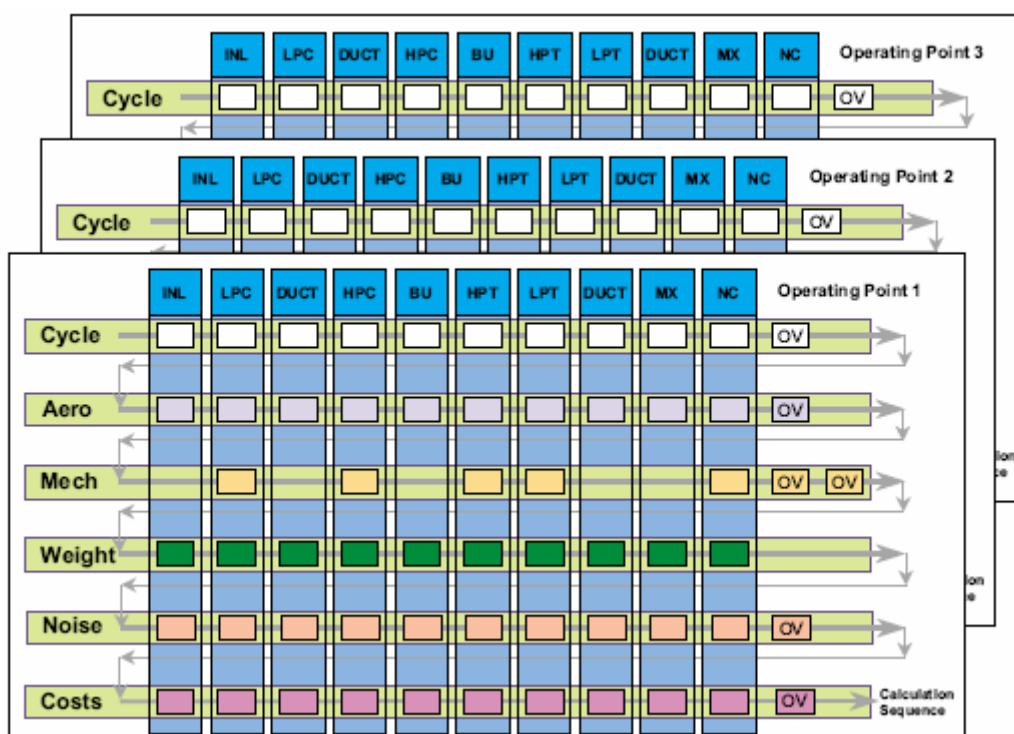


**Figure 5.4: Program Structure of MOPEDS.**

For each operating point an inner loop is required for finding a valid solution for the thermodynamic cycle and the other disciplines. An outer loop over all the operating points completes the process. Each module's variables are uniquely defined at each operating point and are treated as independent or dependent variables, constraints, or figures of merit depending on the problem under concern. There is no maximum value for the number of operating points, variables or constraints to be considered apart from the user's choice to limit the complexity of the problem.

Zooming is implemented in such a way that the methods that are used in the specialist's departments are called by MOPEDS. Specialists from any discipline are able to add even more detail to the design and – by running MOPEDS in parallel – may see how their changes affect the performance of other components and the overall engine.

### **Potential Benefits**

The overall system simulation employing the component specialists tools guarantees a smooth transfer of the pre-design results to the detailed design and vice versa. The latter is important for building a consistent data base of lessons learnt during the early phases of any new gas turbine design and also in engine growth studies.

The integration of the most important disciplines into one tool has the benefit that much more criteria can be considered simultaneously than with the conventional approach of iterating between specialists from different departments.

### **Cited Example**

- Jeschke, P., Kurzke, J., Schaber, R. and Riegler, C., "Preliminary Gas Turbine Design Using the Multidisciplinary Design System MOPEDS", Journal of Engineering for Gas Turbine and Power, Vol. 126, April 2004, pp. 258-264. [\[5.4\]](#)

What makes the preliminary design task so challenging are the many design variables and constraints to be considered at several operating points of the flight mission. The strong coupling of the effects of all disciplines as well as the strong interrelation of all engine components puts up the need to consider many variables and constraints simultaneously. For example, the constraints for the turbine metal temperatures at Take-Off rating are a direct function of the cycle variables and the component efficiencies at the cycle design point which coincides with the Max Climb rating. Moreover, the component efficiencies are a direct function of the aero design variables set at the aerodynamic design point which is usually the Cruise condition at high altitude. Thus there is a direct correlation between several design variables of different disciplines at the three operating points Take-Off, Max Climb and Cruise.

The paper describes first the multi-disciplinary tool MOPEDS which has been developed for use by a gas turbine manufacturer. As an application example the optimisation of the high pressure compressor for a conventional turbofan with respect to exit radius ratio, spool speed and stage number is used. Numerical optimisation is employed for finding the best solution and parametric studies are done to explore the surroundings of the optimum found.

The example described in the paper illustrates the value of the tool. Even though the investigated problem is somehow ‘academic’, it comprises a truly multi-disciplinary, multi-operating-point investigation of the complete gas turbine engine. A preliminary designer could by no means produce results like these – not to speak of a more realistic problem with more variables – in such a short time without an integral tool like MOPEDS.

### ***Limitations of Chosen Modeling Technique***

There obviously can be several pitfalls when numerically investigating a problem of high complexity. Especially the physical accuracy of the models used must always be checked carefully. This is even more true if numerical optimisation is employed which finds the optimum of the model only as opposed to the optimum in the real world. The numerically best solution might be outside of the design space for which the model is validated.

Another limitation of this modelling approach is the lack of detail available during the preliminary phase. Moreover, the results are strongly dependent on the constraints applied to the design task and the choice of the figure of merit.

Last but not least one needs very capable engineers who can make reasonable use of any highly complex multi-disciplinary tool. It is not adequate to simply accept what the computer presents as the optimum solution of a complex design problem – each result must be scrutinized carefully before accepting it.

## **5.3 GASTURB**

The big programs used within industry for performance simulations all have one common problem. They require an experienced engineer to operate them. Mostly there is no user-friendly interface and the user has to deal with the sometimes-complex component matching issues.

When predefined engine configurations are employed, it is possible to hide all the mathematics from the user of the program. This makes the program applicable for a much wider audience than the traditional gas turbine performance programs.

An example of a 0-D model with predefined gas turbine configurations is GasTurb [5.5], see **Figure 5.5**. GasTurb was originally developed as a Turbo Pascal program and was later transferred to Delphi. It has a traditional Pascal program structure (i.e. a main program with subroutines and data blocks) where each engine configuration is implemented as a program unit.

## GasTurb 10

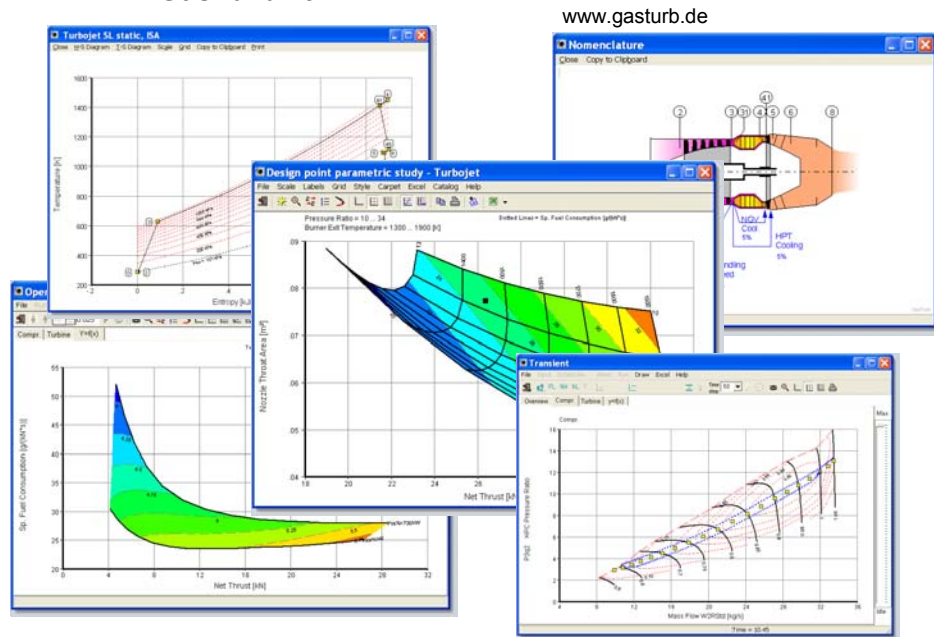


**Figure 5.5: GasTurb Model Selection Window.**

GasTurb is run on common desktop PCs with the Microsoft Windows operating system (Windows 95/98 or Windows NT4.0/2000/XP). The development environment is Borland Delphi®, which is based on the Object-Oriented Pascal programming (‘OOPascal’) language.

Apart from the user interface, GasTurb does not make use of the object-oriented features that are offered by Delphi.

The majority of the GasTurb code is devoted to the user interface. As a Windows program it is an event driven program in contrary to the traditional FORTRAN codes that are typically run using a command line interface or in batch mode.

Event driven programs pose a new challenge to the programmer because the user may click the buttons in any sequence. The user can be provided with much more powerful control (he can perform his tasks in different orders). However, the program must then also prevent unreasonable actions and provide hints and error messages when it cannot perform an action for some reason.

**Figure 5.6** shows the architecture of GasTurb where the different engine configurations are all (non-visible) sub-items of the box marked ‘Gas Turbine Physics’. All parts of the schematic above this box deal with the hidden mathematics and with many task specific user interfaces.

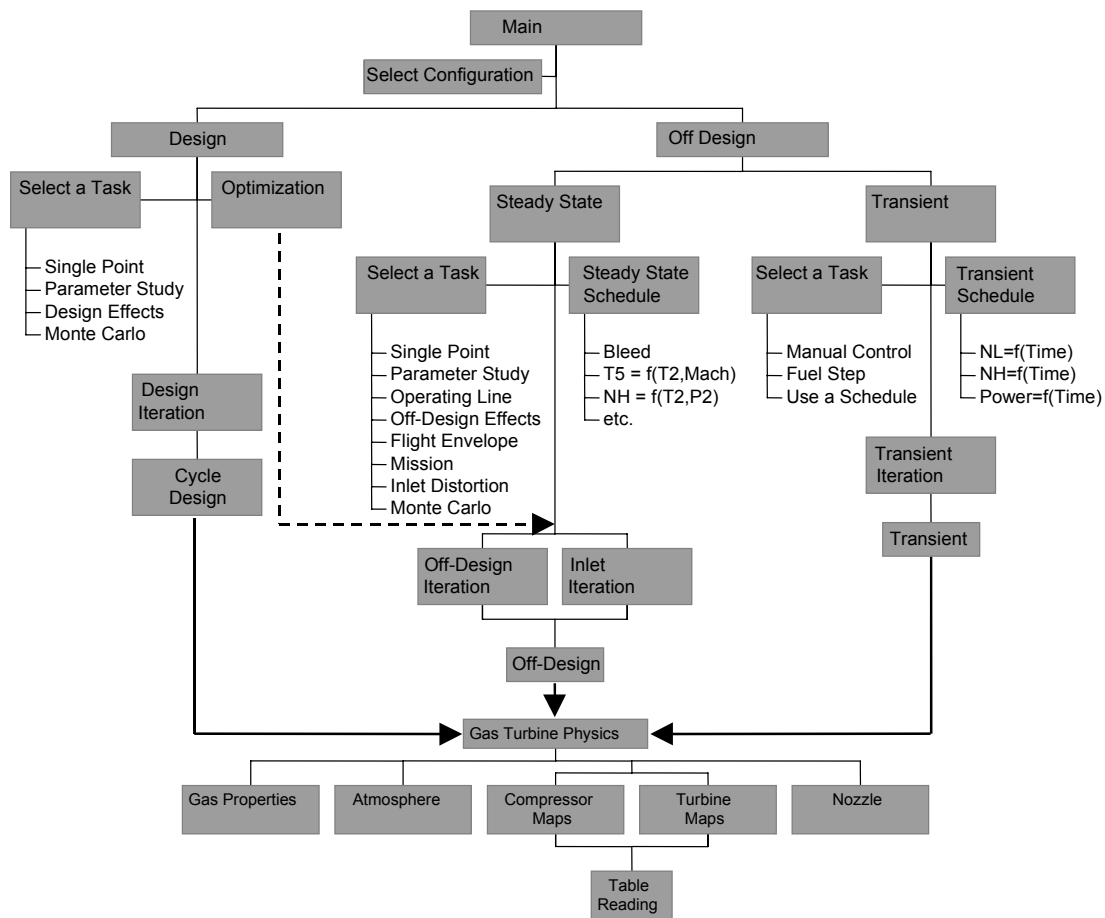


**Figure 5.6: GasTurb Architecture.**

A simplified version of GasTurb can be downloaded for evaluation purposes from the following website: <http://www.gasturb.de>.

## 5.4 THE GSP OBJECT-ORIENTED MODELING ENVIRONMENT

NLR's 'Gas Turbine Simulation Program' [5.6] is a component based modeling environment for gas turbines and related systems. Both steady-state and transient simulation of any kind of gas turbine configuration can be performed by establishing a specific arrangement of component models in a model window as displayed in Figure 5.7.

## EXAMPLES OF 0-D NUMERICAL SIMULATIONS

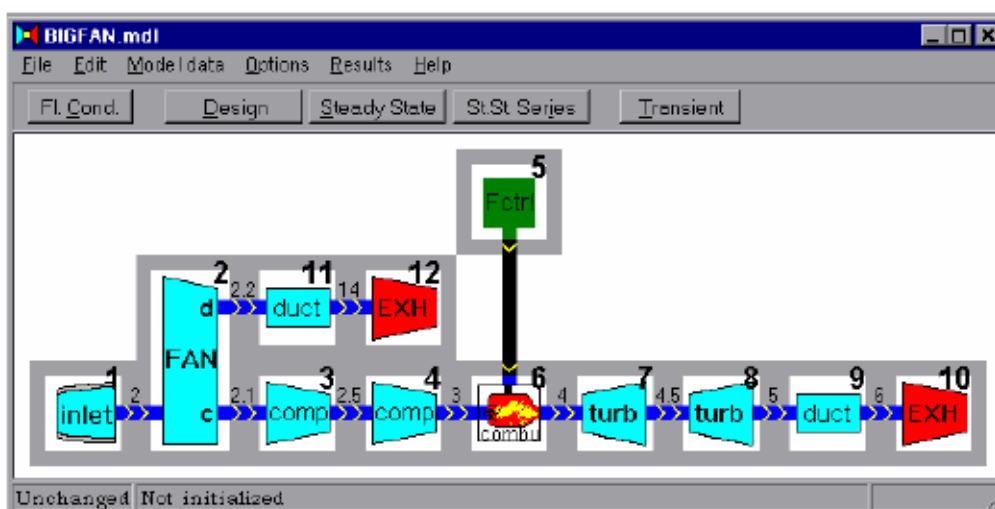


**Figure 5.7: GSP Model Window with Simple Turbofan Model.**

GSP is run on common desktop PCs with the Microsoft Windows platform (Windows 95/98/ME or Windows NT4.0/2000). The development environment is Borland Delphi®, which is based on the Object-Oriented Pascal programming ‘OOPascal’ language.

GSP is a highly flexible tool for analysis of operating condition effects on steady-state and transient performance. Typical effects are:

- Ambient and flight conditions;
- Installation losses;
- Deterioration; and
- Malfunctions of control and other subsystems.

Both the flexibility and user-friendly interface are owed to GSP’s *object-oriented* architecture, which has been designed with primarily these two qualities in mind.

The flexibility is to a large extent reflected in the component modeling approach. With efficient ways to develop or adapt component models, simulations of new gas turbine configurations and models with different levels of (local) detail or fidelity can easily be realized. For this approach a solver is required that is able to handle any configuration of components (and thus *states*) in a model. In effect, a generic solver is needed for a *virtual* set of *abstract components* with an undefined number of states. This also implies a specific approach for the user-interface, i.e. an interface focused on the component level.

**Object orientation** offers an excellent mechanism for this problem. *Inheritance* is used to concentrate code common to multiple component types (e.g. both compressor and turbines have some similarities) in ‘*abstract*’ component object types or “*classes*”. From these abstract classes, component classes are derived and ‘*instantiated*’ as real gas turbine components in an engine model. See **Figure 5.8** for the GSP component class hierarchy.

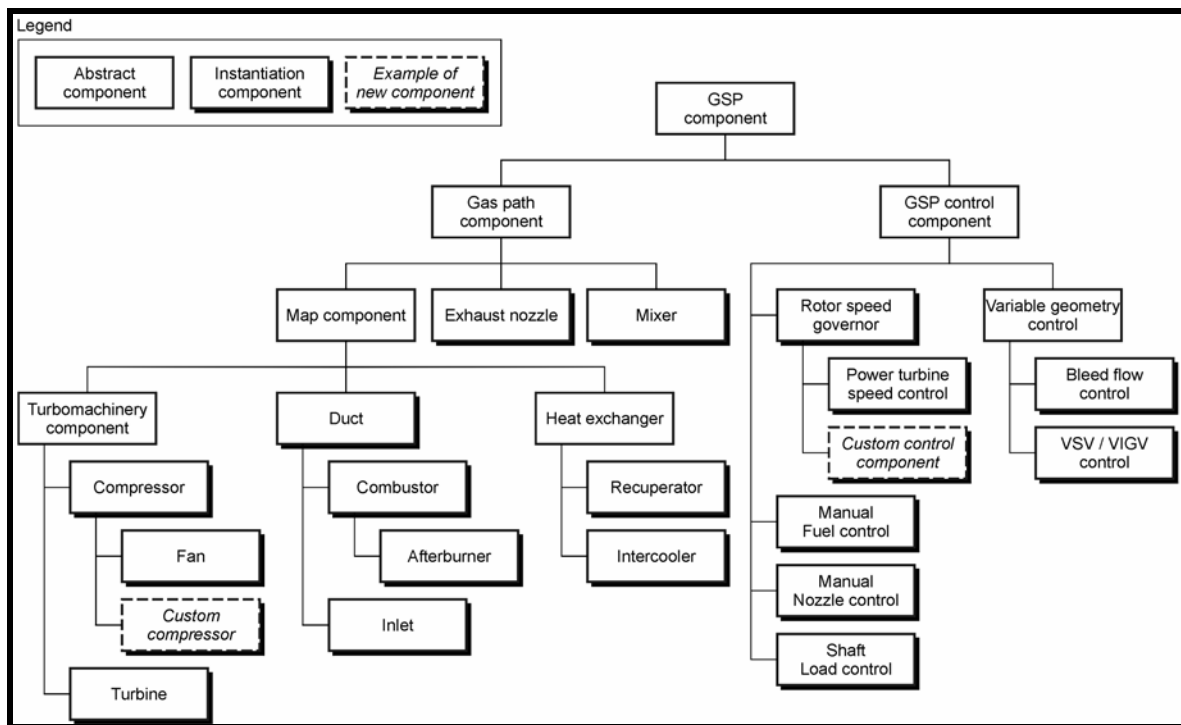


**Figure 5.8: Standard Component Architecture.**

Many publications on object-oriented software designs (and also on object-oriented gas turbine simulation tools exist and show the three basic principles of object orientation: *encapsulation*, *inheritance* and *polymorphism*. These principles offer significant potential to efficient gas turbine simulation software development.

**Encapsulation** enhances code maintainability and readability by concentrating both the routine code (representing behavior) and data block code (representing the properties and state of operation) of a particular component in a single component *object class*. Contrary to conventional software design practice (i.e. FORTRAN), all data declarations and procedures (in OOD terminology *methods*, both for interface and simulation calculations) are concentrated in a single code unit.

**Inheritance** facilitates concentration of code common to multiple component classes in one or more *abstract ancestor classes*. This is to eliminate code duplication. The turbo-machinery component class in **Figure 5.8** for example represents all functionality common to compressors, fans and turbines. Code maintainability is also enhanced because single code adaptations in ancestor classes are effected in all descendant classes. **Polymorphism** is the ability of abstract parameters to represent different object classes. This principle is extensively applied in GSP. Every component class for example has a 'Calc' method for running the simulation code. The system model code has an abstract (*polymorphic*) component object identifier able to represent any real component object instance in the model. During simulation, the system model subsequently lets the abstract identifier point to successive components, calling their 'Calc' methods. The abstract component object has an abstract 'Calc' method that is a token representation of the real simulation code. During runtime a mechanism called *late binding* replaces this abstract 'Calc' code with the actual 'Calc' code of the component it is representing.

Using inheritance, code development effort and maintainability can be drastically reduced. Many gas turbine components have similarities in the model and user interface code. Common or generic code elements can be concentrated in (and inherited from) a single abstract ancestor class (an abstract class cannot be instantiated, i.e. cannot represent an actual component model). Also, when a new component

## EXAMPLES OF 0-D NUMERICAL SIMULATIONS

model is needed, or needs a small adaptation (for example a ‘customized compressor model’), a child class may be derived and only the new code needs to be implemented. Any type of custom component model may be derived and stored in additional ‘custom component libraries’ to be provided to specific GSP users in the form of separate Dynamically Linked Libraries (DLL’s, or if intended for use only with Delphi applications, BPL files). This has the advantage that GSP’s core code for the standard components does not need adaptation.

In GSP, similar inheritance structures are used for modeling of secondary airflows, control sub-systems models, etc. Component models for external systems *interfacing* with the gas turbine can be developed for simulation of gas turbine integrated thermal systems. Examples are:

- Turbine Powered Simulator engine models. These are compressed air driven wind tunnel engine models, including a pressure vessel and control valve;
- Models of Power Generating Systems with a bio-mass gasifier delivering low calorific value fuel to a gas turbine;
- Aircraft Environmental Control Systems, employing turbo-machinery and heat exchangers;
- STOVL propulsion systems including lift fans or swiveling vertical thrust nozzles; and
- Systems with heat exchangers for extra steam cycles, heating systems, etc.

Naturally, a separate mechanism is needed to link component models into a whole engine model. GSP employs dynamic instantiation and linking of component models to set up models of any gas turbine configuration. Also multiple gas turbine installations, such as two interconnected helicopter engines, can be simulated simultaneously. **Figure 5.9** shows the model level architecture. To the user a whole engine model is represented by a window such as shown in **Figure 5.7**.

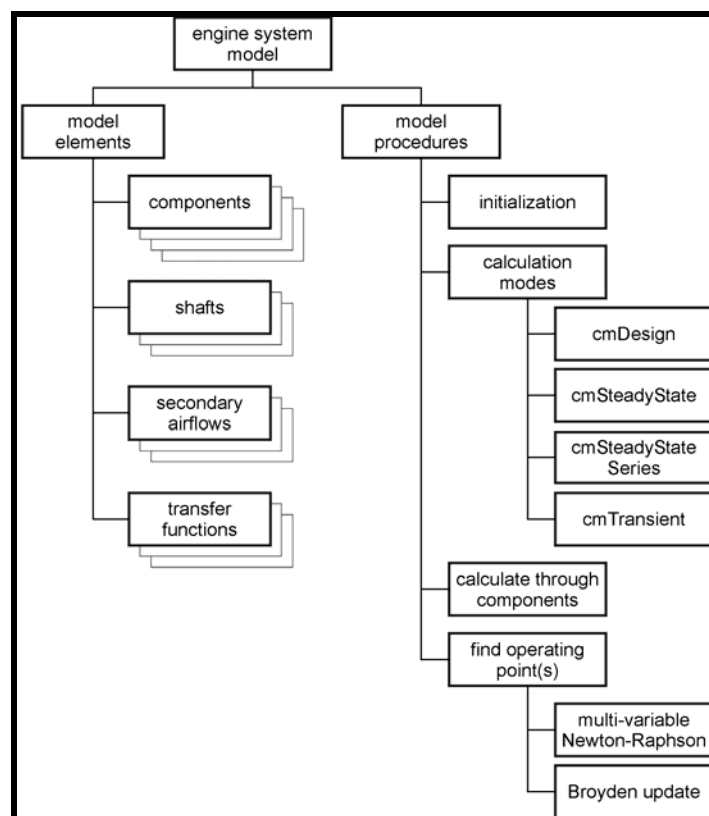


**Figure 5.9: Engine System Model Architecture.**

GSP's graphical user interface fully reflects the object-oriented architecture for the component models. It is also fully event driven, which allows the user to perform his tasks in any order.

A gas turbine system model is represented by a window that incorporates general model I/O features (such as ambient/flight conditions, options, etc.) and a work bench sheet on which a number of component icons are arranged to form a valid gas turbine configuration. Another example of a typical representation is shown in **Figure 5.10**. A component icon represents a gas turbine component model including the component user interface. Double-clicking the icon opens the component user interface: see **Figure 5.11** for an example of a simple compressor component window. **Figure 5.12** shows component performance results in a map window, also accessed through the component window. The drag and drop interface allows the copying of multiple instances of components between models, enabling the user to build his own specific component repositories and save them as a generic model.

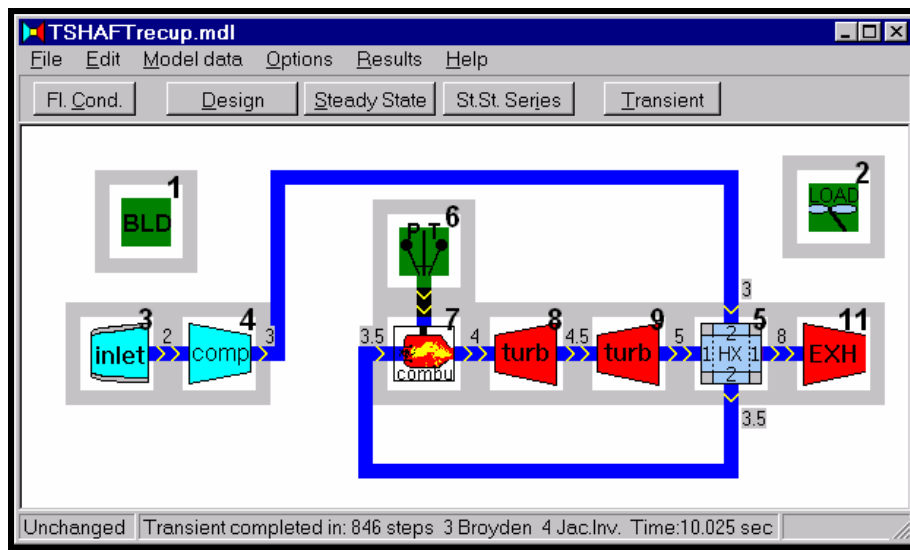


**Figure 5.10:** GSP Model Window with Recuperated Turbo-Shaft Engine Model.

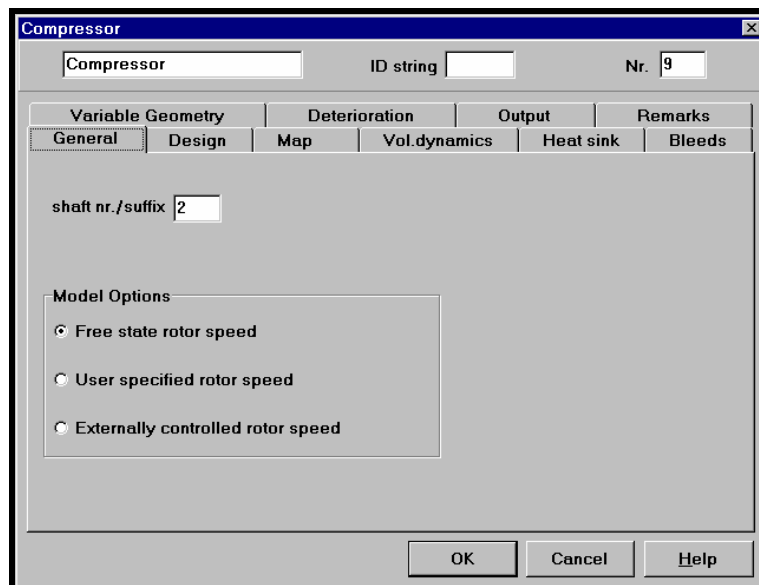


**Figure 5.11:** Compressor Component Window.

## EXAMPLES OF 0-D NUMERICAL SIMULATIONS

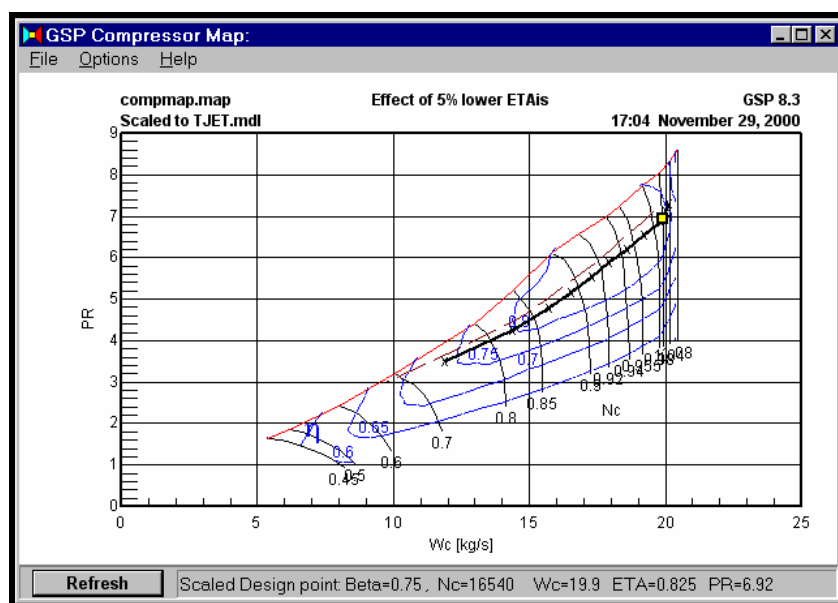


**Figure 5.12: Component Performance Output Results.**

When deriving a new component from an existing one (not a user but rather a developer task), the user-interface is also inherited and often only a few elements need to be added to the component interface window. See **Figure 5.13** for the interface architecture.

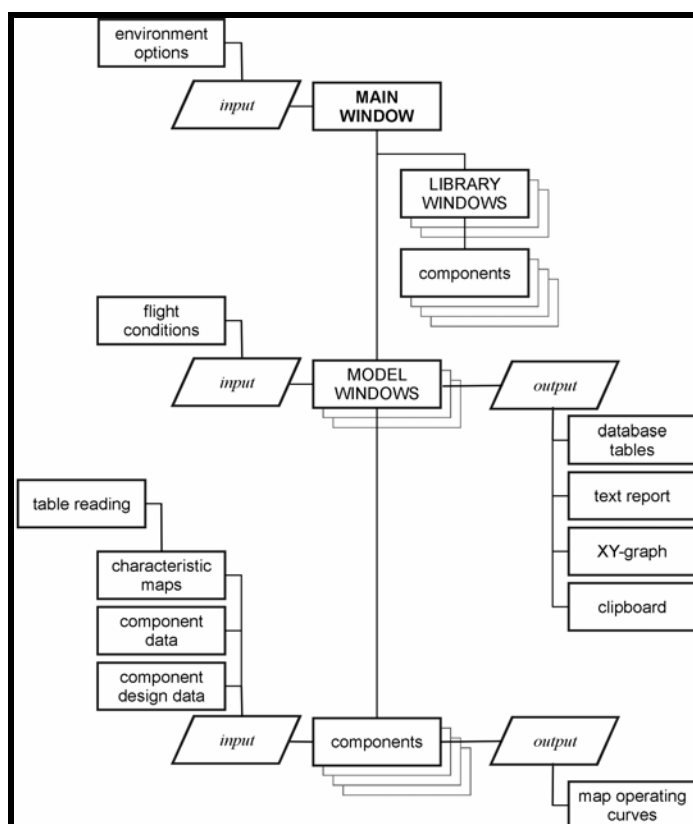


**Figure 5.13: GSP Interface Architecture.**

## 5.5 TERTS (TURBINE ENGINE REAL TIME SIMULATOR)

TERTS [5.7] is an example of a real-time 0-D component stacking model. TERTS is built with MATLAB Simulink, and offers a component-based predefined configuration. In order to comply with the requirement of limited computation time per time step (for real-time simulation), the ‘one iteration per time step’ method was applied, which offers good accuracy with high update frequencies (time steps smaller than 0.02 s). Figure 5.14 displays the TERTS thermodynamic engine model level.

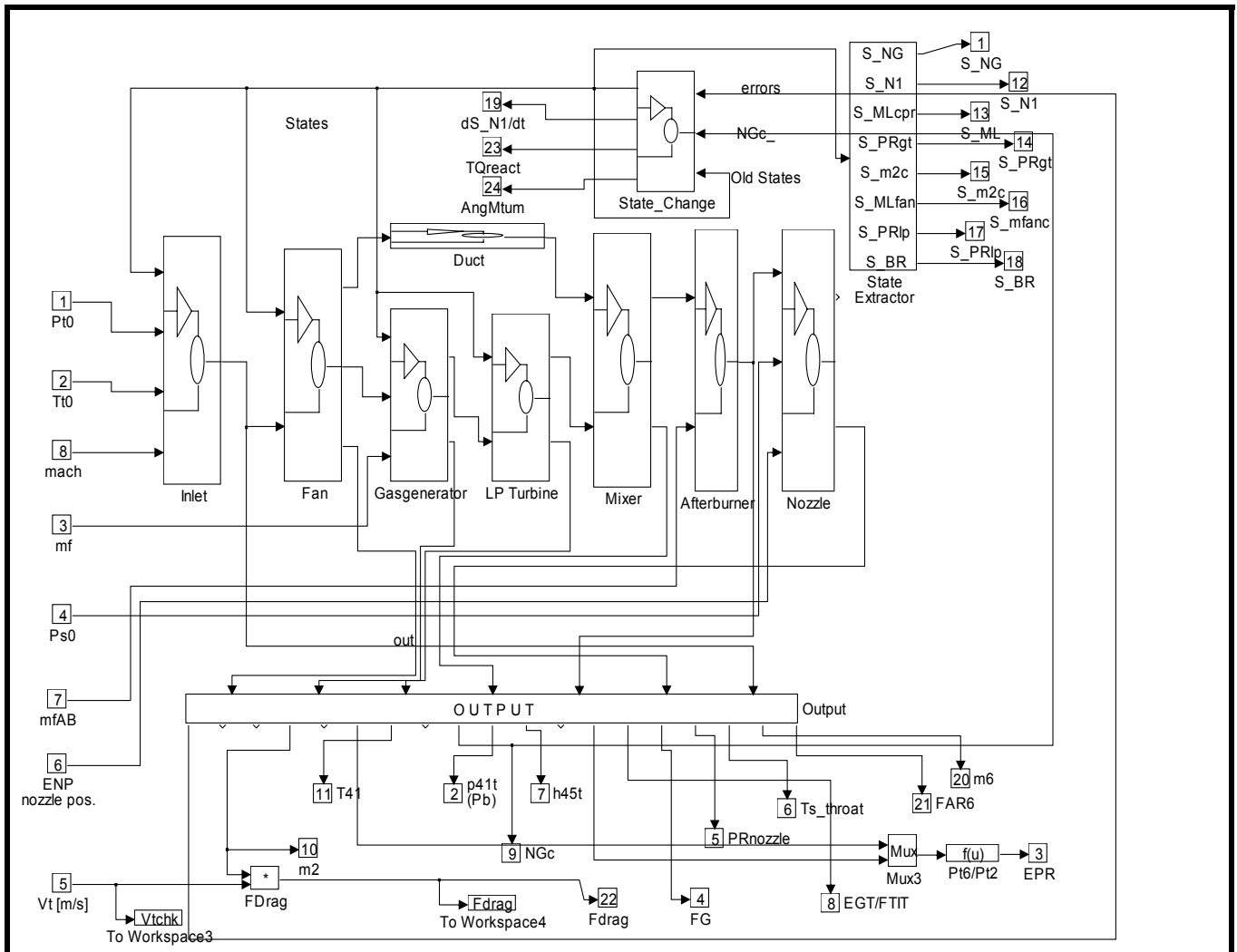
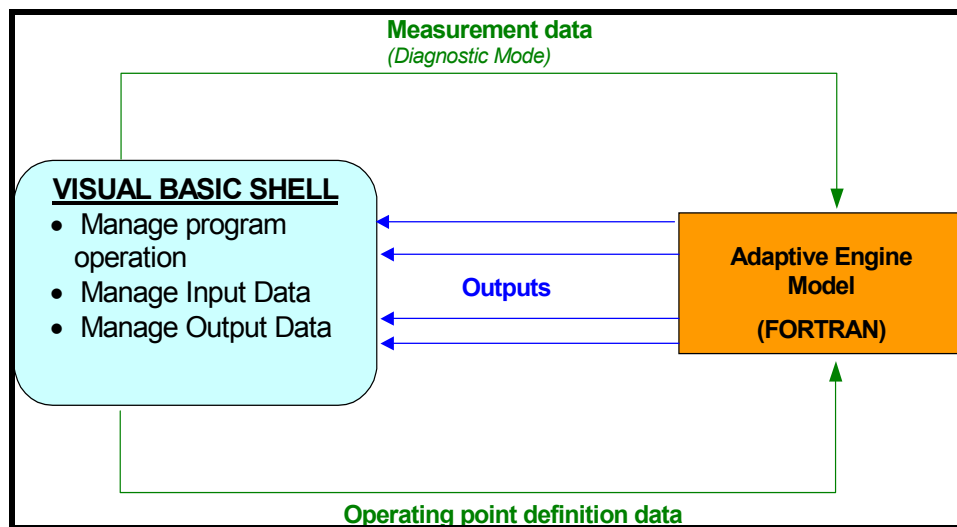


Figure 5.14: NLR TERTS Thermodynamic Engine-Model, with Sub-Levels.

TERTS uses MATLAB Simulink. This is a multiple-level architecture with which a large number of subsequent sub-model levels can be specified. More than 10 levels are used in TERTS, and the compressor for example includes a number of sub-models for the various thermodynamic processes and also reading of the maps. With the Simulink interface, the user easily gets into sub-level detail by clicking a sub-component model icon. Simulink’s component-oriented architecture has the object-oriented *encapsulation* feature but lacks *inheritance* and *polymorphism* (see Section 5.4).

### 5.6 SIMULATION MODELS FOR ENGINE DIAGNOSTICS

Models offering the possibility of use for gas turbine engine fault diagnosis have been developed by the Diagnostics Group of the Lab of Thermal Turbo-machines and the National Technical University of Athens [5.8, 5.9 and 5.10]. The TEACHES model has been built with VISUAL BASIC™ programming language for a building a shell and a Graphic User's Interface (GUI), operating in a MS Windows 98 environment. An engine performance calculation module performs the key aero-thermodynamic calculations. This is a dynamic link library (DLL) written in FORTRAN. Information is passed between the Visual Basic shell and the performance calculation module whenever performance calculations are requested, as shown schematically in Figure 5.15.



**Figure 5.15:** The Structure of a Modeling Environment Offering the Possibility of Fault Diagnosis.

The FORTRAN code forms the core of the modeling system. It employs the Adaptive Modeling technique (described in Chapter 2) to perform fault diagnosis. By appropriate selection of input data it can perform either direct simulation of engine operation at any desired operating point ('Simulation mode') or a diagnosis of the condition of the engine components, once a set of measurement data is available ('Diagnostic mode').

The GUI interface Figure 5.16, allows the user to choose between different modes of operation and to perform various tasks with input and output information. The interactive main window is used to control the most common actions and to get the most significant information from the calculations. Less common functions are available via a menu system. The two modes of program operation – Simulation and Diagnostic – are selected from this window.

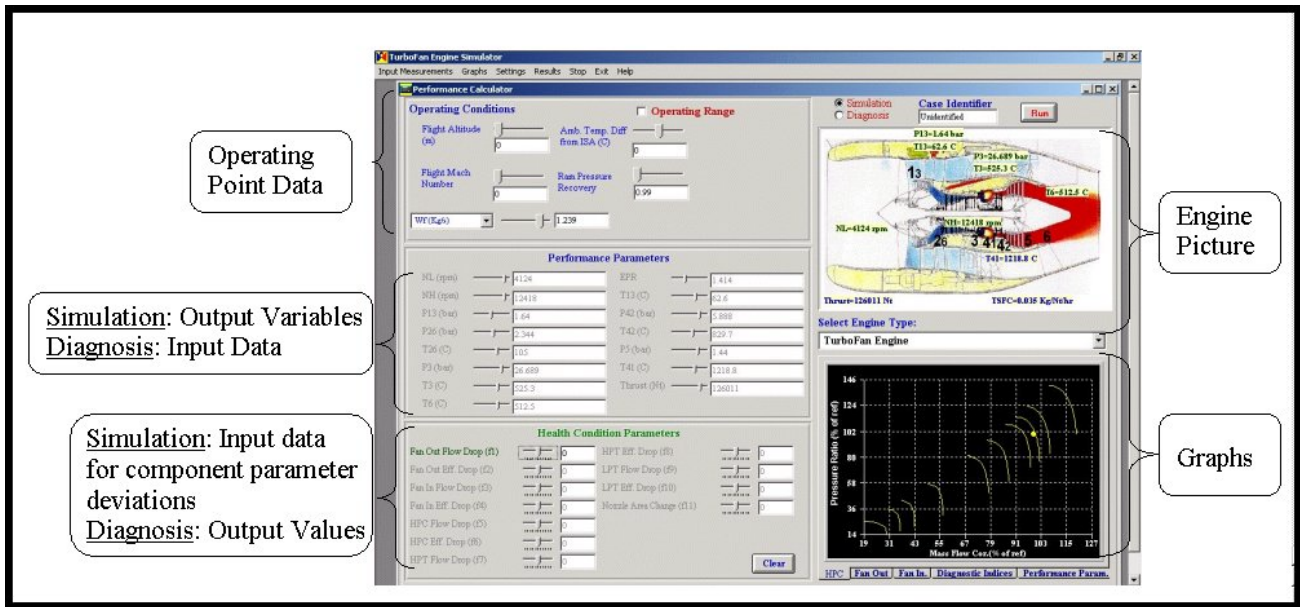


**Figure 5.16: Main User Interface of TEACHES Package.**

The architecture of the interface is shown in **Figure 5.17**. It is to be noticed that the role of different sections of the interface is different for different mode of operation. Operating point data are always inputs. They include ambient conditions and a set point variable chosen from a menu offering different possibilities as shown in **Figure 5.18**. The values of measured quantities are outputs in the ‘Simulation’ mode, while they are inputs for the ‘Diagnostic’ mode, when measurement data are used to produce a diagnosis. Component parameters are inputs when component malfunctions are simulated and outputs when a diagnostic run has been performed with measured input data.

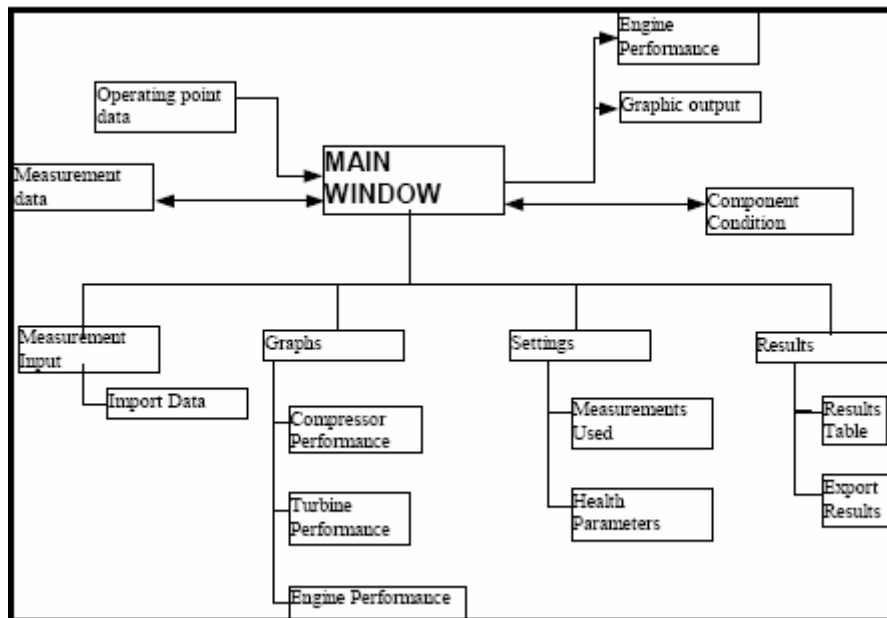


**Figure 5.17: Interface Architecture Schematic.**

## EXAMPLES OF 0-D NUMERICAL SIMULATIONS

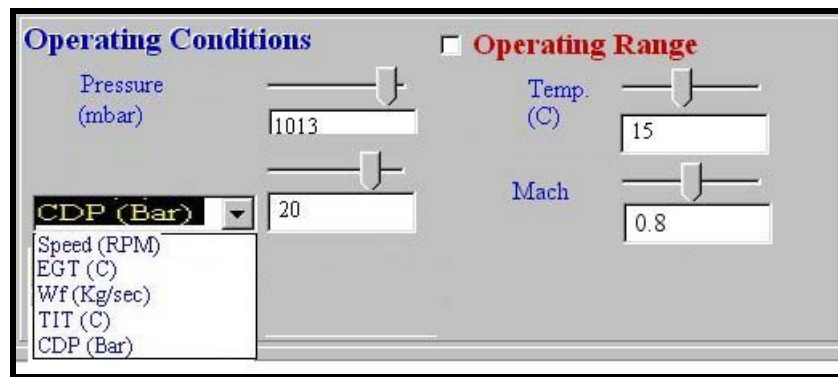


**Figure 5.18:** The Operational Parameters Input Section of the Visual Interface.

The overall structure of this modeling package is characterized by modularity in three levels:

- The code for the GUI is modular, so different engines can be modeled by supplying a different DLL.
- The code of the DLL is built by using individual subroutines for each type of component, so that the engine layout can be easily modified.
- For a DLL built for a certain gas turbine configuration (single-shaft, twin-shaft, etc.), engine data and component map data can be provided to represent different individual engines of this type.

### 5.6.1 Examples of Results

#### 5.6.1.1 Examining the Effects of Component Malfunctions

Modifying the performance characteristics of the components simulates different faults. The engine performance for these modified characteristics is then calculated. The deviations from nominal component performance are introduced as percentages in the corresponding section of the main window, and using scalars, multiplying the component performance-parameter effects map modifications. The modification factors are explained in *Chapter 4*. For example, setting the value of modification factor  $f_1$  to a value of 0.98 represents a reduction in pumping capacity of the compressor by 2%. The modified component characteristics can be visualized, in comparison to the initial intact ones, as for example shown in **Figure 5.19**.

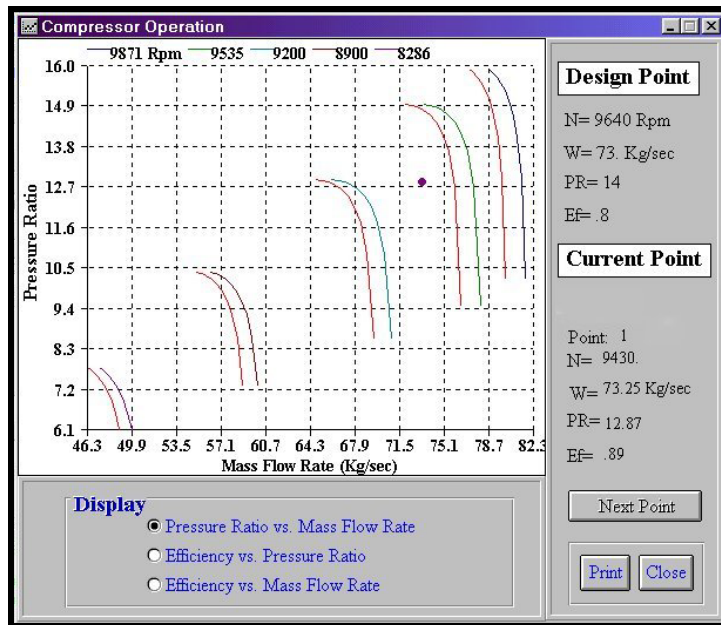


**Figure 5.19: Output from a Compressor Model.**

When such a calculation is performed in addition to all the cycle variables, ‘fault signatures’ are also calculated and displayed. A picture of a fault signature in the form of measurement deviations from reference values provided by the model is shown in **Figure 5.20**.

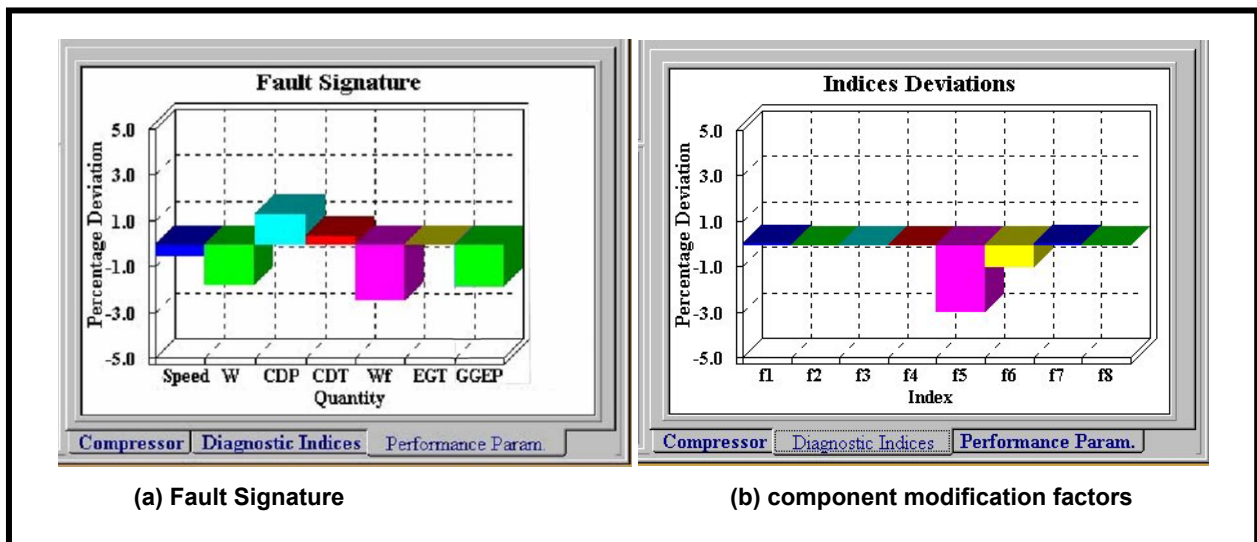


**Figure 5.20: Examples of Graphic Information Related to Diagnostics.**

## 5.6.2 Direct Component Condition Diagnosis

When a set of measurement data is available from an engine with a suspected fault, it is fed to the model in ‘Diagnostic’ mode. The model then calculates the corresponding values of health indices (MF). Changes in MF values indicate the occurrence of a fault. The pattern of change of MFs can then be used to help identify the fault itself. A display of the model output for diagnostic application is shown in

## EXAMPLES OF 0-D NUMERICAL SIMULATIONS

**Figure 5.20.** The results of this figure come from an engine with a turbine suffering a deterioration, which led to a 3% reduction in swallowing capacity and 1% efficiency reduction.

### 5.7 NUMERICAL PROPULSION SYSTEM SIMULATION (NPSS)

#### 5.7.1 Overview

The Numerical Propulsion System Simulation, NPSS, [5.11 and 5.12] is a concerted effort by NASA Glenn Research Center, the aerospace industry and academia to develop an advanced engineering environment – or integrated collection of software programs – for the analysis and design of aircraft engines and, eventually, space transportation components<sup>1</sup>. Its purpose is to dramatically reduce the time, effort and expense necessary to design and test jet engines. It accomplishes that by generating sophisticated computer simulations of an aerospace object or system, thus permitting an engineer to “test” various design options without having to conduct costly and time-consuming real-life tests. A schematic of the NPSS concept is illustrated in **Figure 5.21**. The ultimate goal of NPSS is to create a “numerical test cell” that enables engineers to create complete engine simulations overnight on cost-effective computing platforms. Using NPSS, engine designers will be able to:

- Analyze different parts of the engine simultaneously;
- Perform different types of analysis simultaneously (e.g. aerodynamic and structural); and
- Perform analysis faster, better and cheaper.

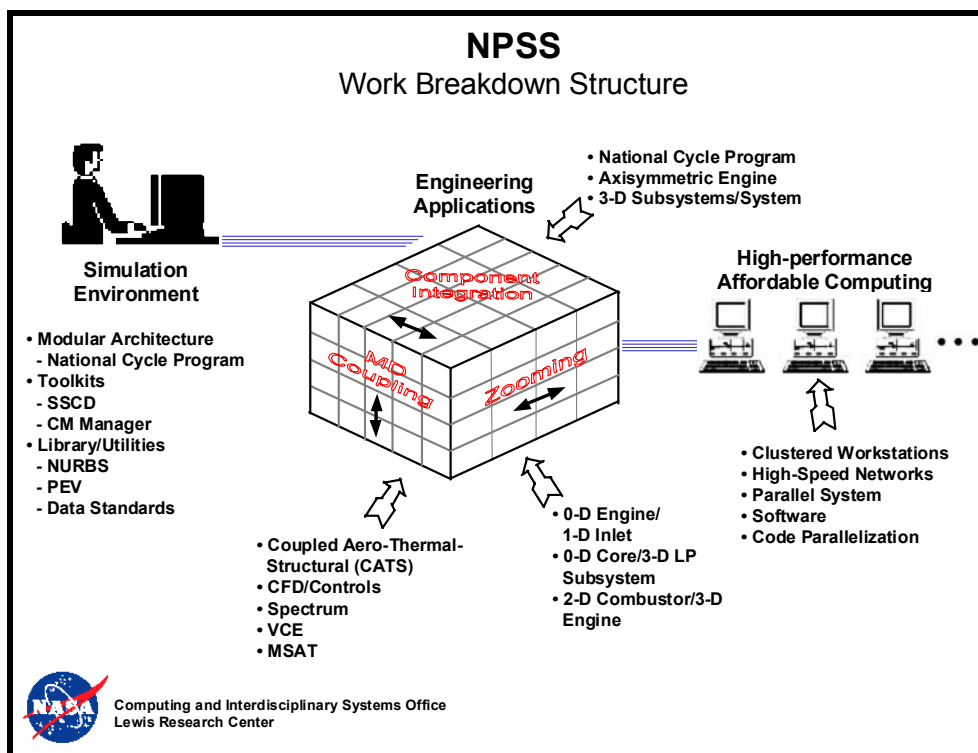


**Figure 5.21:** Overview of NPSS.

<sup>1</sup> Parts of this section were copied from (see for further information): <http://hpcc.grc.nasa.gov/npssintro.shtml>.

All of which is consistent with the CAS goal of accelerating the development and availability of high-performance computing hardware and software to the United States aerospace community.

NPSS attempts to create a propulsion system simulation system covering a wide range of disciplines and levels of fidelity. It is unlikely that a simulation including all disciplines and all components at the highest level of fidelity will be possible (or even desired) in the near future. However, the potential to use higher fidelity representations for key portions of a propulsion simulation, ‘Zooming’, for better accuracy or extended insight into important behavior is of interest and well within current computational capabilities. Zooming has been limited to technology demonstration efforts because of the difficulty and complexity in creating these simulations in a consistent manner, while still providing effective access to the required high performance computing capability. Reducing the complexity of multi-disciplinary analysis at varying levels of fidelity is being addressed by creating standard APIs. Computing availability is being addressed by allowing for distributed computing using CORBA.

### **5.7.2 NPSS Architecture and Object-Oriented Software Design**

The underlying framework of NPSS – the architecture that links together the different computer codes – is already in use. Several aerospace companies and NASA Glenn Research Center, using an object-oriented approach to software design, built the framework for NPSS.

Object-oriented software design is a way of organizing data and procedures in a computer program into manageable packages called “objects.” The object-oriented approach was chosen for NPSS because it allows new codes to be introduced into the system quickly and easily. In other words, if a company develops a powerful new code for one engine component – such as a compressor, combustor, turbine or shaft - the object-oriented framework permits use of that code with all the other codes in NPSS – even if that new code runs on a different type of computer.

NPSS provides another important capability to engine developers called zooming. As in photography, zooming or magnifying allows an engine developer to analyze the performance of an engine component by zooming in on that component to evaluate its performance in great detail. This is a major step forward because engineers can now analyze engine components within a system (the entire engine) rather than in isolation.

### **5.7.3 NPSS and Conceptual Design**

NPSS is advancing the process of conceptual design – the initial stage of engine development when engineers are making educated guesses about an engine’s performance, size, and weight. During the conceptual design phase, engine developers provide a computer code called a cycle deck to airplane developers, who have their own computer models. Since the engine and aircraft manufacturers make many changes during the design phase, they must be able to exchange information and design changes quickly and accurately in order to ensure that the final product performs effectively and safely. NASA and industry are developing a common model that engine and airframe companies will use to collaborate on the design of engines. The common model facilitates collaboration by establishing a standard set of data that all partners share, understand and can readily implement in their individual design tools.

NPSS, although still being improved, is being used by aircraft and aircraft engine developers to create better cycle deck codes. For example, it has been used to model the turbofan engine for a supersonic passenger aircraft. And, in the future, NPSS will be applied to the extremely difficult task of simulating jet engine combustion systems (i.e. the part of the engine that burns the fuel to produce high-energy air for turning the engine’s turbine).

NASA, the Department of Defense, the Department of Energy, and industry are developing the National Combustion Code (NCC) – a system that integrates the entire set of computer codes needed for the design

## EXAMPLES OF 0-D NUMERICAL SIMULATIONS

and analysis of combustion systems. The National Combustion Code will be used in the design of current engine technology as well as in future combustion technologies that will yield cleaner, more powerful engines.

### 5.7.4 Standards and Zooming

As part of the NPSS system development, standard application interfaces for engine components have been developed, as well as standards for links between the components at varying levels of fidelity. Within the component are standard sub-element representations that can capture different methods for representing portions of the component behavior. A key benefit of this object-oriented approach is that components and component sub-elements can be developed, tested and shared with minimal coordination between users and minimal limitations in user applications. The functional behaviors of low and high fidelity components are the same. The complexity of the conversion of boundary conditions among different levels of fidelity and component modeling issues are available to the system modeler, but do not require the same level of expertise from the user. At the system level, these standards are captured in the SAE ARP4868 standard [5.13] developed by the SAE S-15 committee.

### 5.7.5 Examples

Shown here is output from a software tool called ENG10, [5.14], (see Figure 5.22) which was developed through the Numerical Propulsion System Simulation (NPSS) Project at NASA Glenn Research Center. The ENG10 code is used to analyze the airflow through modern jet engines. One of the strengths of this code is its ability to use the results of studies of individual components of an engine to model how the overall engine system behaves and how various components influence each other.

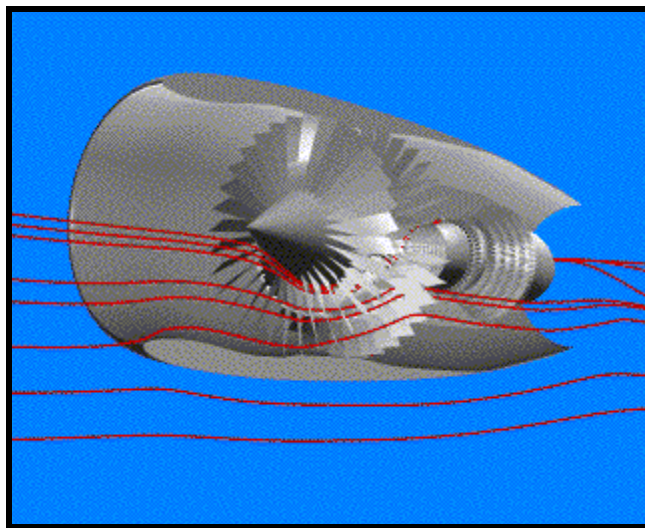
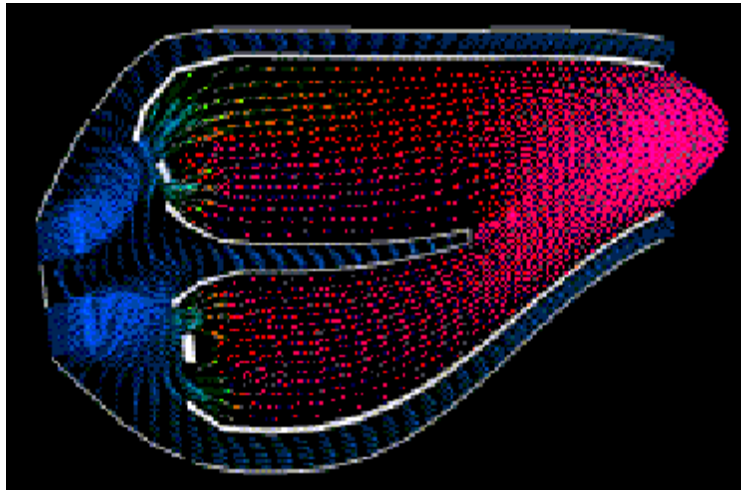


Figure 5.22: Output from ENG10 Modeling Tool.

Some codes developed through NPSS analyze individual engine components. Shown in Figure 5.23 is a simulation of the Energy Efficient Engine's combustor using ALLSPD-3D [5.15 and 5.16], a Glenn – developed combustor code. Component design teams use simulation codes such as ALLSPD-3D to simulate and design engine components in detail.



**Figure 5.23: ALLSPD Simulation of a Combustor.**

## 5.8 OTHER 0-D MODELING SYSTEMS

There are a number of proprietary or limited distribution programs used in the industry:

- SOAPP (P&W);
- CWS/ICS (GE);
- GECAT/NEPP (SRS Technologies) [5.17];
- TERMAP (Allison/USAF) [5.18];
- RRAP (Rolls Royce);
- JANUS (Snecma);
- ON-X/OFF-X (Jack Mattingly) [5.19];
- PYTHIA (Cranfield) [5.20];
- TURBOMATCH (Cranfield) [5.21];
- FAST (Honeywell Allied Signal);
- TESS (Univ. Toledo) [5.22]; and
- ATEST (AEDC) [5.23].

MOPS and TESS are similar to GSP in that they provide a configurable modeling system with a suite of components. These systems typically include other features to allow productive use in the engine design and analysis process. Examples are communication to test data systems, provisions for matching models to test data and configuration management for the various component and engine models for multiple users of multiple engine models. NPSS (see **Section 5.7**) is also a configurable modeling system for both 0-D and multi-dimensional modeling.

## 5.9 REFERENCES

- [5.1] SAE Standard, AS681: Gas Turbine Engine Steady-State and Transient Performance Presentation for Digital Computer Programs, March 1999.

## EXAMPLES OF 0-D NUMERICAL SIMULATIONS

---

- [5.2] SAE Standard, AS755: Aircraft Propulsion System Performance Station Designation and Nomenclature, August 2004.
- [5.3] Kurzke, J., "Calculation of Installation Effects within Performance Computer Programs", AGARD-LS-183, 1992.
- [5.4] Jeschke, P., Kurzke, J., Schaber, R. and Riegler, C., "Preliminary Gas Turbine Design Using the Multidisciplinary Design System MOPEDS", Journal of Engineering for Gas Turbine and Power, Vol. 126, April 2004, pp. 258-264.
- [5.5] Kurzke, J., "Gas Turbine Performance Simulation with GasTurb™", [www.gasturb.de/](http://www.gasturb.de/).
- [5.6] Visser, W.P.J. and Broomhead, M.J., "GSP, A Generic Object-Oriented Gas Turbine Simulation Environment", ASME Paper # 2000-GT-0002, ASME Conference Munich, June 2000.
- [5.7] Visser, W.P.J. et al., "TERTS: A Generic Real-Time Gas Turbine Simulation Environment", ASME Paper # 2001-GT-446, June 2001.
- [5.8] Mathioudakis, K., Stamatis, A., Tsalavoutas, A. and Aretakis, N., "Performance Analysis of Industrial Gas Turbines for Engine Condition Monitoring", Presented at: First International Conference on Engineering Thermophysics", Beijing, China, August 18-21, 1999 (ICET '99).
- [5.9] Mathioudakis, K., Stamatis, A., Tsalavoutas, A. and Aretakis N., "Instructing the Principles of Gas Turbine Performance Monitoring and Diagnostics by Means of Interactive Computer Models", Paper # 2000-GT-0584, May 2000.
- [5.10] Tsalavoutas, A., Aretakis, N., Stamatis, A. and Mathioudakis, K., "Combining Advanced Data Analysis Methods for the Constitution of an Integrated Gas Turbine Condition Monitoring as Diagnostic System", Paper # 2000-GT-0034, May 2000.
- [5.11] Claus, R.W. et al., "Multidisciplinary Propulsion Simulation Using NPSS", AIAA-92-4709-CP.
- [5.12] Evans, A.L. et al., "An Integrated Computed and Interdisciplinary Systems Approach to Aeropropulsion Simulation", ASME Paper # 97-GT-303.
- [5.13] SAE Standard, ARP4868: Application Programming Interface Requirements for the Presentation of Gas Turbine Engine Performance on Digital Computers, October 2001.
- [5.14] Stewart, M., "Axisymmetric Aerodynamic Numerical Analysis of a Turbofan Engine", ASME Paper # 95-GT-338.
- [5.15] Chen, K.H. et al., "Three-Dimensional Coupled Implicit Methods for Spray Combustion at All Speeds", AIAA-94-3047, June 1994.
- [5.16] Fricker, D.M., "[Parallel ALLSPD-3D: Speeding Up Combustor Analysis via Parallel Processing](#)", AIAA-97-3295, July 1997.
- [5.17] "Graphical Engine Cycle Analysis Tool, GECAT", SRS Technologies, [www.stg.srs.com](http://www.stg.srs.com).
- [5.18] "Innovative Visual Modeling Environment for Turbine Engine Reverse Modeling Aid Program (TERMAP)", January 2000, SRS Technologies, [www.stg.srs.com](http://www.stg.srs.com).

- [5.19] Mattingly, J.D., “Elements of Gas Turbine Propulsion”, 1996, McGraw-Hill.
- [5.20] Pachidis, V., “Gas Turbine Simulation – PYTHIA Workshop Guide”, ASME/IGTI Aero Engine Life Management Conference, London, March 2004.
- [5.21] Palmer, J.R., “The TURBOMATCH Scheme for Aero/Industrial Gas Turbine Engine Design Point/Off Design Performance Calculation” SME, Thermal Power Group, Cranfield University, 1990.
- [5.22] Reed, J.A. and Afjeh, A.A., “Development of an Interactive Graphical Propulsion System Simulator”, AIAA-94-3216, June 1994.
- [5.23] Chappell, M.A. and McLaughlin, P.W., “Approach to Modeling Continuous Turbine Engine Operation from Startup to Shutdown”, *Journal of Propulsion and Power*, Vol. 9, No. 3, May-June 1993, pp. 466-471.

## EXAMPLES OF 0-D NUMERICAL SIMULATIONS

---



## **Annex A – HIGHER ORDER MODELS**

### **INTRODUCTORY COMMENTS**

This Annex provides the reader with an insight into a whole category of simulation techniques that have been developed and continue to be developed for phenomena that have been observed in gas turbine engines but can't be simulated within the 0-D cycle model concept. The 1-D dynamic models used for compression system and engine operability (such as surge and rotating stall) are especially highlighted and several examples have been given to indicate how these models have been used.

### **A.1 DETAILED 1-DIMENSIONAL (1-D) MODELS**

A 1-D model typically tries to extend a 0-D cycle model representation by physically modeling an additional dimension. The most commonly used 1-D models are for dynamic simulations where 0-D models require the addition of a length dimension to adequately model high frequency behavior. The next most common use is where components or local areas of the engine are modeled at a higher level of fidelity in either the radial, circumferential or axial direction to address specific concerns. Often these models remain at 0-D fidelity in other parts of the engine. 0-D and 1-D models may be used predict 2-D and 3-D variations in engine conditions and may use a physical model to do it. But the physical models stay at the lesser level of detail. An example is the use of a more detailed compressor model, which predicts the variation in driving pressures at the hub and tip, and then uses these to model internal leakage and cooling circuits.

#### **A.1.1 Steady State 1-D Models**

Steady state 1-D models are typically used to provide detailed information inside one or more components such as:

- Blade row, cooling passage or cavity level information. In some cases this may not be a true 1-D model but merely a 0-D model taken to a greater than normal level of detail.
- Tracing radial or circumferential information through the engine. This could be inlet pressure or temperature distortion, water or fuel cloud, or a non-uniform condition created inside the engine. This might be in the burner due to a fuel nozzle variation, or in a compressor due to a locally off-angle sector of stators.

When providing more detail inside a component, more detailed boundary conditions may not be required. For models addressing radial or circumferential behavior through the engine, creation and transfer of the additional boundary conditions is the key part of transient 1-D models.

#### **A.1.2 Transient 1-D Models**

Often these models are identical to a steady state 1-D model and only include the transient extensions found in 0-D models. This includes models of low frequency phenomena such as rotor accelerations, heat transfer and active or passive geometry changes. Active geometry changes modeling can include dynamics associated with variable stators, variable bleed-valves, or modulated cooling flows such as anti-ice air or variable exhaust nozzles. Passive geometry changes can include turbine or exhaust nozzle areas, which change with temperature or tip clearance. Heat transfer effects must typically cover a range of time constants (from a few seconds to a few minutes) to accurately model engine behavior. These models may include volume dynamics to address leakage or cavity flows or to meet other accuracy needs. However, these models are generally not intended to address acoustic level phenomena such as stall, surge or combustion instability.

### A.1.3 1-D Dynamic Engine Simulations

The purpose of this section is to describe recent advances in modeling gas turbine engine dynamic behavior. A dynamic turbine-engine combustor model and simulation, VPICOMB, which was developed at Virginia Polytechnic Institute and State University, [A.1] will be discussed. The integration of the VPICOMB combustion model equations with the DYNamic Turbine Engine Compressor Code (DYNTTECC), conducted at the Arnold Engineering Development Center (AEDC), [A.2 and A.3] will then be discussed. Finally, a full gas turbine engine model and simulation, the Aerodynamic Turbine Engine Code (ATEC), also developed at AEDC, [A.4 and A.5] will be described. ATEC currently has the ability to simulate a turbojet engine with the compressor system operating post-stall, and a turbofan engine operating up to the point of compressor stall.

The governing equations are derived by the application of mass, momentum, and energy conservation to the elemental control volume where:

$$\frac{\partial \mathbf{U}}{\partial t} + \frac{\partial \mathbf{F}}{\partial x} = \mathbf{G} \quad \text{Eq. A-1}$$

where:

$$\mathbf{U} = \begin{bmatrix} A\rho \\ \rho Au \\ AE \end{bmatrix} \quad \mathbf{F} = \begin{bmatrix} \rho Au \\ \rho Au^2 + AP \\ u(AE + AP) \end{bmatrix} \quad \mathbf{G} = \begin{bmatrix} -W_{Bx} \\ FX_x \\ Q_x + SW_x - H_{Bx} \end{bmatrix} \quad \text{Eq. A-2}$$

Additionally, a perfect gas is assumed and the equation of state,

$$P = \rho RT \quad \text{Eq. A-3}$$

is used. The assumption of constant specific heats ( $C_p$ ) and ratio of specific heats ( $\gamma$ ) in the property calculations, while computationally efficient, does result in predicted temperature levels in the combustor that are too high during rich combustion. This effect will be shown in the following sections. The distributed turbomachinery source terms  $-w_{B_x}, F_x, Q_x + SW_x - H_{B_x}$  are supplied to the overall model by the user. Models for the source terms will be discussed in each of the respective sections.

The time dependent flow-field within the system of interest is obtained by solving the time dependent system of equations using one of two numerical approaches. The VPICOMB model [A.1] uses an explicit Roe's flux-differencing scheme adapted to the Euler equations with source terms to evaluate the face fluxes, and then uses a second-order four step Runge-Kutta algorithm to solve for the time dependent equations. DYNTTECC [A.2 and A.3] and ATEC [A.4 and A.5] use a flux-difference-splitting scheme based upon characteristic theory to solve for the face fluxes. A first order Euler method is used to solve for the time dependent equations.

#### A.1.3.1 Combustor Component – VPICOMB

The VPICOMB model and simulation provides a one-dimensional tool running on the personal computer for analyzing dynamic gas turbine engine combustor operation. With VPICOMB, the user can analyze the influence of varying inlet conditions, fuel pulses, exit flow restrictions, and many other possible dynamic events. The user provides the simulation with appropriate initial and boundary conditions, plus any time dependent variations in the boundary conditions, and then exercises the program to determine the time dependent flow-field.

For the inlet boundary conditions, the user specifies inlet total pressure, total temperature, and flow rate. The user can also specify the friction factor along the wall of the combustor. No pressure loss due to combustion is assumed. The exit boundary condition assumes a constant value for the mass flow parameter:

$$\frac{W\sqrt{T_T}}{P_TA} = \text{Const} \quad \text{Eq. A-4}$$

The value of the mass flow function is obtained during the initial condition calculations. It is assumed that the fuel mass flow addition occurs in the first control volume. The heat release due to combustion occurs in the control volumes specified by the user as the zone of heat release. The heat release is equally distributed across the zone of heat release control volumes. The amount of energy released in the zone of heat release control volumes is a function of fuel flow rate, the combustion efficiency, the lower heating value of the fuel, and the combustor flammability limits.

The combustor flammability limits are determined by using steady state engineering correlations developed by Herbert, 1957. In order for stable combustion to occur, the primary zone equivalence ratio ( $\phi_{PZ}$ ) must fall within a rich and lean limit:

$$\phi_L \leq \phi_{PZ} \leq \phi_R \quad \text{Eq. A-5}$$

Based on experimental data, Herbert defined a Combined Air Loading Factor to calibrate the light off and blow off data. A polynomial curve fit of Herbert's flammability data for a generic can type combustor is used in the VPICOMB model. Combustion efficiency is determined by using steady state engineering correlations developed by Lefebvre, 1985 [A.6]. Lefebvre assumed that the efficiency of fuel evaporation and the reaction efficiency limit the overall combustion efficiency. Further modification to the Lefebvre work was done by Derr and Mellor, 1990 [A.7].

Because of the dynamic operation of the combustor, it is possible for heat release to occur for a short period of time even though the combustor equivalence ratio may lie outside the steady state flammability limits. Likewise, the heat release process may not resume immediately after the combustor equivalence ratio re-enters the flammability bounds. To account for these effects, a first order lag on the heat release rate has been incorporated in the model:

$$\tau \frac{d\dot{Q}}{dt} + \dot{Q} = \dot{Q}_{ss}(t) \quad \text{Eq. A-6}$$

### A.1.3.2 Compressor Component – DYNTECC

DYNTECC [A.2 and A.3] is a one-dimensional, stage-by-stage, compression system mathematical model that is able to analyze any generic compression system. DYNTECC uses a finite difference numerical technique to simultaneously solve the mass, momentum, and energy equations with turbomachinery source terms (mass bleed, blade forces, heat transfer, and shaft work). The source terms are determined from a complete set of stage pressure and temperature characteristics provided by the user.

Illustrated in **Figure A.1** is a representative, single-spool, multi-stage compressor and ducting system. An overall control volume models the compressor and ducting system. Acting on the fluid control volume is an axial-force distribution,  $FX$ , attributable to the effects of the compressor blading and the walls of the system. Appropriate inlet and outlet boundary conditions are applied at the inflow and outflow boundary

## ANNEX A – HIGHER ORDER MODELS

locations. Energy supplied to the control volume includes the rate of heat added to the fluid,  $Q$ , and shaft work done on the fluid,  $SW$ . Mass transfer rates across boundaries other than the inlet or exit, such as the case of inter-stage bleeds, are represented by the distribution,  $W_B$ .

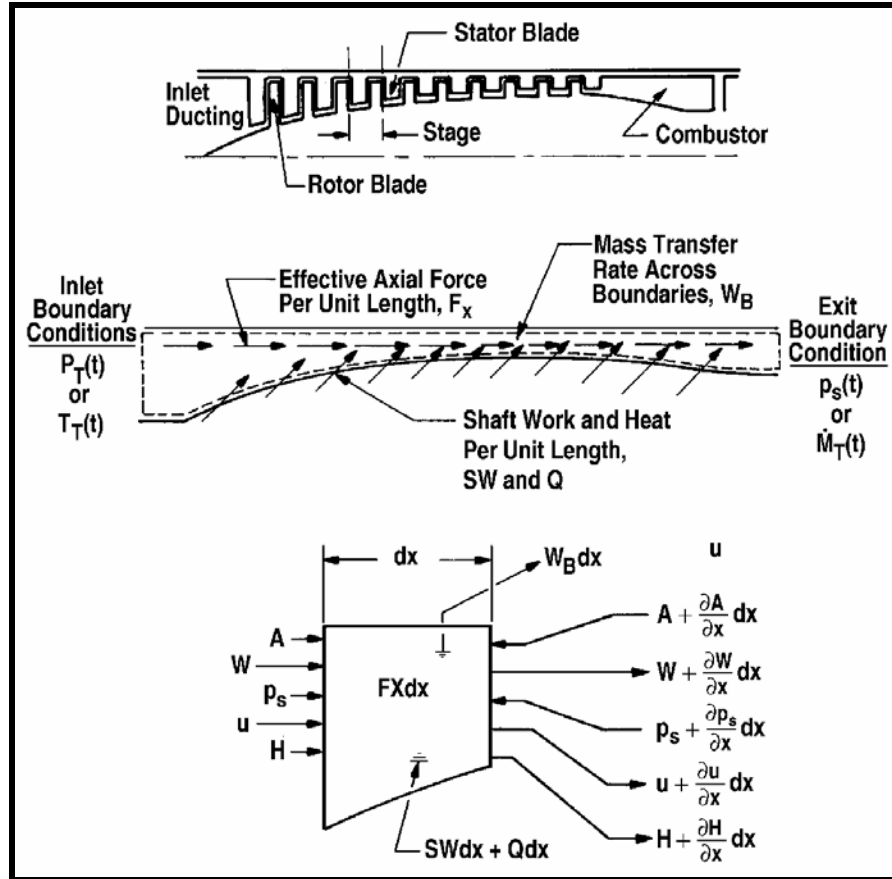


**Figure A.1: DYNTTECC Control Volume Technique.**

The overall control volume is subdivided into a set of elemental control volumes. Typically, the compressor section is subdivided by stages either as rotor-stator or vice versa depending on the way experimental stage characteristics may have been obtained. All other duct control volumes are divided to ensure an appropriate frequency response. The governing equations are derived from the application of mass, momentum, and energy conservation principles to each elemental control volume.

To provide stage force,  $FX$ , and shaft work,  $SW$ , inputs to the momentum and energy equations, a set of quasi-steady stage characteristics must be available for closure. The stage characteristics provide the pressure and temperature rise across each stage as a function of steady airflow. Using pressure rise, temperature rise, and airflow, a calculation can be made for stage steady-state forces and shaft work. A typical set of stage characteristics is presented in **Figure A.2**.

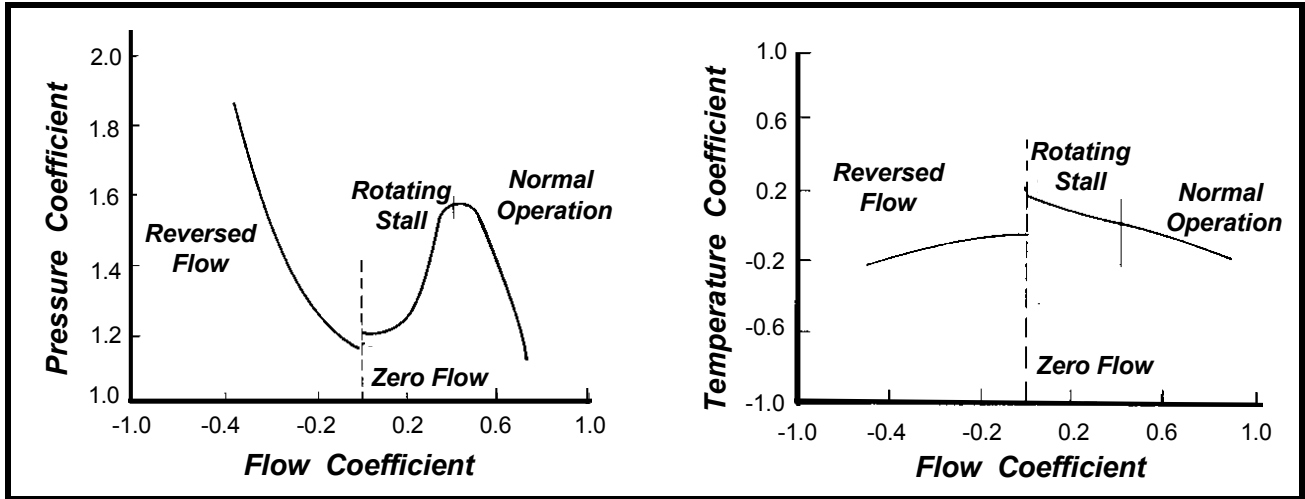


**Figure A.2:** Typical Set of Stage Characteristics.

The above discussion centers on the steady characteristic. During transition to surge and development of rotating stall, the steady stage forces derived from the steady characteristics are modified for dynamic behavior via a first-order lag equation of the form:

$$\tau \frac{d(FX)}{dt} + FX = FX_{ss} \quad \text{Eq. A-7}$$

The time constant,  $\tau$ , is used to calibrate the model to provide the correct post-stall behavior. The inflow boundary during normal forward flow is the specification of total pressure and temperature. The exit boundary condition is the specification of exit Mach number or static pressure. During reverse flow the inlet is converted to an exit boundary with the specification of the ambient static pressure. Therefore, both the inlet and the exit boundary function as exit boundaries during a surge cycle.

An explicit split-flux finite-difference algorithm is used to numerically solve the area weighted quasi-one-dimensional Euler equations. The quasi-one-dimensional Euler equations with source terms (**Eq. A-1** and **Eq. A-2**) are written in conservation Cartesian form and applied to a fixed grid. A finite difference representation of **Eq. A-1** can be applied over an interval between grid points  $j$  and  $j+1$  with the fluxes evaluated at the nodes and the sources evaluated at the center of the volume given by

$$\left( \frac{\Delta U}{\Delta t} \right)_j = I_{j-\frac{1}{2}}^+ \left( \frac{\Delta U}{\Delta t} \right)_{j-\frac{1}{2}} + I_{j+\frac{1}{2}}^- \left( \frac{\Delta U}{\Delta t} \right)_{j+\frac{1}{2}} \quad \text{Eq. A-8}$$

where

$$\left( \frac{\Delta U}{\Delta t} \right)_{j-\frac{1}{2}} = \left[ G_{j-\frac{1}{2}} - \frac{(F_j - F_{j-1})}{(x_j - x_{j-1})} \right]; \quad \left( \frac{\Delta U}{\Delta t} \right)_{j+\frac{1}{2}} = \left[ G_{j+\frac{1}{2}} - \frac{(F_{j+1} - F_j)}{(x_{j+1} - x_j)} \right] \quad \text{Eq. A-9}$$

Characteristic theory is used to develop weighting terms ( $I^+, I^-$ ) for splitting the time derivatives to the adjacent nodes as illustrated in **Figure A.3**.

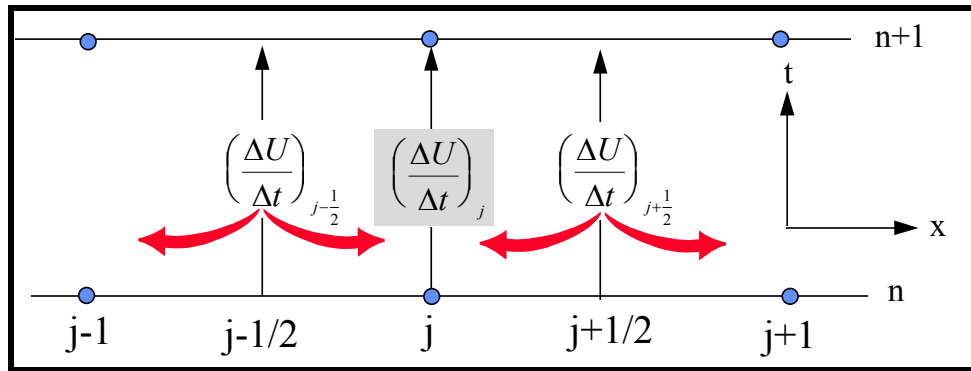


**Figure A.3:** Schematic of DYNTTECC Explicit Split Flux-Differencing Scheme.

The time derivatives at the nodes can be obtained by summing the left characteristic weighted time derivative from an upstream interval and the right characteristic weighted time derivative from the downstream interval. A solution is now obtainable at the  $n+1$  time step by a forward Euler time integration procedure.

When circumferential inlet distortion effects are important, DYNTTECC can be operated as a parallel compressor model with or without circumferential and radial cross-flow approximations. This is illustrated in **Figure A.4**. Modified parallel compressor theory (Shahrokhi, 1995), [A.8] has been applied to permit the simulation of dynamic inlet distortion. The overall compression system control volume is sub-divided into a series of circumferential and parallel tubes. Each segment or tube then acts in parallel with each other segment, exiting to the same exit boundary condition. Different magnitudes of inlet total pressure and temperature can then be imposed upon each segment of the parallel compressor. In the purest sense, each segment is independent of all other segments, except through the exit boundary condition. For complex distortion patterns the circumferential and radial cross-flow terms are approximated. System instability occurs when any one segment becomes unstable as a result of the inlet and exit conditions imposed upon it.

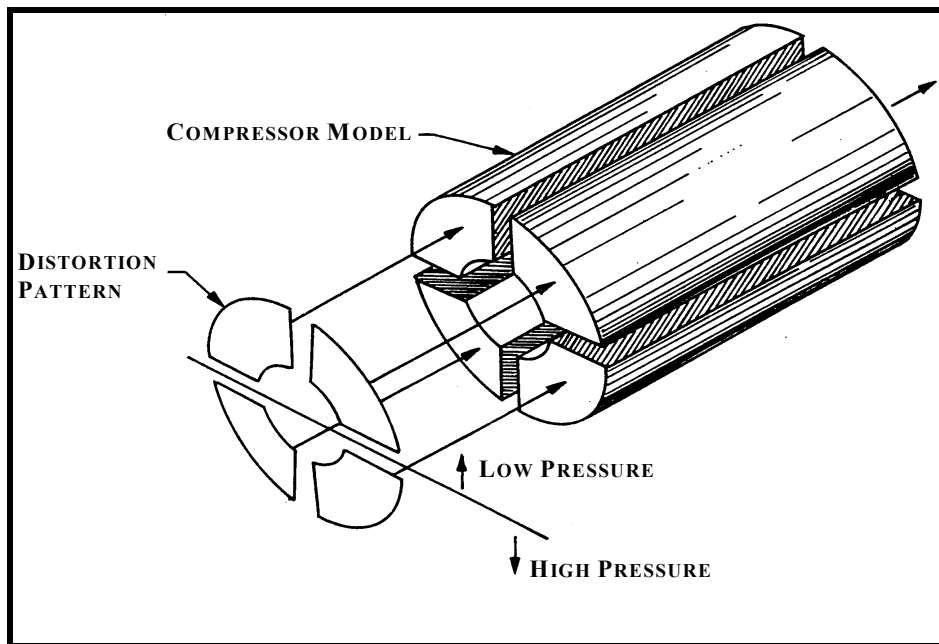


**Figure A.4:** Compressor with Circumferential Segments and Applied Inlet Distortion.

Parallel compressor theory is generally valid if the segment arc is greater than 60 degrees, also known as the critical angle. Secondary flow mechanisms become more significant for segments with arcs less than the critical angle. The parallel compressor theory's predictive capabilities deteriorate when segments of less than the critical angle are used.

Both pressure and temperature characteristics are required. During pre-stall operation, the steady state compressor characteristics are used as given. During post-stall operation, the change in compressor operating conditions is lagged using the same first order equation used in lagging the VPICOMB combustion heat release rate. The most recent version of DYNTECC has been upgraded to include the VPI developed combustor model discussed above. This new feature will permit the user to study dynamic compressor and combustor interactions.

### A.1.3.3 Full Engine Simulation – ATEC

With the inclusion of the VPICOMB combustor model equations into the DYNTECC program, development of a gas turbine engine model and simulation required was completed with the addition of a turbine model. Because of the modularity of the DYNTECC coding, integrating the turbine model into the existing code required specifying the performance characteristics in a fashion similar to the compressor performance (shaft work and blade forces) and as shown in **Figure A.5** and compared to a component level modeling scheme.

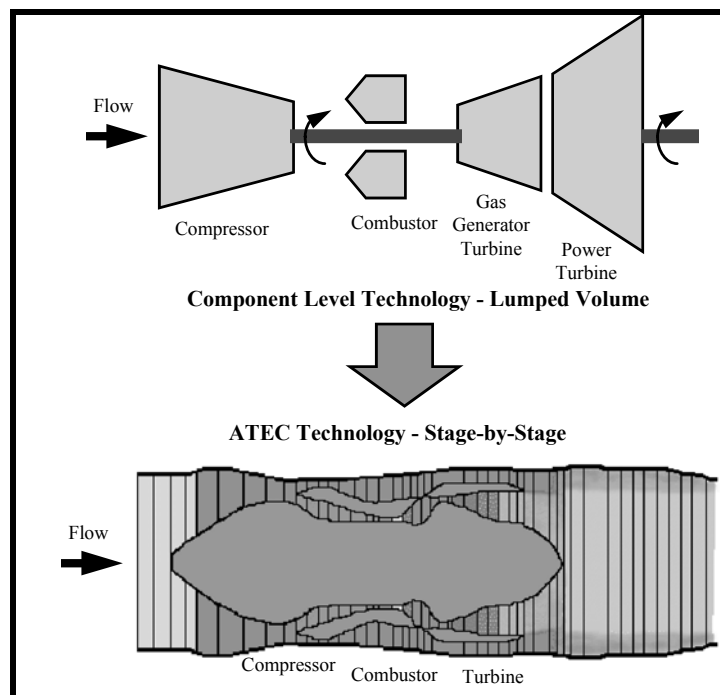


**Figure A.5: ATEC Code Compared to Component Level Modeling Technique.**

ATEC (Garrard, 1996), [A.4 and A.5] is currently configured to support two gas generator turbines coupled to compressor systems through up to two shafts, and one power turbine. To determine the amount of work extracted across a given turbine during the initial condition calculations, the gas generator turbine is assumed to exactly provide the power required by the compressor system. The user initially specifies work output from the power turbine. Once the time integration starts, energy extraction is given by the pressure ratio across the turbine and the turbine inlet flow function.

## ANNEX A – HIGHER ORDER MODELS

Operational demonstration of the dynamic engine model has been accomplished by using the T-55 turboshaft and the J-85 turbojet engines. Characteristics for each of the turbines are overall, not stage-by-stage, due to lack of inter-stage data. The shaft work and blade forces in each turbine were equally distributed across multiple control volumes, however, to keep the overall length of any given control volume on the same order as the rest of the grid. This helps maximize model dynamic fidelity and, with the explicit flow solver routine, numerical stability.

Steady state results of the engine system are compared to the engine manufacturer's steady state engine model. The comparison results are shown in **Figure A.6**. Close agreement between the two models was obtained. It is judged that the majority of the differences can be attributed to the fact that the compressor characteristics for ATEC were based on compressor rig data, which was not the same as used in the steady state model. Even with this difference, the maximum error was less than seven percent.

	Total Pressure ( $P/P_{ref}$ )			Total Temperature ( $T/T_{ref}$ )		
Location	Mfg	ATEC	%Delta	Mfg	ATEC	%Delta
Inlet	0.29	0.29	0.00	0.26	0.26	0.00
Compressor Exit	2.38	2.36	0.73	0.51	0.51	0.72
Burner Exit	2.29	2.25	1.76	1.16	1.15	0.47
Gas Generator Turbine Exit	0.81	0.87	-6.27	0.93	0.96	-3.63
Power Generator Turbine Exit	0.30	0.30	-0.75	0.75	0.79	-5.22

**Figure A.6: Comparison of ATEC and Engine Model Results.**

To demonstrate dynamic operation of ATEC, the same test case as was used to demonstrate the integration of the VPICOMB model equations into DYNTTECC has been exercised.

Variation of the relative total pressure in the engine is shown in **Figure A.6**. During the initial steady state operation, the total pressure increases through the compressor system. In the combustor, a small total pressure loss occurs. Work extraction in the turbines reduces the pressure back to near atmospheric before the flow exits the engine. As with the DYNTTECC test case, the fuel flow pulse forces the compressor into surge. Rather than being driven by a constant Mach number exit boundary condition, however, the pressure increase is tied to the turbine choking as explicitly defined by the turbine steady state operating characteristics. Steady state operation is not re-established until the fuel flow rate is decreased back to the original flow rate. The frequency of the surge cycles is reduced due to the increased volume of the calculation domain.

Relative total temperature in the engine as a function of time is also shown in **Figure A.6**. As the compressor enters the surge cycle, the reduction of air mass flow rate causes the combustor temperature to increase dramatically, until the equivalence ratio rises to the rich flammability limit. After the surge cycle

is completed, the combustion process is re-established until the next cycle forces the equivalence ratio to rise above the flammability limit.

Relative mass flow rate in the engine as a function of time is shown in **Figure A.7**. In addition to the bleed extraction occurring in the axial compressor and the fuel addition occurring in the combustor, turbine-cooling bleed is injected into the flow in the last gas-generator turbine control-volume. As with the DYNTECC test case, during each of the surge cycles, the mass flow rate in the front section of the engine reverses and becomes negative. In the back section of the engine, the flow rate is greatly reduced, but it does not reverse.

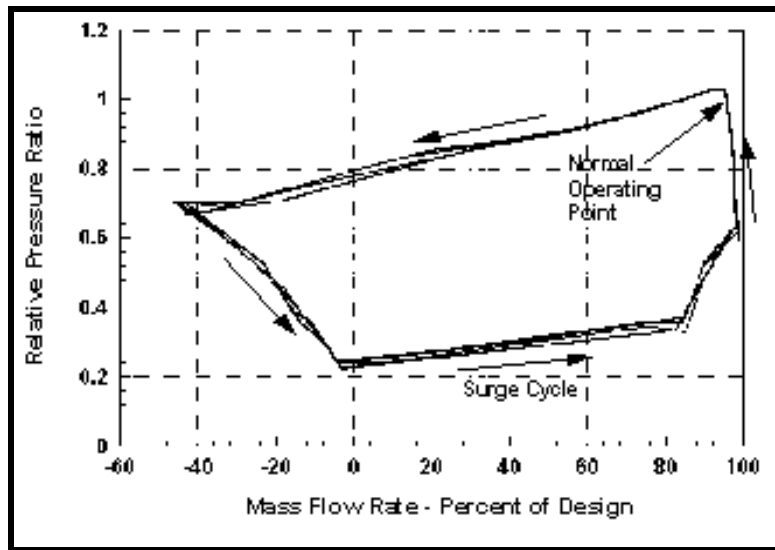


**Figure A.7: System Response with Small Lag.**

To demonstrate the capability of the model and simulation to simulate rotating stall in the compressor system, the above test case was repeated with a modification to the time-lag constant used with the compressor characteristics in the rotating stall regime. By increasing the time constant of each stage of the compressor system, the operational characteristics change. This results in the compressor system being unable to return to the normal operating mode. The effect is shown by comparing the compressor pressure ratio curves as a function of mass flow rate through the system for both cases. This comparison is shown in **Figure A.8**. With a relatively small time constant, the dynamics of the system allow the compressor to return back to the normal pre-stall operating speed line before re-entering the surge cycle, as is shown in **Figure A.7**. As is shown in the various figures, once the perturbation in fuel flow rate is removed, the system returns to normal, steady state operation. An increase in the compression system time constants forces the system into rotating stall, as is shown in **Figure A.8**. Even when the fuel flow rate is reduced back to the original level, the system is unable to recover back to the original steady state operating point.

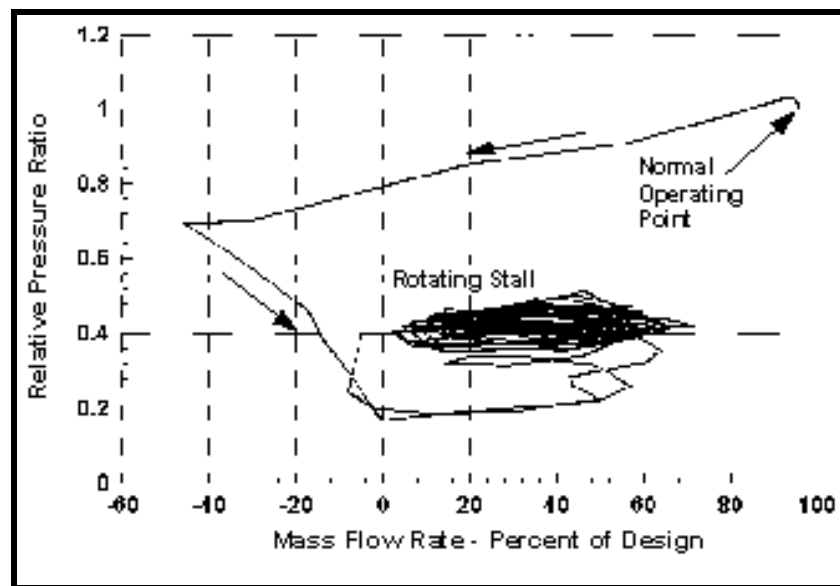


**Figure A.8: System Response with Large Lag.**

### A.1.4 Benefits of 1-D vs. 0-D Models

1-D models provide additional boundary condition details not covered by 0-D models. The reason for using a more detailed model in place of a purely empirical correlation based on 0-D conditions is to obtain greater accuracy or better fidelity in response to changing conditions. Correlations to extend 0-D models are often difficult to create and require significant effort to recreate if engine operating conditions or component representations change.

Detailed 1-D models are generally well adapted to desktop PC and UNIX workstations. They do not represent a significant computational barrier unless near real-time transient performance is required or they are to be part of a larger simulation or a study requiring a large number of runs.

## A.2 HIGH FIDELITY 2-D/3-D MODELS

2-D and 3-D models not only predict but also attempt to model the physics at this higher level of detail.

0-D or 1-D models may be used predict 2-D and 3-D variations in engine conditions, and may use a physical model to do it, but the physical models stay at the lesser level of detail. Engine system level models at this level of detail are just becoming practical from both computation and component modeling needs.

Detailed models provide potential for closer modeling of the physics, reducing the need for empiricism and to provide insight into the component operation and variation. The primary near term benefit of using 2-D and 3-D models of an engine system is to provide insight into the component operation details that 0-D and 1-D models cannot.

### A.2.1 Zooming of 2-D Models

2-D Axisymmetric models have been the workhorses for compressor and turbine design for many years. 3-D tools are gradually replacing them. The primary benefit of using 2-D system models is to facilitate the design and detail analysis of a particular component across the range of possible boundary conditions. In the past, running lower fidelity models did this. More detailed boundary conditions were created through

an empirical process, and then the 2-D code was run in isolation. Computing capacity made this process the only reasonable option.

It is now possible to run a 2-D component simulation, in conjunction with a simplified model of the rest of the engine, in a few minutes and to even run the entire engine in less than an hour. The choice now falls between:

- Modeling a component or the entire engine at the 2-D level, which must be justified in terms of the extra model development complexity and effort required to add value to the results; and
- Obtaining estimates that can be made based on a simpler model.

Currently, it is only in the design and detailed insight into the turbo-machinery where the added information justifies the more detailed modeling. The engine level performance impact of this greater detail is generally lost in the overall empiricism and modeling uncertainty. For example, 2-D modeling of clearance effects can be of interest in the analysis and design of the compressor. However, the predictive accuracy and stability of currently available models does not justify their use in a whole engine model. **Figure A.9** indicates typical characteristics for different types of model.

<b>Model Type</b>	<b>Accuracy</b>	<b>Stability</b>	<b>Computation Speed</b>
<b>Component Design</b>	High	Low	Low
<b>Component Analysis</b>	Medium	Medium	Medium
<b>Engine Analysis</b>	Low	High	High

**Figure A.9: Model Attributes for Design and Analysis.**

### **A.2.2 3-D Models (Euler and RANS)**

Full physics 3-D CFD models for single blade rows and components are beginning to see use outside of research areas. For system models, virtually all require some level of empiricism or simplification such as use of source terms or body forces for the turbo-machinery or an average passage or mixing plane assumption.

Two types of 3-D codes may be encountered: Euler and Reynolds Averaged Navier-Stokes (RANS). Examples of Euler codes include the dynamic Turbine Engine Analysis Compressor code, TEACC, [A.9] and the steady state NASA ENG10 [A.10] code. These codes generally use some modeling simplifications (source terms, streamline curvature methods) to allow solution on a single workstation in minutes to hours. They can generally run multiple points or even transients. As computing power grows, these limitations may be reduced. However, the need to accept simplifying assumptions to allow for the desired level of full engine analysis will remain for some time.

An example of RANS codes are: The NASA Average Passage Code (APNASA) [A.11] is an example of a component code which has been extended to cover all the blade rows in an engine. Simplified component models or boundary conditions inputs are used to address portions of the engine that can not be addressed using the component code. In some instances two multi-dimension components codes are joined to address the interaction between different component types. The NPARC and ADPAC code have been combined to study Fan and Inlet interaction [A.12]. Models based on combining or extending detailed component codes require the highest level of computer resources. To run a single point, these codes may

## ANNEX A – HIGHER ORDER MODELS

---

require in dozens or even hundreds of workstations. Codes have been developed for the purpose of multi-dimensional simulation throughout the engine.

Three-dimensional codes require a level of geometry detail not generally required for 0-D system performance models. The detailed component models often require gridding and application to different disciplines may put additional compatibility constraints on the solution. Often the bookkeeping of the geometry and gridding exceeds the complexity of other parts of the simulation. This process is often facilitated by use of a CAD package to manage geometry and geometry centered information. Linking this information to a CAD system designed to address these issues greatly simplifies the already complicated job of creating and managing the simulation. Some more details on these types of codes can be found in *Annex B*.

### A.3 HIGHER ORDER MODELING APPLICATIONS

Included in this Annex are synoptics or examples of applications using higher order (1-D, 2-D and 3-D) component or engine simulations. The format established in *Chapter 2* has been retained to provide the reader with a sense of what the code can do and an applicable reference for further enlightenment.

#### A.3.1 1-D Dynamic Model Applications

An important component of the gas turbine engine is the compression system. In today's military turbine engines, the compression system consists of one or more axial compressors. These axial compressors must operate in a stable manner even with severe inlet pressure or temperature distortion. Many experimental and analytical investigations have been conducted in the past three or four decades to separately quantify the effects of pressure or temperature distortion on the compression system. While little experimental work has been performed on combined time-variant total pressure and temperature distortions, some investigations have been carried out to examine the effects of combined steady-state pressure and temperature distortion on compression system stability. With the advent of highly agile maneuvering aircraft with weapons release near the engine inlets, there exists a requirement to quantify the combined effects of severe pressure and temperature distortion, both transiently and in the steady state.

##### A.3.1.1 Rotating Stall and Surge Investigation Using 1-D Compressor Model

In most aircraft gas turbine engines, the compression system consists of one or more aerodynamically coupled axial-flow compressors. It is the function of the compression system to increase the static pressure and density of the working fluid. Without stable aerodynamic operation, the compression system cannot deliver the desired increase in static pressure and density. During operation of axial-flow multi-stage compression systems in gas turbine engines, undesired system phenomena known as surge and rotating stall have been observed. Several modeling techniques have been developed over the last decade to investigate surge and rotating stall. One technique involves a stage-by-stage one-dimensional approach described below.

##### *Modeling Techniques Used*

DYNTECC is a one-dimensional, stage-by-stage, compression system mathematical model, [A.2 and A.3], which is able to analyze any generic compression system (see *Section A.1.3.2*). DYNTECC uses a finite difference numerical technique to simultaneously solve the mass, momentum, and energy equations with turbomachinery source terms (mass bleed, blade forces, heat transfer, and shaft work). The source terms are determined from a complete set of stage pressure and temperature characteristics provided by the user.

### ***Potential Benefits***

Mathematical compressor models have become a major tool for understanding compression system behavior during dynamic events, such as inlet distortions. A validated compression system model can be used to extend the range of the experimental test results to the untested regime. Using a validated stage-by-stage compression system model, a parametric investigation can be conducted to determine the qualitative effects of various recovery actions or design changes on system operability.

### ***Cited Examples***

- Hale, A.A. and Davis, Jr., M.W., “Dynamic Turbine Engine Compressor Code, DYNTTECC – Theory and Capabilities”, AIAA Paper # 92-3190, June 1992. [\[A.2\]](#)
- Davis, Jr., M.W. et al., “Euler Modeling Techniques for the Investigation of Unsteady Dynamic Compression System Behavior”, Loss Mechanisms and Unsteady Flows in Turbomachines, AGARD-CP-571, January 1996. [\[A.3\]](#)

DYNTTECC was configured to aid in the analysis of a ten-stage compressor rig test conducted at the Compressor Research Facility to investigate the boundary between surge and rotating stall for high-pressure ratio compressors. The model was executed at the experimentally determined stall and surge boundary where the recovery hysteresis was most severe. DYNTTECC was calibrated at the stall and surge boundary by adjusting calibration constants to produce rotating stall. The constants were held fixed for subsequent analysis that investigated possible hardware modifications to reduce the sensitivity of the compressor to rotating stall.

Calibration of DYNTTECC with experimental data matched the overall performance and individual stage performance of the 10-stage compressor rig. As illustrated in [Figure A.10](#), the compressor initially experiences a partial surge cycle, then transitions to rotating stall. DYNTTECC individual stage performance is also compared to that obtained experimentally. For both overall and individual stage behaviors, DYNTTECC reproduced the experimental results fairly accurately during the dynamic event.

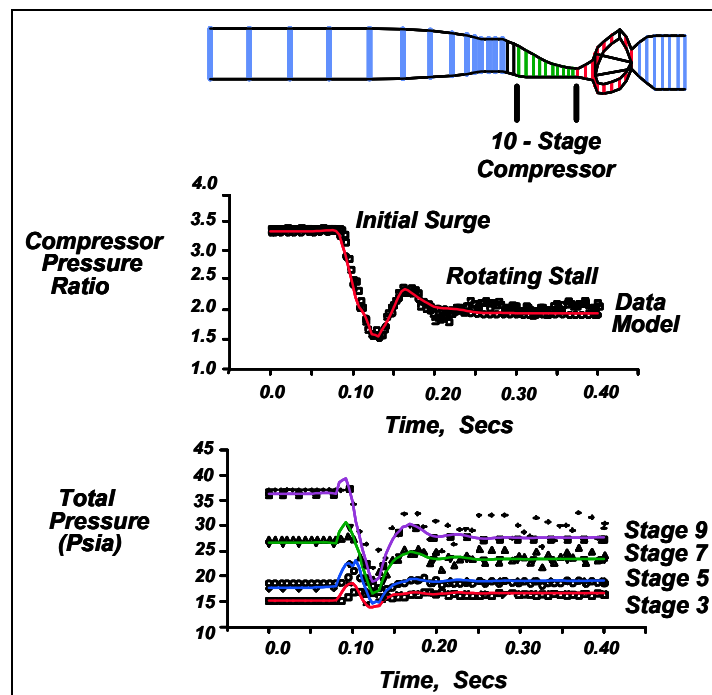


**Figure A.10: Post-Stall Dynamic Event – DYNTTECC.**

### ***Limitations of Chosen Modeling Technique***

For the stage-by-stage compression system modeling technique chosen, the biggest issue is the development of stage characteristics. Generally, even compressor rig tests are not instrumented well enough to get proper stage characteristic information. If blade shapes are known, a mean-line or streamline curvature technique can be used to generate characteristics. However, these types of codes rely on empirical inputs based upon cascade test results and generic correlations. In addition the DYNTECC code, even though the single spool version has a parallel compressor capability, does not handle radial distortion well and the dual-spool version of DYNTECC is currently not configured for parallel compressors.

### **A.3.1.2 Engine Stall Using One-Dimensional Modeling**

The gas turbine engine has played a significant role in the advancement of the flight capabilities of modern day aircraft. In order for a gas turbine engine to operate at the performance, operability, and durability level for which it was designed, stable operation of the various engine components must be ensured. Transient and dynamic instabilities, which could push the engine components beyond their operational limits, could result in loss of thrust, loss of engine control, or possible engine damage due to high heat loads and high cyclic stresses. The influence of operating instabilities must be quantified not only from the individual component considerations, but also from the point of view of any interaction between the various components.

### ***Modeling Techniques Used***

The turbine engine modeling technique was the Aerodynamic Turbine Engine Code, or ATEC, [A.4 and A.5], a time-dependent turbine engine model and simulation capable of simulating a turbojet engine operating in both transient and dynamic modes. Other gas turbine engine models and simulations have typically focused on providing a transient, component-level representation of the overall engine, or a dynamic representation of a single component. The ATEC simulation provides a bridge between the two types of simulations. It provides the computational efficiency that is desired when simulating the gas turbine engine during transient events, but it also provides the appropriate simulation techniques to address overall engine operation during a dynamic event such as compressor surge or combustor blow-out. ATEC provides the detailed system resolution needed to analyze a dynamic event (such as a stage-by-stage representation of the compression system), but uses the same type of component performance information used in standard transient simulations.

The Aerodynamic Turbine Engine Code (ATEC) solves the one-dimensional, time dependent, compressible, inviscid flow-field solution for internal flows by solving the Euler equations for the conservation of mass, momentum, and energy. The solution is obtained over the computational domain using both implicit and explicit numerical integration routines. The effects of the various engine system components are modeled using turbomachinery source terms in the governing equations.

### ***Potential Benefits***

The ATEC model and simulation can simulate on and off-design steady-state operation, as well as transient and dynamic engine responses to perturbations in a wide range of operational and control conditions. By example, it has been shown that the ATEC simulation can handle a wide variety of conditions that occur during normal and abnormal gas turbine engine operation. The benefits of the variable time-step routine, which uses a combination of the explicit and implicit numerical solvers, were also demonstrated. Test cases were presented that demonstrated that the ATEC simulation could: be calibrated to a steady-state data set; extended the steady-state calibration to a transient fuel variation; presented results from an engine operation that resulted in compressor surge; and addressed a turboshaft engine going through the start process. The ATEC results were shown to agree closely with test data where available.

## Cited Examples

- Garrard, G.D., “ATEC: The Aerodynamic Turbine Engine Code for the Analysis of Transient and Dynamic Gas Turbine Engine System Operations – Part 1: Model Development”, ASME Paper # 96-GT-193, June 1996. [A.4]
- Garrard, G.D., “ATEC: The Aerodynamic Turbine Engine Code for the Analysis of Transient and Dynamic Gas Turbine Engine System Operations – Part 2: Numerical Simulations”, ASME Paper # 96-GT-194, June 1996. [A.5]

This example demonstrates the real benefit of a dynamic simulation, by computing post-stall operation of a compressor and engine system, which cannot be modeled with a cycle-type simulation. The test case simulated a transient throttle movement using the T55-L-712 that resulted in the gas generator portion of the engine decelerating from 100 percent speed to approximately 90 percent speed. After a brief pause at the 90 percent speed, the engine was accelerated back to the 100 percent speed condition. The change in fuel flow rate during the acceleration was fast enough to force the compressor into surge cycles. The relative compressor pressure ratio as a function of time is illustrated in the figure below. The multiple surge cycles cause a significant drop in the total pressure throughout the engine and a corresponding flow reversal as indicated in **Figure A.11**.

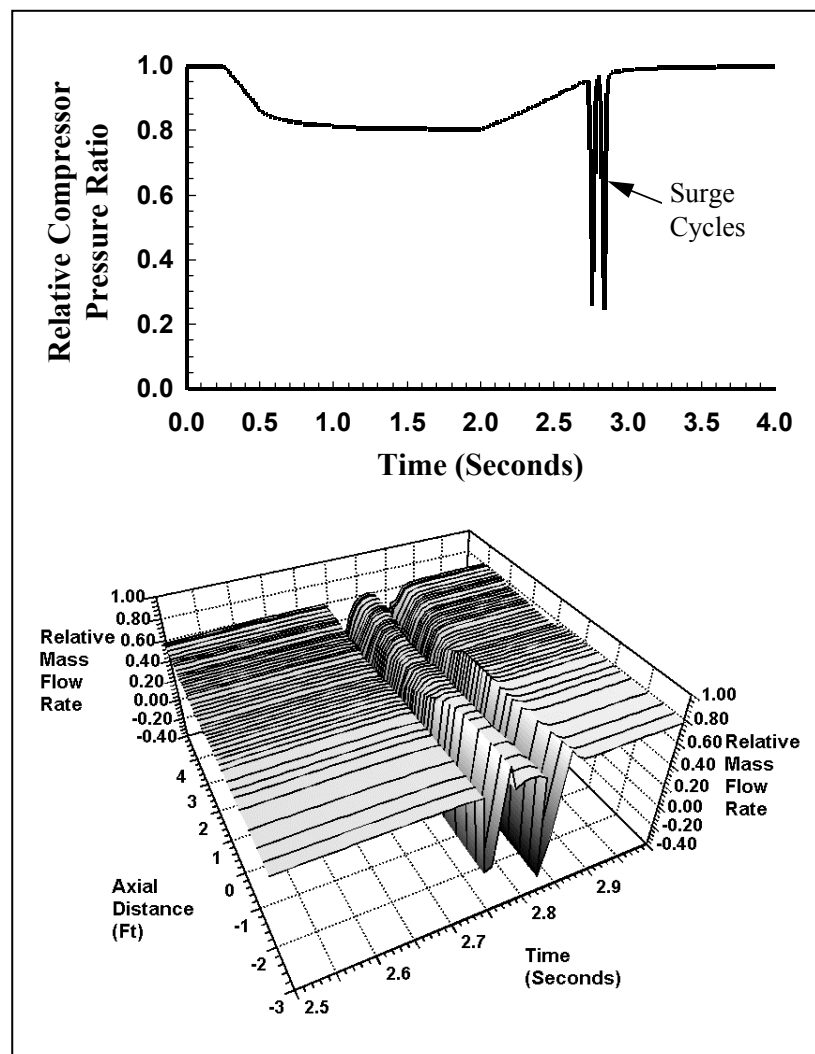


**Figure A.11:** Surge Cycles during Engine Re-Acceleration.

***Limitations of Chosen Modeling Technique***

The simulation described in the cited reference uses a one-dimensional approach. Thus, the interaction associated with inlet spatial distortion can not be analyzed with this modeling technique. It is, however, an excellent technique to investigate control actions that can be initiated because of some destabilizing event such as an inlet by-pass door malfunction or an engine surge.

**A.3.1.3 Combustor Dynamics**

Due to the inherent dynamics of the fluid system, transient performance of a gas turbine engine can differ significantly from that predicted from quasi-steady operating assumptions. The consequences of these can be quite dramatic, including unexpected crossing of the compressor surge line while changing operating points. Beyond the surge line, compressor rotating stall and surge serve as the forcing function for a complex dynamic interaction between engine components. Because these unsteady operating cycles produce substantially reduced performance and durability the recovery from the instability is an important issue facing the gas turbine designer. Because of this, significant efforts have been made to accurately simulate the performance of a compressor undergoing a surge transient. As these techniques have matured, the focus increasingly has shifted to an extension of these methods to encompass the entire engine, and thus capture the important compressor-combustor interactions that occur during engine surge.

***Modeling Techniques Used***

Design methods for gas turbine engine combustors require mathematical models that satisfy two simultaneous and often-conflicting requirements. These are to provide an accurate description of the highly complex geometry and physics involved, and be sufficiently inexpensive in computational requirements to allow its incorporation in a design cycle involving the evaluation of a great number of operating conditions. For these reasons, a one-dimensional, finite-rate, unsteady combustor model has been developed that incorporates most elements found in modern gas turbine burners, and yet is simple enough to be implemented in desktop computers.

Combustor models for dynamic behavior may have a division of the flow path into annular and primary streams with finite-rate effects within the primary flow and interaction between hot and cold gases through dilution holes. Over the past 50 years there have been numerous efforts at modeling gas-turbine combustor performance. Physical models and numerical techniques have primarily been developed for the simulation of steady flow in combustors. In the past 20 years, particular emphasis has been placed on engine pollution. One of the key difficulties in modeling dynamic engine behavior has been the limited knowledge of transient combustion phenomena, or more specifically post-stall combustor dynamics. Initial efforts employed a quasi-steady heat release formulation based on the fuel-air ratio and only simple combustion efficiency degradation was modeled. Two recent modeling efforts have made improvements based on finite-rate chemistry for incorporation into a dynamic gas turbine engine model.

***Potential Benefits***

Dynamic modeling of combustor and compressor interaction can lead to a better understanding of the relationship between combustor blowout and re-light during engine surge. When a multi-zoned model is used, combustor flow within the primary zone can be modeled with finite-rate chemistry to allow predictions of blowout and the effects of perturbation in boundary and operating conditions.

***Cited Examples***

- Rodriguez, C.G. and O'Brien, W.F., "Unsteady, Finite-Rate Model for Application in the Design of Complete Gas-Turbine Combustor Configurations", Design Principles and Methods for Aircraft Gas Turbine Engines, RTO-MP-8, February 1999. [\[A.1\]](#)

- Costura, D.M. et al., “A Model for Combustor Dynamics for Inclusion in a Dynamic Gas Turbine Simulation Code”, AIAA Paper # 97-3336, Presented at the 33rd AIAA/ASME/SAE/ASEE Joint Propulsion Conference, July 6-9, 1997, Seattle, WA. [A.13]

Indicated in **Figure A.12**, is a solution grid for a generic reverse flow combustor used in an analysis as presented in **Ref. [A.1]**. The main issues associated with the layout of the grid from the point of view of a one-dimensional theory are division of the main flow into primary and annular paths, and interaction between flow paths through the presence of dilution holes. Once the grid has been selected, analysis can be conducted to determine the effects of perturbations in boundary and operating conditions. Indicated in **Figure A.13**, are the effects of an imposed fuel flow oscillation on total pressure.

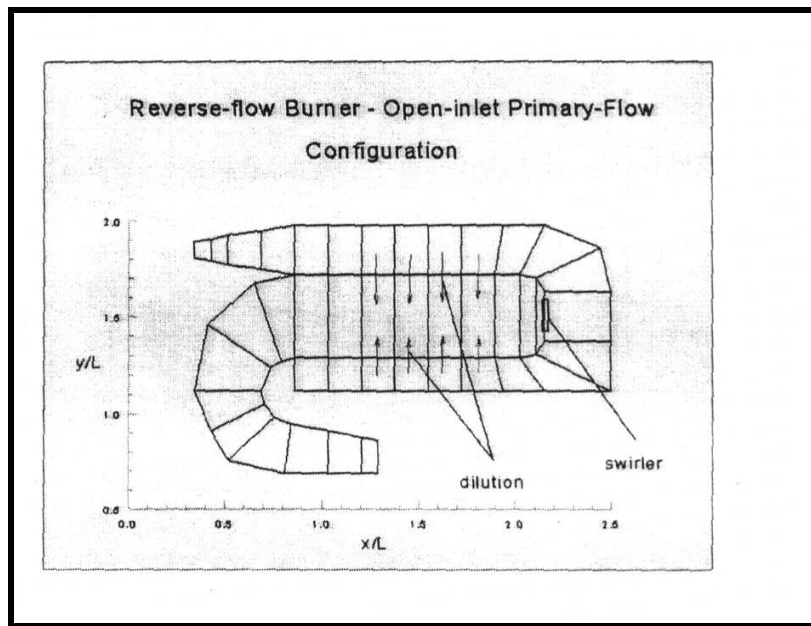


**Figure A.12: Grid of Reverse Flow Burner.**

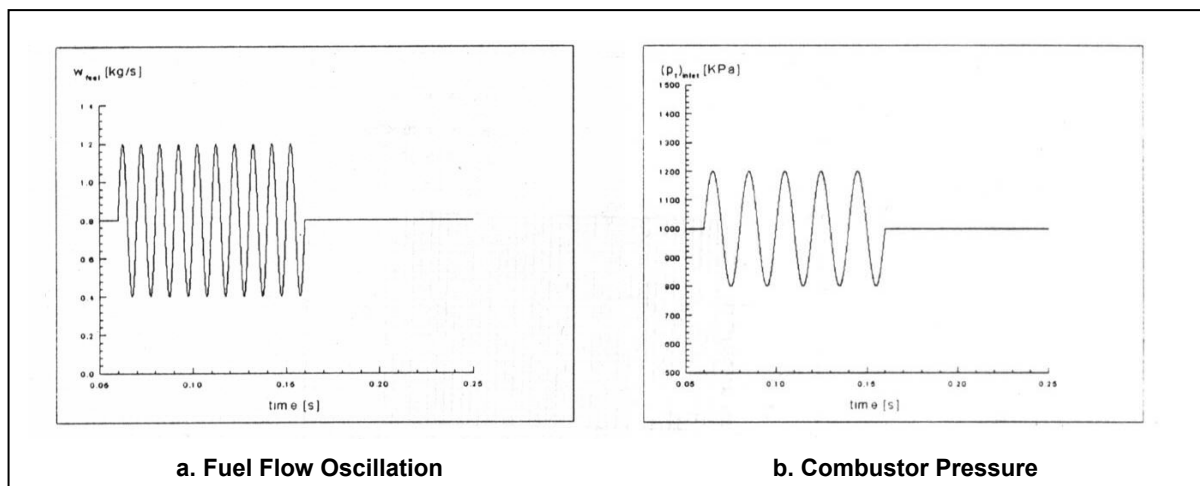


**Figure A.13: Effects of an Imposed Fuel Flow Oscillation on Combustor Pressure.**

Combustor performance for a dump combustor as illustrated in **Figure A.14** during ignition and blowout are illustrated in **Figure A.15** and **Figure A.16**, taken from **Ref. [A.13]**. During the ignition event, airflow

## ANNEX A – HIGHER ORDER MODELS

unsteadiness was quite high during the period of ignition from  $t = 6$  to  $t = 7$  seconds. An oscillation of 8 psi in magnitude and 50 Hz frequency is seen, indicative of an initial instability in the combustor. For a lean blowout case, a gradual fuel reduction began at 7 seconds with complete fuel shut-off achieved near  $t = 13$  seconds. Note the minimum fuel flow that can be recorded is 0.5 gph, and thus the exact point of fuel extinction is expected between  $t = 13$  and  $t = 14$  seconds.

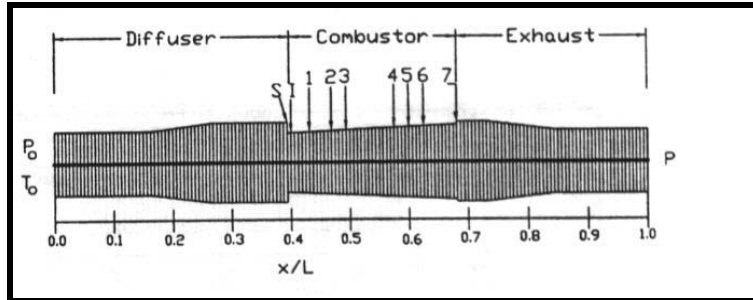


Figure A.14: Grid for Dump Combustor.

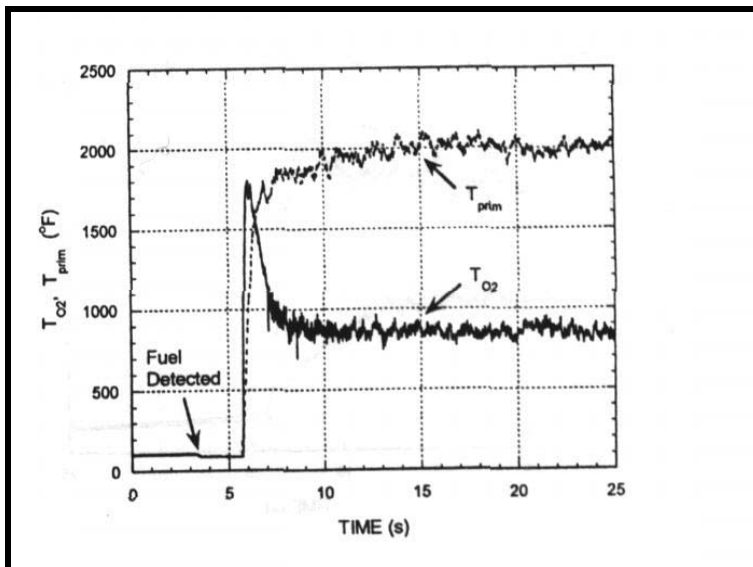


Figure A.15: Ignition Event.

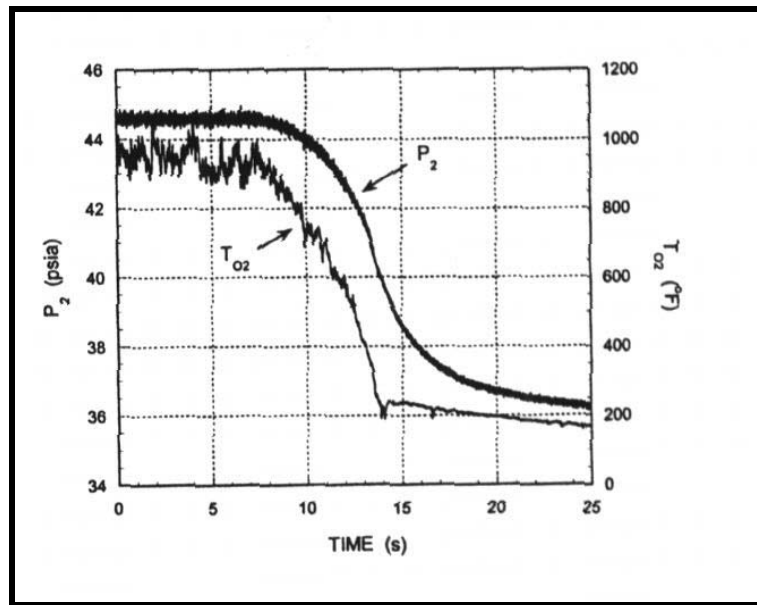


Figure A.16: Blowout Event.

#### Limitations of Chosen Modeling Technique

Unsteady models, based on the fundamental governing equations for flows with non-equilibrium chemistry, have been developed for gas turbine configurations. The chosen approach in both models is a one-dimensional fluid dynamics approach with integral conservation equations for multi-species flows with chemical reactions. All the effects that could not be handled by the usual one-dimensional ideal flow (Euler) equations (i.e. area changes and friction) were included in source terms on the right-hand side of the system. In [Ref. \[A.1\]](#), a one-step chemistry model was used and in [Ref. \[A.13\]](#), a two step model was used. Both models can provide steady state and dynamic results. The results from these models were satisfactory, but showed some limitation of any one-dimensional approach in that pressure losses could not be modeled by simple fluid dynamics, and were provided to the model.

#### A.3.1.4 Engine-Inlet Integration

The economic viability of a commercial supersonic transport, such as the High Speed Civil Transport (HSCT), is highly dependent on the development of a high-performance propulsion system. Typically, these propulsion systems mate a supersonic mixed-compression inlet with a turbojet or turbofan engine. The nature of such propulsion systems offers the potential for undesirable component interactions, which must be thoroughly understood for proper design. Therefore, it is imperative to have tools that allow investigation of inlet-engine integration issues.

The inlet must provide the engine with the correct mass flow rate at the highest possible pressure with minimum drag. Additionally, flow angularity and distortion must be minimized at the compressor face if the engine is to function appropriately. Maximum thrust with a minimum of fuel consumption will not be obtained without the inlet operating close to peak performance. Unfortunately, operating near peak performance can result in an inlet unstart (expulsion of the normal shock) followed by engine stall and possibly surge. When that happens, proper control action must be taken to recover the system as quickly as possible. Thus the operability of the overall system must also be addressed, because stable time dependent operation of the system must be ensured for both scheduled and non-scheduled events.

Because of the complexity of the inlet and engine systems, and the high cost of experimentally determining overall performance, numerical simulations of the components can be of significant benefit.

## ANNEX A – HIGHER ORDER MODELS

For example, dynamic simulations provide a means for investigating the potential interactions mentioned above, as well as providing a test bed for guiding the design, testing and validation of propulsion controls.

### *Modeling Techniques Used*

The simulation system, operating under the Application Portable Parallel Library (APPL), closely coupled a supersonic inlet with a gas turbine engine. The supersonic inlet was modeled using the Large Perturbation Inlet (LAPIN) computer code, and the gas turbine engine was modeled using the Aerodynamic Turbine Engine Code (ATEC) as illustrated in **Figure A.17**.

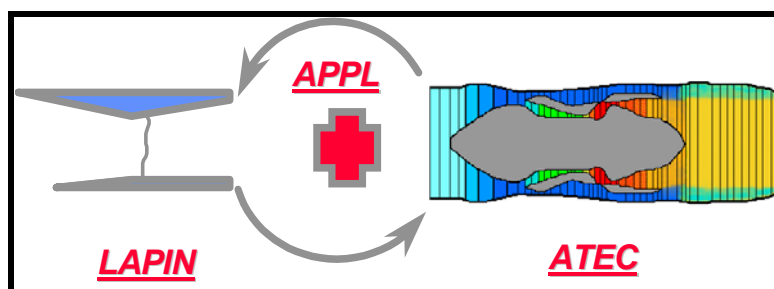


**Figure A.17: Schematic of the Coupled Inlet-Engine Codes.**

Both LAPIN and ATEC provide a one-dimensional, compressible, time dependent flow solution by solving the one-dimensional Euler equations for the conservation of mass, momentum, and energy. Source terms are used to model features such as bleed flows, turbomachinery component characteristics, and inlet subsonic spillage while unstated. High frequency events, such as compressor surge and inlet unstart, can be simulated with a high degree of fidelity. The simulation system was exercised using a supersonic inlet with sixty percent of the supersonic area contraction occurring internally, and a GE J85-13 turbojet engine as illustrated in **Figure A.18**.

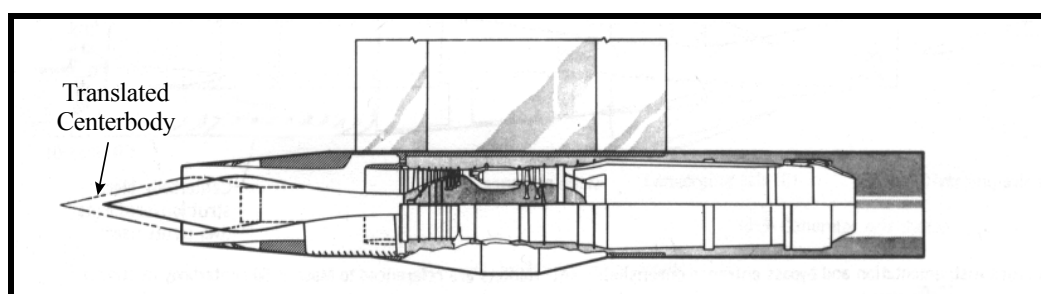


**Figure A.18: Cross-Section View of the 4060 Inlet and J85-13 Turbojet Installation.**

The cited paper [A.14] describes the general modeling techniques used in the simulations, and the approach taken to implement the simulations under the APPL environment. It presents results from selected test cases.

### *Potential Benefits*

Traditionally, aircraft inlet performance and propulsion performance have been designed separately and latter mated together via flight-testing. In today's atmosphere of declining resources, it is imperative that more productive ways of designing and verifying aircraft and propulsion performance be made available to the aerospace industry. One method of obtaining a more productive design and evaluation capability is

with numerical simulations. Numerical simulations can provide insight into physical phenomena that may not be understood by test data alone. Simulations can fill information gaps and extend the range of test results to areas not tested. In addition, once a simulation has been validated, it can become a numerical experiment and the analysis engineer can conduct ‘what-if’ studies to determine possible solutions to performance or operability problems.

### ***Cited Example***

- Garrard, G.D., Davis, Jr., M.W., Wehofer, S. and Cole, G., “A One-Dimensional, Time Dependent Inlet/Engine Numerical Simulation for Aircraft Propulsion Systems”, ASME Paper # 97-GT-333, June 1997. [\[A.14\]](#)

The simulation system was exercised using a supersonic inlet with sixty percent of the supersonic area contraction occurring internally, and a GE J85-13 turbojet engine. The inlet-engine simulation combination of LAPIN and ATEC was compared to experimental results. A transient event was initiated at a flight Mach number of 2.5 by pulsing the bypass doors in the closed direction. The result was an inlet unstart followed by an engine compression system stall. During the given transient, the majority of the system instabilities can be traced to the fact that the normal shock, located initially downstream of the inlet throat, was expelled outside of the inlet. The location of the shock is plotted as a function of time in [Figure A.19](#). The shock location is normalized by the inlet cowl lip radius, and referenced to the centerbody tip. The cowl lip is axially located two cowl-lip-radii downstream of the centerbody tip. The act of closing the bypass valve forces the shock structure to be expelled from the inlet. Moving the centerbody forward in conjunction with proper modulation of the bypass doors allows the shock to be re-ingested.

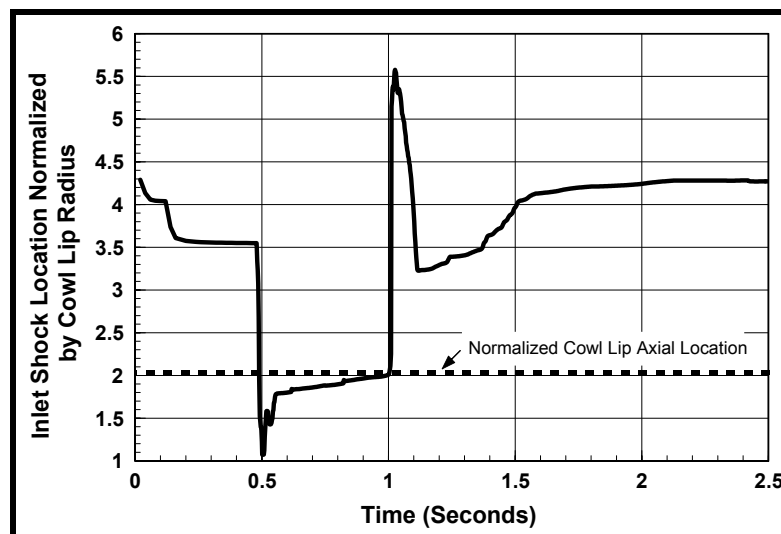


**Figure A.19: Inlet Shock Location.**

Total pressure across the compressor is lost once the inlet system unstarts. At the instant of unstart there is a sharp spike in pressure ratio to a value exceeding 5.0 which (probably) exceeds the steady-state stall line, resulting in stall. Although the system begins to recover the original level of compressor operating pressure ratio, the compressor total pressure ratio is lower. The relative compressor pressure ratio is plotted as a function of the inlet corrected mass flow rate, expressed as a percentage of the design mass flow rate, in [Figure A.20](#). It is evident from the figure that there is one engine surge cycle, with a rotating stall event. Recovery takes place at a lower corrected inlet mass flow rate due to the lower engine shaft speed.

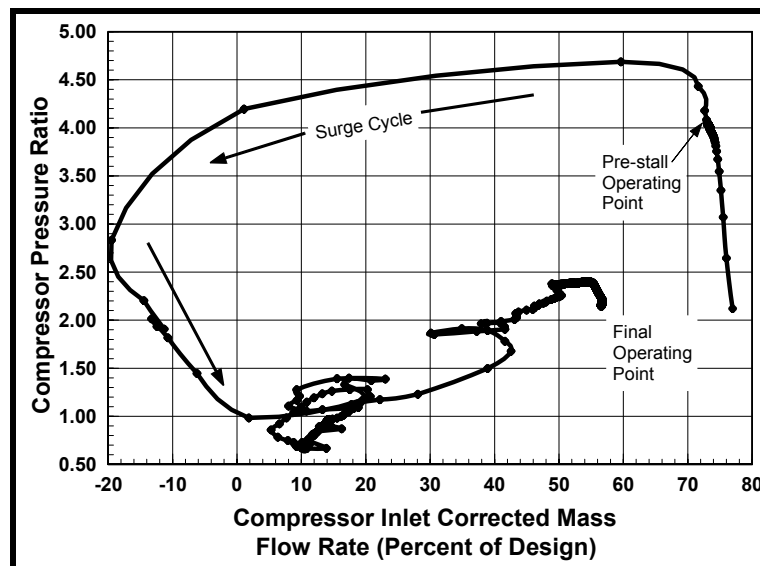


**Figure A.20:** Compressor Pressure Ratio as a Function of Compressor Inlet Corrected Mass Flow Rate.

#### *Limitations of Chosen Modeling Technique*

The simulation described in the cited reference uses a one-dimensional approach. Thus, the interaction associated with inlet spatial distortion cannot be analyzed with this modeling technique. It is, however, an excellent technique to investigate control actions that can be initiated by some destabilizing event such as an inlet by-pass door malfunction or an engine surge.

#### **A.3.1.5 Hot Gas Ingestion**

Engine stability problems have occurred when exhaust products from rocket or gun firings are ingested into the engine. The most common form of instability is axial compressor stall which, depending on engine type and the aircraft flight envelop, can lead to surge with serious and damaging effects. From previous investigations, it has been determined that the rapid inlet temperature increase is probably the predominant factor causing compression system instability in these situations. Tests with rapid inlet temperature transient rates in the range of 2000 – 8000 K/sec are typical of those experienced during gun or rocket gas ingestion.

#### *Modeling Techniques Used*

The numerical simulation used for this type of application was a stage-by-stage compression system model known as *DYNTECC* (*DYN*amic *TECC* Engine Compressor Code) [A.2]. *DYNTECC* is able to analyze post-stall behavior and predict the onset of compression system instability. Stability limit analysis can be conducted for single-spool and dual-spool systems with and without temperature or pressure distortion. *DYNTECC* requires a full set of stage characteristics and annulus geometry as inputs. *DYNTECC* was configured and applied to the geometry of the TF30 compression system as illustrated in **Figure A.21**, for an investigation into the effects of temperature ramps on system stability. The TF30 compression system has dual-spool rotors, but with three compressors: fan, low-pressure and high-pressure compressors.

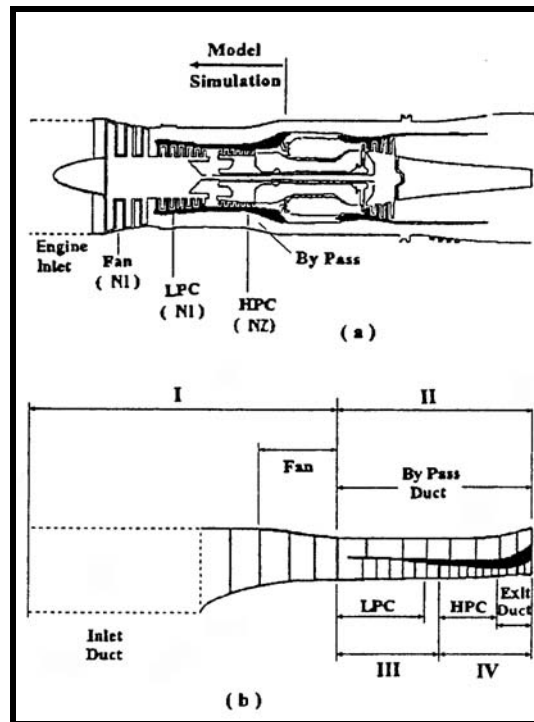


**Figure A.21: Schematic of TF30 Compression System Modeled.**

### Potential Benefits

Mathematical compressor models have become a major tool for understanding compression system behavior during dynamic events such as inlet distortions. A validated compression system model can be used to extend the range of the experimental test results to the untested regime. Using a validated stage-by-stage compression system model, a parametric investigation can determine the qualitative effects of gas ingestion effects on system operability.

### Cited Example

- Abdel-Fattah, A.M., “Response of a Turbofan Engine Compression System to Disturbed Inlet Conditions”, Journal of Turbomachinery, Vol. 119, No. 4, October 1997. [\[A.15\]](#)

Using the DYNTECC stage-by-stage compression system simulation, the following observations were made with regard to the TF30 gas ingestion investigation:

- The stability limit of the system in response to inlet temperature ramps improved with increasing low rotor speed.
- The stability limit, in terms of temperature rise required to surge the compressor, was found to be independent of the rise rate as illustrated in [Figure A.23](#).
- At the time of instability because of inlet temperature ramps, the DYNTECC model predicted the possibility of the third stage of the fan as the critical stage responsible for compression system surge initiation as illustrated in [Figure A.22](#).

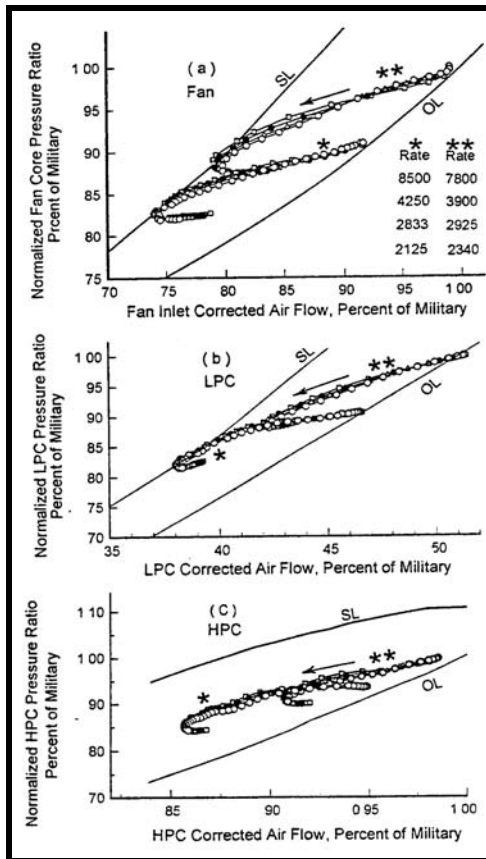


**Figure A.22: Ops Line Migration due to Temperature Ramps.**

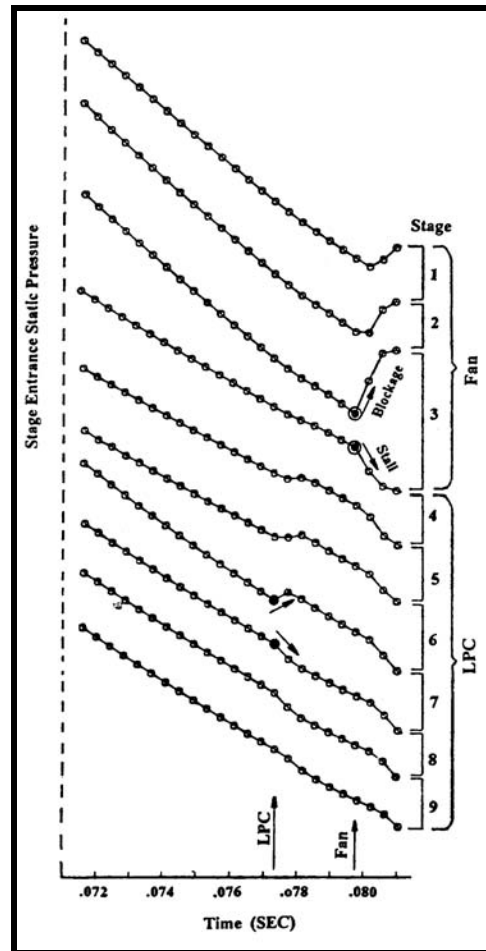


**Figure A.23: Static Pressure Signature.**

## Limitations of Chosen Modeling Technique

For the stage-by-stage compression system modeling technique chosen, the biggest issue is the development of stage characteristics. Generally, even compressor rig tests are not instrumented well enough to get proper stage characteristic information. If blade shapes are known, a mean-line or streamline curvature technique can be used to generate characteristics. However, these types of codes rely on empirical inputs based upon cascade test results and generic correlation. In addition, the DYNTECC code does not handle radial distortion well, even though the single spool version has a parallel compressor capability. The dual-spool version of DYNTECC is currently not configured for parallel compressors.

### A.3.1.6 Distortion Investigation Using Parallel Compressor Model

Modern high-performance military aircraft are subjected to rapid flight maneuvers, which place great operational demands on their air-breathing gas turbine engines. One component of the engine that is particularly sensitive to the fluid dynamic transients that result from rapid aircraft maneuvers is the compressor. The compressor should operate in a stable manner during all aspects of flight. However, rapid flight transients cause the aircraft intake to present a highly distorted total pressure flow-field to the compressor inlet. High distortion levels may cause the compressor to surge at high rotational speeds or slip into rotating stall at lower rotational speeds. Since total pressure distortion is the primary reason

for reaching the engine stability limit, its effects on system performance and operability need to be understood.

### ***Modeling Techniques Used***

For this investigation, a one-dimensional compression system model with a parallel compression system modeling technique was used (DYNTECC). Parallel compressor theory states that the overall control volume representing the compressor and inlet or exit duct system may be circumferentially divided into segments. Each segment then acts in parallel with each other segment, exiting to the same exit boundary condition. Different magnitudes of inlet total pressure and temperature can then be imposed upon each segment of the parallel compressor as illustrated in **Figure A.24**. In the purest sense, each segment is independent of all other segments, except through the exit boundary condition.

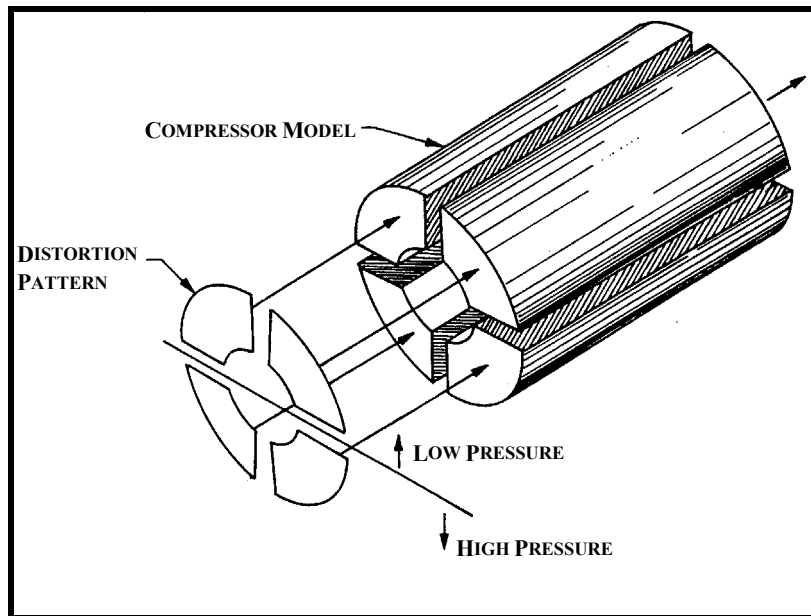


**Figure A.24: Parallel Compressor Theory.**

Each circumferential segment was modeled using a one-dimensional approach with an overall control volume for each. Each overall control volume was then subdivided into elemental control volumes. The governing equations were derived by the application of mass, momentum, and energy conservation principles to the elemental control volume. In the compressor section, a stage elemental control volume consists of a rotor followed by a stator and associated volume representing the complete stage. Acting on this fluid control volume is an axial-force distribution,  $F_X$ , attributable to the effects of the compressor blading and walls of the system. In addition, the rate of heat transfer to the fluid and shaft work done on the fluid are represented by distributions,  $Q$  and  $SW$ , respectively.

### ***Potential Benefits***

Mathematical compressor models have become a major tool for understanding compression system behavior during dynamic events such as inlet distortions. A validated compression system model can be used to extend the range of the experimental test results to the untested regime. Using a validated parallel compressor model, a parametric investigation can be conducted to determine the qualitative effects of certain combinations of transient and steady state pressure and temperature distortions on system operability.

## ANNEX A – HIGHER ORDER MODELS

### Cited Example

- Davis, Jr., M.W. et al., “Euler Modeling Techniques for the Investigation of Unsteady Dynamic Compression System Behavior”, Loss Mechanisms and Unsteady Flows in Turbomachines, AGARD-CP-571, January 1996. [A.3]

DYNTECC can be configured to analyze inlet total pressure distortion using a modified parallel compressor theory. DYNTECC was used to analyze the effects of inlet distortion on a two-stage, low aspect ratio fan. The model was initially calibrated against the experimental clean inlet performance of the compressor. The modified model was then validated using the compressor performance with a pure circumferential inlet distortion pattern. The inlet distortion pattern was generated from a 1/rev circumferential distortion screen shown in **Figure A.25**.

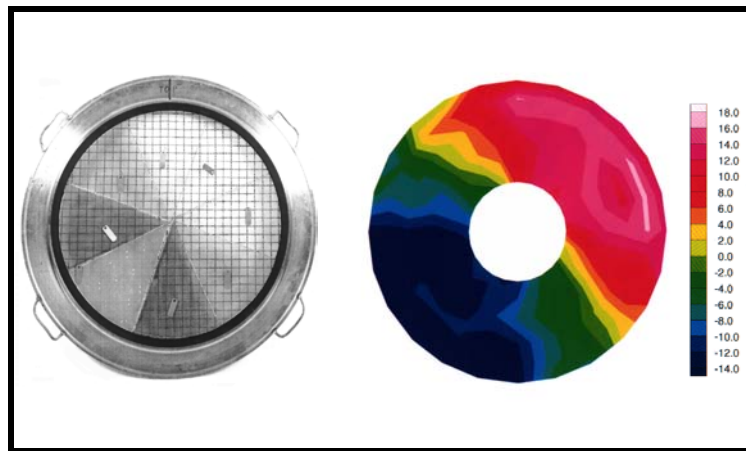


**Figure A.25:** Imposed Distortion Pattern, Produced by Distortion Screen.

This screen produces a total pressure inlet distortion that is purely circumferential. The simulation was run with the model modifications, as well as with the pure parallel compressor theory for comparison purposes. Shown in **Figure A.26** are the model predictions, compared to the experimental results at 98.6% speed. The inlet distortion pattern has a significant impact on both compressor performance and operability.

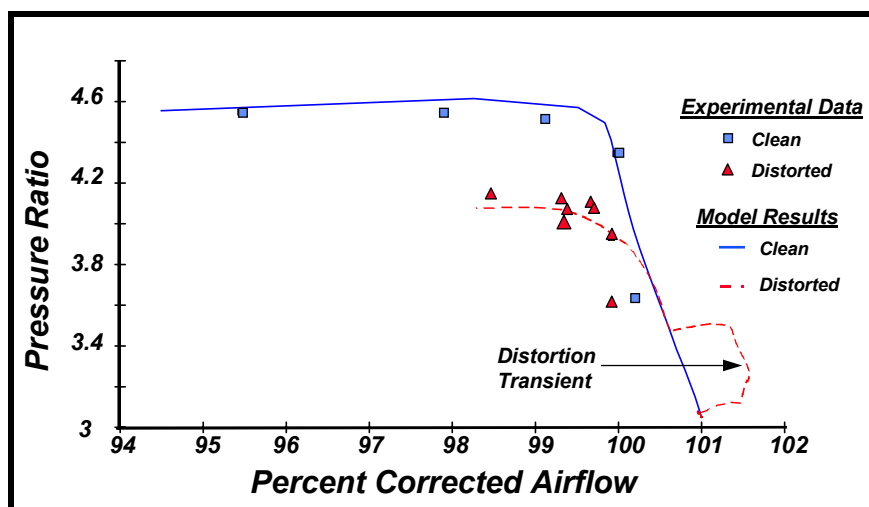


**Figure A.26:** Model Prediction and Comparison.

### ***Limitations of Chosen Modeling Technique***

For the parallel compressor theory, system instability occurs when any one segment becomes unstable as a result of the inlet and exit conditions imposed upon it. This assumption has been successful when the simulation is limited to few segments. The assumption becomes invalid when the simulation uses many circumferential segments without a mechanism to redistribute circumferential flow. Some simulations have improved upon this concept by allowing circumferential cross-flow or radial redistribution. However, these improvements are usually empirical in nature and rely upon specific databases.

### **A.3.2 Three-Dimensional Model Applications**

The following applications use modeling techniques that range from solving the 3-D Euler equations to full 3-D Navier-Stokes equations. Each has their advantages and disadvantages and contributes in specific areas. No one 3-D modeling technique can solve all types of problems and as such each is suited to a specific type of application. The reader is encouraged to investigate the references since what is presented in this section is a summary of each reference.

#### **A.3.2.1 Distortion Investigation**

Modern high-performance military aircraft are subjected to rapid flight maneuvers, which place great operational demands on their air-breathing gas turbine engines. One component of the engine that is particularly sensitive to the fluid dynamic transients that result from rapid aircraft maneuvers is the compressor. The compressor should operate in a stable manner during all aspects of flight. However, rapid flight transients cause the inlet to produce a highly distorted total pressure flow-field to the compressor inlet. High distortion levels may cause the compressor to surge at high rotational speeds or slip into rotating stall at lower rotational speeds. Since total pressure distortion may cause the compression system to reach the stability limit earlier, its effects on system performance and operability need to be understood. Distortion imposed on a circumferentially swirling flow was shown by Greitzer and Strand (1978) to have a three-dimensional (3-D) nature, which is fundamental to the development of both inlets and compressors. Design or analysis engineers are interested in understanding the details of the flow-field to determine the effects of inlet total pressure distortion on the compressor. One way to quantify the effects of distortion is to test for that effect in a ground test facility. Another way is to analyze the flow-field using a computational technique.

### ***Modeling Techniques Used***

Parallel compressor theory has been used successfully in the past to develop an understanding of compressor performance with inlet distortion. However, parallel compressor theory has been generally restricted to simple inlet distortion patterns and is generally conservative at estimating the stability limit. Investigators have made extensive modifications to parallel compressor theory through modeling techniques to account for the transfer of mass, momentum, and energy transfer between segments. These techniques are empirically based and have to be applied on a case-by-case basis. Recent developments of three-dimensional simulations can automatically account for the transfer of conservation properties.

A 3-D numerical simulation for analysis of inlet distortion has been developed and is known as the Turbine Engine Analysis Compressor Code (TEACC) [A.9]. TEACC solves the compressible three-dimensional (3-D) Euler equations over a finite-volume grid domain through each blade row. The Euler equations are modified to include turbomachinery source terms of bleed flow, blade forces (in the three Cartesian directions), and shaft work, which model the effect of the blades. The source terms are calculated for each circumferential grid section of each blade row by the application of a streamline curvature code. A methodology was developed for distributing the turbomachinery source terms axially, radially, and circumferentially through the bladed region. The overall TEACC development methodology is conceptually presented in **Figure A.27**.

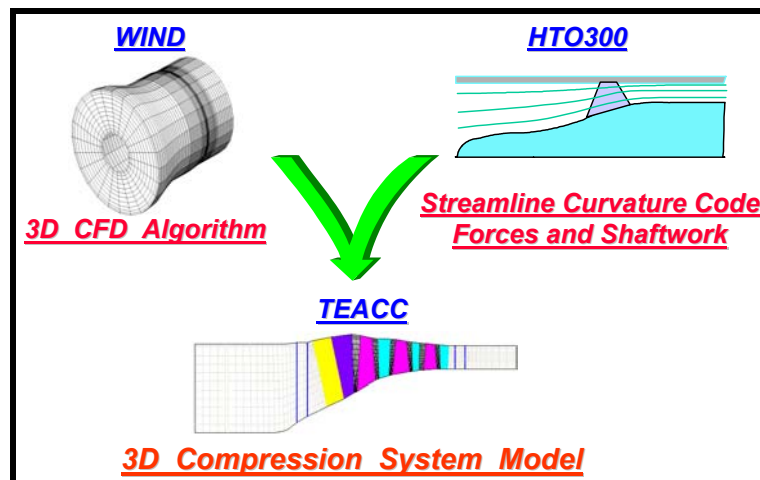


**Figure A.27:** General Technical Approach for 3-D Dynamic Compression System Model, TEACC.

### Potential Benefits

Distortion imposed on a circumferentially swirling flow has been shown to be three-dimensional (3-D) in nature. Design or analysis engineers are interested in understanding the details of the flow-field to determine the effects of inlet total pressure distortion on the compressor. One way to quantify the effects of distortion is to test for that effect in a ground test facility. Currently, the inlet and engine are tested separately. Typically, the aircraft fuselage is too big to fit in a wind tunnel. A forebody simulator is used in conjunction with the inlet to characterize its flow-field. The forebody simulator is designed to produce a flow-field at the inlet reference plane (IRP) similar to the flow-field produced by the aircraft. Screens are constructed to capture the most severe dynamic patterns produced by the inlet and are then placed in front of the engine to measure the loss of stall margin produced by the steady-state inlet distortion. However, it is expensive to instrument a compressor and perform the necessary number of tests to adequately understand the compressor flow-field. Numerical simulations have been developed to support the testing community in this area.

### Cited Examples

- Hale, A.A. and O'Brien, W.F., "A Three-Dimensional Turbine Engine Analysis Compressor Code (TEACC) for Steady-State Inlet Distortion", *Journal of Turbomachinery*, Vol. 120, July 1998, pp. 422-430. [A.9]
- Hale, A.A., Chalk, J., Klepper, J. and Kneile, K., "Turbine Engine Analysis Compressor Code: TEACC – Part II: Multi-Stage Compressors and Inlet Distortion", AIAA Paper # 99-3214, Presented at the 17th AIAA Applied Aerodynamics Conference, June 1999. [A.16]

A three-stage fan, representing a modern, high-performance military fan was modeled. It consists of a structural strut, a variable inlet guide vane (IGV) attached to the back of the strut, and three rotor-stator pairs. Only overall experimental performance data were available for comparison. No blade-row by blade-row or radial distributions of flow quantities were available. Consequently, only overall performance was compared with data. An axial-radial representation of the grid used for the three-stage fan is shown in **Figure A.28**. The three-dimensional grid on which the flow-field solution was obtained was uniformly spaced in the circumferential direction at 15-degree intervals.

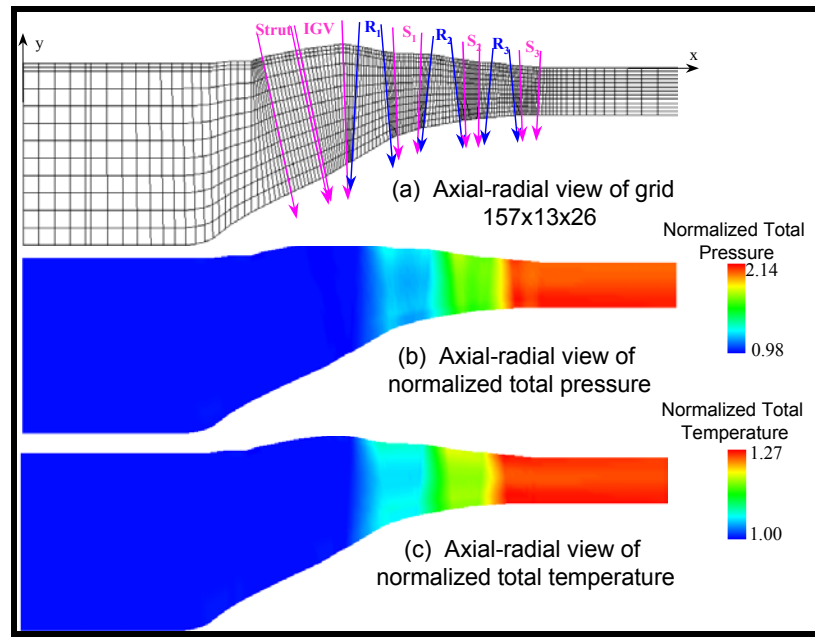


**Figure A.28: Grid and Performance for Three-Stage Fan at 80-percent Corrected Speed.**

The fan was executed with clean, standard-day inlet conditions. The results of the TEACC fan simulation are at 68% of the design corrected mass flow on the 80% speed line. Both the normalized pressure ratio and the normalized temperature ratio achieved at this point were within 0.5% of the experimental data. These results were achieved with uncalibrated loss and deviation correlations obtained from the open literature. As expected, there is an increase in both total pressure and total temperature through the machine. **Figure A.28** provides an insight into the general character of how the total pressure and temperature vary radially and axially throughout the machine.

Illustrated in **Figure A.29** is the calibrated clean inlet performance of the three-stage fan at various speeds and a corresponding flow-field for one particular point on the map. Illustrated in the flow-field view are streamlines, colored with Mach number, through the fan. This figure clearly illustrates the rotors turning the flow and the stators straightening the flow. The total turning of the flow through the entire machine is about 45 degrees. The hub has the highest Mach number through the entire fan. The streamlines illustrate that the flow is almost completely axial at the exit of the fan.

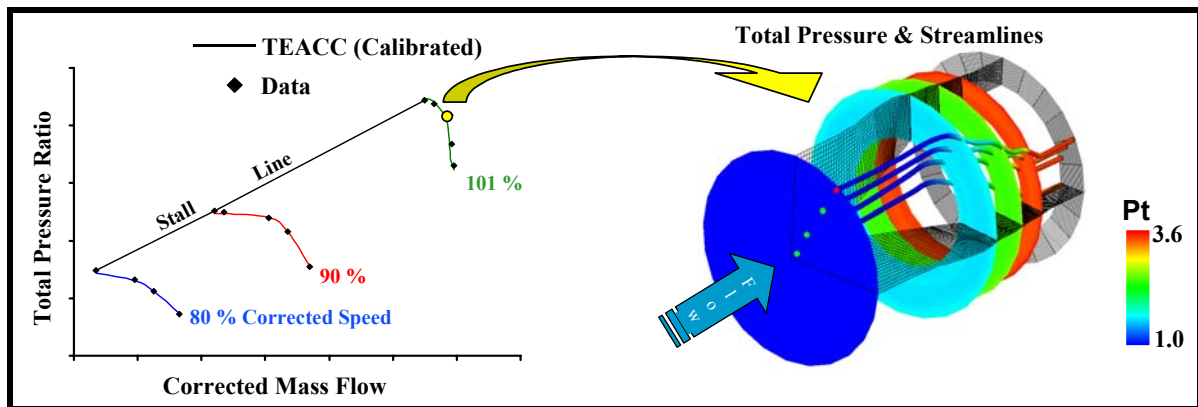


**Figure A.29: Point Inlet Performance and Corresponding Flow-Field for a Typical Three-Stage Military Fan.**

## ANNEX A – HIGHER ORDER MODELS

This same three-stage fan was exercised with a total pressure distortion flow-field imposed upon its inlet as illustrated in **Figure A.30**. The distortion was simulated with as a steady state pattern produced by an inlet distortion screen, a standard ground test method for simulating distortion at the engine inlet plane. Although, the model results are not compared to experimental results there is enough information to make an engineering judgment as to the validity of the results.

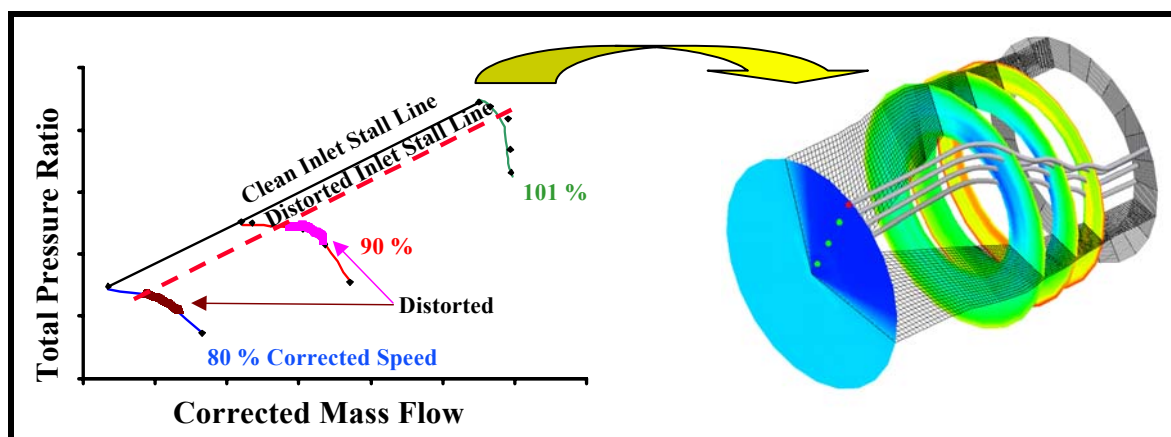


**Figure A.30: Predicted Performance with Imposed 90° Circumferential Distortion.**

### *Limitations of Chosen Modeling Technique*

This modeling technique has its strengths and weakness. The approach allows for a relatively quick computation of distortion when compared to traditional CFD turbomachinery, but because there is a level of empiricism the flow-field may not be accurately represented at a detailed level suitable for design. This modeling technique is best suited for studying potential design changes that can be quantified as to their effects on blade performance and system response to inlet distortion.

### **A.3.2.2 Rotating Stall and Surge Investigation**

Compressor instability is a major limiting factor on gas turbine engine operating range, performance, and reliability. The instability, either in a form known as rotating stall or surge, occurs at an operating point with low mass-flow and a large pressure rise. To avoid such instabilities, the compressor has to run at an operating point corresponding to a lower pressure ratio so that an adequate stall margin is maintained. The stall margin can be badly reduced in operating environments for which the inlet conditions are non-uniform. Predicting the condition at which instability will occur in a compressor requires an understanding of the flow process leading to the onset of the instability. The transition from initial disturbance to final stall or surge can usefully be divided into three stages: (1) inception, (2) development, and (3) final flow pattern. The inception stage is the period when disturbances start to grow (flow becomes unstable). It defines the operating point and conditions at which instability occurs. In practice, the disturbances will take a finite amount of time, ranging from a few to several hundred rotor-revolutions, to grow into final stall or surge. So, the inception stage can be viewed as the early development of the unstable flow. The development stage, which includes all the processes after the inception stage through to the final flow pattern, is usually of less importance. It is often the case that one final form of instability in one compressor could be the pre-stage of the final form in another compressor.

### *Modeling Techniques Used*

A non-linear three-dimensional computational model aimed at simulating 3-D finite amplitude disturbances such as inlet distortions, short wavelength stall inception processes, and part-span stall cells

has been developed as outlined in the cited reference [A.17]. To make the model practicable in terms of currently available computational resource, the following simplifications were made:

- Infinite number of blades assumption – the resolution of flow-field in every blade passage is not computationally feasible with currently available computational resources.
- A local pressure rise characteristic in every small portion of a blade passage can be defined. It is essential for a blade row to respond in a local manner, since flow redistribution is expected within a blade row. This assumption is consistent with the infinite number of blade assumption and is thus good for a blade passage of high solidity.

Since the number of blades is infinite in a bladed region, the flow at each circumferential position can be regarded as axisymmetric flow in a coordinate frame that is fixed to the blade row. The pressure rise and flow turning due to blades can thus be simulated by a body force field. Due to the presence of the blades, the flow-fields between any row blade passages can be different. Therefore, a three-dimensional flow-field in a blade row can be composed of an infinite number of axisymmetric flow-fields. This idea is illustrated in **Figure A.31**.

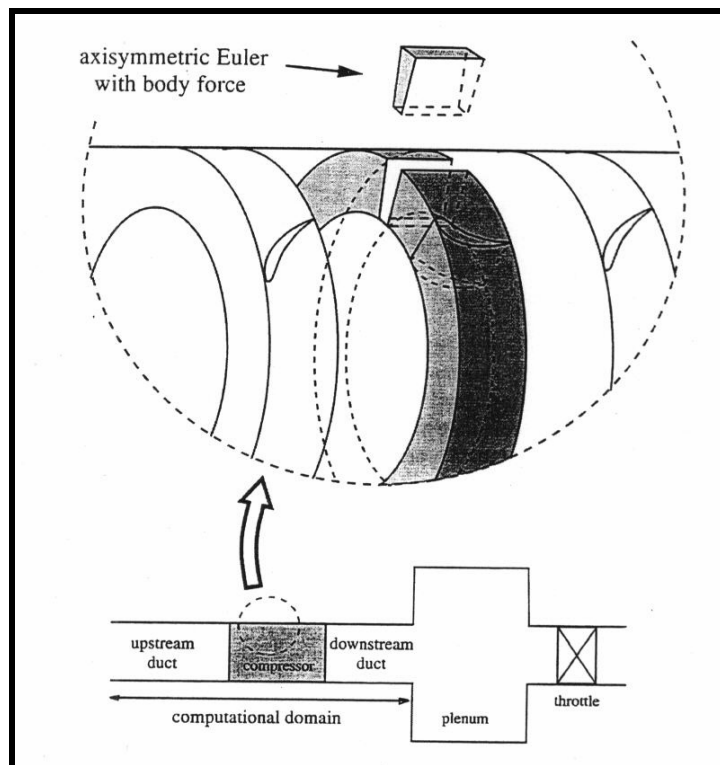


**Figure A.31: Typical Blade Row Characteristics.**

The requirements on the body force field are:

- In steady axisymmetric conditions, the body force should be capable of reproducing the required pressure rise and flow turning;
- The body force should be capable of responding to the flow disturbances for both the steady situations (e.g. inlet distortions) and unsteady flow situations;
- The body force field is formulated from the following given compression system characteristics:
  - Pressure rise characteristic in each blade row,

## ANNEX A – HIGHER ORDER MODELS

- Exit relative flow angle, and
- Blade metal angle distribution.

A notional characteristic set is illustrated in **Figure A.32**. This type of characteristic is similar to that used in the 1-D models such as DYNTECC (see **Section A.1.3.2**).

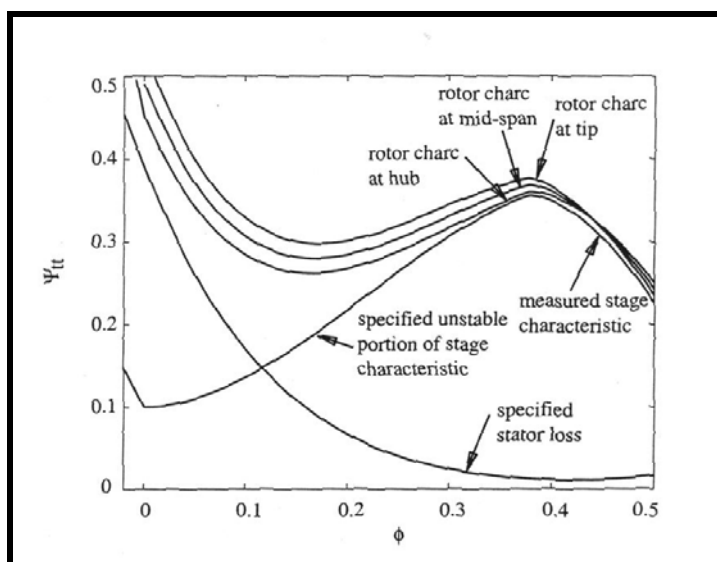


**Figure A.32: Euler Approach with Body Forces.**

### Potential Benefits

Having a model to emulate the inception of rotating stall or surge provides a means for improving the operational characteristics of any compression system. Understanding the mechanisms of rotating stall inception will provide compression system designers a means to prevent or delay the onset of this type of instability. A strength of this type of modeling technique is that the model can be used to investigate the interactions between the compressor and other components. Some types of investigations that could be conducted are:

- Interaction between the inlet and the compressor with distortions and its impact on the performance and stability margin;
- Hot gas ingestion into the engine and its impact on stability;
- The behavior of an inlet vortex in an intake and its impact on the performance and stall margin; and
- The model could become a component in an engine system to model the dynamic behavior of a whole engine under various dynamic situations.

### Cited Examples

- Gong, Y., “A Computational Model for Rotating Stall and Inlet Distortions in Multistage Compressors”, GTL Report #230, March 1999, Gas Turbine Laboratory, Massachusetts Institute of Technology, Cambridge, MA. [\[A.17\]](#)
- Longley, J.P. et al., “Effects of Rotating Inlet Distortion on Multistage Compressor Stability”, ASME Paper # 94-GT-220, June 1994. [\[A.18\]](#)

In the work by Gong, the model is used to simulate stall inception. Two major inception types have been experimentally identified: modal waves and spikes. Modal waves are exponentially growing long wavelength (length scale comparable to the annulus) small amplitude disturbances. Modal waves penetrate the whole compressor in the axial direction, so they can be detected by sensors at any locations at the inlet, exit, or with the compressor. The other inception mechanism is the growth of localized non-linear short wavelength (with length scale of several blade pitches) disturbances, often referred to as ‘spikes’. The inception starts as one or several spike-shaped finite amplitude disturbances within the tip region of a particular stage. Usually, the disturbance develops into a large full span stall cell within three-to-five rotor revolutions. The simulation was executed such that a short wavelength stall inception was initiated by a spike-shaped disturbance.

The flow coefficient traces shown in **Figure A.33**, as taken from the tip region of the first rotor inlet of a four-stage GE low-speed compressor, show that the disturbance is sustained and the disturbance leads to compressor stall subsequently. The overall inception is similar to the measurements as illustrated in **Figure A.34**. A quantitative comparison shows that the stall inception initiated by the spike-shaped disturbance has an initial disturbance rotating speed of 83% of rotor speed, and a transition time of about three-rotor revolutions and compares reasonably well with experimental results.

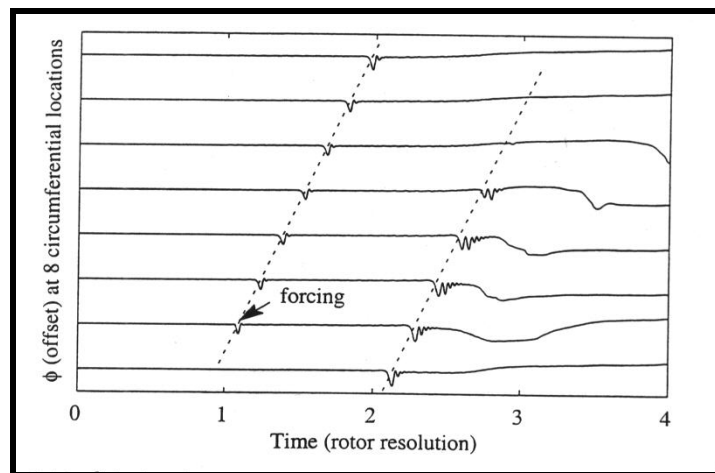


**Figure A.33: Model Prediction of Stall Inception Process for Short Wavelength (Spike) Stalls.**

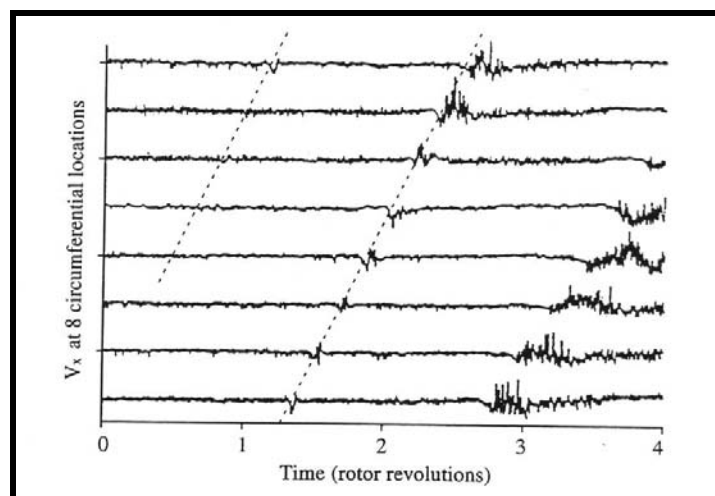


**Figure A.34: Experimental Data of Stall Inception Process for Short Wavelength (Spike) Stalls.**

In multi-spool engines, rotating stall in an upstream compressor will impose a rotating distortion on the downstream compressor, thereby affecting its stability margin. Inlet distortion can modify the flow rate at which rotating stall occurs, degrading the range over which stable operation is possible. The investigation reported by Longley [A.18] addresses the relationship between speed and direction at which the inlet distortion pattern rotates around the compressor annulus and the severity of the degradation in stability margin. Imposition of a rotating distortion can also be thought of as a type of forced response experiment to probe the compressor dynamic behavior. The measured mean flow coefficients at stall inception as a function of screen rotation speed, the means by which rotating distortion was imposed, for the GE four-stage compressor is presented in **Figure A.35**. The calculations from the modeling technique, described in the paper by Gong are shown in the figure as solid lines. Both the data and the model indicated that there is less stability margin available with co-rotating distortion than with the counter-rotating screen.

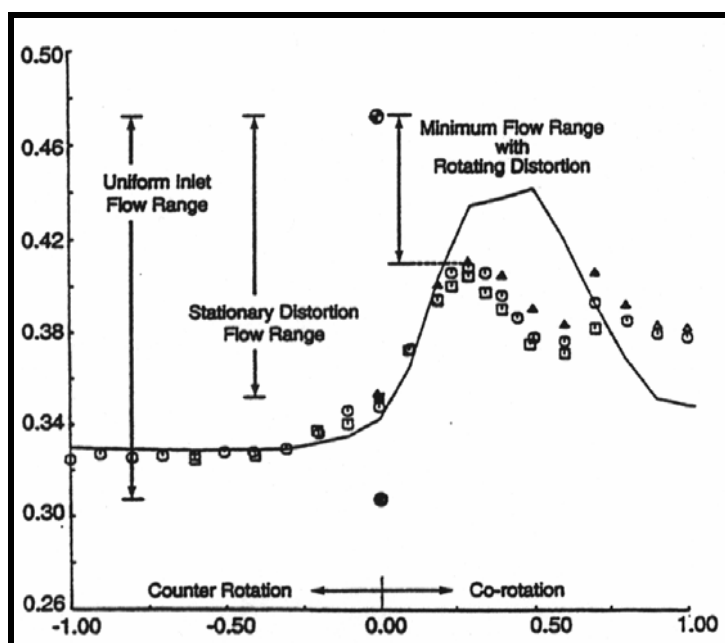


**Figure A.35:** The Effects of Co- and Counter-Screen Rotation on Compressor Stability Limit.

### *Limitations of Chosen Modeling Technique*

This modeling technique has its strengths and weaknesses. The approach allows for a relatively quick computation of distortion as compared to traditional CFD turbomachinery, but because there is a level of empiricism the flow-field may not be accurately represented at a detailed level suitable for design. This modeling technique is best suited for studying potential design changes that can be quantified as to their effects on blade performance and system response to inlet distortion effects.

### **A.3.2.3 Multi-Disciplinary Interaction for Durability**

Traditionally, aeropropulsive and structural performance have been designed separately and later mated together via flight-testing. In today's atmosphere of declining resources, it is imperative that more productive ways of designing, optimizing and verifying aeropropulsive performance and structural aerodynamic interaction are made available to the aerospace industry. One method of obtaining a more productive design and evaluation capability is through numerical simulations. Recent advances in turbomachinery design are leading to very high thrust, lightweight engines that challenge all fronts of technology development. High temperature super alloys with single crystal construction offer tremendous resilience in extremely harsh turbine engine operating environments. Similarly, the high-bypass wide-

chord, lightweight hollow, or composite, fan blade offers tremendous strength during bird strikes, hail ingestion, and surge cycles.

### ***Modeling Techniques Used***

There are two technical approaches for analyzing aerodynamic-structural interactions. The more traditional approach is to use a computational fluid dynamic code to obtain aerodynamic forcing functions, and then pass that information to a finite-element structural code. The second approach is to use a code that integrates both the structures and aerodynamics. This approach has been demonstrated with a code known as ALE3D, developed by Lawrence Livermore National Laboratory. This code is capable of characterizing fluid and structural interaction for components such as the combustor, fan and stators, inlet and nozzles. This code solves the 3-D Euler equations and has been applied to several aeropropulsive applications, such as a supersonic inlet and a combustor rupture simulation.

ALE3D was developed from a version of DYNA3D. It uses the basic Lagrangian finite element techniques developed there but has not maintained an identical set of algorithms as the two code efforts evolved along different paths. The fluid dynamic treatment of solid elements has been completely rewritten. However, the coding and the available models for treating beam and shell elements have been kept consistent with the equivalent DYNA3D models, although only a subset are currently available. Fluid mechanics and ALE techniques from JOY and CALE were modified for application to unstructured meshes and incorporated into ALE3D. Thermal and structural analysis techniques are generally developed first in DYNA3D and TOPAZ3D then migrated to ALE3D as required. (See [A.19] for specific references to the Lawrence Livermore suite of codes listed in this paragraph).

The basic computational step consists of a Lagrangian step followed by an advection, or remap step. This combination of operations is formally equivalent to an Eulerian solution while providing increased flexibility and, in some cases, greater accuracy. In the Lagrangian phase, nodal forces are accumulated and an updated nodal acceleration is computed. Following DYNA3D, the stress gradients and strain rates are evaluated by a lowest order finite-element method. At the end of the Lagrangian phase of the cycle, the velocities and nodal positions are updated. At this point, several options are available. If the user wishes to run the code in a pure-Lagrangian mode, no further action is taken and the code proceeds to the next time step. If a pure-Eulerian calculation is desired, the nodes are placed back in their original positions. This nodal motion or relaxation generates inter-element fluxes that must be used to update velocities, masses, energies, stresses and other constitutive properties. This re-mapping process is referred to as advection. Second-order schemes are required to perform this operation with sufficient accuracy. In addition, it is not generally adequate to allow advection only within material boundaries. ALE3D has the ability to treat multi-material elements, thus allowing relaxation to take place across material boundaries.

### ***Potential Benefits***

With this coupled approach, a numerical tool is available to the aeropropulsion community that will allow fully interactive analysis between the traditionally uncoupled aerodynamics and structural disciplines. A system level approach, which would allow internal engine component and sub-components (compressor stage or blade row) to interact with the full turbine engine system and thus with external aircraft structures, is envisioned. If analysis of an internal engine component were desired, a more traditional CFD approach would be available through zooming.

### ***Cited Example***

- Nazir, J., Couch, R. and Davis, M., “An Approach for the Development of an Aerodynamic-Structural Interaction Numerical Simulation for Aeropropulsion Systems”, ASME Paper # 96-GT-480, June 1996. [A.19]

An engine-inlet configuration associated with the HSCT program was analyzed in terms of inlet unstart and the effect of the regurgitated shock wave. Inlet start is a complex three-dimensional phenomenon where a supersonic flow, which comes through the inlet, is stabilized to some acceptable subsonic condition before entering the fan. This produces a shock wave that sits strategically somewhere in the HSCT inlet, thus creating a transition zone from supersonic flow to subsonic flow within the inlet itself. If, for whatever reason, the engine undergoes a transient such as an engine surge, the stable shock wave will be disrupted, and may become unstable, possibly spilling out around the engine. This bubble or plume will spread and produce loading on the surrounding structure, such as the wing, and can affect the aircraft attitude-control surfaces. These will try to compensate for such pulse loading, as illustrated in **Figure A.36**. If large enough, the bubble or plume could be sucked in by the adjacent engine, causing it also to unstart. This will obviously intensify the dynamics for the control system to compensate, thus requiring a thorough understanding of this phenomenon.

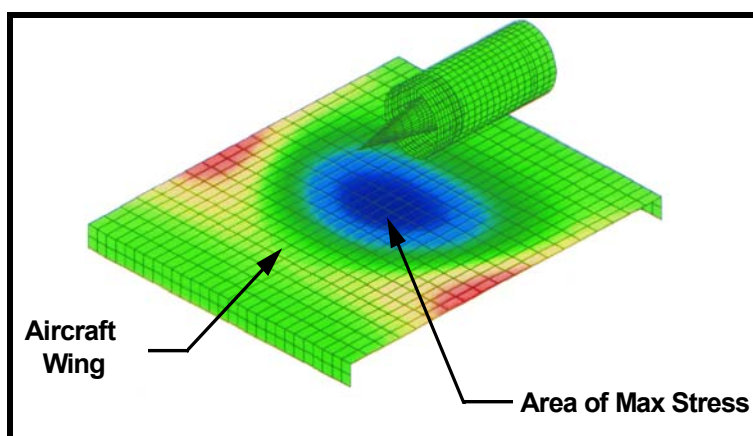


**Figure A.36:** Effect of Inlet Unstart on Aircraft Wing Assembly.

The initial approach has been to analyze this coupled aerodynamic-structural interaction with a de-coupled numerical technique. The approach that was taken was to model the surge cycle frequencies and intensity using a one-dimensional compression system model, DYNTECC [A.2], for a typical high-pressure compressor. This scaled pressure loading at the fan face was then introduced as a boundary condition to ALE3D, which characterized the inlet steady state shock location in a three-dimensional inlet. The appropriate boundary conditions were applied and the equilibrium flow was obtained as described in the previous section. The surge conditions were then applied as a time-variant one-dimensional pressure boundary condition. The initial spike and rapid drop-off occurs within the first 10 to 15 milliseconds after the event is initiated. The highly cyclic nature of the blowdown part of the cycle was not represented by the boundary condition. However, the cyclic oscillations cease to play a role in the inlet unstart once it has begun.

### ***Limitations of Chosen Modeling Technique***

The major limitation with this technique was the need to loosely couple the compression system code to the ALE3D simulation. The output of the DYNTECC code had to be used as a boundary condition to the ALE code. Full interaction was not realized with this technique. In addition, when using a highly coupled approach, some compromises had to be made in the development of the code. These compromises can manifest themselves in reduced capability that might otherwise be available in a separate computational fluid dynamics code or finite-element structural code.

#### **A.3.2.4 Component Aerodynamic Design**

Turbomachinery aerodynamicists have long realized that the flow within multi-stage turbomachinery is complex. In addition, to the non-deterministic, small-scale chaotic unsteadiness due to turbulence, at a large scale the flow is also unsteady and periodic from blade passage to blade passage. The flow features associated with these large scales are deterministic. It is because of the unsteady deterministic flow that turbomachinery is able to either impart or extract energy from a flow. The challenge is to develop an analytical model of sufficient fidelity to address key design issues. At the same time, the cost and time of executing a simulation based on the model, and the cost of acquiring and maintaining the empirical database that underpins the model must be compatible with the design environment.

##### ***Modeling Techniques Used***

Within the last ten years, there has been a steady infusion of 3-D CFD-based models into axial flow multi-stage turbo-machinery design systems. In part this has been due to the useful role these models have played in the analysis of isolated blade rows. The performance level of the fan rotor of the current generation of high-bypass-ratio turbofan engines is directly tied to the advances made in the use of 3-D CFD-based models. A through-flow or a quasi-three-dimensional system may provide the initial fan-rotor geometry, but the final shape of the rotor is evolved exclusively using 3-D CFD-based models. The rotor shape is tailored to control the interaction of shock waves with the blade surface boundary layers to avoid separation and to minimize loss. In addition, using these 3-D CFD models one is able to resolve the tip clearance flow as well as the stator hub leakage flow, and establish their impact on aerodynamic performance. From this activity guidelines have been established for use in aerodynamic design.

The 3-D CFD-based models that were initially introduced into multi-stage axial flow turbo-machinery design systems ignored the impact of the unsteady, deterministic flow existing within axial flow multi-stage turbo-machines. The unsteady, deterministic flow is produced by the surrounding blade rows and its frequency content is linked to shaft rotational speed. These 3-D models have two forms. The first is simply an isolated 3-D blade row CFD-based model linked to a through-flow code. The initial geometry and the inlet and exit flow conditions to the blade row being designed are established by the through-flow or quasi-3-D system. The established inlet and exit flow conditions to a blade row set the boundary conditions for the 3-D model. 3-D simulations are executed with geometry updates until a blade configuration is found whose inlet and exit flows closely match that of the through-flow system. The aerodynamic matching of stages within a machine is established by the through-flow system.

Another approach is based on the flow model derived from the work of Adamczyk [A.11]. This model and its off-shoots have proven useful in design applications. The model developed by Adamczyk is referred to as the average-passage flow model. This flow model describes the time-averaged flow-field within a typical passage of a blade row embedded within a multi-stage configuration. The resulting flow-field is periodic over the pitch of the blade row of interest. The average-passage flow model is an analysis model, as are all the others that have been referred to thus far. This means that geometry is the input and the output is the flow-field generated by the geometry.

When using the average-passage flow model in aerodynamic design, the initial geometry is defined by a through-flow system. During the design process, geometry updates are done exclusively based on simulation results from the average-passage model. No output from an axisymmetric through-flow system or a data match that implicitly or explicitly sets the aerodynamic matching of stages within a turbomachine is provided to the average-passage simulations. The credibility of an average-passage flow simulation is not tied to aerodynamic matching information provided by a through-flow system or a data match. The credibility is tied to the models used to account for the effects of the unsteady flow environment on the average-passage flow-field. The effect of the unsteady deterministic flow-field on aerodynamic matching of stages is accounted for by velocity correlation within the momentum equations associated with the

## ANNEX A – HIGHER ORDER MODELS

---

average-passage flow-field and by a velocity total enthalpy correlation within the energy equation associated with the average-passage flow-field. The term unsteady deterministic refers to all time-dependent behavior that is linked to shaft rotational speed. All unsteady behavior not linked to shaft rotational speed is referred to as non-deterministic.

### *Potential Benefits*

Up until recently (the late 90's), the aerodynamic design of most axial flow multi-stage turbomachinery has been executed using various axisymmetric flow models. The use of these models is iterative. A design has been executed based on the existing database. Data obtained from tests of the fabricated hardware are used to update empirical correlations embedded within these models. The updated axisymmetric flow model is then used to support the next design of the configuration. This bootstrap approach to the aerodynamic design of axial flow multi-stage turbomachinery results in some truly impressive machines, as evidenced by the aerodynamic performance they achieve. However, because of strong economic forces, the turbomachinery industry has been forced to re-examine this iterative approach to aerodynamic design. These economic forces mandated that industry reduce the time and cost of developing a turbomachinery component and, at the same time, required the design of machinery whose performance goals lay outside the then-existing experience base. As a result, a strong need to develop a new methodology, for executing the aerodynamic design of axial flow multi-stage turbomachinery, has arisen. The foundation of this new methodology requires aerodynamic models whose resolution is greater than that of the axisymmetric flow models. These models have to allow for overnight turnaround using computer resources compatible with the design environment. Finally, the model has to be capable of addressing the aerodynamic issues associated with the design of advanced configurations.

### *Cited Example*

- Adamczyk, J.J., “Aerodynamic Analysis of Multistage Turbomachinery Flows in Support of Aerodynamic Design”, 1999 International Gas Turbine Institute Scholar Lecture, Transactions of the ASME, Journal of Turbomachinery, Vol. 122, April 2000, pp. 189-217. [\[A.11\]](#)

**Figure A.37** shows the measured pressure rise characteristic along with simulation results at a flow coefficient of 0.395 and 0.375 for the Lewis low-speed axial compressor (LSAC). LSAC is a four-stage machine with an inlet IGV, which is representative of the rear stages of a high-pressure (HP) compressor. The compressor is of a modern design employing hub-shrouded stators with end-bends. The four stages are geometrically identical. The simulation accounted for the rotor tip clearance. The simulation did not include the stator hub cavities nor did the simulations account for stator hub leakage.

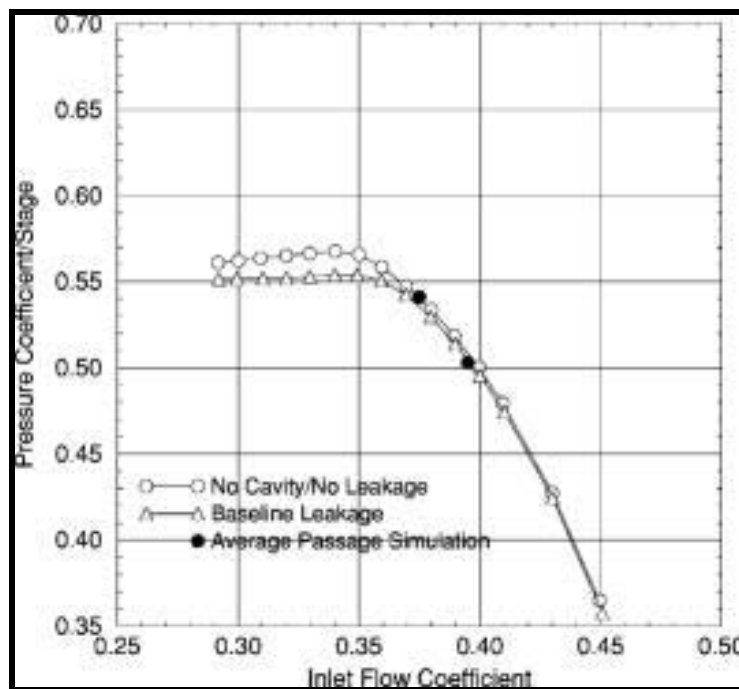


**Figure A.37: Overall Performance Characteristic.**

At the flow coefficient of 0.395 (which is near the measured peak efficiency operating point) and at the flow coefficient of 0.375, the simulation results are in good agreement with the measurement. An attempt to simulate an operating condition near peak pressure failed to converge. The simulation did not account for casing treatment over the first rotor present in the experiment. Tests with the casing treatment removed show that the compressor stalls at a flow coefficient near the peak pressure point of the characteristic. **Figure A.38** shows the measured static pressure rise characteristic for each stage along with results from the simulations. The agreement between the simulation results and the data is very good. For the flow coefficient of 0.395, **Figure A.39** shows plots of the total and static pressure coefficient, the axial and absolute tangential velocity, and the absolute and relative flow angle as a function of span for the simulation and the experiment. The plots are for an axial location behind the second stator. Once again, the agreement between the simulation results and the data is good. The slight difference between the static pressure coefficient derived from the simulation and that measured inboard at 40 percent span is unknown.

## ANNEX A – HIGHER ORDER MODELS

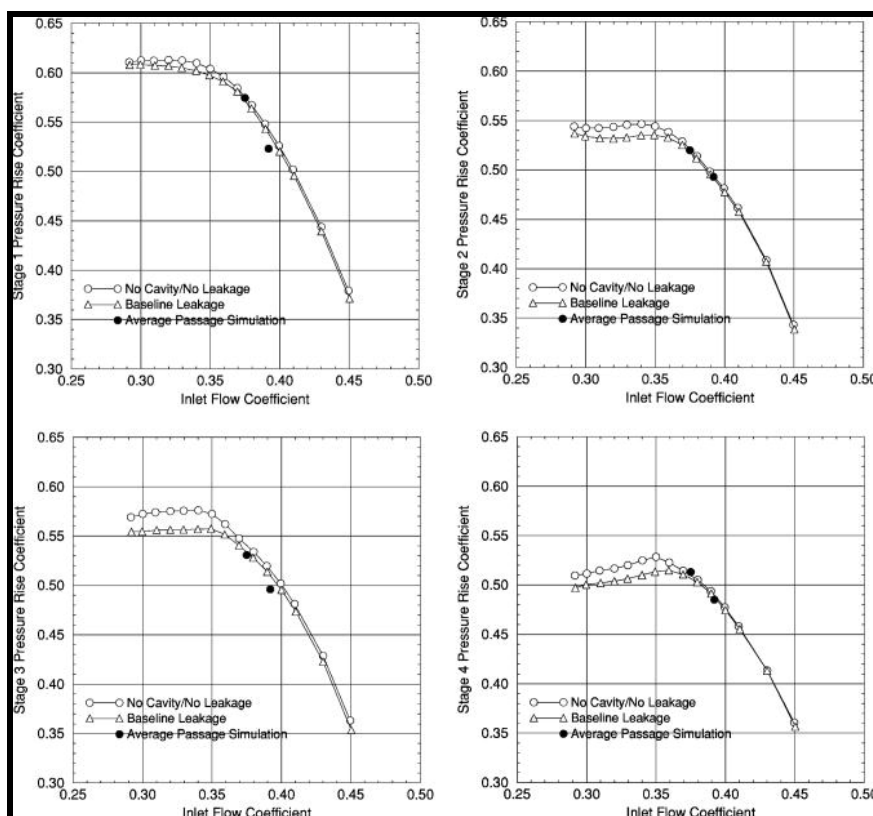
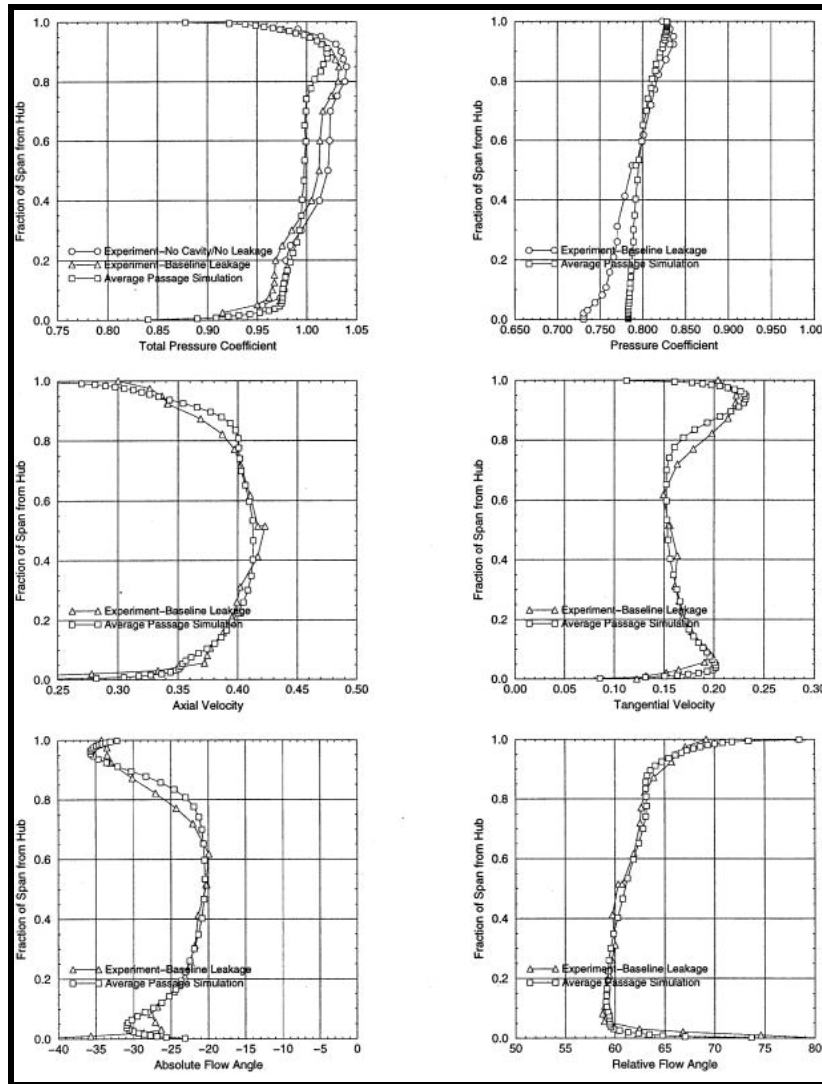


Figure A.38: Individual Stage Pressure Rise Coefficient.



**Figure A.39: Axisymmetric Flow Variables, Exiting the Second Stage Rotor.**

### Limitations of Chosen Modeling Technique

There is no doubt that 3-D CFD-based models with aerodynamic input from through-flow models have provided credible designs. These models will continue to provide credible designs as long as the design parameters are within the bounds of the database underpinning well-calibrated through-flow or quasi 3-D design systems. However, reliance on through-flow or quasi-3-D models to set key aerodynamic design parameters such as the aerodynamic matching of stages greatly impedes the utility of these models. Specifically, they are limited in their ability to uncover the fluid mechanics controlling the performance of multi-stage axial flow turbomachines at design and off-design operating conditions. The objective of 3-D CFD-based modeling should be to break free of the dependence on through-flow or quasi 3-D design systems except for providing the initial geometry. If such 3-D CFD-based models are proven credible, their use would allow aerodynamic designs of machinery whose parameters lay outside the bounds of the database, allowing through-flow systems to be used with confidence. This would include both design and off-design operation, and in the case of compressors, prediction of maps including the surge line.

**A.4 REFERENCES**

- [A.1] Rodriguez, C.G. and O'Brien, W.F., "Unsteady, Finite-Rate Model for Application in the Design of Complete Gas-Turbine Combustor Configurations", Design Principles and Methods for Aircraft Gas Turbine Engines, RTO-MP-8, February 1999.
- [A.2] Hale, A.A. and Davis, Jr., M.W., "Dynamic Turbine Engine Compressor Code, DYNTTECC – Theory and Capabilities", AIAA Paper # 92-3190, June 1992.
- [A.3] Davis, Jr., M.W. et al., "Euler Modeling Techniques for the Investigation of Unsteady Dynamic Compression System Behavior", Loss Mechanisms and Unsteady Flows in Turbomachines, AGARD-CP-571, January 1996.
- [A.4] Garrard, G.D., "ATEC: The Aerodynamic Turbine Engine Code for the Analysis of Transient and Dynamic Gas Turbine Engine System Operations – Part 1: Model Development", ASME Paper # 96-GT-193, June 1996.
- [A.5] Garrard, G.D., "ATEC: The Aerodynamic Turbine Engine Code for the Analysis of Transient and Dynamic Gas Turbine Engine System Operations – Part 2: Numerical Simulations", ASME Paper # 96-GT-194, June 1996.
- [A.6] Lefebvre, A.H., "Fuel Effects on Gas Turbine Combustion – Ignition, Stability, and Combustion Efficiency," *Journal of Engineering for Gas Turbines and Power*, Vol. 107, January 1985, pp. 24-37.
- [A.7] Derr, W.S. and Mellor, A.M., "Recent Developments," in *Design of Modern Turbine Combustors*, edited by A.M. Mellor, Academic Press, Harcourt Brace Jovanovich, New York, NY, © 1990.
- [A.8] Shahroohi, K.A. and Davis, Jr., M.W., "Application of a Modified Dynamic Compression System Model to a Low-Aspect Ratio Fan: Effects of Distortion", AIAA-95-0301, Presented at the 33rd Aerospace Science Meeting, Reno, NV, January 1995.
- [A.9] Hale, A.A. and O'Brien, W.F., "A Three-Dimensional Turbine Engine Analysis Compressor Code (TEACC) for Steady-State Inlet Distortion," *Journal of Turbomachinery*, Vol. 120, July 1998, pp. 422-430.
- [A.10] Stewart, M.E.M., "Axisymmetric Aerodynamic Numerical Analysis of a Jet Engine", ASME Paper # 95-GT-338, June 1995.
- [A.11] Adameczyk, J.J., "Aerodynamic Analysis of Multistage Turbomachinery Flows in Support of Aerodynamic Design", 1999 International Gas Turbine Institute Scholar Lecture, Transactions of the ASME, *Journal of Turbomachinery*, Vol. 122, April 2000, pp. 189-217.
- [A.12] Suresh, A. et al., "Analysis of Compressor-Inlet Acoustic Interactions Using Coupled Component Codes", AIAA Paper # 99-0749, 1999.
- [A.13] Costura, D.M. et al., "A Model for Combustor Dynamics for Inclusion in a Dynamic Gas Turbine Simulation Code", AIAA Paper # 97-3336, Presented at the 33rd AIAA/ASME/SAE/ASEE Joint Propulsion Conference, July 6-9, 1997, Seattle, WA.
- [A.14] Garrard, G.D., Davis, Jr., M.W., Wehofer, S. and Cole, G., "A One-Dimensional Time Dependent Inlet/Engine Numerical Simulation for Aircraft Propulsion Systems", ASME Paper # 97-GT-333, June 1997.

- [A.15] Abdel-Fattah, A.M., “Response of a Turbofan Engine Compression System to Disturbed Inlet Conditions”, Journal of Turbomachinery, Vol. 119, No. 4, October 1997.
- [A.16] Hale, A.A., Chalk, J., Klepper, J. and Kneile, K., “Turbine Engine Analysis Compressor Code: TEACC – Part II: Multi-Stage Compressors and Inlet Distortion”, AIAA Paper # 99-3214, Presented at the 17th AIAA Applied Aerodynamics Conference, June 1999.
- [A.17] Gong, Y., “A Computational Model for Rotating Stall and Inlet Distortions in Multistage Compressors”, GTL Report #230, March 1999, Gas Turbine Laboratory, Massachusetts Institute of Technology, Cambridge, MA.
- [A.18] Longley, J.P. et al., “Effects of Rotating Inlet Distortion on Multistage Compressor Stability”, ASME Paper # 94-GT-220, June 1994.
- [A.19] Nazir, J., Couch, R. and Davis, M., “An Approach for the Development of an Aerodynamic-Structural Interaction Numerical Simulation for Aeropropulsion Systems”, ASME Paper # 96-GT-480, June 1996.



## Annex B – ADVANCED TOPICS AND RECENT PROGRESS

### INTRODUCTORY COMMENTS

This Annex provides an overall view of the recent progress made on the prediction and simulation of aspects of gas turbine engine component performance. These components are inlet, compressor, combustor, turbine, afterburner, nozzle, splitters, mixers, and secondary flow systems. It also includes a section on control systems modeling. The Annex is arranged as follows. We begin with the rotating components (compressor and turbines); this is then followed by the non-rotating components.

### B.1 COMPRESSOR SYSTEMS PERFORMANCE

Engine compressor performance is represented by the basic compressor map, as illustrated in **Figure B.1**. Total Pressure Ratio versus Corrected Airflow characteristics are shown for various percent corrected (referred) speeds. Efficiency islands and the surge line complete the performance definition of the compression system.

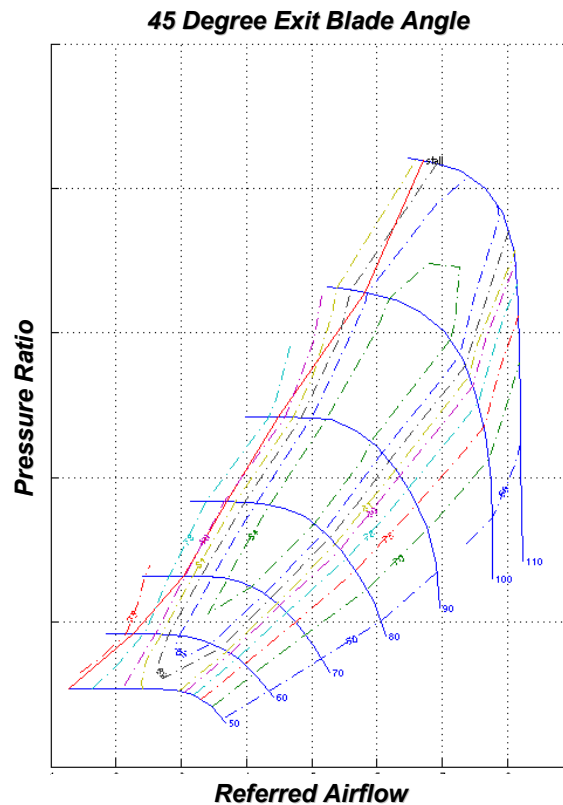


**Figure B.1: Basic Compressor Map.**

The Performance level of a compression system is dependent on a number of variables; air flow and pressure ratio requirements, speed compatibility with the turbine, the type of application, and cost considerations. The type of compression system is determined by the same parameters. The primary configurations consist of multi-stage axial, multi-stage axial + centrifugal, and single or multi-stage centrifugal compressors. A Mixed-flow compressor configuration has been applied in a few applications. **Figure B.2** depicts these various compression systems.

## ANNEX B – ADVANCED TOPICS AND RECENT PROGRESS

Performance comparisons of these configurations are shown in **Figure B.3**. Overall compressor efficiency is plotted versus overall compressor exit corrected flow. Exit corrected flow was selected as the abscissa as it collapses the data into the 3 curves shown and removes Pressure Ratio as a parameter. It is well established that for large size compression systems, axial type compressors have a significant efficiency advantage over centrifugal configurations. As airflow requirements decrease, the performance of the axial compressor starts to decrease due to the reduction in physical size. Clearance and secondary flow losses begin to dominate and better performance can be obtained with a centrifugal stage.

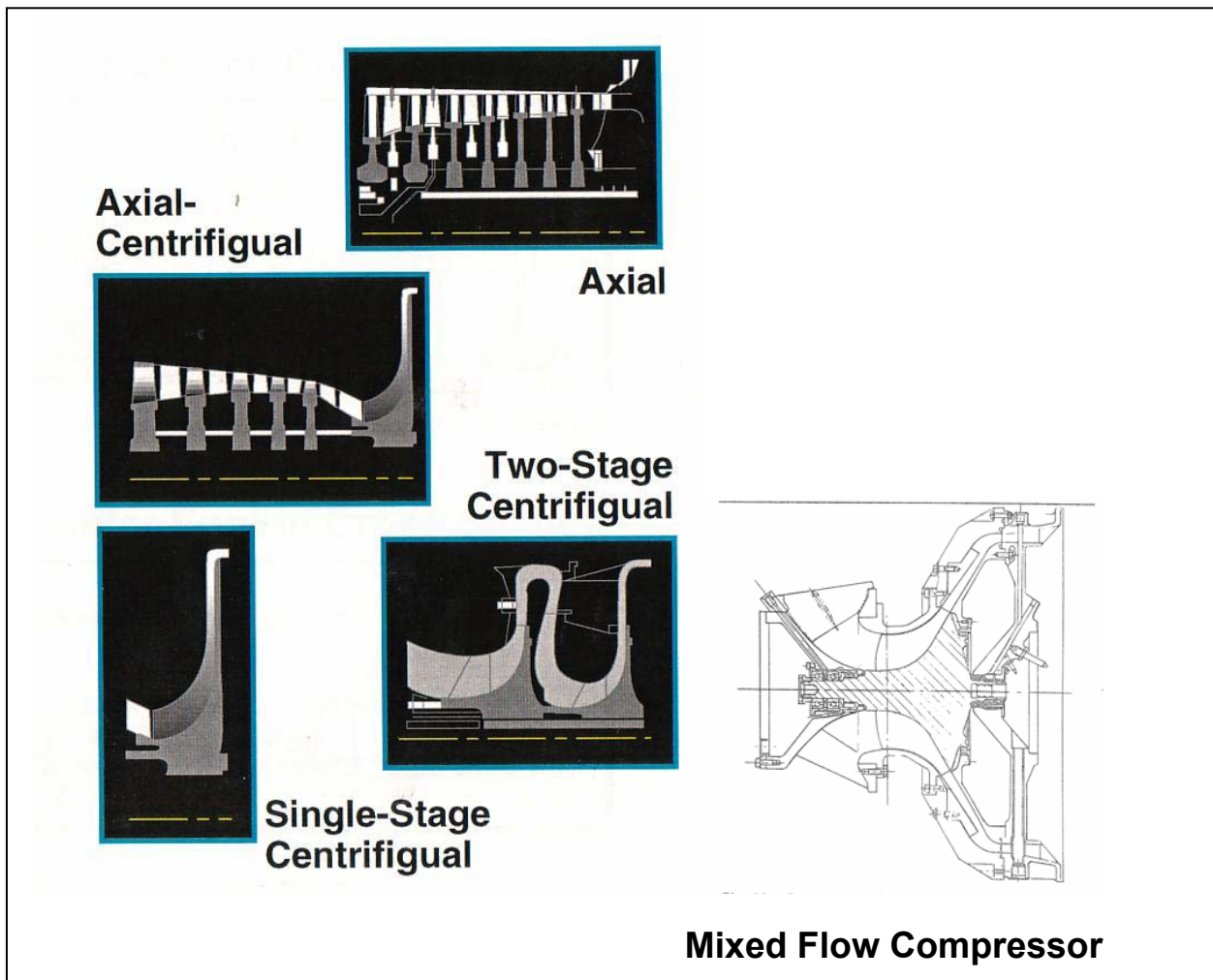


**Figure B.2: Types of Compressors.**

Another method used to select the type of compressor configuration is shown in **Figure B.4** where Compressor Exit Corrected Flow is plotted versus Pressure Ratio. Curves are generated for constant compressor Inlet Corrected Flow. Indicated at the top of the figure is the area where axial compressors should be used, and the area at the bottom of the figure where centrifugal compressors will have better performance. In the middle of the figure is a “gray” area where either type of compressor may be used from an efficiency point of view. This figure may also be used to determine in a multi-stage axial + centrifugal configuration the point at which a designer should consider changing from an axial stage to a centrifugal stage. As the overall pressure ratio increases and axial stages are added, the exit corrected flow decreases. At the combination of lower inlet corrected flow and higher pressure ratio, performance of centrifugal compressors will be better than that of axial compressors. Based on the selection of the axial

pressure ratio per stage, this figure can be used in determining the appropriate number of axial stages in a multi-stage axial + centrifugal configuration.

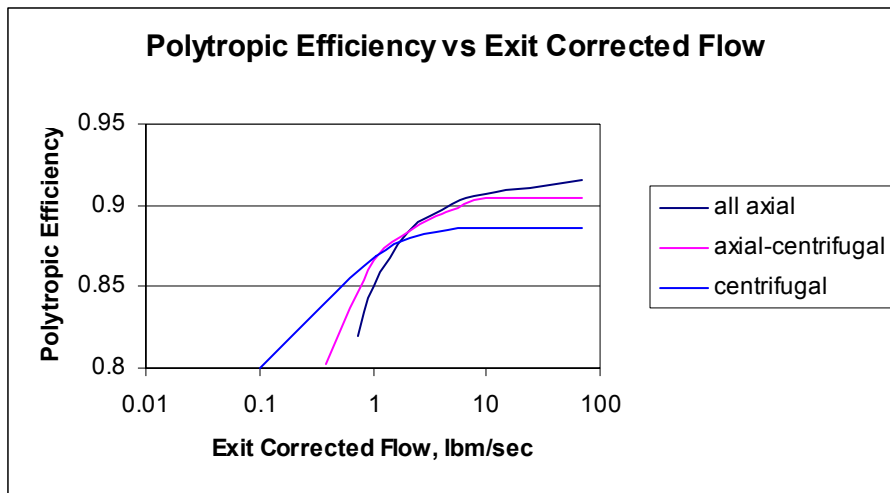


**Figure B.3: Polytopic Efficiency for Various Types of Compression Systems.**

Up to this point, considerations have been given to primarily aerodynamic parameters as far as determining the type of compressor configuration. As mentioned in the initial paragraphs, application and cost considerations can be of equal importance. For prime commercial and large military applications which require extremely large thrust and therefore very large inlet airflow, all axial configurations are preferred, as evident from **Figure B.3**. For these types of applications, the following section describes the performance and simulation of axial compressors.

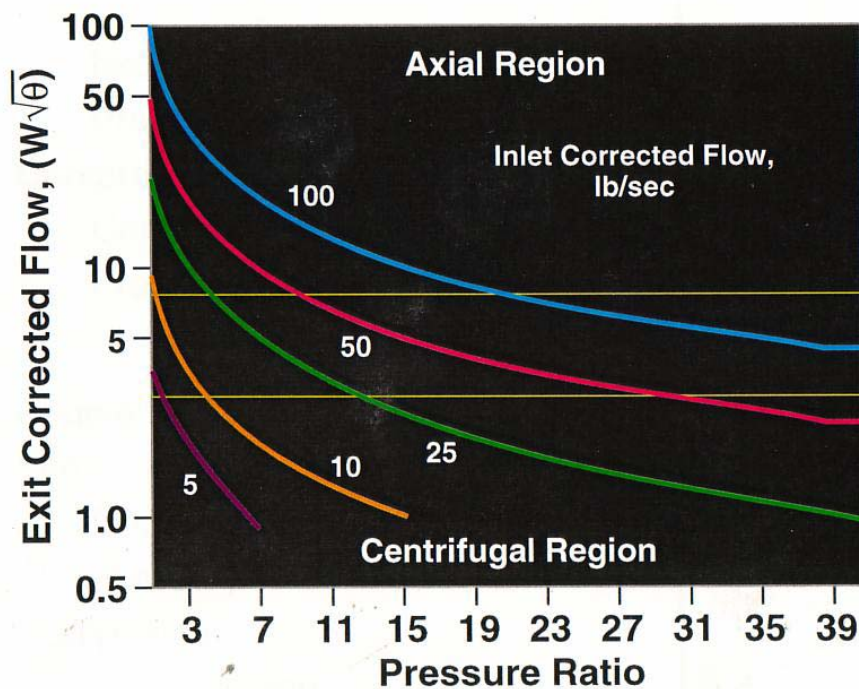


**Figure B.4: Compressor Configuration as a Function of Flow and Pressure Ratio.**

For military helicopters, turboprops, and auxiliary power unit (APU) applications, the inclusion of axial-centrifugal and centrifugal compressor stages is preferred as inlet flow requirements are much smaller for these types of applications. In addition, cost has become a significant consideration during engine selection. Minimizing the number of parts and variable geometry components translates into increased compressor reliability and maintainability and thus have become major factors in the selection of new engine configurations. Centrifugal stages have inherent advantages in these applications. *Section B.2.2* describes examples and attributes of centrifugal compressor configurations.

Engine performance is computed by utilizing the basic component maps for each of the turbomachinery components. Depending on the type of compressor and the amount of variable geometry and interstage bleed configurations, numerous maps may have to be included in the cycle deck. Alternatively, map scalars are supplied to represent various effects. These scalars may also vary with corrected speed. The remaining sections discuss in detail the most critical parameters that can change the performance of compressors and provide information on how to include these effects in the overall engine simulation model.

### B.1.1 Simulation of Axial Compressor Performance

The performance map for a specific compressor configuration can be obtained through both systematic experimental measurements and computations. With the recent advances made in numerical techniques [B.1 and B.2], and the availability of computational resources, it is now possible to evaluate the performance and the design changes in multi-stage compressor, on a three-dimensional flow basis using a computational flow solver. It is intended to provide a concise delineation of those factors that can potentially modify baseline compressor performance-characteristics, rather than to discuss the details of the measurement and computation techniques for compressor performance maps. These factors are commonly referred to as characteristic modifiers.

There are thus two items of interest in this chapter, shown in *Figure B.5*:

- The generation of a baseline compressor map for a specific configuration; and
- The change in the pressure rise characteristic, the efficiency, and the operability limit (the surge line and the flutter boundary).

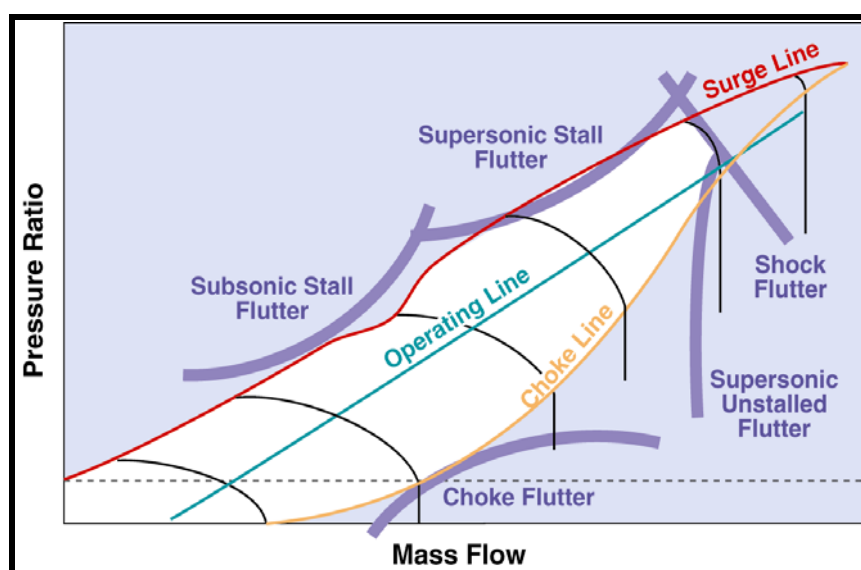


**Figure B.5:** Representative Compressor-Map, with Surge-Line, Speed-Line, Efficiency Contours, and Flutter Boundary.

In particular the specific focus will be on compressor performance changes associated with:

- Changes in compressor tip clearance;
- Stationary and rotating distortion, either self-induced (due to asymmetric compressor tip clearance) or externally imposed (due inlet distortion);
- Changes in intra-blade row gap;
- Blade surface roughness and Reynolds number effect;
- Changes in bleeds;
- Changes in stator schedule and position;
- Blade untwist associated centrifugal effect (this is of particular significance in fan rotor); and
- Heat transfer to compressor.

In this, it is assumed that the baseline compressor-performance characteristics are known and that one would like to determine the change in compressor characteristics and operability range, for instance, due to changes in compressor tip clearance. As such, the material present here is not meant to be exhaustive and extensive; it is aimed at providing the readers with an adequate knowledge base (in line with the objective of the monograph) to aid the readers in:

- Interpreting data from gas turbine engine; and
- Implementing gas turbine engine system simulation.

The readers are strongly advised to refer to the wealth of information on compressor aerodynamics, in the excellent book by Cumpsty [B.3] and ASME Journal of Turbomachinery [B.4].

This section is organized as follows, based on work reported in journal publications up to 1999, of which the authors are aware:

- Generation of the baseline compressor map;
- Effects of changes in (axisymmetric) compressor tip clearance on compressor pressure rise characteristics, efficiency and stall inception point;
- Response of compressors to stationary and rotating distortion, induced by inlet distortion and asymmetric compressor tip clearance;
- How changes in blade row gap can alter the performance characteristics of compressor (Experimental data is first presented to elucidate the consequence of changing the axial spacing between compressor blade rows. Unsteady computational results are then used to establish the causes for the observed changes in compressor performance);
- The impact of blade surface roughness and Reynolds number on compressor performance;
- Changes associated with bleeds, stator schedule and position and heat transfer effects;
- Because the fan and the bypass duct system are distinct from the core compressor, we devote a separate section to the fan and factors that modify its performance characteristics. An example is the blade structural deformation associated with high-speed rotation of the fan rotor;
- A concise description of the importance of aeromechanics (flutter and forced response) on the operability of high performance aircraft engines; and
- Recent progress made in the development of computational compressor flow models and computational fluid dynamics for predicting and simulating flow phenomena of interest in multi-stage compressors.

**B.1.1.1 Generation of Baseline Compressor Map**

A compressor map is the 0-D representation of its performance, showing the mass flow and efficiency of the compressor for a range of operating conditions. It may also include stall line operating limits and various flutter boundaries, as shown in **Figure B.5**. The requirements for the map vary with their application. For engine and control system design, maps may be required to run from near zero speed to extreme over speed conditions that are beyond shaft break limits, and from stall down to windmill pressure ratios less than unity. For special studies, post-stall maps may be required.

A map represents the performance for a nominal set of conditions that may include:

- Stator position;
- Bleed amount and location;
- Entrance temperature, pressure and gas properties (including Reynolds number, gas composition changes such as water vapor or combustion products); and
- Tip clearance.

**B.1.1.2 Effect of Axisymmetric Compressor Tip Clearance on Performance**

Compressor tip clearance causes a leakage of gas across the blade tip from the pressure surface to the suction surface. This tip leakage interacts with the primary gas stream and the wall boundary layer. Indeed, the tip leakage flow dominates the aerothermodynamic behavior of the end-wall flow and the blade-to-blade flow in the tip regions. As such it has a strong impact on compressor efficiency and stability. The influence of tip leakage flow manifests itself in two ways:

- Fluid dynamic blockage that effectively reduced the flow area; and
- A thermodynamic effect, in that the work done in the tip region is different from that in the free stream.

The measured impact on compressor or fan performance due to increased tip clearance is shown in **Figure B.6** and **Figure B.7 [B.4]**. As shown in **Figure B.6** when the tip clearance was increased from the baseline value of 1.38 to 2.8 per cent of span for a low speed multi-stage compressor:

- Peak efficiency reduced by 1.5 points;
- Peak pressure rise dropped by 9.7 per cent; and
- Operability range reduced from 17.5 to 9.7 per cent (a reduction in stall margin).

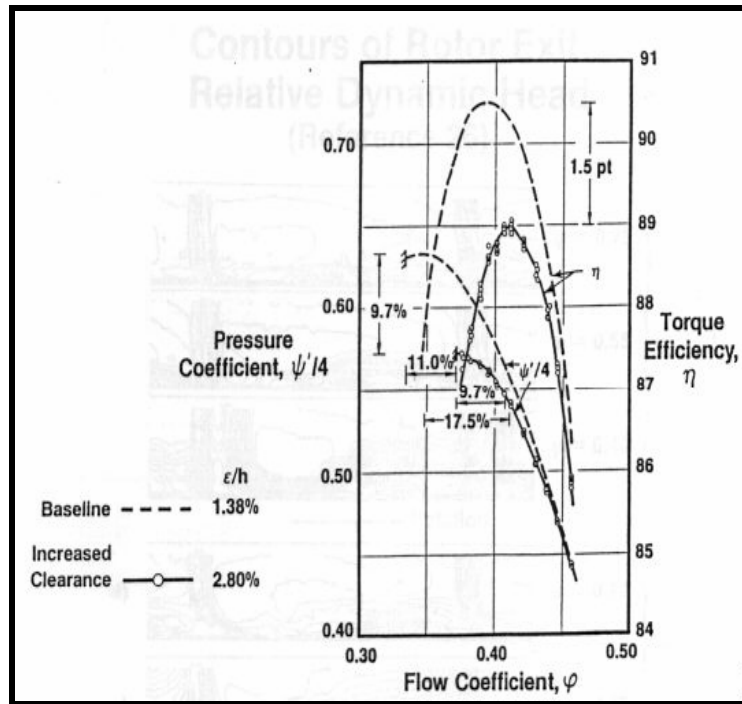


**Figure B.6:** Effect of Increased Tip Clearance on Overall Compressor Performance for a Low-Speed Compressor [B.4].

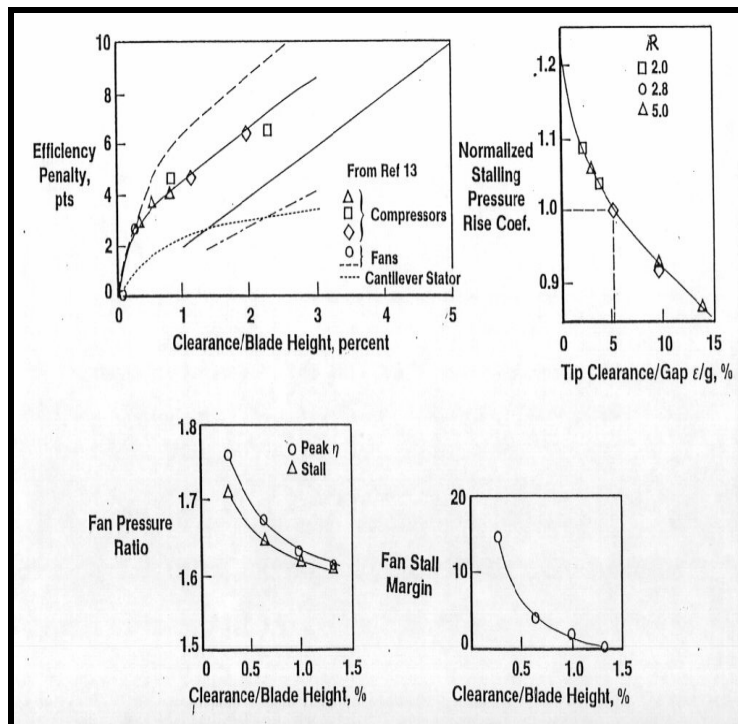


**Figure B.7:** Effect of Tip Clearance on Overall Compressor and Fan Performance [B.4].

The parametric trend of loss in performance (in terms of efficiency, pressure rise or pressure ratio and stalling pressure rise coefficient or stall margin) with increased tip clearance is further brought out in

## ANNEX B – ADVANCED TOPICS AND RECENT PROGRESS

**Figure B.7.** L. Smith [B.5] has developed a correlative approach for estimating the effect of end-wall flow on multi-stage compressor efficiency. This works in terms of:

- Efficiency, uncorrected for end-wall effects;
- Averaged staggered-spacing-to-blade-height ratio;
- Displacement thickness; and
- Tangential force thickness associated with end-wall flows.

The analysis that derives this correlation is based on a repeating stage assumption, and uses data from a set of multi-stage designs or builds.

While the approach does not provide information about the flow, it is apparently a useful approach as elucidated in the results shown in **Figure B.8** [B.5]. More recently a slight more complex correlation has been developed by Khalid et al. [B.6] for the pressure rise capability across a rotor v blockage associated with the tip leakage flow; as the results in **Figure B.9** show it has a behavior analogous to the diffusion factor used for correlating cascade data. While these approaches appear correlative, their utility could lie in enabling the post-processing of vast amounts of computed data (e.g. from the use of CFD to simulate flow in multi-blade rows compressor). This data could then be used for simulating gas turbine engine systems.

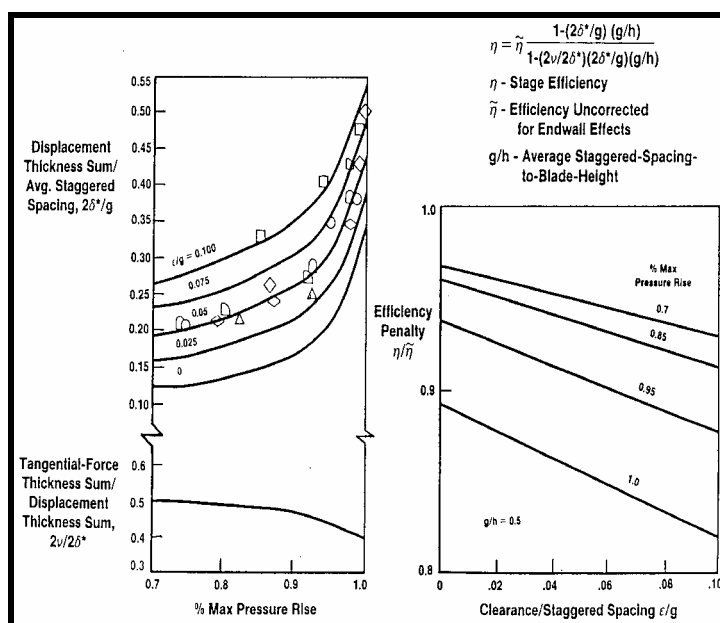


**Figure B.8:** Effect of Tip Clearance on Overall Compressor and Fan Performance [B.5].

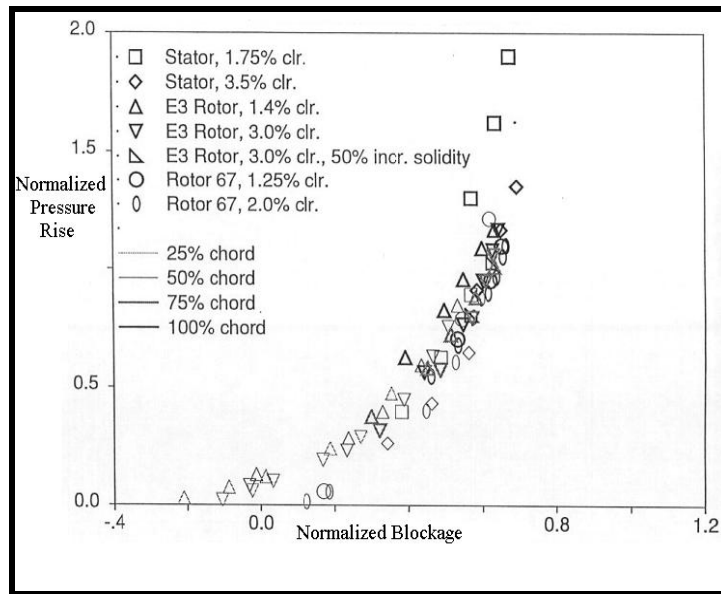


**Figure B.9: Correlation of Rotor Pressure Rise Capability Against Flow Blockage Associated with Tip Leakage Flow [B.6].**

Useful measured information on tip clearance effects in high-speed compressors was given in a paper by Freeman [B.7] and Schmucker [B.10]. Figure B.10 (taken from a lecture at VKI by Freeman) and Figure B.11 (taken from [B.10]) show the impact of increased tip clearance on the efficiency and pressure ratio of high-pressure compressors. Not only do the efficiency and pressure ratio deteriorate with increased tip clearance, but also the loss or gain in efficiency is not monotonic with increasing or decreasing tip clearance. Indeed, for tip clearances below a threshold value, the efficiency deteriorates and the surge line moves considerably to the right so that the compressor would surge at higher mass flows. All these measured effects are highly detrimental to the operability of a compressor.

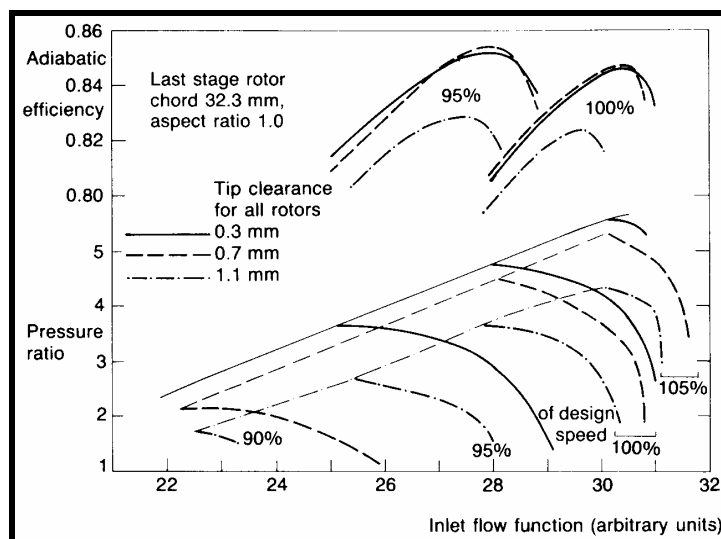


**Figure B.10: Effect of Tip Clearance on Pressure Ratio, Surge Line and Efficiency of 6-Stage, High-Speed Compressor [B.7].**

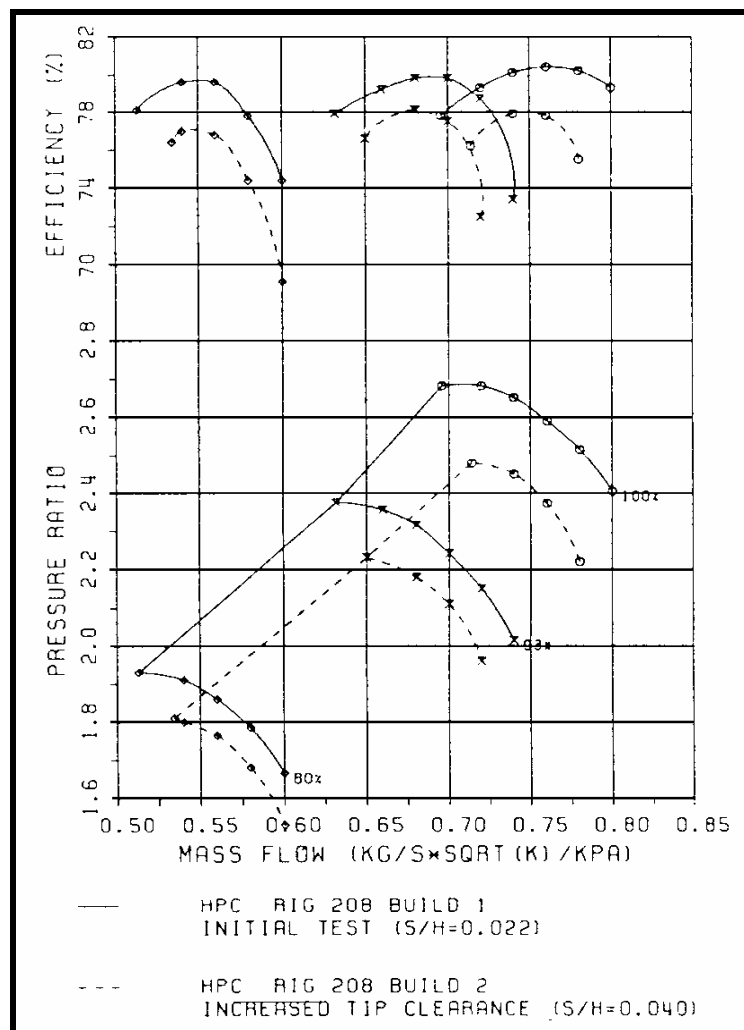


**Figure B.11: Influence of Tip Clearance on Performance – Measurements from HPC-Rig [B.10].**

In a multi-stage compressor environment the effect of changes in tip clearance would generate additional blockage and loss (say for instance to the front stages), altering the matching of the downstream stages. Likewise, the alteration in the performance of a specific stage, due to changes in tip clearance, could influence the aerodynamic matching with the upstream stage. These aspects of tip clearance together with the consequential impact on stage matching have yet to be defined on a quantitative basis. This is required if they are to be incorporated into a simulation procedure for gas turbine engine performance changes associated with changes in tip clearance.

Measurement of detailed flow in the rotor tip region has always been difficult. The advances in computational fluid dynamics and computer technology have enabled the simulation of unsteady three-dimensional flow for rotors with tip clearance, both in isolation and in multi-stage environments. This opens up an entirely new way of probing the physics of tip leakage flow, with the objective of establishing its role on compressor performance on a non-correlative basis.

To summarize, we have reviewed physical measurements to show compressor performance deterioration with increased compressor tip clearance. This may be attributed to the response of the flow behavior in the tip region, which is essentially dominated by the tip leakage vortices. While the overall performance of compressor is set by the pressure rise characteristics, its change is determined by the fluid dynamic event

local to the compressor blade passage and the flow conditions set by the preceding and succeeding blade row.

### B.1.1.3 Stationary and Rotating Distortion

An operating compressor or fan may be subjected to various types of flow distortion. In general, the distortion is of the combined radial-circumferential type. Purely radial distortion can be assessed or analyzed using standard streamline-curvature methods for computing steady-state axisymmetric flows. Circumferential distortion introduces additional fluid dynamic effects that are associated with flow unsteadiness. Thus, a different class of methods is needed to assess the response of compressors to circumferential distortions.

In this section, we shall consider the impact of following types of distortion on compressor performance:

- Stationary inlet distortion, such as that due to flow separation in an inlet (e.g. due to cross-winds or aircraft maneuver) upstream of the fan or compressor;
- Rotating distortion, which can occur in a multi-spool compressors when rotating stall occurs in an upstream compressor, thus imposing a rotating distortion on the downstream compressor;
- Self-induced stationary distortion, associated with tip clearance asymmetry due to an off-centered rotor or oval casing, **Figure B.12**; and
- Self-induced rotating distortion associated with rotating tip clearance asymmetry due to non-uniform blade height or whirling rotor, **Figure B.12**. Whenever a compressor is subjected to an externally imposed distortion or self-induced distortion, its stall margin and performance are degraded and that there could be aeromechanical consequences as well.

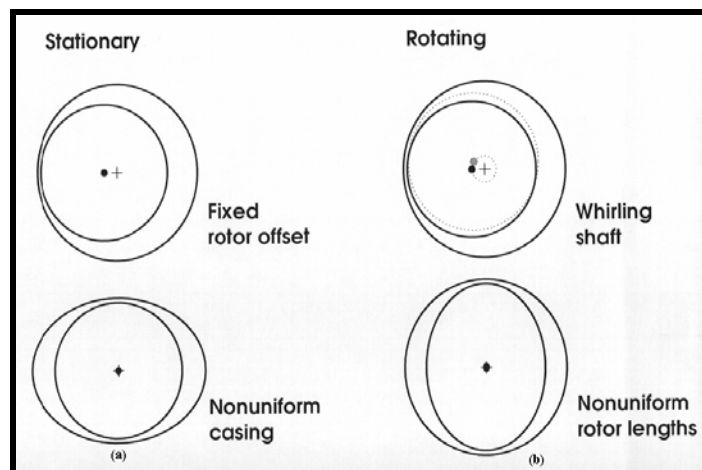


**Figure B.12: Non-Axisymmetric Tip Clearance: (a) Stationary Caused by Off-Centered Rotor and Oval Casing; (b) Rotating Caused by Whirling Shaft and Non-Uniform Rotor Heights.**

Because of the significant impact circumferential-flow distortion has on compressor performance, empirical and correlative approaches (SAE AIR 1419 [B.8], SAE ARP 1420 [B.9]), based on laborious compressor testing, have been developed for estimating the aerodynamic consequence. The parallel or multi-segments compressor model [B.11] provides useful results in certain class of problems and gives an overall view of the associated fluid dynamics. For instance, for a compressor subjected to circumferential distortion it yields a loss in stability margin and stalling pressure ratio. It also gives the result that for effective attenuation of distortion; a given compressor should have a steeper slope in the unstalled pressure rise characteristics. However, the method does not provide an adequate stall point prediction. Advances in

## ANNEX B – ADVANCED TOPICS AND RECENT PROGRESS

analytical and computational techniques for assessing compressor response to flow distortion will be described in the section on methodologies.

### B.1.1.3.1 Stationary and Rotating Inlet Distortion

The measured effects of inlet distortion on the performance of a 9-stage axial compressor are shown in **Figure B.13**. The measurements showed that the stall line with circumferential inlet distortion moved considerably to the right, a degradation in compressor stall margin. The general trends of compressor performance with different inlet distortions are elucidated through a series of experiments undertaken by Reid [B.12]. A representative set of these results is shown in **Figure B.14**, which shows the compressor delivery pressure at the surge line for different types of distortions. Two key aspects may be deduced from these data:

- As the angular extent of the spoiled sector (low inlet total pressure) is increased, there is an angle above which the exit static pressure changes little (**Figure B.14**). This angular extent is often referred to as the critical sector angle.
- Fixing the total angular extent of the distortion, the effect of sub-dividing it into different number of equal sections is shown in **Figure B.15**. The greatest effect on the loss of peak pressure rise is observed when there is only one region. This suggests that inlet distortion patterns, which have a longer length scale and a lower circumferential harmonic content, are the most important.

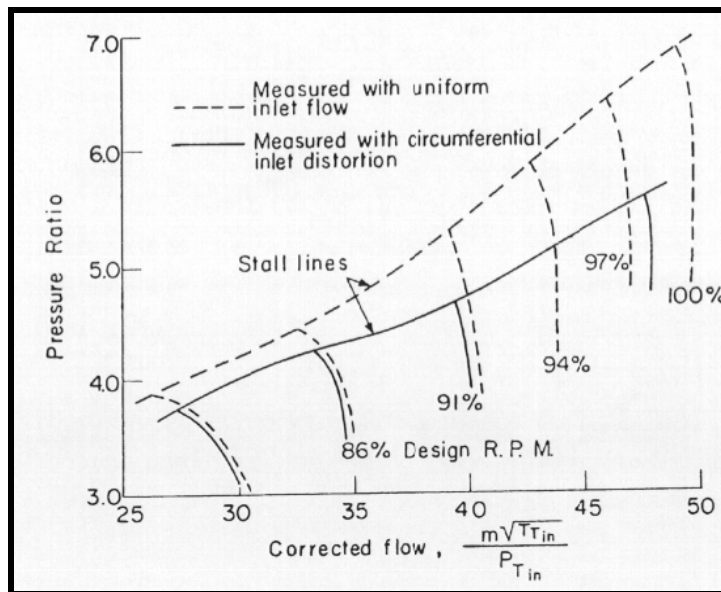


**Figure B.13: Effects of Circumferential Inlet Distortion on Multi-Stage Axial Compressor Performance.**

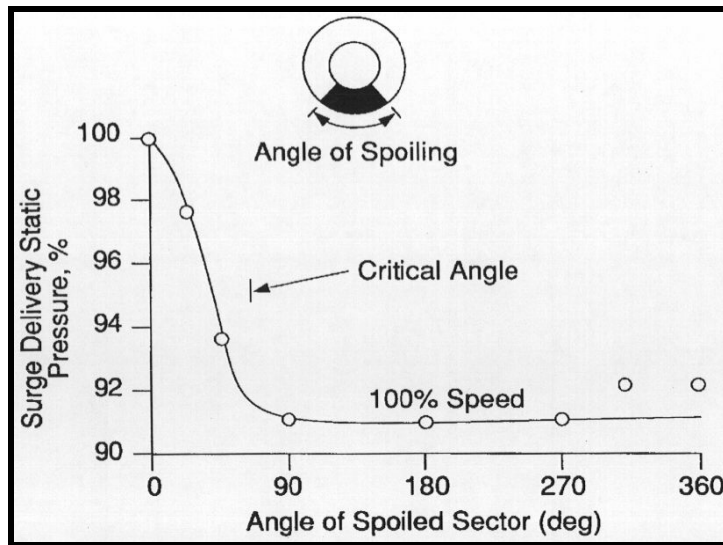


**Figure B.14:** Effect of Circumferential Distortion Sector Angle on Surge Pressure Ratio.

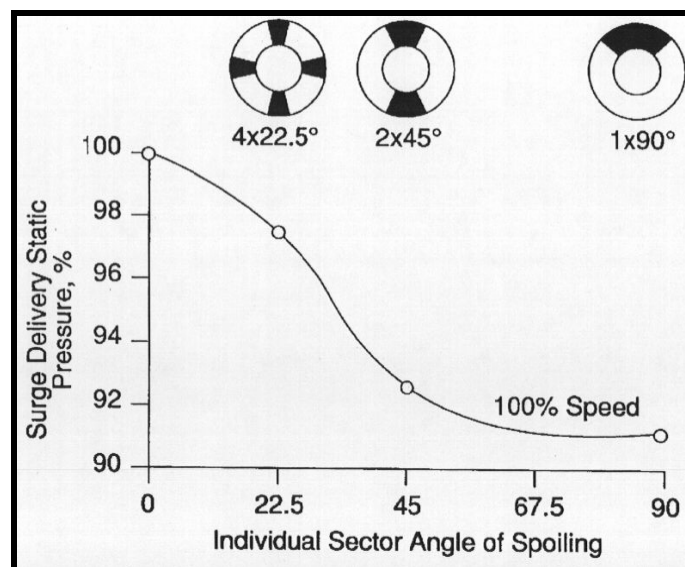


**Figure B.15:** Effect of Number of Sectors, on Surge Pressure Ratio.

While there is a considerable database on the response of compressor to stationary inlet distortion, only limited physical measurements are available on the degradation in performance (particularly in stall margin) when compressors are subjected to a rotating inlet distortion. Experiments by Ludwig et al. [B.13] for an isolated rotor show clearly that the stall margin is strongly affected by the speed at which distortion rotates. Co-rotating distortions have a larger impact than counter-rotating distortions, with the maximum loss in stability when speed of rotating distortion is near that at which a rotating stall cell would propagate if the compressor were throttled to stall. Kozarev et al. (1983) [B.14] has obtained similar results for a two-stage compressor.

A more thorough investigation on the effects of rotating inlet distortion on (low speed) multi-stage compressor stability was undertaken by Longley et al. [B.15]. A representative set of measurements from Longley et al. in Figure B.16 showed measured mean flow coefficients at stall inception against inlet

## ANNEX B – ADVANCED TOPICS AND RECENT PROGRESS

distortion speed (normalized by rotor rotation speed) for two types of compressors with respectively different characteristic responses. The two types of compressors are distinguished by the two different routes to rotating stall inception known to occur in compressors:

- ‘Modal Stall Inception’ with a length scale of the order of compressor diameter; and
- Short length scale (spike) inception of the order of few blade pitches with a marked three-dimensional structure local to the rotor tip (Silkowski [B.16], Day [B.17]). The calculations from a theoretical model (described below in a separate section) are shown as solid lines in the figures. The stalling flow coefficients with no distortion and the design flow coefficients are included in the figure as reference.

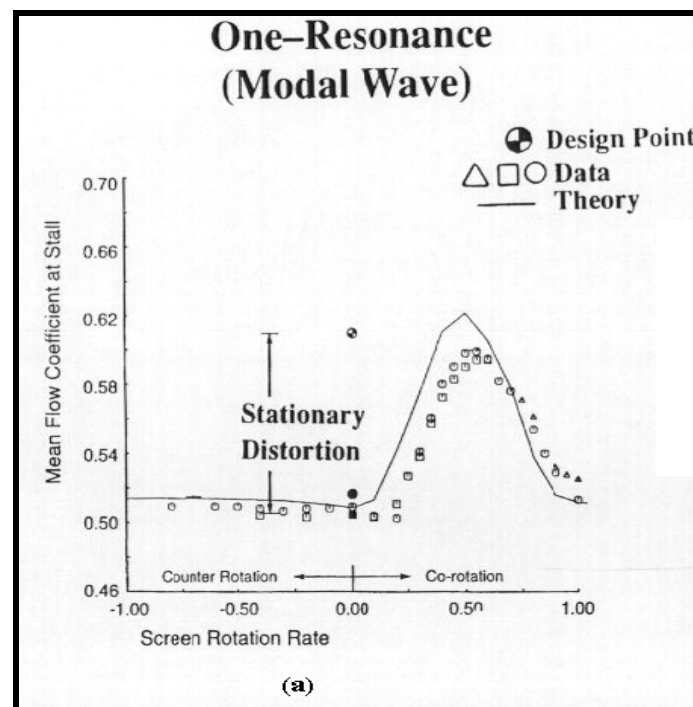


**Figure B.16: Flow Coefficient at Stall versus Distortion Rate, for Single-Resonance-Peak Type of Compressor.**

These measurements showed that the distortion rotational speed has a dramatic effect on the stability point, with the co-rotating one having a stronger impact. Specifically, the change in the stalling flow coefficient is a substantial fraction of the difference between that for stationary distortion and the design flow, providing a measure of the extent to which stability margin has been degraded by co-rotating distortion. For the response of the compressor shown in **Figure B.16**, the degradation of compressor stability margin is greatest when the co-rotating speed is near the measured propagating speed of modal stall inception disturbance (i.e. one resonance peak). This is approximately 40 to 50% of rotor speed, if the compressor is allowed to stall in the absence of any flow distortions. For the compressor shown in **Figure B.17**, compressor stability margin degrades considerably at two co-rotating speeds: one at 20 to 30% of rotor speed and the other at about 70% (i.e. two resonance peaks). The response of compressor to inlet distortion is an example for which the distortion-induced flow unsteadiness clearly changes the steady state compressor characteristics/performance.

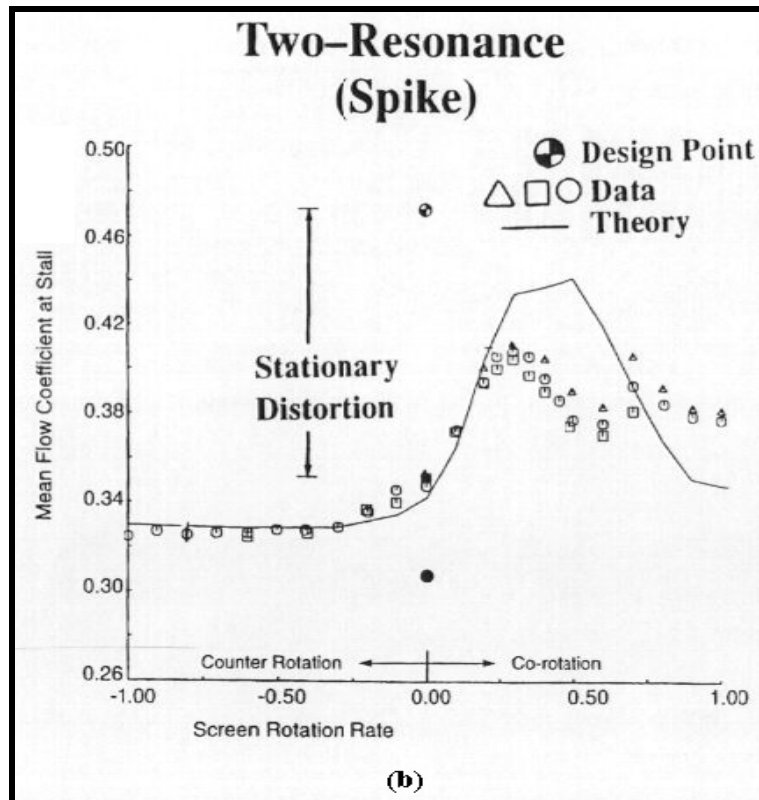


**Figure B.17:** Flow Coefficient at Stall versus Distortion Rate. Two Resonance Peak Type of Compressor.

In the presence of rotating distortion [B.17], the compressor performance deteriorates with a drop in pressure rise capability and a decrease in stability margin (due to a resulting increase in compressor face axial velocity non-uniformity) as the distortion co-rotating speed. For a co-rotating stall at 0.3 rotor speed, there is only a small flow regime for which the compressor is stable. A dramatic decrease in compressor stall margin can be the result when the inlet distortion is co-rotating at a speed corresponding to the propagating speed of the stall inception disturbance.

#### B.1.1.3.2 Aerodynamic Coupling between Inlet-Induced Distortion and Compressor

The above discussion has so far been confined to the response of compressors to a distortion pattern that was specified far upstream. However such is not often the situation encountered in practice. The development of the flow within the inlet can be substantially altered by the presence of the compressor. This aspect of the flow interaction has been clearly elucidated in the set of measurements taken by Hodder [B.18] shown in **Figure B.18**. In the absence of the compressor and with the inlet at 30-degree incidence there was a large region of low total pressure flow due to flow separation. In the presence of the compressor, and at an even larger incidence of 35-degrees, the region of low total pressure fluid was much smaller because the compressor acted to equalize the velocities. This reduced the extent of the separated flow region.

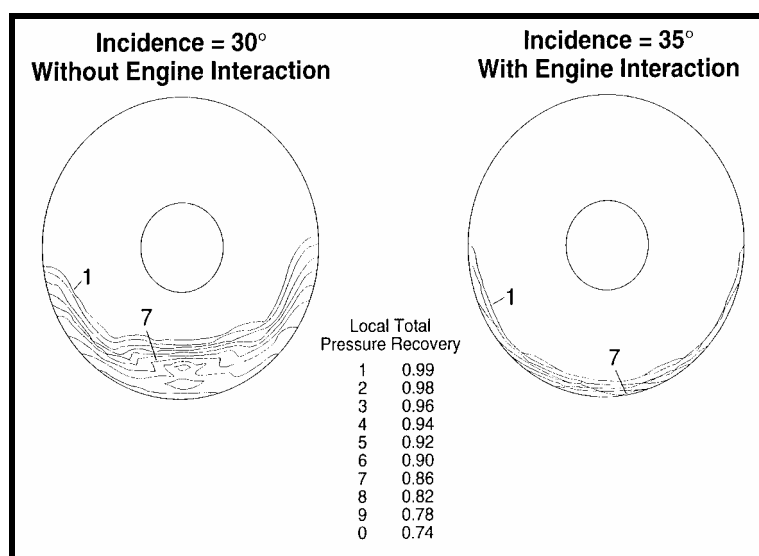


**Figure B.18: Effect of Engine Presence on Total Pressure Distribution within Inlet.**

One may thus infer from this that when undertaking experimental and analytical work on compressor response to inlet-induced flow distortion it is necessary to take steps to ensure correct inlet-compressor interaction. To say this differently: the assessment of engine response to flow distortion should be implemented from the global context of the airframe-inlet-engine system. Proper airframe-inlet-engine matching is needed to ensure the desired vehicle performance for the intended flight envelope. A poorly integrated inlet could result in a flight-vehicle performance penalty (see Airframe-Inlet-Engine Integration).

## B.1.1.3.3 Summary on Rotating Inlet Distortion

Compressors subjected to co-rotating distortions show a significant loss in stability margin if the distortion speed matches a characteristic speed of the compressor flow-field. Measurements indicate that there are two groups of compressors:

- Those with a single peak stall margin decrement; and
- Those with a double peak stall margin decrement (a multi-stage compressor can have more than one characteristic resonance).

Compressor response to rotating inlet distortion can be linked to the disturbance structure at the onset of the stall. The results provide a clear illustration of a situation in which the unsteady flow effects directly affect the time-averaged performance of the compressor.

## B.1.1.4 Stationary and Rotating Asymmetric Tip Clearance

We have examined the change in compressor performance associated with changes in compressor axisymmetric tip clearance. However, the circumferential distribution of tip clearance may become asymmetric due to engine usage and overhauls. An operational question of engineering interest is thus “Can one regard the asymmetry in tip clearance as just an effect of ‘time and circumferentially averaged’ clearance?”

Experimental and analytical investigations have been carried out on a low-speed multi-stage compressor [B.19] where a single and a two-lobed approximately sinusoidal variation in tip clearance had been separately introduced. The baseline configuration had an axisymmetric clearance of 4% chord. The quoted

clearances are relative to the baseline, so that +2% and –2% chord clearance corresponds to tip clearance of 6% and 2% chord respectively. The asymmetric clearance was introduced by varying the casing so that the circumferential average clearance was the same as the baseline clearance.

These results presented in **Figures B.15 to Figure B.19**, show that clearance asymmetry reduces both the compressor stability margin and efficiency. The single lobe variation has a larger impact than two and higher lobe patterns, which is a frequency effect. The reduction in stability margin is closer to the maximum than would be given by the circumferential average clearance. The sensitivity of performance to clearance asymmetry is a function of the steady state compressor response and unsteady response. The computed results from the theoretical model are in general agreement with the measurements. While no experimental data is available to depict the effect of rotating tip clearance asymmetry on compressor performance, calculations, based on the model presented in the section on methodology, show that the effect is analogous to that of rotating inlet distortion. In this case, the impact on compressor performance deterioration is greatest when tip clearance is co-rotating at a speed close to that at which the rotating stall inception would propagate.

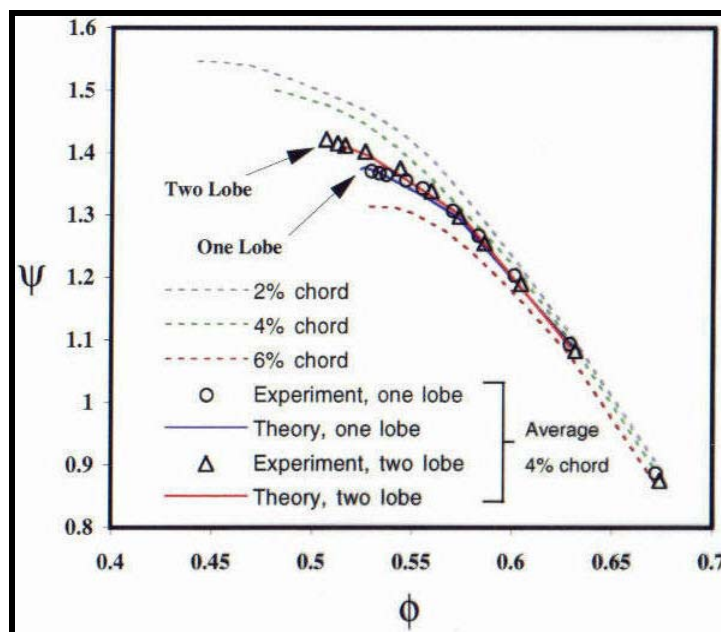


**Figure B.19:** Effect of Tip Clearance Distribution on Pressure Rise Characteristics and Stall Margin.

### B.1.1.5 Effect of Compressor Axial Gap

The performance of axial compressors is known to depend on axial gapping between blade rows. Experimental data, published from General Electric (Smith [B.5]), Rolls Royce (Hetherington and Moritz [B.20]) and Pratt & Whitney (Mikolajczak [B.21]) and shown in **Figure B.24**, clearly show that the performance (efficiency) of axial flow compressors can be increased by optimizing the axial gap between adjacent airfoil rows. The results of **Figure B.20**, while interesting, provide neither a quantitative guideline nor an understanding of how to improve the performance of the machine. Smith's results showed a one to two per cent gain in efficiency, and a two to four per cent gain in the stage pressure rise in a low-speed research compressor, by reducing the blade row gap from 0.37 to 0.07 chords. Mikolajczak obtained similar results in a moderate speed compressor. Hetherington and Moritz, however, obtained a 2 per cent gain in efficiency by increasing the gap in front of the rotor rows in a multi-stage compressor. The experiments of Smith and Mikolajczak suggest that reduced axial gap improves performance,

## ANNEX B – ADVANCED TOPICS AND RECENT PROGRESS

while Hetherington and Moritz's investigation indicates increased axial gap can also be beneficial. A wake recovery model, developed by Smith [B.22], establishes a connection between blade row interaction and performance and is further substantiated by the computed results of Valkov and Tan [B.25] to include the tip leakage vortex flow.

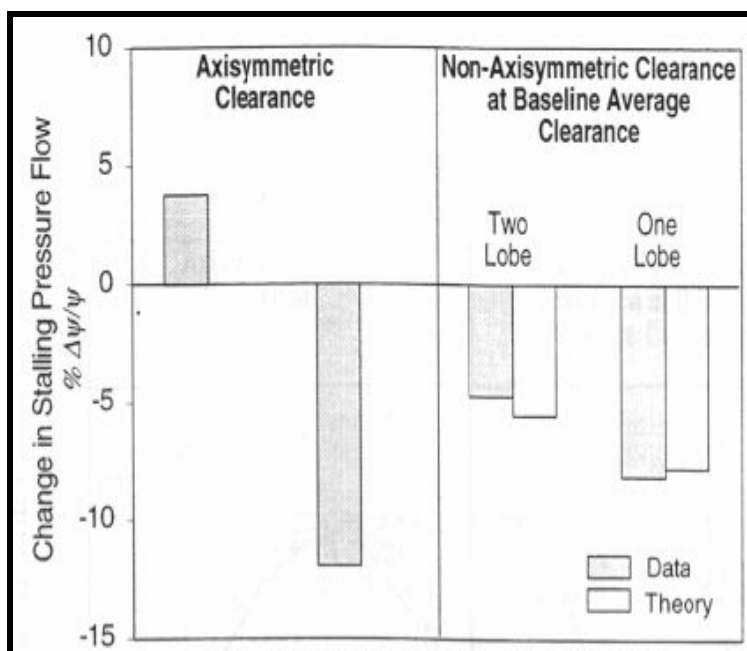


**Figure B.20:** Changes in Stalling Pressure Rise with Axisymmetric and Non-Axisymmetric Clearance.

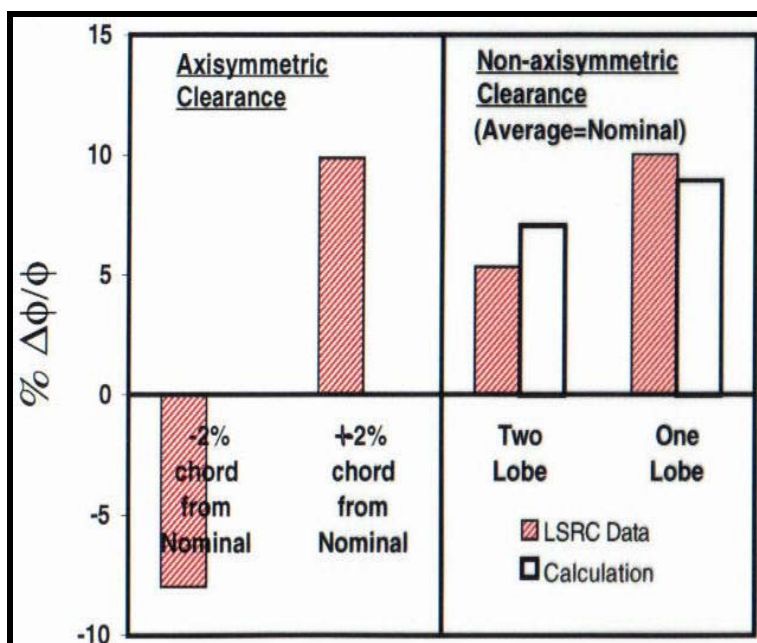


**Figure B.21:** Changes in Flow Coefficient with Axisymmetric and Non-Axisymmetric Clearance.

## B.1.1.6 Effect of Axial Gap on Stalling Pressure Rise

Data, taken from Koch [B.24] and shown in Figure B.22, shows that the stalling pressure can increase by as much as 10% when the axial gap between the blade row is reduced by a factor of 3. The implication is that axial gap not only changes the performance at design but can also potentially change the stability margin.

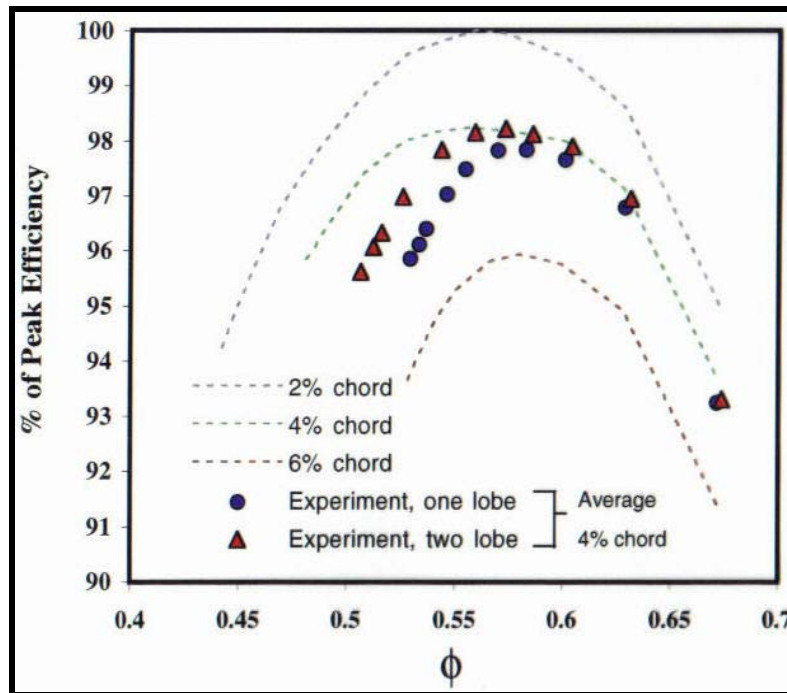


Figure B.22: Effect of Tip Clearance Distribution on Compressor Efficiency.

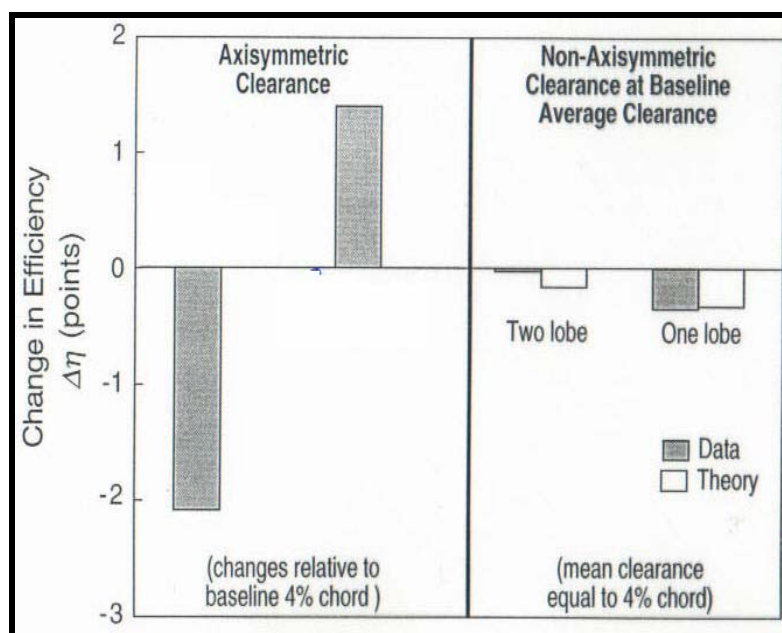
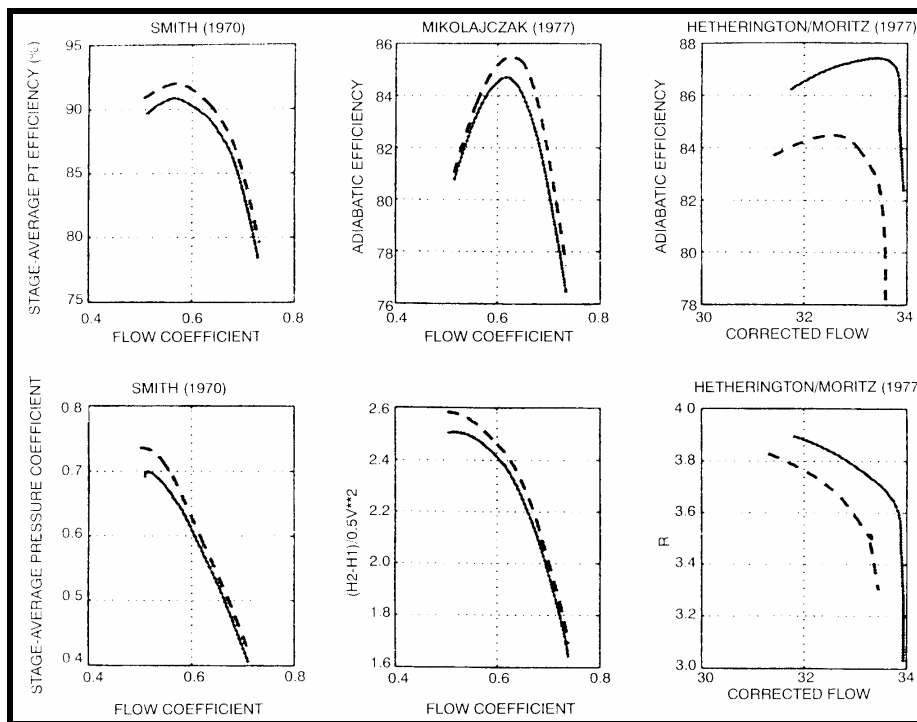
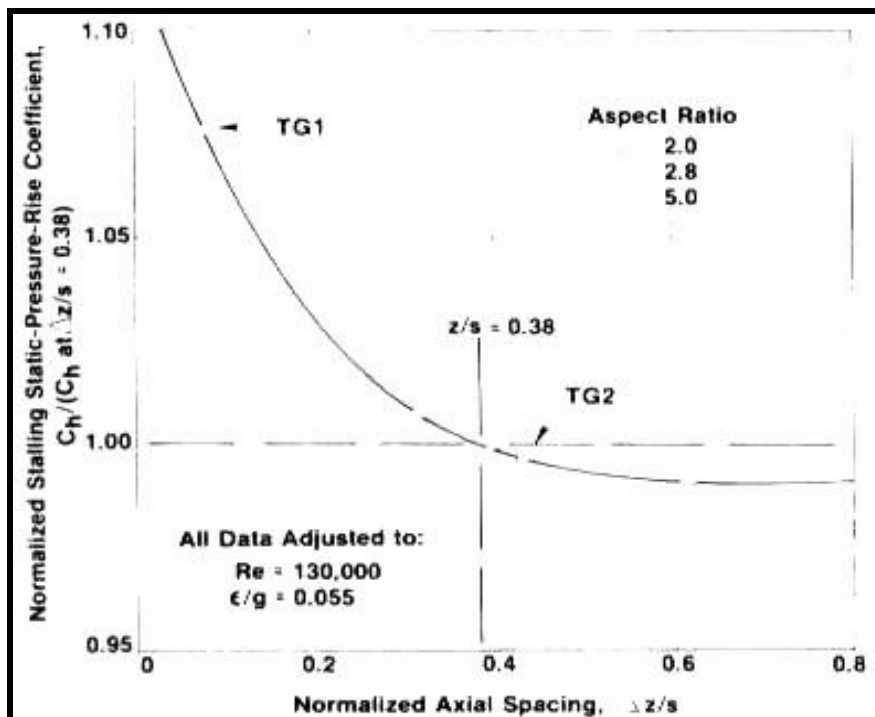


Figure B.23: Changes in Peak Efficiency with Asymmetric Clearance, with the Flow Condition Corresponding to the Peak Efficiency Points in Next Figure.



**Figure B.24:** Variation of Compressor Efficiency (top) and Pressure Rise (bottom) for Closely-Spaced (dashed lines) and Widely-Spaced (solid lines) Blade Rows.



**Figure B.25:** Effect of Axial Spacing on Stalling Pressure Coefficient.

This section discusses how changing the axial spacing between compressor blade rows can alter the compressor performance in terms of its pressure rise capability and efficiency. Often in compressor testing

one may attempt to increase the axial spacing between blade rows to accommodate placement of instrumentation; it is to be borne in mind that this will modify the compressor performance characteristics undesirably.

## B.1.1.7 Effect of Reynolds Number and Blade Surface Roughness

The performance deterioration of a high speed axial compressor rotor due to changes in Reynolds number and blade surface roughness and airfoil thickness variations has been investigated on an experimental and on an analytical and computational basis by Schaffler [B.26], Koch [B.24] and K. Suder et al. [B.27]. Within the flight envelope for a typical modern fighter aircraft indicated in Figure B.26 [B.26], the operational Reynolds number can change by a factor of 10 (from 100,000 to 1,400,000).

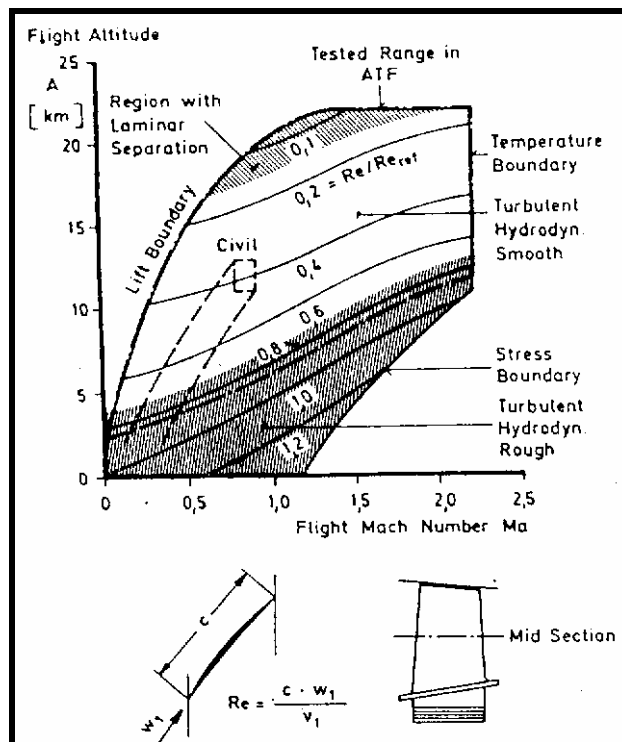


**Figure B.26:** Range of Operational Reynolds Number of a High-Pressure Compressor within the Flight Envelope [B.26].

Three flow regimes corresponding to this range of Reynolds number can readily be identified. These are:

- Low Reynolds number regime where laminar separation occurs at least in the front stages, resulting in reduced flow and efficiency levels and stall margin. This corresponds to operation at high altitude.
- Intermediate regime with a turbulent attached boundary layer flow and hydrodynamically smooth blade surfaces.
- High Reynolds number regime where the middle and back stages of high pressure ratio compression systems experience turbulent attached boundary layer flow with hydrodynamically rough blade surfaces. This corresponds to operation at low altitude.

A multi-stage compressor can be expected to show the following behavior over a wide Reynolds number range:

## ANNEX B – ADVANCED TOPICS AND RECENT PROGRESS

- Mass flow increases steadily with Reynolds number up to the choking condition in the blade passage;
- The surge line is essentially unaffected by Reynolds number until there is severe flow separation corresponding to operation at Reynolds number less than 100,000; and
- Polytropic efficiency varies with distinct slope changes that are dictated by specific boundary layer behavior.

The impact of boundary layer behavior on the functional dependence of efficiency on Reynolds number is shown in **Figure B.27 [B.26]** for an axial compressor at design point operation. As to be expected there are again three different regimes demarcated by a lower and an upper critical Reynolds number that define the laminar separation boundary and the surface roughness boundary. The consequence on compressor performance changes corresponding to each of the regimes is indicated in **Figure B.28**. If the Reynolds number is sufficiently high, the efficiency essentially becomes independent of the Reynolds number. Under this condition the blade surface roughness elements protrude through the laminar sub-layer of the turbulent boundary layer.

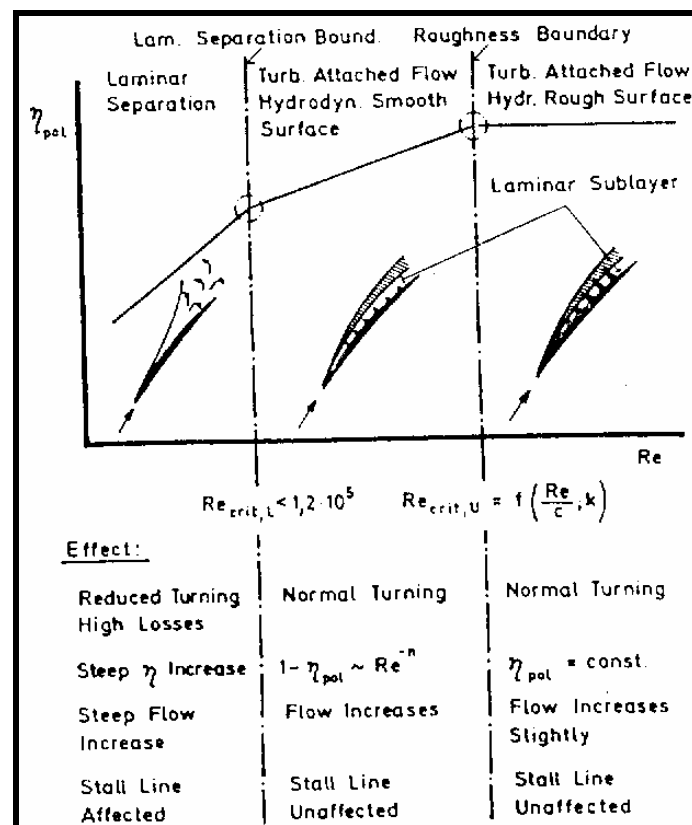


**Figure B.27: Effect of Boundary Layer Condition on Compressor Behavior [B.26].**

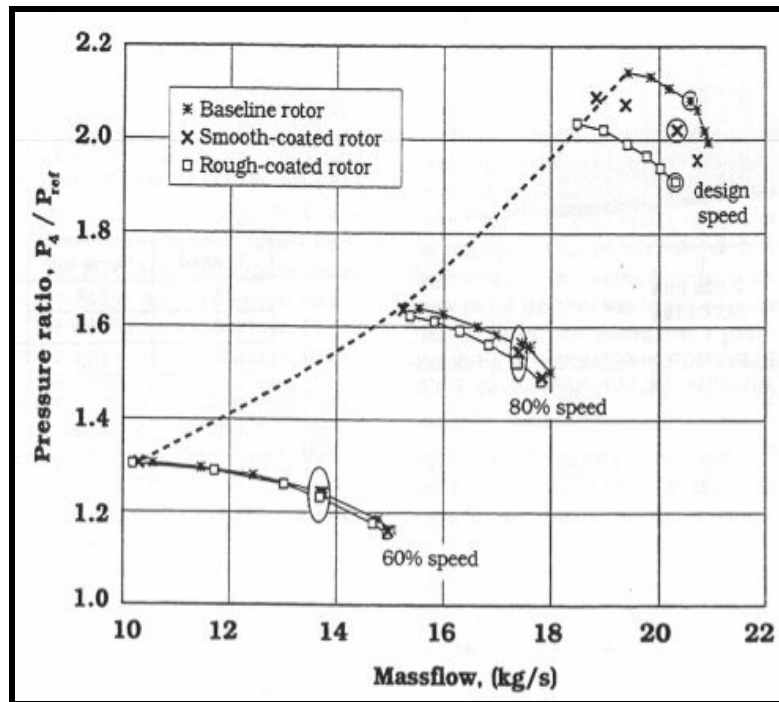


**Figure B.28:** Effect of Surface Roughness on Compressor Pressure Characteristics.

Results that show the effects of Reynolds number and blade surface roughness on compressor performance changes are drawn from Schaffler, Koch and Suder. The impact of blade surface roughness on the pressure ratio, efficiency, and pressure rise v mass flow characteristics of a high-speed fan stage are respectively shown in **Figure B.28** to **Figure B.30**. Likewise the influence of Reynolds number on compressor efficiency and pressure ratio of an intermediate pressure compressor and a high pressure compressor is shown in **Figure B.31**, while its influence on the stalling pressure rise coefficient (taken from Koch, 1981) is shown in **Figure B.32**.

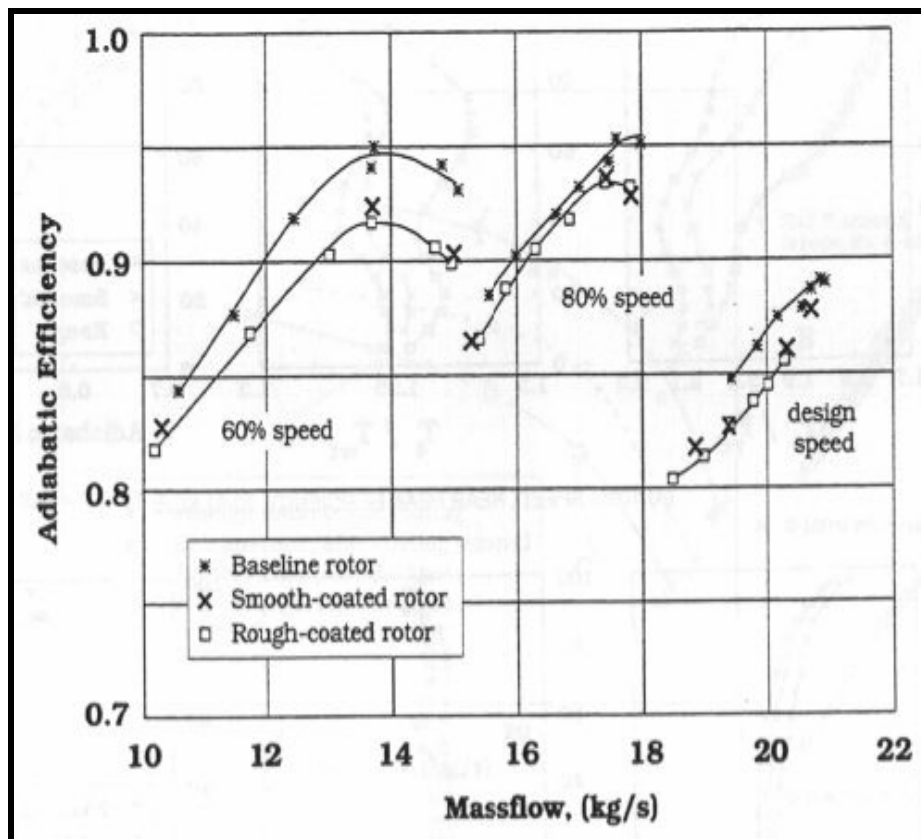


Figure B.29: Effect of Blade Surface Roughness on Compressor Efficiency.

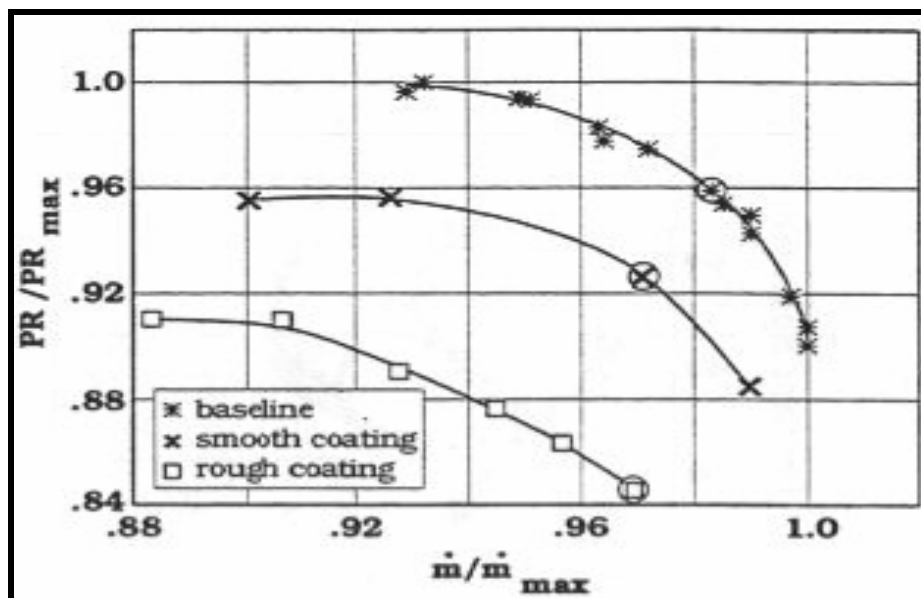
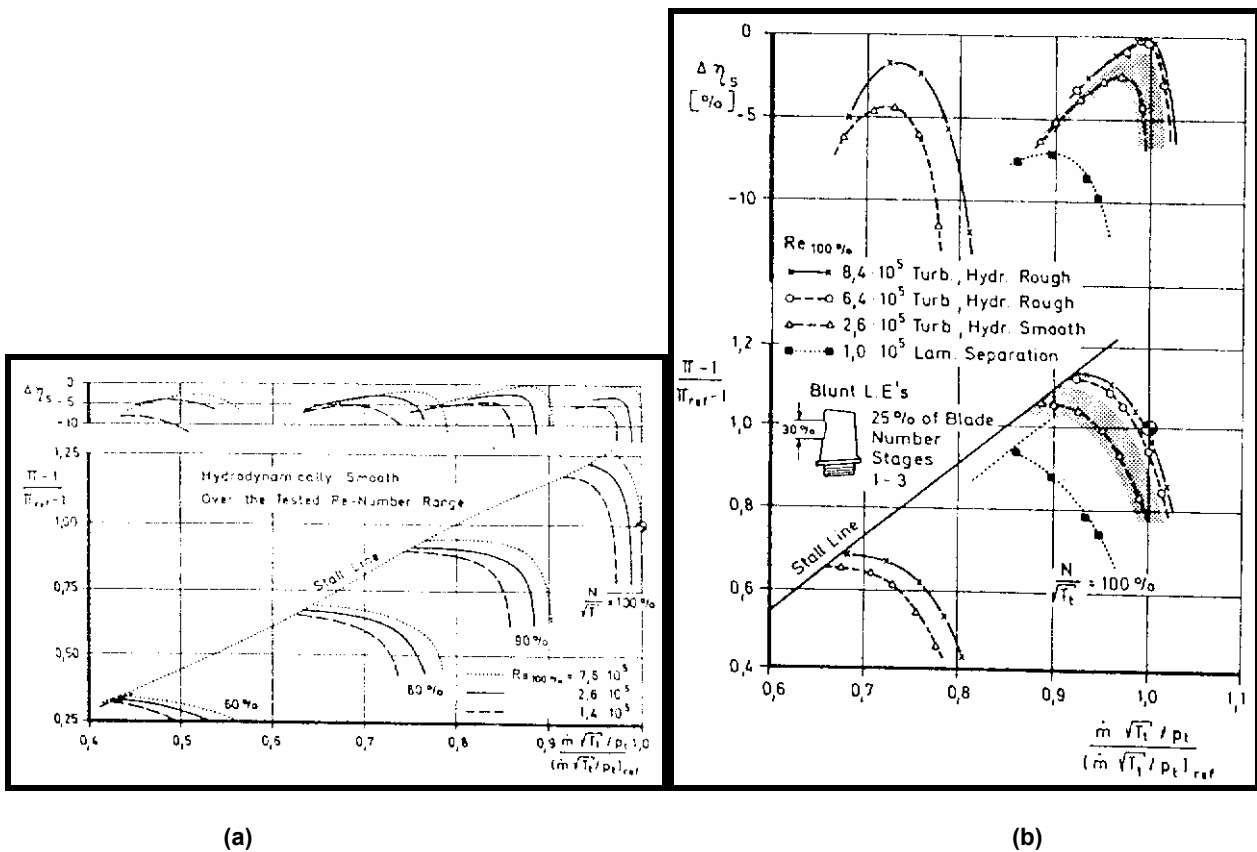
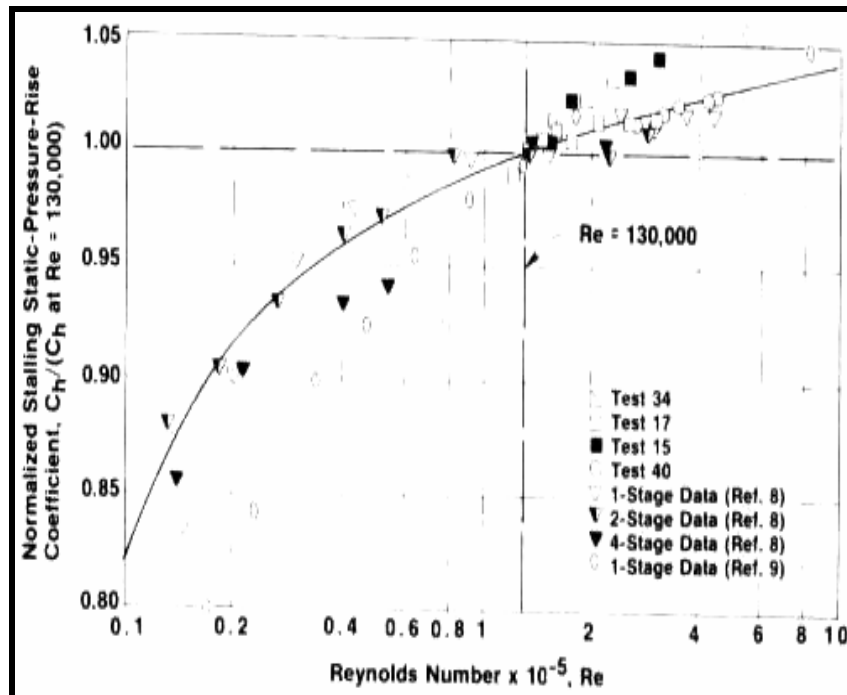


Figure B.30: Effect of Variation in Blade Surface Roughness on Pressure Ratio versus Mass Flow Characteristics at 70-Percent Span.



**Figure B.31:** Effect of Reynolds Number on the Performance of: (a) A Three-Stage Intermediate Pressure Compressor; and (b) A Six-Stage High Pressure Compressor [B.26].



**Figure B.32:** Effect of Reynolds Number on Compressor Stalling Pressure Rise Coefficient.

As will be indicated in the section on methodology, present computational resources do not allow one to assess the influence of Reynolds number and blade surface roughness on compressor performance on an adequate basis. This is because one would have to resort to the use of direct numerical simulation (DNS), and presently such techniques have been applied only to very simplistic flow situations.

## B.1.1.8 Variable Stator Vane Effects

Variable stator vanes (VSV) are used to optimize performance and operating stability of compression components. Compressors often operate with stator positions differing from the nominal schedule that is consistent with the map. For single stage machines, the stator angle can be used directly although an intermediate stator position indicator is often used rather than the actual airfoil angle. For multi-stage machines with multiple variable stators, the variable stators are generally ganged together and one average stator angle is used to represent the overall stator movement. Tabular 0-D compression component maps may address VSV effects by providing separate maps for different average stator positions relative to a nominal setting and interpolating between these maps for intermediate stator settings. Analytical 0-D component maps can do the same or use the implied change in the average stage characteristic and flow coefficient to indirectly model the impact of stator movement based on a simplified physical model. Stator movements change the overall performance of the component and the matching between stages, which can affect the predicted inter-stage conditions for the same overall operating conditions. This can be important for bleed and cooling flow extraction in full engine use. **Figure B.33** shows the impact of stator position on flow and efficiency as a function of speed for a particular operating line.

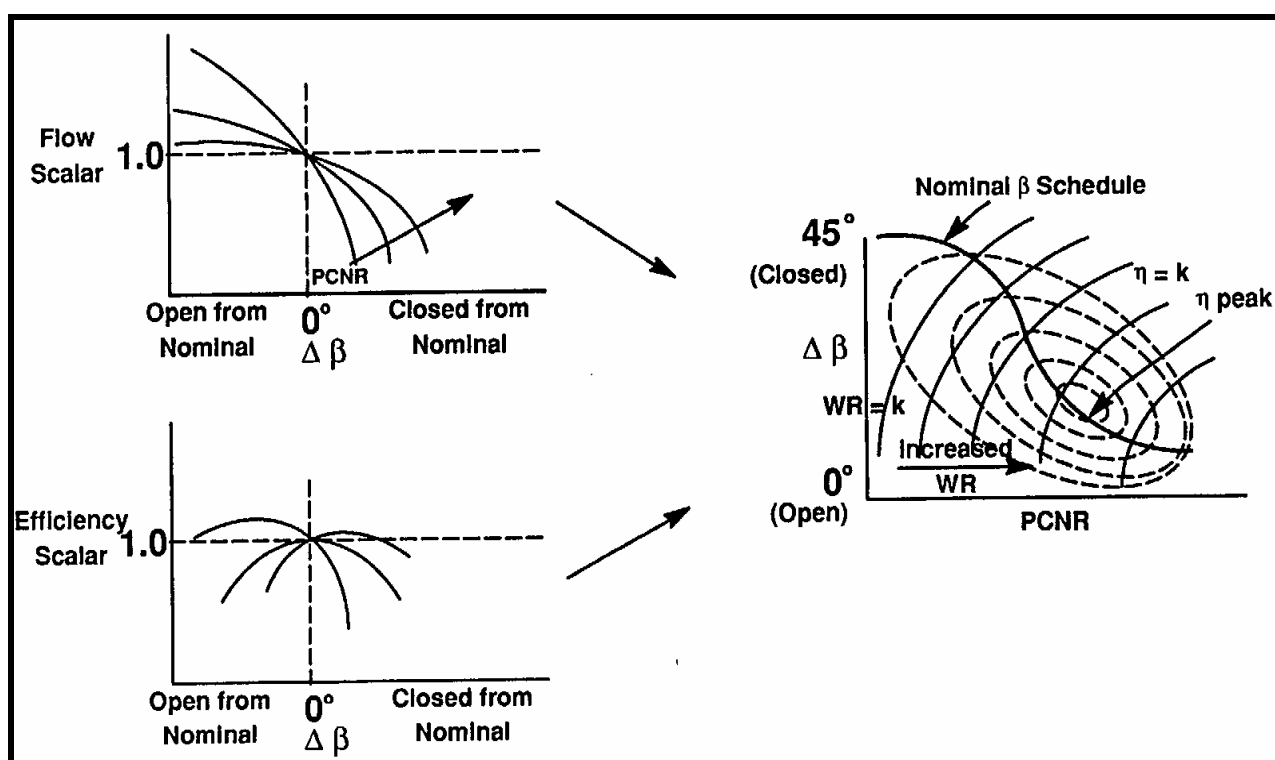


**Figure B.33:** Impact of Stator Position on Flow and Efficiency as a Function of Speed for a Particular Operating Line.

Higher fidelity models that require specific geometry will generally model the effect of stator position directly as part of the component representation. Stator position accuracy is critical to obtain accurate results from these high fidelity models. Stators and their position sensors are a frequent source of difficulty

in validating component models with real data due to hysteresis and variation between the indicated and actual stator position.

### **B.1.1.9 Effects of Thermal Origins**

#### *B.1.1.9.1 Temperature and Gas Property Effects*

A compressor map generated for a specific set of entrance conditions may not be accurate at other entrance conditions due to the effects noted above. Many of these effects are compounded. Temperature changes affect clearance as the case grows. The relationship between the mechanical and corrected speed changes affects both blade untwist and blade growth. Unless the entrance pressure changes to match, entrance temperature also changes the Reynolds number. Even if all these effects are ignored, the use of temperature corrected parameters still ignores the change in the speed of sound with gas properties due to temperature and gas composition. So-called ‘gamma-R’ corrections are commonly used with most 0-D models to adjust base map predictions to a constant average Mach number similarity parameter. This is to allow for gas property changes. Due to lack of test data to separate these effects, it is common to select a few key effects such as clearance, Reynolds number and VSV (variable stator vane) angle to cover empirically all the effects not modeled hitherto.

#### *B.1.1.9.2 Heat Transfer Effect*

For 1-D, 2-D and 3-D models, the effect of heat transfer from the blades and static parts to the gas path flow can be modeled directly. The change in temperature will modify the stage-by-stage performance and result in an overall re-matching of the compressor. At a 0-D level, it is generally not possible to create an adjustment to the compressor performance that can be distinguished from the empirical bulk heat-transfer effects in the overall engine model. The heat transfer impact on compressor performance depends on the controlling stage in the machine and whether heat transfer at that particular operating condition moves that stage to a less or more favorable condition.

Heat-transfer effects on 0-D compressor maps are difficult to model, because performance depends on the controlling stage in the machine and whether heat transfer at that particular operating condition moves that stage to a less or more favorable conditions. However, simple approaches allow the main consequences of heat transfer to be caught.

### **B.1.1.10 Fan and Bypass Duct System**

As shown in **Figure B.34**, the fan-bypass duct system consists of a fan followed by a splitter that subdivides the fan flow into a stream through the bypass duct and another through-the-core compressor. The core compressor may also include a row of exit guide vane and supporting struts.

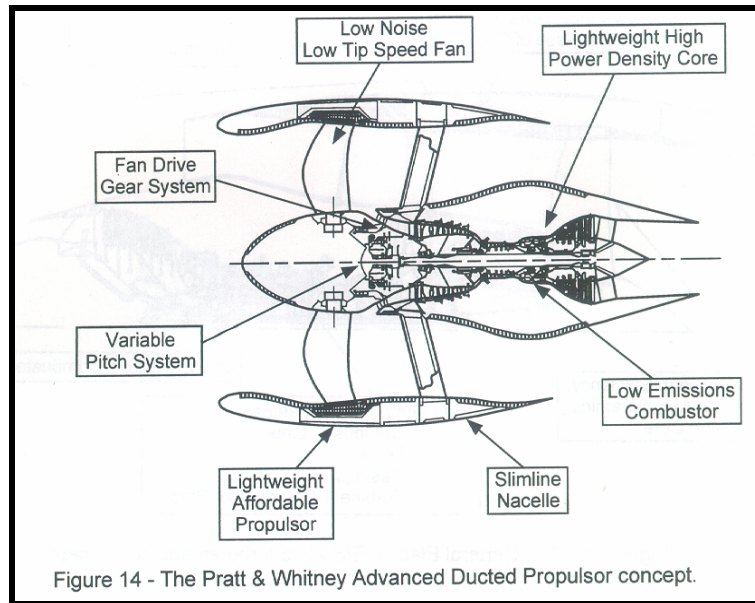


**Figure B.34: Advanced Fan-By-Pass Core-Engine Duct System.**

Fans have a hub-to-tip ratio ranging from 0.3 to 0.6, while core compressors have a much higher hub-to-tip ratio of 0.7 and above. Thus the outer portion of the fan generates the pressure ratio needed to maintain the required flow in the bypass duct and the inner portion of the fan generates the pressure ratio for the flow into the core compressor. The dividing streamline that demarcates the inner and outer stream of the fan is the stagnation streamline with the stagnation point located on the leading edge of the splitter.

The performance of the fan-bypass duct system can be represented through the following set of maps:

Fan OD map  $F\left(\frac{P_{t12.5}}{P_{t12}}, \frac{N}{\sqrt{\theta_{t2}}}, \frac{W_{tot}\sqrt{\theta_{t2}}}{\delta_2}, \eta_{fanOD}\right)$ , surge line, see **Figure B.35**.

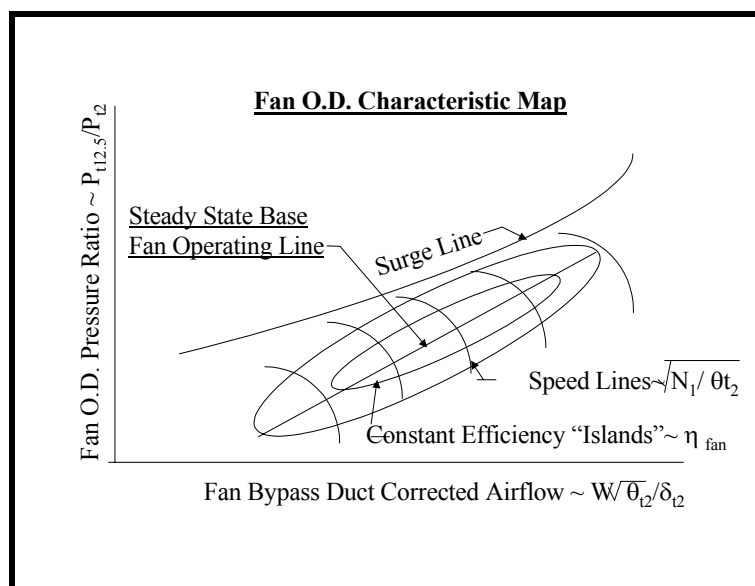


**Figure B.35: Fan O. D. Map.**

Fan exit guide vane (FEGV) map  $F\left[\left(\frac{\Delta P}{P}\right)_{fegv}, \frac{W_{fan OD} \sqrt{\theta_{t12.5}}}{\delta_{t12.5}}, \frac{N}{\sqrt{\theta_{t12.5}}}\right]$ , see **Figure B.36**.

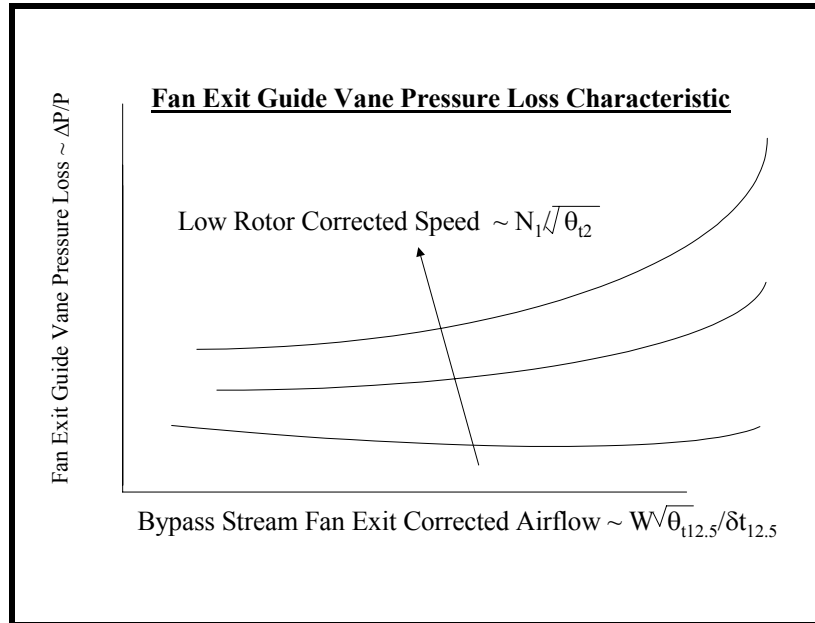


**Figure B.36:** Fan Exit Guide Vane (FEGV) Map.

Low pressure compressor map, including fan ID  $F\left(\frac{P_{t2.5}}{P_{t2}}, \frac{N}{\sqrt{\theta_{t2.5}}}, \frac{W_2 \sqrt{\theta_{t2.5}}}{\delta_{2.5}}, \eta_{LPC}, \text{surge line}\right)$ , see **Figure B.37**.

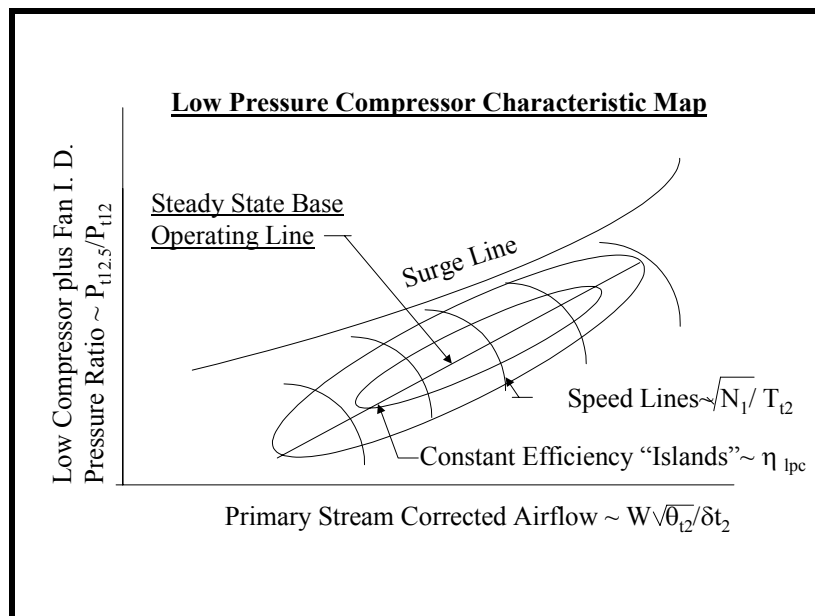


**Figure B.37:** Low Pressure Compressor Map, including Fan ID.

## ANNEX B – ADVANCED TOPICS AND RECENT PROGRESS

Super charging curve for primary stream  $F\left[\Delta\left(\frac{P_{t2.5}}{P_{t2}}\right), \frac{N}{\sqrt{\theta_{t2}}}, BPR, \eta_{LPC}\right]$ , see **Figure B.38**.

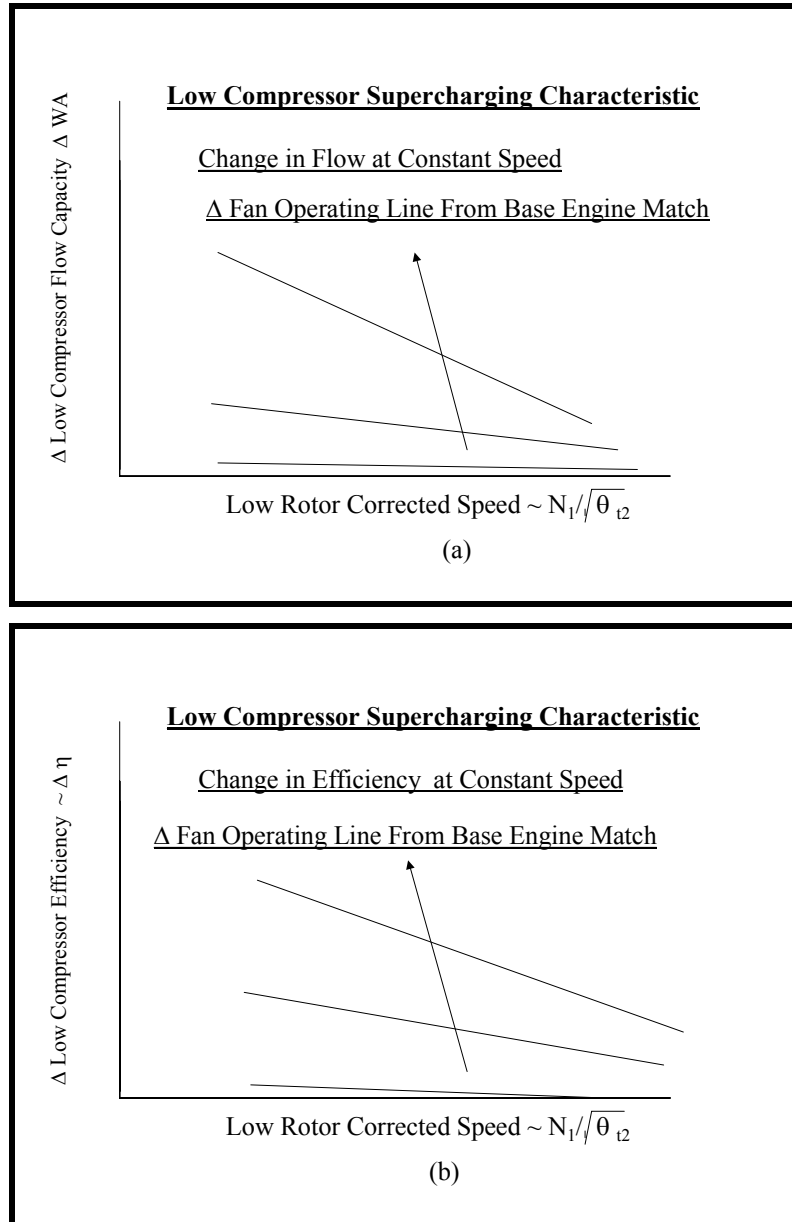


**Figure B.38: Super Charging Curve for Primary Stream.**

In addition to the characteristic modifiers described above there are two additional characteristic modifiers unique to the fan system. These are the fan blade untwist and stratification, which will be described below.

### B.1.1.11 Blade Untwist

#### B.1.1.11.1 Description

Blade untwist is a mechanical phenomenon where the leading edge blade angle varies with operating condition. Typically this is due to the loads from centripetal acceleration and changing pressure forces on the

blade. It is primarily of concern for low hub/tip radius ratio blades (high bypass fans and the first stages of multi-stage medium bypass fans), but can be an issue for accurate detailed predictions of off-design behavior in highly loaded multi-stage compressors. **Figure B.39** shows an example of untwist for a high bypass fan. The change with flight condition shows the need to model more than just the centripetal accelerations. **Figure B.40** shows the impact of pressure and mechanical loading on the blade. The fan is designed with some nominal untwist which changes with both engine power setting and environmental conditions. **Figure B.41** shows the definition and conventions for untwist angle.

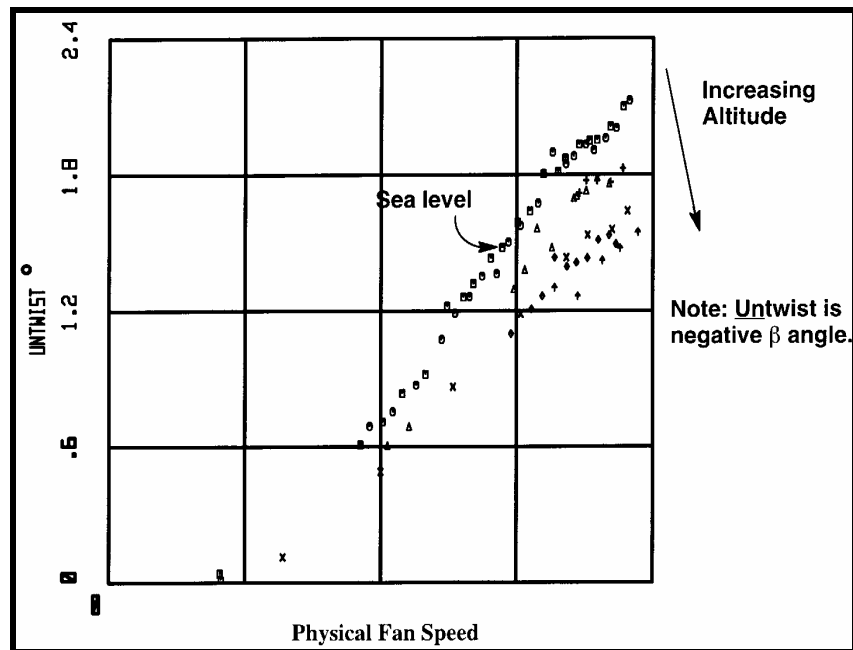


**Figure B.39:** Level of Untwist for a High Bypass Fan.

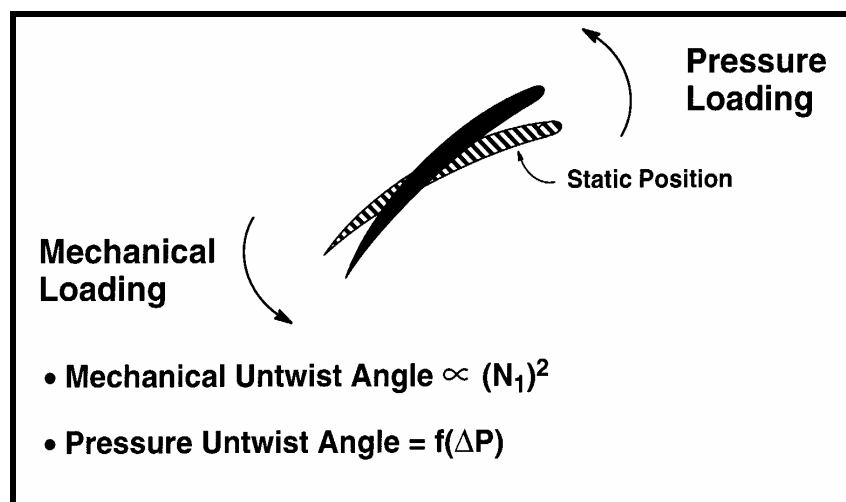


**Figure B.40:** Impact of Pressure and Mechanical Loading on Blade.

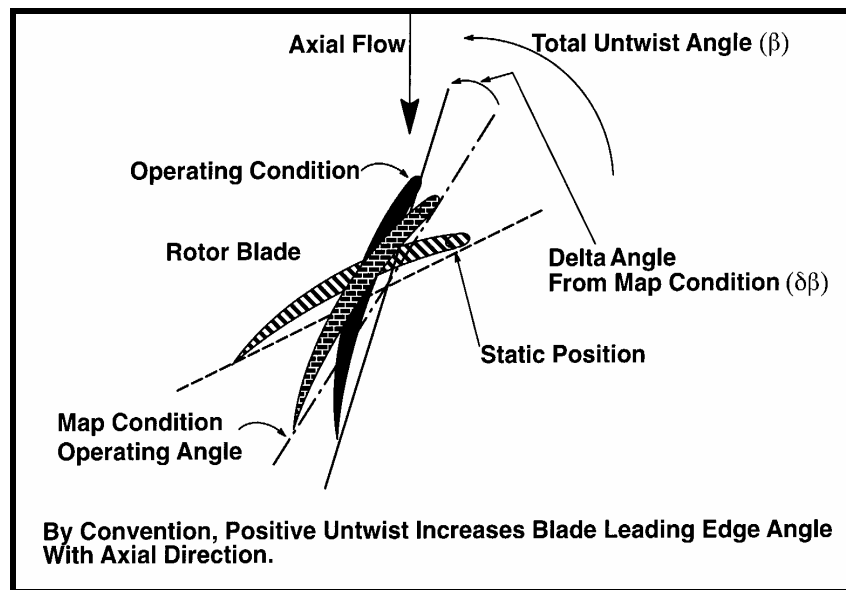


**Figure B.41:** Definition and Conventions for Untwist Angle.

## B.1.1.11.2 Impact on Component Modeling

The primary impact of untwist is on flow capacity for high bypass fans. The same tools used to generate the basic fan model can often be used to identify the flow impact per degree of untwist. For multi-stage machines even a few tenths of a degree in blade angle can impact the stage matching and component performance, particularly with supersonic airfoils. This becomes an issue for compressor design but is rarely considered for component modeling. Blade untwist effect is typically in the order of 1% per degree at low speeds and will often double that at the maximum flow capacity of the machine as shown in **Figure B.42**.

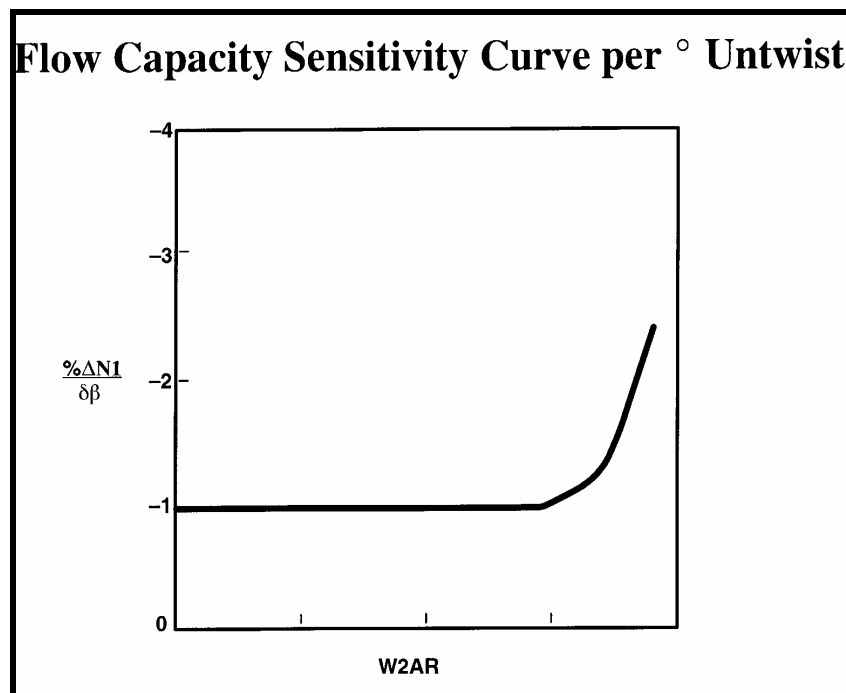


**Figure B.42:** Blade Untwist Effect vs. Speed.

#### *B.1.1.11.3 Modeling Approach*

Although it is possible to use a mechanical model to provide the actual change in blade angle with operating condition, a correlation is typically used for both engine design and component simulation. For engine design these correlations can be quite involved. For 0-D and 1-D models, a correlation with mechanical speed and pressure rise is usual. **Figure B.42** shows typical behavior vs. speed and flight conditions and can adequately be correlated with speed and stage pressure rise for use in a 0-D or 1-D model.

A problem with untwist modeling in multi-stage machines is the complexity of the behavior and the confounding with clearance and Reynolds number effects. Since both of these are a function of flight conditions and clearance is a function of mechanical speed, inadequacies in the models for these three effects are difficult to separate. A good model for one will be misleading when comparing the model with test data where these other effects are ignored. For high bypass fans the impact is large enough to be obvious but even there the ability to make accurate estimates may be limited by the lack of an asymmetric clearance model.

Finally for 2-D and 3-D situations, NASTRAN can be used to calculate the blade untwist effects as a function of radius.

#### **B.1.1.12 Stratification**

Stratification is the radial variation in temperature and pressure at the exit of a fan. In a mixed flow turbofan, the average conditions at the fan exit are stratified to generate the separate conditions entering the bypass duct and core. The relationship of these split conditions to the average condition varies with the operating-line, speed and engine-bypass-ratio. Although separate maps can be used for the hub portion and tip portion of the fan, as is often done on high bypass turbofans, the bypass ratio effect may still be significant. Changes in down stream geometry can also affect this behavior as shown in **Figure B.43**. If the splitter is close enough to the fan, the stream line movements to turn the flow to the splitter leading edge can change the splitting streamline position across the fan affecting both the average and stratified performance.

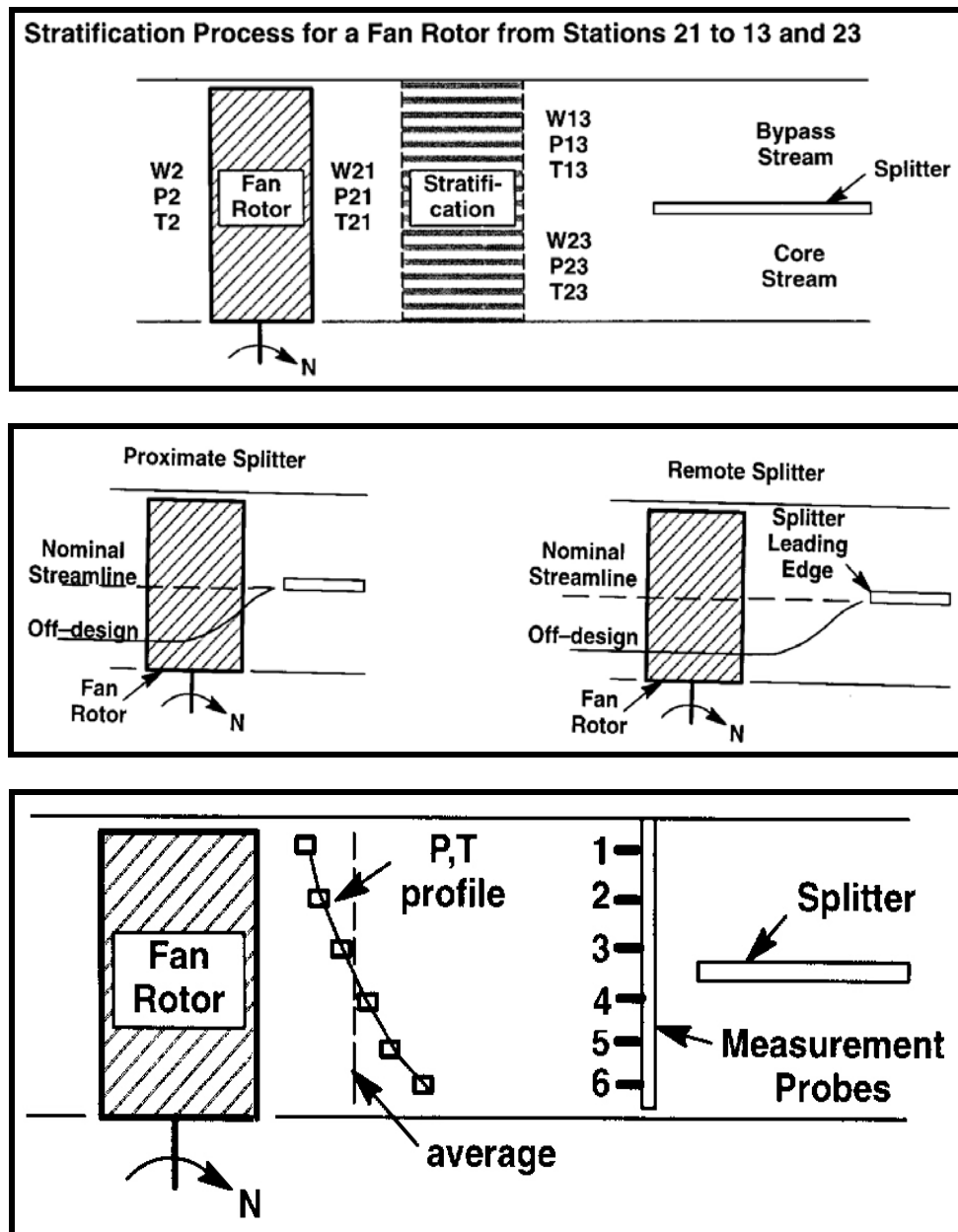


**Figure B.43: Effects Associated with Stratification.**

For 0-D and 1-D performance, the change in exit pressure and temperature at the tip relative to the average is usually correlated from test data or detailed model prediction. The hub values are then calculated based on conservation. For higher bypass engines the correlation basis may switch, and be based on the hub.

## B.1.1.13 Parametric Analysis of Aeroengine Flutter for Flutter Clearance

So far, we have mainly focused on the aerodynamic aspects. Here we will touch on the aeromechanical aspects. Successful aeroengine designs must be free from turbomachinery flutter under all operating conditions. Flutter is a vibrational instability of the rotor blades, which can rapidly promote High Cycle Fatigue (HCF) failure. If not caught during testing and corrected before entry into service use, flutter problems can impact the readiness on a fleet-wide basis (Kandebo, 1994) [B.28].

The work of A. Khalak [B.29] addresses the problem of constructing a rational testing procedure to ensure flutter clearance throughout the operational flight regime of a turbomachine. In so doing, a new set of similarity parameters has been developed for operability assessment. This set consists of four parameters: ( $m_c$ ,  $N_c$ ,  $K_0^*$ ,  $g/\rho^*$ ), where the first two parameters are the corrected mass flow,  $m_c$ , and corrected rotor speed,  $N_c$ , and the latter two parameters are new. These we term the compressible reduced frequency,  $K_0^*$ , and the reduced damping,  $g/\rho^*$ .

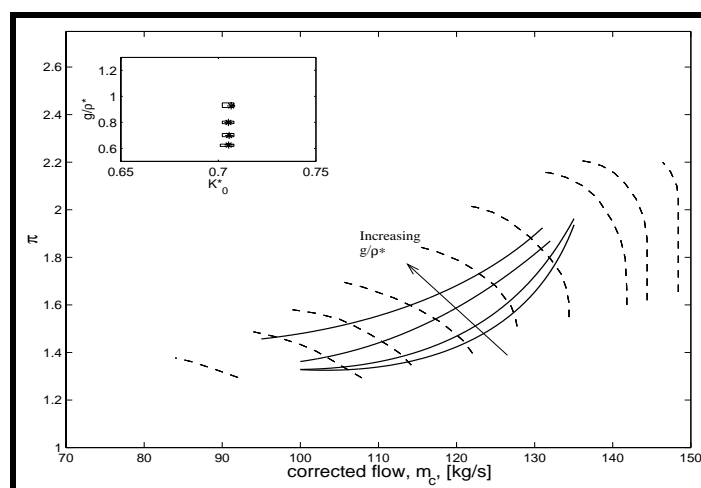
$$\frac{g}{\rho^*} = \frac{gm_0}{c^2 \rho_0} = \frac{4}{\pi} g \mu$$

The reduced damping,  $g/\rho^*$ , combines the mechanical damping,  $g$ , and the mass ratio,  $\mu$ , into a single non-dimensional parameter, useful for linear stability purposes. This parameter is defined such that  $m_0$  is the modal mass (per unit length),  $c$  is the chord, and  $\rho_0$  is the inlet density. The  $g/\rho^*$  label emphasizes the dependence upon inlet density. For cases with frictional damping (e.g. inserted blades), the reduced damping is order 1 and has a significant impact on flutter stability.

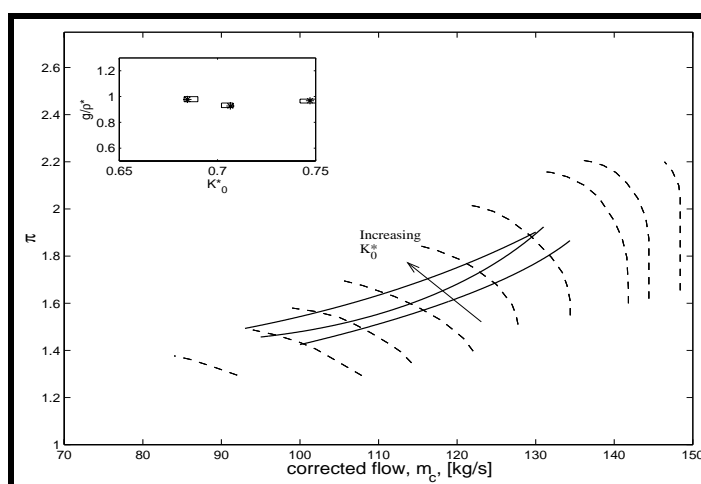
The compressible reduced frequency,  $K_0^*$ , is defined as  $\omega_0 c / (\gamma RT)^{1/2}$ , where  $\omega_0$  is the blade natural frequency at rest, and  $(\gamma RT)^{1/2}$  is the inlet speed of sound (which varies with inlet temperature,  $T$ ). The  $K_0^*$  parameter comes from a decoupling of corrected performance effects from purely aeroelastic effects. Roughly speaking, for a constant structure (i.e. constant  $\omega_0 c$ ) the parameter  $K_0^*$  varies with the temperature, a parameter for which the performance is “corrected”.

The first two parameters of the set,  $m_c$  and  $N_c$ , account for the corrected performance, as normally measured for high speed turbomachines. For constant structural parameters, the latter two parameters,  $K_0^*$  and  $g/\rho^*$ , span the inlet temperature and density. These can be related to the flight conditions in terms of flight Mach number and altitude. An implication of this four-parameter viewpoint is that the flutter clearance of a machine depends on the corrected performance point, and the intended flight envelope of the aircraft.

These parameters were applied to the analysis of full-scale test data. **Figure B.44** shows the trends with  $K_0^*$  and  $g/\rho^*$ . Both increasing  $K_0^*$  and increasing  $g/\rho^*$  (at constant  $m_c$  and  $N_c$ ) have stabilizing effects upon flutter stability. It is proposed that these trends hold generally. The trend with  $g/\rho^*$  is analytically based in the equations of motion, and is equivalent (by similarity) to the statement that increasing the mechanical damping is stabilizing. The trend with  $K_0^*$  is ultimately empirical, but it is supported by several previous studies and is equivalent (by similarity) to the widely-held design principle that increasing the natural frequency stabilizes flutter.



a)



b)

**Figure B.44: Trends of Performance Map Flutter Boundary with  $K_0^*$  and  $g/\rho^*$  from Full-Scale Engine Data.**

Figure (a) shows the effect of varying  $g/\rho^*$ , and (b) shows the effect of varying  $K_0^*$ . Increases in both  $K_0^*$  and  $g/\rho^*$  are stabilizing.

With the relevant similarity parameters spanning a four-dimensional space, the range of comprehensive testing is vast. The proposed trends with  $K_0^*$  and  $g/\rho^*$ , however, suggest a way to simplify the requirements for comprehensive testing. Since increasing  $K_0^*$  and increasing  $g/\rho^*$  are both stabilizing, it follows that the worst case at a particular  $(m_c, N_c)$  are the minimum values of  $K_0^*$  and  $g/\rho^*$ . Thus, clearance for the engine at the minimum  $K_0^*$  and  $g/\rho^*$  implies clearance throughout the flight regime.

## B.1.2 Simulation of Centrifugal Compressor Performance

The Performance of a centrifugal compressor simulated in an engine performance model is very similar to the modeling for axial compressors. A basic compressor map is generated based either on test data or by an analytical process in the case of a new compressor. This section will discuss the primary differences

between a centrifugal stage and an axial stage and then describe the effects of various parameters on the performance of centrifugal compressors.

### B.1.2.1 Key Centrifugal Compressor Characteristics

**Figure B.45** shows the comparison of a typical axial stage and a centrifugal stage. An excellent description of both types of compressors is given in Cumptsy, N.A. [B.3]. A short summary is presented to highlight the differences that affect performance. For this discussion, centrifugal stages will be assumed to have an impeller inlet (inducer) region that is similar to an axial stage as is typical of aircraft applications. Process and industrial compressors often may not include an inducer section.

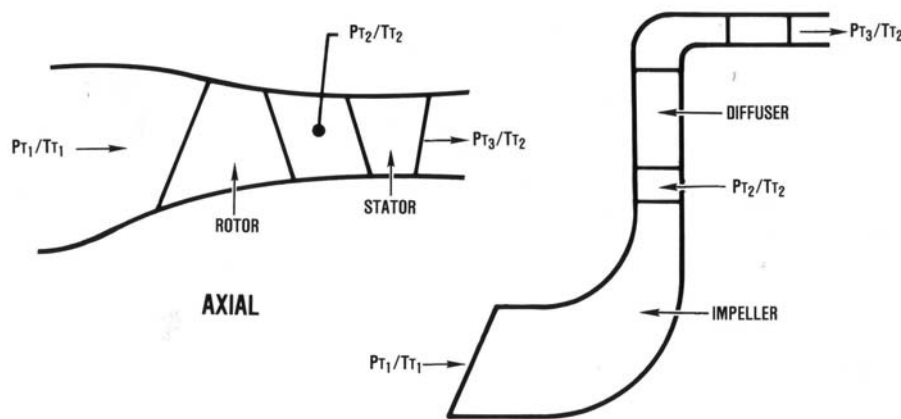


**Figure B.45: Comparison of Centrifugal and Axial Stage Flowpaths.**

Whereas the inlet regions of the two types of stages are similar, the exit regions are entirely different in that the impeller flowpath turns from axial at the inlet towards vertical at the exit (usually 90 degrees relative to the engine centerline). The exit radius is significantly larger than the mean inlet radius. This much larger exit radius means that the centrifugal stage can produce much higher Pressure Ratio than a single stage axial compressor. This is evident by examining the basic angular momentum equation of turbomachinery:

$$(H_{0x} - H_{0i}) \sim (U_x * V_{\theta x} - U_i * V_{\theta i}) \quad \text{Eq. B-1}$$

For a centrifugal impeller, the exit tip speed,  $U_x$  can be much higher than the inlet tip speed,  $U_i$  and therefore the Work ( or P/P) per stage can be much higher than for an axial stage. A typical curve of P/P versus impeller exit tip speed is shown in **Figure B.46** assuming no inlet swirl ( $V_{\theta i} = 0$ ). Of course a multi-stage axial compressor can achieve a similar P/P by adding stages. The trade-off of axial length versus diameter and weight often determine the type of configuration selected for a given application.

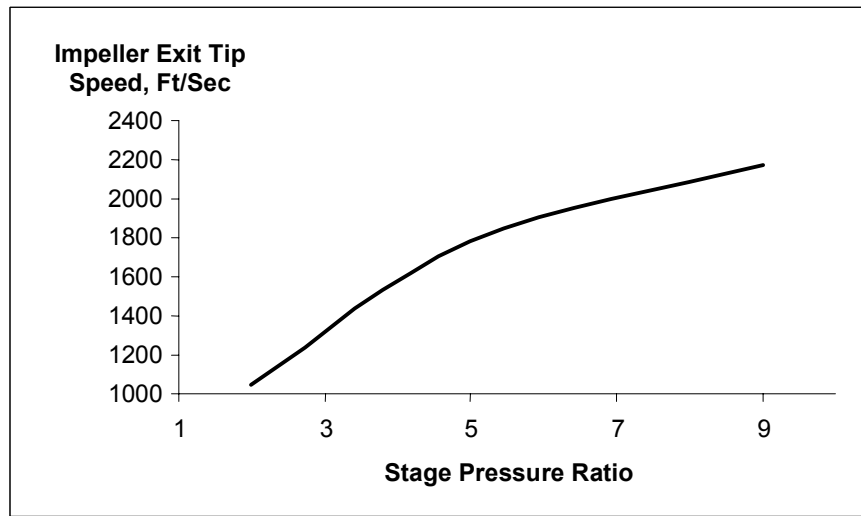


**Figure B.46: Impeller Exit Tip Speed vs. Stage Pressure Ratio.**

Another critical parameter for centrifugal stages is the exit blade angle of the impeller. **Eq. B-1** can be rewritten as:

$$(H_{0x} - H_{0i}) \sim (U_x * V_{mx} * \tan(\beta_x) - U_i * V_{mi} * \tan(\beta_i)) \quad \text{Eq. B-2}$$

where  $V_m$  is the meridional velocity and  $\beta$  is the relative air angle. Correlations have been established to relate the exit air angle and blade angle. Again assuming no inlet swirl, **Figure B.47** shows the impact of exit blade angle on centrifugal stage Pressure Ratio for a fixed impeller diameter.

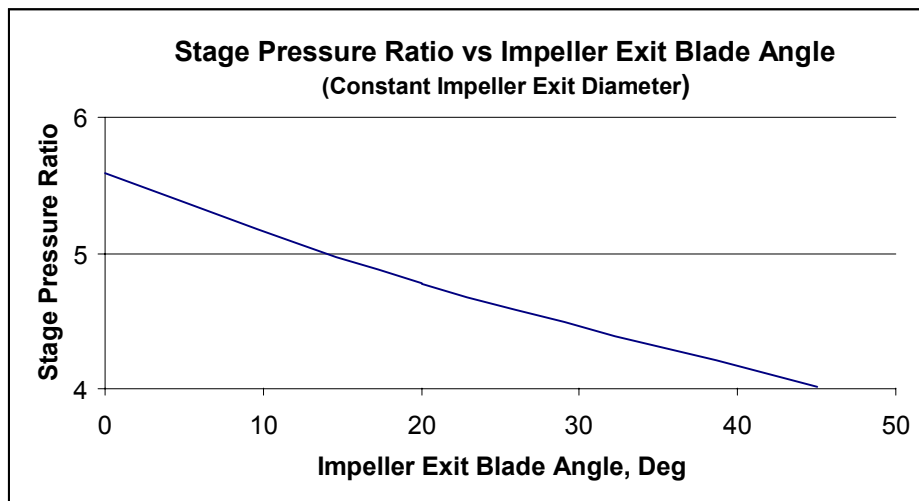


**Figure B.47: Stage Pressure Ratio vs. Impeller Exit Blade Angle.**

This curve clearly shows that reducing the impeller exit blade angle increases the Pressure Ratio capability of a given impeller diameter. The key missing element is the variation of stage efficiency with exit blade angle. Current technology centrifugal stages now routinely use impeller exit blade angles varying from 30 – 50 degrees. The reason for incorporating this level of exit blade angle is illustrated in **Figure B.48**, which compares the compressor maps of two stages designed for the same Pressure Ratio. The first

compressor has 0 degree exit blade angle (radial) whereas the second compressor utilizes 40+ degree of exit blade angle. Whereas the two compressors have similar Flow-Pressure Ratio characteristics and similar stall margins at design speed, the stage with the higher exit blade angle has peak efficiency at the operating line. The stage with 0 degree exit blade angle has the same level of peak efficiency but it occurs at the stall line. Efficiency at the operating line is 2+ points lower. It is clear that unless there are engine constraints such as axial thrust requirements or engine diameter constraints, impellers should use a reasonable level of exit blade angle.

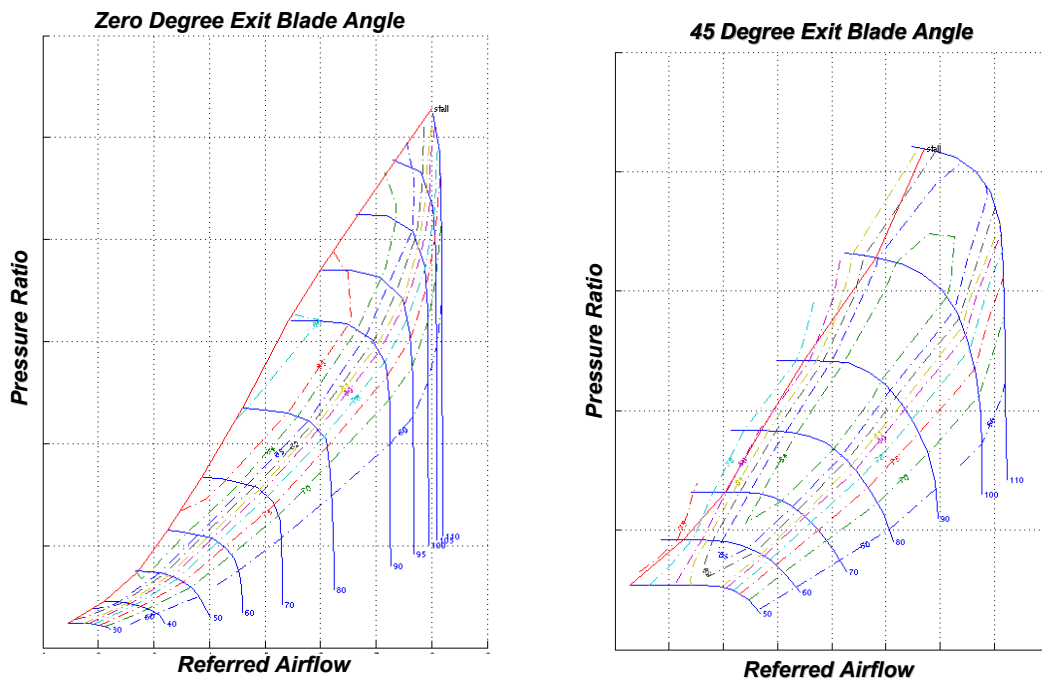


**Figure B.48:** Comparison of Centrifugal Compressor Maps with 0 deg and 45 deg Exit Blade Angles.

The primary materials for centrifugal impellers in aircraft applications are steel and titanium. Depending on costs, life, and environment, each material has distinct applications. Mechanically, material capability is a function of operating stress levels and temperature. This latter capability is depicted in **Figure B.49**, which shows approximate impeller tip speed versus impeller exit temperature for the two materials. The final shapes of these curves are a function of the detailed shape of the impeller disk.

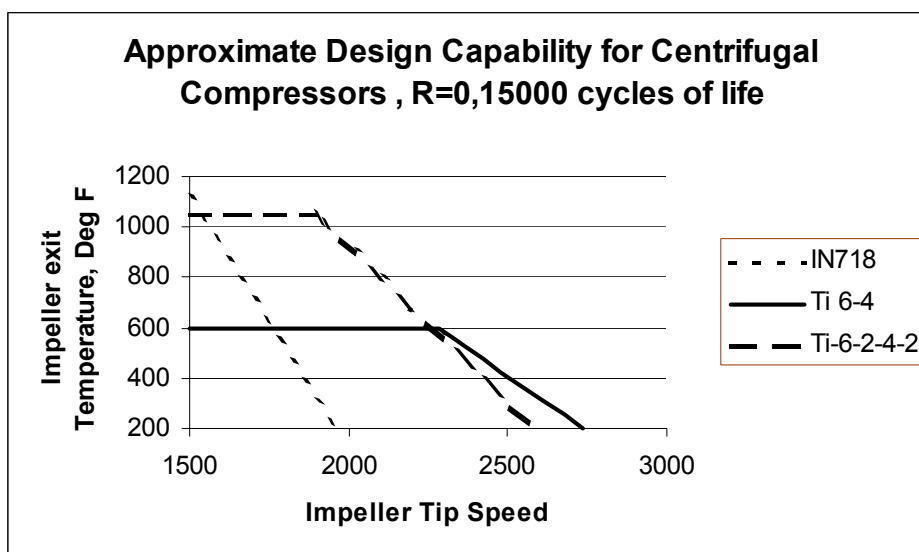


**Figure B.49: Impeller Exit Temperature vs. Impeller Tip Speed Material Capability.**

The diffuser is the other key component for centrifugal stages. For nearly all aircraft and APU applications, it consists of a vaneless space, radial diffuser, and either a 90 degree bend and deswirl system or a collecting scroll device. Multi-stage centrifugal compressors utilize a return duct system to return the flow back to the inducer of the following stage. All aspects of modern centrifugal stages can be seen in **Figure B.50**, which shows the engine cross-section of a modern Auxiliary Power Unit. The Power section consists of a single-stage centrifugal compressor and a Load compressor, which includes a variable inlet guide vane and collecting scroll. (**Figure B.51** added as an example of integral bleed engine, but not yet described or discussed.)

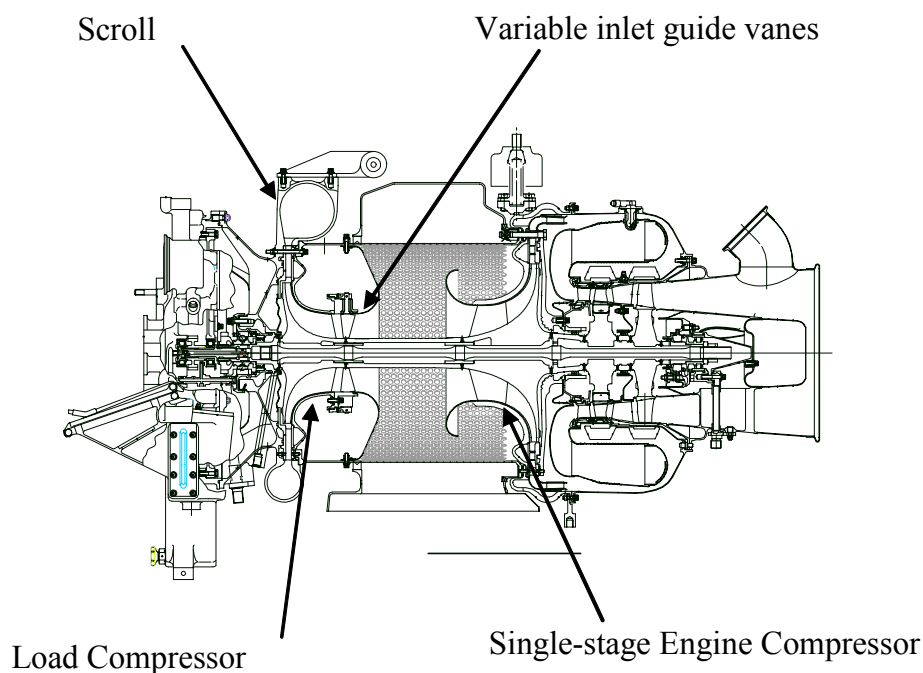


**Figure B.50: Load Compressor Auxiliary Power Unit Engine Cross-Section.**

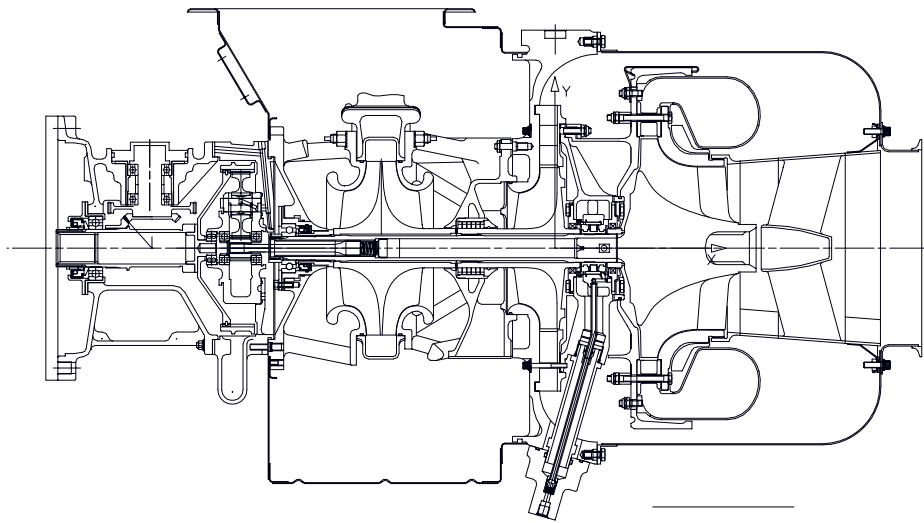


**Figure B.51: Integral Bleed Auxiliary Power Unit Engine Cross-Section.**

Again, Cumptsy [B.3] has an excellent description of the basic diffusion system and its performance characteristics. He points out that the static pressure rise in the diffusion system is all accomplished by decelerating the flow and converting kinetic energy into static pressure. For centrifugal compressors, this diffusion process is even more significant than for axial stages as the exit Mach number requirements are usually much lower. For two-stage centrifugal compressors, the Mach number in the return duct system can be near the second stage inlet Mach number to minimize losses. Pressure recoveries of 75 – 80% can be achieved in many diffusion systems by minimizing the flow separation in the diffusing passages.

A properly matched centrifugal stage is depicted in Figure B.52. The impeller usually has a much larger flow range from choke to stall than the diffusion system. When the stages are matched properly, the stall and choke flow at design speed is often set by the diffuser. At higher corrected speeds, the impeller controls flow capacity. At part speed the diffuser controls flow capacity when the stages are well matched. Peak impeller efficiency and minimum diffuser loss occur at nearly the same flow point at design speed.

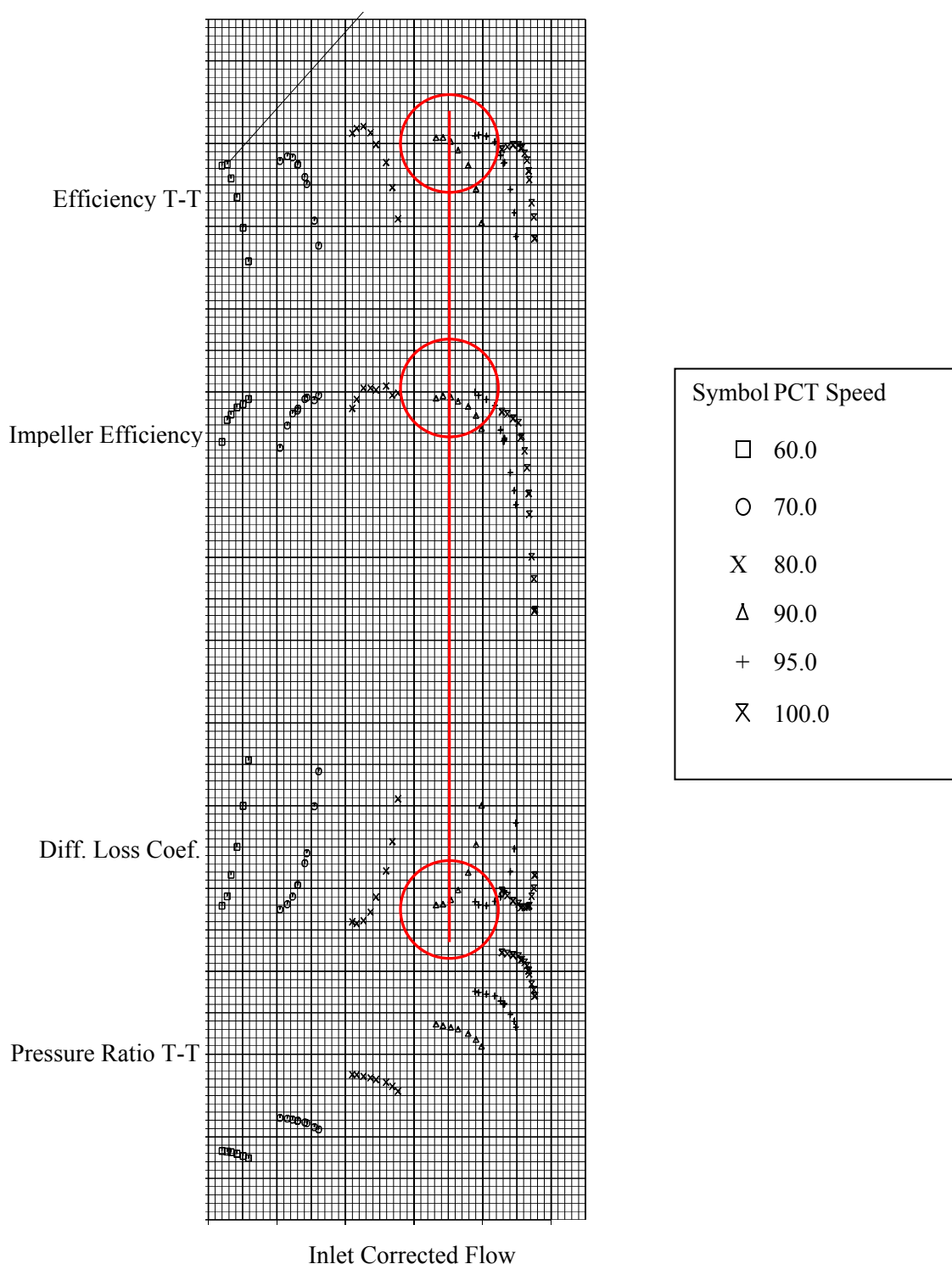


**Figure B.52: Impeller-Diffuser Matching.**

The Load Compressor APU is used in both military and commercial aircraft applications as a means of supplying variable air requirements for the main propulsion engine. The cross-section in **Figure B.50** illustrates the load compressor on the left side attached to the same shaft as the power section with a

common inlet. An inlet guide vane is used to essentially shut off the flow capacity of the Load Compressor during starting. An APU for aircraft applications is essentially a single speed device and runs at design physical speed for most of its operating conditions. This constant speed operation can simplify the mechanical challenges of the impeller design. Due to the significant variation in corrected speed due to ambient air changes with altitude, an APU compressor usually operates from 90% corrected (referred) speed on hot days to 115% corrected speed at high altitude, cold day. Due to the wide range of IGV positions from nearly shut-off to over open at max power, there can be significant inlet distortion patterns generated due to the unique inlet plenum configurations that are often used in APUs. These distortion patterns are very complex and are usually not symmetric circumferentially. **Figure B.53** shows a typical pattern entering an impeller from an inlet plenum.

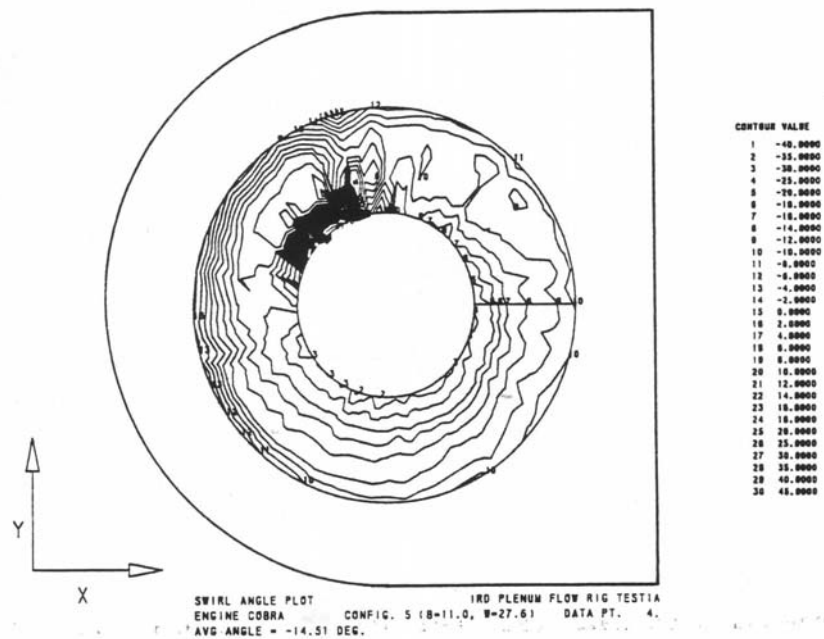


**Figure B.53: Swirl Pattern Entering a Centrifugal Compressor from a Typical Plenum.**

The reason for discussing the effects of these basic parameters here is for information that may useful to people who may be doing field repair work. Care must be taken in the blend repair of nicked parts both from a structural and aerodynamic viewpoint. Reworking leading and trailing edges of impellers and diffusers can significantly affected the performance of the stage. Leading edge blending can affect part speed stall margin as well as efficiency. Cutting back the trailing edge of an impeller will lower the Pressure Ratio capability of the stage and change the match with the downstream diffuser usually reducing flow capacity and potentially increasing diffuser losses. Blending a diffuser leading edge nick will change the match between the impeller and diffuser and will probably reduce the stall margin of the stage.

### B.1.2.2 Effects of Tip Clearance

Due to the significant reduction in blade height as the flow passes from the inlet to the exit, tip clearance sensitivity is much larger at impeller exit than at the inlet. Correlations have been developed through significant testing to express the variation in stage efficiency as a function of impeller exit clearance to impeller exit blade height. The large scatter in the data is related to the detailed blade shapes defined in the design process. This significant variation was illustrated in Palmer and Waterman's ASME Paper [\[B.30\]](#) and is presented in **Figure B.54**.

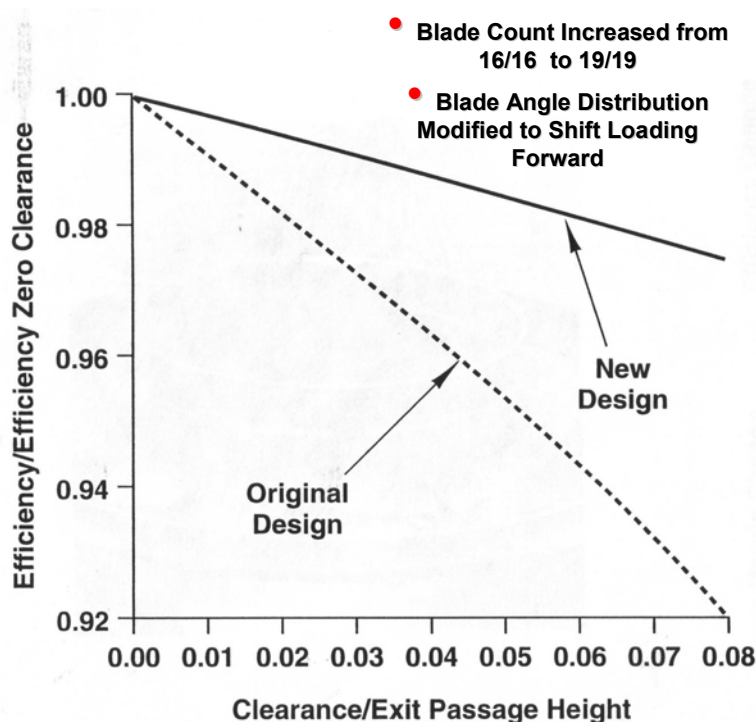


**Figure B.54: Improved Clearance Sensitivity by Reduced Blade Loading.**

This figure compares the clearance sensitivity of an original 16 main blade/16 splitter bladed second-stage impeller to a new design having 19 main blades/19 splitters. Clearly, the reduced impeller loadings due to increased blade count and revised blade angle distribution has had a significant effect on the rate of efficiency loss with increasing axial tip clearance. The low clearance sensitivity allows the second stage to operate efficiently at a robust 6 percent axial clearance-to-exit blade height needed for the extremely rapid helicopter acceleration requirements for this particular application.

## B.1.2.3 Effects of Surface Roughness on Performance

Centrifugal compressor performance is significantly affected by the stationary shroud surface roughness over a rotating impeller. The small clearance gap makes this scrubbing flow very sensitivity to the surface roughness of the shroud. This sensitivity is illustrated in **Figure B.55** taken from Palmer and Waterman's ASME paper, [B.30]. Using a pipe-flow analogy for a centrifugal stage, the characteristic length for similarity is the hydraulic diameter (which is nearly equal to the impeller exit tip width). On this basis, centrifugal compressor Reynolds number effects can be correlated, as shown in the figure, to illustrate the effects of surface roughness at high Reynolds numbers. The Reynolds number of the selected second stage compressor is indicated on the figure ( $Re_b = 3.5 \times 10^5$ ). As can be seen, the second stage lies in the hydraulically rough regime with a roughness of 350 micro-inches and in the transition region between hydraulically rough and hydraulically smooth with a roughness of 70 micro-inches. The predicted change in efficiency is 4.0 points which converts to approximately 1.6 points in the overall two-stage efficiency for the compressor configuration. The tested performance change for the overall two-stage efficiency was 2.0 points at the design point, verifying the criticality of stationary shroud surface roughness on compressor performance.

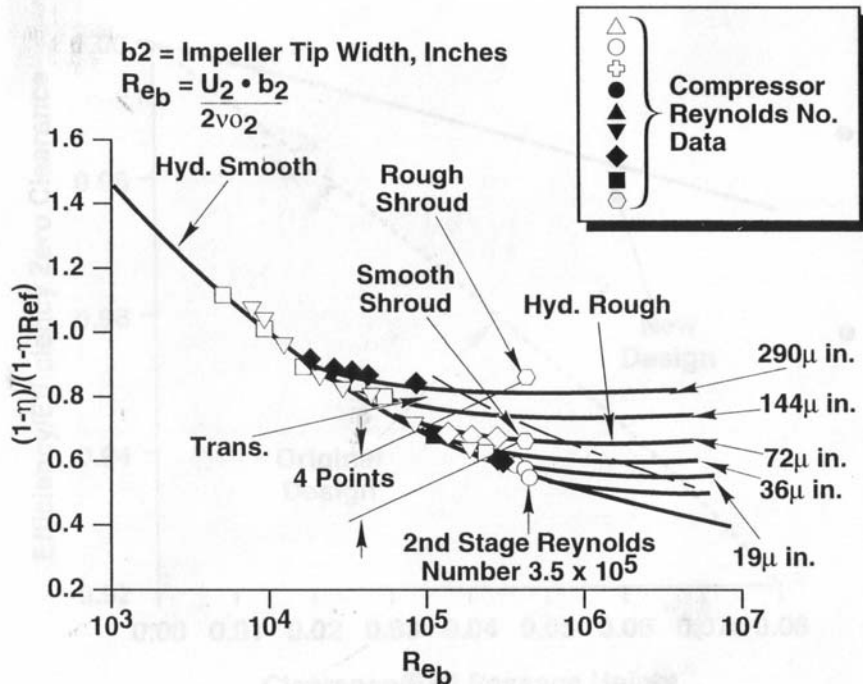


**Figure B.55:** Single-stage Centrifugal Compressor's Loss versus Reynolds Number.

#### B.1.2.4 Effect of Erosion on Performance

The effect of erosion, particularly sand erosion can have a large performance impact on turbomachinery components. Axial compressors are more sensitive to erosion compared to centrifugal stages for the same material. Quite often the first stage of axial compressors will be manufactured from steel if the compressor is utilized in a helicopter application. This section describes the results of a 50-hour sand ingestion test on a helicopter engine as reported in [B.30]. The engine was subjected to a 50-hour C-spec sand ingest test, an AC-fine sand test, and an AC-course sand test. The C-spec sand is generally considered to have the most potential for damage due to the high percentage of large particles. This test encompassed 50 hours of engine operation at maximum continuous rated power with sand contaminant introduced into the engine inlet at 53 mg per cubic meter of engine inlet air. The engine was equipped with an integral particle separator with a very high separation efficiency, therefore, most of the sand did not reach the compressor. However approximately 2.39 pounds of sand went through the engine core.

Engine performance deterioration was less than 5 percent horsepower at 25 hours and 10 percent at 50 hours. Diagnostic analysis of the pre- and post-test data indicated the compressor efficiency degraded over the range of 85 to 100 percent speed and was the major cause of the engine performance loss.

Post-test inspection of the compressor hardware showed:

- The leading edges of the first stage impeller blades were eroded as shown in Figure B.56 with higher value near the hub.
- A slight channel on the pressure side of each blade and splitter at the exducer of the first-stage impeller.
- An increase in roughness on the first-stage shroud abrasion coating.
- No visual signs of second-stage impeller leading edge erosion was noted.

## ANNEX B – ADVANCED TOPICS AND RECENT PROGRESS

- The second-stage shroud had a polished appearance.
- Only minor evidence of erosion was noted on the first- and second-stage diffusers and deswirl assembly.

This example shows the robustness of centrifugal compressors to sand and dust erosion.

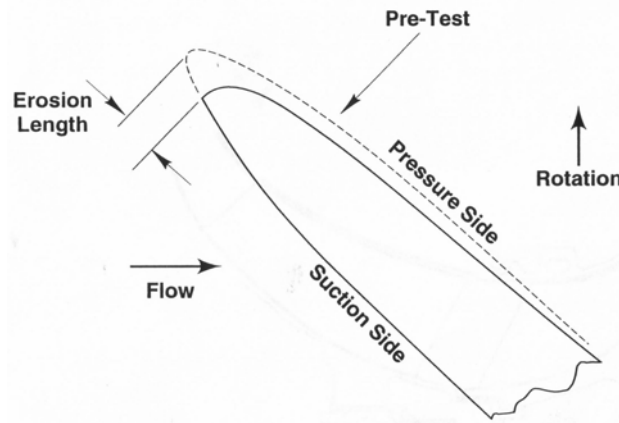
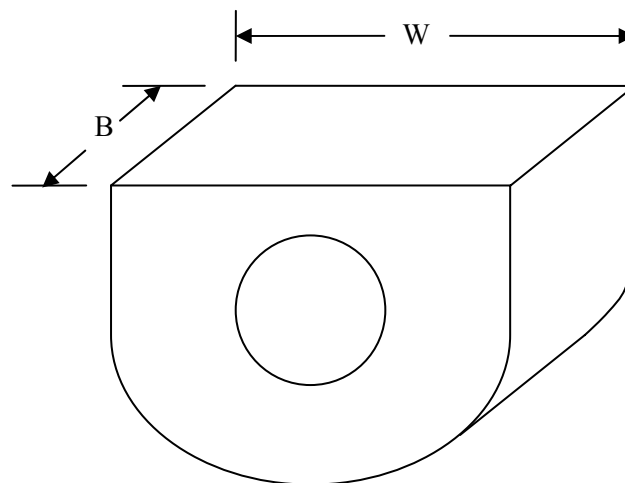


**Figure B.56: First-Stage Impeller Leading Edge Sand Erosion.**

### B.1.2.5 Effect of Inlet Plenum on Performance

With the “buried” installations of APUs and with some helicopter applications, the effect of the inlet on compressor performance can be significant. The typical inlet plenum for an APU is shown in **Figure B.57**. The two most significant parameters that can impact compressor performance are:

- The ratio of the impeller inlet annulus area to the inlet plenum area ( $B \times W$ ); and
- The inlet plenum aspect ratio ( $B/W$ ).



Aspect Ratio =  $B/W$

Area Ratio = Impeller Eye/ $B \cdot W$

**Figure B.57: Inlet Plenum Cross-Section.**

Systematic testing with an inlet plenum flow rig that measured the pressure loss across the plenum is presented in **Figure B.58** and shows the rapid increase in plenum loss when the aspect ratio is less than 0.4. Keeping the aspect above 0.4 is essential to minimize plenum effects. In addition to aspect ratio, the plenum area ratio is the other significant parameter. This effect is best evaluated by comparing the efficiency of the entire compressor configuration including the inlet plenum. The reason for this is that the inlet distortion from the plenum affects the basic performance of the compressor in addition to the inlet plenum loss. **Figure B.59** shows that compressor efficiency can decrease as much as 3+ points in efficiency when a plenum with a poor aspect ratio ( $B/W = .27$ ) and Area Ratio of 0.25 is added to a base compressor. This data is not necessarily in disagreement with data presented by Colin Rodgers [B.31]. He states that area ratios of .25 or smaller result in low loss plenums. This paper does not reference the aspect ratio of the plenum tested. The above data indicates that both parameters are important.

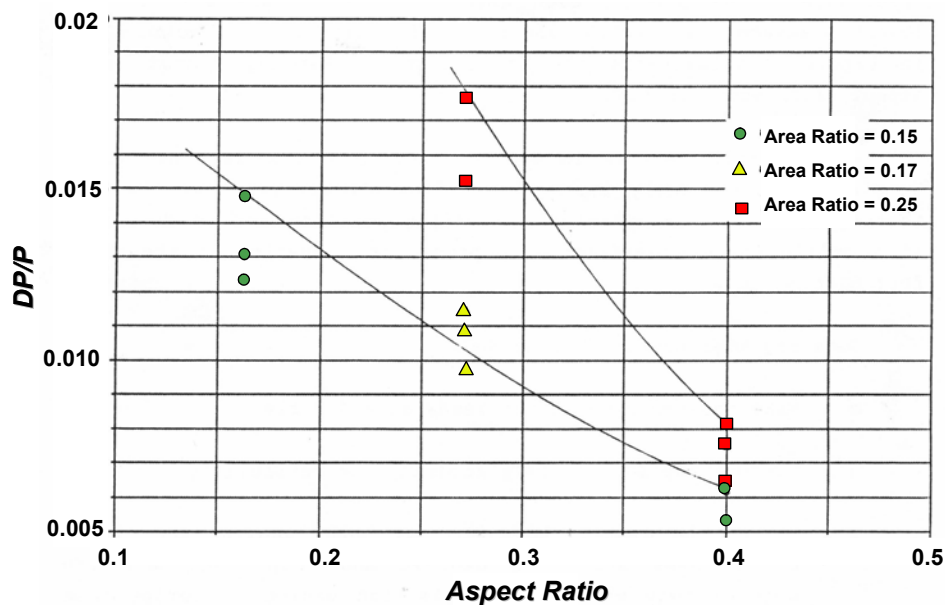


**Figure B.58:** Effect of Plenum Aspect Ratio and Area Ratio on Plenum Loss.

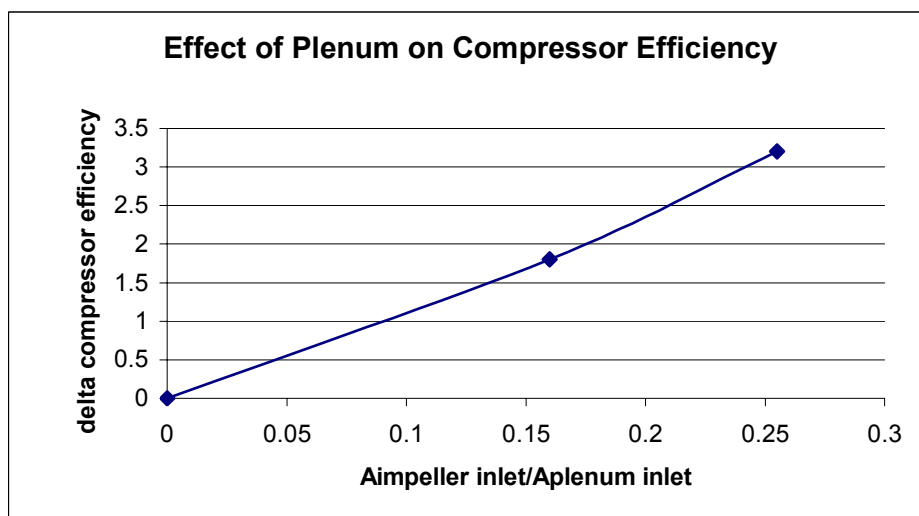


**Figure B.59:** Effect of Plenum Area Ratio on Compressor Efficiency.

### B.1.2.6 Effect of Leakage on Performance

Due to the high pressure ratio achieved with centrifugal compressors, leakage can have large effects on compressor efficiency. There are two types of leakage that are most serious, recirculation and diffuser endwall leakages. These leakage paths are indicated in **Figure B.60**. Recirculation leakage can be from the exit of 1 component back to the inlet of that component or back to the inlet of the compressor. Another type of recirculation leakage can be from the turbine component to the backside of the compressor. All of these can result in loss of compressor flow capacity and or compressor efficiency. Testing has shown efficiency loss of over two points from just diffuser leakage from compressor exit back to diffuser inlet. This flow jetting back into the diffuser inlet region usually results in 2 – 4 percent loss in flow and pressure ratio along an operating line.

Diffuser endwall leakage can be just as serious. To minimize cost, compressors are manufactured with radial diffusers that are butted together at one endwall instead of brazing or securing the vanes to the endwall with studs or bolts. At operating temperature, the structures move significantly and diffuser endwall gaps develop especially near the leading edge region. Significant loss in diffuser pressure recovery was a result. A variable vane diffuser (via a button near the leading edge) was tested at various diffuser endwall clearances. The test results indicated over a 7-point reduction in compressor efficiency when the vane clearance gap was increased from zero to one percent of the diffuser vane height in order to be able to rotate the vanes. It is important to have minimal leakage in the compressor section. Developing and incorporating leakage models into engine simulation is critical to diagnosing the correct components to examine as engine performance changes with time.

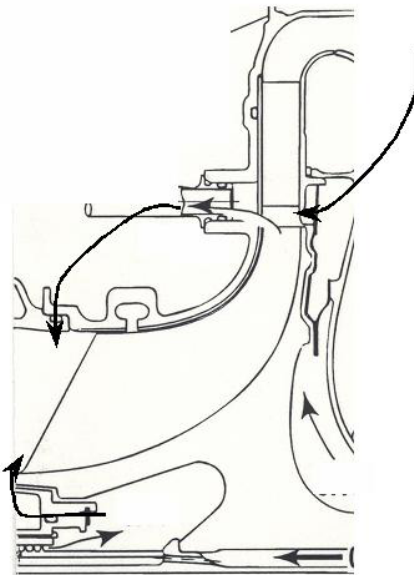


**Figure B.60:** Cross-Section of Centrifugal Stage Showing Leakage Paths.

### B.1.2.7 Effect of Flowpath Steps

Conventional wisdom would say that flowpath steps should always be down, i.e. like a waterfall. However, looking at **Figure B.61**, which is reproduced directly from Hoener, [B.32], the figure shows the drag coefficient for a variety of types of steps (steps up, steps down, blunt, rounded, etc.) on the sheet metal skin of aircraft, but is equally applicable to internal ducting of modern gas turbine engines. The higher the drag coefficient, the greater the loss in pressure.

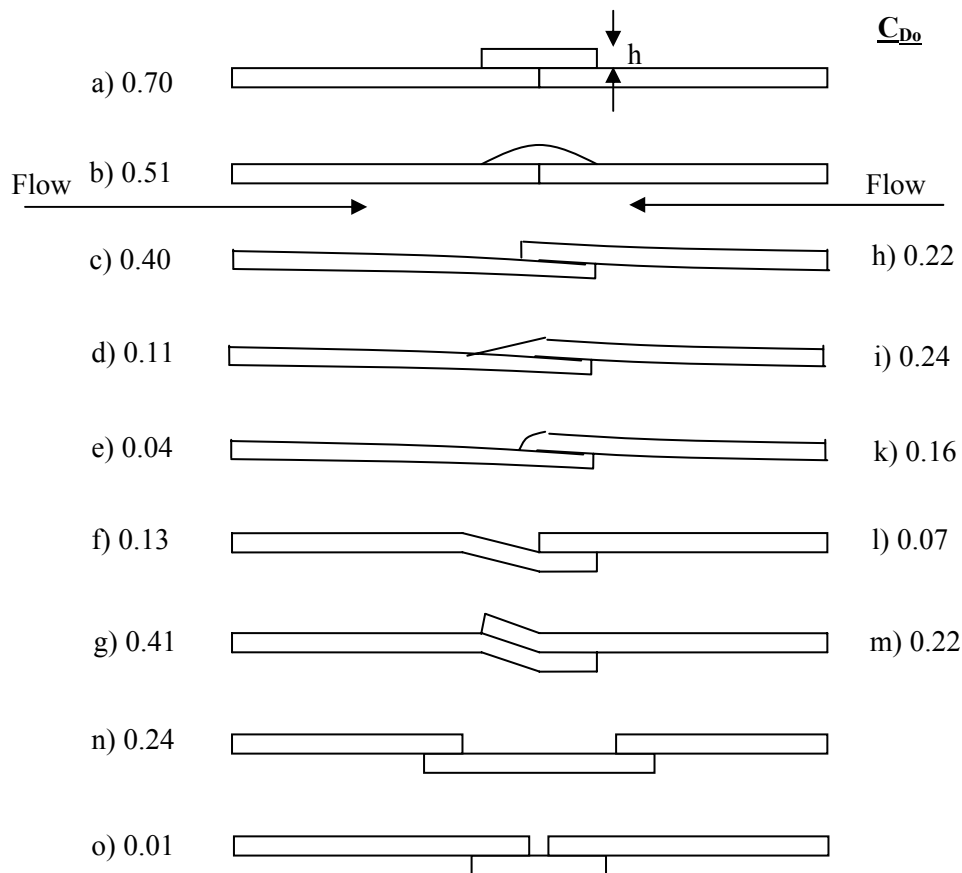


**Figure B.61: Independent Drag Coefficient of Various Sheet Metal Joints, Based on Thickness, “h”.**

Drag coefficient is defined as

$$C_d = \text{Drag} / (q * S)$$

where  $q$  = velocity head ( $P_{\text{total}} - P_{\text{static}}$  or  $1/2 * \text{density} * V^2$ )

$S$  = a representative area (like wing area or a pipe area)

Note that coefficients are shown in the figure for flow from either direction, left or right, thereby for a step up or down. The following observations can be made:

- Comparing c (a blunt step up) to e (a rounded well treated step up) in the flowpath, the well treated step up reduces the drag by a factor of 10.
- Comparing h (a blunt step down) to e (the same rounded step up), the well shaped step UP is 5 times better than a step down.
- Even a 30 degree ramp (bevel) up (i) is half the drag of a beveled step down.

A “rounded well treated step up” is one that has the step shaped with a quadrant of an ellipse, preferably a 4:1 major/minor diameters (meaning blending the length over 2 times the height of the positive step). This is analogous to an entry bellmouth, which is continuously accelerating with little or no loss-producing diffusion. The above comparisons were made to counter the “conventional wisdom”; other comparisons are left to the reader (with an open mind). This data applies only to Mach numbers below

about 0.5 where there is little danger of local shocks forming on sharp corners, etc. Also, this applies only to small steps and ignores area changes.

### **B.1.3 Methodologies**

We have so far been examining physical factors that impact the compressor performance and stability margin; these have been referred as compressor characteristic modifiers. In this section we will discuss analytical or computational models for assessing the effects of some of these characteristic modifiers on a quantitative basis. In principle one can proceed to build a correlative database for defining the effects these have on compressor performance through extensive testing. Such an approach, while of engineering utility, does not provide a rigorous scientific approach or basis that would allow one to predict changes in performance due to changes in the modifiers. Computational techniques have often been suggested as the ultimate means to predict component performance and its change with subsequent alteration of parameters such as tip clearance and operating conditions from those it is designed for. However as articulated by Adamczyk [B.1], the range of time scales and length scales encountered in flows through multi-stage compressors are so broad that it is unlikely that direct computation is feasible in the foreseeable future. Adamczyk suggested that one way to overcome this is to calculate fluid dynamic effects when the computational timescales are acceptable, and to model them on other occasions. Such an approach has been adopted by Adamczyk [B.1] and Rhie et al. [B.2] to develop procedures to compute the performance of a multi-stage compressor. In the following, methodologies to provide quantitative assessment of the impact of characteristic modifiers, via the simulation of flow phenomena in multi-stage compressors, are described.

#### **B.1.3.1 Approximations at Global Level**

In the development of techniques for simulating flow phenomena in multi-stage compressors with the aim of extracting quantitative information on compressor characteristics and its modifiers, there are two levels of approximation:

- Physical Approximations to problem under consideration; here we first ask the following question:
  - What is it that is important to include?
- Numerical approximations to partial differential equations (PDE) for the problem.

In general the various levels of physical approximation for flow phenomena can broadly be given as follows:

- Navier-Stokes equations (direct numerical simulation);
- Large eddy simulation;
- ‘Reynolds averaged’ Navier-Stokes equations – this would require the use of a turbulence model;
- Thin shear layer approximation;
- Inviscid Euler equations;
- Steady flow vs. unsteady flow;
- Three-dimensional vs. two-dimensional flow;
- Streamline curvature;
- Throughflow methods (hub-to-tip and blade-to-blade);
- Potential flow equations;
- Incompressible flow; and
- One-dimensional flow (control volume approach).

Because of the large range of length and time scales involved in the multi-stage environment, high-speed multi-stage turbomachinery flows are not presently amenable to direct numerical simulation (Adamczyk). Thus it is still necessary to develop multi-row geometry models that yield ‘averaged’ descriptions. These provide useful information that can be used to generate compressor performance maps and to quantify changes associated with characteristic modifiers. Hence we have to address the basic question of “What is the proper level to average at?” Furthermore the flow in multi-stage compressors is inherently unsteady. One is thus interested in assessing the time averaged impact of flow unsteadiness on compressor performance. (The characteristic modifier associated with changes in axial gap is a good example to illustrate this aspect of the problem.) In view of this it is useful to draw on the equation of hierarchy for turbomachinery flow given by Adamczyk:

- Navier-Stokes Equation – No closure, direct simulation;
- Reynolds-averaged Navier-Stokes Equation – Reynolds stresses, energy correlations;
- Time-averaged equations – Body forces, energy sources, correlations;
- Averaged passage equations – Body forces, energy sources, correlations;
- Axisymmetric equations – Body forces, energy sources, correlations; and
- Quasi-one-dimensional equations (control volume approach).

It is clear from the above that as one proceeds downward through this list, the degree of empiricism increases. Or more positively, one needs to do an ever better job of flow modeling. Conversely, the requirement for computational resources increases as one proceeds upward through the list.

#### **B.1.3.2 Discrete Approximations to PDE**

The result of physical approximation to the problem is a set of partial differential equations. To solve this set of PDE, one needs to discretize the PDE both on the spatial and on the temporal basis. These discretizations are summarized below:

- For spatial discretization:
  - Finite difference method (FDM);
  - Finite element method (FEM);
  - Spectral methods;
  - Finite volume method;
  - Hybrid method; and
  - Vortex methods – singularity methods.
- For temporal discretization:
  - Finite difference method;
  - Finite element method; and
  - Spectral method.

In the following, we will present examples that involve both levels of approximation for assessing changes in compressor performance.

#### **B.1.4 Theoretical Model**

The computed or predicted results shown as a solid line in **Figure B.16** and **Figure B.17** are based on the theoretical model of Hynes and Greitzer [B.33]. It addresses the behavior of two-dimensional flow-field

## ANNEX B – ADVANCED TOPICS AND RECENT PROGRESS

---

disturbances that have a length scale of the order of the compressor circumference (larger than the blade pitch). The model is thus strictly applicable only to situations where the flow through the compressor may be considered as radially uniform. In the model, the pressure rise across any blade row in the compressor is taken to consist of: that achieved in steady uniform flow, at the local inlet conditions plus that necessary to balance the acceleration of the fluid, within the blade row. The upstream and downstream flow-fields, and the overall flow system within which the compressor operates, are described in terms of the flow equations. In addition, the instantaneous loss across the blade-row lags the incidence changes with a timescale in the order of the convection time through the blade.

Assessing the effect of inlet distortion on flow stability through the compressor is inherently a nonlinear problem. This is apparent from the nonlinear relationship between compressor performance and flow coefficient. However the nonlinearity associated with the flow-fields upstream and downstream of the compressor are of lesser importance than those associated with the compressor performance. Hence a linear treatment is appropriate and is shown to be so, through assessment of the computed results from the model against measurements. Because the background flow is non-uniform the unsteady disturbance flow-field will not have a purely sinusoidal distribution round the annulus. Furthermore, the annulus averaged mass flow is not generally zero (in contrast to the situation of uniform background flow). This implies that the global compression system behavior is coupled to the local compressor behavior.

The compression system model essentially consists of a compressor pumping to a plenum that exhausts through an ideal throttle. The length of compressor ducting is assumed to be sufficiently long to ensure that there is no asymmetric potential flow interaction with the inlet and exit duct terminations. The inlet distortion, in total pressure terms, is specified as a function of circumferential position and time. This is at a location upstream of the asymmetric static pressure field ahead of the compressor. The background flow corresponding to the specified inlet distortion in the absence of flow instabilities can now be determined. To assess the stability of the compression system, an arbitrary small, unsteady flow disturbance is added to the background flow. If any such flow disturbance grows with time, the flow through the compressor is considered unstable. Such an approach is a standard technique in stability theory and constitutes an eigenmode and eigenvalue problem. The unsteady flow disturbances can be viewed as incipient stall cells when they propagate around the annulus and as small amplitude, surge-like system transients when they are predominantly one-dimensional in character.

The results of **Figure B.16** show that the computed stability degradation is in good agreement with the measurements for one-resonance-peak response compressor, implying that the stability margin degradation is associated with two-dimensional long circumferential-length-scale phenomena. However the model does not accurately capture the measured stability margin degradation for two-resonance-peak response compressors, **Figure B.17**.

When the model was applied to the determination of the overall compressor pressure rise characteristic in the presence of rotating distortion **[B.34]**, the compressor performance deteriorated with a drop in pressure rise capability and a decrease in stability margin as the distortion co-rotating speed increased. For a co-rotating speed of 0.3 rotor speed, there is only a small flow regime for which the compressor is stable. This is indicated by the progressive shift to the right of the neutral stability points indicated as solid circles. A drastic decrease in compressor stall margin can be the result when the inlet distortion is co-rotating at a speed corresponding to the propagating speed of the stall inception disturbance. An analogous drop in compressor stability margin occurs when:

- The system frequency (the one-dimensional surge-like instability mode) coincides with the frequency at which rotating stall would propagate.
- When the difference between the co-rotating speed of the imposed rotating inlet distortion and that of rotating stall coincides with the frequency of the one-dimensional surge-like mode **[B.34]**.

### B.1.5 Application of CFD and Flow Models for Compressor Performance Assessment

In addressing the overall performance of multi-stage axial compressors, it is useful to characterize the flow variation on the following two length scales:

- The blade pitch; and
- The scale through which the blade row components interact, which is larger than the blade pitch.

In the following, we describe an approach used to develop a methodology that allows one to address flow instabilities in a multi-stage compressor in a practical manner. The procedure has the potential of establishing the design characteristics of each blade row so that the multi-stage compressor may have more desirable stability properties. This offers the possibility of designing a local component for optimal performance of the integrated system.

In essence, the approach takes advantage of modern CFD where it is appropriate to do so, and would take advantage of modeling the response and dynamics of the component when it is expeditious to do so. The modeling of the response and dynamics of the component can be implemented through the use of modern CFD tools. For instance, the pressure rise characteristic and the loss characteristic of a blade row can be established through local blade-row calculations. This information can then be used to represent each blade row as an appropriate body force distribution for compressor stability analysis or simulation. The flow-field in the blade-free regions can be described by the Navier-Stokes equations so that the presence of each blade row then appears as a source term to the Navier-Stokes equation. The aerodynamic coupling among the components would perceive the presence of the blade as a region of continuous body force distribution, rather than the detailed events in the individual blade passage. This is so because the interaction occurs on a length scale larger than the spacing between the blades.

However, the effects of the blade passage event should be reflected in the representation of the blade row by a continuous body force distribution. Thus, in the stability analysis of the multi-stage axial compressor, local calculations are made, for components such as the fan, fan exit guide vane, and rotor-stator pair, to establish the physical information needed for representation of a body force distribution (see **Figure B.62** local to system level). This is then used in the multi-stage compressor-stability calculations [B.35].

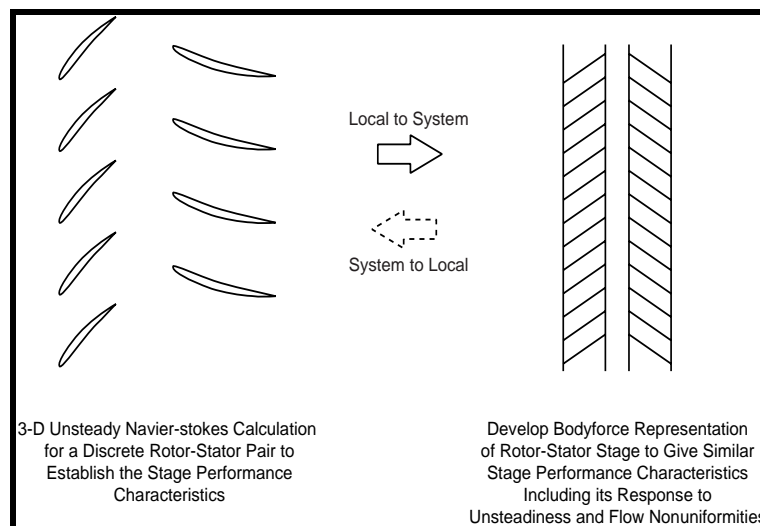


**Figure B.62: Duality of Local and System Calculations.**

Conversely, the multi-stage compressor-stability calculation can be used to establish the desired design characteristics of each blade row that will result in a compressor design that has the desirable stability

## ANNEX B – ADVANCED TOPICS AND RECENT PROGRESS

properties. This is then followed by a detailed design of the blade row to yield the desired design characteristics.

In summary, the proposed approach consists of two levels of analysis or simulation:

- Global system level analysis/calculation: The blade rows are represented as a body force distribution appearing as a source term to the flow equation describing the flow through the system. This has been applied successfully at the MIT Gas Turbine Laboratory to the development of a computational model for simulating inception and development of three-dimensional aerodynamic instabilities in a multi-stage compressor and its response to inlet distortion [B.35].
- Local level CFD calculation at the component level: This is used to establish information for use in the representation of the blade row as a body-force (i.e. local to system level). Likewise, this can also be used to design the blade row to yield the desired component characteristic to result in a compressor with good operability characteristics (i.e. system to local level).

To assess the impact of adjacent blade rows or adjacent stages, we can first implement unsteady 3-D flow in a discrete rotor-stator environment. (The computed results in this situation can be post-processed to examine the influence of adjacent blade rows on the resulting unsteady blade loads associated with rotor tip vortices and blade wakes.) The computed results for a discrete rotor-stator can then be used to establish the equivalent body force representation.

Now we can envision embedding a discrete rotor-stator pair in a multi-stage environment with the remaining stages represented as body force distribution as indicated in **Figure B.63**. Computed results from this situation can be assessed against calculations from the discrete rotor-stator pair alone to quantify multi-stage effects on time-average performance. For instance, the aero forces and moments as dictated by the multi-stage environment on a specific blade row can be viewed as an input for local aeroelastic calculation (as implied in **Figure B.62**). The local aeroelastic calculation would now redistribute the body force representation of the specific blade row under consideration. This is then in turn used in the multi-stage environment to update the flow-field and the associated blade response. Thus, this provides a conceptual model for implementing multi-stage aeroelastic calculations on a consistent basis. For application of this methodology for assessing the stability properties of multi-stage compressor, the reader is referred to [B.35].

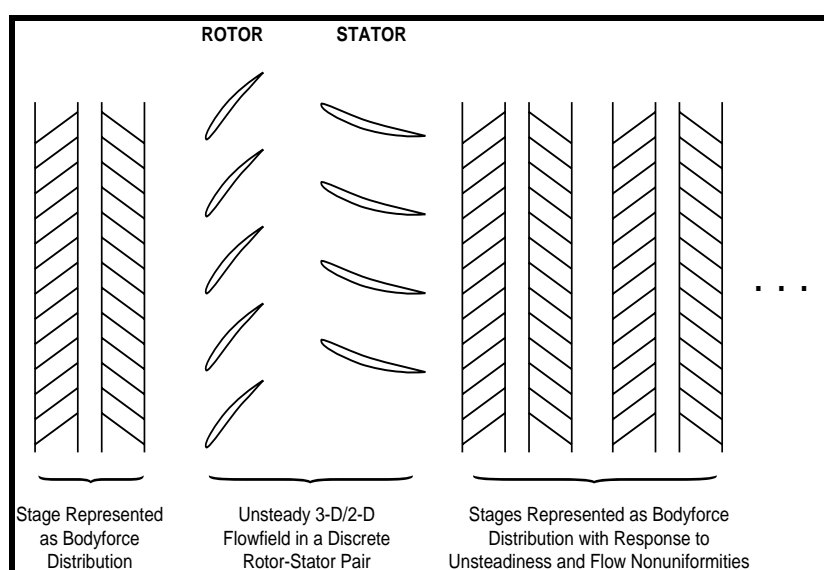


**Figure B.63: Physical Model of Multi-Stage Compressor.**

On a conceptual basis one can even extrapolate the methodology to the computation of compressor characteristics as delineated in **Figure B.5** provided a rigorous basis has been established for linking the factors that modify the characteristics for inclusion in the body force representation. Presently streamline curvature with correlative data base is routinely used to generate the compressor characteristics though modern CFD is playing an increasingly important role in this.

The methodology described in this section can readily be integrated seamlessly into an airframe-inlet-engine system for simulating the dynamic behavior of such a system.

### **B.1.6 Different Levels of Modeling**

There are essentially three levels of physical approximations that one can use to generate compressor characteristics and/or its modification; these can be broadly classified as follows.

- System lumped parameters level (low-order) models:
  - 1-D model (ordinary differential equations); and
  - 2-D model with compressor represented as single actuator disk (ordinary differential equations or rudimentary partial differential equations for flow distortion problem in compressor and compression system dynamics).
- Macro-level model:
  - 3-D model with blade-row by blade-row body force representation (i.e. actuator duct representation for each blade-row) (partial differential equations).
- Physical level model:
  - 3-D distributed model with discrete blades in each blade row; and
  - 3-D flow simulation in multi-blade and multi-blade rows environment (partial differential equations).

#### **B.1.6.1 Lumped Parameter (Low-Order) Models**

This type of model captures all key system dynamic behavior but does so:

- With fast calculations (preferably analytical, rather than numerical);
- In a form that permits the designer to assess any effects of design variation;
- In a form suitable for incorporating into system level simulation for:
  - Assessing whether dynamic behavior requirements are met, and
  - Developing active control techniques for instability avoidance or performance enhancement.

#### **B.1.6.2 Attributes of Macro-Level Models**

This level of model satisfies physical laws on a blade passage average basis:

- Mass, momentum, energy conservation; and
- Entropy production in dissipative systems.

It has the correct dependencies on engine geometry and is preferably directly usable by designers. The results should agree with results of 3-D flow simulation and physical experiments.

**B.1.6.3 Physical Level Model**

At this level the method uses the full 3-D geometry that includes:

- Blade geometry details;
- Multi-blade passages; and
- Multi-blade rows.

This constitutes a full unsteady 3-D flow simulation in the complex geometrical configuration of a modern compressor.

**B.1.6.4 Role of Each Level of Modeling**

System designers specify component dynamic-behavior requirements while component designers specify constraints (what is feasible and what is not). Thus, the different levels of modeling enable system and component designers to communicate with one another on a rational basis.

**B.1.7 Compressor Overall Summary**

In this section we have reviewed the impact of tip clearance, stationary and rotating flow distortion, flow unsteadiness (axial spacing), Reynolds number, and blade surface roughness on compressor performance. We have also reviewed effects of thermal origin, and effects associated with blade untwist in high-speed fans. Recent progress made in the development of techniques for simulating and predicting flow effects that affect the operability of the compressor is also discussed. These techniques take advantage of modern CFD but physically model those aspects of the flow phenomena that are still beyond the feasibility of currently available computational resources.

**B.1.8 Cited References for Compressor Section**

- [B.1] Adamczyk, J.A., “Model Equation for Simulating Flows in Multistage Compressor,” ASME Paper # 85-GT-226, 1985.
- [B.2] Rhie, C.M. et al., “Development and Application of a Multistage Navier-Stokes Solver: Part I”, ASME Journal of Turbomachinery, Vol. 120, No. 2, April 1998.
- [B.3] Cumpsty, N.A., “Compressor Aerodynamics”, Longman Scientific & Technical, 1989.
- [B.4] Wisler, D.C., “Advanced Compressor and Fan Systems”, GE Aircraft Engines, Cincinnati, Ohio, USA. Copyright @ 1988 by General Electric Co. USA, All Rights Reserved. (Also 1986 Lecture to ASME Turbomachinery Institute, Ames Iowa)
- [B.5] Smith, L.H., “Casing Boundary Layers in Multistage Compressors”, Proceeding of the Symposium on Flow Research on Blading, Brown Boveri & Co. Ltd, Baden, Switzerland 1969, In Dzung, L.S. (ed) Flow Research on Blading, Elsevier Publishing Company, 1970.
- [B.6] Khalid, A. et al., “Effect of Tip Clearance on Compressor Endwall Blockage and Pressure Rise Capability”, Presented at 43rd IGTI Conference, Stockholm, 1998.
- [B.7] Freeman, C., “Effect of Tip Clearance Flow on Compressor Stability and Engine Performance”, VKI Lecture Series 1985-05, 1985.
- [B.8] SAE Aerospace Information Report, AIR-1419, “Inlet Total-Pressure Distortion Considerations for Gas Turbine Engines”, May 1983.

- [B.9] SAE Aerospace Recommended Practice, ARP-1420, “Gas Turbine Engine Inlet Flow Distortion Guidelines”, March 1978.
- [B.10] Schmucker, J. et al., “Erosion, Corrosion and Foreign Object Damage Effects in Gas Turbines”, AGARD-CP-558, 1994.
- [B.11] Mazzawy, R.S., “Multiple Segment Parallel Compressor Model for Circumferential Flow Distortion”, ASME J. Engineering for Power, 99, pp. 288-296, 1977.
- [B.12] Reid, C., “The Response of Axial Flow Compressors to Intake Flow Distortions”, ASME Paper # 69-GT-29, 1969.
- [B.13] Ludwig, G.R., Nenni, J.P. and Arendt, R.H., “Investigation of Rotating Stall in Axial Flow Compressors and Development of a Prototype Stall Control System”, Technical Report USAF-APL-TR-73-45, 1973.
- [B.14] Kozarev, L.A. and Federov, R.M., “Aspects of the Appearance and Elimination of Breakdown in an Axial-Flow Compressor in the Presence of a Rotating Non-Uniformity at the Inlet”, Izevstinya vuz Aviatsionnaya Tekhnika, 26(1), pp. 33-37 (translated), 1983.
- [B.15] Longley, J.P., Shin, H.-W., Plumley, R.E., Silkowski, P.D., Day, I.J., Greitzer, E.M., Tan, C.S. and Wisler, D.C., “Effects of Rotating Inlet Distortion on Multistage Compressor Stability”, *ASME Journal of Turbomachinery*.
- [B.16] Silkowski, P.D., “Measurements of Rotor Stalling in Matched and Mismatched Multistage Compressor”, MIT Gas Turbine Report No. 221, Massachusetts Institute of Technology, 1995.
- [B.17] Day, J.J., “Stall Inception in Axial Flow Compressors”, *ASME Journal of Turbomachinery*, Vol. 115, pp. 1-9, 1993.
- [B.18] Hodder, B.K., “An Investigation of Engine Influence on Inlet Performance”, NASA CR-166136, 1981.
- [B.19] Graf, M., Wong, T., Greitzer, E.M., Tan, C.S., Marble, F.E., Shin, H.-W. and Wisler, D., “Effects of Asymmetric Tip Clearance on Compressor Stability”, accepted for publication in *ASME Journal of Turbomachinery*, 1997.
- [B.20] Hetherington, R. and Morritz, R.R., “The Influence of Unsteady Flow Phenomena on the Design and Operation of Aero Engines”, in *Unsteady Phenomena in Turbomachinery*, AGARD CP-144, 1977.
- [B.21] Mikolajczak, A.A., “The Practical Importance of Unsteady Flow Phenomena on Design and Operation of Aero Engines”, in *AGARD CP-144, Unsteady Phenomena in Turbomachinery*, 1977.
- [B.22] Smith, L.H., “Wake Dispersion in Turbomachines”, *ASME Journal of Basic Engineering*, September 1966.
- [B.23] Smith, L.H., Discussion of ASME Paper # 96-GT-029, Birmingham, United Kingdom, June 1996.
- [B.24] Koch, C.C., “Stalling Pressure Rise Capability of Axial Flow Compressor Stages”, ASME Paper # 81-GT-3, 1981.

---

**ANNEX B – ADVANCED TOPICS AND RECENT PROGRESS**

---

- [B.25] Valkov, T.V., “The Effect of Upstream Rotor Vortical Disturbances on the Time-Average Performance of Axial Compressor Stators”, MIT, GTL, Report # 227, August 1997.
- [B.26] Schaffler, A., “Experimental and Analytical Investigation of the Effects of Reynolds Number and Blade Surface Roughness on Multistage Axial Flow Compressors”, ASME Paper # 79-GT-2, 1979.
- [B.27] Suder, K.L., Chima, R.V., Strazisar, A.J. and Roberts, W.B., “The Effect of Adding Roughness and Thickness to a Transonic Axial Compressor Rotor”, ASME Paper # 94-GT-339, 1994.
- [B.28] Kandebo, S.E., “F100-PW-229 Failures Affect F-15E Readiness”, Aviation Week and Space Technology, June 27 1994.
- [B.29] Khalak, “Parametric Dependencies of Aeroengine Flutter for Flutter Clearance Applications”, Phd Thesis, MIT Aero & Astro, 2000.
- [B.30] Palmer, D.L. and Waterman, W.F., “Design and Development of an Advanced Two-Stage Centrifugal Compressor”, ASME Paper # 94-GT-202, 1994.
- [B.31] Rodgers, C., “Effect of Inlet Geometry on the Performance of Small Centrifugal Compressors”, AIAA-88-2812, 1988.
- [B.32] Hoener, S.F., “Fluid-Dynamic Drag”, Published by the Author, 1965.
- [B.33] Hynes, T.P. and Greitzer, E.M., “A Method for Assessing Effects of Inlet Flow Distortion on Compressor Stability”, ASME J. of Turbomachinery, 109, pp. 371-379, 1987.
- [B.34] Chue, R., Hynes, T.P., Greitzer, E.M., Tan, C.S. and Longley, J.P., “Calculations of Inlet Distortion Induced Compressor Flowfield Instability”, *Int. Journal of Heat and Fluid Flow*, 10, pp. 211-223, September 1989.
- [B.35] Gong, Y., Tan, C.S., Gordon, K. and Greitzer, E., “A Three-dimensional Computational Flow Model for Short Length Scale Instability in Multistage Axial Compressor”, Submitted for consideration of publication in ASME Journal of Turbomachinery 1998.

**B.1.9 Additional Bibliography for Compressor Section**

- Graf, M.B. and Sharma, O.P., “Effects of Downstream Stator Pressure Field on Upstream Rotor Performance”, ASME Paper # 96-GT-507, 1996.
- Walker, G.J., “The Unsteady Nature of Boundary Layer Transition on an Axial-Flow Compressor Blade”, ASME Paper # 74-GT-135, 1974.
- Pfeil, H., Herbst, R. and Schroder, T., “Investigation of the Laminar-Turbulent Transition of Boundary Layers Disturbed by Wakes”, ASME Journal of Engineering and Power, 105, 1983.
- Hodson, H.P., “Modeling Unsteady Transition and Its Effect on Profile Loss”, ASME Journal of Turbomachinery, 112, October 1990.
- Sharma, O.P. et al., “Assessment of Unsteady Flows in Turbines”, ASME Paper # 90-GT-150, 1990.
- Dong, Y. and Cumpsty, N.A., “Compressor Blade Boundary Layers: Part 1 – Test Facility and Measurements with Incident Wakes”, ASME Journal of Turbomachinery, 112, 1990a.

Dong, Y. and Cumpsty, N.A., “Compressor Blade Boundary Layers: Part 2 – Measurements with Incident”, ASME Journal of Turbomachinery, 112, 1990b.

Halstead, D.E., Wisler, D.C., Okiishi, T.H., Walker, G.J., Hodson, H.P. and Hsin, H.W., “Boundary Layer Development in Axial Compressors and Turbines – Part 1 of 4: Composite Picture”, ASME Paper # 95-GT-461, 1995.

Halstead, D.E., Wisler, D.C., Okiishi, T.H., Walker, J., Hodson, H.P. and Hsin, H.W., “Boundary Layer Development in Axial Compressors and Turbines – Part 2 of 4: Compressors”, ASME Paper # 95-GT-462, 1995.

Schulz, H.D., Gallus, H.E. and Lakshminarayana, B., “Three-Dimensional Separated Flow Field in the Endwall Region of An Annular Compressor Cascade in the Presence of Rotor-Stator Interaction – Part 1: Quasi-Steady Flow Field and Comparison with Steady-State Data”, ASME Journal of Turbomachinery, 112, October 1990.

Kerrebrock, J.L. and Mikolajczak, A.A., “Intra-Stator Transport of Rotor Wakes and Its Effect on Compressor Performance”, ASME Journal of Engineering and Power, October 1970, pp. 359-368.

Dawes, W.N., “A Numerical Study of the Interaction of a Transonic Compressor Rotor Overtip Leakage Vortex with the following Stator Blade Row”, ASME Paper # 94-GT-156, 1994.

Valkov, T. and Tan, C.S., “Control of the Unsteady Flow in a Stator Blade Row Interacting with Upstream Moving Wakes”, ASME J. Turbomachinery, 1995, Vol. 117, pp. 97-105.

Howard, M.A., Ivey, P.C., Barton, J.P. and Young, K.F., “Endwall Effects at Two Tip Clearances in a Multi-Stage Axial Flow Compressor with Controlled-Diffusion Blading”, ASME Journal of Turbomachinery, 116, 1994.

Poensgen, C. and Gallus, H.E., “Three-Dimensional Wake Decay Inside of a Compressor Cascade and Its Influence on the Downstream Unsteady Flow Field: Part I – Wake Decay Characteristics in the Flow Passage”, ASME Journal of Turbomachinery, 113, 1991a.

Poensgen, C. and Gallus, H.E., “Three-Dimensional Wake Decay Inside of a Compressor Cascade and Its Influence on the Downstream Unsteady Flow Field: Part II – Unsteady Flow Field Downstream of the Stator”, ASME Journal of Turbomachinery, 113, 1991b.

Denton, J.D., “Loss Mechanism in Turbomachines”, ASME Journal of Turbomachines, 115, No. 4, 1993.

Valkov, T. and Tan, C.S., “Effects of Upstream Rotor Vortical Disturbances on Time-Average Performance of Axial Compressor Stator: Part 1 – Framework of Technical Approach and Rotor Wakes – Stator Blade Interaction”, Accepted for Presentation at 43rd International Gas Turbine and Aeroengine Congress and Exposition, Stockholm, June 1998.

Valkov, T. and Tan, C.S., “Effects of Upstream Rotor Vortical Disturbances on Time-Average Performance of Axial Compressor Stator: Part 2 – Rotor Tip Leakage and Discrete Streamwise Vortex – Stator Blade Interaction”, Accepted for Presentation at 43rd International Gas Turbine and Aeroengine Congress and Exposition, Stockholm, June 1998.

Hendricks, G.J., Bonnaure, L.P., Longley, J.P., Gretizer, E.M. and Epstein, A.M., “Analysis of Rotating Stall Onset in High Speed Axial Compressors”, AIAA Paper # 93-2233, 1993.

## ANNEX B – ADVANCED TOPICS AND RECENT PROGRESS

---

Hoying, D.A., Tan, C.S., Vo, H.D. and Greitzer, E.M., “Role of Blade Passage Flow Structures in Axial Compressor Rotating Stall Inception”, Paper submitted for TurboExpo ‘98, Stockholm, Sweden, 1998.

Wisler, D.C., “Core Compressor Exit Stage Study, Vol. IV – Data and Performance Report for the Best Stage Configuration”, NASA CR-165357, NASA Lewis Research Center, 1981.

Park, H.G., “Unsteady Disturbance Structures in Axial Flow Compressor Stall Inception”, Master’s Thesis, Massachusetts Institute of Technology, 1994.

LeJambre, C.R., Zacharias, R.M., Biederman, B.P., Gleixner, A.J. and Yetka, C.J., “Development and Application of Multistage Navier-Stokes Solver, Part II: Application to a High Pressure Compressor Design”, ASME Journal of Turbomachinery, Vol. 120, No. 2, April 1998.

Dring, R.P., Sprout, W.D. and Weingold, H.D., “A Navier-Stokes Analysis of the Effect of Tip Clearance on Compressor Stall Margin”, ASME Paper # 95-GT-190, 1995.

## B.2 PERFORMANCE OF TURBINE SUB-SYSTEMS

### B.2.1 Overview of Turbine Sub-System Performance

The turbine system of the gas turbine engine is a complex integration and balancing of the disciplines of aerodynamics, internal and external heat transfer, stressing, material properties, and manufacturing capability. During the design phase of the engine it is important to consider the expansion system in totality, i.e. high pressure turbine, interduct, low pressure turbine, exhaust diffuser and jet pipe. By so doing, the optimal engine may be derived. This may or may not mean that each turbine stage is at its peak aerodynamic performance point. Turbine interducts are potential sources of high losses, with high mach number swirling flow, highly rotational flow, and often with large radius changes. The turbine turbomachinery behaves in similar ways to that of the compressor’s. Reynolds dependency on profile losses, shock-boundary layer interactions, tip clearance effects, and many of the references given under the compressor section are relevant to both environments.

This section of the report aims to give the reader an understanding of the way in which turbine performance is predicted, measured and analysed, highlighting areas of particular sensitivity.

### B.2.2 High Pressure Turbines

#### B.2.2.1 General Performance

High pressure turbines operate for most of the time at a fixed expansion ratio with small changes in aerodynamic speed. Depending on the performance of the compressors, the LP turbine, the combustor pressure loss and efficiency, and the capacity and efficiency of the HP turbine, the turbine may, or may not, operate at its design expansion ratio and aerodynamic speed. In order to develop the engine it is important to have a characteristic of the turbine for use in the synthesis of the engine. In early design stages and simplified cycle calculations it is sufficient to hold a constant efficiency due to the relatively small variation in operating point.

The turbine has to convert energy from the hot gas stream to drive the compressor on the same shaft. In its simplest form, assuming constant flow through the gas turbine, the energy balance is:

$$\text{Compressor enthalpy rise} = \text{Turbine enthalpy drop}$$

In practice this is moderated in varying degrees by the following:

### Compressor:

- External bleed bypassing the turbine;
- Internal bleed, partially or wholly bypassing the turbine;
- Leaks (i.e. from variable geometry vanes) bypassing the turbine; and
- Radiated heat from casings.

### Secondary Air System:

- Windage losses on shaft and discs.

### Bearings and Power Off-Take Shaft:

- Heat to oil and windage losses; power extraction.

### Turbine:

- Position of cooling air return relative to rotor throat(s);
- Energy state of returned secondary air; and
- Heat losses through casings.

These modifiers of the simplified arrangement all need quantification for a real assessment of the turbine performance in the engine. Some of the above are amenable to direct measurement, whilst others are reliant on calculation and separate experimentation with subsequent superposition.

Two of the above are closely linked and are the two that are most difficult to assess. They are: 1) the secondary air system; and 2) the energy state of returned secondary air. Both these systems are driven by main gas stream pressure differentials, which are themselves subject to changes throughout the running range, and are strongly subject to engine deterioration. A typified cooling and secondary air system is indicated in **Figure B.64**.

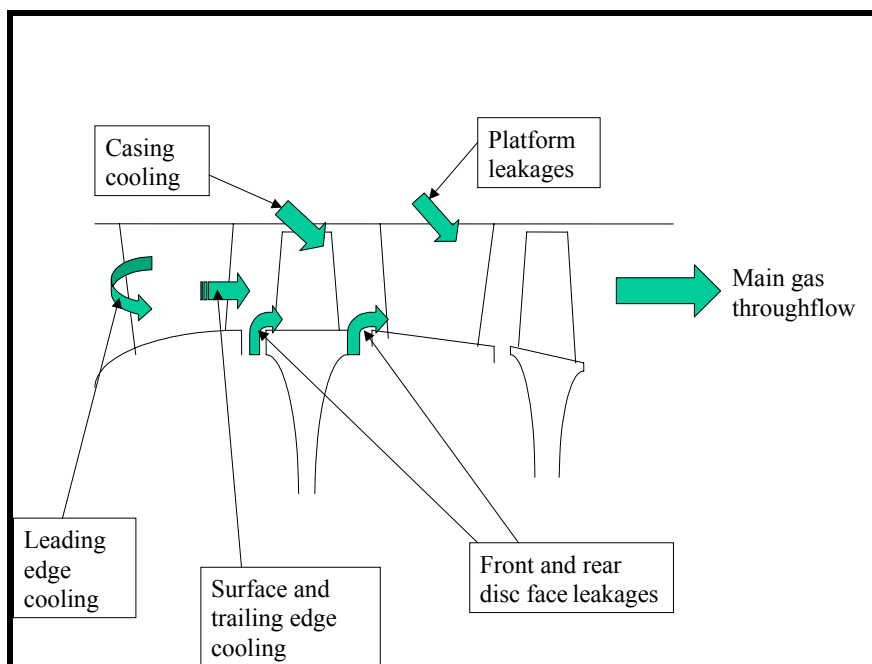


**Figure B.64:** Typical Secondary-Air-System Returns to Main Throughflow Bleed Network.

## ANNEX B – ADVANCED TOPICS AND RECENT PROGRESS

---

### Nozzle:

- Airfoil leading edge cooling;
- Airfoil surface cooling;
- Airfoil trailing edge cooling;
- Platform cooling returned at platform trailing edge – inner and outer;
- Platform leakage, blade to blade direction, inner and outer; and
- Shroud well cooling.

### Rotor:

- Airfoil leading edge cooling;
- Airfoil surface cooling;
- Airfoil trailing edge cooling;
- Front face of disc cooling;
- Front face of disc leakage;
- Rear face of disc cooling;
- Rear face of disc leakage;
- Platform leakage; and
- Overtip cooling flow.

It is normal convention that bleeds are treated in the following manner:

- Bleed flows introduced in the preceding blade row are treated as available for work in subsequent blade rows.
- Platform and disc bleed flows introduced upstream of the throat affect throat sizing, but are not available for work.
- Airfoil bleeds upstream of the throat contribute to the work in the turbine.
- Bleed flows downstream of the throat contribute no work in that blade row.

The astute reader will recognize that such a convention is not academically correct. This highlights the importance of clarity of the turbine efficiency definition being used.

### B.2.2.2 Characteristic Generation

The potential efficiency of the turbine stage, or stages, is dependent on the basic velocity triangles, i.e. work, blade speed, and through-flow velocities. These have to be considered in the context of the turbine physical size and the hub/tip ratio of the stage concerned. Such physical considerations determine the effects of trailing edge thickness on the potential efficiency, the influence of tip clearance, and the Reynolds regime that the turbine will operate in.

Optimization of the airfoil profile, shock and secondary losses leads to the design point efficiency of the turbine, when the effects of cooling and secondary air flows have been incorporated. In order to generate a turbine characteristic for use in the synthesis of the gas turbine engine one of three actions can be taken.

Scaling of a previously measured turbine characteristic which has similar leading parameters, i.e. work, hub/tip ratio, through-flow axial mach numbers, and reaction.

Prediction based on blade row stacking. Based on regression analysis of previous turbines, the generic performance of the turbine can be predicted over a wide range of operation. Such methodology works adequately well with consistent and progressive small changes in the designs. It may however lead to substantive errors when more radical changes in design are pursued [B.36, B.37 and B.38].

Quasi 3-D/3-D simulation of the turbine stage(s). This methodology has proven itself capable of simulating widely different types of design with good results. The speed range and expansion ratio range is more limited than methods 1 and 2, normally due to the range of applicability of the boundary layer methods and calculation stability at off-design flow conditions. The flow conditions along the hub and casings allow better analysis of the secondary air system, and from the knowledge of the changes in lift distribution on the airfoil, so improved blade cooling assessments can be made [B.39]. This method does have the following added potential benefits: identifying the effects of upstream wakes, and downstream perturbations from struts or instrumentation; assessing the exit profile from the turbine at the various operating conditions. This is particularly important if inter-turbine ducts (especially with large radius change) are used, and if the downstream turbine is sensitive to pressure and temperature profiles.

### B.2.2.3 Rig Testing

The HP turbine lives in a hostile environment and hence there are associated difficulties of measuring, as opposed to deducing, its in-engine performance. Consequently, much turbine development has used ‘cold flow’ rigs, which replicate the turbine unit and are operated at substantially lower temperatures. Without the complexity of combustor or following turbine, more accurate measurements may be taken over wide operating regimes, but which need accounting systems to transpose from the rig to the engine environment.

Four major types of rig have been used in the development of turbines, viz.

- **2-D or Annular Cascades** – These facilities are capable of high accuracy measurement of the aerodynamics of the airfoil over a wide range of operation and Reynolds number. The necessity to control the end wall boundary layer, and its effect on the mid height aerodynamics led to development of methods such as porous walls, and each tunnel has its own particular characteristic. Due to the potential of high quality test results these tunnels have formed the foundation of improvement to the analytical approach to airfoil design [B.40].
- This can be further subdivided into two sections:
  - **Internal Cooling** – Investigations of the effectiveness of internal cooling passage designs, including the residual pressure that is key to the selection of the location of the exhausting of the coolant, and its impact on the external aerodynamics [B.41].
  - **External Cooling** – Used to determine the optimum pitching and direction of the coolant ejection holes for effective filming of the surface. Such rigs also indicate the sensitivity of the film to the hole shape and the pressure ratio between the main gas passage and the source [B.42].

Both of these rig types need to be able to evaluate the effects of Coriolis forces from within the gas flow, and superimposed centrifugal forces, and their consequential effects on the localized heat transfer rates.

- **‘Cold Flow’ Turbine Rigs** – The cold-flow turbine rig simplifies the instrumentation and measurement difficulties that are encountered in the high temperature in engine situation. It allows for easier full spatial inlet, inter-blade row, and exit traverse, and can exercise the turbine over a wide of operation. As such these facilities provide the first insight to the measured performance of the turbine, as opposed to the predicted performance. There are corrections to be made to the

measured performance, such as disc windage and bearing losses, and gas conditions from rig to engine. In uncooled, or low flow cooled turbines the cold flow rig has close similarity to the engine environment. Most of the modern engines now rely on relatively high proportions of the main gas flow being used for cooling and secondary air systems. Consequently, the cold flow rig with solid blading has to attempt to emulate these effects. The experimenter can elect to maintain the blades as per the engine, test the turbine over the range of expansion ratios, and then manipulate the turbine results for the correct engine reaction. Alternatively, it may be preferred to redesign the nozzle, such that the correct reaction is achieved at the design expansion ratio. Such considerations are compounded with increasing stage numbers. Both approaches ignore the effects that cooling films have on the basic loss of the airfoil, and potential shock-interaction changes, and further modification to the measured characteristics must be made.

- **‘Warm Flow’ Turbine Rigs** – These facilities have the advantages of the cold flow rig plus the capability to introduce cooling and secondary air into the turbine. The spoiling effects of these return bleeds, their effects on disc windage and the blade row to blade row throat distribution and hence stage reaction, lead to a better simulation. Some facilities use vitiated cooling air that has been combined with other gases in order to better approximate the relative densities between the cooling and the main stream air. They therefore represent very closely the in-engine performance. Due to their complexity, the cost of the unit and plant on which the unit is tested is substantially greater than that of cold flow testing. Since the airfoils contain either engine or emulated engine cooling systems, the availability of these complex parts may be late in the lifespan of the engine development. So although good measurement of the turbine characteristic can be accomplished, the timing may be so late that the only gain may be an understanding of how to make improvements for the next mark of engine!

The experimenter must decide how best to run the unit to generate the required characteristics. Options include: running the cooling or secondary air at constant feed to re-entrant point pressure difference; or holding feed pressure constant over a small expansion ratio variation; varying the leading edge feed pressure in conjunction with trailing edge; or only varying trailing edge feed as expansion ratio changes. It must also be noted that as the feed pressures change, so may, the windage levels on the turbine disc and the thrust bearing losses. This depends on the detailed design of the rig.

Because of the cost of these units, their relative inflexibility, and the experimental accuracy available, the use of warm-flow turbine rigs is often reserved for exceptional occasions.

#### **B.2.2.4 Engine Testing**

In the engine environment the turbine experiences the radial and circumferential patterns generated by the combustor, and the upstream influence of the LP turbine. Both of these can lead to differences between cold and warm flow tests, usually in minor ways. The difficulty in engine testing is to achieve a high experimental accuracy on all of the parameters (see above), such that the resulting assessment of the turbine is of high integrity.

In order to measure correctly the energy state of the gas entering and exiting the turbine, full area traverses are required. These are difficult to achieve in the strictures of the engine architecture. This often leads to the use of separate engine core testing, without the LP spool, with greater access for measurement, and yet retaining the temperatures and secondary air systems and clearances as experienced in the whole engine. The quality of the primary factors in the calculation of turbine efficiency, mass flow, work in the compressor and average inlet and exit temperatures can all be substantially better than those of the engine.

Unlike the engine, where it is extremely difficult to change the operating point of the turbine, the HP spool vehicle enables the experimenter to explore a wide range of operation. Changes to the downstream control nozzle change the operating point, giving a limited turbine characteristic. If available, then alterations to

the compressor variable-geometry allow for a range of turbine aerodynamic speed to be assessed. Extra turbine load can be added by absorbing power at the power off-take shaft. This is normally done by use of hydraulic motors. Whilst these investigations are underway it remains important for the secondary air and cooling air system to be monitored, along with changes in tip clearance in order to gain a correct assessment of the turbine.

The table below summarizes the methods of turbine characteristic measurement and gives guidance to the validity of the resulting performance map.

**Table B-1: Method of Turbine Characteristic Measurement**

Method	Representative Conditions	Measurement or Sampling Difficulty	Measurement Accuracy	Nett Assessment	
				<i>HP Turbines</i>	<i>LP (uncooled) Turbines</i>
<b>Cold Flow Rig</b>	Poor	Low	High	No. 5	No. 2
<b>Engine Parts Cold Flow Rig</b>	Good	Low	High	No. 3	Best
<b>HP Spool</b>	Best (with intermediate op. range)	Intermediate	Intermediate	No. 2	N/A
<b>Direct on Engine</b>	Best (but limited range)	High	Intermediate	No. 4	No.4
<b>On Engine with performance simulation</b>	Best (but limited range)	High	Intermediate	Best	No.3

#### **B.2.2.5 Transient and Abnormal Operations**

During rapid throttle movement, the combustor may not complete the combustion process. Hence, the gas entering the turbine may also contain a relatively high degree of unburned fuel. This causes insignificant blockage of the turbine throat and does not affect engine matching. The major area of concern under transient operation is that of tip clearance, and the effect on turbine efficiency. Time constants for the tip clearance changes are substantially greater than those of the gas flow are. Consequently, turbine performance can be treated as pseudo steady state with the effects of the tip clearance changes added by superposition.

Whilst the aerodynamicist will be able to justify the use of continuous curvature on the blade surfaces, and the use of polished surfaces to gain that last point of efficiency, once developed, turbines are generally extremely resilient to damage. It is not infrequent that operators will only detect damaged turbines either by boroscope visual inspection or by indicated out of balance. Missing blades, burnt trailing edges of nozzles, impact damaged leading edges, erosion by volcanic ash, all are found in service and have to be severe to reduce the engine performance. It is essential though to maintain the mechanical integrity of the engine.

### **B.2.3 Low Pressure Turbines**

#### **B.2.3.1 General Performance**

The low pressure turbine of aero gas turbines operates over relatively wide aerodynamic speed ranges and expansion ratios. It is therefore more important to have a characteristic that reflects the turbine performance

## ANNEX B – ADVANCED TOPICS AND RECENT PROGRESS

---

when engine performance calculations are made. Two different types of turbine need to be considered. They are:

- **High Specific Thrust Engines** – These turbines, often single-stage units, are usually cooled, and due to the effects of the reheat system, variable final nozzle and the wide flight regime, operate over a wide range of aerodynamics.
- **Low Specific Thrust Engines** – These multi-stage units are usually uncooled, at least in the airfoil, and changes in expansion ratio reflect the changes in aerodynamic speed. Generally, the aerodynamic excursions of the blades are substantially less than the high specific thrust units.

A modern exception to the above is the ‘Remote fan’ solution for one of the contenders in the Joint Strike Fighter – Vertical landing scenario. In this gas turbine, a clutched fan is driven by a low-pressure turbine that also drives the main engine low-pressure compressor. For up and away flight the turbine operates as a lightly loaded unit and is subject to normal high specific thrust engine changes of operation. In the vertical land mode the turbine operates as a highly loaded, but low specific thrust unit. At similar aerodynamic speeds the turbine changes its expansion ratio by approximately 2:1 as the load of the ‘Remote fan’ is demanded from the turbine. Similar operations have been considered for civil low noise supersonic engines. These ranges of operation demand that representative characteristics are available early in the project design phase as critical thrust conditions have to be met in both methods of operation.

The exhaust diffuser is the last aerodynamic unit before the gas enters the jetpipe. It has an arduous task, taking swirling flow from the exit of the turbine, turning it to the axial direction and diffusing from typically 0.6 Mn to 0.2 Mn. As the turbine aerodynamic loading varies so does the swirl and mach number into the diffuser. Since the performance analyst is primarily concerned with jetpipe gas conditions, it is often convenient to incorporate the losses of the exhaust diffuser into the LP turbine characteristic. Otherwise it is necessary for the diffuser losses to be expressed as a function of the turbine operating point, i.e. exit swirl, Mach number.

### B.2.3.2 Characteristic Generation

Methods for estimating or measuring the LP turbine performance are essentially the same as for the HP turbine. Due to the variation in aerodynamic operation of the LP turbine, the cooling flow source to sink pressure ratios are not as constant as for the HP turbine. Consequently, it is important to include the variations in the ‘warm flow’ testing that may be done. As an alternative, the influence, normally by calculation, of the varying cooling flows can be superpositioned on the test results of a solid bladed ‘cold flow’ rig result.

### B.2.3.3 Rig and Engine Testing

Similar requirements and concerns exist for LP turbine testing as those of the HP turbine. The cooled LP turbine may be subjected to the same options for rig tests as those for the HP turbine. Uncooled LP turbines, usually associated with the high power civil engines generate large powers, and need large capital investment in facilities if they are to be tested at engine conditions. It had been common practice to use scaled models of these units to overcome these difficulties. When model rigs are used it remains important to emulate the blading of the turbine as it will exist in the full scale unit. This means that representative features, such as trailing edge thickness and tip clearances are replicated in the rig. Due to the change of centrifugal and gas bending loads it is usually necessary to design such that the scaled turbine is representative at design aerodynamic speed, and account the small variances that will be present at off-design aerodynamic speeds. With modern blading methods that are strongly Reynolds number, turbulence level and unsteadiness level dependant, the use of model LP turbines is reducing. [B.43]

Engine testing of the LP turbine has a variety of technical areas that need consideration. The necessary quality measurements of the gas parameters, both inlet and outlet are difficult to achieve, as per the HP

turbine. The work done by the turbine is attributed from the analysis of the low pressure compressor, and the working mass flow is deduced from the analysis of the core engine. These factors accumulate such that the of the turbomachinery analysis the LP turbine performance has the highest uncertainty. However given these reservations, with careful analysis over a series of engine tests, then changes in efficiency and capacity of the turbine over a reasonably wide operation can be established.

## **B.2.4 The Exceptions**

### **B.2.4.1 Variable Area Turbines**

The concept of the variable area turbine has been considered for a variety of applications. Classically such turbines are designed to reduce their inlet flow usually by changing the stagger of the nozzle, whilst maintaining specific work at near fixed inlet temperatures. In order to predict their characteristic it is essential to have robust off-design incidence calculations of the blading. It is usual to compromise on the rotor ~ stator-throat ratios so that as the turbine is increased in flow so the flow controlling cascade remains the stator. Such modes of operation challenge the computational capabilities, especially at high or low incidence where separation bubbles can be generated on either the suction or pressure surface. Normal design and operation of turbines is given to eliminating such features from the blading. Modern variable bypass military engines use the variable turbine in conjunction with the variable geometry in the core compression system to improve the matching between the supersonic inlet characteristics, the propulsion nozzle drag characteristics and the flow ~ speed ~ combustion temperature relationships of the gas turbine. Since the benefit to the propulsion system is dominated by the inlet efficiency and exhaust losses, the compromise is sometimes to operate the turbine at less than optimal aerodynamics.

Alternative use of variable turbines is to improve spool matching, or to thermodynamically down flow the engine, whilst retaining overall pressure ratio and turbine temperature. This enables the lower power to be achieved with similar thermal efficiencies to the full power. Significant reductions in part power specific fuel consumption can initially be calculated, but changes to the internal bleed network, and reduction of component efficiencies at off-design conditions can rapidly erode initial indicated advantages. It remains the responsibility of the turbine designer to be able to predict with reasonable accuracy the performance at these extremes of operation.

A variety of potential solutions for changing the throat size of the turbine have been tried ranging from:

- Variable stagger (complete vane or trailing edge);
- Moving casing;
- Variable camber (or profile);
- Switchable high pressure air bleed at the throat; and
- Physical obstruction at the throat.

Many of the test results remain either company proprietary or classified.

### **B.2.4.2 Statorless Contra Rotating Turbines**

Adoption of an expansion system where there is no direct control of the LP turbine flow capacity by use of a fixed nozzle between the HP and LP spools has seen limited application. There are clear advantages by deletion of the inter-turbine vane, such as the length, weight, and cooling flow savings along with potential aerodynamic improvements in the net expansion system efficiency. These turbines benefit from having close axial spacing, but this may be in conflict with the disc designs, which usually demand a reasonable disc width at the hub to accommodate the stressing and life requirements. Close coupling of the discs also leads to air system losses as the contra rotating discs create high shearing forces between their faces.

## ANNEX B – ADVANCED TOPICS AND RECENT PROGRESS

---

This can, in turn demand higher intercavity flows to prevent excessive heat build up and the possibility of induced disc vibrations from the secondary air flow behavior.

Prediction of these turbines is more complex than for nozzled turbines. The entry conditions for the following turbine are dependent on the through flow and work level of the preceding turbine as these determine the swirl angle and Mach number of the flow. It is therefore necessary to generate a turbine characteristic that is dependent on the compressor performance. This characteristic will vary with degradation, distortion and build scatter, and where an appropriate influence of variable vane and bleed off-take schedules, including tolerances, have been included.

### B.2.5 Cited References for Turbine Section

Also refer to the Compressor section.

- [B.36] Ainley, D.G. and Matheson, G.C.R., “A Method of Performance Estimation for Axial Flow Turbines”, Aeronautical Research Council, R & M 2974 (1957).
- [B.37] Craig, H.R.M. and Cox, H.J.A., “Performance Estimation of Axial Flow Turbines”, Proc Inst. Mech. Engrs, Vol. 185, 32/71, 1971.
- [B.38] Kacker, S.C. and Okapu, U., “A Mean-Line Prediction Method for Axial Turbine Efficiency”, ASME Paper # 81-GT-58, 1981.
- [B.39] Various, “Loss Mechanisms and Unsteady Flows in Turbomachinery”, AGARD CP-571, 1996.
- [B.40] Various, “CFD Validation for Propulsion System Components”, AGARD AR-355, 1998.
- [B.41] Ardoy, Fottner, Beversdorff and Weyer, “Laser 2-Focus Measurements on a Turbine Cascade with Leading Edge Cooling”, AGARD CP-598, 1998.
- [B.42] Guo, Lai, Jeony, Jones and Oldfield, “Use of Liquid Crystal Techniques to Measure Film Cooling Heat Transfer and Effectiveness”, AGARD CP-598, 1998.
- [B.43] Various, “Unsteady Aerodynamic Phenomena in Turbomachinery”, AGARD CP-468, 1990.

## B.3 COMBUSTOR SYSTEMS

### B.3.1 Flowpath and Exit Temperature

One of the main issues for combustor design and performance is compliance with the high-pressure distributor and turbine specifications for durability and thermodynamic efficiency. Life and durability specifications are directly linked with the limiting thermal and mechanical point-stresses of the turbine nozzle and rotating parts and their associated cooling requirements. The circumferential and radial temperature and velocity profile envelopes and maximum temperature threshold compliance conditions at the exhaust of the combustor derive from these limits. These requirements are generally established in accordance with extreme design points for the engine operation and various representative fuelling mode effects, especially for staged or double combustors.

Additionally, profile distortions at the exit of the combustor can be generated during transient phases of the engine operation. These distortions due to air supply and air-to-fuel ratio variations can directly impact the global thermodynamic efficiency of the engine, through combustor and HP-turbine efficiency variations. Of course, these specifications have also to take into account the machining and tooling variations from both

the turbine and combustor points of view. The cost-effectiveness and technological compromise between the two modules also affects the outcome.

For design points, 1-D and 2-D engineering methods and 3-D CFD reactive calculations for isolated combustion, or coupled with the turbine nozzle module, are currently used to determine the most effective interface compliance conditions. Transient aspects are generally considered through 1-D and 2-D transient global modeling of the engine fitted on experimental data resulting from core engine tests and combustion rig tests on other engines. Inert and reactive 3-D and 2-D CFD calculations can also be considered for fuelling transient considerations.

### **B.3.1.1 Modeling**

Classically, the design requirements have been obtained through numerous tests, leading to the practice where all of a manufacturer's experience is recorded and codified and some rules are given as advice. In the last ten years, CFD has been used to reduce the number of tests needed, but one is always kept as a reference point for calibrating the various constants involved in the different models. Today the main goal for the manufacturer is to design new concepts for advanced combustion, which usually represent technological progress regarding in-house experience and ability. Consequently, a better understanding of all the involved physical phenomena, combined with related improvements in CFD tools is greatly needed. Although all phenomena are linked in turbulent two-phase reactive flow the prediction of a good temperature field is of primary importance. Without a correct temperature field, a correct flow-field cannot be obtained. (Because the density is false the solution of the conservation equation for momentum is false.)

Two phenomena are particularly crucial in the prediction of all the performances related to combustion. These are:

- Two phase flow in turbulent combustion; and
- The interactions between turbulence and chemistry.

Both need to be represented simultaneously, with accuracy, by the model to get reliable CFD tools.

The most attractive approach for modeling turbulent combustion is the laminar flamelet concept. Within the laminar flamelet concept, a turbulent flame is regarded as an ensemble of stationary laminar, locally one-dimensional flame elements, stretched and distorted by the turbulent flow.

Two assumptions are commonly introduced: the reaction zone is thin in comparison to the typical length of the turbulent flow, and the chemistry is fast in comparison to diffusion and convective transport. Then the reaction zone can be modeled as a one-dimensional reaction diffusion layer. This method is based on the local mixture fraction, and includes an extinction mechanism due to high local strain.

In applications of flamelets, stationary laminar flame solutions are stored in a flamelet library. During the CFD calculation, the flamelet library is consulted to determine the local distribution of reactants.

However, laminar-flamelet concept drawbacks are:

- This method works well only if the reaction zone is small compared to turbulent lengths; and
- The turbulence influence appears through a presumed PDF (Probability Density Function) that required an 'a priori' knowledge of the composition PDF.

The second approach concerns the calculated PDF method. The main characteristic is that this method combines an exact treatment of chemical reactions with the influence of turbulence. It does so by solving a

balance equation for the one-point composition PDF wherein the chemical reaction terms are in closed form. All PDF codes use notional particles that obey stochastic differential equations, solved by a Monte Carlo method.

The PDF contains random variables representing all chemical species at a particular spatial location. However, it contains no information concerning local fluctuations in the scalar gradient (2-point information). Thus, a model is needed for this micromixing term.

PDF codes are more CPU intensive than moment closure, but still tractable for process engineering calculations. In order to predict pollutants, detailed kinetic mechanisms can be combined with composition PDF, but this application is restricted by CPU and computer memory limits on laboratory flames. Since the reaction rates usually vary by several orders of magnitude, a stiff ODE (Ordinary Differential Equations) solver is required, and complex kinetics involving many reactants can be computationally intensive. In principle, the number of scalars is limited to five or six reactants with a reduced chemical mechanism, and with a reaction look-up table.

Presently, considerable effort is being applied to develop reliable models for micro mixing and to represent the effect of the evaporation of the droplets.

#### **B.3.1.2 Dissociation/Recombination/Emission**

Because of strict environmental regulations for aircraft engines, emissions from carbon monoxide, unburned hydrocarbons, oxides of nitrogen and smoke must be reduced. Moreover, especially at high combustion temperatures ( $>1800$  K), dissociation of  $\text{CO}_2$  and  $\text{H}_2\text{O}$  into  $\text{CO}$  and  $\text{H}_2$ , result in a decreased heat release.

The combustion system is more affected by concerns about pollutant emission than any other part of a gas turbine. The combustor can be separated into two zones:

- A relatively small primary zone, where fast reactions produce radicals ( $\text{H}$ ,  $\text{OH}$ ). High temperatures are reached in this zone, which corresponds to the  $\text{CO}$  production region.
- A bigger secondary zone downstream, where  $\text{CO}$  is oxidized into  $\text{CO}_2$  and  $\text{NO}_x$  appears.

$\text{CO}$  and  $\text{NO}_x$  emissions from combustion chamber are influenced by engine power setting. First, carbon monoxide and hydrocarbon emissions are lowest at full throttle operations. As thrust is increased, inlet temperature and pressure in the combustion are higher, as is fuel-air ratio. The increased fuel flow results in improved fuel atomization, and a higher combustion inlet temperature increases the vaporization rate. Because of the greater fuel-air ratio (FAR), the flame temperature increases and the chemical reaction rates responsible for  $\text{CO}$  and  $\text{HC}$  consumption are also sharply increased. Secondly, oxides of nitrogen emissions are greatest at high power operating conditions.  $\text{NO}_x$  formation is extremely temperature sensitive. Since the combustion inlet temperature and consequently the stoichiometric flame temperature is increased with the power setting, the  $\text{NO}_x$  emission level is important for high design. Hence, new combustion concepts are being developed in order to reduce  $\text{NO}_x$  and  $\text{CO}$  emissions, with respect to their conflicting trends.

Combustion efficiency is a parameter of paramount importance for the performance engineer. It is customary to define the combustion efficiency as the ratio of the released energy to the maximum possible energy that can theoretically be released during the combustion process.

Hence, it is common practice in cycle decks to use the combustion efficiency as the ratio of the ‘actually burned’ fuel to the input fuel. The fuel air ratio (FAR) used for all subsequent calculations up to the engine exit is then based on this ‘actually burned’ fuel. The ‘remaining fuel’ (which has not been burned)

disappears from the engine thermodynamic calculation, with the exception of the Specific Fuel Consumption (SFC).

Until recently, because combustion efficiency was close to the maximum and exit combustion temperature ( $T_4$ ) was not very high, this way of working suited engine performance calculations. In recent years, the maximum cycle pressures and temperatures of jet engines have increased considerably. When temperatures are in excess of 1650 K, the dissociation effects become important.

The combustion inefficiency can be measured from the percentages of the exhaust products containing chemical energy (i.e. unburned hydrocarbons, carbon monoxide and hydrogen). To obtain the combustion inefficiency, only the amounts in excess of those formed at dissociation at equilibrium are considered (we cannot blame the combustion designers for the dissociation at equilibrium...). These concentrations in excess of those formed at equilibrium may be due to the non-uniformity of the temperature or combustion profile.

The dissociation energy at equilibrium can be very important, depending on the pressure and final temperature. At 39 bars and 2200 K the energy of dissociation accounts for 0.76% of the total fuel energy; at 2600 K the dissociation energy rises to 6%.

At these high temperatures, it is necessary to account for the molecular dissociation and recombination mechanism beyond station 4, because recombination is an exothermic reaction.

The engine makers frequently use one of two extreme assumptions:

- Local equilibrium is assumed (i.e. infinitely rapid chemical kinetics); and
- A frozen composition is assumed (i.e. no recombination) from the combustion exit to the engine exhaust.

From an engine test-analysis viewpoint, the assumption on the chemical composition is closely related to the turbine efficiency. Let's say that on a test bed there is an engine running at a very high turbine-entry temperature. If the frozen assumption is used to analyze the test data, the energy available for the turbines is less than the energy available if the local equilibrium assumption is used. Therefore, the turbine efficiency will be higher with the frozen assumption than with the local equilibrium assumption. Of course, the engine SFC is the same, what changes is the trade-off between chemical composition and turbine aerodynamics. This means that there is no clear cut-off (station 4) between the combustion (i.e. chemical reactions) and the turbine designer.

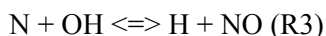
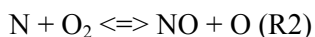
As has been mentioned above, the energy of dissociation becomes very important at high temperatures, making it is necessary to determine how much energy is recovered by the recombination reactions downstream of the combustion. There are few publications dealing with aerodynamics and chemistry through the turbine expansion. The cited publication is based on one-dimensional flow in the first nozzle (without cooling flows). This study shows that, except for the NO concentration, local equilibrium is attained at the exit of the nozzle.

Because NO has a much slower reaction rate, in this reference it is assumed that the concentration at equilibrium cannot be achieved at the end of the combustion. However, as the fluid progresses through the nozzle more NO is produced. In order to guarantee low emissions, turbine designers should consider NO formation.

From a performance viewpoint, the combustion efficiency is not enough, the chemical reactions downstream of the combustion cannot be ignored. The problem is very complex, aerodynamics and chemistry are involved, and 3-D effects may be important. The turbine blade cooling technique may have a strong influence on the recombination mechanism.

### B.3.1.3 NO<sub>x</sub> Modeling

NO<sub>x</sub> is defined by the regulatory authorities as the sum of nitric oxide (NO) and nitrogen dioxide (NO<sub>2</sub>). Many mechanisms have been developed to represent NO<sub>x</sub> formation under a variety of thermo-chemistry conditions. In classical combustion, characterized by the presence of diffusion flames ‘Thermal NO<sub>x</sub>’ is the principal route to NO<sub>x</sub> formation. It is well described by the Zeldovich equations.



A combustion kinetics model for NO<sub>x</sub>, with a classical hypothesis of steadiness and partial equilibrium, is applied as a post-processing step after a converged two-phase turbulent reactive computation has been obtained. The model for turbulent combustion is based on a presumed PDF approach where chemistry is very fast compared to the turbulent micro-mixing and where liquid fuel is represented by an ensemble of droplets in a Lagrangian framework. From the expression of the chemical reaction rate we can see that two characteristics of the flow-field have to be very well predicted by the reactive computation. They are the temperature and equivalence ratio fields. Temperature acts directly on the k’s constants while equivalence ratio is used to estimate the equilibrium values for all the radicals. This method is currently applied in the design process at Snecma and the other engine manufacturers use similar methods. All the users have demonstrated that this approach works well only for high level pressures (>30b), and that more information about chemistry must be included in the combustion model as a first step, and in the NO<sub>x</sub> mechanism as a second step. The reasons for the method breaking down when finite-rate chemistry effects become important (when the pressure is reduced) lie principally in the combustion model. If we try to apply a very fast chemistry turbulent combustion model to situations where we get a false temperature field the consequence is a bad flow-field associated with a bad equivalence ratio field. Super equilibrium concentrations for the O radical have been frequently observed or computed with more powerful tools. This is directly the consequence of slow three body recombination reactions. Only the integration of more detailed chemistry to the turbulent combustion model can give us solution to this problem. This is currently the case at Snecma where work has been oriented toward the use of the PDF techniques associated with complex chemistry.

Applied to a research tubular combustor the simplified method has given the following results, which are a good illustration of the considerations above.

**Table B-2: Simplified Method Results**

EINO <sub>x</sub> Computed	EINO <sub>x</sub> Measured	Pressure	Equivalence Ratio	Error %
5	7	15.6	8.6	28,6%
5	8	15.5	9.8	37,5%
5,5	10	15.3	13.7	45,0%
20	20	32.9	11.2	0,0%
22	27	32.6	15.3	18,5%
27	35	33.4	18.4	22,9%
28	28	37.6	12.8	0,0%
31	31	37.6	13.7	0,0%
32	38	37.3	16.8	15,8%

Improvements can be obtained in the framework of PDF transported methods using the coupled kinetics of kerosene and  $\text{NO}_x$ , and taking into account more information about the  $\text{NO}_x$  production mechanism. Although  $\text{NO}_x$  modeling is compatible with flamelet model capabilities, it seems CO prediction is limited by this assumption. The flamelet approach for CO prediction can be improved by the inclusion of turbulent and chemistry models. However CO formation is very complex, and flamelet hypothesis is not necessarily appropriate for this pollutant.

In combustors, CO oxidation can take place in lean post-flame zones, far from the flame front, where the flamelet approach may be incorrect. CO emissions are greatly influenced by high mixing rates in combustors, so the statistics of fluctuations need to be well predicted.

Therefore, the PDF transport method, which is able to model the non-equilibrium effects, works well for CO predictions, and should improve results. Finally, two aspects are important for CO modeling: the kinetic mechanism must be enough detailed, and the PDF method must be accurate with scalar fluctuations, and account for finite rate and non-equilibrium effects.

#### **B.3.1.4 Hail and Water Ingestion**

Exposed to various climatic conditions, the jet engine ingests different forms of water contained in the atmosphere: vapor, liquid, hail, snow; and ice crystals. The operating conditions where these forms of water can be met are below 20,000 ft. For higher altitudes, the atmospheric water content is insignificant. Depending upon flight speed (i.e. the ratio between the free stream area and the inlet area) and engine rotor speed, the fluid flow at the compressor outlet might include water vapor, liquid or solid water. The lower the corrected speed, the more important these phenomena are. The impacted flight phases are then low altitude cruise, taxiing, and descent. Engine performance predictions and risk assessments for flight safety in severe climatic conditions require an understanding of the different factors characterizing the behavior of the combustion chamber. If the working fluid has a high water content, the specific fuel consumption (SFC) rises and the operational range of the aircraft decreases. With liquid water at the combustion inlet, several cases must be considered. With low liquid water content, vaporizing takes place in the combustion chamber, but combustion efficiency is deteriorated. The fuel flow rate must then be increased. Beyond some threshold, extinction might occur.

Two modeling approaches are required:

- Modeling of reductions in flame temperature and efficiency as a function of water content; and
- Calculation of extinction limits due to the presence of liquid and solid water in the combustor.

### **B.3.2 Transient and Dynamic Modeling**

#### **B.3.2.1 Flame Blow-Out and Relight**

The engine operational envelope at high altitude or during fast transient or descent operations can be severely restricted by flame blow-out and combustor re-light capabilities (see **Figure B.65**). For example, flame blow-out effects can lead to very high thermal stress on turbine elements, nozzles and other parts located at the rear of the combustor.

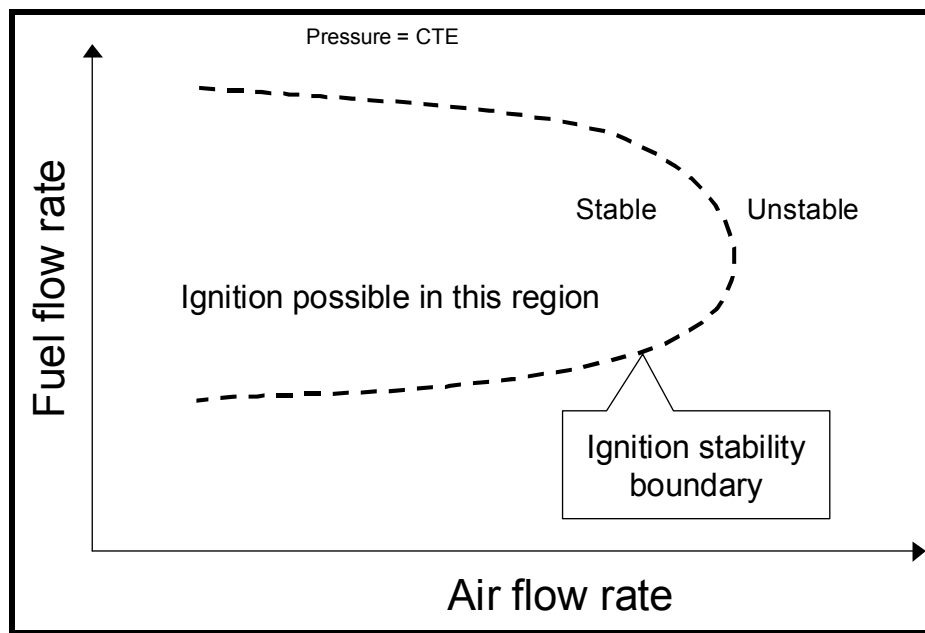


**Figure B.65: Region of Stable Ignition.**

Due to flight safety considerations and civil regulations, combustor ignition capability and operability requirements are generally defined through sub-domains and included in the flight envelope specifications. Complementary specifications on fuel temperature and atmospheric conditions such as temperature and hygrometry, rain and hailstone precipitation are also taken into account. Thermal limitations of the pumps and injection systems require minimal fuel flow rates for cooling and these can also reduce the operability of the combustor.

From the control system view of the combustor, these constraints are translated into fuelling and actuation laws that are dependent on engine operating conditions. All these conditions must be integrated in the global engine performance model in order to specify module performance and control systems, and help to define in-flight emergency procedures. Sensitivity to various control options, especially for staged or double combustion, have also to be considered: commutation laws between pilot, main and mixed modes in combustor fueling have to be considered in order to prevent such effects. Sensitivity to power off-take and air bleed, which can induce fuel–air ratio variations, also must be taken into account.

A re-light control system needs simulation models of extinction and light up capacities of the combustion. These transient models have to provide extinction detection and light up information. They integrate time-delay modeling for fuelling and spark operations, and combustion energy efficiency, which is correlated with the compression efficiency, fuel flow and engine power setting of the engine. Alarm temperature on turbine parts and engine rotor speed information generally is considered in this loop in order to detect a blow out risk or light up failure.

A particular aspect of the problem is the windmilling starting process, which requires:

- A precise knowledge of the airflow conditions at the combustor entry (pressure and temperature).
- After re-light, a good understanding of thermal and kinetic inertia of all other parts of the engine.

Of course, the control system and engine performance models have also to take into account the global variations in the quality of components such as the compressor, fueling system, combustor, sensor systems and others elements of the core engine.

Regarding the operational limits of the combustion, operation capacities and flame-out performances can be expressed in terms of fuel-air ratio and air-loading envelopes. These stability and re-light performance envelopes are determined from 3-D CFD combustion calculations, experimental results and engine tests. As spark energy intensity and frequency at the ignition plug system has a direct influence on the combustion re-light and light up performance, it is also taken into account by 3-D CFD. The windmilling envelope re-light capacity is directly derived from this, incorporating the compressor effects through a simulation model of the engine for these particular conditions.

Unsteady and instability effects of the combustion preceding the flame-out event are currently incorporated in these models. Due to recent progress in computing, Large Eddy Simulation CFD calculations are progressively supplying an improving representation of these phenomena and providing new methodologies for building such simulation models.

On another point, blow out and relight performances are directly affected by the variation in quality of components and fueling and air flow distortions at the combustor inlet. CFD simulations and specific rig tests of the hydraulic chain including pump, manifold, valves and injectors currently provide models for the fuel system. However, a multi-module coupled CFD analysis from compressor to the combustor exit is needed to provide a sensitivity analysis of blow out risk and relight capacity to component variations and flow distortions.

#### **B.3.2.2 Modeling Relight**

Today, empirical rules are used to determine the primary zone airflow rate required for an acceptable altitude relight capability. The size of an aircraft combustor is, for the major part, fixed by this capacity. Ignition begins when power is supplied to the igniter plug to make a spark inside the combustor. We can then distinguish four steps, which are necessary in order to restart the engine:

- The kernel formed by the spark must be able to burn. This is the result of the competition between energy losses (turbulent conduction outside the kernel, conduction to the droplets inside the kernel, evaporation, heat release chemical kinetics ) and the source of energy for the kernel (density of energy injected by the spark, energy coming from initiated combustion).
- Once the kernel is burning it must be captured by a stable eddy to maintain stable combustion. This process may be tuned by positioning of the igniter combined with the general flow organization.
- The flame, which is anchored to one sector of the combustor, must propagate to the whole combustor.
- When the flame has been established throughout the entire combustor, the combustion efficiency must be sufficient to ensure that the engine will accelerate. (Inertia and turbine/compressor power balance).

Failure of one single step will cause failure of the engine restart or re-light. For example doubling the energy to the igniter has no influence on the final ignition if step two fails. On the other hand optimizing the location of the igniter is a bad strategy if step one fails.

With only empirical rules that do not lead to any understanding of the underlying mechanism, significant improvements in ignition capability cannot be obtained. Note that if we are able to reduce the size of the combustor while keeping the ignition capacity constant, or improving it, we will have gains related to mass and weight because combustor chamber may be made more compact. For civil aircraft engines a reduction of combustor size can lead to reduction in  $\text{NO}_x$  emissions.

Making predictive models for this phenomenon becomes very hard when we try to connect the spark process through the related kernel growth to the turbulent flow inside the combustion. Many length scales

## ANNEX B – ADVANCED TOPICS AND RECENT PROGRESS

---

are involved with at least four orders of magnitude of difference. It is then impossible in the same computation to represent all those scales except with DNS (Direct Navier-Stokes) tools. Unfortunately due to CPU limitations DNS is not at present a viable strategy for the calculation of turbulent reactive two-phase flows with complex geometry in industrial applications, where Reynolds numbers are always high.

Once again, two-phase flow has a major role in the ignition process. If we consider step one in more detail we can see that the distribution of droplet size inside the ignition kernel will affect its future growth. This distribution is a function of the injector system and the location of the igniter inside the combustor. As already mentioned, the precise representation of the evaporation process inside the kernel is a key to success in building a reliable predictive computational tool. The method chosen at Snecma consists of: computing a two-phase flow with 3-D code to represent all the fields in the combustor related to engine windmilling before starting; applying a 1-D code at every point to determine the minimum ignition energy.

Although it is theoretically possible to make those computations by means of the PDF transport equation associated with detailed chemistry, we must keep in mind that we have to compute ignition curves corresponding to many points in the plane (fuel flow, air flow). Therefore, simplified methods are preferred.

### B.3.2.3 Combustion Efficiency and Compressor Limits

Combustion efficiency is mainly controlled by evaporation, mixing and chemical reaction. When the chemical reactions govern the combustion process, the theta parameter (air loading) obtained by A.H. Lefebvre [B.44], which is based on the burning velocity model in the primary zone, allows correlation of efficiency to the main operating variables (pressure, temperature, mass flow and geometry). J. Odgers [B.45] has also obtained an empirical correlation, which allows combustion efficiency to be represented as a function of the fuel loading.

When mixing governs the combustion process, a quasi-empirical correlation due to Tipler and Wilson [B.46] is very often used. It has been claimed by A.H. Lefebvre that at low pressures (100 KPa), combustion is governed by chemical reactions and at high pressures (>300 KPa), combustion is dominated by mixing. As jet engines operate in a wide range of operating conditions, combustion efficiency may be determined by chemical reactions, mixing or both at the same time.

During transient operation, fuel evaporation may become important when dealing with rapid or severe (slam acceleration) transients. Evaporation rates depend strongly on the Sauter Mean Diameter (SMD), which in turns depends on the fuel properties, flow rate, geometry, etc. A.H. Lefebvre gives some correlation to obtain the combustion efficiency when evaporation is predominant. Moreover during a transient, there is a heat flux between the gas and the surrounding material (convection and radiation). This heat transfer affects combustor efficiency. When predicting compressor surge, it is very important to know accurately the combustion efficiency. Compressor surge is a very fast process, therefore all factors affecting combustion must be taken into account.

Compressor surge is a major consideration in the design of gas turbine engines and their control systems. The compliance with specified operability constraints requires a high level of agreement between the different component characteristics (aerodynamics, thermal conduction...) and the related control commands. It is customary to use both transient simulation tools and rig tests (components, HP core, and bench engine). The prediction of the surge and operating lines during various fast transients is therefore required.

Models for engine transient behavior prediction are required for the determination of:

- The fuel and stator schedules during acceleration and deceleration, with the computation of the operating and surge lines.

- The available surge margin.
- Process viability, for example fuel cut-off and re-light transients, for surge recovery.

Stability margins are evaluated on the engine to ensure that sufficient margin is available to meet the operational requirements. Compression system surge lines may differ on the engine from the rig test because of differing dimensional, thermodynamic and dynamic properties. To characterize the engine installed HP compressor surge line position or shift the following method is commonly used. The fuel step technique allows HPC operating point to be moved very quickly towards the HPC surge line. By using the continuity equation in the choked turbine nozzle the compressor mass flow is then solved.

With the aforementioned applications in mind, the following investigations are of interest:

- Modeling of outlet temperature, efficiency, stability domain, relaxation time, and heat soak characteristics as a function of gradients in fuel, FAR, and inlet conditions.
- Method to analyze compressor operating line excursions during fuel step transients.

### **B.3.3 Reheat System**

#### **B.3.3.1 Stability and Blow-Out**

As for main combustors, fast transient from idle to full throttle operations can be severely restricted by flame blowout and instability in reheat system. There are different risks linked with this. From the pilot's viewpoint, and depending on the flight point considered, this phenomenon can be felt as an important and instantaneous lost of operability. This may lead to safety issues during heavily loaded take-off or dog-fight phases of flight. Less critical issues, such as thrust loss during supersonic operations, may also appear.

From the engine point of view and depending on the engine control system loop, the criticality of instability or a blowout varies. A local extinction or a local blow out of the combustion between different gutters of the flame holder system may have limited impact on the combustion efficiency and the thrust efficiency. However, due to consequential exhaust nozzle operation, the engine rating, the internal pressure of the reheat pipe, and eventually the compressor stall margin, the internal cooling distribution and the integrity of the liner, may all be affected. Due to the fuel release, it may also induce uncontrolled re-light phenomena in the nozzle or in the plume with undesirable effects on the infrared signature.

Reheat operability requirements expressed in terms of fuel-rate-range are generally defined through sub-domains and included into the flight envelope specifications, together with aircraft incidence parameters. These specifications have to integrate for instance the compressor stall margin transcribed in terms of maximum fuel rate and nozzle section amplitude. Complementary specifications on fuel temperature, and atmosphere conditions such as temperature and hygrometry also have to be taken into account.

All these conditions must be integrated in the global performance engine model in order to specify module performances, and control systems operation, and help to define in-flight re-light procedures. Sensitivity to various control options, especially for staged fueling and distribution laws of the fueling of the various manifolds and gutters of the flame-holder systems have also to be considered. Transient models have to integrate time-delay modeling for fuelling, spark and nozzle operations, reheat system energy efficiency variation and correlation with internal pressure, nozzle section, and fuel flow and engine speed.

Of course, these models have also to take into account the global variations in quality of components such as the fueling system, flame-holder geometry, by-pass ratio and nozzle section variations, regulation measurement systems and other elements of the engine.

## ANNEX B – ADVANCED TOPICS AND RECENT PROGRESS

---

With regard to the isolated module view of the reheat system, stability and blow out performance can be expressed in terms of fuel-air ratio and air-loading envelopes or limits. Specific sub-domains concerning fuel-staging modes of the different gutters and flame-holder regions are generally associated with these limits.

These stability and blow-out envelopes can be determined both from 3-D CFD calculations and experimental results on sub-components and engine tests.

Unsteady and instability effects of the combustion preceding the blow out or the unsteady process are currently incorporated in these models. Due to recent progress in computing, Large Eddy Simulation CFD calculations are progressively supplying a better representation of these phenomena and providing new methodologies for building such compartmental models. These may be further developed to take into account the influence of the aircraft incidence and the consequences on fan efficiency and combustion quality.

Blowout and stability performances are directly affected by the variations in the components of the fuelling system, by-pass ratio variations, and the vitiation and airflow distortions in mixer regions. CFD simulations and specific rig tests of the hydraulic chain including pump, manifold, valves and injectors currently provide compartmental models for the fuelling system.

### B.3.3.2 Screech and Rumble

Screech and rumble phenomena in reheat systems may impose severe mechanical stress on the engine and may rapidly create safety issues for the engine and the aircraft. Due to combustion and acoustically coupled effects, the combustion amplified energy release may induce extensive physical to the exhaust duct structure. Because of the closeness of fuel pipes and fuel tanks, these problems can directly affect aircraft safety.

These instabilities can suddenly appear during transient operations, like fuel staging or engine acceleration, and continue until the pilot or the control system switches off the reheat mode. These phenomena are generally amplified in regimes of high fuel-air-ratio. Hence, free-screech and free-rumble operating conditions have to be precisely defined in the engine cycle models. These conditions can be transcribed from terms of fuel rate and air-fuel ratio interaction limits into fuel operating and staging regulation and intake airflow conditions. These limits have to take into account fuel flow restrictions or staging options directly connected to the fuel-system operating-regime, and include margins for distortion effects and component variations.

Screech and rumble margin safety domains can be transcribed into fuel-air ratio or air-loading envelopes or limits. Specific sub-domains concerning fuelling staging modes of the different gutters and flame holder regions are generally associated with these limits.

Experiments on full-scale engines and sub-component tests are required to determine these limits and build compartmental models for the whole flight envelope. Large Eddy Simulation CFD calculations are also useful to confirm these limits.

Screech and rumble sensitivity are affected by variations in components which may influence the fuelling regions, the by-pass ratio variations, and the vitiation and air flow distortions at the core and bypass mixer. CFD simulations and specific rig tests of the hydraulic chain including pump, manifold, valves and injectors currently provide compartmental models for the fuelling system.

Transient aspects are generally considered through 1-D and 2-D transient global modeling of the engine. This is typically based on experimental data resulting from full engine and reheat component tests on other

engines. Inert and reactive 3-D and 2-D CFD calculations can also be considered for fuelling transient considerations.

#### *B.3.3.2.1 Modeling*

The problem of combustion instabilities is classical, difficult and critical. It is classical and has been under study for at least sixty years. The first large effort on the subject was in the area of rocket propulsion with solid fuel during the two decades following WWII. It is difficult because the same term in fact applies to a wide variety of mechanisms, coupling several physical phenomena such as combustion itself, convection, fuel atomization and vaporization, mixing, hydrodynamic instabilities and acoustics. It should be noted that instabilities are generally named after the way they sound to the ear, and not after the underlying mechanism, which is often complex and ill understood. Examples are groaning, screech, organ noise, chugging, and growl. The problem is critical because combustion oscillations may lead to very large disturbances that jeopardize combustor operability, especially for advanced, low-emission designs.

It is useful to consider a classification of instabilities in three groups:

- Intrinsic combustion instabilities;
- Chamber instabilities; and
- System instabilities.

Intrinsic instabilities deal with the combustion process itself. The LBO limit, and flashback or auto-ignition phenomena may be treated within this class. By definition these instabilities do not involve complex coupling between various physical phenomena, and the modeling challenge is not as difficult as with the two other types, which will be our main concern from now on.

Chamber instabilities involve, in a strong way, the acoustic eigenmodes of the combustor. Given the scales typically encountered in aeronautical combustors, these instabilities can also be identified as high frequency instabilities, which are based on a coupling between acoustics and combustion. Indeed the frequency range is related to the acoustic characteristic frequency  $c/L$ , where  $c$  is the speed of sound and  $L$  the size of the combustor. The speed of sound is the highest velocity scalar available, especially at high temperature, and frequencies tend to be high.

System instabilities involve the whole combustion system, which not only includes the combustor itself, but also the fuel line, injection system and exhaust. In the case of a full engine, the system can go as far as including elements of the compressor and turbine. This type of instability is the most difficult to tackle since the first difficulty is to choose the limit of the ‘system’ under study. These instabilities can also be referred to as low frequency instabilities. The time scale is defined either by the acoustics of the system, with longer length scales than the combustor alone, or by slower physical processes, such as hydraulics, convection or vaporization.

#### **B.3.3.3 High Frequency Instabilities**

We will identify high frequency instabilities with instabilities based on a strong coupling of the combustion with the cavity modes of the chamber. These instabilities have been known for a long time in rocket engines, and in jet engine reheat systems. As far as the main chamber of a jet engine is concerned, ‘high frequency’ instabilities could be relevant to organ noise problems, related to the first circumferential modes of an annular combustor.

Modeling approaches for these problems are typically based on writing a classical acoustic equation where the combustion influence is relegated to a source term [B.47]:

$$\nabla(c^2 \nabla p) - \frac{\partial^2 p}{\partial t^2} = H \quad \text{Eq. B-3}$$

Generally speaking the source term,  $H$ , is complex, and some techniques aim at providing a model for  $H$ . Before detailing this, it is useful to derive an acoustic energy transport equation, with a source term relating to [B.48]:

$$S \propto p' \dot{q}, \quad \text{Eq. B-4}$$

where  $p'$  is the acoustic pressure and  $\dot{q}$  the unsteady heat release rate. By integrating this over time, the classical Rayleigh criterion is obtained. A combustion oscillation tends to amplify if the heat release is in phase with the pressure. One approach consists in writing the heat release and pressure correlation in the  $(n, \tau)$  form initially proposed by Crocco [B.49]:

$$\dot{q}(t) = n \cdot p(t - \tau) \quad \text{Eq. B-5}$$

where  $n$  is a sensitivity factor and  $\tau$  a time lag accounting for the time it takes for the flame to respond to a pressure perturbation. This time lag typically includes convection or vaporization time, and could be measured. In principle, it is then possible to build instability models. The only information that needs to be evaluated is the  $(n, \tau)$  couple. However, the theory has the drawback that it implies a simple causal relationship between pressure or velocity fluctuation and flame response, while in a real instability the coupling is highly non-linear. Therefore, even with more complex definitions, the  $(n, \tau)$  nomenclature remains a formal description, which is more useful in forming a visual representation of the phenomenon of high frequency instabilities rather than in actually predicting it.

As high frequency instabilities are strongly linked to the acoustic eigenmodes of the combustor, these modes are useful information in themselves. Computing the modes will give no information as to which modes will actually be excited, but will at least identify the higher risk frequencies. Moreover, the spatial structure of these modes can suggest locations where passive-damping techniques may be more efficiently applied. The extraction of the acoustic modes of a cavity is a classical problem with well-known solutions for an homogeneous medium in basic geometric configurations. For application in combustors, more general solving techniques have been developed for arbitrary geometric configurations with a non-homogeneous base temperature (hence speed of sound) field [B.50]. Let us recall that the computed eigenmodes are the solution of equation (1) with no source term: it is supposed that the combustion oscillation simply locks onto a cavity mode, without strongly affecting it, which is of course a strong assumption.

A more difficult problem is to define boundary conditions, while it is relatively simple to define boundaries themselves. The only boundaries that are easily handled are rigid solid boundaries, or zero pressure conditions, which are both energy conserving. The nozzle throat or turbine in the case of rocket engines or afterburners, and the compressor and turbines in the case of the main combustor in a jet engine, lead to complex boundary conditions. Generally speaking they involve frequency-dependent impedance conditions, which are not so easily modeled. Models are available for various types of problem [B.51], but the boundary problem remains a critical point in these approaches.

Given that the basic acoustic modes were accurately captured, attempts have been made to account for a complex non linear interaction with combustion, namely by actually keeping the source term  $H$  in equation (1) and decomposing the perturbed modes on the free acoustic eigenbase. This is essentially Culick's approach [B.52]. Given the free cavity modes  $\Psi_n(x)$  associated to frequencies  $\omega_n$ :

$$\nabla(c^2 \nabla \Psi_n) + \omega_n^2 \Psi_n = 0 \quad \text{Eq. B-6}$$

The solutions perturbed (by combustion) are decomposed on the  $\Psi_n$  base:

$$p(x,t) = \sum_n a_n(t) \Psi_n(x) \quad \text{Eq. B-7}$$

Applying **Eq. B-3**, the amplitudes  $a_n(t)$  are solution of the following equation:

$$\left(\frac{d^2}{dt^2} + \omega_n^2\right) a_n(t) = \int H \cdot \Psi_n dV \quad \text{Eq. B-8}$$

Of course, with zero source term,  $a_n$  is a simple sine wave with frequency  $\omega_n$ . Let us assume that  $a_n$  has the form

$$a_n(t) = \exp(-i\omega t) \quad \text{Eq. B-9}$$

With no source term we recover of course  $\omega = \omega_n$ . The source term represents the influence of combustion and will therefore lead to a frequency shift (real part of the frequency), and a growth or decay (imaginary part of the frequency) of the eigenmode. Starting from an unperturbed acoustic mode computation, this method is therefore able to predict the alteration of the combustor acoustic modes by interaction with combustion, and provides the amplification factor of each modified mode. These are attractive features of the approach. On the other hand, all the difficulty consists in evaluating and modeling  $H$ , and more precisely response functions in the form  $H/a_n$ .

### **B.3.4 Liner Cooling**

Because of the interactions resulting from the reheat chamber pressure and the air flow distribution between the liner and the reheat system, it is necessary to consider a coupled approach to modeling the liner cooling and the mixing of the core and fan flows.

These two functions directly influence the reheat combustion efficiency, the global pressure drop performances and the cooling efficiency. They also may influence the core rating and performances.

1-D models can be sufficient to give an average representation of the exhaust and liner flow rates. However, because recent non axisymmetric flame-holder geometries and cooling configurations may also induce local pressure drop and flows distortions in the exhaust pipe, 2-D and 3-D CFD analyses may be necessary to build a derived compartmental model.

### **B.3.5 Cited References for Combustor Section**

- [B. 44] Lefebvre, H., “Gas Turbine Combustion”, Second Edition 1999 Taylor & Francis.
- [B.45] Odgers, J. and Carrier, C., “Modelling of Gas Turbine Combustors; Considerations of Combustion Efficiency and Stability”, Journal of Engineering for Power, pp. 105-113, April 1973.
- [B.46] Tipler, W. and Wilson, A.W., “Combustion in Gas Turbines”, Paper B9 in Proceedings of the Congrès International des Machines à Combustion (CIMAC), Paris, pp. 897-927, 1959.
- [B.47] Schönfeld, T. and Rudgyard, M.A., “Steady and Unsteady Flow Simulations Using the Hybrid Flow Solver AVBP”, AIAA Journal, 37(11), November 1999, pp. 1378-1385.
- [B.48] Schönfeld, T. and Rudgyard, M.A., “COUPL and Its Use within Hybrid Mesh CFD Applications”, Proc. of the 10th Intl Conference on Parallel CFD 98, pp. 433-440, Eds A. Ecer, D. Emerson,

## ANNEX B – ADVANCED TOPICS AND RECENT PROGRESS

---

J. Periaux and N. Satofuka, Elsevier Science Publishers, 1998, AIAA 98-1027, 36th AIAA Aerospace Sciences, January 12-15, 1998, Reno.

[B.49] Crocco, L. and Cheng, S.-I., “Theory of Combustion Instability Liquid Propellant Rocket Motor”, AGARDograph No. 8, 1956.

[B.50] Colin, O., Ducros, F., Veynante, D. and Poinso, T., “A Thickened Flame Model for Large Eddy Simulations of Turbulent Premixed Combustion”, Physics of Fluids 2000, In Press.

[B.51] Cazalens, M., Lecourt, R. and Quintilla, V., “Predicting Ignition Performance for Altitude Relight”, XV ISABE 2001, September 2-7 2001, Bangalore, Inde.

[B.52] Culick, F.E. and Yang, V., “Overview of Combustion Instabilities in Liquid-Propellant Rocket Engines”, Progress in Astronautics and Aeronautics, 169, 1995.

### B.3.6 Additional Bibliography for Combustor Section

Bray, K.N.C., “The Challenge of Turbulent Combustion”, 26th Symposium (International) on Combustion, The Combustion Institute, Pittsburgh, 1996, pp. 1-26.

Pitsch, H., Chen, M. and Peters, N., “Unsteady Flamelet Modeling of Turbulent Hydrogen-Air Diffusion Flames”, 27th Symposium (International) on Combustion, The Combustion Institute, Pittsburgh, 1998, pp. 1057-1064.

Barths, H., Peters, N., Brehm, N., Mack, A., Pfitzner, M. and Smiljanovski, V., “Simulation of Pollutant Formation in a Gas-Turbine Combustor Using Unsteady Flamelets”, 27th Symposium (International) on Combustion, The Combustion Institute, Pittsburgh, 1998, pp. 1841-1847.

Dopazo, C., “Turbulent Reacting Flows”, (Libby, P.A. and Williams, F.A., Eds), Academic Press, London, 1994, pp. 375-474.

Larroya, J.C., François, C., Cazalens, M. and Vervisch, L., “Testing a New Monte Carlo Method for Solving PDF Equation in Turbulent Combustion”, In 5th International Conference on Technologies and Combustion for a Clean Environment, Vol. I, pp. 177-183, 1999.

Leide, B. and Stouffs, P., “Residual Reactivity of Burnt Gases in the Early Expansion Process of Future Gas Turbines”, Gas Turbine and Power.

Visser, W.P.J. and Kluiters, S.C.M., “Modelling the Effects of Operating Conditions and Alternative Fuels on Gas Turbine Performance and Emissions”, Research and Technology Organisation, RTO-MP-14, 1999.

Ravet, F. and Vervisch, L., “Modelling Non-Premixed Turbulent Combustion in Aeronautical Engines using PDF Generator”, AIAA Paper # 98-1027, 36th AIAA Aerospace Sciences, January 12-15, 1998, Reno.

Cazalens, M., Beule, F. and David, E., “Design of Advanced Low Emission Combustor”, CEAS European Propulsion Forum Programme 2001.

Angelberger, C., Veynante, D., Egolfopoulos, F. and Poinso, T., “Large Eddy Simulations of Combustion Instabilities in Premixed Flames”, Proc. of the Summer Program 1998, Center for Turbulence Research, Stanford.

Williams, F.A., “Combustion Theory”, Menlo Park: Benjamin/Cummings, 1985.

Laverdant, Poinso, T. and Candel, S., "Influence of the Mean Temperature Field on the Acoustic Mode Structure in a Dump Combustor", J. Propulsion and Power, 2, pp. 311-316, 1986.

Vuillot, F. "Acoustic Mode Determination in Solid Rocket Motor Stability Analysis", AIAA Journal, July-August 1987.

## B.4 EXHAUST NOZZLE COMPONENT SYSTEMS

The nozzle exhaust system is a major component of an aircraft gas turbine powerplant. It is the device by which the energy from the gas generator is converted into useful thrust. It has efficiency just like other components. Turbofan and turbojet engines are especially sensitive to nozzle losses in because they operate on all of the flow from both an airflow and thrust standpoint. Careful design to keep losses low is necessary to achieve goal performance.

The exhaust nozzle component system serves the following functions in the aircraft gas turbine powerplant:

- The exhaust nozzle component contains the exit throttling area (throat) of the powerplant. It meters flow and sets the turbine back-pressure, thereby controlling turbine work. It is one of the primary metering areas in the engine, regulating the cycle. For the case of a dual stream bypass engine, the exit nozzle is the principle controller of the back-pressure to the fan thereby setting fan pressure ratio.
- The nozzle functions as an aerodynamic component that accelerates the gas exiting the turbine to produce thrust from available energy (see **Figure B.66**).
- A variable area nozzle plays an important role in providing optimum performance and assuring engine operability. Variable throat area is essential for control of engine matching and fan back-pressure during augmentation.
- A variable geometry nozzle can be designed to generate pitch and yaw forces to control the air vehicle.
- The exhaust nozzle can be designed to produce reverse thrust.

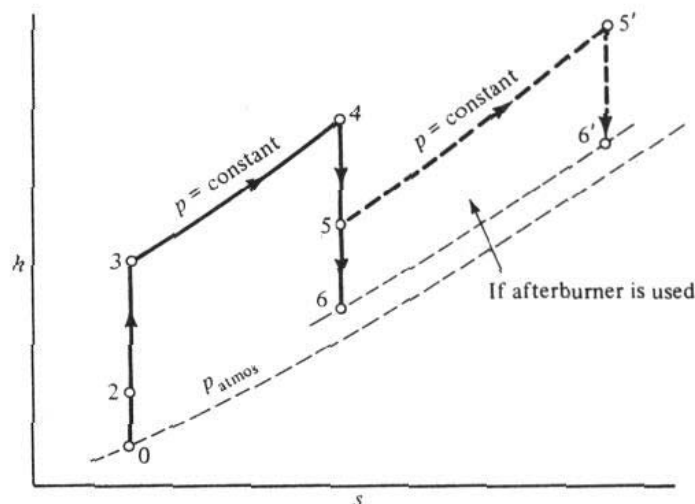


**Figure B.66: Energy Available to Produce Thrust from Thermodynamic Cycle.**

This chapter will develop and define the standard theory and practice for assessing exhaust system performance in aircraft gas turbine engine analytical simulations. That is, the analytical determination of

the efficiency of the exhaust and nozzle systems in passing flow and producing thrust. We begin with a simple single-stream turbojet and continue to more complex dual stream and variable geometry examples.

### B.4.1 Zero Dimensional Analysis

#### B.4.1.1 Definition of Nozzle Coefficients

Definition and evaluation of the gross and specific thrust and flow coefficients requires a definition of ‘ideal’ thrust. The ideal thrust can be defined on a basis of an ideal convergent/divergent nozzle, an ideal convergent nozzle, or variations in between. It is recommended that the ideal thrust be defined based on fully expanded convergent/divergent nozzle theory.

The true performance of the nozzle system remains of course unchanged by the choice of the ideal definition; often the ideal definition is simply a choice of a reference datum for bookkeeping purposes. However, it is also a measure of maximum potential of the nozzle component to produce thrust. Insight into potential nozzle system improvements may be gained by analysis and understanding of the various real gas and mechanical design effects causing the actual thrust and nozzle coefficient to be less than ideal.

#### B.4.1.2 Single Stream Exhaust System

Gas turbine rotating machinery produces hot gas at the turbine exit, station 5, shown schematically for a single-stream turbojet engine in **Figure B.67**.

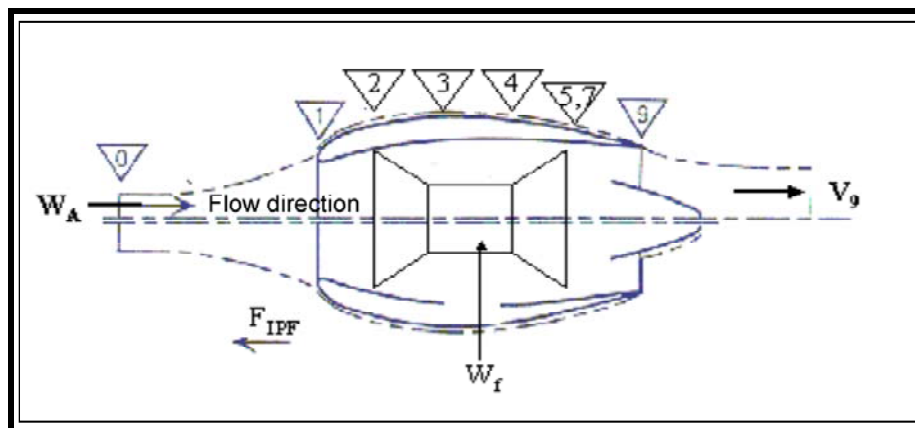


**Figure B.67: Turbojet Schematic Showing Engine and Nozzle Station Designations.**

For this simple configuration the forward boundary of the nozzle component, Station 7 (also called the nozzle ‘charging station’), coincides with the turbine exit Station 5. The nozzle throat is designated Station 8 and the nozzle exit, Station 9. Station designations between 5 and 7 are reserved for ducting, mixers, and augmentors in more complicated engine configurations.

The gas flow at the turbine exit consists of combustion products produced by air entering the engine minus any leakage and customer bleed prior to Station 7 plus the fuel flow entering the combustor.

$$W_{g7} = W_2 - W_{bl} + W_f \quad \text{Eq. B-10}$$

The total energy available for thrust is equal to  $W_{g7} * h_{t7}$  where  $h_{t7}$  is the total specific enthalpy of the turbine exit gas.

The gas expands through the nozzle to ambient pressure at Station 9 for a fully expanded ideal convergent/divergent nozzle. This acceleration process transforms available heat energy in the gas to kinetic energy in the expanding jet, which produces useful thrust to propel the aircraft.

The flow velocity at the nozzle exit will be:

$$V_{9,ideal} = \sqrt{2 * (h_{t7} - h_{amb})} \quad \text{Eq. B-11}$$

The resultant ideal gross thrust is:

$$F_{g9,ideal} = W_{g7} * V_{9,ideal} \quad \text{Eq. B-12}$$

The ideal gross thrust can also be evaluated as a function of nozzle pressure ratio:

$$F_{g9,ideal} = W_{g7} * M_9 * a_9 = W_{g7} * \sqrt{T_{t7}} * f_1(\gamma, R, P_{t7} / P_{amb}) \quad \text{Eq. B-13}$$

Where  $M_9$  and  $a_9$  are the corresponding Mach number and speed of sound for the exhaust gas expanded to ambient conditions at the nozzle pressure ratio,  $P_{t7}/P_{amb}$ .

$$F_{g9,ideal} = \left[ F_{g9} / (W_{g7} * \sqrt{T_{t7}}) \right]_{ideal} W_{g7} * \sqrt{T_{t7}} \quad \text{Eq. B-14}$$

$[F_{g9}/(W_{g7} * \sqrt{T_{t7}})]_{ideal}$  developed in **Eq. B-14** is called the ‘ideal specific thrust parameter’ and is an analytic function of isentropic exponent, gamma, gas constant and nozzle pressure ratio.

An alternate equivalent expression for gross thrust, based on full expansion, is

$$F_{g9,ideal} = \left[ F_{g9} / (A_8 * P_{amb}) \right]_{ideal} * A_8 * P_{amb} \quad \text{Eq. B-15}$$

$[F_{g9}/(A_8 * P_{amb})]_{ideal}$  in **Eq. B-15** is called the ‘ideal thrust function’ and is a second analytic function of gamma, gas constant and nozzle expansion ratio.

These definitions are used for both converging and converging/diverging (C/D) nozzles, both choked and unchoked. The definitions assume that the controlling area of the nozzle is at station 8. However, for an unchoked C/D nozzle, the controlling area shifts to station 9. Because of this shift, it is not unusual to calculate nozzle throat flow (discharge) coefficients greater than unity for unchoked C/D nozzles.

The expansion process in real nozzles is not isentropic. Losses occur relative to the ideal, because of real gas effects and other reasons listed below:

- Leakage;
- Cooling;
- Thermal expansion;
- Reverser links;
- Steps and gaps;
- Surface roughness and friction;
- Acoustic treatment;

## ANNEX B – ADVANCED TOPICS AND RECENT PROGRESS

- Gas mixing;
- Temperature profile;
- Pressure profile;
- Non-axial exit flow vector;
- Swirl;
- Over or under expansion;
- Shock losses; and
- Separation.

Because of these losses, the actual thrust is less than the ideal.

The nozzle gross thrust coefficient that quantifies this loss is defined as:

$C_g$  is called the ‘gross thrust coefficient’ and can be expressed as

$$C_g = F_{g9,actual} / F_{g9,ideal} \quad \text{Eq. B-16}$$

$C_g$  can also be expressed as:

$$C_g = [F_g / (A_{8,actual} * P_{amb})]_{actual} / [F_g / (A_{8,ideal} * P_{amb})]_{ideal} \quad \text{Eq. B-17}$$

Actual nozzle gross thrust can be evaluated using **Eq. B-18** if  $C_g$  is known.

$$F_{g9,actual} = [F_g / (A_8 * P_{amb})]_{ideal} * C_g * A_8 * P_{amb} \quad \text{Eq. B-18}$$

The actual gas flow will also be less in a real nozzle than in an ideal nozzle. The ‘flow’ coefficient,  $C_d$ , quantifies this loss, **Eq. B-19**.

$$\begin{aligned} C_d &= W_{g7,actual} / W_{g7,ideal} = A_{8,ideal} / A_{8,actual} \\ &= [W_{g7} * \sqrt{T_{t7}} / (A_8 * P_{t7})]_{actual} / [W_{g7} * \sqrt{T_{t7}} / (A_8 * P_{t7})]_{ideal} \end{aligned} \quad \text{Eq. B-19}$$

The specific thrust coefficient,  $C_v$  is defined in **Eq. B-20**.

$$C_v = [F_g / (W_{g7} * \sqrt{T_{t7}})]_{actual} / [F_g / (W_{g7} * \sqrt{T_{t7}})]_{ideal} \quad \text{Eq. B-20}$$

An alternate equivalent method to calculate gross thrust uses the ‘specific thrust coefficient’,  $C_v$ .

$$F_{g9} = [F_g / (W_{g7} * \sqrt{T_{t7}})]_{ideal} * C_v * W_{g7} * \sqrt{T_{t7}} \quad \text{Eq. B-21}$$

Actual gross thrust expressions defined by equations 8 and 11 are equivalent.

$$C_v = \frac{F_{g9,actual} / (W_{g7} * \sqrt{T_{t7}})_{actual}}{F_{g9,ideal} / (W_{g7} * \sqrt{T_{t7}})_{ideal}} = C_g * \frac{(W_{g7} * \sqrt{T_{t7}})_{ideal}}{(W_{g7} * \sqrt{T_{t7}})_{actual}} = \frac{C_g}{C_d}$$

The relationship between the coefficients is given by **Eq. B-22**.

$$C_g = C_v * C_d \quad \text{Eq. B-22}$$

From the definition of  $C_g$ , **Eq. B-17**, the following correlation may be derived:

$$\begin{aligned} C_g &= F_{g9,actual} / F_{g9,ideal} = [W_{g7} * V_9]_{actual} / [W_{g7} * V_9]_{ideal} \\ &= C_d * [V_{9,actual} / V_{9,ideal}] \end{aligned} \quad \text{Eq. B-23}$$

Comparing **Eq. B-22** with **Eq. B-23**, shows that:

$$C_v = [V_{9,actual} / V_{9,ideal}] \quad \text{Eq. B-24}$$

Therefore the specific thrust coefficient,  $C_v$ , is also the ratio of actual to ideal jet velocity and is commonly referred to as the ‘velocity coefficient’, **Eq. B-22**. This relationship is very useful to adjust to actual thrust in cycle-match computer simulations where the ideal jet velocity is calculated from energy deltas, **Eq. B-11**.

#### B.4.1.3 Thrust Definitions

A control volume for a single stream turbojet is shown in **Figure B.68**.

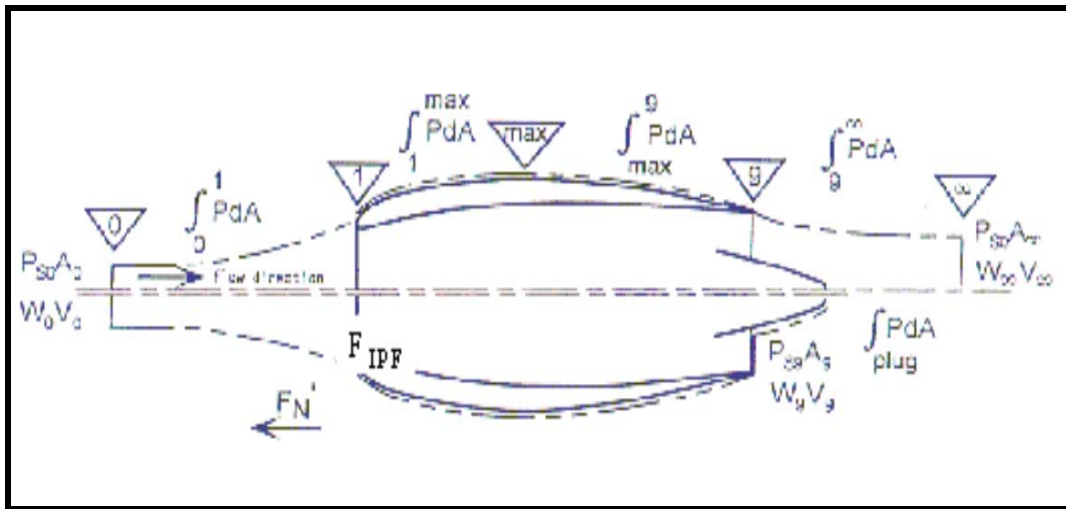


**Figure B.68: Single Stream Control Volume for Thrust Definition.**

The sum of the forces called ‘Installed Propulsive Force’, ( $F_{IPF}$ ), acting on the single stream turbojet control volume shown in **Figure B.68** is

$$F_{IPF} = -A_0 P_{amb} - W_0 * V_0 + \int_0^1 P_s * dA + \int_1^{\max} P_s * dA + \int_{\max}^9 P_s * dA + A_9 * P_{s9} + W_9 * V_9 + \int_{plug} P_s * dA \quad \text{Eq. B-25}$$

Friction has been set to zero to simplify the equation.

## ANNEX B – ADVANCED TOPICS AND RECENT PROGRESS

Algebraic adjustment, to refer pressure forces to ambient, yields:

$$F_{IPF} = -W_0 * V_0 + \int_0^1 (P_s - P_{amb}) * dA - \int_1^{\max} (P_s - P_{amb}) * dA + \int_{\max}^9 (P_s - P_{amb}) * dA$$

$$+ A_9 * (P_{s9} - P_{amb}) + W_9 * V_9 + \int_{plug} (P_s - P_{amb}) * dA$$

**Eq. B-26**

The terms in **Eq. B-26** are also known as:

Ram Drag  $-W_0 * V_0$

Additive Drag  $\int_0^1 (P_s - P_{amb}) * dA$

Lip Suction  $\int_1^{\max} (P_s - P_{amb}) * dA$

Exhaust Recompression Force  $\Delta F_{EXH} \int_{\max}^9 (P_s - P_{amb}) * dA$

Engine Gross Thrust  $F_{gg} A_9 * (P_{s9} - P_{amb}) + W_9 * V_9 + \int_{plug} (P_s - P_{amb}) * dA$

Spillage drag  $\Delta F_{INL}$  is the sum of additive drag and lip suction.

$$F_{IPF} = -W_{a0} * V_0 + \underbrace{\int_0^1 (P_s - P_{amb}) dA}_{\text{ADDITIVE DRAG}} - \underbrace{\int_1^{\max} (P_s - P_{amb}) dA}_{\text{LIP SUCTION}} + \int_{\max}^9 (P_s - P_{amb}) dA$$

$$\underbrace{-W_{a0} * V_0}_{\text{RAM DRAG}} \quad \underbrace{- \int_1^{\max} (P_s - P_{amb}) dA}_{\text{INLET SPILLAGE DRAG}} \quad \underbrace{+ \int_{\max}^9 (P_s - P_{amb}) dA}_{\text{EXHAUST RECOMPRESSION FORCE}}$$

$$+ A_9 (P_{s9} - P_{amb}) + W_9 * V_9 + \int_{plug} (P_s - P_{amb}) dA = F_{IPF}$$

**ENGINE GROSS THRUST**

**Eq. B-27**

$$= F_{G9}$$

**Eq. B-26** and **Eq. B-27** do not account for friction forces. Including friction uses the definition of  $\Phi$  which describes the axial force component of the combined pressure and friction force on a surface in axisymmetric flow:

$$\Phi = \int_{surface} [(P_s - P_{amb}) + \tau * \cot \Theta] * dA$$

**Eq. B-28**

where,  $\Theta$  = angle between free stream flow direction and plane tangent to the surface element  $ds$

$\tau$  = shear stress acting on surface element  $ds$

$dA = \sin\Theta \, ds$  = area of a surface element  $ds$  projected on a plane normal to the free stream flow direction

Rewriting **Eq. B-28** including friction forces leads to **Eq. B-29**:

$$F_{IPF} = -W_0 * V_0 + \int_0^1 (P_s - P_{amb}) * dA - \Phi_{inlet} + \Phi_{Exhaust} + A_9 * (P_{s9} - P_{amb}) + W_9 * V_9 + \Phi_{Plug} \quad \text{Eq. B-29}$$

The installed propulsive force  $F_{IPF}$  acting on the pylon consists of engine net thrust reduced by nacelle drag and is equal to the airframe system drag,  $D_{afs}$ , **Eq. B-30**. SAE AIR 1703, [B.53].

$$F_{IPF} = F_{g9} - W_0 * V_0 - \Delta F_{INL} - \Delta F_{EXH} = D_{afs} \quad \text{Eq. B-30}$$

The powerplant net thrust,  $F_n$ , is defined in **Eq. B-31**.

$$F_{net} = F_{g9} - W_0 * V_0 \quad \text{Eq. B-31}$$

Summarizing for the single stream turbojet:

$$F_{g9} = [W_9 * V_9]_{actual} - A_9 * (P_{s9} - P_{amb}) + \int_{plug} (P_s - P_{amb}) * dA \quad \text{Eq. B-32}$$

$$= [F_{g9} / (A_8 * P_{amb})]_{ideal} * C_g * A_8 * P_{amb} \quad \text{Eq. B-33}$$

$$= [F_{g9} / (W_{g9} * \sqrt{T_t})]_{ideal} * C_v * W_{g7} * \sqrt{T_{t7}} \quad \text{Eq. B-34}$$

$$= W_{g7,actual} * V_{9,ideal} * C_v \quad \text{Eq. B-35}$$

$$= W_{g7} * C_v * \sqrt{2 * (h_{t7} - h_{amb})} \quad \text{Eq. B-36}$$

A representative plot of the nozzle coefficients is shown in **Figure B.69**.

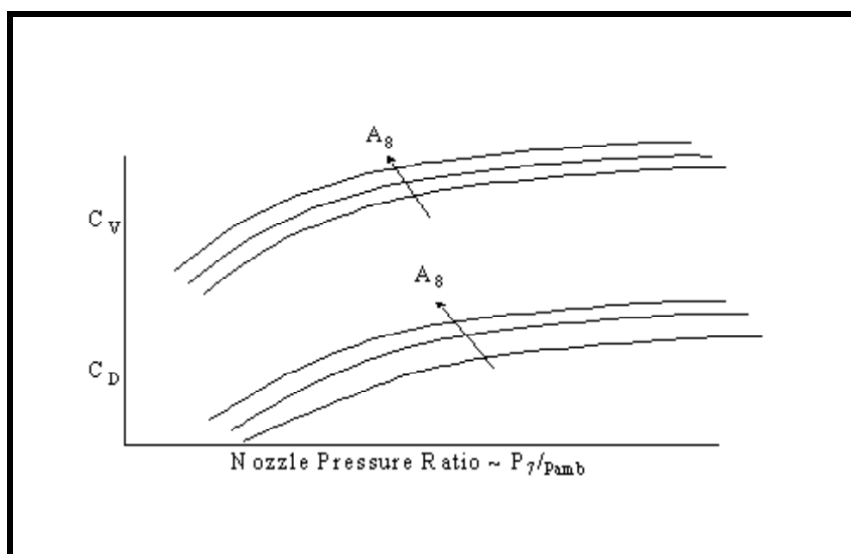


**Figure B.69:** Representative Thrust and Flow Coefficients vs. Nozzle Pressure Ratio.

## B.4.1.4 Dual Stream Engine Configuration

The foregoing relationships can be extrapolated to dual-stream by-pass engines (see **Figure B.70**). Station numbers in the bypass stream are similar to those in the primary stream but increase by ten; e.g. station 9 primary becomes station 19 in the by-pass duct. Force accounting and thrust definitions are shown in **Eq. B-38**, the no friction case.

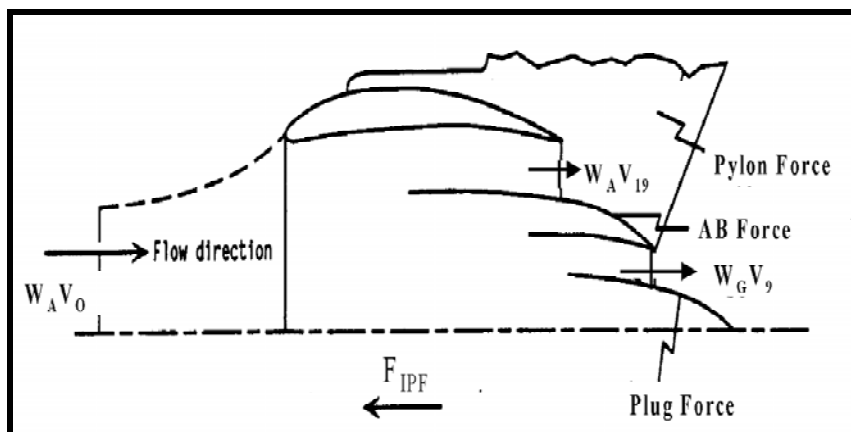


**Figure B.70:** Schematic of a Dual-Stream Bypass Engine.

$$\begin{aligned}
 F_{IPF} = & -W_{a0} * V_0 + \underbrace{\int_0^1 (P_s - P_{amb}) dA}_{\text{ADDITIVE DRAG}} - \underbrace{\int_1^{\max} (P_s - P_{amb}) dA}_{\text{LIP SUCTION}} + \int_{\max}^9 (P_s - P_{amb}) dA \\
 & \underbrace{= F_R}_{\text{RAM DRAG}} \quad \underbrace{\text{INLET}}_{\text{SPILLAGE DRAG} = \Delta F_{INL}} \quad \underbrace{\text{EXHAUST}}_{\text{RECOMPRESSION FORCE} = \Delta F_{EXH}} \\
 & + A_9 (P_{s9} - P_{amb}) + W_9 * V_9 + \int_{\text{external plug}} (P_s - P_{amb}) dA \\
 & \underbrace{\hspace{10em}}_{\text{PRIMARY STREAM GROSS THRUST} = F_{G9}} \\
 & + A_{19} (P_{s19} - P_{amb}) + W_{19} * V_{19} + \underbrace{\int_{\text{core cowl}} (P_s - P_{amb}) dA}_{\text{BYPASS STREAM GROSS THRUST} = F_{G19}}
 \end{aligned}$$

**Eq. B-37**

$$\begin{aligned}
 F_{IPF} = & -W_0 * V_0 + \int_0^1 (P_s - P_{amb}) * dA + \int_1^{\max} (P_s - P_{amb}) * dA + \int_{\max}^9 (P_s - P_{amb}) * dA \\
 & + A_9 * (P_{s9} - P_{amb}) + W_9 * V_9 + \int_{\text{plug}} (P_s - P_{amb}) * dA \\
 & + A_{19} * (P_{s19} - P_{amb}) + W_{19} * V_{19} + \int_{\text{core cowl}} (P_s - P_{amb}) * dA
 \end{aligned}$$

**Eq. B-38**

The terms in **Eq. B-38** are also known as:

Ram Drag  $-W_0 * V_0$

Additive Drag  $\int_0^1 (P_s - P_{amb}) * dA$

Lip Suction  $\int_1^{\max} (P_s - P_{amb}) * dA$

Exhaust Recompression Force  $\Delta F_{EXH} \int_{\max}^9 (P_s - P_{amb}) * dA$

Primary Stream Gross Thrust  $F_{G9}^* A_9 * (P_{s9} - P_{amb}) + W_9 * V_9 + \int_{\text{plug}} (P_s - P_{amb}) * dA$

Bypass Stream Gross Thrust  $F_{G19}^* A_{19} * (P_{s19} - P_{amb}) + W_{19} * V_{19} + \int_{\text{core cowl}} (P_s - P_{amb}) * dA$

## ANNEX B – ADVANCED TOPICS AND RECENT PROGRESS

Spillage drag  $\Delta F_{INL}$  is the sum of additive drag and lip suction.

If friction forces are included, then **Eq. B-38** becomes

$$F_{IPF} = -W_0 * V_0 + \int_0^1 (P_s - P_{amb}) * dA - \Phi_{inlet} + \Phi_{Exhaust} +$$

$$+ A_9 * (P_{s9} - P_{amb}) + W_9 * V_9 + \Phi_{plug}$$

$$+ A_{19} * (P_{s19} - P_{amb}) + W_{19} * V_{19} + \Phi_{core cowl}$$

**Eq. B-39**

Inlet and exhaust system forces defined in installed propulsive force equations (**Eq. B-25**, **Eq. B-30**, and **Eq. B-39**) have been accounted entirely as thrust terms to the propulsion system for bookkeeping. They are customarily apportioned partially to the propulsion system and partially to the airframe system depending on the scope of scale model tests done to define the thrust-drag bookkeeping system. Further details may be found in references SAE AIR 1703 [B.53] and SAE AIR 5020 [B.54].

A PW4000 two-stream separate nozzle flow example is shown in **Figure B.71**.

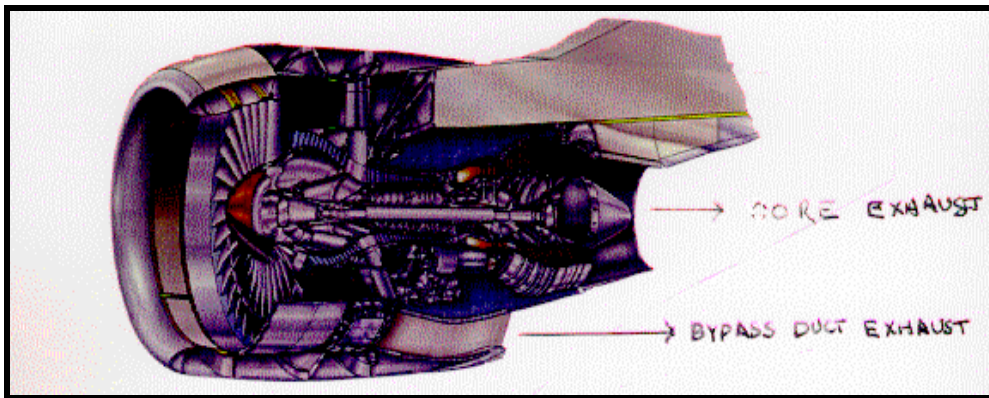


**Figure B.71:** PW4000 Example of Dual-Stream Exhaust System.

### B.4.1.5 Mixed Flow Example

A schematic of a two-stream mixed flow powerplant is shown in **Figure B.72**. For this case, the primary and by-pass flows mix before they enter the nozzle. The mixing process in a particular configuration is further complicated if augmentation is also present. These processes must be precisely defined to produce average pressure, temperature, and gas constituents entering the nozzle charging station. Systematic errors in these calculations will be transferred to the nozzle and complicate understanding between measured (real) and ideal conditions. The mixed configuration is then handled the same as for a single stream engine. **Figure B.73** and **Figure B.74** show examples of mixed flow configurations. **Figure B.75** shows an example with an augmentor in the F100.

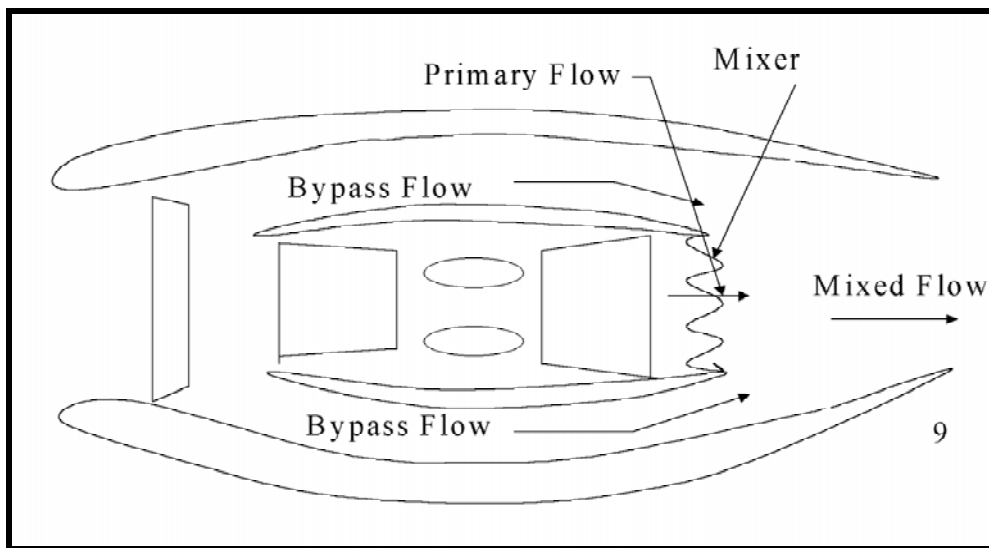


Figure B.72: Schematic of Mixed Flow Turbofan Engine.

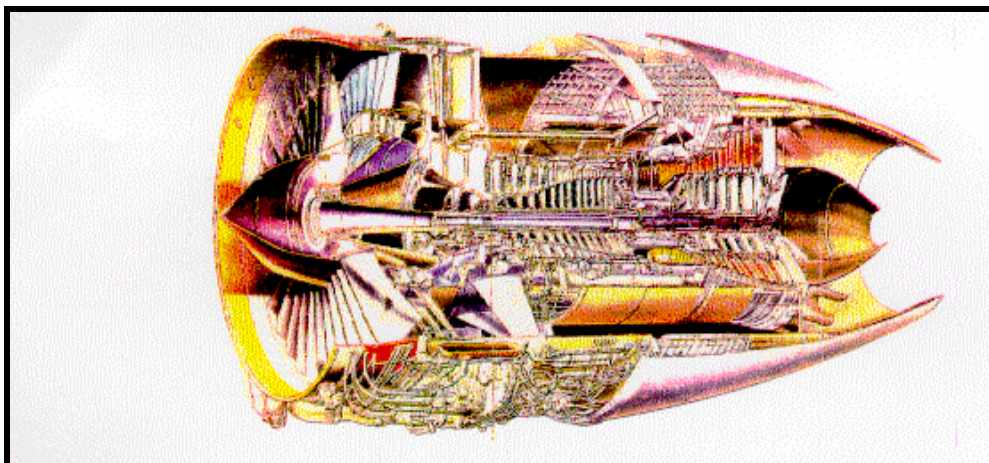


Figure B.73: Mixed Flow Configuration Example, PS-90P.

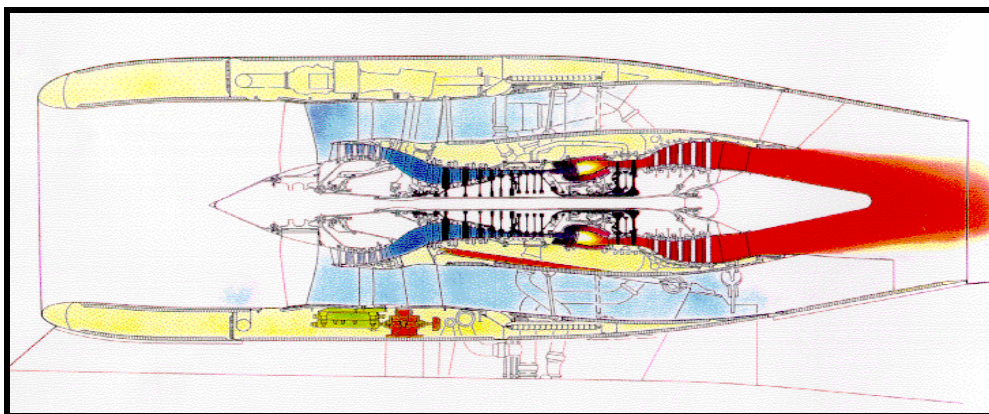
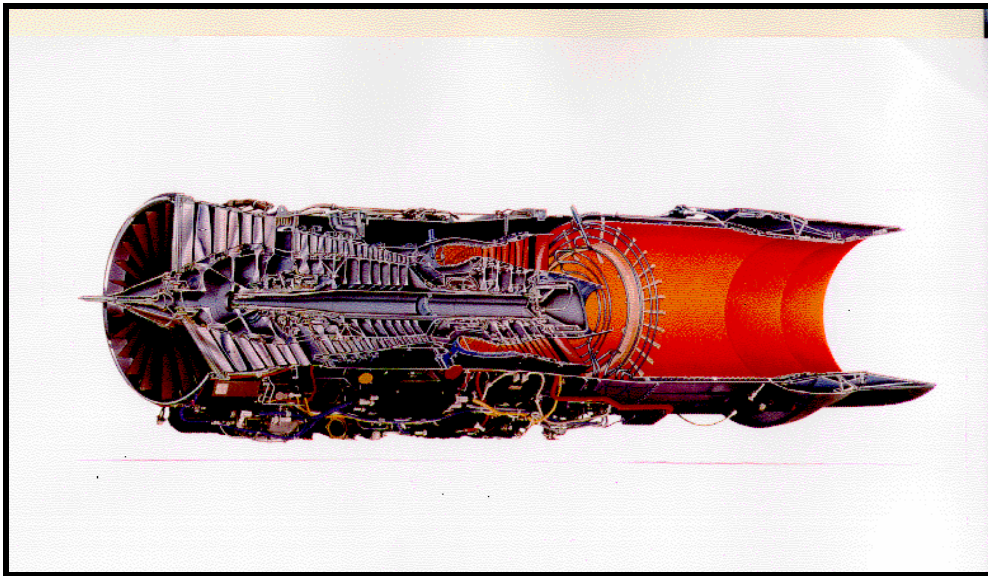


Figure B.74: Mixed Flow Example, V-2500.



**Figure B.75:** Military Mixed Flow with Augmentor Example, PW-F-100.

Modern military aircraft need extensive cooling in the nozzle, which must be accounted for in the definition of ideal thrust and flow coefficients.

### B.4.1.6 Evaluation of Nozzle Coefficients

Nozzle coefficients discussed in the foregoing paragraphs are measured using a full-scale engine testing in sea level and altitude test facilities, **Figure B.76** and **Figure B.77**. They are also measured using sub-scale models tested in rigs and wind tunnels. Methodology for doing this utilizes the same definitions and equations as discussed above. For evaluation testing, however, the thrust and airflow are measured and the nozzle coefficients calculated. The coefficients are then used in the engine simulation and aircraft in-flight thrust determination process. Methods and examples for determining nozzle coefficients are described in detail in references **[B.53, B.54 and B.55]**.

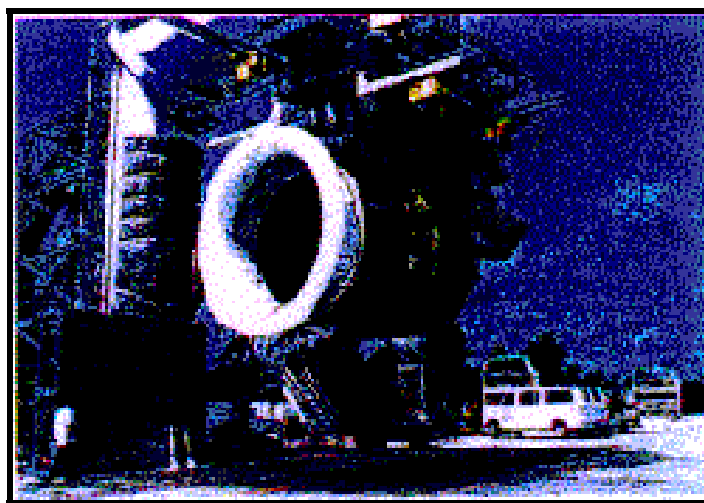


**Figure B.76:** Sea Level Engine Test Facility to Measure Thrust, Airflow and Nozzle Coefficients.

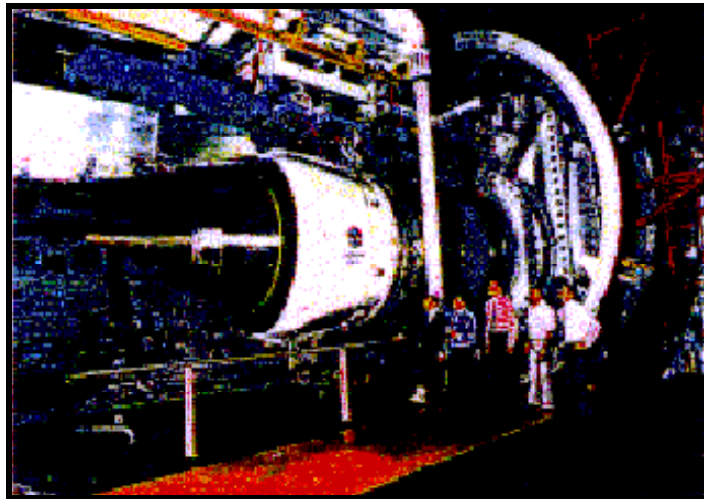


**Figure B.77: Altitude Engine Test Facility to Measure Thrust, Airflow, and Nozzle Coefficients.**

When measuring nozzle coefficients, in either the full-scale engine or sub-scale model, the test measurement and data analysis process must account for the differences between the test article and the flight engines, see the earlier list. Scale models must be corrected to (adjusted to full scale) and measurements in full-scale engines must be designed to provide, or be adjusted to, an average one-dimensional  $T_7$  or  $P_7$  value, for example. Any error in adjusting the measurements will be propagated to the nozzle coefficient through the calculation of ideal thrust and airflow, [B.55].

## B.4.1.7 Variable Nozzle Benefits and Examples

The calculation for thrust and performance for all foregoing definitions are applicable for variable geometry nozzles. The nozzle coefficients are a function of both nozzle expansion ratio and jet area. The coefficients must be measured during full-scale engine or sub-scale model testing. The F-100 military-turbofan engine, shown in Figure B.75, provides an example of a variable geometry nozzle.

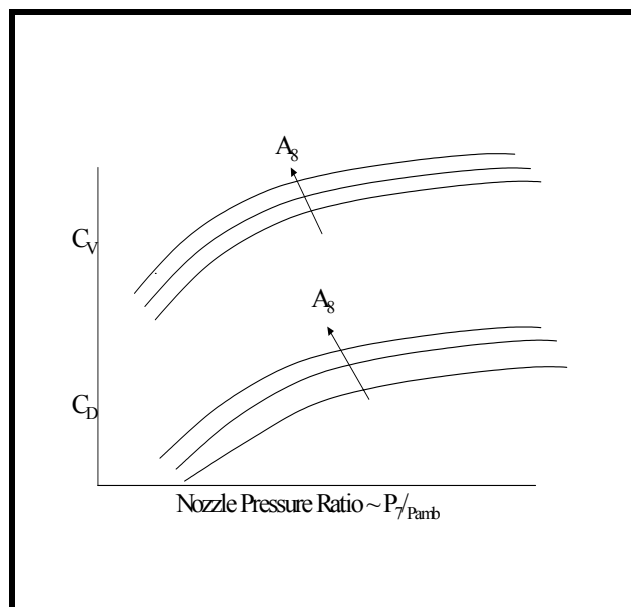


**Figure B.78: Nozzle Coefficients with Variable Jet Nozzle Area.**

A variable jet nozzle area is of benefit to aircraft gas turbine engines for three reasons:

- 1) **Operability** – The variable geometry nozzle is used to regulate the backpressure to the fan thereby maintaining stall free operation throughout the operating envelope. This is especially important for an engine with augmentation. The jet area must be increased when the afterburner is operating to maintain stall free fan operation. This accomplished with modern control systems by closed loop logic, where pressure ratio measured with high response transducers, is maintained by control of a variable nozzle area.
- 2) **Performance Optimization** – Since the nozzle throat meters the exit flow, it regulates the backpressure of the gas generator. Variation of the backpressure affects the cycle match and therefore powerplant thermal efficiency. The throat area also affects jet velocity, which impacts propulsive efficiency. A variable throat area may be optimized to provide best performance at a given flight condition. Generally, non-augmented engines require minimal or no throat area variation to optimize engine thrust. Augmented engines, however, require throat areas as much as 100% larger than the corresponding non-augmented area.

Improved performance may also be obtained from a variable expansion ratio (exit area) convergent/divergent nozzle when a large operating range of nozzle pressure ratio (NPR) is required (most transonic/supersonic vehicles), see [Figure B.78](#). The maximum thrust that the nozzle can produce for a given expansion ratio is obtained when the nozzle flow is fully expanded to ambient pressure at station 9 (see [Figure B.79](#)). The potential improvement for a convergent-divergent nozzle relative to a convergent nozzle is a function of nozzle pressure ratio. It may be calculated as the ratio of the ideal thrust functions and is shown in [Figure B.80](#). The actual improvement for a convergent/divergent section will be reduced because of additional pressure loss. Inspection of [Figure B.78](#) shows that the convergent nozzle is better than the C/D nozzle at low nozzle-pressure ratios. The improvement for a C/D nozzle occurs when the C/D nozzle over-expansion losses are less than the convergent nozzle under-expansion losses.

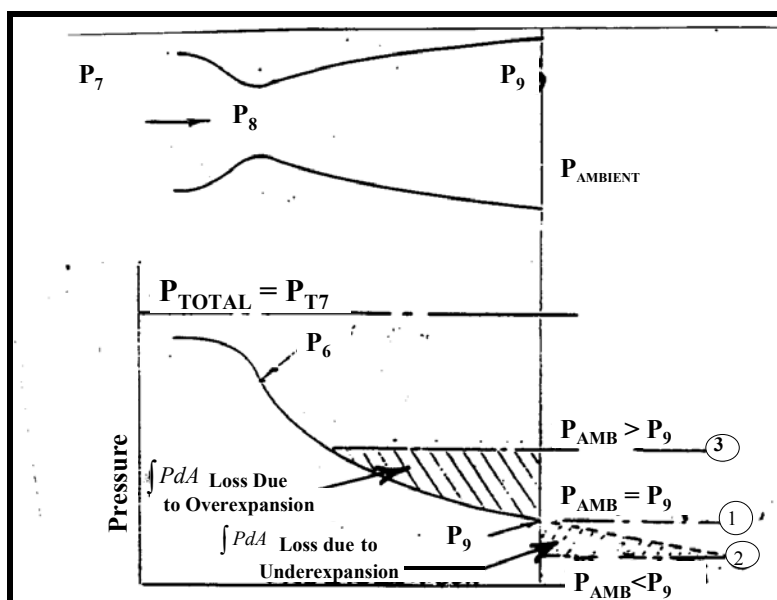


**Figure B.79:** Schematic Showing Pressure-Forces on C-D Divergent Section.

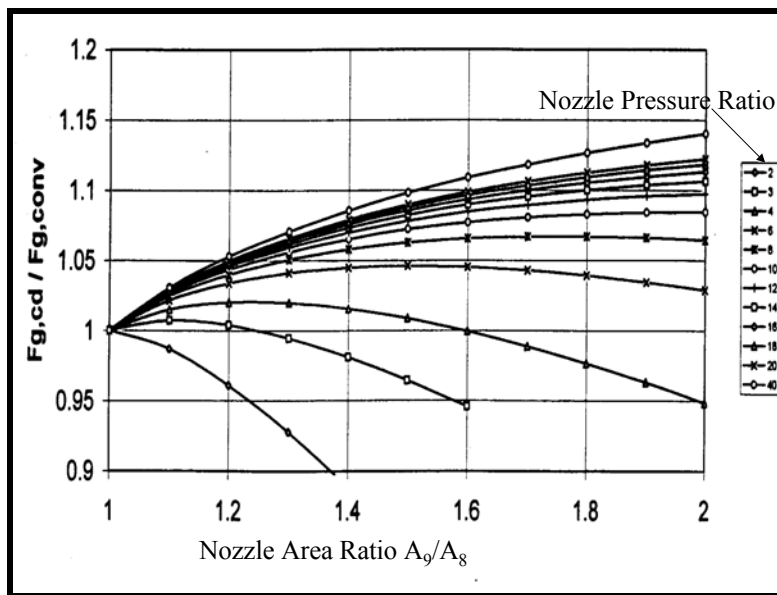


**Figure B.80:** Theoretical Improvement for C-D Relative to a Convergent Nozzle.

Commercial and transport engines are normally high bypass – low nozzle pressure ratio configurations to maximize propulsive efficiency and reduce fuel consumption. They do not have augmentors or operate over a large range of nozzle pressure ratio so variable nozzle areas are not required. The optimum nozzle is usually a convergent or fixed convergent/divergent with a small area ratio.

High thrust-to-weight ratio military engine configurations operate over a much wider range of nozzle pressure ratios and flight Mach numbers, and benefit greatly from variable-area-ratio nozzles.

- 3) **Air Vehicle Maneuverability** – The nozzle may be designed to turn the exhaust thrust vector to provide forces in the pitch and yaw directions as well as the normal thrust direction. This feature may be used by the pilot to direct additional pitch and yaw control to the aircraft. Special configurations may also provide lift control. An example is provided by the F-119-PW-100 shown in **Figure B.81**.

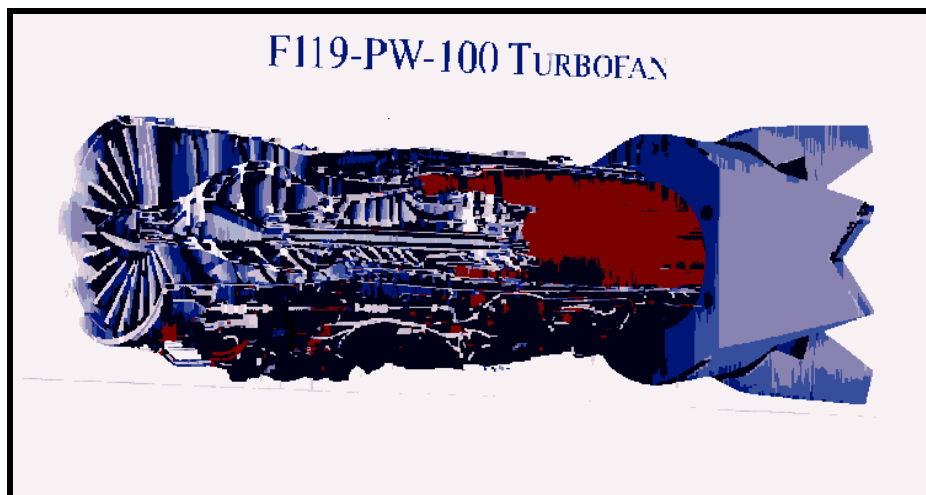


**Figure B.81:** F-119 Example.

## B.4.2 Multi-Dimensional Considerations for Variable Area Nozzle Simulation

The foregoing discussions have been focused on a ‘zero’ dimensional simulation of the nozzle wherein all nozzle losses have been accounted for in the thrust and flow coefficients, based on an ideal flexible convergent/divergent nozzle. Simulation of an engine with variable geometry nozzles (which include all engines with reheat) may be sufficiently complicated as to require consideration of the true nozzle geometry, internal nozzle mechanical characteristics and aerothermodynamic processes for accurate results. For that case, a one (or greater) dimensional treatment of the nozzle is necessary to obtain reliable and robust calculation of the match points and efficiencies in the rotating machinery and augmentor. This applies to both predictive simulations and simulations used in the test data reduction process. These nozzle exhaust system requirements are similar to those which drive improvement from ‘zero dimensional’ compressor and turbine maps to higher dimensional ‘physics based’ FD representations of rotating components.

### B.4.2.1 Multi-Dimensional Representation of Convergent Nozzles

#### B.4.2.1.1 Flow

The effective area of the nozzle is the product of the geometric area and the discharge flow coefficient,  $A_8 C_{d8}$ , as defined by **Eq. B-19** referenced to station 8, (nozzle exit and throat). The magnitude of  $C_{d8}$  depends on the nozzle pressure ratio,  $P_7/P_{amb}$ , and the nozzle design features, e.g. relative petal length ( $L/D$ ), and petal angle,  $\alpha$ . **Figure B.82**. For the case where the pressure loss between Stations 7 and 8 is small then  $P_7/P_{amb}$  is approximately equal to  $P_8/P_{amb}$ . The development below is based on this assumption.

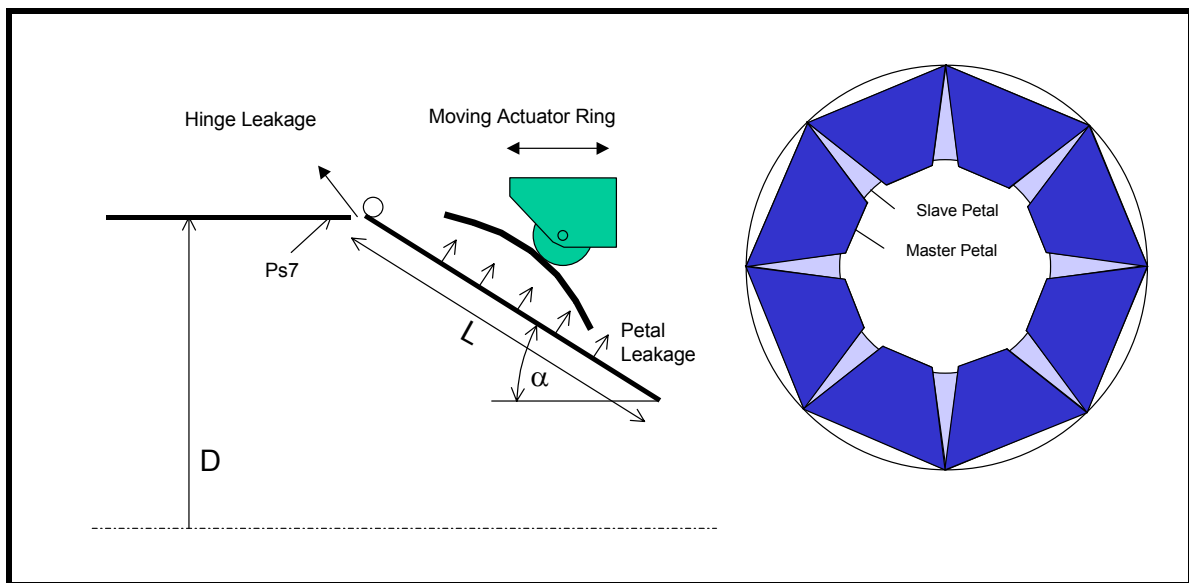


**Figure B.82: Schematic of Variable Convergent Nozzle.**

Note that in the text below, the total pressures and temperatures are designated without the subscript,  $t$ .

The flow at the nozzle throat  $W_8$  may be calculated from  $P_8/P_{amb}$ ,  $T_8$  and  $A_8$  from the formulae for isentropic flow.

#### B.4.2.1.2 Engine Test Analysis Method

Design to calculate nozzle exit area,  $A_8$ , from other measured parameters and sub-scale model correlations:

- Calculate  $T_8$  from measured  $W_2$ ,  $W_f$ , overboard leakage, and main burner efficiency utilizing conservation of energy considerations. This calculation utilizes an iteration which begins with an initial value for petal angle ( $\alpha$ ) (see **Figure B.82**).
- $P_7$  and  $P_8$  are determined from sub-scale model correlations of  $P_7/P_{s7} = f(\alpha)$  and  $P_{s7}/P_{s7wall} = f(\alpha)$ .
- $A_8 \cdot C_{d8}$  is then calculated from  $W_8$ ,  $T_8$ , and  $P_8$ .
- Actual  $A_8$  is calculated from Step 3 and sub-scale model correlation of  $C_d = f(P_7/P_{amb}, \alpha)$ .
- Solve (iterate) till  $A_8$  and petal angle, ( $\alpha$ ), are consistent.

### B.4.2.1.3 Simulation and Measurement Validation Criteria

The calculated and measured nozzle jet areas  $A_8$  are compared. The difference can be used to ‘calibrate’ the nozzle jet area measurement process. If the difference is large and unexpected then a re-evaluation of the simulation and measurement process should be undertaken. A detailed uncertainty analysis should be available to assist in evaluating the result, Ref. SAE Aerospace Information Report 1678, **[B.55]**.

### B.4.2.1.4 Scale Model Basis for Flow and Thrust Coefficient Definition

For a given design the discharge flow coefficient may be measured as a function of nozzle pressure ratio and petal angle during sub-scale model tests encompassing the full range of pressure ratio and petal angle. Good practice requires that model nozzles be made of one piece to preclude leakage during the tests. Furthermore, it is good practice to measure  $P_{s7,wall}$  upstream of the petal hinge to establish the correlation,  $P_{s7}/P_{s7,wall}$  to be used to determine  $P_{s7}$  from measured  $P_{s7,wall}$  during full scale test analysis.

### B.4.2.1.5 Nozzle Leakage Considerations

To calculate airflow at the nozzle charging station, it is necessary to account for flow path and nozzle leakage. Proper accounting requires accurate inlet airflow, fuel flow and main burner efficiency correlation which must be determined/calibrated from dry engine test results over the full range of nozzle inlet conditions.

For the full scale variable nozzle there will be some leakage at the hinge of the petals as well as at the intersection of adjacent petals between the hinge and the throat, **Figure B.82**. The analytical model must account for this leakage in order to obtain consistency between the scale model and full scale flow and thrust coefficients,  $C_d$  and  $C_g$ . Further discussion of the thrust and thrust coefficients is contained in the next section.

The leakage at the hinge can be calculated from the pressure ratio across the hinge,  $P_{s7}/P_{amb}$  and the effective area of the leakage path. Along the petals between the hinge and the throat, there is a straight-line contact between the ‘master’ (outer) and ‘slave’ (inner) petals. The effective leakage gap height and area decreases with increasing pressure difference,  $P_s - P_{amb}$ . Since the static pressure inside the nozzle varies significantly along the petals, it is recommended to subdivide the leakage calculation into several parts.

### B.4.2.1.6 Nozzle Area Measurement Considerations

Accurate measurement of a variable nozzle throat area is a difficult task. One method utilizes a Moving Actuator Ring (MAR). It is positioned by hydraulics or air motor, and has rollers running on curved tracks which are mounted on master petals. Measurement of the axial position of the MAR is used with a correlation to determine actual nozzle throat area,  $A_8$ . This measurement is very difficult to perform because the position sensor is located in a very harsh environment. Moreover, if there is only 1 MAR sensor, any misalignment of the MAR relative to the nozzle centerline will result in additional

measurement error. The widely varying mechanical loads and metal temperatures are elements causing an additional nozzle-area measurement error. A large resulting error in nozzle-area will propagate to unacceptably large uncertainties in calculated and measured airflow and thrust.

### B.4.2.1.7 Nozzle Position Sensor Calibration

The nozzle position sensor requires calibration, which can be done utilizing the full-scale static pressure at the nozzle charging station (inlet)  $P_{s7wall}$ , and the  $P_{s7wall}/P_{am}$  and  $C_d$  from sub-scale model tests (or alternatively CFD calculations).

### B.4.2.1.8 Thrust

The gross thrust of a convergent nozzle may be defined as

$$F_{g8 \text{ actual}} = A_8 (P_{s8} - P_0) + W_8 * V_{8,ideal} * C_{v8} \quad \text{Eq. B-40}$$

This equation is consistent with the thrust-accounting control volume for a single stream convergent exhaust system shown in **Figure B.67** and **Eq. B-25** adjusted to a convergent throat at station 8. The nozzle coefficient is defined here as the ratio of the actual to the ideal jet velocity of a convergent nozzle.

For the example of **Figure B.82**, the velocity coefficient,  $C_{v8}$ , is a function of nozzle design, the petal angle, the nozzle pressure ratio, and many other loss causing effects.

### B.4.2.1.9 Mixing

Incomplete mixing of the gas streams in a turbofan engine will result in a thrust loss, which is properly assessed against the mixer, not the nozzle. This loss has been accounted as a ‘mixer efficiency’, **Eq. B-41**.

$$\eta_{\text{mix}} = (F_{g8} - F_{g8,unmixed}) / (F_{g8 \text{ fully mixed}} - F_{g8 \text{ unmixed}}) \quad \text{Eq. B-41}$$

The application of  $\eta_{\text{mix}}$  requires the calculation of the fully mixed and unmixed thrust, i.e. separate expansion of the cold and hot streams. This makes the nozzle calculation complex because one must now define two nozzle entry stations: one for the hot and one for the cold expansion. In addition, the nozzle area must be apportioned for the hot and cold streams. Inconsistencies in throat Mach number for the separate streams also arise due to gas property effects. When different turbofan cycles or different mixers are to be compared, the concept of partial mixing is very useful, both to describe and to help understand effects on thrust. On an existing engine, although it is much simpler to book-keep the effects of non-uniform temperature and pressure to the nozzle thrust coefficient, it must be recognized that a significant contributor to the level of the thrust coefficient derives from an effect generated outside the nozzle.

### B.4.2.1.10 Clear Definition of Ideal Thrust Required

It is important in any particular program to avoid ambiguity by clear understanding and agreement at the outset among all stakeholders regarding the definition of nozzle ideal thrust.

A common definition for the ideal expansion process is to ambient pressure in an ideal convergent/divergent nozzle. Other definitions are possible depending on how the averaging calculations at the nozzle charging station, the flow mixing calculations, bleed and leakage calculations, and multi-stream evaluation are handled. The definitions may become complicated especially as the complexity (dimensionality) of nozzle model increases.

The actual thrust for an existing engine will not change regardless of how the ideal nozzle coefficient is defined. Understanding of the components including the nozzle can be improved by more complex ‘physics based’ nozzle component representations.

#### B.4.2.2 Multi-Dimensional Representation of Convergent-Divergent Nozzles

The addition of a divergent section to the exhaust nozzle increases the usefulness and in some cases need for one plus dimensional analysis and simulation of the system. For the example discussed here, **Figure B.83**, a precise description of the geometry for all positions is necessary. The primary petal angle is an important parameter; the metal temperature of the primary petal is also important. Thermal expansion of the primary master petals causes an increase in  $A_9$ . This happens because the length of the strut which holds the divergent petals remains unchanged because its temperature does not change, **Figure B.83b**. The multi-dimensional geometry model is necessary to properly evaluate the values for the throat area,  $A_8$  and the exit area,  $A_9$ , and thus nozzle area ratio  $A_9/A_8$  for all operating conditions.

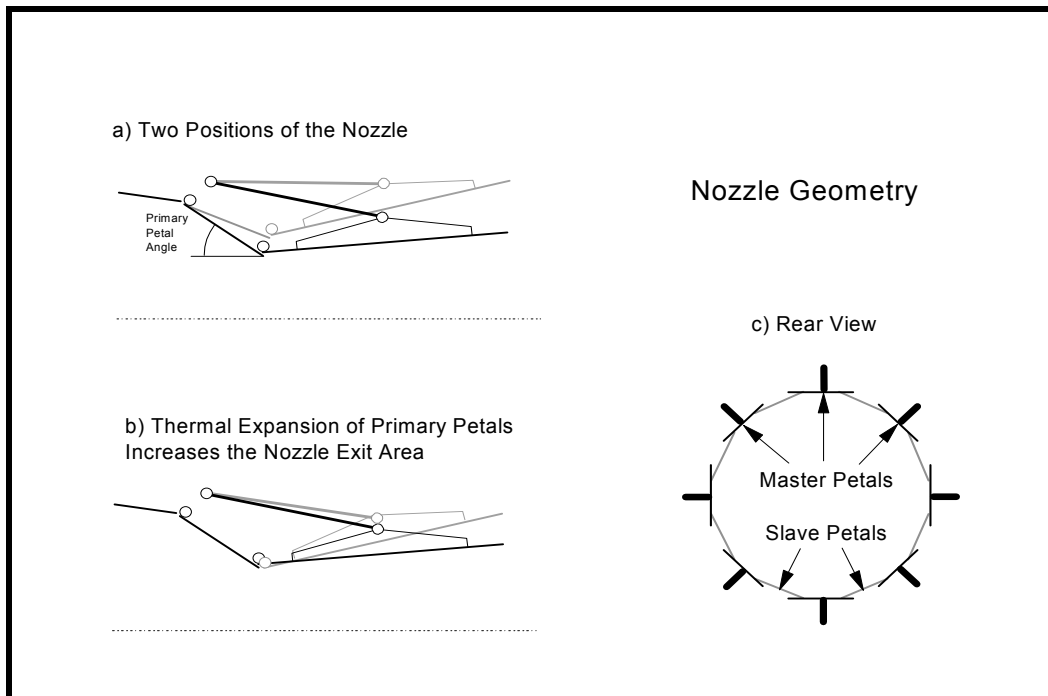


**Figure B.83: Geometry of Variable Convergent Divergent Nozzle.**

Once the geometry is determined from the mathematical model, the static pressure along the nozzle inside surface can be calculated. In the convergent section, the static pressure along the wall can be calculated from the local area ratio  $A_{\text{local}}/A_7$  and one-dimensional isentropic relationships. In the divergent section, the wall pressures can be determined from isentropic relationships with corrections, Rebolo et al. (1993) [B.56].

##### B.4.2.2.1 Flow

The flow characteristics of a convergent/divergent nozzle can be described according to Eq. B-42.

$$C_d = W_{g-\text{actual}} / W_{g-\text{ideal}} = A_{8-\text{ideal}} / A_{8-\text{actual}}$$

$$= \left[ W_g * \sqrt{T_t} / (A * P_t) \right]_{\text{actual}} / \left[ W_g * \sqrt{T_t} / (A * P_t) \right]_{\text{ideal}} \quad \text{Eq. B-42}$$

## ANNEX B – ADVANCED TOPICS AND RECENT PROGRESS

In order for the definitions of equation 9 to be valid, flows, temperatures and pressures must be consistently calculated at Station 8.

When the ideal flow,  $W_{g8,ideal}$ , is calculated from  $W_g - W_{leak}$ , the total temperature  $T_g$  and pressure ratio  $P_g/P_{amb}$ , a flow coefficient calculated from  $C_d = W_{act}/W_{ideal}$  will provide coefficients greater than 1.0 at low pressure ratios. Proper physics in the computation of the coefficient will always result in a value less than 1.0. More realistic computation, of the flow-conditions at the throat, is no additional burden for this simulation because it is needed for the calculation of forces and nozzle leakage.

At sufficiently high nozzle pressure ratios (when the flow is under-expanded or only slightly over-expanded) the discharge flow coefficient can be closely approximated as a function of petal angle ( $\alpha$ ) only, **Eq. B-43**.

$$C_d = -1.25 \cdot 10^{-5} \cdot \alpha^2 - 0.001425 \cdot \alpha + 0.995 \quad \text{Eq. B-43}$$

When the pressure ratio is low, the flow in the divergent section of the nozzle detaches and  $C_d$  becomes a function of both  $\alpha$  and  $P_g/P_{amb}$ .

The nozzle exit discharge flow coefficient  $C_{D9}$  is very nearly constant and has a value of  $\sim 0.995$ , for under expanded operation and becomes a function of pressure ratio and area for low  $P_g/P_{amb}$ .

### B.4.2.2.2 Leakage Considerations

The leakage through the hinges and between the master and slave petals depends on the difference between the pressures within and around the nozzle. A description of how to evaluate the pressure distribution inside the convergent part of the nozzle can be found in the foregoing description.

As long as the pressure outside the nozzle is lower than inside, the effect of leakage can be directly evaluated. However, there are many operating conditions, sea level static for example, for which static pressure in the throat and divergent sections is lower than pressure outside, and air is consequently sucked in.

During engine testing of the EJ200 (a mixed flow turbofan engine), for example, one could easily identify when the pressure inside the divergent nozzle section is lower than outside. Inspection of **Figure B.84** shows that the slave petals are sucked in and a gap opens between the master and the slave petals.

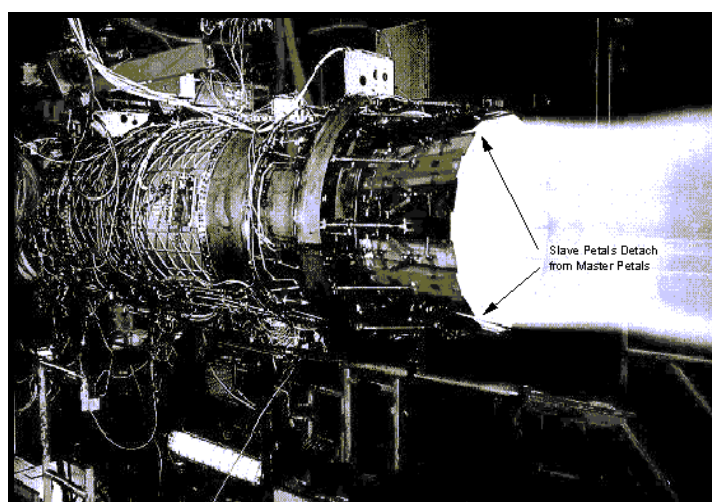


**Figure B.84:** Over-Expanded Operation of a Convergent-Divergent Nozzle.

#### B.4.2.2.3 Thrust

A nozzle located downstream of a mixed flow turbofan gas-generator will have non-uniform pressure and temperature profiles at the nozzle inlet Station 7. It is possible to model the thrust loss caused by the non-uniform flow conditions by using the mixing efficiency approach described in the previous convergent nozzle discussion. However, the calculation process of the unmixed flow conditions in the convergent/divergent nozzle becomes unnecessary complex. It is much better to base the calculation of the ideal nozzle performance on the fully mixed flow and properties at the nozzle entry charging station 7. Losses due to incomplete mixing can be addressed by the nozzle thrust coefficient.

#### B.4.2.2.4 Definition of Thrust Coefficient

The performance of a convergent/divergent can be characterized by the thrust coefficient  $C_g$  defined in **Eq. B-44**, repeated.

$$C_g = F_{g9_{actual}} / F_{g9_{ideal}} \quad \text{Eq. B-44}$$

The thrust coefficient  $C_g$  can also be calculated consistent with the flow coefficient.

$$C_g = [F_g / (A_8 * P_{am})]_{actual} / [F_g / (A_8 * P_{am})]_{ideal} \quad \text{Eq. B-45}$$

The gross thrust coefficient compares the actual thrust (measured) with an ideal definition of thrust produced by an ideal expansion to ambient pressure.  $C_g$  will also be a function of nozzle throat to exit area ratio,  $A_8/A_9$ .

#### B.4.2.2.5 All Stake-Holders Should be Aware of Thrust and Coefficient Definitions

The definition of ideal  $C_g$  based fully expanded variable geometry results in a lower numerical value for the calculated real nozzle system. This is because it is not possible for the nozzle to fully expand to ambient pressures at off-design conditions. Several experimenters have opted to define the ideal coefficient as the maximum achievable for a given hardware geometry. This has the advantage, that the thrust respectively velocity coefficient becomes a true measure of nozzle flow quality. The coefficient defined in such a way is independent from nozzle area ratio  $A_9/A_8$ , pressure ratio  $P_8/P_{amb}$  and nozzle leakage provided a sufficiently detailed mathematical model of the nozzle is employed.

Although other definitions for ideal thrust are possible, they are generally non-standard and should only be used for sound reasons, related to a particular geometry. All parties should fully understand and use the definitions including nozzle designers, sub-scale modelers, analytical simulation engineers, test analysis engineers, technical manager/system evaluators, customers and sometimes suppliers.

An alternate formulation of the thrust equation reported in the literature is shown in **Eq. B-46**.

$$F_{g9_{actual}} = A_9 (P_{s9} - P_{amb}) + W_9 * V_{9_{ideal}} * C^*_{v9} * C_a * C_f \quad \text{Eq. B-46}$$

In this formulation  $C_a$  is the angularity coefficient from the Reference [B.57] Fig. 5 – 12 that accounts for the losses due to non-axial exit flow velocity. The coefficient  $C_f$  from the Reference [B.57] Fig. 5.13 accounts for the effect of boundary layer momentum loss caused by friction in the nozzle. Both these coefficients depend on the nozzle area and the primary petal angle. The velocity coefficient  $C^*_{v9}$  is held to represent a nozzle efficiency. The advantage to define the coefficient is this way is discussed in the next section.

## ANNEX B – ADVANCED TOPICS AND RECENT PROGRESS

Note that in the turbofan engine this coefficient accounts mainly for losses due to incomplete mixing of the core flow, bypass flow and nozzle cooling air and is not the same as the velocity coefficient  $C_v$  as defined earlier.

### B.4.2.3 Special Considerations for Multi-Dimensional Modeling and Simulation of Nozzles

#### B.4.2.3.1 High Nozzle-Pressure Ratios

When the nozzle pressure is large, and the flow is under-expanded, the flow tends to remain attached to the nozzle ‘wall’ and follow the contours of the divergent petals. Using a nozzle analytical model based on geometry provides excellent correlation with test results. An example of velocity coefficient  $C_{v9}^*$  test results for a turbofan engine measured over a wide range of engine ratings, altitude and Mach number flight conditions is shown in **Figure B.85**. When the nozzle pressure ratio is greater than 3.5, the velocity coefficient has a unique value of 0.99. The 1% reduction from the ideal value of 1.0 is caused by incomplete mixing of the core and bypass gas streams, and losses due to nozzle cooling.

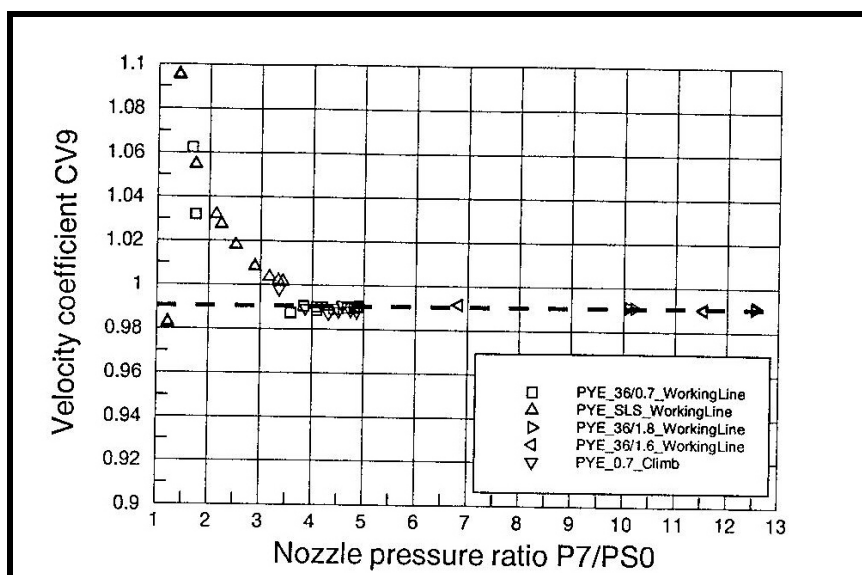


**Figure B.85:** Test Result for Nozzle Velocity Coefficient Using 1-D Geometry Model.

For high-pressure ratio nozzles with significant cooling flow, the assumptions in treating the cooling flow can change the nozzle thrust coefficient. Typically cooling air entering upstream of the nozzle throat is treated as part of the primary flow, even if the injection location does not allow for effective mixing and the momentum of the flow is not considered. Cooling flow on the expansion flaps is generally not included in the thrust calculation. As cooling becomes more significant, the modeler may choose to treat these cooling flows as separate streams with their own thrust contribution and thrust coefficient, rather than try to develop a thrust coefficient representation to cover the nozzle behavior over a wide range of cooling flow and nozzle pressure ratio levels.

#### B.4.2.3.2 Low Nozzle-Pressure Ratios

When the nozzle pressure ratio is less than 3.5 to 4.0 the  $C_{v9}^*$  increases rapidly as nozzle pressure-ratio decreases, **Figure B.85**. This occurs because the calculated force on the struts holding the secondary petals becomes negative. In turn, this is because the pressure inside the divergent section is lower than ambient causing the forces on the divergent master petals to exert a “pull” on the struts, see **Figure B.86**. Under

these conditions, the slave petals detach from the master petals as can be clearly seen in **Figure B.84**. Airflows from outside to inside the nozzle, which reduces the effective nozzle exit area ratio  $A_9/A_8$ . This results in a better match of the effective nozzle area ratio at the low-pressure ratio condition and the nozzle appears to perform better than calculated with the standard assumption,  $C_d = 0.995$ .

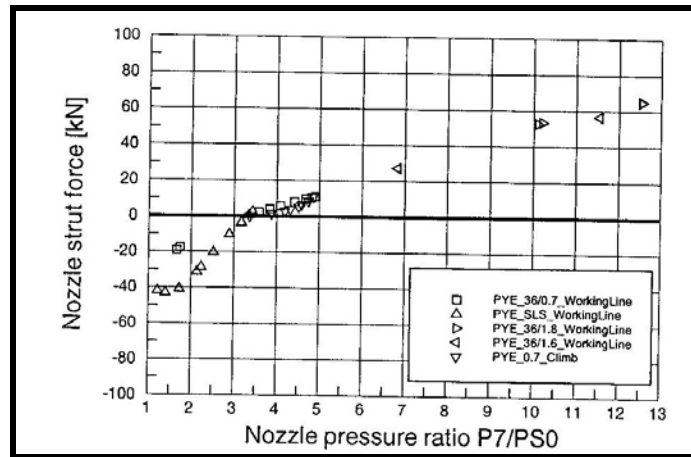


**Figure B.86:** Nozzle Strut Forces; Positive when Struts are Compressed.

This point is illustrated in **Figure B.87** in which the calculated thrust coefficient, ( $C_g$ ) is plotted as a function of nozzle pressure ratio for lines of constant nozzle area ratio. For example, when the flow follows the nozzle geometry at a pressure ratio of 2.4 and nozzle area ratio of 1.35 the ideal thrust coefficient is 0.95. If the flow were detached in the divergent section leading to an effective area ratio of only 1.2, the gross thrust would improve by 3.0%.

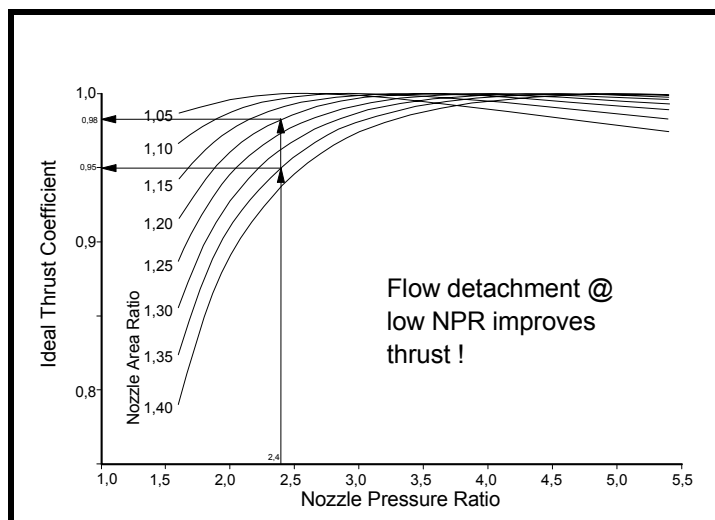


**Figure B.87:** Thrust Gain Due to Flow Detachment at Low Nozzle Pressure Ratios.

## B.4.2.3.3 Operation at Windmilling Conditions (ISABAE Paper Excerpt on Windmilling)

For separate flow high bypass engines at very low nozzle pressure ratios and extreme bypass ratios (windmilling conditions), the assumption of independent expansion of the two exhaust nozzles begins to break down and the thrust coefficient characteristics begin to vary significantly. Mixed flow nozzles thrust

## ANNEX B – ADVANCED TOPICS AND RECENT PROGRESS

coefficient characteristics tend to be less sensitive since they have already captured this effect in the mixing calculation. To allow continued use of the base nozzles thrust coefficient characteristic at windmilling conditions, a base drag term is often added for separate flow engines to approximate the thrust impact of the downstream mixing of the two streams. (ISABAE paper reference with chart on relative effect).

### B.4.2.3.4 Partially Mixed Nozzles

Most low to medium bypass turbofan engines incorporate mixed flow nozzles. Very high-bypass ratio engines are typically separate flow. Use of mixed flow nozzles on high bypass engines often results in behavior that does not match well with the results from a fully mixed nozzle analysis. Rather than trying to capture this behavior in a unique thrust coefficient characteristic, a partially mixed nozzle analysis may be used. In this case, the results from a separate flow and mixed flow nozzle analysis are used and the results are interpolated using the two limiting cases.

### B.4.2.3.5 Useful Correlation from Test Results

Improved understanding of the characteristics of the divergent section of the nozzle may be achieved from analysis of correlation of the ratio of static pressure measured at the nozzle exit wall to  $P_{amb}$ ,  $P_{s9,wall}/P_{amb}$ , vs. nozzle pressure ratio,  $P_7/P_{amb}$ , **Figure B.88**. Test results for a turbofan engine are plotted in **Figure B.89**. Also plotted in the figure are of constant divergent section area ratio,  $A_9/A_8$ , based on one-dimensional analysis with  $C_{d8} = C_{d9} = 1$ . Note that the range of the constant-area-ratio lines extends well below 1.0. The lower limit of the measured pressures for this example is approximately 0.91.

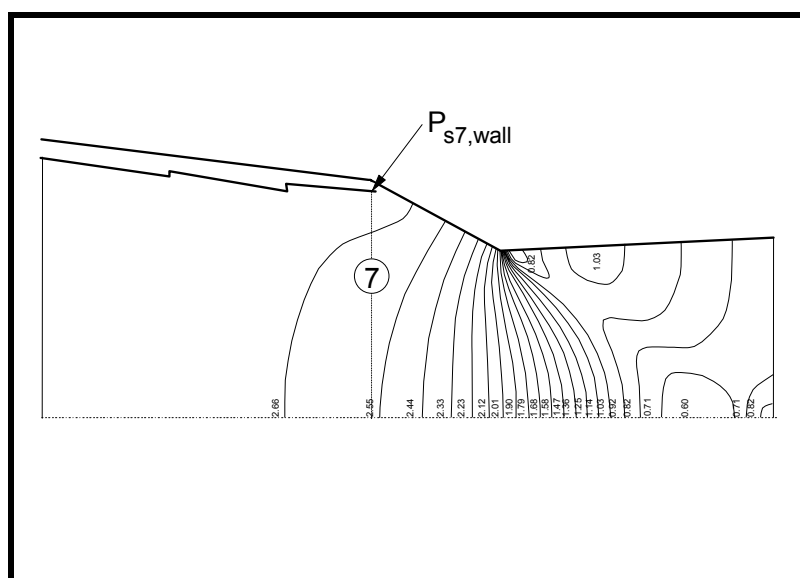


**Figure B.88: Schematic of Divergent Nozzle Wall Section with Pressure Instrumentation Locations.**

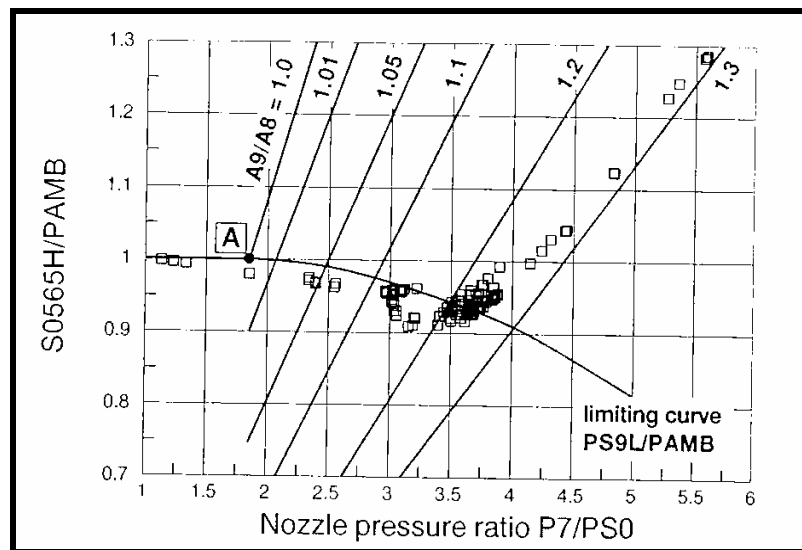


**Figure B.89: Correlation of Static Pressure near the Nozzle Exit with Nozzle Pressure Ratio.**

If one hypothesizes the requirement that the Nozzle throat area,  $A_8$ , always controls the flow, i.e. the effective nozzle area ratio,  $A_{e9}/A_{e8}$ , is always greater than 1, an empirical correlation to calculate nozzle exit discharge coefficient,  $C_{d9}$ , may be defined. In this example the nozzle operates much like a convergent nozzle and expands the flow to ambient pressure for nozzle pressure ratios below the sonic limit of  $\sim 1.8$ , ( $P_{s9wall}/P_{amb} = \sim 1.0$ ). At nozzle pressure ratios above 1.8 the level of measured  $P_{s9wall}/P_{amb}$  trends lower. The curve labeled  $P_{s9L}/P_{amb}$  in **Figure B.89** is a best-fit curve through the measured data; it represents the lower limit of the  $P_{s9}/P_{amb}$  for the given nozzle. Lines of constant divergent nozzle area ratio calculated from one-dimensional considerations are also shown in the figure.

The limiting curve of  $P_{s9L}/P_{amb} = f(P_7/P_{amb})$  is used in the simulation in the determination of  $C_{d9}$  as follows:

- 1) Assume  $C_{d9} = 0.995$  and calculate a tentative value for  $P_{s9}$ .
- 2) If  $P_{s9}/P_{amb}$  is greater than the limiting value from **Figure B.89**, then  $C_{d9} = 0.995$ .
- 3) If  $P_{s9}/P_{amb}$  is lower than  $P_{s9L}/P_{amb}$  In **Figure B.89**, then use the theoretical  $(A_9/A_8)_{eff}$  from the limiting curve.
- 4) Calculate the required  $C_{d9}$ , and recalculate the exit flow conditions.

This procedure requires that the static pressure at the nozzle exit never be lower than that consistent with the limiting curve; therefore the simulation calculations may be slightly different than the measured values for  $C_d$ . The method provided good consistency of the thrust coefficient,  $C_{v9}^*$ , however, and therefore provides a useful correlation for characterizing nozzle thrust performance, **Figure B.90**.

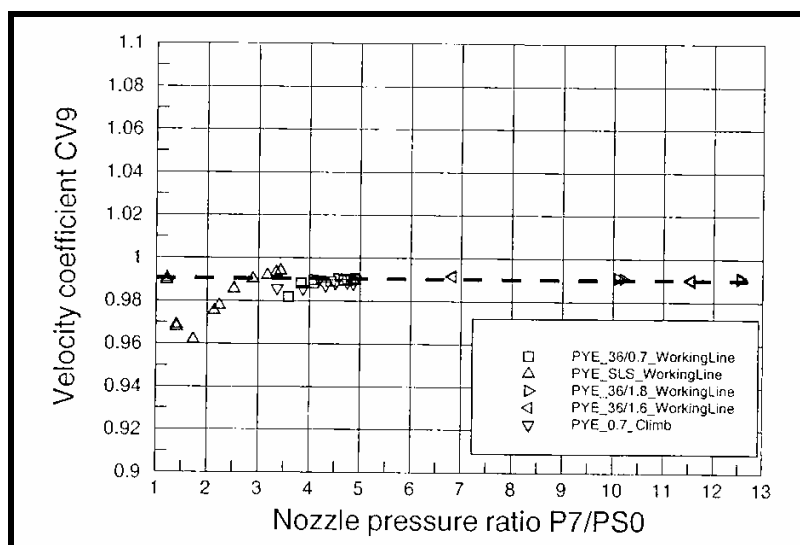


**Figure B.90: Adjusted Correlation for Nozzle Velocity Coefficient.**

## B.5 INLET SYSTEMS

The inlet aerodynamic design characteristics of the powerplant have significant effects on the engine performance and stability and are of vital concern to the engine designer. Inlets are designed to guide required engine flow into the front face of the engine with minimum loss and distortion. For sub-sonic flight velocity this generally means properly faired inlet surfaces to minimize flow separation. For supersonic flight velocity, the design must minimize losses due to formation of shock waves. In any case to assure engine stability, the inlet design must provide low flow distortion and, in the supersonic case, stable shock structures. The inlet design will also have important effects on overall flight vehicle drag.

The inlet functions as follows in the overall powerplant system:

- It accelerates or decelerates ambient air to the engine forward flange station to achieve the entering flow Mach number that will provide most efficient operation of the engine turbomachinery.
- It is part of the cycle compression process.
- It transforms the dynamic pressure generated by flight velocity to increased cycle static pressure.
- It produces total pressure loss in the outer bypass stream.
- It produces total pressure loss in inner core stream by means of spinner scrubbing.
- It affects distortion entering the engine.
- It affects noise generated by powerplant.
- It contains instrumentation required for power setting and engine control.
- It produces ‘spillage drag force’ due to non-isentropic effects.
- It produces additional air vehicle drag due to scrubbing and pressure forces generated by free stream flow over the external cowl.

Inlet drag and pressure loss should be faithfully modeled in the engine simulation to calculate accurate average total pressures for the core stream and the bypass stream at the fan inlet face. Clear definitions are required for thrust-drag bookkeeping.

### B.5.1 Diffusion and Acceleration of Airflow into the Propulsion System

The inlet is designed to induct air into the powerplant with minimum loss at the aircraft design flight condition. For subsonic and low supersonic aircraft the design is usually a fixed inlet area with significant external diffusion and accompanying rise in static pressure, see **Figure B.91**. The energy contribution of the velocity of the airflow to the engine cycle is depicted in the H-S diagram shown in **Figure B.92**. A typical subsonic aircraft design condition would have the inlet area approximately 20% larger than the area of the entering stream tube far upstream of the engine where the flow which will enter the engine is unaffected by air vehicle velocity. The diffusion process from station 0 far upstream to station 1 at the inlet lip is very nearly isentropic at the design condition and the static pressure rise is an ideal function of the flight velocity, equation 22 and **Figure B.92**.

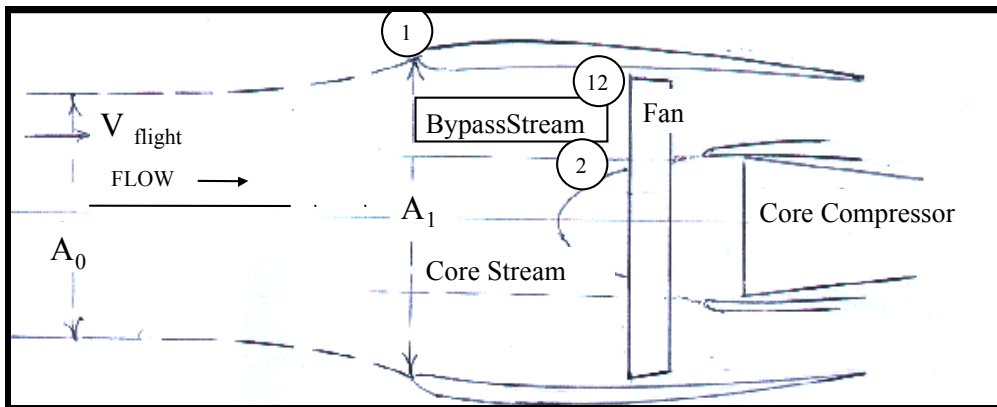


**Figure B.91: Fixed Inlet Area Schematic.**

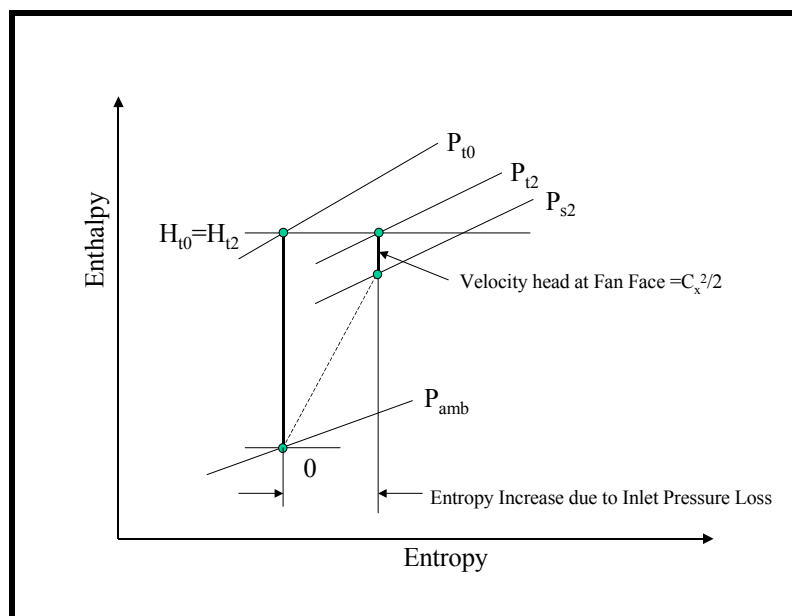


**Figure B.92: Flight Velocity and Inlet Contribution to Engine Cycle.**

An exception to this would be off-design conditions like sea level static where the engine flow required is very large relative to the inlet area and some of the entering flow comes from behind the inlet and may actually intersect the ground. Engine test installations minimize this effect by using a bellmouth inlet

which is designed to minimize lip overspeed, **Figure B.93**. Another exception at the aircraft design condition would be a case where external heating of the flow occurs due to hot gas ingestion from a missile. For supersonic inlets losses due to shock wave formation internal and external to the inlet must be considered and will be discussed below.

$$\Delta h = V^2/2$$

Eq. B-47

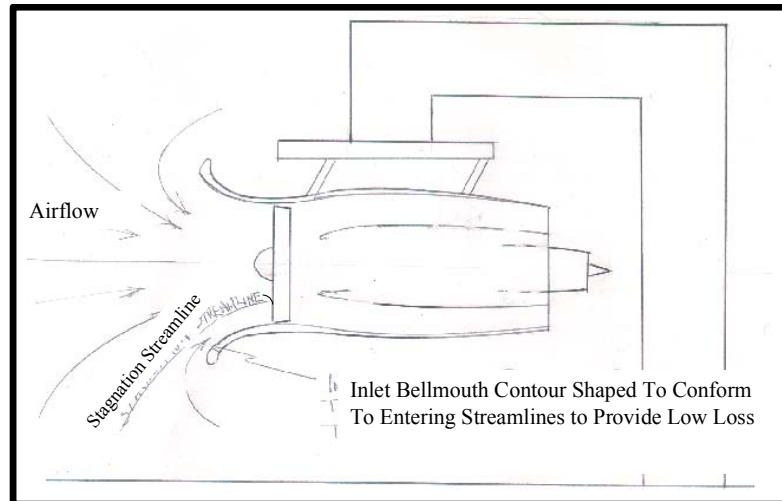


**Figure B.93: Schematic of Sea Level Test Inlet.**

### B.5.2 Inlet External Loss: Spillage Drag

Forces are generated on the inlet cowl from pressure differentials along the external surface and from viscous effects such as scrubbing skin friction, flow separation at the inlet lip, and shock losses. The sum of these forces defines the total drag of the Inlet.

The 'INLET SPILLAGE DRAG' force term consists of three components:

- Additive drag, which is the force from the static pressure integral along the entering streamline from station 0 far upstream to the engine inlet lip, Station 1;
- Lip suction, which consists of the static pressure force integrals along the external surface from the inlet lip, Station 1 to the rear of the inlet cowl, Station MAX; and
- Scrubbing Friction.

#### B.5.2.1 Subsonic Case

For ideal non-viscous flow the additive drag is balanced by the forward force generated by low pressures on the forward facing surface of the inlet lip. In real (viscous) flow the "lip suction force is reduced from the ideal due to turbulence and separation effects and a net force in the drag direction occurs which is defined as 'spillage drag', equation 23. Spillage drag is minimized by proper inlet design, at the primary aircraft operating condition. The spillage drag is a result of the viscous losses generated at the inlet lip and increases when the flow Mach numbers around the lip increase. These losses are a function of inlet mass flow ratio, (Area of inlet at lip)/(Area of entering stream tube), see **Figure B.94**.

$$\text{Additive Drag} + \text{Lip suction} + \text{Scrubbing Friction} = \text{Spillage Drag}$$

Eq. B-48

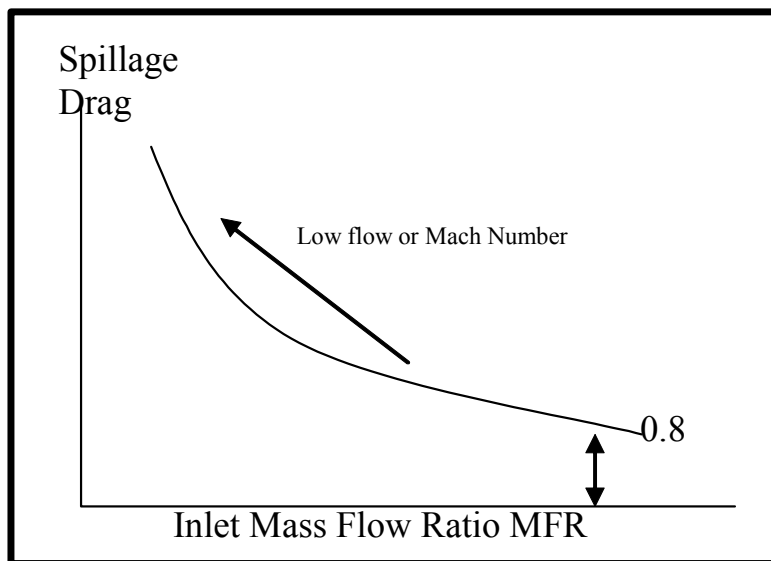


**Figure B.94:** Inlet Spillage Drag is a Function of Mass Flow Ratio.

### B.5.2.2 Supersonic Case

For supersonic flight velocity, a shock wave can form at the inlet lip. At velocities higher than the inlet design condition, the shock may be positioned forward of the inlet, **Figure B.95**. The supersonic inlet lip design will generally be sharper than for the subsonic case and will not support a forward lip-suction force. A portion of the flow in the potential ‘inlet capture area’ will spill around the lip with little or no flow acceleration around the lip generating compensating ‘lip suction’. The resultant spillage drag will be large and approximately equal to the additive drag.

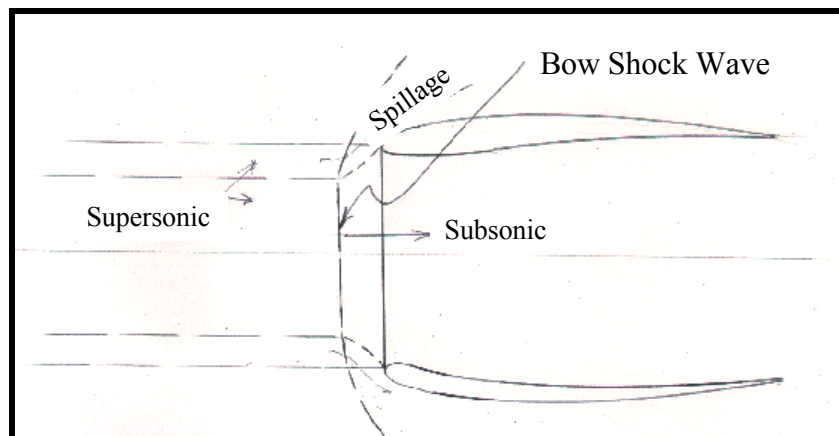


**Figure B.95:** Fixed Area Inlet in Supersonic Flow.

Fixed inlet area normal shock losses are generally acceptable for Mach numbers up to about 1.6. To reduce the shock losses at higher flight Mach numbers, the inlet is designed with external centerbody ramps that compress the flow externally. The ramps create a series of oblique shocks having lower total loss than a single normal shock near the inlet lip. Forward force can also be generated on a center inlet plug, **Figure B.96**. For Mach numbers above about ~2.5 optimum inlet loss can be obtained using an inlet design having both external and internal compression, **Figure B.97**.

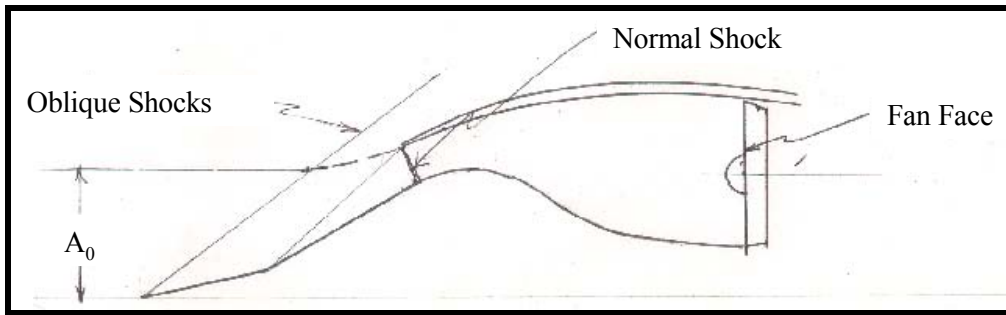


**Figure B.96: Supersonic Inlet with External Compression.**

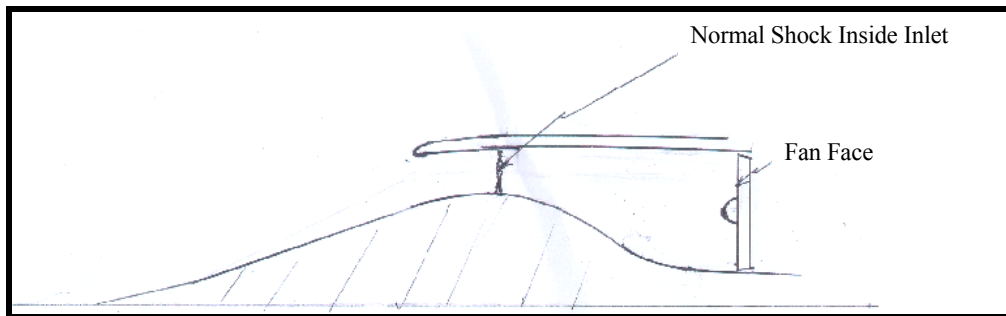


**Figure B.97: Supersonic Inlet with External and Internal Compression.**

Simulation of the propulsion system requires accounting for all shock and other viscous losses between Station 0 and Station 1. External forces must be accounted for between Station 2 and the inlet max-external diameter. Internal drag forces must be accounted for between Station 1 and the fan face.

### B.5.3 Inlet Internal Losses: Inlet Recovery

The entering flow stream tube has a stagnation point at the inlet lip. Flow within the stream tube enters the engine and scrubs the inner surface of the inlet creating a boundary layer and reducing the effective total pressure of the flow in the fan tip region. Additional loss due to flow distortion may be generated by inlet lip-separation effects. The flow also scrubs the center spinner producing an additional pressure loss in the core stream. These losses reduce  $P_{12}$  and  $P_2$  at the fan face inlet, and are correlated for simulation as functions of the corrected airflow. This is shown schematically in **Figure B.98**.

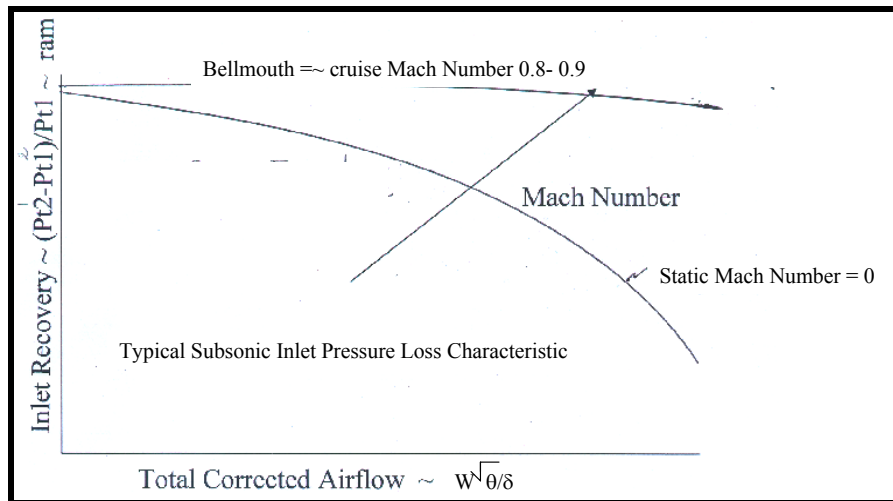


**Figure B.98: Inlet Recovery Loss.**

For sea-level testing a special bellmouth inlet is used to reduce inlet recovery loss. These losses correlate with inlet airflow, and are shown in **Figure B.98**.

For supersonic applications in the early design stage, the inlet recovery is estimated using a convention shown in **Eq. B-49** which is taken from Mil-E-5007D.

$$\begin{aligned} Pt2 &= 1.0 - .075 (M_0 - 1)^{1.35} & 1.0 < M < 5.0 & \text{Eq. B-49} \\ Pt2 &= 800 / (M_0^4 + 935) & M > 5.0 & \end{aligned}$$

## B.5.4 Cited References for Nozzles and Inlets

- [B.53] SAE Standard, IR1703: In-Flight Thrust Determination.
- [B.54] SAE Standard, AIR5020: Time Dependent In-Flight Thrust Determination.
- [B.55] SAE Standard, AIR1678: Uncertainty of In-Flight Thrust Determination.
- [B.56] Rebolo et al., “Aerodynamic Design of Convergent-Divergent Nozzles”, AIAA-93-2574, 1993.
- [B.57] Oates, G., “Aircraft Propulsion Systems Technology and Design”, AIAA Education Series, 1989.

## B.6 AERODYNAMICS OF AIR SYSTEMS

### B.6.1 Introduction

Three important subjects of the physics of air systems have been chosen:

- Part 1: Tappings/Bleeds and Pre-Swirl Systems;
- Part 2: Rotating Holes and Two Phase Flow; and
- Part 3: Labyrinth Seals.

In these fields, many new papers are available. Correlations out of the literature for the discharge coefficients, which include the most important parameters are compared and discussed. For two-phase

flow, simple correlations for engineering purposes are recommended, especially for vent lines of aero engines. It is concluded that much more effort is required in order to push knowledge beyond the state of current literature that is partly controversial and not comprehensive enough for computerized engineering.

The aim of this review is to collect the major aspects for air systems calculations. It does not contain all the different correlations out of the literature. The choice presented in the following is based on a subjective judgment of the authors based on their experience. Furthermore it is aimed to keep it simple; therefore, the effects of only the most important parameters are taken into account.

### **B.6.2 Tappings/Bleeds**

Air is tapped off outwards for several purposes: Cooling air (C/A), engine bleeds, i.e. for starting or for pneumatic purposes and customer bleeds. Inwards the air is only used for cooling purposes.

In order to minimize the performance impact of the tapped air on the engine cycle, it is important to choose the lowest possible compressor stage. The purpose for which the air is used dictates a certain pressure level and necessitates tapping off with a minimum of pressure losses. On the other hand, from a design point-of-view it is required to keep the number of tappings to a minimum.

To calculate overall engine secondary-air-system characteristics with a computer program, accurate correlations for all flow elements are necessary. For tappings they are usually presented in form of  $C_d$ -values as a function of pressure ratio.

Results from rig tests or from numerical calculations are usually from three-dimensional models and a transformation into 1-D correlations is necessary. In this process a lot of information is lost, this and further reasons are responsible that only moderate accuracy can be expected.

#### **B.6.2.1 Outward Tappings**

The following geometries are encountered:

- Plain;
- With a step;
- Radiused;
- With subsequent diffuser; and
- Between vanes.

Plain tappings are the most common ones, but they have relatively high pressure losses.

A stepped design can only be adopted, if there is a permanent bleed, since otherwise the pressure losses in the main channel become high. If there is space for a radius at the upstream corner or a subsequent diffuser the pressure losses of the tapping configuration can be significantly reduced. (**Figure B.99** gives an example of a tapping with a step, a radius and a subsequent diffuser). Tapping in between vanes has high-pressure losses and leads to an elaborate design but it minimizes the axial length of the compressor.

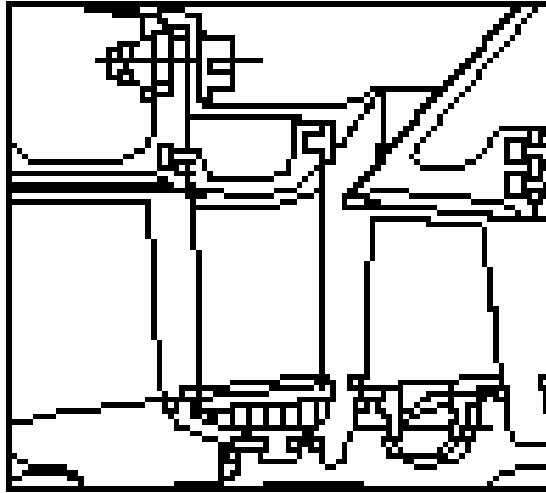


**Figure B.99:** Example for an Outward Tapping.

The following correlations are commonly used:

$$C_d = m_{ol} / m_{id} \quad \text{Eq. B-50}$$

$$m_{id} = \frac{P_{t1} \cdot A_{bl}}{\sqrt{R \cdot T_{t1}}} \left( \frac{P_{s2}}{P_{t1}} \right)^{\frac{1}{\kappa}} \sqrt{\frac{2\kappa}{\kappa-1} \left[ 1 - \left( \frac{P_{s2}}{P_{t1}} \right)^{\frac{\kappa-1}{\kappa}} \right]} \quad \text{Eq. B-51}$$

$$C_d = f(DAB) \quad \text{Eq. B-52}$$

$$DAB = \frac{P_{t1} - P_{s2}}{P_{t1} - P_{s1}} \quad \text{Eq. B-53}$$

In order to fit all configurations it is convenient to base the DAB-parameter on total upstream and the static downstream pressure. Otherwise, if the upstream static pressure is used it becomes difficult in case the downstream static pressure is higher than the upstream one.

The influence of a diffuser can be seen from **Figure B.100**, details can be obtained from Möller (1990) [B.58]. In **Figure B.101** the  $C_d$ -values of rectangular holes are compared with those of angled holes. The influence of slot length and lip height can be seen on **Figure B.102** and **Figure B.103** for tappings with a step, details again from Möller (1990). Further characteristics can be obtained from Dittrichs and Graves (1956) [B.59] and Rohde et al. (1996) [B.60].

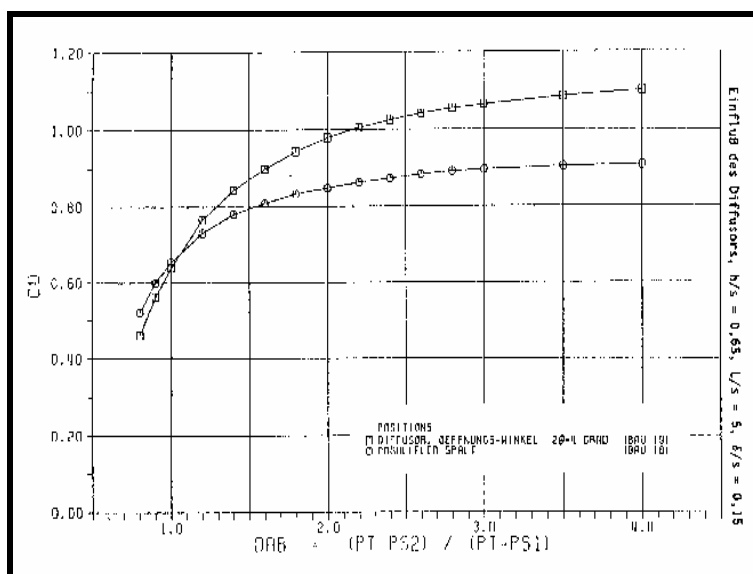


**Figure B.100:** Influence of a Diffuser on the Cd-Value.

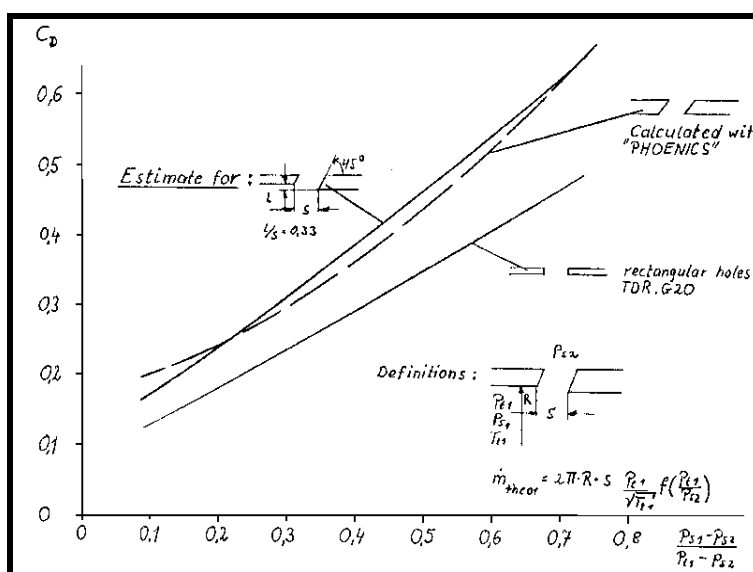


**Figure B.101:** Comparison of a Rectangular with an Angled Hole.

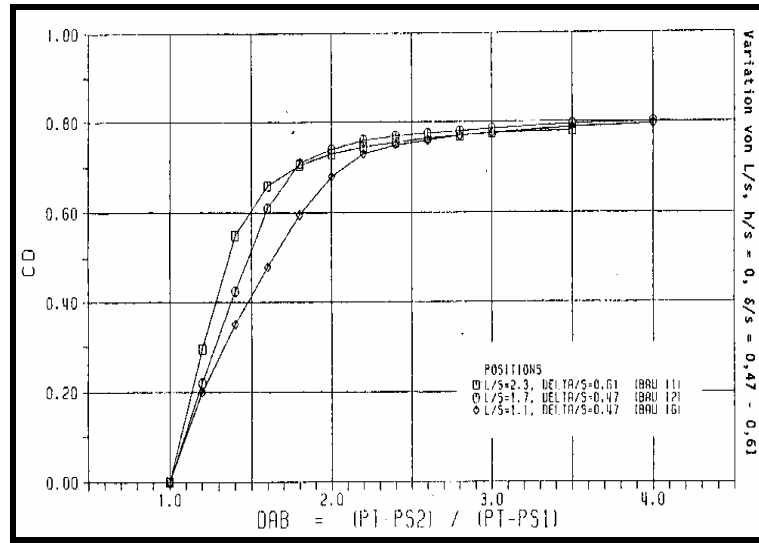


**Figure B.102: Influence of Slot Length on the Cd-Value.**

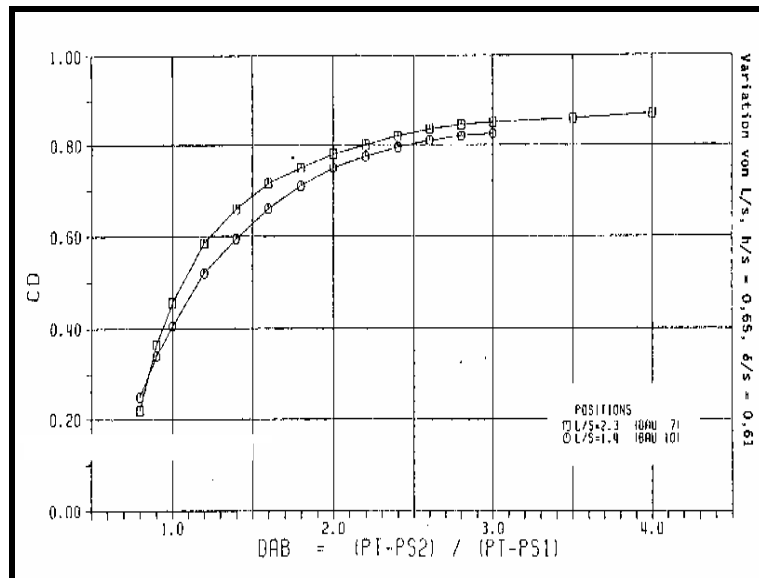


**Figure B.103: Influence of Step Height and Slot Length on the Cd-Value.**

For a bleed port with diffuser, assuming that  $P_{t1} = P_{t2}$

$$DAB_{dif} = DAB * (1 - C_p) = \frac{P_{t1} - P_{dif,s2}}{P_{t1} - P_{s1}} \quad \text{Eq. B-54}$$

$$C_p = \frac{P_{dif,s2} - P_{dif,s1}}{P_{dif,t1} - P_{dif,s1}} \quad \text{Eq. B-55}$$

Assuming further that the diffuser behaves like an ordinary one, i.e. the distortion of the inlet velocity profile is neglected, bleed port characteristics with a diffuser can be obtained from the basic DAB with a  $C_p$  from diffuser charts and vice versa. Of course, DAB could be derived from  $DAB_{dif}$ .

### B.6.2.2 Inward Tappings

To design an efficient inward tapping needs much more sophisticated skills than the outward case. This results from aerodynamic as well as from mechanical reasons and the relevant engine and rig tests are very expensive.

An example for an inward tapping of air is presented in **Figure B.104**. There are several difficulties encountered in designing such a system: The swirl between the inner radius of the main stream and the rotor drum must be known to get the correct inlet conditions for the holes in the drum. Next, the swirl originating from the holes and its development down to the inlet of the tubes influence the pressure drop in the upper cavity and the inlet losses to the tubes. The tubes are used to avoid the high-pressure drop of a free vortex, which would strongly limit the amount of flow which can be bled inward. The radial position of the tube entry can be optimized to the end that the circumferential velocities of the tube and the entry swirl are matched. On the other hand a stream tube between the holes and the entry of the tubes may form without diffusing the radial velocity.

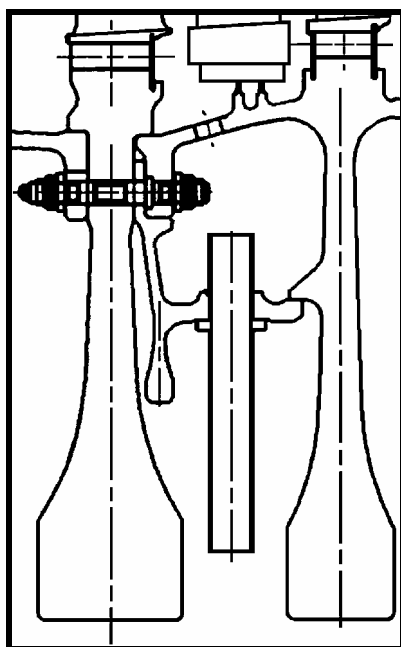


**Figure B.104: Inward Tapping with Tubes.**

This situation can best be investigated with the help of CFD (computational fluid dynamics). This should be done already in the design phase, where normally only correlations are used. But the swirl changes and entry losses into the tubes can only roughly be calculated using correlations. The pressure changes and losses inside the tubes could as well be calculated by CFD, though this might not be worthwhile. To generate correlations from model tests will not yield results that can be generalized and applied to all engine conditions.

It is considered that this is the only case in internal engine aerodynamics, where mainly CFD is recommended. Variation calculations should be performed for different swirl levels and tube positions.

Stable inward tapping without tubes is only possible for a small amount of bleed and the pressure drop calculation is not at all accurate which leads to a considerable uncertainty of the calculated bleed flow. A calculation method can be based on Farthing et al. (1989) [B.61], but their investigation was done for low Reynolds and Rossby numbers only.

### B.6.3 Pre-Swirl Systems

Two types, radial and axial pre-swirl systems are in use. There was an opinion, that the two types of systems should behave considerably different. Rig tests have shown that for practical applications it is fair enough to apply the same correlations for both. The whole problem can be divided into four parts:

- Characteristics of the pre-swirl nozzles.
- Swirl loss and mixing in of boundary layer fluid in the pre-swirl chamber.
- Pressure and swirl losses in the receiver.
- Cover plates.

The second point might be different for radial and axial pre-swirl systems, but there are not enough test results available to quantify the matter. Uncertainties arise from rig results, which are specific to engine configurations and up to now no telemetry tests results are available. Furthermore, it is recommended to agree on a nomenclature and the basic theory in order to facilitate comparisons.

The temperature drop into the rotating system is:

$$T_t - T_{t,rel} = C^2 / 2Cp - W^2 / 2Cp = U * C_{ta} / Cp - U^2 / 2Cp \quad \text{Eq. B-56}$$

$$\text{with } C_{ta} = C * \cos \alpha \quad \text{Eq. B-57}$$

Using for C according to Meierhofer and Franklin (1981) (see **Section B.6.8** for full reference):

$$C = f_s * C_n \quad \text{Eq. B-58}$$

$$\text{and} \quad C_n = C_v * C_{id} \quad \text{Eq. B-59}$$

$$\text{it follows} \quad C = C_v * f_s * C_{id} \quad \text{Eq. B-60}$$

$$\text{with } C_{id} = \sqrt{\frac{2\kappa}{\kappa-1} R * T_t \left[ 1 - \left( \frac{P_{s,n,2}}{P_{t,n,1}} \right)^{\frac{\kappa-1}{\kappa}} \right]} \quad \text{Eq. B-61}$$

Cv depends on nozzle shape, surface roughness and pressure ratio, it is in the order of 0.9 to 0.95. The swirl factor  $f_s$  comprises wall friction and turbulence losses and mixing in of boundary layer fluid. It is in the order of 0.8.

#### B.6.3.1 Pre-Swirl Nozzles

The shape of the nozzles can be optimized by CFD methods without big effort. It is important to get a nearly rectangular velocity profile, in order to get a good discharge coefficient and, more important, a good velocity coefficient, which is coupled with the Cd-value. The discharge coefficient in itself is not so important as there is usually enough space available to have the required amount of pre-swirl nozzles. A low velocity coefficient, however, would reduce the pre-swirl with the consequence of higher temperatures in the rotating system. An important means of achieving a high Cd and Cv is a low roughness of the pre-swirl nozzles.

### B.6.3.2 Pre-Swirl Chamber

The size of the chamber is not very important, but the distance nozzle exit and receiver entry should at least be larger than  $1.2 d_n$  to avoid an interaction between the two flow-fields: that of the nozzle jet and that of the receiver.

Radial nozzles have the advantage that there is no boundary layer due to disk pumping which can mix into the receiver flow.

The swirl loss results from a complex 3-D flow structure including a powerful chamber vortex.

### B.6.3.3 Receiver

The receiver holes are normally large and consequently the pressure losses small.

If the swirl can be utilized, i.e. if there is a coverplate or an annular space for a free vortex downstream of the receiver the swirl losses are of importance.

The swirl loss of the receiver is a function of length over diameter ratio of the holes and of the ratio of receiver to nozzle area. The receiver swirl factor is defined as:

$$f_{s,rec} = W_{ta,rec2} / W_{ta,rec1} \quad \text{Eq. B-62}$$

The pressure loss can be described by a Cd-value:

$$Cd = m / m_{id} \quad \text{Eq. B-63}$$

or by a pressure loss coefficient:

$$\zeta = \frac{P_{t,rel,1} - P_{t,rel,2}}{\frac{\rho}{2} \cdot W_{rel,1}^2} \quad \text{Eq. B-64}$$

The difficulty is, to define a pressure ratio across the receiver. A pressure loss is a total pressure difference and would have to be determined by averaging the velocity profiles up- and downstream of the receiver. Normally these profiles are not available, furthermore the pressure losses are small and the pressure profiles very uneven which would render these results questionable. In Schmitz [B.62] and Popp et al. [B.63] the pressure and swirl losses of different receiver configurations are plotted.

### B.6.3.4 Coverplates

In Hasan et al. [B.64], and Zimmermann [B.65] it is shown, that the free vortex flow between coverplate and turbine disc can be fairly well calculated by CFD, the same applies for a forced vortex. Many engine applications have no coverplate, i.e. the swirl is lost by the transition into the disc. The main reason for having a coverplate is to enable good seals on both sides of the swirl chamber in order to minimize leakages and to achieve a sufficiently high pressure for a good blade cooling air supply.

### B.6.3.5 Conclusions for Tappings

- For outward tapings correlations are available.
- For designing inward tapings CFD is recommended.

- To get reliable coverplate receiver characteristics, more investigations are necessary.
- On the whole more research is required.

### B.6.4 Labyrinth Seals

Most companies in the turbomachinery industry have a wealth of unpublished test results, which are partly transformed into company restricted correlations. Therefore, the opinion in this review is necessarily based on the knowledge of the authors. If this paper initiates more research and exchange of ideas, or even correlations, the authors would meet part of their targets.

This chapter comprises labyrinth seals. There are several books for these subjects, e.g. Trutnovsky [B.66] and others. Since there is a good basis, progress needs much effort, but there are still some geometrical and physical parameters, which are not fully covered up to now.

On the other hand, seal clearances will hardly be known very accurately and there are other uncertainties, which overall results in moderate accuracy of air system calculations.

It is important to cover the main parameters for optimizing purposes and to give analytical engineers more confidence into their calculations.

Labyrinth flow has been a subject of research for more than 100 years. Therefore a wealth of literature exists, but complete combined correlations for all parameters are missing. In this paper it is aimed to give a set of correlations for practical applications. Contributions from other authors to complete or improve this set are welcomed.

The authors have produced several quite different methods of correlating labyrinth seal leakage, but only one method each for straight through and stepped seals will be described.

For straight through labyrinth seals most of the important geometrical parameters can be covered, for stepped seals there are significant gaps of knowledge. In this paper, it is not intended to quote every investigation into the effects of the different geometrical parameters. Only if there is a correlation that covers a large fraction of the field of practical application, is it taken into account. It is considered that the forthcoming correlation method based on ideal labyrinth flow, carry over factors (in case of straight through seals) and Cd-values are most useful. A disadvantage of that method is, that ideal labyrinth correlation and carry over factors are strictly speaking not fully correct models. Therefore, many corrections have to be bundled in a Cd-value, if not, for the benefit of better practical application of a simpler model, slightly larger discrepancies from reality are accepted.

#### B.6.4.1 Straight Through Labyrinth Seals

**Figure B.105** shows the flow function for the ideal labyrinth, derived from the linearized gas dynamic equations, as a function of pressure ratio. It can be seen that for 1 fin up to conditions of maximum flow function the difference between linearized and compressible flow functions are small. Therefore, the forthcoming correction factors are based on the linearized functions:

$$Q_{id} = \sqrt{\frac{1 - (P_s / P_t)^2}{R(n - \ln(P_s / P_t))}} = \frac{m_{id} \cdot \sqrt{T_t}}{A \cdot P_t} \quad \text{Eq. B-65}$$

$$m = k_2 \cdot Cd \cdot m_{id} \quad \text{Eq. B-66}$$

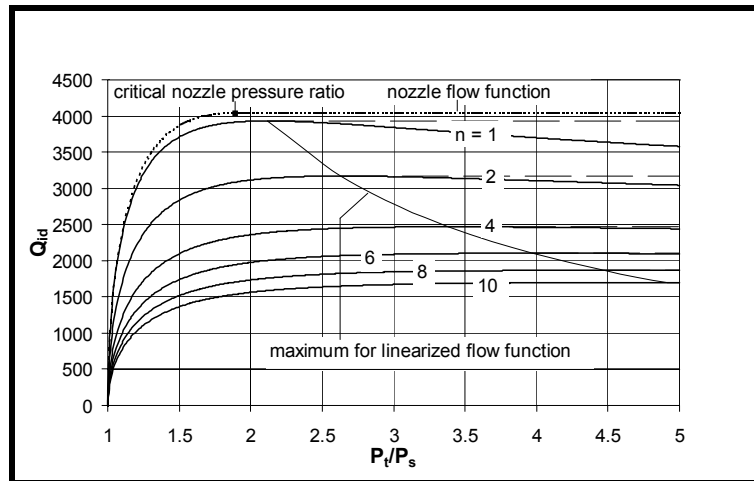


**Figure B.105: Ideal Labyrinth Flow.**

Eq. B-65, Eq. B-66, and **Figure B.105** are based on the so-called ‘Martin Equation’ for a series of identical restrictions with vertical fins. **Eq. B-66** defines  $k_2$  and  $C_d$ .

## B.6.4.1.1 Carry-Over Factor

The ideal labyrinth flow functions (**Figure B.105**) imply one dynamic head pressure loss downstream of each fin. The carry-over factor should account for the effect that only a fraction of the dynamic head is lost, i.e. some dynamic head is carried over. Test results have shown, that this effect depends on the number of fins, which can easily be understood, because the first and the last fin play an extra role and thus it is important how many fins are in between.

**Figure B.106** shows the carry-over factor from Hodkinson [B.67] and **Figure B.107** shows correction factors as a function of number of fins.

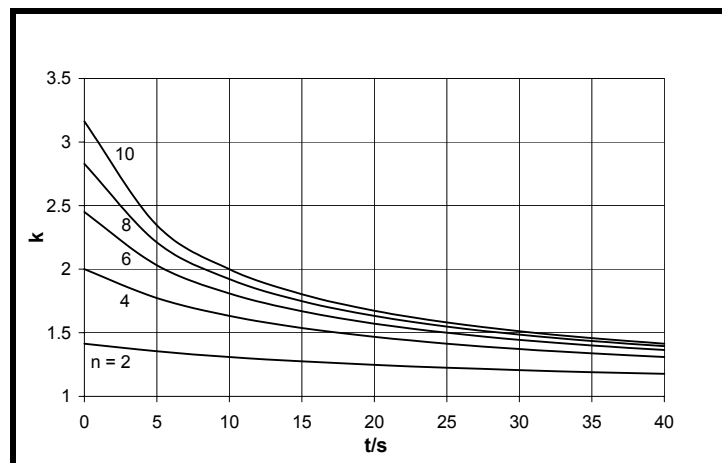


**Figure B.106: Carry-Over Factor from Hodkinson.**

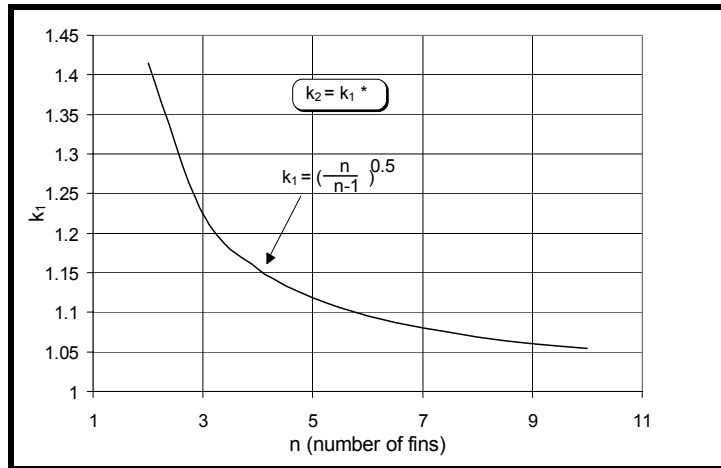


**Figure B.107: Correction Term for Carry-Over Factor.**

The carry-over factor proposed by Hodkinson [B.67] is:

$$k = \sqrt{\frac{1}{1 - \frac{n-1}{n} \cdot \frac{s/t}{s/t + 0,02}}} \quad \text{Eq. B-67}$$

With the new correction factor from unpublished test results:

$$k_1 = \sqrt{\frac{n}{n-1}} \quad \text{Eq. B-68}$$

A revised carry-over factor  $k_2$ , which describes better the effect of  $n$ , than the correlation  $k$  from Hodkinson [B.67], is obtained by:

$$k_2 = k_1 \cdot k \quad \text{Eq. B-69}$$

Carry-over factors derived from CFD calculations as tabulated in Zimmermann and Wolff [B.68] compared with those from equivalent conditions in Figure B.106 and Figure B.107, are in the same order, i.e. they are in line with physical understanding.

#### B.6.4.1.2 Coefficient of Discharge

The  $C_d$ -values in Figure B.108 and Figure B.109 comprise the effect of flow contraction and various corrections, they are plotted against the stream-wise Reynolds number ( $Re = U \cdot d_h / \nu$  with  $U$ , the velocity at the fin tip). Above  $Re = 2 \times 10^4$  there is only an effect of  $s/b$  for small seal clearances, where friction losses are of larger influence.

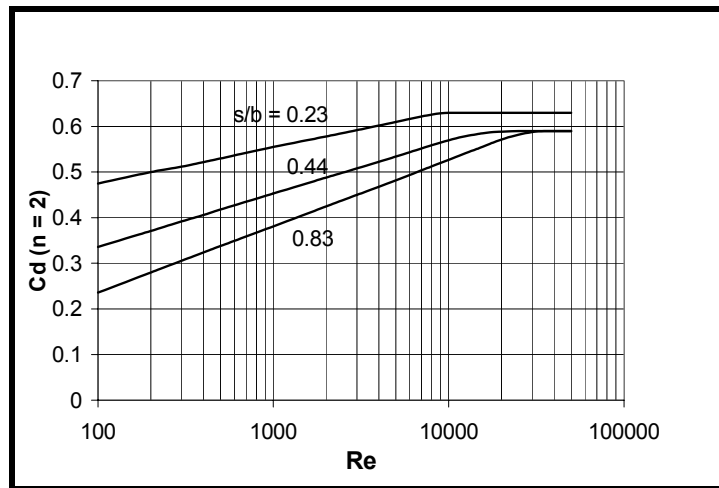


**Figure B.108:** Discharge Coefficients for  $n = 2$ .

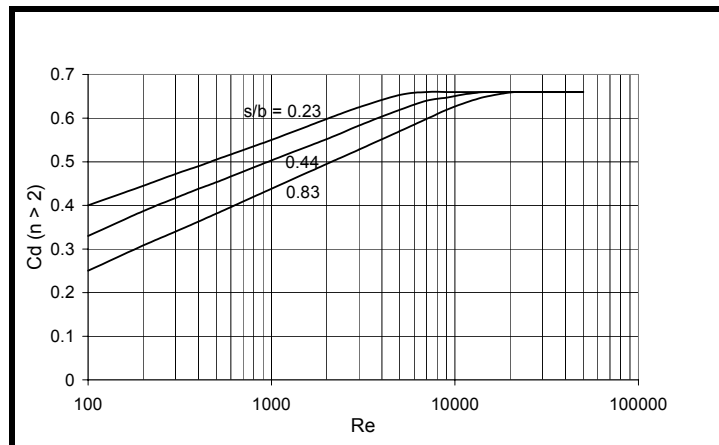


**Figure B.109:** Discharge Coefficient for  $n > 2$ .

The plotted correlations represent test results from a data bank, containing a mixture of test results from literature and company owned data. It is considered, that for low Reynolds numbers, friction factors would give better correlations.

## B.6.4.1.3 Grooves

With the use of coatings on the stator, the design is often such, that running into the liner is allowed under certain extreme operating conditions. Therefore, it is important to know the performance of a labyrinth seal running in a groove. **Figure B.110**, derived from Zimmermann et al. [B.69], shows a correction factor for Cd-values without grooves as a function of the groove depth related to gap width and with the groove width related to groove depth as parameter. It can be seen that large increases of the throughflow up to a factor of approximately 2.5 can occur.

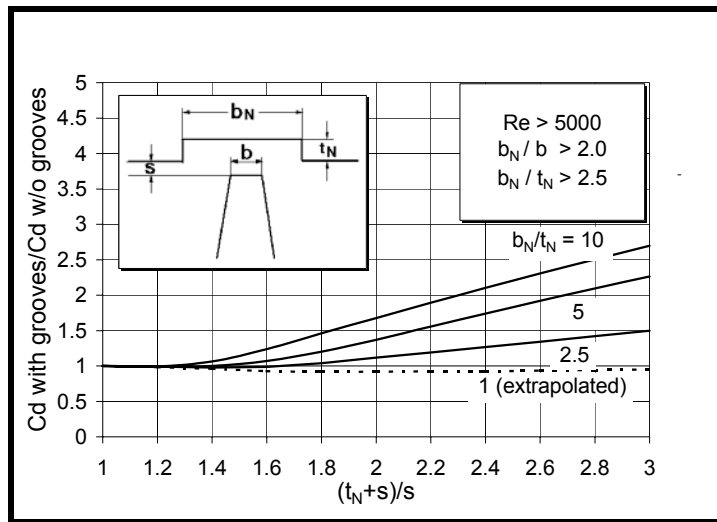


**Figure B.110: Correction Factor for Straight-Through Labyrinth Seals with Stator Grooves.**

Honeycomb on the stator layers with three different sizes as a function of labyrinth gap width related to cell size, where  $\delta_m$  is the increase or decrease of the leakage flow induced by the honeycomb. The correction is derived from Stocker [B.70] and agrees well with company owned data. For big seal clearances the negative  $\delta_m$  arises from the increased roughness of the outer wall. For small seal clearances, the effective gap is enlarged. Figure B.111 shows a correction for honeycomb.

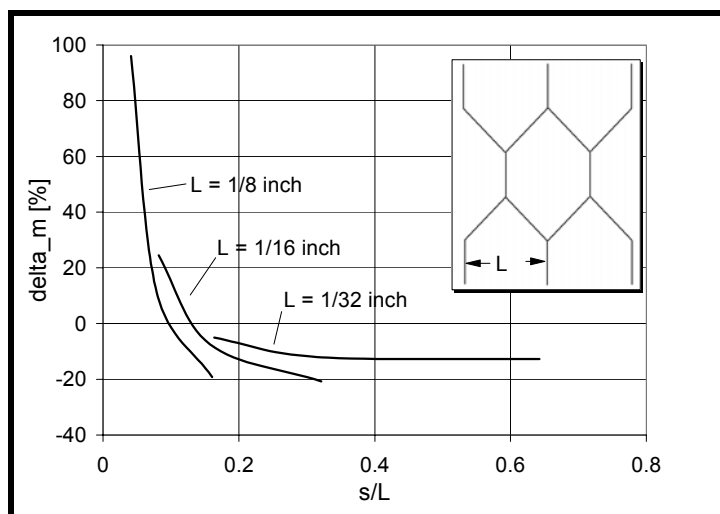


**Figure B.111: Mass Flow Differences for Honeycomb Layers on the Stator.**

## B.6.4.1.4 Corner Radius

The effect of corner rounding on  $C_d$  can be obtained from Zimmermann et al. and is shown in Figure B.112. The correction factor on  $C_d$  is plotted versus corner radius related to hydraulic diameter for an orifice, for stepped and straight through labyrinth seals. Because of the carry-over effect in straight through labyrinth seals, the effect of the corner radius is much smaller than for stepped seals. A relative small rounding of  $r/d_h = 0.2$  yields already most of the effect.

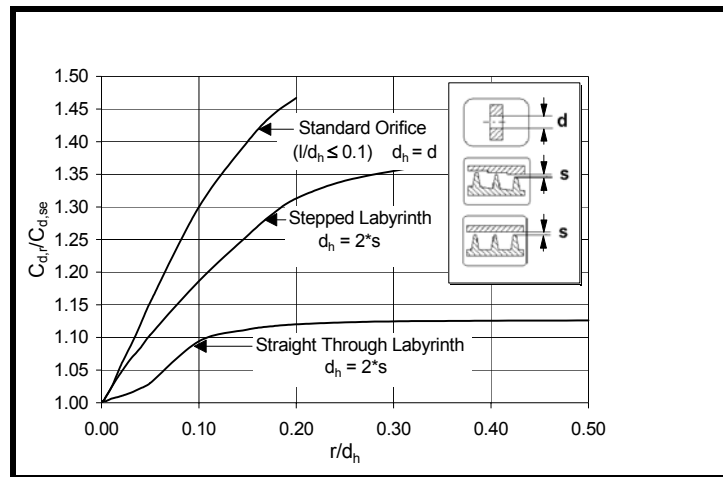


**Figure B.112: Effect of Rounding Radius.**

## B.6.4.1.5 Chamber Depth

In **Figure B.113** the influence of chamber depth on the labyrinth through-flow from Trutnovsky and Komotori [B.66] is shown. It can be seen that up to 15 % improvement can be obtained. As the minimum is independent of gap width always at  $h/t = 0.25$  it is possible to realize it on an engine and to sustain the effect under all operating conditions. But very likely will not be realized in practice, because shorter teeth tend to be thermally unstable in a rub case, i.e. the situation might escalate into a failure case.

## B.6.4.1.6 Labyrinth Seal Windage

A set of formulae is from McGreehan and Ko [B.71], a verification by test results can be found in Millward and Edwards [B.72]. This effect, however, is not directly related to the calculation of labyrinth seal leakage. Therefore, it is not discussed here in more depth.

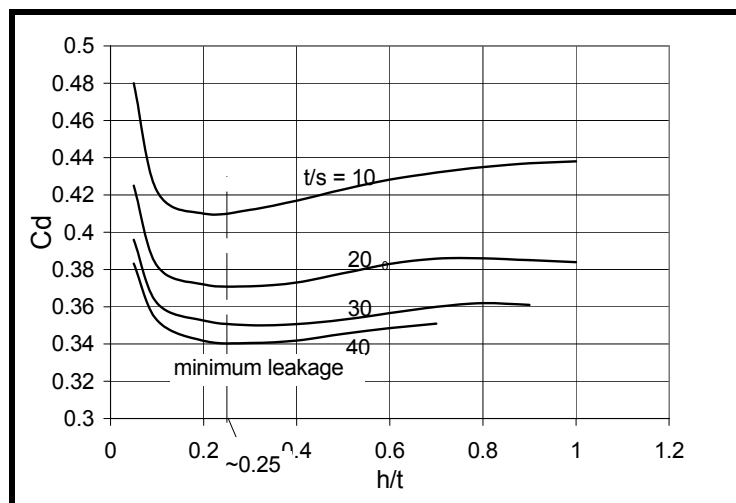


**Figure B.113: Effect of Chamber Depth.**

## B.6.4.1.7 Rotation

From Waschka et al. [B.73] it can be seen that for  $Re = 10000$  the influence of rotation on throughflow is negligible. But for laminar flow, especially for low Reynolds numbers the effect is high. As the pressure

losses for laminar flow are due to increasing friction losses with decreasing Reynolds numbers they depend on surface area and form. Therefore, a generalized correlation cannot be very accurate.

## B.6.4.2 Stepped Labyrinth Seals

The flow function of the ideal labyrinth in **Figure B.105** is as well valid for stepped seals.

$$m = k_s \cdot C_d \cdot m_{id} \quad \text{Eq. B-70}$$

with  $C_d$  from **Figure B.114** and  $k_s$  from **Figure B.115**.

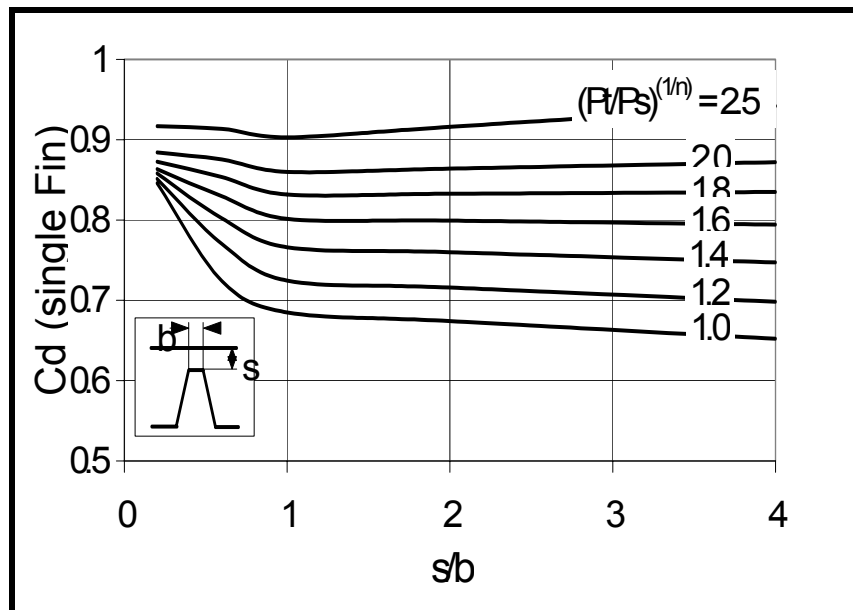


**Figure B.114:** Discharge Coefficients for Stepped Labyrinth Seals (single fin).

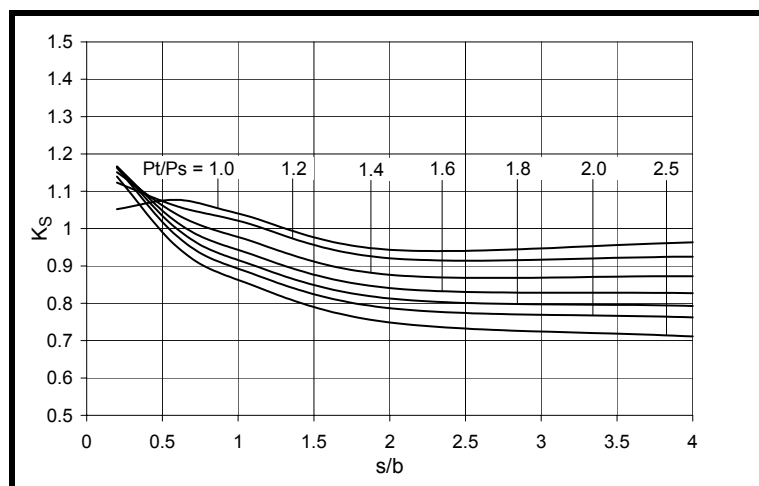


**Figure B.115:** Correction Factor for  $C_d$ .

## ANNEX B – ADVANCED TOPICS AND RECENT PROGRESS

Though the literature is manifold, there is not enough information available to cover all influencing parameters.

### B.6.4.2.1 Ideal Cd-Values

**Figure B.114** contains the Cd-values for single fins derived from Snow [B.74] to be applied for stepped seals because of the assumption that there is a one dynamic head loss after every fin. It is furthermore assumed that the pressure ratios are equal for each fin.

### B.6.4.2.2 Cd Correction Factor

As the assumption above is not fully applicable, a correction factor is necessary. **Figure B.115** shows this factor as a function of gap width related to fin width. It represents test results with  $\pm 5\%$  accuracy.

### B.6.4.2.3 Corner Radius

See **Figure B.112** and the associated section, where the effect of corner rounding for stepped seals is included.

### B.6.4.2.4 Flow Reversal

From Waschka [B.73] it can be seen that the influence of flow reversal on the Cd-value of stepped labyrinth seals is small. Only for  $Re \leq 10^3$  there is an effect of approximately 10 to 20%, but that rarely occurs with stepped seals in aero engines, see Zimmermann et al. [B.69].

### B.6.4.2.5 Rotation

Waschka et al. [B.73] have shown that for approximately  $Re \geq 3 \cdot 10^2$  the influence of rotation on through-flow is negligible.

### B.6.4.2.6 Step Height

**Figure B.116** based on unpublished company owned data shows that there is a flat minimum at  $H/t$  equal to 0.075. It is recommended to place practical applications around that value. For decreasing  $s/b$   $Cd \cdot k_s$  increases, because in the then relatively longer gap the flow reattaches and thus increases Cd.

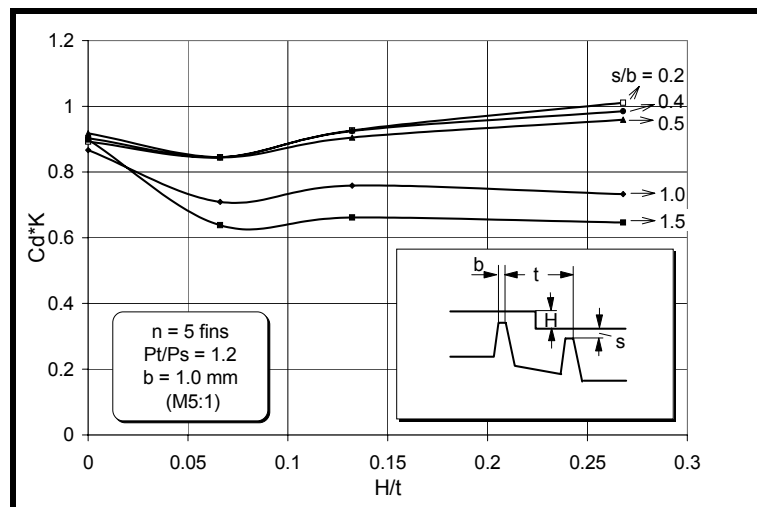


**Figure B.116: Influence of Step Height.**

### **B.6.4.3 Conclusions for Labyrinth Seals**

- For both, stepped and straight through labyrinth seals the influence of Reynolds number is only significant for laminar flow.
- It is advantageous to design straight through labyrinth seals with flat chambers. But the thermal stability of the fins in a rub situation has to be watched.
- It is as well advantageous to realize flat steps and small chambers for stepped labyrinth seals. The influence of flow reversal on the Cd-values of stepped seals is small.
- There is a strong need for further research, especially concerning whole models and correlations for all important parameters.
- All correlations in this paper could be refined.
- Better or new correlations are required for Reynolds number effect, influence of rotation, especially at low Reynolds numbers, furthermore for the influence of chamber depth (or step height) and for the axial displacement of stepped seals.
- There is a wealth of literature but it is difficult to create complete correlations from individual research projects that do not fit together.

### **B.6.5 Rotating Holes**

The aim of this review is to collect the major aspects for systems calculations. It does not contain all different possibilities out of the literature, thus it is based on a subjective judgement of the author. For simplicity, only the effects of the most important parameters are taken into account.

Rotating holes are often the bottleneck to sections of the air system network, because the discharge coefficients are small. Consequently, large areas in rotating pieces are required which is often critical, especially with respect to the stressing of these parts. For rotating holes the final method of correlation has yet to be found. Therefore, in this chapter four methods are compared to each other and discussed.

#### **B.6.5.1 Sharp-Edged Holes**

For sharp edged holes with small l/d all sources quote similar test results. The more it is astonishing that for the other cases there are so large discrepancies.

#### **B.6.5.2 Rounded Holes**

There is only little and contradictory literature available on the influence of the rounding radius and the interaction with the l/d effect.

Several methods of correlation are in use. The definitions of Cd are the following:

$$Cd = \frac{m}{m_{id}} \quad \text{Eq. B-71}$$

$$m_{id} = A \cdot P \sqrt{\frac{1}{RT}} \sqrt{\frac{2\gamma}{\gamma-1} \left(\frac{P_{S\infty}}{P}\right)^{\frac{2}{\gamma}} \left(1 - \left(\frac{P_{S\infty}}{P}\right)^{\frac{\gamma-1}{\gamma}}\right)} \quad \text{Eq. B-72}$$

P and T may be expressed either in the absolute or in the relative frame of reference. In the absolute frame of reference, P and T are P<sub>0</sub> and T<sub>0</sub>, whereas in the relative frame of reference P<sub>rel</sub> and T<sub>rel</sub> have to be used:

$$P_{rel} = P_0 \left(1 + \frac{\gamma-1}{2} Ma^2\right)^{\frac{\gamma}{\gamma-1}} \quad \text{Eq. B-73}$$

$$T_{rel} = T_0 \left(1 + \frac{\gamma-1}{2} Ma^2\right) \quad \text{with} \quad \text{Eq. B-74}$$

$$Ma = \frac{U}{\sqrt{\gamma \cdot R \cdot T_0}} \quad \text{Eq. B-75}$$

Samoilowich [B.75], Meyfarth and Shine [B.76] and McGreehan and Schotsch [B.77] plot  $C_d$  in the absolute system against  $U/C_{ax,id}$ :

$$C_{ax,id} = \frac{m_{id}}{\rho A} = \sqrt{\frac{2\gamma}{\gamma-1} RT_0 \left(1 - \left(\frac{P_{s\infty}}{P_0}\right)^{\frac{\gamma-1}{\gamma}}\right)} \quad \text{Eq. B-76}$$

More recently Weissert [B.78] presents  $C_d$  in the relative frame of reference versus  $C_{ax}$ :

$$C_{ax} = \frac{C_d \cdot m_{id}}{\rho A} \quad \text{Eq. B-77}$$

For  $\rho$ , the density in the vena contracta has to be used. This necessitates iteration and the first  $C_d$  has to be guessed. Another method would be to plot  $C_d$  in the relative system against  $U/W_{id}$  with:

$$W_{id} = \sqrt{\frac{2\gamma}{\gamma-1} RT_{rel} \left(1 - \left(\frac{P_{s\infty}}{P_{rel}}\right)^{\frac{\gamma-1}{\gamma}}\right)} \quad \text{Eq. B-78}$$

Because  $U/W_{id}$  approaches 1 for  $U$  approaching infinity,  $U/W_{id}$  is limited between 0 and 1 and not between 0 and infinity as is the case with  $U/C_{ax}$  and  $U/C_{ax,id}$ . Therefore,  $U/W_{id}$  is advantageous, especially if limited test data have to be extrapolated.

In the following diagrams the different correlations are transformed to the same basis, in order to allow a comparison. The upstream total equals the static condition. From **Figure B.117** it can be seen that in the absolute frame of reference  $C_{d,rot,abs}$  may exceed 1. This is the more the case the greater  $Rk/D$  is.  $C_{d,rot,rel}$  in the relative frame of reference.

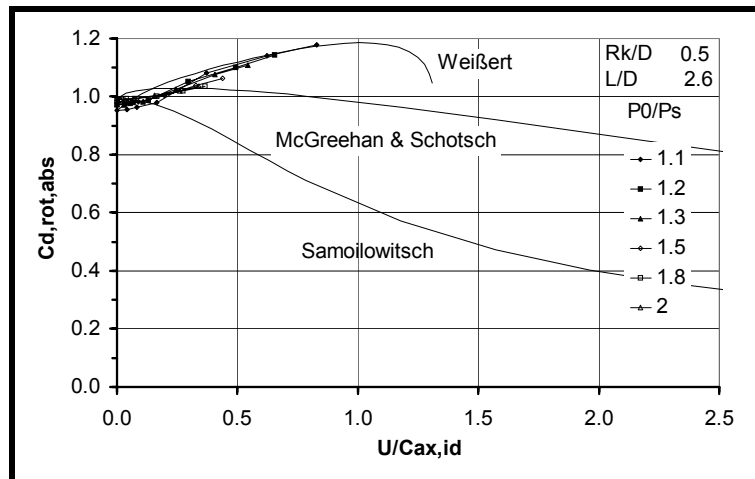


**Figure B.117:** Comparison of Different Cd Correlations, Absolute Frame of Reference.

**Figure B.118** on the contrary stays at or only slightly above 1 which is in line with the notion of an engineer, that such ratios describing a comparison to an ideal condition should stay below 1.

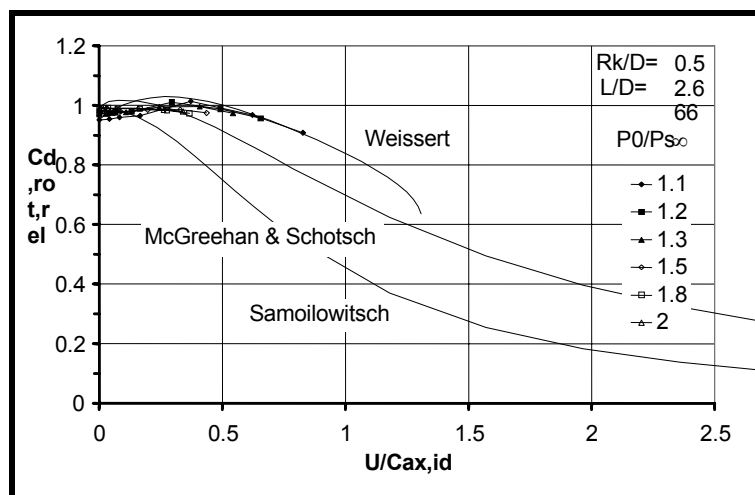


**Figure B.118:** Comparison of Different Cd Correlations, Relative Frame of Reference.

In the forthcoming figures  $C_{d,rot,rel}$  will be related to the static  $C_d$  which is labeled as  $C_{d,0}$ . This has the advantage, that the scatter of the test results is reduced. From **Figure B.119** and **Figure B.120** it can be seen that the rotating  $C_d$  for low  $U/C_{ax,id}$  is higher than the static  $C_d$ , because of the work done to the distorted flow with strong secondary vortices.

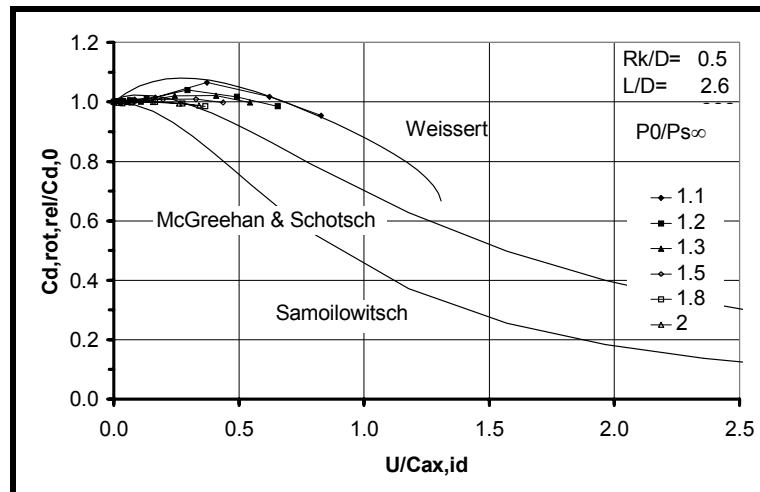


**Figure B.119:**  $C_{d,rot,rel}$  Referred to  $C_{d,static}$  as Function of  $U/C_{ax,id}$ .

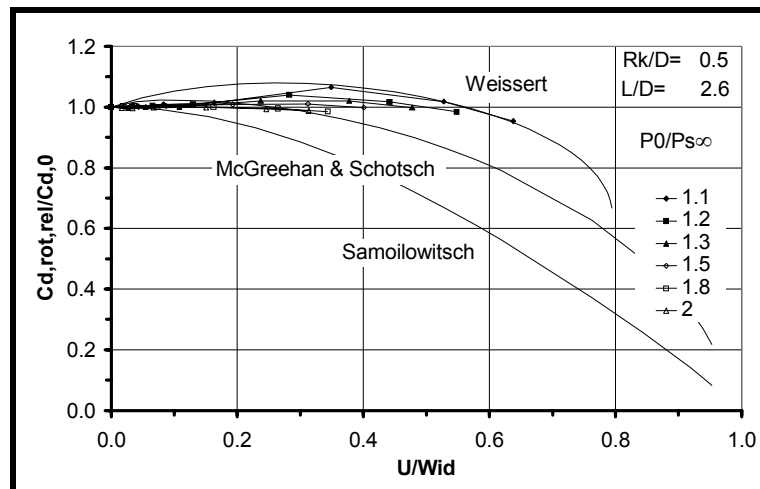


**Figure B.120:**  $C_{d,rot,rel}$  Referred to  $C_{d,static}$  as Function of  $U/W_{id}$ .

With large  $L/d$  the work done is mainly independent of the corner radius, but influences the efficiency, i.e. the conversion into pressure rise which yields higher  $C_d$ -values than for shorter  $L/d$ . In **Figure B.117** to **Figure B.119** the  $C_d$ -values are plotted against  $U/C_{ax,id}$ , whereas in **Figure B.120** against  $U/W_{id}$ . This has the clear advantage that the  $C_d$ -values have to approach different  $C_d$  Correlations 0 at  $U/W_{id} = 1$  on the abscissa. This is advantageous if, due to the limited extent of available test data, extrapolations become necessary. The difference between the three compared correlations partly results from the difference in the test results. Only Weissert [B.78] has modeled the maximum in the relative system on the left hand side of the diagrams which is due to the work done to the secondary flows.

## B.6.5.3 Discharge Coefficient Correlations

In this section four methods to correlate discharge coefficients will be described and discussed. They differ by the use of different test results. All four methods could be improved and developed to the preferred one in practical use.

## B.6.5.3.1 Method by McGreehan and Schotsch (1987)

This method is mainly based on test data of stationary holes, i.e. Rohde et al. (1969) [B.60], with inlet tangential velocity. For small  $U/C_{ax,id}$  the correlations were checked by McGreehan and Schotsch [B.77] against test results from rotating holes, Grimm (1969) [B.79], Meyfarth and Shine (1965) [B.76]. For  $U/C_{ax,id}$  between 0 to 1, where most of the practical applications are placed, the maximum as shown in Weissert (1997) [B.78], is not modeled adequately, whereas for  $U/C_{ax,id}$  from 2 to 5 it can be seen from the original paper that the correlation should yield smaller  $C_d$ -values. All this could be adjusted in the light of more recent test results or CFD calculations.

## B.6.5.3.2 Method by Weissert (1997)

The Thesis of Weissert (1997) [B.78] will not yet be known to most of the readers. It contains very useful CFD results, which show the complex flow pattern in rotating holes and, here of more interest, presents a  $C_d$  correlation.

In **Figure B.121** the related  $C_d$ -values are plotted against  $U/C_{ax}$ , which on the first sight shows no difference to **Figure B.119**, a plot against  $U/C_{ax,id}$ . When **Figure B.120** and **Figure B.122** are analyzed, it becomes evident, especially on **Figure B.122** that  $W_{id}$  derived from  $C_{ax}$  can lead to erroneous values. This is insofar as it tends to show a maximum and will not reach the theoretical limit of 1.

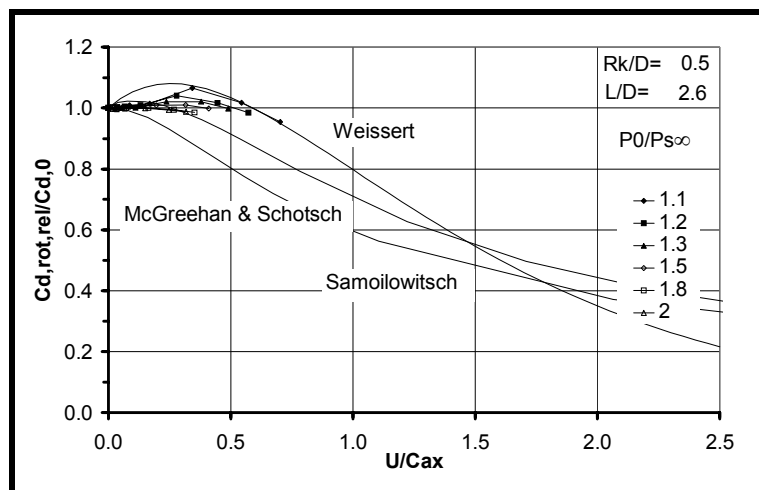


**Figure B.121:**  $C_{d,rot,rel}$  Referred to  $C_{d,static}$  as Function of  $U/C_{ax}$ .

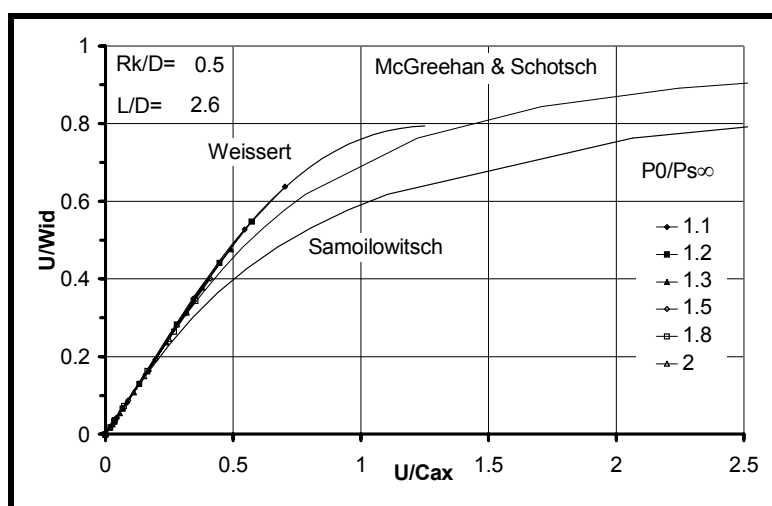


**Figure B.122: Comparison of U/Wid vs. U/Cax.**

It can be shown that  $C_{ax} = C_d \cdot W_{id}$ . With  $C_d = f(U/C_{ax})$  it follows that  $U/W_{id} = U/C_{ax} \cdot f(U/C_{ax})$ . Because  $U/W_{id}$  approaches 1 for  $U/C_{ax, id}$  or  $U/C_{ax}$  approaching infinity, as mentioned already above, only such functions  $C_d = f(U/C_{ax})$  are allowed which do not produce a maximum of  $U/W_{id}$ , i.e. the slope  $dC_d/d(U/C_{ax})$  has to be greater than -1. Therefore, the validity of the correlation from Weissert (1997) [B.78] has to be limited to  $U/C_{ax} < 1.5$ , where most of the practical applications take place. In order to obtain  $C_{ax}$ , a  $C_d$ -value is required, the relevant iteration can lead to big discrepancies with the test results the correlation is based on.

## B.6.5.3.3 Method Based on Samoilowich [B.75]

A previous method of MTU is fully based on Samoilowich (1957) [B.75] and, therefore, is somehow superseded by more recent publications. The following correlation has been developed:

$$C_{d, rot, abs} = (C_{d, 0}^{-1/z} + 2 \cdot (U / C_{ax, id})^2)^{-z} \quad \text{Eq. B-79}$$

with:

$$l/d \quad 0 \quad 0.5 \quad 1.0 \quad 1.5 \quad 2.0 \quad 2.5 \quad 3.0 \quad 3.50$$

$$z \quad 0.65 \quad 0.65 \quad 0.65 \quad 0.65 \quad 0.53 \quad 0.44 \quad 0.38 \quad 0.33$$

$$l/d \quad 4.0 \quad 4.5 \quad 5.0 \quad 5.5 \quad 6.00$$

$$z \quad 0.30 \quad 0.28 \quad 0.26 \quad 0.25 \quad 0.24$$

The influence of a corner radius is taken from McGreehan and Schotsch (1987) [B.77]. The correlation (equation 23) has been included as the test data from Samoilowich are still the most comprehensive ones and can be used to check the other methods. It is easier to do the comparison with a formula that can easily be programmed, than to use test results from diagrams, which are often not very clear.

## B.6.5.3.4 Method by Reichert et al. (1997) [B.80]

This method can only be recommended for long orifices. It differentiates between three parts: Entry losses, friction losses in the middle and exit losses. Details can be obtained from the paper.

This method should be used as a basis for a new method of correlating all three parts (entry, friction, and exit losses) separately, mainly as a function of RPM. Weissert (1997) [B.78] has demonstrated by CFD calculations that the velocity profiles are heavily distorted. The entry losses can be described by a flow contraction defined as a Cd-value and a subsequent expansion loss (Carnot shock). The exit loss is as well determined by a Cd-value, which describes the contraction. A full dynamic head pressure loss from the velocity in the restricted area then yields the exit loss.

It is considered that a method where all three parts are assessed separately would yield better results than a complex formula with all three parts mixed.

#### **B.6.5.4 Comments on the Correlation Methods**

Each method has its merits, the main difference among method 1 to 3 may arise from the test results used. It is not understood why the discrepancies are so large, which is not the case for sharp edged holes. In Samoilowich (1957) [B.75], the test arrangement was different to that of Weissert (1997) [B.78] with respect to the pre-swirl and the pre-swirl was varied. With static test data, i.e. McGreehan and Schotsch (1987) [B.77] the pre-swirl effect is excluded. For rotating holes with corner rounding the pre-swirl is much more important than for sharp edged holes.

Furthermore, it is suggested to differentiate between disc windage and the associated flow-field and flow through rotating holes. Both are at least to a small extent coupled according to the design of the different test facilities. The disc windage yields the boundary conditions for the rotating holes and both should be assessed separately (laser measurements). It is mainly important to know the core rotation factor and to use it as input to calculate the Cd-value of the rotating holes from the amount of pre-swirl.

#### **B.6.5.5 Conclusions for Rotating Holes**

- It is recommended to plot related Cd-values in the relative frame of reference against  $U/Wid$ .
- If  $U/Cax$  is used on the horizontal axis, errors due to the coupling with Cd can occur in case the correlation is used for extrapolating beyond the test data.
- The difference between the various test results is not understood.
- New test results are required to clarify the latter point and to refine the correlations.

#### **B.6.6 Two Phase Flow**

Only those correlations are chosen for this chapter which are easy to handle for engineering purposes and as there is not much experience in this field, test data are added to give more confidence into the application.

In Zimmermann et al. (1991) [B.81] a review was published mainly based on water/air test results. Since then, new correlations have come forward and oil/air test results are available. Because of limited space the formulas or basic diagrams are not reproduced, they have to be taken from the references. The air/oil test data are taken from an ongoing research program and a forthcoming thesis from R. Fischer.

##### **B.6.6.1 Pipe Flow**

The Lockart and Martinelli (1949) [B.82] correlation is still in use, therefore it has been compared with those of Storek and Brauer (1980) [B.83], Friedel (1978) [B.84] and air/oil test results (Figure B.123). As already stated in Zimmermann et al. (1991) [B.81] the correlation of Friedel is recommended.

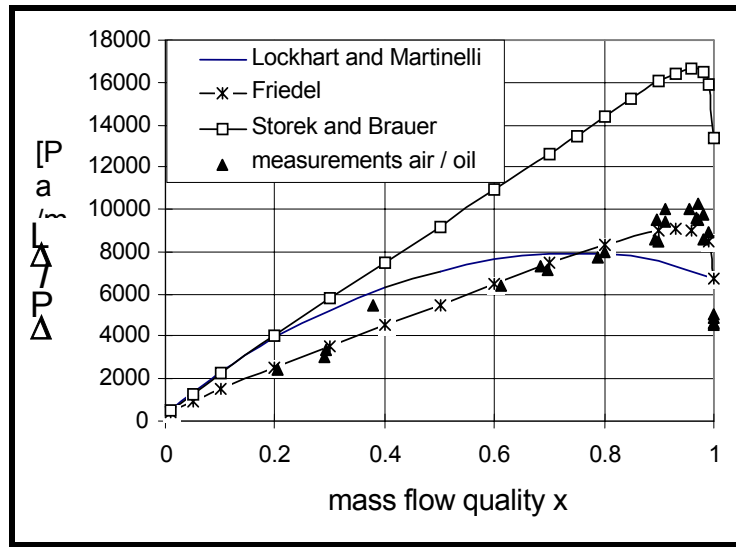


**Figure B.123: Comparison of Available Correlations with Air/Oil Measurements.**

## B.6.6.2 Bends

In order to take into account the effect of de-mixing the pressure loss in the exit line has to be considered. For bends two calculation methods are available, which both are simple combinations of pure bend losses, Chisholm (1980) [B.85], and pipe losses Friedel (1978) [B.84] or Storek and Brauer (1980) [B.83]. It can be seen from **Figure B.124** that both have their shortcomings if it is assumed that the test data are representative for engine conditions.

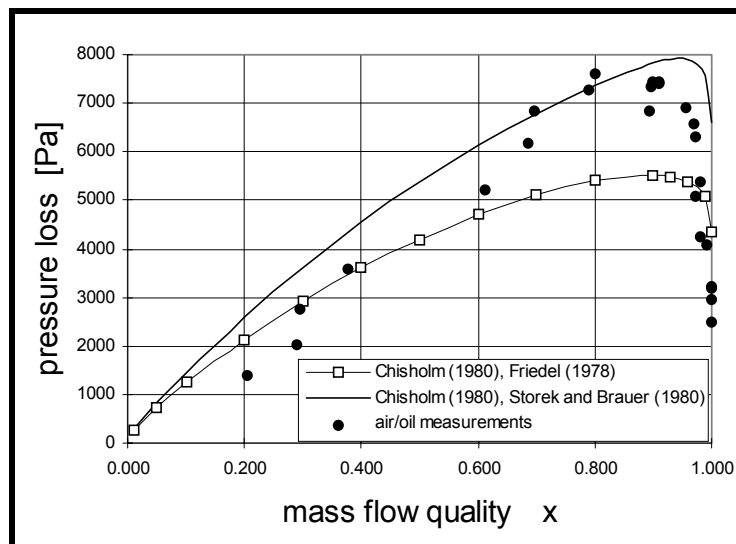


**Figure B.124: Pressure Loss of a 90° Bend – Comparison of Available Correlations with Air/Oil Measurements.**

## B.6.6.3 Mitre Bends

**Figure B.124** shows the pressure loss comparison of a 90° mitre bend with correlations from Chisholm (1980) [B.85] and from Theissing (1980) [B.86], it can be seen that the Chisholm correlation fits better but for pure air there is a big discrepancy. For a 60° mitre bend the situation is very similar, **Figure B.125**.

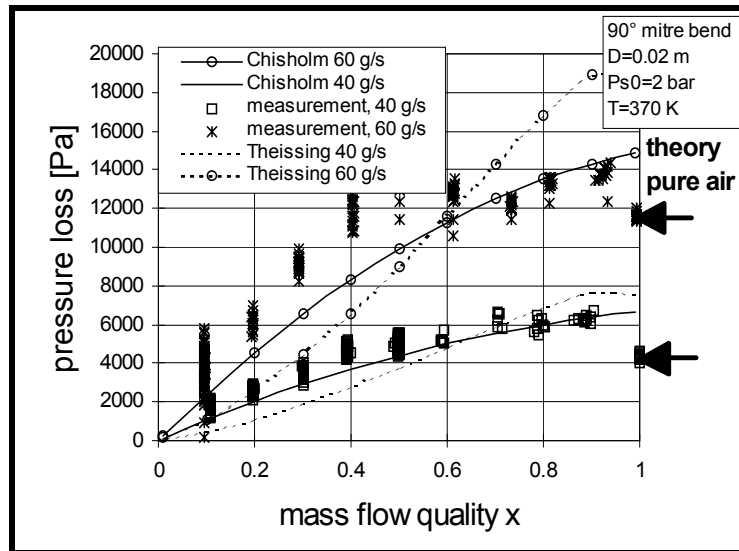


**Figure B.125: Pressure Loss of a 90° Mitre Bend.**

## B.6.6.4 Stationary Orifices

In **Figure B.126** the data resulting from Fischer (1995) [B.87] are compared to air/oil test data. It can be seen that the comparison is favorable. The measurements are obtained from a mixture of sharp edged and chamfered entry configurations of the orifice. It seems that the oil smoothes the edges and, therefore, it is questionable whether there is a vena contracta at all.

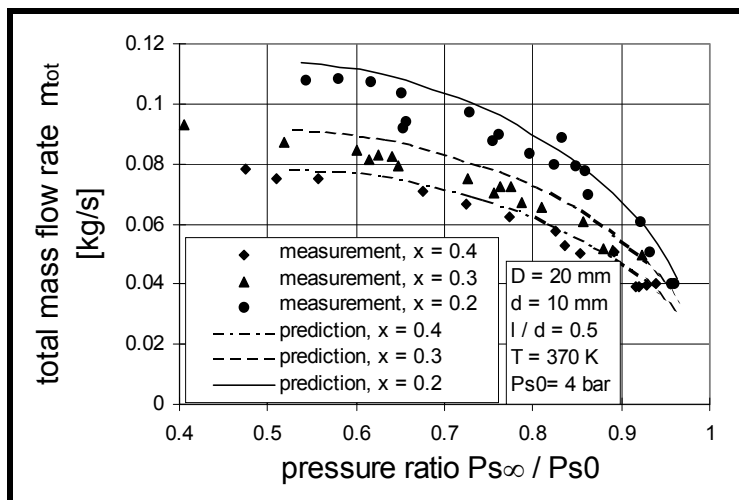


**Figure B.126: Subcritical Mass Flow Rate through an Orifice – Comparison between Prediction and Measurement.**

**Figure B.127** shows the critical mass flow rate as a function of mass flow quality. Again, it can be seen that there is no difference between sharp edged and chamfered orifices. The comparison is very good.

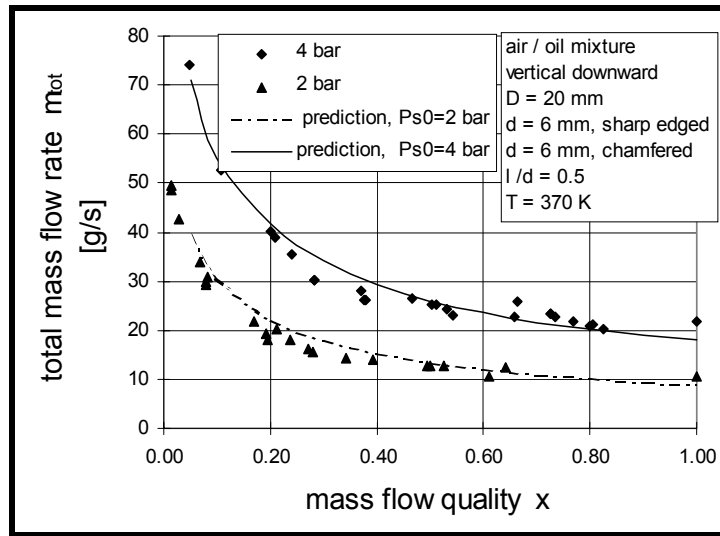


**Figure B.127: Critical Mass Flow Rate through an Orifice – Comparison between Prediction and Measurement.**

The two phase flow through orifices can be described by the following formula:

$$\left( \frac{m x^{0.44} \sqrt{T}}{P_o A} \right) = C_d' \cdot \left( \frac{P_{s, \infty}}{P_o} \right)^{1/\gamma} \sqrt{\frac{2\gamma}{R(\gamma-1)} \left[ 1 - \left( \frac{P_{s, \infty}}{P_o} \right)^{\frac{\gamma-1}{\gamma}} \right]} \quad \text{Eq. B-80}$$

$C_d'$  can be obtained from pure air correlations for instance from Parker and Kercher (see [Section B.6.8](#) for full reference).

The relevant critical mass flow function equals:

$$\frac{m x^{0.44} \sqrt{T}}{P_o \cdot A} = 3322.1 = Q_{crit} \quad \text{Eq. B-81}$$

**Figure B.128** summarizes all the test results, which show a scatter band of approximately +/- 10 % which is not bad for two phase flow.

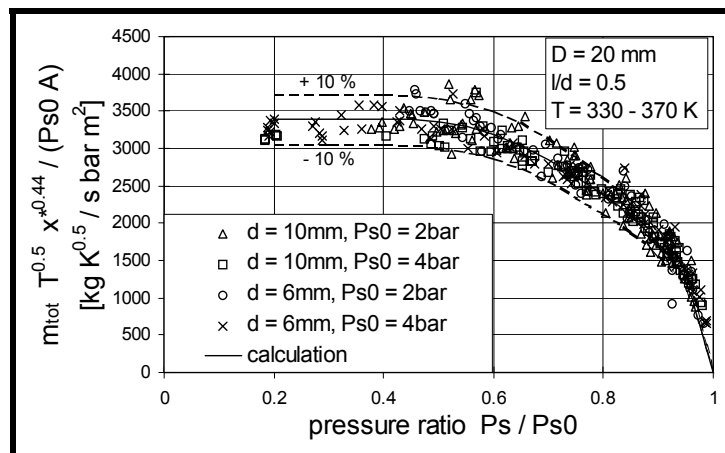


**Figure B.128: Two Phase Orifice Flow Characteristic.**

In **Figure B.129** the critical mass flow for orifices from different authors are compared to rig and engine measurements, which are in line with the already quoted value of  $Q_{crit}$  of 3322.1. It is considered that the difference arises from the method of generating air/oil mixtures. In the literature, frozen conditions are the objective. The rig results from the forthcoming thesis are obtained from a rig set up which simulates the engine conditions.

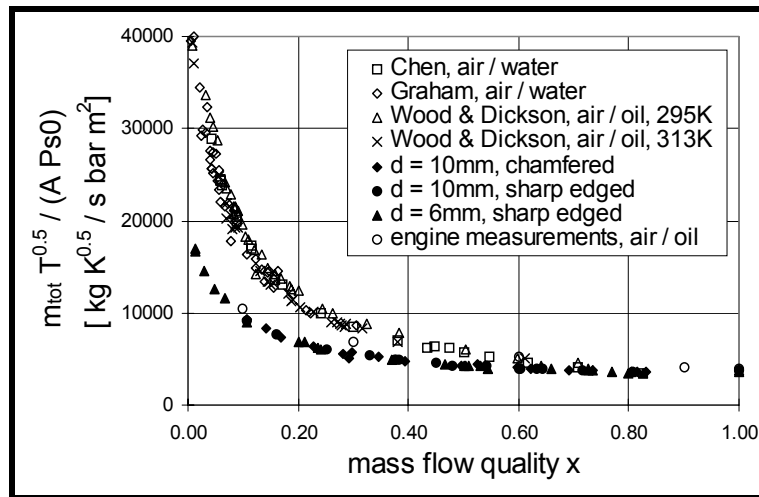


**Figure B.129: Mass Flow Function of Critical Orifice Flows.**

#### B.6.6.5 Conclusions for Two Phase Flows

- For straight pipes the correlation of Friedel (1978) [B.84] is recommended.
- The correlations for bends are not satisfactory. More research is required.
- The correlations for mitre bends from Chisholm (1980) [B.85] have to be adjusted for pure air.
- For orifices satisfactory correlations for practical applications are put forward.

#### B.6.7 References for Aerodynamics for Air Systems

- [B.58] Möller, M., “EJ 200: Durchflußbeiwerte für Spaltabzweigungen in Verdichtern”, Technischer MTU Bericht, Liu, X., 1997, “Flow in a Corotation Radial Inflow Cavity Between Turbine Disc and Coverplate”, ASME Paper # 97-GT-137, 1990.
- [B.59] Dittrich, R.T. and Graves, C.C., “Discharge Coefficients for Combustor-Liner Air Entry Holes: Circular Holes with Parallel Flow”, NACA-TN3663, 1956.
- [B.60] Rohde, R.E., Richards, H.T. and Metger, G.W., “Discharge Coefficients for Thick Plate Orifices with Approach Flow Perpendicular and Inclined to the Orifice Axis”, NASA TN D- 5467, 1969.
- [B.61] Farthing, P.R., “The Use of Deswirl Nozzles to Reduce the Pressure Drop in a Rotating Cavity with a Radial Inflow”, ASME Paper # 89-GT-184, 1989.
- [B.62] Schmitz, D., “Analyse von Axialen und Radialen Vordralldüsensystemen”, Technischer MTU Bericht, 1995.
- [B.63] Popp, O., Kutz, J. and Zimmermann, H., “CFD-Analysis of Coverplate Receiver Flow”, ASME Paper # 96-GT-357.

## ANNEX B – ADVANCED TOPICS AND RECENT PROGRESS

---

- [B.64] Hasan, J.C., “Flow in a Cover-Plate Pre-Swirl Rotor-Stator System”, ASME Paper # 97-GT-243, 1997.
- [B.65] Zimmermann, H., “Some Aerodynamic Aspects of Engine Secondary Air Systems”, ASME Paper # 89-GT-209, 1989.
- [B.66] Trutnovsky, K. and Komotori, K., “Berührungsfreie Dichtungen”, VDI – Verlag, 1981.
- [B.67] Hodkinson, B., “Estimation of the Leakage Through a Labyrinth Gland”, Proceedings Inst. Mech. Eng. Vol. 141, pp. 283-288, 1940.
- [B.68] Zimmermann, H. and Wolff, K.H., “Comparison between Empirical and Numerical Labyrinth Flow Correlations”, ASME Paper # 87-GT-86, 1987.
- [B.69] Zimmermann, H., Kammerer, A. and Wolff, K.H., “Performance of Worn Labyrinth Seals”, ASME Paper # 94-GT-131, 1994.
- [B.70] Stocker, H.L., “Determining and Improving Labyrinth Seal Performance in Current and Advanced High Performance Gas Turbines”, AGARD-CP-273, 1978.
- [B.71] McGreehan, W.F. and Ko, S.H., “Power Dissipation in Smooth and Honeycomb Labyrinth Seals”, ASME Paper # 89-GT-220, 1989.
- [B.72] Millward, J.A. and Edwards, M.F., “Windage Heating of Air Passing Through Labyrinth Seals”, ASME Paper # 94-GT-56, 1994.
- [B.73] Waschka, W., “Zum Einfluß der Rotation auf das Durchfluß- und Wärmeübergangsverhalten in Labyrinthdichtungen und Wellenduchführungen”, Dissertation, Universität Karlsruhe, 1991.
- [B.74] Snow, E.W., “Diskussionsbeitrag”, Proc. Inst. Mech. Engrs., Vol. 166, 1952.
- [B.75] Samoilowich, G.S., “Coefficients of Flow Through Pressure Equalizing Holes in Turbine Discs”, D. S. I. R. Translation C. T. S. No. 541, 1957.
- [B.76] Meyfarth, P.F. and Shine, A.J., “Experimental Study of Flow Through Moving Orifices”, J. of Basic Engineering, pp. 1082-1083, 1965.
- [B.77] McGreehan, W.F. and Schotsch, M.J., “Flow Characteristics of Long Orifices with Rotation and Corner Radiusing”, ASME Paper # 87-GT-162, 1987.
- [B.78] Weissert, I., “Numerische Simulation reidimensionaler Strömungen in Sekundärluftsystemen von Gasturbinen unter besonderer Berücksichtigung der Rotation”, 1997, VDI Fortschrittsbericht, Reihe 7, Nr. 313.
- [B.79] Grim, R.E., “Fluid Flow Characteristics Through Orifices in Enclosed Rotating Discs”, M.S. Thesis, AFIT, 1969.
- [B.80] Reichert, A.W., Birillert, D. and Simon, H., “Loss Prediction for Rotating Passages in Secondary Air Systems”, ASME Paper # 97-GT-215, 1997.
- [B.81] Zimmermann, H., Kammerer, A., Fischer, R. and Rebhan, D., “Two-Phase Flow Correlations in Air/Oil Systems of Aero Engines”, ASME Paper # 91-GT-54.

- [B.82] Lockart, R.W. and Martinelli, R., “Proposed Correlation of Data for Isothermal Two Phase, Two Component Flow in Pipes”, Journ. Chem. Eng. Progr., Vol. 45, pp. 39-48, 1949.
- [B.83] Storek, H. and Brauer, H., “Reibungsdruck-verlust der Adiabaten Gas/Flüssigkeits- Strömung in Horizontalen und Vertikalen Röhren”, VDI Forschungsheft Nr. 599, 1980.
- [B.84] Friedel, L., “Druckabfall bei der Strömung von Gas/Dampf-Flüssigkeits-Gemischen in Röhren”, Chem. Ing. Technik, Vol. 50, pp. 167-180, 1978.
- [B.85] Chisholm, D., “Two-Phase Flow in Bends”, Int. J. Multiph. Flow, Vol. 6, pp. 363-367, 1980.
- [B.86] Theissing, P., “Eine allgemeingültige Methode zur Berechnung des Reibungsdruckverlustes der Mehrphasenströmung”, Chemie-Ing.-Techn. 52, Heft 4 (1980).
- [B.87] Fischer, R., “Calculation of the Discharge Characteristic of an Orifice for Gas-Liquid Annular Mist Flow”, Int. J. Multiph. Flow, Vol. 21, 1995.

### **B.6.8 Additional Bibliography for Aerodynamics for Air Systems**

- Idel’chic, I.E., “Handbook of Hydraulic Resistance”, Atomic Energy Com. And Nat. Science Found, AEC - TR 6630, 1960.
- Oates, G., “Aircraft Propulsion Systems Technology and Design”, AIAA Education Series, 1989.
- Chen, D.K., Chen, Z.H., Zhao, Z.S. and Zhua, N., “The Local Resistance of a Gas-Liquid Two-Phase Flow through an Orifice”, Int. Journal of Heat and Fluid Flow, Vol. Nr. 3, pp. 231-238, 1986.
- Graham, E.J., “The Flow of Air-Water Mixtures through Nozzles”, NEL Report, No. 308, 1967.
- Parker, D.M. and Kercher, D.M., “An Enhanced Method to Compute the Compressible Discharge Coefficient of Thin and Long Orifices with Inlet Corner Radiusing”, HDT- Vol. 183, Heat Transfer in Gas Turbine Engines, ASME 1991.
- Meierhofer, B. and Franklin, C.J., “An Investigation of a Preswirled Cooling Airflow to a Turbine Disc by Measuring the Air Temperature in the Rotating Channels”, ASME Paper # 81-GT-132, 1981.
- Wood, J.D. and Dickson, A.N., “Metering of Air-Oil Mixtures with Sharp-Edged Orifices”, Dep. Mech. Eng. Rep., Heriot-Watt University, Ricarton, Edinburgh, UK, 1973.

## **B.7 CONTROL SYSTEMS MODELING**

### **B.7.1 Requirements for Modeling Control Systems**

The standard of fuel system and actuator modeling that is required depends on the objective for the work. When the objective is to analyze and develop a control-system, then very detailed models of the hardware and software will be required. When the basic control is functioning satisfactorily, and the objective is to evaluate engine performance and handling, the control system models can usually be simplified significantly.

Simplification of the control system models for engine handling and performance work is required to obtain acceptable run times for the model. The detailed control models normally require shorter integration time steps than are acceptable for engine handling work.

## ANNEX B – ADVANCED TOPICS AND RECENT PROGRESS

---

Acceptable control-system models for engine handling work can be developed using simple transfer-functions and the steady-state characteristics of the control. It may be necessary to change the coefficients of the transfer functions with engine operating conditions. The information required to define suitable transfer functions for the control systems can be obtained from the more detailed models that should have been built to facilitate control design.

Where control-system dynamics must be modeled accurately, then all dynamic valves need to be modeled as first or second-order systems. For all valves, fluid pressure, spring force, friction effects, leakage and the effect of fluid masses should be considered and included where appropriate. Fluid pressure-drop-to-flow relations and fuel compressibility should be modeled throughout the system. The effects of flow forces (Bernoulli Forces) should be included in valves that operate at low force levels.

It is not practicable to model the effects of heat transfer and other thermal effects in a dynamic control-system model. Where such effects are of interest, a separate model should be built for this purpose, using simplified control modeling.

The effect of manufacturing tolerances can be simulated, in a detailed control-system model, by changing parameters within the model. It is rarely practical to include terms for all components where tolerances could influence control performance, so engineering judgment must be used in determining how to model particular scenarios. The same constraints apply to modeling of failures within the control system.

Modern controls are built around electrohydraulic and electromechanical transducers and actuators. These can often be modeled satisfactorily using the manufacturer's declared characteristics and response data, but more detailed modeling is advisable if performance is marginal. It is also advisable to model delays incurred in the signal conditioning associated with many transducers.

Modeling of the DECU will depend on how detailed the control system models are and what the objectives for the model are. The engine control laws will normally be modeled, but the functionality associated with transducers and output devices may be omitted for the simpler models.

Clearly, control-laws, which are implemented digitally, are bespoke and modeling can only exist at a certain level for a given logical feature. However, a decision may be made to omit a certain branch of logic depending on the application of the model.

There will be other features of a fuel system, which require modeling at the appropriate level of detail, examples being heat-to-fuel, filtration, fuel chemistry changes, pressure losses, and compressibility effects.

### **B.7.1.1 Types of Models**

There are two main types of pump used in modern fuel systems: the fixed displacement type and centrifugal flow pumps. Gear pumps are the most common form of fixed displacement pump and are widely used in modern, main-engine fuel-systems. Centrifugal pumps are used primarily in low-pressure fuel supply systems but are increasingly finding applications in reheat controls.

In the past, variable stroke piston pumps were used in many main engine fuel systems, and vapor core pumps (inlet throttled C.F. Pumps) were used for reheat applications. Although these pumps are to be found on many engines still in operation, they are unlikely to be used on new engine controls and are not described in this report.

#### *B.7.1.1.1 Modeling the Fixed Displacement Pump*

This type of pump is probably the simplest to model. The steady state characteristic, **Figure B.130** is used to determine pump delivery flow given pump speed and delivery pressure. There are no dynamics in the pump to be represented.

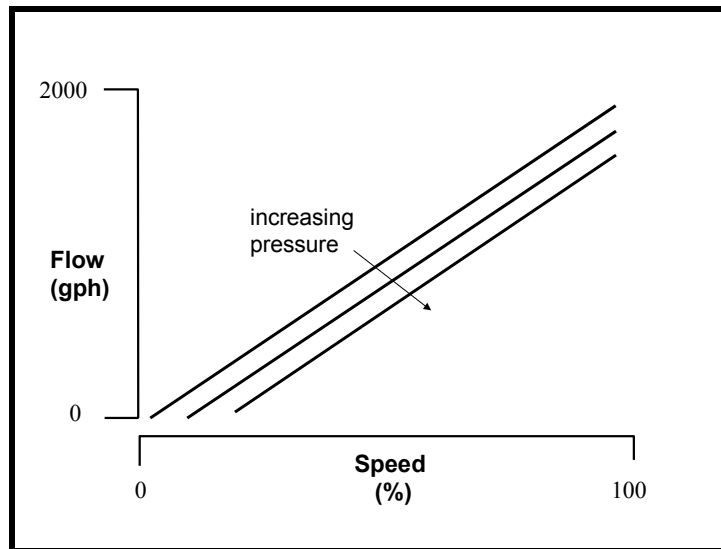


**Figure B.130: Fixed Displacement Pump Characteristic.**

## B.7.1.1.2 Modeling the Centrifugal Pump

The CF pump characteristic (see **Figure B.131**) is more complex than for a fixed displacement pump. Modeling of pump dynamics is not necessary, and pump delivery pressure is determined from the pump characteristics for given speed and delivery flow rate.

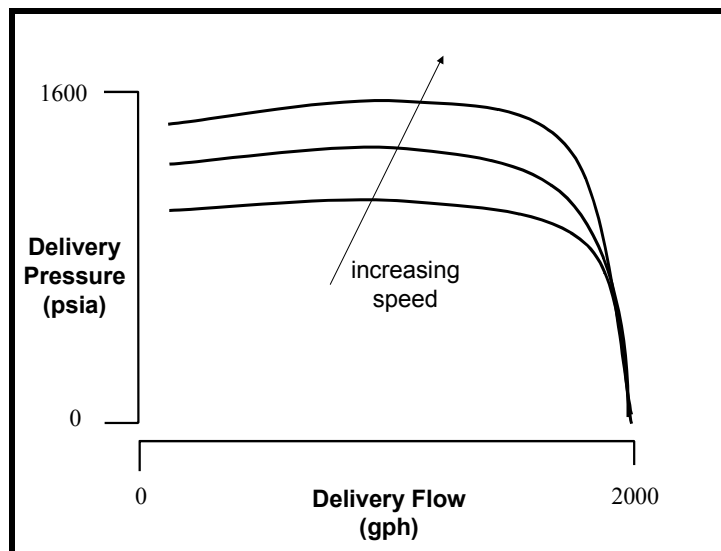


**Figure B.131: Centrifugal Pump Characteristic.**

To avoid algebraic loops in the model, it may be necessary to include a first order lag as shown in **Figure B.132**. The lag should not exceed 0.01 seconds.

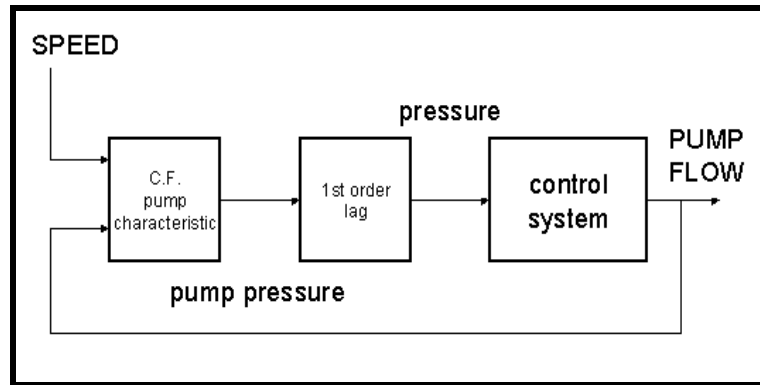


**Figure B.132: Avoidance of Algebraic Loops.**

## B.7.1.2 Equations Used in Hydraulic Control Systems

The following equations are widely used in modeling aero engine control systems and components.

Where:

- Flow: Volume flow rate through orifice;
- Cd: Discharge coefficient;
- CSA: Orifice flow area;
- P: Pressure;
- ΔP: Pressure drop;
- ρ: Fluid density;
- Area: Pressure sensing area;
- Acc: Acceleration;
- Force: Applied force;
- Mass: Effective mass;
- K: Fluid bulk modulus;
- Qnet: Net flow into a chamber; and
- Vol: Volume of chamber.

The equations are valid for any consistent set of units (**Figure B.133**).

$$\begin{aligned}
 flow &= Cd.CSA.\sqrt{\frac{2\Delta P}{\rho}} \\
 force &= P.area \\
 acc &= \frac{force}{mass} \\
 P &= \int K.\frac{Q_{net}}{vol}.dt
 \end{aligned}$$

**Figure B.133: Hydraulic Control System Equations.**

### B.7.1.3 Electro-Hydraulic Servo Valves

Modern engine control systems are operated using several types of electrohydraulic servo valve. The most common types are:

- Solenoid;
- Single stage servo valve – flapper, jet deflector and jet pipe types; and
- Two-stage servo valve – using one of the above first stages to drive a second stage spool.

Response of these servo valves can normally be ignored for engine handling work, as the bandwidth of the devices is typically above 100 Hz. For more detailed work, the manufacturer's response data can be used, and an example of a two-stage servo valve is shown later. For detailed analysis of the control systems, it is often necessary to model individual components within the servo valves, but this is beyond the scope of this document.

The solenoid valve is usually used for on-off operations and can often be treated as a simple switch. Where the response is critical, the device can be represented as a first order lag with a time constant obtained from the manufacturer's data.

A schematic of a single-stage flapper-valve is shown in **Figure B.134**, the jet deflector and jet pipe devices are similar, although the steady state characteristics need to be treated differently when detailed models are required.

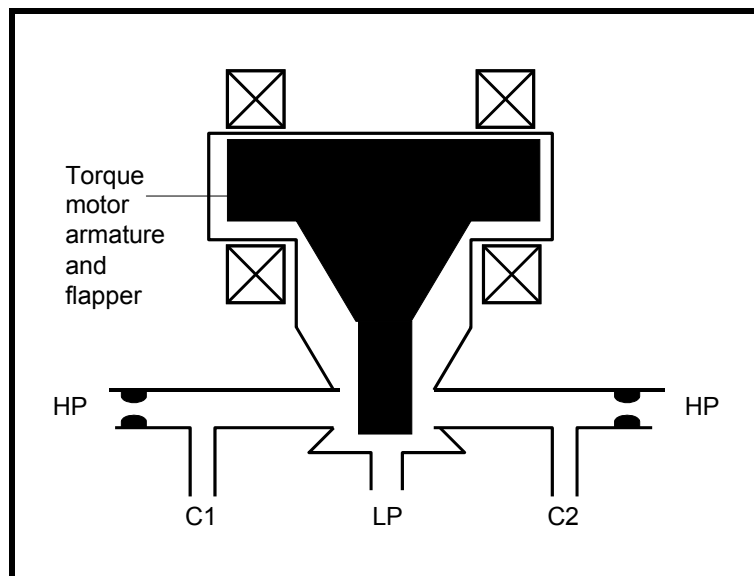


**Figure B.134: Single Stage Flapper Valve.**

For engine handling work the single stage servo valve response can normally be ignored, because the bandwidth is typically above 100 Hz. Use of a flapper-type servo-valve as the first stage of a two-stage servo valve is shown, as an example, in a later section.

### B.7.1.4 Metering Valve

The metering valve (**Figure B.135**) is a variable orifice, usually controlled by a spool valve. The flow through the metering valve is proportional to the orifice area and the square root of the pressure drop across the orifice, which is set by a pressure drop regulator.

The metering orifice is normally machined in a sleeve and is opened and closed by varying the travel of a spool inside the sleeve (see below). An LVDT or other transducer measures the metering valve travel, and a single or two-stage servo valve controls it (see example of two-stage valve). The control loop is closed by the DECU.

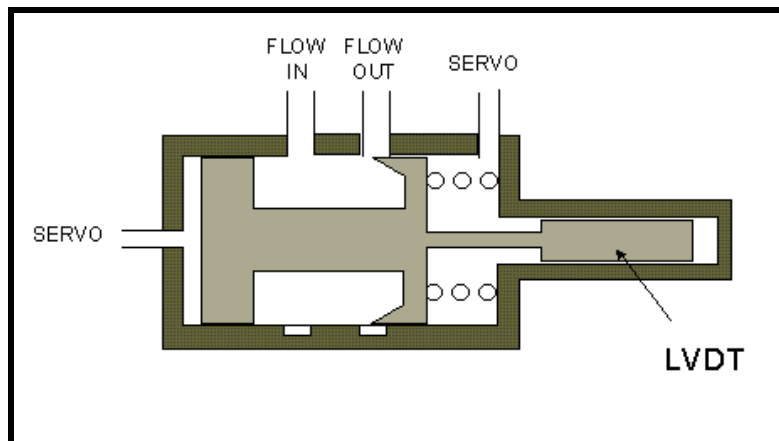


**Figure B.135: Metering Valve.**

The response of the loop will be a function of: the control algorithm in the computer, the response and gain of the servo valve, the diameter of the metering valve spool, the supply and return pressures available, and any loads on the metering spool.

Typically, the metering valve loop can be represented by a first order response with a time constant of 0.015 to 0.03 seconds. This should be adequate for engine handling work, but more detailed modeling is required to investigate any problems with the control.

### B.7.1.5 Pressure Drop Regulator

The purpose of the pressure drop regulator is to set the required pressure drop across the metering orifice. The required pressure drop may be constant or, if correction for fuel temperature is required, the pressure drop may be made a linear function of fuel temperature.

The metering pressure drop is controlled by spilling excess flow when a fixed displacement pump is used, or by throttling when a C.F. pump is used. Both direct acting and servo pressure-drop regulators may be used.

The response of the pressure drop regulator is normally much faster than that of the metering valve, and can be ignored for engine handling work; only the steady state characteristics of the valve need be included. Where fuel system problems are to be investigated, a more detailed PDR model is required, but this is beyond the scope of this document.

### B.7.1.6 Power Actuators

These are used to control IGVs, nozzle area and other engine components. Typically the power actuator is a ram, with the servo supply set by a two-stage servo valve (**Figure B.136**). An LVDT or other transducer measures Ram position, and a digital computer is used to close the loop. Provided that the control has been correctly designed, the response of the servo valve will be insignificant in the overall control loop. An acceptable model can be obtained by setting the ram velocity as a function of DECU drive current and available pressure drop across the servo valve, after allowing for the pressure required to overcome actuator loads.

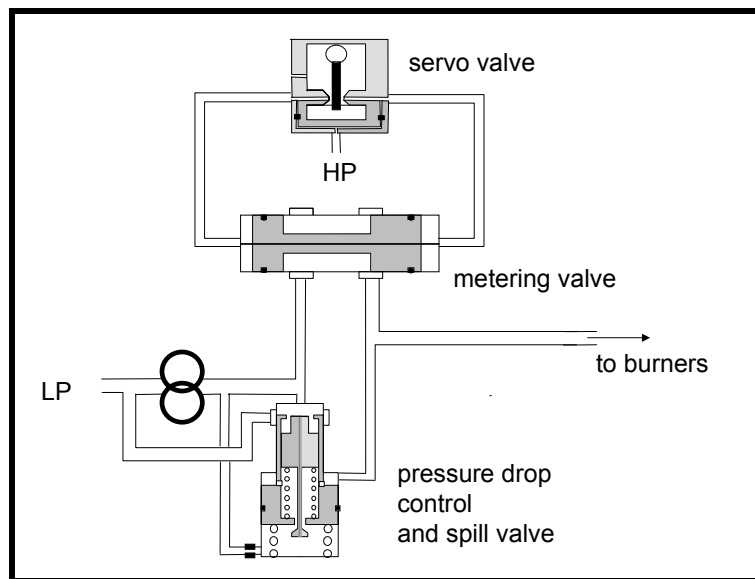


**Figure B.136: Schematic of Main System Components.**

## B.7.1.7 Modeling a Two-Stage Servo Valve (Moog Type)

A schematic of the valve is shown in **Figure B.137**.

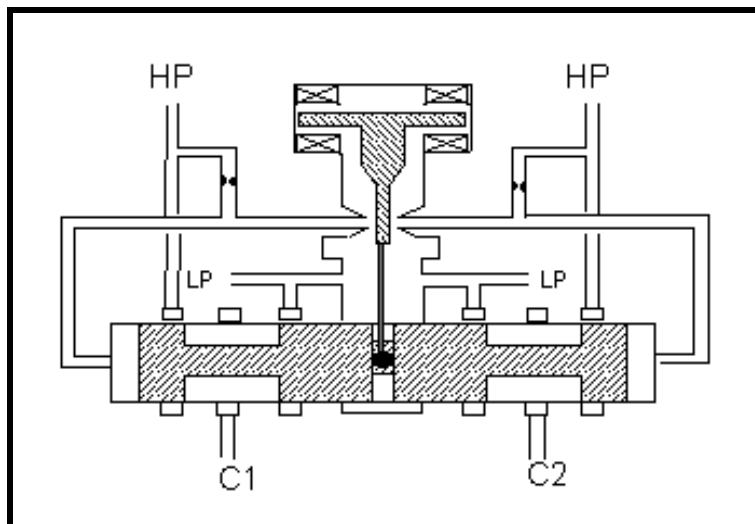


**Figure B.137: A Two-Stage Moog Valve.**

In the steady state condition, servo fluid, at servo supply pressure, passes through identical restrictors to the nozzles on each side of the flapper. The flapper is equidistant from each nozzle, so equal pressures and flows are generated at each side of the flapper. The pressures at the flapper are felt on the spool ends and, as the pressures are equal, the spool remains stationary.

When drive current is applied to the motor, it produces torque on the first stage, and the flapper and motor armature deflect. With the flapper deflected, the nozzle flows are no longer equal and the difference in flow results in spool displacement. As the spool displaces, it bends the feedback wire producing a torque at the armature to balance the motor torque. A new equilibrium position will occur when the flapper is

## ANNEX B – ADVANCED TOPICS AND RECENT PROGRESS

again centered between the nozzles and the feedback wire torque balances the motor torque, with the spool displaced from its null position.

As the spool moves, it varies the flow numbers between its output ports (C1 and C2) and the supply and return pressures. These flow numbers may vary linearly with spool travel or be profiled for custom applications.

An external driven device (e.g. a metering valve) will be connected to ports C1 and C2 so that the velocity of the driven valve will be a function of the control spool displacement, the supply and return pressures available and the loads on the driven valve.

**Figure B.138** shows a relatively detailed model of the above valve and the equations **Figure B.139** used to build it. For any detailed dynamic analysis of engine and control systems, a model of this complexity will be required but, for engine handling work, the response of the valve may be reduced to a first-order transfer-function with break frequency =  $K_v$  rad/sec.

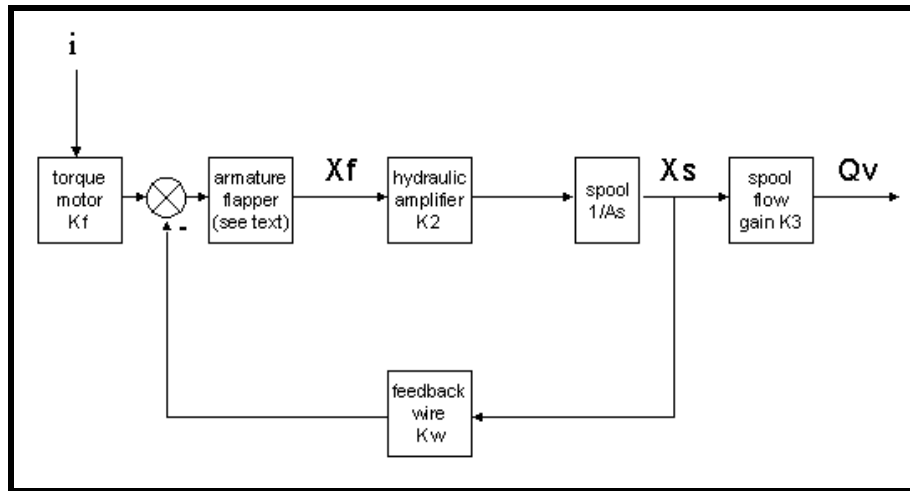


**Figure B.138: Two-Stage Servo Valve Block Diagram.**

Armature flapper characteristic	
$\frac{1}{K_f} \cdot \frac{1}{1 + \left( \frac{2\zeta}{\omega_n} \right) s + \left( \frac{s}{\omega_n} \right)^2}$	
where :	
$\omega_n = \sqrt{\frac{K_f}{L_f}}$	first stage natural frequency
$\zeta = \frac{B_f}{2 \cdot K_f} \cdot \omega_n$	first stage damping ratio
$K_v = \frac{K_2 \cdot K_w}{K_f \cdot A}$	servo valve loop gain

**Figure B.139: Valve Control Laws.**

Where performance variations of the valve need to be investigated, or a possible problem with the valve is suspected, the *hydraulic amplifier* block will need to be modeled in more detail, but the degree of complexity required is beyond the scope of this report.

The manufacturer for each valve design can supply the following data.

- I: Torque motor current;
- Xf: Flapper displacement at nozzles;
- Xs: Spool displacement;
- Qv: Servo valve control flow;
- K1: Torque motor gain;
- K2: Hydraulic amplifier flow gain;
- K3: Flow gain of spool;
- A: Spool end area;
- Kf: Net stiffness of armature/flapper;
- Kw: Feedback wire stiffness;
- Bf: Net damping on armature/flapper; and
- Lf: Rotational mass of armature/flapper.

### **B.7.2 Control Integration with Engine Model**

Consider the *traditional* roles of the performance and controls engineers, in terms of the engine functional definition. The performance engineer determines the appropriate way to control the engine to meet certain performance requirements within thermodynamic constraints. This will cover both transient and steady state aspects of the engine performance. The controls engineer will determine suitable control laws to allow the engine to operate according to the identified constraints, such as control loops. There is, of course, a considerable *gray area* between the two, the extent of which increases with engine complexity. It is sometimes difficult to distinguish between the *performance requirements for engine control* and *feasible ways of controlling gas-turbine engines*. It is therefore important to remove as many of the working barriers between the two areas as possible, so that the functional definition process becomes co-operative, thus facilitating an iterative engineering approach. The final solution may be a compromise of the ideals perceived by each area.

Each area may use different computing environments and tools for the differing engineering tasks. *Pure* performance work is generally based around development of an engine understanding through synthesis and analysis of engine test data. Where a control-system model is required to support this work, it is usually of a known, bespoke standard. In the past it has been common to see control-system models coded independently in the performance area, without reference to any similar model existing in the controls area. Such a duplication of effort has clear disadvantages in operational, program and risk terms Marcus S Horobin May (1998) [B.88].

There are two fundamental issues:

- Provision and interfacing of a single *engine model*, used across all functional engineering activities; and
- Provision and interfacing of a single *control-system model* used across all functional engineering activities.

### B.7.2.1 Common Engine Model

Configuration control of the models is essential, and has the same importance as configuration control of the end products – engines. Engine models must be released to the controls area, and controller models must be released to the performance area. A central repository containing all models may be the ideal, but network constraints may force the use of copies in each area; this needs careful handling.

**Figure B.140** shows the common scenario of an engine model supplied by a specialist area for control-system development work using a proprietary development environment such as MATRIXx or MATLAB.

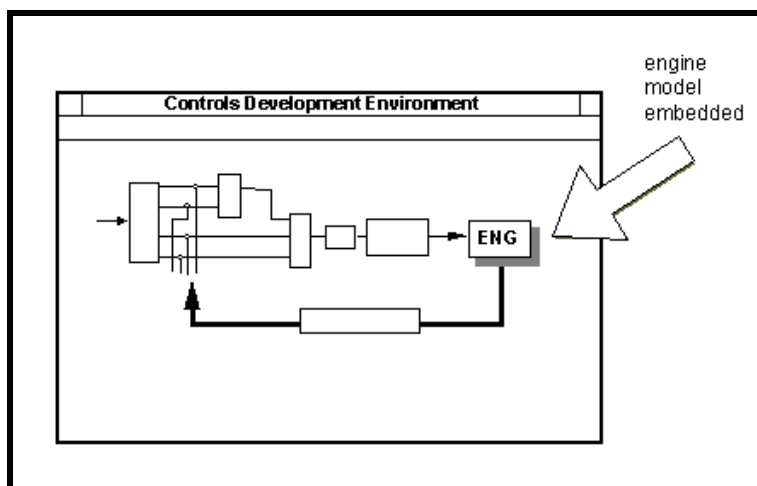


**Figure B.140:** Engine Model Imported (Embedded) in Controls Development Environment.

The main challenges arise from the interface of different modeling tools. Embedding sub-system models into other host environments is one approach; the use of shared memory or other inter-process communication interfaces such as CORBA (Common Object-Request Brokerage Architecture) may be more appropriate. This is because it offers greater flexibility arising from the separate configuration of the models. A CORBA based model can be cross language, cross operating system and cross hardware platform. The combined model is not a single executable, but consists of separate elements that are based on object-oriented design. This has advantages in keeping the accountability for the subsystem models with the model creator. **Figure B.141** below shows the engine and controller each running in their home environments, communicating by shared memory. For the controls user, there is no significant difference to the setup as shown in **Figure B.140**. However, there is now the potential to drive the simulation from the performance environment as may be required (see below).

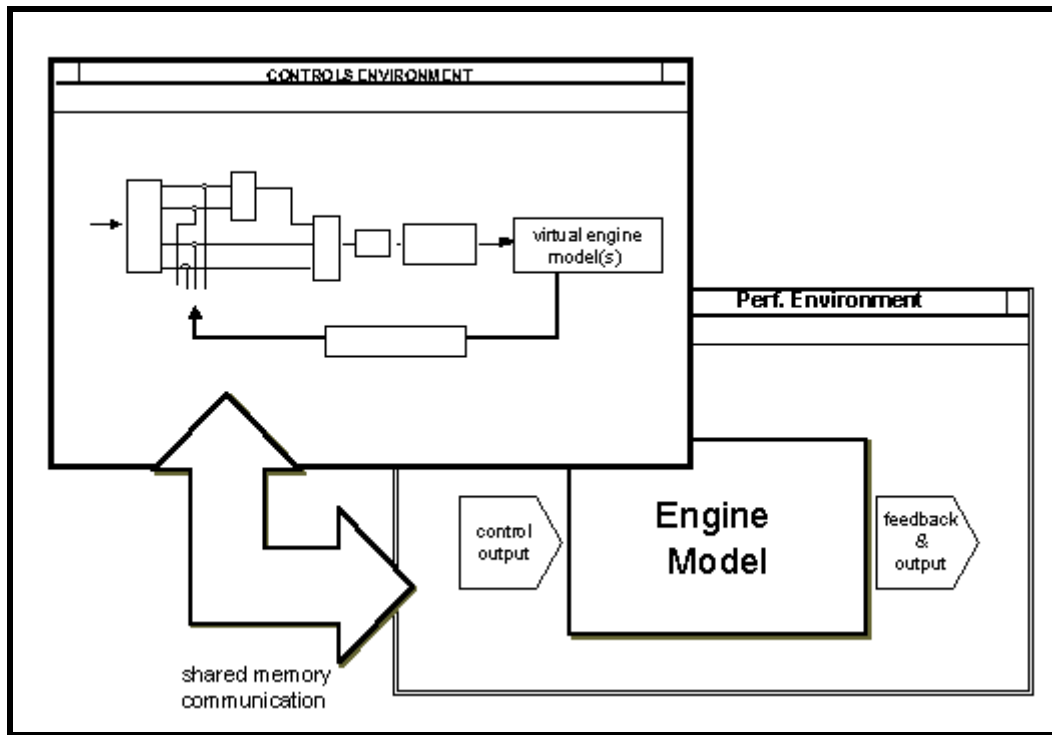


**Figure B.141: Engine and Control-System Models Running Together with Inter-Process Communication.**

It is common practice for engine models to be written in FORTRAN although the emphasis is shifting towards C. As such, an engine model may be imported into proprietary development environments in the form of a user code block. Custom interface routines may be required. The interface routines should allow easy routing of additional signals if required.

Development environments such as MATLAB or MATRIXx have suites of tools (toolboxes) with which the model must be compatible. It is common practice for all dynamic elements in a system to be numerically integrated by the host environment. Several integration algorithms are available; the most appropriate for the particular dynamics present, can be chosen. This said, some engine models might perform their own integration internally. Iterative techniques used in thermodynamic solutions facilitate implicit integration approaches that may have certain advantages in numerical stability. Engine models are also manipulated to generate linear models in state-space form.

In the early stages of a project, it is common to find that some control variables are not modeled as independent program input variables. For example, a variable mixer may be present in the engine concept, but early performance studies do not need a geometry-to-thermodynamic-effect calculation. This is because the model can be matched by prescribing what such a feature has to achieve, rather than predicting the effect of a specified geometry. Clearly, in the case of control-system design, a geometry model is required, although some simplification may be acceptable at the preliminary stage.

### B.7.2.2 Using Performance (Cycle-Match) Models for Control-System Design and Analysis

Control engineers are perhaps most familiar with engine models presented in the form shown in **Figure B.142** below. The engine is a dynamic simulation, which requires the host environment to perform the numerical integration of state derivatives. Often explicit integration techniques are used such as Runge-Kutta 4<sup>th</sup> order. A model presented in this form is also able to be linearized (see below). Whereas this is the

standard model form used in many areas of dynamic modeling, it is one particular form (of several) in which a performance model may be presented. It can be thought as a *states-matching mode*. This reflects the model's function of finding a solution (by iteration) to a *question* posed in terms of specified values of inputs  $[u]$  and states  $[x]$ .

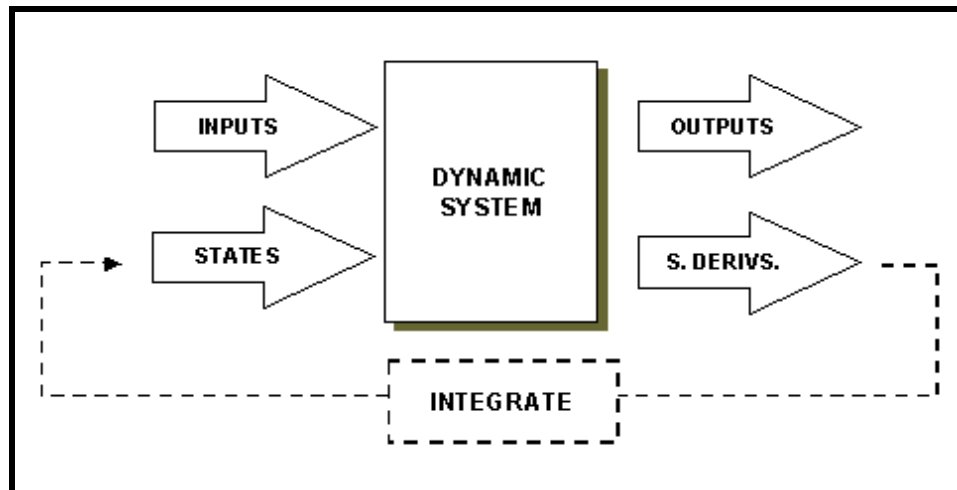


**Figure B.142: A General Form of Dynamic Model using External Integration for Simulation.**

- **Inputs**  $[u]$  are boundary terms, e.g. environmental temps, pressures, fuel-flows and geometry for an engine;
- **Outputs**  $[y]$  are parameters of interest, e.g. thrust, specific-fuel consumption, surge margin;
- **States**  $[x]$  are those parameters whose responses are governed by a differential (dynamic) equation, e.g. shaft speed; and
- **State Derivatives**  $[\dot{x}]$  are the time differentials of the state variables.

### B.7.2.2.1 Linearization

In order to linearize the engine model, it must be presented in this form – i.e. with states set up as program input, and state derivatives as output. Thus the model may be manipulated (by parametric perturbation of states and inputs) around a base point to generate the linear (partial-derivative or state-space) engine representation which is necessary for standard controller design and analysis methods.

### B.7.2.2.2 Steady-State Synthesis (Initialization)

Consider the engine model presented as shown in **Figure B.143**. In order to generate a steady-state solution for a prescribed set of boundary conditions (inputs, e.g. fuel flow), the values of the state variables have to be ascertained. With a performance model, this is achieved by the iteration that is also used for the thermodynamic solution. With other types of engine model which do not use iteration, the initial values of states can be determined in several ways:

- By invoking an external iteration function, *trimming*, which varies the states to achieve a zero state-derivative (at fixed inputs).
- By running a *settling transient* where the states are initialized at arbitrary values and the simulation run over a period of time at constant inputs until steady state is achieved. Thus the initial combination of *arbitrary states* and *prescribed (fixed) inputs* combine to give a non-zero state-derivative. This is numerically integrated to predict the next time-step value of state variable. The model should eventually achieve steady state where  $\dot{x} = 0$ .

- By using table look-ups of states vs. inputs for steady-conditions.
- By setting the inputs and states at values stored from a previous run (not necessarily a steady-condition), moving the input variables to the required values over a time-base, and allowing the model to achieve steady-state.

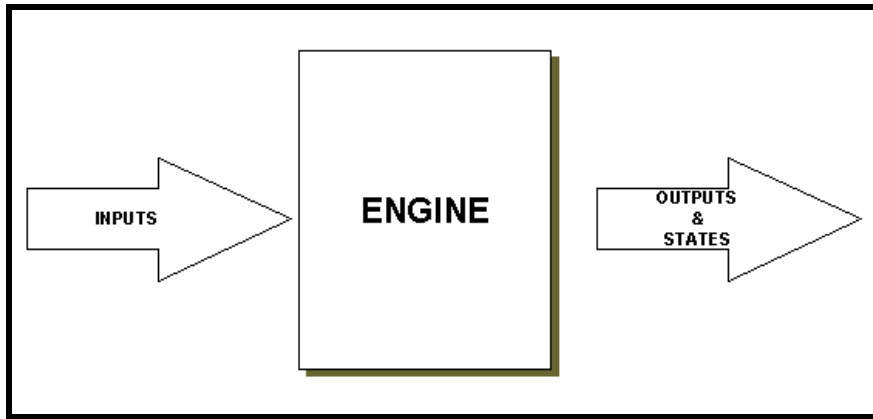


**Figure B.143: Performance Model Showing Steady-State Mode.**

None of this is necessary with a performance model running in *steady-state* mode.

Given fixed values of control inputs, a steady-state solution is generated. The steady condition may also be specified in terms of a specified level of output parameter (e.g. thrust) or internal engine parameter (e.g. compressor operating point).

*Steady-state* mode can be used to define the base points around which the model may be linearized. *States-matching* mode is selected after the steady-state point has been generated.

If a control-system model is present, this can be initialized separately or as part of the combined system using the methods described above.

### B.7.2.2.3 Simulation (Dynamic or Transient Synthesis)

Although simulation can be achieved using *states-matching* mode (using the host system to integrate), performance models can simulate transients by performing integration internally. Iteration allows integration to be performed implicitly which gives certain advantages in numerical stability. Thus there is a third *transient* mode (**Figure B.144**).

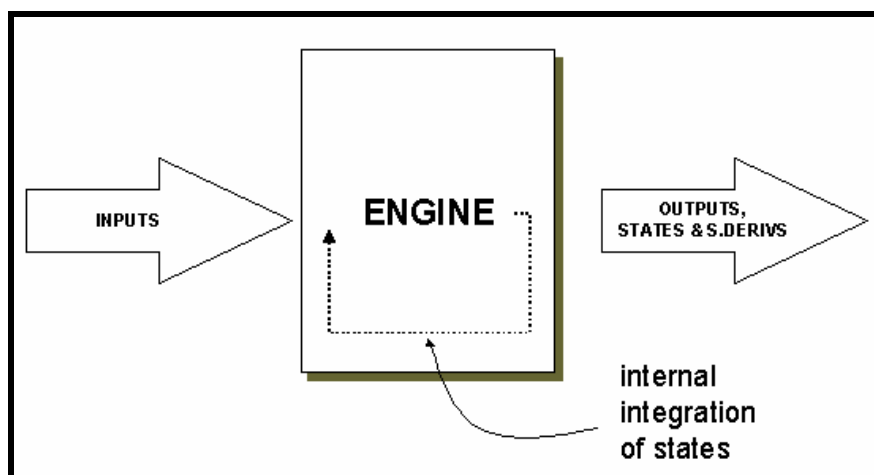


**Figure B.144: A Performance Model Running in Transient Mode using Internal Integration.**

The base points for linearization are not necessarily at steady-state conditions. Any mid-transient point (generated by *transient* mode) can be selected as a base point for linearization.

Generalization:

- The three modes are fundamentally distinguished by the iteration matching-scheme used to produce the solution in each case (which is transparent to the user). In addition, the dynamics routines are not called in steady-state mode.
- The steady-state matching-scheme is the simplest and does not allow excess power on any shaft, nor any stored W, P or T within a volume. This matching scheme is extended for the states-matching mode and for the transient mode, where an extra matching pair is added for each dynamic equation being considered. Ref. 1 expands on this using a simple example.
- Iterative models are not dependent on the solution of gas dynamics equations for dynamic or transient simulation – valid simulation can be achieved by modeling only the shaft dynamics. Modeling of gas dynamics (volume packing) can be added if required.
- When gas dynamics are *not* modeled, the model sampling frequency is around 5 Hz. With gas dynamics, the bandwidth is increased to 30 – 40 Hz.
- The performance process is largely preoccupied with the prediction and analysis of steady-state performance. Solution by iteration is essential for this type of work. Performance engineers often regard transient synthesis as an extension of the steady-state model. Controls engineers often see things the other way around with the steady state being a particular state of a dynamic system, which is perhaps never truly achievable. However regarded, the modeling techniques are the same.

## B.7.2.2.4 Using Control-System Models in Performance and Operability Assessment

Integrated engine and controller models are seldom required in traditional performance activities. However, for operability studies, such as compressor stability assessment, a control-system model is essential. The emphasis is placed on the understanding of engine behavior in response to control-system action. Data interface requirements therefore differ – the performance engineer wants full visibility of internal engine parameters and engine analysis tools. It is also the case that other sub-systems, for instance the secondary air-system and oil systems, should be represented in the best possible way.

Clearly, if a controller model has been developed in a controls development environment, it is desirable that this should also run in the performance environment. Models constructed using Graphical User Interfaces

(GUI) can be represented in pure code forms using proprietary code-writing tools. This facility offers potential for inter-environment use. C and ADA are common languages for this task.

**Figure B.145** shows a controller model derived using picture-to-code tool in a performance development environment.

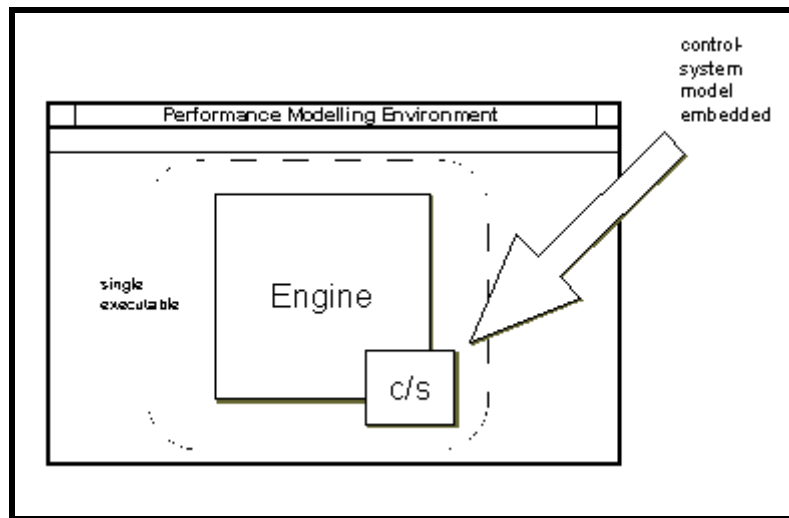


**Figure B.145: Control-System Model Imported (Embedded) into Performance Modeling Environment.**

Several issues arise:

- Interface of dissimilar languages (e.g. FORTRAN and C);
- Ideally, the control-system and engine model should be separately configurable items;
- The integrated model in this environment should be technically equivalent (in simulation terms) to the alternative scenario of the engine-model imported as a subservient element in the controls environment; and
- Initialization.

In the case of FORTRAN and C, there is little technological challenge in interfacing. It is more a case of careful handling of the different conventions used in the two languages. Naturally, the platform must support both languages.

It is possible to avoid embedding the controller within the engine model, by using the inter-process communication technique shown in **Figure B.141**. For work centered on performance studies, it is desirable that the combined model should be run from the performance domain.

Performance work often involves the prediction of nominal steady-state performance under the action of the control-system, at, say, a particular power demand or rating. For example, as expressed by a certain pilot-lever angle. Ideally, the full, integrated model should be used to generate these points. However, the computing task can become a burden because of the requirement to initialize certain dynamic terms in the combined model.

A control-system (or other engine sub-systems) can also be structured to take on the form in **Figure B.141**. Thus a combined controller and engine model, both exhibiting the form in **Figure B.141** and running in a

## ANNEX B – ADVANCED TOPICS AND RECENT PROGRESS

---

development environment (such as MATRIXx or MATLAB) can be initialized in the ways discussed above. Initialization is *not* so straightforward when:

- Any constituent part of a whole system is not in the standard form (**Figure B.142**);
- When constituent parts of the model are spread across different environments (**Figure B.141**); and
- When the whole model is running in an environment that does not feature the *trimming* function (**Figure B.145**).

1 is solved by providing ensuring a standard form, or providing models which are self-initializing.

2 ought not be a fundamental problem if 1) is solved; inter-process communication will be increased for the initialization phase.

3 becomes an issue when using combined models in the performance environment. Often, a *series* of steady-state flight points (for given values of pilot demand) is to be generated. This can require initialization for each point. In such a case, the settling transient method is an excessive burden on execution time. However, there are ways of alleviating this overhead. The transients are not of interest, so some dynamic terms can be muted or modified to reduce settling time (e.g. heat-soakage can be muted and shaft inertia reduced). A problem can arise if this measure is taken to extremes: the whole-system stability may be compromised and therefore prevent a steady condition being achieved! A *trimming* function may be used, however such a facility may not be available in all environments. Also, with an extended iteration scheme, there is a potential convergence hazard with the number of control-system states that may need initialization.

An alternative approach is to use a subset of the controller: the ratings structure, to establish the level of performance in terms of the engine rating parameters. An iterative engine model can be run to such parameters (with due regard to engine limit loops) and converge on a steady-state solution (either on the prescribed rating or on an overriding limit) without any settling period. From this point, the initial conditions in the controller may be determined either by back-calculation or by including controller terms in the iteration loop. The engine condition thus obtained should be identical (within iteration tolerance) to that obtained by transient settling. However, there are some situations when this approach is not feasible. Even with iteration; the time-settling technique is sometimes essential, for instance for engines with switching bleeds or with unusual ‘pecking–order’ of limits and ratings. The full model is, of course, the best means of determining the steady-state performance, if indeed such a condition exists.

Where the model is being used for *true* transient simulation, the execution time associated with the start point is less significant and so the transient settling method may be acceptable. It may be beneficial in this case to initialize the engine model at an arbitrary fuel flow first, thus giving the controller a feedback consistent with the initial engine input. The combined model can then *bootstrap* to the required steady-state condition, at which point the controller state variables (e.g. numerical integrators) are correctly initialized for the forthcoming maneuver of interest. From the user’s point of view, the settling method can be made virtually transparent. The settling transient can be hidden and discarded after steady state has been achieved. The only symptom will be in the execution time.

The issues discussed above extend to other systems such as intakes and secondary air system that interact with the engine.

### B.7.3 References for Control Models

- [B.88] Horobin, M.S., “Cycle-Match Models Used in Functional Engine Design – An Overview”, Presented at the RTO Symposium: Design Principles and Methods for Aircraft Gas Turbine Engines, May 1998.

## **B.8 EFFECT OF WATER/STEAM INJECTION ON THE PERFORMANCE OF POWER GENERATION GAS**

### **B.8.1 Introduction**

The increasing use of gas turbines in the power generation industry has created an additional incentive for the further improvement of their performances. In the last years several techniques have been proposed for gas turbine power and efficiency augmentation, such as steam or water injection at different locations along the gas path.

A first possible location for water injection is the compressor inlet duct. The fact that gas turbine output and efficiency drop during high ambient temperature periods, when demand usually increases, has led to the broad application of inlet air cooling through evaporation of water injected in the form of fine droplets, a technique called inlet fogging. Water injection at some location along the compression path is a means of compression intercooling for performance augmentation. Steam can be injected at a location along the expansion path, as for example between a high pressure and a low pressure turbine of a twin spool engine. The most widely used technique; however, is the injection of water or steam at the exit of the compressor.

Injection of water or steam in the combustion chamber of gas turbines is one of the means to reduce  $\text{NO}_x$  emissions while it leads to augmentation of power output. Steam injection, in particular, is also a means of improving efficiency. If it is produced with the use of the heat of the exhaust gases, it increases the net efficiency of the gas turbine cycle, by exploiting some of the heat that would otherwise be wasted through the exhaust gases. The term diluent will be used hereafter to denote either steam or water injected in the combustion chamber of a gas turbine.

The reduction of  $\text{NO}_x$  emission levels through diluent injection has been the subject of many studies. Reviews of such techniques have been reported in [B.89, B.90 and B.91]. Relations between the amount of water used and the emissions reduction achieved have been presented in [B.89 and B.92]. On the other hand, since steam injection has a beneficial effect on performance, study of its effects on the overall performance of gas turbine cycles has been the subject of many publications, as for example [B.93, B.94, B.95 and B.96]. Summaries of the technology and the achievements up to the early nineties have been provided in [B.97 and B.98].

The effects of the injection on the performance of the gas turbine engine are qualitatively known, (see for example [B.99]). Curves of performance parameters dependence on the amount of injected water or steam have been presented by some authors (for example [B.100 and B.101]). Such curves are usually produced with the aid of computational performance models for specific gas turbines. The effect of diluent injection is evaluated by introducing the appropriate parameters in a thermodynamic engine model and comparing the results to those with no injection. A study of this type was also reported in [B.102].

Methods for evaluating the effects of water or steam injection on the performance of a gas turbine will be discussed in the following. The case of diluent injection in the combustion chamber will be covered in more detail, as it has been more extensively studied. Before presenting the techniques for evaluating effects on performance, it is useful to overview the physical mechanisms through which performance is altered.

### **B.8.2 The Physics of Operational Parameter Deviations**

Water or steam injection at some station along an engine has the following consequences:

- Mixing of the injected media with the gas, alters the thermodynamic state of the main gas flow. The mixing can be considered to be at constant pressure. A small pressure drop due to mixing

## ANNEX B – ADVANCED TOPICS AND RECENT PROGRESS

---

may occur, but this drop is of small magnitude. Temperature change can be more significant, especially if liquid water is injected and it absorbs heat for its evaporation.

- The thermodynamic properties of the gases are different after the mixing, since their constitution changes, containing a larger amount of steam.
- The mass flow rate of the gases is larger by the amount of injected media after the injection position. The mass flow compatibility may lead to alteration of turbomachinery components (compressor or turbine) operating point.

Let's consider the case of injection in the combustion chamber in more detail. Injection of a diluent between the compressor outlet and the turbine inlet results in the change of several operational parameters. The way of change depends on the mode of operation. For example, different changes occur if the controller maintains a constant turbine inlet temperature (TIT) or if the load demand is kept constant. We will discuss here the changes for operation with given TIT, since this is the mode of operation used for defining turbine ratings.

Since the diluent is injected at a temperature that is lower than the TIT, some additional heat is needed to bring it to the required TIT level. The engine controller gives thus a command for additional fuel injection into the combustion chamber. The amount of additional fuel depends on the condition of the diluent. When water is injected, the amount of additional fuel is larger than for steam, since the heat needed includes the latent heat of evaporation of the water, which is of considerable magnitude.

Diluent injection results in an increase of the mass flow that has to pass through the turbine. This means that for a given TIT, the pressure has to increase (since the referred mass flow rate though the turbine is fixed). Therefore, the compressor is required to operate at higher pressure ratio. Compressor outlet pressure and temperature are thus altered, in comparison to operation with no injection. The movement of the operating point on the compressor map will depend on the shaft configuration, namely single or twin shaft.

The turbine is fed with a larger amount of gas, at a pressure higher than for dry operation. Additionally, this gas has a larger steam content, and therefore a larger heat capacity (the heat capacity of steam is roughly double that of air), while the isentropic exponent also changes. The expansion process is thus different and the turbine produces more power. The immediate consequence of these changes is that overall engine performance, namely power output and efficiency, are altered.

As a result of these changes, the matching between compressor and turbine is influenced, leading to different operating points on their corresponding characteristic curves. Typical positions of operating points on the compressor map of a single shaft gas turbine for different cases of operation are shown in **Figure B.146**. The three points correspond to the same TIT. It is observed that water injection drives the operating point to higher pressure ratio. The change is larger for larger amount of water.

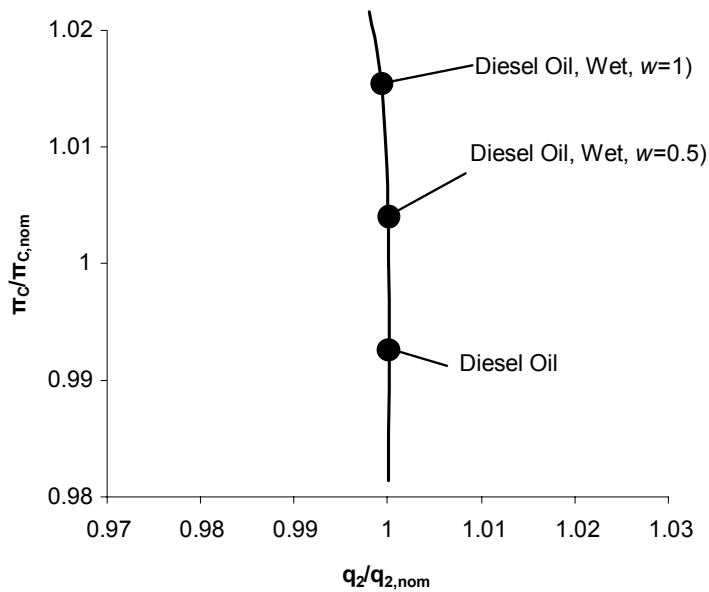


**Figure B.146: Compressor Operating Point of a Single Shaft Gas Turbine. Constant TIT, Operation with Different Fuels and Water Injection.**

### B.8.3 Computer Models for Water Injected Operation

#### B.8.3.1 Constitution of a Performance Model

In order to build a performance model, a Gas Turbine is viewed as an assembly of different components (modules). Each component is identified according to the kind of process it accomplishes. The working fluid is assumed to be a perfect gas and its thermodynamic properties are interrelated through the compressible flow relations. If  $\bar{Y}_{IN}$  is the vector of independent variables at a component inlet and  $\bar{Y}_{OUT}$  the corresponding vector at its outlet, then in order to find the values at the components exit an equation of the following form must be solved

$$g(\bar{Y}_{IN}, \bar{Y}_{out}) = 0 \quad \text{Eq. B-82}$$

This equation usually derives from conservation laws, as well as existing experience in components operation. It can be an analytical relation, possibly including empirical constants (e.g. duct pressure loss), or a set of curves (e.g. turbomachinery component maps). Additional equations express the compatibility between the different components operation. A set of equations which have to be simultaneously satisfied by the fluid parameters, is thus formed. The solution of this system of equations, non-linear in nature, is achieved numerically. Different types of numerical techniques can be employed, as for example described by Stamatis et al. [B.104]. The solution of this system for one operating point gives the full cycle details, and the performance parameters are uniquely defined.

A schematic representation of a twin spool gas turbine of interest to the present paper and its subdivision to individual components is shown in **Figure B.147**. The layout shown has provision for inlet cooling, intercooling, combustion chamber injection and interturbine steam injection.

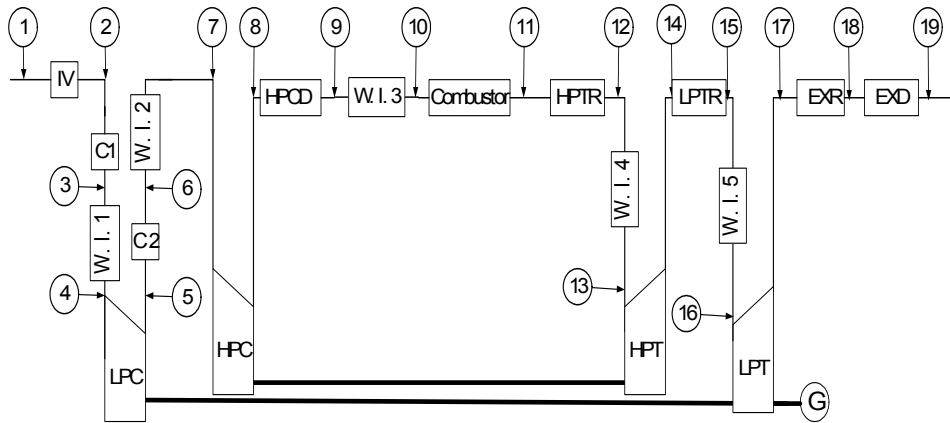


**Figure B.147: Schematic Representation of a Twin Spool Gas Turbine and Discrimination of its Components.**

### B.8.3.2 Modelling for Water Injection

#### B.8.3.2.1 Gas – Water Mixing

Mixing of gas, namely air or combustion products, with water can take place at different stations along the engine: compressor inlet, between the compressors, at compressor outlet (in the form of liquid water or steam), steam between the turbines. In zero dimensional modeling it is considered that when water is injected, it is always fully evaporated before entering the downstream component. The way that properties are calculated for mixing at any of these stations is described below.

The flow in the cooling component is assumed to be steady, one-dimensional and adiabatic. The droplets partial pressure along with the volume occupied by the droplets is neglected. At cooling component inlet (station 1) the thermodynamic conditions of the air mixture and the injected water, are considered known.



Conditions downstream of the cooling component (station 2) can be computed through the application of the conservation laws of continuity, energy and momentum which in the case of water injection form the following set of equations:

$$\dot{m}_{da} \left( h_{da1} + \frac{V_1^2}{2} \right) + \dot{m}_{w1} \left( h_{w1} + \frac{V_1^2}{2} \right) + \dot{m}_{w1} h_{w1} - \left[ \dot{m}_{da} \left( h_{da2} + \frac{V_2^2}{2} \right) + \dot{m}_{v2} \cdot \left( h_{v2} + \frac{V_2^2}{2} \right) + (\dot{m}_{w1} - (\dot{m}_{v2} - \dot{m}_{w1})) \cdot h_{w2} \right] = 0 \quad \text{Eq. B-83}$$

$$p_1 \cdot A_1 + \rho_{m1} \cdot (V_1 \cos(\alpha_1))^2 \cdot A_1 = p_2 \cdot A_2 + \rho_{m2} (V_2 \cos(\alpha_1))^2 \cdot A_2 \quad \text{Eq. B-84}$$

$$\rho_{m1} \cdot V_1 \cdot \cos(\alpha_1) \cdot A_1 = \rho_{m2} \cdot V_2 \cos(\alpha_1) \cdot A_2 \quad \text{Eq. B-85}$$

Dry air enthalpy is a function of temperature while vapour and water enthalpy is a function of both pressure and temperature.

These relations can express the case that no full evaporation occurs, along with the case of possible condensation. A mixing component is assumed of constant cross-sectional area.

The non-linear algebraic equations are solved through a numerical procedure, taking into consideration the variation of the composition and the variation of thermodynamic properties of the mixture. The criterion whether saturation occurs is the correlation between vapour partial pressure and vapour saturation pressure at the temperature at component exit. In the case that the mixture is saturated vapour partial pressure is equal to vapour saturation pressure at the same temperature:

$$p_{v2} = p_{sat}(T_2) \quad \text{Eq. B-86}$$

## B.8.3.2.2 Gas Properties

Calculations of thermodynamic processes use properties of a working medium, which is a mixture of gasses. The properties of individual mixture constituents are calculated by means of polynomial functions and the mixture properties are evaluated from its mass composition, through a relation of the form:

$$P = \sum_i X_i \cdot P_i \quad \text{Eq. B-87}$$

P is a property of the mixture and  $X_i$ ,  $P_i$  is the mass composition and the corresponding property value for the i-element of the mixture respectively. Inlet air is handled as a mixture of gases, including steam due to ambient humidity. The composition of gases at the combustor outlet is computed on the basis of stoichiometric calculations, and depends on the composition of the fuel used. When water is injected, it also accounted for as an additional amount in the gas composition.

The variation of  $c_p$  of the mixture of combustion gases and steam, for the range of temperatures of interest to gas turbine applications, is shown in **Figure B.148**. The values have been calculated by considering the gases as a mixture of ideal gasses, and the properties of the constituents are derived by polynomial relations [B.99]. The variation of isentropic exponent  $\gamma$  is also shown.

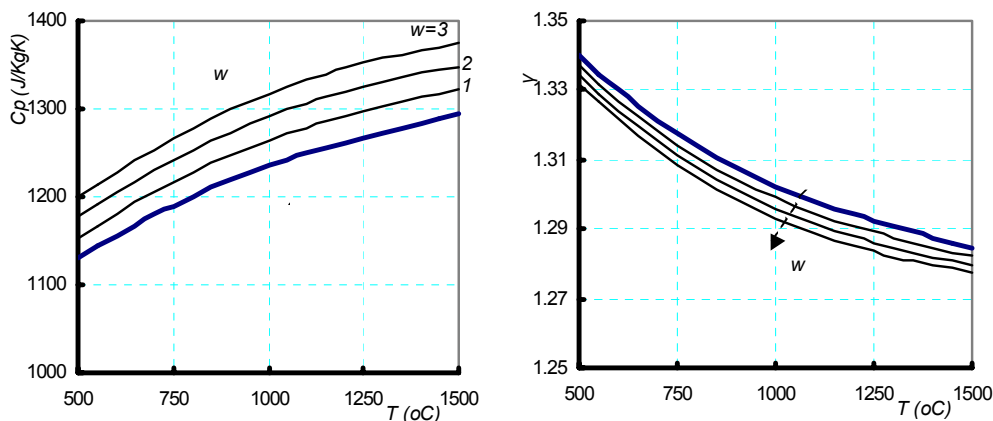


**Figure B.148: Values of Specific Heat  $C_p$  and Isentropic Exponent  $\gamma$ , for Temperatures Usual in the Hot Section of Gas Turbines.**

Variation of gas properties for typical rates of water injection is shown in **Figure B.149**. The changes of properties of gases after water is injected, with respect to the values with no water injected are shown.

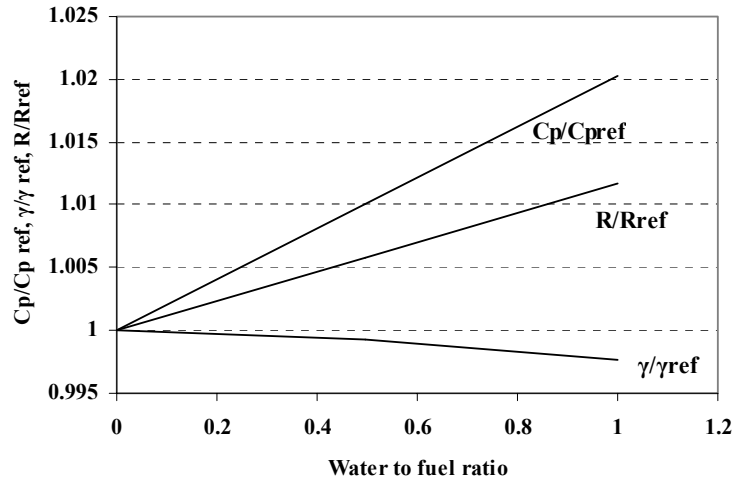


**Figure B.149:** Change in Gas Properties for Different Amount of Injected Water ( $f = 0.02$ ).

#### B.8.3.2.3 Turbomachinery Components

Calculation of component performance parameters is based on performance maps for each component, which are expressed in a generalized form to account for the use of different gases. The quantities that remain invariant for a map can be found in many references (e.g. AGARD [B.105], Walsh and Fletcher [B.99], Mathioudakis and Tsalavoutas [B.106]). When the map is expressed in function of these parameters it remains unique, independently of the working medium.

For water/steam injection at the compressor outlet, the variation of the quantities related to the turbine is of interest, since it is the turbine that faces this gas composition changes. The quantities that remain invariant and are interrelated through the map, when gas composition changes are:

$$\left( \frac{N}{\sqrt{T}} \right) / \left( \frac{N}{\sqrt{T}} \right)_0 = \sqrt{R \cdot \gamma \cdot (1 + \gamma_0) / R_0 \cdot \gamma_0 \cdot (1 + \gamma)} \quad \text{Eq. B-88}$$

$$\left( \frac{W\sqrt{T}}{P} \right) / \left( \frac{W\sqrt{T}}{P} \right)_0 = \sqrt{\frac{R_0 \cdot \gamma}{R \cdot \gamma_0}} \cdot \left( \frac{2}{1 + \gamma} \right)^{\frac{\gamma + 1}{2(\gamma - 1)}} \cdot \left( \frac{1 + \gamma_0}{2} \right)^{\frac{\gamma_0 + 1}{2(\gamma_0 - 1)}} \quad \text{Eq. B-89}$$

$$\left( \frac{\Delta h}{T} \right) / \left( \frac{\Delta h}{T} \right)_0 = R \cdot \gamma \cdot (1 + \gamma_0) / R_0 \cdot \gamma_0 \cdot (1 + \gamma) \quad \text{Eq. B-90}$$

Subscript 0 in all the above relations denotes properties of working medium at a condition that is considered to be the reference. The choice of reference condition depends on how the map was obtained. It could be dry air, combustion gases with dry air at the inlet and reference gas fuel or other.

It is worth noting here that the expression for reduced flow rate through the turbine, Eq. B-89 can be used to understand some of the effects of fuel change or water injection. When the turbine is choked (which is actually the case for most gas turbines today, at least for operating conditions in the vicinity of full load),

reduced mass flow remains constant. It can be easily shown that the term to the right of the radical, in the right hand side of **Eq. B-89** changes very little for the range of values obtained by  $\gamma$ . This means that the quantity that remains unchanged is:

$$q_4 = \left( \frac{W_4 \sqrt{T_4}}{P_4} \right) \sqrt{\frac{R}{\gamma}} \quad \text{Eq. B-91}$$

Using this fact and also the fact that compressor inlet reduced mass flow changes very little (“vertical” characteristic on compressor map), changes in pressure ratio can be evaluated.

#### *B.8.3.2.4 Sample Results of Effects on Performance*

Once a model that can simulate engine performance in all these situations is constituted, it is possible to examine how water injection can influence engine performance. Before going into the detailed study, it is useful to remark that assessment of these effects can be done in two levels: It is possible to have an assessment using analytic relations. Such analysis for fuel changes has been presented by Mathioudakis [B.106] and for water injection effects by Mathioudakis as well [B.107]. They give an understanding of the related effects and the possibility for fast calculations, helpful for a quick engineering judgment. The accuracy of predictions can be good, especially if small deviations occur from what is considered to be the reference condition. Accurate calculations, irrespective of the size of deviations, necessitate the use of a non-linear computer simulation model.

### **B.8.3.3 Estimation of Performance Deviations using Analytical Relations**

The information derived by computer models is valid for a specific gas turbine modeled, but it is not known how general the predictions are or what are the factors governing the phenomena studied. If another gas turbine is considered, it is not known to what extent information already available can be used for assessing these effects.

These drawbacks are overcome when explicit relations can be used. If such relations are available, then it is possible to study any given gas turbine, provided that the necessary design data are available. Additionally, the use of relations allows an understanding of the effect of diluent injection and provides a means for a quick estimation of such effects. Such relations have been published by Mathioudakis [B.103], for studying the effect of water injection on the performance of a gas turbine. In the present paper, this approach is extended to study the effects of steam injection. The analysis is further extended to study the movement of the compressor operating point and thus allow implementation on twin shaft gas turbines. Differences for the effects of steam or water injection will be highlighted and explained. The study is concentrated on the behaviour of the gas turbine engine and it is shown that it can be used to interpret the changes observed on cycle performances.

#### *B.8.3.3.1 Fuel/Air Ratio and Gas Properties Changes*

An important mechanism behind overall performance parameter changes lies in the fact that additional fuel is needed for keeping the turbine inlet temperature constant, as mentioned above. The fuel to air ratio  $f'$  when diluent is injected, with a proportion to fuel denoted by  $w$  can be evaluated from the ratio  $f$  without injection, through the following relation:

$$f' = \frac{f}{1 - r w f} \quad \text{Eq. B-92}$$

Eq. B-92 can also be written as

$$\frac{\delta f}{f} = \frac{f' - f}{f} = \frac{rwf}{1 - rwf} \quad \text{Eq. B-93}$$

The parameter that determines how  $f$  changes with  $w$  is the relative enthalpy rise of steam  $r$ . This parameter takes characteristic values, which are different for water or steam, and do not change very much for practical gas turbine designs. Its value depends on TIT, compressor delivery temperature and the condition of the injected diluent. It can be shown that  $r$  does not vary very much for existing gas turbine designs and a typical value that can be used for steam injection is  $r \approx 2$  and for water injection  $r \approx 5$ .

Predictions of fuel/air ratio for different diluent flow rates, using Eq. B-93, are shown in Figure B.150. They are compared to predictions of a detailed thermodynamic computer model. The test case of a single shaft gas turbine, the modeling of which has been reported in [B.108] was used. The predictions of Eq. B-93 are shown to almost coincide with those of the full model, for either steam or water injection. The slope of the change for water is larger than for steam, due to the larger value of  $r$ , reflecting the larger amount of fuel needed to evaporate the water, as mentioned in the previous section.

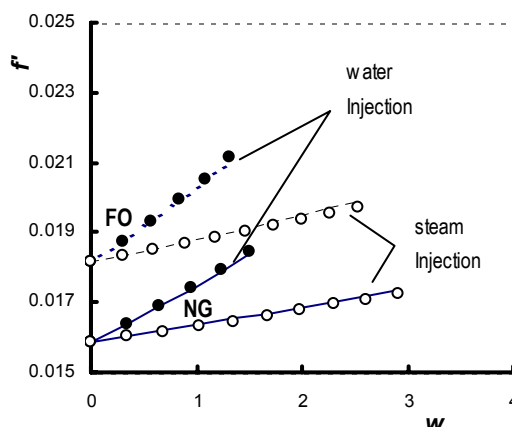


**Figure B.150: Typical Variation of Fuel/Air Ratio, with Water and Steam Injection (TG20 Simulation). Operation with Fuel Oil and Natural Gas. Points: Computer Model, Lines: eq (1).**

The range of variation of  $w$  for water injection is chosen narrower than for steam. This choice is made to reflect the fact that water is used mainly for  $\text{NO}_x$  abatement, and it is more effective than steam for that purpose (It is mentioned in [B.90] that the same level of emissions reduction can be achieved by steam using 1.6 times the amount of water). Typically, the maximum reduction can be achieved with a one-to-one proportion of liquid water to fuel. On the other hand, steam may be chosen to be used in larger amounts, not simply for  $\text{NO}_x$  abatement, but also for performance improvement purposes. For example, a large engine manufacturer uses a typical level of steam content for performance augmentation of the order of 5% of inlet airflow, while recent improvements have allowed increasing this level to 9%, as reported in [B.109].

#### B.8.3.3.2 Gas Properties Changes

The derivation of  $C_p$  and  $\gamma$  from the dry combustion gas values can be evaluated by means of simplified relation. If property values are known for dry combustion gases, then the change of  $c_p$  because of the injection of water or steam can be evaluated though the relation:

$$\frac{\delta c_{pg}}{c_{pg}} = war \left( \frac{c_{ps}}{c_{pg}} - 1 \right) \quad \text{Eq. B-94}$$

The specific heat of the dry combustion products can be considered to be the same as the one before the diluent is injected. A similar relation can be derived for the change in the value of the gas constant R:

$$\frac{\delta R_g}{R_g} = war \left( \frac{R_s}{R_g} - 1 \right) \quad \text{Eq. B-95}$$

The change in the isentropic exponent  $\gamma$  results from its definition and the previous expressions, to get:

$$\frac{\delta \gamma}{\gamma} = (\gamma - 1) \left( \frac{\delta R_g}{R_g} - \frac{\delta c_{pg}}{c_{pg}} \right) = (\gamma - 1) \left( \frac{R_s}{R_g} - \frac{c_{ps}}{c_{pg}} \right) war \quad \text{Eq. B-96}$$

The product ( $f \cdot w$ ) appearing in these relations is equal to the water-to-air ratio  $war$ . If this quantity is substituted in the previous expressions, they could also be used for changes in inlet air properties due to varying ambient humidity.

We note that the above expressions can be further simplified for gas turbine combustion gases, by taking into account that the specific heat of steam is roughly double the specific heat of the combustion gases, as can be seen from **Figure B.151**. For the range of turbine inlet temperatures encountered in today's turbines, and representative values of fuel/air ratio,  $C_{ps}/C_{pg}$  is shown to take values very close to **Eq. B-94**.

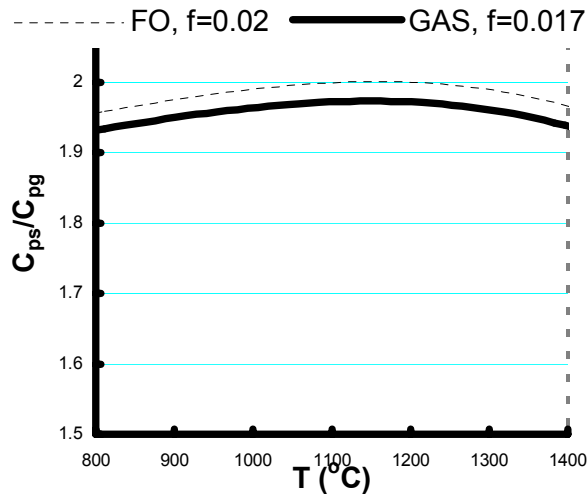


**Figure B.151: Ratio of Specific Heats of Steam and Combustion Gases.**

By virtue of this observation, **Eq. B-94** for  $C_p$  becomes:

$$\frac{\delta c_{pg}}{c_{pg}} \approx war \quad \text{Eq. B-97}$$

For the gas constant  $R$ , for  $R_s = 461.5$  and  $R_g = 287$ , **Eq. B-95** gives:

$$\frac{\delta R_g}{R_g} = 0.61 war \quad \text{Eq. B-98}$$

and for the isentropic exponent,

$$\frac{\delta \gamma}{\gamma} \approx 0.33(1.61 - 2)war = -0.13 war \quad \text{Eq. B-99}$$

#### B.8.3.3.3 Performance Deviations

With the help of the formulas for the fuel/air ratio and specific heat deviations, simplified expressions for the deviations of power output, and efficiency can be derived. We will show that use of such expressions allows the evaluation of the effects of diluent injection on the performance of a gas turbine. Power output and efficiency are examined first, followed by the effect on the compressor operating point and exhaust gas temperature.

#### B.8.3.3.4 Power Output

The fractional change in power output is given by the following approximate relation:

$$\frac{\Delta P}{P} = \frac{\Delta \dot{m}_2}{\dot{m}_2} + 2 \frac{P_T}{P} f' w \quad \text{Eq. B-100}$$

The first term is the fractional change of air mass flow rate caused by the change in the operating point of the compressor. The second term represents the change in power produced by the turbine, swallowing extra fluid, namely the injected diluent. The factor two comes from the fact that steam produces twice the power produced by the same mass flow rate of combustion gas, when expanding over the same temperature limits, due to its thermal capacity being double that of the combustion gas. can be modified to use only data from the dry operating point at the same TIT, by substituting  $f'$  from **Eq. B-92**.

$$\frac{\Delta P}{P} = \frac{\Delta \dot{m}_2}{\dot{m}_2} + 2 \frac{P_T}{P} \frac{f' w}{1 - r_w f} \quad \text{Eq. B-101}$$

For a modern single shaft turbine used in electricity generation, operation with fixed compressor geometry implies almost no change in inlet mass flow rate. Therefore, the change in power will depend only on the water/fuel ratio  $w$ , since the first term on the right hand side of **Eq. B-100** will be almost zero. When variable geometry exists and is used for engine control, mass flow changes will have to be accounted for according to this relation. This also holds for a twin shaft gas turbine.

Variation of the power output of a single shaft gas turbine with constant IGV setting, as a function of the water-to-fuel ratio, is shown in **Figure B.152**. Results for operation with fuel oil or natural gas and injection of water or steam are shown. The lines represent the prediction using **Eq. B-100** and the points prediction of the same conditions with a detailed thermodynamic computer model of the engine considered **[B.108]**. It is shown that predictions with **Eq. B-100** are in very close agreement with the predictions of the full model, and thus **Eq. B-100** can accurately represent changes due to diluent injection for different fuels. It can also be used to interpret the differences in operation for the different cases, shown in **Figure B.152**.

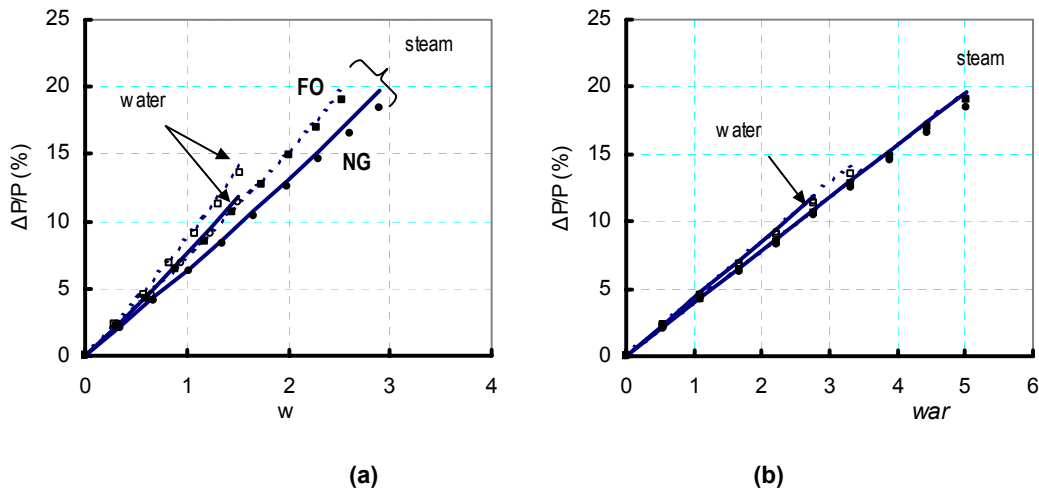


**Figure B.152: Power Output Deviation with Diluent Injection. (a) As a Function of Water/Fuel Ratio, (b) As a Function of Water/Air Ratio. Points: Computer Model, Lines: eq (6).**

Water injection produces a larger power output than the same quantity of steam, irrespective of the kind of fuel. **Eq. B-101** can be used to explain this trend: for a given operating point and fuel (given  $PT/P$ ), the slope of the power increase versus  $w$  is higher in the case of water, since the parameter  $r$  takes a larger value, and thus the denominator in **Eq. B-101** becomes smaller. It is also observed in **Figure B.152**, that the change in power output is smaller when the fuel is gas, as compared to liquid. The reason for this behaviour is two fold: First, the term  $PT/P$  is slightly smaller ( $PT$  increases due to a larger gas specific heat and therefore  $PT/P(=1/(1-P_c/PT))$  slightly decreases), and secondly, the slope is proportional to  $f$  which is smaller for typical natural gas (due to its LHV being about 20% higher than fuel oil). The difference is much smaller if  $war(=f \cdot w)$  is plotted on the abscissa, as shown in **Figure B.152b**. The use of this independent variable, virtually eliminates thus the dependence on the kind of fuel.

The values of the predictions presented in **Figure B.152**, are in very close agreement with data published by gas turbine manufacturers [**B.100** and **B.101**].

#### B.8.3.3.5 Efficiency

The deviation of thermal efficiency is given by the relation:

$$\frac{\Delta(\eta_{th})}{\eta_{th}} = (2 \frac{P_r}{P} - r) f' w \quad \text{Eq. B-102}$$

which can be further transformed, using **Eq. B-92**

$$\frac{\Delta(\eta_{th})}{\eta_{th}} = (2 \frac{P_r}{P} - r) \frac{f w}{1 - r f w} \quad \text{Eq. B-103}$$

The efficiency deviation, as a function of the water-to-fuel ratio, is shown in **Figure B.153**, where data for water injection and different fuels are also included, similar to **Figure B.153**. The good agreement with predictions of the full computer model can be observed in this case too, while the trends predicted here are close to the trends published by engine manufacturers, shown in **Figure B.153**. In this case too, it can be shown that use of the water to air ratio as an independent variable produces curves which demonstrate a very weak dependence on the kind of fuel.

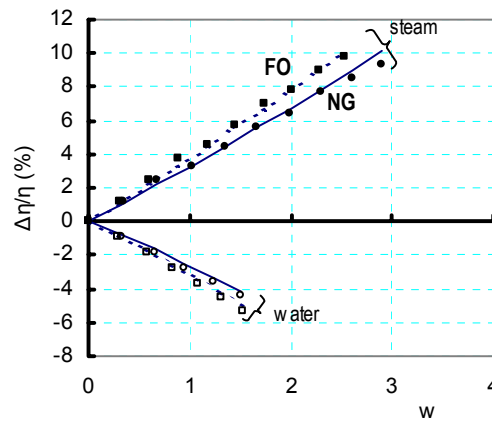


**Figure B.153: Gas Turbine Efficiency Deviation with Diluent Injection.**

The first observation is that while both steam and water injection result in an output increase, they have the opposite effects on efficiency: steam injection increases efficiency while water injection decreases it. The reason for this behaviour can be explained by looking at **Eq. B-102**. As discussed above,  $r$  is very large for water injection, and thus the coefficient in **Eq. B-102** becomes negative. It has a much smaller value for steam and hence the positive slope.

The change in efficiency can be further interpreted physically, as the resultant of two effects in opposite directions: More power is produced due to the increased flow through the turbine and increase in heat capacity. This power increase is achieved with an increase in the fuel consumed, to heat the diluent injected. This heat is proportionally higher than the extra power, in the case of water injection, as it includes the heat of vaporization. This proportionality is expressed by the value of  $r$ . For water  $r$  is very large, and offsets the advantage in power. It should be noted that this effect can also be seen from the cycle point of view: In the case of steam the average temperature of heat addition to the cycle is slightly increased, while the temperature of heat rejection is lowered, since part of the exhaust heat is used to produce the steam. In the case of water, the heat rejection is at the same temperature, while heat addition occurs at a lower temperature (a large part of it is used to evaporate the water).

#### B.8.3.3.6 Compressor Operating Conditions

Movement of the operating point on the compressor map is of interest for different operating conditions, mainly to monitor surge margins and to ensure that the risk of encountering unstable operation is minimized. The fact that steam injection reduces surge margin means that compressor operation has to be monitored, to avoid the occurrence of such conditions, as discussed in **[B.110]**.

The operating point of the compressor is defined by the pressure ratio  $\pi_c$  and reduced mass flow rate  $q_2$ . For operation without and with water injection and dividing the two equations gives:

$$\frac{\pi_c'}{\pi_c} = \frac{q_2'}{q_2} \frac{1 + f'(1+w)}{1+f} \sqrt{\frac{R_4' \gamma_4' T_4' T_2}{R_4 \gamma_4 T_4 T_2'}} \quad \text{Eq. B-104}$$

This relation can be used to predict the pressure ratio at any operating condition once the pressure ratio at one operating point is known (e.g. at base load) and can be applied to both dry and wet operation. It can be used to estimate the change in pressure ratio, which will result from the injection of water. For constant TIT, this equation gives:

$$\frac{\pi_c'}{\pi_c} = \frac{q_2'}{q_2} \frac{1 + f'(1 + w)}{1 + f} \sqrt{\frac{R_4'}{R_4} \frac{\gamma_4}{\gamma_4'}} \quad \text{Eq. B-105}$$

Using the small  $f'w$  approximation and eq. (23), it can be transformed as follows:

$$\frac{\pi_c'}{\pi_c} \frac{q_2'}{q_2} \approx (1 + f'w)(1 + 0.37f'w) \approx 1 + 1.37 \frac{f'w}{1 - r'w} \quad \text{Eq. B-106}$$

At this point it must be noted that operation of a single shaft configuration and a configuration with a free power turbine is different. The relations for change in pressure ratio, presented above, can be used to estimate the shift of operating points for the two cases.

#### B.8.3.3.6.1 Single Shaft Gas Turbine

The typical application for this configuration is electricity generation. In such applications the shaft mechanical speed is constant. This means that for given ambient conditions the compressor operating point will be moving along a constant speed line. For operation with constant geometry, namely with no variation of stator vane angles, it is usual that the nominal constant speed characteristic is approximately vertical to the flow axis, namely  $q_2 = \text{constant}$ , especially for high pressure ratio transonic axial compressors. Operation at constant turbine inlet temperature, allows thus a further simplification of **Eq. B-105**:

$$\frac{\pi_c'}{\pi_c} = \frac{1 + f'(1 + w)}{1 + f} \sqrt{\frac{R_4'}{R_4} \frac{\gamma_4}{\gamma_4'}} \approx (1 + f'w) \sqrt{\frac{R_4'}{R_4} \frac{\gamma_4}{\gamma_4'}} \quad \text{Eq. B-107}$$

This relation shows that pressure ratio changes as a result of two effects: change of mass flow through the turbine and change of gas properties as a result of increased water content. Therefore, diluent injection will force the pressure ratio to increase.

**Eq. B-107** can be used to evaluate change in pressure ratio and thus estimate the new position of the compressor operating point. An example of a calculated change in pressure ratio is shown in **Figure B.154**, where it is also shown that predictions of **Eq. B-107** are in close agreement to those of a full computer model. The way the operating point moves is shown in **Figure B.154**.

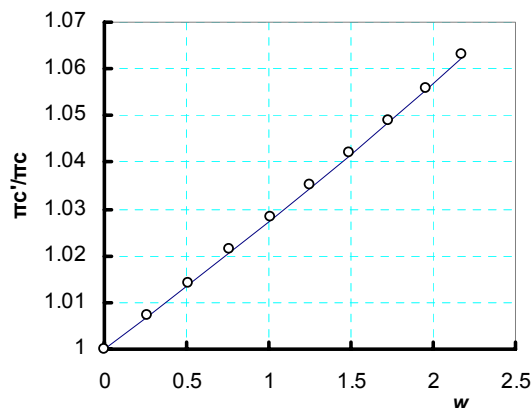


**Figure B.154:** Variation of Compressor Pressure Ratio as a Function of the Amount of Injected Steam for a Single Shaft Gas Turbine.

## ANNEX B – ADVANCED TOPICS AND RECENT PROGRESS

### B.8.3.3.6.2 Twin Shaft Gas Turbine

For dry operation, the gas generator operating point moves along the operating line. For a single spool gas generator, the movement of the operating point can be assessed by using the power balance equation. This equation can be written as follows:

$$\pi_C^{\frac{\gamma-1}{\gamma}} - 1 = \frac{m_4}{m_2} \frac{c_{pg}}{c_{pa}} \frac{T_4}{T_2} \left( 1 - \frac{T_{41}}{T_4} \right) \eta_{Cis} \quad \text{Eq. B-108}$$

For operation with the power turbine choked, the temperature ratio of the gas generator turbine  $T_{41}/T_4$  remains approximately constant (see for example [B.111]). If we consider operation with a given  $T_4$ , write this equation for operation with and without injection, divide the two equations and use also eq (18), we get:

$$\frac{\pi'_C{}^{\frac{\gamma-1}{\gamma}} - 1}{\pi_C{}^{\frac{\gamma-1}{\gamma}} - 1} = \frac{1 + f'(1+w)}{1 + f} \frac{c'_{pg}}{c_{pg}} \quad \text{Eq. B-109}$$

This equation can be used to predict the change in pressure ratio. A comparison of prediction of this equation and prediction using a full computer model of a twin shaft gas turbine (the one described in [B.112]), is shown in **Figure B.155**.

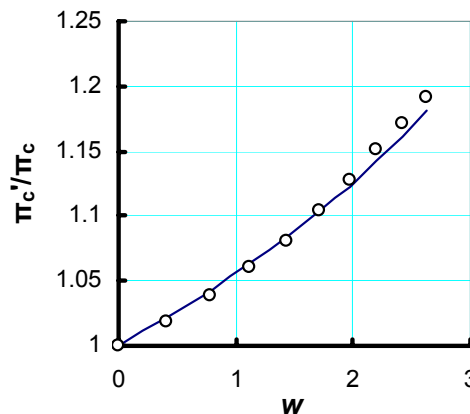


**Figure B.155:** Change of Compressor Pressure Ratio with Water Injection for a Twin Shaft Gas Turbine. Points: Computer Model, Line: Eq. B-109.

Once the pressure ratio is estimated, the compressor flow function  $q_2$  can be estimated using **Eq. B-105**. The movement of the operating point on the compressor map, corresponding to the predictions of **Figure B.155**, is shown in **Figure B.156**, where prediction of this equation are compared to those of the full computer model. It is observed that pressure ratio varies with mass flow rate and compressor speed. The increase in power caused by diluent injection drives the compressor to operate at higher rotational speed, the surge margin is however reduced.

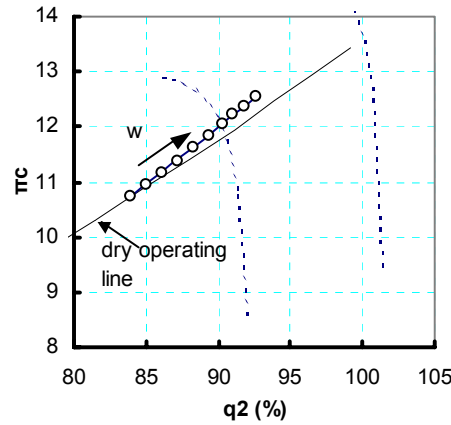


**Figure B.156:** Change of Compressor Operating Conditions with Diluent Injection for a Twin Shaft Gas Turbine. ° Operating Points when Water is Injected at Constant TIT.

The estimated deviations of the compressor flow function provide directly the deviations of mass flow rate from the value at the dry operating point. This means that both terms of **Eq. B-100** are known and thus the deviation in power output can be assessed for the case of the twin shaft gas turbine as well. A comparison of the deviation evaluated through **Eq. B-101** and the detailed computer model is shown in **Figure B.157**.

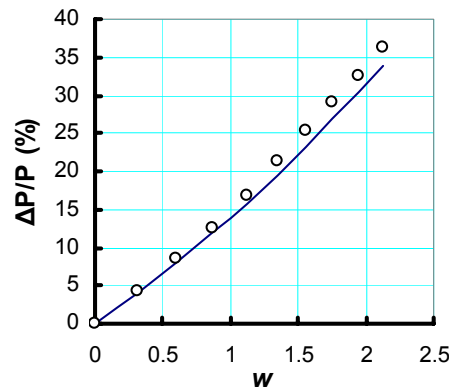


**Figure B.157:** Deviation of Power Output with Water Injection, for a Twin Shaft Gas Turbine.

## B.8.4 Water/Steam Ingestion Effects Discussion

All the relations presented above for evaluating the deviations of performance parameters contain the term  $f'w$ . This term is equal to the water/air ratio, since:

$$f'w = \frac{m_f}{m_a} \frac{m_w}{m_f} = \frac{m_w}{m_a} = war \quad \text{Eq. B-110}$$

This means that this parameter can also be considered as the governing parameter for the deviations. We have also shown that when this parameter is used, the change in power output and efficiency depends very little on the type of fuel, while when  $w$  is the independent variable, different slopes are observed for different fuels. On the other hand, the use of  $w$  may be preferable since this parameter is the one that determines the reduction in  $\text{NO}_x$  emissions, as discussed in the introduction.

The formulas for power output and efficiency are valid, independently of shaft arrangement. It was discussed previously that in the case of a single shaft gas turbine with constant geometry, the amount of water alone determines the power change. If variable IGVs are used their control law would need to be known, for evaluating the power change (this law would allow determination of the term  $\Delta m/m$  in **Eq. B-100**). For the twin shaft gas turbine, the mass flow change is evaluated from the power and flow matching relations, as discussed in the previous section.

It is interesting to examine how the sensitivity of power and efficiency variations are expected to vary for the range of design parameters encountered in today's gas turbines. The main parameters that influence sensitivity to diluent injection are the ratio of turbine power to power output  $PT/P$  and the relative enthalpy rise of the steam expressed by the parameter  $r$ . The range of values of these two parameters for today's gas turbines is discussed in *Annex B*. On the basis of these values, the range of variation of the power versus water to air ratio for constant geometry single shaft gas turbines, is shown in **Figure B.158**.  $war$  is chosen as the abscissa, since the corresponding lines are then almost independent of the fuel type. It is observed that for a large variety of designs, the rate of power change with water-to-air ratio varies within a relatively narrow range. The range for water injection is also narrow with slightly higher slope. From this figure we could claim that for any gas turbine, a rule of thumb would be that there is an increase of 5% in power for every 1% of injected water or steam, expressed as a percentage of inlet air, for operation at nominal conditions.

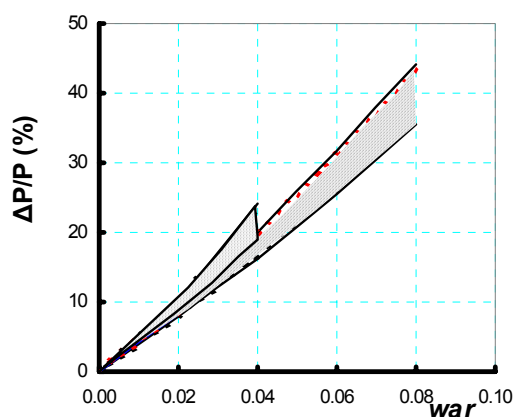


**Figure B.158: Range of Variation of Power Deviation for Existing Gas Turbines. Single Shaft, Constant Geometry.**

At this point it should be commented that the increase in output for a twin shaft gas turbine is larger, for the same amount of injected water or steam. For this case, diluent injection results in an increase of mass flow rate, resulting in an additional power increase, as indicated from **Eq. B-100**. The simultaneous increase in pressure ratio, results in general in larger values of the ratio  $PT/P$ , giving finally a larger increase of output per unit diluent mass flow injection. Analysis of **Eq. B-106** and **Eq. B-109** can show that for this case an additional output increase of about 1.5% per 1% of injected diluent, should be expected. We note here an increase of 6.5% per 1% of injected steam in a twin spool, twin shaft gas turbine was reported, which is in agreement with the previous observations.

The corresponding changes of efficiency are shown in **Figure B.159**. It is observed here that the efficiency increase due to steam injection is bounded within a relatively narrow band. The range of variation for the efficiency drop for water injection is rather wide however.

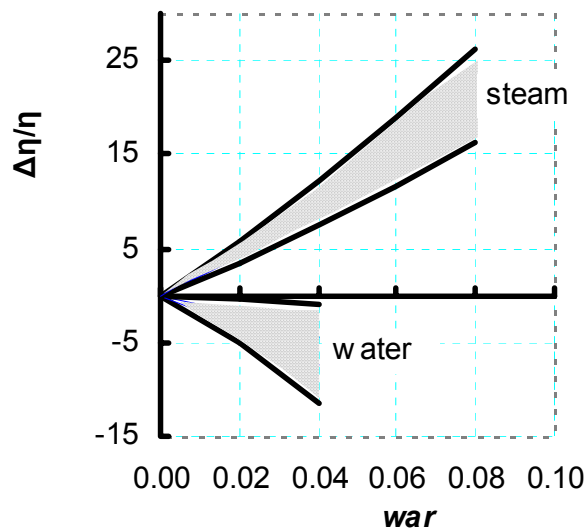


**Figure B.159: Range of Variation of Efficiency Deviation for Existing Gas Turbines. Single Shaft, Constant Geometry.**

Both **Figure B.158** and **Figure B.159** have been derived on the basis of design point data. When off-design operation of a given gas turbine is considered, the curves may differ considerably, since the parameter  $PT/P$  may change.

### B.8.5 Conclusions for Water/Steam Ingestion

The possibility of predicting the main gas turbine performance parameter deviations due to the injection of water or steam into the combustion chamber, by means of simple analytical relations has been demonstrated. It was shown that with minimum design data, it is possible to predict deviations in performance with an accuracy comparable to that of more detailed models.

These relations allow an interpretation of the difference in behavior observed between water and steam injection, or even different fuels. It was thus explained why both water and steam injection have the same influence on output, while they produce opposite trends in efficiency.

Apart from the overall performance, it was shown that the movement of the operating point on the compressor characteristic can also be predicted.

The generality of the predictions was discussed and it was shown that some general trends exist for current gas turbine designs, as demonstrated by using published design data from a large number of industrial gas turbines.

It was also shown that the main parameters influencing the magnitude of the deviations caused by diluent injection are bounded within certain limits. Some generalized conclusions can thus be derived for any application.

### B.8.6 Further Discussions

The layout of a gas turbine considered for the present study is shown in **Figure B.160**. This layout covers both types of shaft arrangement. For the twin shaft gas turbine, station 41 is the station between compressor and power turbine.

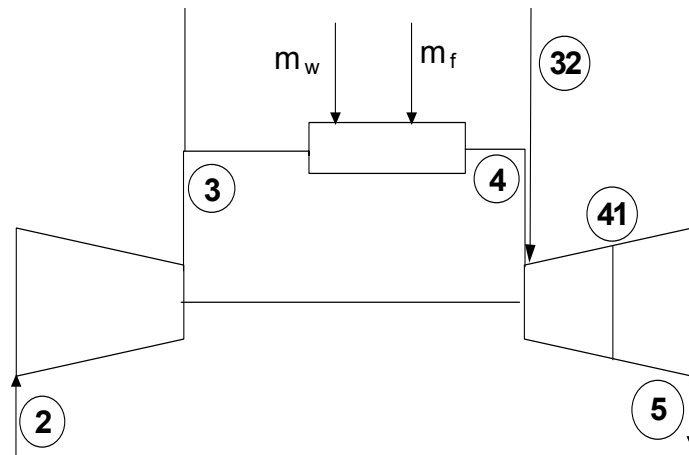


**Figure B.160: Schematic of the Gas Turbine Layout Studied.**

The formulas used to calculate performance parameter changes have been derived by the author in [B.103], for water injection. The approach followed is to consider an operating point without diluent injection and to derive formulas for the deviations of performances from the values at that operating point. From the derivation, it is deduced that they are applicable to steam injection as well. Injection at compressor outlet or within the combustion chamber are equivalent from a performance point of view.

Derivation of simplified relations becomes possible by taking advantage of the fact that the fuel air ratio of a gas turbine is a small number, with a value usually around 0.02 for base load operation. Terms containing higher power of this quantity can thus be neglected without loss of accuracy. A summary of the procedure for derivation of the equations is given in the following.

### B.8.6.1 Gas Properties

Diluent injection increases the steam content of the hot gases into the turbine, in comparison to the case with no diluent injection. The new specific heat can be calculated if the gas is considered to be a mixture of water vapour and gas produced from dry combustion:

$$c'_{pg} = \frac{(1 + f')c_{pg} + f'w c_{ps}}{1 + f'(1 + w)} \quad \text{Eq. B-111}$$

Taking into account that  $f', f'w \ll 1$  this relation can be simplified to give:

$$\frac{c'_{pg}}{c_{pg}} \approx (1 + f'w(\frac{c_{ps}}{c_{pg}} - 1)) \quad \text{Eq. B-112}$$

From this relation, Eq. B-93 is derived.

### B.8.6.2 Fuel-Air Ratio

The change in fuel flow rate when diluent is injected can be evaluated by applying the steady flow energy equation (SFEE) to the combustion chamber for operation with and without injection. The flows into and out of the combustion chamber are shown schematically in Figure B.161.

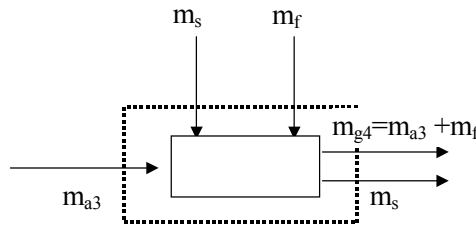


**Figure B.161: Control Volume for Application of the SFEE over the Combustion Chamber.**

The SFEE for the combustion chamber is:

$$(1 + f')(h_{g4} - h_{g0}) = (h'_{a3} - h_{a0}) + f' LHV - w f' (h_{s4} - h_w) \quad \text{Eq. B-113}$$

Writing this equation for dry and wet operation and eliminating the quantity LHV, gives the following relation for fuel air ratio:

$$\frac{f'}{f} = r w f' + a \quad \text{Eq. B-114}$$

where

$$a = \frac{(h_{g4} - h_{g0}) - (h'_{a3} - h_{a0})}{(h_{g4} - h_{g0}) - (h_{a3} - h_{a0})}, \quad r = \frac{h_{s4} - h_w}{(h_{g4} - h_{g0}) - (h_{a3} - h_{a0})} \quad \text{Eq. B-115}$$

The value of  $a$  in this relation is very close to unity. Compressor outlet enthalpy  $h'_{a3}$  differs from the dry value  $h_{a3}$  by a relatively small amount, compared to the enthalpy rise in the combustion chamber. The numerator and denominator of the fraction are therefore almost equal. We thus have:

$$\frac{f'}{f} \approx r w f' + 1 \quad \text{Eq. B-116}$$

which gives **Eq. B-92** of the main text.

We note that  $r$  expresses the relative specific enthalpy rise of the injected diluent with respect to the enthalpy rise for transformation of the air into combustion products.

### B.8.6.3 Power Output

The deviation of power output has been derived in **[B.103]**. The derivation is also summarized here for completeness.

Power output is derived by relating the net output to the difference between the turbine and compressor power:

$$P = \dot{m}_2 C_{pa} T_2 \left[ \overbrace{\frac{\dot{m}_4}{\dot{m}_2} \frac{c_{pg}}{c_{pa}} \frac{T_4}{T_2} \eta_{Tis}}^{P_h} \left( 1 - \frac{1}{\pi_T^{\frac{\gamma_g - 1}{\gamma_g}}} \right) - \frac{1}{\eta_{cis}} \left( \pi_C^{\frac{\gamma_a - 1}{\gamma_a}} - 1 \right) \right] \quad \text{Eq. B-117}$$

## ANNEX B – ADVANCED TOPICS AND RECENT PROGRESS

This is a simplified expression, as it does not take into account the effect of parasitic flows, such as those used for cooling. It provides a better approximation when  $T_4$  is the ISO turbine inlet temperature (derived on the assumption of mixing parasitic flows at turbine inlet). Deviations, when water or steam is injected, are calculated more accurately, provided that the cooling flows remain unchanged. This is a good approximation, since these flows are driven by pressure differences which remain practically unaltered.

For given ambient temperature and turbine inlet temperature, taking logarithms and differentiating, we obtain:

$$\frac{\delta P}{P} = \frac{\delta \dot{m}_2}{\dot{m}_2} + \frac{m_2 C_{pg} T_2}{P} \delta P_h \quad \text{Eq. B-118}$$

where  $P_h$  is the term in brackets in eq (17). The deviation  $\delta P_h$  can be further evaluated as follows:

$$\delta P_h = Y_T \cdot \delta \left( \frac{\dot{m}_4 C_{pg} T_4}{\dot{m}_2 C_{pa} T_2} \right) + \left[ \frac{\dot{m}_4 C_{pg} T_4}{\dot{m}_2 C_{pa} T_2} \delta Y_T - \delta Y_c \right] \quad \text{Eq. B-119}$$

$$\text{where we have put: } Y_c = \left( \pi_c^{\frac{\gamma_a - 1}{\gamma_a}} - 1 \right) / \eta_{cis}, \quad Y_T = \eta_{tis} \left( 1 - 1 / \pi_T^{\frac{\gamma_g - 1}{\gamma_g}} \right) \quad \text{Eq. B-120}$$

For evaluation of the first term of the right hand side of eq (18a), when ambient and turbine inlet temperature are constant, we have:

$$\delta \left( \frac{\dot{m}_4 C_{pg}}{\dot{m}_2 C_{pa}} \right) = \frac{\dot{m}_4 C_{pg}}{\dot{m}_2 C_{pa}} \left( \frac{\delta \left( \frac{\dot{m}_4}{\dot{m}_2} \right)}{\frac{\dot{m}_4}{\dot{m}_2}} + \frac{\delta C_{pg}}{C_{pg}} \right) \quad \text{Eq. B-121}$$

The mass balance for the combustion chamber gives the following relation between the turbine inlet and compressor inlet mass flow rates:

$$\frac{\dot{m}_4}{\dot{m}_2} = \frac{\dot{m}_4}{\dot{m}_3} \frac{\dot{m}_3}{\dot{m}_2} = (1 + f'(1 + w)) \cdot (1 - b) \quad \text{Eq. B-122}$$

where  $b$  is the fraction of the total air flow bled from the compressor, before entry to the combustion chamber. Application of this equation without and with water injection, gives:

$$\delta \left( \frac{\dot{m}_4}{\dot{m}_2} \right) / \left( \frac{\dot{m}_4}{\dot{m}_2} \right) = \frac{f w}{1 + f} \quad \text{Eq. B-123}$$

Coming to the second term of the right hand side of **Eq. B-119**, it expresses the rate of change of specific power with pressure ratio, for given isentropic efficiencies of compressor and turbine. This term is very small and can be neglected for the following reason: gas turbine designers usually choose the design point of an engine in the ‘flat’ region of the specific-power versus pressure ratio curve, where derivative over pressure ratio has a value close to zero.

Using now **Eq. B-119**, **Eq. B-121**, **Eq. B-123** and **Eq. B-92**, gives:

$$\frac{\delta P}{P} = \frac{\delta \dot{m}_2}{\dot{m}_2} + \frac{P_T}{P} \left( \frac{C_{ps}}{C_{pg}} - \frac{f}{1+f} \right) f' w \quad \text{Eq. B-124}$$

For  $C_{ps}/C_{pg} \approx 2$  and  $f \ll 1$ , this relation gives **Eq. B-100** of the main text.

#### **B.8.6.4 Efficiency**

The relation for estimating efficiency deviation can be derived from the equation of definition of gas turbine efficiency:

$$\eta_{th} = \frac{P}{\dot{m}_f LHV} = \frac{P}{f \dot{m}_3 LHV} \quad \text{Eq. B-125}$$

Efficiency change can be derived from this relation, by taking logarithms and then differentiating:

$$\frac{\delta(\eta_{th})}{\eta_{th}} = \frac{\delta P}{P} - \frac{\delta f}{f} - \frac{\delta \dot{m}_3}{\dot{m}_3} \quad \text{Eq. B-126}$$

It is noted here that the gas turbine alone is considered in the definition of efficiency. When steam is injected, the heat of producing it is not accounted for in this expression. This represents the case that steam is produced from the gas turbine exhaust gases and no additional fuel is used.

#### **B.8.6.5 Compressor Pressure Ratio**

Pressure ratio can be related to turbine and compressor flow capacities through flow matching relations. Using the definition of turbine and compressor reduced mass flow rates, and **Eq. B-122** that links the inlet mass flow rate to the two components, it is easily deduced that the following relation holds:

$$\pi_c = \frac{q_2}{q_4} (1 + f' (1 + w)) (1 - b) (1 - K_b) \sqrt{\frac{R_4}{R_2} \frac{\gamma_2}{\gamma_4}} \sqrt{\frac{T_4}{T_2}} \quad \text{Eq. B-127}$$

This relation holds for any operating condition, with or without diluent injection. It is also realistic to assume that the bleed air fraction  $b$  and loss factor  $K_b$  do not change with diluent injection, namely the term  $(1-b)(1-K_b)$  remains constant. It is also noted that the turbine flow function  $q_4$  remains constant for a choked turbine, which is the case for the largest part of the operating envelope of modern gas turbines.

Using **Eq. B-99** for gas constant and isentropic exponent deviations we get:

$$\frac{R'_4}{R_4} \frac{\gamma_4}{\gamma'_4} = \frac{(1 + \delta R / R)}{(1 + \delta \gamma / \gamma)} = \frac{(1 + 0.61 f' w)}{(1 - 0.13 f' w)} \approx 1 + 0.74 f' w \Rightarrow \sqrt{\frac{R'_4}{R_4} \frac{\gamma_4}{\gamma'_4}} \cong 1 + 0.37 f' w \quad \text{Eq. B-128}$$

#### **B.8.7 References in Section B.8, Water/Steam Ingestion**

[B.89] Lefebvre, A.H., “The Role of Fuel Preparation in Low Emission Combustion”, Journal of Engineering for Gas Turbines and Power, October, Vol. 117, pp. 617-654, 1995.

---

**ANNEX B – ADVANCED TOPICS AND RECENT PROGRESS**

---

- [B.90] Pavri, R. and Moore, G.D., “Gas Turbine Emissions and Control”, GE Reference Library, GER-4211, 03/01, 2001.
- [B.91] Schetter, B., “Gas Turbine Combustion and Emission Control”, Lecture Series 1993-08, Combined Cycles for Power Plants, von Kármán Institute for Fluid Dynamics, 1993.
- [B.92] Shaw, H., “The Effects of Water, Pressure, and Equivalence Ratio on Nitric Oxide Production in Gas Turbines”, ASME Journal of Engineering for Power, July 1974, pp. 240-246.
- [B.93] Digumarthy, R. et al., “Cheng-Cycle Implementation on a Small Gas Turbine Engine”, Journal of Engineering for Gas Turbines and Power, Vol. 106, pp. 699-702, 1984.
- [B.94] Kolp, D.A. and Moeller, D.J., “World’s First Full STIG LM5000 Installed at Simpson Paper Company”, ASME Journal of Engineering for Gas Turbines and Power, Vol. 111, pp. 200-210, 1989.
- [B.95] Fraize, W.E. and Kinney, C., “Effects of Steam Injection on the Performance of Gas Turbine Power Cycles”, ASME Journal of Engineering for Gas Turbines and Power, Vol. 101, pp. 217-227.
- [B.96] Burnham, J.B., Giuliani, M.H. and Moeller, D.J., “Development, Installation and Operating Results of a Steam Injection System (STIG) in a General Electric LM5000 Gas Generator”, ASME Journal of Engineering for Gas Turbines and Power, Vol. 109, pp. 257-262, pp. 699-702, 1987.
- [B.97] Larson, E.D. and Williams, R.H., “Steam-Injected Gas Turbines”, ASME Journal of Engineering for Gas Turbines and Power, Vol. 109, pp. 55-63.
- [B.98] Tuzson, J., “Status of Steam-Injected Gas Turbines”, Journal of Engineering for Gas Turbines and Power, Vol. 114, October 1992, pp. 682-686.
- [B.99] Walsh, P.P. and Fletcher, P., “Gas Turbine Performance”, Blackwell Science Ltd, ISBN 0-632-04874-3, 1998.
- [B.100] Kreitmeier, F., Fruttschi, H.U. and Vogel, M., “Economic Evaluation of Methods for Reducing NO<sub>x</sub> Emissions of Gas Turbines and Combined Cycle Plants”, ABB Review 1/92, pp. 29-36, 1992.
- [B.101] Cloyd, S.T. and Harris, A.J., “Gas Turbine Performance – New Application and Test Correction Curves”, ASME Paper # 95-GT-167, 1995.
- [B.102] Noymer, P.D. and Wilson, D.G., “Thermodynamic Design Considerations for Steam-Injected Gas Turbines”, ASME Paper # 93-GT-432, 1993.
- [B.103] Mathioudakis, K., “Analysis of the Effects of Water Injection on the Performance of a Gas Turbine”, ASME Journal of Engineering for Gas Turbines and Power, July 2002, Vol. 124, pp. 489-495.
- [B.104] Stamatis, A., Kamboukos, Ph., Aretakis, N. and Mathioudakis, K., “On Board Adaptive Models: A General Framework and Implementation Aspects”, Proceedings of ASME Turbo Expo 2002 June 3-6, 2002, Amsterdam, The Netherlands, ASME Paper # GT-2002-30622.
- [B.105] AGARD-AR-332, “Recommended Practices for the Assessment of the Effects of Atmospheric Water Ingestion on the Performance and Operability of Gas Turbines Engines”, September 1995, ISBN 92-836-1022-9.

- [B.106] Mathioudakis, K., Aretakis, N. and Tsalavoutas, A., “Increasing Diagnostic Effectiveness by Inclusion of Fuel Composition and Water Injection Effects”, Proceedings of ASME Turbo Expo June 3-6, 2002, Amsterdam, The Netherlands, ASME Paper # GT-2002-30032.
- [B.107] Mathioudakis, K., “Evaluation of Steam and Water Injection Effects on Gas Turbine Operation Using Explicit Analytical Relations”, Proceedings of the Institution of Mechanical Engineers, Part A, Journal of Power and Energy, Vol. 216, No. A6, December 2002, pp. 419-431.
- [B.108] Tsalavoutas, A., Aretakis, N., Stamatis, A. and Mathioudakis, K., “Combining Advanced Data Analysis Methods for the Constitution of an Integrated Gas Turbine Condition Monitoring and Diagnostic System”, ASME Paper # 2000-GT-0034, 2000.
- [B.109] Johnston, J.R., “Performance and Reliability Improvements for Heavy-Duty Gas Turbines”, GE Reference Library, GER-3571H, 10/00, 2000.
- [B.110] Dundas, R., Sullivan, D. and Abegg, F., “Performance Monitoring of Gas Turbines for Failure Prevention”, ASME Paper # 92-GT-267, 1992.
- [B.111] Cohen, C. and Rogers, G.F.C. and Saravanamutto, H.I.H., “Gas Turbine Theory”, 4th Edition, Addison Wesley Longman Ltd, 1996, ISBN 0-321-04346-4.
- [B.112] Mathioudakis, K., Stamatis, A., Tsalavoutas, A. and Aretakis, N., “Performance Analysis of Industrial Gas Turbines for Engine Condition Monitoring”, Proceedings of Institution of Mechanical Engineers, Part A: Journal of Power and Energy, Vol. 215, March 2000, pp. 173-184.

### **B.8.8 Additional Bibliography for Section B.8**

- Hoefl, R. and Gebhardt, E., “Heavy Duty Gas Turbine Operating and Maintenance Considerations”, GE Reference Library, GER-3620G, 10/00, 2000.
- Turbomachinery International: Handbook 2001-2002, Vol. 42, No. 6, and Handbook/1996, Vol. 37, No. 6.
- Horlock, J.H., “The Evaporative Gas Turbine [EGT] Cycle”, ASME Paper # 97-GT-408, 1997.
- Utamura, M., Takehara, I. and Karasawa, H., “MAT, A NOVEL, Open Cycle Gas Turbine for Power Augmentation”, Energy Convers. Mgmt, Vol. 39, No. 16-18, pp. 1631-1642, 1998.
- Meher Homji, C.B. and Mee III, T.R., “Inlet Fogging of Gas Turbine Engines Part A: Theory, Psychrometrics and Fog Generation”, ASME Paper # 2000-GT-307, 2000.
- RTO-TR-044, “Performance Prediction and Simulation of Gas Turbine Engine Operation”, RTO Technical Report 44, April 2002, AC/323(AVT-018)TP/29, ISBN 92-837-1083-5.
- Mathioudakis, K. and Tsalavoutas, A., “Uncertainty Reduction in Gas Turbine Performance Diagnostics by Accounting for Humidity Effects”, Proceedings of ASME Turbo Expo 2001 June 4-7, 2001, New Orleans, Louisiana, ASME Paper # 2001-GT-0010, 2001.
- Stamatis, A., Mathioudakis, K. and Papailiou, D.K., “Adaptive Simulation of Gas Turbine Performance”, Journal of Engineering for Gas Turbine and Power, April 1990, Vol. 112.
- Kurzke, J., “Performance Maps for Gas Turbine Performance Computer Programs”, GASTURB Program Manuals, 1996.

## ANNEX B – ADVANCED TOPICS AND RECENT PROGRESS

---

Saravanamuttoo, H.I.H. and McIsaac, B.D., “Thermodynamic Models for Pipeline Gas Turbine Diagnostics”, ASME Paper # 83-GT-235, Transaction of the ASME, Vol. 105, Series A, 1983, pp. 875-884.

Kurzke, J. and Riegler, C., “A New Compressor Map Scaling Procedure for Preliminary Conceptual Design of Gas Turbines”, ASME Paper # 2000-GT-006, 2000.

Tsalavoutas, A., Stamatis, K. and Mathioudakis, K., “Derivation of Compressor Stage Characteristic, for Accurate Overall Performance Map Prediction”, ASME Paper # 94-GT-32, 1994.

Kamboukos, Ph., Oikonomou, P., Stamatis, A. and Mathioudakis, K., “Optimizing Diagnostic Effectiveness of Mixed Turbofans by Means of Adaptive Modeling and Choice of Appropriate Monitoring Parameters”, AVT Symposium on “Monitoring and Management of Gas Turbine Fleets for Extended Life and Reduced Costs”, Manchester, UK, 8-11 October 2000.

Stamatis, A., Mathioudakis, K., Berios, G. and Papailiou, K., “Jet Engine Fault Detection with Differential Gas Path Analysis at Discrete Operating Points”, Journal of Propulsion and Power, Vol. 7, No 6, November-December 1991, pp. 1043-1048.

Burnham, J.B., Giuliani, M.H. and Moeller, D.J., “Development, Installation and Operating Results of a Steam Injection System (STIGTM) in a General Electric LM5000 Gas Generator”, Journal of Engineering for Gas Turbine and Power, July 1987, Vol. 109.

Anon., “LM6000 Control Solutions Benefit Operations”, Woodward Governor Company, Application Sheet 51178, 1997.

Pavri, R. and Moore, G.D., “Gas Turbine Emissions and Control”, GE Reference Library, GER-4211, 03/01, 2001.

Organowski, G., “GE LM6000 Development of the First 40% Thermal Efficiency Gas Turbine”, GE Marine & Industrial Engine and Service Division”.

Meher Homji, C.B. and Mee III, T.R., “Gas Turbine Power Augmentation by Fogging of Inlet Air”, Proceedings of the 28th Turbomachinery Symposium, Texas A&M University, 1999.

Mathioudakis, K., “Gas Turbine Test Parameters Corrections including Operation with Water Injection”, ASME Turbo Expo 2002, Paper # GT-2002-30466.

Mathioudakis, K., Stamatis, A., Tsalavoutas, A. and Aretakis, N., “Computer Models for Education on Performance Monitoring and Diagnostics of Gas Turbines”, Journal of Mechanical Engineering Education, July 2002, Vol. 30, (3), pp. 204-218.

## Annex C – COMPUTER PLATFORMS

### C.1 COMPUTER PLATFORMS

The computer platform is the combination of the hardware and software needed for gas turbine performance calculations. The *hardware* is the actual computer; the *operating system* represents the software required to use the hardware. A specific gas turbine simulation application is implemented on the platform using *application development software*. Together, they form the *development environment*.

Many varieties of development environments exist for gas turbine simulation. A gas turbine model type can be characterized by three needs:

- Application;
- Model fidelity; and
- Computing performance requirements.

The level of model fidelity directly depends on the type of simulation application (see **Chapter 2 – Applications**). Application types include:

- R&D (competitive, for product development);
- Fundamental R&D (often performed at research institutions and universities);
- Cycle decks (both for testing and customer cycle decks);
- Real-time simulation (flight simulators);
- Maintenance/diagnostics (models used to enhance maintenance procedures and diagnostics);
- Probabilistic effects simulations (e.g. Monte-Carlo simulations); and
- Integrated simulations (engine simulations integrated into other models such as aircraft models).

Currently, 2-D and 3-D simulations often focus on component R&D applications while 0-D models usually simulate the whole engine for a large variety of purposes such as a customer cycle deck. 0-D models also include parametric, non-thermodynamic or non-component based models, which may be considered the simpler 0-D models.

Model fidelity directly relates to required computer performance. Full 3-D Navier-Stokes simulations still require special high performance hardware while 0-D models can now be run on PCs. Consequently, computing performance requirements strongly relate to the computer platform.

#### C.1.1 Hardware

Four major hardware categories can be identified:

- High performance computers (including parallel computing);
- Mainframes;
- UNIX workstations; and
- PCs.

High performance computers are generally used for high-fidelity simulation for R&D purposes, such as 2-D and 3-D CFD. Use of 0-D or 1-D engine models for integration within a larger system simulation or

## ANNEX C – COMPUTER PLATFORMS

for probabilistic analysis may also require high performance computers. High-fidelity CFD has become indispensable for gas turbine R&D and can be regarded as heading the (fidelity) frontier of the modeling spectrum. The most important limitation for high fidelity computing is available computing power, both in terms of memory and processing speed. Mainframe computers are rapidly being replaced by other systems such as PC and workstation networks, but are still used for running older applications such as 0-D (cycle decks) and 1-D models. UNIX workstations are widely applied and used for medium fidelity simulation or visualization and data processing of high-performance computing results.

PCs are rapidly increasing their share of the entire computing market. Due to rapid increase in computer power, PCs are now able to run medium fidelity 0-D and 1-D models and to a limited extent (coarse grid) even 3-D CFD simulations (e.g. FLUENT). An important issue at this end of the spectrum is the efficient use and development of new gas turbine simulation applications for the operational field (e.g. maintenance and diagnostics tools). Powerful PCs may well be considered ‘workstations’ now, since they can easily be configured to match the conventional UNIX workstations in performance but then require disk space and memory beyond that of a typical office PC, even with the fastest CPU. Networked UNIX workstations or PCs can be used in parallel for some problems with properly configured software. In some circumstances performance can equal or exceed that of a supercomputer. **Figure C.1** presents the relation between model fidelity, computer platform hardware and application.

NUMBER OF DIMENSIONS (time and space)	SUPER/HIGH PERFORMANCE COMPUTING	MAINFRAME or NETWORKED WORKSTATIONS	SINGLE UNIX WORKSTATION	SINGLE PC
0	Cycle decks. Probabilistic. Multi-disciplinary.	Cycle decks. Maintenance or Diagnostics. Probabilistic. Multi-disciplinary.	Cycle decks. Maintenance or Diagnostics. Probabilistic. Multi-disciplinary.	Cycle decks. Maintenance or Diagnostics. Probabilistic.
1	Cycle decks. Probabilistic. Multi-disciplinary.	Cycle decks. Real-time.	Cycle decks. Real-time.	Cycle decks. Real-time.
2	Cycle match CFD.	Cycle match CFD.	Cycle match CFD.	Component CFD.
3	Cycle match CFD.	Component CFD.	Component CFD.	none <sup>1</sup>
4	Component CFD.	Component CFD.	Component CFD.	none <sup>1</sup>

**Figure C.1: Model Fidelity and Computing Platforms (Status Year 2005).**

### C.1.2 Operating Systems

With the retirement of the old mainframe systems, the number of different operating systems is reduced. In general it can be stated that there are two main streams: UNIX which is commonly used from workstations up to higher performance systems and Windows (Windows 95/98, NT 4.0, 2000 and XP) for the PC based systems. The need to perform simulations on legacy platforms (such as old mainframe systems) can become a barrier and must be identified early on.

Windows NT is also available on a number of high-performance 64-bit systems like the DEC-Alpha, providing a combination of high-computing power with the ability to use the customary PC office software suites.

### **C.1.3 Development Environments**

A large number of development environments exist, both for the UNIX and the Windows systems. Traditionally these environments consisted of 3<sup>rd</sup> Generation Languages (3GL), the most widely used being FORTRAN in the scientific world. Newer 3GL languages include C and the object-oriented languages C++ and ADA. More modern are the 4<sup>th</sup> Generation Languages (4GL). Often these are wrapped around a 3GL language in order to reduce developer effort when building (graphical) user interfaces. Many 4GL tools automatically generate most of the user interface parts of the application. Examples are Visual Basic<sup>®</sup>, Delphi<sup>®</sup>, C++Builder<sup>®</sup>, JBuilder<sup>®</sup> and Visual C++<sup>®</sup>. There are also a number of development environments dedicated to simulation in general or sometimes even to gas turbine simulation (i.e. generic gas turbine simulation tools). Examples are MATLAB Simulink<sup>®</sup> and MathCad<sup>®</sup>. Examples of turbo-machinery CFD tools are CFX-TASCflow<sup>®</sup> with Turbogrid<sup>®</sup>, NUMECA<sup>®</sup> Fine/Turbo<sup>®</sup>.

FORTRAN is still the standard programming language for gas turbine simulation. If FORTRAN is used without platform specific code (such as user interface shells), it can be compiled and run on most platforms. This will be the dominant advantage of FORTRAN until alternative standards become widely accepted. *Chapter 5* lists a number of simulation systems including descriptions of the development environments.

## **C.2 TRENDS AND NEW TECHNOLOGIES**

The Internet and the PC have dominated computer related technological development since the nineties. Both technologies require ‘low cost platforms’ which offer great potential for gas turbine simulation by offering distributed computing, a good user interface, and high power, especially at the lower fidelity end (i.e. operational use) of the spectrum.

High performance computing technology may not have as much public attention, but is also developing at a rapid pace and offering ever more power for high fidelity computing.

With distributed parallel computing technology improving, PC and high performance computer technologies may well merge into a single type of environment or platform. High-speed networks have made remote distribution common in simulations and remote computing is becoming a reality.

### **C.2.1 Computing Power**

Since the introduction of the digital computer, computing power has increased at a rapid rate, see **Figure C.2**. Interesting to note is that the low cost PC is increasing its share of the entire spectrum, while high performance computing is maintaining the top high-fidelity part of it.

## ANNEX C – COMPUTER PLATFORMS

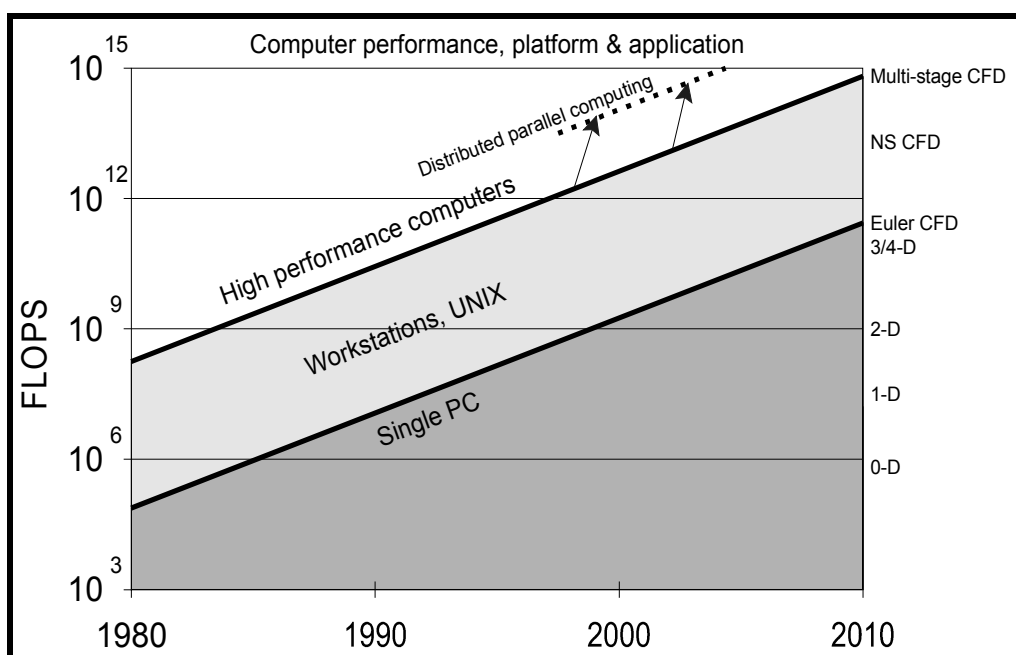


**Figure C.2: Trends in Computing Power.**

As a consequence, computer power has ceased to be the bottleneck for all but the high-fidelity CFD gas turbine simulations. For all types of simulations, implementation effort, user interface including visualization and code maintenance have become critical for successful and efficient use of the models.

For high fidelity CFD simulations a bottleneck remains in the available computer power, especially when the time domain is added as an extra dimension for dynamic simulations. Simultaneous simulation at high spatial resolution and high time domain resolution for instance remains limited as indicated by **Figure C.3**.

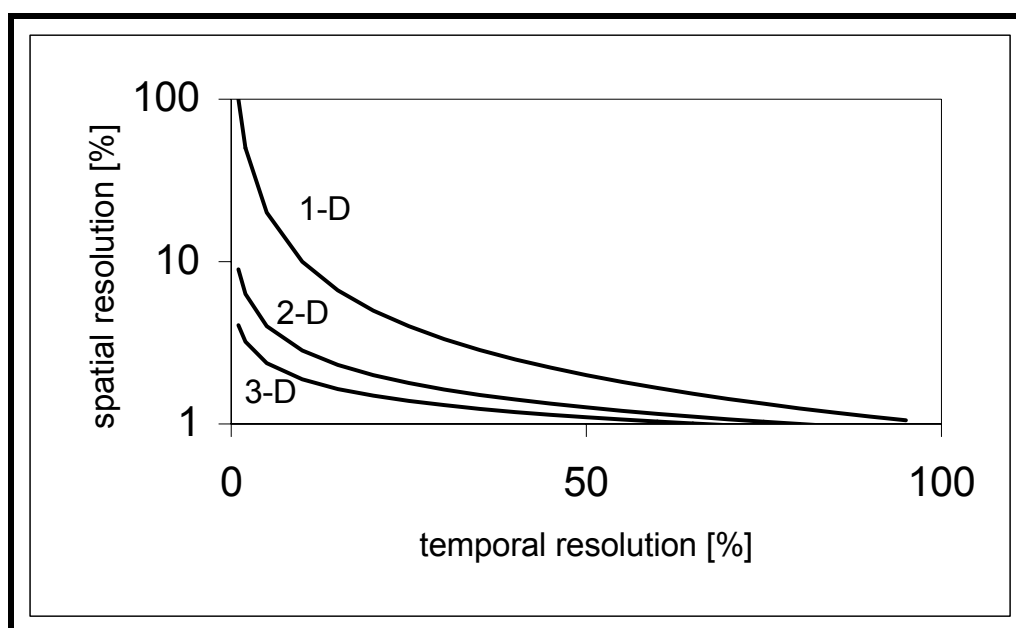


**Figure C.3: Spatial versus Temporal Resolution for a Given Computing Power.**

For a given amount of computer execution time, a trade-off must be made, between temporal and spatial resolution, depending on the purposes and the requirements of the simulation in terms of accuracy. When allowing unlimited computation time, temporal resolution requirements are no longer a restriction and spatial resolution becomes limited by available computer memory. For high-resolution simulations over larger flow areas in engine components, computer memory is critical. With limited computing memory, certain problems cannot be simulated at all while limited processing power only affects computation time without making the simulation totally impossible.

Simultaneous high-fidelity simulations of multiple compressor stages or even multiple components remains impossible without compromises in terms of assumptions or application of the zooming concept (see **Section C.2.7**). *Multi-disciplinary modeling* as in the NPSS program [C.1 and C.2] also requires compromises to compensate for limited computing power.

### **C.2.2 Computing Costs**

In general it can be stated that the cost/benefit ratio of using simulations for various purposes is decreasing rapidly. This becomes evident from **Figure C.1** and the fact that the prices of state-of-the-art PC systems have not risen over the years. 1-D whole-engine thermodynamic performance calculations and simulations can be run at costs many times lower than a few decades ago. This is demonstrated by the emerging PC applications for gas turbine simulation, which allow 0-D simulations at very low cost.

At the other end of the spectrum, the increasing power of high-performance computers offers new opportunities to optimize aero-thermodynamic designs with high-fidelity CFD. Especially when using distributed parallel computing using clustered low cost workstations or PCs this can be done at relatively low costs. Many large gas turbine R&D programs focus on greater CFD detail at limited costs, which is critical to gas turbine technology progress.

As a consequence, established simulation technologies and tools move to lower cost platforms, yet retain their speed and fidelity. High-performance computer technology benefits from low cost technology in the form of distributed parallel computing (see **Section C.2.3**) to satisfy the ever-increasing hunger for CFD calculation power. While computing power remains critical for the high fidelity CFD challenges, the established simulation technology basically needs improvements in order to make their use more efficient (i.e. at lower costs). This means greater attention to user interface, code portability and maintainability aspects is needed.

### **C.2.3 Parallel and Distributed Computing**

Symmetric Multi-Processor (SMP) technology is becoming common in servers. This technology uses several processors in a single computer, and offers the ability to run several tasks in parallel, under the control of the operating system. These tasks are usually distributed at *task* or *thread* level. A thread is a small piece of a program that is capable of performing a task that is largely independent of other threads. To distribute processing at thread level requires design effort from the programmers. Whether using an SMP computer will provide worthwhile gains in speed depends on the amount of data that is used, and the amount of processing that is done to it. If the application is data bound and the CPU is not highly loaded, any investment may be better spent on a faster disk. Similarly, a processor that could run at twice normal speed would not carry the operating system overheads associated with SMP and 2 normal speed processors.

To share tasks between multiple processors:

- The CPUs must have SMP enabling features.
- The operating system must support SMP.

## ANNEX C – COMPUTER PLATFORMS

---

Most new CPU's now are SMP enabled. Different OS versions support different numbers of processors. Windows NT has crept up from 2 to about 8; Windows2000 supports up to 64 processors! Other versions of Windows do not support SMP. Linux 2.2 theoretically supports up to 16 processors on Pentium, UltraSparc, SparcServer, Alpha and PowerPC machines.

Parallel computing is a new development, in which tasks are shared between several processors. Ideally little effort is required from the programmer, with the effort being provided by the operating system. This has great potential for high-performance computing. Such techniques are used internally in many current processors. Optimally, parallel computing could offer a way to increase computing performance in direct proportion to the number of processors used. In reality, the performance gain is less due to the problem of how to distribute the computing tasks over the processors.

Early applications that exploited parallel computing had to include the computing task distribution themselves, requiring large efforts in software development. Now, the trend is to have the operating system or development environment handle that task with solutions like the *Parallel Virtual Machine* (PVM) [C.3]. Although becoming easier to use, this still requires that special actions be taken in defining the problem to facilitate parallel operation. Other examples are: Windows PVM and Bulk Synchronous Parallelism (BSP) '*A new programming model for parallel processing simplifies writing programs and promises code portability*' [C.4].

### C.2.3.1 Multi-Threading

Multi-threading is basically time slicing by the OS. The OS must make these features available to compilers. The language and compiler must in turn make the necessary commands available to the programmer. All 32-bit Windows platforms support multi-threading. This was necessary, so that memory could be shared between related processes, and to prevent Windows applications from being slowed down (frozen) by a single very intensive process. Multi-threading enables the processor to start another process parallel to the slow process and also to be able to interrupt or control the slow process from another thread.

Whether the OS makes SMP available between applications and also between threads within an application, is OS dependent.

With web servers, Windows based systems are typically thread based, usually via reference counted DLLs (ISAPI, NSAPI), while Unix systems spawn new processes (CGI) that typically return data via files. The target platform therefore affects the architecture of a new application, and the way in which efficient code is ported between platforms. This means that multi-threading gas turbine simulation applications will be difficult to port to other platforms.

All modern programming languages have features to use parallel computing and the modern development environments like Delphi come with tools to facilitate multi-processor and parallel computing using *multi-threading*. It is interesting to note that recent computing performance records have been set with parallel computers using large numbers of cheap processors like the Intel 386.

Parallel computing is often applied in super-computers and high-performance workstations operating multiple processors. A new trend is to apply parallel computing to multiple computers that are interconnected over a network. This *distributed parallel computing* requires special software controlling the distribution of different computing tasks in a simulation.

It is expected that eventually software will become available to control parallel distributed computing using a large number of ordinary network environment PCs. This would allow simulations, which could traditionally only be run on super-computers, to run at a fraction of the current cost. This is already being done with networked UNIX workstations.

A critical new technology for distributed computing is object orientation (see **Section C.2.5**). Object orientation offers modularity and common interface mechanisms required for distributed computing. Each computer in a network is executing the simulation of an ‘object’ as part of the entire simulation session across the network.

Most distributed computing has been limited to the same type of processor and operating system. Computers networked over the Internet (or an Intranet) can be used to perform a distributed computation task with Sun’s JAVA technology and the CORBA (Common Object Request Broker Architecture) technology. The JAVA gas turbine simulator **[C.5 and C.6]** is an example of this new trend. Microsoft Windows uses a similar technology called variously ActiveX or DCOM (Distributed Component Object Model).

An example of a distributed-parallel computing project is the Visual Computing Environment (VCE) project at NASA Glenn Research Center **[C.1]**. One of VCE’s objectives is ‘...to develop a visual computing environment for controlling the execution of individual simulation codes that are running in parallel and are distributed on heterogeneous host machines in a networked environment...’. VCE was designed to provide a distributed, object-oriented environment including a parallel virtual machine (PVM) for distributed processing. Users can interactively select and couple any set of codes that have been modified to run in a parallel-distributed fashion on a cluster of heterogeneous workstations.

### **C.2.3.2 Distributed Computing and CORBA**

Common Object Request Brokering Architecture (CORBA) is a standard for cross-platform and cross-network communication. It uses an *Object Request Broker* (ORB) that resides on different computers (either as part a web browser, a part of other analysis software or as an independent server application). Once an application is registered with the ORB, any other CORBA based application with appropriate permissions and access can utilize the services available from that application that have been registered with the ORB. The DCOM standards for MS-Windows applications provide a similar functionality for applications on MS-Windows computers and networks. A number of CORBA-DCOM interface packages have been developed. Most are focused on facilitating CORBA based systems access to MS-Windows DCOM applications.

In this way, simulations or portions of the simulation can be used and implemented in a way that is somewhat independent of the local computing infrastructure. A user of a model at one location can easily and transparently point to a model on a different computer platform and network. Even components within an engine simulation may reside on different computers on different networks. As use of web environments and data management systems grow in the future, the distinction of where (or even if) a simulation is performed become less important to the user. If the requested simulation data is generated and is returned in the desired form and location, then whether the simulation was run on a local computer, a remote computer or pulled from previous results stored in a database can be a transparent detail to the end user.

The main advantages of CORBA are that it is slightly easier to use than DCOM, and works on all platforms, whereas DCOM works only on Windows platforms. However, DCOM is provided free by Microsoft and requires no additional licenses for distribution, while CORBA ‘broker’ software must be purchased under license from a variety of suppliers.

## **C.2.4 Interfaces**

### **C.2.4.1 User Interfaces**

Most modern computer applications have replaced the command line interface with the graphical user interface (GUI). This offers significant benefits in terms of user friendliness. The older gas turbine modeling

## ANNEX C – COMPUTER PLATFORMS

---

environments, especially the 3GL based ones such as FORTRAN, still use the command line interface. Many of them have been updated and wrapped inside 4GL GUI structures.

To specify input-data for complex models, sophisticated user interfaces are required to prevent unacceptable time-consuming data-entry tasks. Across the spectrum of modeling platforms, attempts are made to accomplish this with advanced GUI's. As an example, component maps for 0-D simulation are usually presented to the program in tabular format. To use the tabular format for user data entry (for specification of new or modified maps) is very time consuming and therefore graphical tools are used to have the user edit the data using the graphical map representation to actually 'draw' the map. SmoothC and SmoothT [C.7] are examples of stand-alone Windows applications able to do that task.

With the increase in computing power, the size and detail of the results increases drastically. Graphical visualization and sometimes animation tools are required for their analysis, such as the VCE [C.1] for example.

As a result the user-interface issue tends to become separated from the modeling issue. The modularization of the simulation environments reflects this trend also. In programs like NPSS, sub-programs are defined to address user-interface issues such as visualization of CFD results.

Needs of the expert user or the user with specific highly repetitive tasks can conflict with the needs of the low-end user who needs easy access without being confused by the features and options which aren't relevant to simpler applications. Some GUIs (such as GasTurb, see [Section 5.3](#), and GSP see [Section 5.4](#)) are designed so those more advanced options are hidden or separated from the low-end user options.

### C.2.4.2 External Interfaces

Interfaces with data acquisition systems and measurement databases are often platform specific. The advantages of having these systems on the same platform as the simulation system are often the reason for maintaining legacy systems.

### C.2.4.3 Event Driven User Interfaces

Traditional coding techniques are known as procedural because when a program is started, it runs through a predetermined sequence. At certain points the program may stop and wait for user input and then proceed. A more modern Graphical User Interface (GUI) typically looks like a Windows or Apple screen. It is usually *event driven* which means that code can be executed in any order, depending for example on the order in which the user operates (clicks) buttons or other visual controls. When first introduced, this created additional problems for the programmer, who had to take into account all of the ways in which the user may wish to work. Nowadays, few programmers would welcome a return to the legacy thought patterns, and most users prefer the clarity of function and ease of use of a GUI.

### C.2.5 Object Orientation

Object orientation (OO) is an approach in software development that was defined during the seventies. Before this, the program design was entirely up to the programmer, and the relationship between data and the procedures that operated on it could be unnecessarily complicated and inconsistent. For instance several procedures could operate on the same data, causing a problem if one procedure was changed and another not. The basic idea of object-oriented design (OOD) is *encapsulation*. This means that everything is described as an object, and that every object has methods, properties and data. For illustration, an object called *airplane* might have methods called *take-off*, *fly* and *land*, properties called *all-up-weight*, *number-of-engines* and *maximum-number-of-passengers*, and data called *elapsed-flight-time*, *number-of-passengers* and *current-speed*. The key idea is that only the methods contained within the object can

change the properties and data, thus ensuring integrity. Depending on the programming language, objects may be known as types or classes. Two additional principles of object orientation are:

**Inheritance**, which means that specific types of airplane may be defined by changing the properties of the generic *airplane* object, and by adding new or subtracting existing methods, properties and data. In some languages an object may inherit from more than one parent.

**Polymorphism**, which means that different methods may have the same name, but operate differently depending on the context. For example *take-off* could apply to the start of flight or the removal of equipment.

Inheritance and polymorphism offer significant extra benefits in terms of software design but are not fully included in some development environments. Although OOD promised many benefits in terms of code development effort and maintainability the OOD approach was widely adopted only during the nineties. One of the reasons was that the requirement for software developer skills was underestimated. Most popular object-oriented programming languages are traditional languages extended with object-oriented features like C++ and OOPascal. ADA is an object-oriented language widely used by the US military, but does not include all OOD features (such as inheritance and polymorphism).

Especially in 4GL languages, OOD is commonly applied for GUI development and OO code is generated automatically.

It is up to the developer to decide the extent to which the actual functional (in this case simulation) code will be object-oriented and event driven. For gas turbine simulation, there is great potential in object orientation since in many cases the simulated process can be divided into objects directly. For example, in a non-dimensional whole-engine simulation, engine components such as compressors, turbines, control systems, etc. can easily be defined (encapsulated) as objects. With the OOD principles of inheritance and polymorphism, code development effort, reusability, maintainability and flexibility can be significantly enhanced. An example is the Visual Computing Environment VCE [C.1]. See **Section 5.4** or **5.7** for an example of an OO gas turbine modeling architecture.

### **C.2.6 PC Technology**

Since the eighties, PC technology has drastically changed the IT world. With its continuing and rapid increase in performance the PC is increasing its share in the overall computer market. With the increasing need for computing power for gas turbine simulation, this development offers great potential. Also the PC is becoming the platform on which most efforts to improve development and user environments are focused. This means that all gas-turbine-simulation applications except the high-fidelity simulations requiring high-performance computers will probably be most efficiently developed on PC platforms. If distributed-parallel computing technology becomes mature for networked PCs (see **Section C.2.3**) the high-performance simulation jobs may also benefit from PC technology.

The major corporate operating system used on PCs is Windows (W95/98/NT4.0/2000/XP). An interesting development is the use of UNIX on PCs such as SCO-UNIX and Linux, the Free Software Foundation open UNIX clone.

### **C.2.7 Zooming**

The ‘Zooming’ concept allows high-fidelity simulation of local phenomena of interest in a gas turbine, together with lower fidelity simulation of the rest of the engine system. This approach is necessary to reduce computing power, development time and complexity where higher fidelity analysis is not required. High-fidelity CFD simulation of the aero-thermodynamic processes throughout the entire engine would

require computing power far beyond what is feasible. With the zooming concept, detailed CFD simulation of flow around specific compressor blades, for example, can be performed while the rest of the engine is simulated with lower detail.

An example of the application of the zooming concept is the NPSS program, described in *Section 5.7*.

### **C.2.8 Development Environments**

There are trends towards using new developments like 4GL languages and C++ in the global IT world. The scientific world still generally considers FORTRAN the standard, basically due to the lack of a new clear standard for more modern environments. Only the 3<sup>rd</sup> generation (3GL) languages C, C++ and ADA seem to be able to receive confidence enough to be adopted by some organizations as a standard for gas turbine simulation. Even these can become a problem since they expose low-end computer users to details beyond their level of interest.

On the lower fidelity end of the spectrum with PC simulations and applications, for engine operators and maintenance (e.g. diagnostic tools), new 4GL tools are applied. In the Architectures section, **C.2.9**, two examples are given of 0-D modeling environments using the Delphi 4GL tool based on Object Pascal. C++Builder is another Borland product that uses the same back end compiler as Delphi. This also runs on AS400 and Windows platforms. Linux (Unix) compatibility was launched in June 2001 with the Kylx product. Cross-platform independence depends on programmers not using platform specific Application Programming Interface calls in the code that they write. A graphical library called CLX (pronounced ‘clicks’) has been made available for both Windows and Linux to allow this. Other 4GL tools that could be used for 0-D modeling are Microsoft Visual Basic and Visual C++, although Visual Basic is not an object-oriented language. At the time of writing Microsoft have started to introduce a new language called C# (C Sharp), which is designed to compete with Java, but only to run on WinTel platforms.

With the large amounts of existing and proven FORTRAN code, 4GL environments based on modern languages are often applied to encapsulate FORTRAN sub-routines with a modern front end.

Generic simulation tools like MATLAB Simulink and MatrixX have become popular for 0-D modeling for some types of performance analysis (e.g. real-time modeling and control system design). An important advantage of these tools is that they usually employ ‘auto-solvers’, hiding the details of numerical methods. The user only needs to specify the required accuracy. However, under some circumstances auto-solvers may use inappropriate methods that produce instability due to rounding and other computational errors and solvers specifically developed for gas turbine simulation may give better results by applying plausibility checks.

In *Section 5.5* an example is given of a Simulink real-time thermodynamic 0-D model. The figure only shows the whole engine model level and hides the top level including the control system, and many sub-levels as well as.

### **C.2.9 Architectures**

The gas turbine model architecture represents the way the model is built up of sub-models, components, finite elements, etc. Several types exist; ranging from non-component based parametric models where no gas turbine components can be identified, to high-fidelity CFD models of flows in particular sub-components like compressor blades. These may include large numbers of finite elements.

The model architecture is important both to the model developer and the model user.

For the developer, for example, a modular approach may be adopted for 0-D and 1-D models with sub-modules representing typical components like compressors and turbines. Generic sub-modules may be

developed using object orientation offering significant benefits in terms of software development and maintenance effort. This approach may also be used when using generic simulation tools like MATLAB-Simulink.

In *Chapter 5* the architectures of some simulation environments are described.

### **C.2.10 Configuration Management**

Management of gas turbine model software and data requires specific attention, especially when large numbers of different model versions are involved. Also when the number of people involved with using or developing a model increases, configuration management becomes increasingly important. Often special tasks need to be defined in order to maintain integrity of the model configurations. These tasks may well be performed using special software tools.

Configuration and system management are general information technology issues and detailed information is therefore considered beyond the scope of this report.

### **C.2.11 Windows versus UNIX**

Currently, there is fierce competition between the UNIX and Windows operating systems. UNIX systems originate from the expensive high end and lack tight standards. Windows (Microsoft) offers solutions at lower costs for PCs and a number of other hardware systems, and currently is increasing its market share at the cost of UNIX. Windows focuses on user friendliness for the consumer market and consequently generates enormous (financial) momentum for further development.

Although Windows 95/98 offers significant potential for simple (0-D) gas turbine simulation, the more powerful Windows NT4.0 (or Windows2000) is the environment to be compared with UNIX. Currently, Windows NT and UNIX have no significant differences in performance for single workstation applications.

UNIX still has advantages when sharing data among many users (for large user-base engineering applications) and security related issues are important. It is also considered slightly superior in terms of stability. It has already been noted that UNIX is the platform most widely used for parallel computing, and with clustered workstations.

Windows has advantages in user friendliness, commonality with the common desktop PC environment and low (system maintenance and purchase) cost when used in simple networked configurations. For the future, the expectation is that Windows will rapidly (within a few years) fix the remaining drawbacks when compared to UNIX. Then, parallel computing with clustered Windows workstations, which already has been demonstrated experimentally, may well become reality.

The unknown factor is the influence that Linux, the UNIX clone, may have. Competition against Microsoft is fierce, and Corel have launched an easy to install and use version of Linux, together with a complete office software suite. During the writing and compilation of this document, Linux achieved as good a GUI interface as Windows, and Redhat and Suse also launched easy graphical installation procedures for Linux. Because of the inherent client/server design of the graphical sub-systems in UNIX like computers they can easily run applications on one computer, and view the graphical results on another. The binding of the graphical subsystems in Windows to the OS kernel provides faster 'in PC' operation but brings severe penalties for 'between platform' operations. Web style client/server applications do not completely overcome these limitations.

## C.3 CHALLENGES

### C.3.1 General

In general it can be stated that with the rapid increase in available computing power and high bandwidth networks at low cost, the challenge is to efficiently use that power for gas turbine simulation. The growth rate of the PC's performance/cost ratio indicates there are significant opportunities. Moore's Law, reported in 1965 predicted a doubling in the number of elements on a chip every 18 months. This was when the largest chip contained 64 elements. From 1970 to 1990 Intel chips doubled their complexity every 2 years. Since that time the doubling period for Intel has become 2.5 years (ref <http://www.physics.udel.edu/wwwusers/watson/scen103/intel.html>), and 28 million elements are contained in a Pentium 3 cpu. To benefit from these opportunities, new technologies for (gas turbine) simulation software development and user-interfaces software maintenance and new standards must be developed.

### C.3.2 Reducing Development Effort

Closely related to maintainability is the aspect of development effort. With increasing complexity, advanced development environments are needed for automating many tasks previously performed with line-by-line coding. This implies distribution of software development tasks, e.g. 4GL tools to develop GUI and general software structure. Ideally, the line-by-line coding should be limited to the implementation of the actual equations being used in the model, but this will not easily be accomplished. With the hand written code being reduced to the actual equations, advanced development environments should also enhance maintainability. However, this may be at the cost of code efficiency. This is illustrated by the fact that some of the current 4GL systems, with automated code generation, carry significant 'Safe practice' coding overheads that are simply irrelevant to many applications.

Object-oriented technology (see **Section C.2.5**) offers reduction in development efforts with the inheritance principle. This has the potential to allow the engineer to quickly do tasks that are currently limited to Information Technology professionals or methodology experts.

### C.3.3 Generic Tools

An approach to reduce gas turbine model development effort is to use generic gas turbine or turbo-machinery specific tools. For the 0-D models several tools already exist for modeling performance of any kind of gas turbine) (see **Chapter 5**). Also specific simulation tools like MATLAB Simulink may be applied for certain simulation tasks (see **Section 5.5**).

For the entire spectrum, more attention can be expected to more intensive use of existing generic tools instead of redeveloping code repeatedly. This may also be in the form of reusing generic objects in OO environments.

### C.3.4 Standardization

Standards for gas turbine modeling code and interfaces are critical for large, comprehensive multi-disciplinary models, created by large numbers of developers. *Portability* is also enhanced when standards for development environments, languages, etc. are observed. Current standards for gas turbine simulation are SAE Aerospace Recommended Practice (ARP) 755 and 681 [**C.8** and **C.9**]. These are based on shared FORTRAN common blocks. These lowest common denominator standards severely limit simulation options for future simulation development. A new ARP recognizing the needs of modern computer systems, development environment and providing the option for an Application Programming Interface (API) type interface is being developed as part of ARP 4868 (Draft) limitations.

Standards are indispensable to interface gas turbine models with other models (e.g. aircraft system models) and to benefit from modern development environments, such as CORBA and DCOM (see **Section C.2.3**). These will reduce development efforts, increase maintainability and improve user interfaces. Without them the R&D gas turbine world will remain committed to FORTRAN, at least for implementation of the fundamental algorithms. As has happened before, the market will probably define the new standard. So for now it seems the technical community will have to wait and see what happens.

MATLAB Simulink and similar environments are becoming common for lower fidelity models, non-component models, real-time models and even simplified 0-D models. For the higher fidelity models, new standards may become available to wrap interfaces and objects around existing FORTRAN codes in order to maintain backward compatibility. New standards for modern OO languages may then be used for developing new codes.

So far, the lack of standards and legacy system compatibility needs have caused most model makers and engine manufacturers to hesitate to move from FORTRAN to another modern development environment. The development of new standards and the gradual disappearance of these legacy systems are causing this change to begin.

### **C.3.5 User Interfaces**

In general, the different tasks involved in developing and using engine performance models become dispersed over a large variety of applications. When using engine-modeling tools in the operational area, interface aspects are very important. For example, an engine diagnostic tool based on an engine performance model must have a good user-interface, dedicated to a maintenance engineer instead of a research engineer. Often the engine model is isolated from the user interface so that it can be tailored to specific tasks such as trending, testing and data visualization.

### **C.3.6 Visualization**

Visualization, both static and animated graphical representations, will become more and more important for the presentation of gas turbine simulation results, especially for high fidelity CFD. With the increasing fidelity of modeled flows, new visualization technologies will be necessary to present results from the large amounts of data. For 0-D models visualization needs are often driven by the needs of the data system and the application. Keeping the simulation tool independent of the visualization package should be a goal for flexibility.

### **C.3.7 Maintainability**

Maintainability is a big issue for the entire IT world. General trends trying to enhance maintainability are new programming languages (object-oriented), CASE tools, documentation tools. Terms involved are: modularity, OOD, portability, documentation, debugging tools.

Currently, much gas turbine code is still in the FORTRAN language. This allows maintenance by those with low-end computer skills but often requires specialized knowledge of the simulation tool and application, which are impractical. However, the need to exploit software technologies and move to new development environments and languages or to complement FORTRAN models with new tools is growing.

Object-oriented technology offers improvements in maintainability because the encapsulation principle offers highly modular code. Used well this can capture the knowledge necessary for maintenance with the tool and the application. Previously this only resided in the minds of those intimately familiar with the development of the application.

### **C.3.8 Grid Generation**

For high fidelity simulations, grid generation software is used to specify hardware geometry and can therefore benefit from direct coupling to a CAD system or geometry database. Developments in user interface technology are required to improve the complex tasks of grid generation. However, it is usually handled outside of the engine simulation and is therefore considered as a data input issue beyond the scope of this report.

### **C.3.9 Distributed Parallel Computing**

A big challenge lies in exploiting the large amount of cheap computing power becoming available with PCs and PC processors. The development of software, for efficient distribution of computing tasks over a large number of networked PCs, will be critical. This is a need across all engineering computing tasks and is also being developed for more powerful stress analysis.

An important issue is how data is managed among distributed parallel computing tasks. Remote computers have data sharing limitations due to limited network transfer speed. This is, in essence, no different from disk accessing speed limitations on a fast singleton PC. With distributed processing, a workflow management system is likely to be needed. Such systems are already commonly used to coordinate complex commercial Customer Relationship Management, Credit Checking, Accounting, Service Provisioning, Trouble Ticketing and Billing systems.

### **C.3.10 Probabilistic Analysis**

It is becoming necessary for performance simulations to both predict an expected or mean performance and to indicate the relative uncertainty of the predictions. For diagnostic models, 95% confidence level bands may be used as indicators of real vs. random observations. In engine selection or design, the best choice will often be the technology combination that balances the highest probability of meeting minimum objectives and providing the best overall mission performance.

The most common method of generating these estimates is to assign uncertainty levels to key requirements, technology assumptions or component performance characteristics and then run simulations to estimate the resulting uncertainty in the performance parameters of interest. For simple 0-D models with a small number of uncertainty values, a Monte-Carlo analysis may be practical on a PC or the same computer system may be used for single point analysis. With more complicated models, such as combined engine-aircraft mission analysis models or with a large number of uncertainty variables, Monte-Carlo evaluations become impractical without greater computing power (see *Chapter 2*).

In some cases, design of experiments (DOE), response surface methods or fast probabilistic integration (FPI) may be used to reduce the computing requirements for probabilistic analysis. For high-fidelity models, probabilistic evaluations are generally limited to small areas of the simulation where it improves the accuracy of the basic prediction, an example being probabilistic kinetics models used for combustor emission predictions.

Thus, detailed probabilistic analysis with multi-dimensional simulation requires high-performance computers. Efficient approaches for these applications (see *Chapter 2*), require new developments. Although a challenge, probabilistic analysis is naturally configured for parallel computing. It is particularly well suited to off-hours use of PC or UNIX workstations since the computation requirements of the basic models are fairly modest.

## **C.4 FUTURE**

In general, developments in computer platform technologies will have a significant impact on the potential of gas turbine simulations. The current rapid pace of developments like Internet technology, PC technology, and distributed parallel computing indicate the importance of carefully monitoring these developments in order to continuously exploit all possible benefits for gas turbine simulation. This however requires a significant effort, and few new trends can be adopted with the certainty that they will become standards.

FORTRAN will probably remain the standard language for the higher fidelity R&D applications. C/C++ will continue to make inroads. Moreover, C++ and other object-oriented languages are used often in conjunction with 4GL development environments, which offer significant benefits in terms of user interface development, code maintainability, debugging and code documentation and readability. For the lower fidelity modeling applications, especially for operational users, these newer environments will continue to be adopted.

Distributed parallel computing will provide large potential to satisfy the increasing hunger for computing power high-fidelity simulations for R&D purposes. With the rapid increase in available computing power, the traditional bottleneck in computer power becomes replaced by implementation issues like development effort, visualization, and software for (distributed) parallel computing.

Modern computer platforms and development environments will be applied for new types of model such as those applied in operational areas like maintenance, diagnostic tools or even customer cycle decks. The past decades have shown it is hard to predict very far into the future of information technology. However, it is clear that we can expect significant progress in the following areas:

- Computing power: As is visualized in **Figure C.2**, there is no reason to assume the current rate of progress in available computer power will not be maintained. This means there is a great challenge in efficient use for even higher-fidelity simulation for gas turbine R&D. Also, increasing power means the pressure to develop efficient code will decrease and the focus can be moved to reducing development effort instead (see **Section C.3.2**).
- Costs: The increasing computing power will become available at lower cost. PCs will be able to do higher fidelity simulations, meaning current simulation tasks will become cheaper.
- Distributed-parallel computing: High-performance computing will be done more and more, using clustered or networked low-cost systems working in parallel. This will also lower the cost of high fidelity simulations.
- Model development environment: Development environments for gas turbine simulation will move from traditional 3GL languages to environments specific to simulation (CFD) or environments including readily available user interface and visualization tools. This will enable research engineers to concentrate on the actual modeling tasks when developing gas turbine models.
- Standards: Standards will evolve from those driven by legacy requirements to those consistent with commercial software tools, databases and development environments.

## **C.5 CITED REFERENCES**

- [C.1] Claus, R.W. et al., “Multidisciplinary Propulsion Simulation Using NPSS”, AIAA-92-4709-CP.
- [C.2] Evans, A.L. et al., “An Integrated Computed and Interdisciplinary Systems Approach to Aeropropulsion Simulation”, ASME Paper # 97-GT-303.

## ANNEX C – COMPUTER PLATFORMS

---

- [C.3] Geist et al., “PVM: Parallel Virtual Machine, A Users’ Guide and Tutorial for Networked Parallel Computing”, MIT Press, ISBN 0-262-57108 (on the WWW: <http://www.netlib.org/pvm3/book/pvm-book.html>).
- [C.4] Reed, J.A. and Afjeh, A.A., “Intelligent Visualization and Control System for Multidisciplinary Numerical Propulsion System Simulation”, AIAA Paper # 96-4034, 6th AIAA/USAF/NASA/ISSMO Multidisciplinary and Optimization Conference, Bellevue, WA, September 1996.
- [C.5] Reed, J.A. and Afjeh, A.A., “Computational Simulation of Gas Turbines: Part I – Foundations of Component-Based Models”, ASME Paper # 99-GT-346.
- [C.6] Reed, J.A. and Afjeh, A.A., “Computational Simulation of Gas Turbines: Part II – Extensible Domain Frameworks”, ASME Paper # 99-GT-347.
- [C.7] Kurzke, J., “How to Get Component Maps for Aircraft Gas Turbine Performance Calculations”, ASME Paper # 96-GT-164.
- [C.8] SAE Aerospace Recommended Practice (ARP) 755.
- [C.9] SAE Aerospace Recommended Practice (ARP) 681.

### C.6 ADDITIONAL BIBLIOGRAPHY

Visser, W.P.J. and Broomhead, M.J., “GSP, A Generic Object-Oriented Gas Turbine Simulation Environment”, ASME Paper # 2000-GT-2, May 2000.

Mathioudakis, K., Stamatis, A., Tsalavoutas, A. and Aretakis, N., “Performance Analysis of Industrial Gas Turbines for Engine Condition Monitoring”, Presented at: First International Conference on Engineering Thermophysics, Beijing, China, August 18-21, 1999 (ICET ‘99).

Mathioudakis, K., Stamatis, A., Tsalavoutas, A. and Aretakis, N., “Instructing the Principles of Gas Turbine Performance Monitoring and Diagnostics by Means of Interactive Computer Models”, Paper # 2000-GT-0584, The 45th ASME International Gas Turbine & Aeroengine Technical Congress, Munich, Germany, 8-11 May 2000.

Tsalavoutas, A., Aretakis, N., Stamatis, A. and Mathioudakis, K., “Combining Advanced Data Analysis Methods for the Constitution of an Integrated Gas Turbine Condition Monitoring as Diagnostic System”, Paper # 2000-GT-0034, The 45th ASME International Gas Turbine & Aeroengine Technical Congress, Munich, Germany, 8-11 May 2000.

Visser, W.P.J., “Gas Turbine Simulation at NLR”, “Making it REAL”, CEAS Symposium on Simulation Technology (Paper MOD05), Delft, The Netherlands, 1995.

Kurzke, J., “Advanced User-friendly Gas Turbine Performance Calculations on a Personal Computer”, ASME Paper # 95-GT-147.

Sellers, J.J. and Daniels, C.J., “DYNGEN – A Program for Calculating Steady-State and Transient Performance of Turbojet and Turbofan Engines”, NASA TN D-7901, 1975.

Visser, W.P.J. and Kluiters, S.C.M., “Modeling the Effects of Operating Conditions and Alternative Fuels on Gas Turbine Performance and Emissions”, NLR Technical Publication NLR-TP-98629 or Research and Technology Organisation, RTO-MP-14, 1999.

Booch, G., “Object-Oriented Analysis and Design with Applications”, Addison-Wesley Object Technology Series, 2nd edition (February 1994) Addison-Wesley Pub Co; ISBN: 0805353402.

Bush, R.H., Power, G.D. and Towne, C.E., “WIND: The Production Flow Solver of the NPARC Alliance”, AIAA Paper # 98-0935.

Barber, T. et al., “Preliminary Findings in Certification of ADPAC”, AIAA Paper # 94-2240, June 1994.

Stewart, M., “Axisymmetric Aerodynamic Numerical Analysis of a Turbofan Engine”, ASME Paper # 95-GT-338.

“WPVM: Parallel Computing for the People”, Proceedings of HPCN’95, High Performance Computing and Networking Conference, in Springer Verlag Lecture Notes in Computer Science, pp. 582-587, Milan, Italy, 1995. (on the WWW: <http://winpar.iit.uni-miskolc.hu/onldoc/wpvm/kk.html>)

“A New Multistage Axial Compressor Designed with APNASA Multistage CFD Code: Part 2”, Application to a New Compressor Design”, Paper # 2001-GT-0350 (from IGTI 2001 paper list).

Hale, A., Chalk, J., Klepper, J. and Kneile, K., “3-D Technique to Calculate Total Temperature and Total Pressure Inlet Distortion”, Sverdrup Technology, Inc., Arnold Engineering Development Center, Arnold AFB, TN.

## **C.7 ACRONYMS**

3GL	3 <sup>rd</sup> Generation Language, conventional computer language for structured programming of line-by-line code according to a specific syntax; requires a compiler for translation to machine code. Examples are FORTRAN, C, ADA, PASCAL, ALGOL, BASIC.
4GL	4 <sup>th</sup> Generation Language, employs code generation using a visual interface. Often generated 3 <sup>rd</sup> GL code. Code generation is usually focused on the user interface, database structures or other specific tasks. Examples are Visual Basic, Visual C++, Jbuilder, and Delphi, which are focused on generating code for the interface. They are also designed to make working with a wide variety of databases very easy. MATLAB Simulink may be regarded as a 4GL environment for simulation (it generates C code for off-line and real-time simulation).
CAD	Computer Aided Design
FLOPS	FLoating point Operations Per Second (computer speed unit)
ICT	Information and Communication Technology
IT	Information Technology
PVM	Parallel Virtual Machine



## Annex D – GAS TURBINE ENGINE SIMULATIONS FOR EDUCATIONAL PURPOSES

Gas turbine theory is being well documented nowadays. The basic principles of gas turbine and aircraft engines are clearly described in many excellent books. Two books from the AIAA Education Series edited by Gordon C. Oates are excellent, introducing the basic gas dynamics for gas turbine components and their performance calculation as well as design methods. Cohen, Rogers and Saravanamuttoo's book is one of the best books for introducing gas turbine theory and many universities use it as a reference book during lectures.

Recently, Walsh and Fletcher from Rolls Royce wrote a book of gas turbine performance, which has an excellent description of gas turbine performance theory from a gas turbine manufacturer's viewpoint. Gas turbine engines consist of intakes, compressors, fans, turbines, ducts, combustor, mixer, afterburner, heat exchangers and nozzles. Gas turbine performance means *Design Point Performance*, *Off-Design Performance* and *Transient Performance*. Design Point Performance is central to the engine concept design process. Off-Design Performance is the steady state performance of gas turbine as its operational condition is changed. Transient Performance deals with the operating regime, where engine performance parameters are changing with time.

Gas turbine engine simulations can be useful tools for teaching engineering students while in an academic situation or for on-the-job training for engineers within industry. Many of the models discussed in **Chapter 5** can be and are used in educational settings. Many textbooks, such as those written by Jack Mattingly, supply software (e.g. ONX, OFFX) for use in propulsion classes. Both educational institutions and industry use GASTURB, the cycle model developed by Kurkze, for in-house training. An extensive listing and description of the available models are provided in **Chapter 5**.

### D.1 INTRODUCTION TO TRANSIENT MODELING

This is a real example based on current practice in an engine company. The purpose of this section is to introduce the student to the following concepts:

- General form of a dynamic model;
- Dynamic and steady-state terms within a dynamic model;
- Initialization of a dynamic model;
- Dynamic simulation;
- Explicit, implicit and trapezoidal integration;
- Linear state-space representation of a dynamic model; and
- Linearization of dynamic model.

#### D.1.1 Audience

This education is aimed at those who have some experience of steady-state performance synthesis (and may have 'black-box' dynamic modeling experience), who want to understand some of the related issues. This particular module is part of a series of tutorials covering the techniques used in interfacing control-systems and engine models.

### D.1.2 Format

The module uses a *very simple* engine model – hardly credible as a model itself but featuring clearly identifiable elements: input, output, state and state-derivative i/o (handled as vectors by the modeling system):

- A dynamic equation for shaft speed;
- A basic fuelling characteristic (fuel flow for a speed); and
- Quasi steady-state ‘characteristics’ (output parameters as a function of speed and overfueling).

The model can be set up easily in any dynamic modeling system, e.g. MATRIXx. The student is encouraged to do this rather than pick up the one already supplied. **Figure D.1** shows the model used in the exercise.

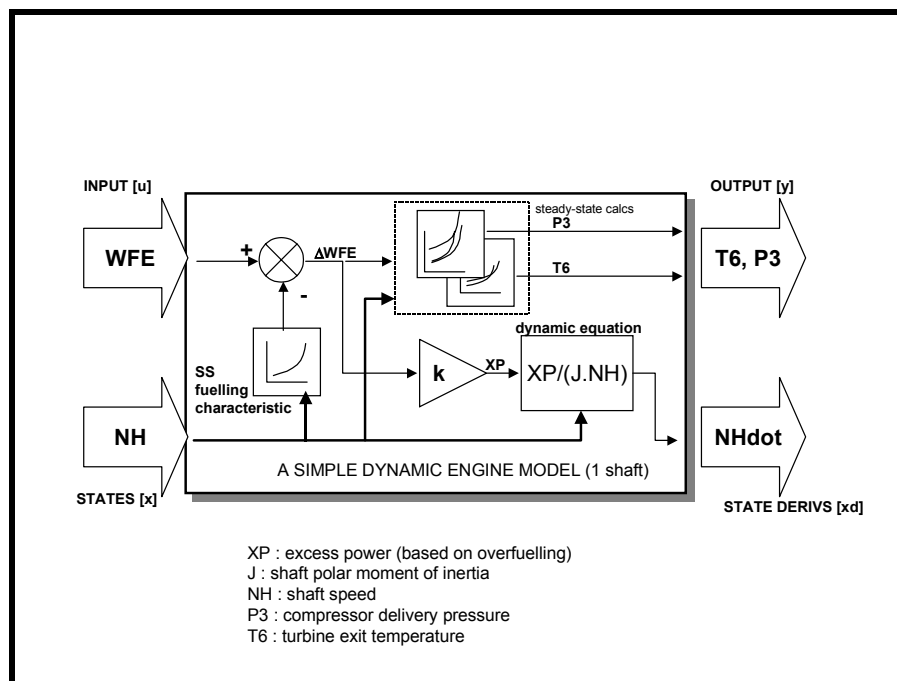


**Figure D.1: The Exercise Model.**

The model exhibits standard dynamic form and the problems of initialization are clear. In order to generate a steady-state solution for a specified value of fuel (WFE), a corresponding value of shaft-speed (NH) must be found. This is the main issue of initialization, which can be approached in different ways. The model can be set up in two ways:

- First Method: With arbitrary values of the state and be allowed to settle over time.
- Second Method: The implicit form of Euler’s method is often used in full dynamic cycle-match engine models.

An external iteration routine can be used to determine the value of NH (at the specified WFE), for which the state derivative (NHdot) = 0 (within tolerance). This is the principle employed by the ‘trimming’ tools in some modeling packages.

Simulation (running the model to a specified trace of input vs. time) requires the numerical integration of state-derivatives. The clearest explanation of this process uses Euler’s explicit method, where the value of shaft speed for the next timestep is predicted from the derivative obtained at the current timestep.

$$x_{(t + \Delta t)} = x_t + \left. \frac{dx}{dt} \right|_t \cdot \Delta t$$

This integration method may be viewed as over-simplistic for many gas-turbine systems. However, it is the principle being explored here rather than the accuracy or stability of a particular method.

The student is encouraged to run the model and observe the effects of varying the simulation timestep. The results can be compared with the model run using a more advanced explicit integration methods such as Runge-Kutta 4th order.

For control-system design, the model is used to generate the linear representation of the engine at a particular ‘set points’. From examination of the model, it can be appreciated that a set of partial derivatives can be obtained by parametric perturbation of inputs and states. Again, the student is encouraged to use the automatic linearization function within the modeling environment to generate the linear engine model, which can then be simulated and compared with the non-linear version.

The implicit form of Euler’s method is often used in *full* dynamic cycle-match engine models.

$$x_t = x_{(t - \Delta t)} + \left. \frac{dx}{dt} \right|_t \cdot \Delta t$$

The principles of implicit integration can be explored here at the simplest level. For this, the student must construct an outer iteration loop as shown in **Figure D.2**. Here the value of NH at t is varied until the two different derivations of  $Nh_{dot}$  are numerically equal.

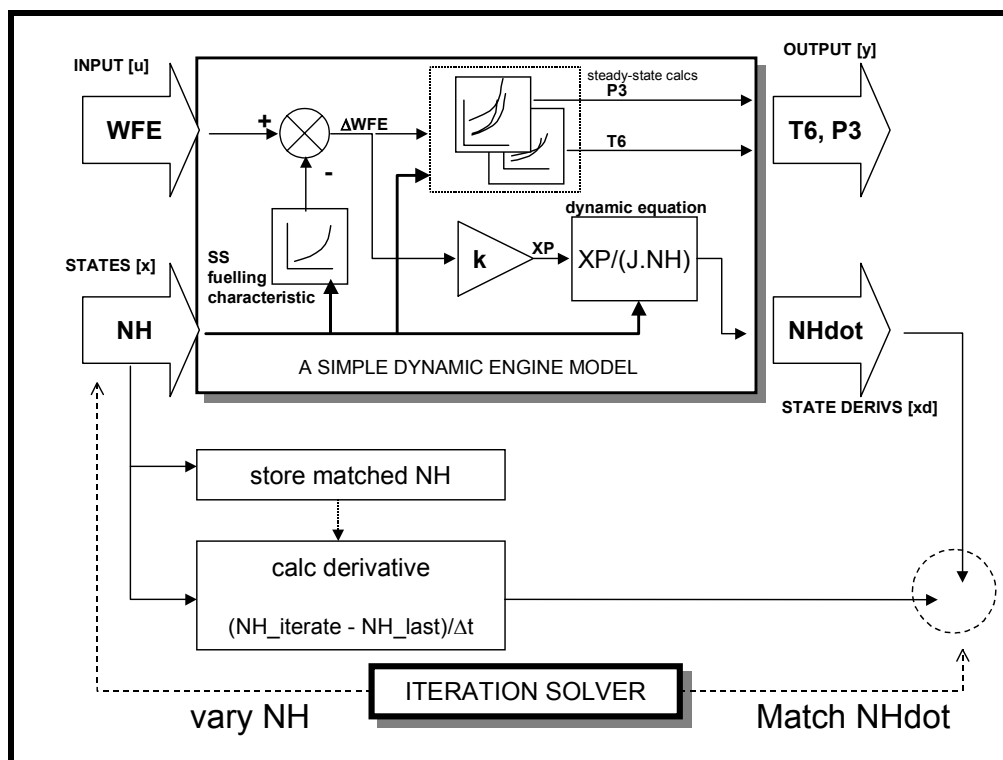


**Figure D.2:** The Exercise Model, with Implicit Integration Added.

As with the explicit implementation, the student is encouraged to run the model with various different timesteps and compare the behavior. It should be seen that the implicit approach is more stable than the explicit approach. The trapezoidal integration concept can be introduced at this point, which can be seen as being essentially a hybrid of both explicit and implicit methods.

### **D.1.3 Value**

Once these principles are understood at the simplest level, it is much easier to see how they are implemented in a more complex modeling system. In such cases, the implementation is often obscure and tied closely to the advanced thermodynamic calculations employed. Also, iteration is often used in the steady-state elements of the model, and its specific role for implicit integration can be difficult to identify.

It should become clear that iteration and integration are purely means to an end and are not a real part of the engine model. Ideally, these processes are kept transparent to the user. However, it is often found that iteration in particular is an impenetrable subject, and a simple treatment such as this can be of value in explaining the operation of the more complex multi-variable solvers needed for ‘proper’ engine models.

The exercise also serves as a hands-on introduction to the modeling tool – taking in formulation of the model, population with data, use of associated tools (linearization and trimming) and data visualization. The student works from an intranet-based set of instructions.

## **D.2 INTRODUCTION TO GAS TURBINE CYCLES**

This is a real example based on current practice in an engine company. The purpose of this section is to introduce the thermodynamic interactions and dependencies within a gas turbine engine.

### **D.2.1 Audience**

This education is aimed at the new-start in the performance discipline, although it can be used as refresher material for those with more experience. It can also be used at a more basic level, for students aged around 17 – 18 who are considering aeronautical engineering courses at university. Students such as these usually pass through industry on specially arranged work-experience periods. Experience has shown that the same basic learning material can be used for each group of learners – the difference is in the depth of discussion which is a fundamental part of the education.

The following issues are covered:

- Engine design point performance;
- Off-design performance;
- Ratings; and
- Transients.

### **D.2.2 Format**

There are three training modules.

#### **D.2.2.1 Module #1: Hand Calculation**

This exercise enables the design point performance of a simple single-spool engine, based on an existing engine, to be determined solely with the use of ‘hand calculations’. The basic principles of the thermodynamic calculations are demonstrated using engine design point data.

The engine design point performance calculations use standard gas property charts where necessary. The compression and combustion calculations are also performed using the standard methods employed in the corporate engine modeling system, by hand, without the use of charts, replicating the methods used on the computer. Solutions are included for both exercises while a computer program is used to obtain a solution for comparison purposes.

#### **D.2.2.2 Module #2: Design Point Calculation**

This module uses a PC-based program to explore the parameters that influence the functional definition of civil and military engines. The input and output of the program are relatively non-complex and so facilitate the learning process rather than requiring much effort to be put into the means of driving the model.

The module addresses the design of a two spool (unmixed and mixed) turbofan. The following is an extract from the electronic module notes.

##### ***Objectives:***

- To investigate the effects of changing the design Stator Outlet Temperature (SOT) and design Overall Pressure Ratio (OPR) on Specific Fuel Consumption (SFC), Specific Thrust and engine mechanical configuration for a two spool unmixed turbofan engine.
- To investigate the effects of changing design Fan pressure ratio on SFC for a range of engine bypass ratios.
- To investigate the effect of changing the design Stator Outlet Temperature (SOT) on By-Pass Ratio (BPR) and Specific Thrust for a range of design Fan Pressure Ratios (FPR) on a two-spool mixed turbofan engine.

These results will indicate the reasons for the choice of military and civil turbofan engine functional designs.

A PC-based computer program will be used to perform the calculations. The software also produces a schematic of the engine at a specified technology level (a program input expressed as an in-service date). This is a valuable visualization of the physical manifestation of cycle thermodynamics. The student is given the information that allows him to generate and plot (electronically) various fundamental parameters for various different cycles. Questions are set and discussed later with an experienced engineer.

#### **D.2.2.3 Module #3: Off-Design Calculation**

Design point studies as covered above enable optimum component and engine design parameters (e.g. bypass ratio and SOT) to be established. However, in order to calculate the steady state and transient performance of a gas turbine engine over a range of operating powers and ambient conditions, it is necessary to consider the interaction of all the components in an engine. The off-design or part-load performance calculations are necessary to ensure that the engine is capable of operating throughout its flight envelope and power range in a safe, stable and efficient manner. The exercise uses a proprietary PC-based cycle synthesis program to examine the off-design performance issues of a 2-spool mixed turbofan.

The following is an extract from the electronic module notes.

##### ***Objectives:***

- To investigate the effects of two engine rating methods, fixed Stator Outlet Temperature (SOT) and fixed HP compressor aerodynamic speed ( $NH/\sqrt{T}$ ) on performance parameters such as net thrust (FN), over a range of ambient temperatures at sea level static.

- Investigate the effects of fixing the SOT and HPC aerodynamic speed on performance parameters over a range of Mach numbers at sea level, ISA.
- Produce HPC and fan-operating lines (i.e. flow function vs. pressure ratio). Assess the effect of HP turbine and HP compressor deterioration on the engine.
- Investigate transient performance effects.

As before, questions are set throughout the exercise and are followed up in the discussion phase. With all of these modules, use of the computer could have been avoided. However, the hands-on experience (the generation of the data) is considered valuable. The figures could be merely supplied and subsequently discussed. However, the student feels no *ownership* of the data in this case.

#### **D.2.2.4 Value**

Objective 1 from module #2 leads the student to generate several figures, depicting the relationships between various cycle parameters. The following figure is such an example and is generated by synthesizing cycles at various values of Stator Outlet Temperature, bypass ratio, fan and HPC pressure ratio.

**Figure D.3** illustrates the following:

- Minimum SFC is obtained with high overall pressure ratio (OPR);
- Maximum specific thrust is obtained at high SOT and moderate OPR; and
- Maximum thrust and minimum SFC are mutually exclusive.

Thus, the discussion leads into the compromises required in cycle design – especially at early stages.

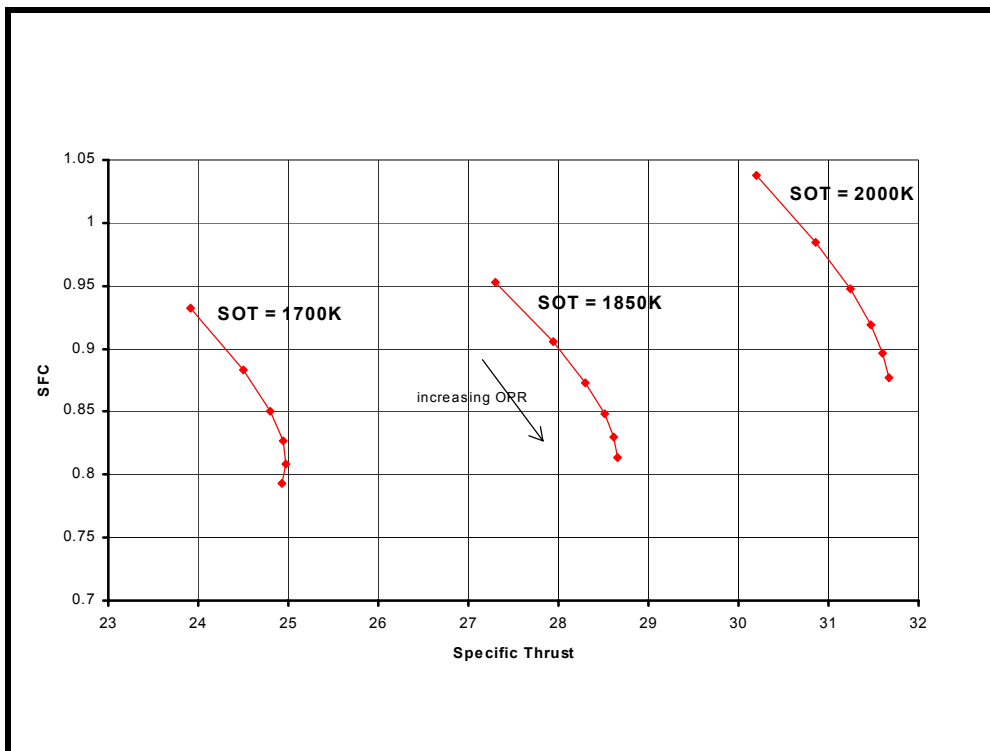


**Figure D.3: Results from Module #2.**

For the work-experience student, the three structured exercises lead into a further case study or mini-project concerning the selection of a replacement powerplant for the Concorde SST. A datum model of the existing powerplant is supplied which can be run using the packages used in the earlier modules.

The case study aims to explore the basic facets of aeronautical engineering *viz.* technical knowledge, modeling, teamwork, compromise, assumption, simplification (where appropriate), research, assessment of options, technical review, presentation of ideas, requirements management, project management, etc.

**Objectives:**

- Reduce operating costs of supersonic transport aircraft by modifications to existing engine only.
- Further reduce operating costs by selecting new powerplant.
- Add an extra constraint: minimize noise at take-off (development and retrofitting costs may be ignored).
- Consider the implications (fuel vs. passengers) for transpacific SST capability.

The students are given various data pertaining to the aircraft and the London to New-York flight. The Breguet range equation and other simplified relationships are also supplied. The problem is fairly unconstrained which can encourage the student to think *out-of-the-box* (e.g. consider variable cycle solutions – albeit at a very simple, conceptual level).

The students, usually operating in a small group of three or four, inevitably require some guidance on approaching the problem. However, with help they emerge from the experience with an appreciation of the preliminary design process, and of the difficulties inherent with providing large-scale supersonic transport. Perhaps most importantly, it brings the foundation modules to life, and provides a focus for the lessons learnt previously.

### **D.3 BIBLIOGRAPHY**

Stricker, J.M., “The Gas Turbine Engine Conceptual Design Process – An Integrated Approach”, Design Principles and Methods for Aircraft Gas Turbine Engines, RTO-MP-8, February 1999.

Schaffler, A. and Lauer, W., “Design of a New Fighter Engine – The Dream in an Engine Man’s Life”, Design Principles and Methods for Aircraft Gas Turbine Engines, RTO-MP-8, February 1999.

Khalid, S.J., “Role of Dynamic Simulation in Fighter Engine Design and Development”, Journal of Propulsion and Power, Vol. 8, No. 1, January-February 1992, pp. 219-226.

Horobin, M., “Cycle-Match Models Used in Functional Engine Design – An Overview”, Design Principles and Methods for Aircraft Gas Turbine Engines, RTO-MP-8, February 1999.

Kurkze, J., “Gas Turbine Cycle Design Methodology: A Comparison of Parameter Variation with Numerical Optimization”, Journal of Engineering for Gas Turbine and Power, Vol. 121, January 1999, pp. 6-11.



## Annex E – GLOSSARY

Term	Description of Term
0-D model	A model which presents the gas conditions at discrete stations along the engine and where no physical length is implied.
1-D model	A model which presents the gas conditions at stations along the engine where the longitudinal location is defined in units of length.
2-D model	A model, which presents the gas, conditions at stations along the engine and provides profile information either in the radial or circumferential sense (usually radial).
3-D model	A model, which presents the gas, conditions at stations along the engine and provides profile information both radially and circumferentially.
A8	Exhaust nozzle throat area.
Accuracy	The measure of a model's ability to replicate the true physical entity.
Adaptive model	A model which adjusts itself to a set of observations.
Additive drag	Pressure force on external stream tube surface in front of inlet.
Adiabatic	A process which occurs without loss or gain of heat.
Adjusted performance	The performance, which is a result of trimming, engine inputs following an analysis process – automated or manual.
Adverse weather	Phenomena, such as clear air turbulence, thunderstorms, and low altitude wind shear that may affect safety of flight on each route to be flown and at each airport to be used.
Aero acoustics	The study of sound transmission through the air, in terms of the effects of environmental noise from machinery, vehicles, aircraft.
Aerodynamic forcing functions	Force on blade(s) due to aerodynamic flow over the blade; in conjunction with blade vibration analysis.
Aero-elastics	Coupled motion of solid surfaces due to elasticity of solid materials and aerodynamic forces.
Aerothermo-dynamics	The analysis of aerodynamic phenomena at high gas speeds incorporating the essential thermodynamic properties of gas into the examination.
Afterburning, Reheat, Post Combustion, Augmentation	Addition of fuel and combustion after the last turbine to provide additional thrust.
AIR	Aerospace Information Report (SAE).
Airframe designers	Project team in charge for the entire process of vehicle definition/development: from requirement and specification to production, qualification and in service use.
Airframe propulsion integration	Optimization of the airframe and propulsion flow-field interactions: Lower drag, inlet characteristics, and nozzle characteristics.
Analog simulation	Simulation of processes on an analog computer. An analog computer represents data using continuous rather than digital signals. Analog computers are not frequently used anymore.
Analysis	The process of understanding the behavior of an engine by inspection of measured data from test.
Annular cascade	Set of blade profiles set up axi-symmetrically.
AnSyn	Analysis by Synthesis: the process of replicating a set of measured data by the automated varying of a model's thermodynamic assumptions.
ANSYN Factors (matching)	The factors on a model's baseline assumptions which are generated in the AnSyn process.
API	Application Programming Interface. An API is a series of functions that application programs (such as gas turbine simulation programs) can use to make the operating system do specific tasks.

## ANNEX E – GLOSSARY

Application software	The application software represents the programs that are executed on a computer to perform tasks for the user such as gas turbine simulation calculations.
APU (Auxiliary Power Unit)	Generally addition gas turbine engines to provide electrical power to other aircraft components.
ARP	Aerospace Recommended Practice (SAE).
AS	Aerospace Standard (SAE).
Average engine	Fictitious engine, described by nominal/mean global performance or operability (thrust/surge margin/fuel flow/bleeds/turbine temperature).
Average passage	A method of averaging blade flow conditions to be able to provide conditions for the next blade row.
Axi-symmetric model	A 2D representation of a flow process.
Bandwidth	The range of input frequency over which a model gives valid results.
Beta lines	Set of external lines draw on a compressor map to aid in the construction of appropriate tables that describe compressor performance in a numerical simulation.
Blade geometry	Turbomachinery blade description in terms of blade shape, stagger, lean, inlet and exit metal angles, camber, thickness, solidity, etc.
Blade loading	The work capacity of a stage; Loading is increased as angle of attach is increased until flow separation occurs.
Blade row stacking	Stacking of steady state blade performance to provide overall compressor performance.
Blade surface roughness	Surface roughness that can effect aerodynamic and thermodynamic performance over a compressor or turbine blade.
Blade untwist	Compressor blades are usually twisted from hub to tip to obtain an optimum angle of attack or loading at all radii; Aerodynamic forces can untwist the blade while in motion.
Bleed flows	Airflows to or from a component used for cooling or external air condition within the aircraft.
Body forces	Any external force that act on a volume element of a body and is proportional to the volume, such as gravity force.
Buzz	Usually associate with the inlet where the shock is moving back-and-forth in the throat causing a “buzzing” sound.
Bypass ratio	The ratio of cold stream mass flow-rate to hot stream mass flow rate in a turbofan engine. Ratio of the amount of air that bypasses the core of the engine to the amount of air that passes through the core.
CAD	Computer Aided Design. CAD programs help engineers in the design processes. For example, CAD programs can help design gas turbine components and check compatibility of parts in an assembly. CAD tools often have advanced visualization capabilities to show the geometry of parts and assemblies.
Calibration	The process of adjusting a model to replicate a specific set of data.
Camber	The difference in the inlet and outlet blade angles.
Casing treatment	Refers to compressor or fan tip casing refinements to increase stall margin; may be in the form of circumferential grooves or cross-blade slots.
Cause-effect relationship	An empirical or computer-generated exchange rate of an input to an output of a physical process.
CFD	Computational fluid dynamics – a numerical simulation technique usually solving 3D viscous equations.
CFD turbomachinery	Computational Fluid Dynamics simulation using Navier-Stokes equations for turbomachinery applications.
Choked nozzle operation	An operating point corresponding to the maximum mass flow-rate through the nozzle.
Class	A class defines the structure of an <i>object</i> in <i>object-oriented</i> software code. A synonym for class would be ‘object type’.
Clean inlet performance	No inlet distortion present.

Closed loop control	Control system with a feedback mechanism from the output.
Cold flow rigs	Testing facility providing ambient inlet temperature generating conditions in the test section.
Combustion aerodynamic load	The effects of mass flow rate, combustion volume, and pressure on the stability of the combustion process.
Combustion efficiency	A measure of the combustion process; measures the completeness of the combustion process.
Combustor blowout	Flame-out of the primary combustor.
Combustor primary zone	Part of combustor where combustion is stoichiometric (i.e. all fuel is burned with 100% $O_2$ ).
Combustor relight	Re-ignition of the primary combustor.
Compact engine model	A simplified engine model.
Complexity	A measure of the rigor of thermodynamic treatment within a model.
Component characteristics (CHICS)	Representative performance of an engine component such as a compressor map; Overall pressure ratio and efficiency as a function of corrected airflow rate and corrected speed.
Component level cycle code (CLM)	See Cycle Deck.
Component matching	The process of integrating engine components such that each component operates at the appropriate operating point, working line or trajectory.
Compressor axial gap	The axial spacing between rotor and stator blades of a compressor.
Compressor recovery	Compressor operation that recovers from stall or surge.
Computer platform	The computer platform is the combination of the hardware and software needed for gas turbine performance calculations. The <i>hardware</i> is the physical part of the computer; the <i>operating system</i> represents the software required to use the hardware with application software such as gas turbine simulation programs.
Configuration management	Management of a computer program either by software or by a manual process that sets version control and checks out code to users and checks it back in without ‘stepping’ on the work of others.
Consistency	The measure of a model’s ability to replicate the reference database.
Control logic	Process by which the engine is controlled; usually imbedded within an on-board computer.
Control loops	Feedback loops in a control system. Deviation from a desired output is detected, and an input related to the difference is applied to reduce the deviation.
Control volume	An imaginary boundary encompassing a component which allows it to be considered as a gross entity.
Convergence	The ‘homing’ onto a solution by iteration.
Convergent-divergent nozzle	Type of exhaust nozzle to accelerate the gas flow to supersonic speeds.
CORBA	Common Object Request Broker Architecture. CORBA provides an <i>object-oriented</i> approach to writing <i>distributed applications</i> . Distributed applications and CORBA would enable integral gas turbine simulations using simultaneous execution of different programs simulating separate engine modules, on separate computers at separate locations.
Core flow	Fractional flow that runs gas generator of the turbofan engine; hot stream flow.
Corrected parameters (referred parameters)	Turbomachinery operating point characterizing parameters corrected by inlet thermodynamic conditions to eliminate the dependence (sometimes referred to as non dimensional parameters (mass-flow, rotational speed, pressure ratio ) although not truly non-dimensional).
Cowl lip	Front part of an inlet; usually where an oblique shock develops.
Cradle drag	Loads, induced by parasitic airflows, on the engine installation in the test cell.
Customer bleed	External bleed generally used for aircraft air conditioning.
Cycle decks	An engine model/program (usually 0D type) using the cycle match technique.
Cycle match model	A model using iteration to achieve flow compatibility between engine components.

## ANNEX E – GLOSSARY

Data base	A collection of organized data, usually residing in a number of files in a computer system. A database can be as simple as a shopping list or as complex as a collection of thousands of sounds, graphics, and related text files.
Data validation	The process by which input (and output) data is checked for correctness.
Debugging tools	Computer programs that help find errors in computer program code. Often, debugging tools are integrated in the <i>development environment</i> . Modern debugging tools enable computer programmers to monitor the execution of the program, line-by-line in the program code while being able to query all relevant program parameter values.
Deck	Originally describing the set of punched cards comprising a computer program – this term is still used to refer to digital computer models.
Degree of reaction	A measure of the extent to which the rotor contributes to the overall static pressure change in a turbomachinery stage.
Design	1) An operating point corresponding to the design values of mass flow-rate, pressure ratio and rotational speed in a turbo-machine.
Design and verification	Also known as the Program Definition and Risk Reduction phase.
Deterioration	Loss in engine performance due to mechanical degradation of components.
Deterministic	Describes a process which given the same inputs will always produce the same outputs.
Development and validation	Also known as the Engineering and Manufacturing phase.
Development environment	Software (and sometimes hardware) used to develop software. Usually at least including a programming language such as FORTRAN. Often additional software tools are used for design, documentation, version control, etc.
Development process	Begins as soon as hardware to new design is available; main phase complete at production/service release; is also known as Engineering and Manufacturing Development.
Development testers	Team in charge of the evolution of the system definition, gradually implementing improvements to an initial design in order to enhance its physical/ industrial capabilities.
Diagnosis mode	A mode of operation of a model where measured data is used as input.
Diagnosis techniques	Techniques applied to the determination of the condition of an engine.
Digital simulation	Simulation of processes on a digital computer. A digital computer represents data using digital signals in electronics corresponding to binary formats (arrays of “0”s and “1”s). Almost all computers in use to date are digital computers.
Direct numerical simulation	No approximations are made such as the Reynolds averaging technique of mean flow and fluctuating flow.
Discretization	The breaking down of a continuous process into several portions.
Displacement pumps	Pumps that physically displace a volume of fluid, rather than inducing flow via a pressure difference.
Dissociation	The process by which a chemical combination breaks up into simpler constituents by collision with a second body.
Distortion (circumferential and radial)	Airflow distortion to the compressor or fan face commonly caused by high angle of attack or roll rates; usually manifests itself as total pressure distortion but could be temperature or inlet swirl.
Distributed computing	A new trend is to apply <i>parallel computing</i> to multiple computers that are interconnected over a network. This <i>distributed parallel computing</i> requires special software controlling the distribution of different computing tasks in a simulation.
DLL (Dynamic Link Library)	A DLL file contains a library of functions and other information that can be accessed by a Windows program. DLL files allow programs to share common resources, such as memory and hard drive space, and use them more efficiently.
Dry/wet operation (Afterburner)	Dry operation = non augmented operation; Wet operation = with augmentation.
Durability	Engineering methodologies related to the life characteristics: by considering mission profile segment power usage, operational severity exposure of the engine components and maintenance and support factors.

Dynamic model	A model having high bandwidth (e.g. 30Hz).
Effective nozzle area ratio, A9/A8	Exhaust nozzle exit to throat area reduced by boundary layer effects.
EGT (Exhaust Gas Temperature)	The flow weighted mean total temperature of the working fluid at a plane immediately downstream of the last turbine stage.
Electro hydraulic servo units	Hydraulically powered servo units that are electrically controlled.
Embedded engine model	An engine model implemented as part of a control system.
EMD (Engine Manufacturing Development)	Life cycle phase that translates the most promising design approach into a stable, interoperable, producible, supportable, and cost-effective design; validate the manufacturing or production process; and demonstrate system capabilities through testing.
Emissions index	The ratio of mass of pollutants to unit mass of fuel.
Empirical model	A representation of an engine set up in terms of a priori observations.
End wall effects	The boundary layer formation effects at the hub and casing of a turbo-machine causing pressure losses and blockage.
Engine aging	cf. deterioration.
Engine altitude facility	Wind tunnel whose working section can simulate altitude conditions of pressure, temperature and humidity.
Engine anomalies	Difference between current engine behavior and the predicted one.
Engine component model	A simulation of a gas turbine engine using major components (compressor, burner, turbine, etc.) as the smallest breakdown.
Engine condition monitoring	The process of inspecting measured data in order to determine the health of an engine.
Engine configurations	A list of engine specific components, type and model or designation.
Engine controls	Hardware and/or software (depending upon the age of the engine) that controls the fuel flow and the size of holes that the gas flow must flow through.
Engine cycle	The set of thermodynamic processes (often depicted as a trajectory on a Enthalpy-Entropy chart) which constitute an engine.
Engine design process	The succession of the various phases, from requirement/specification to project definition.
Engine deterioration	Worsening of components in terms of performance and mechanical potential.
Engine fleet management	Activity of analyzing operation data for aircraft engines to ensure engine safety by adapted repair and maintenance planning.
Engine health	Quantified performance engine status described by component characteristics difference relative to a status.
Engine model	A set of thermodynamic assumptions representing an engine.
Engine operators	People or company involved in engine operation/usage.
Engine simulation	A computer implementation of a model run to give the time response of an engine.
Engine to engine scatter	Diversity of engine behavior due to: component characteristics variance, generated by the bill of material tolerance transducer/controller accuracy causing dispersion of component throttling and command.
Environmental effects	Extraneous effects on an engine imposed by environmental conditions.
EPR (Engine Pressure Ratio)	The pressure ratio of an engine cycle available to the turbine and nozzle.
Euler equations	The equation of motion for frictionless flow.
Evaluation testers	Team in charge of the assessment of a technical proposal (design or hardware) usually by an engine-to-engine comparative basis or by comparison with an expected behavior (from simulation or requirement).
Event driven	A computer program that executes tasks after receiving messages. The transmission of a message is called an 'event'. Event driven programs usually are <i>object-oriented</i> with the messages transmitted among objects and the input and output devices of the program.
Exhaust nozzle	The gas path exhaust nozzle used to accelerate the gas flow to produce thrust.
External loads	External engine loads to run auxiliary equipment.

## ANNEX E – GLOSSARY

Factors, deltas (adders, scalars)	Adjustment scalars or multipliers to aid in the calibration of turbine engine component maps.
FADEC, DECU	Full Authority Digital Electronic Control; Digital Electronic Control Unit.
FAR (Fuel Air Ratio)	The ratio of the mass of air to the mass of fuel for a combustion chamber.
Fault detection	The process by which malfunctions in a system are identified.
FHV (Fuel Heating Value), LHV	Amount of energy available in the fuel; Lower Heating Value; Amount of energy available in the fuel with all water from the combustion process in a vapor state.
Finite element model	The solution of (typically) heat transfer, stress or aerodynamic systems by subdivision (meshing) of the problem to local, small linear subsets, compatibility of which must be assured.
Finite rate chemistry	Modeling the combustion process considering forward and backward reaction rates.
Flame-holder	Combustor or augmentor hardware which aids in the stabilization of the combustion process by developing eddies and swirl to allow combustion to take place.
Flat rated engine	An engine designed to deliver constant power or thrust over a range of ambient temperature.
Flight simulators	Devices that are able to simulate the operation of an aircraft to a pilot. These may range from just computers with screens and keyboards (e.g. Microsoft Flight Simulator for the PC) to 'moving base' systems including a fully equipped cockpit.
Flow coefficient CD	Nozzle discharge coefficient; Ratio of actual flow rate to ideal flow rate.
Flowpath	The path that the working fluid follows during the flow through a machine.
Fluid dynamic blockage	The available flow area excluding the flow blockage due to boundary layer growth or separation in a duct, nozzle, and intake or within a compressor. (Net flow area / Total area)
Flutter	A self-induced (flow induced) oscillating motion of improperly designed fan or rotor blades.
FOD	Foreign Object Damage, damage caused by ingestion of external material.
FORTTRAN	FORmula TRANslater. One of the earliest 'third generation <i>programming languages</i> ' with origins going back to the 1950's. FORTRAN is the traditional computer language for the scientific community and the majority of gas turbine simulation code to date is implemented in FORTRAN.
Free vortex	Flow with concentric circles in which there is no change of total energy per unit weight with radius.
Frozen	When the time for a change in state of a chemical process is shorter than the relaxation time, than the gas is said to be frozen at a fixed composition.
Functionality	Logical process action expected from the system.
Fundamental pressure losses	The stagnation pressure drop in a combustion chamber associated with the rise in the temperature due to combustion.
Gas generator	Compressor-burner-turbine; the internal gas path power cycle.
Gas path analysis	See Analysis.
Gas properties effects	Effects of gas properties on a thermodynamic process.
Gas sampling	Specific process of chemical analysis by gas extraction for combustion efficiency, emissions and temperature assessments.
Global iteration	An iteration loop around a complete engine model.
Global system level analysis	Overall characterization of the system described by sole inputs/outputs relationships.
Grid generation	Division of 2 or 3 dimensional flow domain into 'finite volumes'. For <i>CFD</i> , grid generation is required to divide the space in which the flow is analyzed in small grid elements: spatial discretization.
Groaning, screech, organ noise, chugging, and growl	Colorful ways of describing unsteady gas path behavior; Usually associated with Combustion.
Grooves	Type of compressor tip casing treatment to increase stall margin.

Gross thrust	Total thrust of a jet engine without deduction of the momentum drag of the incoming air (momentum thrust plus pressure thrust).
GUI (Graphical User Interface)	Graphical User Interface (pronounce “gooey”).
Gutter	A flame holder in an afterburner system.
Hardware in the loop	Set of components (ECU, actuators and sensors) which change the actual engine/plane state into the desired state by the pilot connected to the simulation loop.
HCF high cycle fatigue	Blade failure due to rotor stator interaction or rotor interaction with inlet distortion.
Heat balance method	A method of calculating engine core flow by considering the balance of energy into and out of the cycle.
Heat released	The amount of heat given in a reaction or combustion process.
Heat soakage (heat transfer)	Time for thermal equilibrium to take place usually between the gas path and the engine metal components.
Heat transfer effects	Effects of heat transfer on component performance.
Honeycomb	Type of compressor tip casing treatment to increase stall margin; Type of seal.
Hot gas ingestion	Inlet ingestion of exhaust gases from a missile, rocket or from another engine or the engine itself (VSTOL, reverse).
Ideal thrust	Thrust without any irreversibility; i.e. friction or shocks in the system not accounted for.
Idle	Engine power at which the system is at minimum power; ground idle or flight idle.
IGV & VSV	Inlet Guide Vane and Variable Stator Vane.
Incipient stall cells	Stall cells that initiate rotating stall; may be multiple cells prior to full stall.
Incompressible flow	The flow of a fluid where the changes in density with other thermodynamic parameters is negligible (low Mach number flows).
In-flight thrust	Thrust of an engine while in flight; fully installed.
Influence coefficients	Partial derivatives.
Initialization	The process of setting up a model such that the initial conditions are as required (often at steady-state).
Inlet capture area	Inlet airflow area.
Inlet engine compatibility	The ability of the inlet and the engine to interface for prolonged periods without interference under prescribed environmental conditions.
Inlet engine compatibility	The ability of the inlet and the engine to interface for prolonged periods without interference under prescribed environmental conditions.
Inlet recovery factor	Intake losses expressed in terms of the ratio of total pressure at the compressor inlet to that defined in front of the intake.
Inlet spillage drag	Drag due to more air.
Inlet unstart	The inlet normal shock is not at the minimum area and may be expelled out the front of the inlet.
Input	A parameter which perturbs a system, e.g. fuel flow, intake conditions.
In-service support	Technical and commercial activities involving the engine operators, with a technology to operate satisfactorily the engine population provided by engine manufacturers.
Installed performance	Engine performance with all external bleeds and power extraction activated.
Intakes	The entry duct into an engine, which may be used to induce compression.
Integration (implicit and explicit)	The process of estimating the time-dependent behavior of state variables.
Integration time step	The time increment in a numerical integration technique.
Internal air system (secondary air system)	Airflow pathways between the rotors and disks used for transferring cooling air between compressor and turbines.
Iron bird	Ground rig to test major aircraft system.
Isentropic	A process which takes place without change of entropy.
IT&E	Integrated Test and Evaluation; Alludes to the intertwining of experimental data and numerical simulation results to provide a full analysis process.

## ANNEX E – GLOSSARY

Iteration	A mathematical process where a set of inputs are varied to achieve a required set of constraints.
Jacobian matrix	A matrix of partial derivatives of constraints w.r.t. variables.
Kalman filtering	An analysis method using linear theory to produce a 'best estimate' of system performance.
Kernel	The innermost part of an operating system.
Labyrinth seals	Seals between the primary and secondary flow systems.
Labyrinth seals windage	Losses due to leakage and turbulence, retarding torque.
Large eddy simulation	Solution of the time-dependent Navier-Stokes equations for the evolution of the large eddies with model(s) for the smallest, sub-grid scale, eddies.
Legacy system or code	The term 'legacy system' or 'legacy code' usually refers to computer systems respectively programs of an outdated technology level designed in the past, but still in use because of complications and costs of migrating to state-of-the-art systems.
Level of detail	See Fidelity.
Life assessment	Estimation of the allowable total period of operation of hardware item.
Life cycle	The set of phases which define the 'cradle to grave' lifespan of an engine.
Lifing model	Computer models for the estimation of the allowable total period of operation of hardware item.
Linear cascade	Set of blade profiles set up in a planar fashion for profile loss assessment purposes in rig test.
Linearization	The process by which the partial derivatives which characterize the dynamic behavior of a system are derived.
Liner cooling	Airflow used to cool combustor or augmentor liner metal temperature.
Local equilibrium	The condition of having thermal, mechanical and chemical equilibrium at a specified point in a thermodynamic system.
LPP (Lean Premix Pre-vaporized)	Type of combustion process; fuel is premixed and already vaporized; very lean.
LRU (Line Replacement Unit)	Component that can be replaced at a first line maintenance unit.
Lubrication and fuel systems	Pipes, pumps, and controls for the oil lubrication process and the fuel delivery process.
LVDT	Linear Variable Differential Transformer – a type of displacement transducer.
Man in the loop	Human-piloted action for generating demands to the hardware by visual monitoring of states engine/plane indicators connected to the simulation loop.
Manufacturers	Company in charge of a product (from design through development to manufacturing and certification) with specified technical use.
Manufacturing tolerances	Range of acceptable characteristics described in the bill of materials.
Maps (CHICS)	Component performance characteristics, generally steady state.
MAR (Moving Actuator Ring)	Nozzle hardware to allow the changing of a convergent nozzle to a CD type nozzle.
Mass flow function	Mass flow times square root of the temperature all divided by the pressure times the flow area; can be viewed as an inlet Mach number.
Mass, momentum, energy conservation	IN GENERAL: Conservation laws of nature namely continuity of flow, Newton's second law and first law of thermodynamics respectively.
Master/Slave petals	Nozzle hardware to allow the changing of a convergent nozzle to a CD type nozzle.
Mathematical engine model	A set of equations defining the behavior of a physical system.
Max AB	Gas turbine engine running at near design conditions with maximum afterburner.
Mean line , row-row model	Blade row stacking model using mean-line blade information (not a function of radius).
Measurement uncertainty	The scatter inherent in measured parameters.
Mil power	Gas turbine engine running at near design conditions without afterburner.
Mil specification	Official standards of requirements in the military aircraft business.
Min AB	Gas turbine engine running at near design conditions with minimum afterburner.

Minimum engine	Individuals of the engine population, minimum in global performance or operability (thrust/surge margin/fuel flow/bleeds/turbine temperature) – to be described statistically.
Mixer	A device used to mix the flow; can be a device to mix flow within a mixed flow turbofan augmentor or a device to mix the exhaust jet flow.
Mixer efficiency	Efficiency of a mixing device.
Model assumptions	The assumed behavior of the various subsets of an engine model, e.g. compressor characteristic and associated scaling factors.
Model creators	The people who build or develop the simulation code, reproducing synthetically a functioning system.
Model fidelity	The level of detail inherent in a model.
Model user	The operator of the engine computer simulation code, reproducing a functioning system synthetically.
Monte Carlo	A statistical method whereby a information is obtained based on the exposure of the model to a (large) set of random variances on inputs and assumptions.
Moore's law	More than 25 years ago, when Intel was developing the first microprocessor, company cofounder Gordon Moore predicted that the number of transistors on a microprocessor would double approximately every 18 months. To date, Moore's law has proven remarkably accurate.
Multi-disciplinary	Work by combining several (academic) disciplines or methods.
Multi-stream model	A model where the flow conditions are assumed to be some combination of two or more modeled flow-paths, each of which describe some specific aspect of the total stream (e.g. stalled and unstalled flows, multi-phase flow).
Navier-Stokes equations	The non-linear differential equation of motion applicable to incompressible, viscous fluid and fundamental to all aspects of fluid dynamics.
Net thrust	Gross thrust minus the momentum drag in a propulsion engine.
NGV	Nozzle Guide Vane – Refers to the inlet guide vanes of the turbine.
NH, N2, XNH	Rotational speed of a high pressure rotor of a multi-spool engine.
NL, N1, XNL	Rotational speed of a low pressure rotor of a multi-spool engine.
Non-recoverable stall	Engine can not recover from a compressor stall condition without shutting the engine off; Usually caused by development of rotating stall in the HPC.
NO <sub>x</sub>	Oxides of Nitrogen, pollutants created in the combustion chamber.
Nozzle area ratio	Exit to throat area ratio for a CD nozzle.
NPR	Nozzle pressure ratio; Ratio of mean total pressure at a plane at the entry of a nozzle to the back pressure.
NPSS	The Numerical Propulsion System Simulation NPSS [Ref. 17 in Ch. 4] is a concerted effort by NASA Glenn Research Center, the aerospace industry and academia to develop an advanced engineering environment – or integrated collection of software programs – for the analysis and design of aircraft engines and, eventually, space transportation components.
Numerical optimization	A mathematical process aimed at minimizing a certain function.
Numerical stability	The property of a numerical process to behave in an orderly manner.
Object	Primary entity of <i>object-oriented</i> software. An object is the <i>instantiation</i> of a specific <i>object class</i> . Instantiation is the actual creation (claim of a chunk of computer memory) of an object variable of a specific class.
Object-oriented	Object Orientated Design (OOD) provides significant benefits in terms of software development efficiency and maintainability.
Off-design	Any operating point of a turbo-machine, which is not the design operating-point.
On-board engine performance	Installed-engine characteristics comprising aircraft/engine interaction effects such as inlet efficiency, bleeds, power off-takes, nozzle efficiency, scrubbing drags.
One stream model	A model where the properties of any flow path is modeled using a single calculation process.
Open loop control	Control system with no feedback mechanism.

## ANNEX E – GLOSSARY

Operability	Engineering methodologies dealing with maneuverability envelope and engine handling quality achievement: by implementation of satisfactory compressor surge margins, combustor/reheat blow out limit margins...and adapted control system characteristics.
Operating point	The thermodynamic and flow and engine operating conditions (pressure, temperature, flow-rate and rotational speed) represented by a point on the compressor or turbine characteristics.
Operating system	The operating system represents the software required to use the computer hardware with application software.
Operation	Planned activity or mission involving many actions aimed at a specific result on the utilized system or hardware.
Output	Calculated parameter.
Over under expansion	The expansion of a nozzle to a pressure above or below nozzle design pressure, where there is no shock formation within the nozzle (but oblique shock or expansion wave formation happen outside the nozzle) respectively.
Parallel compressor	An example of a multi-stream model.
Parallel computing	Technology to perform several tasks of the same calculation (simulation) job simultaneously, on different processors in one or more computers.
PC-based	(Program or software) able to be executed on a desktop or laptop PC (Personal Computer).
PDF (Probability Density Function)	A mathematical function describing the shape of a statistical distribution.
Perfect gas	A gas for which the product of the pressure and volume is proportional to the absolute temperature.
Performance	Overall engine characteristics contributing to aircraft propulsion requirements.
Performance seeking control	A control technique making use of optimization techniques to locate a peak in a particular function.
Physical model	A model that represents a physical process; A physical model can then be represented in a numerical simulation.
Piecewise linear	A set of linear models linked by scheduling a base parameter.
PLA	Power Lever Angle: The pilot's throttle.
Plausibility check	A check for a credible answer on the basis of basic engineering judgement.
Polytropic, isentropic efficiency	Isentropic efficiency is the ratio of ideal to actual work transfers of an isentropic process in a compressor or vice versa in a turbine. Polytropic efficiency is the isentropic efficiency of an infinitesimal stage in the process such that it is constant throughout the whole process (compression or expansion).
Portability	Ability of the software to run on different <i>computer platforms</i> without (large) efforts to adapt the program code or recompile the program.
Post certification	Check – during engine service – compliance with MIL specifications requirements, expected from the engine qualification process.
Post stall	Compressor operation beyond instability on-set; usually involves reverse flow.
Power balance	Power compatibility between the compressor, the turbine and/or shaft power output of a gas turbine.
Power off-take	External power requirement to run some axially equipment.
Power turbine	Turbine used solely for extraction of power for an external shaft; Usually, the last turbine in a series of turbines.
Preliminary design	Also known as the Concept Exploration phase; consists of competitive, short-term concept studies: define and evaluate the feasibility of alternative concepts and assessing their relative merits.
Pressure loss	Pressure changes due to (changes in elevation, flow velocity, and ) viscous effects.
Pre-swirl system	A system to adjust the direction of the flow to provide a circumferential component of the flow.
Profile losses	Pressure losses associated with friction across a turbomachinery blade.

Programming languages	A programming language is the set of commands that can be used to tell a computer what to do in a computer program. Usually strict rules apply to using the programming commands and arranging them in a certain sequence.
Pump and tap architecture	A pump design that maintains fluid at a high pressure and controls the outflow by modulating a downstream valve.
Quasi 3-D	Three-dimensional representation usually with some form of empiricism – not a true 3D simulation.
Ram drag	Drag produced by the momentum of air entering the inlet of an engine in flight.
Reactive chemistry	Combustion process that allows for differing species of products to exist during the process.
Real gas	A gas whose properties deviate from those of the hypothetical ideal gas due to interactions between the gas molecules.
Real-time engine models	A model where the outputs are produced commensurate with the rate at which the inputs are changing.
Relaxation	A method of iteration which converges rapidly.
Research	Intellectual process of collecting and analyzing facts and information in order to achieve reliable/physical understanding of the processes involved in the technical system behavior.
Reverse flow combustor	Combustor design process involving combustion gases flowing in a channel back toward the front of the engine; usually to accommodate radial compressors.
Reverse flow compressor	Airflow going the wrong way; caused by compressor instability such as surge or rotating stall.
Reynolds number	Non dimensional number which represents the ratio of the inertial forces to viscous forces.
Rig-engine effects	Engine components behave in a different way when tested on rig test and when installed on the engine.
Risk reduction	Diminution in the combined effect of the likelihood of unfavorable occurrence and the potential impact of that occurrence.
RNI (Reynolds Numbers Index)	It relates Reynolds numbers of installed compressor to altitude and flight Mach number, at a defined engine corrected flow.
Robustness	Quality of a computer program to handle errors without causing abnormal termination or ‘hanging’ (program stops to respond to user commands) of the program.
Rossby number	Ratio of inertial forces to the Coriolis force for a rotating fluid.
Rotating distortion	Inlet pressure distortion that is rotational; can be simulated by a rotating screen.
Rotating holes	Holes in a rotating component.
Rotating stall	Blade stall that seems to rotate in the direction of rotor revolution; usually near 50% rotor speed.
Rotor moments of inertia	Moment of inertia used to determine shaft spool-up timing.
RQL (Rich Quench Lean)	A combustor type, using an over-stoichiometric stage followed by a rapid quench, with dilution air followed by a lean burn region.
Rumble	Description of a combustion instability which sounds like a “rumble” due to its low frequency(50 Hz) content pressure perturbation.
Safe operational limits	Limits on certain engine performance for safe and correct operation.
Sauter mean diameter	The ratio of the sum of all volumes of droplets in a spray to the total surface area of all droplets.
Schedule	Refers to a variation of a parameter or hardware (such as fuel flow or variable vane position) as a function of some measure of flight condition (such as burner pressure for fuel flow and rotor speed for variable vane position).
Screech	Description of a combustion instability which sounds like a “screech” due to its high frequency (400 Hz) content pressure perturbation.
Scrubbing	Cleaning of exhaust gases.
Secondary air system	Airflow system used to bring relatively cool air to hotter parts of the engine such as turbine blades; Airflow system uses cavities within the rotor shafts and bladed disks to transfer cool air to hotter parts.

## ANNEX E – GLOSSARY

Sensors	Instrumentation to provide information to control logic for proper engine operation.
Separation	A situation occurring when the streamlines cannot follow the contour of the body because of the adverse pressure gradients.
Shell	A computer program that provides an external interface for another program. This may be an operating system shell (such as the various UNIX shells) that provide enhanced user interfaces, or shells that provide a <i>GUI</i> around a particular application program.
Shock boundary layer interactions	Transonic or supersonic flow interacting with the boundary layer resulting in shocks and boundary layer separations and causing losses in intakes nozzles or turbomachinery.
Shock wave	A pressure wave passing through a fluid medium in which the pressure, density and particle velocity undergo drastic changes.
Signal noise	Parasitic measurement perturbation induced by measurement system (acquisition electronics).
Simulation mode	A mode of operation of a model where measured data is used as input. Frequently relates to models that can describe transient behavior.
SLS (Sea Level Static)	Ambient conditions represented by air at a temperature of 15 °C (59 °F), a barometric pressure of 1.01325 bar (14.696 psia) corresponding to average sea level atmospheric conditions at middling latitudes.
SOT (Stator Outlet Temperature)	The flow weighted mean total temperature of the working fluid at a plane immediately upstream of the first stage turbine rotor blades. (See TET)
Spatial resolution	A measure of the ability of a model to resolve differences in properties in terms of physical proximity.
Specific fuel consumption	Fuel consumption per unit thrust or per unit specific work output.
Specific thrust	Net thrust per unit mass flow-rate of air inflow.
Splitters	Generally a flow splitter between the fan and the high pressure compressor.
Spool down	The deceleration of a shaft rotor usually due to combustor extinction.
Stage by stage	Modeling each stage of turbomachinery as a separate thermodynamic process.
Stagger	Angle between the blade camber line and the axial direction.
Stall	Compressor instability; Sometimes synonymous with Surge. May be rotating stall or non-recoverable stall.
Stall line	Locus of stability points for all speeds beyond which the compressor will stall or surge.
Stall margin	Measured at a constant airflow rate; the amount of pressure rise available between the stall line and the operating line: stall margin can be affected by inlet distortion, engine-to-engine tolerances, deterioration, and clearances.
Stalling pressure rise	The pressure rise @ constant corrected airflow that will cause the compressor to stall.
Standard atmosphere	Ambient conditions represented by air at a temperature of 15 °C (59 °F), a barometric pressure of 1.01325 bar (14.696 psia). ISA corresponds to average values of temperature and pressure at middling latitudes.
Standards	Technical requirements expressed by certifying organizations.
State space model	A linear representation of a dynamic system.
State variables	Parameters in a model whose rate of change is defined by a dynamic equation.
Steady-state	The description of a system where there are no unbalanced forces or energies.
Stepped labyrinth seals	A type of seal design.
Straight model	The model that satisfy the engine matching equations for a given component characteristics.
Stratification	Separation into layers.
Stream line curvature code	A type of 2D turbomachinery code which uses blade geometry, correlations of blade loss and flow exit deviation to determine blade steady performance.
Sub idle	Engine power at which the system is in start up mode.
Surface cooling	Associated with cooling across a metal surface by convection using cooler airflow from some source within the engine.

Surge	Compressor instability; Violent reversing of flow within the compressor; Usually 3 – 15 Hz.
Surge cycle	Reoccurring compressor surge with periods of recovery; Cyclic in nature 3 – 15 Hz.
Surge line	Locus of stability points for all speeds beyond which the compressor will stall or surge.
Swirl losses	Pressure losses in a duct or turbo-machine due to the swirl component of flow.
Swirling flow	Flow that has a circular motion on top of its principal direction.
Synthesis	The generation of a prediction based on a collection of component assumptions.
System identification	A process by which the transfer function of a dynamic process can be derived by observing its outputs.
T&E (Test and Evaluation)	Strong coupling between modeling and simulation technology with experimental data during the development process.
Tappings (bleed ports)	Holes or slots in the casing for extraction or introduction of air from some other source.
Temporal resolution	Dealing with time stepping or time domain.
Test cell	Installation embedding the engine or component to reproduce their actual theoretical environment for characterization of global and detailed behaviors.
TET (Turbine <i>Exit</i> Temperature) OR (Turbine <i>Entry</i> Temperature)	1) The flow weighted mean total temperature of the working fluid at a plane immediately downstream of the last stage turbine rotor blades. 2) The flow weighted mean total temperature of the working fluid at a plane immediately upstream of the first stage turbine rotor blades.
Thermal efficiency	The ratio of the net power output to the heat consumption based on the lower heating value of the fuel.
Thermal management system	A design that controls the temperature of a component or region.
Thermodynamic parameters	Parameters defining the state of the working fluid during the engine cycle, such as temperature, pressure, enthalpy, entropy, etc.
Through flow code	Another name for streamline curvature or meridional type codes.
Thrust	Unbalanced force caused by the pressure forces across and the difference in the momentum of air entering and the exhaust gasses leaving a gas turbine engine.
Thrust coefficient $C_g$	Ratio of actual thrust to ideal thrust.
Thrust vectoring	Off centerline axis thrust produced by a vectoring exhaust nozzle.
Time average equations	Equations that do not consider fluctuating pressure perturbations – mean flow type equations.
Time between overhauls	Time spent on wing between required major planned maintenance action on engine component to restore hot parts temperature margin – relative to the declared red-line.
Time lag	A time-based delay or skew.
Tip clearances	Physical distance between the rotor tip and the casing; generally the larger the clearances the worse the performance.
TIT (Turbine Inlet Temperature)	The flow weighted mean total temperature of the working fluid at a plane immediately upstream of the first stage rotor blades.
Total/static conditions	Static Conditions refer to thermodynamic properties not considering the flow velocity. Total (or Stagnation) Conditions refer to thermodynamic conditions hypothetically reachable by decelerating the flow to zero speed (Stagnation) isentropically.
Transfer function	A mathematical expression defining the dynamic response of a system.
Transient	Unsteady state. Also used to described low bandwidth dynamic models.
Trending	A process of averaging/smoothing a time series of data.
Trim setting	Engine control settings to provide a certain engine performance.
Trimming	The process of obtaining a set of initial states which give a steady state.
Turbine flow capacity method	An method of deriving core flow by assuming a value for HP turbine flow capacity.
Turbine nozzle	Turbine inlet guide vane used to direct the gas flow at an optimum angle on to the first turbine rotor.

## ANNEX E – GLOSSARY

Turbofan	A gas turbine engine propulsion where a portion of flow bypasses the gas generator.
Turbojet	An engine where the turbine(s) produce just enough power to drive the compressor(s), the remaining energy is used for propulsion, expanding through a nozzle.
Turbomachinery matching	Matching the operation of compressors and turbines operating in line in a gas turbine engine to give the desired equilibrium operating point.
Turboshaft	A gas turbine engine where all the power produced is shaft power as in helicopters, marine applications and electrical power production.
Turbulence model	Model of the Reynolds Stress terms of the Navier-Stokes Equations. Models turbulence generation – variety of models used, some better than others depending upon the application.
Two phase flow	Any combination of two distinct phases under flow conditions: gas-liquid, liquid-liquid, or gas-solid particles.
Two-spool or Dual-spool	Twin shafts; Low pressure turbine usually turns fan compressor; High pressure turbine turns high pressure compressor.
Unsteady	Description of a process which is time-varying.
User environment	User interface of a computer plus additional peripherals such as printers, scanners and network connections.
User friendly	“Easy to use by the user”. Qualification for a software user-interface that requires a relatively small learning effort from the user before he can operate the program. User friendly interfaces are usually <i>GUI</i> 's that “speak for themselves” as to how the user can perform certain tasks.
Utilities	Auxiliary software programs that provide additional capabilities to application programs or the operating system. Examples are file format conversion programs, separate visualization programs, corrupt file repair programs and disk compression tools.
Variable area turbine	Turbine design that allows adjustment of the nozzle guide vanes or downstream stator vanes. Usually done to optimize turbine performance.
Variable cycle engine	Jet engine in which path of working fluid can be altered by shutters/valves/doors, thereby modulating gross engine properties such as SFC and specific thrust.
Variable geometry	Refers to changes in gas path geometry such as variable inlet guide vanes (IGV) or variable exit nozzle area such as CD nozzle.
Variable nozzle	Variable area nozzle; A nozzle design that allows the exhaust nozzle to change area ratios and/or go from convergent nozzle to CD nozzle; Most commonly used in military turbofan engines.
Velocity coefficient, $C_v$	Nozzle Coefficient base upon ratio of actual velocity to ideal velocity.
Velocity triangles	Turbomachinery velocity triangles describing the absolute and relative velocity magnitudes and direction.
Vitiated air	Air with products of combustion; usually experienced when the objective is to get heat air via combustion; sometimes $O_2$ is injected in the air to make up the loss due to combustion.
Volume dynamics	Volume changes usually due to acoustic pressure changes.
Warm flow rigs	Testing facility providing controlled inlet temperature generating conditions in the test section (more representative of the actual system environment – but not actual conditions).
Weak extinction	Combustion flameout due to fuel lean conditions.
WFB burner fuel flow	The total fuel flow-rate to the combustor.
Wind tunnel	Any of family of devices in which fluid is pumped through duct to flow past object under test.
Windage losses	External energy loss occurring on the disc surfaces, etc. due to air friction.
Windmilling	Phenomena in which the fan rotation is caused by the momentum of the incoming air only.
Zero order model	A model which has no dynamic content.
Zooming	A process where the fidelity of a model can be modified at user request.

REPORT DOCUMENTATION PAGE																					
<b>1. Recipient's Reference</b>	<b>2. Originator's References</b>	<b>3. Further Reference</b>	<b>4. Security Classification of Document</b>																		
	RTO-TR-AVT-036 AC/323(AVT-036)TP/106	ISBN 978-92-837-0061-6	UNCLASSIFIED/ UNLIMITED																		
<b>5. Originator</b>	Research and Technology Organisation North Atlantic Treaty Organisation BP 25, F-92201 Neuilly-sur-Seine Cedex, France																				
<b>6. Title</b>	Performance Prediction and Simulation of Gas Turbine Engine Operation for Aircraft, Marine, Vehicular, and Power Generation																				
<b>7. Presented at/Sponsored by</b>	The RTO Applied Vehicle Technology Panel (AVT) Task Group – Final Report of AVT-036.																				
<b>8. Author(s)/Editor(s)</b>	Multiple		<b>9. Date</b> February 2007																		
<b>10. Author's/Editor's Address</b>	Multiple		<b>11. Pages</b> 652																		
<b>12. Distribution Statement</b>	There are no restrictions on the distribution of this document. Information about the availability of this and other RTO unclassified publications is given on the back cover.																				
<b>13. Keywords/Descriptors</b>	<table border="0"> <tbody> <tr> <td>Aircraft engines</td> <td>Mathematical models</td> <td>Models</td> </tr> <tr> <td>Computer programs</td> <td>Methodology</td> <td>Performance evaluation</td> </tr> <tr> <td>Computerized simulation</td> <td>Military vehicle</td> <td>Performance modelling</td> </tr> <tr> <td>Cycle codes</td> <td>Model validation</td> <td>Reviews</td> </tr> <tr> <td>Gas turbine engines</td> <td>Model verification</td> <td>V &amp; V (Verification and Validation)</td> </tr> <tr> <td>Marine propulsion</td> <td></td> <td></td> </tr> </tbody> </table>			Aircraft engines	Mathematical models	Models	Computer programs	Methodology	Performance evaluation	Computerized simulation	Military vehicle	Performance modelling	Cycle codes	Model validation	Reviews	Gas turbine engines	Model verification	V & V (Verification and Validation)	Marine propulsion		
Aircraft engines	Mathematical models	Models																			
Computer programs	Methodology	Performance evaluation																			
Computerized simulation	Military vehicle	Performance modelling																			
Cycle codes	Model validation	Reviews																			
Gas turbine engines	Model verification	V & V (Verification and Validation)																			
Marine propulsion																					
<b>14. Abstract</b>	<p>A Technical Team of the NATO RTO has created a report on gas turbine simulation, ranging from applications to latest methodology of modeling techniques for gas turbine propulsion applications. The report includes examples of how gas turbine numerical simulations have been utilized for aircraft, marine, and vehicular propulsion applications. The major numerical simulation presented in the report is the gas turbine engine cycle code which provides performance for both steady state and transient operation. In addition to examples of how cycle codes are used, an in-depth discussion of how cycle codes are constructed and what basic assumptions are involved is given in the report. Additional higher order and specific numerical simulations for component design and operation are presented in the appendices to this report. Present computer platforms in use for such models are reviewed, and an outlook on development is given. The report aims at increasing the use and the value of engine computer simulations in NATO Nations and NATO's design and use of engines.</p>																				





BP 25

F-92201 NEUILLY-SUR-SEINE CEDEX • FRANCE  
Télécopie 0(1)55.61.22.99 • E-mail [mailbox@rta.nato.int](mailto:mailbox@rta.nato.int)



## DIFFUSION DES PUBLICATIONS RTO NON CLASSIFIEES

Les publications de l'AGARD et de la RTO peuvent parfois être obtenues auprès des centres nationaux de distribution indiqués ci-dessous. Si vous souhaitez recevoir toutes les publications de la RTO, ou simplement celles qui concernent certains Panels, vous pouvez demander d'être inclus soit à titre personnel, soit au nom de votre organisation, sur la liste d'envoi.

Les publications de la RTO et de l'AGARD sont également en vente auprès des agences de vente indiquées ci-dessous.

Les demandes de documents RTO ou AGARD doivent comporter la dénomination « RTO » ou « AGARD » selon le cas, suivi du numéro de série. Des informations analogues, telles que le titre et la date de publication sont souhaitables.

Si vous souhaitez recevoir une notification électronique de la disponibilité des rapports de la RTO au fur et à mesure de leur publication, vous pouvez consulter notre site Web ([www.rta.nato.int](http://www.rta.nato.int)) et vous abonner à ce service.

### CENTRES DE DIFFUSION NATIONAUX

#### ALLEMAGNE

Streitkräfteamt / Abteilung III  
Fachinformationszentrum der  
Bundeswehr (FIZBW)  
Gorch-Fock-Straße 7, D-53229 Bonn

#### BELGIQUE

Etat-Major de la Défense  
Département d'Etat-Major Stratégie  
ACOS-STRAT – Coord. RTO  
Quartier Reine Elisabeth  
Rue d'Evère, B-1140 Bruxelles

#### CANADA

DSIGRD2 – Bibliothécaire des ressources du savoir  
R et D pour la défense Canada  
Ministère de la Défense nationale  
305, rue Rideau, 9<sup>e</sup> étage  
Ottawa, Ontario K1A 0K2

#### DANEMARK

Danish Acquisition and Logistics  
Organization (DALO)  
Lautrupbjerg 1-5  
2750 Ballerup

#### ESPAGNE

SDG TECEN / DGAM  
C/ Arturo Soria 289  
Madrid 28033

#### ETATS-UNIS

NASA Center for AeroSpace  
Information (CASI)  
Parkway Center, 7121 Standard Drive  
Hanover, MD 21076-1320

#### FRANCE

O.N.E.R.A. (ISP)  
29, Avenue de la Division Leclerc  
BP 72, 92322 Châtillon Cedex

#### GRECE (Correspondant)

Defence Industry & Research  
General Directorate  
Research Directorate  
Fakinos Base Camp, S.T.G. 1020  
Holargos, Athens

#### HONGRIE

Department for Scientific Analysis  
Institute of Military Technology  
Ministry of Defence  
P O Box 26  
H-1525 Budapest

#### ISLANDE

Director of Aviation  
c/o Flugrad  
Reykjavik

#### ITALIE

Centro di Documentazione  
Tecnico-Scientifica della Difesa  
Via XX Settembre 123  
00187 Roma

#### LUXEMBOURG

Voir Belgique

#### NORVEGE

Norwegian Defence Research  
Establishment  
Attn: Biblioteket  
P.O. Box 25  
NO-2007 Kjeller

#### PAYS-BAS

Royal Netherlands Military  
Academy Library  
P.O. Box 90.002  
4800 PA Breda

#### POLOGNE

Centralny Ośrodek Naukowej  
Informacji Wojskowej  
Al. Jerozolimskie 97  
00-909 Warszawa

#### PORTUGAL

Estado Maior da Força Aérea  
SDFA – Centro de Documentação  
Alfragide  
P-2720 Amadora

#### REPUBLIQUE TCHEQUE

LOM PRAHA s. p.  
o. z. VTÚLaPVO  
Mladoboleslavská 944  
PO Box 18  
197 21 Praha 9

#### ROUMANIE

Romanian National Distribution  
Centre  
Armaments Department  
9-11, Drumul Taberei Street  
Sector 6, 061353, Bucharest

#### ROYAUME-UNI

Dstl Knowledge Services  
Information Centre  
Building 247  
Dstl Porton Down  
Salisbury  
Wiltshire SP4 0JQ

#### TURQUIE

Milli Savunma Bakanlığı (MSB)  
ARGE ve Teknoloji Dairesi  
Başkanlığı  
06650 Bakanlıklar – Ankara

### AGENCES DE VENTE

#### NASA Center for AeroSpace Information (CASI)

Parkway Center, 7121 Standard Drive  
Hanover, MD 21076-1320  
ETATS-UNIS

#### The British Library Document Supply Centre

Boston Spa, Wetherby  
West Yorkshire LS23 7BQ  
ROYAUME-UNI

#### Canada Institute for Scientific and Technical Information (CISTI)

National Research Council  
Acquisitions, Montreal Road, Building M-55  
Ottawa K1A 0S2, CANADA

Les demandes de documents RTO ou AGARD doivent comporter la dénomination « RTO » ou « AGARD » selon le cas, suivie du numéro de série (par exemple AGARD-AG-315). Des informations analogues, telles que le titre et la date de publication sont souhaitables. Des références bibliographiques complètes ainsi que des résumés des publications RTO et AGARD figurent dans les journaux suivants :

#### Scientific and Technical Aerospace Reports (STAR)

STAR peut être consulté en ligne au localisateur de ressources uniformes (URL) suivant :

<http://www.sti.nasa.gov/Pubs/star/Star.html>

STAR est édité par CASI dans le cadre du programme NASA d'information scientifique et technique (STI)  
STI Program Office, MS 157A  
NASA Langley Research Center  
Hampton, Virginia 23681-0001  
ETATS-UNIS

#### Government Reports Announcements & Index (GRA&I)

publié par le National Technical Information Service  
Springfield

Virginia 2216

ETATS-UNIS

(accessible également en mode interactif dans la base de données bibliographiques en ligne du NTIS, et sur CD-ROM)



BP 25

F-92201 NEUILLY-SUR-SEINE CEDEX • FRANCE  
Télécopie 0(1)55.61.22.99 • E-mail [mailbox@rta.nato.int](mailto:mailbox@rta.nato.int)



## DISTRIBUTION OF UNCLASSIFIED RTO PUBLICATIONS

AGARD & RTO publications are sometimes available from the National Distribution Centres listed below. If you wish to receive all RTO reports, or just those relating to one or more specific RTO Panels, they may be willing to include you (or your Organisation) in their distribution.

RTO and AGARD reports may also be purchased from the Sales Agencies listed below.

Requests for RTO or AGARD documents should include the word 'RTO' or 'AGARD', as appropriate, followed by the serial number. Collateral information such as title and publication date is desirable.

If you wish to receive electronic notification of RTO reports as they are published, please visit our website ([www.rta.nato.int](http://www.rta.nato.int)) from where you can register for this service.

### NATIONAL DISTRIBUTION CENTRES

#### BELGIUM

Etat-Major de la Défense  
Département d'Etat-Major Stratégie  
ACOS-STRAT – Coord. RTO  
Quartier Reine Elisabeth  
Rue d'Evère  
B-1140 Bruxelles

#### CANADA

DRDKIM2  
Knowledge Resources Librarian  
Defence R&D Canada  
Department of National Defence  
305 Rideau Street, 9<sup>th</sup> Floor  
Ottawa, Ontario K1A 0K2

#### CZECH REPUBLIC

LOM PRAHA s. p.  
o. z. VTÚLaPVO  
Mladoboleslavská 944  
PO Box 18  
197 21 Praha 9

#### DENMARK

Danish Acquisition and Logistics  
Organization (DALO)  
Lautrupbjerg 1-5  
2750 Ballerup

#### FRANCE

O.N.E.R.A. (ISP)  
29, Avenue de la Division Leclerc  
BP 72  
92322 Châtillon Cedex

#### GERMANY

Streitkräfteamt / Abteilung III  
Fachinformationszentrum der  
Bundeswehr (FIZBw)  
Gorch-Fock-Straße 7  
D-53229 Bonn

#### GREECE (Point of Contact)

Defence Industry & Research  
General Directorate  
Research Directorate  
Fakinos Base Camp  
S.T.G. 1020  
Holargos, Athens

#### HUNGARY

Department for Scientific Analysis  
Institute of Military Technology  
Ministry of Defence  
P O Box 26  
H-1525 Budapest

#### ICELAND

Director of Aviation  
c/o Flugrad, Reykjavik

#### ITALY

Centro di Documentazione  
Tecnico-Scientifica della Difesa  
Via XX Settembre 123  
00187 Roma

#### LUXEMBOURG

See Belgium

#### NETHERLANDS

Royal Netherlands Military  
Academy Library  
P.O. Box 90.002  
4800 PA Breda

#### NORWAY

Norwegian Defence Research  
Establishment  
Attn: Biblioteket  
P.O. Box 25  
NO-2007 Kjeller

#### POLAND

Centralny Ośrodek Naukowej  
Informacji Wojskowej  
Al. Jerozolimskie 97  
00-909 Warszawa

#### PORTUGAL

Estado Maior da Força Aérea  
SDFA – Centro de Documentação  
Alfragide  
P-2720 Amadora

#### ROMANIA

Romanian National Distribution Centre  
Armaments Department  
9-11, Drumul Taberei Street  
Sector 6, 061353, Bucharest

#### SPAIN

SDG TECEN / DGAM  
C/ Arturo Soria 289  
Madrid 28033

#### TURKEY

Milli Savunma Bakanlığı (MSB)  
ARGE ve Teknoloji Dairesi Başkanlığı  
06650 Bakanlıklar – Ankara

#### UNITED KINGDOM

Dstl Knowledge Services  
Information Centre  
Building 247  
Dstl Porton Down  
Salisbury, Wiltshire SP4 0JQ

#### UNITED STATES

NASA Center for AeroSpace  
Information (CASI)  
Parkway Center  
7121 Standard Drive  
Hanover, MD 21076-1320

### SALES AGENCIES

#### NASA Center for AeroSpace Information (CASI)

Parkway Center  
7121 Standard Drive  
Hanover, MD 21076-1320  
UNITED STATES

#### The British Library Document Supply Centre

Boston Spa, Wetherby  
West Yorkshire LS23 7BQ  
UNITED KINGDOM

#### Canada Institute for Scientific and Technical Information (CISTI)

National Research Council  
Acquisitions  
Montreal Road, Building M-55  
Ottawa K1A 0S2, CANADA

Requests for RTO or AGARD documents should include the word 'RTO' or 'AGARD', as appropriate, followed by the serial number (for example AGARD-AG-315). Collateral information such as title and publication date is desirable. Full bibliographical references and abstracts of RTO and AGARD publications are given in the following journals:

#### Scientific and Technical Aerospace Reports (STAR)

STAR is available on-line at the following uniform resource locator:

<http://www.sti.nasa.gov/Pubs/star/Star.html>

STAR is published by CASI for the NASA Scientific and Technical Information (STI) Program  
STI Program Office, MS 157A  
NASA Langley Research Center  
Hampton, Virginia 23681-0001  
UNITED STATES

#### Government Reports Announcements & Index (GRA&I)

published by the National Technical Information Service  
Springfield  
Virginia 2216  
UNITED STATES  
(also available online in the NTIS Bibliographic Database or on CD-ROM)